SOLID-PHASE SYNTHESIS OF 5-ARYLHISTIDINE-CONTAINING PEPTIDES: FROM LINEAR ANTIMICROBIAL PEPTIDES TO CYCLIC PEPTIDES DERIVED FROM ARYLOMYCINS AND ACICULITINS

I-teng Montserrat Ng Choi

Universitat de Girona

DOCTORAL THESIS

SOLID-PHASE SYNTHESIS OF 5-ARYLHISTIDINE-CONTAINING PEPTIDES: FROM LINEAR ANTIMICROBIAL PEPTIDES TO CYCLIC PEPTIDES DERIVED FROM ARYLOMYCINS AND ACICULITINS

I-teng Montserrat Ng Choi

2015

Doctoral Programme in Experimental Sciences and Sustainability

Supervised by: Dr. Marta Planas Grabuleda and Dr. Lidia Feliu Soley

This manuscript has been presented to opt for the **Doctoral Degree** from the **University of Girona**

Dr. Marta Planas Grabuleda and Dr. Lidia Feliu Soley, of the Universitat de Girona,

WE DECLARE:

That the thesis entitled "Solid-phase synthesis of 5-arylhistidine-containing peptides: from linear antimicrobial peptides to cyclic peptides derived from arylomycins and aciculitins", presented by I-teng Montserrat Ng Choi to obtain a doctoral degree, has been completed under our supervision and meets the requirements to opt for an International Doctorate.

For all intents and purposes, we hereby sign this document.

Dr. Marta Planas Grabuleda

Dr. Lidia Feliu Soley

Girona, 08/09/2015

"The only way to do great work is to love what you do."

(Steve Jobs)

"Without music, life would be a mistake."

(Friedrich Nietzsche)

A LA MEVA FAMILIA

FULL LIST OF PUBLICATIONS

Publications derived from this thesis

Chapter 3: Ng-Choi, I.; Soler, M.; Cerezo, V.; Badosa, E.; Montesinos, E.; Planas, M.; Feliu, L. Solid-phase synthesis of 5-arylhistidine-containing peptides with antimicrobial activity through a microwave assisted Suzuki-Miyaura cross-coupling. *Eur. J. Org. Chem.* **2012**, 4321-4332.

Chapter 3: Ng-Choi, I.; Soler, M.; Güell, I.; Badosa, E.; Cabrefiga, J.; Bardají, E.; Montesinos, E.; Planas, M.; Feliu, L. Antimicrobial peptides incorporating non-natural amino acids as agents for plant protection. *Protein Pept. Lett.* **2014**, *21*, 357-367. (Review article)

Manuscripts in preparation derived from this thesis

Chapter 4: Ng-Choi, I.; Feliu, L.; Planas, M. Solid-phase synthesis of biaryl cyclic peptides containing a histidine-phenylalanine linkage.

Chapter 5: Ng-Choi, I.; Planas, M.; Feliu, L. Solid-phase peptide macrocyclization via a microwave-assisted Suzuki-Miyaura reaction between a histidine and a tyrosine derivative.

Chapter 6: Ng-Choi, I.; Figueras, E.; Feliu, L.; Planas, M. Solid-phase synthesis of biaryl cyclic lipopeptides derived from arylomycins.

Chapter 7: Ng-Choi, I.; Planas, M.; Feliu, L. Solid-phase synthesis of analogues of the northern and southern hemispheres of aciculitins.

Chapter 8: Ng-Choi, I.; Feliu, L.; Planas, M. Solid-phase synthesis of biaryl bicyclic peptide analogues of aciculitins.

ABBREVIATIONS

Ac	Acetyl
Ar	Aryl
Aq.	Aqueous
L-BPA	4-Borono-L-phenylalanine
Bn	Benzyl
B_2Pin_2	Bis(pinacolato)diboron
Boc	*tert*-Butyloxycarbonyl
br. s	Broad singlet
*t*Bu	*tert*-Butyl
Cbz	Carboxybenzyl
CFU	Colony-forming unit
CM	Aminomethyl ChemMatrix
COMU	1-[(1-(Cyano-2-ethoxy-2-oxoethylideneaminooxy)-dimethylamino-morpholinomethylene)] methanaminium hexafluorophosphate
dba	*trans*,*trans*-Dibenzylideneacetone
DBU	1,8-Diazabicyclo[5.4.0]undec-7-ene
DCC	*N*,*N'*-Dicyclohexylcarbodiimide
d	Doublet
dd	Doublet of doublets
DG	Directing group
DIAD	Diisopropyl azodicarboxylate
DIEA	*N*,*N*-Diisopropylethylamine
DIPCDI	*N*,*N'*-Diisopropylcarbodiimide
DME	1,2-Dimethoxyethane
DMF	*N*,*N*-Dimethylformamide
DMSO	Dimethyl sulfoxide
dppf	1,1'-Bis(diphenylphosphino)ferrocene
DVB	Divinylbenzene
EDC	1-Ethyl-3-(3-dimethylaminopropyl)carbodiimide
EDTA	Ethylenediaminetetraacetic acid

equiv.	Equivalent(s)
ESI-MS	Electrospray mass spectrometry
Et	Ethyl
Fmoc	9-Fluorenylmethoxycarbonyl
Fmoc-OSu	*N*-(9-Fluorenylmethoxycarbonyloxy)succinimide
HATU	*O*-(7-Aza-1*H*-benzotriazole-1-yl)-*N*,*N*,*N'*,*N'*-tetramethyluronium hexafluorophosphate
HBTU	*O*-(Benzotriazol-1-yl)-*N*,*N*,*N'*,*N'*-tetramethyluronium hexafluorophosphate
HCTU	*O*-(6-Chlorobenzotriazol-1-yl)-*N*,*N*,*N'*,*N'*-tetramethyluronium hexafluorophosphate
HOAt	*N*-Hydroxy-7-azabenzotriazole
HOBt	*N*-Hydroxybenzotriazole
HPLC	High performance liquid chromatography
HRMS	High resolution mass spectrometry
J	Coupling constant
LB	Luria Bertani
LC/MS	Liquid chromatography-mass spectrometry
liq.	Liquid
m	Multiplet
MBHA	4-Methylbenzhydrylamine
Me	Methyl
MIC	Minimum inhibitory concentration
MOM	Methoxymethyl ether
MW	Microwave irradiation
m/z	Mass-to-charge ratio
*p*NB	*para*-Nitrobenzyl
NBS	*N*-Bromosuccinimide
*o*NBS	*ortho*-Nitrobenzenesulfonyl
NMP	*N*-Methyl-2-pyrrolidone
NMR	Nuclear magnetic resonance
NsCl	*para*-Nitrobenzenesulfonyl
OTf	Trifluoromethanesulfonate
Oxyma	Ethyl 2-cyano-2-(hydroxyimino)acetate

Pbf	2,2,4,6,7-Pentamethyldihydrobenzofuran-5-sulfonyl
PCy	Tricyclohexylphosphine
PDA	Potato dextrose agar
PDB	Potato dextrose broth
PEG	Poly(ethylene glycol)
PEGA	Poly(acryloyl-bis(aminopropyl)polyethylene glycol)
PG	Protecting group
Ph	Phenyl
Pin	Pinacolato
PivOH	Pivalic acid
PMe_3	Trimethylphosphine
PMP	*para*-Methoxyphenyl
PPh_3	Triphenylphosphine
ppm	Parts per million
PS	Polystyrene
P(*o*-tolyl)$_3$	Tri(*ortho*-tolyl)phosphine
PyBOP	Benzotriazol-1-yloxytri(pyrrolidino)phosphonium hexafluorophosphate
PyOxim	*O*-[(Cyano(ethoxycarbonyl)methyliden)-amino]-yloxytri(pyrrolidino)phosphonium hexafluorophosphate
r.t.	Room temperature
s	Singlet
SEM	2-(Trimethylsilyl)ethoxymethyl
SPhos	2-Dicyclohexylphosphino-2’,6’-dimethoxybiphenyl
SPPS	Solid-phase peptide synthesis
t	Triplet
TBS	*tert*-Butyldimethylsilyl ether
TES	Triethylsilyl ether
TFA	Trifluoroacetic acid
THF	Tetrahydrofuran
TIS	Triisopropylsilane
Tmob	2,4,6-Trimethoxybenzyl
TMS	Trimethylsilyl
TPPTS	tri(*meta*-sulfonatedphenyl)phosphine

t_R	Retention time
Tr	Trityl
TRIS	Tris(hydroxymethyl)aminomethane
Ts	*para*-Toluenesulfonyl
TSB	Trypticase soy broth
UV	Ultraviolet
vis	Visible
XPhos	2-Dicyclohexylphosphino-2',4',6'-triisopropylbiphenyl
δ	Chemical shift
λ	Wavelength

Amino acids

Name	Three letter code	One letter code
Alanine	Ala	A
Arginine	Arg	R
Asparagine	Asn	N
Aspartic acid	Asp	D
Cysteine	Cys	C
Glutamic acid	Glu	E
Glutamine	Gln	Q
Glycine	Gly	G
Histidine	His	H
Isoleucine	Ile	I
Leucine	Leu	L
Lysine	Lys	K
Methionine	Met	M
Phenylalanine	Phe	F
Proline	Pro	P
Serine	Ser	S
Threonine	Thr	T
Tryptophan	Trp	W
Tyrosine	Tyr	Y
Valine	Val	V

LIST OF FIGURES

LIST OF TABLES

LIST OF SCHEMES

ACKNOWLEDGEMENTS

Arribats en aquest punt, és moment de reconèixer l'esforç de totes aquelles persones que, d'una manera o altra, m'han donat suport i han fet possible que en aquest instant pugui escriure aquestes paraules. Per això, m'agradaria que aquestes línies serveixin per expressar el meu agraïment a tots els que han estat al meu costat al llarg d'aquesta aventura.

En primer lloc, voldria agrair a les meves supervisores, la Dra. Marta Planas i la Dra. Lidia Feliu, per l'ajuda, suport i confiança dipositada en mi al llarg d'aquest temps. També m'agradaria donar les gràcies al Dr. Eduard Bardají i a la Dra. Montse Heras pels vostres consells i gran suport incondicional, els quals m'han permès el més important d'aquesta etapa, aprendre.

Tot seguit, voldria agrair a totes les persones que formen part dels Serveis Tècnics de Recerca de la Universitat de Girona, en especial, a la Dra. Lluïsa Matas per l'atenció que he rebut durant les estones a ressonància, a la Laura Gómez per haver realitzat gran part de les proves de HRMS, i a la senyora Anna Costa per les proves d'ESI-MS i sobretot per la paciència, atenció i professionalitat que en tot moment m'ha mostrat. De la mateixa manera, voldria donar les gràcies a la Dra. Esther Badosa del CIDSAV per haver portat a terme les proves biològiques del capítol 3 d'aquesta tesi.

No em puc oblidar de la persona gràcies a la qual he après tantes coses a nivell de laboratori, la Dra. Vane Cerezo (la d'en Tuck!). Gràcies per haver-me ajudat en tot durant els meus inicis al LIPPSO i pel granet de sorra que has aportat en aquesta tesi.

També m'agradaria expressar el meu agraïment a totes aquelles persones que formen o varen formar part del grup LIPPSO. Seguint la trajectòria d'aquest "viatge", a l'Ana Afonso pels dubtes existencials i per les nostres xerrades com a companyes de laboratori; A la Imma Güell (Sra. Güell!) pel bon ambient, treball en equip i per les nostres xerrades matinals; A en Rafael (el creador de "La Show") i a en Tiffa (tampoc revelaré l'alias que em vas assignar) per portar l'alegria al grup amb les vostres bromes constants fent que

les estones de feina fossin encara més agradables; A la Marta D. i a la Montse T. pels bons consells a nivell de laboratori i per la confiança que m'heu mostrat a nivell personal durant tan poc temps. No voldria oblidar-me de la Marta S. (i els nostres afterworks!), de la Sílvia (vale, també de les teves mascotes) i de la Cris R. (la mangui) per tots els moments que hem compartit al despatx, al laboratori i sobretot fora del món de la química. Seguint el recorregut, m'agradaria agrair a totes aquelles persones amb les que he pogut treballar directament: A la Sonia, a la Natàlia A., a la Marta S. (una altra vegada), i a l'Eduard F. (L'Edw!!) per la contribució en aquest treball. Ja al final del trajecte, no em puc oblidar de les persones amb les que he compartit laboratori durant l'any més dur, l'últim de la tesi. Sense intenció d'oblidar-me de ningú, gràcies Àngel, Nerea, Eduard (una altra vegada), Alberto, Eila, Ricard, Mireya i Christian per les vostres ganes d'aprendre i les bones estones al laboratori. Sempre em dieu que sóc molt alegre, però sense gent com vosaltres això no seria possible. Finalment, tot i haver coincidit poc a nivell de laboratori, m'agradaria destacar el meu agraïment a la Cris Camó, especialment a nivell personal durant els darrers mesos de tesi. Gràcies pel suport, per les nostres xerrades i sobretot pels moments de desconnexió que m'han ajudat a mantenir el meu positivisme, no és fàcil escriure una tesi.

No puc deixar de banda a tots els companys del Departament de Química amb qui he compartit bones estones entre dinars al bar d'en Paco, sopars, sortides i celebracions.

A nivell d'aprenentatge internacional, m'agradaria expressar el meu agraïment a totes aquelles persones amb les que he tingut la oportunitat de compartir 3 mesos molt agradables durant la meva estada a Itàlia. I would like to express my sincere gratitude to Prof. Alessandro Tossi at the University of Trieste for giving me the opportunity to expand my knowledge in his research group in the "Dip. di Scienze della Vita" and for his guidance during my research visit in Trieste. Many thanks for my lab mates Mario, Caterina, Annalisa, Michela, Matteo, Nicole, and Silvia P., and especially for Daniella, Monica and Valentina for their help and friendship. I would also like to thank Marija and Jusip for all our funny moments outside the laboratory, especially the time we spent in Piazza dell'Unità watching soccer. Inoltre, grazie mille a tutte le persone della Casa

dello Studente che ho avuto il piacere di incontrare, per farmi sentire come a casa. Siete tutti molto gentili e grandi compagni di stanza.

Ja fora del món de la química, m'agradaria agrair a tots els meus amics, per la vostra alegria i optimisme, el suport constant i les llargues xerrades sobre el dia a dia.

Finalment, vull donar les gràcies i dedicar aquest treball a la meva família els quals estan sempre al meu costat. A la meva mare pel recolzament i pels moments de desconnexió a la cuina; Al meu germà, en Gnai-yim, per escoltar-me, per estar disposat a donar-me consells, i sobretot pel gran suport incomparable que he rebut durant aquest darrer any; Al meu pare, la persona més especial i que més estimo. Gràcies per estar sempre atent, per la teva gran paciència i per ser tan fort.

A tots vosaltres, moltíssimes gràcies!

TABLE OF CONTENTS

Supplementary Digital Information

- ✓ PhD thesis (pdf file)
- ✓ ANNEX: Electronic supporting information for Chapter 3 – 8 (pdf file)

ABSTRACT

The incorporation of arylated amino acids into peptide sequences results in an increase of the conformational flexibility restriction and, therefore, in peptides with improved biological properties. In this context, considering the significance of 4(5)-arylimidazoles in many functional biomolecules, the preparation of peptides containing a 5-arylhistidines has received much attention in recent years. However, due to the difficulty of arylating the 4(5)-position of the imidazole ring, the formation of 5-arylhistidines is scarcely reported. The palladium-catalyzed Suzuki-Miyaura reaction is one of the most advantageous and often used cross-couplings for biaryl formation.

This thesis focuses on the preparation of linear and cyclic peptides containing a 5-arylhistidine, a 4-arylphenylalanine or a 3-aryltyrosine residue through catalytic inter- or intramolecular arylation of halopeptides on solid support. In particular, in Chapter 3, 5-arylhistidine-containing linear peptides are synthesized based on the structure of lead antimicrobial undecapeptides previously described in our group. These biaryl peptides have been designed by replacing a phenylalanine residue located at the 1- or 4-position in the lead undecapeptides by a 5-arylhistidine. The resulting biaryl linear peptides are less hemolytic than the corresponding parent peptide. In the following Chapters 4 and 5, our methodology is extended to the preparation of biaryl cyclic peptides incorporating a His-Phe or a His-Tyr biaryl linkage. The microwave-assisted intramolecular Suzuki-Miyaura reaction has allowed the synthesis of biaryl macrocycles of different ring sizes containing a histidine residue at the N- or C-terminus. Next, in Chapter 6 we describe the total solid-phase synthesis of biaryl cyclic lipopeptides derived from arylomycins, containing a Phe-Tyr, a Tyr-Tyr, a His-Tyr or a phenylglycine (Phg)-Tyr linkage in their structure. The key steps of our solid-phase methodology are a Miyaura borylation reaction, the cyclization via an intramolecular Suzuki-Miyaura arylation, a Mitsunobu N-methylation and the N-terminus acylation. Finally, based on our interest in aciculitins, in Chapters 7 and 8, we investigate the synthesis of analogues of the northern and the southern hemispheres of these marine bicyclic peptides, as well as the preparation of biaryl bicyclic peptide analogues containing a Phe-Phe, a Phe-Tyr, a His-Tyr or a Tyr-Tyr linkage. Several Suzuki-Miyaura conditions have been tested to enable the biaryl bond formation. Interestingly, the macroarylation step should preceed the macrolactamization for the formation of the bicyclic analogues.

RESUM

La incorporació d'aminoàcids arilats en seqüències peptídiques suposa un augment de la restricció de la flexibilitat conformacional i, per tant, dóna lloc a pèptids amb millors propietats biològiques. En aquest context, tenint en compte la importància de l'anell de 4(5)-arilimidazole en moltes biomolècules funcionals, la preparació de pèptids que continguin un residu de 5-arilhistidina ha rebut molta atenció en els darrers anys. No obstant això, degut a la dificultat d'arilar la posició 4(5) de l'anell d'imidazole, la formació de 5-arilhistidines pràcticament no s'ha publicat. La reacció de Suzuki-Miyaura catalitzada per pal·ladi és una de les reaccions d'acoblament creuat més avantatjoses i més utilitzades.

Aquesta tesi es centra en la preparació de pèptids lineals i cíclics que contenen un residu de 5-arilhistidina, un de 4-arilfenilalanina o un de 3-ariltirosina a través d'una arilació inter- o intramolecular d'halopèptids units a un suport sòlid. Concretament, en el capítol 3, es sintetizen pèptids lineals contenint un residu de 5-arilhistidina, els quals es basen en l'estructura d'undecapèptids antimicrobians *lead* prèviament descrits en el nostre grup. Aquests pèptids biarílics s'han dissenyat per substitució del residu de fenilalanina present a la posició 1 o 4 dels undecapèptids *lead* per una 5-arilhistidina. Els pèptids biarílics lineals resultants són menys hemolítics que el corresponent pèptid *lead*. En els següents capítols 4 i 5, la nostra metodologia s'aplica a la preparació de pèptids biarílics cíclics que incorporen un enllaç His-Phe o His-Tyr. La reacció intramolecular de Suzuki-Miyaura sota irradiació de microones ha permès la síntesi de macrocicles biarílics de diferents mides d'anell que contenen un residu d'histidina a la posició N- o C-terminal. Seguidament, en el capítol 6 es descriu la síntesi total en fase sòlida de lipopèptids biarílics cíclics derivats de les arilomicines, contenint en la seva estructura una enllaç Phe-Tyr, Tyr-Tyr, His-Tyr o fenilglicina (Phg)-Tyr. Les etapes clau de la nostra metodologia en fase sòlida són una reacció de borilació de Miyaura, la ciclació a través d'una arilació de Suzuki-Miyaura intramolecular, una reacció de Mitsunobu d'N-metilació i l'acilació de l'extrem N-terminal. Finalment, basant-nos en el nostre interès en les aciculitines, en els capítols 7 i 8, s'investiga la síntesi d'anàlegs dels hemisferis nord i del sud d'aquests pèptids bicíclics marins, així com la preparació de pèptids biarílics bicíclics anàlegs contenint un pont Phe-Phe, Phe-Tyr, His-Tyr o Tyr-Tyr. S'han assajat diverses condicions de la reacció de Suzuki-Miyaura per a la formació de

l’enllaç biarílic. Cal destacar que l’etapa de macroarilació ha de precedir a l’etapa de macrolactamització per a la formació dels anàlegs bicíclics.

RESUMEN

La incorporación de aminoacidos arilados en secuencias peptídicas supone un aumento de la restricción de la flexibilidad conformacional y, por lo tanto, da lugar a peptidos con mejores propiedades biológicas. En este contexto, considerando la importancia del anillo de 4(5)-arilimidazol en muchas biomoléculas funcionales, la preparación de péptidos que contengan un residuo de 5-arilhistidinas ha despertado un gran interés en los últimos años. Sin embargo, la formación de 5-arilhistidinas apenas se ha publicado debido a la dificultad para arilar la posición 4(5) del anillo de imidazol. La reacción de Suzuki-Miyaura catalizada por paladio es una de las reacciones de acoplamiento cruzado más útiles y ventajosas.

Esta tesis doctoral se centra en la preparación de péptidos lineales y cíclicos que contienen un residuo de 5-arilhistidina, uno de 4-arilfenilalanina o uno de 3-ariltirosina mediante una arilación inter- o intramolecular de halopéptidos unidos a un soporte sólido. Concretamente, en el capítulo 3, se sintetizan péptidos lineales que contienen un residuo de 5-arilhistidina, los cuales se basan estructuralmente en undecapéptidos antimicrobianos *lead* previamente descritos en nuestro grupo. Estos péptidos lineales han sido diseñados por sustitución de un residuo de fenilalanina presente en la posición 1 o 4 de los undecapéptidos *lead* por una 5-arilhistidina. Los péptidos biarílicos lineales resultantes son menos hemolíticos que el correspondiente péptido *lead*. En los siguientes capítulos 4 y 5, extendemos nuestra metodología se aplica a la preparación de péptidos biarílicos cíclicos que incorporan un enlace His-Phe o His-Tyr. La reacción intramolecular de Suzuki-Miyaura bajo irradiación de microondas ha permitido la síntesis de macrociclos biarílicos de diferentes tamaños de anillo que contienen un residuo de histidina en la posición N- o C-terminal. A continuación, en el capítulo 6 se describe la síntesis total en fase sólida de lipopéptidos biarílicos cíclicos derivados de las arilomicinas, conteniendo en su estructura un enlace Phe-Tyr, Tyr-Tyr, His-Tyr o fenilglicina (Phg)-Tyr. Las etapas clave de nuestra metodología en fase sólida son una reacción de borilación de Miyaura, la ciclación a través de una arilación de Suzuki-Miyaura intramolecular, una reacción de Mitsunobu de N-metilación y la acilación del extremo N-terminal. Finalmente, teniendo en cuenta nuestro interés en las aciculitinas, en los capítulos 7 y 8, se investiga la síntesis de análogos de los hemisferios norte y sur de estos péptidos marinos, así como la preparación de péptidos biarílicos bicíclicos análogos conteniendo un puente Phe-Phe,

Phe-Tyr, His-Tyr o Tyr-Tyr. Se han ensayado varias condiciones de la reacción de Suzuki-Miyaura para la formación del enlace biarílico. Es de destacar que la etapa de macroarilación debe preceder a la etapa de macrolactamización para la formación de los análogos bicíclicos.

CHAPTER 1

Introduction

CHAPTER 1

1.1. BIARYL NATURAL PRODUCTS

1.1.1. Importance of biaryl compounds

Biaryl compounds contain two aromatic rings joined through a sigma carbon-carbon bond. This biaryl motif has been of great interest over the last century, because it has been proven to be the key structural feature responsible for the activity of many biologically active molecules, including natural products, pharmaceuticals, fine chemicals, agrochemical compounds, and chiral catalysts (Torborg and Beller, 2009; Magano and Dunetz, 2011; Burke and Marques, 2015).

For instance, the biaryl moiety is present in many pharmaceutical drugs currently in the market, such as losartan (antihypertensive, Merck), valsartan (antihypertensive, Novartis), felbinac (antiinflammatory, Pfizer), imatinib (antitumor, Novartis), crizotinib (antitumor, Pfizer), and zolpidem (hypnotic, Sandoz) (Figure 1.1) (Johansson et al., 2012; Burke and Marques, 2015).

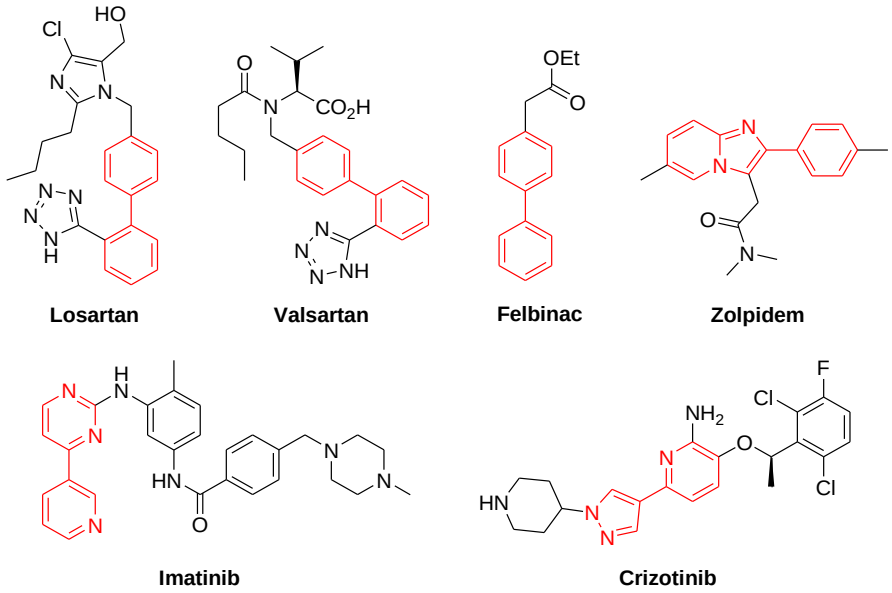

Figure 1.1. Chemical structures of some biologically active biaryl-containing drugs.

Furthermore, several biaryl natural products have been isolated and identified from a large number of marine and terrestrial sources (Lewis, 2000; Jin, 2006; Morris,

2013). Sponges, soft coral and ascidians are some of the most widespread sources found in the marine environment, which are able of producing a variety of bioactive compounds (Figure 1.2). Topsentins A-C are bis(indolyl)imidazoles isolated from the marine sponge *Topsentia genitrix*, being antitumor and antiviral agents. Nortopsentins A-B are cytotoxic and antifungal bis(indolyl)imidazoles isolated from the marine sponge *Spongosorites ruetzleri*. Dictyodendrin A is a marine substituted pyrrolocarbazole alkaloid from the sponge *Dictyodendrilla verongiformis* that displays inhibitory activity against telomerase. Polycarpine is a marine imidazole-type alkaloid from the ascidian *Polycarpa aurata*, which exhibits antitumor and cytotoxic activities. Diazonamide A is a heteroaromatic biaryl macrocycle with an indole bis-oxazole core, isolated from the marine ascidian *Diazona angulata*, and that it is a cytotoxic agent. Rigidin is a marine pyrrolopyrimidine alkaloid from the tunicate *Eudistoma cf. rigida*, which possesses calmodulin antagonistic activity, and cinnamide dimer is an antibacterial and antifungal *ortho*-hydroxylated biphenyl alkaloid from the marine soft coral *Sinularia flexibilis*.

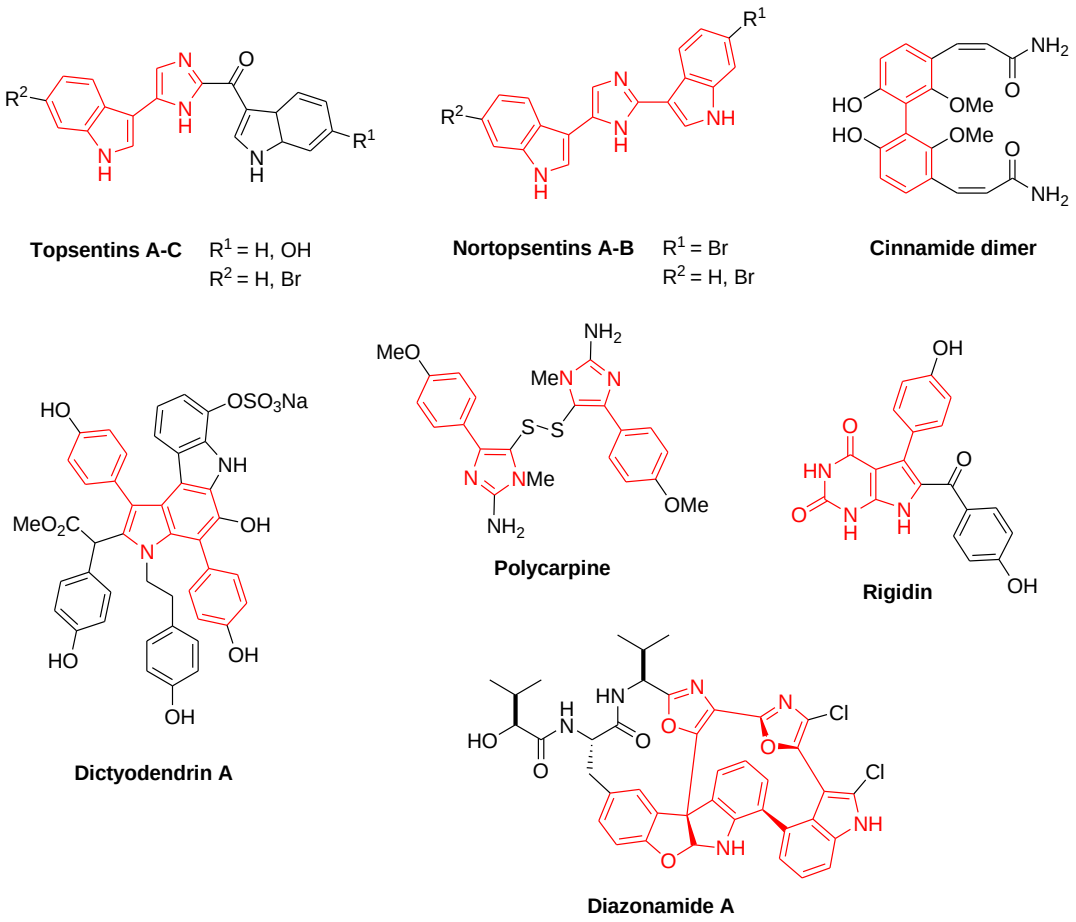

Figure 1.2. Examples of biaryl natural products from marine sources.

Biaryl compounds isolated from terrestrial sources have also been described to exhibit high biological activity, ranging from antimicrobial, antiviral, cytotoxic, antiplasmodial, antioxidant or enzyme inhibitory. Some of these natural products are the anti-human immunodeficiency virus (HIV) alkaloid michellamine B and the antimalarial alkaloid korupensamine A, both from the tropical plant *Ancistrocladus korupensis*; knipholone, an antiplasmodial anthraquinone derivative isolated from the roots of *Kniphofia foliosa*; gossypol, a polyphenolic pigment from the cotton plant *Gossypium*, being an antifertility agent; schizandrin, an antioxidant lignin from the fruit of *Schisandra chinensis*; and acerogenin E, a diarylheptanoid with inhibitory activity on nitric oxide production, isolated from *Acer nikoense* (Figure 1.3) (Kozlowski et al., 2009).

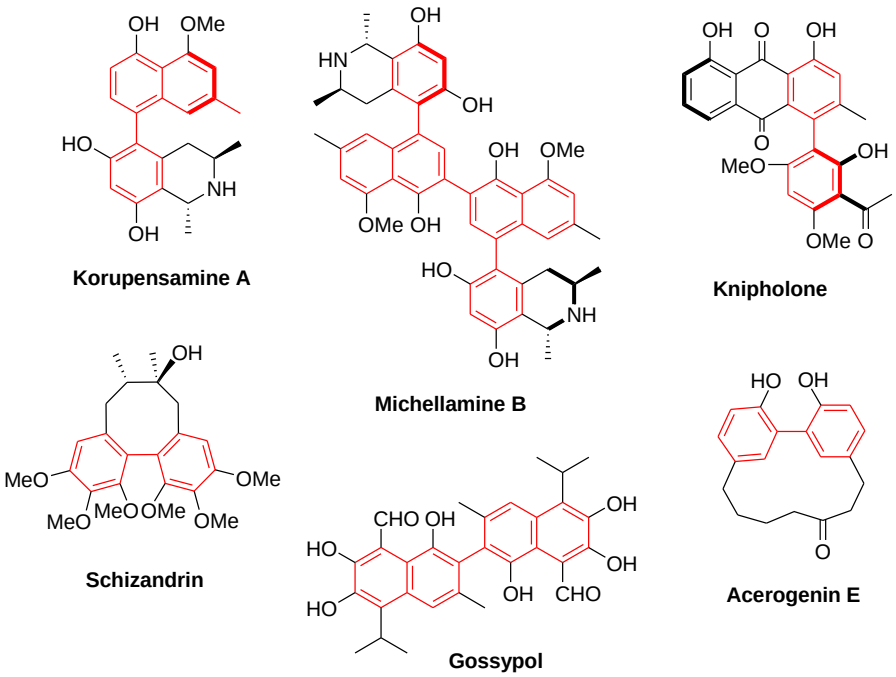

Figure 1.3. Examples of biaryl natural products from terrestrial sources.

1.1.2. Natural biaryl cyclic peptides

Unsymmetrical biaryl systems are also found in a great diversity of bioactive naturally occurring cyclic peptides from relatively simple to complex macrocycles (Feliu and Planas, 2005). These aryl-aryl moieties are commonly formed through the linkage between the side-chains of two aromatic amino acids, including histidines, tyrosines, phenylalanines, and tryptophans. These natural peptides are monocyclic or bicyclic. Some of the earliest reported biaryl-containing monocyclic peptides are himastatin, TMC-95A-D, biphenomycins A-B, and arylomycins A-B (Figure 1.4). Himastatin is a dimeric peptide containing two cyclohexadepsipeptide units joined through a biphenyl linkage between the aromatic side chains of two oxidized tryptophan derivatives. It was isolated from the cultured broth of *Streptomyces hygroscopus*, and displays antitumor activity against localized P388 leukemia and B16 melanoma (Leet et al., 1996). TMC-95A-D are cyclic tripeptides incorporating a phenol-oxindole biaryl system resulting from the linkage of the side chains of a tyrosine residue and a tryptophan. These proteasome inhibitors, isolated from the fermentation broth of *Apiospora montagnei*, are useful therapeutic agents for the treatment of cancer, inflammatory disorders, and immune diseases (Kohno et al., 2000). Biphenomycins A-B are biaryl cyclic tripeptides with a biphenyl system formed by cross-linking the aromatic side chains of 2-hydroxyphenylalanine residues. They were isolated from the culture broth *Streptomyces griseorubiginosus* and are potent antibacterial agents against strains of gram-positive bacteria, such as *Staphylococcus aureus* 2508 and 2485 (Ezaki et al., 1985). Arylomycins A-B are unique biaryl-bridged lipohexapeptides bearing a lipotripeptide tail attached to a biaryl cyclic tripeptide. The biaryl motif results from the linkage between a 4-hydroxyphenylglycine and a tyrosine residue. Arylomycins, which were isolated from the fermentation broth of a *Streptomyces* strain, display moderate antibacterial activity against a variety of gram-positive bacteria, and also exhibit weak antifungal activity against *Mucor hiemalis* Tü 179/180 (Schimana et al., 2002).

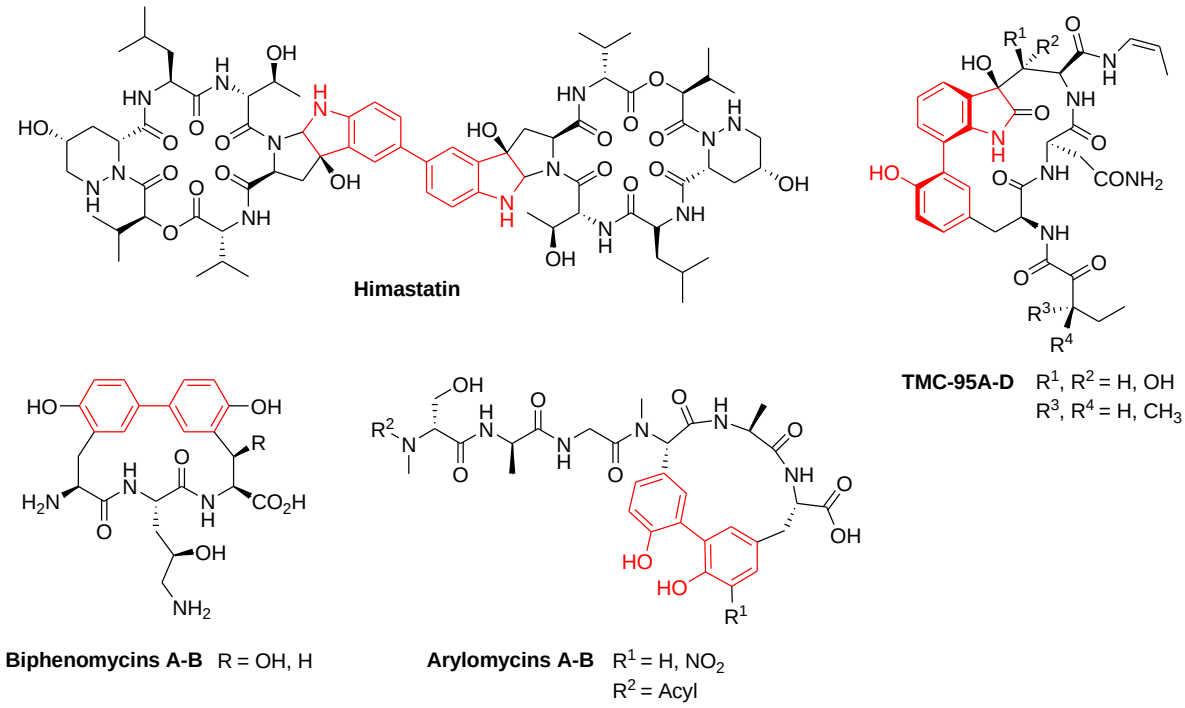

Figure 1.4. Natural biaryl monocyclic peptides.

Among the naturally occurring bicyclic peptides, vancomycin, RP-66453, neo-RA-V, and aciculitins A-C are some of the reported bioactive peptides that contain a biaryl and/or a biaryl ether bridge (Figure 1.5). Vancomycin belongs to a class of clinically important glycopeptide antibiotics that contain both biaryl and biaryl ether linkages in their structures. It was isolated from the fermentation broth of the actinomycete *Amicolatopsis orientalis*. Due to its effectiveness in the treatment of serious gram-positive bacterial infections, vancomycin is currently used in hospitals as antibiotic of last resort (Van Bambeke et al., 2004; Pace and Yang, 2006). RP-66453, a bicyclic tetrapeptide possessing a biaryl and a biaryl ether bridge formed by the linkage between the phenol groups of three tyrosine residues, was isolated from an *Astinomycetes* strain and it is a potent neurotensin receptor antagonist, useful for the treatment of depression, schizophrenia as well as Alzheimer's and Parkinson's diseases (Helynck et al., 1998). Neo-RA-V is an antitumor bicyclic hexapeptide that is characterized by the presence of a linkage between the 3-position of the phenol ring of two tyrosine residues. It was isolated from the roots of *Rubia cordifolia* L (*Galium cordifolium*) (Hitotsuyanagi et al., 2012). Aciculitins A-C were the first described bioactive natural glycopeptidolipids and they

were isolated from the marine sponge *Aciculites orientalis*. Structurally, they are bicyclic peptides that contain an unusual histidine-tyrosine bridge, which is formed from the linkage between the 5-position of the imidazole ring of a histidine and the 3-position of the phenol ring of a tyrosine. This uncommon bridge plays an important role in the biological activity of these compounds, being cytotoxic to the human-colon tumor cell line HCT-116 and antifungal against *Candida albicans* (Bewley et al., 1996).

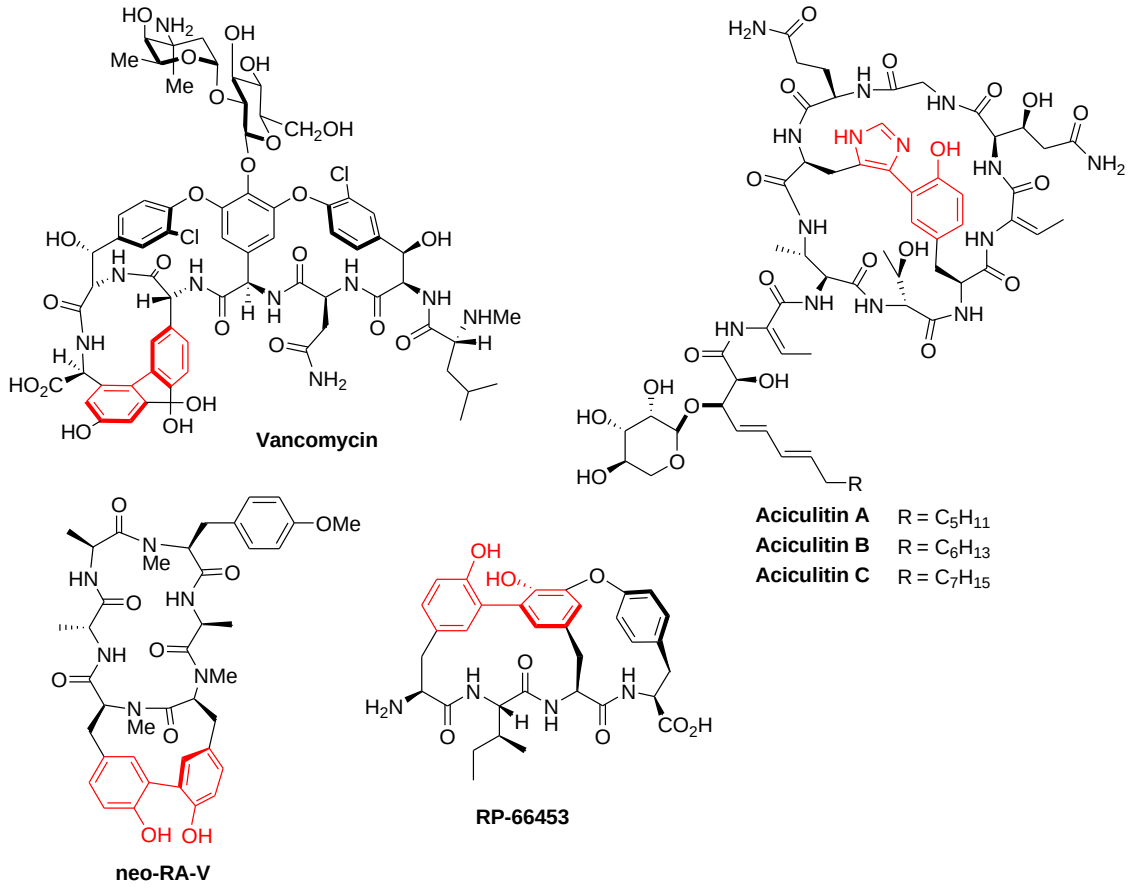

Figure 1.5. Natural biaryl bicyclic peptides.

1.2. METHODS FOR BIARYL BOND FORMATION

The difficulty to isolate biaryl natural products in enough quantities from terrestrial and especially from marine sources has encouraged organic chemists to develop efficient methods for the total synthesis of these compounds. The preparation of large amounts of these biologically active products and even of new analogues would allow further accurate studies related to their structural complexity as well as to other biological applications of such biaryl-containing products. Nowadays, cross-coupling reactions and direct arylation catalyzed by palladium are reported to be the most common and efficient methods for the formation of biaryl bonds.

Palladium-catalyzed cross-coupling reactions, such as the Negishi, Stille and Suzuki-Miyaura reactions, involve the use of an aryl electrophile (Ar^1-X), e.g. an arylhalide or an aryltriflate, and an arylmetal reagent (Ar^2-M) (Scheme 1.1). In particular, in the Negishi reactions, the organometallic reagent is an arylzinc, while the Stille and the Suzuki-Miyaura cross-couplings require the use of an aryltin and an arylboron derivative, respectively. Professors Ei-ichi Negishi, Akira Suzuki and Richard Fred Heck were awarded the Nobel Prize in Chemistry 2010 for their important contribution in the development of palladium-catalyzed cross-coupling reactions, which play an essential role in organic synthesis, both in research laboratories and industrial processes (Nicolaou et al., 2005; Johansson et al., 2012; Burke and Marques, 2015). The palladium-catalyzed direct C-H arylation of an aryl electrophile with a simple arene has also proven to be a useful method for the preparation of small biaryl molecules (Scheme 1.1). The main advantage of this arylation is that it avoids the preparation of the organometallic derivative. However, it has some limitations, because most organic compounds usually contain multiple C-H bonds and, in some cases, most of them are kinetically inert.

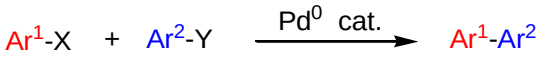

Reaction	X	Y	
Negishi	Br, I, OTf, OTs	ZnBr, ZnCl, ZnI	
Stille	Br, Cl, I, OAc, OTf	SnR_3	(R = alkyl)
Suzuki-Miyaura	Br, Cl, I, OAc, OTs, OTf	$B(OR)_2$	(R = H, alkyl)
Direct arylation	Br, Cl, I, OTf	H	

Scheme 1.1. Common palladium-catalyzed reactions for biaryl bond formation.

1.2.1. Suzuki-Miyaura cross-coupling reaction

The Suzuki-Miyaura reaction, first published in 1979, was discovered by Akira Suzuki and Norio Miyaura, and it is one of the most popular methods to selectively generate new carbon-carbon bonds. This transition metal-catalyzed process involves the cross-coupling of an organoboron compound with an organic electrophile, such as an aryl halide or triflate, in the presence of a base and catalyzed by a Pd(0) active complex (Suzuki, 1999). The first example of this reaction described the formation of biphenyls via the palladium-mediated cross-coupling of phenylboronic acid with several halobenzenes using benzene as solvent and $Pd(PPh_3)_4$ as catalyst (Miyaura et al., 1981) (Scheme 1.2).

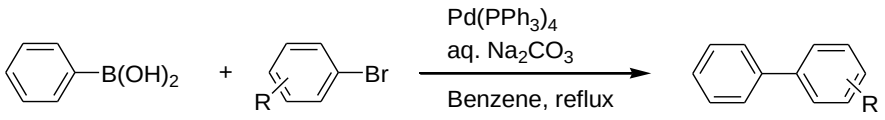

Scheme 1.2. Suzuki-Miyaura reaction.

This reaction has received much attention by researchers due to the wide range of advantages that it provides over the other palladium-catalyzed cross-coupling reactions (Corbet and Mignani, 2006; Suzuki, 2011), including the high stability of the starting materials, the high different functional group tolerance, the commercial availability of a wide range of boronic acid reagents, the use of small amounts of palladium catalyst, the insignificant effect of steric hindrance, the high regio- and stereoselectivity of the reaction, the mild reaction conditions, and the high possibility of using a wide variety of water soluble reagents because water can be used as solvent or co-solvent. Moreover, boron containing byproducts are non-toxic and can be easily removed by work-up, leading to high product purities and yields, and allowing its application in one-pot synthesis.

The general mechanism of the Suzuki-Miyaura cross-coupling reaction is shown in Scheme 1.3. The main steps of this catalytic cycle are a catalyst pre-activation, an oxidative addition, a Pd(II) complex activation, a transmetallation and a reductive

elimination (Martin and Yang, 1993; Miyaura and Suzuki, 1995; Corbet and Mignani, 2006; Alonso et al., 2008; García-Melchor et al., 2013). In particular, the Pd-catalyst pre-activation occurs when two ligands are dissociated from the pre-catalyst to generate a highly active 14-electron Pd(0) complex **A**. After the oxidative addition of the aryl halide Ar^1-X (**B**) into the active Pd(0) catalyst **A**, whose insertion is commonly known as the rate-determining step of this catalytic cycle, the resulting 16-electron Pd(II) complex **C** is activated by an inorganic base by replacing the halide of the coordination sphere of Pd to give the arylpalladium intermediate **D**, which incorporates an active bond. Then, the negatively charged base coordinates to the boron atom of the arylboron compound Ar^2-$B(OH)_2$ (**E**) generating a more nucleophilic complex **F**, which accelerates the transmetallation rate. In this step, the aryl group (Ar^2) of **F** is transferred to the palladium complex **D** to give the diarylpalladium complex **G**. Finally, the biaryl compound Ar^1-Ar^2 (**H**) is released from the diarylpalladium complex **G** during the reductive elimination step, and consequently the active Pd(0) complex **A** is regenerated, closing the catalytic cycle.

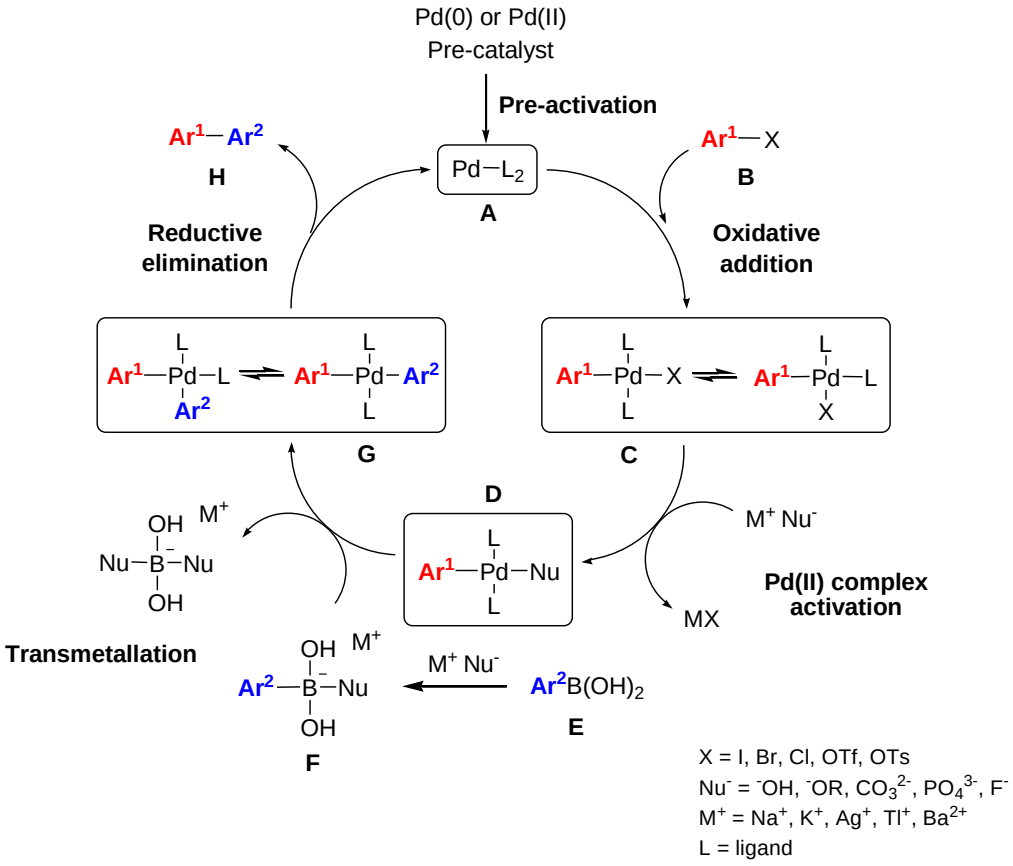

Scheme 1.3. Proposed mechanism of the Suzuki-Miyaura cross-coupling reaction.

The use of appropriate starting materials and reagents plays an important role in the Suzuki-Miyaura reaction. The most important issues of the catalyst, the ligand, the base, the arylboronic derivative, and the aryl halide are highlighted below (Miyaura and Suzuki, 1995; Martin and Yang, 1993; Kotha et al., 2002; Miyaura, 2002; Suzuki, 2011).

Due to their high thermal stability, the most frequently employed **catalysts** are phosphine-based Pd(II) or Pd(0) complexes. Among them, $Pd(PPh_3)_4$ is the most common. $PdCl_2(PPh_3)_2$, $Pd(OAc)_2$, $PdCl_2$(dppf) and $Pd_2(dba)_3$ are also efficient.

The addition of a convenient **ligand** has attracted particular interest, since it can accelerate the activation of the palladium pre-catalyst. Moreover, bulky and electron-rich ligands are able to stabilize the palladium intermediates. Phosphines, such as PPh_3, tri(*ortho*-tolyl)phosphine (P(*o*-tolyl)$_3$) and tricyclohexylphosphine (PCy_3), are commonly used, being the former the most popular. However, nowadays, several monodentate, bulky and electron-rich dialkylbiaryl phosphines, such as 2-dicyclohexylphosphino-2',6'-dimethoxybiphenyl (SPhos) and 2-dicyclohexylphosphino-2',4',6'-triisopropylbiphenyl (XPhos), have gained considerable attention and have been successfully applied to a wide variety of Pd-catalyzed cross-coupling reactions (Barder et al., 2005; Martin and Buchwald, 2008; Prieto et al., 2009).

The nature of the **aryl halide** or aryl triflate (Ar^1-X) can directly affect the activation energy of the catalytic process, specifically of the oxidative addition step. Generally, the rate of reactivity of Ar^1-X decreases as follows: Ar^1-I > Ar^1-OTf > Ar^1-Br >> Ar^1-Cl. Aryl halides incorporating an electron-withdrawing group are more active than those with an electron-donating group.

The presence of a negatively charged **base** has a remarkable effect on the acceleration of the cross-coupling of boronic acids. It has been assumed that the addition of a suitable inorganic base, such as Na_2CO_3, Cs_2CO_3, K_2CO_3, $Ba(OH)_2$, K_3PO_4, NaOH or the mild bases KF or CsF, is essential to increase the nucleophilicity of the organoboron compound, facilitating the formation of the diarylpalladium complex in the transmetallation step. Moreover, it can also activate the arylpalladium complex resulting from the oxidative addition step by replacing the halide group, forming a palladium complex which easily reacts with the nucleophilic organoboron compound.

The **organoboron compound**, which is typically an arylboronic ester (Ar^2-$B(OR)_2$) or arylboronic acid (Ar^2-$B(OH)_2$), is the most important reagent in the Suzuki-Miyaura coupling reaction. Nowadays, these compounds are commercially available or several functionalized derivatives can be easily prepared (Hall, 2005; Lennox and Lloyd-Jones, 2014). The general approaches to the synthesis of arylboronic acids are detailed in the next section.

1.2.2. Synthesis of arylboronic acids and esters

The traditional and most economical way to prepare arylboronic acids on large scale involves the reaction of an organometallic reagent, such as an aryllithium or an arylmagnesium, with a trialkylborate (Scheme 1.4a and b). The resulting arylboronic ester is then hydrolyzed to the arylboronic acid by addition of aqueous acid. The organometallic reagent can be generated by a metal-halogen exchange reaction of an aryl halide (Scheme 1.4a) or by a direct *ortho*-metallation of a functionalized arene (Scheme 1.4b). Another method for synthesizing arylboronic acids involves the transmetallation of an arylsilane or an arylstannane with boron tribromide followed by final acidolytic hydrolysis under mild conditions (Scheme 1.4c) (Hall, 2005).

However, these methods possess some important limitations, including the toxicity of the organostannane reagents, and the low functional group tolerance associated with the use of organometallic reagents of silane, lithium or magnesium (Miyaura, 2002; Lennox and Lloyd-Jones, 2014). Alternatively, the palladium-catalyzed Miyaura borylation reaction has been developed as a more efficient strategy for the borylation of aryl halides without using organolithium, organomagnesium, organosilane or organostannane reagents.

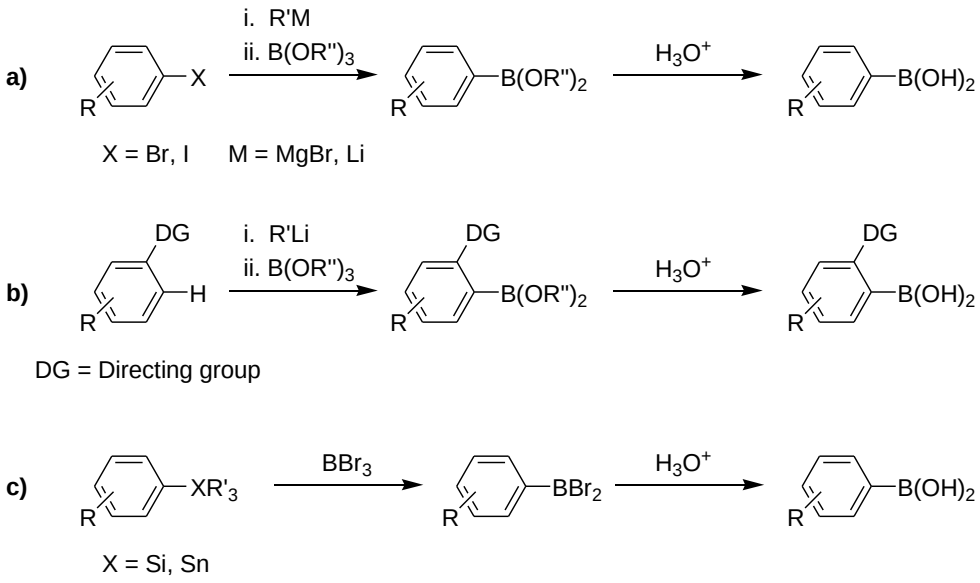

Scheme 1.4. Classical methods for the synthesis of aylboronic acids from a) aryl halides, b) arenes with an *ortho*-directing group, c) arylsilanes and arylstannanes.

1.2.2.1. Miyaura borylation reaction

In 1995, Ishiyama et al. reported an one-step approach for the preparation of arylboronic esters by the palladium(0)-catalyzed cross-coupling of bis(pinacolato)diboron (B_2Pin_2) with an aryl halide. The most suitable conditions for this so-called Miyaura borylation reaction were $PdCl_2$(dppf) and KOAc in dimethyl sulfoxide (DMSO) at 80 ºC (Scheme 1.5) (Ishiyama et al., 1995).

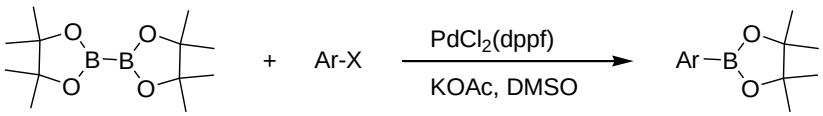

Scheme 1.5. Synthesis of arylboronic esters through the Miyaura borylation reaction.

The general catalytic cycle for the Miyaura borylation reaction is depicted in Scheme 1.6. The reaction proceeds through an oxidative addition step, the activation of a Pd(II) complex, a transmetallation, and a reductive elimination (Ishiyama et al., 1995). In particular, the oxidative addition involves the addition of the aryl halide Ar^2-X (**B**) to the Pd(0) complex **A** to generate the arylpalladium(II) complex **C**. This complex is then activated by replacement of the halide from the coordination sphere of Pd with acetate to give the (acetoxo)palladium(II) intermediate **D**, the reactivity of which is attributed to the presence of an active Pd-O bond. Next, the transmetallation occurs when the boron group from B_2Pin_2 (**E**) is transferred to the (acetoxo)palladium(II) intermediate **D** to provide the palladium complex **F**. Finally, the desired arylboronic ester Ar^2-BPin (**G**) is obtained from the Pd(II) complex **F** during the reductive elimination, leading to the regeneration of the Pd(0) complex **A**.

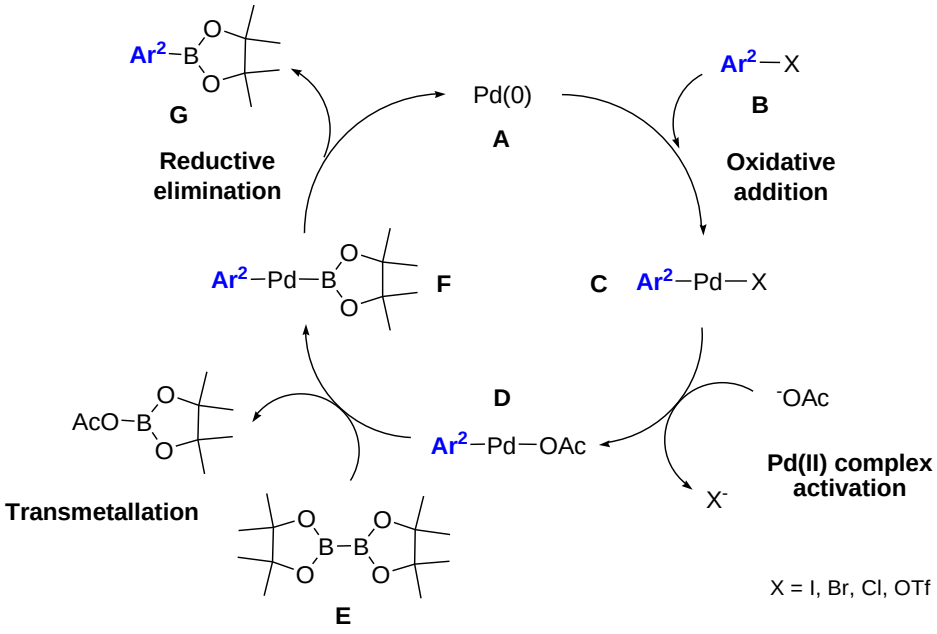

Scheme 1.6. Mechanism for the Miyaura borylation of aryl halides.

Many examples of preparation of boronophenylalanines and boronotyrosines have been reported. Malan and Morin described the first synthesis of 4-borono-L-phenylalanine in solution by direct C-B bond formation through a palladium-catalyzed Miyaura borylation of N^{α}-*tert*-butyloxycarbonyl (Boc)-protected 4-iodo-L-phenylalanine with B_2Pin_2, followed by removal of the Boc group and hydrolysis of the boronate (Scheme 1.7) (Malan and Morin, 1998).

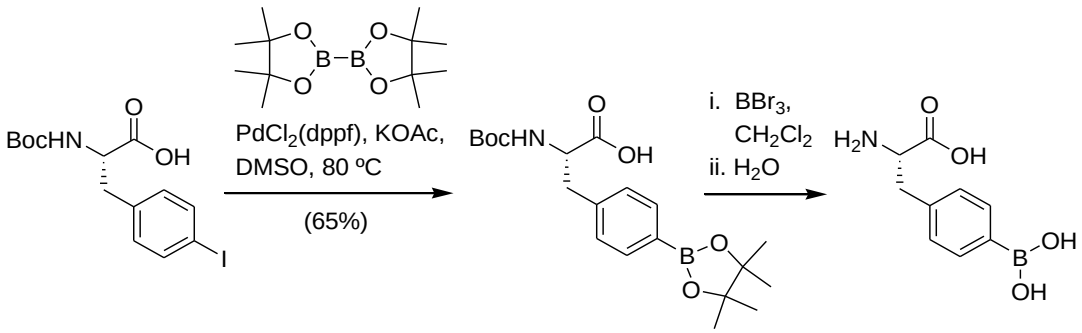

Scheme 1.7. Synthesis of 4-borono-L-phenylalanine.

One example of preparation of 3-borono-L-tyrosines in solution was published by Hutton and Skaff. It involves the conversion of N^{α}-carboxybenzyl (Cbz)-protected 3-iodo-L-tyrosine derivatives to the corresponding boronotyrosine under standard Miyaura borylation conditions (Scheme 1.8) (Hutton and Skaff, 2003).

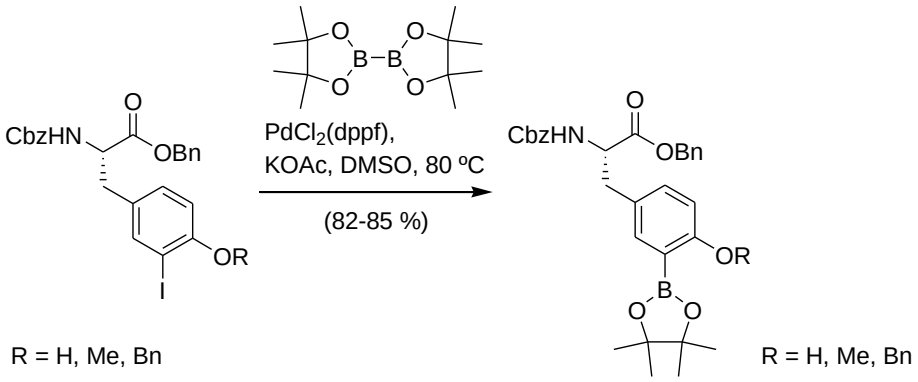

Scheme 1.8. Synthesis of N^{α}-Cbz-protected 3-borono-L-tyrosines.

Despite the Suzuki-Miyaura cross-coupling reaction has been adapted to the solid phase synthesis of biaryl compounds, the solid-phase borylation of haloamino acids has not been reported prior to the publication of Afonso and coworkers (Afonso et al., 2010). These authors developed for the first time an efficient strategy for the formation of a polymer-bound amino acid bearing a boronic ester. In particular, a N^{α}-Boc-protected 4-iodo-L-phenylalanine-containing tripeptidyl resin was treated with B_2Pin_2, $PdCl_2$(dppf), and KOAc in DMSO at 80 ºC (Scheme 1.9).

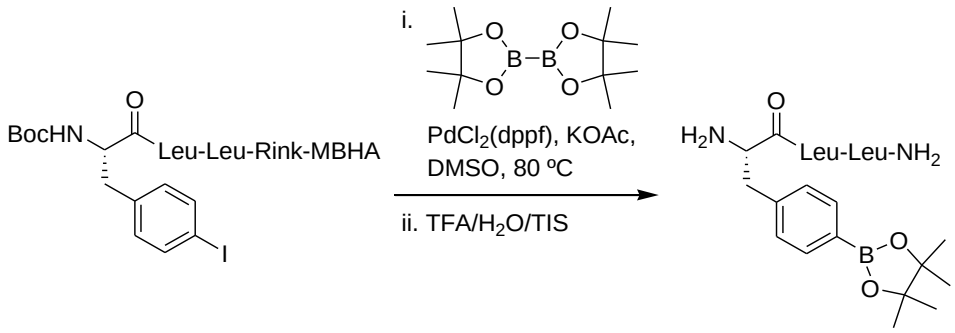

Scheme 1.9. Solid-phase synthesis of a 4-borono-L-phenylalanine-containing tripeptide.

1.2.3. Common side products from arylboronic acids in the Suzuki-Miyaura reaction

The synthesis and application of arylboronic acids (Ar-$B(OH)_2$) have risen in popularity since many of them are air and water stable. However, some arylboronic acids are reported to undergo slow protodeboronation (C-B bond cleavage), oxidation, and biaryl homocoupling (coupling of two identical molecules) during the Suzuki-Miyaura cross-coupling reaction (Miyaura, 2002; Hall, 2005; Lennox and Lloyd-Jones, 2014). The protodeboronated (Ar-H), the oxidized (Ar-OH), and the homocoupling (Ar-Ar) side products are often generated when the reaction mixture is exposed to air and the solvent is incompletely degassed. Moreover, the use of an inappropriate base as well as a prolonged heating may also prompt these side reactions.

The proposed mechanism for the protodeboronation of arylboronic acids is depicted in Scheme 1.10. The C-B bond is cleaved in the presence of aqueous base conditions to form the protodeboronated product (Ar-H) (Lennox and Lloyd-Jones, 2014).

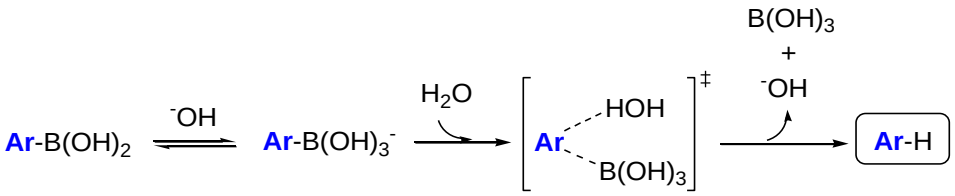

Scheme 1.10. Proposed base catalyzed protodeboronation of arylboronic acids.

The proposed mechanism for the palladium catalyzed homocoupling of arylboronic acids occurs in the presence of an oxygenated atmosphere, which is generated when air enters through the system. If the work atmosphere is not inert, the Pd(0) complex **A** reacts with oxygen to form the Pd(II) peroxo complex **B**, which consumes an arylboronic acid to generate the Pd(II) complex **C**, as illustrated in Scheme 1.11. The hydrolysis of the latter complex produces the Pd(II) complex **D**, together with a perboric acid ($B(OH)_2OOH$). A second molecule of arylboronic acid is added to the Pd(II) complex **D** to give the diarylpalladium complex **E**, from which the homocoupled product (Ar-Ar) is released to regenerate the active Pd(0) complex **A**. In addition, when the perboric acid co-product reacts with a third molecule of the arylboronic acid, the oxidized product (Ar-OH) is generated (Lennox and Lloyd-Jones, 2014).

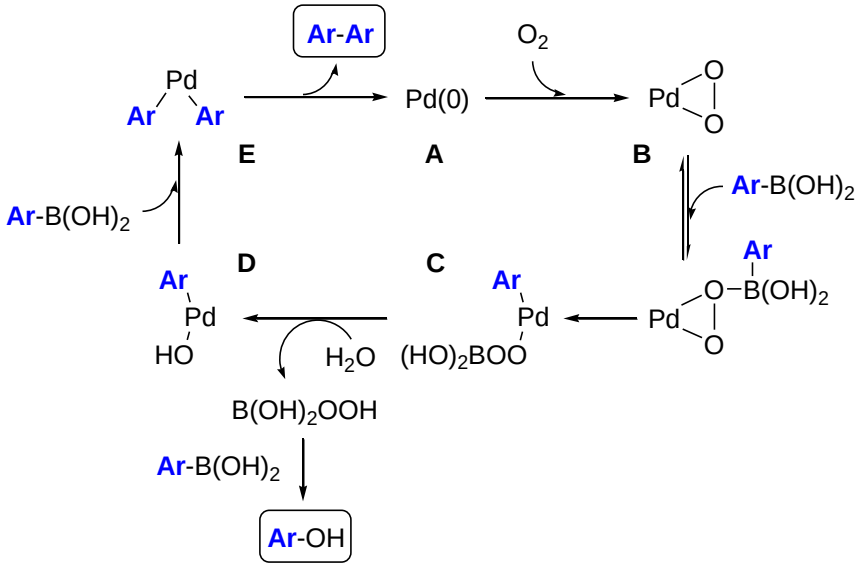

Scheme 1.11. Proposed mechanism of the oxidative homocoupling of arylboronic acids.

These side reactions can be suppressed by optimizing the base, solvent, and temperature. Therefore, the application of arylboronic acids in organic synthesis is nowadays of great interest for scientific research.

1.3. SYNTHESIS OF BIARYL PEPTIDES VIA A SUZUKI-MIYAURA REACTION IN SOLUTION

In view of the great importance of peptides in biological processes and also of the diversity and broad range of applications of the naturally occurring biaryl peptides, many researchers are recently interested in the preparation of new analogues incorporating biaryl amino acids in their sequence. This modification also overcomes the problems associated with the high conformational flexibility, and low bioavailability and enzymatic stability of natural peptides (Haug 2007; Le Quement et al., 2011; Kotha et al., 2013). Up to now, many examples on the synthesis of biaryl systems are well described in the literature, ranging from aryl-heteroaryl compounds (e.g. arylazoles, arylindoles, arylpyrimidines) to simple arylphenyl or arylphenol derivatives (Burke and Marques, 2015). Some of the conditions used to obtain these biaryl systems have been applied to the preparation of biaryl amino acids and biaryl peptides as described below.

1.3.1. Synthesis of biaryl amino acids

1.3.1.1. 5-Arylhistidines

The synthesis of 5-arylhistidines has been scarcely reported. However, considering the significance of 4(5)-arylimidazoles in biologically and pharmacologically active compounds, e.g. topsentins, nortopsentins, polycarpine and aciculitins, much attention has been recently paid to the preparation of these biaryl systems (Bellina et al., 2007). The arylation of the imidazole ring at the 4(5)-position has been accomplished through palladium-catalyzed direct C-H arylation, or via the Negishi, Stille or Suzuki-Miyaura cross-coupling reactions (Li and Gribble, 2000; Schnürch et al., 2006; Katritzky et al., 2008; Bellina and Rossi, 2010). Few recent examples of arylation of N-protected imidazoles are shown in Scheme 1.12. Baghbanzadeh et al. described a microwave-assisted procedure for the direct C-H arylation of N-methylimidazoles with different aryl bromides (Scheme 1.12a) (Baghbanzadeh et al., 2011). Dobler reported a three-step Negishi cross-coupling C-4 arylation of 4-iodo-5-(4-methoxyphenyl)-*N*-methylimidazole with 2-bromopyridine (Scheme 1.12b) (Dobler, 2003). Reversz et al. published a Stille-type cross-coupling reaction between a 2-(trimethylsilyl)ethoxymethyl (SEM)-protected 4,5-dibromoimidazole and several aryl bromides (Scheme 1.12c)

(Revesz et al., 1998). Cerezo et al. reported the Suzuki-Miyaura cross-coupling reaction between a regioisomeric mixture of benzyl (Bn)-protected 5(4)-bromo-4(5)-methylimidazole and phenylboronic acid to yield 4(5)-methyl-5(4)-phenylimidazole (Scheme 1.12d) (Cerezo et al., 2007).

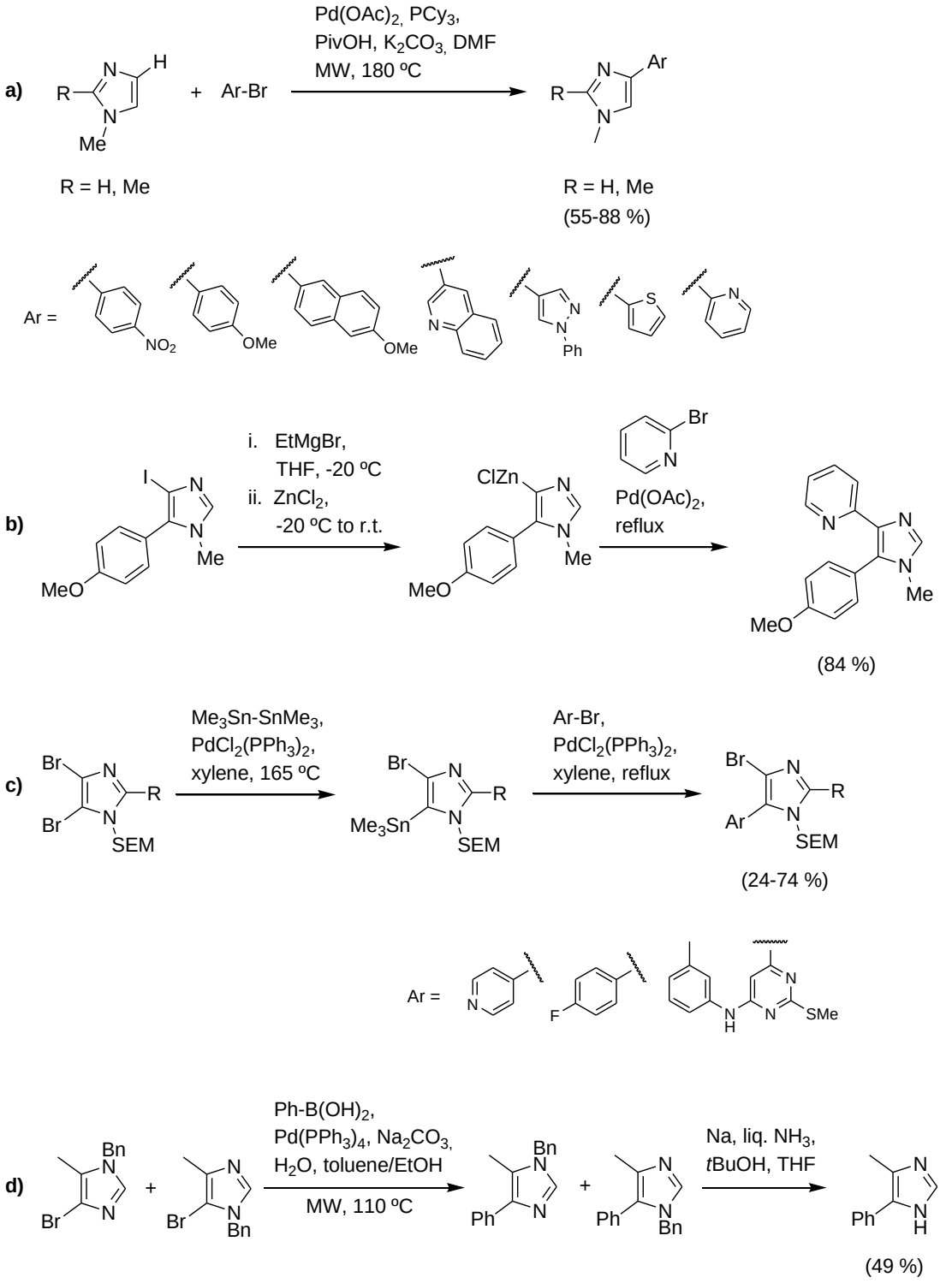

Scheme 1.12. Synthesis of 4(5)-arylimidazoles in solution. a) Direct C-H arylation; b) Negishi arylation; c) Stille arylation; d) Suzuki-Miyaura arylation.

Due to the difficulty of arylating the 4(5)-position of the imidazole ring, up to now only two reports on the preparation of 5-aryl-L-histidines have been published. In particular, Cerezo et al. developed the first efficient approach for the synthesis of these biaryl amino acids through a microwave-assisted Suzuki-Miyaura cross-coupling reaction of a conveniently protected 5-bromo-L-histidine with various arylboronic acids (Cerezo et al., 2007). The SEM group was selected as imidazole protection and it was removed under acidolytic conditions after the arylation step. The reaction conditions were optimized for the preparation of 5-phenyl-L-histidines, and the best results were obtained using $Pd_2(dba)_3$ and KF under microwave irradiation at 110 ºC for 10 min. (Scheme 1.13). These conditions were extended to the synthesis of histidines bearing at position 5 a substituted phenyl, a piridyl or a thienyl ring.

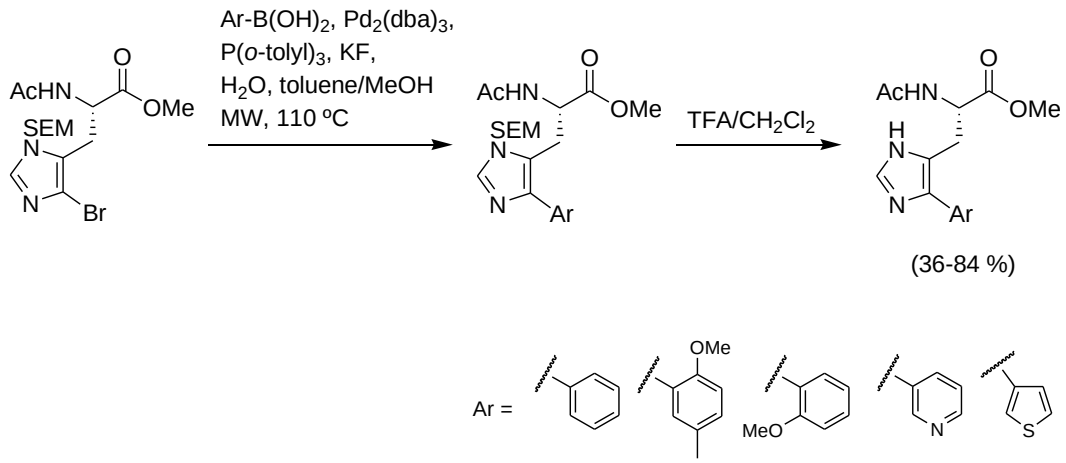

Scheme 1.13. Synthesis of 5-aryl-L-histidines via a palladium-catalyzed Suzuki-Miyaura cross-coupling reaction in solution.

Later, Mahindra and coworkers reported the regioselective direct C-5 arylation of a conveniently protected L-histidine with various aryl iodides under microwave irradiation. The best result was obtained when this reaction was carried out in the presence of $Pd(MeCN)_2$-PCy_3 as catalytic system, K_2CO_3 as base, and pivalic acid (PivOH) as additive in *N*,*N*-dimethylformamide (DMF) under microwave irradiation at 140 ºC for 45 to 60 min, depending on the aryl iodide used. (Scheme 1.14) (Mahindra et al., 2013).

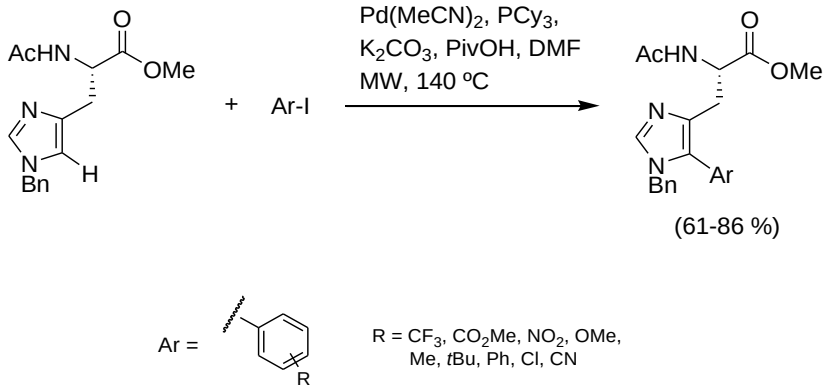

Scheme 1.14. Synthesis of 5-aryl-L-histidines via palladium-catalyzed direct C-H arylation in solution.

1.3.1.2. 4-Arylphenylalanines

The Suzuki-Miyaura cross-coupling is one of the most applied reactions for the arylation of the C-4 position of a phenylalanine (Kotha et al., 2002). The synthesis of 4-arylphenylalanines has been carried out by arylating a 4-halophenylalanine with an arylboronic acid or, by contrast, by arylating a 4-boronophenylalanine with an aryl halide.

In 1994, Burk et al. reported the cross-coupling of an acyl-protected 2-, 3- or 4-bromo-D-phenylalanine with various arylboronic acids in presence of $Pd(OAc)_2$ and P(*o*-tolyl)$_3$ under conventional heating at 80 ºC (Scheme 1.15) (Burk et al., 1994).

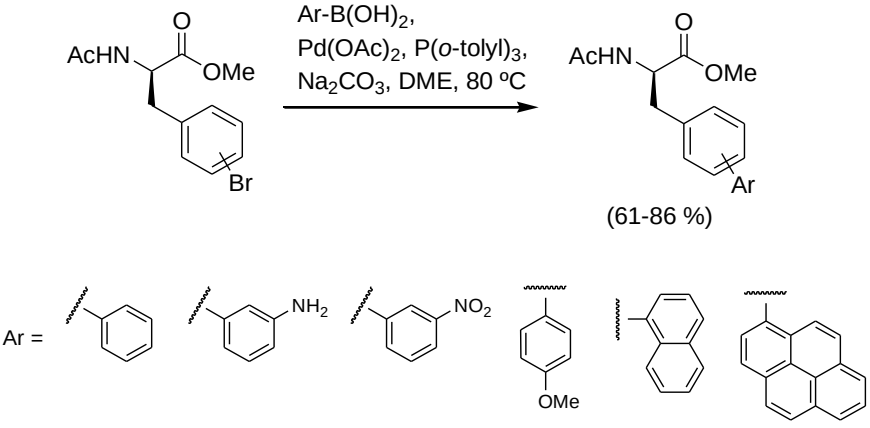

Scheme 1.15. Synthesis of 2-, 3- and 4-aryl-D-phenylalanines under conventional heating starting from a bromo-D-phenylalanine.

This methodology was later used by Kotha and Lahiri to synthesize Boc-protected 4-aryl-L-phenylalanines from Boc-protected-4-iodo-L-phenylalanines using $Pd(PPh_3)_4$ under conventional heating at 80 ºC (Scheme 1.16) (Kotha and Lahiri, 2001; Kotha and Lahiri, 2003).

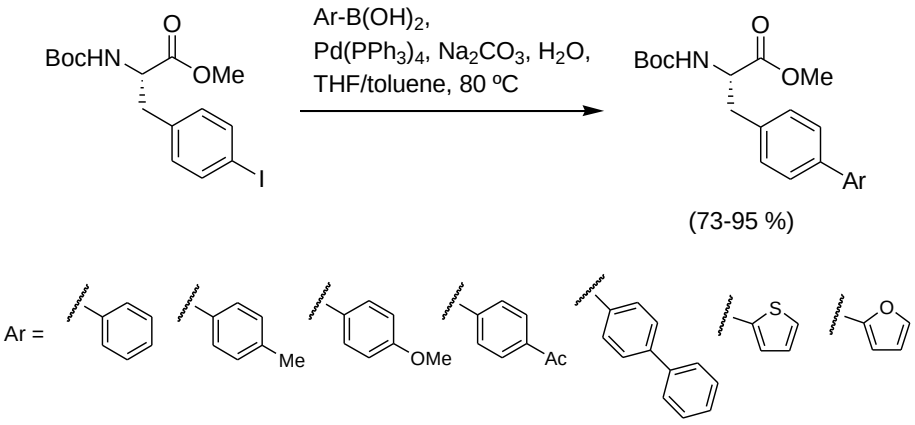

Scheme 1.16. Synthesis of 4-aryl-L-phenylalanines under conventional heating starting from a 4-iodo-L-phenylalanine.

The preparation of 4-arylphenylalanines through a Suzuki-Miyaura cross-coupling of a 4-boronophenylalanine and an aryl halide or triflate was investigated by Firooznia and coworkers. They described the enantioselective synthesis of Boc-protected 4-aryl-L-phenylalanines from a 4-pinacolylborono-L-phenylalanine derivative and several aryl halides or triflates using $PdCl_2$(dppf) and K_2CO_3 in 1,2-dimethoxyethane (DME) under conventional heating at 80 ºC (Scheme 1.17) (Firooznia et al., 1999).

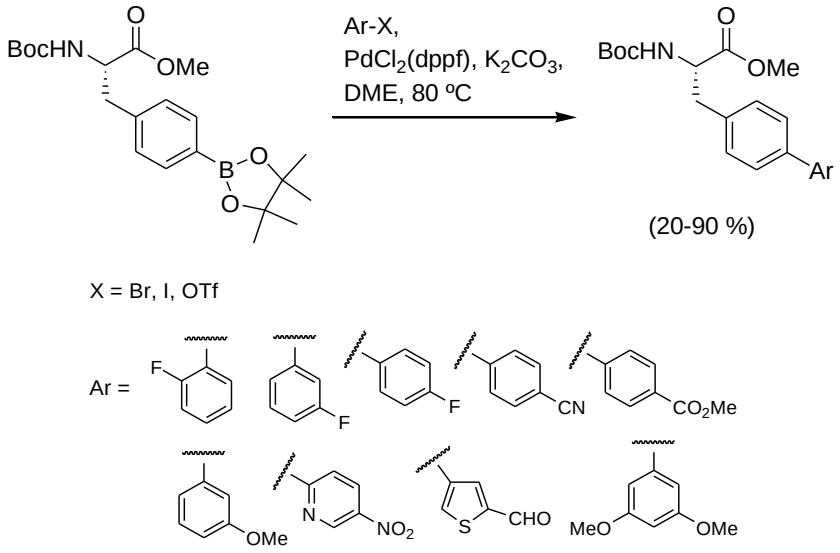

Scheme 1.17. Synthesis of 4-aryl-L-phenylalanines under conventional heating starting from a 4-borono-L-phenylalanine.

Similarly, Gong and He successfully described in 2002 the synthesis of racemic 4-arylphenylalanines through a Suzuki-Miyaura cross-coupling reaction of unprotected 4-boronophenylalanine with aryl halides in presence of $Pd(PPh_3)_2Cl_2$ under microwave heating at 150 ºC (Scheme 1.18) (Gong and He, 2002).

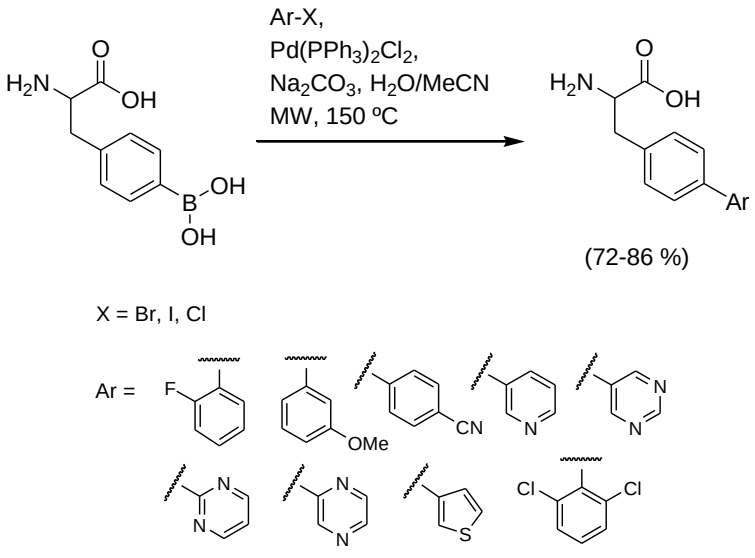

Scheme 1.18. Synthesis of 4-arylphenylalanines under microwave irradiation starting from 4-boronophenylalanine.

1.3.1.3. 3-Aryltyrosines

Over the years, many strategies have been developed for the synthesis of 3-aryl-L-tyrosines in solution based on the Suzuki-Miyaura cross-coupling. These biaryl amino acids are important motifs in a large number of natural products, such as the proteasome inhibitors TMC-95, the antimicrobial arylomycins, the antibiotic vancomycin, the neurotensin antagonist RP-66453, the antitumoral neo-RA-V, or the antifungal aciculitins, as previously mentioned in this thesis. Similarly to 4-arylphenylalanines, 3-aryl-L-tyrosines can be prepared either starting from a 3-halo-L-tyrosine or from a 3-borono-L-tyrosine.

As an example, 3-aryl-L-tyrosines were obtained by Knör and coworkers via a Suzuki-Miyaura cross-coupling of a Boc-protected 3-iodo-L-tyrosine derivative with several arylboronic acids using $Pd(OAc)_2$ and P(*o*-tolyl)$_3$ under conventional heating at 80 ºC (Scheme 1.19) (Knör et al., 2006).

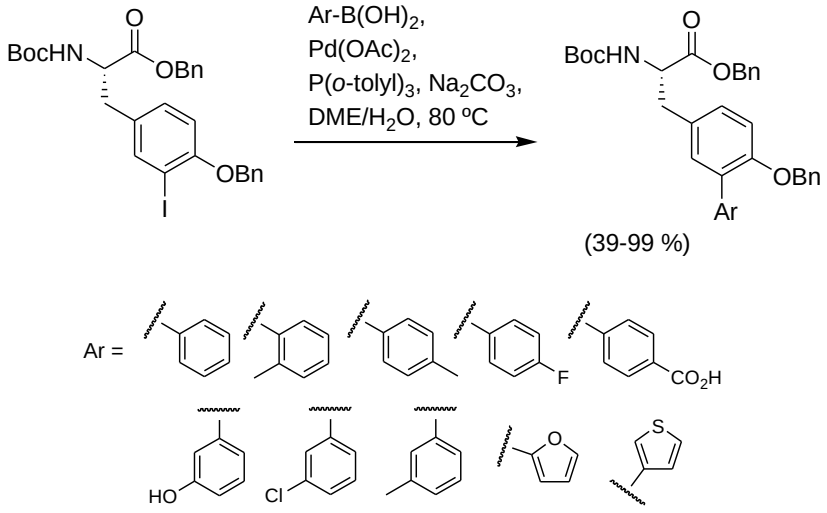

Scheme 1.19. Synthesis of 3-aryl-L-tyrosines under conventional heating starting from a 3-iodo-L-tyrosine.

Interestingly, Hutton and Skaff developed an efficient strategy for the preparation of dityrosines through the Suzuki-Miyaura cross-coupling between a Cbz-protected 3-iodo-L-tyrosine and a Cbz-protected 3-borono-L-tyrosine (Scheme 1.20a). In addition, they also described the direct conversion of 3-iodo-L-tyrosine derivatives to dityrosines in a one-pot borylation-arylation strategy (Scheme 1.20b) (Hutton and Skaff, 2003).

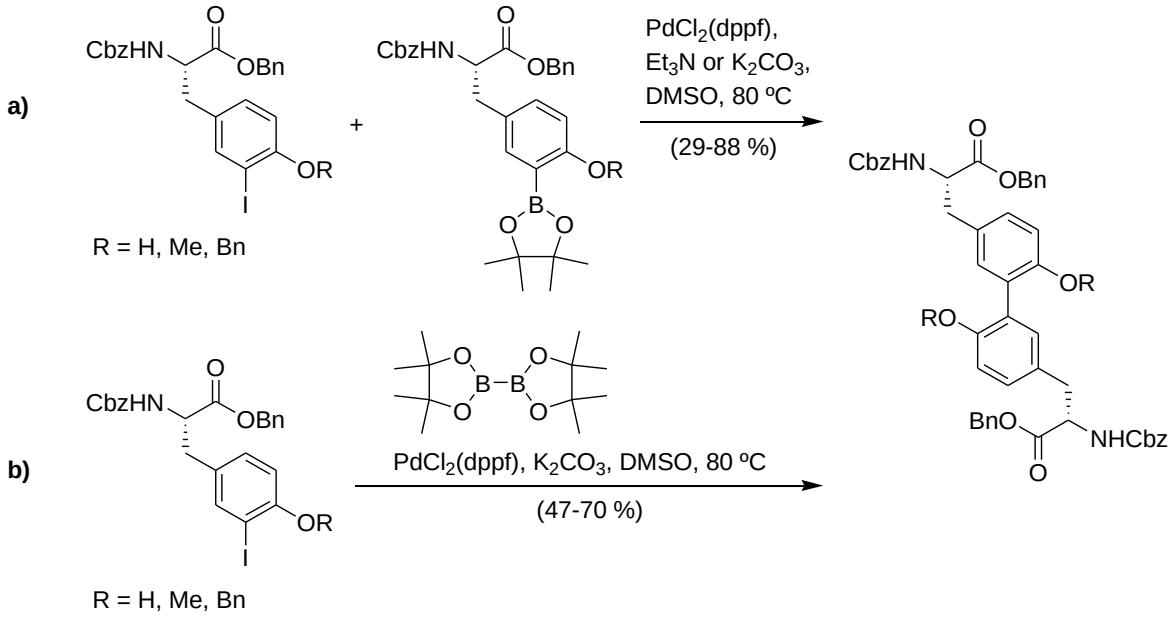

Scheme 1.20. Synthesis of dityrosines in solution. a) Suzuki-Miyaura cross-coupling between a 3-iodo-L-tyrosine and a 3-borono-L-tyrosine; b) one-pot borylation-arylation.

1.3.2. Synthesis of biaryl linear peptides

The Suzuki-Miyaura cross-coupling has been used as the key step in the preparation of biaryl linear peptides. For instance, Kotha and Lahiri designed and synthesized a set of 4-aryl-L-phenylalanine-containing linear tripeptides and pentapeptides through the arylation of a 4-iodo-L-phenylalanine residue with different arylboronic acids by applying the same conditions depicted in Scheme 1.16 for the obtention of 4-aryl-L-phenylalanines (Scheme 1.21) (Kotha and Lahiri, 2001; Kotha and Lahiri, 2003).

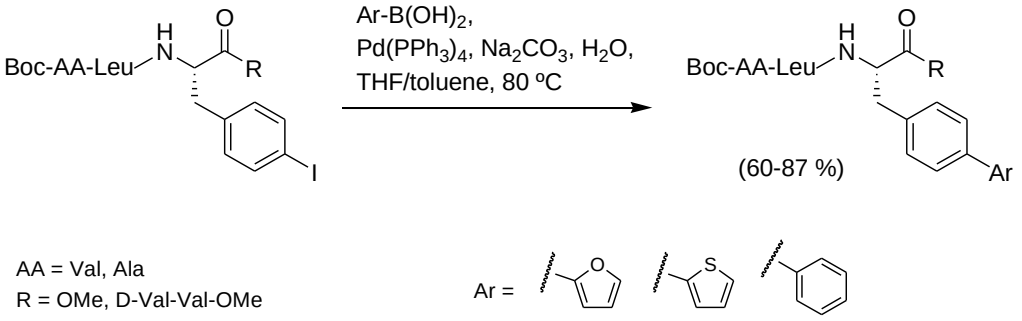

Scheme 1.21. Synthesis of 4-aryl-L-phenylalanine-containing tripeptides and pentapeptides in solution.

Vilaró and coworkers reported the preparation of biaryl linear peptides of different chain length containing a 4-aryl-L-phenylalanine or a 3,5-diaryl-L-tyrosine residue through a Suzuki-Miyaura cross-coupling of the corresponding unprotected iodopeptide with two different aryltrifluoroborates (Scheme 1.22 and Scheme 1.23) (Vilaró et al., 2008). The reaction was carried out at 50 ºC in aqueous media using $Pd(OAc)_2$ as catalyst.

a)

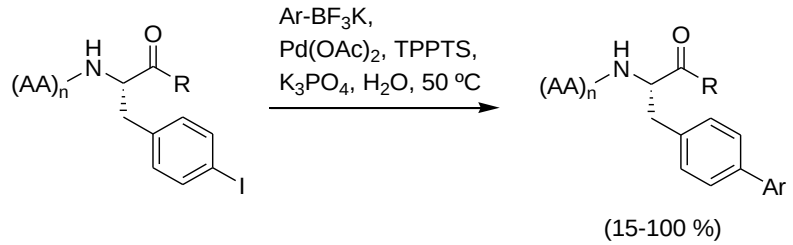

$(AA)_n$	R
H-Tyr-Tyr-Gly-Gly	Leu-OH
H-Gly-Gly	Leu-OH
For-Met-Leu	OH
H-Tyr-Gly-Gly	Met-OH
H-Tyr-D-Ala	Gly-Tyr-Pro-Ser-NH_2
H-Met-Glu-His	Arg-Trp-Gly-OH

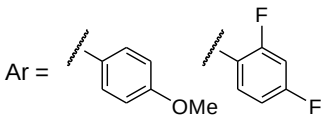

Scheme 1.22. Synthesis of 4-aryl-L-phenylalanine-containing peptides in solution.

b)

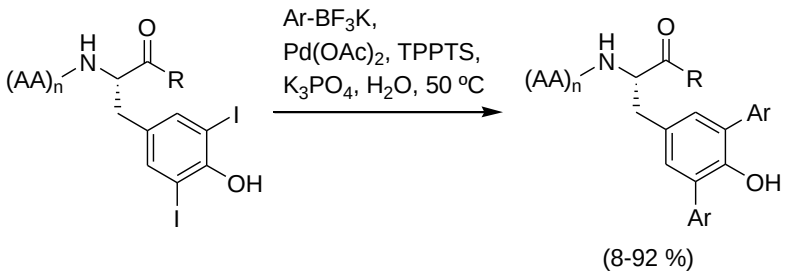

$(AA)_n$	R
Ac-Phe	OH
H	Gly-Gly-Phe-Leu-OH
H	Gly-Gly-Phe-Leu-OH
H	Gly-Gly-Phe-Met-OH
H	D-Ala-Phe-Gly-Tyr-Pro-Ser-NH_2

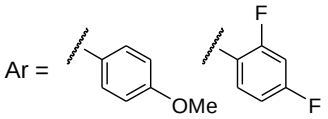

Scheme 1.23. Synthesis of 3,5-diaryl-L-tyrosine-containing peptides in solution.

1.3.3. Synthesis of natural biaryl cyclic peptides

In recent years, the aforementioned synthetic protocols have been successfully extended to the preparation of naturally occurring biaryl cyclic and bicyclic peptides and of some analogues (Feliu and Planas, 2005). The key step of the synthesis of these compounds is the macrocyclization, which can be performed either by standard macrolactamization (route A) or by macroarylation (route B) (Scheme 1.24). In particular, route A involves the formation of a biaryl linear precursor through an intermolecular Suzuki-Miyaura reaction between the corresponding aromatic amino acid derivatives prior to the macrolactamization. Otherwise, route B implies the synthesis of the linear sequence incorporating both the haloamino acid and the boronoamino acid derivatives, followed by an intramolecular Suzuki-Miyaura cross-coupling reaction (Heravi and Hashemi, 2012). The latter approach resulted to be the most versatile.

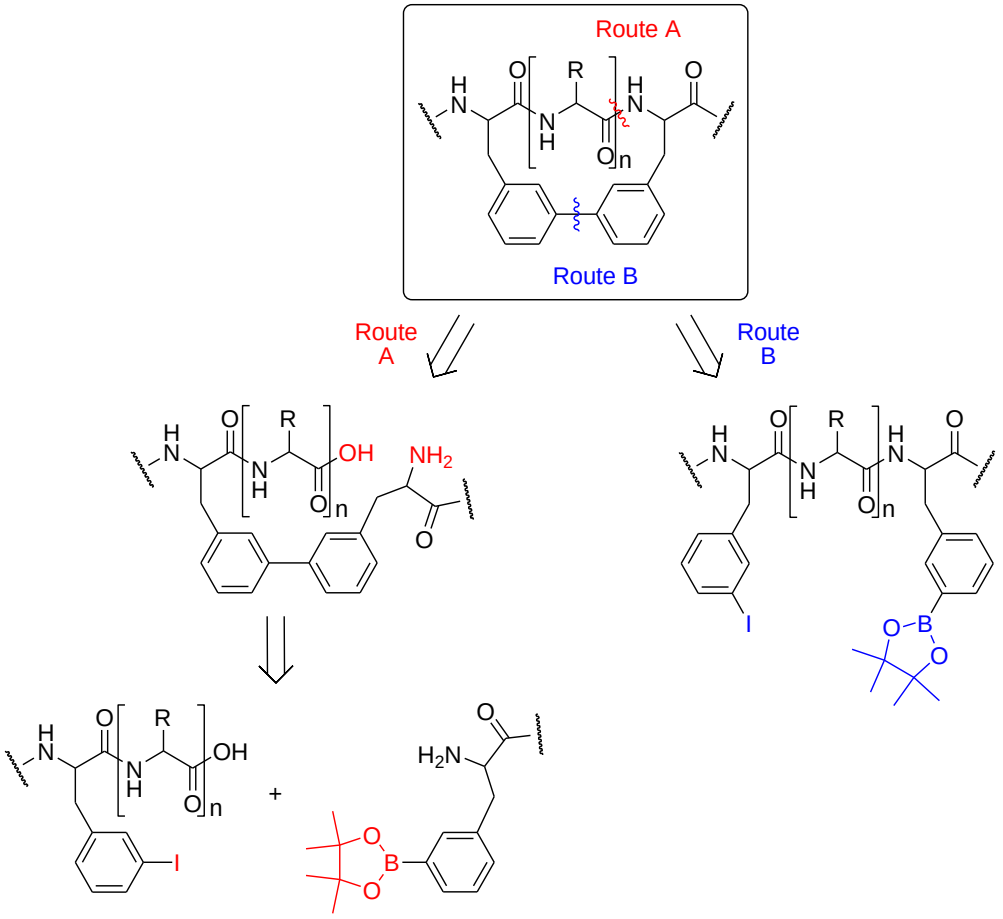

Scheme 1.24. Retrosynthetic analysis of biaryl cyclic peptides.

Inoue et al. reported in 2003 the total synthesis of the macrocyclic core of TMC-95A following route A (Inoue et al., 2003). In this case, the biaryl bond was formed by treatment of an oxidized iodotryptophan derivative with a dipeptide bearing a 3-borono-L-tyrosine in presence of $Pd(PPh_3)_4$ and Na_2CO_3 in aqueous DME at 95 ºC (Scheme 1.25). Then, subsequent hydrolysis of the methyl ester, coupling of L-asparagine benzyl ester, and hydrogenolysis to remove the Cbz and Bn protecting groups was followed by the final macrolactamization step.

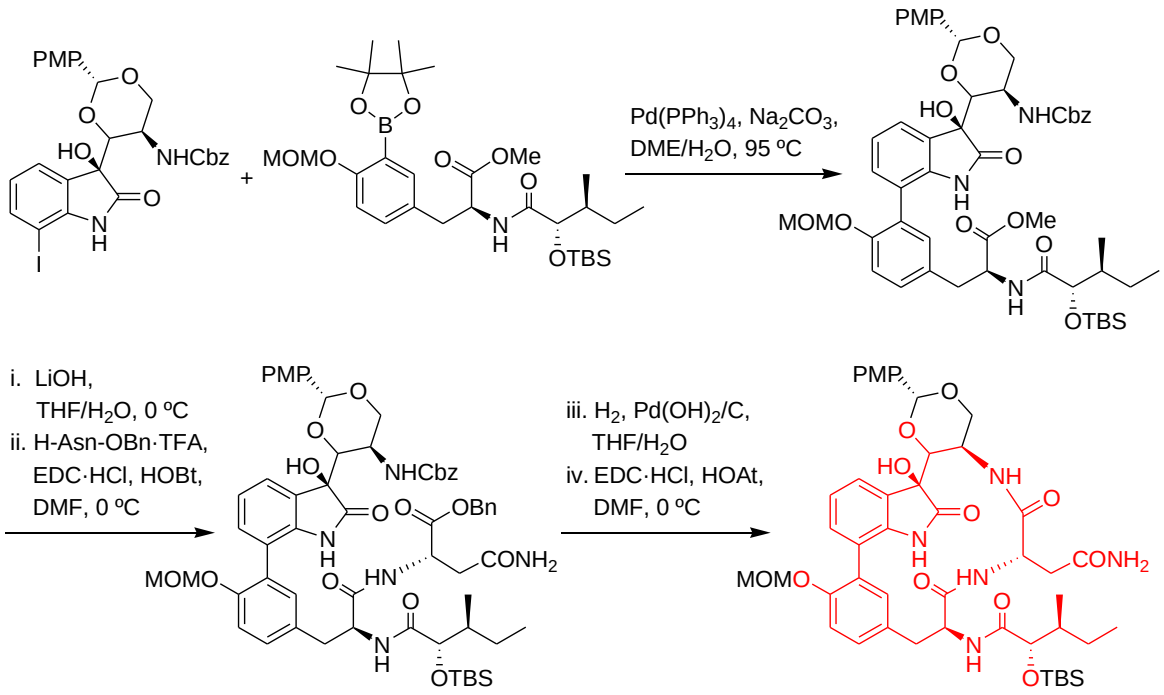

Scheme 1.25. Synthesis of the macrocyclic core of TMC-95A following route A.

More recently, Coste and coworkers developed a synthetic approach to the macrocyclic core of TMC-95A based on route B (Scheme 1.26) (Coste et al., 2014). Accordingly, they prepared a linear precursor containing the required iodotryptophan and 3-borono-L-tyrosine derivatives. The final macroarylation step using $PdCl_2$(dppf) and K_2CO_3 in aqueous DME at 80 ºC successfully generated the desired macrocyclic core of TMC-95A.

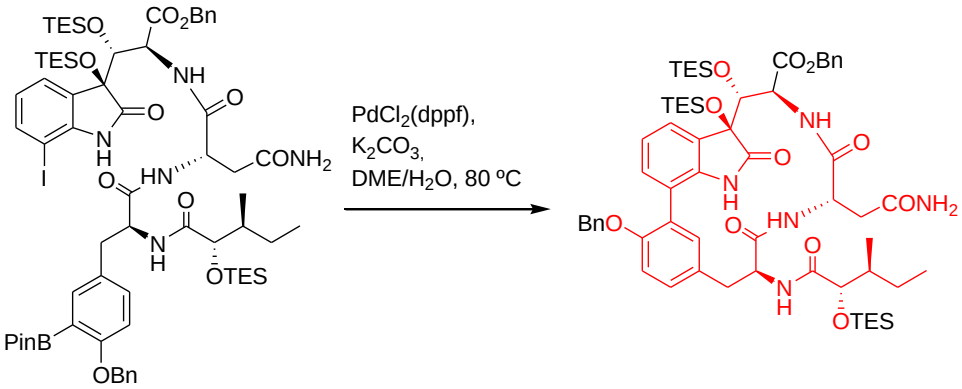

Scheme 1.26. Synthesis of the macrocyclic core of TMC-95A following route B.

In 2007, Roberts and coworkers described the total synthesis of arylomycin A_2 following both routes A and B (Roberts et al., 2007). In route A, the linear precursor was obtained through a Suzuki-Miyaura arylation of a dipeptide containing a 3-iodo-L-phenylglycine with a conveniently protected 3-borono-L-tyrosine derivative in presence of $PdCl_2$(dppf) and K_2CO_3 in DMSO at 80 ºC. Then, simultaneous hydrogenolysis of the Cbz and Bn groups followed by macrolactamization afforded the macrocyclic core of arylomycin A_2 (Scheme 1.27a). In route B, the intramolecular Suzuki-Miyaura macrocyclization of the linear precursor incorporating both the 3-iodo-L-phenylglycine and the 3-borono-L-tyrosine residues was tested. The desired biaryl macrocyclic core was obtained in good yields using $PdCl_2$(dppf), K_2CO_3 in MeCN at 80 ºC (Scheme 1.27b).

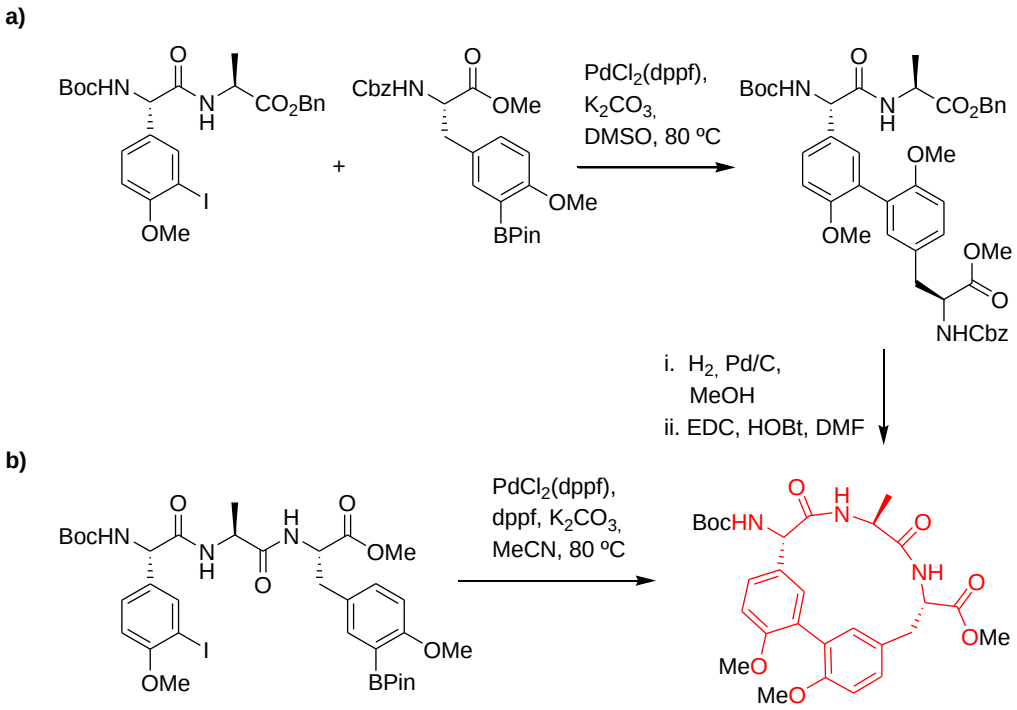

Scheme 1.27. Synthesis of the macrocyclic core of arylomycin A_2. a) Route A; b) route B.

The total synthesis of the lipohexapeptide arylomycin A_2 was accomplished by subsequent N-methylation of the biaryl macrocyclic tripeptide, coupling of Boc-protected glycine, incorporation of a previously prepared lipodipeptide at the N-terminus via amide bond formation, and final removal of the protecting groups (Scheme 1.28).

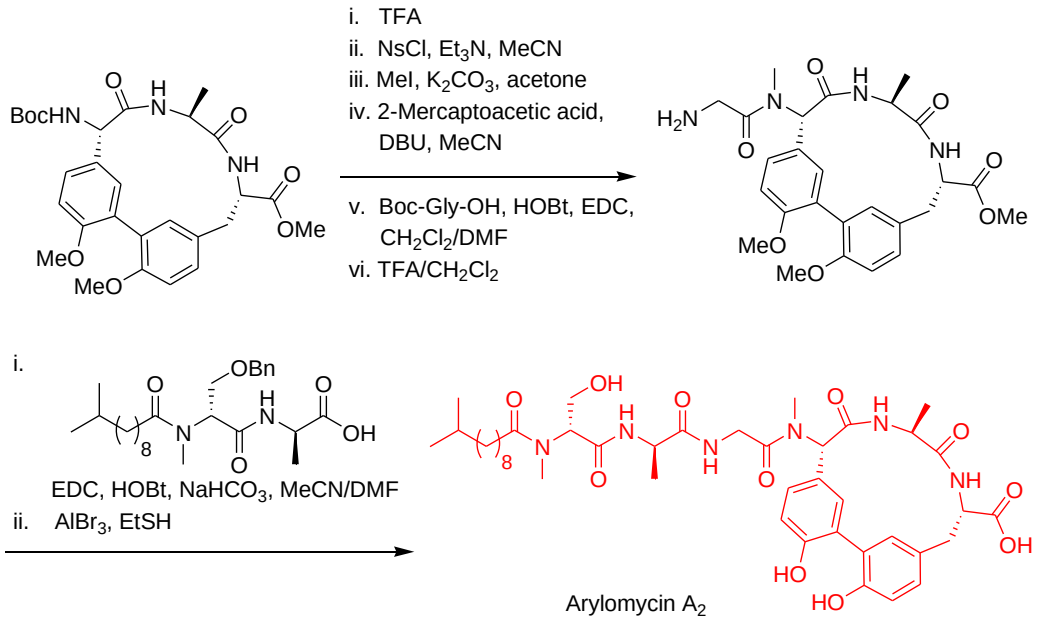

Scheme 1.28. Total synthesis of arylomycin A_2.

The biaryl antibiotic biphenomycin B has been efficiently synthesized either via route A or B (Scheme 1.29). Waldmann et al. published a strategy based on route A that included a cross-coupling reaction to give a biaryl linear intermediate, which was then coupled to a protected hydroxyornithine derivative. The macrolactamization of the resulting biaryl linear tripeptide followed by removal of the protecting groups provided the natural product (Scheme 1.29a) (Waldmann et al., 2008). Following route B, Lépine and Zhu employed a microwave-assisted intramolecular macroarylation of the conveniently functionalized linear tripeptide for the ring-closure step (Scheme 1.29b) (Lépine and Zhu, 2005).

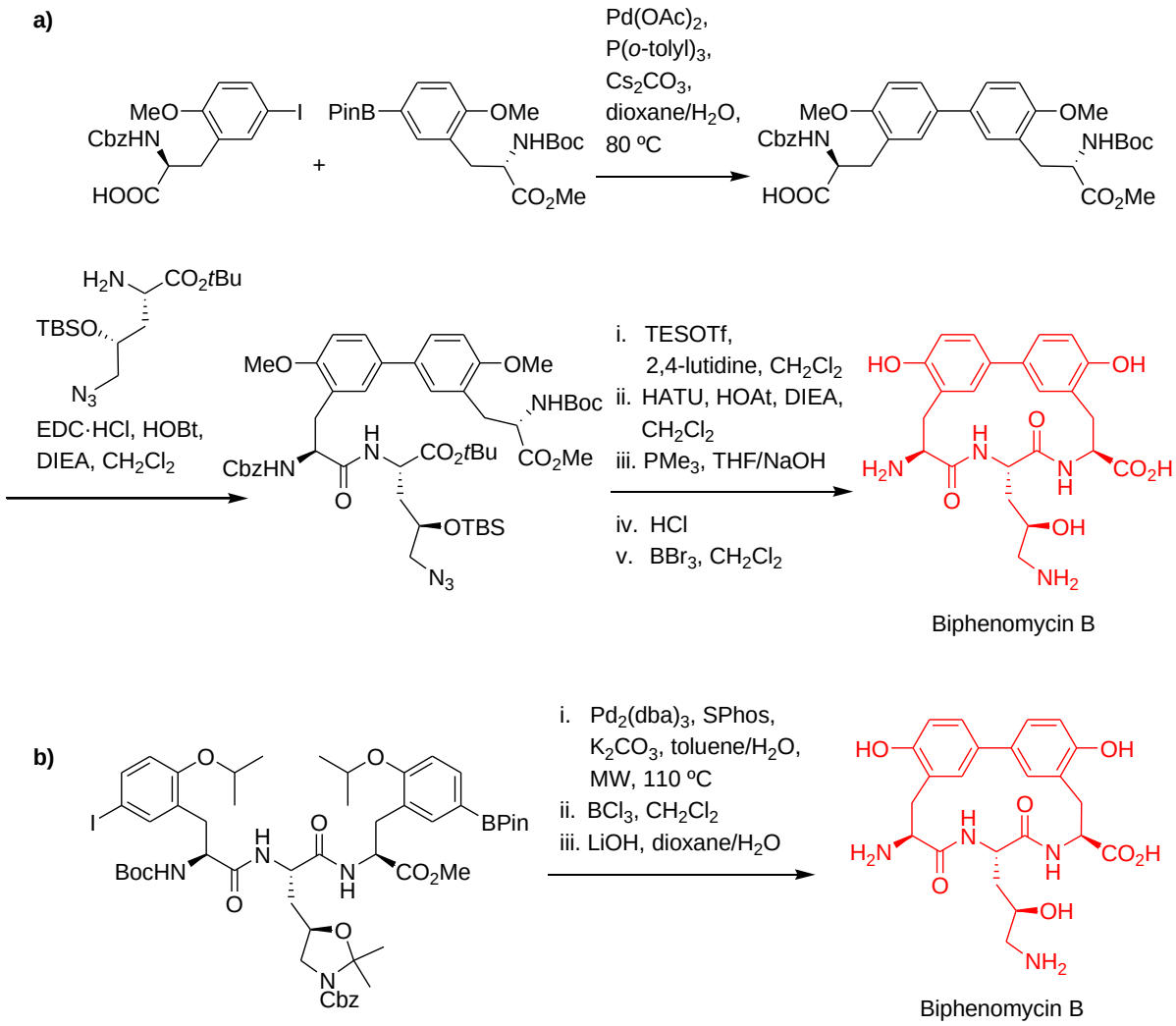

Scheme 1.29. Total synthesis of biphenomycin B. a) Route A; b) route B.

1.4. SOLID-PHASE SYNTHESIS OF BIARYL PEPTIDES VIA A SUZUKI-MIYAURA REACTION

Since conventional solution-phase synthesis generally requires very long and tedious work-up procedures as well as troublesome purifications after each reaction step, a powerful method for accelerating such process was established. Hence, the solid-phase organic synthesis has become the method of choice for an increased production of many chemical compounds, including peptides and small molecules. Moreover, much attention has also been paid to the application of the palladium-catalyzed Suzuki-Miyaura cross-coupling reaction on solid-phase for the incorporation of biaryl amino acids into peptide sequences (Scott, 2012; Zaragoza, 2000; Bräse et al., 2003). The immobilization of the desired product allows the facile elimination of the soluble palladium catalyst as well as the excess of soluble reagents and non-toxic byproducts. This powerful synthetic methodology has been recently used for the preparation of biaryl linear and cyclic peptides.

1.4.1. Solid-phase peptide synthesis (SPPS)

The solid-phase peptide synthesis (SPPS) is considered the most efficient method for the preparation of peptides. It was first developed by Robert Bruce Merrifield (1963), which was awarded in the Nobel Prize in Chemistry 1984 for the development of this methodology for chemical synthesis on a solid matrix (Merrifield, 1963; Merrifield, 1968; Merrifield, 1985). The SPPS is based on the peptide chain elongation on an insoluble polymeric support by sequential amide bond formation, generally, in the C → N direction (Grant, 2002; Zaragoza, 2000; Palomo, 2014; Pires et al., 2014). The solid support is a polymeric support which consists of particles that must be mechanically stable, chemically inert to the reaction conditions, chemically functionalized, and completely insoluble in the reaction solvents. Moreover, this polymeric support must swell extensively in the solvents that are used. There are several types of solid support, which are generally classified according to their composition, such as polystyrene (PS), polyacrylamide, poly(ethylene glycol) (PEG) and PEG-PS-based resins (Lloyd-Williams et al., 1997; Zaragoza, 2000; Palomo, 2014). Among them, the most widely used

PS-divinylbenzene (DVB) support, the 4-methylbenzhydrylamine (MBHA) resin (Sarin et al., 1980; Santini et al., 1998; Lee et al., 2008), and the aminomethyl ChemMatrix (CM) resin, a totally PEG-based support (García-Martin et al., 2006; García-Ramos et al., 2010), are the two solid supports used in this thesis. These resins are well swollen by the typical solvents employed in solid-phase synthesis, such as CH_2Cl_2, DMF and *N*-methyl-2-pyrrolidone (NMP) (Figure 1.6).

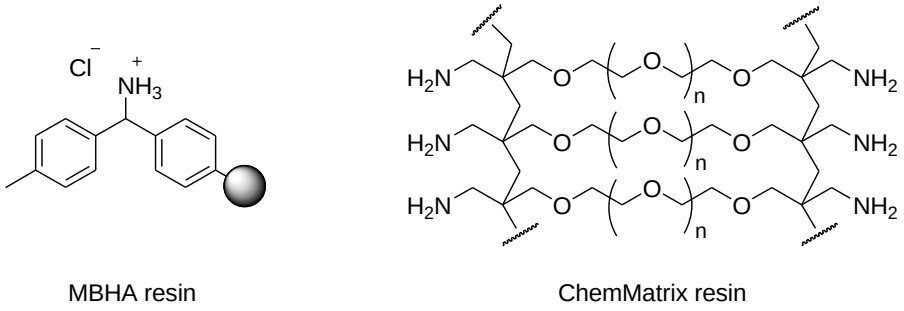

Figure 1.6. MBHA and ChemMatrix resin.

The solid support of choice must be initially derivatized with a bifunctional linker before the attachment to the polymeric support of the first amino acid of the peptide to be synthesized. The linker would allow the final peptide release from the resin once the sequence is complete (James, 1999; Guillier et al., 2000; Zaragoza, 2000; Góngora-Benítez et al., 2013). The linker-resin bond must be stable and inert under both peptide chain elongation and cleavage conditions, while the peptide-linker bond must be labile to the cleavage conditions, leading to the release of the desired C-terminal functionalized peptide from the resin (James, 1999; Guillier et al., 2000). The correct choice of an adequate linker depends on the nature of the C-terminal functional group of the peptide of interest and also on the cleavage conditions. The 9-fluorenylmethoxycarbonyl (Fmoc)-Rink amide linker is one of the most common acid-labile linkers used in Fmoc chemistry to yield peptide amides (Figure 1.7). In this case, trifluoroacetic acid (TFA) is required to cleave the peptide from the resin.

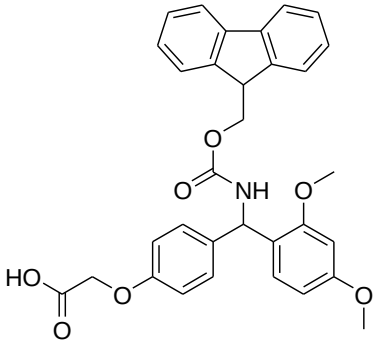

Figure 1.7. Fmoc-Rink amide linker.

In order to prevent possible side reactions during the solid-phase peptide synthesis, N^{α}-amino group and the side-chain function (if necessary) or even the C^{α}-carboxyl group of the amino acids to be attached must be masked by using orthogonal protecting groups. A standard orthogonal protection includes at least two different types of protecting groups, each one of which can be selectively removed by different cleavage mechanisms, in any order and in the presence of the others (Isidro-Llobet et al., 2009; Palomo, 2014; Pires et al., 2014).

The Fmoc/*tert*-butyl (*t*Bu) strategy is the most common solid-phase peptide synthesis strategy based on the use of orthogonal protecting groups. In this case, the Fmoc group is employed as base-labile temporary N^{α}-amino protecting group, which is removed from each coupled amino acid to allow the peptide chain elongation. By contrast, acid-labile groups, including *t*Bu, Boc or trityl (Tr) groups, are used as permanent side-chain protecting groups. These permanent groups remain during all the peptide synthesis and they are simultaneously removed during the cleavage, the last step of the synthesis. Moreover, when cyclic peptides must be synthesized, the C^{α}-carboxyl group is usually protected with a semipermanent protecting group that may be selectively removed without deprotecting the other functional groups (Lloyd-Williams et al., 1997; Greene, 1999; Isidro-Llobet et al., 2009). The following table summarizes the cleavage conditions of all the protecting groups used in this thesis (Table 1.1).

Table 1.1. Amino acid protecting groups used in this thesis.

Protecting group	**Abbreviation**	**Structure**	**Cleavage conditions**
tert-Butyloxycarbonyl	Boc	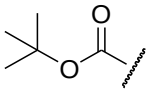	25-50% TFA in CH_2Cl_2 TIS (scavenger)
tert-Butyl	*t*Bu		90% TFA in CH_2Cl_2 TIS (scavenger)
9-Fluorenylmethoxycarbonyl	Fmoc	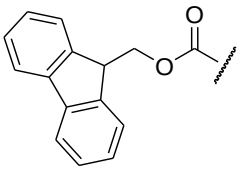	20% Piperidine in DMF
ortho-Nitrobenzenesulfonyl	*o*NBS	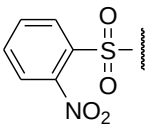	β-Mercarptoethanol and DBU
para-Nitrobenzyl	*p*NB	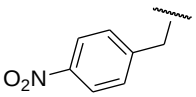	$SnCl_2$ in DMF
2,4,6-Trimethoxybenzyl	Tmob	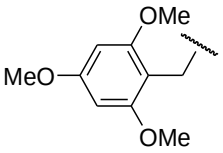	95% TFA TIS (scavenger)
2-(Trimethylsilyl)ethoxymethyl	SEM	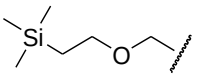	TFA/CH_2Cl_2 (2:1)
Trityl	Tr	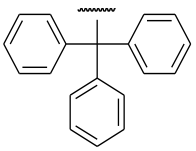	1% TFA in CH_2Cl_2 TIS (scavenger)

In particular, the steps involved in this peptide synthesis process are shown in Scheme 1.30, and include (i) the coupling of the first protected amino acid, by reaction of its C^{α}-carboxyl group with the free functional group of the linker, (ii) the selective removal of the N^{α}-amino protecting group from the previously attached amino acid, without affecting the side-chain protecting group, (iii) the coupling of the next protected amino acid, (iv) sequential N^{α}-deprotection and amino acid coupling steps for the peptide chain elongation, and finally, (v) the N^{α}-deprotection (if necessary) and the cleavage of the covalent peptide-linker bond to release the peptide from the resin, and to simultaneously remove the side-chain protecting groups (Lloyd-Williams et al., 1997; Grant, 2002; Palomo, 2014).

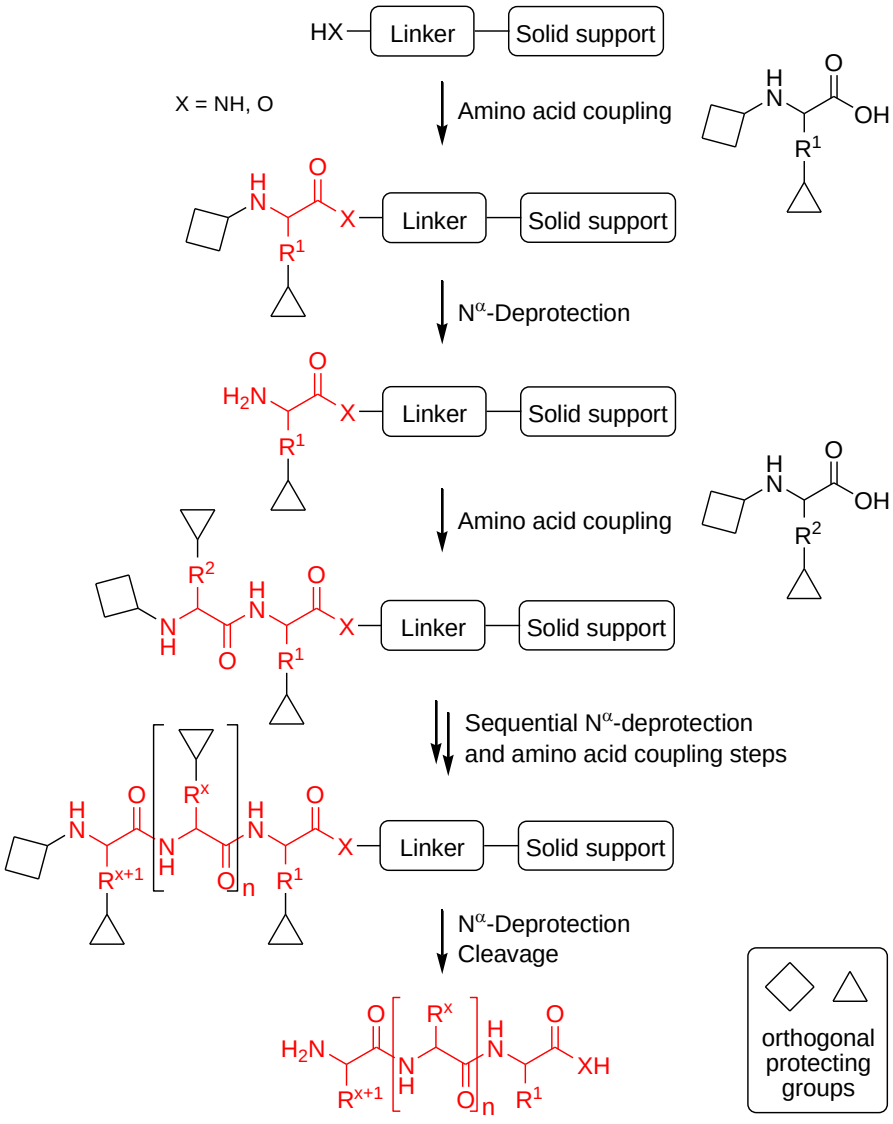

Scheme 1.30. General steps of the standard solid-phase peptide synthesis (SPPS).

The coupling of amino acids requires the activation of the C^{α}-carboxyl group by reaction with a suitable coupling reagent which leads to an active-ester intermediate that can easily react with the free N^{α}-amino group of the peptidyl resin. Until now, several coupling reagents, such as carbodiimides (e.g. DIPCDI, DCC, EDC), aminium salts (e.g. HBTU, HATU, HCTU), phosphonium salts (e.g. PyBOP), and new uronium salts (e.g. COMU, PyOxim) have been used. These reagents are often employed in the presence of a nucleophilic additive (e.g. HOBt, Oxyma) to suppress racemization and other undesired side reactions (Table 1.2) (Palomo, 2014; Pires et al., 2014). Carbodiimide aminium and phosphonium reagents are usually used in combination with HOBt. Apart from this additive, the two latter reagents also require the presence of a base, such as *N*,*N*-diisopropylethylamine (DIEA) (Palomo, 2014). However, the potentially explosive character of the benzotriazole-based additives (Wehrstedt et al., 2005) as well as its potential to cause allergic reactions, including skin irritation and respiratory problems, has limited its application in organic chemistry. Otherwise, the use of carbodiimides in combination with the new ethyl 2-cyano-2-(hydroxyimino)acetate (Oxyma) additive has attracted much attention in peptide synthesis (Subirós-Funosas et al., 2009a). Moreover, 1-[(1-(cyano-2-ethoxy-2-oxoethylideneaminooxy)-dimethylamino-morpholinomethylene)] methanaminium hexafluorophosphate (COMU), a new coupling reagent based on the Oxyma structure, has been reported to be a safer and more efficient coupling reagent in comparison to the classic benzotriazole-based reagents (El-Faham et al., 2009; Subiros-Funosas et al., 2009b; El-Faham and Albericio, 2010).

Table 1.2. Coupling reagents and additives.

Coupling reagents / Additives	**Structure**		
Carbodiimides	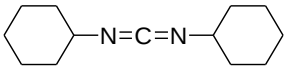 **DCC**	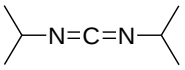 **DIPCDI**	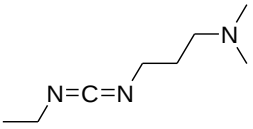 **EDC**
Aminium salts	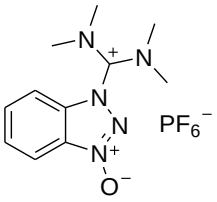 **HBTU**	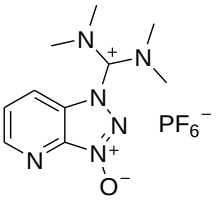 **HATU**	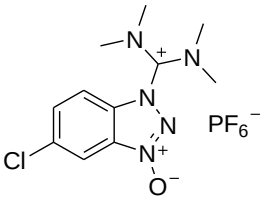 **HCTU**
Phosphonium salts	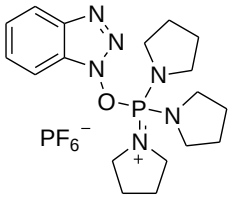 **PyBOP**		
Uronium salts	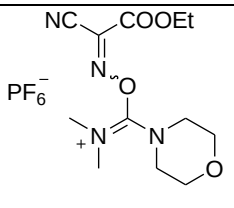 **COMU**	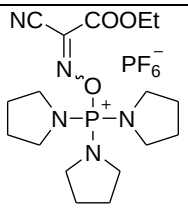 **PyOxim**	
Additives	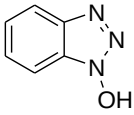 **HOBt**	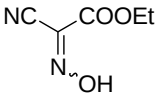 **Oxyma**	

1.4.2. Solid-phase synthesis of biaryl linear peptides

Despite the advantages of the solid-phase synthesis, up to now, only few examples of peptide modification through a Suzuki-Miyaura arylation on solid support are found in the literature. The most common approach for the formation of biaryl amino acids involves the previous attachment of the corresponding haloamino acid on the solid support and its subsequent arylation with an arylboronic acid in solution. In 2007, Haug and coworkers reported the first solid-phase synthesis of biaryl linear peptides following this approach. In particular, they prepared a library of biaryl tripeptides using a Rink amide NovaGel resin (Haug et al., 2007). The biaryl bond was formed via a Suzuki-Miyaura reaction between a 4-iodo-L-phenylalanine-containing tripeptidyl resin and several commercially available arylboronic acids (Scheme 1.31). This reaction was carried out by using $Pd(OAc)_2$ as catalyst, P(*o*-tolyl)$_3$ as ligand and Na_2CO_3 as base, under conventional heating at 80 ºC.

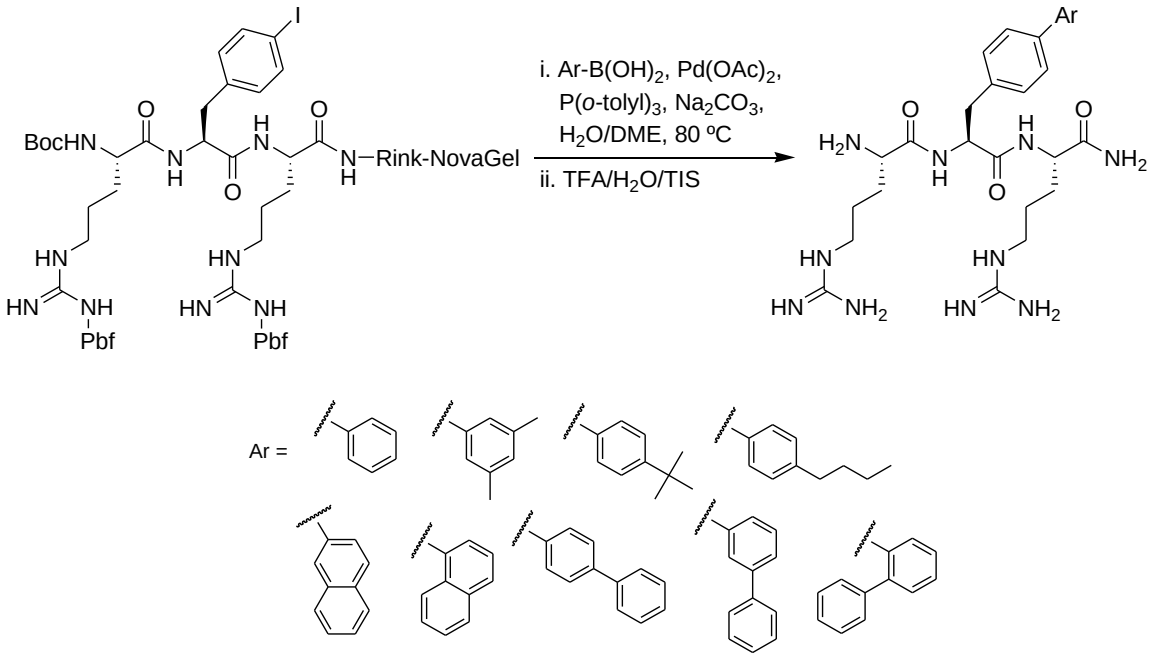

Scheme 1.31. Solid-phase synthesis of 4-aryl-L-phenylalanine-containing tripeptides.

Doan et al. described a library of biaryl octapeptides which were prepared on a Wang resin. The key step of the synthesis was the arylation of a 4-iodo-L-phenylalanine-containing octapeptidyl resin with various arylboronic acids. $Pd(PPh_3)_4$ was used as catalyst and K_3PO_4 as base, and the reaction was performed under conventional heating at 80 ºC (Scheme 1.32) (Doan et al., 2008).

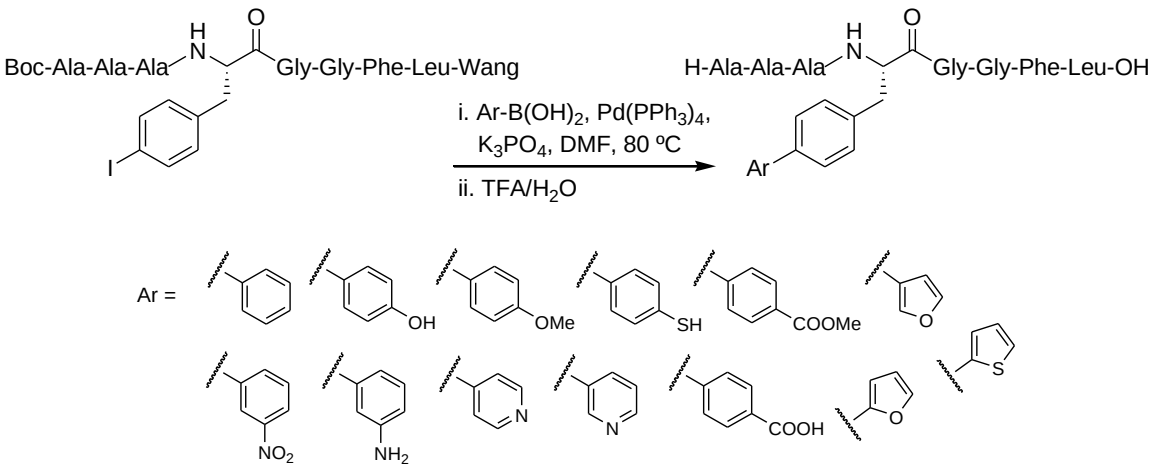

Scheme 1.32. Solid-phase synthesis of 4-aryl-L-phenylalanine-containing octapeptides.

A similar procedure was recently reported by Le Quement and coworkers. They examined the Suzuki-Miyaura cross-coupling reaction between a 3- or 4-iodo-L-phenylalanine-containing tetrapeptidyl resin and a set of arylboronic acids. A $PEGA_{800}$ resin was used as solid support and, after extensive optimization, the best results were achieved with $PdCl_2$(dppf) and K_3PO_4 in *tert*-butyl alcohol (*t*BuOH)/toluene/H_2O at room temperature (Scheme 1.33) (Le Quement et al., 2011).

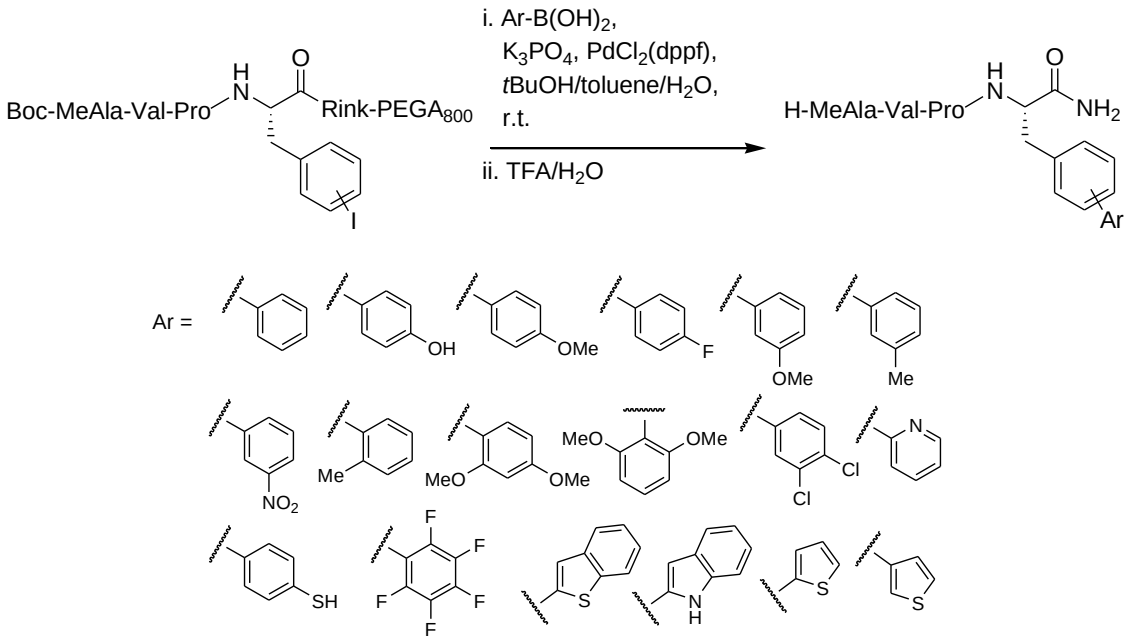

Scheme 1.33. Solid-phase synthesis of 3- and 4-aryl-L-phenylalanine-containing tetrapeptides.

Cerezo and coworkers described in 2008 the preparation of short linear peptides containing a 5-aryl-L-histidine by means of a microwave-assisted Suzuki-Miyaura cross-coupling of a 5-bromohistidine-containing tripeptidyl resin with several commercially available arylboronic acids (Scheme 1.34) (Cerezo et al., 2008). This was the first example of a solid-phase Suzuki-Miyaura cross-coupling involving the imidazole ring of a histidine residue. The synthesis was carried out on a MBHA resin in presence of $Pd_2(dba)_3$, P(*o*-tolyl)$_3$ and KF in DME/EtOH/H_2O under microwave irradiation at 170 ºC. These conditions, but at 140 ºC, allowed the cross-coupling of the bromotripeptidyl resin with a Boc-protected 3-borono-L-tyrosine derivative leading to a biaryl linear tetrapeptide containing a His-Tyr linkage (Scheme 1.34).

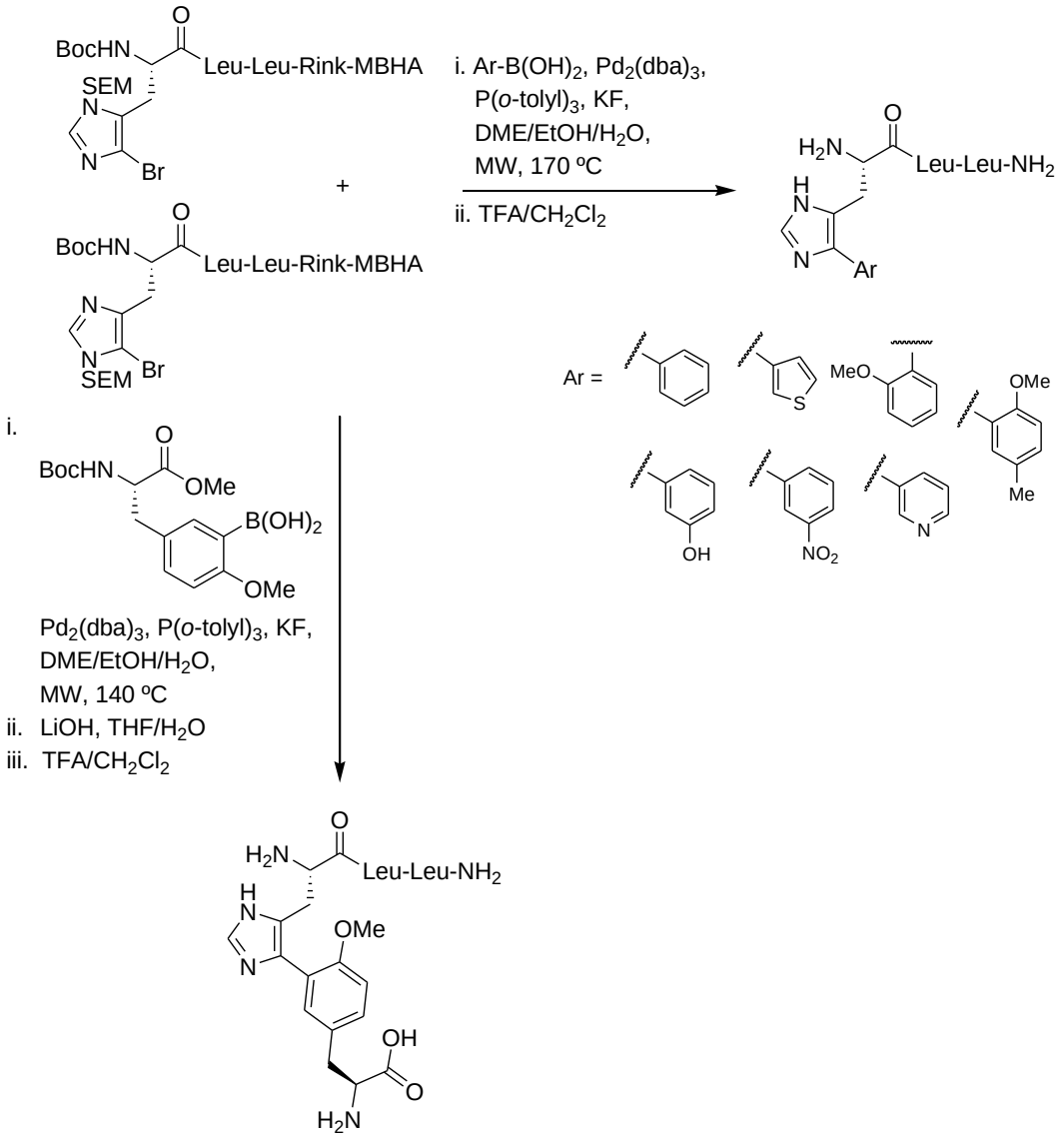

Scheme 1.34. Solid-phase synthesis of 5-aryl-L-histidine-containing tri- and tetrapeptides.

As an alternative to the preparation of biaryl peptides through the arylation of an halopeptidyl resin with an arylboronic acid, Afonso and coworkers investigated a more flexible approach, which involved the Suzuki-Miyaura arylation of a boronopeptidyl resin with an aryl halide in solution. The main advantages of Afonso's approach over the previous mentioned one are the higher commercial availability of aryl halides compared to arylboronic acids, and that all the synthetic steps are performed on solid support, including the formation of the boronic acid derivative. Thus, this approach does not require the preparation in solution of non-commercially available arylboronic acids and, therefore, it avoids the tedious work-up of solution reactions and the subsequent

purification step. Using this approach, Afonso and coworkers reported the preparation of a set of 4-aryl-L-phenylalanine-containing linear peptides through: (i) solid-phase Miyaura borylation of a 4-iodo-L-phenylalanine-containing tripeptidyl resin following the same procedure described in Scheme 1.9, and (ii) subsequent Suzuki-Miyaura cross-coupling of the resulting 4-boronopeptidyl resin Boc-Phe(4-BPin)-Leu-Leu-Rink-MBHA with several aryl halides using $Pd_2(dba)_3$, P(*o*-tolyl)$_3$ and KF under microwave irradiation at 120 ºC for 30 min (Scheme 1.35a) (Afonso et al., 2010). Moreover, the arylation of the resin Boc-Phe(4-BPin)-Leu-Leu-Rink-MBHA with halogenated aromatic amino acids afforded biaryl linear tetrapeptides incorporating a Phe-Phe, a Tyr-Phe or a His-Phe linkage (Scheme 1.35b) (Afonso et al., 2011).

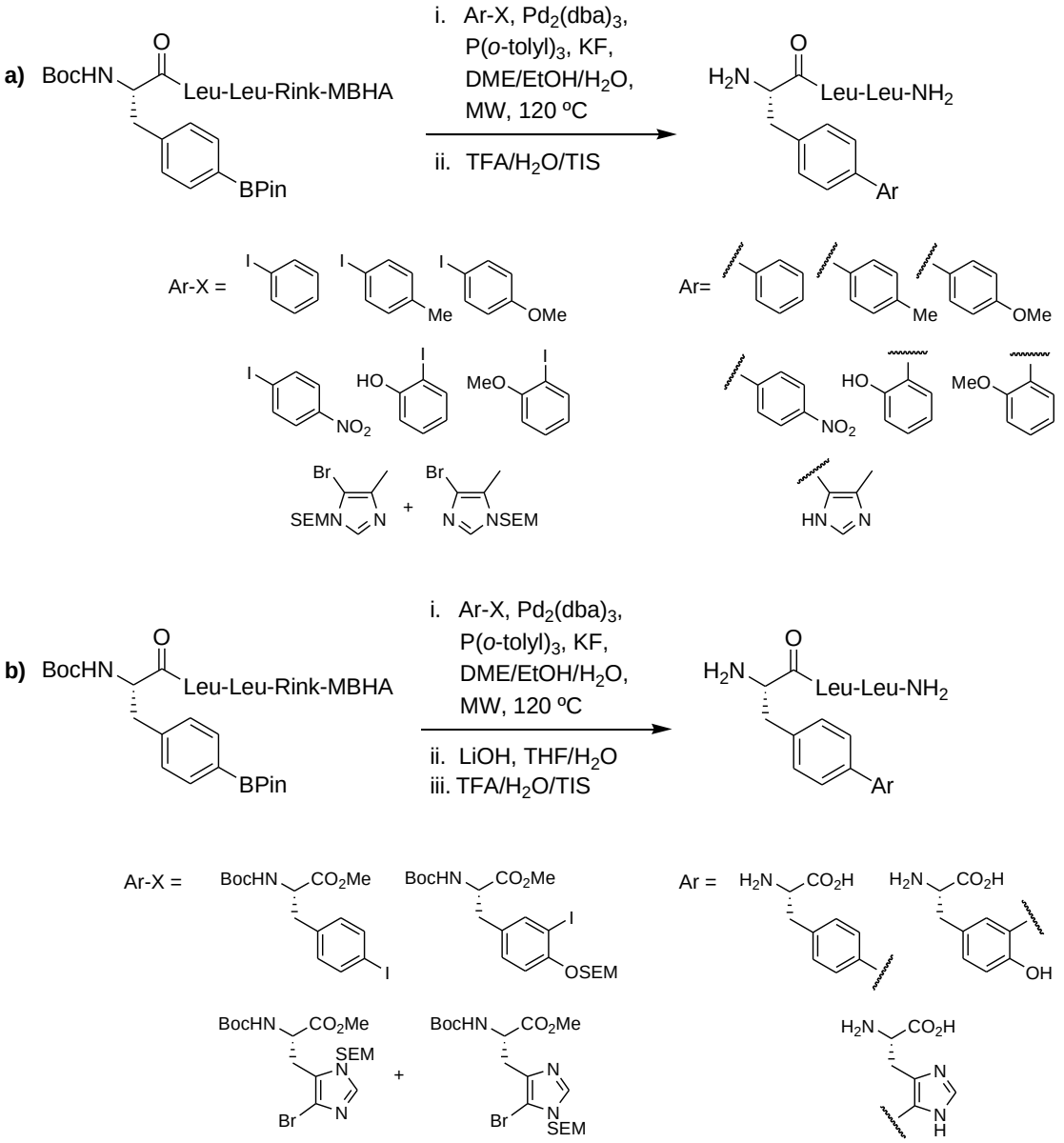

Scheme 1.35. Synthesis of biaryl linear tri- and tetrapeptides via a microwave-assisted Suzuki-Miyaura arylation of: a) a resin-bound phenylalanine boronic ester with various aryl halides; b) a resin-bound phenylalanine boronic ester with halogenated aromatic amino acids.

Afterwards, the previous strategy was extended to the preparation of a 3-phenyl-L-tyrosine-containing linear tripeptide (Scheme 1.36a), and biaryl linear tetrapeptides incorporating a Phe-Tyr or a Tyr-Tyr linkage (Scheme 1.36b) (Afonso et al., 2012). In both cases, the solid-phase Miyaura borylation of a 3-iodo-L-tyrosine-containing tripeptidyl resin was achieved as described in Scheme 1.9, being the reaction time of 8 h,

while the Suzuki-Miyaura arylation was performed under the same reaction conditions described in Scheme 1.35 for phenylalanine.

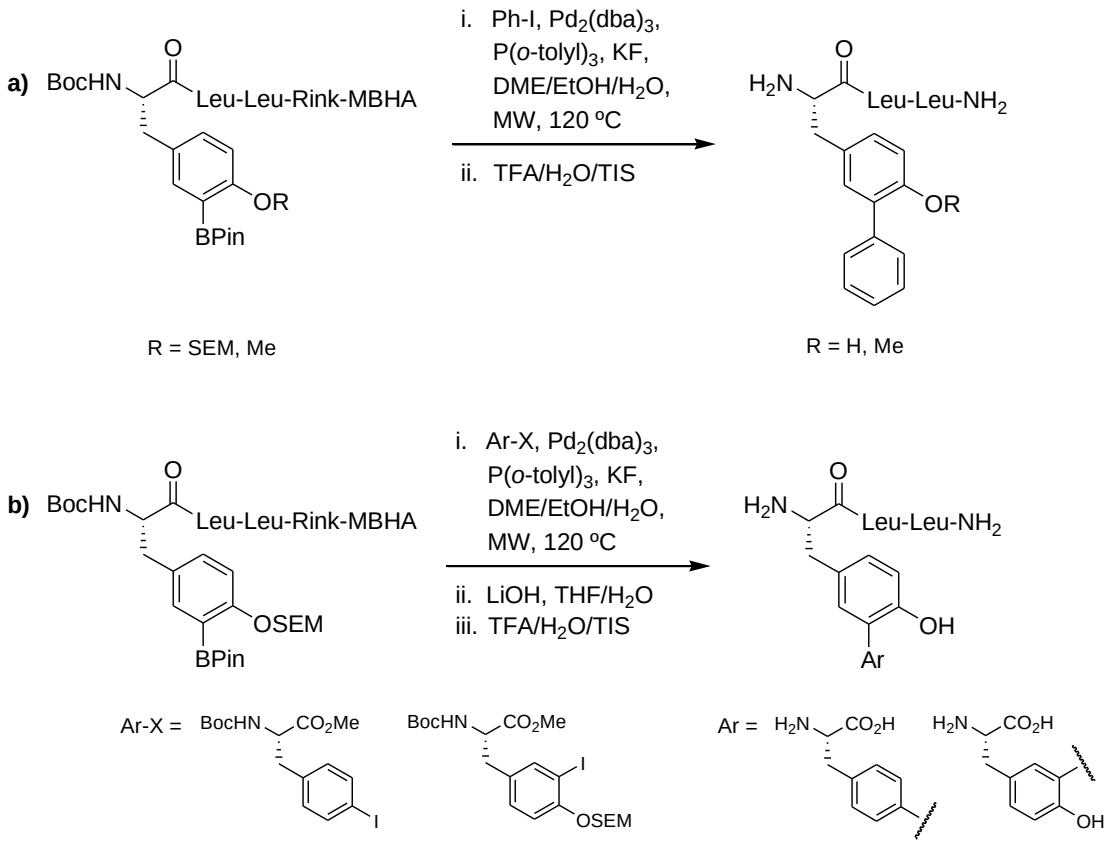

Scheme 1.36. Synthesis of biaryl linear tri- or tetrapeptides via microwave-assisted Suzuki-Miyaura arylation of: a) a resin-bound tyrosine boronic ester with iodobenzene and; b) a resin-bound tyrosine boronic ester with halogenated aromatic amino acids.

1.4.3. Solid-phase synthesis of biaryl cyclic peptides

In the last years, two examples on the solid-phase synthesis of biaryl cyclic peptides have been reported. Peptide macrocyclization has been accomplished via an intramolecular Suzuki-Miyaura cross-coupling.

Afonso and coworkers extended the previous methodology developed for the preparation of biaryl linear peptides (Scheme 1.35 andScheme 1.36) to the synthesis of biaryl cyclic peptides of different ring sizes incorporating a Phe-Phe, Phe-Tyr, Tyr-Phe or

Tyr-Tyr biaryl linkage (Afonso et al., 2011; Afonso et al., 2012) (Figure 1.8). The key steps of this approach were the synthesis of a linear peptidyl resin containing both the borono and the halogenated amino acid derivatives, and its cyclization via a microwave-assisted Suzuki-Miyaura reaction. The linear precursors were obtained by Miyaura borylation of a trityl-protected iodopeptidyl resin, followed by subsequent trityl group removal and coupling of the halogenated amino acid. This methodology is depicted in Scheme 1.37 for the preparation of biaryl cyclic peptides containing a Phe-Phe linkage (Figure 1.8a) (Afonso et al., 2011). It was then extended to the synthesis of sequences containing a biaryl bond between the side-chains of a Phe and a Tyr, or between two Tyr residues (Figure 1.1b-d) (Afonso et al., 2011; Alonso et al., 2012). Interestingly, the intramolecular Suzuki-Miyaura arylation of the linear peptidyl resins incorporating the 3-borono-L-tyrosine residue at the C-terminus was accomplished by using SPhos instead of P(*o*-tolyl)$_3$ as ligand.

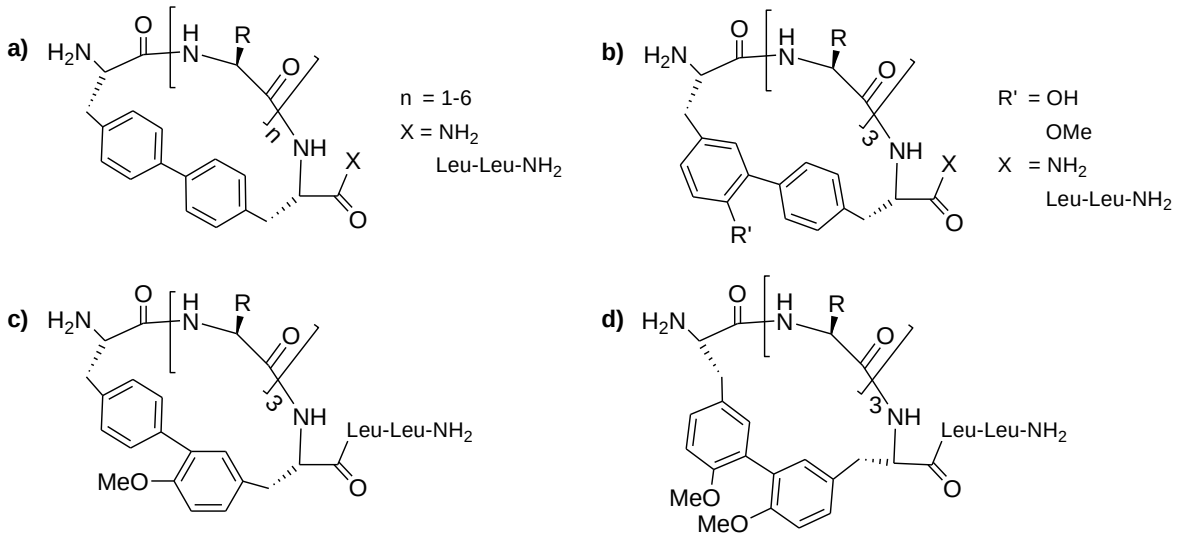

Figure 1.8. Biaryl cyclic peptides containing: a) a Phe-Phe; b) a Tyr-Phe; c) a Phe-Tyr; or d) a Tyr-Tyr linkage.

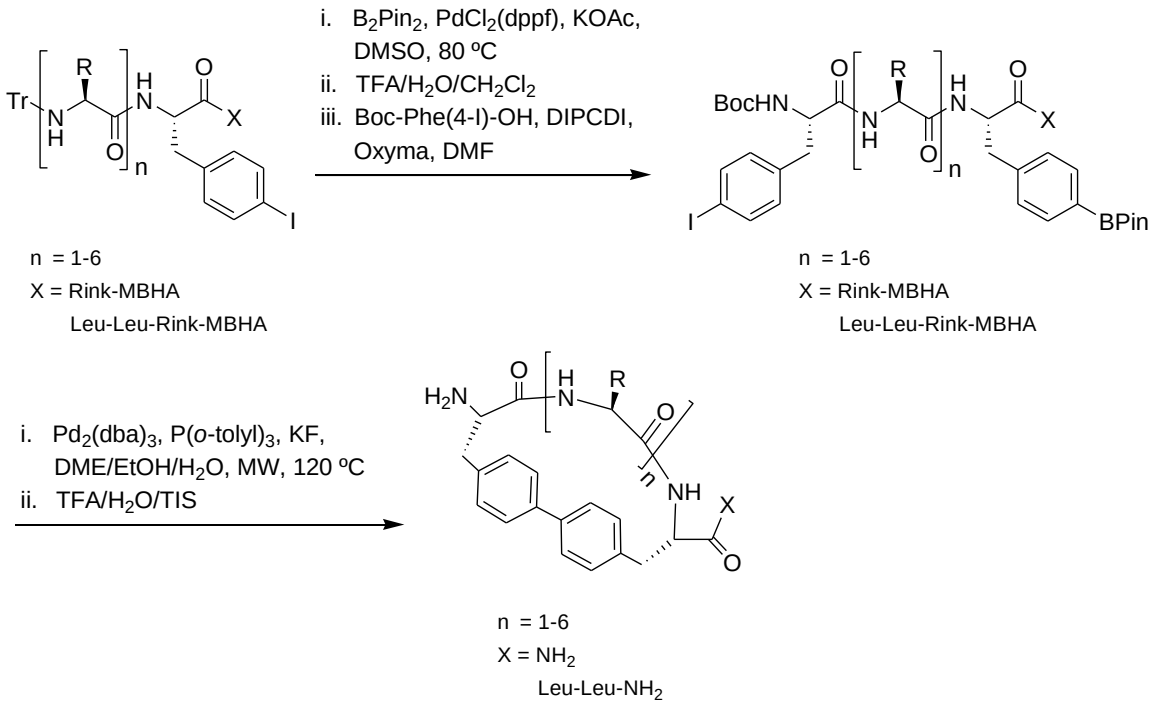

Scheme 1.37. Solid-phase synthesis of biaryl cyclic peptides incorporating a Phe-Phe linkage.

Following a similar methodology, in 2012, Meyer and coworkers prepared a library of *m,m*-, *m,o*- and *o,m*-biaryl-bridged macrocyclic peptides (Figure 1.9). They synthesized linear peptidyl resins containing a *m*- or *o*-boronophenylalanine at the N-terminus and a *m*- or *o*-halogenated phenylalanine at the C-terminus, which were then cyclized via an intramolecular Suzuki-Miyaura reaction (Meyer et al., 2012). In this case, the borono amino acid was prepared in solution and coupled to the N-terminus of the corresponding peptidyl resin. The intramolecular arylation for the synthesis of the *m,m*-biaryl-bridged macrocyclic peptide (Figure 1.9a) was initially tested and was achieved using $Pd(OAc)_2$, dppf and CsF in dioxane and H_2O at 90 ºC, as detailed in Scheme 1.38. This methodology was then applied to the preparation of *m,o*- and *o,m*-biaryl-bridged macrocyclic peptides with general structure depicted in Figure 1.9b-c, respectively. The formation of the latter *o,m*-system required the use of $Pd(PPh_3)_4$ and K_2CO_3 in DME at 140 ºC in the cyclization step.

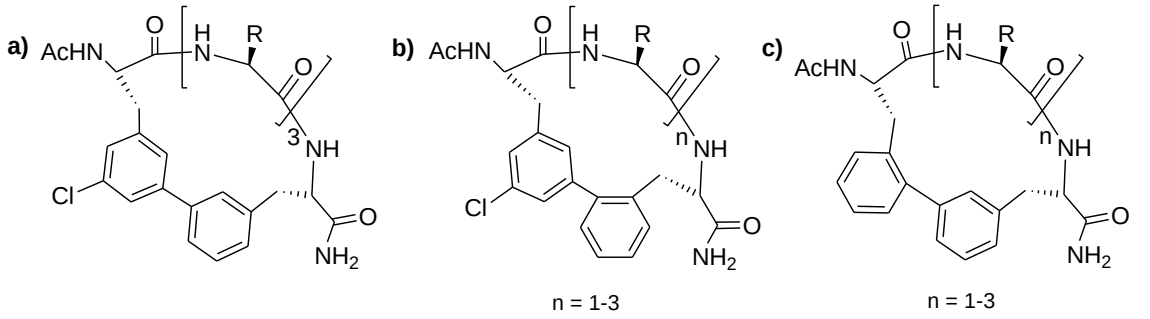

Figure 1.9. Biaryl-bridged macrocyclic peptides incorporating: a) a *m*,*m*-system; b) a *m*,*o*-system; and c) a *o*,*m*-system.

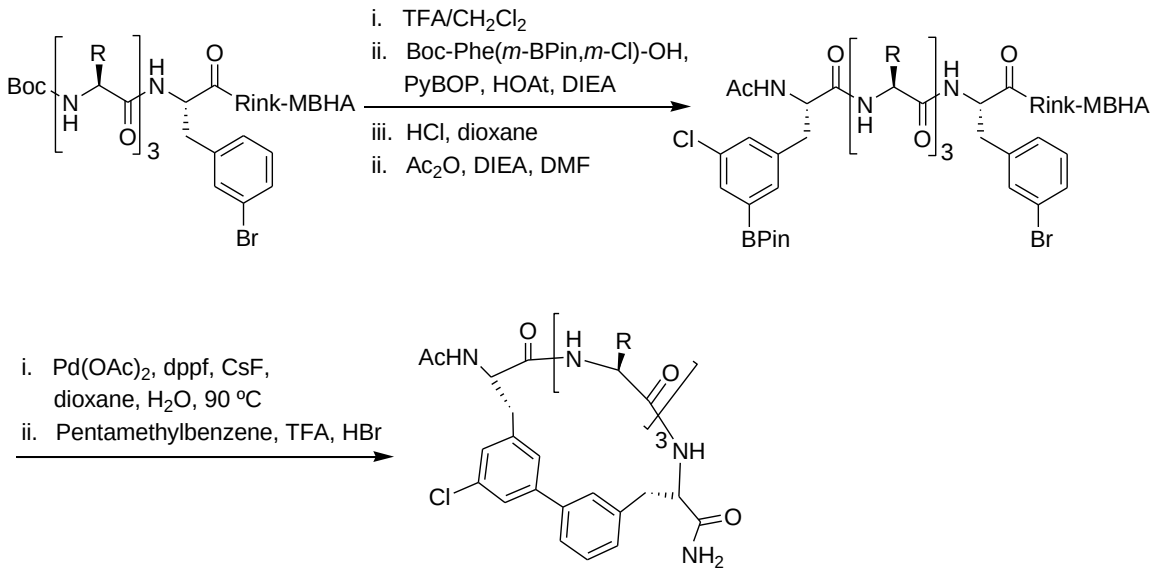

Scheme 1.38. Solid-phase synthesis of *m*,*m*-biaryl-bridged macrocyclic peptide.

Thus, the above examples constitute the first solid-phase synthesis of biaryl cyclic compounds bearing a biaryl linkage involving a phenylalanine or a tyrosine residue. However, despite the importance of 5-arylhistidines in the biological activity of naturally occurring biaryl cyclic peptides, and due to the difficulty of arylating the 4(5)-position of the imidazole ring, the formation of biaryl-bridged cyclic peptides involving the arylation of the imidazole ring of a histidine residue has not still been reported.

1.5. BIBLIOGRAPHY

Afonso, A.; Cussó, O.; Feliu, L.; Planas, M. Solid-phase synthesis of biaryl cyclic peptides containing a 3-aryltyrosine. *Eur. J. Org. Chem.* **2012**, 6204-6211.

Afonso, A.; Feliu, L.; Planas, M. Solid-phase synthesis of biaryl cyclic peptides by borylation and microwave-assisted intramolecular Suzuki-Miyaura reaction. *Tetrahedron* **2011**, *67*, 2238-2245.

Afonso, A.; Rosés, C.; Planas, M.; Feliu, L. Biaryl peptides from 4-iodophenylalanine by solid-phase borylation and Suzuki-Miyaura cross-coupling. *Eur. J. Org. Chem.* **2010**, 1461-1468.

Alonso, F.; Beletskaya, I. P.; Yus, M. Non-conventional methodologies for transition-metal catalysed carbon-carbon coupling: a critical overview. Part 2: The Suzuki reaction. *Tetrahedron* **2008**, *64*, 3047-3101.

Baghbanzadeh, M.; Pilger, C.; Kappe, O. Palladium-catalyzed direct arylation of heteroaromatic compounds: Improved conditions utilizing controlled microwave heating. *J. Org. Chem.* **2011**, *76*, 8138-8142.

Barder, T. E.; Walker, S. D.; Martinelli, J. R.; Buchwald, S. L. Catalysts for Suzuki-Miyaura coupling processes. Scope and studies of the effect of ligand structure. *J. Am. Chem. Soc.* **2005**, *127*, 4685-4696.

Bellina, F.; Cauteruccio, S.; Rossi, R. Synthesis and biological activity of vicinal diaryl-substituted-1H-imidazoles. *Tetrahedron* **2007**, *63*, 4571-4624.

Bellina, F.; Rossi, R. Regioselective functionalization of the imidazole ring via transition metal-catalyzed C-N and C-C bond forming reactions. *Adv. Synth. Catal.* **2010**, *352*, 1223-1276.

Bewley, C. A.; He, H.; Williams, D. H.; Faulkner, D. J. Aciculitins A-C: Cytotoxic and antifungal cyclic peptides from the lithistid sponge *Aciculites orientalis*. *J. Am. Chem. Soc.* **1996**, *118*, 4314-4321.

Bräse, S.; Kirchhoff, J. H.; Köbberling, J. Palladium-catalysed reactions in solid phase organic synthesis. *Tetrahedron* **2003**, *59*, 885-939.

Burk, M. J.; Lee, J. R.; Martinez, J. P. A versatile tandem catalysis procedure for the preparation of novel amino acids and peptides. *J. Am. Chem. Soc.* **1994**, *116*, 10847-10848.

Burke, A. J.; Silva Marques, C. Catalytic arylation methods. From the academic lab to industrial processes. Wiley-VCH Verlag: Weinheim, 2015.

Cerezo, V.; Afonso, A.; Planas, M.; Feliu, L. Synthesis of 5-arylhistidines via a Suzuki-Miyaura cross-coupling. *Tetrahedron* **2007**, *63*, 10445-10453.

Cerezo, V.; Amblard, M.; Martinez, J.; Verdié, P.; Planas, M.; Feliu, L. Solid-phase synthesis of 5-arylhistidines via a microwave-assisted Suzuki-Miyaura cross-coupling. *Tetrahedron* **2008**, *64*, 10538-10545.

Corbet, J.; Mignani, G. Selected patented cross-coupling reaction technologies. *Chem. Rev.* **2006**, *106*, 2651-2710.

Coste, A.; Bayle, A.; Marrot, J.; Evano, G. A convergent synthesis of the fully elaborated macrocyclic core of TMC-95A. *Org. Lett.* **2014**, *16*, 1306-1309.

Doan, N.; Bourgault, S.; Létourneau, M.; Fournier, A. Effectiveness of the Suzuki-Miyaura cross-coupling reaction for solid-phase peptide modification. *J. Comb. Chem.* **2008**, *10*, 44-51.

Dobler, M. R. Design and novel synthesis of aryl-heteroaryl-imidazole MAP kinase inhibitors. *Tetrahedron Lett.* **2003**, *44*, 7115-7117.

El-Faham, A.; Albericio, F. COMU: A third generation of uranium-type coupling reagents. *J. Pept. Sci.* **2010**, *16*, 6-9.

El-Faham, A.; Subirós-Funosas, R.; Prohens, R.; Albericio, F. COMU: A safer and more efficient replacement for benzotriazole-based uranium coupling reagents. *Chem. Eur. J.* **2009**, *15*, 9404-9416.

Ezaki, M.; Iwami, M.; Yamashita, M.; Hashimoto, S.; Komori, T.; Umehara, K.; Mine, Y.; Kohsaka, M.; Aoki, H.; Imanaka, H. Biphenomycins A and B, novel peptide antibiotics I. Taxonomy, fermentation, isolation and characterization. *J. Antibiot.* **1985**, *38*, 1453-1461.

Feliu, L.; Planas, M. Cyclic peptides containing biaryl and biaryl ether linkages. *Int. J. Pept. Res. Ther.* **2005**, *11*, 53-97.

Firooznia, F.; Gude, C.; Chan, K.; Marcopulos, N.; Satoh, Y. Enantioselective synthesis of 4-substituted phenylalanines by cross-coupling reactions. *Tetrahedron Lett.* **1999**, *40*, 213-216.

García-Martín, F.; Quintanar-Audelo, M.; García-Ramos, Y.; Cruz, L. J.; Gravel, C.; Furic, R.; Côte, S.; Tulla-Puche, J.; Albericio, F. ChemMatrix, a poly(ethylene glycol)-based support for the solid-phase synthesis of complex peptides. *J. Comb. Chem.* **2006**, *8*, 213-220.

García-Melchor, M.; Braga, A. A. C.; Lledós, A.; Ujaque, G.; Maseras, F. Computational perspective on Pd-catalyzed C-C cross-coupling reaction mechanisms. *Acc. Chem. Res.* **2013**, *46*, 2626-2634.

García-Ramos, Y.; Paradís-Bas, M.; Tulla-Puche, J.; Albericio, F. ChemMatrix for complex peptides and combinatorial chemistry. *J. Pept. Sci.* **2010**, *16*, 675-678.

Gong, Y.; He, W. Direct synthesis of unprotected 4-aryl phenylalanines via the Suzuki reaction under microwave irradiation. *Org. Lett.* **2002**, *4*, 3803-3805.

Góngora-Benítez, M.; Tulla-Puche, J.; Albericio, F. Handles for Fmoc solid-phase synthesis of protected peptides. *ACS Comb. Sci.* **2013**, *15*, 217-228.

Grant, G. A. Synthetic peptides. A user's guide. Oxfort University Press: New York, 2002.

Greene, T. W. Protective groups in organic synthesis., John Wiley & Sons, INC.: Canada, 1999.

Guillier, F.; Orain, D.; Bradley, M. Linkers and cleavage strategies in solid-phase organic synthesis and combinatorial chemistry. *Chem. Rev.* **2000**, *100*, 2091-2157.

Hall, D. G. Boronic acids. Wiley-VCH Verlag: Weinheim, 2005.

Haug, B. E.; Stensen, W.; Svendsen, J. S. Application of the Suzuki-Miyaura cross-coupling to increase antimicrobial potency generates promising novel antibacterials. *Bioorg. Med. Chem. Lett.* **2007**, *17*, 2361-2364.

Helynck, G.; Dubertret, C.; Frechet, D.; Leboul, J. Isolation of RP 66453, a new secondary peptide metabolite from *Streptomyces* sp. useful as a lead for neurotensin antagonists. *J. Antibiot.* **1998**, *51*, 512-514.

Heravi, M. M.; Hashemi, E. Recent advances in application of intramolecular Suzuki cross-coupling in cyclization and heterocyclization. *Monatsh. Chem.* **2012**, *143*, 861-880.

Hitotsuyanagi, Y.; Odagiri, M.; Kato, S.; Kusano, J.; Hasuda, T.; Fukaya, H.; Takya, K. Isolation, structure determination, and synthesis of allo-RA-V and neo-RA-V, RA-series bicyclic peptides from *Rubia cordifolia* L. *Chem. Eur. J.* **2012**, *18*, 2839-2846.

Hutton, C. A; Skaff, O. A convenient preparation of dityrosine via Miyaura borylation-Suzuki coupling of iodotyrosine derivatives. *Tetrahedron Lett.* **2003**, *44*, 4895-4898.

Inoue, M.; Sakazaki, H.; Furuyama, H.; Hirama, M. Total synthesis of TMC-95A. *Angew. Chem. Int. Ed.* **2003**, *42*, 2654-2657.

Ishiyama, T.; Murata, M.; Miyaura, N. Palladium(0)-catalyzed cross-coupling reaction of alkoxydiboron with haloarenes: A direct procedure for arylboronic esters. *J. Org. Chem.* **1995**, *60*, 7508-7510.

Isidro-Llobet, A.; Álvarez, M.; Albericio, F. Amino acid-protecting groups. *Chem. Rev.* **2009**, *109*, 2455-2504.

James, J. W. Linkers for solid phase organic synthesis. *Tetrahedron* **1999**, *55*, 4855-4946.

Jin, Z. Imidazole, oxazole and thiazole alkaloids. *Nat. Prod. Rep.* **2006**, *23*, 464-496.

Johansson, C. C. C.; Kitching, M. O.; Colacot, T. J.; Snieckus, V. Palladium-catalyzed cross-coupling: A historical contextual perspective to the 2010 Nobel prize. *Angew. Chem. Int. Ed.* **2012**, *51*, 5062-5085.

Katritzky, A. R.; Ramsden, C. A.; Scriven, E. F. V.; Taylor, R. J. K. Comprehensive heterocyclic chemistry III. A review of the literature 1995-2007. *vol. 4*, Elsevier Science: Oxford, 2008.

Knör, S.; Laufer, B.; Kessler, H. Efficient enantioselective synthesis of condensed and aromatic-ring-substituted tyrosine derivatives. *J. Org. Chem.* **2006**, *71*, 5625-5630.

Kohno, J.; Koguchi Y.; Nishio, M.; Nakao, K.; Kuroda, M.; Shimizu, R.; Ohnuki, T.; Komatsubara, S. Structures of TMC-95A-D: Novel proteasome inhibitors from *Apiospora montagnei* Sacc. TC1093. *J. Org. Chem.* **2000**, *65*, 990-995.

Kotha, S.; Goyal, D.; Chavan, A. S. Diversity-oriented approaches to unusual α-amino acids and peptides: Step economy, atom economy, redox economy, and beyond. *J. Org. Chem.* **2013**, *78*, 12288-12313.

Kotha, S.; Lahiri, K. A new approach for modification of phenylalanine peptides by Suzuki-Miyaura coupling reaction. *Bioorg. Med. Chem. Lett.* **2001**, *11*, 2887-2890.

Kotha, S.; Lahiri, K. Application of the Suzuki-Miyaura cross-coupling reaction for the modification of phenylalanine peptides. *Biopolymers* **2003**, *69*, 517-528.

Kotha, S.; Lahiri, K.; Kashinath, D. Recent applications of the Suzuki-Miyaura cross-coupling reaction in organic synthesis. *Tetrahedron* **2002**, *58*, 9633-9695.

Kozlowski, M. C.; Morgan, B. J.; Linton, E. C. Total synthesis of chiral biaryl natural products by asymmetric biaryl coupling. *Chem. Soc. Rev.* **2009**, *38*, 3193-3207.

Le Quement, S. T.; Ishoey, M.; Petersen, M. T.; Thastrup, J.; Hagel, G.; Nielsen, T. E. Solid-phase synthesis of Smac peptidomimetics incorporating triazoloprolines and biarylalanines. *ACS Comb. Sci.* **2011**, *13*, 667-675.

Lee, T.; Choi, J.; Byun, J.; Lee, Y. Preparation of MBHA resin by benzotriazole-mediated amidoalkylation. *Tetrahedron Lett.* **2008**, *49*, 5380-5382.

Leet, J. E.; Schroeder, D. R.; Golik, J.; Matson, J. A.; Doyle, T. W.; Lam, K. S.; Hill, S. E.; Lee, M. S.; Whitney, J. L.; Krishnan, B. S. Himastatin, a new antitumor antibiotic from *Streptomyces hygroscopicus* III. Structural elucidation. *J. Antibiot.* **1996**, *49*, 299-311.

Lennox, A. J. J.; Lloyd-Jones, G. C. Selection of boron reagents for Suzuki-Miyaura coupling. *Chem. Soc. Rev.* **2014**, *43*, 412-443.

Lépine, R.; Zhu, J. Microwave-assisted intramolecular Suzuki-Miyaura reaction to macrocycle, a concise asymmetric total synthesis of Biphenomycin B. *Org. Lett.* **2005**, *7*, 2981-2984.

Lewis, J. R. Amaryllidaceae, muscarine, imidazole, oxazole, thiazole and peptide alkaloids, and other miscellaneous alkaloids. *Nat. Prod. Rep.* **2000**, *17*, 57-84.

Li, J. J.; Gribble, G. W. Palladium in heterocyclic chemistry. A guide for the synthetic chemist., *vol. 20*, Pergamon, 2000.

Lloyd-Williams, P.; Albericio, F.; Giralt, E. Chemical approaches to the synthesis of peptides and proteins. CRC Press LLC: Florida, 1997.

Magano, J.; Dunetz, J. R. Large-scale applications of transition metal-catalyzed couplings for the synthesis of pharmaceuticals. *Chem. Rev.* **2011**, *111*, 2177-2250.

Mahindra, A.; Bagra, N.; Jain, R. Palladium-catalyzed regioselective C-5 arylation of protected L-histidine: Microwave-assisted C-H activation adjacent to donor arm. *J. Org. Chem.* **2013**, *78*, 10954-10959.

Malan, C.; Morin, C. A concise preparation of 4-borono-L-phenylalanine (L-BPA) from L-phenylalanine. *J. Org. Chem.* **1998**, *63*, 8019-8020.

Martin, R.; Buchwald, S. L. Palladium-catalyzed Suzuki-Miyaura cross-coupling reactions employing dialkylbiaryl phosphine ligands. *Acc. Chem. Res.* **2008**, *41*, 1461-1473.

Martin, A. R.; Yang, Y. Palladium-catalyzed cross-coupling reactions of organoboronic acids with organic electrophiles. *Acta Chem. Scand.* **1993**, *47*, 221-230.

Merrifield, R. B. Solid phase peptide synthesis. I. The synthesis of a tetrapeptide. *J. Am. Chem. Soc.* **1963**, *85*, 2149-2154.

Merrifield, R. B. Solid phase peptide synthesis. *Science.* **1968**, *232*, 341-347.

Merrifield, R. B. Solid phase synthesis (Nobel Lecture). *Angew. Chem. Int. Ed.* **1985**, *24*, 799-810.

Meyer, F.; Collins, J. C.; Borin, B.; Bradow, J.; Liras, S.; Limberakis, C.; Mathiowetz, A. M.; Philippe, L.; Price, D.; Song, K.; James, K. Biaryl-bridged macrocyclic

peptides: Conformational constraint via carbogenic fusion of natural amino acid side chains. *J. Org. Chem.* **2012**, *77*, 3099-3114.

Miyaura, N. Topics in current chemistry., *vol. 219*, Springer-Verlag: Berlin Heidelberg, 2002.

Miyaura, N.; Suzuki, A. Palladium-catalyzed cross-coupling reaction of organoboron compounds. *Chem. Rev.* **1995**, *95*, 2457-2483.

Miyaura, N.; Yanagi, T.; Suzuki, A. The palladium-catalyzed cross-coupling reaction of phenylboronic acid with haloarenes in the presence of bases. *Synth. Commun.* **1981**, *11*, 513-519.

Morris, J. C. Marine natural products: synthetic aspects. *Nat. Prod. Rep.* **2013**, *30*, 783-805.

Nicolaou, K. C.; Bulger, P. G.; Sarlah, D. Palladium-catalyzed cross-coupling reactions in total synthesis. *Angew. Chem. Int. Ed.* **2005**, *44*, 4442-4489.

Pace, J. L.; Yang, G. Glycopeptides: Update on an old successful antibiotic class. *Biochem. Pharmacol.* **2006**, *71*, 968-980.

Palomo, J. M. Solid-phase peptide synthesis: an overview focused on the preparation of biologically relevant peptides. *RSC Adv.* **2014**, *4*, 32658-32672.

Pires, D. A. T.; Bemquerer, M. P.; Nascimento, C. J. Some mechanistic aspects on Fmoc solid phase peptide synthesis. *Int. J. Pept. Res. Ther.* **2014**, *20*, 53-69.

Prieto, M.; Mayor, S.; Lloyd-Williams, P.; Giralt, E. Use of the SPhos ligand to suppress racemization in arylpinacolboronate ester Suzuki couplings involving α-amino acids. Synthesis of biaryl derivatives of 4-hydroxyphenylglycine, tyrosine and tryptophan. *J. Org. Chem.* **2009**, *74*, 9202-9205.

Revesz, L.; Bonne, F.; Makavou, P. Vicinal bromostannanes as novel building blocks for the preparation of di- and tribustituted imidazoles. *Tetrahedron Lett.* **1998**, *39*, 5171-5174.

Roberts, T. C.; Smith, P. A.; Cirz, R. T.; Romesberg, F. E. Structural and initial biological analysis of synthetic Arylomycin A_2. *J. Am. Chem. Soc.* **2007**, *129*, 15830-15838.

Santini, R.; Griffith, M. C.; Qi, M. A measure of solvent effects on swelling of resins for solid phase organic synthesis. *Tetrahedron Lett.* **1998**, *39*, 8951-8954.

Sarin, V.; Kent, S. B. H.; Merrifield, R. B. Properties of swollen polymer networks. Solvation and swelling of peptide-containing resins in solid-phase peptide synthesis. *J. Am. Chem. Soc.* **1980**, *102*, 5463-5470.

Schimana, J.; Gebhardt, K.; Höltzel, A.; Schmid, D. G.; Süssmuth, R.; Müller, J.; Pukall, R.; Fiedler, H. P. Arylomycins A and B, new biaryl-bridged lipopeptide antibiotics produced by *Streptomyces* sp. Tu 6075. I. Taxonomy, fermentation, isolation and biological activities. *J. Antibiot.* **2002**, *55*, 565-570.

Schnürch, M.; Flasik, R.; Khan, A. F.; Spina, M.; Mihovilovic, M. D.; Stanetty, P. Cross-coupling reactions on azoles with two and more heteroatoms. *Eur. J. Org. Chem.* **2006**, 3283-3307.

Scott, P. T. H. Solid-phase organic syntheses. Solid-phase palladium chemistry., *vol. 2*, John Wiley & Sons, INC.: New Jersey, 2012.

Subirós-Funosas, R.; Acosta, G. A.; El-Faham, A.; Albericio, F. Microwave irradiation and COMU: a potent combination for solid-phase peptide synthesis. *Tetrahedron Lett.* **2009**, *50*, 6200-6202 (b).

Subirós-Funosas, R.; Prohens, R.; Barbas, R.; El-Faham, A.; Albericio, F. Oxyma: An efficient additive for peptide synthesis to replace the benzotriazole-based HOBt and HOAt with a lower risk of explosion. *Chem. Eur. J.* **2009**, *15*, 9394-9403 (a).

Suzuki, A. Recent advances in the cross-coupling reaction of organoboron derivatives with organic electrophiles, 1995-1998. *J. Organom. Chem.* **1999**, *576*, 147-168.

Suzuki, A. Cross-coupling reactions of organoboranes: An easy way to construct C-C bonds (Nobel lecture). *Angew. Chem. Int. Ed.* **2011**, *50*, 6723-6737.

Torborg, C.; Beller, M. Recent applications of palladium-catalyzed coupling reactions in the pharmaceutical, agrochemical, and fine chemical industries. *Adv. Synth. Catal.* **2009**, *351*, 3027-3043.

Van Bambeke, F.; Van Laethem, Y.; Courvalin, P.; Tulkens, P. M. Glycopeptides antibiotics from conventional molecules to new derivatives. *Drugs* **2004**, *64*, 913-936.

Vilaró, M.; Arsequell, G.; Valencia, G.; Ballesteros, A.; Barluenga, J. Arylation of Phe and Tyr side chains of unprotected peptides by a Suzuki-Miyaura reaction in water. *Org. Lett.* **2008**, *10*, 3243-3245.

Waldmann, H.; He, Y.; Tan, H.; Arve, L.; Arndt, H. Flexible total synthesis of Biphenomycin B. *Chem. Commun.* **2008**, 5562-5564.

Wehrstedt, K. D.; Wandrey, P. A.; Heitkamp, D. Explosive properties of 1-hydroxybenzotriazoles. *J. Hazard. Mater*. **2005**, *126*, 1-7.

Zaragoza, F. Organic synthesis on solid phase. Supports, linkers, reactions. Wiley-VCH Verlag: Weinheim, 2000.

CHAPTER 2

General Objectives

CHAPTER 2: General objectives

This thesis deals with the development of a solid-phase synthetic approach for the preparation of biaryl linear and cyclic peptides incorporating a 5-arylhistidine residue through a microwave-assisted Suzuki-Miyaura cross-coupling reaction. In particular, the main objectives were:

- The investigation of an efficient methodology for the solid-phase synthesis of linear undecapeptides incorporating a 5-arylhistidine residue at the 1- or 4-position, and their biological evaluation (Chapter 3).

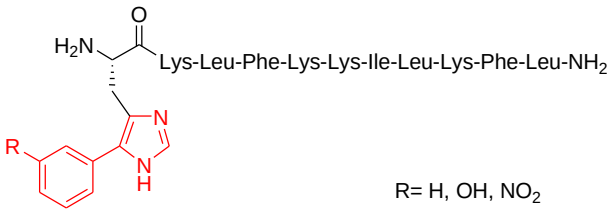

- The extension of the above methodology to the solid-phase synthesis of biaryl cyclic peptides of different ring sizes containing a His-Phe linkage, and the evaluation of the influence of the peptide length, the presence of a C-terminus spacer and the position of the histidine residue at the N- or C-terminus (Chapter 4).

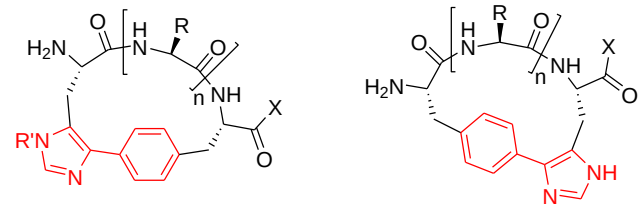

- The application of the previous methodology to the preparation of biaryl cyclic peptides containing a 3- or 5-amino acid ring with a His-Tyr linkage (Chapter 5).

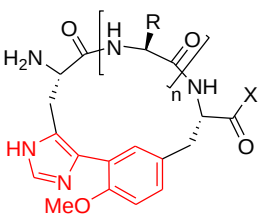

I

X = NH_2
Leu-Leu-NH_2

n = 1, 3

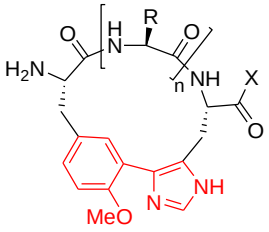

II

X = NH_2
Leu-Leu-NH_2

n = 1, 3

- The study of the total solid-phase synthesis of biaryl cyclic lipopeptide derivatives of arylomycins containing a Phe-Tyr, a Tyr-Tyr, a His-Tyr, or a phenylglycine (Phg)-Tyr biaryl linkage (Chapter 6).

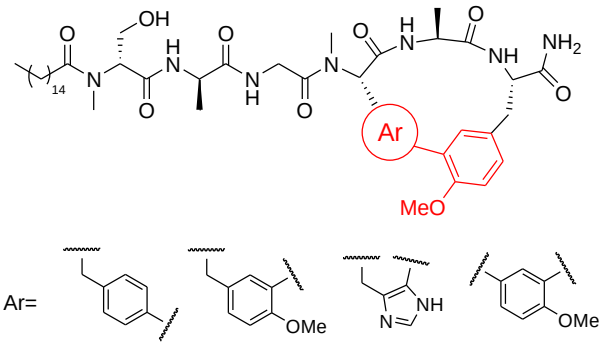

- The synthesis of biaryl cyclic peptide analogues of the northern and the southern hemispheres of aciculitins.

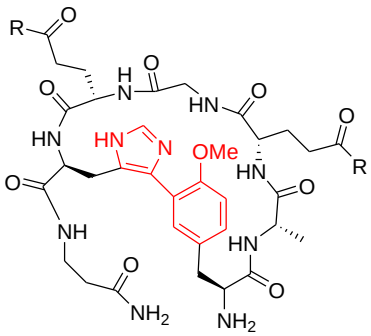

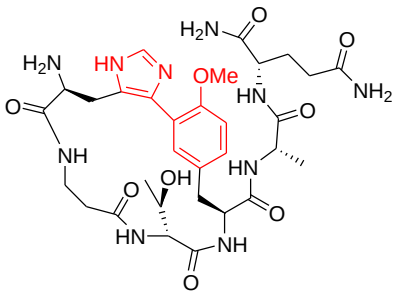

- The development of a solid-phase methodology for the preparation of biaryl bicyclic peptide analogues of aciculitins containing a Phe-Phe, a Phe-Tyr, a His-Tyr and a Tyr-Tyr linkage.

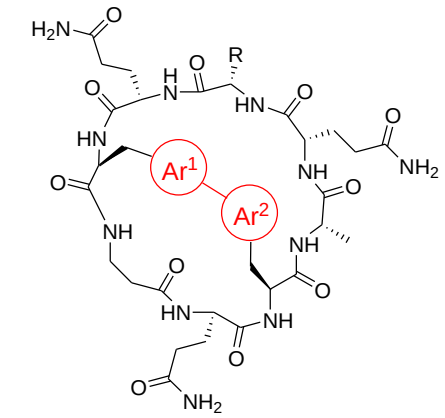

CHAPTER 3

Solid-Phase Synthesis of 5-Arylhistidine-Containing Peptides with Antimicrobial Activity Through a Microwave-Assisted Suzuki-Miyaura Cross-Coupling

*This chapter corresponds to the following publication:

Ng-Choi, I.; Soler, M.; Cerezo, V.; Badosa, E.; Montesinos, E.; Planas, M.; Feliu, L. Solid-phase synthesis of 5-arylhistidine-containing peptides with antimicrobial activity through a microwave-assisted Suzuki-Miyaura cross-coupling. *Eur. J. Org. Chem.* **2012**, 4321-4332.

CHAPTER 3

A microwave-assisted solid-phase Suzuki-Miyaura reaction has been employed for the synthesis of 5-arylhistidine-containing peptides. In particular, sequences containing a 5-arylhistidine at the 1- or 4-positions have been designed based on lead antimicrobial peptides. The cross-coupling involved the arylation of a resin-bound 5-bromohistidine with an arylboronic acid in solution under microwave irradiation. This protocol is compatible with common protecting groups used in peptide chemistry. The resulting biaryl linear undecapeptides were screened for their antibacterial, antifungal and hemolytic activities. The results showed that the presence of an imidazole ring significantly decreases the cytotoxicity.

3.1. INTRODUCTION

Antimicrobial peptides have attracted considerable attention as an alternative to traditional antibiotics for human, veterinary and plant disease control owing to their broad spectrum of activity, low intrinsic cytotoxicity and novel mode of action (Bulet et al., 2004; Huang, 2006; Jenssen et al., 2006; Montesinos, 2007; Marcos and Gandía, 2009). Unlike conventional antibiotics, it has been postulated that most of these peptides selectively disrupt cell membranes. The cationic nature of antimicrobial peptides and the ability to assume an amphipathic structure are responsible for this distinct mode of action. Moreover, several models have been proposed to account for the morphological changes in the membrane induced by antimicrobial peptides, such us pore formation, lysis or peptide translocation into the cytoplasm (Yeaman and Yount, 2003; Brogden, 2005; Bechinger and Lohner, 2006; Hancock and Sahl, 2006; Nicolas, 2009; Marcos and Gandía, 2009). On the basis of this mode of action, these peptides are unlikely to cause rapid emergence of resistance because it would require significant alteration of membrane composition, which would be difficult (Brogden, 2005; Yount and Yeaman, 2005; Peschel and Sahl, 2006).

Several methodologies have been described for the modification of peptides either in solution or in solid-phase (Kotha and Lahiri, 2001; Kotha et al., 2002; Kotha and Lahiri, 2003; Kotha and Lahiri, 2005; Nielsen et al., 2005; Haug et al., 2007; Doan et al., 2008; Kazmaier and Deska, 2008; Afonso et al., 2011). In particular, one strategy that has been used to improve the biological profile of antimicrobial peptides is the introduction in their sequence of biaryl amino acids, which may lead to peptidomimetics with restricted conformational flexibility, increased proteolytic stability, and enhanced selectivity and biological activity (Perdih and Dolenc, 2007; Haldar, 2008). In fact, biaryl amino acids are present in a wide variety of naturally occurring biaryl peptides that display important biological properties (Feliu and Planas, 2005). Among them, 5-arylhistidines have been described to be the central structures of cytotoxic and antifungal marine peptides, with the imidazole ring being the key element to its activity (Faulkner et al., 1993; Bewley et al., 1996; Tomson et al., 2002).

Despite their interest, a general strategy for the solid-phase synthesis of biaryl peptides containing 5-arylhistidines has not been reported. In fact, arylation of the 4(5)-position of an imidazole ring has proven challenging. Such strategy would benefit from the advantages inherent to solid-phase synthesis. It would represent a convergent and versatile approach for the preparation of biaryl linear compounds, because it would allow the preparation of a large diversity of biaryl peptides from a single 5-bromohistidine-containing peptide intermediate. Toward this end, we have recently established suitable conditions for the solid-phase arylation of a 5-bromohistidine residue through a microwave-assisted Suzuki-Miyaura cross-coupling with an arylboronic acid (Cerezo et al., 2008). This strategy allowed the preparation of biaryl peptides containing three and four residues with good purity.

During our current research into the development of new antimicrobial agents, we identified linear undecapeptides with high activity against the gram-negative bacteria *Erwinia amylovora*, *Xanthomonas axonopodis* pv. *vesicatoria*, and *Pseudomonas syringae* pv. *syringae*, and the fungi *Fusarium oxysporum* and *Penicillium expansum* (Ferre et al., 2006; Badosa et al., 2007; Badosa et al., 2009). The most active peptides also showed minimal cytotoxicity. In the present study, we decided to incorporate a 5-arylhistidine residue in the peptide sequence of the best analogues and study its influence on their biological activity profile. With this aim, we investigated whether our previous methodology for the preparation of short peptides bearing a 5-arylhistidine

residue is compatible with common protecting groups used in solid-phase peptide synthesis and whether it could be extended to the synthesis of longer peptide sequences. Herein, we report the feasibility of this methodology for the solid-phase synthesis of 5-arylhistidine-containing undecapeptides. We also describe the evaluation of their antimicrobial and hemolytic activities.

3.2. RESULTS AND DISCUSSION

3.2.1. Design of the 5-arylhistidine-containing undecapeptides

We designed undecapeptides containing a 5-arylhistidine residue at the 1- or 4-positions (Figure 3.1). Their structure was based on lead peptides selected from a 125-member library (Badosa et al., 2007; Badosa et al. 2009). In particular, FKLFKKILKFL-NH_2 (**BP66**) was chosen for its high antibacterial activity and served as a model for the synthesis of biaryl peptide analogues **BP281**-**BP283** bearing a 5-arylhistidine at the 1-position. These analogues differ at the aryl substituent on the histidine residue between a phenyl (**BP281**), a 3-hydroxyphenyl (**BP282**) or a 3-nitrophenyl (**BP283**) group.

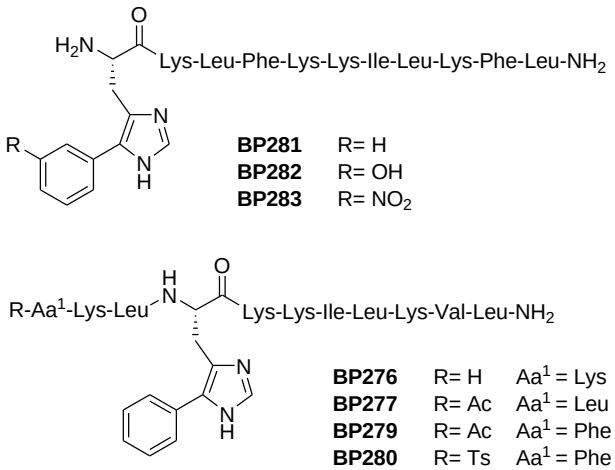

Figure 3.1. Structures of 5-arylhistidine-containing peptides.

The biaryl undecapeptides **BP276**, **BP277**, **BP279** and **BP280**, which incorporate a 5-arylhistidine at the 4-position, were designed from the sequence of the antifungal peptides KKLFKKILKVL-NH_2 (**BP15**), Ac-FKLFKKILKVL-NH_2 (**BP21**), Ts-FKLFKKILKVL-NH_2 (**BP22**), and Ac-LKLFKKILKVL-NH_2 (**BP34**). In these cases, the phenylalanine residue at the 4-position was replaced by a 5-phenylhistidine.

For comparison purposes, and based on the above lead undecapeptides, analogues **BP270**-**BP275**, **BP284**, **BP285**, **BP305**, and **BP306**, bearing a histidine residue at the 1-, 4- and/or 10-positions, were also designed (Table 3.1).

Table 3.1. Structures of the histidine-containing peptides.

Peptide	Sequence	t_R (min)[a]	Purity (%)[b]	ESI-MS $[M+H]^+$
BP270	KKLHKKILKVL-NH_2	5.87[c]	92	1346.7
BP271	Ac-LKLHKKILKVL-NH_2	6.32[c]	85	1373.7
BP272	Ac-HKLHKKILKVL-NH_2	5.98[c]	91	1397.8
BP273	Ac-FKLHKKILKVL-NH_2	6.46[c]	87	1407.6
BP274	Ts-HKLHKKILKVL-NH_2	6.17[c]	80	1509.7
BP275	Ts-FKLHKKILKVL-NH_2	6.78[c]	85	1519.7
BP284	HKLFKKILKFL-NH_2	17.16[d]	76	1413.6
BP285	FKLFKKILKHL-NH_2	17.03[d]	82	1413.7
BP305	HKLFKKILKHL-NH_2	6.02[c]	91	1404.1
BP306	HKLHKKILKHL-NH_2	5.63[c]	94	1394.1

[a] HPLC retention time. [b] Percentage determined by HPLC at 220 nm. [c] Conditions A (Experimental section). [d] Conditions B (Experimental section)

3.2.2. Synthesis of H-His(5-Ph)-Lys-Lys-Ile-Leu-Lys-Tyr-Leu-NH_2 (1)

Firstly, we investigated the compatibility of our methodology for the solid-phase synthesis of 5-arylhistidines with common protecting groups used in peptide chemistry. This strategy involves the microwave-assisted Suzuki-Miyaura reaction between a resin-bound 5-bromohistidine residue and an arylboronic acid. For this purpose, we chose the synthesis of the octapeptide H-His(5-Ph)-Lys-Lys-Ile-Leu-Lys-Tyr-Leu-NH_2 (**1**) as a model system (Scheme 3.1). Starting from a 9-fluorenylmethyloxycarbonyl-protected (Fmoc)-Rink-MBHA resin, we prepared the heptapeptidyl resin Fmoc-Lys(Boc)-Lys(Boc)-Ile-Leu-Lys(Boc)-Tyr(*t*Bu)-Leu-Rink-MBHA (**2**) following a Fmoc/*t*Bu strategy by sequential coupling and deprotection steps under standard conditions. After Fmoc removal, the regioisomeric mixture Boc-His(5-Br,1-SEM)-OH (**3a**) and Boc-His(5-Br,3-SEM)-OH (**3b**), obtained as previously reported (Cerezo et al., 2008), was coupled to the resulting resin affording the bromooctapeptidyl resin **4** as a mixture of two regioisomers (**4a** and **4b**). An aliquot of **4** was treated with trifluoroacetic acid (TFA)/CH_2Cl_2 and stirred for 3 h, providing H-His(5-Br)-Lys-Lys-Ile-Leu-Lys-Tyr-Leu-NH_2 (**5**), with HPLC purity of 99%.

The Suzuki-Miyaura reaction was initially attempted by treating **4** with $PhB(OH)_2$ (4 equiv.), $Pd_2(dba)_3$ (0.2 equiv.), KF (4 equiv.) and P(*o*-tolyl)$_3$ (0.4 equiv.) in 1,2-dimethoxyethane (DME)/EtOH/H_2O (9:9:2) under microwave irradiation at 140 ºC for 15 min (Scheme 3.1). After acidolytic cleavage, these conditions led to H-His(5-Ph)-Lys-Lys-Ile-Leu-Lys-Tyr-Leu-NH_2 (**1**; 56% purity) together with brominated peptide **5** (22% purity) and dehalogenated derivative H-His-Lys-Lys-Ile-Leu-Lys-Tyr-Leu-NH2 (**6**; 22% purity). The latter compound derives from the reductive dehalogenation of the bromohistidine residue of **4** which is reported to be a common side-reaction of Suzuki-Miyaura cross-couplings. When increasing the reaction time to 30 min, **6** was still detected (20%) but the purity of the expected biaryl peptide **1** was improved to 72%.

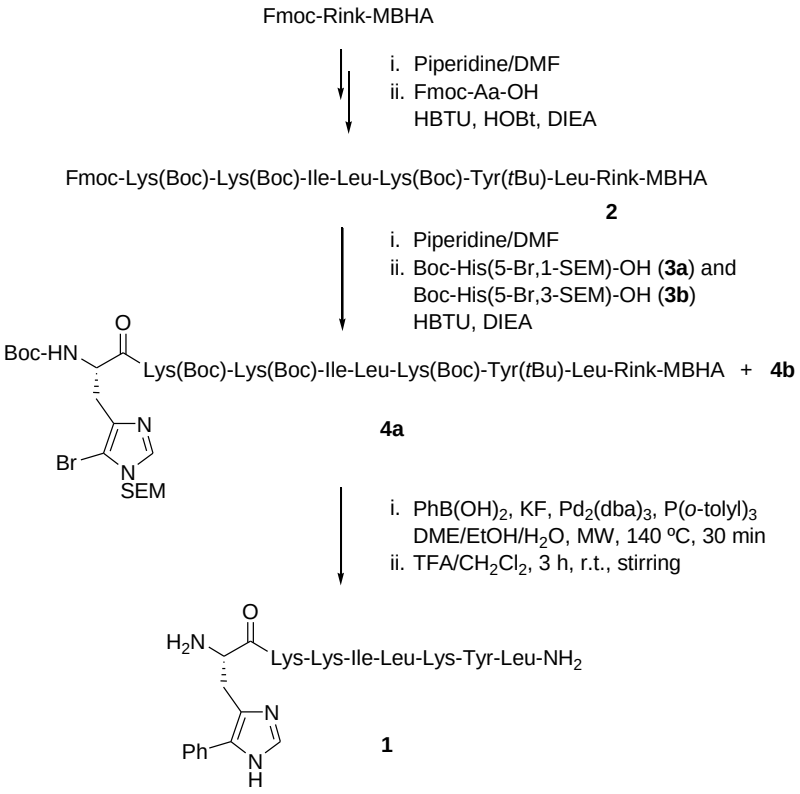

Scheme 3.1. Synthesis of the 5-phenylhistidine octapeptide **1**.

3.2.3. Synthesis of undecapeptides containing a 5-arylhistidine at the 1-position

We extended the above methodology to the synthesis of biaryl peptides **BP281**-**BP283** derived from the lead antibacterial peptide **BP66** (Scheme 3.2). Following a similar strategy to that described for **4**, we prepared the regioisomeric bromopeptidyl resins **7a** and **7b**. An aliquot of **7** was subjected to TFA/CH_2Cl_2 and stirred for 3 h to give H-His(5-Br)-Lys-Leu-Phe-Lys-Lys-Ile-Leu-Lys-Phe-Leu-NH_2 (**8**) with a purity of 82%.

The arylation of **7** with $PhB(OH)_2$ was first carried out under the conditions that gave the best result for the preparation of **1**. Microwave irradiation at 140 ºC for 30 min and subsequent acidolytic treatment resulted in H-His(5-Ph)-Lys-Leu-Phe-Lys-Lys-Ile-Leu-Lys-Phe-Leu-NH_2 (**BP281**) with a purity of only 9%. A decrease of the reaction time to 15 min did not significantly improve the results, and **BP281** was obtained with a purity of 12%. The use of SPhos instead of P(*o*-tolyl)$_3$ improved the purity of **BP281** to 37%. However, when the reaction was performed at 110 ºC for 30 min with P(*o*-tolyl)$_3$, the

purity of **BP281** increased to 72%. These conditions were applied to the arylation of **7** with 3-hydroxyphenylboronic acid and with 3-nitrophenylboronic acid. The cross-coupling reaction with 3-hydroxyphenylboronic acid led to the biaryl peptide **BP282** with a purity of 81%. In contrast, the reaction with 3-nitrophenylboronic acid was more difficult, and the corresponding biaryl peptide **BP283** was obtained with a purity of only 35%. The crude reaction mixture also proved to contain a 15-33% of the dehalogenated derivative H-His-Lys-Leu-Phe-Lys-Lys-Ile-Leu-Lys-Phe-Leu-NH_2 (**BP284**). Thus, according to our results, the presence of an electron-withdrawing group such as NO_2 hinders the cross-coupling. However, other studies showed that the electronic properties of the aromatic ring do not correlate with the reactivity of the boronic acid derivative (Doan et al., 2008; Cerezo et al., 2008).

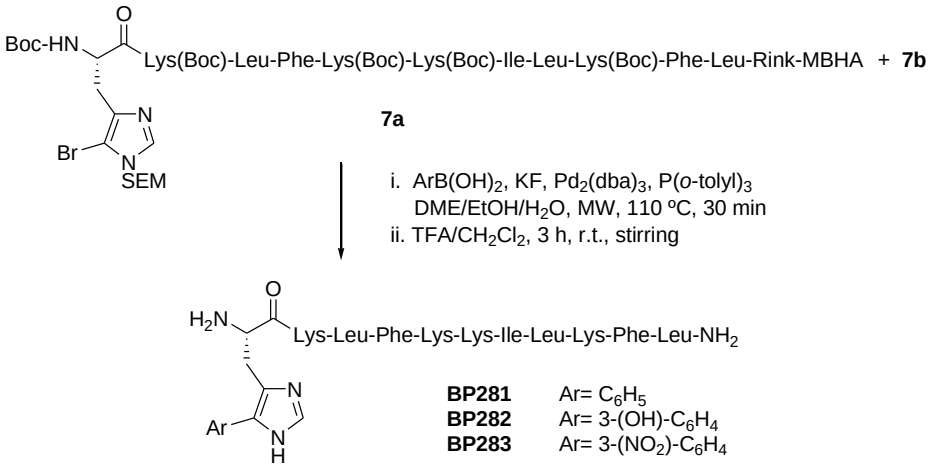

Scheme 3.2. Synthesis of **BP281**, **BP282**, and **BP283**.

3.2.4. Synthesis of undecapeptides containing a 5-phenylhistidine at the 4-position

Next, we studied the synthesis of the biaryl peptides **BP276**, **BP277**, **BP279**, and **BP280** that all contained a 5-phenylhistidine at the 4-position. The preparation of the corresponding bromopeptidyl resins following a Fmoc/*t*Bu strategy required the use of a 5-bromohistidine derivative protected with a Fmoc group at the N-terminus and with a 2-(trimethylsilyl)ethoxymethyl (SEM) group on the imidazole ring. The regioisomeric mixture Fmoc-His(5-Br,1-SEM)-OH (**9a**) and Fmoc-His(5-Br,3-SEM)-OH (**9b**) was prepared from commercially available Boc-His-OMe through bromination, introduction

of the SEM group, selective removal of the Boc group, methyl ester hydrolysis, and protection with the Fmoc group (Scheme 3.3). All reactions proceeded smoothly and the protected histidines **9** were fully characterized by NMR and mass spectrometry.

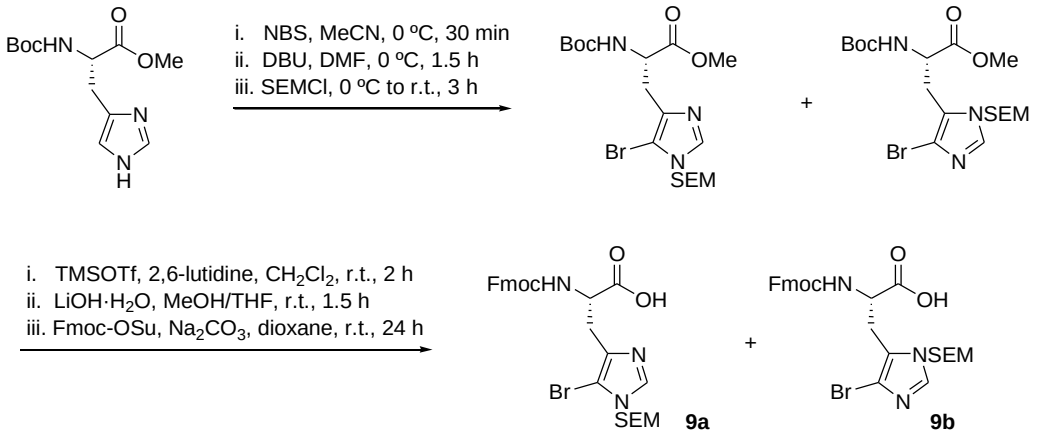

Scheme 3.3. Synthesis of Fmoc-His(5-Br,1-SEM)-OH (**9a**) and Fmoc-His(5-Br,3-SEM)-OH (**9b**).

We first attempted the synthesis of **BP276** starting from a Fmoc-Rink-MBHA resin. The regioisomeric peptidyl resins Fmoc-Lys(Boc)-Lys(Boc)-Leu-His(5-Br,1-SEM)-Lys(Boc)-Lys(Boc)-Ile-Leu-Lys(Boc)-Val-Leu-Rink-MBHA and Fmoc-Lys(Boc)-Lys(Boc)-Leu-His(5-Br,3-SEM)-Lys(Boc)-Lys(Boc)-Ile-Leu-Lys(Boc)-Val-Leu-Rink-MBHA were prepared by sequential Fmoc group removal and amino acid coupling steps. The Fmoc group was removed by treatment with piperidine/*N*,*N*-dimethylformamide (DMF), and the amino acid couplings were mediated by *N*,*N'*-diisopropylcarbodiimide (DIPCDI) and ethyl 2-cyano-2-(hydroxyimino)acetate (Oxyma), except for the bromohistidines **9** that were incorporated with 1-[(1-(cyano-2-ethoxy-2-oxoethylideneaminooxy)-dimethylamino-morpholinomethylene)]methanaminium hexafluorophosphate (COMU), Oxyma and *N*,*N*-diisopropylethylamine (DIEA). An aliquot of these resins was subjected to TFA/H_2O/triisopropylsilane (TIS) and stirred for 3 h, yielding Fmoc-Lys-Lys-Leu-His(5-Br)-Lys-Lys-Ile-Leu-Lys-Val-Leu-NH_2 with a purity of 78%. Next, we investigated replacing the Fmoc group for a trityl to overcome its instability under the conditions of the Suzuki-Miyaura cross-coupling. The Fmoc group was removed and the resulting resin was treated with trityl chloride (TrCl; 10 equiv.) and DIEA (10 equiv.) in *N*-methyl-2-pyrrolidone (NMP) for 4 h. This reaction proved difficult and eight treatments were required for a negative Kaiser test (Kaiser et al., 1970).

Cleavage of the final resin afforded H-Lys-Lys-Leu-His(5-Br)-Lys-Lys-Ile-Leu-Lys-Val-Leu-NH_2 with a purity of 73%.

This result was improved using a ChemMatrix resin (Scheme 3.4). Following a similar strategy, the regioisomeric peptidyl resins **10** were prepared and an aliquot was cleaved providing Fmoc-Lys-Lys-Leu-His(5-Br)-Lys-Lys-Ile-Leu-Lys-Val-Leu-NH_2 with a purity of 90%. Next, the N-terminal Fmoc group of **10** was replaced by a trityl group. The incorporation of this group was easier than when MBHA resin was used, only three treatments with TrCl (10 equiv.) and DIEA (10 equiv.) in NMP for 4 h were required. An aliquot of the resulting resins **11** were treated with TFA/H_2O/TIS under stirring for 3 h, and H-Lys-Lys-Leu-His(5-Br)-Lys-Lys-Ile-Leu-Lys-Val-Leu-NH_2 was obtained with a purity of 82%.

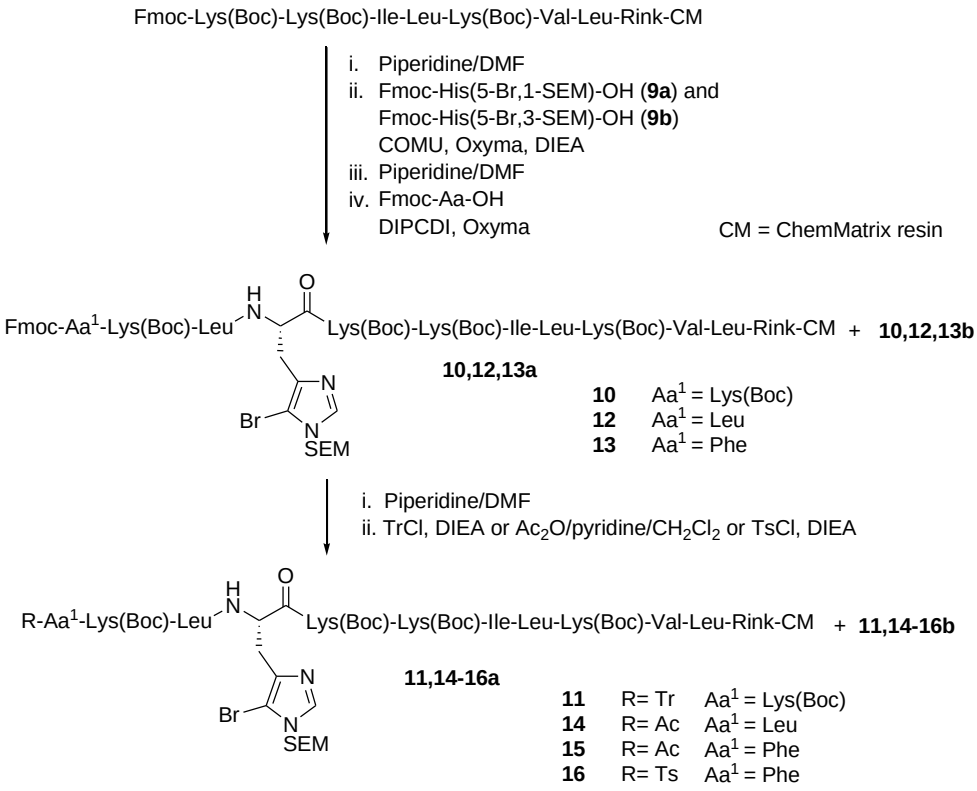

Scheme 3.4. Synthesis of 5-bromopeptidyl resins **11** and **14-16**.

Given the good results obtained, bromopeptidyl resins **12** and **13** were prepared following the same protocol. Fmoc removal of resins **12** followed by acetylation with

Ac_2O/pyridine/CH_2Cl_2, afforded resins **14**, which after cleavage of an aliquot, led to Ac-Leu-Lys-Leu-His(5-Br)-Lys-Lys-Ile-Leu-Lys-Val-Leu-NH_2 with a purity of 77%. Resins **13** were deprotected and then either acetylated, providing resins **15**, or tosylated with *para*-toluenesulfonyl chloride (TsCl) and DIEA to give resins **16**. Acidolytic cleavage of aliquots of **15** and **16** furnished the bromopeptides Ac-Phe-Lys-Leu-His(5-Br)-Lys-Lys-Ile-Leu-Lys-Val-Leu-NH_2 and Ts-Phe-Lys-Leu-His(5-Br)-Lys-Lys-Ile-Leu-Lys-Val-Leu-NH_2 with purities of 77 and 86%, respectively.

Resins **11** were arylated with $PhB(OH)_2$ (4 equiv.), $Pd_2(dba)_3$ (0.2 equiv.), KF (4 equiv.) and P(*o*-tolyl)$_3$ (0.4 equiv.) in DME/EtOH/H_2O (9:9:2) under microwave irradiation at 110 ºC for 30 min (Scheme 3.5). The resulting resin was cleaved and HPLC and ESI-MS analysis of the crude reaction mixture revealed the presence of starting material. When the arylation was carried out with SPhos, HPLC analysis showed one broad peak. Analysis by ESI-MS revealed the formation of the expected biaryl peptide **BP276** together with the dehalogenated peptide H-Lys-Lys-Leu-His-Lys-Lys-Ile-Leu-Lys-Val-Leu-NH_2 (**BP270**) in a 4:3 ratio, and other compounds that could not be identified. Performing the arylation at higher temperature, 140 ºC for 30 min, slightly improved the results. Two major peaks were observed by HPLC and **BP276** and **BP270** were detected by ESI-MS in a 4:3 ratio. **BP276** was isolated by reverse-phase column chromatography and obtained with a purity of 95%.

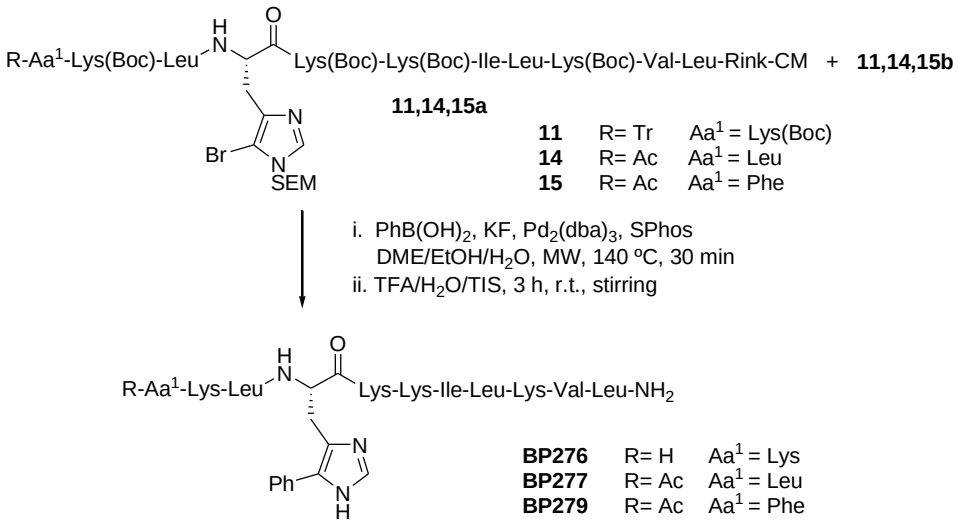

Scheme 3.5. Synthesis of **BP276**, **BP277**, and **BP279**.

These reaction conditions were applied to the arylation of resins **14** and **15**. After cleavage, ESI-MS analysis showed the presence of the expected biaryl peptides **BP277** and **BP279**, respectively. In both cases, these biaryl peptides were also obtained along with the corresponding dehalogenated compound Ac-Leu-Lys-Leu-His-Lys-Lys-Ile-Leu-Lys-Val-Leu-NH_2 (**BP271**) or Ac-Phe-Lys-Leu-His-Lys-Lys-Ile-Leu-Lys-Val-Leu-NH_2 (**BP273**) in a 4:3 ratio. **BP277** was isolated by reverse-phase column chromatography and obtained with a purity of 95%.

In contrast, arylation of resins **16** did not afford the biaryl peptide **BP280**. In this case, the dehalogenated peptide Ts-Phe-Lys-Leu-His-Lys-Lys-Ile-Leu-Lys-Val-Leu-NH_2 (**BP275**) was the major product. This result was attributed to the N-terminal tosyl group of the bromopeptidyl resins **16**. Thus, we decided to carry out the arylation step before the tosylation step. For this reason, bromopeptidyl resins **13** were transformed into the N-terminal tritylated bromopeptidyl resins **17**, which were subjected to arylation with $PhB(OH)_2$ (Scheme 3.6). The crude reaction mixture proved to contain biaryl peptide H-Phe-Lys-Leu-His(5-Ph)-Lys-Lys-Ile-Leu-Lys-Val-Leu-NH_2 and the dehalogenated compound H-Phe-Lys-Leu-His-Lys-Lys-Ile-Leu-Lys-Val-Leu-NH_2 in a 4:3 ratio. Selective trityl group removal of **17** with TFA/H_2O/CH_2Cl_2 (0.2:1:98.8), followed by tosylation and cleavage afforded **BP280** and Ts-Phe-Lys-Leu-His-Lys-Lys-Ile-Leu-Lys-Val-Leu-NH_2 (**BP275**) in a 4:3 ratio.

Relative to the arylation of peptides containing a 5-bromohistidine residue at the 1-position, the synthesis of **BP276**, **BP277** and **BP279** revealed that arylation at the 4-position is more difficult, as shown by the formation of the dehalogenated byproduct. This result could be attributed to the fact that the 5-bromohistidine residue in peptidyl resins **11**, **14**, and **15** is located at a less accessible position than in **7**.

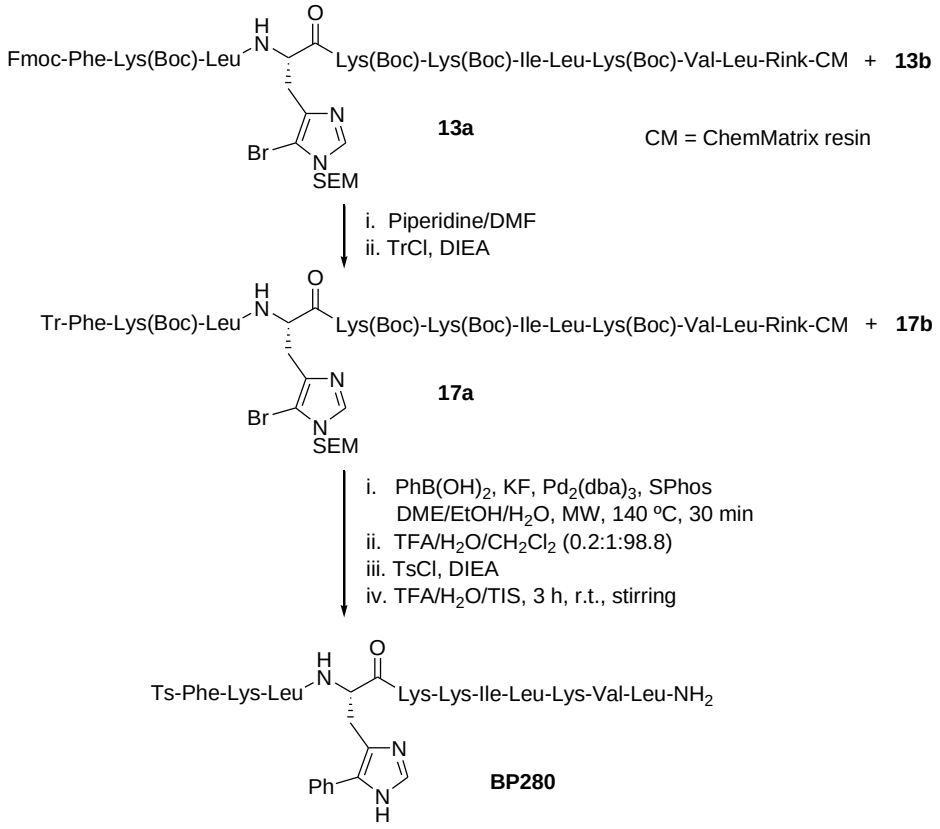

Scheme 3.6. Synthesis of **BP280**.

3.2.5. Synthesis of peptides containing histidine residues

For comparison purposes, histidine-containing peptides **BP270**-**BP275**, **BP284**, **BP285**, **BP305** and **BP306** were prepared by the solid-phase method using Fmoc-type chemistry on a Fmoc-Rink-MBHA resin (Table 3.1). Coupling of the Fmoc-amino acids were mediated by DIPCDI and Oxyma in DMF. The Fmoc group was removed by treating the resin with a mixture of piperidine/DMF. Once the chain assembly was completed, the N-terminal Fmoc group was removed and the resulting resin was cleaved with TFA/H_2O/TIS for 2 h or subjected to N-terminus derivatization. Acetylation was performed by treatment with Ac_2O/pyridine/CH_2Cl_2, and tosylation was carried out by treatment with TsCl and DIEA. Following the derivatization step, peptides were released from the resin. All compounds synthesized were obtained in good purities, 74-99% as determined by HPLC. ESI-MS was used to confirm peptide identity.

3.2.6. Biological activity

Peptides synthesized were screened for their antimicrobial activity against *E. amylovora*, *X. axonopodis* pv. vesicatoria, P. syringae pv. syringae, F. oxysporum and *P. expansum*. In general, *E. amylovora* and *P. expansum* were the least sensitive pathogens to these peptides. Against *X. axonopodis* pv. *vesicatoria*, *P. syringae* pv. syringae, and *F. oxysporum*, most peptides exhibited an antimicrobial activity ranging from 3.1 to 25 μM (Table 3.2). Moreover, **BP281**, **BP284**, and **BP305** showed a MIC <3.1 μM against *F. oxysporum*, being more active than the parent peptide **BP66**. Among the peptides bearing a histidine residue, **BP275** was the most active, with MIC values of 3.1 to 6.2 μM against *F. oxysporum*, *X. axonopodis* pv. *vesicatoria*, and *P. syringae* pv. *syringae*, with the activity against the latter higher than that of the parent peptide **BP22**. Results showed that the arylation of the histidine residue do not significantly influence the antimicrobial activity and both arylated and non-arylated peptides displayed similar activity. Moreover, we did not observe differences between the antimicrobial activity of the purified and non-purified samples of peptides **BP276** and **BP277**. Therefore, we decided to test **BP279** and **BP280** as mixtures. These samples together with **BP281** and **BP282** were the 5-arylhistidine-containing peptides that displayed the highest antimicrobial activity.

Interestingly, substitution of a phenylalanine by a histidine or a 5-arylhistidine resulted in a significant decrease in hemolytic activity. These results are in good agreement with previous studies on antimicrobial peptides reporting that an increase of the peptide hydrophilicity is related to a decrease of the cytotoxicity (Blondelle and Lohner, 2000; Oh et al., 2000; Ferre et al., 2006; Badosa et al., 2007; Badosa et al., 2009). Thus, peptides incorporating a histidine residue were low hemolytic, 0-26% at 150 μM. Notably, the most active peptide **BP275** only showed a hemolysis of 4% at this concentration, being much lower than that of the parent peptide **BP22** (73%). Even though the arylation of the imidazole ring increased the cytotoxicity, the 5-arylhistidine-containing peptides were less hemolytic (25-55%) than the corresponding phenylalanine analogues (16-85%), except for **BP276** that showed similar hemolysis than **BP15**. These results suggest that the imidazole ring of histidine confers to peptides a higher hydrophilicity than the benzene ring of phenylalanine. Therefore, despite the introduction of a histidine or a 5-arylhistidine does not improve the antimicrobial activity, this modification leads to significantly less cytotoxic peptides.

Table 3.2. Antimicrobial activity (MIC) and cytotoxicity of histidine- and 5-arylhistidine-containing peptides, and of the corresponding parent peptides

Peptide	MIC (μM)					Hemolysis[a] (%)
	Ea[b]	*Pss*[b]	*Xav*[b]	*Fo*[b]	*Pe*[b]	150 μM
BP15 (KKLFKKILKVL-NH_2)	3.1-6.2	3.1-6.2	12.5-25	<3.1	12.5-25	16 ± 2.9
BP270	>50	12.5-25	>50	6.2-12.5	>50	0 ± 1.1
BP276	25-50	6.2-12.5	12.5-25	6.2-12.5	>50	19 ± 2.4
BP21 (Ac-FKLFKKILKVL-NH_2)	6.2-12.5	6.2-12.5	3.1-6.2	3.1-6.2	<6.2	85 ± 1.4
BP272	>50	12.5-25	>50	6.2-12.5	>50	0 ± 0.1
BP273	>50	12.5-25	25-50	6.2-12.5	>50	0 ± 0.5
BP279	12.5-25	12.5-25	3.1-6.2	3.1-6.2	>50	25 ± 0.2
BP22 (Ts-FKLFKKILKVL-NH_2)	6.2-12.5	6.2-12.5	3.1-6.2	3.1-6.2	6.2-12.5	73 ± 1.5
BP274	25-50	6.2-12.5	6.2-12.5	3.1-6.2	>50	0 ± 0.1
BP275	12.5-25	3.1-6.2	3.1-6.2	3.1-6.2	>50	4 ± 1.3
BP280	12.5-25	12.5-25	3.1-6.2	6.2-12.5	>50	43 ± 2.1
BP34 (Ac-LKLFKKILKVL-NH_2)	6.2-12.5	6.2-12.5	3.1-6.2	3.1-6.2	<6.2	45 ± 2.8
BP271	>50	12.5-25	>50	12.5-25	>50	0 ± 0.3
BP277	>25	>25	>25	6.2-12.5	>50	0 ± 0.1
BP66 (FKLFKKILKFL-NH_2)	6.2-12.5	3.1-6.2	3.1-6.2	3.1-6.2	25-50	63 ± 5.9
BP284	6.2-12.5	6.2-12.5	6.2-12.5	<3.1	25-50	16 ± 5.4
BP285	>25	>25	>50	3.1-6.2	>50	26 ± 0.8
BP305	>25	12.5-25	12.5-25	<3.1	>50	0 ± 0.2
BP306	>25	>25	>50	6.2-12.5	>50	0 ± 0.3
BP281	6.2-12.5	6.2-12.5	3.1-6.2	<3.1	25-50	54 ± 8.5
BP282	6.2-12.5	6.2-12.5	3.1-6.2	3.1-6.2	>50	55 ± 4.6

[a] Percentage hemolysis plus confidence interval. [b] *Ea*, *Erwinia amylovora*; *Pss*, *Pseudomonas syringae* pv. *syringae*; *Xav*, *Xanthomonas axonopodis* pv. *vesicatoria*; *Fo*, *Fusarium oxysporum*; *Pe*, *Penicillium expansum*.

3.3. CONCLUSIONS

In summary, we have established the viability of the solid-phase Suzuki-Miyaura reaction for the synthesis of 5-arylhistidine undecapeptides. This work shows that the Suzuki-Miyaura reaction can be applied to the cross-coupling of a resin bound 5-bromohistidine residue, either at the 1- or 4-position, with an arylboronic acid. Moreover, this work constitutes the first example of a solid-phase Suzuki-Miyaura cross-coupling for the formation of long biaryl linear peptides containing a 5-arylhistidine. These biaryl peptides displayed antibacterial and antifungal activity and were low hemolytic. This low cytotoxicity has been attributed to the presence of the imidazole ring of histidine. We expect that this methodology could be useful for the development of new antimicrobial agents.

3.4. EXPERIMENTAL SECTION

3.4.1. General methods

Manual peptide synthesis was performed in polypropylene syringes fitted with a polyethylene porous disk. Solvents and soluble reagents were removed in vacuo. Most chemicals were purchased from commercial suppliers Sigma–Aldrich, Fluka, NovaBiochem (Schwalbach, Germany), Iris Biotech GmbH (Marktredwitz, Germany), Scharlab (Sentmenat, Spain), Merck (Mollet del Vallès, Spain) or Panreac (Castellar del Vallès, Spain) and used without further purification.

Peptides were analyzed under standard analytical HPLC conditions with a Dionex liquid chromatography instrument composed of an UV/Vis Dionex UVD170U detector, a P680 Dionex bomb, an ASI-100 Dionex automatic injector, and CHROMELEON 6.60 software. Detection was performed at 220 nm. Solvent A was 0.1% aq. TFA and solvent B was 0.1% TFA in MeCN. Conditions A: Analysis was carried out with a Kromasil 100 C_{18} (4.6 mm × 40 mm, 3.5 μm) column with a 2–100% B over 7 min at a flow rate of 1 mL/min. Conditions B: Analysis was carried out with a Kromasil 100 C_{18} (4.6 mm × 250 mm, 3.5 μm) column with a 2–100% B over 30 min at a flow rate of 1 mL/min.

Flash chromatography purifications were performed on C_{18}-reversed phase silica gel 100 not endcapped (230-400 mesh, Fluka).

ESI-MS analyses were performed with an Esquire 6000 ESI ion Trap LC/MS (Bruker Daltonics) instrument equipped with an electrospray ion source. The instrument was operated in the positive ESI(+) ion mode. Samples (5 μL) were introduced into the mass spectrometer ion source directly through an HPLC autosampler. The mobile phase (80:20 MeCN/H_2O at a flow rate of 100 μL/min) was delivered by a 1100 Series HPLC pump (Agilent). Nitrogen was employed as both the drying and nebulising gas. HRMS were recorded under conditions of ESI with a Bruker MicroTof-Q instrument with a hybrid quadrupole time-of-flight mass spectrometer (University of Zaragoza). Samples were introduced into the mass spectrometer ion source directly through a 1100 Series Agilent HPLC autosampler and were externally calibrated using sodium formate. The instrument was operated in the positive ESI(+) ion mode.

^{1}H and ^{13}C NMR spectra were measured with a Bruker 300 or 400 MHz NMR spectrometer. Chemical shifts were reported as δ values (ppm) directly referenced to the solvent signal.

Microwave-assisted reactions were performed with an Ethos SEL labstation microwave (Milestone) equipped with a dual magnetron (1600 W). The time, temperature, and power were controlled with the EasyControl software. The temperature was monitored through the ATC-400FO Automatic Fiber Optic Temperature Control System immersed in a standard Milestone reference vessel. This equipment regulates the power to achieve and maintain the selected temperature.

3.4.2. Synthesis of amino acids

Methyl 5-bromo-*N*(τ)-[2-(trimethylsilyl)ethoxymethyl]-L-histidinate and methyl 5-bromo-*N*(π)-[2-(trimethylsilyl)ethoxymethyl]-L-histidinate: Trimethylsilyl trifluoromethanesulfonate (TMSOTf) (2.27 mL, 12.54 mmol) and 2,6-lutidine (1.95 mL, 16.72 mmol) were added to a solution of Boc-His(5-Br,1-SEM)-OMe and Boc-His(5-Br,3-SEM)-OMe (Cerezo et al., 2008) (2.0 g, 4.18 mmol) in CH_2Cl_2 (48 mL). The reaction mixture was stirred at room temperature for 2 h. Then, citric acid (10%, 50 mL) was added and the product was extracted with CH_2Cl_2 (3×50 mL). The organic layers were combined, washed with brine (50 mL), and dried over anhydrous magnesium sulphate. Removal of the solvent yielded H-His(5-Br,1-SEM)-OMe and H-His(5-Br,3-SEM)-OMe as a colorless oil (1.36 g, 86% yield). t_R 7.22 and 7.52 min (conditions A). ^{1}H NMR (400 MHz, [D_6]DMSO): δ = 0.07 [s, 9 H, $(CH_3)_3Si$], 0.92-0.96 (m, 2 H, CH_2Si), 3.08 (dd, *J* = 6.8 and 15.4 Hz, 1 H, CH_2-β), 3.14 (dd, *J* = 5.8 and 15.4 Hz, 1 H, CH_2-β), 3.56-3.60 (m, 2 H, OCH_2), 3.73 (s, 0.75 H, OCH_3), 3.76 (s, 2.25 H, OCH_3), 4.37 (t, *J* = 6.4 Hz, 1 H, CH-α), 5.40 (s, 1.5 H, NCH_2O), 5.49 (s, 0.5 H, NCH_2O), 7.99 (s, 0.25 H, CH-2_{imid}), 8.15 (s, 0.75 H, CH-2_{imid}), 8.64 (br. s, 3 H, NH_2) ppm. MS (ESI): *m/z* = 378.0, 380.0 $[M + H]^+$.

5-Bromo-*N*(τ)-[2-(trimethylsilyl)ethoxymethyl]-L-histidine and 5-bromo-*N*(π)-[2-(trimethylsilyl)ethoxymethyl]-L-histidine: An aqueous solution of LiOH (6.5 mL, 10.31 mmol) was added to a solution of H-His(5-Br,1-SEM)-OMe and H-His(5-Br,3-SEM)-OMe (1.3 g, 3.44 mmol) in MeOH/THF (1:1, 13 mL). The reaction mixture was stirred at room temperature for 1.5 h. After this time, the organic solvents were evaporated under reduced pressure and water (25 mL) was added to the resulting residue. The solution was adjusted to pH 6 by addition of glacial AcOH and lyophilized to afford H-His(5-Br,1-SEM)-OH and H-His(5-Br,3-SEM)-OH as a white solid (0.93 g, 75% yield). t_R 6.50 and 6.67 min (conditions A). ^{1}H NMR (400 MHz, [D_6]DMSO): δ = 0.06 [s, 9 H, $(CH_3)_3Si$], 0.91-0.96 (m, 2 H, CH_2Si), 3.06 (dd, *J* = 3.2 and 14.8 Hz, 1 H, CH_2-β), 3.12 (dd, *J* = 4.8 and 14.8 Hz, 1 H, CH_2-β), 3.59-3.61 (m, 2 H, OCH_2), 5.38 (s, 2 H, NCH_2O), 7.81 (s, 0.25 H, CH-2_{imid}), 8.08 (s, 0.75 H, CH-2_{imid}) ppm. MS (ESI): *m/z* 364.1, 366.1 $[M + H]^+$, 370.1, 372.1 $[M + Li]^+$.

5-Bromo-*N*(α)-(9-fluorenylmethyloxycarbonyl)-*N*(τ)-[2-(trimethylsilyl)ethoxymethyl]-L-histidine (9a) and 5-bromo-*N*(α)-(9-fluorenylmethyloxycarbonyl)-*N*(π)-[2-(trimethylsilyl)ethoxymethyl]-L-histidine (9b): A solution of H-His(5-Br,1-SEM)-OH and H-His(5-Br,3-SEM)-OH (0.89 g, 2.44 mmol) in dioxane (9 mL) was neutralized to pH 7-8 by addition of Na_2CO_3 (10%). The reaction mixture was stirred at room temperature for 30 min. After this time, Fmoc-OSu (0.87 g, 2.57 mmol) was added and the mixture was stirred for 24 h at room temperature. The reaction mixture was then concentrated in vacuo, water (30 mL) was added, and the product was extracted with EtOAc (3×30 mL). The organic layers were combined, washed with brine (30 mL), and dried over anhydrous magnesium sulfate. Removal of the solvent followed by digestion of the resulting precipitate in pentane (20 mL) for 3 h afforded a white solid, which was purified by column chromatography. Elution with CH_2Cl_2/MeOH (98:2) gave Fmoc-His(5-Br,1-SEM)-OH (**9a**) and Fmoc-His(5-Br,3-SEM)-OH (**9b**) as a white solid (0.87 g, 61% yield). t_R 8.52 and 8.81 min (conditions A). ^{1}H NMR (400 MHz, $CDCl_3$): δ = -0.01 (s, 9 H, $(CH_3)_3Si$), 0.88-0.93 (m, 2 H, CH_2Si), 3.17-3.30 (m, 2H, CH_2-β), 3.49-3.55 (m, 2 H, OCH_2), 4.22 (t, *J* = 6.8 Hz, 1 H, CH-Fmoc), 4.42-4.46 (m, 2H, CH_2-Fmoc), 4.60-4.61 (m, 1H, CH-α), 5.24-5.28 (m, 2 H, NCH_2O), 5.77 (br. s, 1 H, CONH), 7.31 (t, *J* = 7.2 Hz, 2 H, CH-2_{arom}, CH-7_{arom}), 7.40 (t, *J* = 7.2 Hz, 2 H, CH-3_{arom} and CH-6_{arom}), 7.62 (d, *J* = 7.2 Hz, 2 H, CH-1_{arom}, CH-8_{arom}), 7.77 (d, *J* = 7.2 Hz, 2 H, CH-4_{arom}, CH-5_{arom}), 7.86 (s, 1 H, CH-2_{imid}) ppm. MS (ESI): *m/z* = 586.1, 588.1 $[M + H]^+$.

3.4.3. Synthesis of peptides containing a 5-arylhistidine at the 1-position

Boc-His(5-Br,1-SEM)-Lys(Boc)-Lys(Boc)-Ile-Leu-Lys(Boc)-Tyr(*t*Bu)-Leu-Rink-MBHA (4a) and Boc-His(5-Br,3-SEM)-Lys(Boc)-Lys(Boc)-Ile-Leu-Lys(Boc)-Tyr(*t*Bu)-Leu-Rink-MBHA (4b): The bromopeptidyl resins **4a** and **4b** were synthesized manually by the solid-phase method by using standard Fmoc chemistry. Fmoc-Rink-MBHA resin (0.64 mmol/g) was used as solid support. Couplings of Fmoc amino acids were carried out as follows: Fmoc-Aa-OH (4 equiv.) was dissolved in DMF and preactivated for 5 min with *O*-(benzotriazol-1-yl)-*N*,*N*,*N'*,*N'*-tetramethyluronium hexafluorophosphate (HBTU) (3.8 equiv.), *N*-hydroxybenzotriazole (HOBt) (4 equiv.)

and DIEA (7.8 equiv.). The mixture was added to the resin and shaken for 1 h at room temperature. Coupling of Boc-His(5-Br,1-SEM)-OH (**3a**) and Boc-His(5-Br,3-SEM)-OH (**3b**) (Cerezo et al., 2008) (3 equiv.) was performed with HBTU (3 equiv.) and DIEA (3 equiv.) in DMF whilst stirring for 3 h at room temperature. The completion of the reaction was checked by the Kaiser test (Kaiser et al., 1970). The Fmoc group was removed by treating the resin with a mixture of piperidine/DMF (3:7, 1×3 and 1×7 min). After each coupling and deprotection step, the resin was washed with DMF (3×1 min), MeOH (1×1 min) and CH_2Cl_2 (3×1 min), and air dried. An aliquot of the resulting resins **4a** and **4b** was cleaved with TFA/H_2O/TIS (95:2.5:2.5) whilst stirring for 3 h at room temperature. Following TFA evaporation and diethyl ether extraction, the crude peptide was dissolved in H_2O and lyophilized to afford H-His(5-Br)-Lys-Lys-Ile-Leu-Lys-Tyr-Leu-NH_2 (**5**) (99% purity). t_R 5.89 min (conditions A); MS (ESI): *m/z* = 560.3, 561.4 $[M + 2H]^{2+}$, 1119.6, 1121.6 $[M + H]^+$, 1141.5, 1143.4 $[M+Na]^+$.

Boc-His(5-Br,1-SEM)-Lys(Boc)-Leu-Phe-Lys(Boc)-Lys(Boc)-Ile-Leu-Lys(Boc)-Phe-Leu-Rink-MBHA (7a) and Boc-His(5-Br,3-SEM)-Lys(Boc)-Leu-Phe-Lys(Boc)-Lys(Boc)-Ile-Leu-Lys(Boc)-Phe-Leu-Rink-MBHA (7b): The 5-bromoundecapeptidyl resins **7a** and **7b** were prepared following the same procedure described for **4a** and **4b**. Cleavage of an aliquot of the resulting bromoundecapeptidyl resins **7** by using TFA/H_2O/TIS (95:2.5:2.5) whilst stirring for 3 h at room temperature, followed by TFA evaporation and diethyl ether extraction afforded H-His(5-Br)-Lys-Leu-Phe-Lys-Lys-Ile-Leu-Lys-Phe-Leu-NH_2 (**8**, 82% purity). t_R 6.63 min (conditions A). MS (ESI): m/z = 746.3, 747.3 $[M + 2H]^{2+}$, 1491.6, 1493.6 $[M + H]^+$.

General method for the arylation of bromopeptidyl resins 4 and 7 by using a microwave-assisted solid-phase Suzuki-Miyaura reaction

A 10 mL reaction vessel containing a magnetic stir bar was charged with the corresponding bromopeptidyl resins (50 mg), which was first swelled in a degassed mixture of DME/EtOH/H_2O (9:9:2, 1.2 mL) for 15 min under nitrogen. Then, $Pd_2(dba)_3$ (0.2 equiv.), P(*o*-tolyl)$_3$ (0.4 equiv.), KF (4 equiv.) and the corresponding boronic acid (4 equiv.) were added. The sealed vial was heated under nitrogen in the microwave labstation. A microwave ramp (600 W maximum) was applied for 5 min to reach the reaction temperature. The reaction mixture was irradiated at this temperature for 30 min. After the reaction time, upon cooling, the solvent was removed and the resin was washed with DMF (3×1 min), EtOH (3×1 min), CH_2Cl_2 (3×1 min) and diethyl ether (3×1 min). The biaryl peptides were released from the solid support by treatment with TFA/CH_2Cl_2 (95:5) whilst stirring for 3 h at room temperature. Following TFA evaporation and diethyl ether extraction, the crude peptides were dissolved in H_2O and lyophilized.

H-His(5-Ph)-Lys-Lys-Ile-Leu-Lys-Tyr-Leu-NH_2 (1): Starting from resin Boc-His(5-Br,1-SEM)-Lys(Boc)-Lys(Boc)-Ile-Leu-Lys(Boc)-Tyr(*t*Bu)-Leu-Rink-MBHA (**4a**) and Boc-His(5-Br,3-SEM)-Lys(Boc)-Lys(Boc)-Ile-Leu-Lys(Boc)-Tyr(*t*Bu)-Leu-Rink-MBHA (**4b**), Suzuki-Miyaura reaction with phenylboronic acid at 140 ºC, followed by acidolytic cleavage afforded the biaryl linear peptide **1** (72% purity). t_R 16.09 min (conditions B); MS (ESI): *m/z* = 559.34 $[M + 2H]^{2+}$, 1041.61 $[M - C_6H_5 + H]^+$, 1117.62 $[M + H]^+$.

H-His(5-Ph)-Lys-Leu-Phe-Lys-Lys-Ile-Leu-Lys-Phe-Leu-NH_2 (BP281): Starting from resin Boc-His(5-Br,1-SEM)-Lys(Boc)-Leu-Phe-Lys(Boc)-Lys(Boc)-Ile-Leu-Lys(Boc)-Phe-Leu-Rink-MBHA (**7a**) and Boc-His(5-Br,3-SEM)-Lys(Boc)-Leu-Phe-Lys(Boc)-Lys(Boc)-Ile-Leu-Lys(Boc)-Phe-Leu-Rink-MBHA (**7b**), Suzuki-Miyaura reaction with phenylboronic acid at 110 ºC, followed by acidolytic cleavage afforded the biaryl linear peptide **BP281** (72% purity). t_R 17.70 min (conditions B). MS (ESI): *m/z* = 745.9 $[M + 2H]^{2+}$, 1490.2 $[M + H]^+$, 1512.2 $[M + Na]^+$.

Biaryl peptide BP282: Starting from resin Boc-His(5-Br,1-SEM)-Lys(Boc)-Leu-Phe-Lys(Boc)-Lys(Boc)-Ile-Leu-Lys(Boc)-Phe-Leu-Rink-MBHA (**7a**) and Boc-His(5-Br,3-SEM)-Lys(Boc)-Leu-Phe-Lys(Boc)-Lys(Boc)-Ile-Leu-Lys(Boc)-Phe-Leu-Rink-MBHA (**7b**), Suzuki-Miyaura reaction with 3-hydroxyphenylboronic acid at 110 ºC, followed by acidolytic cleavage afforded the biaryl linear peptide **BP282** (81% purity). t_R 17.44 min (conditions B). MS (ESI): *m/z* = 753.4 $[M + 2H]^{2+}$, 1505.8 $[M + H]^{+}$, 1527.8 $[M + Na]^{+}$.

Biaryl peptide BP283: Starting from resin Boc-His(5-Br,1-SEM)-Lys(Boc)-Leu-Phe-Lys(Boc)-Lys(Boc)-Ile-Leu-Lys(Boc)-Phe-Leu-Rink-MBHA (**7a**) and Boc-His(5-Br,3-SEM)-Lys(Boc)-Leu-Phe-Lys(Boc)-Lys(Boc)-Ile-Leu-Lys(Boc)-Phe-Leu-Rink-MBHA (**7b**), Suzuki-Miyaura reaction with 3-nitrophenylboronic acid at 110 ºC, followed by acidolytic cleavage afforded the biaryl linear peptide **BP283** (35% purity). t_R 17.98 min (conditions B). MS (ESI): *m/z* = 767.9 $[M + 2H]^{2+}$, 1535.8 $[M + H]^{+}$, 1556.7 $[M + Na]^{+}$.

3.4.4. Synthesis of peptides containing a 5-phenylhistidine at the 4-position

Tr-Lys(Boc)-Lys(Boc)-Leu-His(5-Br,1-SEM)-Lys(Boc)-Lys(Boc)-Ile-Leu-Lys(Boc)-Val-Leu-Rink-ChemMatrix (11a) and Tr-Lys(Boc)-Lys(Boc)-Leu-His(5-Br,3-SEM)-Lys(Boc)-Lys(Boc)-Ile-Leu-Lys(Boc)-Val-Leu-Rink-ChemMatrix (11b): The bromotripeptidyl resins **11** were synthesized manually by the solid-phase method using standard Fmoc chemistry. Aminomethyl ChemMatrix resin (0.66 mmol/g) was used as solid support and it was washed before its use with MeOH (2×1 min), DMF (2×1 min), CH_2Cl_2 (3×1 min), TFA/CH_2Cl_2 (1:99, 3×1 min), DIEA/CH_2Cl_2 (1:19, 3×1 min) and CH_2Cl_2 (3×1 min). Coupling of Fmoc-Rink (4 equiv.) was mediated by DIPCDI (4 equiv.) and Oxyma (4 equiv.) in DMF or NMP at room temperature overnight. Couplings of the Fmoc-amino acids (4 equiv.) were performed using DIPCDI (4 equiv.) and Oxyma (4 equiv.) in DMF at room temperature for 1 h, except for coupling of Fmoc-His(5-Br,1-SEM)-OH (**9a**) and Fmoc-His(5-Br,3-SEM)-OH (**9b**) (2 equiv.) which was carried out using COMU (2 equiv.), Oxyma (2 equiv.) and DIEA (4 equiv.) in NMP at room temperature overnight. The completion of the reactions was monitored by the

Kaiser test (Kaiser et al., 1970). Fmoc group removal was achieved with a mixture of piperidine/DMF (3:7, 1×2 and 1×10 min). After each coupling and deprotection step, the resulting resins **10** were washed with DMF or NMP (6×1 min).

An aliquot of resins **10** was cleaved with TFA/H_2O/TIS (95:2.5:2.5) whilst stirring for 3 h at room temperature. Following TFA evaporation and diethyl ether extraction, the crude peptide was dissolved in H_2O and lyophilized, affording Fmoc-Lys-Lys-Leu-His(5-Br)-Lys-Lys-Ile-Leu-Lys-Val-Leu-NH_2 (90% purity). t_R 7.10 min (conditions A).

The rest of resins **10** was subjected to Fmoc removal and washes, followed by three treatments with TrCl (10 equiv.) and DIEA (10 equiv.) in NMP at room temperature for 4 h. Then, the resulting resins **11** were washed with NMP (6×1 min). The completion of this reaction was monitored by the Kaiser test (Kaiser et al., 1970). An aliquot of resins **11** was cleaved with TFA/H_2O/TIS (95:2.5:2.5) under the conditions described above, affording H-Lys-Lys-Leu-His(5-Br)-Lys-Lys-Ile-Leu-Lys-Val-Leu-NH_2 (82% purity). t_R 15.70 min (conditions B). MS (ESI): *m/z* = 712.8, 713.8 $[M + 2H]^{2+}$, 1424.5, 1426.5 $[M + H]^+$.

Ac-Leu-Lys(Boc)-Leu-His(5-Br,1-SEM)-Lys(Boc)-Lys(Boc)-Ile-Leu-Lys(Boc)-Val-Leu-Rink-ChemMatrix (14a) and Ac-Leu-Lys(Boc)-Leu-His(5-Br,3-SEM)-Lys(Boc)-Lys(Boc)-Ile-Leu-Lys(Boc)-Val-Leu-Rink-ChemMatrix (14b): The Fmoc-undecapeptidyl resins **12** were prepared following the procedure described for resins **10**. Once the peptide sequence was completed, resins **12** were subjected to Fmoc removal and washes, followed by treatment with Ac_2O/pyridine/CH_2Cl_2 (1:1:1) at room temperature for 1 h. After this time, the resulting resins **14** were washed with CH_2Cl_2 (6×1 min). The completion of this reaction was monitored by the Kaiser test (Kaiser et al., 1970). An aliquot of resins **14** was cleaved with TFA/H_2O/TIS (95:2.5:2.5) under the conditions described above, affording Ac-Leu-Lys-Leu-His(5-Br)-Lys-Lys-Ile-Leu-Lys-Val-Leu-NH_2 (77% purity). t_R 6.70 min (conditions A). MS (ESI): *m/z* = 1451.4, 1453.4 $[M + H]^+$, 1473.4, 1475.4 $[M + Na]^+$.

Ac-Phe-Lys(Boc)-Leu-His(5-Br,1-SEM)-Lys(Boc)-Lys(Boc)-Ile-Leu-Lys(Boc)-Val-Leu-Rink-ChemMatrix (15a) and Ac-Phe-Lys(Boc)-Leu-His(5-Br,3-SEM)-Lys(Boc)-Lys(Boc)-Ile-Leu-Lys(Boc)-Val-Leu-Rink-ChemMatrix (15b): The Fmoc-undecapeptidyl resins **13** were prepared following the procedure described for resins **10**. Once the peptide sequence was completed, resins **13** were subjected to Fmoc removal and washes, followed by treatment with Ac_2O/pyridine/CH_2Cl_2 (1:1:1) at room temperature for 1 h. After this time, the resulting resins **15** were washed with CH_2Cl_2 (6×1 min). The completion of this reaction was monitored by the Kaiser test (Kaiser et al., 1970). An aliquot of resins **15** was cleaved with TFA/H_2O/TIS (95:2.5:2.5) under the conditions described above, affording Ac-Phe-Lys-Leu-His(5-Br)-Lys-Lys-Ile-Leu-Lys-Val-Leu-NH2 (77% purity). t_R 6.73 min (conditions A). MS (ESI): *m/z* = 1485.4, 1487.4 $[M + H]^+$, 1507.4, 1509.4 $[M + Na]^+$.

Ts-Phe-Lys(Boc)-Leu-His(5-Br,1-SEM)-Lys(Boc)-Lys(Boc)-Ile-Leu-Lys(Boc)-Val-Leu-Rink-ChemMatrix (16a) and Ts-Phe-Lys(Boc)-Leu-His(5-Br,3-SEM)-Lys(Boc)-Lys(Boc)-Ile-Leu-Lys(Boc)-Val-Leu-Rink-ChemMatrix (16b): Resins **13** were subjected to Fmoc removal and washes, followed by treatment with TsCl (40 equiv.) and DIEA (80 equiv.) in a mixture of CH_2Cl_2/NMP (9:1) at room temperature for 1 h. After this time, the resulting resins **16** were washed with CH_2Cl_2 (6×1 min) and NMP (3×1 min). The completion of this reaction was monitored by the Kaiser test (Kaiser et al., 1970). An aliquot of resins **16** was cleaved with TFA/H_2O/TIS (95:2.5:2.5) under the conditions described above, affording Ts-Phe-Lys-Leu-His(5-Br)-Lys-Lys-Ile-Leu-Lys-Val-Leu-NH_2 (86% purity). t_R 6.96 min (conditions A). MS (ESI): *m/z* = 799.4, 800.4 $[M + 2H]^{2+}$, 1597.4, 1599.4 $[M + H]^+$.

Tr-Phe-Lys(Boc)-Leu-His(5-Br,1-SEM)-Lys(Boc)-Lys(Boc)-Ile-Leu-Lys(Boc)-Val-Leu-Rink-ChemMatrix (17a) and Tr-Phe-Lys(Boc)-Leu-His(5-Br,3-SEM)-Lys(Boc)-Lys(Boc)-Ile-Leu-Lys(Boc)-Val-Leu-Rink-ChemMatrix (17b): Resins **13** were subjected to Fmoc removal and washes, followed by treatment with TrCl (10 equiv.) and DIEA (10 equiv.) in NMP at room temperature for 4 h. Then, the resulting resins **17** were washed with NMP (6×1 min). The completion of this reaction was monitored by the

Kaiser test (Kaiser et al., 1970). An aliquot of resins **17** was cleaved with TFA/H_2O/TIS (95:2.5:2.5) under the conditions described above, affording H-Phe-Lys-Leu-His(5-Br)-Lys-Lys-Ile-Leu-Lys-Val-Leu-NH_2 (82% purity). t_R 6.68 min (conditions A). MS (ESI): *m/z* = 722.5, 723.5 $[M + 2H]^{2+}$, 1444.0, 1446.0 $[M + H]^+$, 1465.9, 1467.9 $[M + Na]^+$.

General method for the arylation of bromopeptidyl resins 11, 14, 15 and 17 by using a microwave-assisted solid-phase Suzuki-Miyaura reaction

A 5 mL quartz vial was charged with the corresponding bromopeptidyl resins (50 mg), which were first swelled in a degassed mixture of DME/EtOH/H_2O (9:9:2, 0.84 mL) for 20 min under nitrogen. Then, $Pd_2(dba)_3$ (0.2 equiv.), SPhos (0.4 equiv.), KF (4 equiv.) and phenylboronic acid (4 equiv.) were added. The reaction mixture was heated at 140 ºC under microwave irradiation for 30 min. After this time, the resins were washed with DMF (3×1 min), H_2O (3×1 min), EtOH (3×1 min), CH_2Cl_2 (3×1 min) and diethyl ether (3×1 min). The resulting biaryl linear peptidyl resins were cleaved with TFA/H_2O/TIS (95:2.5:2.5) whilst stirring for 3 h at room temperature. Following TFA evaporation and diethyl ether extraction, the crude peptide was dissolved in H_2O/MeCN and lyophilized.

H-Lys-Lys-Leu-His(5-Ph)-Lys-Lys-Ile-Leu-Lys-Val-Leu-NH_2 (BP276): Starting from resins **11**, Suzuki-Miyaura reaction followed by acidolytic cleavage afforded the biaryl linear peptide **BP276** and H-Lys-Lys-Leu-His-Lys-Lys-Ile-Leu-Lys-Val-Leu-NH_2 (**BP270**) [4:3 ratio by MS (ESI)]. **BP276** was purified by reverse-phase column chromatography (95% purity). t_R 6.41 min (conditions A). MS (ESI): *m/z* = 711.9 $[M + 2H]^{2+}$, 1422.6 $[M + H]^+$, 1444.6 $[M + Na]^+$. HRMS (ESI): calcd for $C_{71}H_{130}N_{19}O_{11}$ $[M + 3H]^{3+}$ 475.0060; found 475.0043; calcd for $C_{71}H_{129}N_{19}O_{11}$ $[M + 2H]^{2+}$ 712.0054; found 712.0012.

Ac-Leu-Lys-Leu-His(5-Ph)-Lys-Lys-Ile-Leu-Lys-Val-Leu-NH_2 (BP277): Starting from resins **14**, Suzuki-Miyaura reaction followed by acidolytic cleavage afforded the biaryl linear peptide **BP277** and Ac-Leu-Lys-Leu-His-Lys-Lys-Ile-Leu-Lys-Val-Leu-NH_2 (**BP271**) [4:3 ratio by MS (ESI)]. **BP277** was purified by reverse-phase column

chromatography (95% purity). t_R 6.61 min (conditions A). MS (ESI): *m/z* = 725.5 [M + 2H]$^{2+}$, 1449.6 [M + H]$^{+}$, 1471.6 [M + Na]$^{+}$. HRMS (ESI): calcd for $C_{73}H_{131}N_{18}O_{12}$ [M + 3H]$^{3+}$ 484.0059; found 484.0049; calcd for $C_{73}H_{130}N_{18}O_{12}$ [M + 2H]$^{2+}$ 725.5052; found 725.4994.

Ac-Phe-Lys-Leu-His(5-Ph)-Lys-Lys-Ile-Leu-Lys-Val-Leu-NH_2 (BP279): Starting from resins **15**, Suzuki-Miyaura reaction followed by acidolytic cleavage afforded the biaryl linear peptide **BP279** and Ac-Phe-Lys-Leu-His-Lys-Lys-Ile-Leu-Lys-Val-Leu-NH_2 (**BP273**) [4:3 ratio by MS (ESI)]. MS (ESI): *m/z* = 705.0 [M + 2H]$^{2+}$, 742.5 [M + 2H]$^{2+}$, 1407.6 [M + H]$^{+}$, 1483.6 [M + H]$^{+}$. HRMS (ESI): calcd for $C_{76}H_{129}N_{18}O_{12}$ [M + 3H]$^{3+}$ 495.3340; found 495.3326; calcd for $C_{76}H_{128}N_{18}O_{12}$ [M + 2H]$^{2+}$ 742.4974; found 742.4936.

Ts-Phe-Lys-Leu-His(5-Ph)-Lys-Lys-Ile-Leu-Lys-Val-Leu-NH2 (BP280): Resins **17** were subjected to Suzuki-Miyaura reaction. The resulting resins were treated with TFA/H_2O/CH_2Cl_2 (0.2:1:98.8, 2×1 min and 1×20 min), and then washed with DMF (3×1 min), DIEA/CH_2Cl_2 (1:19, 3×1 min) and DMF (3×1 min). Then, the resins were treated with TsCl (40 equiv.) and DIEA (80 equiv.) in a mixture of CH_2Cl_2/NMP (9:1) at room temperature for 1 h. After this time, the resins were washed with CH_2Cl_2 (6×1 min) and NMP (3×1 min). Acidolytic cleavage afforded **BP280** and Ts-Phe-Lys-Leu-His-Lys-Lys-Ile-Leu-Lys-Val-Leu-NH2 (**BP275**) [4:3 ratio by MS (ESI)]. MS (ESI): *m/z* = 760.9 [M + 2H]$^{2+}$, 798.4 [M + 2H]$^{2+}$, 1519.4 [M + H]$^{+}$, 1595.4 [M + H]$^{+}$. HRMS (ESI): calcd for $C_{81}H_{133}N_{18}O_{13}S$ [M + 3H]$^{3+}$ 532.6668; found 532.6692; calcd for $C_{81}H_{132}N_{18}O_{13}S$ [M + 2H]$^{2+}$ 798.4965; found 798.4981.

3.4.5. Synthesis of peptides containing histidine residues

General method for the solid-phase synthesis of histidine-containing peptides BP270-BP275, BP284, BP285, BP305, and BP306

Peptides were synthesized manually by the solid-phase method using standard Fmoc chemistry. Fmoc-Rink-MBHA resin (0.56 mmol/g) was used as solid support and it was swelled before its use with CH_2Cl_2 (1×20 min) and DMF (1×20 min). Fmoc removal steps were achieved by treatment with piperidine/DMF (3:7, 1×2 and 1×10 min). Couplings of Fmoc-amino acids were carried out as follows: Fmoc-Aa-OH (4 equiv.) and Oxyma (4 equiv.) were dissolved in DMF, DIPCDI (4 equiv.) was added, and the resulting mixture was added to the resin and shaken for 1 h at room temperature. After each deprotection and coupling step, the resin was washed with DMF (6×1 min). The completion of the reaction was monitored by the Kaiser test (Kaiser et al., 1970). Once the peptide sequence was completed, the Fmoc group was removed. Then, acidolytic cleavage was performed by treatment of the resin with TFA/H_2O/TIS (95:2.5:2.5) for 2 h at room temperature. Following TFA evaporation and diethyl ether extraction, the crude peptides were dissolved in H_2O and lyophilized.

H-Lys-Lys-Leu-His-Lys-Lys-Ile-Leu-Lys-Val-Leu-NH_2 (BP270): Following the general procedure described above, **BP270** was obtained in 92% purity. t_R 5.87 min (conditions A). MS (ESI): *m/z* = 673.9 $[M + 2H]^{2+}$, 1346.8 $[M + H]^+$, 1368.7 $[M + Na]^+$. HRMS (ESI): calcd for $C_{65}H_{126}N_{19}O_{11}$ $[M + 3H]^{3+}$ 449.6623; found 449.6592; calcd for $C_{65}H_{125}N_{19}O_{11}$ $[M + 2H]^{2+}$ 673.9897; found 673.9861.

Ac-Leu-Lys-Leu-His-Lys-Lys-Ile-Leu-Lys-Val-Leu-NH_2 (BP271): Following the general procedure described above, **BP271** was obtained in 85% purity. t_R 6.32 min (conditions A). MS (ESI): *m/z* = 687.4 $[M + 2H]^{2+}$, 1373.7 $[M+H]^+$, 1395.7 $[M+Na]^+$. HRMS (ESI): calcd for $C_{67}H_{127}N_{18}O_{12}$ $[M + 3H]^{3+}$ 458.6621; found 458.6598; calcd for $C_{67}H_{126}N_{18}O_{12}$ $[M + 2H]^{2+}$ 687.4896; found 687.4861.

Ac-His-Lys-Leu-His-Lys-Lys-Ile-Leu-Lys-Val-Leu-NH_2 (BP272): Following the general procedure described above, **BP272** was obtained in 91% purity. t_R 5.98 min (conditions A). MS (ESI): *m/z* 699.4 $[M + 2H]^{2+}$, 1397.8 $[M + H]^+$.

Ac-Phe-Lys-Leu-His-Lys-Lys-Ile-Leu-Lys-Val-Leu-NH_2 (BP273): Following the general procedure described above, **BP273** was obtained in 87% purity. t_R 6.46 min (conditions A). MS (ESI): *m/z* = 704.5 $[M + 2H]^{2+}$, 1407.6 $[M + H]^+$, 1429.5 $[M + Na]^+$. HRMS (ESI): calcd for $C_{70}H_{125}N_{18}O_{12}$ $[M + 3H]^{3+}$ 469.9903; found 469.9880; calcd for $C_{70}H_{124}N_{18}O_{12}$ $[M + 2H]^{2+}$ 704.4818; found 704.4818.

Ts-His-Lys-Leu-His-Lys-Lys-Ile-Leu-Lys-Val-Leu-NH_2 (BP274): Following the general procedure described above, **BP274** was obtained in 80% purity. t_R 6.17 min (conditions A). MS (ESI): *m/z* = 1509.7 $[M + H]^+$, 1531.6 $[M + Na]^+$.

Ts-Phe-Lys-Leu-His-Lys-Lys-Ile-Leu-Lys-Val-Leu-NH_2 (BP275): Following the general procedure described above, **BP275** was obtained in 85% purity. t_R 6.78 min (conditions A). MS (ESI): *m/z* = 760.0 $[M + 2H]^{2+}$, 1519.7 $[M + H]^+$. HRMS (ESI): calcd for $C_{75}H_{129}N_{18}O_{13}S$ $[M + 3H]^{3+}$ 507.3230; found 507.3201; calcd for $C_{75}H_{128}N_{18}O_{13}S$ $[M + 2H]^{2+}$ 760.4809; found 760.4778.

H-His-Lys-Leu-Phe-Lys-Lys-Ile-Leu-Lys-Phe-Leu-NH_2 (BP284): Following the general procedure described above, **BP284** was obtained in 76% purity. t_R 17.16 min (conditions B). MS (ESI): *m/z* = 707.5 $[M + 2H]^{2+}$, 1414.0 $[M + H]^+$, 1436.1 $[M + Na]^+$.

H-Phe-Lys-Leu-Phe-Lys-Lys-Ile-Leu-Lys-His-Leu-NH_2 (BP285): Following the general procedure described above, **BP285** was obtained in 82% purity. t_R 17.03 min (conditions B). MS (ESI): *m/z* 707.4 $[M + 2H]^{2+}$, 1413.7 $[M + H]^+$.

H-His-Lys-Leu-Phe-Lys-Lys-Ile-Leu-Lys-His-Leu-NH_2 (BP305): Following the general procedure described above, **BP305** was obtained in 91% purity. t_R 6.02 min (conditions A). MS (ESI): *m/z* 1404.1 $[M + H]^+$.

H-His-Lys-Leu-His-Lys-Lys-Ile-Leu-Lys-His-Leu-NH_2 (BP306): Following the general procedure described above, **BP306** was obtained in 94% purity. t_R 5.63 min (conditions A). MS (ESI): *m/z* 1394.1 $[M + H]^+$.

3.4.6. Biological assays

3.4.6.1. Bacterial and fungal strains and growth conditions

The following plant pathogenic bacterial strains were used: *Erwinia amylovora* PMV6076 (Institut National de la Recherche Agronomique, Angers, France), *Pseudomonas syringae* pv. *syringae* EPS94 (Institut de Tecnologia Agroalimentària, Universitat de Girona, Spain) and *Xanthomonas axonopodis* pv. *vesicatoria* 2133-2 (Instituto Valenciano de Investigaciones Agrarias, Valencia, Spain). All bacteria were stored in Luria Bertani (LB) broth supplemented with glycerol (20%) and maintained at -80 ºC. *E. amylovora* and *Pss* were scrapped from LB agar after growing for 24 h and *Xav* after growing for 48 h at 25 ºC. The cell material was suspended in sterile water to obtain a suspension of 10^8 CFU ml^{-1}.

The following plant pathogenic fungal strains were used: *Penicillium expansum* EPS 26 (INTEA, University of Girona), *Fusarium oxysporum* f. sp. *lycopersici* FOL 3 race 2 (ATCC 201829, American Type Culture Collection). Strains were cultured on potato dextrose agar (PDA) plates (Difco) using aseptic procedures to avoid contamination. Conidia from fungal mycelium for *P. expansum* were obtained from 5-day-old PDA cultures of the fungus incubated at 25 ºC. Inoculum was prepared by scraping spore material from the culture surfaces with a wet cotton swab and resuspending it in distilled water containing 0.5‰ of Tween 80. Microconidia of F. oxysporum were obtained from 1-week-old potato dextrose broth (PDB) cultures (Oxoid) of the fungus incubated at 25 ºC in the dark in a rotary shaker at 125 rpm. After

incubation, the culture was filtered through several layers of sterile cheesecloth to eliminate macroconidia and mycelial growth of the fungus. Then, the effluent was centrifuged at 8000 × g for 20 min at 4 ºC, and the pellet was resuspended in sterile water. The concentration of conidia was determined by using a hemacytometer and adjusted to 10^4 conidia ml^{-1} for *F. oxysporum*, and 10^3 conidia ml^{-1} for *P. expansum*.

3.4.6.2. Antibacterial and antifungal activity

Lyophilized compounds were solubilized in sterile Milli-Q water to a final concentration of 1000 μM and filter sterilized through a 0.22-μm pore filter. For minimum inhibitory concentration (MIC) assessment, dilutions of the compounds were made to obtain a stock concentration of 500, 250, 125, 62.5 and 31.125 μM. For antibacterial activity 20 μL of each dilution were mixed in a microtiter plate well with 20 μL of the corresponding suspension of the bacterial indicator, 160 μL of Trypticase Soy Broth (TSB) (BioMèrieux, France) to a total volume of 200 μL. For antifungal activity 20 μL of each stock solution were mixed in a microtiter plate well with 80 μL of the corresponding suspension of the fungal pathogen and 100 μL of double concentrated PDB to a total volume of 200 μL containing 0.003% w/v of choramphenicol.

Three replicates for each strain, compound and concentration were used. Positive controls contained water instead of compound and negative controls contained compounds without bacterial suspension. Microbial growth was automatically determined by optical density measurement at 600 nm (Bioscreen C, Labsystem, Helsinki, Finland). For antibacterial activity microplates were incubated at 25 ºC with 20 s shaking before hourly absorbance measurements for 48 h. For antifungal activity microplates were incubated at 20 ºC with 1 min shaking before absorbance measurements that were recorded every two hours for seven days. The experiment was repeated twice. The MIC was taken as the lowest compound concentration with no growth at the end of the experiment.

3.4.6.3. Hemolytic activity

The hemolytic activity of the compounds was evaluated by determining hemoglobin release from erythrocyte suspensions of fresh human blood (5% vol/vol). Blood was aseptically collected with a BD vacutainer K2E System with EDTA (Belliver Industrial State, Plymouth, U.K.) and stored for less than 2 hours at 4 ºC. Blood was centrifuged at 6000 × g, for 5 min, washed three times with TRIS buffer (10 mM TRIS, 150 mM NaCl, pH 7.2) and diluted. Compounds were solubilized in TRIS buffer to a stock concentration of 500, 300 and 100 μM (final concentrations tested were 250, 150 and 50 μM). 65 μL of human red blood cells were mixed with 65 μL of the compound solution and incubated under continuous shaking for 1 h at 37 ºC. Then, the tubes were centrifuged at 3500 × g for 10 min. 80 μL aliquots of the supernatant were transferred to 100-well microplates (Bioscreen) and diluted with 80 μL of Milli-Q water. Hemolysis was measured as the absorbance at 540 nm with a Bioscreen plate reader. Complete hemolysis was determined in TRIS buffer plus melittin at 100 μM final concentration (Sigma-Aldrich Corporation, Madrid, Spain) as a positive control. The percentage of hemolysis (*H*) was calculated using the equation: $H = 100\times[(Op-Ob)/(Om-Ob)]$, where *Op* was the density for a given compound concentration, *Ob* for the buffer, and *Om* for the melittin positive control.

3.5. REFERENCES

Afonso, A.; Feliu, L.; Planas, M. Solid-phase synthesis of biaryl cyclic peptides by borylation and microwave-assisted intramolecular Suzuki-Miyaura reaction. *Tetrahedron* **2011**, *67*, 2238-2245.

Badosa, E.; Ferré, R.; Planas, M.; Feliu, L.; Besalú, E.; Cabrefiga, J.; Bardají, E.; Montesinos, E. A library of linear undecapeptides with bactericidal activity against phytopathogenic bacteria. *Peptides* **2007**, *28*, 2276-2285.

Badosa, E.; Ferré, R.; Francés, J.; Bardají, E.; Feliu, L.; Planas, M.; Montesinos, E. Sporicidal activity of synthetic antifungal undecapeptides and control of *Penicillium* rot of apples. *Appl. Environ. Microbiol.* **2009**, *75*, 5563-5569.

Bechinger, B.; Lohner, K. Detergent-like actions of linear amphipathic cationic antimicrobial peptides. *Biochim. Biophys. Acta* **2006**, *1758*, 1529–1539.

Bewley, C. A.; He, H.; Williams, D. H.; Faulkner, D. J. Aciculitins A-C: Cytotoxic and antifungal cyclic peptides from the lithistid sponge *Aciculites orientalis*. *J. Am. Chem. Soc.* **1996**, *118*, 4314-4321.

Blondelle, S. E.; Lohner, K. Combinatorial libraries: a tool to design antimicrobial and antifungal peptide analogues having lytic specificities for structure-activity relationship studies. *Biopolymers* **2000**, *55*, 74-87.

Brogden, K. A. Antimicrobial peptides: pore formers or metabolic inhibitors in bacteria? *Nat. Rev. Microbiol.* **2005**, *3*, 238–250.

Bulet, P.; Stöcklin, R.; Menin, L. Anti-microbial peptides: from invertebrates to vertebrates. *Immunol. Rev.* **2004**, *198*, 169-184.

Cerezo, V.; Amblard, M.; Martinez, J.; Verdié, P.; Planas, M.; Feliu, L. Solid-phase synthesis of 5-arylhistidines via a microwave-assisted Suzuki-Miyaura cross-coupling. *Tetrahedron* **2008**, *64*, 10538-10545.

Doan, N.; Bourgault, S.; Létourneau, M.; Fournier, A. Effectiveness of the Suzuki-Miyaura cross-coupling reaction for solid-phase peptide modification. *J. Comb. Chem.* **2008**, *10*, 44-51.

Faulkner, D. J.; He, H.; Unson, M. D.; Bewley, C. A.; Garson, M. J. New metabolites from marine sponges: are symbionts important? *Gazz. Chim. Ital.* **1993**, *123*, 301-307.

Feliu, L.; Planas, M. Cyclic peptides containing biaryl and biaryl ether linkages. *Int. J. Pept. Res. Ther.* **2005**, *11*, 53-97.

Ferre, R.; Badosa, E.; Feliu, L.; Planas, M.; Montesinos, E.; Bardají, E. Inhibition of plant-pathogenic bacteria by short synthetic cecropin A-melittin hybrid peptides. *Appl. Environ. Microbiol.* **2006**, *72*, 3302-3308.

Haldar, D. Recent developments in the synthesis of amino acids and analogues for foldamers study. *Curr. Org. Synth.* **2008**, *5*, 61–80.

Hancock, R. E. W.; Sahl, H. G. Antimicrobial and host-defense peptides as new anti-infective therapeutic strategies. *Nature Biotechnol.* **2006**, *24*, 1551–1557.

Haug, B. E.; Stensen, W.; Svendsen, J. S. Application of the Suzuki-Miyaura cross-coupling to increase antimicrobial potency generates promising novel antibacterials. *Bioorg. Med. Chem. Lett.* **2007**, *17*, 2361-2364.

Huang, H. W. Molecular mechanism of antimicrobial peptides: The origin of cooperativity. *Biochim. Biophys. Acta* **2006**, *1758*, 1292–1302.

Jenssen, H.; Hamill, P.; Hancock, R. E. W. Peptide antimicrobial agents. *Clin. Microbiol. Rev.* **2006**, *19*, 491–511.

Kaiser, E.; Colescott, R. L.; Bossinger, C. D.; Cook, P. Color test for detection of free terminal amino groups in the solid-phase synthesis of peptides. *Anal. Biochem.* **1970**, *34*, 595–598.

Kazmaier, U.; Deska, J. Peptide backbone modifications. *Curr. Org. Chem.* **2008**, *12*, 355–385.

Kotha, S.; Lahiri, K. A new approach for modification of phenylalanine peptides by Suzuki-Miyaura coupling reaction. *Bioorg. Med. Chem. Lett.* **2001**, *11*, 2887-2890.

Kotha, S.; Lahiri, K. Application of the Suzuki-Miyaura cross-coupling reaction for the modification of phenylalanine peptides. *Biopolymers* **2003**, *69*, 517-528.

Kotha, S.; Lahiri, K. Post-assembly peptide modifications by chemical methods. *Curr. Med. Chem.* **2005**, *12*, 849–875.

Kotha, S.; Lahiri, K.; Kashinath, D. Recent applications of the Suzuki-Miyaura cross-coupling reaction in organic synthesis. *Tetrahedron* **2002**, *58*, 9633-9695.

Marcos, J. F.; Gandía, M. Antimicrobial peptides: to membranes and beyond. *Expert. Opin. Drug Discov.* **2009**, *4*, 659–671.

Montesinos, E. Antimicrobial peptides and plant disease control. *FEMS Microbiol. Lett.* **2007**, *270*, 1–11.

Nicolas, P. Multifunctional host defense peptides: intracellular-targeting antimicrobial peptides. *FEBS J.* **2009**, *276*, 6483–6496.

Nielsen, T. E.; Le Quement, S.; Meldal, M. Solid-phase synthesis of biarylalanines via Suzuki cross-coupling and intramolecular *N*-acyliminium Pictet-Spengler reactions. *Tetrahedron Lett.* **2005**, *46*, 7959–7962.

Oh, D.; Shin, S. Y.; Lee, S.; Kang, J. H.; Kim, S. D.; Ryu, P. D.; Hahm, K. S.; Kim, Y. Role of the hinge region and the tryptophan residue in the synthetic antimicrobial peptides, cecropin A(1-8)-magainin 2(1-12) and its analogues, on their antibiotic activities and structures. *Biochemistry* **2000**, *39*, 11855-11864.

Perdih, A.; Dolenc, M. S. Recent advances in the synthesis of unnatural α-amino acids. *Curr. Org. Chem.* **2007**, *11*, 801–832.

Peschel, A.; Sahl, H. G. The co-evolution of host cationic antimicrobial peptides and microbial resistance. *Nat. Rev. Microbiol.* **2006**, *4*, 529–536.

Tomson, F.; Bailey, J. A.; Gennis, R. B.; Unkefer, C. J.; Li, Z.; Silks, L. A.; Martinez, R. A.; Donohoe, R. J.; Dyer, R. B.; Woodruff, W. H. Direct infrared detection of the covalently ring linked His-Tyr structure in the active site of the heme-copper oxidases. *Biochemistry* **2002**, *41*, 14383–14390.

Yeaman, M. R.; Yount, N. Y. Mechanisms of antimicrobial peptide action and resistance. *Pharmacol. Rev.* **2003**, *55*, 27–55.

Yount, N. Y.; Yeaman, M. R. Immunocontinuum: perspectives in antimicrobial peptide mechanisms of action and resistance. *Protein Pept. Lett.* **2005**, *12*, 49–67.

CHAPTER 4

Solid-Phase Synthesis of Biaryl Cyclic Peptides Containing a Histidine-Phenylalanine Linkage

*This chapter corresponds to a manuscript in preparation:

Ng-Choi, I.; Feliu, L.; Planas, M. Solid-phase synthesis of biaryl cyclic peptides containing a histidine-phenylalanine linkage. *In preparation*

CHAPTER 4

The feasibility of the solid-phase intramolecular 4(5)-arylation of a histidine residue was established. Biaryl cyclic peptides of different ring sizes and bearing a His-Phe linkage was prepared. These structures contained the His residue at either the N- or the C-terminus. The synthetic strategy involved the preparation of a linear peptidyl resin incorporating a 5-bromohistidine and a 4-boronophenylalanine. The formation of the biaryl bond between the imidazole of His and the phenyl group of Phe was accomplished via a microwave-assisted Suzuki-Miyaura cross-coupling. Following this methodology, the synthesis of biaryl cyclic peptides consisting of a 3- or 5-residue ring, and containing the His at the N-terminus and a Leu-Leu spacer at the C-terminus was the most favorable.

4.1. INTRODUCTION

Unsymmetrical biaryl systems are present in many naturally occurring cyclic peptides that show a variety of important biological activities such as antimicrobial or cytotoxic (Feliu and Planas, 2005). In recent years, much attention has been turned to the incorporation of biaryl amino acids into biologically active peptides (Haug et al., 2007; Le Quement et al., 2011; Ng-Choi et al., 2014). It has been reported that the biaryl motif restricts the conformational flexibility of peptides, enhances their proteolytic stability, increases their selectivity, and improves their bioavailability (Perdih and Dolenc, 2007; Haldar, 2008). In particular, 5-arylhistidines are present in cytotoxic and antifungal marine peptides, and the imidazole ring has been described to be crucial for their activity (Bewley et al., 1996). Moreover, we have shown that the incorporation of a 5-arylhistidine in a linear antimicrobial peptide renders sequences with antibacterial and antifungal activity, and low hemolysis. This low cytotoxicity has been attributed to the presence of the imidazole ring of histidine (Ng-Choi et al., 2012).

CHAPTER 5

Solid-Phase Peptide Macrocyclization via a Microwave-Assisted Suzuki-Miyaura Reaction Between a Histidine and a Tyrosine Derivative

*This chapter corresponds to a manuscript in preparation:

Ng-Choi, I.; Planas, M.; Feliu, L. Solid-phase peptide macrocyclization via a microwave-assisted Suzuki-Miyaura reaction between a histidine and a tyrosine derivative. *In preparation*

CHAPTER 5

A solid-phase strategy for the synthesis of biaryl cyclic peptides containing a His-Tyr linkage was developed. The macrocyclization step was performed through the formation of a biaryl bond between a 5-bromohistidine and a 3-boronotyrosine present in the corresponding linear peptidyl resin via a microwave-assisted Suzuki-Miyaura cross-coupling. This method allowed for direct access to biaryl cyclic peptides containing a 3- or 5-amino acid ring and bearing the histidine residue at the N- or the C-terminus, being especially conducive for analogues in which this amino acid is located at the C-terminus.

5.1. INTRODUCTION

Over the last decades, much attention has been focused on the modification of peptides by selective arylation of aromatic amino acids (Knör et al., 2006; Vilaró et al., 2008; Prieto et al, 2009; Meyer et al., 2012; Coste et al., 2014). On the one hand, the incorporation of arylated amino acids into a peptide sequence results in a higher selectivity and stability against proteolytic degradation due to an increase of the conformational flexibility restriction (Haug et al., 2007; Ng-Choi et al., 2014). On the other hand, biaryl moieties have been reported to play an important role in the biological activity of many naturally occurring molecules (Feliu and Planas, 2005). In particular, aryltyrosines are an important structural motif found in simple peptides as well as in complex macrocycles, such as the antimicrobial peptides arylomycins (Holtzel et al., 2002; Schimana et al., 2002), the proteasome inhibitor TMC-95 (Kohno et al., 2000; Koguchi et al., 2000; Inoue et al., 2003; Coste et al., 2014), the neurotensin antagonist RP-66453 (Helynck et al., 1998; Krenitsky and Boger, 2003), or the antibiotic vancomycin (Van Bambeke et al., 2004; Pace and Yang, 2006). Similarly, arylhistidines are present in the active site of heme-copper oxidases, and in cytotoxic and antifungal marine peptides, such as aciculitins (Faulkner et al., 1993; Bewley et al., 1996; Tomson et al., 2002).

CHAPTER 6

Solid-Phase Synthesis of Biaryl Cyclic Lipopeptides Derived from Arylomycins

*This chapter corresponds to a manuscript in preparation:

Ng-Choi, I.; Figueras, E.; Feliu, L.; Planas, M. Solid-phase synthesis of biaryl cyclic lipopeptides derived from arylomycins. *In preparation*

CHAPTER 6

An efficient approach for the solid-phase synthesis of N-methylated tailed biaryl cyclic lipopeptides based on the structure of arylomycins was established. Each of these analogues incorporates an N-terminal linear lipopeptide attached to a biaryl cyclic tripeptide containing a Phe-Tyr, a Tyr-Tyr, a His-Tyr or a phenylglycine-Tyr linkage. This methodology first involved an intramolecular Suzuki-Miyaura arylation of a linear peptidyl resin incorporating the corresponding halogenated amino acid at the N-terminus and a boronotyrosine at the C-terminus. After N-methylation of the resulting biaryl cyclic peptidyl resin, the N-methylated lipopeptidyl tail was then assembled. The biaryl cyclic lipopeptides were purified and characterized.

6.1. INTRODUCTION

Unsymmetrical biaryl moieties are found in a great diversity of naturally occurring bioactive cyclic peptides from relatively simple to complex macrocycles (Feliu and Planas, 2005). The aryl-aryl bonds in these compounds are commonly formed through the linkage between the side-chains of two aromatic amino acids. Among natural biaryl cyclic peptides, arylomycins A and B are a class of biaryl-containing peptide antibiotics that contain a lipopeptidyl tail attached to a biaryl cyclic tripeptide core. The peptidyl tail is a tripeptide with the N-terminus methylated and acylated with a fatty acid of 12-16 carbon atoms. The cyclic core contains a N-methylated residue and incorporates a biaryl linkage between the phenol groups of a 4-hydroxy-L-phenylglycine derivative and a tyrosine residue (Schimana et al., 2002; Feliu and Planas, 2005; Roberts et al., 2007; Roberts et al., 2011a; Liu et al., 2011) (Figure 6.1). In particular, the A series of arylomycins possess an unmodified core, while the compounds of the B series have a nitro substituent on the phenol ring of tyrosine. Arylomycins were isolated from the fermentation broth of *Streptomyces* sp. Tü 6075 and display moderate antibacterial activity against a variety of gram-positive bacteria (Smith et al., 2010), such as *Staphylococcus epidermidis* (Roberts et al., 2007) and *Streptococcus agalactiae* (Roberts et al., 2011a), and also weak antifungal activity against *Mucor hiemalis* Tü 179/180 (Schimana et al., 2002).

CHAPTER 7

Solid-Phase Synthesis of Analogues of the Northern and Southern Hemispheres of Aciculitins

*This chapter corresponds to a manuscript in preparation:

Ng-Choi, I.; Planas, M.; Feliu, L. Solid-phase synthesis of analogues of the northern and southern hemispheres of aciculitins. *In preparation*

CHAPTER 7

Aciculitins A-C, bicyclic natural peptides incorporating a His-Tyr biaryl linkage in their structure, were isolated from the marine sponge *Aciculites orientalis* and display potent cytotoxic and antifungal activities. Herein, we describe the synthesis of two northern hemisphere analogues and of one southern hemisphere derivative. We devised a solid-phase strategy that involved as key step a microwave-assisted Suzuki-Miyaura macrocyclization of a linear sequence incorporating a 5-bromohistidine and a 3-boronotyrosine. These analogues were purified and obtained in good purities. This study constitutes the first approach towards the synthesis of the naturally occurring biaryl cyclic peptides aciculitins.

7.1. INTRODUCTION

Naturally occurring biaryl cyclic peptides possess interesting biological activities which have been generally attributed to the presence of the biaryl moiety (Feliu and Planas, 2005). Among them, aciculitins A-C, isolated from the marine sponge *Aciculites orientalis*, were the first bioactive natural glycopeptidolipids obtained from a marine source (Bewley et al., 1996) (Figure 7.1). They are cytotoxic to the human-colon tumor cell line HCT-116 and also inhibit the growth of *Candida albicans*. Structurally, aciculitins are bicyclic peptides that contain an unusual His-Tyr biaryl bridge, in which the 5'-position of the imidazole ring of the histidine is linked to the 3'-position of the phenol ring of the tyrosine. In these bicyclic peptides, the northern hemisphere is a macrocycle of 6 amino acids, while the southern one consists of a 4-amino acid ring attached to a glycopeptidolipid tail.

CHAPTER 8

Solid-Phase Synthesis of Biaryl Bicyclic Peptide Analogues of Aciculitins

*This chapter corresponds to a manuscript in preparation:

Ng-Choi, I.; Feliu, L.; Planas, M. Solid-phase synthesis of biaryl bicyclic peptide analogues of aciculitins. *In preparation*

CHAPTER 8

The solid-phase synthesis of biaryl bicyclic peptides analogues of aciculitins bearing a Phe-Phe, a Phe-Tyr, a His-Tyr or a Tyr-Tyr linkage has been accomplished. The first key step is the microwave-assisted Suzuki-Miyaura cyclization of a linear peptidyl resin containing the corresponding halo- and boronoamino acids. The macrolactamization of the resulting biaryl monocyclic peptidyl resins led to the formation of the expected biaryl bicyclic peptides. This is the first report on the solid-phase synthesis of this type of compounds being suitable to obtain other synthetic or naturally occurring biaryl bicyclic peptides.

8.1. INTRODUCTION

Aciculitins A-C are a unique class of biaryl bicyclic glycolipopeptides isolated by Faulkner and coworkers from the lithistid marine sponge *Aciculites orientalis* (Bewley et al., 1996) (Figure 8.1). They are cytotoxic against the human-colon tumor cell line HCT-116 and they also inhibit the growth of *Candida albicans*. The main structural feature of aciculitins is the biaryl bond between the side-chains of a histidine and a tyrosine residue. In particular, this biaryl bond links the 5'-position of the imidazole ring of histidine and the 3'-position of the phenol ring of tyrosine. Moreover, it has been reported that this uncommon biaryl linkage plays an important role in their biological activity. In addition, these bicyclic peptides contain non-natural amino acids and a glycolipid tail consisting of a D-lyxose attached to the 3-hydroxy group of a 2,3-dihydroxy-4,6-dienoic acid unit. Aciculitins A-C differ only in the length of this unsaturated acid moiety.

CHAPTER 9

General Discussion

CHAPTER 9: General discussion

Naturally occurring biaryl peptides have been isolated from several natural sources and have attracted considerable interest due to the significant biological activities that most of them exhibit (Feliu and Planas, 2005). Interestingly, the biaryl system has been proven to be crucial for their activity. Moreover, the incorporation of biaryl amino acids in peptide sequences is considered a useful approach to overcome the problems associated with the high conformation flexibility and low bioavailability of peptides as well as to improve their biological activity.

Nowadays, in view of both the difficulty to isolate biaryl peptides from natural sources and the great importance of biaryl systems, many chemists are interested in the development of strategies for the preparation of a plethora of biaryl linear and cyclic peptides. Among the several synthetic strategies that have been devised for the synthesis of biaryl peptides, the palladium-catalyzed Suzuki-Miyaura cross-coupling reaction of an aryl halide with an arylboronic acid has proven to be one of the most reliable reactions for the formation of the biaryl bond (Kotha and Lahiri, 2001; Kotha and Lahiri, 2003; Inoue et al., 2003; Roberts et al., 2007; Waldmann et al., 2008; Vilaró et al., 2008; Coste et al., 2014). This reaction has been efficiently applied for the preparation of biaryl peptides in solution, but it has been scarcely used for the solid-phase synthesis of this type of compounds (Haug et al., 2007; Cerezo et al., 2008; Doan et al., 2008; Afonso et al., 2010; Afonso et al., 2011; Le Quement et al., 2011; Afonso et al., 2012; Meyer, et al., 2012). In particular, the preparation of 5-arylhistidine-containing peptides has proven to be difficult and there is a need for a general method for their synthesis.

This thesis focused on the development of solid-phase strategies for the preparation of linear, cyclic and bicyclic biaryl peptides based on the structure of synthetic lead antimicrobial peptides and of naturally occurring biaryl peptides. In particular, in Chapter 3 we studied the incorporation of a 5-arylhistidine residue into the sequence of lead linear undecapeptides previously identified in our group with antibacterial and antifungal activity (Badosa et al., 2007; Badosa et al., 2009). The influence of this biaryl moiety in the biological activity profile was also evaluated. In Chapters 4 and 5 a suitable solid-phase methodology for the synthesis of biaryl cyclic peptides of different ring sizes and bearing a His-Phe or a His-Tyr linkage was

established. This methodology was extended in Chapter 6 to the synthesis of biaryl cyclic lipopeptides derived from arylomycins. Finally, in Chapters 7 and 8 the synthesis of biaryl analogues of the northern and the southern hemisphere as well as of the bicyclic structure of aciculitins was studied.

9.1. SYNTHESIS OF BIARYL LINEAR UNDECAPEPTIDES

Biaryl linear undecapeptides were designed by incorporating a 5-arylhistidine into the structure of lead antimicrobial undecapeptides from the 125-member CECMEL11 peptide library (Badosa et al., 2007; Badosa et al., 2009). On the one hand, peptides **BP281**, **BP282** and **BP283** derived from the antibacterial peptide FKLFKKILKFL-NH_2 (**BP66**) and contained at position 1 a 5-phenylhistidine, a 5-(3-hydroxyphenyl)histidine and a 5-(3-nitrophenyl)histidine, respectively (Scheme 9.1). On the other hand, peptides **BP276**, **BP277**, **BP279** and **BP280** were designed from the antifungal peptides KKLFKKILKVL-NH_2 (**BP15**), Ac-FKLFKKILKVL-NH_2 (**BP21**), Ts-FKLFKKILKVL-NH_2 (**BP22**) and Ac-LKLFKKILKVL-NH_2 (**BP34**), respectively, by replacing Phe^4 by a 5-phenylhistidine (Scheme 9.2).

These peptides were synthesized on solid-phase being the key step a microwave-assisted Suzuki-Miyaura reaction between a 5-bromohistidine-containing peptidyl resin and the corresponding arylboronic acid. For peptides **BP281**, **BP282** and **BP283** the synthesis was carried out using a Fmoc-Rink-MBHA resin and the Suzuki-Miyaura reaction was performed using $Pd_2(dba)_3$, P(*o*-tolyl)$_3$ and KF at 110 ºC (Scheme 9.1). The expected biaryl undecapeptides were obtained in HPLC purities ranging from 35-81%. The lowest percentage corresponded to the arylation using 3-nitrophenylboronic acid which showed that the electron-withdrawing nitro group hindered the cross-coupling.

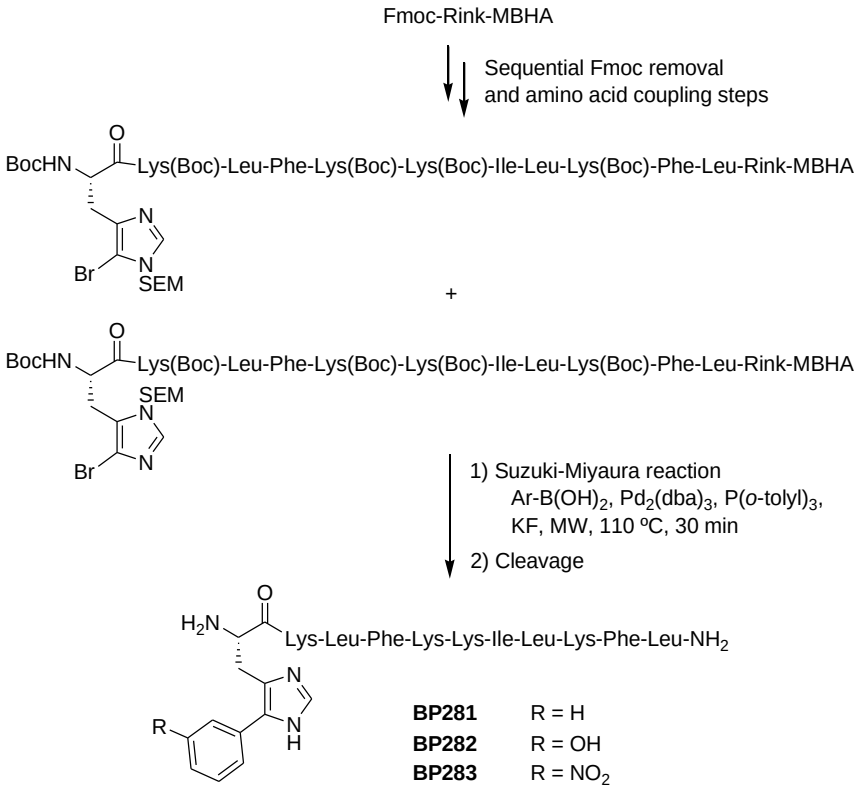

Scheme 9.1. Synthesis of biaryl linear undecapeptides **BP281**, **BP282** and **BP283**.

For the synthesis of peptides **BP276**, **BP277**, **BP279** and **BP280** incorporating a 5-phenylhistidine at position 4 the use of a ChemMatrix resin gave better results than when starting with a Fmoc-Rink-MBHA resin (Scheme 9.2). Once the N-terminal Fmoc-protected 5-bromohistidine peptidyl resins were synthesized, the Fmoc group was removed and the resulting free amine was either tritylated or acetylated. The resulting resins were then subjected to microwave-assisted Suzuki-Miyaura arylation with phenylboronic acid using $Pd_2(dba)_3$, SPhos and KF at 140 ºC. The preparation of tosylated peptide **BP280** required the selective trityl group removal and a subsequent tosylation step. This tosyl group was introduced after the cross-coupling because it was observed that the arylation of the tosylated peptidyl resin led to the formation of a dehalogenated byproduct.

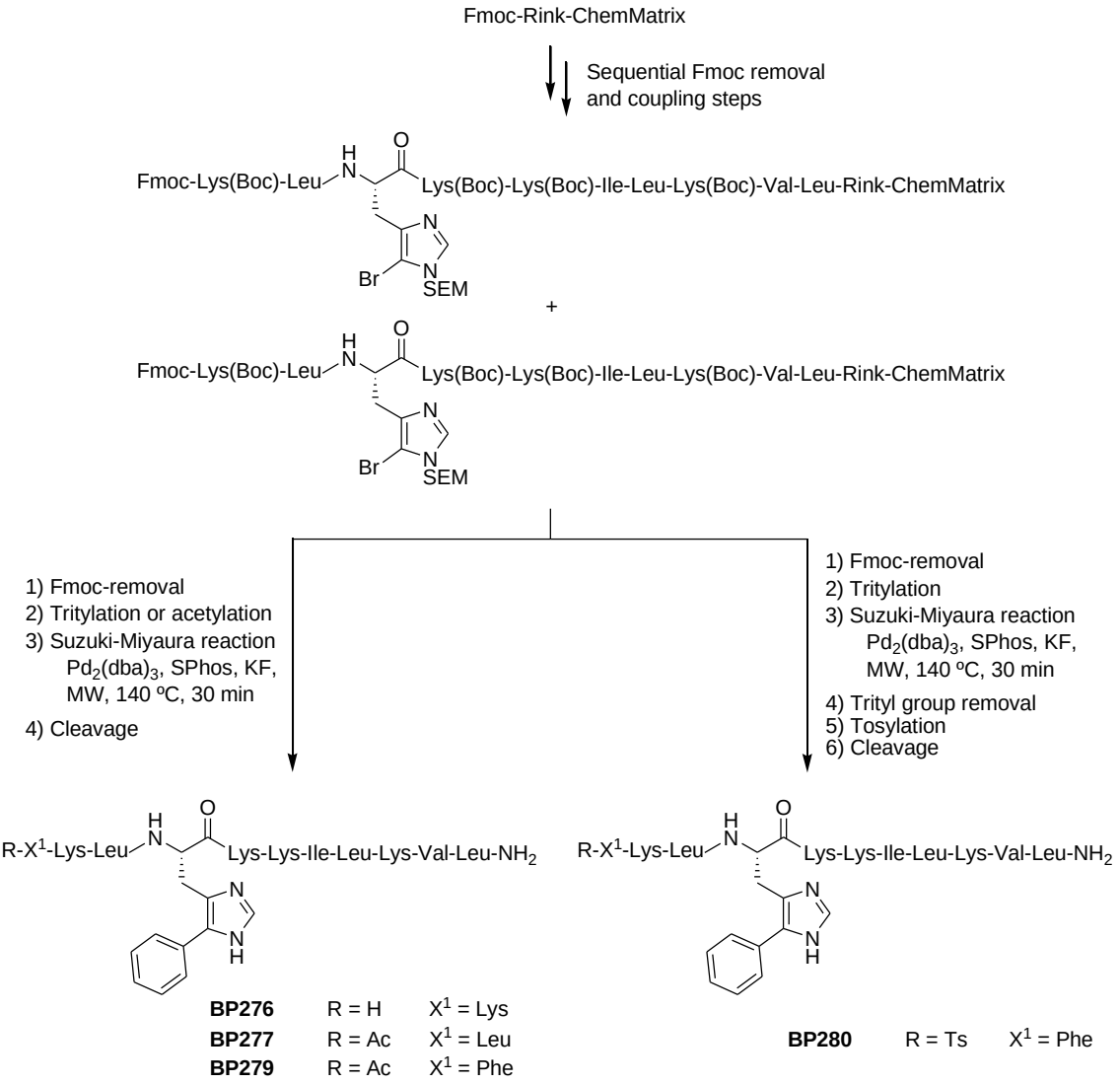

Scheme 9.2. Synthesis of biaryl linear undecapeptides **BP276**, **BP277**, **BP279** and **BP280**.

For comparison purposes, derivatives of the lead peptides **BP15**, **BP21**, **BP22**, **BP34** and **BP66** designed by replacing the phenylalanine residue at position 1, 4 and/or 10 were also synthesized and included in the study.

Biological assays demonstrated that the replacement of the phenylalanine with a 5-arylhistidine or a histidine did not improve the antimicrobial activity but, interestingly, it resulted in a significant decrease of the hemolysis. This reduction of the hemolysis could be attributed to the presence of the imidazole ring of histidine, which suggests that this heterocycle confers to peptides a lower hydrophobicity than the benzene ring of phenylalanine. These results are in agreement with previous reports on antimicrobial

peptides in which a high hydrophobic character is related to a high cytotoxicity (Blondelle and Lohner, 2000; Oh et al., 2000; Ferre et al., 2006; Badosa et al., 2007; Badosa et al., 2009).

9.2. SYNTHESIS OF BIARYL CYCLIC PEPTIDES CONTAINING A HIS-PHE OR A HIS-TYR LINKAGE

The second part of this thesis was focused on the synthesis of biaryl cyclic peptides of different ring sizes containing a His-Phe or a His-Tyr linkage (Figure 9.1). We evaluated the influence of the peptide length (3, 5, 7 or 8 amino acids), the position of the histidine residue (N- or C-terminus), the presence of a spacer at the C-terminus (a 2 or a 5-amino acid spacer) and the protecting group of the imidazole ring of histidine (SEM or Me).

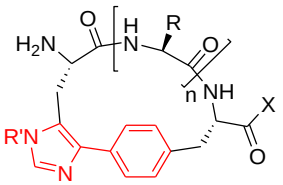

BPC758	n= 3	R' = H	X= Leu-Leu-NH_2
BPC760	n= 1	R' = H	X= Leu-Leu-NH_2
55	n= 5	R' = H	X= Leu-Leu-NH_2
56	n= 6	R' = H	X= Leu-Leu-NH_2
BPC750	n= 3	R' = H	X= NH_2
BPC752	n= 1	R' = H	X= NH_2
BPC754	n= 5	R' = H	X= NH_2
57a-b	n= 3	R' = Me	X= NH_2
BPC772a-b	n= 3	R' = Me	X= Leu-Leu-NH_2
BPC766	n= 3	R' = H	X= Lys-Lys-Leu-Lys-Lys-NH_2
BPC768	n= 1	R' = H	X= Lys-Lys-Leu-Lys-Lys-NH_2

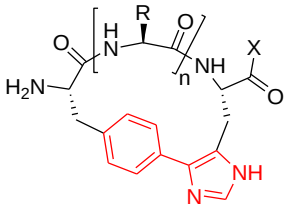

BPC776	n= 1	X= NH_2
BPC778	n= 3	X= Leu-Leu-NH_2
BPC780	n= 1	X= Leu-Leu-NH_2
69	n= 3	X= NH_2

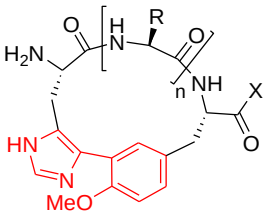

BPC782	n= 3	X= NH_2
BPC784	n= 1	X= NH_2
BPC786	n= 3	X= Leu-Leu-NH_2

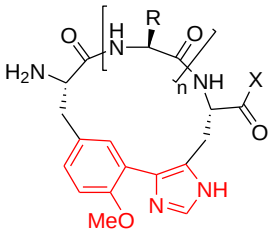

BPC788	n= 3	X= NH_2
BPC790	n= 1	X= NH_2
BPC792	n= 3	X= Leu-Leu-NH_2

Figure 9.1. General structures of biaryl cyclic peptides containing a His-Phe or a His-Tyr linkage.

Biaryl cyclic peptides incorporating a histidine residue at the N-terminus were synthesized from linear peptidyl resins that contain a 5-bromohistidine residue at the N-terminus and a 4-boronophenylalanine or a 3-boronotyrosine at the C-terminus via an intramolecular Suzuki-Miyaura cross-coupling reaction. The general synthetic strategy is depicted in Scheme 9.3 for the derivatives bearing a His-Phe linkage. These linear peptidyl resins were obtained starting from an Fmoc-Rink-MBHA resin and following a standard Fmoc/*t*Bu strategy for peptide elongation. The borylation step was performed on solid-phase using B_2Pin_2, $PdCl_2$(dppf), dppf, and KOAc in anhydrous DMSO at 80 ºC. The reaction time was 24 h for the 4-iodophenylalanine peptidyl resins while it was of 8 h in the case of the 3-iodotyrosine peptidyl resins, because it was observed that longer reaction times promote the protodeborylation and oxidation of the resulting 3-boronotyrosine moiety. Prior to the borylation, the N-terminal Fmoc group was

replaced with a trityl due to instability of the former to basic reaction conditions. Moreover, the borylation was performed just before the coupling of the N-terminal 5-bromohistidine residue because the borono functionality is not stable to several Fmoc removal and amino acid coupling steps (Afonso et al., 2011). The best reaction conditions for the formation of the His-Phe linkage via a Suzuki-Miyaura reaction involved the use of $Pd_2(dba)_3$, P(*o*-tolyl)$_3$ and KF at 140 ºC for 30 min. Similar conditions were employed to obtain biaryl cyclic peptides containing a His-Tyr bond but, in this case, SPhos gave better results than P(*o*-tolyl)$_3$.

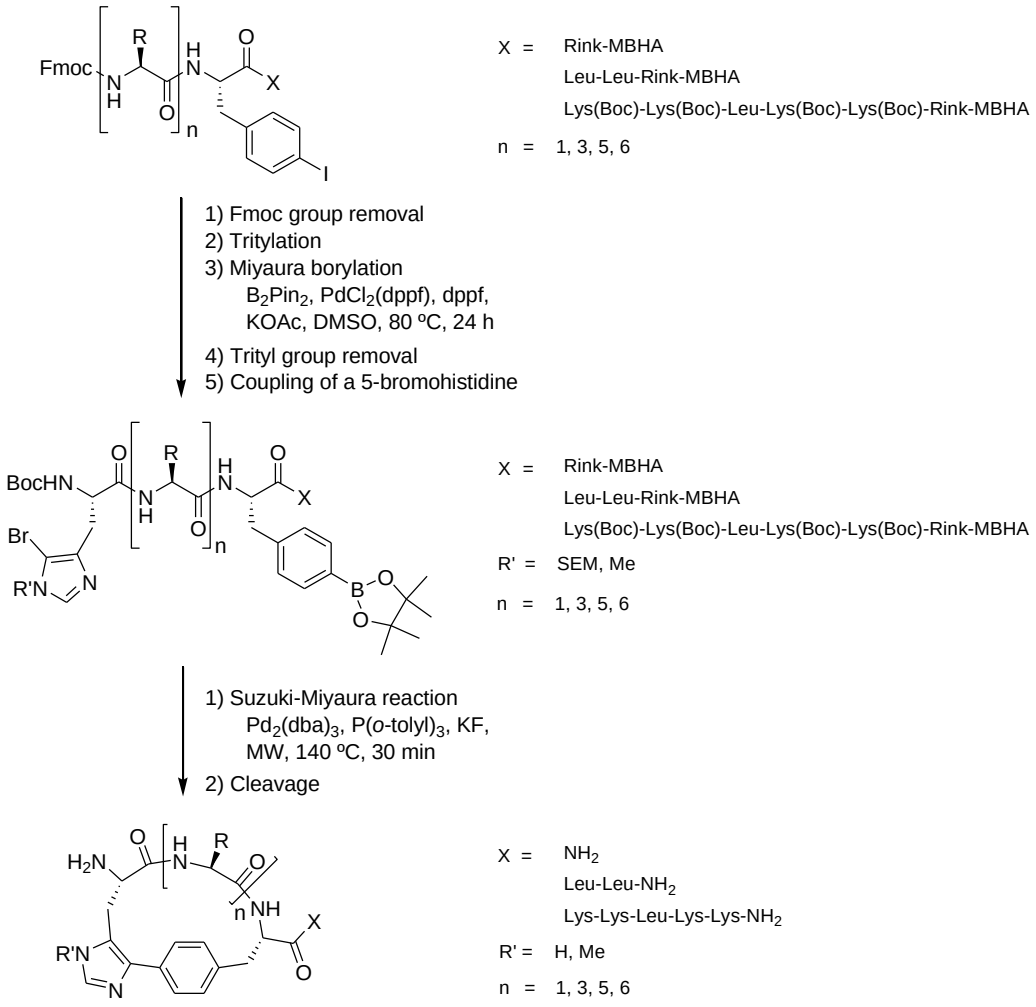

Scheme 9.3. Solid-phase synthesis of biaryl cyclic peptides containing a His-Phe linkage and bearing the histidine residue at the N-terminus.

The synthesis of biaryl cyclic peptides containing the histidine residue at the C-terminus involved the preparation of a linear peptidyl resin incorporating a 4-boronophenylalanine or a 3-boronotyrosine at the N-terminus and a 5-bromohistidine at the C-terminus. Scheme 9.4 exemplifies the general synthetic strategy for the biaryl cyclic peptides containing a His-Phe linkage. These linear peptidyl resins were synthesized following a standard Fmoc/*t*Bu strategy. The required Boc-protected 4-boronophenylalanine and 3-boronotyrosine residues were prepared in solution and coupled to the N-terminus of the corresponding peptidyl resin. Cyclization of the linear peptidyl resins was carried out under the same conditions described above for the biaryl cyclic peptides containing a histidine at the N-terminus.

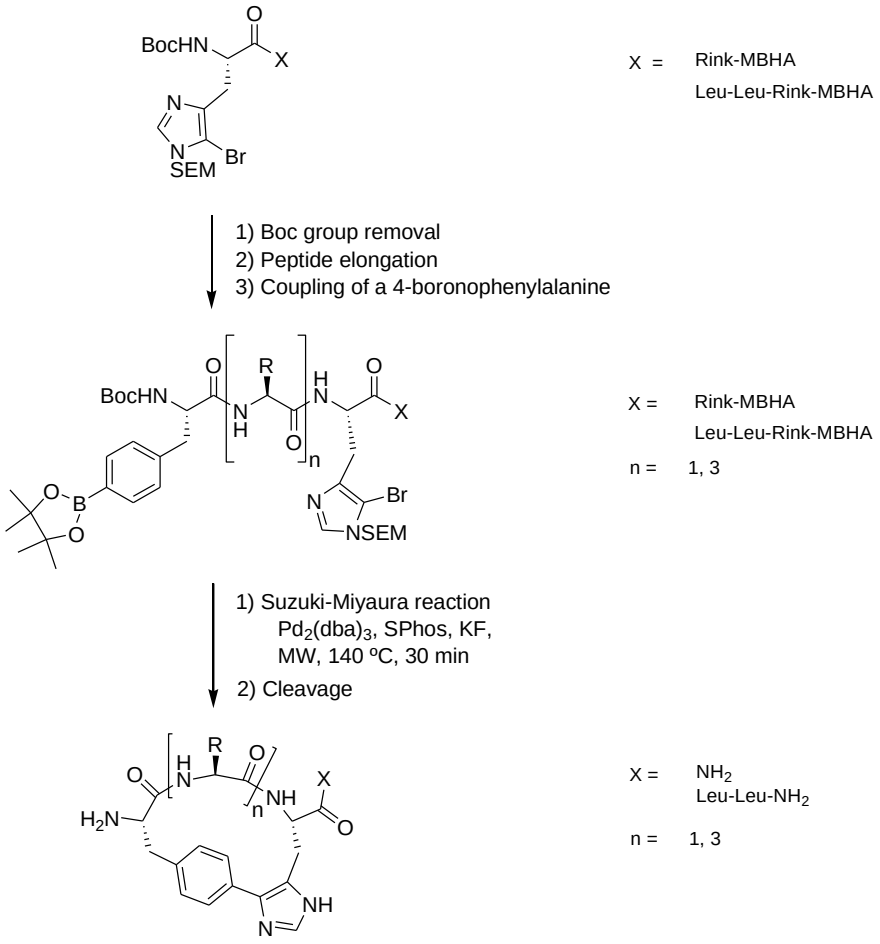

Scheme 9.4. Solid-phase synthesis of biaryl cyclic peptides containing a His-Phe linkage and bearing a histidine residue at the C-terminus.

Analysis of the results obtained revealed that the formation of the biaryl cyclic peptides containing a His-Phe linkage was more favoured when the histidine residue was located at the N-terminus.

For derivatives with the histidine residue at the N-terminus, **BPC760** and **BPC758** incorporating 3 or 5 amino acid residues in their ring, respectively, and a Leu-Leu spacer led to the best results, being the formation of **BPC760** the most favourable. Thus, biaryl cyclic peptides with a 7- or 8-amino acid ring (**55** and **56**) and those with 3 and 5 amino acids that do not contain the C-terminal Leu-Leu spacer (**BPC750** and **BPC752**) were obtained in lower purities. The latter result could be attributed to the steric hindrance posed by the resin. However, the cyclization was not improved by increasing the length of the spacer from 2 to 5 amino acids (**BPC758** and **BPC760** vs **BPC766** and **BPC768**). In addition, it was observed that the cyclization of the SEM-protected linear peptidyl resins gave similar results than the Me-protected ones (**BPC750** and **BPC758** vs **BPC772** and **57**) which pointed out that the presence of the bulkier SEM group at the imidazole ring did not hinder this intramolecular arylation.

Concerning the biaryl cyclic peptides with a His-Phe linkage bearing the histidine residue at the C-terminus, the preparation of **BPC776** and **BPC780** incorporating 3-amino acids in their ring gave the best results, being the formation of their 5-amino acid ring analogues **69** and **BPC778** unsuccessful. Similarly to the derivatives with the histidine at the N-terminus, the presence of a Leu-Leu spacer at the C-terminus improved the intramolecular Suzuki-Miyaura reaction. Accordingly, **BPC780** was obtained in higher purity than **BPC776**.

On the other hand, the biaryl cyclic peptides bearing a His-Tyr linkage were more easily formed than those with a His-Phe bond. However, in this case the macrocyclization leading to a His-Tyr linkage was more favoured when the histidine residue was located at the C-terminus. The synthesis of biaryl cyclic peptides of either 3 or 5 amino acids was accomplished in similar purities irrespective of the position of the histidine residue. Moreover, unlike the His-Phe peptides, the presence of the Leu-Leu spacer did not influence the intramolecular arylation step.

9.3. SYNTHESIS OF ARYLOMYCIN DERIVATIVES

Based on the structural and biological interest arisen from arylomycins (Figure 9.2), and taken into account that their solid-phase synthesis has not yet been reported, we decided to extend our previous methodology to the preparation of biaryl cyclic lipopeptides derived from arylomycins, containing a Phe-Tyr, a Tyr-Tyr, a His-Tyr or a phenylglycine (Phg)-Tyr linkage (Figure 9.3a). Four of these derivatives incorporating an extra lysine residue at the N-terminus of the lipopeptidyl tail were also prepared (Figure 9.3b).

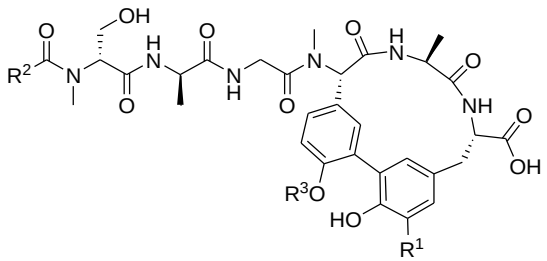

Arylomycins A R^1, R^3 = H, R^2 = fatty acid chain
Arylomycins B $R^1 = NO_2$, R^2 = fatty acid chain, R^3 = H

Figure 9.2. Structure of arylomycins A and B.

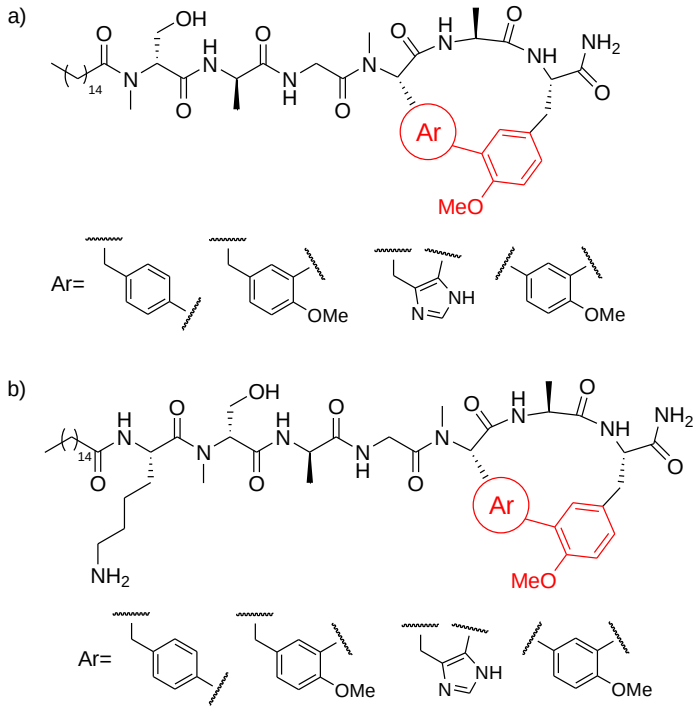

Figure 9.3. Structure of biaryl cyclic lipopeptides derived from arylomycins.

The general strategy for the solid-phase synthesis of the arylomycin analogues is represented in Scheme 9.5 for the biaryl cyclic lipohexapeptides. The first steps included the preparation of the corresponding linear peptidyl resin containing both an haloamino acid and a 3-boronotyrosine residue. These linear resins were obtained by Miyaura borylation of a trityl-protected 3-iodotyrosine dipeptidyl resin and subsequent coupling of the corresponding haloamino acid. The cyclization through the formation of a Phe-Tyr, a Tyr-Tyr or a Phg-Tyr linkage was performed via an intramolecular Suzuki-Miyaura reaction using $Pd_2(dba)_3$, SPhos and KF under microwave irradiation at 120 ºC for 30 min. The formation of the His-Tyr bond required a temperature of 140 ºC. The biaryl cyclic tripeptide cores were obtained in 65-92% HPLC purity and purified by reverse-phase column chromatography (99% purity). In agreement with previous studies, the cyclization involving the histidine residue was the most difficult.

After Boc group removal, the lipotripeptidyl or lipotetrapeptidyl tail was assembled to the biaryl cyclic core through subsequent steps of N-methylation, peptide elongation, N-methylation and acylation (Scheme 9.5). Biaryl cyclic lipopeptides lacking the Lys residue were difficult to analyse and characterize due to their high lipophilicity and their low propensity to ionize during the mass spectrometry analysis. Thus, no consistent data on the formation and purity of these compounds was obtained. In contrast, as expected, the sequences incorporating the extra lysine residue could be easily analysed and characterized by mass spectrometry, and they were obtained in purities ranging from 34-71%.

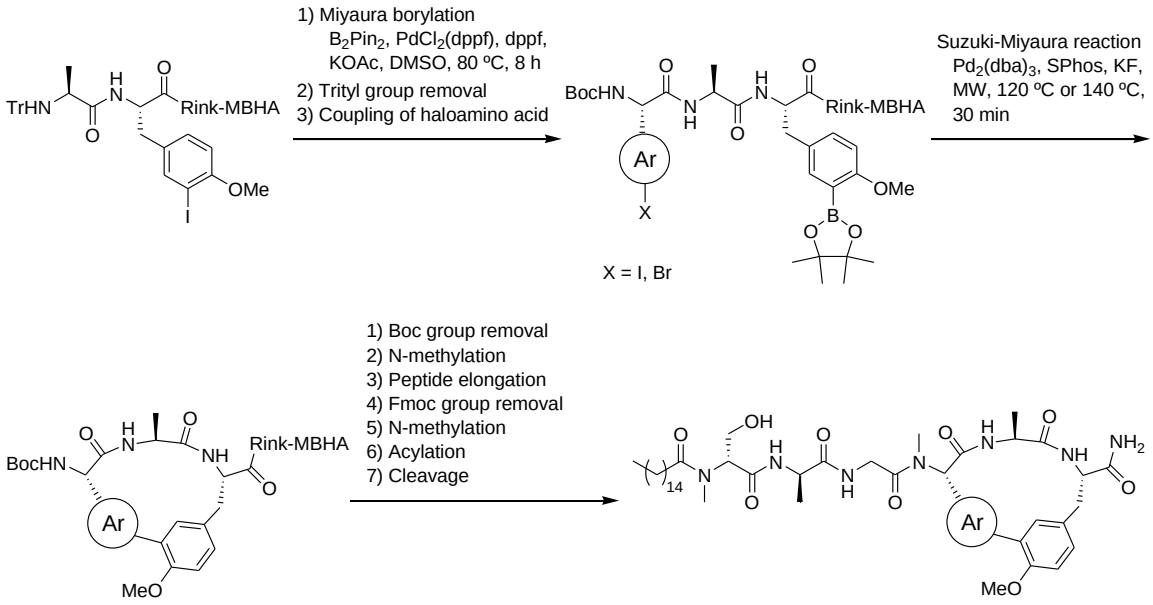

Scheme 9.5. Solid-phase synthesis of biaryl cyclic lipohexapeptides derived from arylomycins.

9.4. SOLID-PHASE SYNTHESIS OF BIARYL PEPTIDE ANALOGUES OF ACICULITINS

In the last part of this PhD thesis biaryl cyclic peptide analogues of aciculitins (Figure 9.4) containing commercially available amino acids were prepared. On the one hand, a strategy for the synthesis of analogues of the northern and the southern hemisphere of aciculitins was established (Figure 9.5a,b). This approach was then extended to the preparation of biaryl bicyclic derivatives incorporating a Phe-Phe, a Phe-Tyr, a His-Tyr or a Tyr-Tyr linkage (Figure 9.5c).

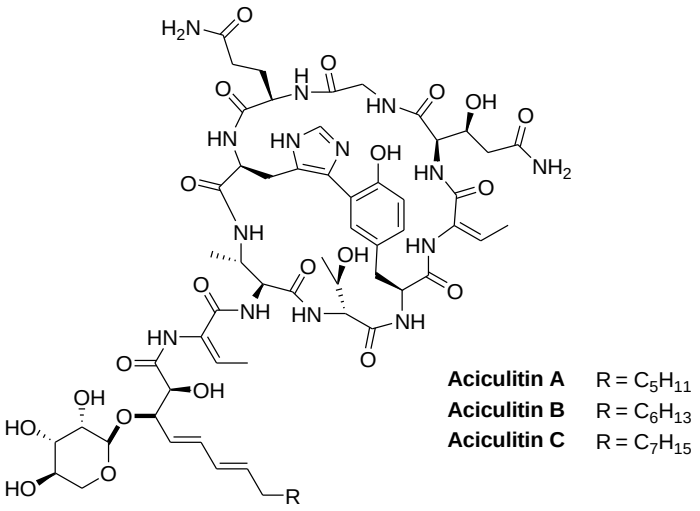

Figure 9.4. Structure of aciculitins A-C.

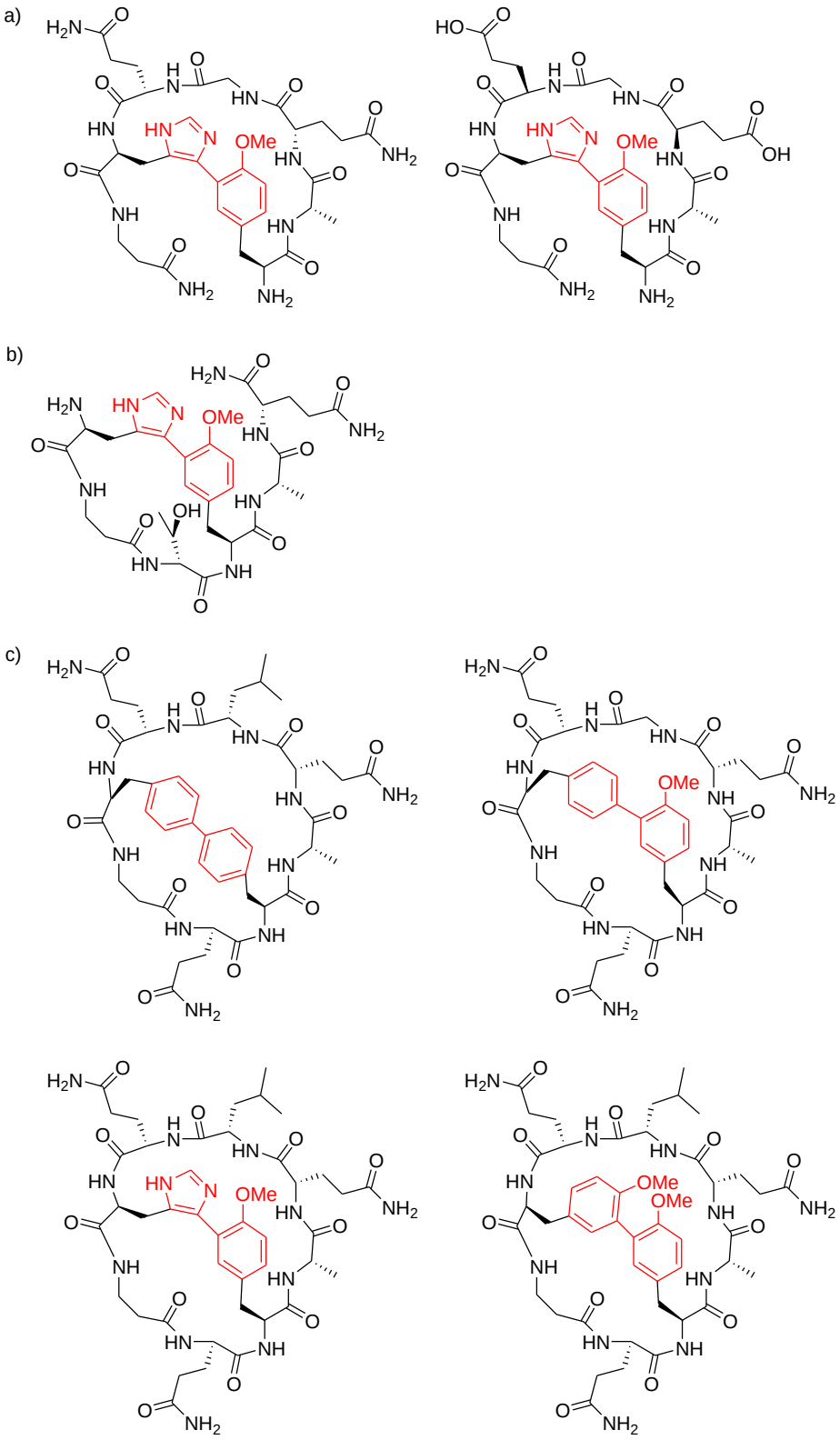

Figure 9.5. Structure of aciculitin derivatives. a) Northern and b) southern hemisphere analogues, c) biaryl bicyclic analogues

The synthesis of the northern analogues started by anchoring Fmoc-βAla-OH to a Fmoc-Rink-MBHA resin and it was followed by peptide elongation to yield the corresponding regioisomeric linear peptidyl resins incorporating a 5-bromohistidine at the C-terminus and a 3-boronotyrosine at the N-terminus (Scheme 9.6). The required Boc-protected 3-boronotyrosine residue was prepared in solution and coupled to the peptidyl resins. After optimizing the cyclization of these linear peptidyl resins by analyzing the influence of the reagent concentration, the catalyst, the ligand, the base, the temperature and the solvent, the best results were achieved using $Pd_2(dba)_3$, SPhos and KF under microwave irradiation at 140 ºC for 30 min in degassed DME/EtOH/H_2O (9:9:2). Moreover, we observed that the side-chain protecting group greatly influenced this cyclization step. Thus, when the bulky trityl group was used, this reaction was unsuccessful while the less sterically hindered Tmob group resulted to be more convenient. Following this procedure and after reverse-phase column chromatography purification, the northern analogues were obtained in 71-73% purity.

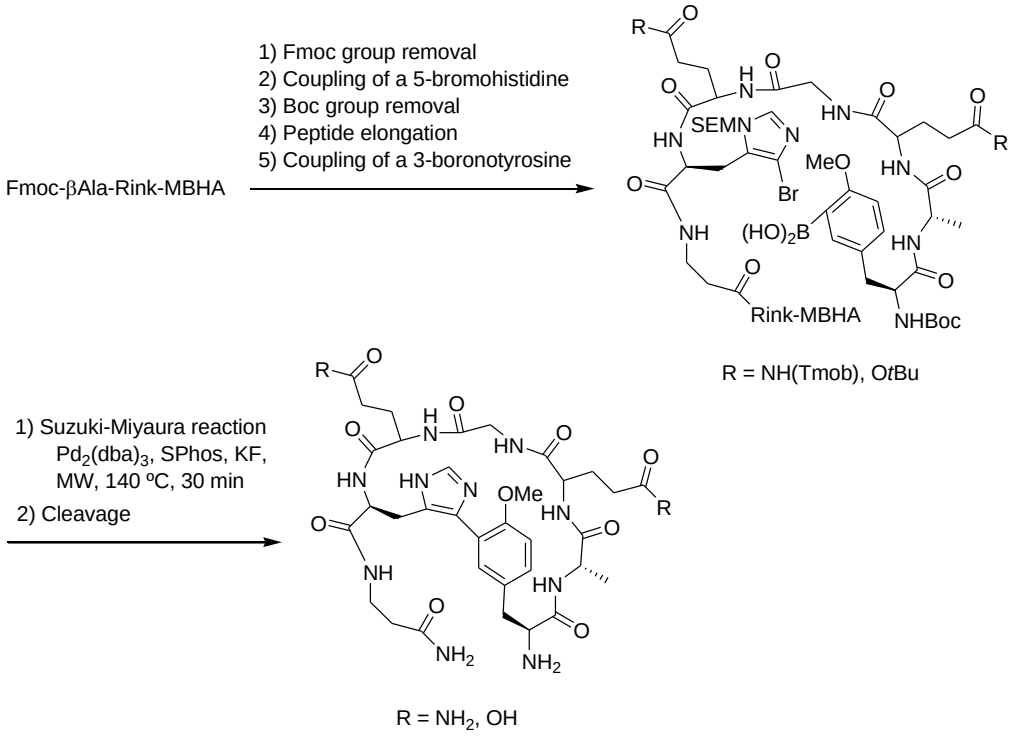

Scheme 9.6. Solid-phase synthesis of the northern hemisphere analogues of aciculitins.

Regarding the southern hemisphere analogue, its synthesis involved coupling of the C-terminal glutamine residue to a Rink-MBHA resin and followed the approach

described in section 9.2 for the biaryl cyclic peptides containing a His-Tyr linkage with the histidine at the N-terminus (Scheme 9.7). Thus, a linear peptidyl resin incorporating a 5-bromohistidine at the N-terminus and a 3-boronotyrosine at the C-terminus was prepared. With this aim, borylation of the corresponding trityl-protected 3-iodotyrosine peptidyl resin was performed prior to the coupling of the N-terminal 5-bromohistidine. Cyclization of this linear peptidyl resin was carried out under the Suzuki-Miyaura conditions described for the northern hemisphere analogues. Reverse-phase column chromatography provided the expected biaryl cyclic peptide in 84% HPLC purity.

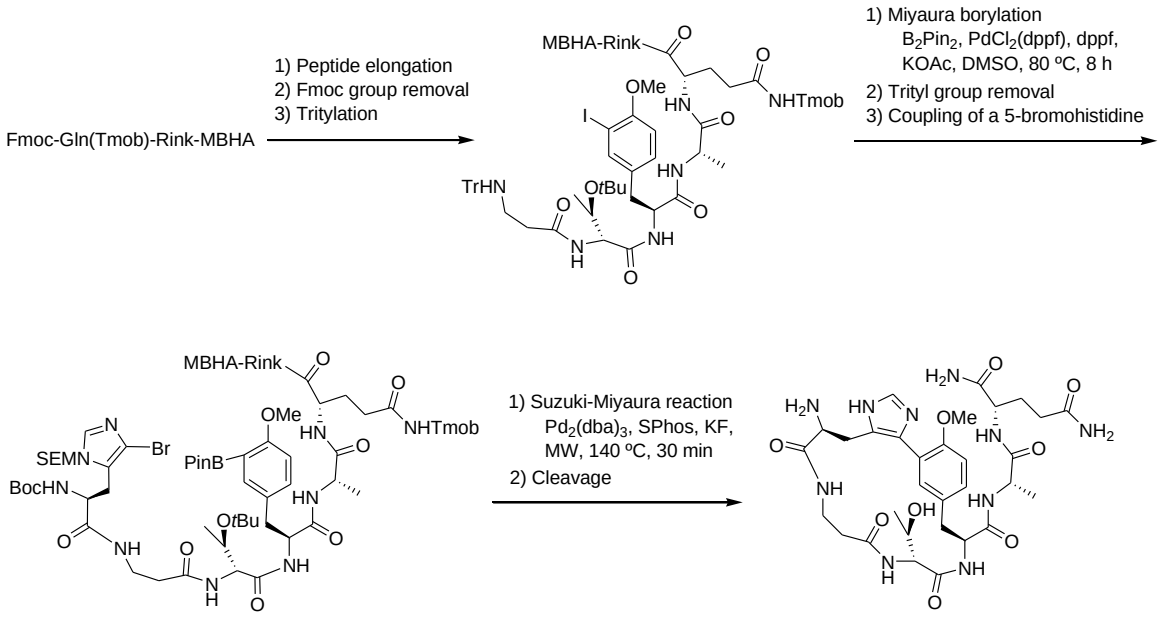

Scheme 9.7. Solid-phase synthesis of the southern hemisphere analogue of aciculitins.

The biaryl bicyclic peptides derived from aciculitins were synthesized following a methodology in which the key steps were the macroarylation and the macrolactamization (Scheme 9.8). In particular, this strategy involved: (i) the coupling of the glutamine residue of the southern hemisphere to a Fmoc-Rink-MBHA resin, (ii) the preparation of the corresponding linear peptidyl resin containing both the haloamino acid and the boronoamino acid, and protected at the N- and C-terminus with a Boc and a *p*NB group, respectively, (iii) the cyclization of this linear peptidyl resin through an intramolecular Suzuki-Miyaura cross-coupling reaction, and (iv) the macrolactamization of the resulting biaryl monocyclic peptide (Scheme 9.8).

Based on our previous results, the Suzuki-Miyaura macroarylation was performed with P(*o*-tolyl)$_3$ or SPhos as ligand depending on whether a 4-boronophenylalanine or a 3-boronotyrosine was involved in the formation of the biaryl bond. Moreover, this reaction was carried out at 120 ºC except for the preparation of the biaryl monocyclic peptide containing a His-Tyr bond which required 140 ºC. In addition, it was observed that these arylation conditions generally promoted the removal of the *p*NB protecting group of the carboxylic acid of the C-terminal glutamine residue. The formation of the expected biaryl bicyclic peptides was demonstrated by mass spectrometry. The spectra showed a peak at $[M - 18 + H]^+$ which was attributed to fragmentation during the analysis, as confirmed by tandem mass spectrometry.

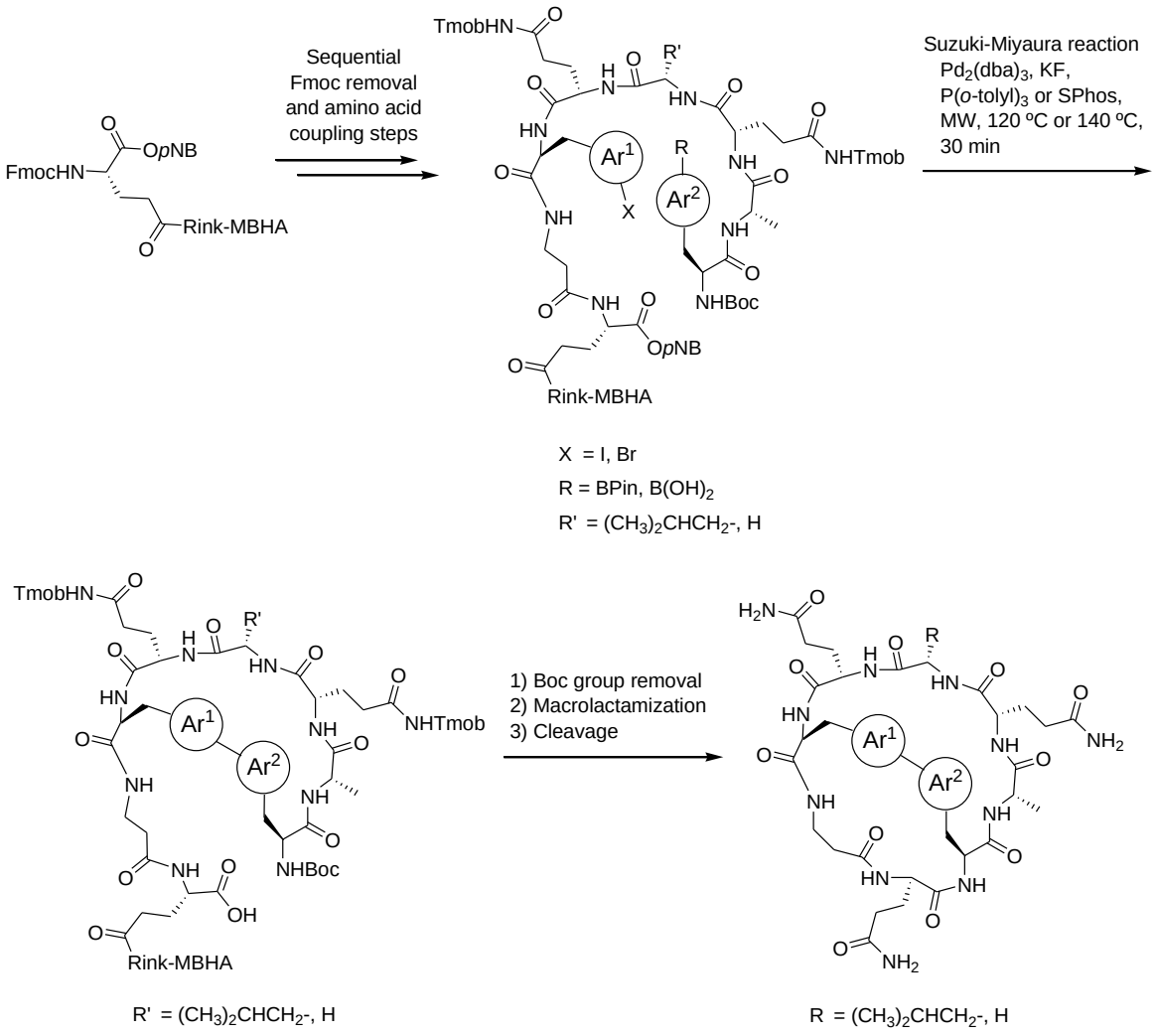

Scheme 9.8. General strategy for the solid-phase synthesis of biaryl bicyclic peptides derived from aciculitins.

To summarize, in this PhD thesis, we developed solid-phase synthetic methodologies for the preparation of biaryl linear, cyclic and bicyclic peptides through a microwave-assisted Suzuki-Miyaura cross-coupling reaction. The application of such methodologies allowed the formation of a wide range of biaryl peptides containing a Phe-Phe, a Phe-Tyr, a Tyr-Tyr, a His-Phe, a His-Tyr or a Phg-Tyr linkage.

9.5. REFERENCES

Afonso, A.; Cussó, O.; Feliu, L.; Planas, M. Solid-phase synthesis of biaryl cyclic peptides containing a 3-aryltyrosine. *Eur. J. Org. Chem.* **2012**, 6204-6211.

Afonso, A.; Feliu, L.; Planas, M. Solid-phase synthesis of biaryl cyclic peptides by borylation and microwave-assisted intramolecular Suzuki-Miyaura reaction. *Tetrahedron* **2011**, *67*, 2238-2245.

Afonso, A.; Rosés, C.; Planas, M.; Feliu, L. Biaryl peptides from 4-iodophenylalanine by solid-phase borylation and Suzuki-Miyaura cross-coupling. *Eur. J. Org. Chem.* **2010**, 1461-1468.

Badosa, E.; Ferré, R.; Planas, M.; Feliu, L.; Besalú, E.; Cabrefiga, J.; Bardají, E.; Montesinos, E. A library of linear undecapeptides with bactericidal activity against phytopathogenic bacteria. *Peptides* **2007**, *28*, 2276-2285.

Badosa, E.; Ferré, R.; Francés, J.; Bardají, E.; Feliu, L.; Planas, M.; Montesinos, E. Sporicidal activity of synthetic antifungal undecapeptides and control of *Penicillium* rot of apples. *Appl. Environ. Microbiol.* **2009**, *75*, 5563-5569.

Blondelle, S. E.; Lohner, K. Combinatorial libraries: a tool to design antimicrobial and antifungal peptide analogues having lytic specificities for structure-activity relationship studies. *Biopolymers* **2000**, *55*, 74-87.

Cerezo, V.; Amblard, M.; Martinez, J.; Verdié, P.; Planas, M.; Feliu, L. Solid-phase synthesis of 5-arylhistidines via a microwave-assisted Suzuki-Miyaura cross-coupling. *Tetrahedron* **2008**, *64*, 10538-10545.

Coste, A.; Bayle, A.; Marrot, J.; Evano, G. A convergent synthesis of the fully elaborated macrocyclic core of TMC-95A. *Org. Lett.* **2014**, *16*, 1306-1309.

Doan, N.; Bourgault, S.; Létourneau, M.; Fournier, A. Effectiveness of the Suzuki-Miyaura cross-coupling reaction for solid-phase peptide modification. *J. Comb. Chem.* **2008**, *10*, 44-51.

Inoue, M.; Sakazaki, H.; Furuyama, H.; Hirama, M. Total synthesis of TMC-95A. *Angew. Chem. Int. Ed.* **2003**, *42*, 2654-2657.

Feliu, L.; Planas, M. Cyclic peptides containing biaryl and biaryl ether linkages. *Int. J. Pept. Res. Ther.* **2005**, *11*, 53-97.

Ferre, R.; Badosa, E.; Feliu, L.; Planas, M.; Montesinos, E.; Bardají, E. Inhibition of plant-pathogenic bacteria by short synthetic cecropin A-melittin hybrid peptides. *Appl. Environ. Microbiol.* **2006**, *72*, 3302-3308.

Haug, B. E.; Stensen, W.; Svendsen, J. S. Application of the Suzuki-Miyaura cross-coupling to increase antimicrobial potency generates promising novel antibacterials. *Bioorg. Med. Chem. Lett.* **2007**, *17*, 2361-2364.

Kotha, S.; Lahiri, K. A new approach for modification of phenylalanine peptides by Suzuki-Miyaura coupling reaction. *Bioorg. Med. Chem. Lett.* **2001**, *11*, 2887-2890.

Kotha, S.; Lahiri, K. Application of the Suzuki-Miyaura cross-coupling reaction for the modification of phenylalanine peptides. *Biopolymers* **2003**, *69*, 517-528.

Le Quement, S. T.; Ishoey, M.; Petersen, M. T.; Thastrup, J.; Hagel, G.; Nielsen, T. E. Solid-phase synthesis of Smac peptidomimetics incorporating triazoloprolines and biarylalanines. *ACS Comb. Sci.* **2011**, *13*, 667-675.

Meyer, F.; Collins, J. C.; Borin, B.; Bradow, J.; Liras, S.; Limberakis, C.; Mathiowetz, A. M.; Philippe, L.; Price, D.; Song, K.; James, K. Biaryl-bridged macrocyclic peptides: Conformational constraint via carbogenic fusion of natural amino acid side chains. *J. Org. Chem.* **2012**, *77*, 3099-3114.

Oh, D.; Shin, S. Y.; Lee, S.; Kang, J. H.; Kim, S. D.; Ryu, P. D.; Hahm, K. S.; Kim, Y. Role of the hinge region and the tryptophan residue in the synthetic antimicrobial

peptides, cecropin A(1-8)-magainin 2(1-12) and its analogues, on their antibiotic activities and structures. *Biochemistry* **2000**, *39*, 11855-11864.

Roberts, T. C.; Smith, P. A.; Cirz, R. T.; Romesberg, F. E. Structural and initial biological analysis of synthetic Arylomycin A_2. *J. Am. Chem. Soc.* **2007**, *129*, 15830-15838.

Vilaró, M.; Arsequell, G.; Valencia, G.; Ballesteros, A.; Barluenga, J. Arylation of Phe and Tyr side chains of unprotected peptides by a Suzuki-Miyaura reaction in water. *Org. Lett.* **2008**, *10*, 3243-3245.

Waldmann, H.; He, Y.; Tan, H.; Arve, L.; Arndt, H. Flexible total synthesis of Biphenomycin B. *Chem. Commun.* **2008**, 5562-5564.

CHAPTER 10

General Conclusions

CHAPTER 10: General conclusions

❖ Biaryl linear antimicrobial undecapeptides

- A suitable solid-phase strategy for the synthesis of 5-arylhistidine-containing linear undecapeptides was established. The arylation of a peptidyl resin incorporating a 5-bromohistidine at position 1 with a commercially available arylboronic acid was accomplished using $Pd_2(dba)_3$, P(*o*-tolyl)$_3$ and KF under microwave irradiation at 110 ºC for 30 min, whereas the use of SPhos as ligand at 140 ºC was more effective when the 5-bromohistidine was at position 4.

- The replacement of a phenylalanine residue of the lead antimicrobial peptides **BP15**, **BP21**, **BP22**, **BP34** and **BP66** with a histidine or a 5-arylhistidine slightly decreased the antibacterial activity against *Erwinia amylovora*, *Pseudomonas syringae* and *Xanthomonas vesicatoria* as well as the antifungal activity against *Fusarium oxysporum*. Interestingly, the presence of the more hydrophilic histidine derivatives compared to phenylalanine led to less hemolytic peptides. The histidine-containing peptide **BP275** showed a better biological profile than its parent peptide **BP22**. Moreover, **BP281** and **BP282** were the most active 5-arylhistidine-containing undecapeptides with MIC values against these pathogens similar to those of their parent peptide **BP66**, being also less hemolytic.

❖ Biaryl cyclic peptides incorporating a His-Phe or a His-Tyr linkage

- It was developed a convenient solid-phase method for the preparation of biaryl cyclic peptides of different ring sizes incorporating a His-Phe or a His-Tyr linkage and bearing the histidine at the N- or C-terminus. The cyclization was achieved through a microwave-assisted intramolecular Suzuki-Miyaura cross-coupling of a linear peptidyl resin incorporating a 5-bromohistidine and a 4-boronophenylalanine or a 3-boronotyrosine. For the derivatives with the histidine at the N-terminus, the borylation step was carried out on solid-phase just before the coupling of the N-terminal 5-bromohistidine residue. In the case of the sequences with the histidine at

the C-terminus, the borono amino acid was prepared in solution and coupled to the N-terminus of the peptidyl resin.

- Formation of the His-Phe linkage required the use of $Pd_2(dba)_3$, P(*o*-tolyl)$_3$ and KF at 140 ºC for 30 min. This reaction was favoured when the His residue was located at the N-terminus. For these derivatives, the best results were obtained for the biaryl cyclic peptides with a 3- or 5-amino acid ring and bearing a C-terminal Leu-Leu spacer. The imidazole protection did not influence the intramolecular arylation. Analogues with the histidine at the C-terminus followed a similar trend. However, in this case, the formation of the 5-amino acid ring derivatives failed.

- The His-Tyr linkage was more easily formed than the His-Phe bond. Its formation was accomplished under the same reaction conditions than those for the preparation of the His-Phe derivatives, but using SPhos as ligand. In this case, the highest purities were obtained for those derivatives with the His at the C-terminus and it was observed that the presence of the Leu-Leu spacer did not influence the cyclization. Biaryl cyclic peptides of 3 or 5 amino acids were prepared incorporating the His at either the N- or the C-terminus.

❖ **Arylomycin derivatives**

- The extension of the above methodology allowed the preparation of arylomycin derivatives containing a Phe-Tyr, a Tyr-Tyr, a His-Tyr or a Phg-Tyr linkage. The key steps of this approach included the synthesis of a linear peptidyl resin incorporating a haloamino acid and a 3-boronotyrosine residue, its cyclization via an intramolecular Suzuki-Miyaura reaction, and the elongation of the lipopeptidyl tail. This work constituted the first report on the total solid-phase synthesis of arylomycin analogues.

- The Suzuki-Miyaura reaction was performed using $Pd_2(dba)_3$, SPhos and KF under microwave irradiation at 120 ºC for 30 min, except for the formation of the His-Tyr linkage that required 140 ºC. Thus, the preparation of the arylomycin analogues incorporating this linkage was the most troublesome.

- Due to the hydrophobicity of these biaryl cyclic lipopeptides and the absence of ionisable groups, the presence of a lysine residue in the lipopeptidyl tail facilitated their HPLC analysis and their mass spectrometry characterization.

❖ **Biaryl peptide analogues of aciculitins**

- Biaryl cyclic peptide analogues of the northern and the southern hemispheres of aciculitins have been successfully prepared. The procedure described above for the synthesis of biaryl cyclic peptides containing a His-Tyr linkage was followed. Thus, the cyclization was accomplished through the intramolecular arylation of the corresponding regioisomeric linear peptidyl resins incorporating a 5-bromohistidine residue and a 3-boronotyrosine residue by using $Pd_2(dba)_3$, SPhos and KF under microwave irradiation at 140 ºC for 30 min.

- The use of a trityl as protecting group of the side-chain glutamine residues difficulted the solid-phase cyclization of the linear peptidyl resins. The less bulky 2,4,6-trimethoxybenzyl (Tmob) protecting group was required.

- The two northern hemisphere analogues where obtained in 71 and 73% purity and the southern hemisphere analogue in 84% purity after chromatographic purification.

- Four biaryl bicyclic peptides derived from aciculitins were synthesized via an intramolecular Suzuki-Miyaura arylation of the corresponding linear peptidyl resins incorporating a 4-iodophenylalanine, a 5-bromohistidine or a 3-iodotyrosine residue at the C-terminus and a 4-boronophenylalanine or 3-boronotyrosine residue at the N-terminus, and subsequent macrolactamization of the resulting biaryl monocyclic peptidyl resin.

- The formation of the biaryl bond involving a 4-boronophenylalanine was performed using P(*o*-tolyl)$_3$, whereas SPhos was employed for the cyclization of sequences containing a 3-boronotyrosine. The reaction temperature was of 120 ºC except for the formation of the His-Tyr linkage which was accomplished at 140 ºC.

- Biaryl bicyclic peptides were characterized by mass spectrometry. This work constituted the first synthetic approach to aciculitins which could be extended to the preparation of other synthetic or naturally occurring biaryl bicyclic peptides.

ANNEX

SOLID-PHASE SYNTHESIS OF 5-ARYLHISTIDINE-CONTAINING PEPTIDES: FROM LINEAR ANTIMICROBIAL PEPTIDES TO CYCLIC PEPTIDES DERIVED FROM ARYLOMYCINS AND ACICULITINS

SUPPORTING INFORMATION CHAPTER 3

Solid-phase synthesis of 5-arylhistidine-containing peptides with antimicrobial activity via a microwave-assisted Suzuki-Miyaura cross-coupling

Iteng Ng Choi, Marta Soler, Vanessa Cerezo, Esther Badosa, Emilio Montesinos, Marta Planas* and Lidia Feliu*

TABLE OF CONTENTS

Copies of HPLC, MS and NMR spectra

1. SEM-protected 5-bromohistidines 9

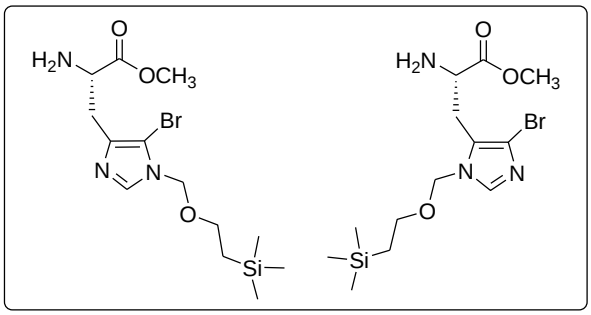

HPLC (λ = 220 nm)

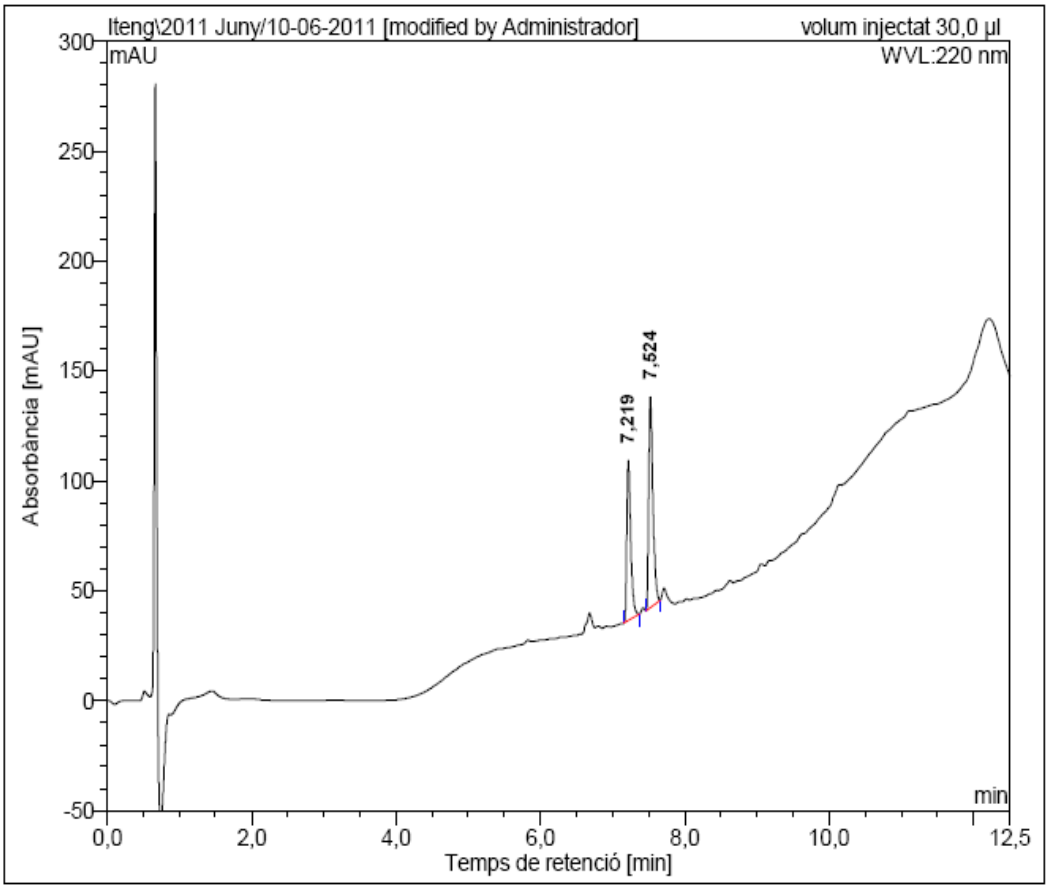

No.	Temps retenció min	alçada mAU	Area mAU*min	Area relativa %
1	7,22	72,787	4,706	41,85
2	7,52	95,613	6,539	58,15
Total:		168,399	11,245	100,00

ESI-MS *m/z* (%)

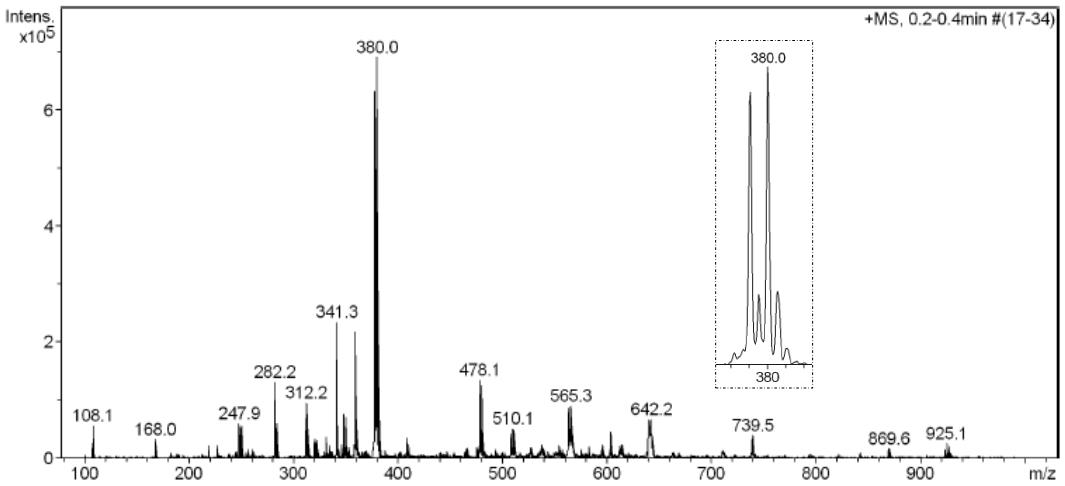

^{1}H-RMN (400 MHz, DMSO-d_6) δ (ppm)

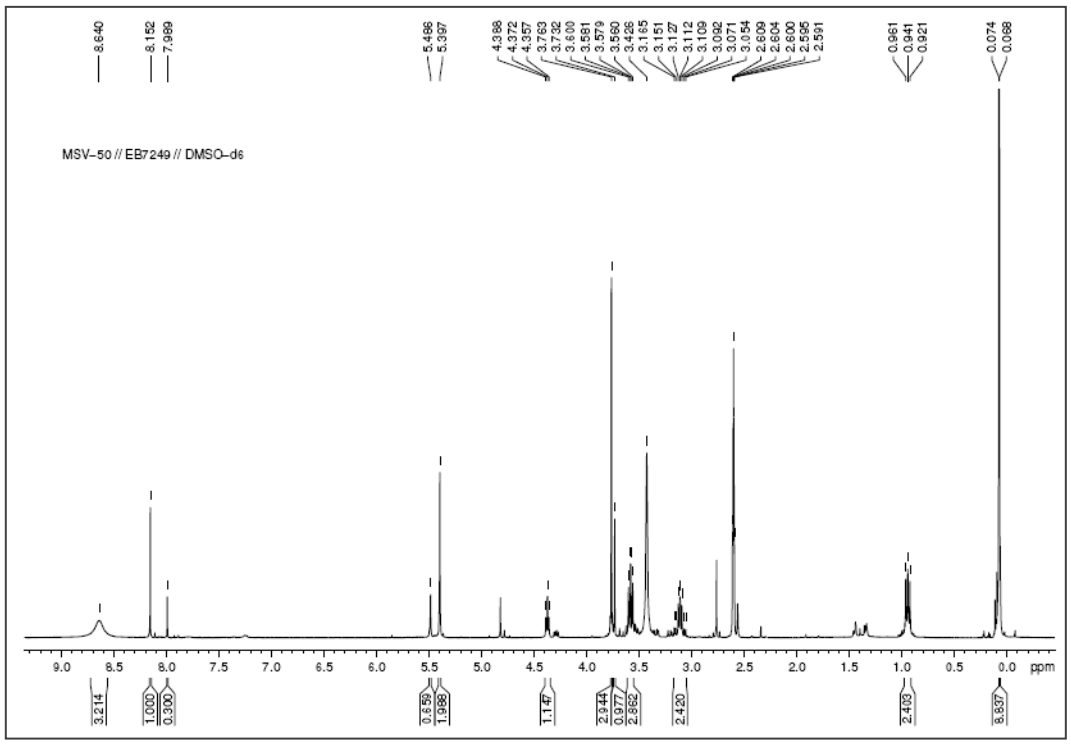

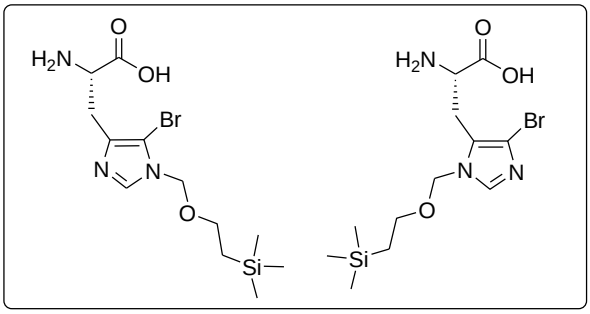

HPLC (λ = 220 nm)

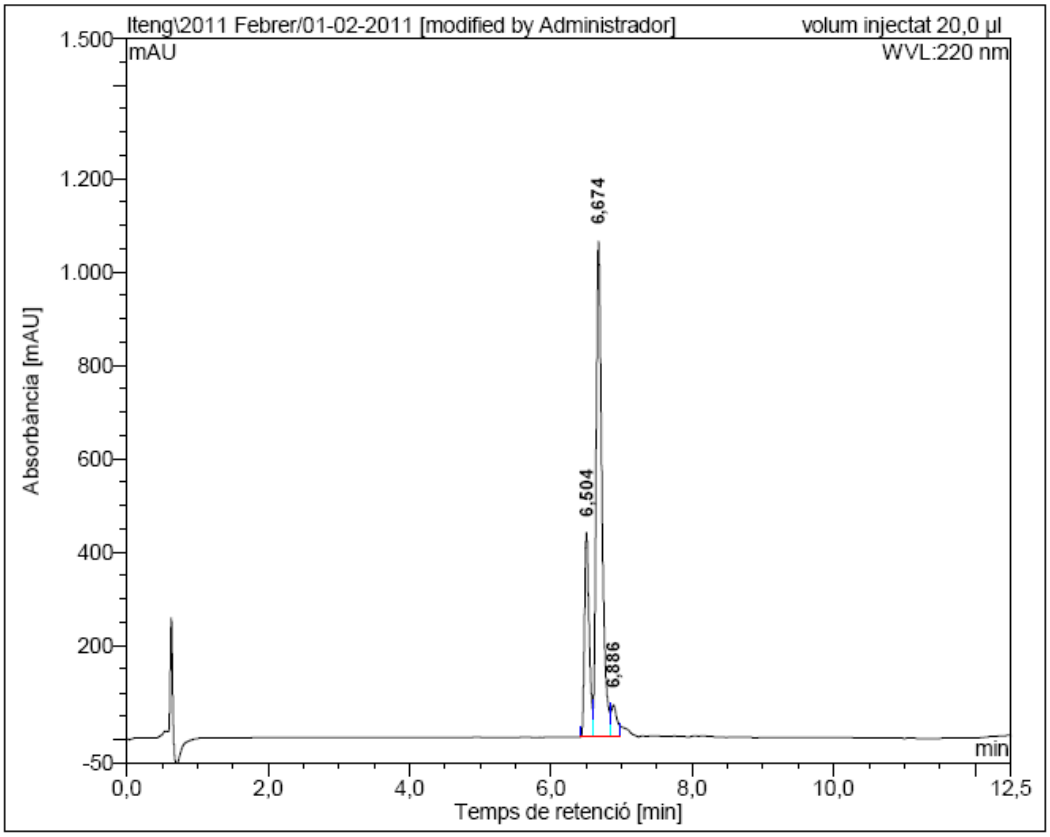

No.	Temps retenció min	alçada mAU	Area mAU*min	Area relativa %
1	6,50	437,158	33,292	23,62
2	6,67	1059,694	101,517	72,03
3	6,89	68,034	6,134	4,35
Total:		1564,885	140,943	100,00

ESI-MS *m/z* (%)

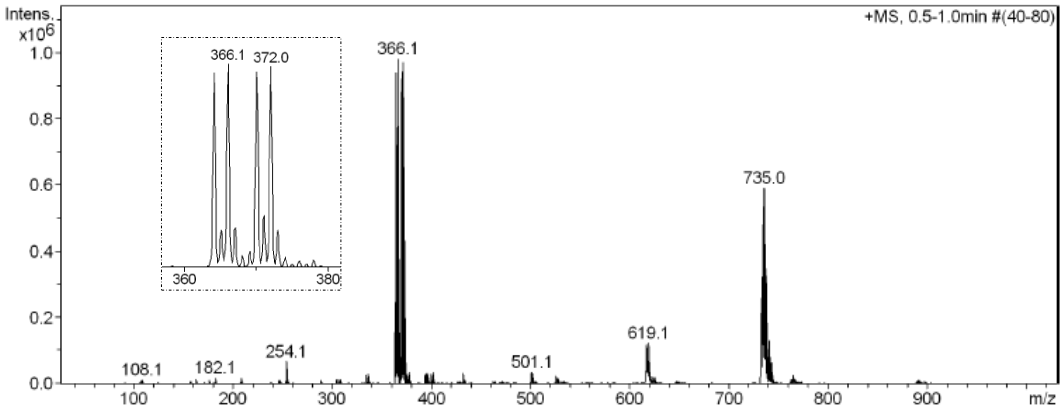

^{1}H-RMN (400 MHz, DMSO-d_6) δ (ppm)

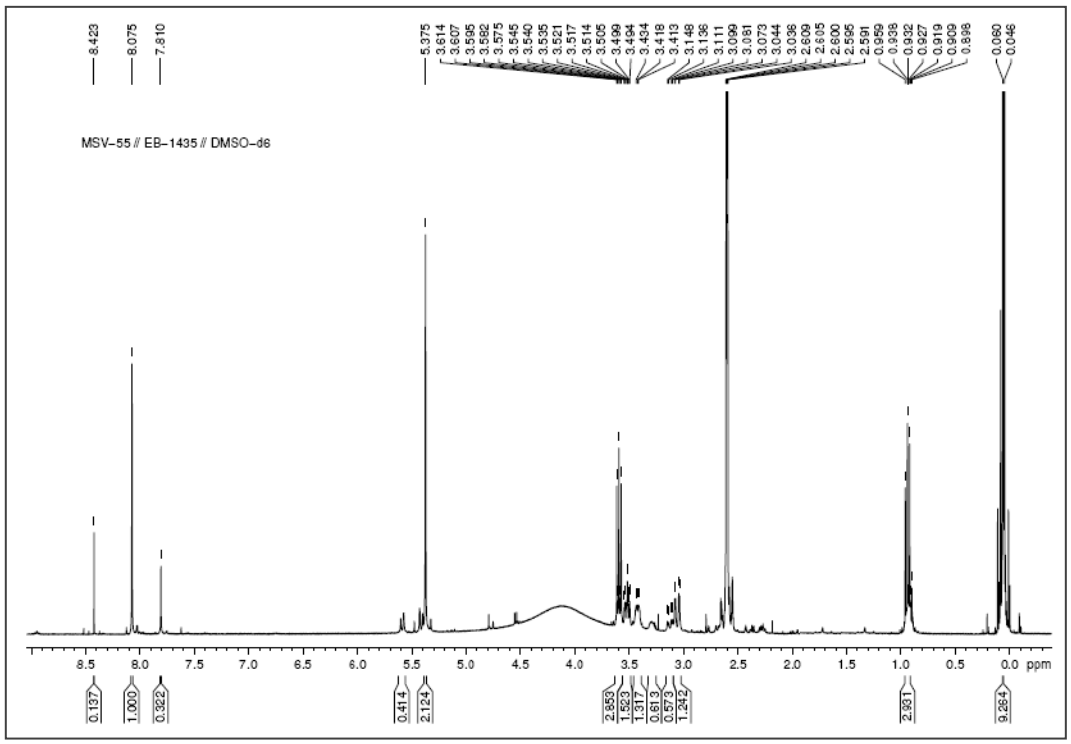

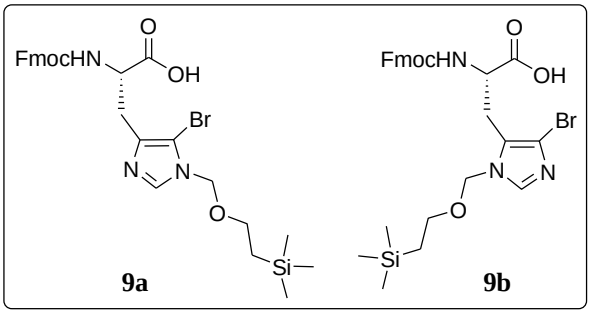

HPLC (λ = 220 nm)

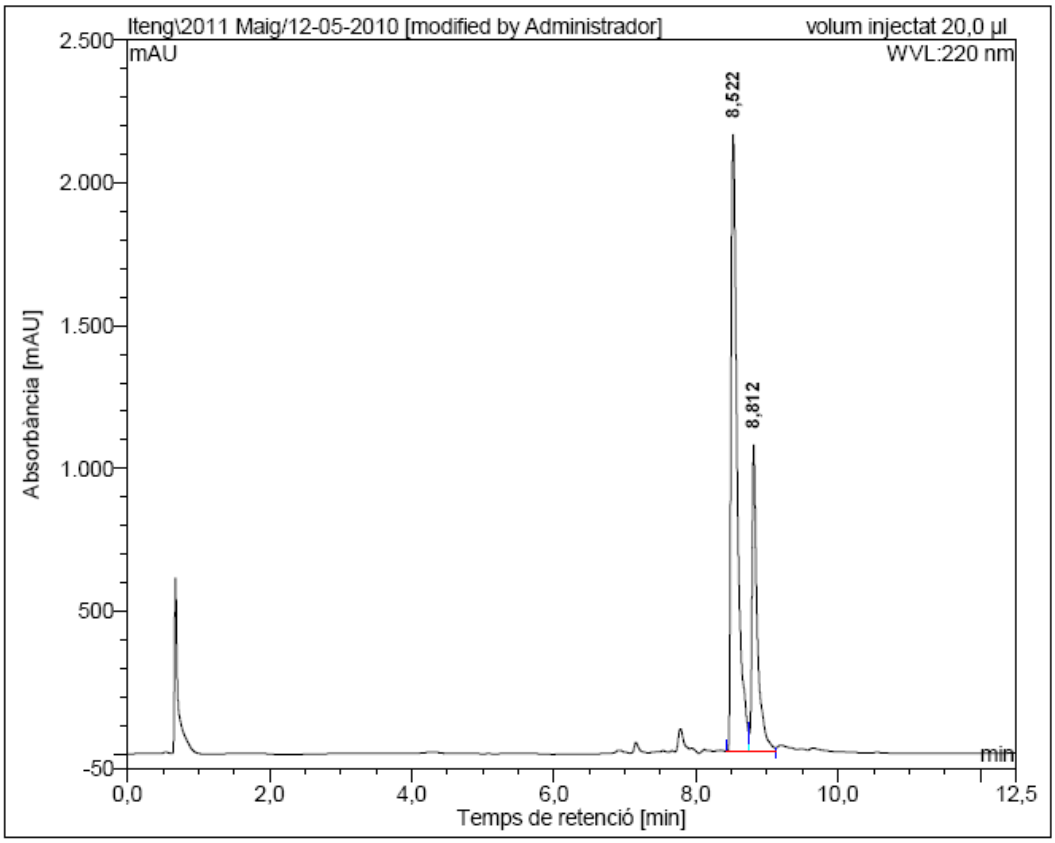

No.	Temps retenció min	alçada mAU	Area mAU*min	Area relativa %
1	8,52	2157,879	220,223	70,77
2	8,81	1071,047	90,949	29,23
Total:		3228,926	311,172	100,00

ESI-MS *m/z* (%)

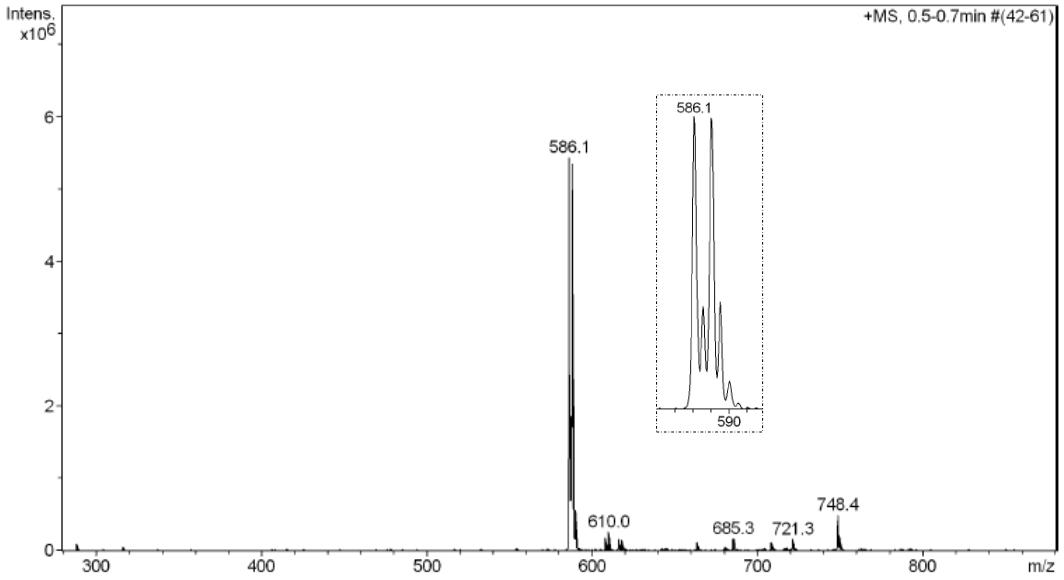

^{1}H-RMN (400 MHz, $CDCl_3$) δ (ppm)

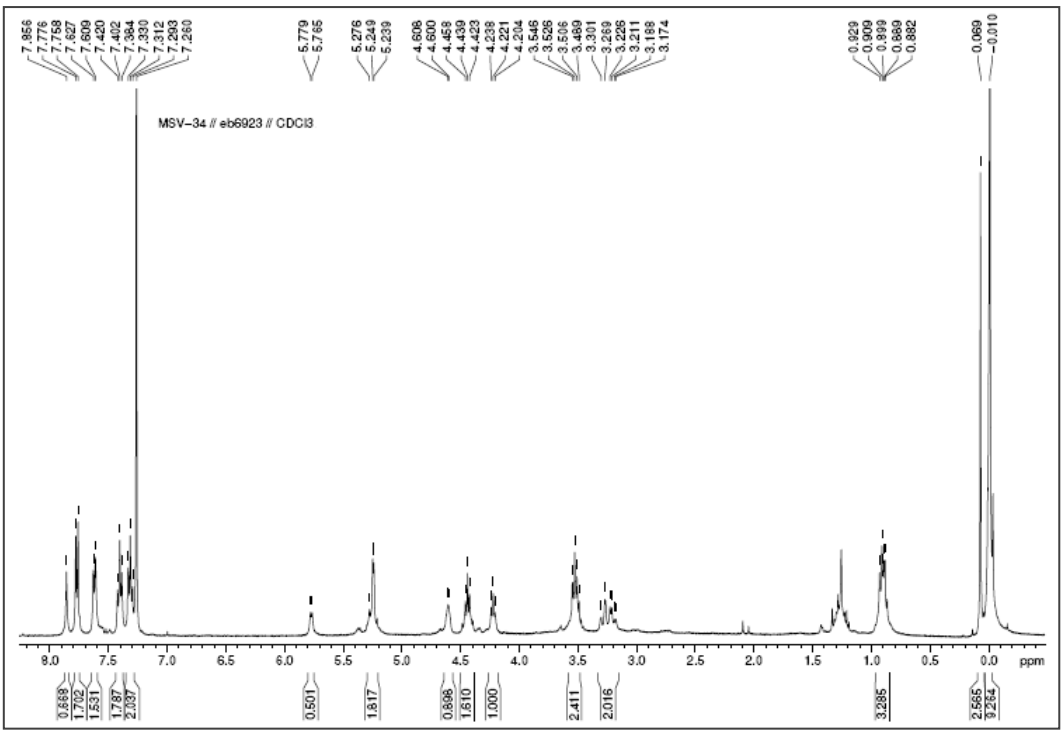

2. H-His(5-Ph)-Lys-Lys-Ile-Leu-Lys-Tyr-Leu-NH_2 (1) and H-His(5-Ar)-Lys-Leu-Phe-Lys-Lys-Ile-Leu-Lys-Phe-Leu-NH_2 (BP281, BP282, and BP283)

H-His(5-Br)-Lys-Lys-Ile-Leu-Lys-Tyr-Leu-NH_2 (5)

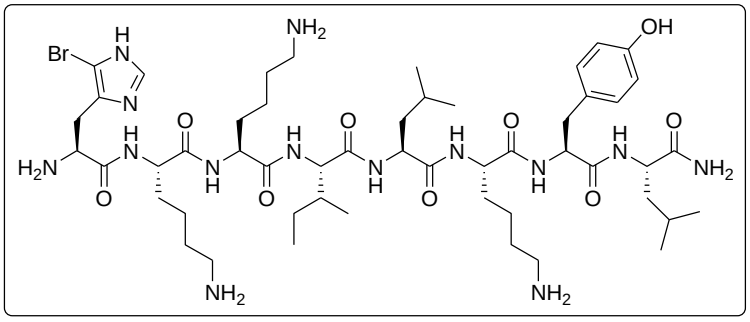

HPLC (λ = 220 nm)

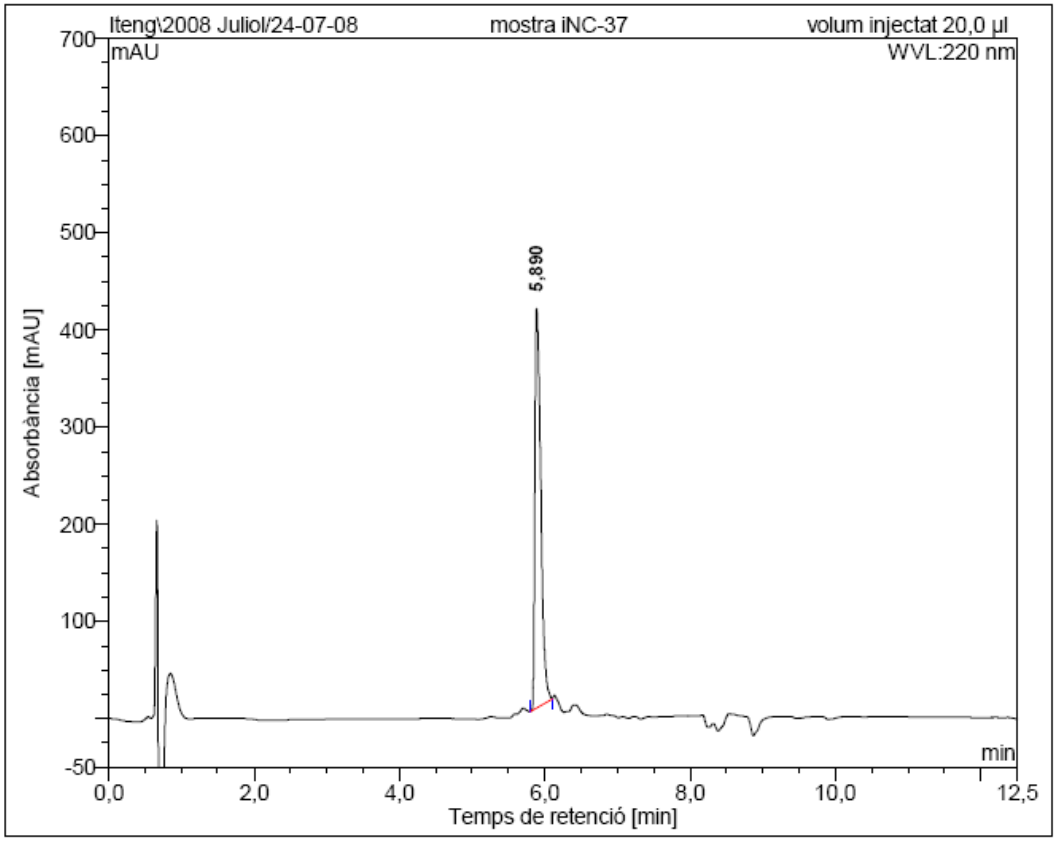

No.	Temps retenció min	alçada mAU	Area mAU*min	Area relativa %
1	5,89	411,031	38,763	100,00
Total:		411,031	38,763	100,00

ESI-MS *m/z* (%)

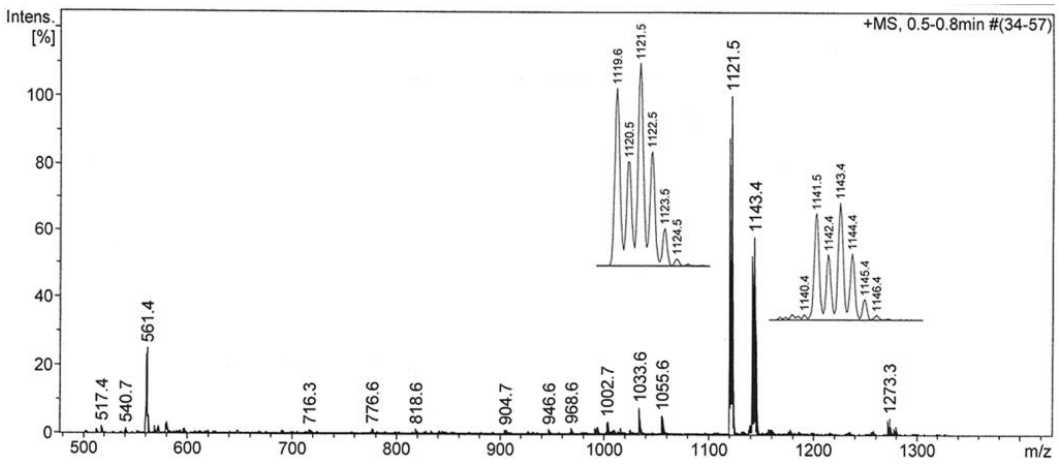
Intens.
[%]
+MS, 0.5-0.8min #(34-57)
100
80
60
40
20
0
500
600
700
800
900
1000
1100
1200
1300
m/z
561.4
517.4
540.7
716.3
776.6
818.6
904.7
946.6
968.6
1002.7
1033.6
1055.6
1121.5
1143.4
1273.3
1119.6
1120.5
1121.5
1122.5
1123.5
1124.5
1140.4
1141.5
1142.4
1143.4
1144.4
1145.4
1146.4

H-His(5-Br)-Lys-Leu-Phe-Lys-Lys-Ile-Leu-Lys-Phe-Leu-NH_2 (8)

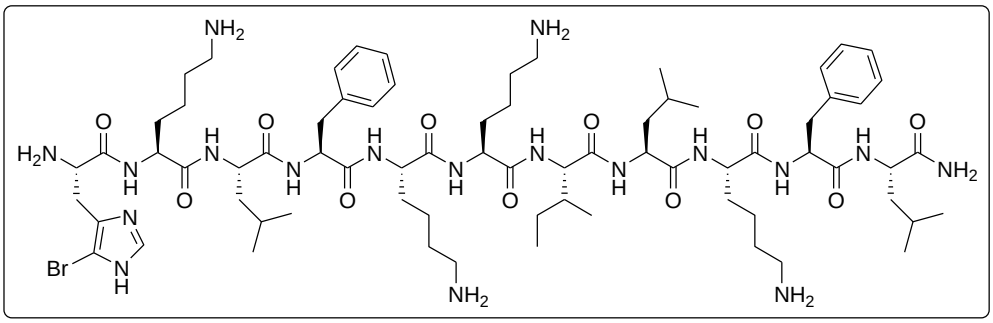

HPLC (λ = 220 nm)

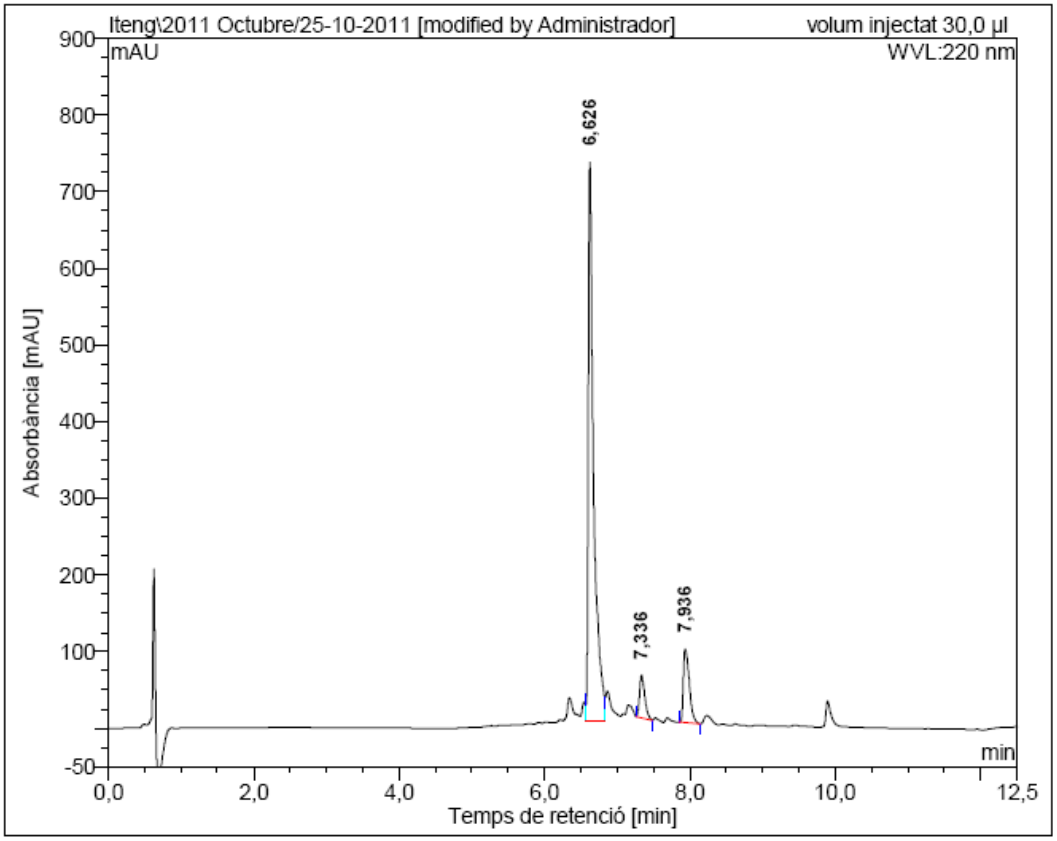

No.	Temps retenció min	alçada mAU	Area mAU*min	Area relativa %
1	6,63	727,733	62,992	82,09
2	7,34	55,213	4,607	6,00
3	7,94	95,883	9,140	11,91
Total:		878,829	76,739	100,00

ESI-MS *m/z* (%)

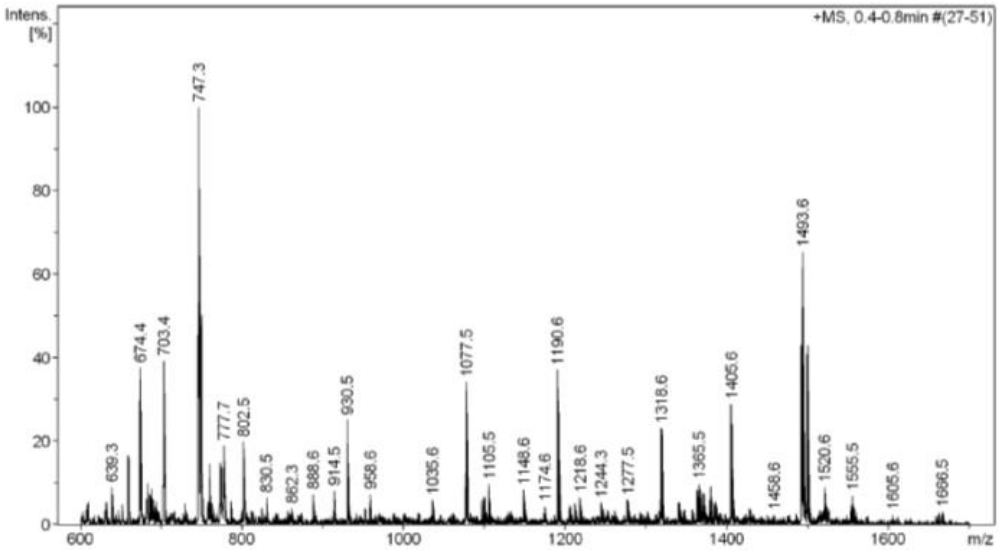
Intens.
[%]
+MS, 0.4-0.8min #(27-51)
747.3
674.4
703.4
1493.6
1077.5
1190.6
930.5
1318.6
1405.6
777.7
802.5
639.3
830.5
862.3
888.6
914.5
958.6
1035.6
1105.5
1148.6
1174.6
1218.6
1244.3
1277.5
1365.5
1458.6
1520.6
1555.5
1605.6
1666.5
100
80
60
40
20
0
600
800
1000
1200
1400
1600
m/z

H-His(5-Ph)-Lys-Lys-Ile-Leu-Lys-Tyr-Leu-NH_2 (1)

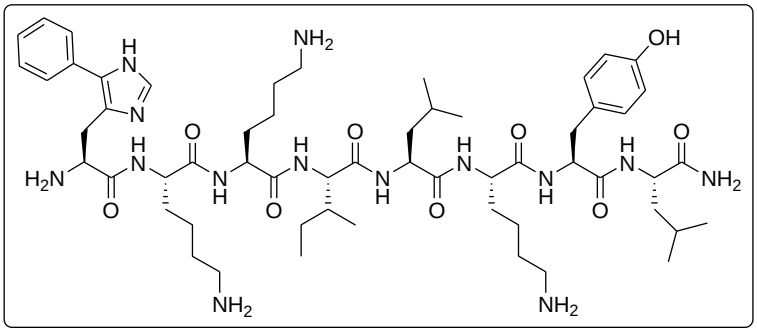

HPLC (λ = 220 nm)

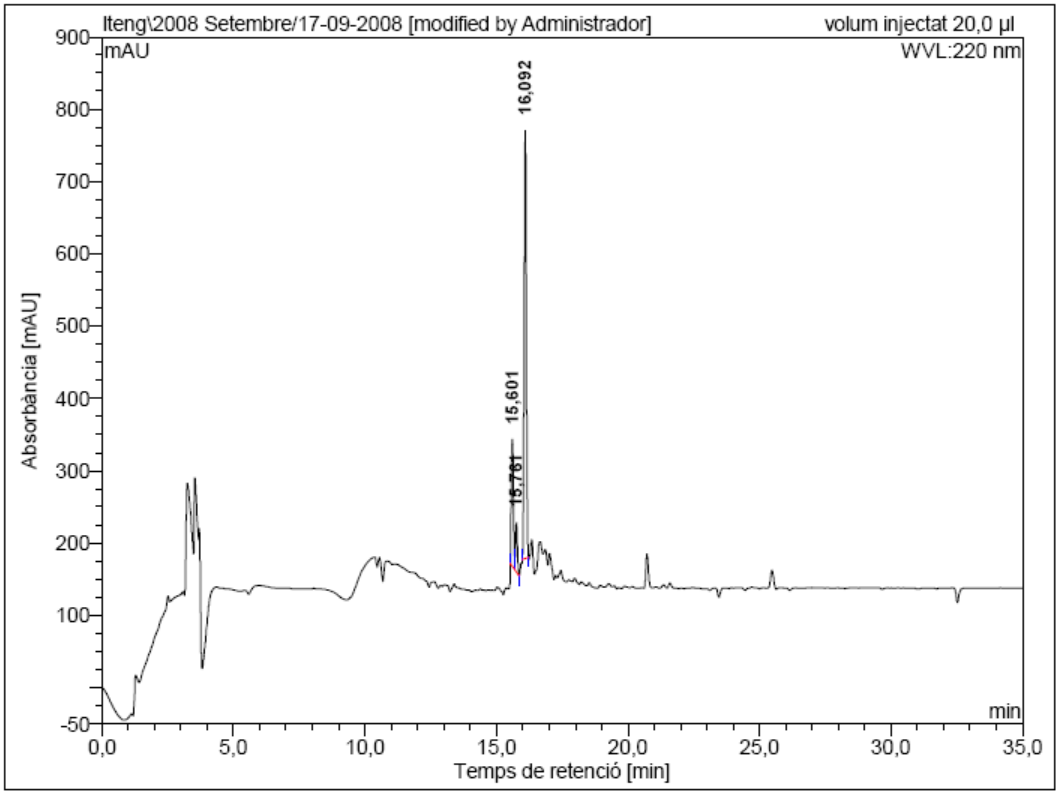

No.	Temps retenció min	alçada mAU	Area mAU*min	Area relativa %
1	15,60	174,742	15,772	20,57
2	15,76	67,602	5,458	7,12
3	16,09	591,758	55,433	72,31
Total:		834,101	76,662	100,00

ESI-MS *m/z* (%)

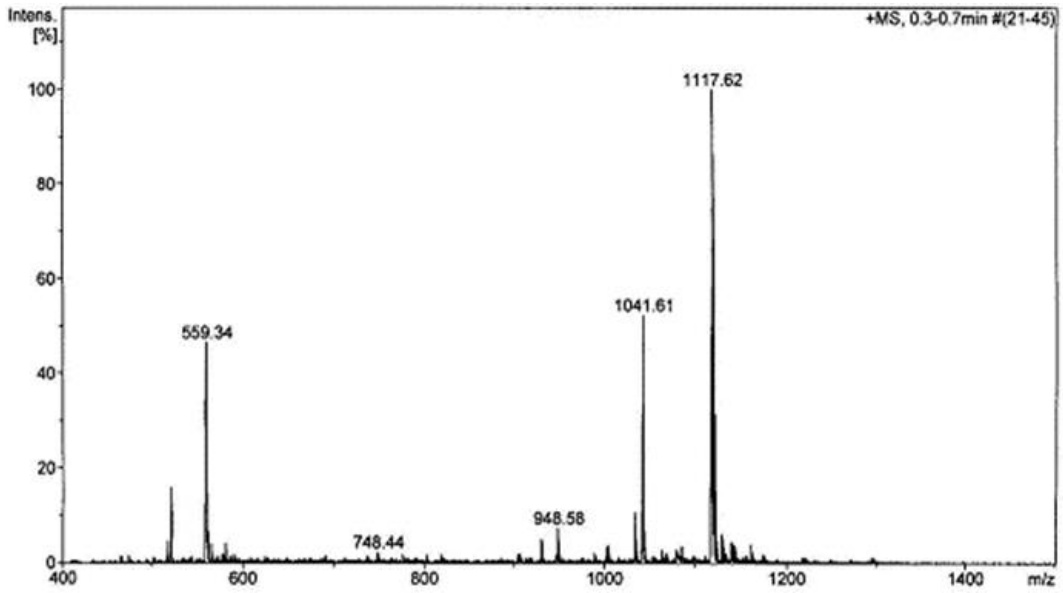
Intens.
[%]
+MS, 0.3-0.7min #(21-45)
1117.62
1041.61
559.34
948.58
748.44
100
80
60
40
20
0
400
600
800
1000
1200
1400
m/z

H-His(5-Ph)-Lys-Leu-Phe-Lys-Lys-Ile-Leu-Lys-Phe-Leu-NH_2 (BP281)

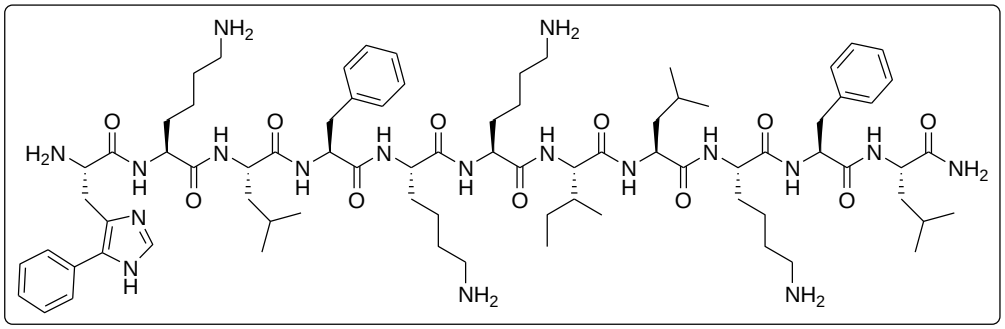

HPLC (λ = 220 nm)

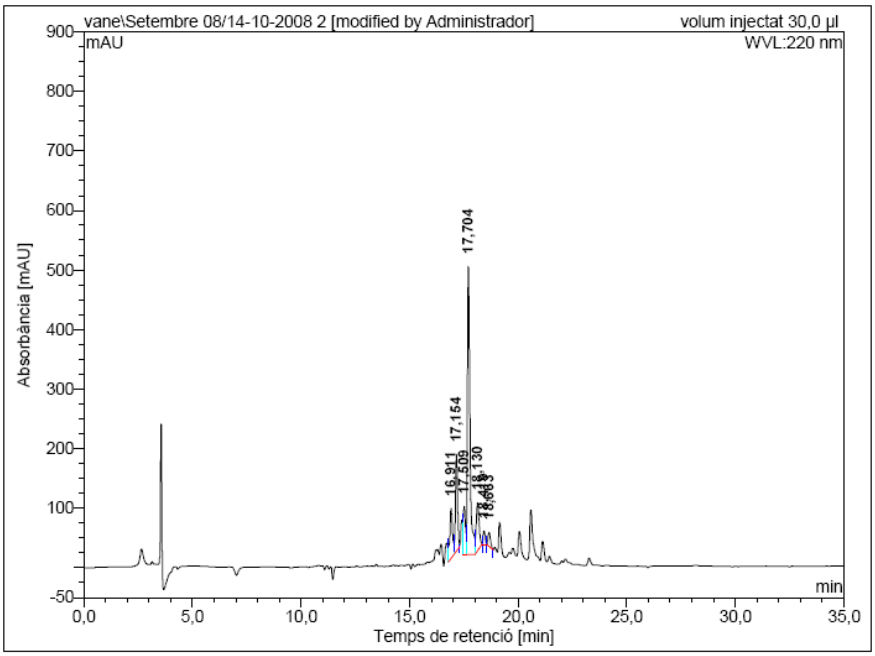

No.	Temps retenció min	alçada mAU	Area mAU*min	Area relativa %
1	16,91	84,215	12,295	9,64
2	17,15	162,647	19,325	15,15
3	17,51	82,318	11,000	8,62
4	17,70	484,164	66,478	52,10
5	18,13	80,438	12,822	10,05
6	18,42	22,328	2,533	1,99
7	18,66	23,673	3,133	2,46
Total:		939,784	127,587	100,00

ESI-MS *m/z* (%)

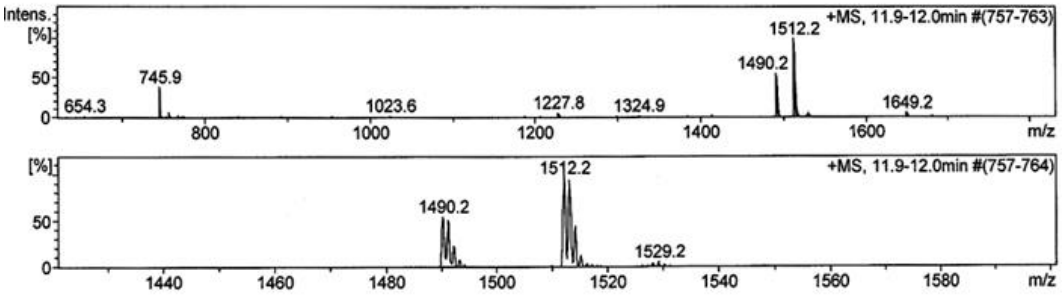

H-His(5-(3-(OH)-C_6H_4))-Lys-Leu-Phe-Lys-Lys-Ile-Leu-Lys-Phe-Leu-NH_2 (BP282)

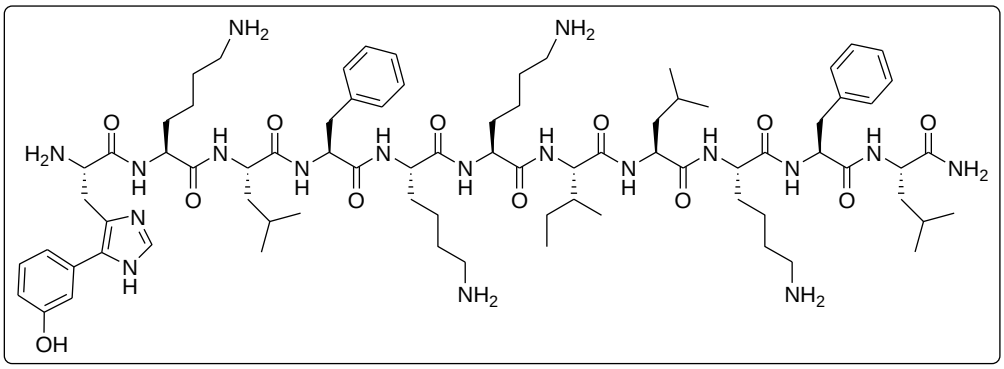

HPLC (λ = 220 nm)

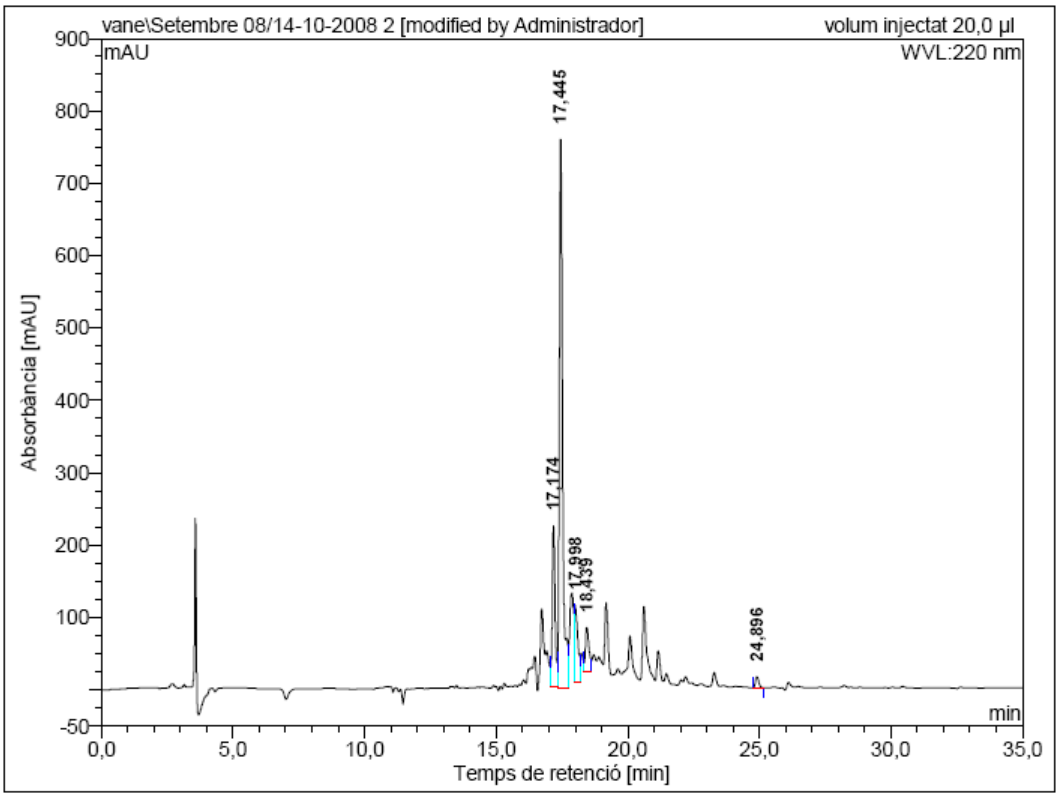

No.	Temps retenció min	alçada mAU	Area mAU*min	Area relativa %
1	17,17	221,730	27,689	16,67
2	17,44	758,243	109,813	66,13
3	18,00	104,584	16,475	9,92
4	18,44	60,377	9,896	5,96
5	24,90	15,262	2,182	1,31
Total:		1160,195	166,054	100,00

ESI-MS *m/z* (%)

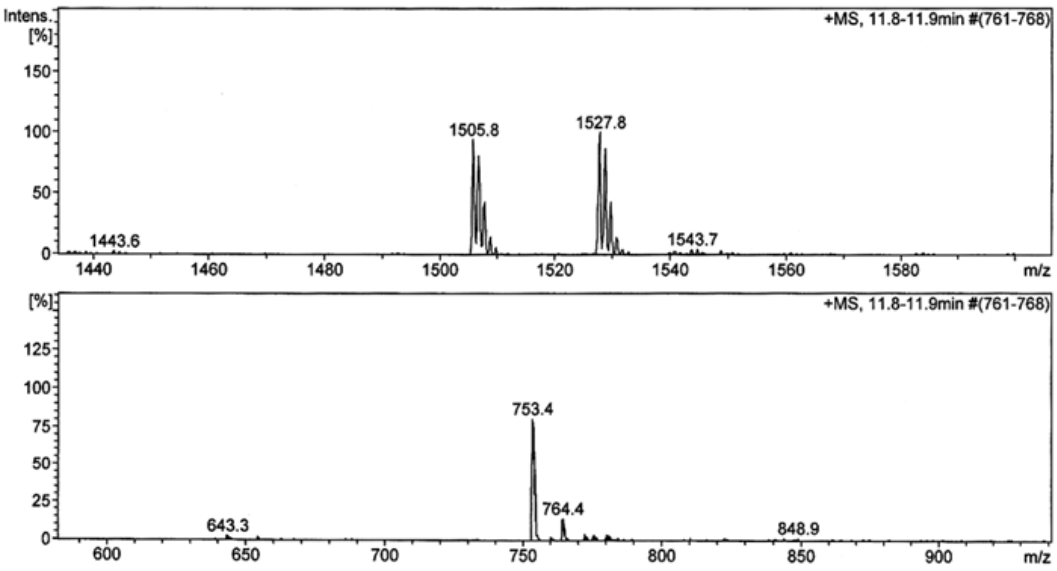
Intens.
[%]
+MS, 11.8-11.9min #(761-768)
150
100
50
0
1505.8
1527.8
1443.6
1543.7
1440
1460
1480
1500
1520
1540
1560
1580
m/z
[%]
+MS, 11.8-11.9min #(761-768)
125
100
75
50
25
0
753.4
764.4
643.3
848.9
600
650
700
750
800
850
900
m/z

H-His(5-(3-(NO_2)-C_6H_4))-Lys-Leu-Phe-Lys-Lys-Ile-Leu-Lys-Phe-Leu-NH_2 (BP283)

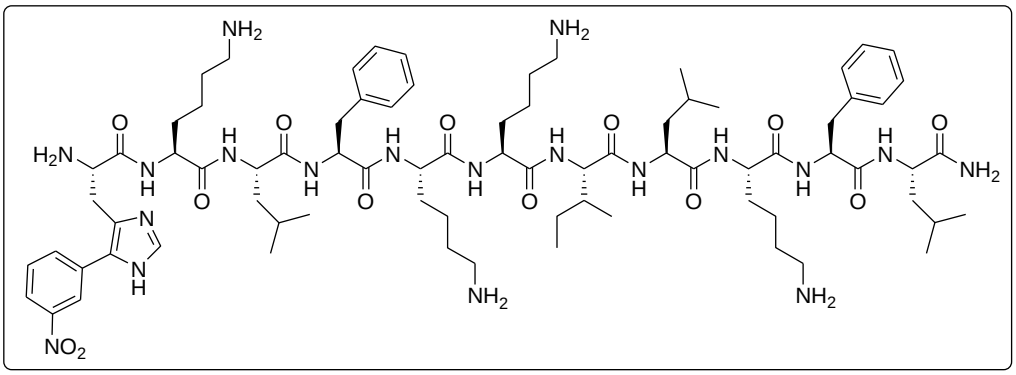

HPLC (λ = 220 nm)

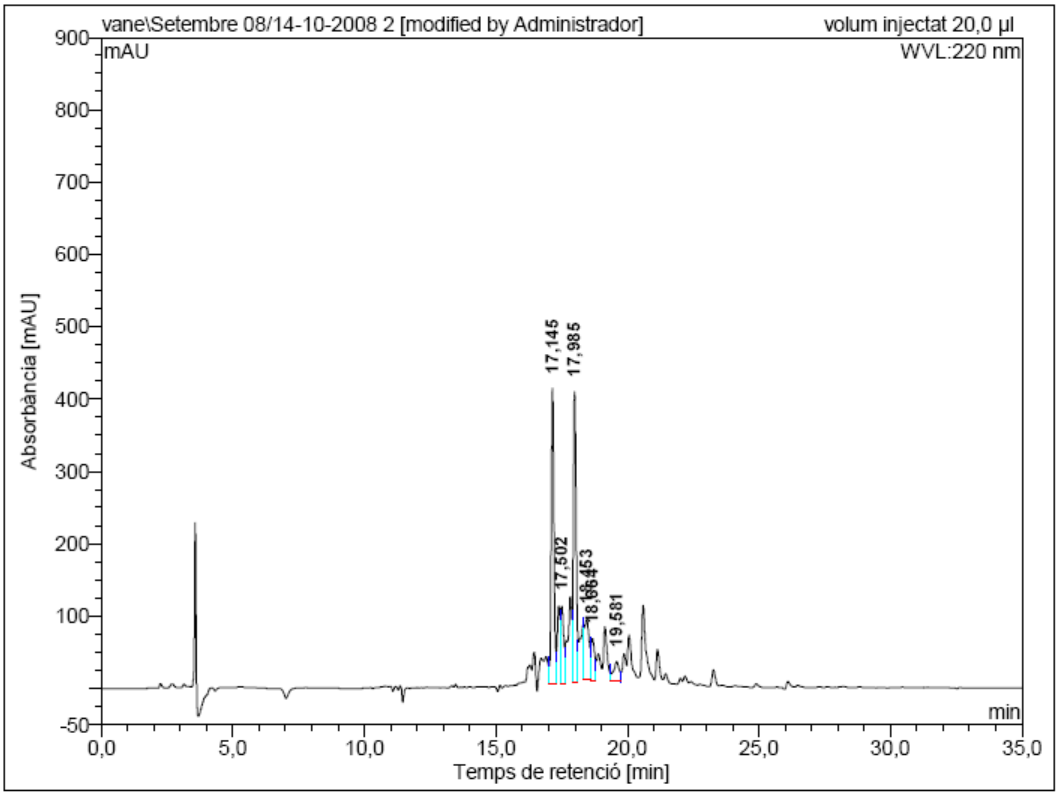

No.	Temps retenció min	alçada mAU	Area mAU*min	Area relativa %
1	17,14	408,793	49,107	32,87
2	17,50	108,052	14,548	9,74
3	17,98	401,112	51,800	34,67
4	18,45	83,460	16,852	11,28
5	18,66	59,627	10,484	7,02
6	19,58	26,350	6,608	4,42
Total:		1087,394	149,399	100,00

ESI-MS *m/z* (%)

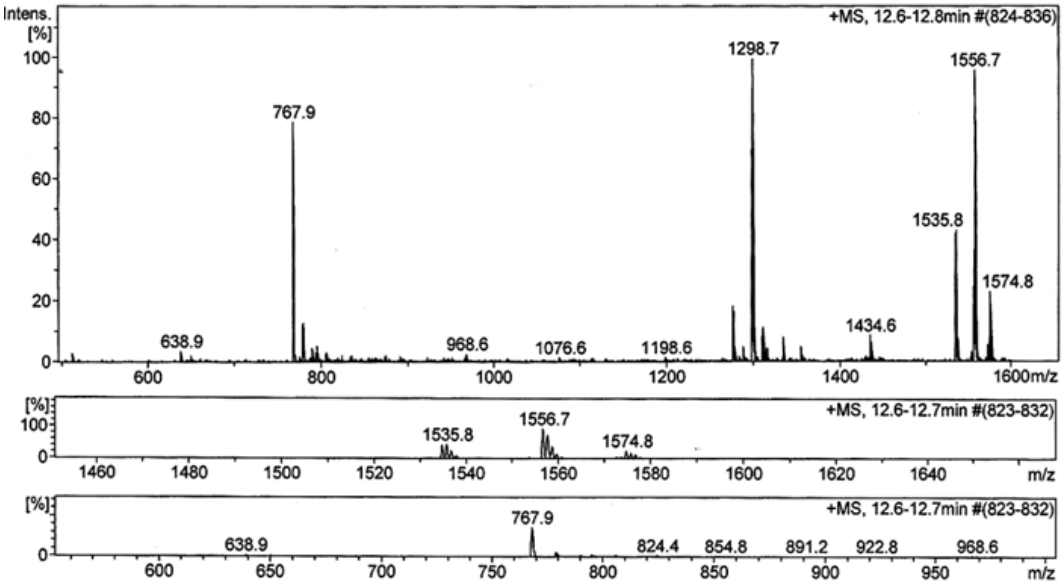
Intens.
[%]
+MS, 12.6-12.8min #(824-836)
1298.7
1556.7
767.9
1535.8
1574.8
1434.6
638.9
968.6
1076.6
1198.6
600
800
1000
1200
1400
1600m/z
+MS, 12.6-12.7min #(823-832)
1556.7
1535.8
1574.8
1460
1480
1500
1520
1540
1560
1580
1600
1620
1640
m/z
+MS, 12.6-12.7min #(823-832)
767.9
638.9
824.4
854.8
891.2
922.8
968.6
600
650
700
750
800
850
900
950
m/z

3. 5-Phenylhistidine-containing peptides BP276, BP277, BP279, and BP280

Fmoc-Lys-Lys-Leu-His(5-Br)-Lys-Lys-Ile-Leu-Lys-Val-Leu-NH_2

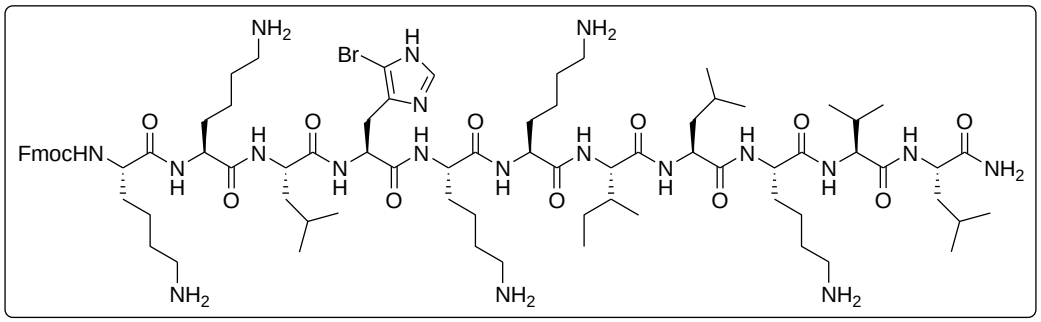

HPLC (λ = 220 nm)

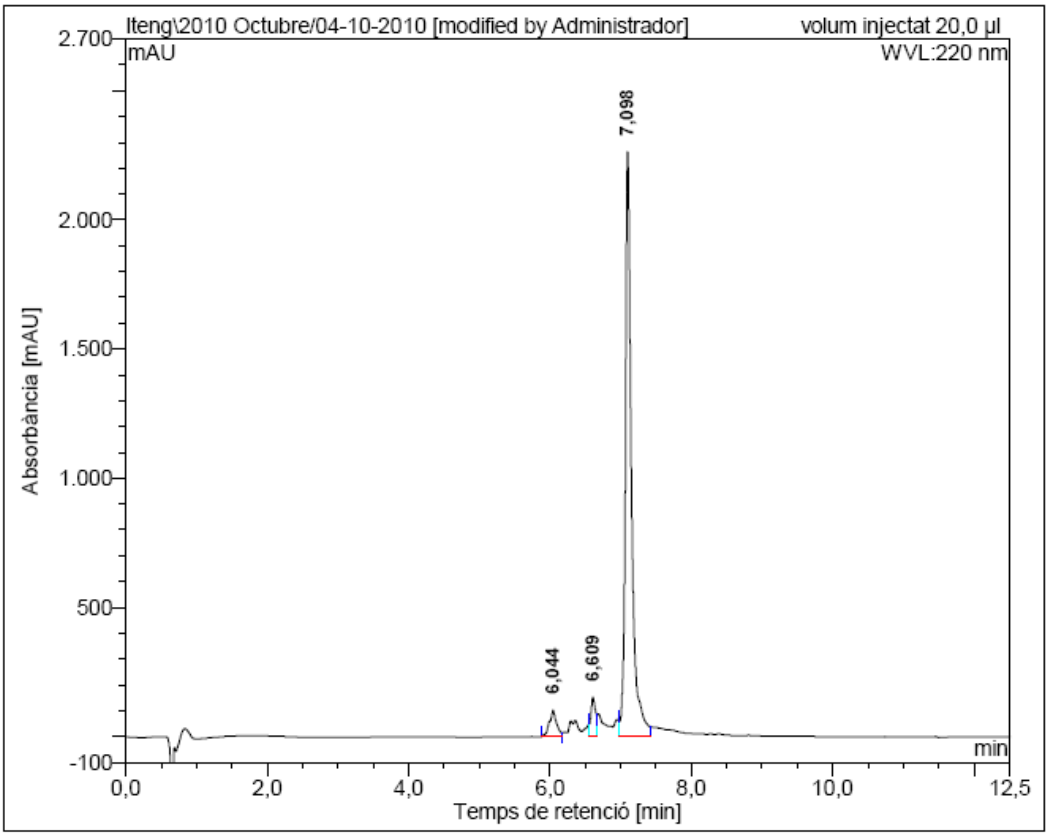

No.	Temps retenció min	alçada mAU	Area mAU*min	Area relativa %
1	6,04	102,232	12,012	4,78
2	6,61	152,408	12,098	4,81
3	7,10	2262,280	227,230	90,41
Total:		2516,919	251,340	100,00

H-Lys-Lys-Leu-His(5-Br)-Lys-Lys-Ile-Leu-Lys-Val-Leu-NH_2

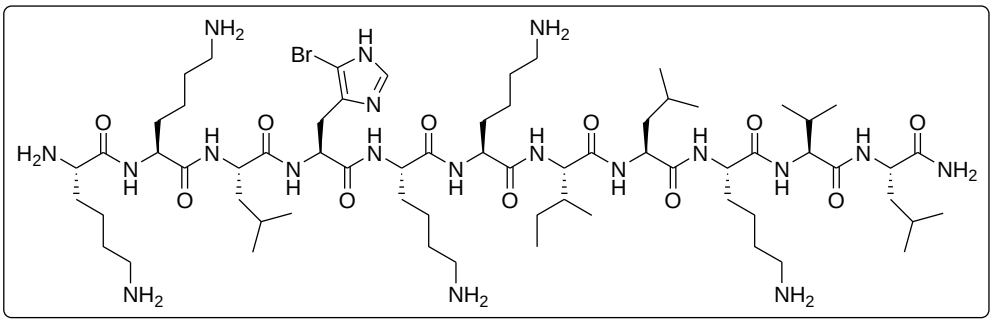

HPLC (λ = 220 nm)

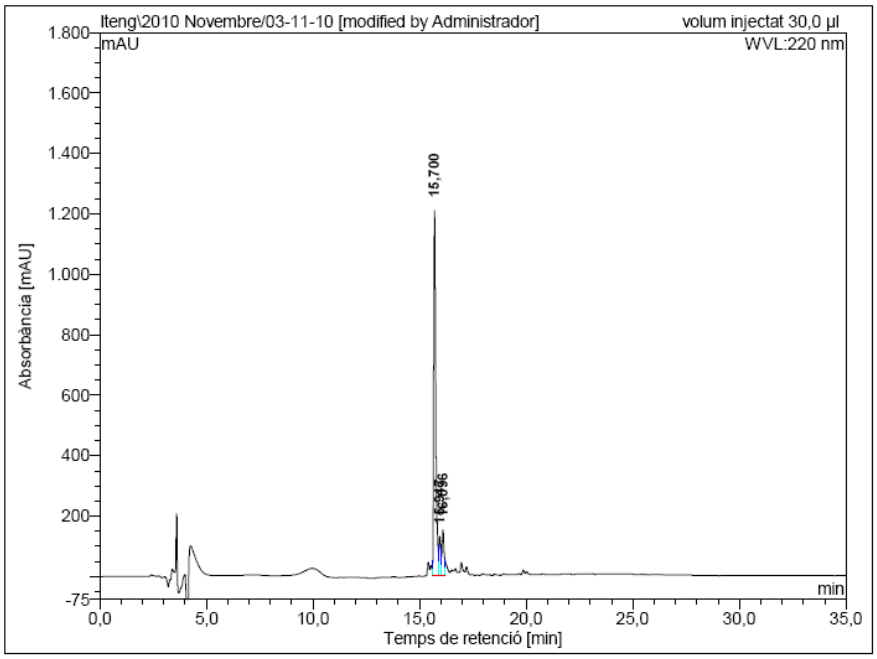

No.	Temps retenció min	alçada mAU	Area mAU*min	Area relativa %
1	15,70	1208,157	133,786	81,68
2	15,95	131,109	13,565	8,28
3	16,10	153,101	16,439	10,04
Total:		1492,367	163,790	100,00

ESI-MS *m/z* (%)

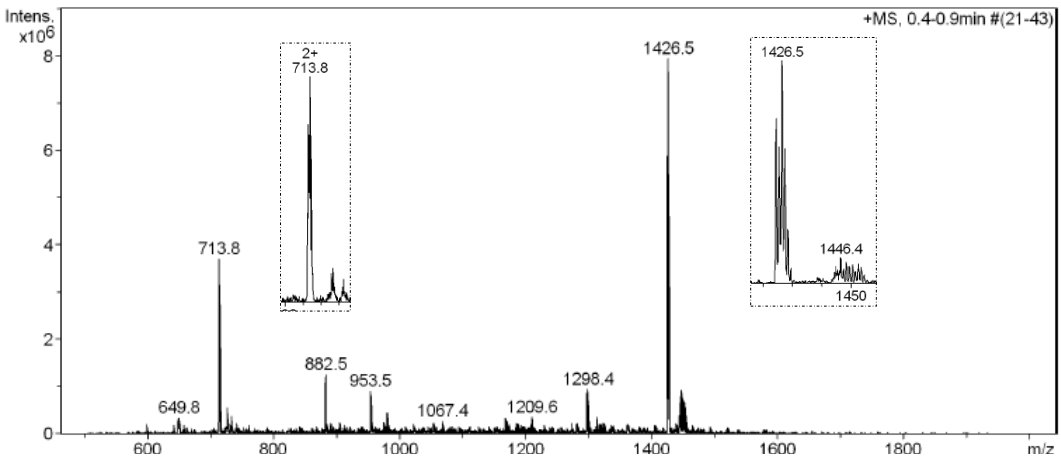

Ac-Leu-Lys-Leu-His(5-Br)-Lys-Lys-Ile-Leu-Lys-Val-Leu-NH_2

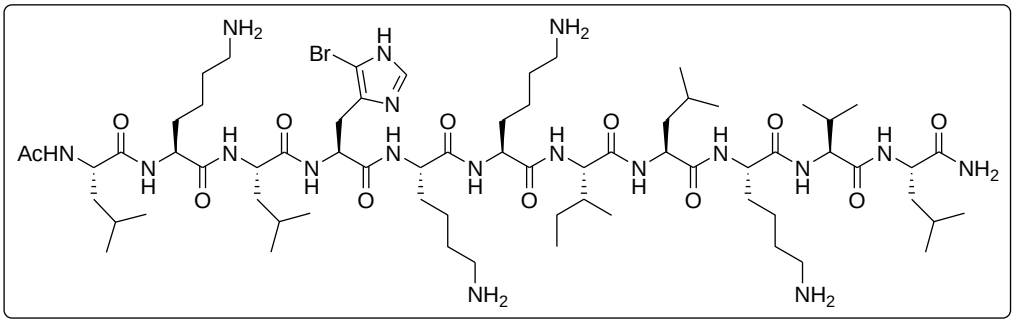

HPLC (λ = 220 nm)

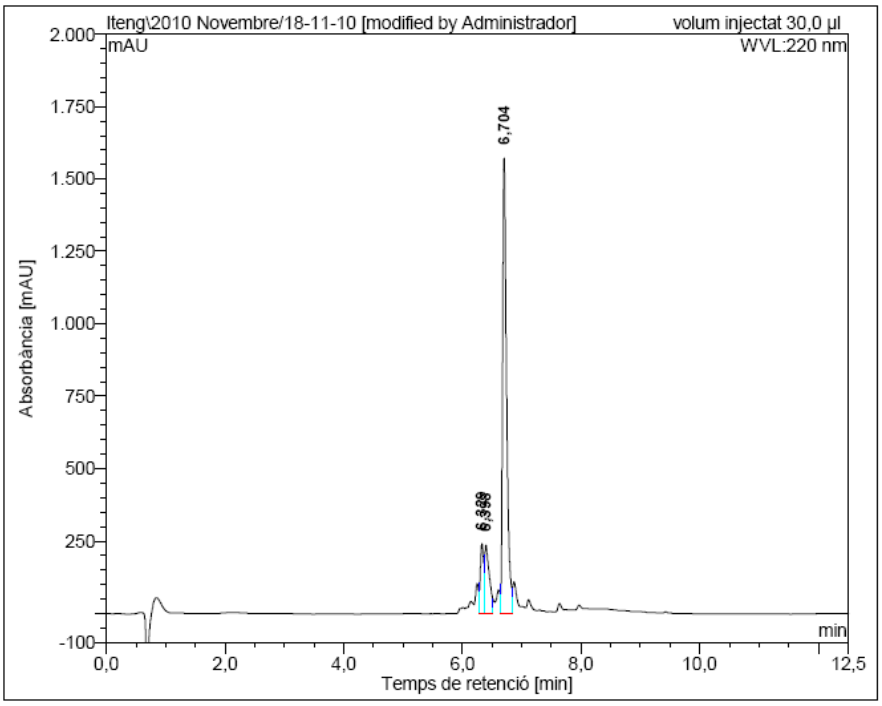

No.	Temps retenció min	alçada mAU	Area mAU*min	Area relativa %
1	6,33	240,250	14,375	8,94
2	6,40	235,217	22,645	14,08
3	6,70	1571,347	123,839	76,99
Total:		2046,814	160,858	100,00

ESI-MS *m/z* (%)

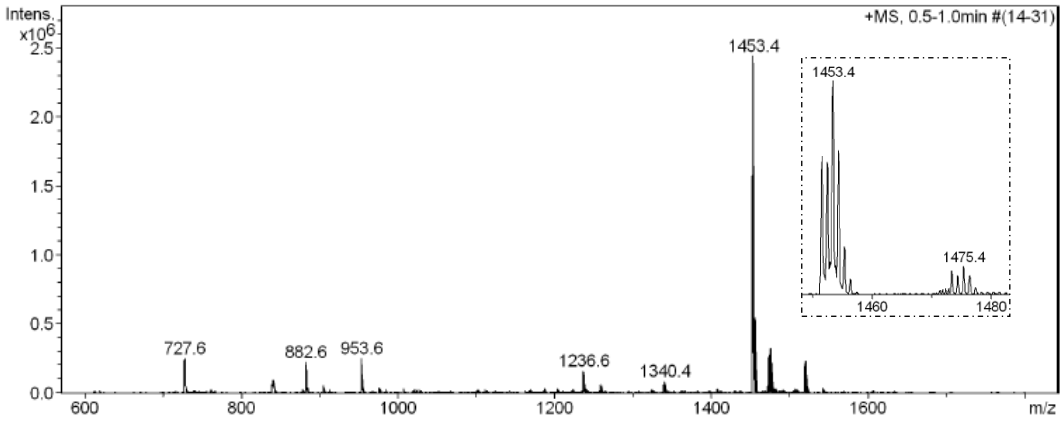

Ac-Phe-Lys-Leu-His(5-Br)-Lys-Lys-Ile-Leu-Lys-Val-Leu-NH_2

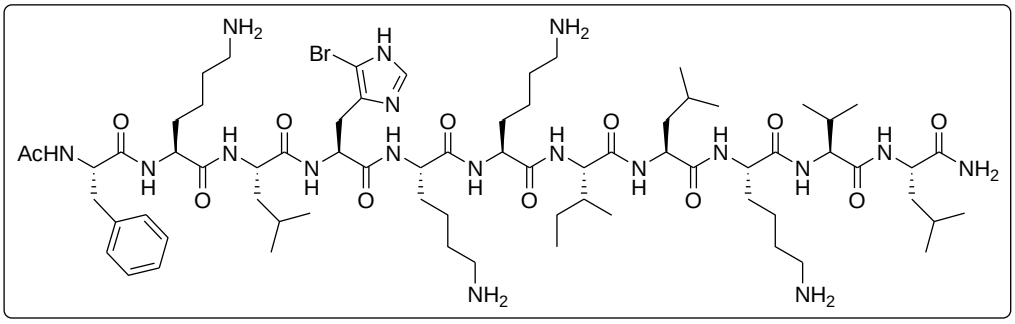

HPLC (λ = 220 nm)

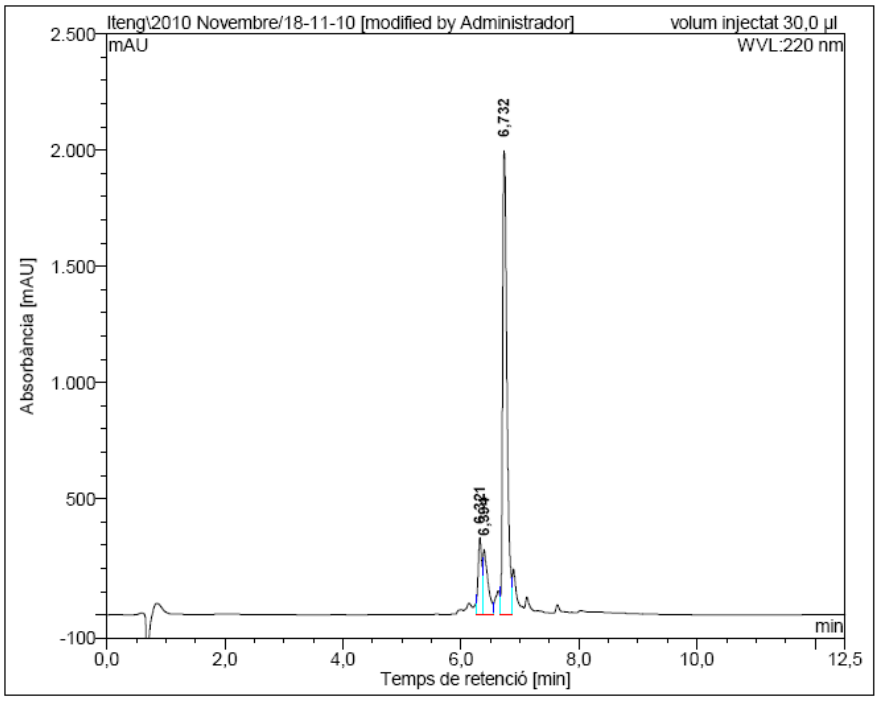

No.	Temps retenció min	alçada mAU	Area mAU*min	Area relativa %
1	6,32	330,144	22,537	10,30
2	6,39	278,663	27,833	12,73
3	6,73	1995,236	168,336	76,97
Total:		2604,043	218,706	100,00

ESI-MS *m/z* (%)

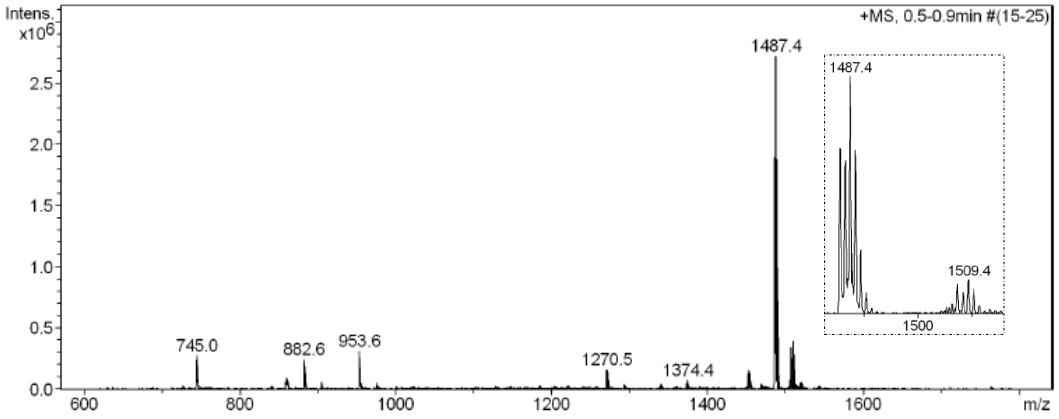

Ts-Phe-Lys-Leu-His(5-Br)-Lys-Lys-Ile-Leu-Lys-Val-Leu-NH_2

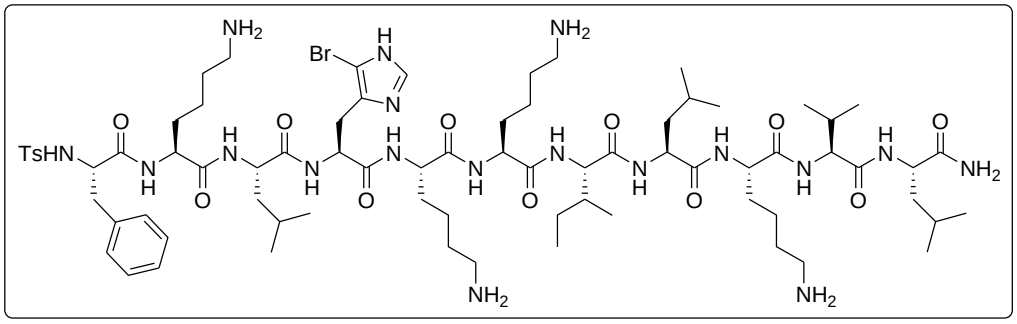

HPLC (λ = 220 nm)

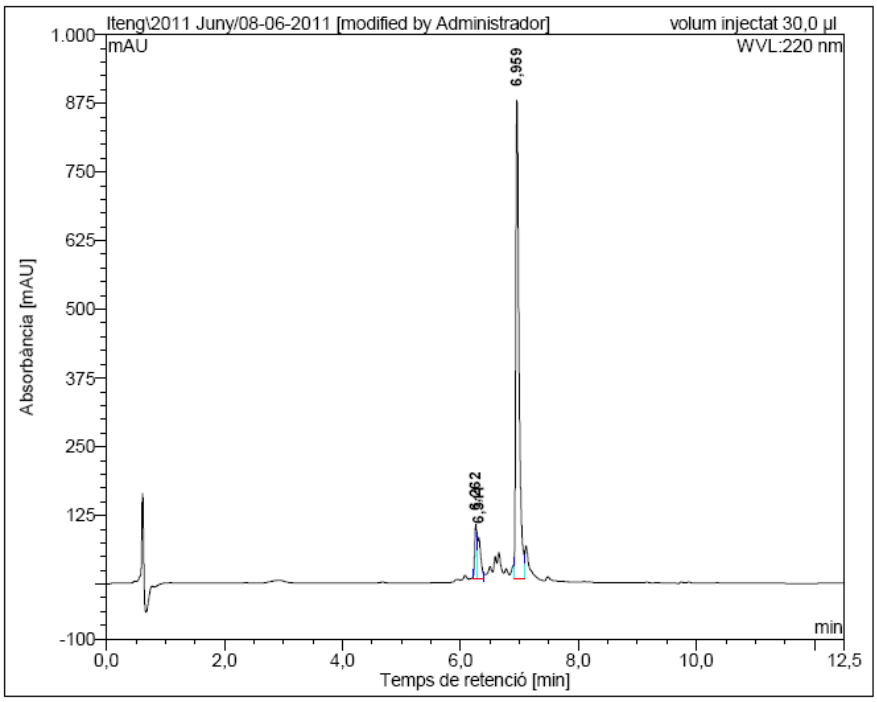

No.	Temps retenció min	alçada mAU	Area mAU*min	Area relativa %
1	6,26	99,388	4,782	7,43
2	6,31	75,792	4,430	6,88
3	6,96	871,861	55,151	85,69
Total:		1047,041	64,363	100,00

ESI-MS *m/z* (%)

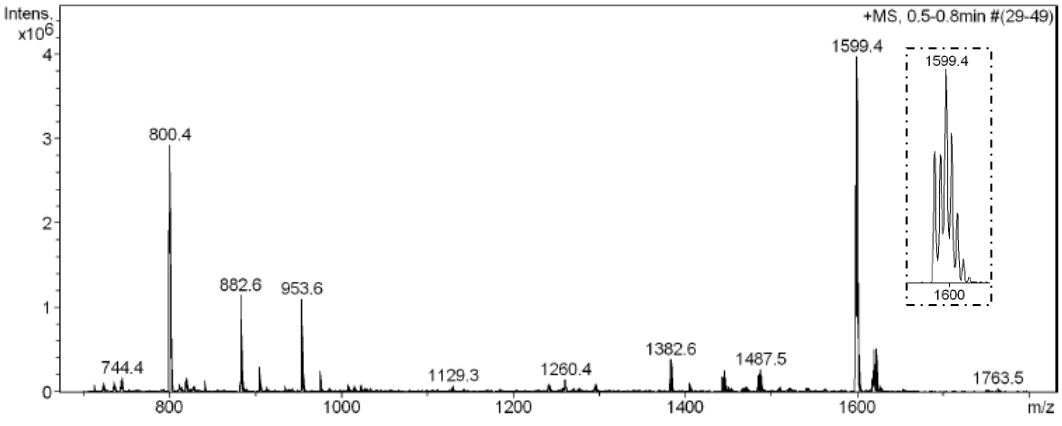

H-Phe-Lys-Leu-His(5-Br)-Lys-Lys-Ile-Leu-Lys-Val-Leu-NH_2

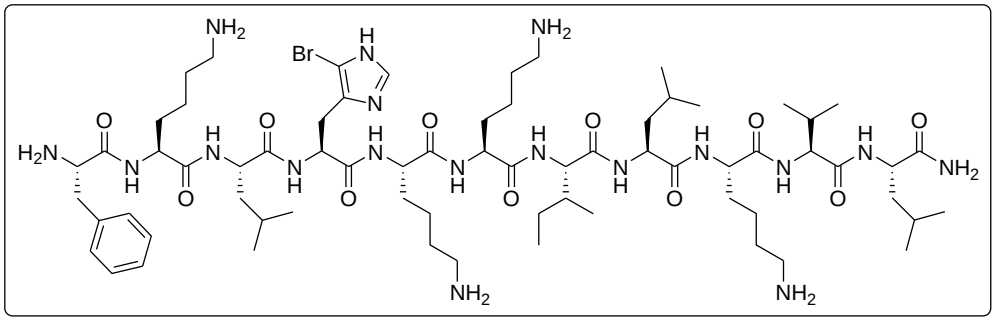

HPLC (λ = 220 nm)

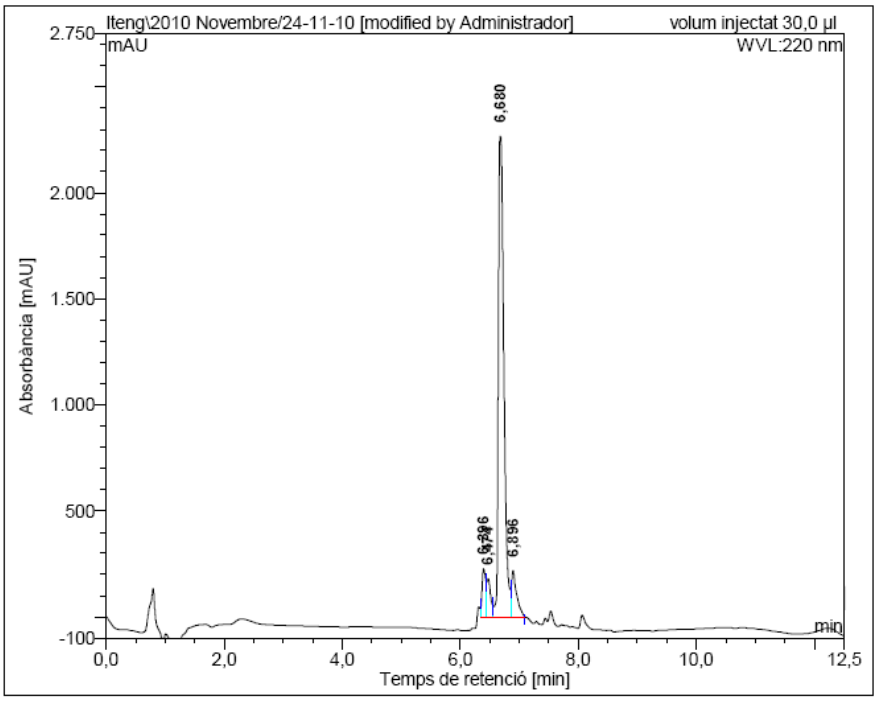

No.	Temps retenció min	alçada mAU	Area mAU*min	Area relativa %
1	6,40	227,440	16,587	5,53
2	6,47	180,091	14,265	4,76
3	6,68	2266,798	246,115	82,11
4	6,90	219,367	22,783	7,60
Total:		2893,696	299,749	100,00

ESI-MS *m/z* (%)

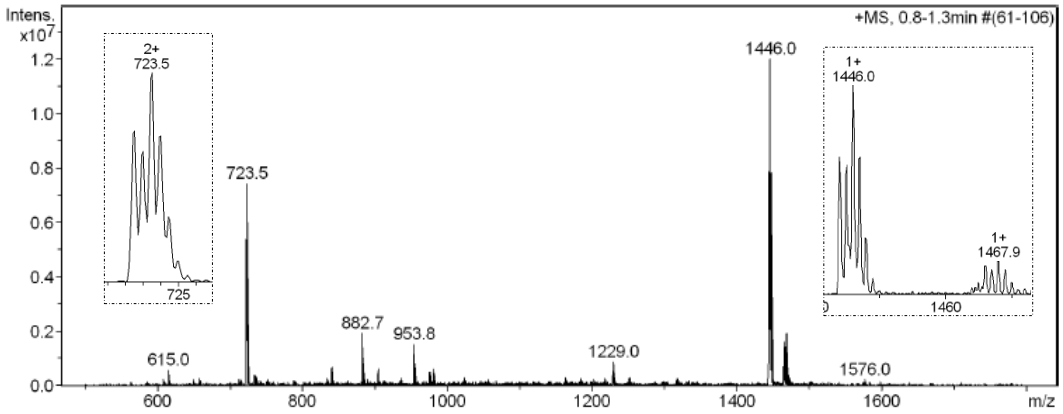
Intens.
x10^7
+MS, 0.8-1.3min #(61-106)
2+
723.5
725
723.5
882.7
953.8
615.0
1229.0
1446.0
1576.0
1+
1446.0
1+
1467.9
1460
600
800
1000
1200
1400
1600
m/z

H-Lys-Lys-Leu-His(5-Ph)-Lys-Lys-Ile-Leu-Lys-Val-Leu-NH_2 (BP276)

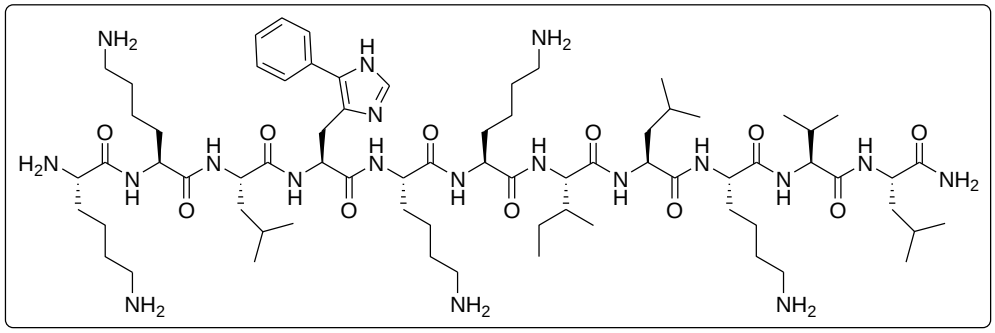

HPLC (λ = 220 nm)

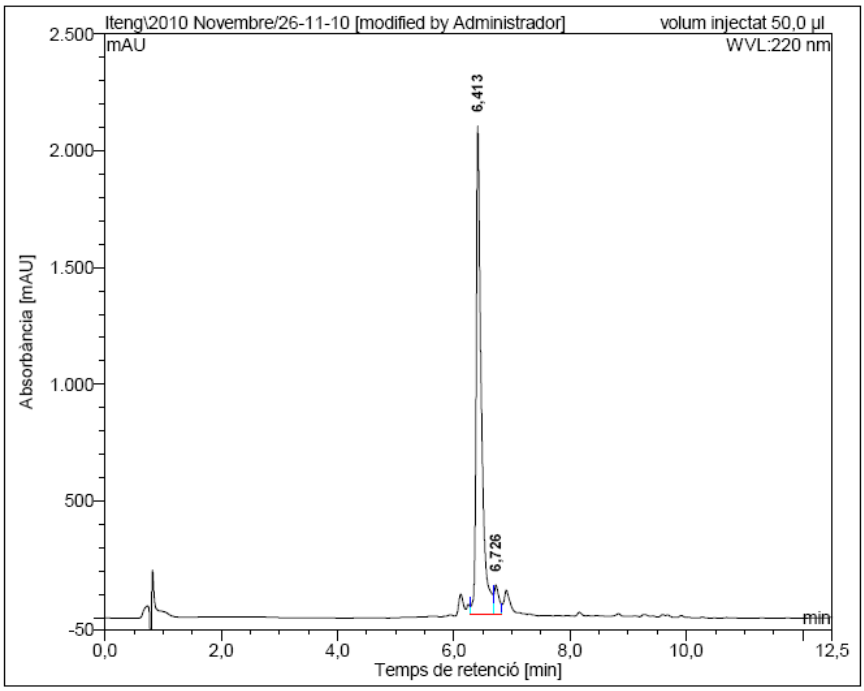

No.	Temps retenció min	alçada mAU	Area mAU*min	Area relativa %
1	6,41	2088,724	212,434	94,85
2	6,73	125,528	11,540	5,15
Total:		2214,252	223,973	100,00

ESI-MS *m/z* (%)

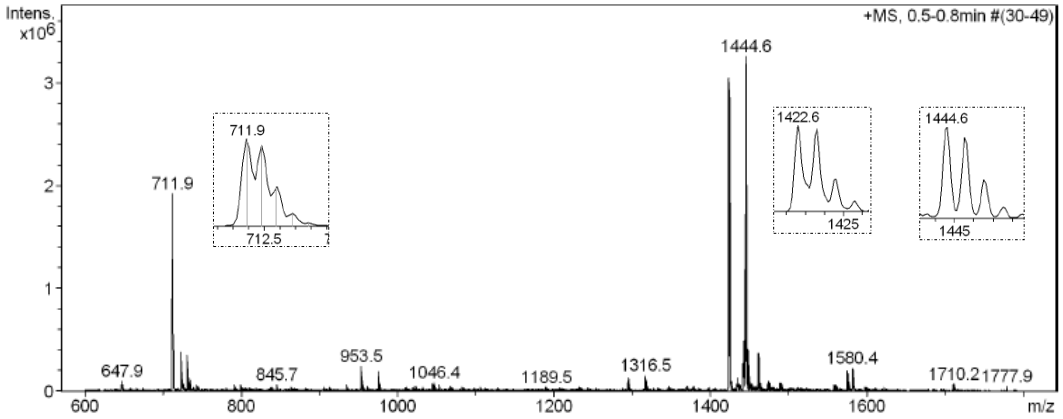

HRMS *m/z* (%)

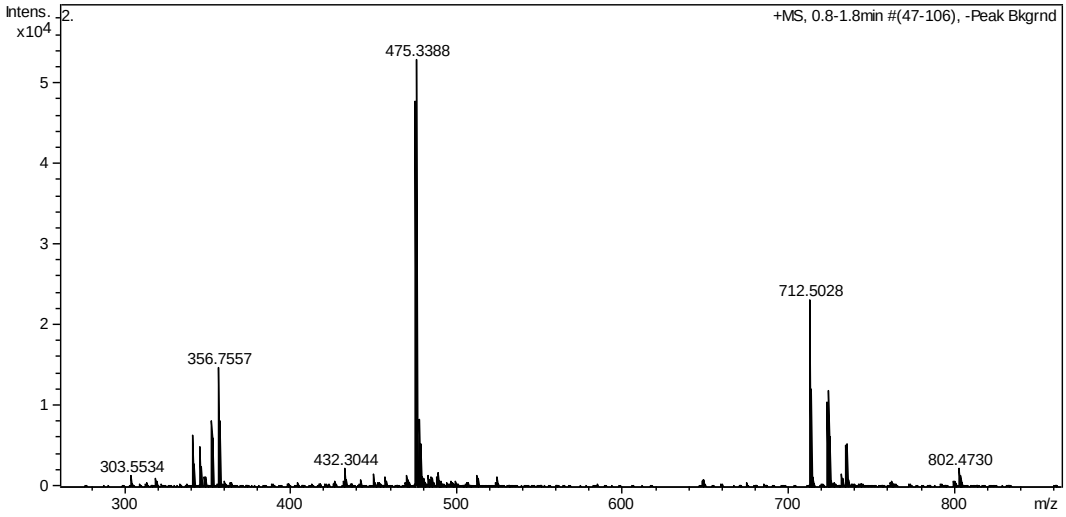

Ac-Leu-Lys-Leu-His(5-Ph)-Lys-Lys-Ile-Leu-Lys-Val-Leu-NH_2 (BP277)

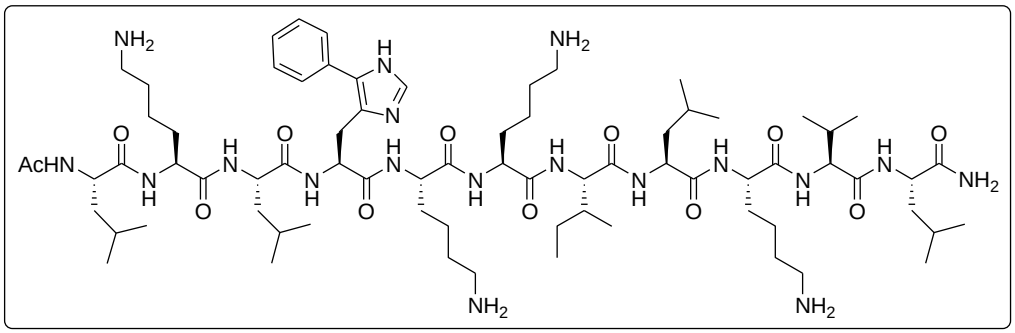

HPLC (λ = 220 nm)

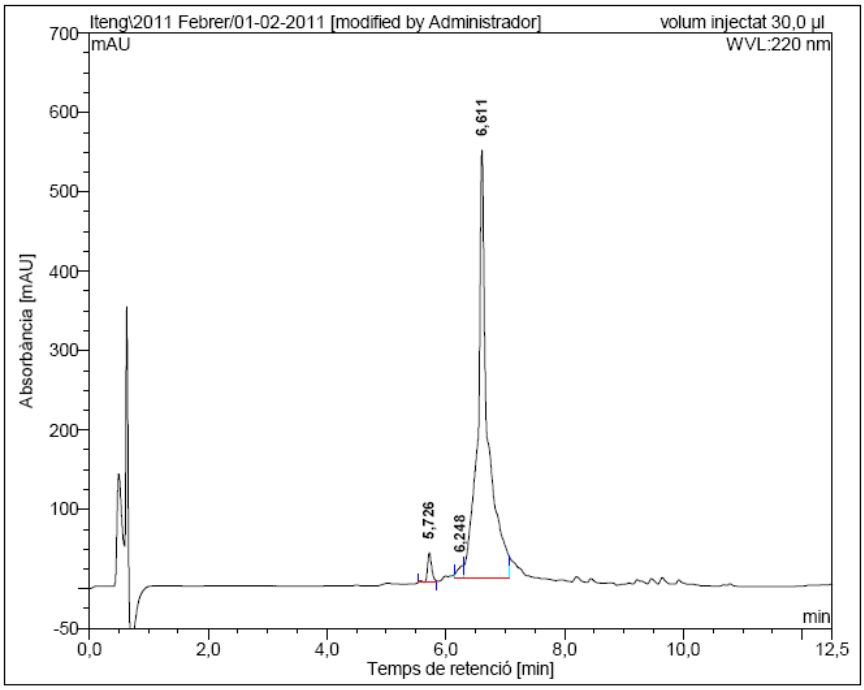

No.	Temps retenció min	alçada mAU	Area mAU*min	Area relativa %
1	5,73	36,973	3,051	2,81
2	6,25	14,621	1,867	1,72
3	6,61	539,377	103,794	95,48
Total:		590,971	108,712	100,00

ESI-MS *m/z* (%)

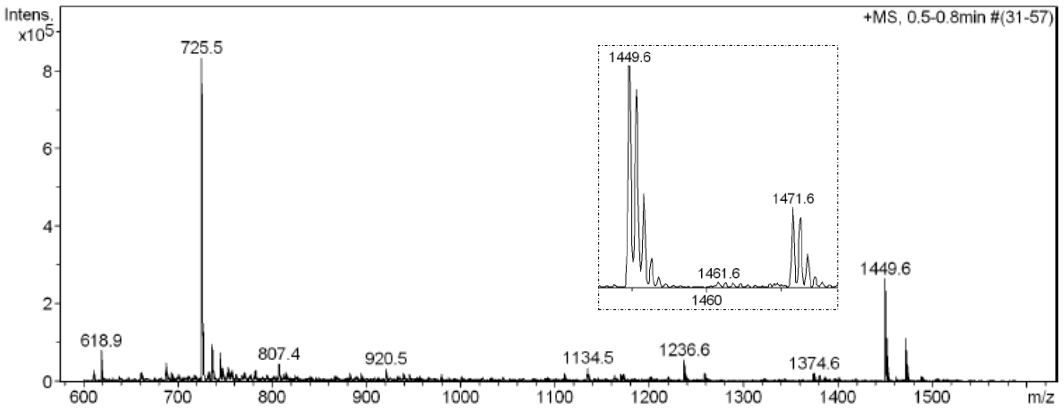

HRMS *m/z* (%)

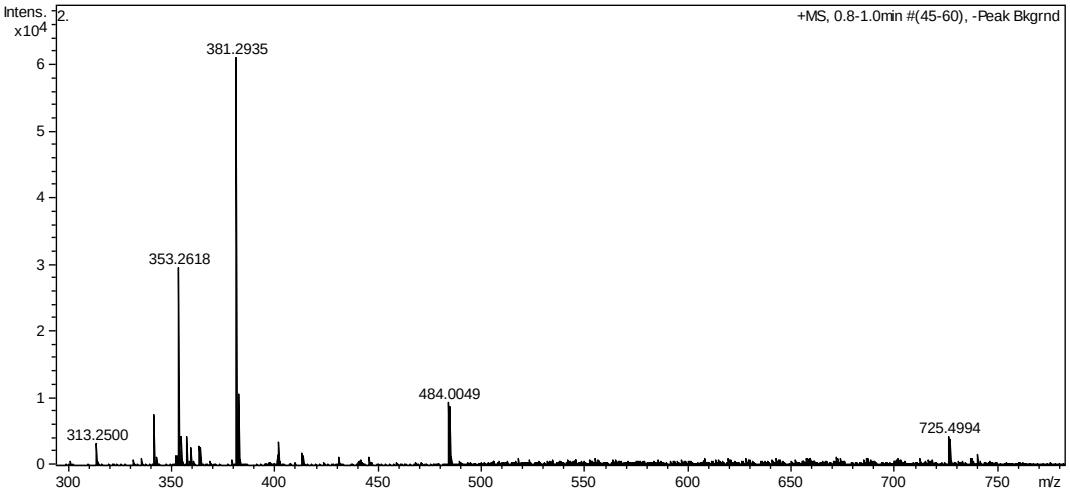

Ac-Phe-Lys-Leu-His(5-Ph)-Lys-Lys-Ile-Leu-Lys-Val-Leu-NH_2 (BP279)

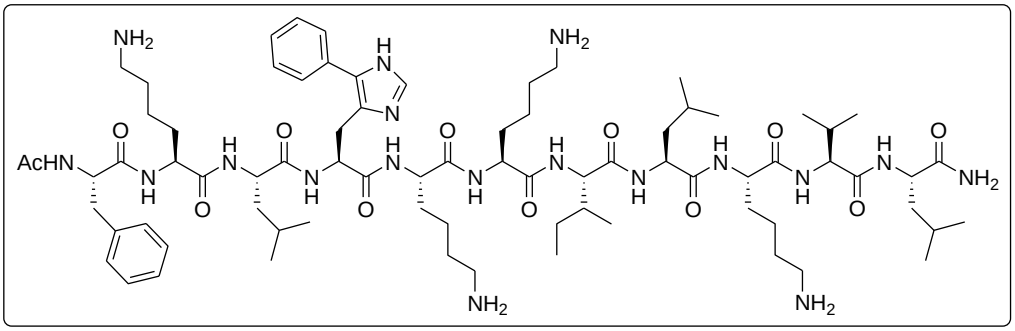

ESI-MS *m/z* (%)

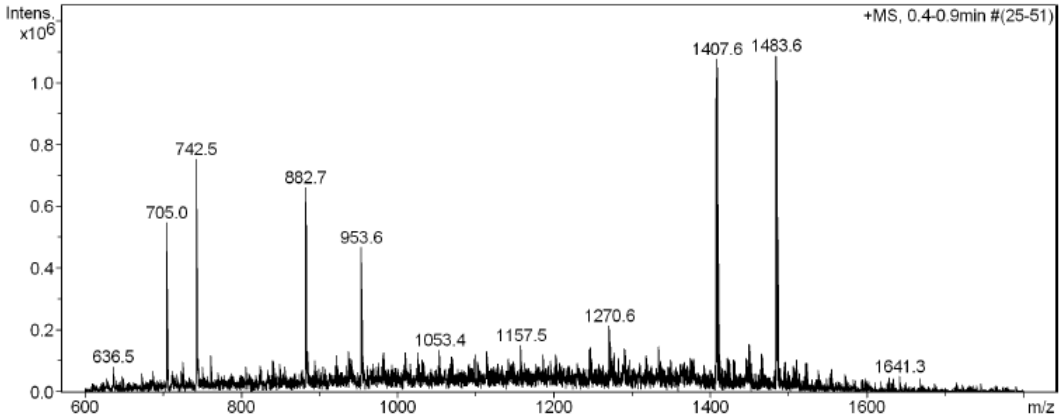

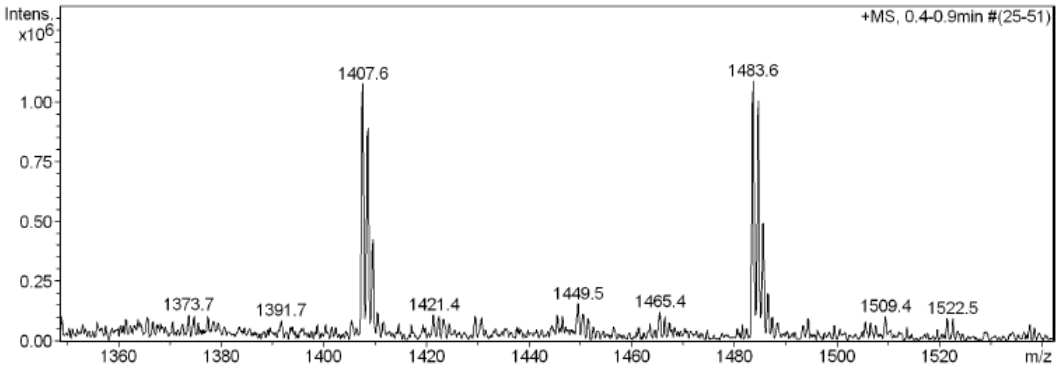

HRMS *m/z* (%)

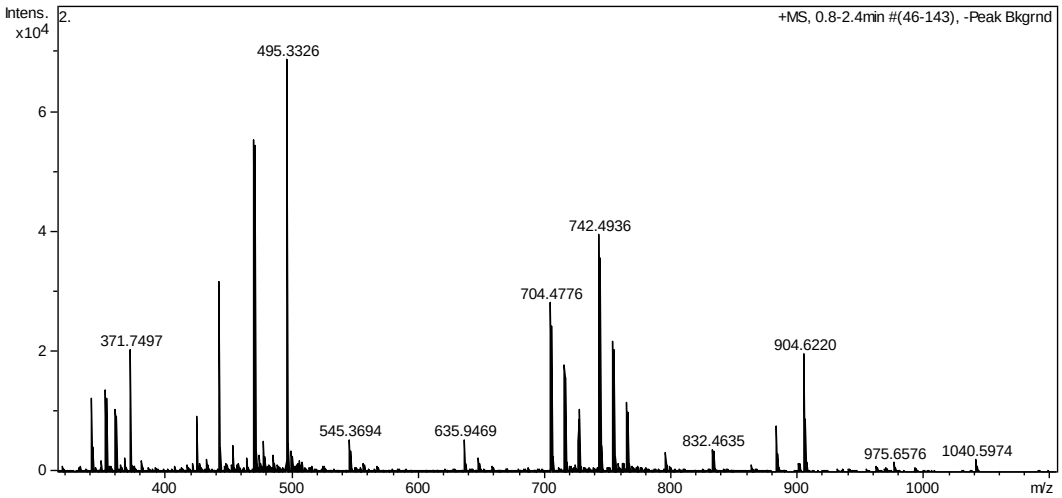

Ts-Phe-Lys-Leu-His(5-Ph)-Lys-Lys-Ile-Leu-Lys-Val-Leu-NH_2 (BP280)

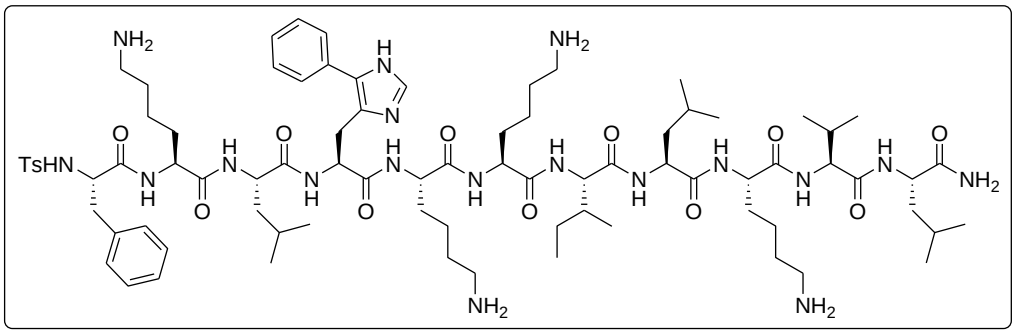

ESI-MS *m/z* (%)

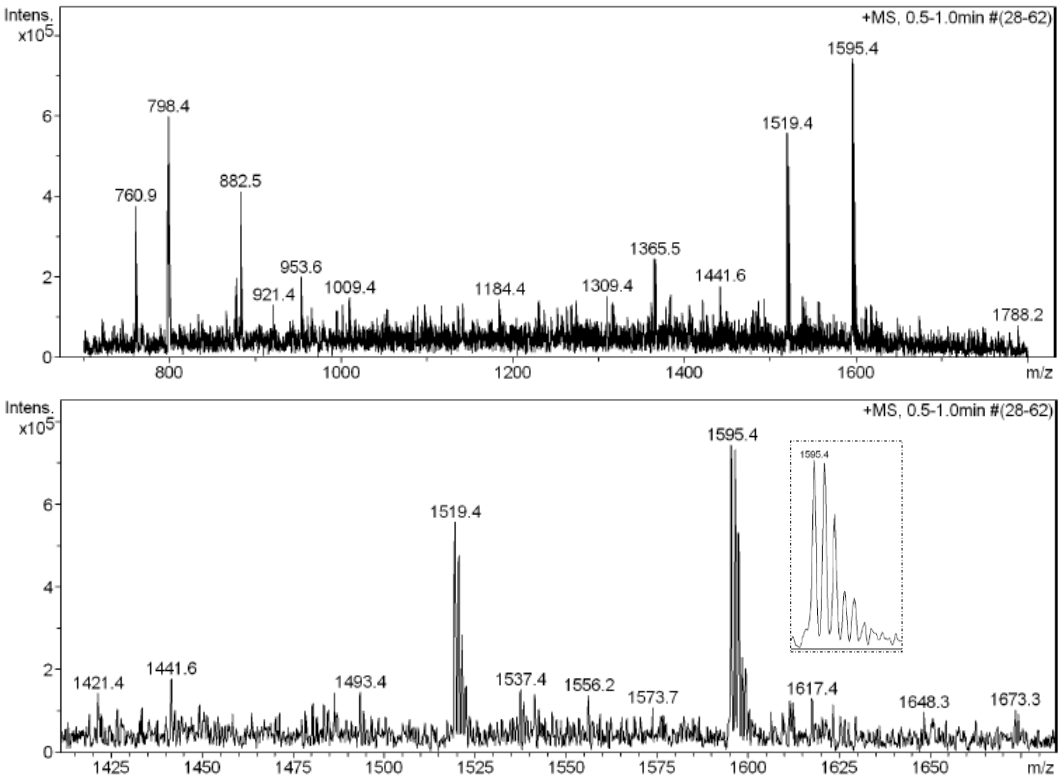

HRMS *m/z* (%)

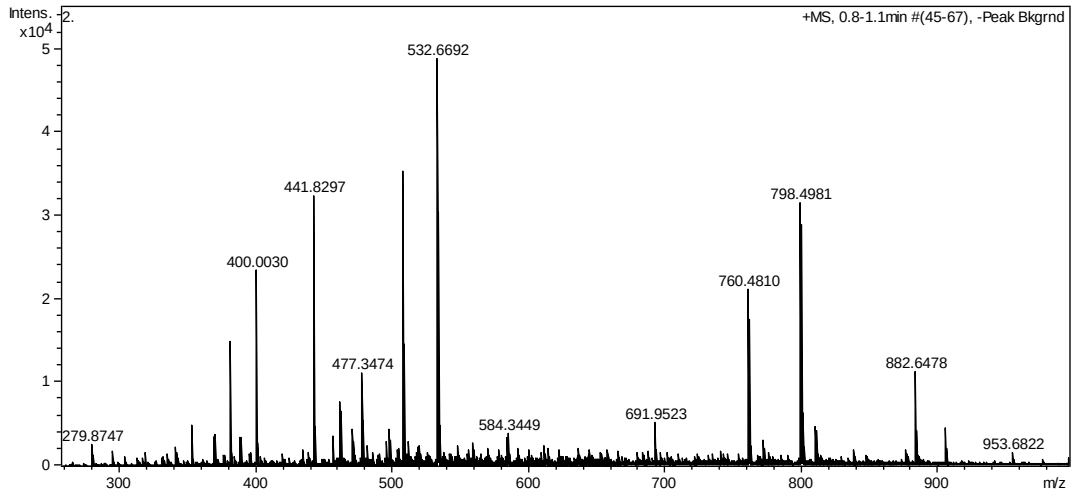

4. Histidine-containing peptides BP270-BP275, BP284, BP285, BP305, and BP306

H-Lys-Lys-Leu-His-Lys-Lys-Ile-Leu-Lys-Val-Leu-NH_2 (BP270)

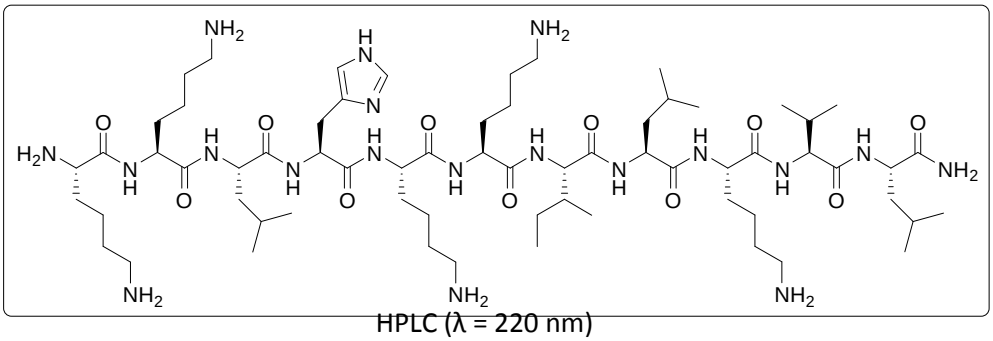

HPLC (λ = 220 nm)

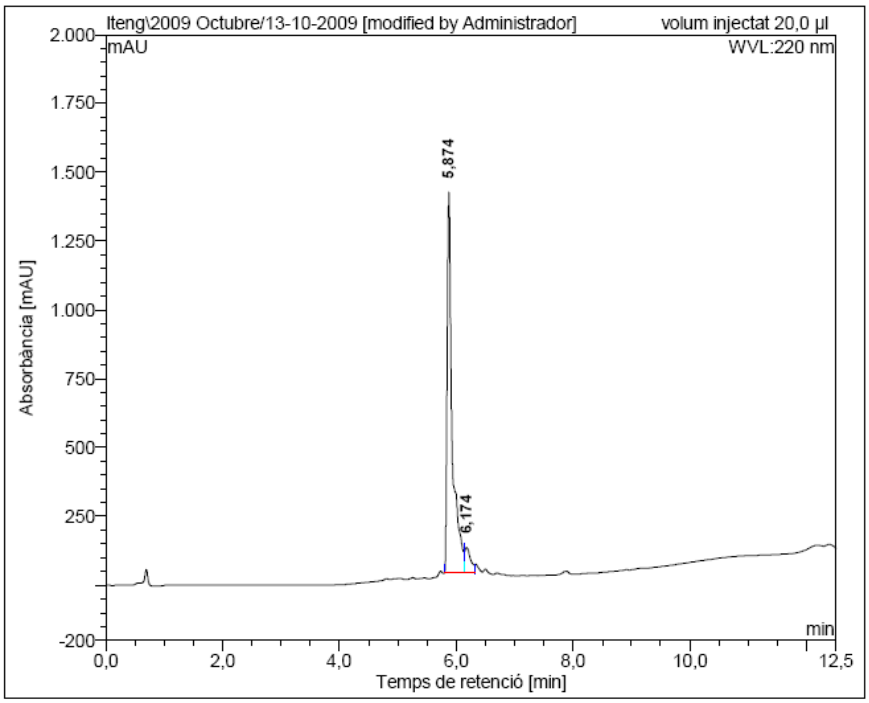

No.	mps retenc min	alçada mAU	Area mAU*min	Area relativa %
1	5,87	1384,452	139,275	92,40
2	6,17	93,183	11,455	7,60
Total:		1477,635	150,730	100,00

ESI-MS *m/z* (%)

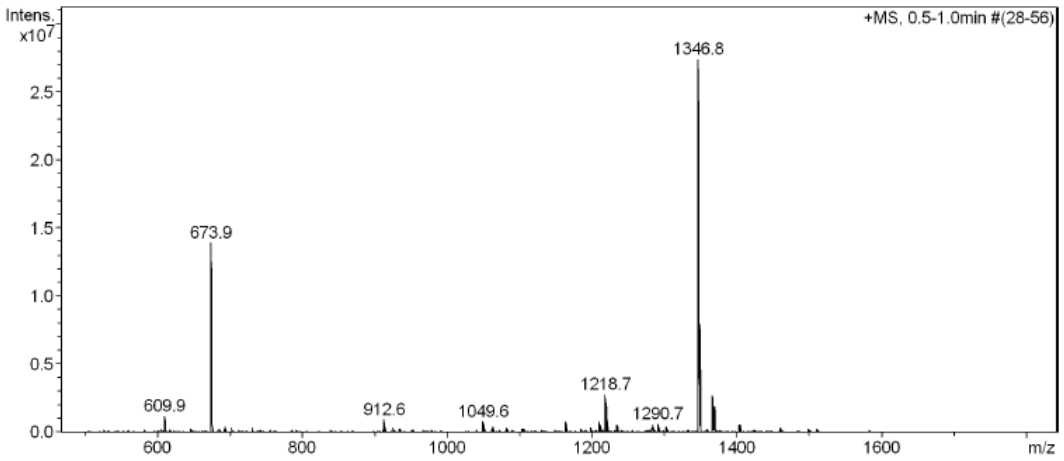

HRMS *m/z* (%)

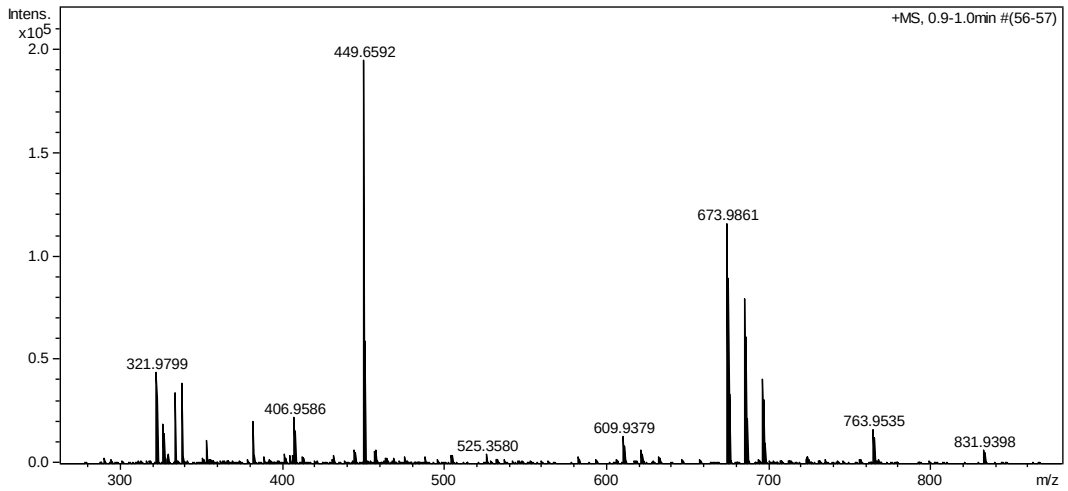

Ac-Leu-Lys-Leu-His-Lys-Lys-Ile-Leu-Lys-Val-Leu-NH_2 (BP271)

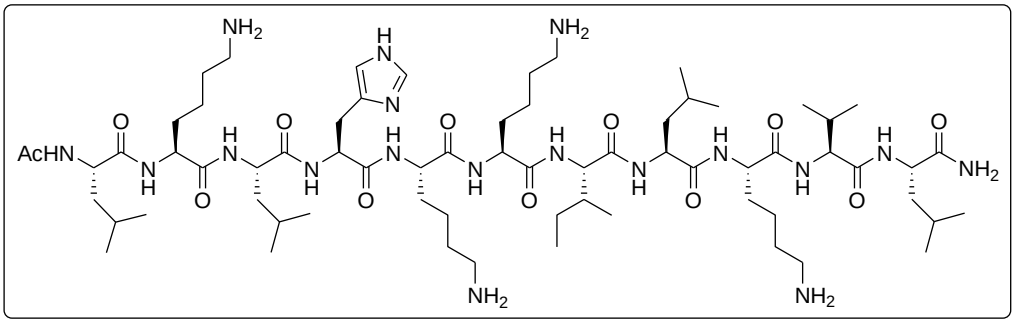

HPLC (λ = 220 nm)

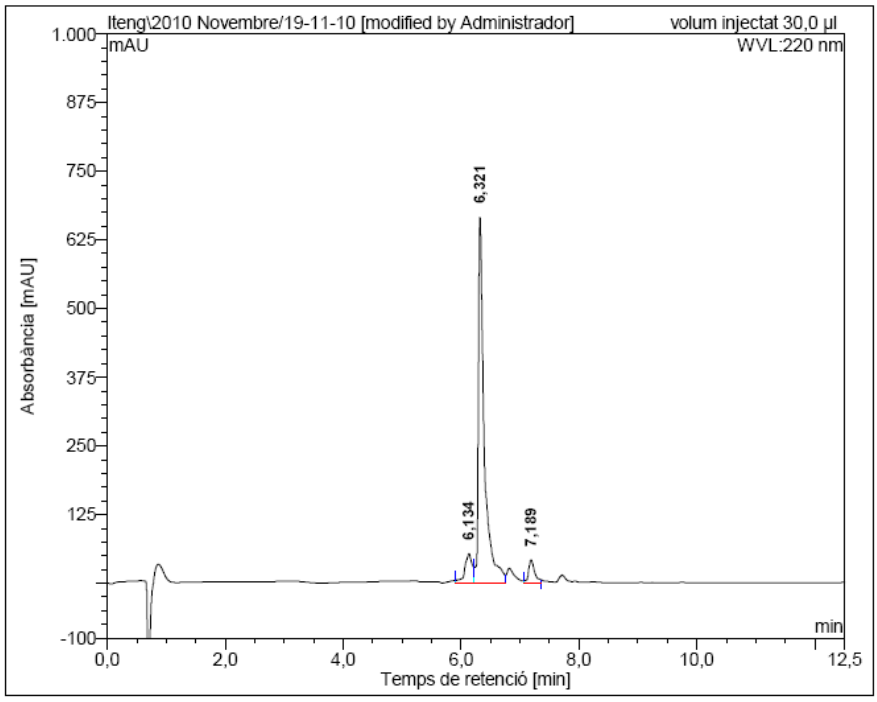

No.	Temps retenció min	alçada mAU	Area mAU*min	Area relativa %
1	6,13	53,725	8,019	8,89
2	6,32	666,510	76,890	85,27
3	7,19	42,647	5,266	5,84
Total:		762,881	90,175	100,00

ESI-MS *m/z* (%)

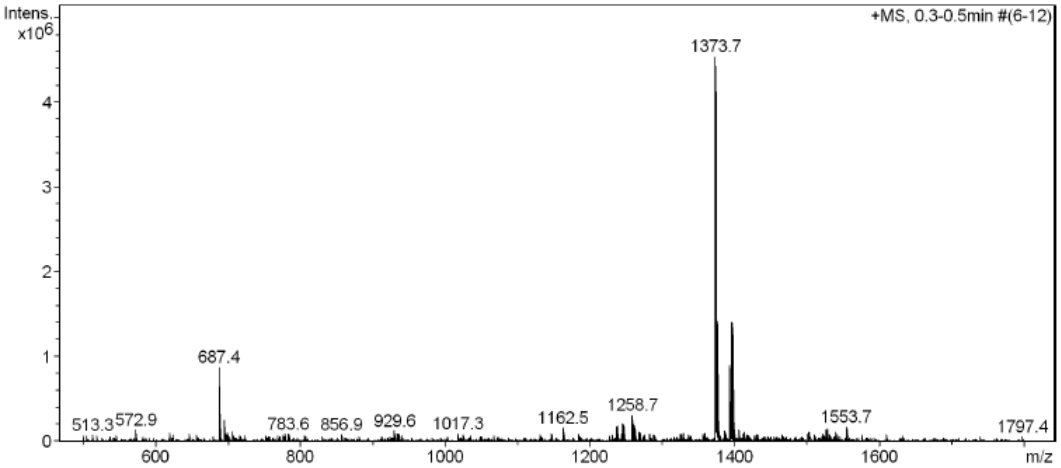

HRMS *m/z* (%)

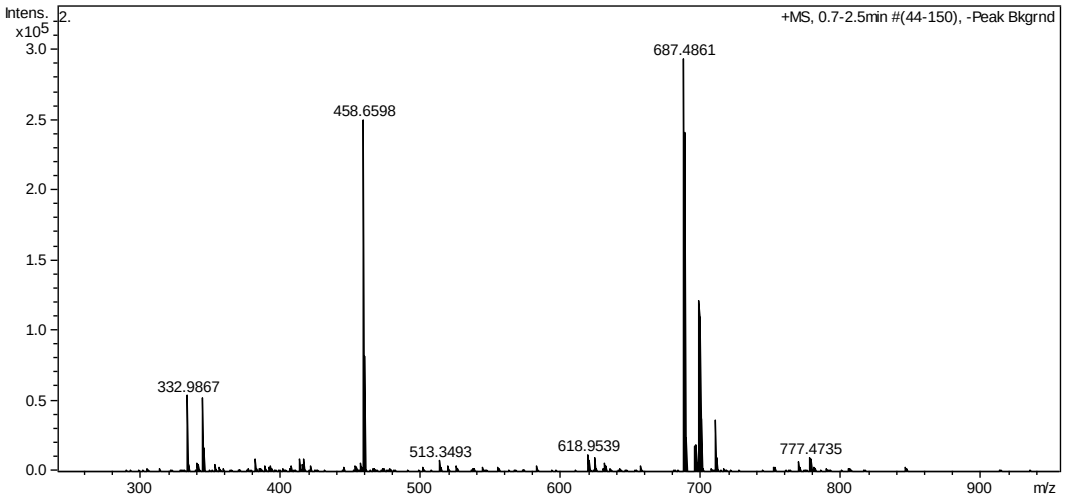

Ac-His-Lys-Leu-His-Lys-Lys-Ile-Leu-Lys-Val-Leu-NH_2 (BP272)

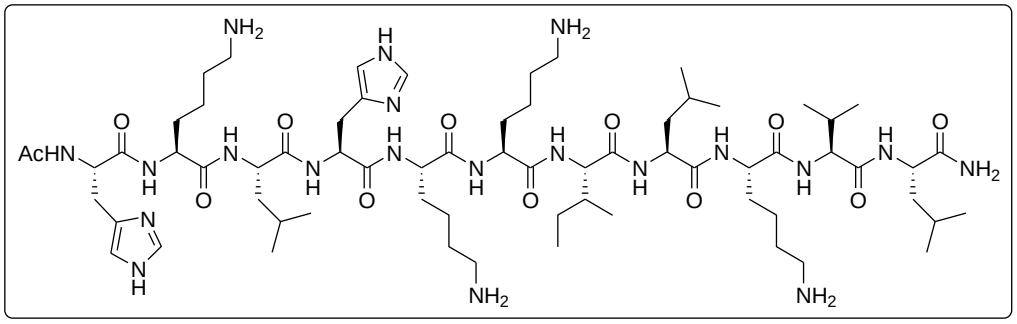

HPLC (λ = 220 nm)

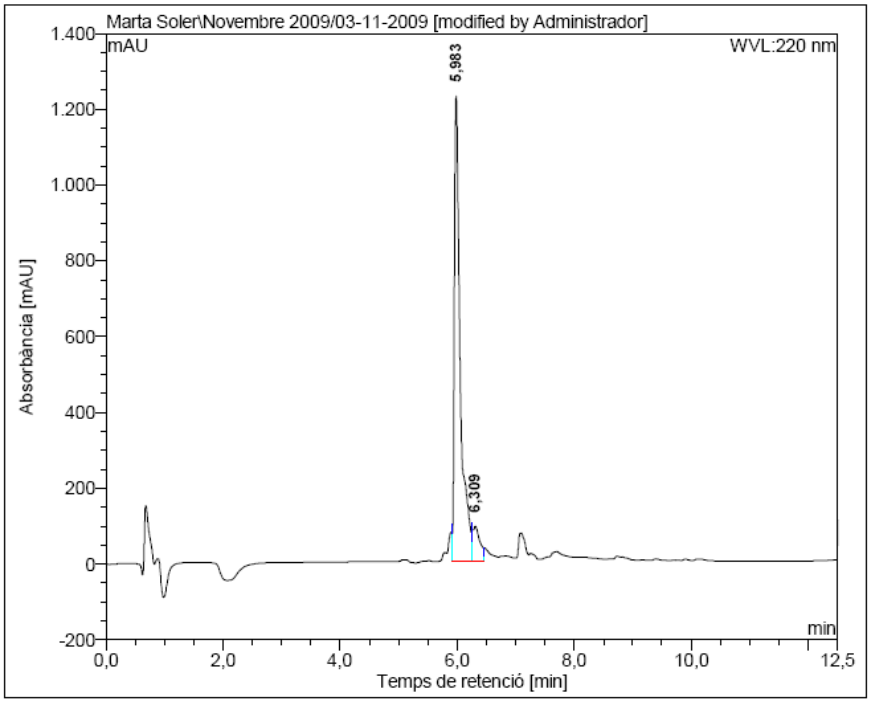

No.	mps retenc min	alçada mAU	Area mAU*min	Area relativa %
1	5,98	1227,443	143,336	91,10
2	6,31	92,387	14,002	8,90
Total:		1319,831	157,339	100,00

ESI-MS *m/z* (%)

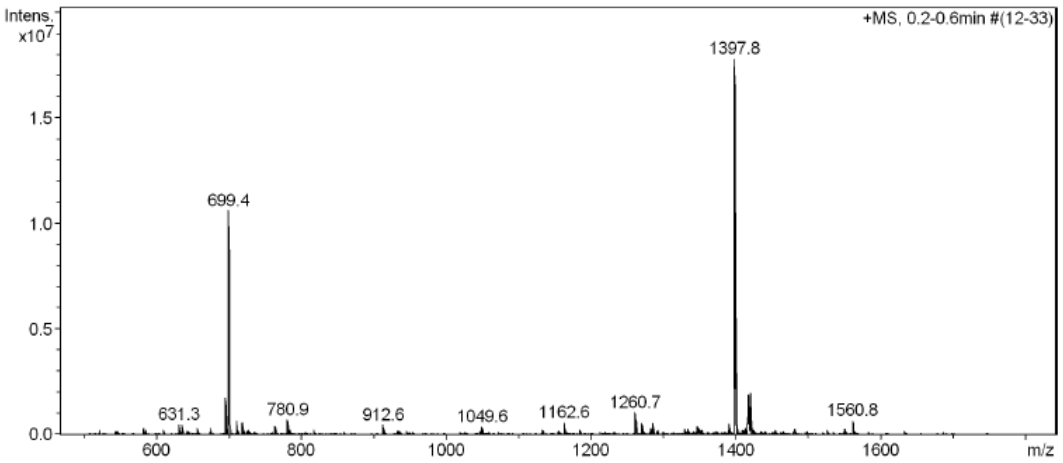

Ac-Phe-Lys-Leu-His-Lys-Lys-Ile-Leu-Lys-Val-Leu-NH_2 (BP273)

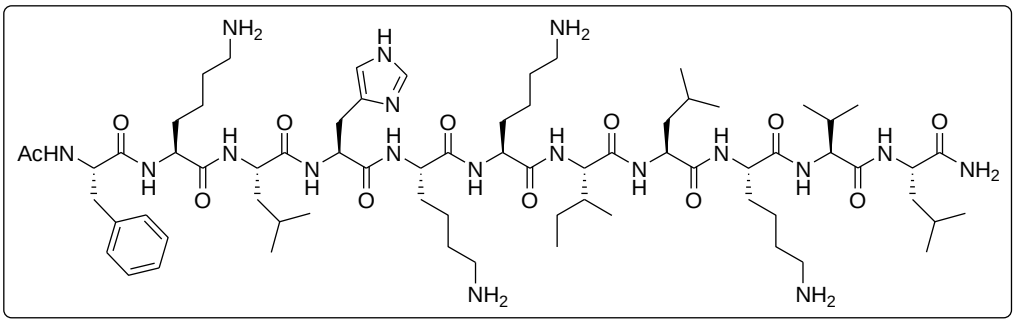

HPLC (λ = 220 nm)

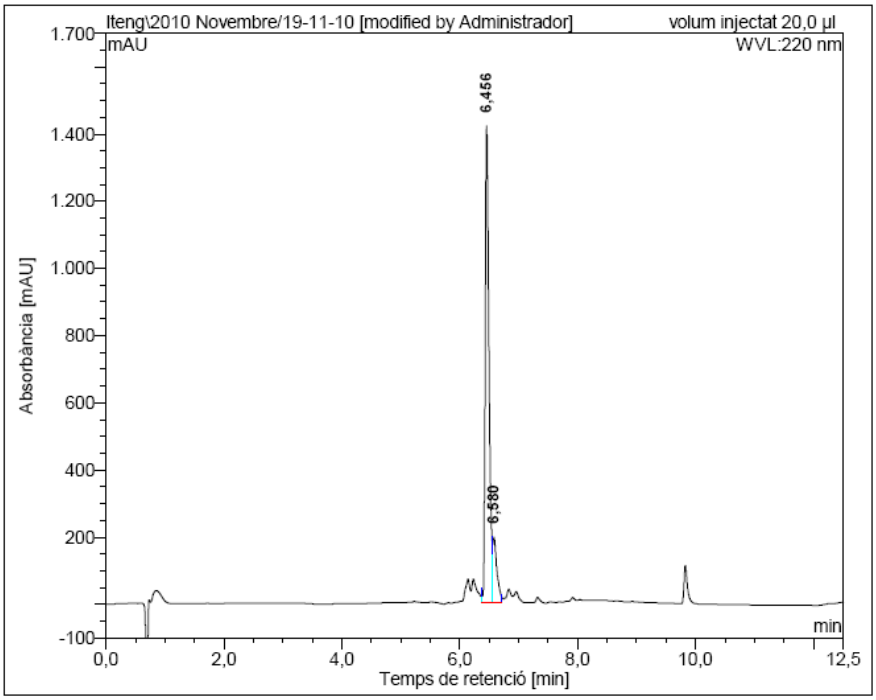

No.	Temps retenció min	alçada mAU	Area mAU*min	Area relativa %
1	6,46	1417,514	106,212	87,22
2	6,58	193,652	15,560	12,78
Total:		1611,166	121,772	100,00

ESI-MS *m/z* (%)

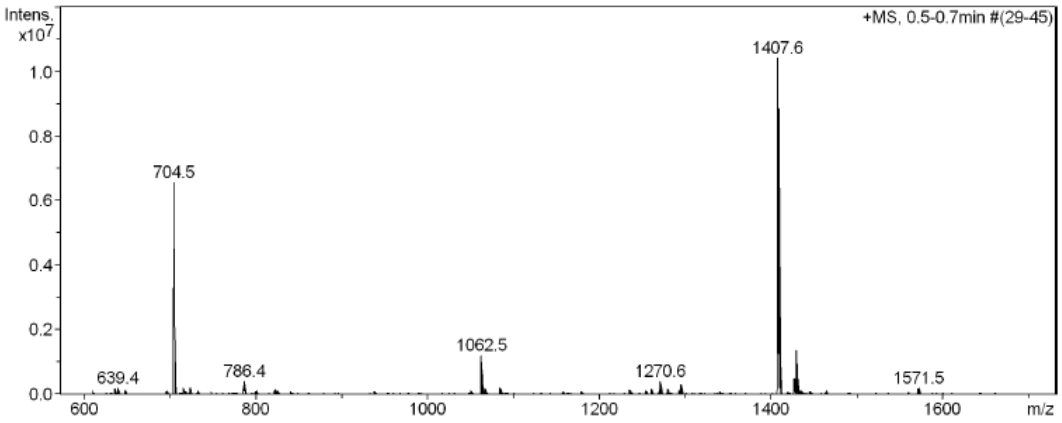

HRMS *m/z* (%)

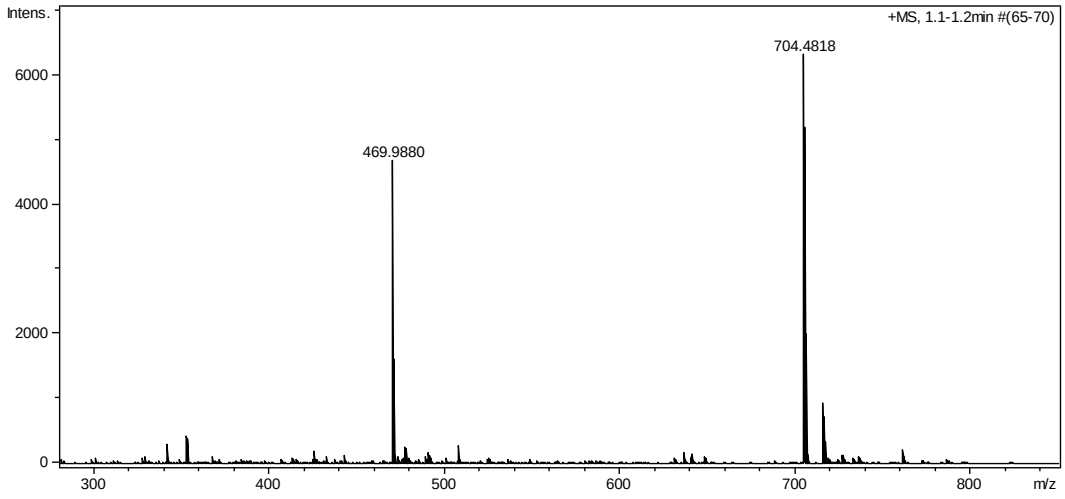

Ts-His-Lys-Leu-His-Lys-Lys-Ile-Leu-Lys-Val-Leu-NH_2 (BP274)

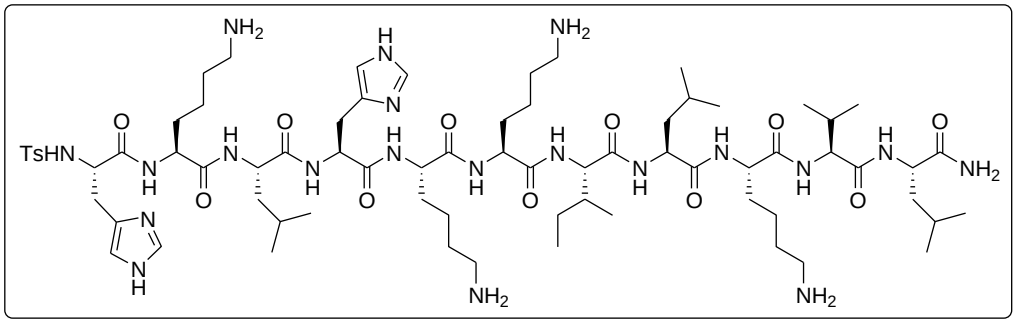

HPLC (λ = 220 nm)

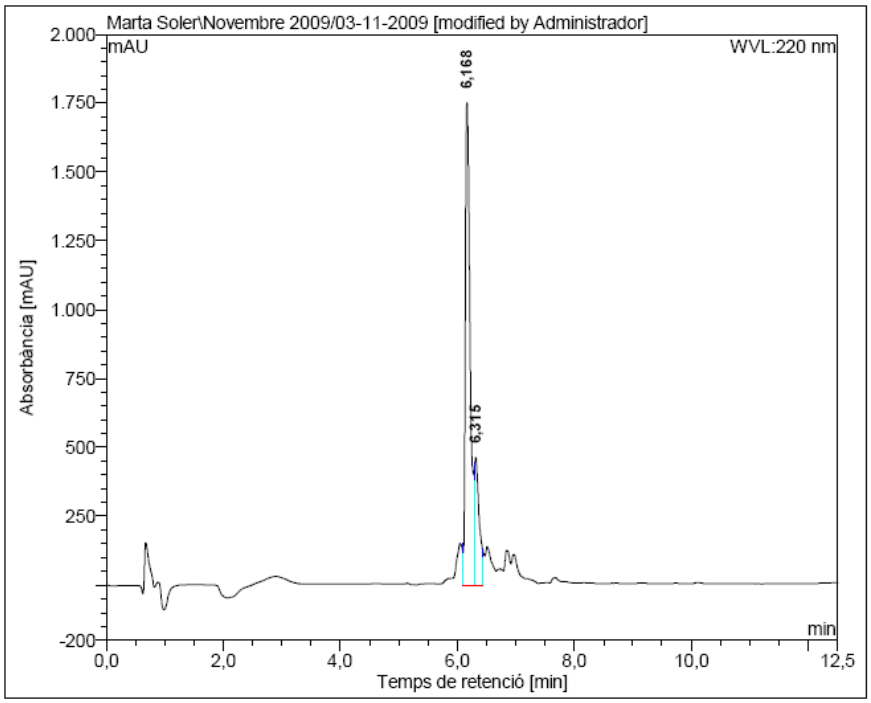

No.	mps retenc min	alçada mAU	Area mAU*min	Area relativa %
1	6,17	1750,550	168,461	79,96
2	6,31	464,518	42,226	20,04
Total:		2215,067	210,687	100,00

ESI-MS *m/z* (%)

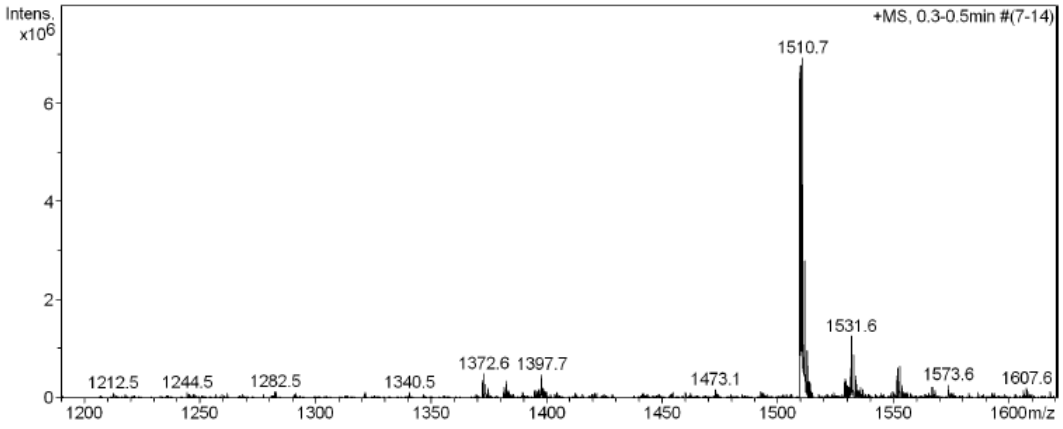

Ts-Phe-Lys-Leu-His-Lys-Lys-Ile-Leu-Lys-Val-Leu-NH_2 (BP275)

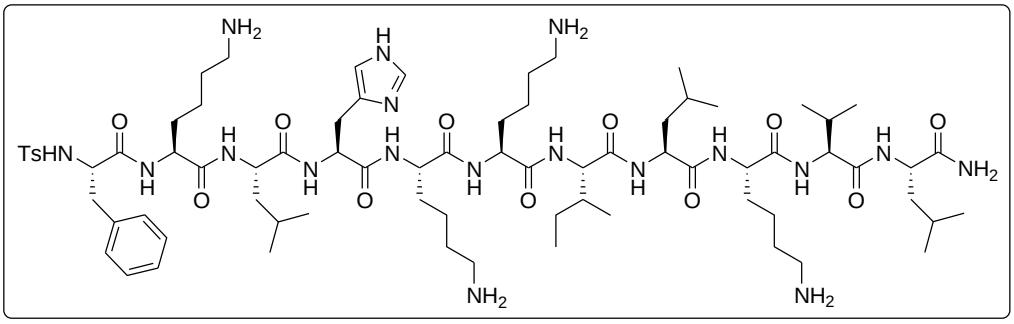

HPLC (λ = 220 nm)

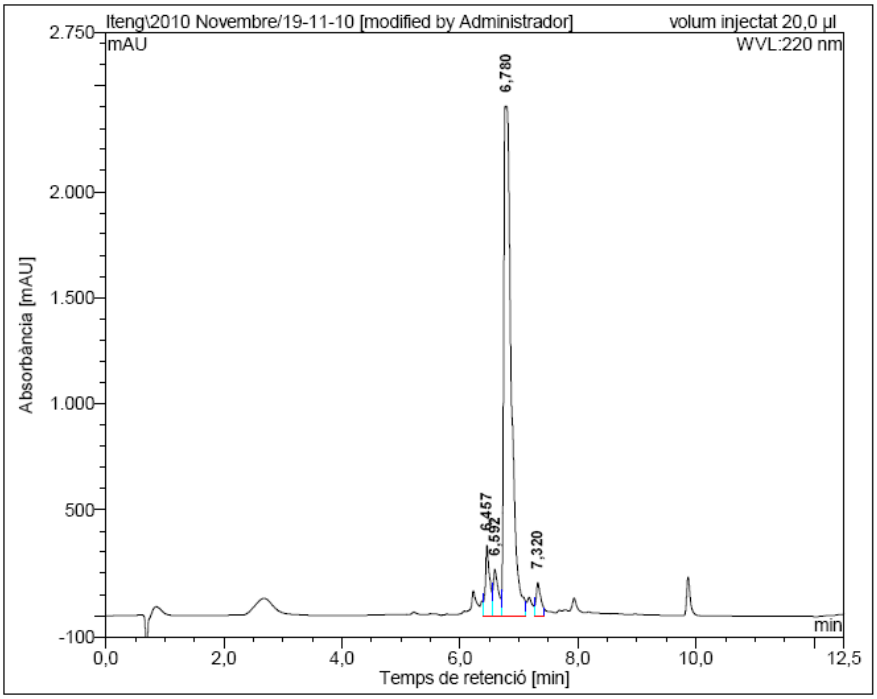

No.	Temps retenció min	alçada mAU	Area mAU*min	Area relativa %
1	6,46	331,718	27,779	6,55
2	6,59	218,288	22,471	5,30
3	6,78	2403,865	358,363	84,51
4	7,32	160,866	15,414	3,64
Total:		3114,737	424,027	100,00

ESI-MS *m/z* (%)

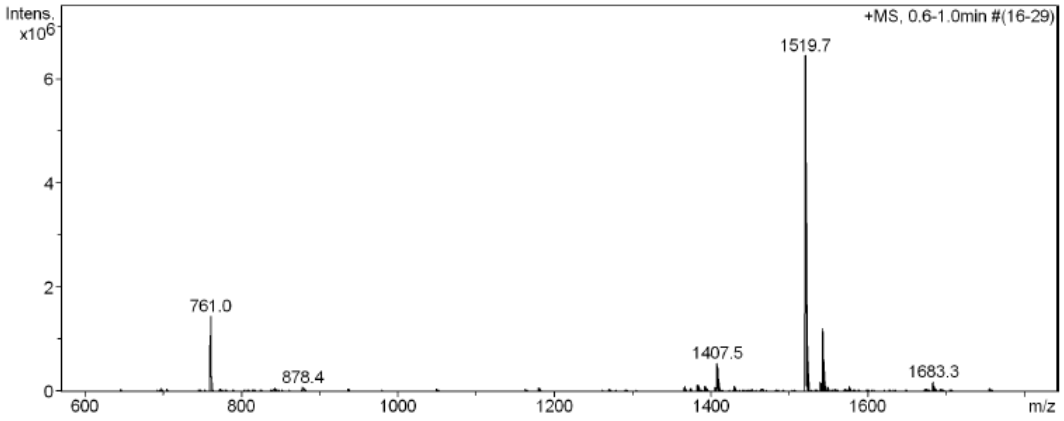

HRMS *m/z* (%)

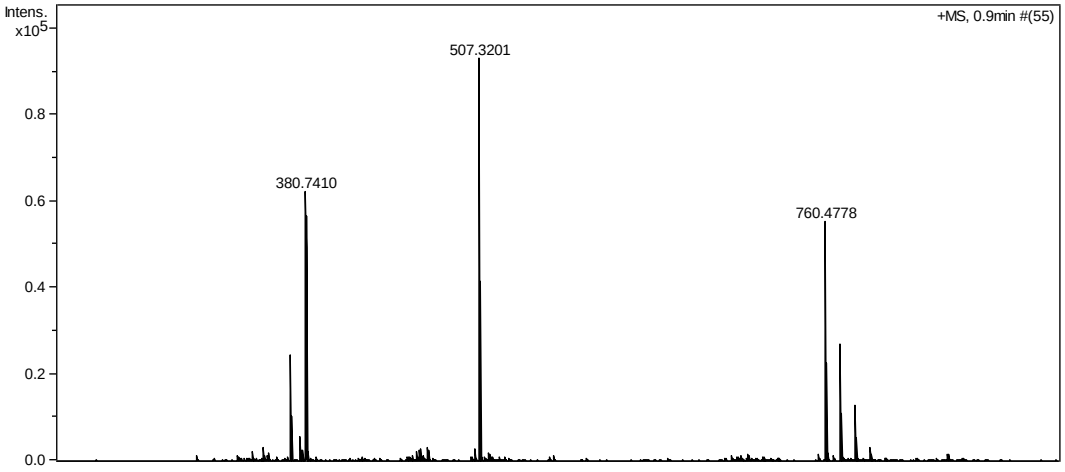

H-His-Lys-Leu-Phe-Lys-Lys-Ile-Leu-Lys-Phe-Leu-NH_2 (BP284)

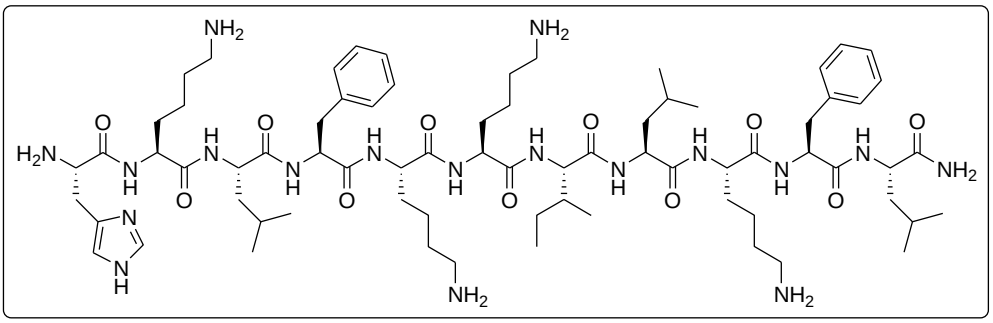

HPLC (λ = 220 nm)

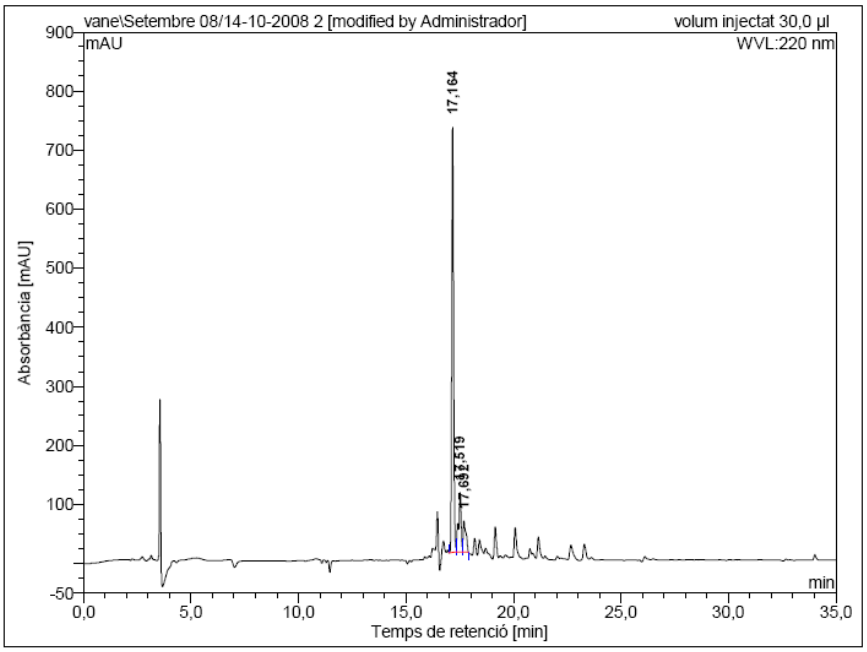

No.	Temps retenció min	alçada mAU	Area mAU*min	Area relativa %
1	17,16	719,258	71,310	76,43
2	17,52	100,179	13,912	14,91
3	17,69	52,007	8,081	8,66
Total:		871,445	93,303	100,00

ESI-MS *m/z* (%)

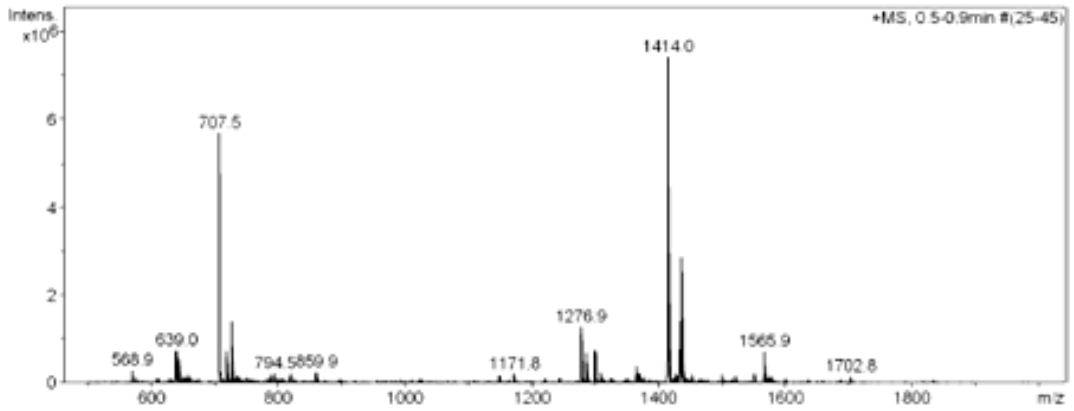
Intens.
x10^6
+MS, 0.5-0.9min #(25-45)
1414.0
707.5
1276.9
639.0
568.9
794.5859.9
1171.8
1565.9
1702.8
6
4
2
0
600
800
1000
1200
1400
1600
1800
m/z

H-Phe-Lys-Leu-Phe-Lys-Lys-Ile-Leu-Lys-His-Leu-NH_2 (BP285)

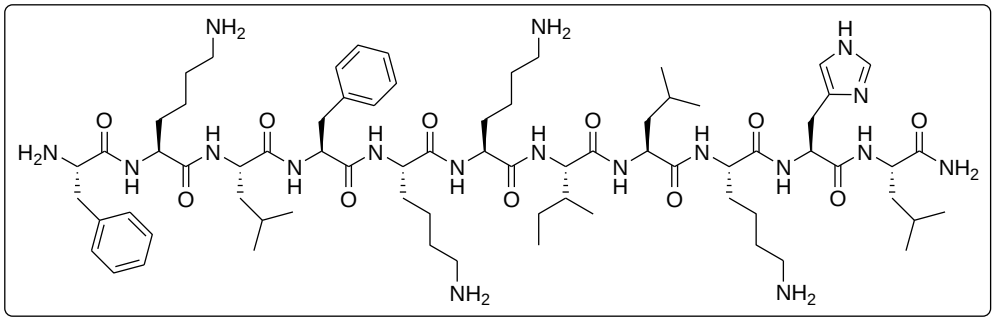

HPLC (λ = 220 nm)

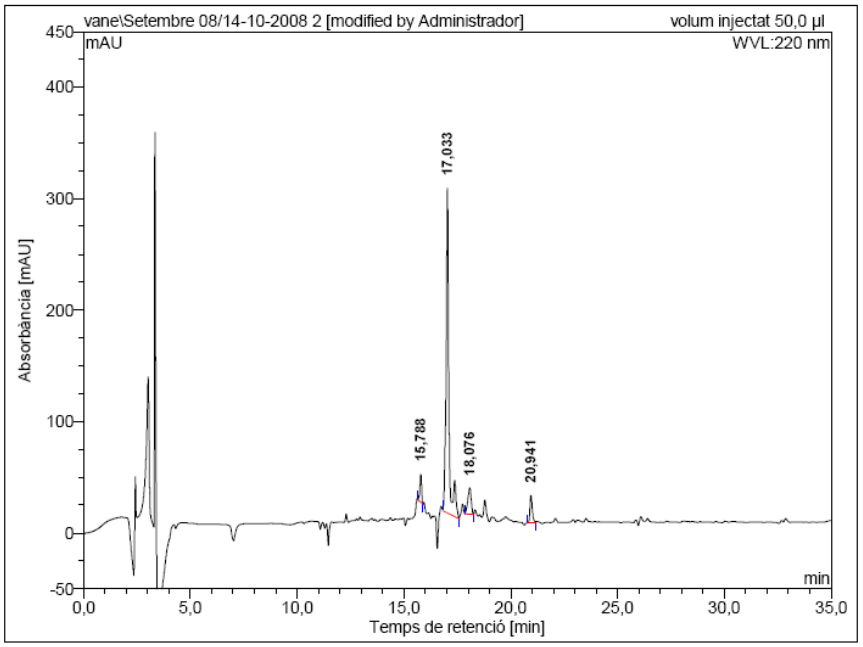

No.	Temps retenció min	alçada mAU	Area mAU*min	Area relativa %
1	15,79	25,009	2,286	4,29
2	17,03	291,403	43,699	81,93
3	18,08	23,502	4,253	7,97
4	20,94	24,215	3,098	5,81
Total:		364,129	53,336	100,00

ESI-MS *m/z* (%)

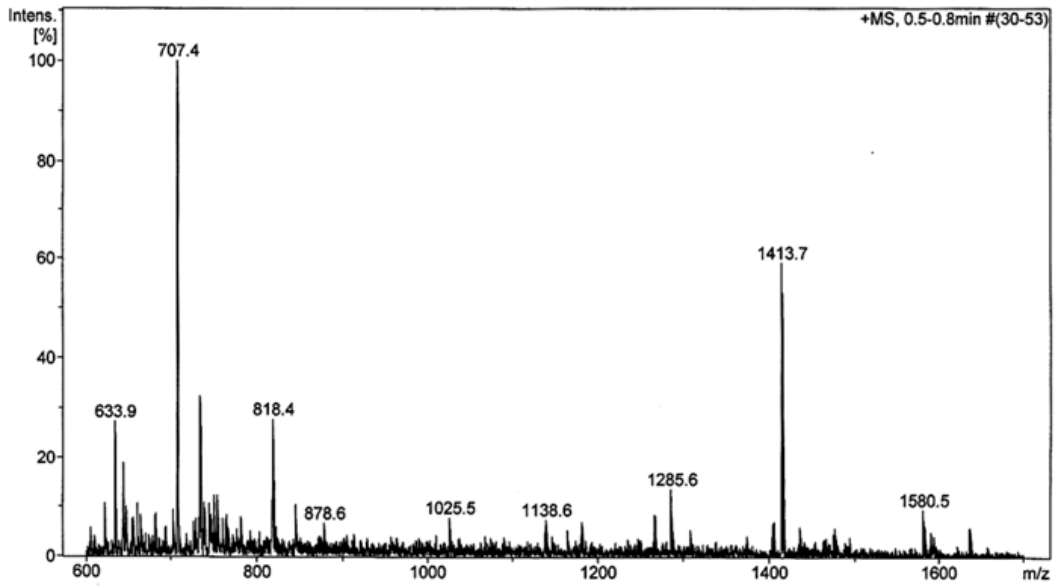
Intens.
[%]
+MS, 0.5-0.8min #(30-53)
707.4
1413.7
633.9
818.4
878.6
1025.5
1138.6
1285.6
1580.5
100
80
60
40
20
0
600
800
1000
1200
1400
1600
m/z

H-His-Lys-Leu-Phe-Lys-Lys-Ile-Leu-Lys-His-Leu-NH_2 (BP305)

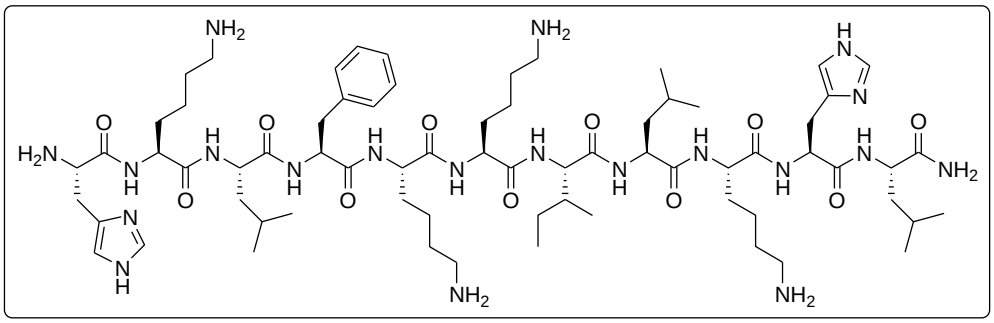

HPLC (λ = 220 nm)

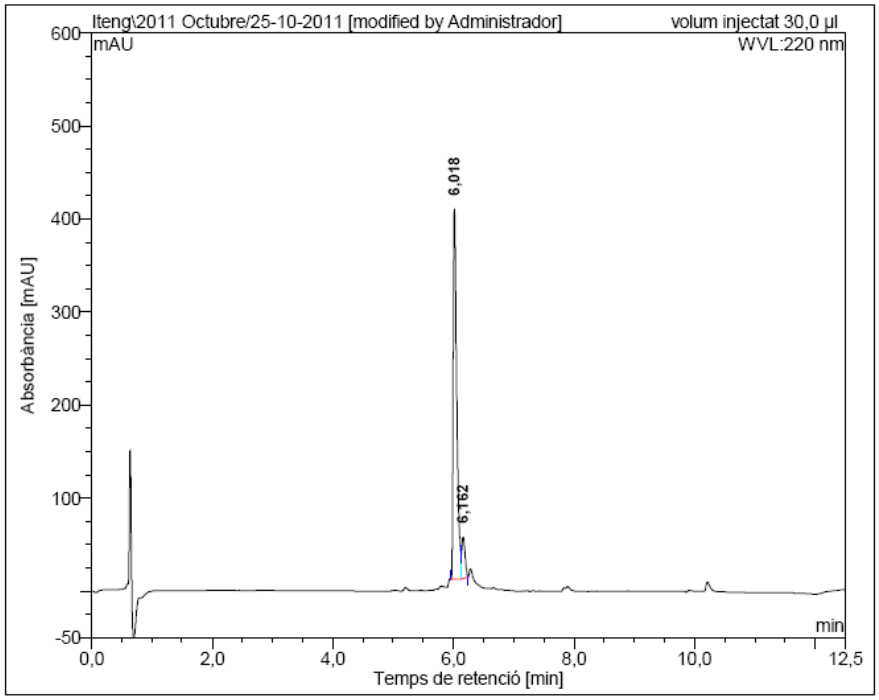

No.	Temps retenció min	alçada mAU	Area mAU*min	Area relativa %
1	6,02	398,123	27,271	90,80
2	6,16	44,528	2,765	9,20
Total:		442,651	30,036	100,00

ESI-MS *m/z* (%)

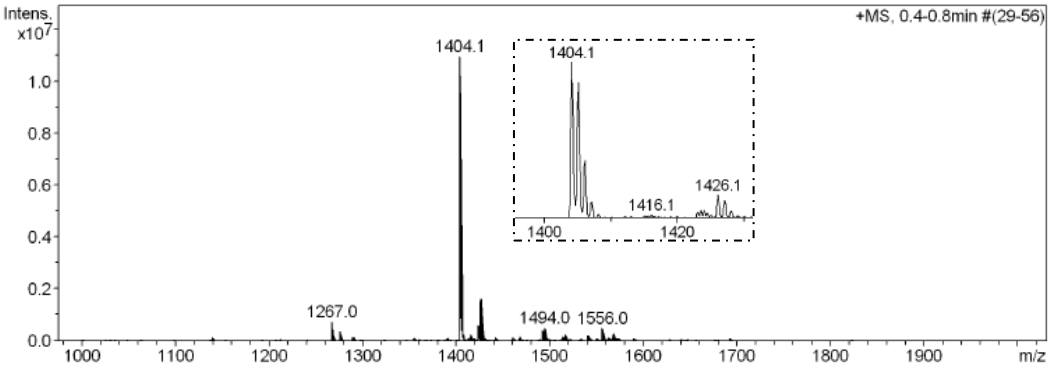
Intens.
x10^7
+MS, 0.4-0.8min #(29-56)
1404.1
1404.1
1426.1
1416.1
1400
1420
1267.0
1494.0
1556.0
1.0
0.8
0.6
0.4
0.2
0.0
1000
1100
1200
1300
1400
1500
1600
1700
1800
1900
m/z

H-His-Lys-Leu-His-Lys-Lys-Ile-Leu-Lys-His-Leu-NH_2 (BP306)

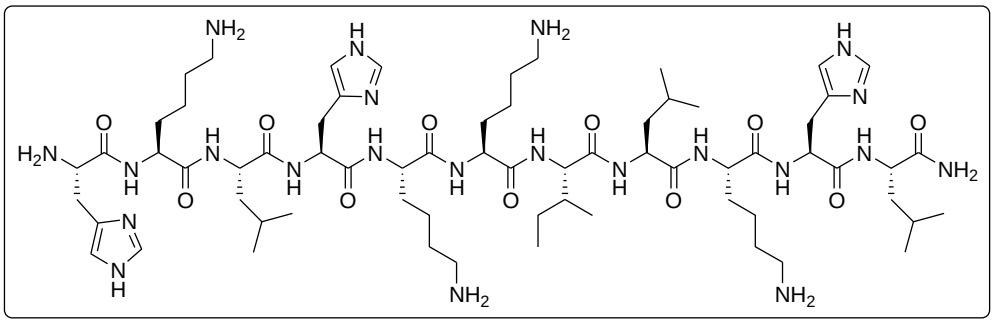

HPLC (λ = 220 nm)

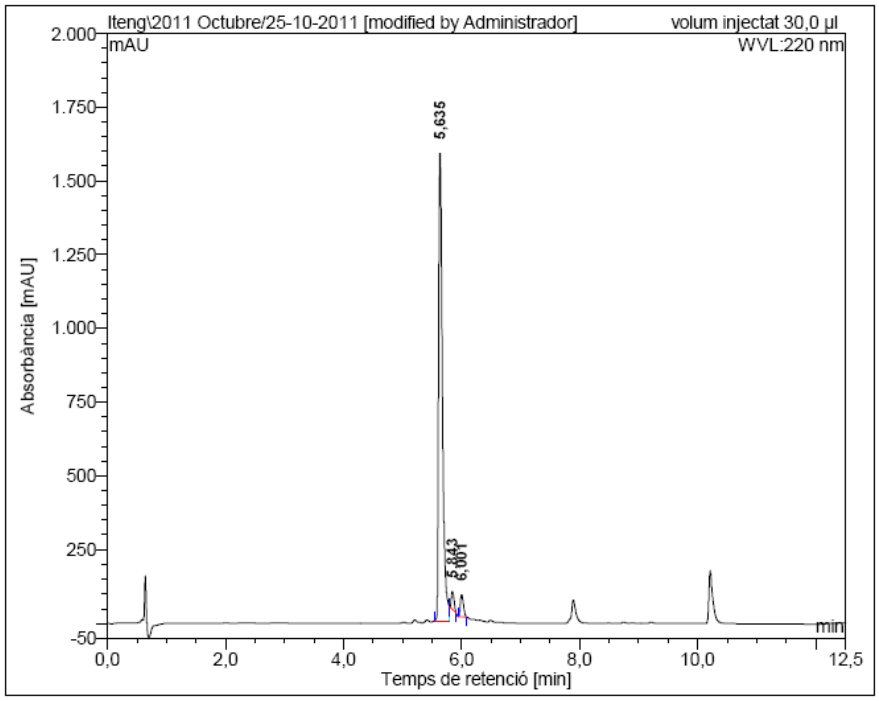

No.	Temps retenció min	alçada mAU	Area mAU*min	Area relativa %
1	5,63	1587,064	120,157	93,97
2	5,84	59,970	3,273	2,56
3	6,00	74,514	4,438	3,47
Total:		1721,547	127,869	100,00

ESI-MS *m/z* (%)

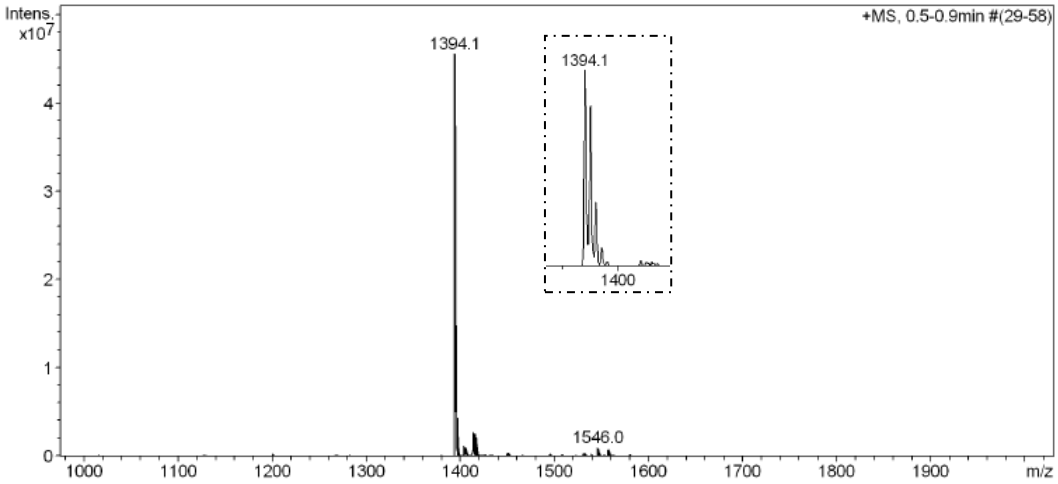
Intens.
x10^7
+MS, 0.5-0.9min #(29-58)
1394.1
1394.1
1400
1546.0
0
1
2
3
4
1000
1100
1200
1300
1400
1500
1600
1700
1800
1900
m/z

SUPPORTING INFORMATION CHAPTER 4

Solid-phase synthesis of biaryl cyclic peptides containing a histidine-phenylalanine linkage

Iteng Ng-Choi,[1] Lidia Feliu[1]* and Marta Planas[1]*

TABLE OF CONTENTS

Copies of HPLC, MS and NMR spectra

1. Synthesis of amino acid derivatives

Fmoc-Phe(4-I)-OH (21)

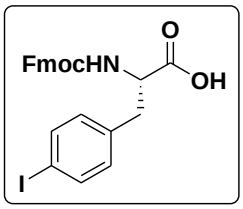

HPLC (λ = 220 nm)

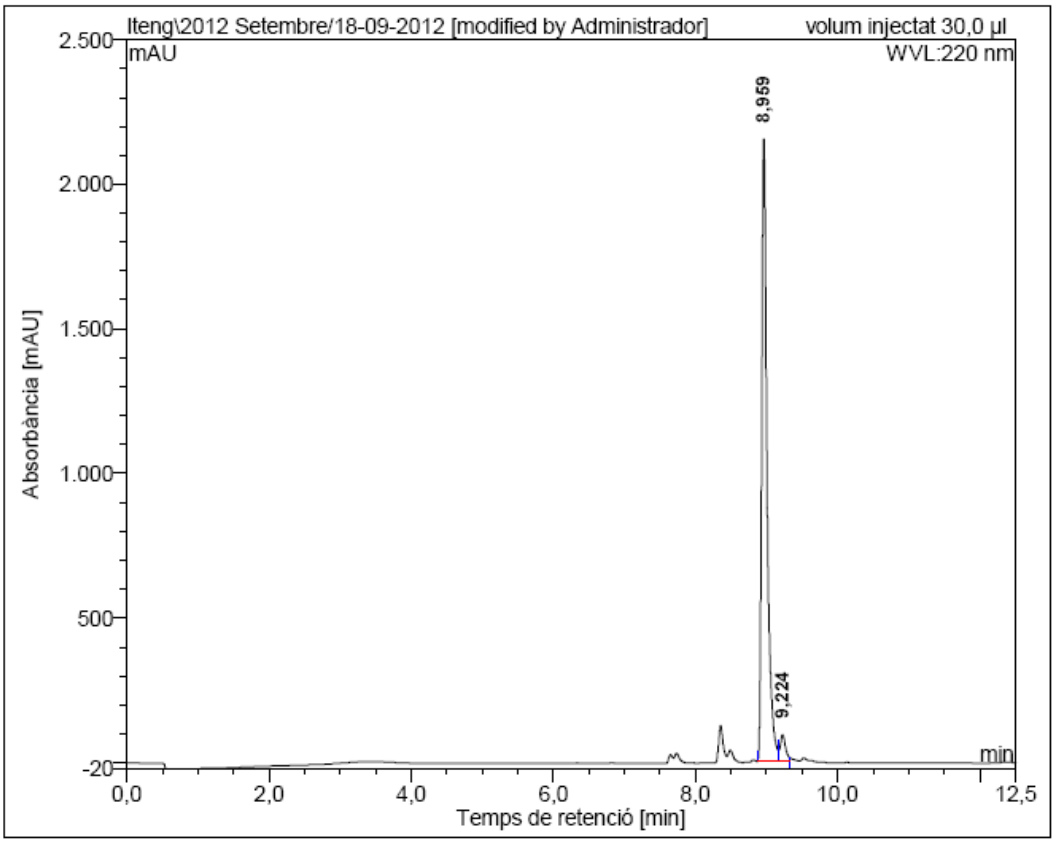

No.	Temps retenció min	alçada mAU	Area mAU*min	Area relativa %
1	8,96	2152,020	190,045	95,93
2	9,22	92,483	8,055	4,07
Total:		2244,503	198,099	100,00

ESI-MS *m/z* (%)

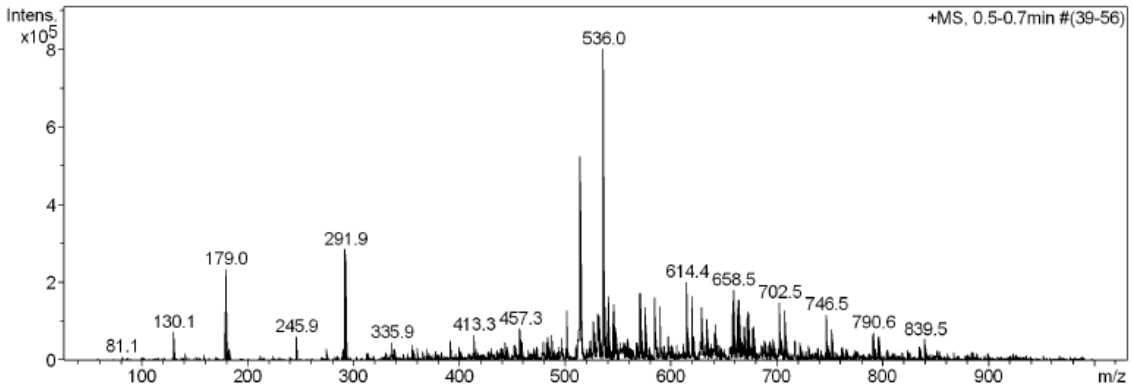

^{1}H-NMR (400 MHz, DMSO-d_6) δ (ppm)

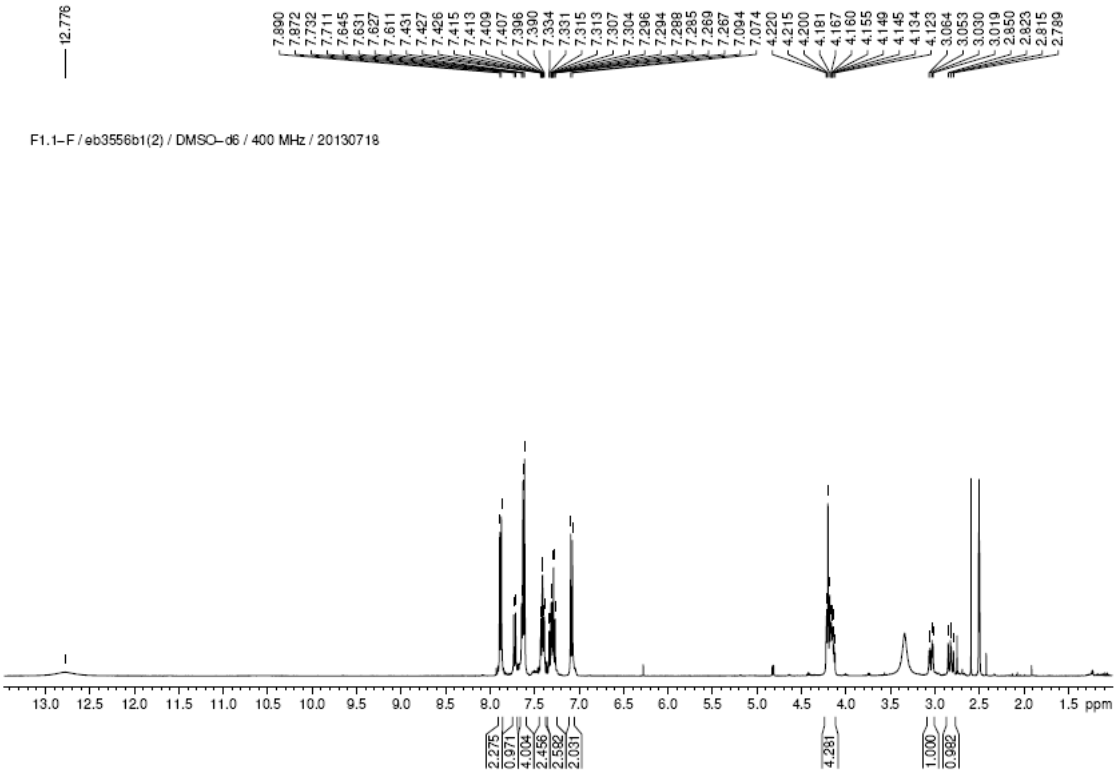

^{13}C-NMR (75 MHz, DMSO-d_6) δ (ppm)

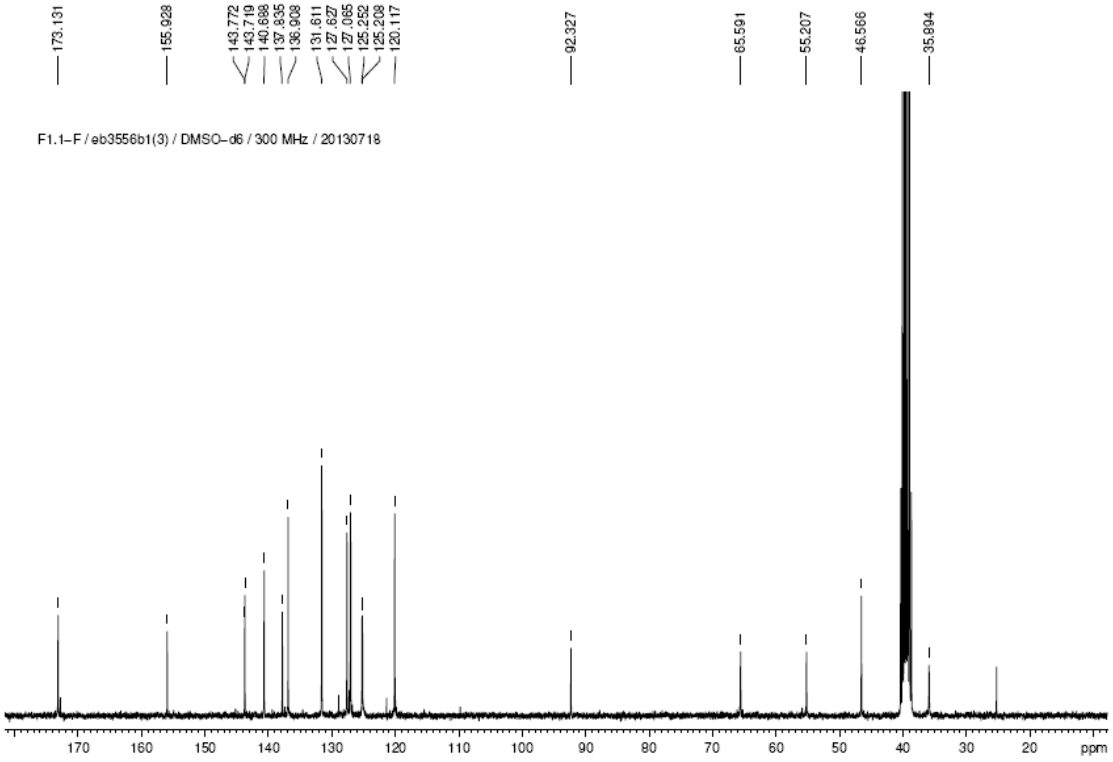

Boc-His(5-Br,1-Me)-OMe and Boc-His(5-Br,3-Me)-OMe

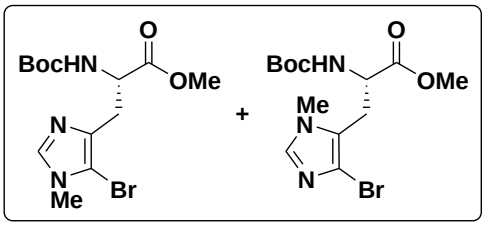

HPLC (λ = 220 nm)

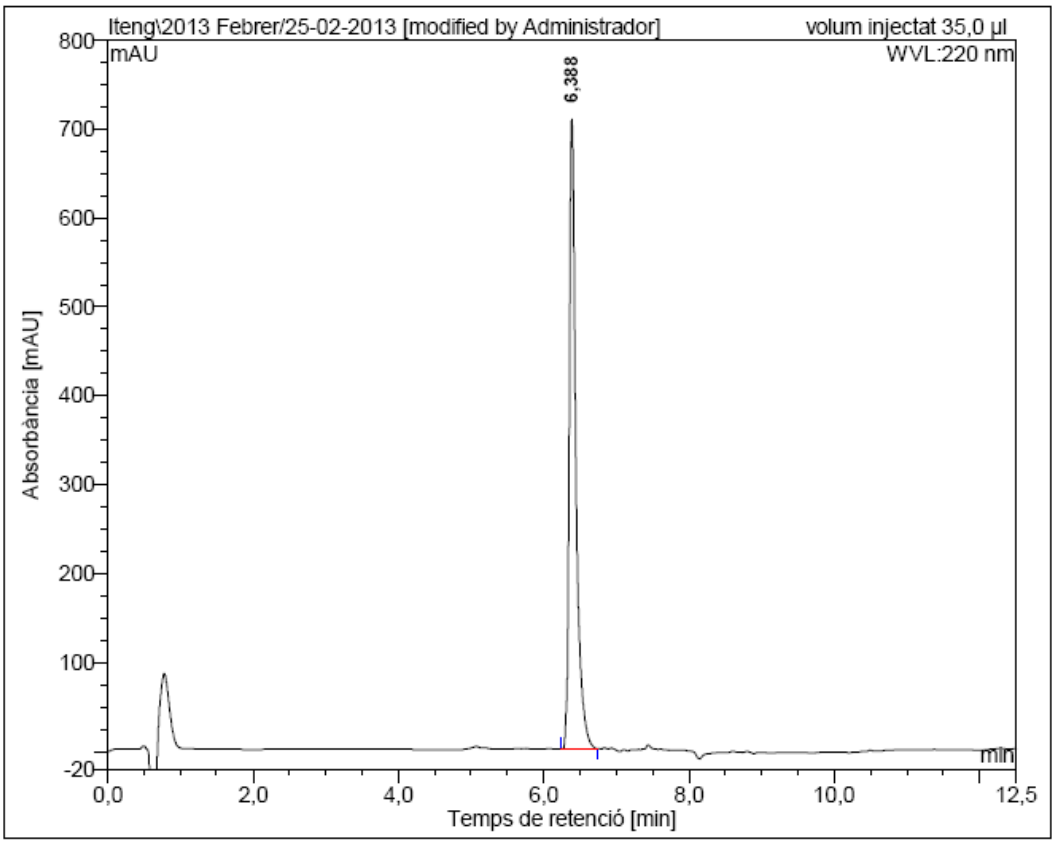

No.	Temps retenció min	alçada mAU	Area mAU*min	Area relativa %
1	6,39	707,993	76,340	100,00
Total:		707,993	76,340	100,00

ESI-MS *m/z* (%)

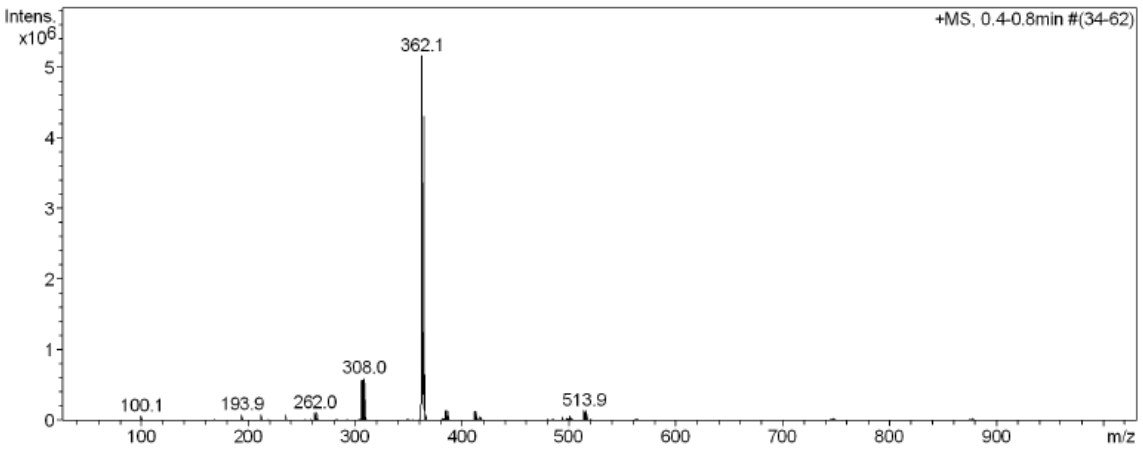

^{1}H-NMR (400 MHz, $CDCl_3$) δ (ppm)

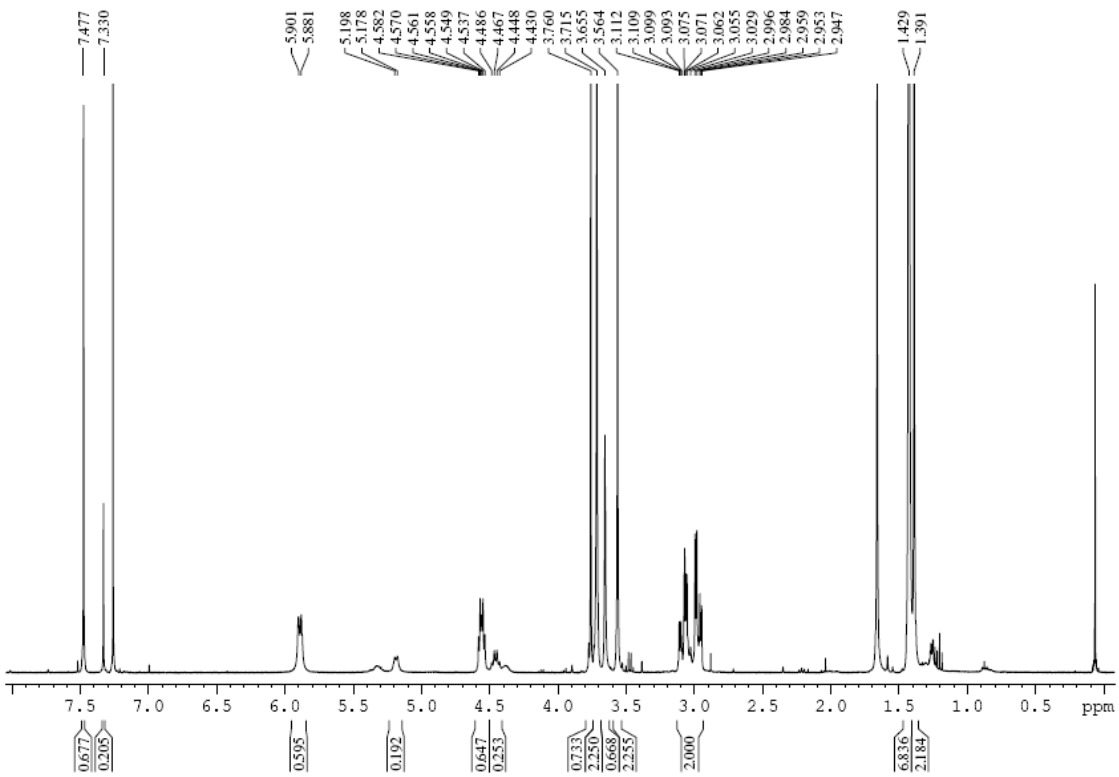

Boc-His(5-Br,1-Me)-OH (41a) and Boc-His(5-Br,3-Me)-OH (41b)

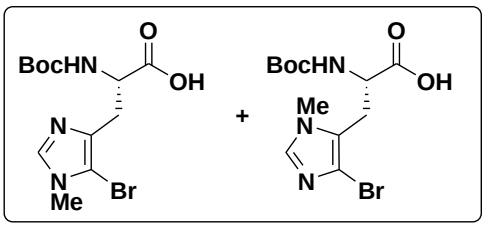

HPLC (λ = 220 nm)

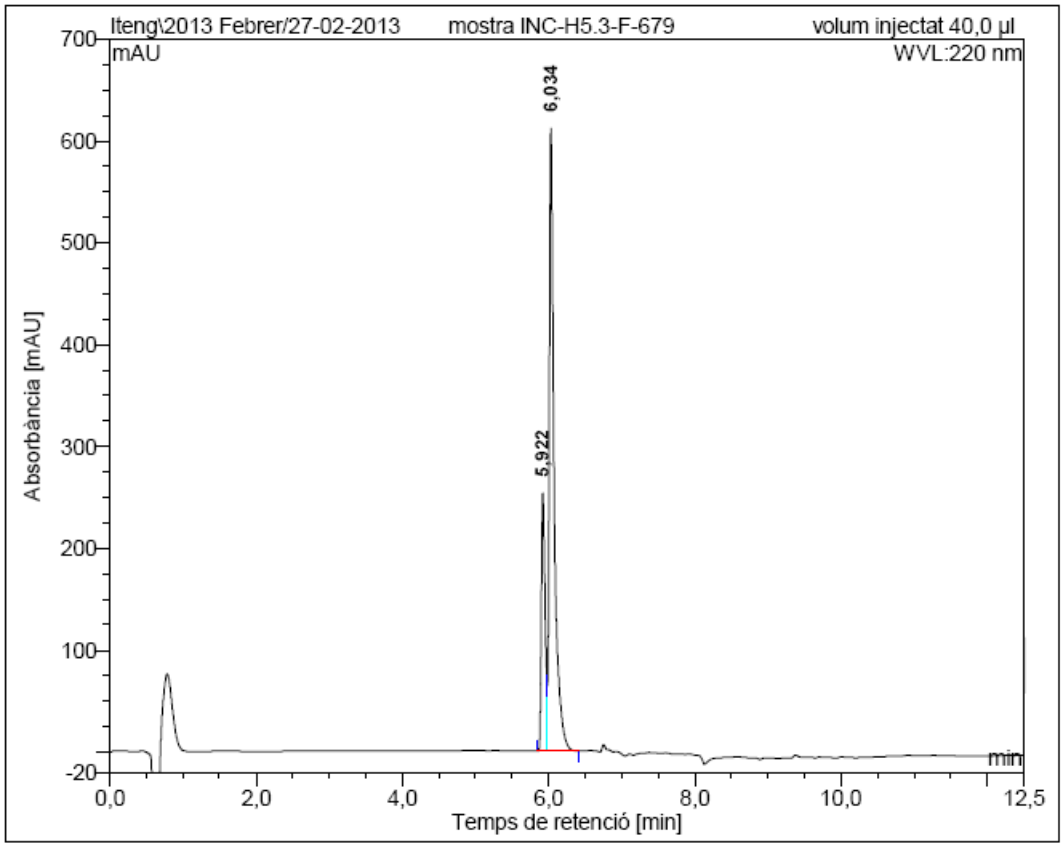

No.	Temps retenció min	alçada mAU	Area mAU*min	Area relativa %
1	5,92	253,428	15,068	24,22
2	6,03	611,533	47,141	75,78
Total:		864,961	62,209	100,00

ESI-MS *m/z* (%)

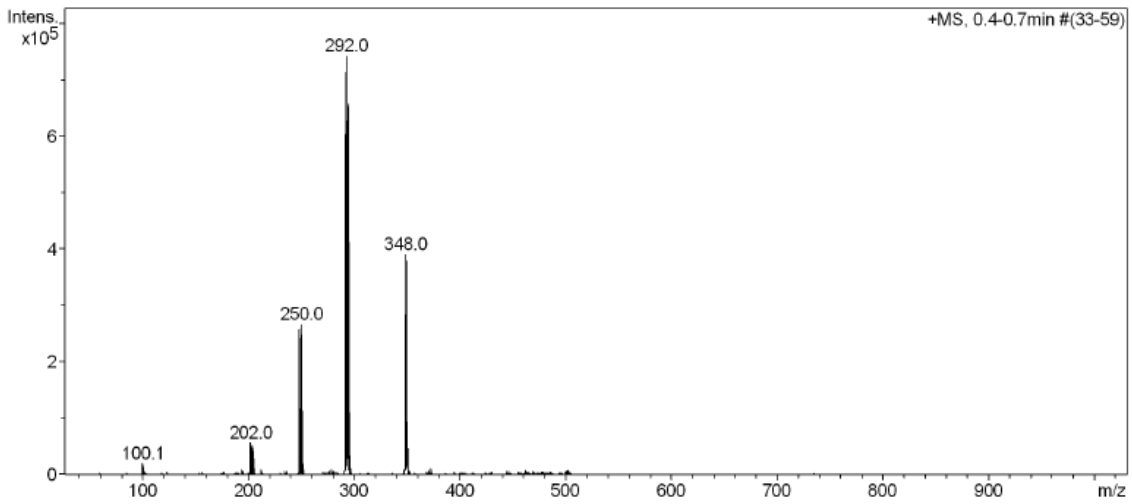

^{1}H-NMR (300 MHz, DMSO-d_6) δ (ppm)

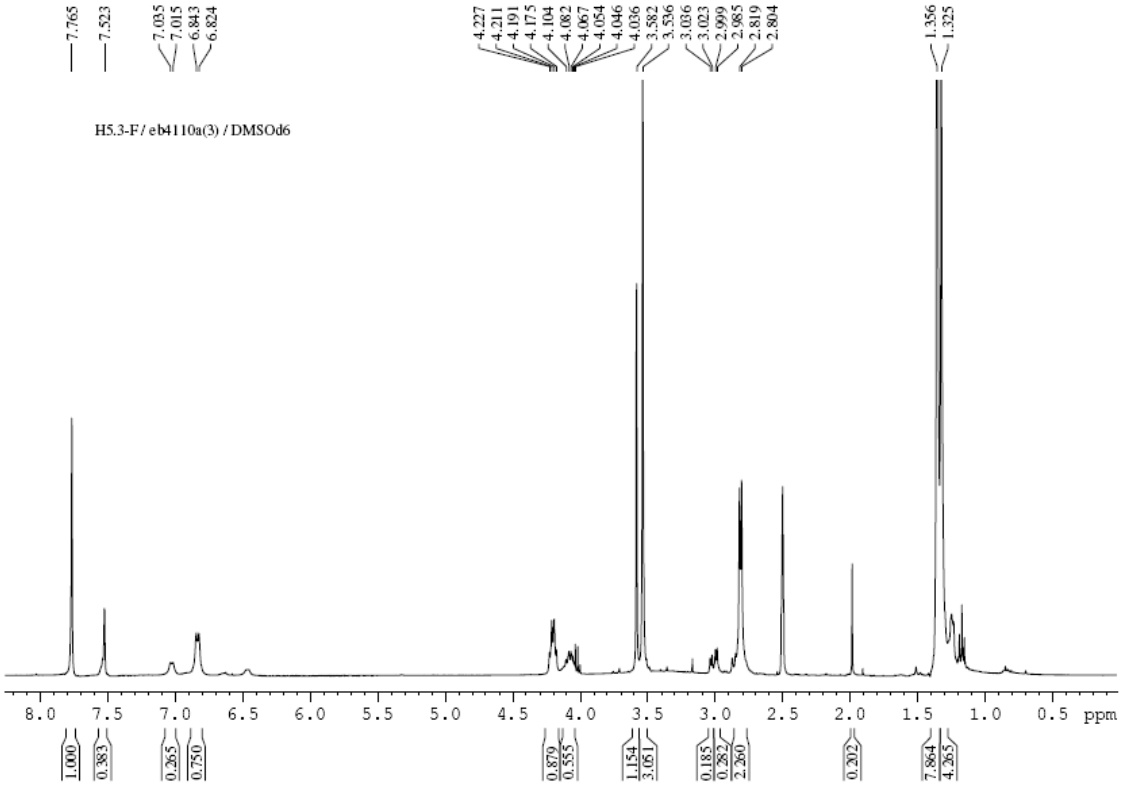

^{13}C-NMR (75 MHz, DMSO-d_6) δ (ppm)

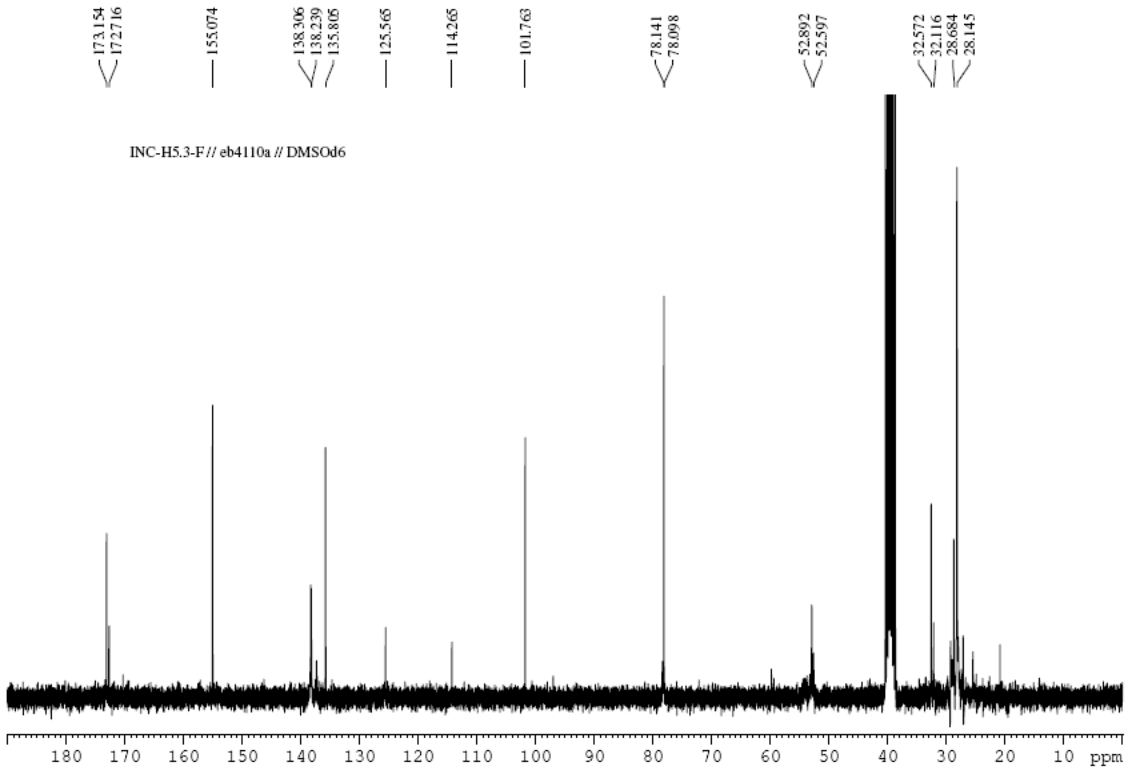

Boc-Phe(4-I)-OMe

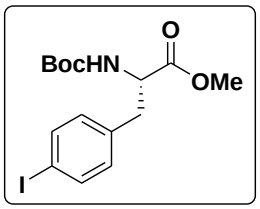

HPLC (λ = 220 nm)

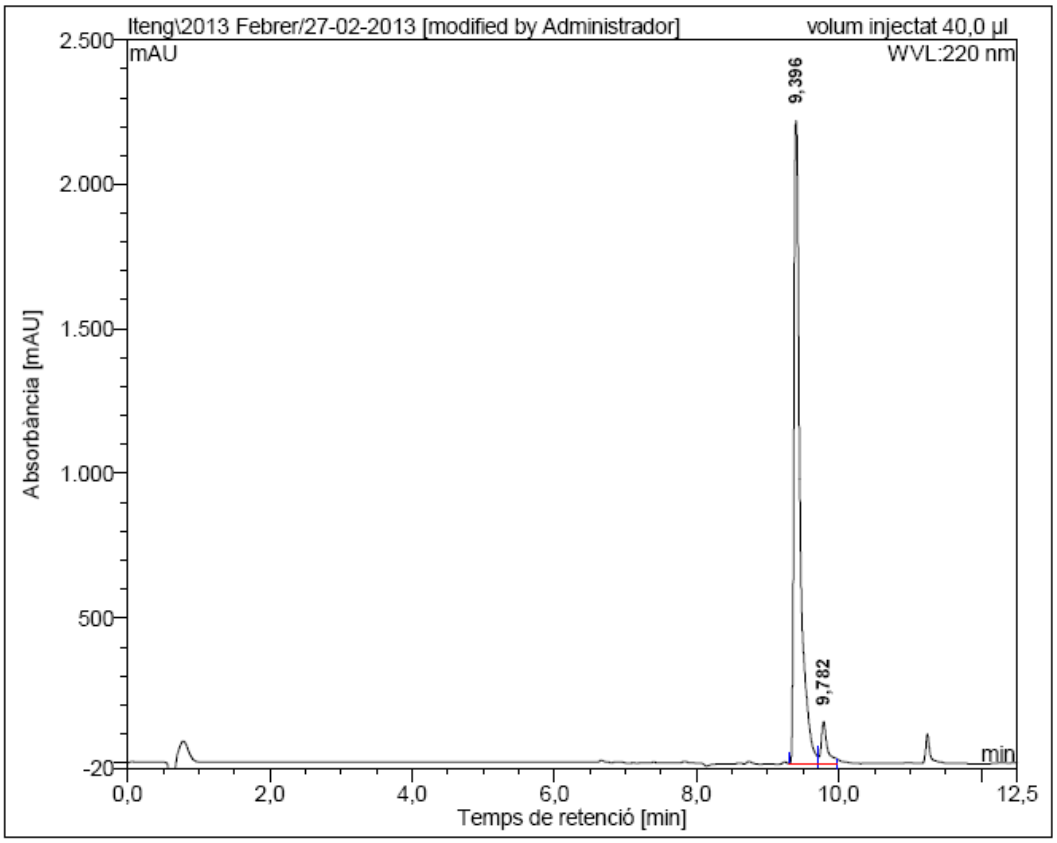

No.	Temps retenció min	alçada mAU	Area mAU*min	Area relativa %
1	9,40	2224,195	224,479	93,96
2	9,78	145,582	14,440	6,04
Total:		2369,777	238,918	100,00

ESI-MS *m/z* (%)

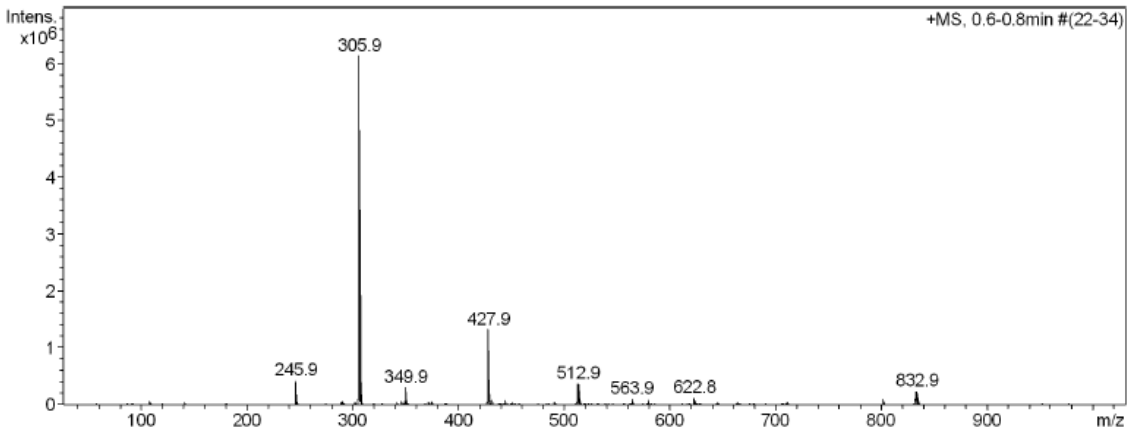

^{1}H-NMR (400 MHz, $CDCl_3$) δ (ppm)

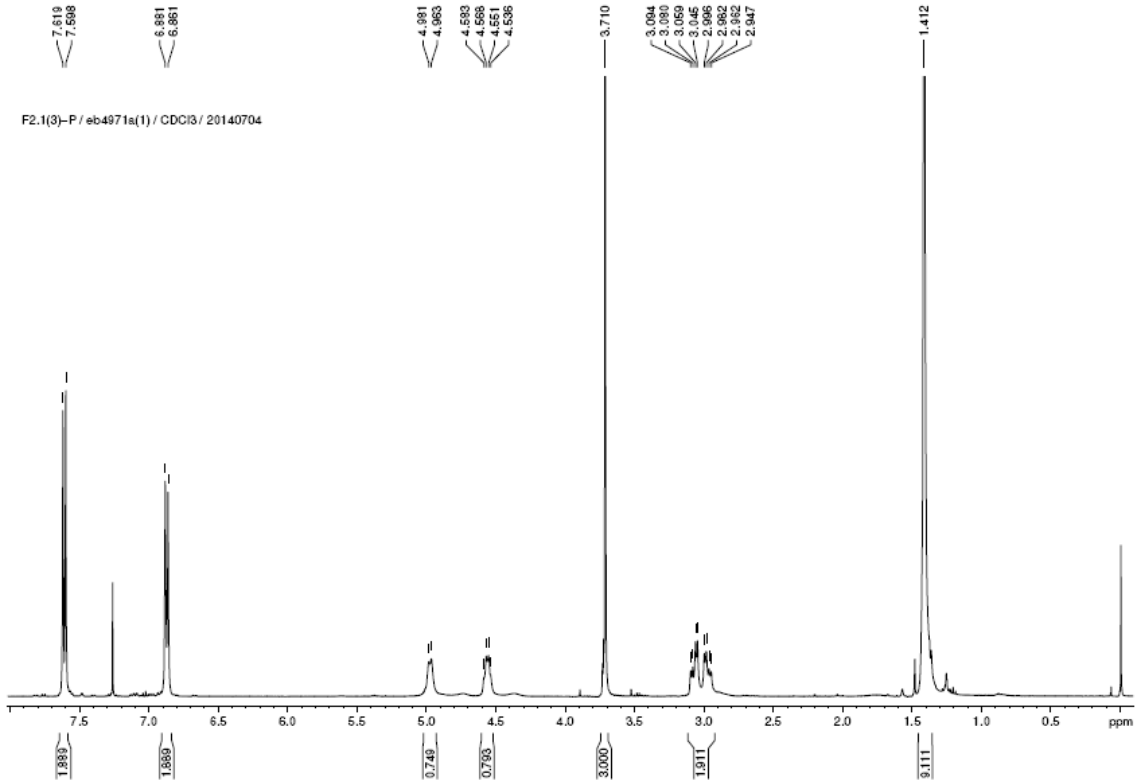

^{13}C-NMR (75 MHz, $CDCl_3$) δ (ppm)

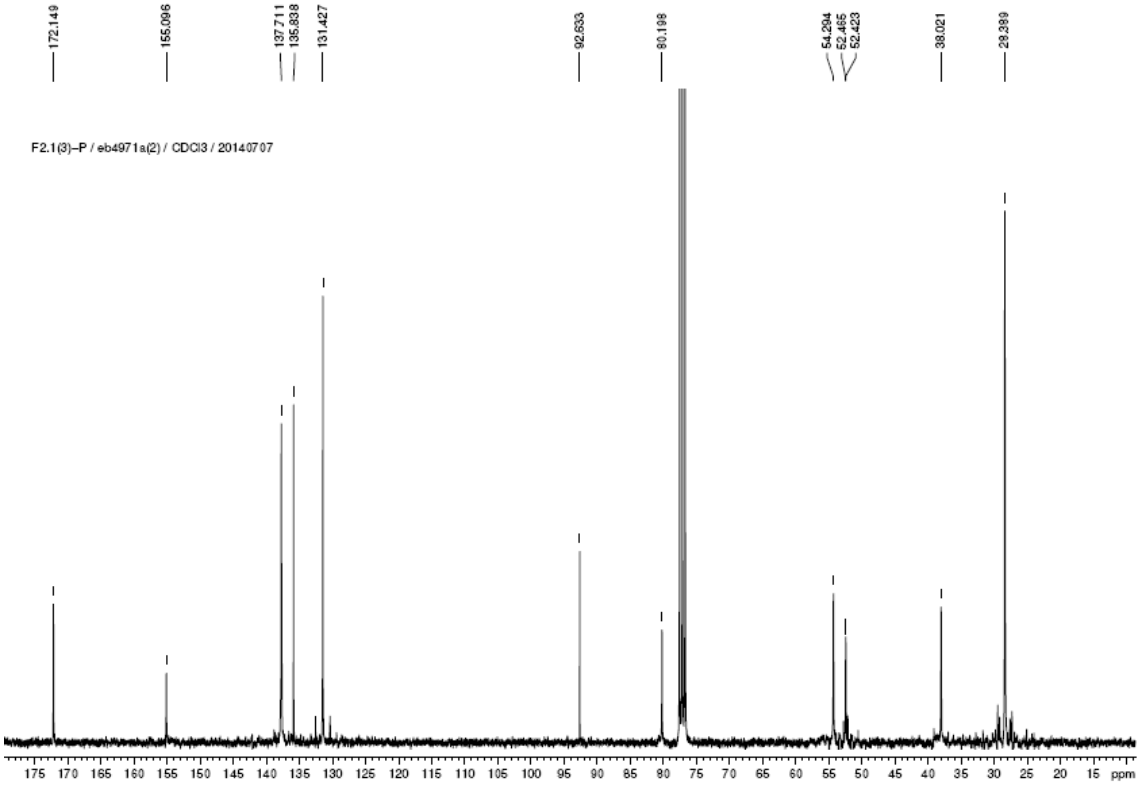

Boc-Phe(4-BPin)-OMe

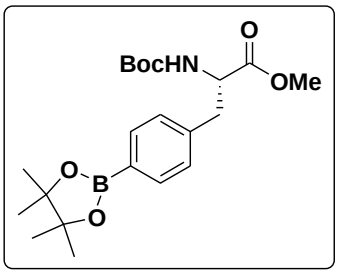

HPLC (λ = 220 nm)

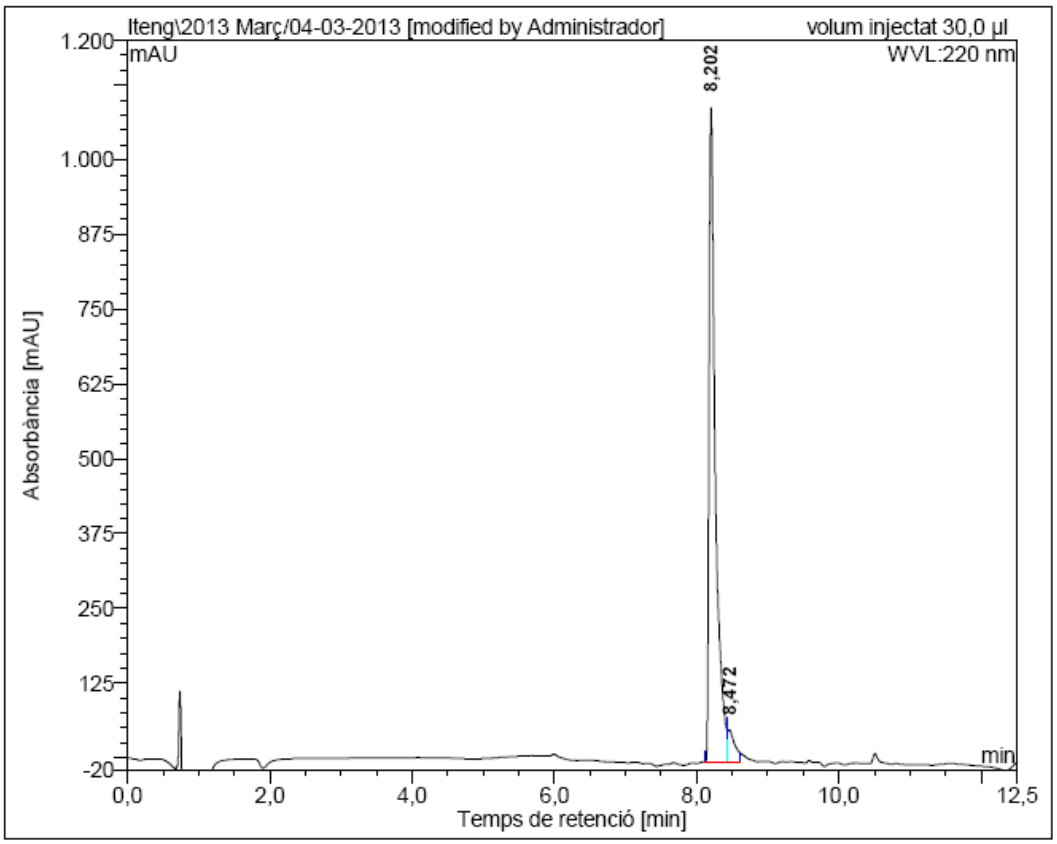

No.	Temps retenció min	alçada mAU	Area mAU*min	Area relativa %
1	8,20	1094,402	112,593	94,14
2	8,47	52,426	7,012	5,86
Total:		1146,827	119,605	100,00

ESI-MS *m/z* (%)

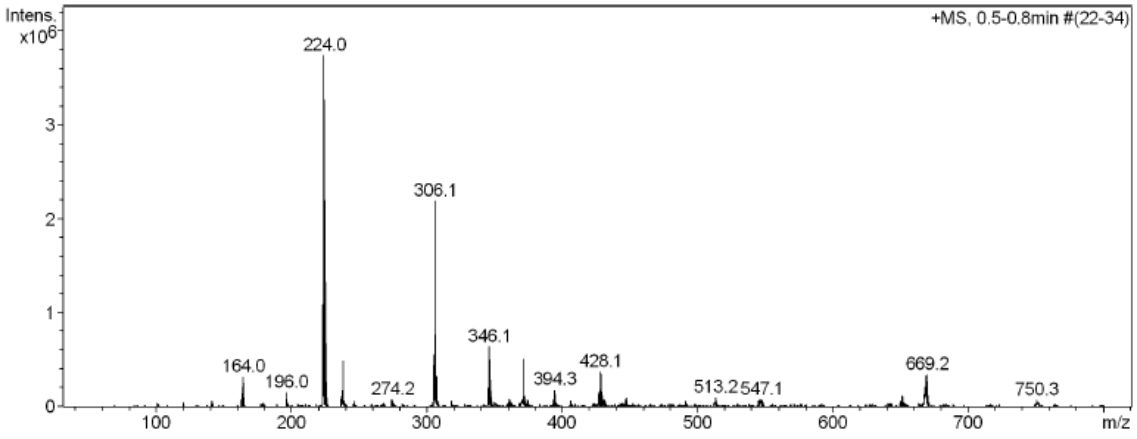

^{1}H-NMR (400 MHz, $CDCl_3$) δ (ppm)

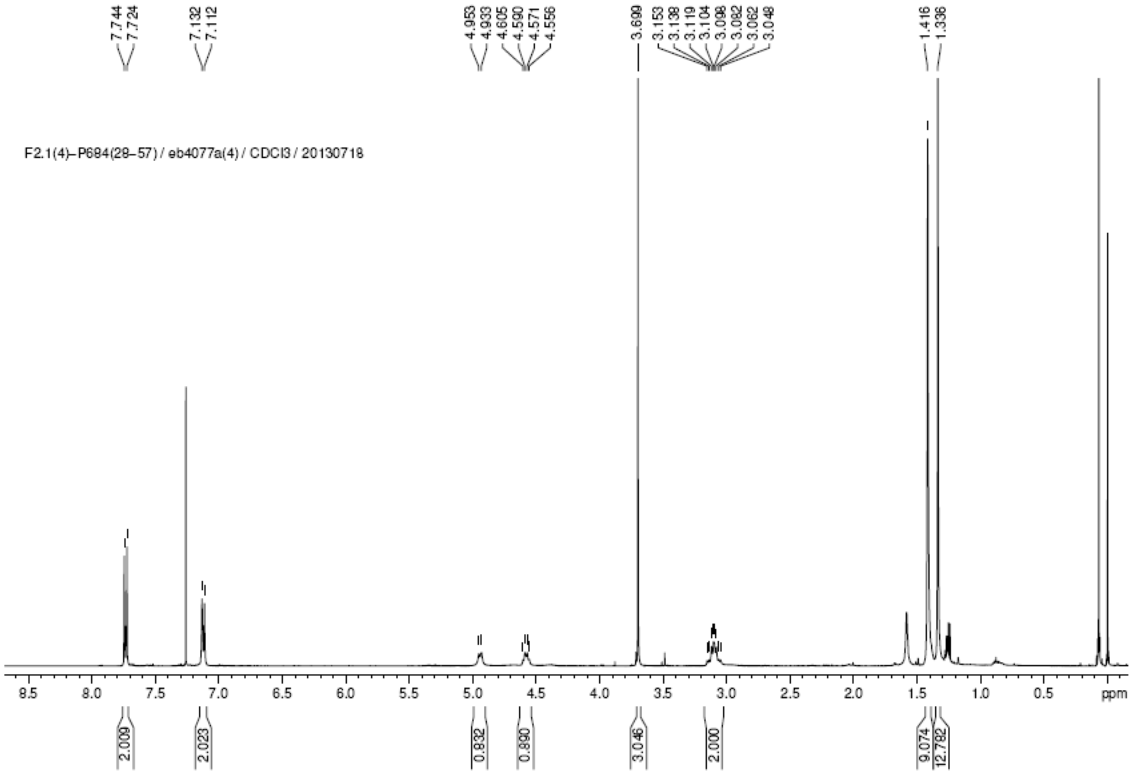

^{13}C-NMR (75 MHz, $CDCl_3$) δ (ppm)

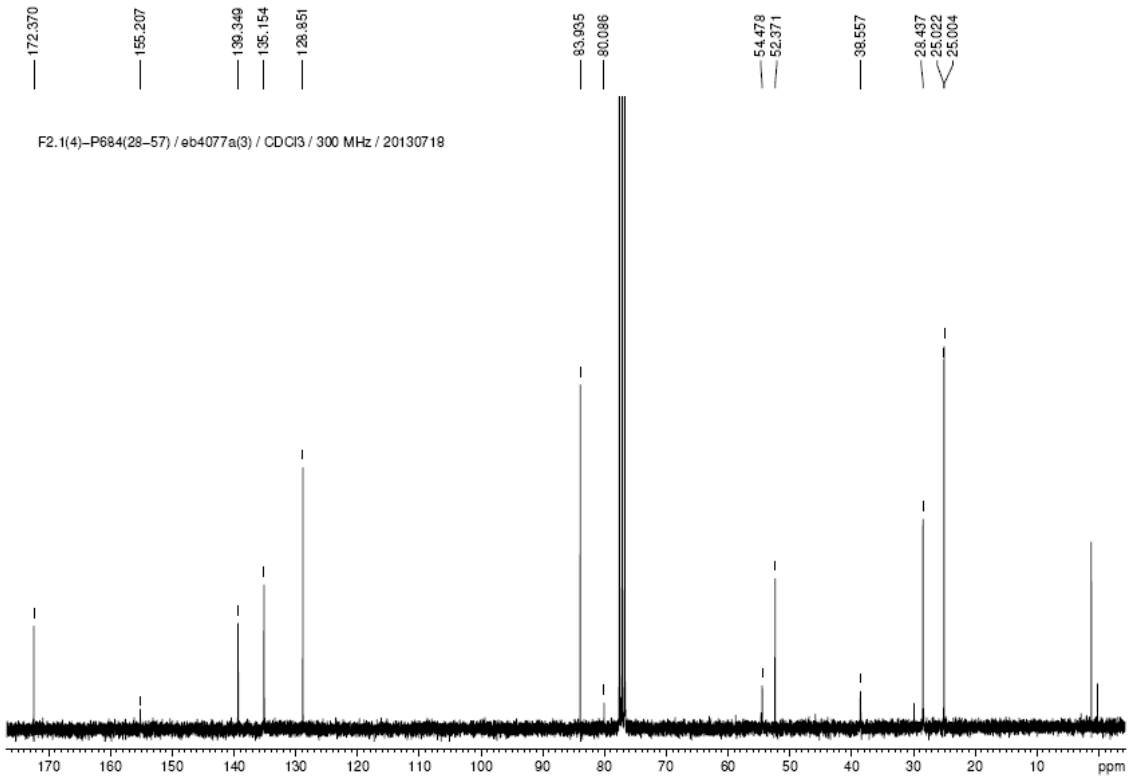

Boc-Phe(4-BPin)-OH (64)

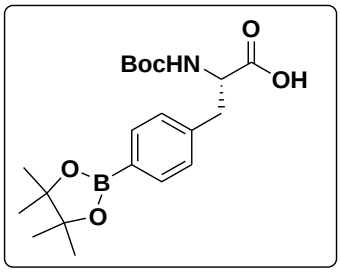

HPLC (λ = 220 nm)

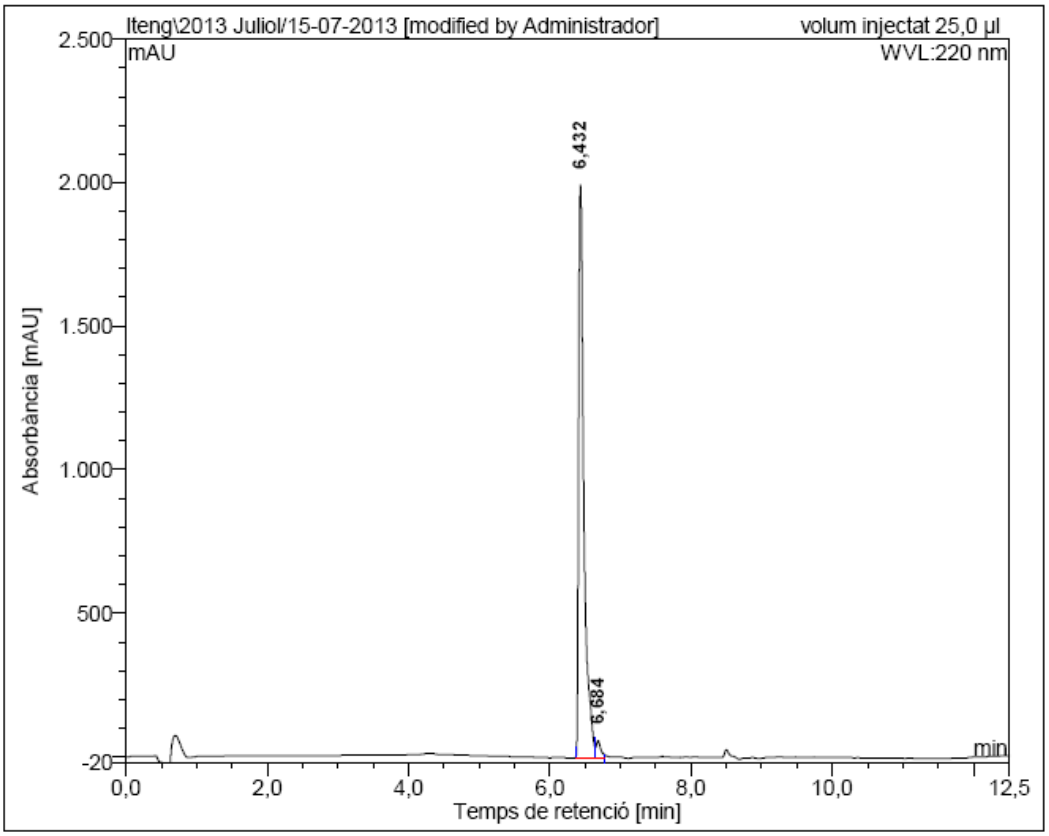

No.	Temps retenció min	alçada mAU	Area mAU*min	Area relativa %
1	6,43	1996,373	172,752	97,52
2	6,68	60,412	4,393	2,48
Total:		2056,784	177,145	100,00

ESI-MS *m/z* (%)

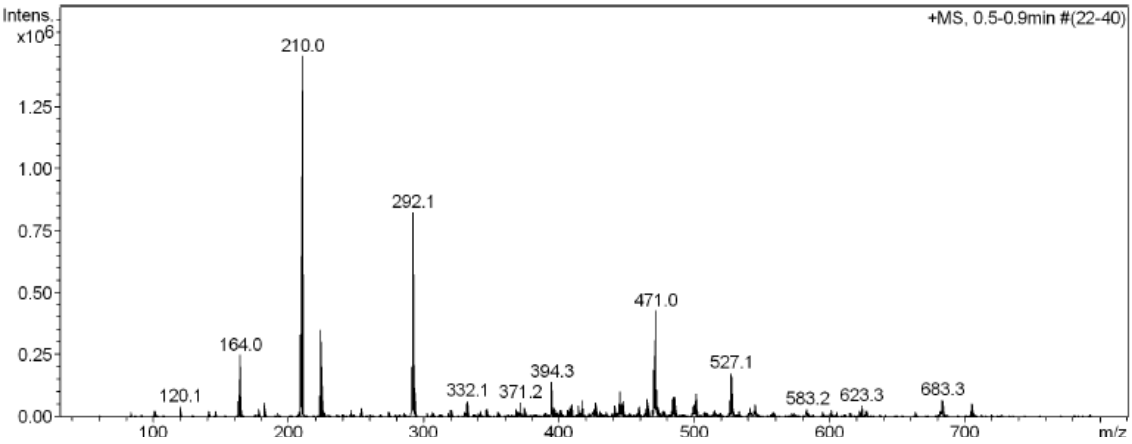

^{1}H-NMR (400 MHz, $CDCl_3$) δ (ppm)

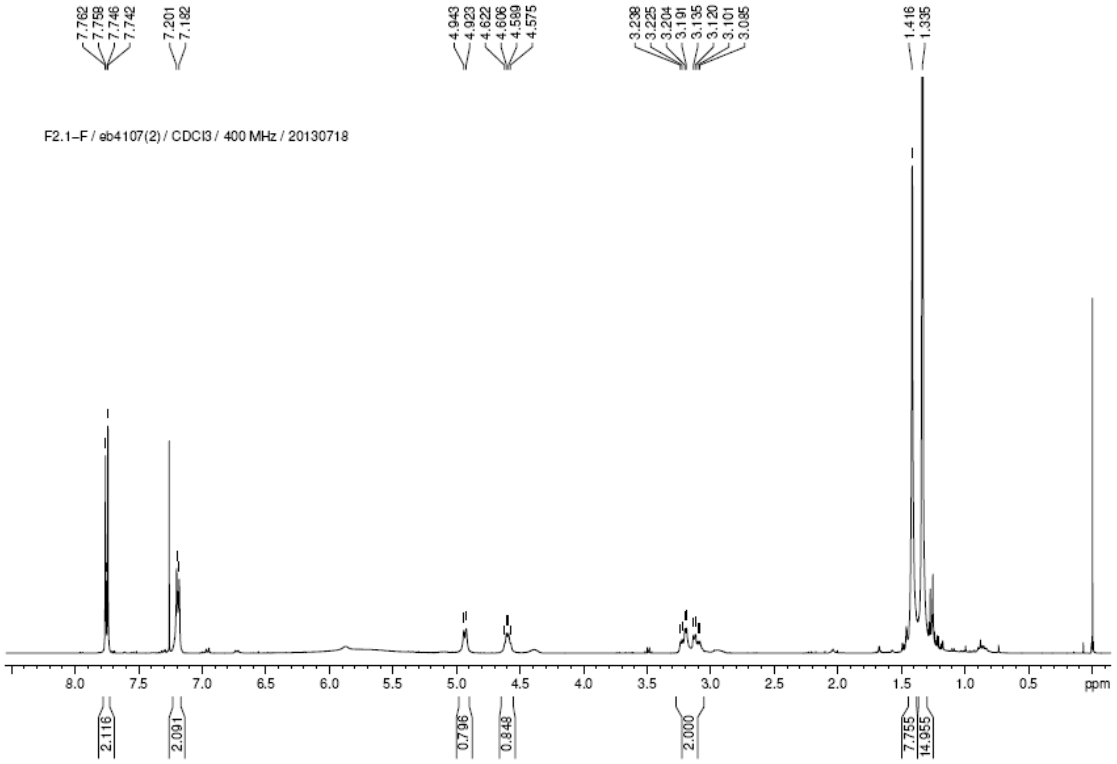

^{13}C-NMR (75 MHz, $CDCl_3$) δ (ppm)

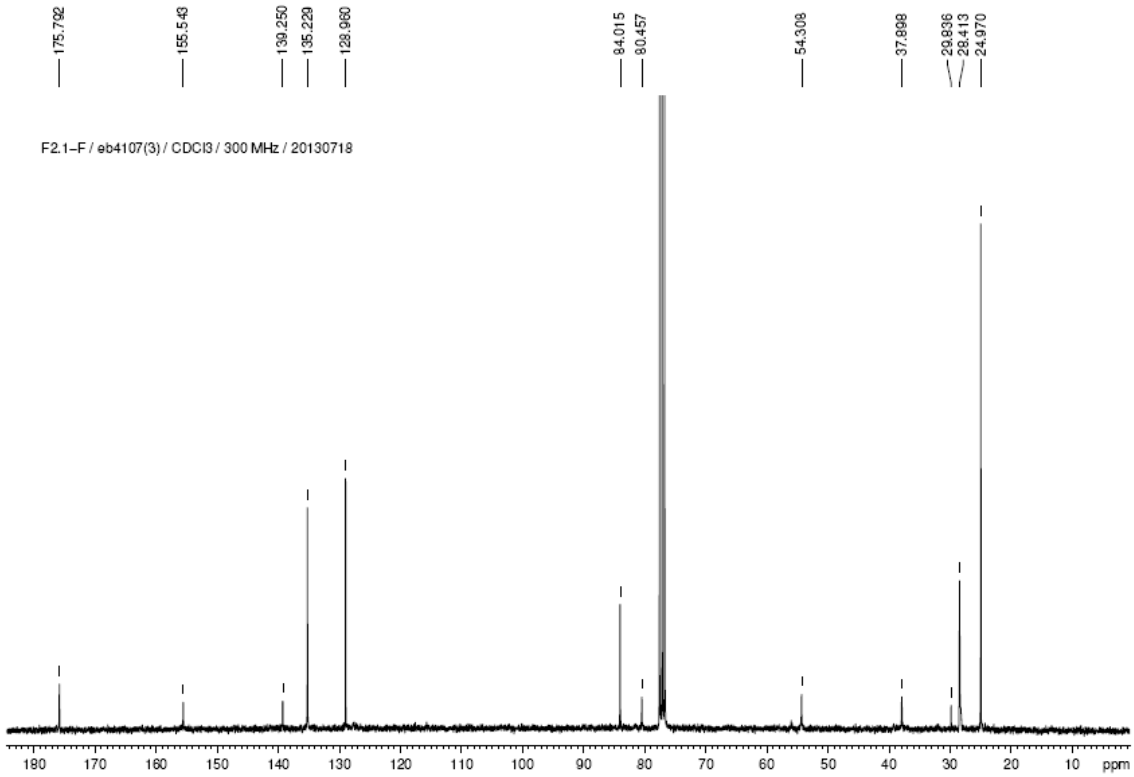

2. Linear peptides containing a 5-bromohistidine at the N-terminus

Iodopeptides

H-Lys-Lys-Leu-Phe(4-I)-Leu-Leu-NH_2

HPLC (λ = 220 nm)

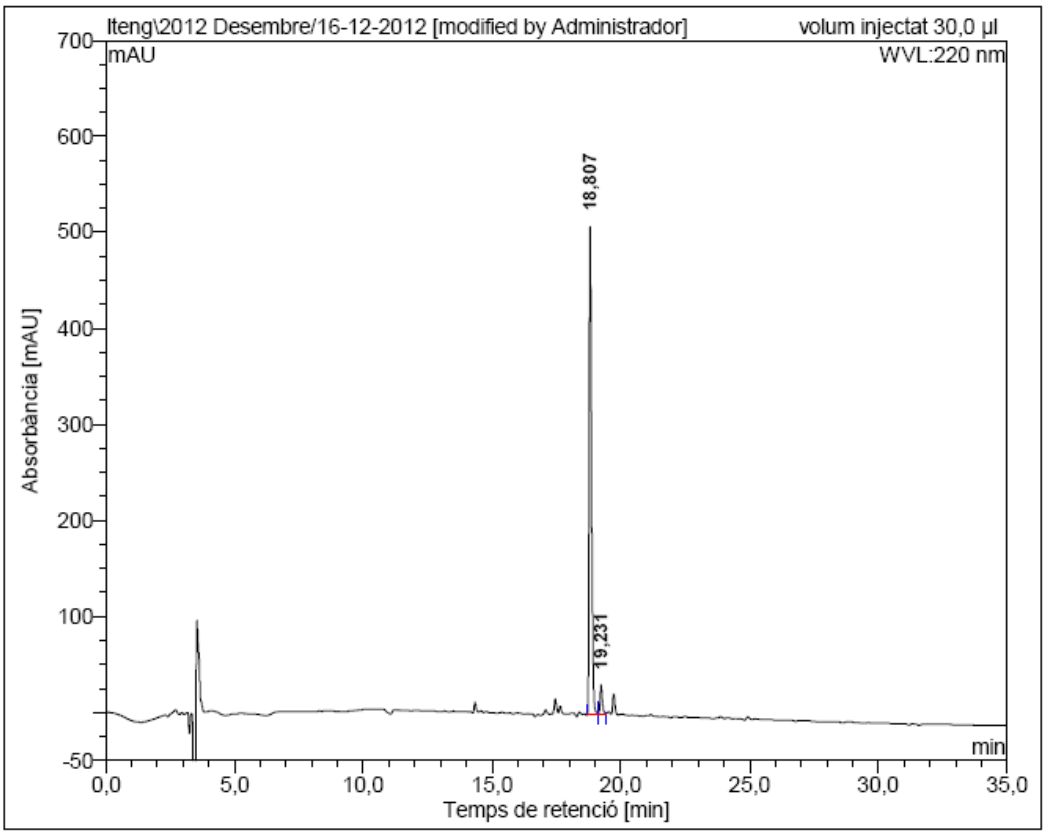

No.	Ret.Time (detected) min	Height mAU	Area mAU*min	Rel.Area %
1	18,81	508,429	54,880	94,15
2	19,23	31,283	3,408	5,85
Total:		539,712	58,289	100,00

ESI-MS *m/z* (%)

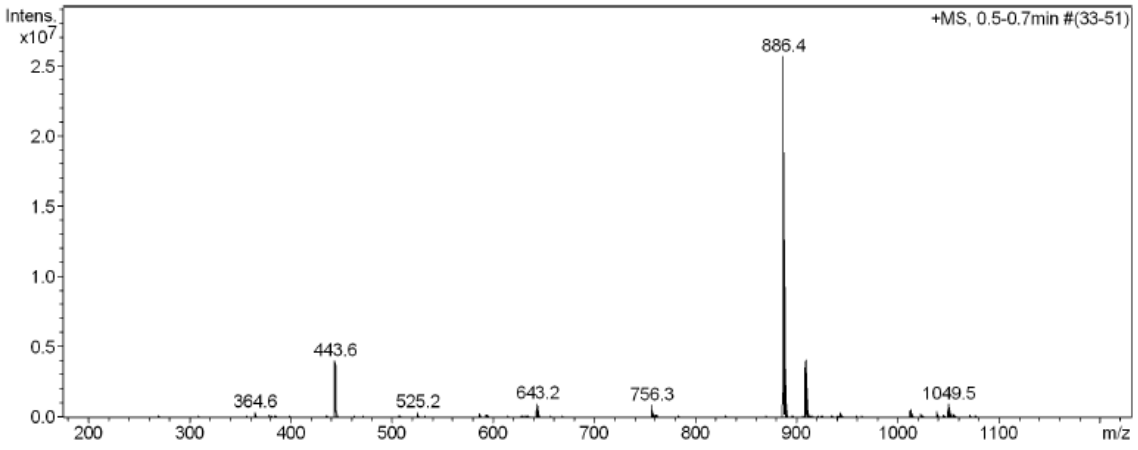

H-Leu-Phe(4-I)-Leu-Leu-NH_2

HPLC (λ = 220 nm)

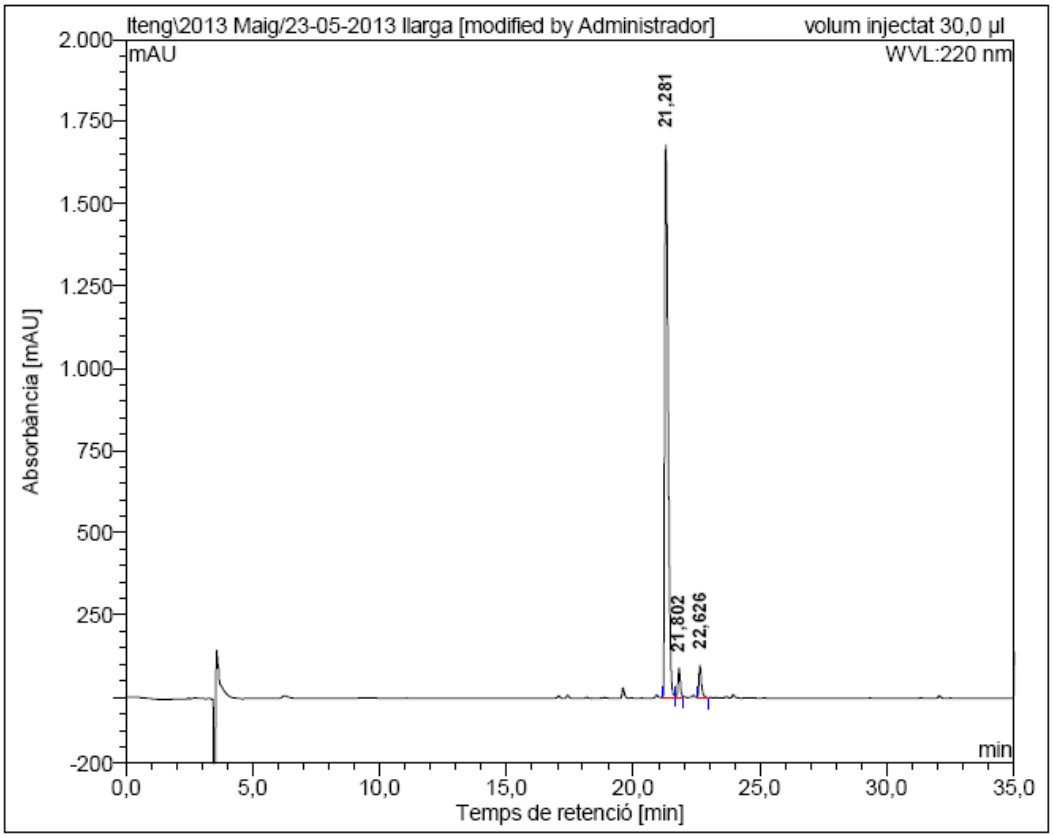

No.	Ret.Time (detected) min	Height mAU	Area mAU*min	Rel.Area %
1	21,28	1680,972	256,894	92,01
2	21,80	90,230	10,300	3,69
3	22,63	100,358	12,018	4,30
Total:		1871,559	279,212	100,00

ESI-MS *m/z* (%)

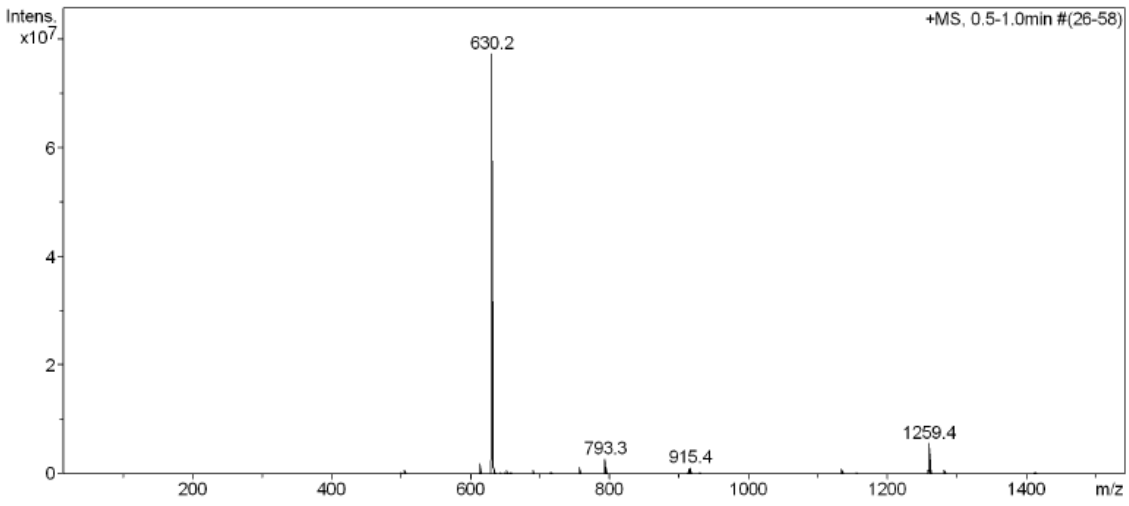

H-Lys-Phe-Lys-Lys-Leu-Phe(4-I)-Leu-Leu-NH_2

HPLC (λ = 220 nm)

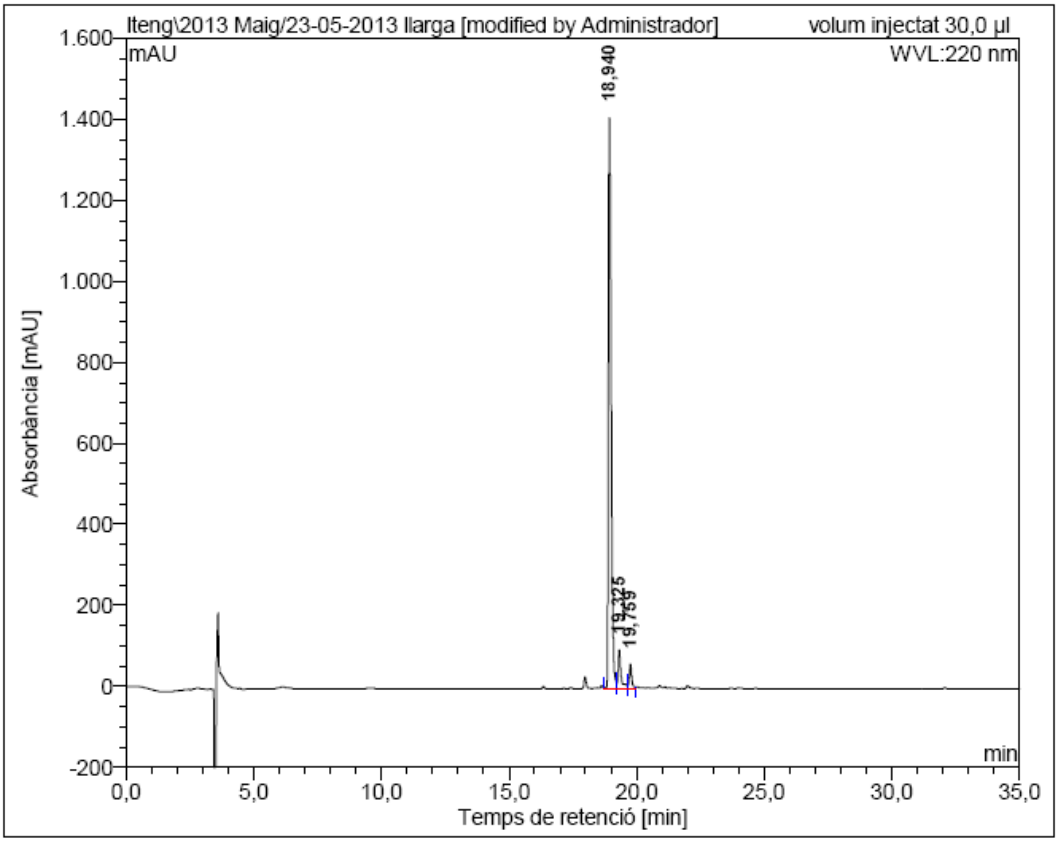

No.	Ret.Time (detected) min	Height mAU	Area mAU*min	Rel.Area %
1	18,94	1409,466	182,971	90,94
2	19,32	93,868	11,803	5,87
3	19,76	59,447	6,428	3,19
Total:		1562,781	201,201	100,00

ESI-MS *m/z* (%)

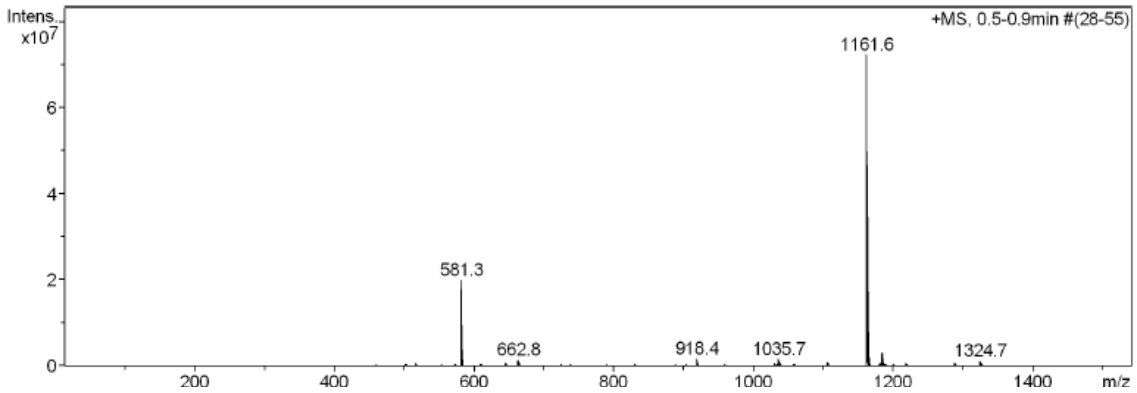

H-Lys-Lys-Phe-Lys-Lys-Leu-Phe(4-I)-Leu-Leu-NH_2

HPLC (λ = 220 nm)

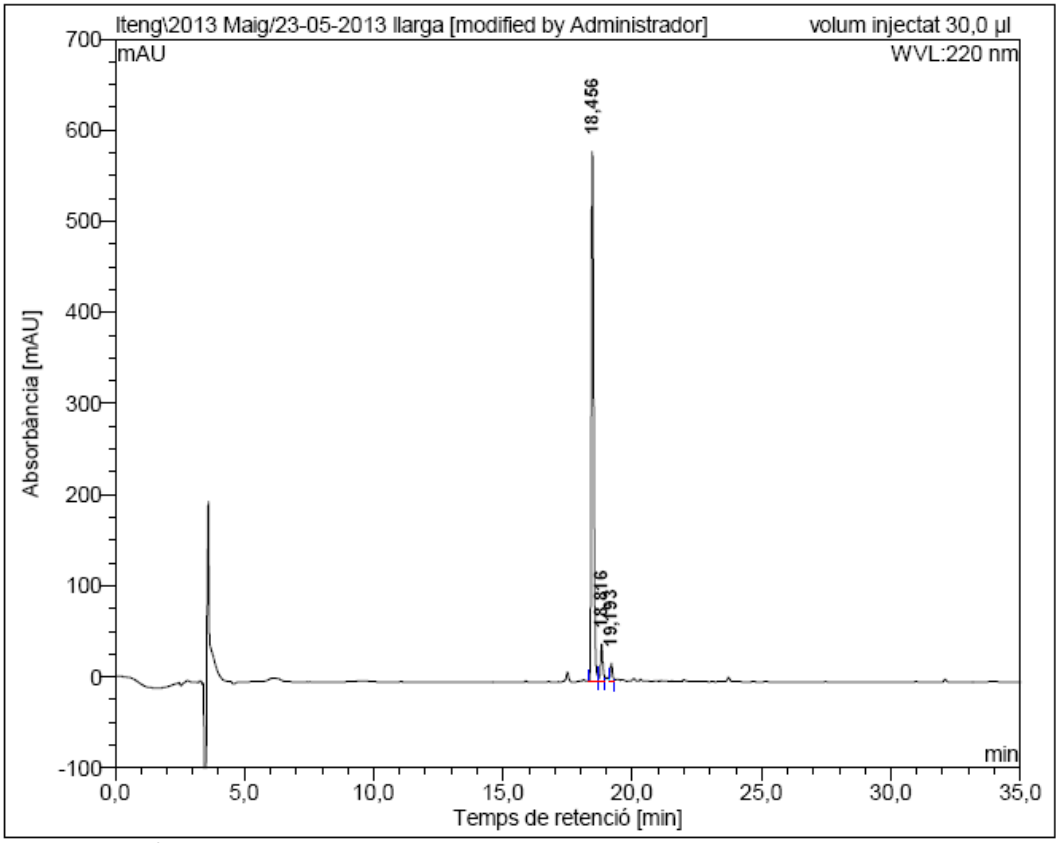

No.	Ret.Time (detected) min	Height mAU	Area mAU*min	Rel.Area %
1	18,46	580,700	61,122	90,83
2	18,82	40,773	4,226	6,28
3	19,19	19,303	1,944	2,89
Total:		640,776	67,292	100,00

ESI-MS *m/z* (%)

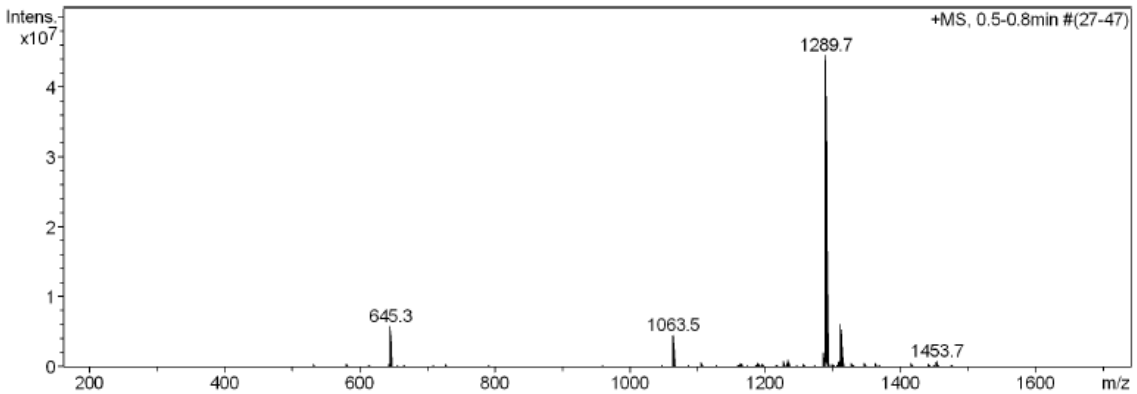

H-Lys-Lys-Leu-Phe(4-I)-NH_2

HPLC (λ = 220 nm)

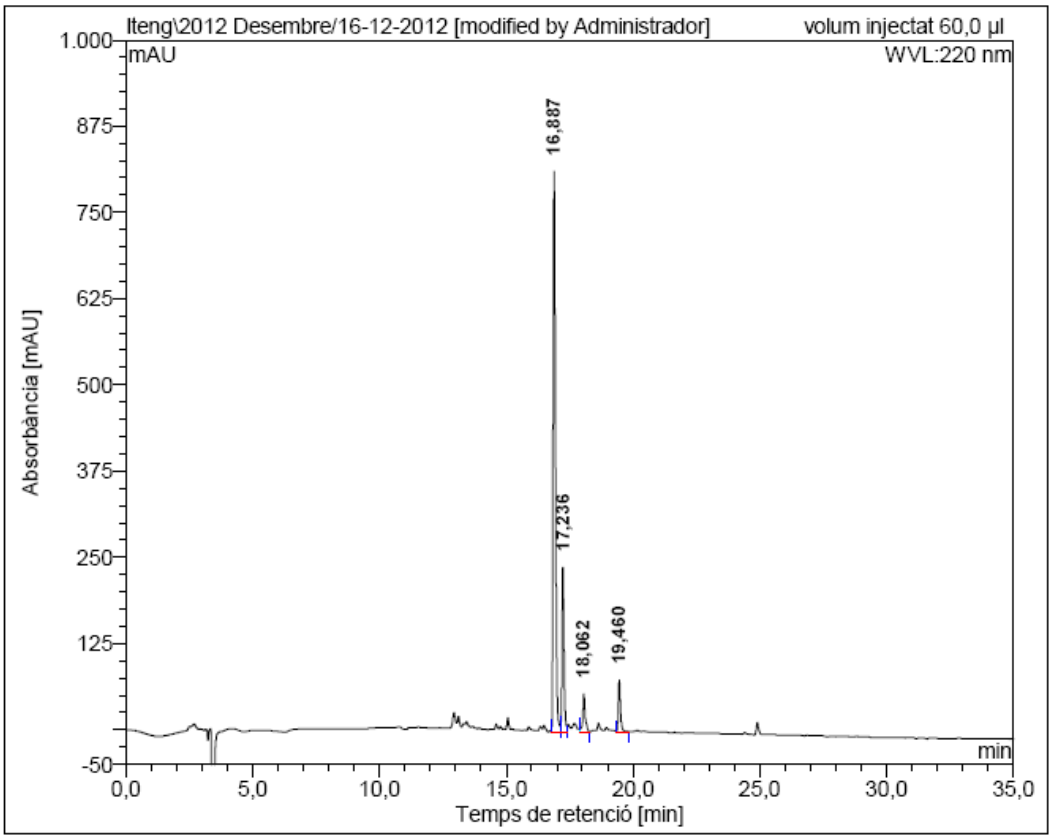

No.	Ret.Time (detected) min	Height mAU	Area mAU*min	Rel.Area %
1	16,89	812,757	85,580	69,91
2	17,24	238,852	22,510	18,39
3	18,06	55,998	6,563	5,36
4	19,46	75,867	7,764	6,34
Total:		1183,474	122,418	100,00

ESI-MS *m/z* (%)

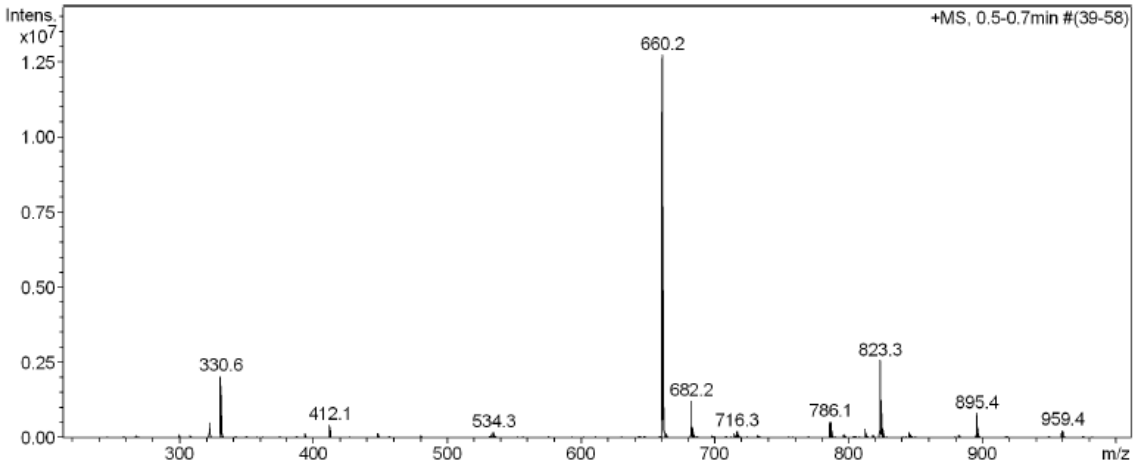

H-Leu-Phe(4-I)-NH_2

HPLC (λ = 220 nm)

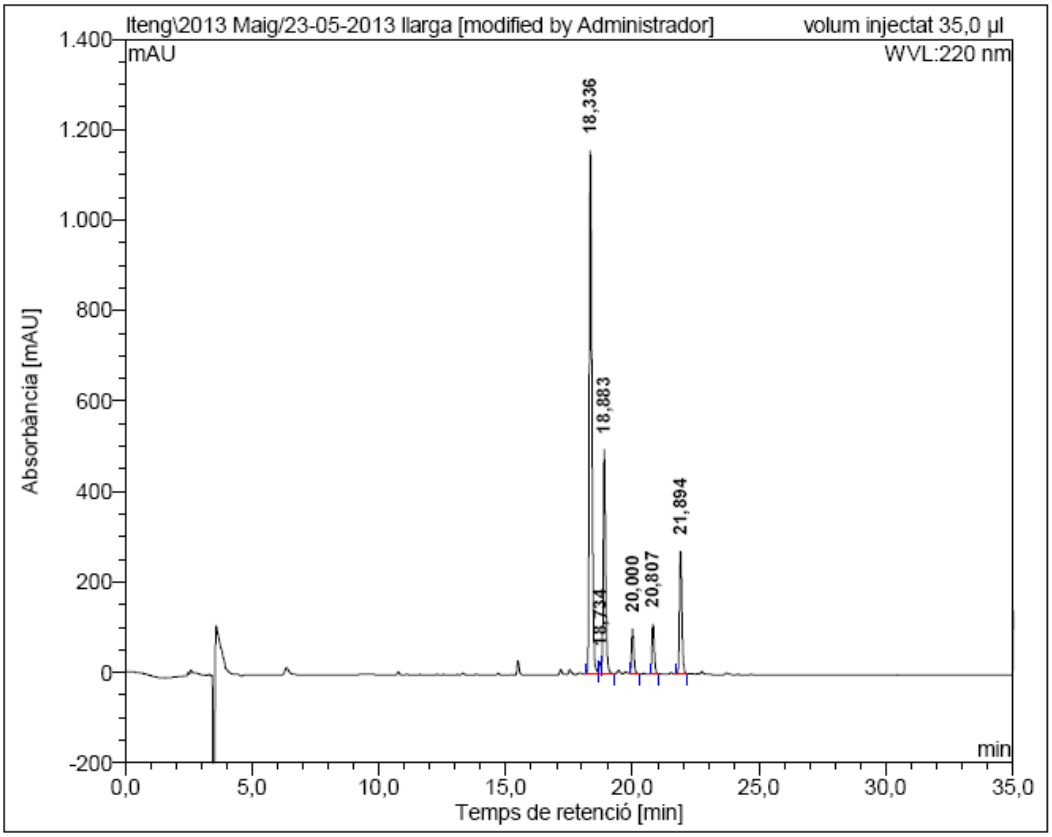

No.	Ret.Time (detected) min	Height mAU	Area mAU*min	Rel.Area %
1	18,34	1156,654	142,637	56,61
2	18,73	26,732	2,577	1,02
3	18,88	495,944	54,319	21,56
4	20,00	100,198	10,865	4,31
5	20,81	110,407	11,664	4,63
6	21,89	272,302	29,895	11,87
Total:		2162,238	251,958	100,00

ESI-MS *m/z* (%)

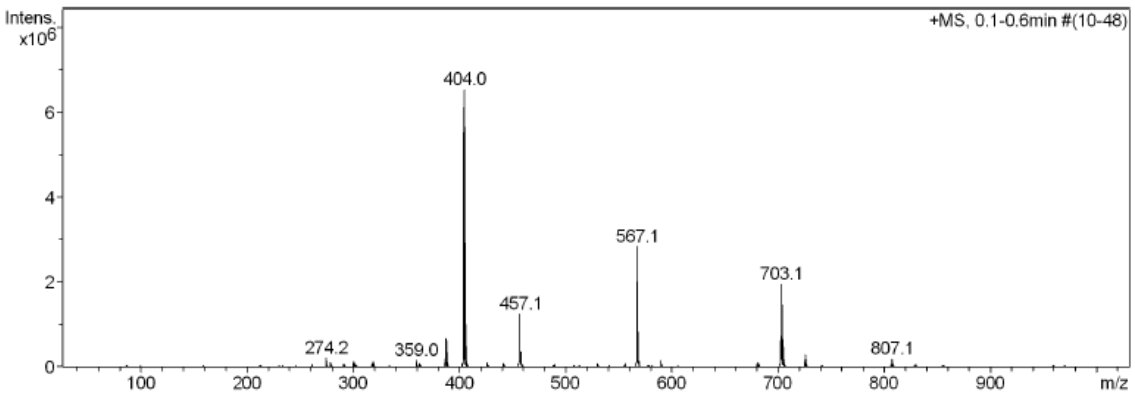

H-Lys-Phe-Lys-Lys-Leu-Phe(4-I)-NH_2

HPLC (λ = 220 nm)

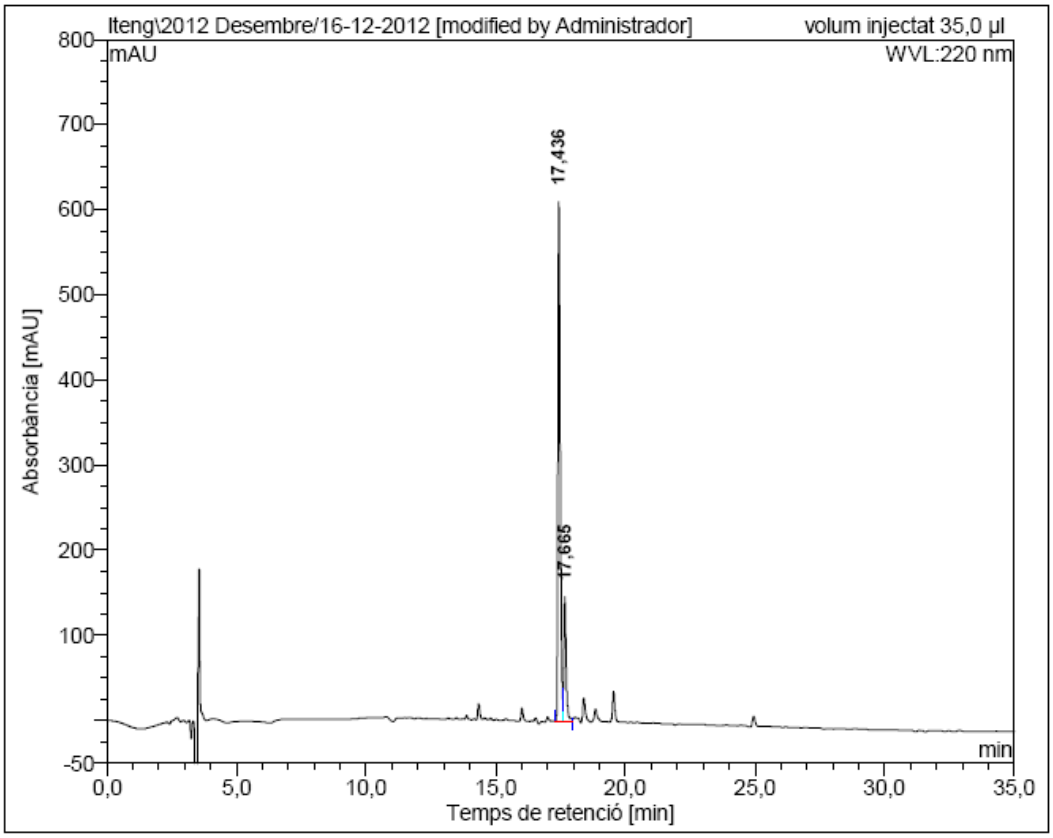

No.	Ret.Time (detected) min	Height mAU	Area mAU*min	Rel.Area %
1	17,44	609,582	63,333	80,43
2	17,66	145,352	15,412	19,57
Total:		754,934	78,745	100,00

ESI-MS *m/z* (%)

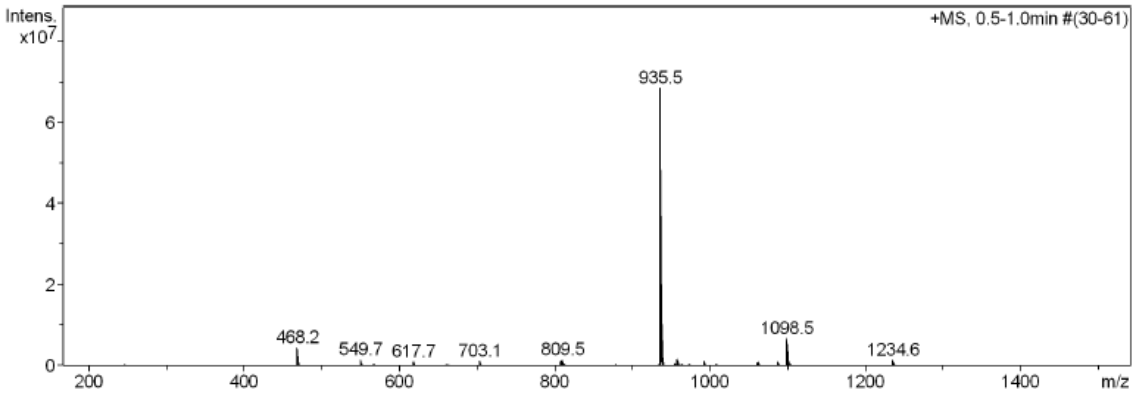

H-Lys-Lys-Leu-Phe(4-I)-Lys-Lys-Leu-Lys-Lys-NH_2

HPLC (λ = 220 nm)

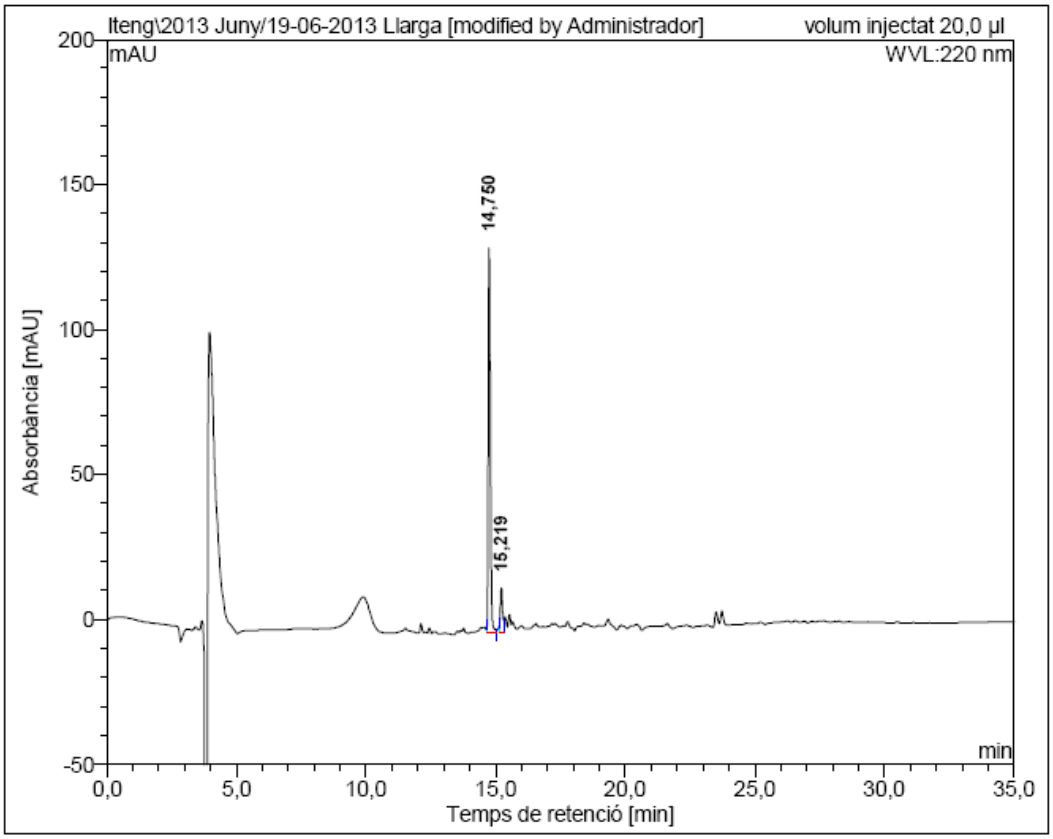

No.	Ret.Time (detected) min	Height mAU	Area mAU*min	Rel.Area %
1	14,75	132,536	12,118	88,11
2	15,22	15,381	1,635	11,89
Total:		147,918	13,753	100,00

ESI-MS *m/z* (%)

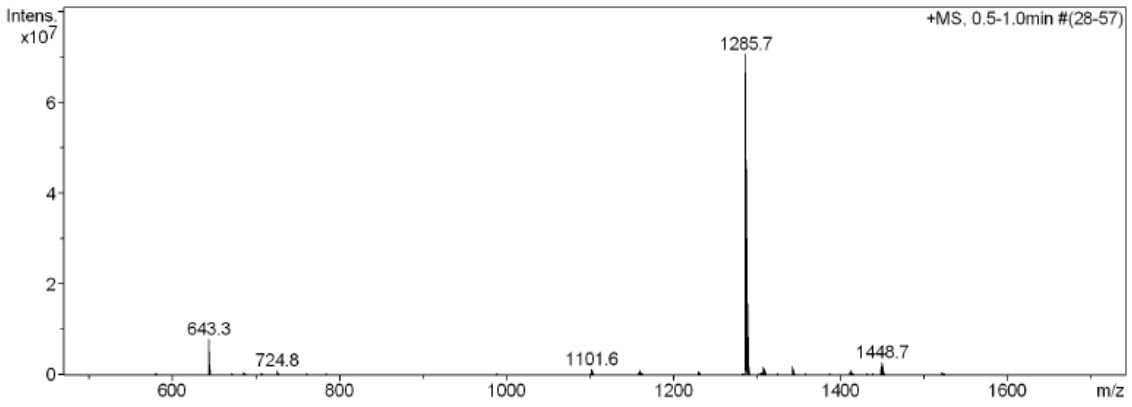

H-Leu-Phe(4-I)-Lys-Lys-Leu-Lys-Lys-NH_2

HPLC (λ = 220 nm)

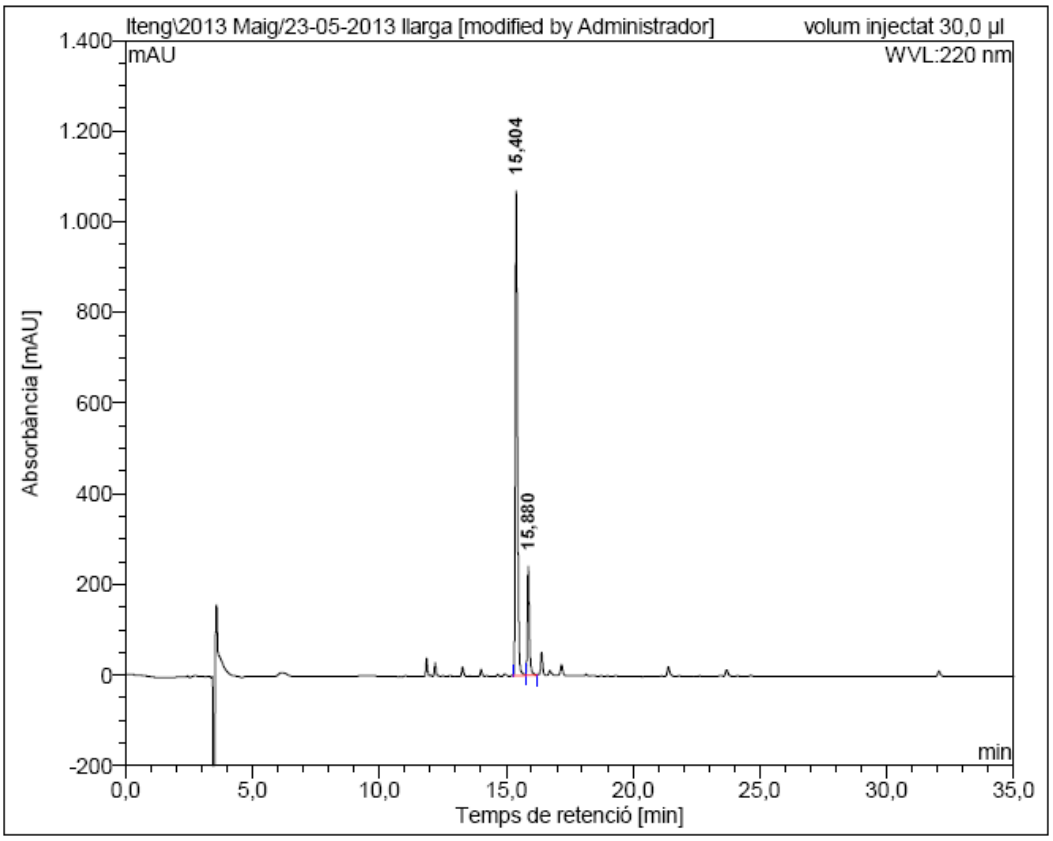

No.	Ret.Time (detected) min	Height mAU	Area mAU*min	Rel.Area %
1	15,40	1068,697	104,014	82,32
2	15,88	240,581	22,333	17,68
Total:		1309,278	126,348	100,00

ESI-MS *m/z* (%)

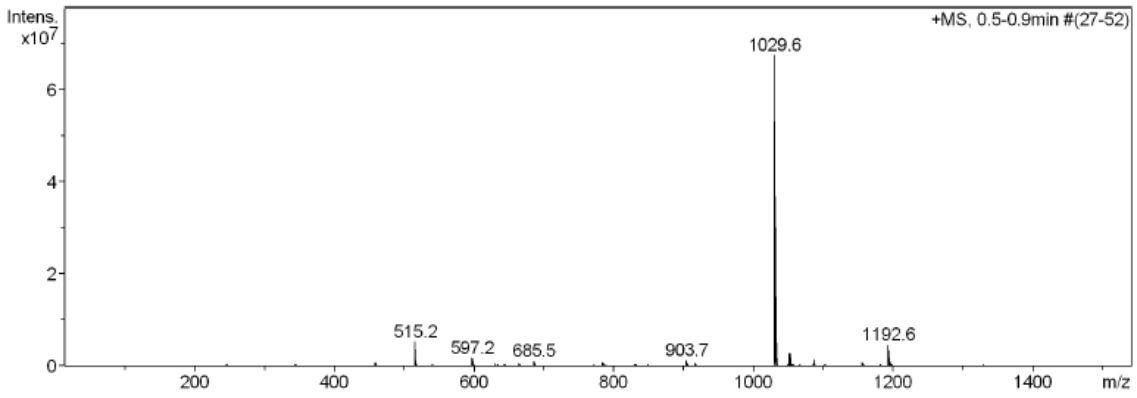

Boronopeptides 31-39

H-Lys-Lys-Leu-Phe(4-B(OH)$_2$)-Leu-Leu-NH$_2$ (31)

HPLC (λ = 220 nm)

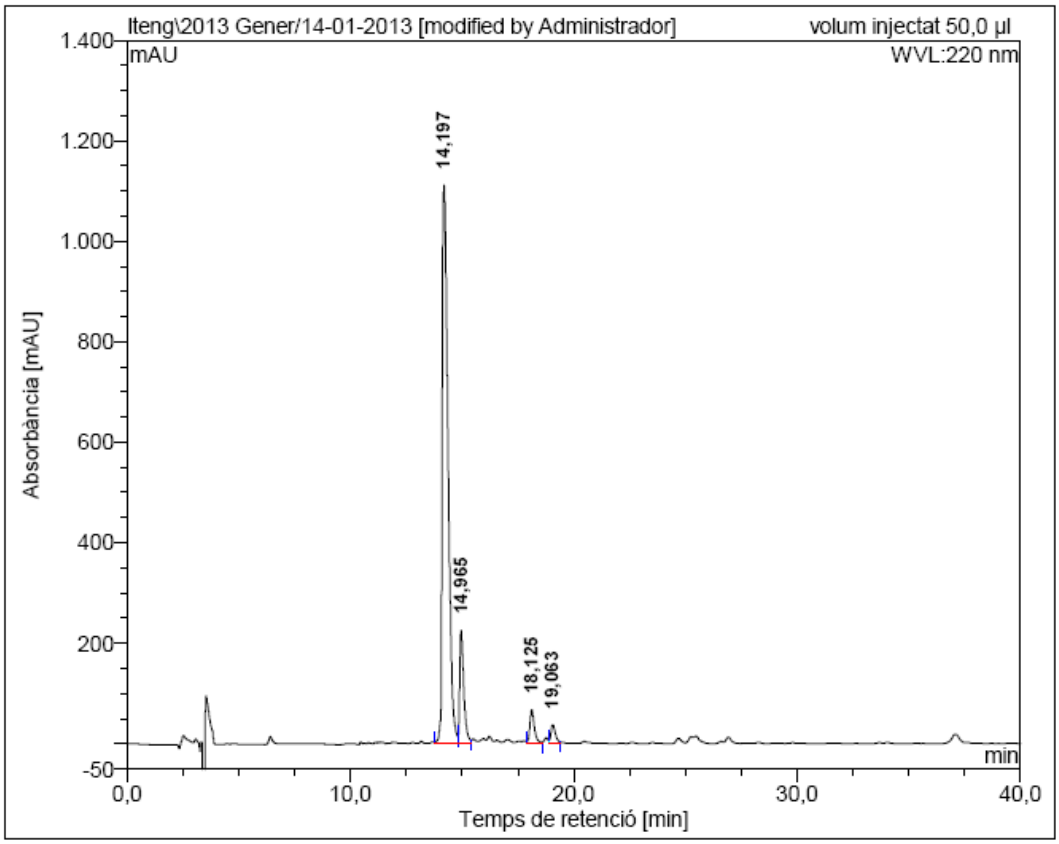

No.	Ret.Time (detected) min	Height mAU	Area mAU*min	Rel.Area %
1	14,20	1109,376	331,846	82,23
2	14,96	224,474	48,038	11,90
3	18,13	65,756	15,402	3,82
4	19,06	35,761	8,254	2,05
Total:		1435,367	403,541	100,00

ESI-MS *m/z* (%)

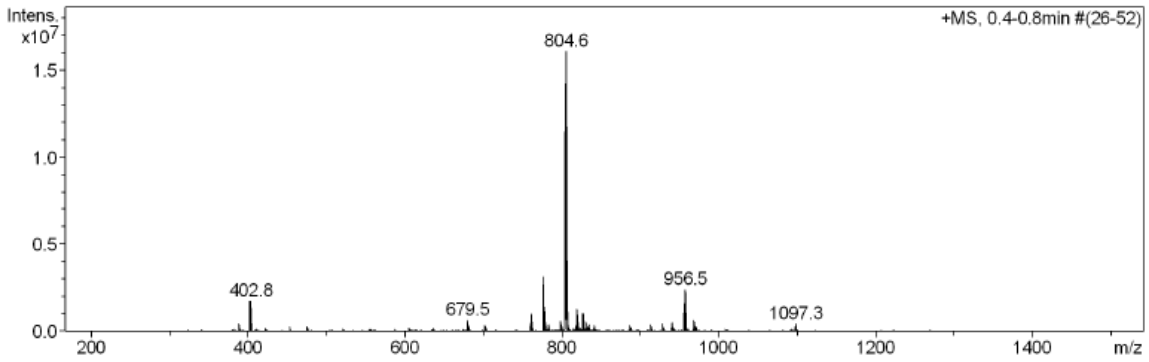

H-Leu-Phe(4-B(OH)$_2$)-Leu-Leu-NH$_2$ (32)

HPLC (λ = 220 nm)

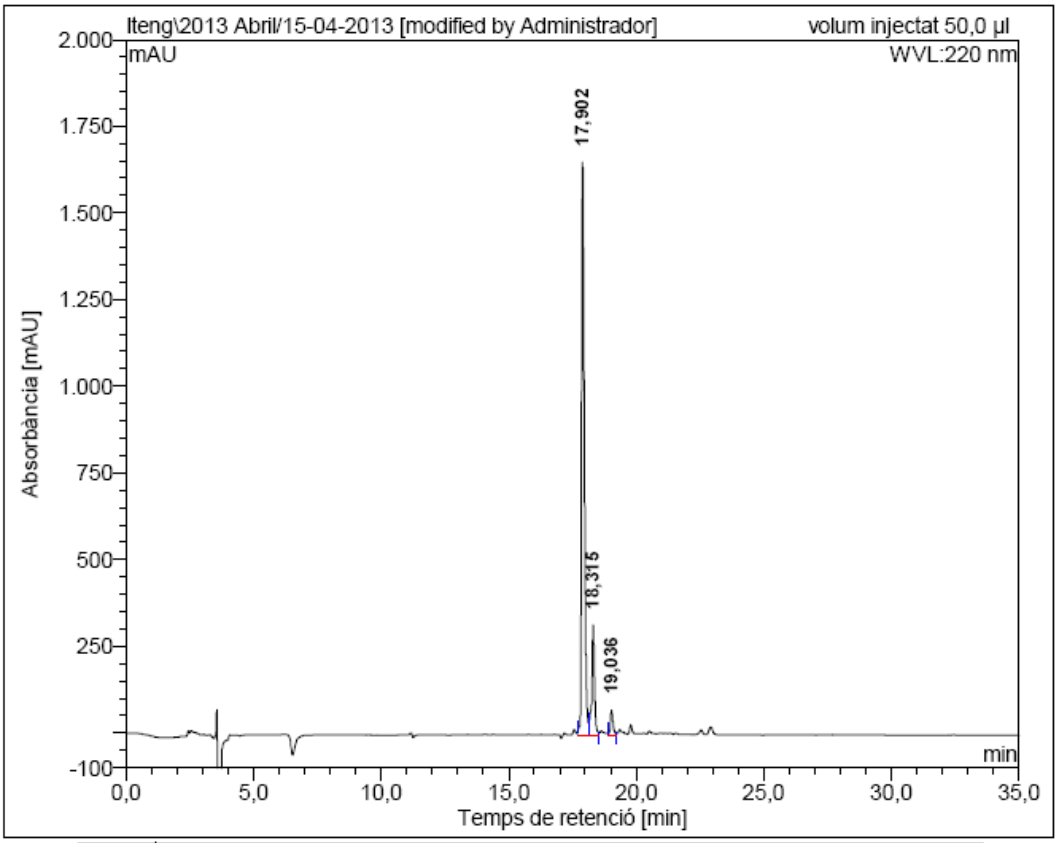

No.	Ret.Time (detected) min	Height mAU	Area mAU*min	Rel.Area %
1	17,90	1650,153	208,915	81,03
2	18,31	315,788	40,800	15,82
3	19,04	70,671	8,119	3,15
Total:		2036,613	257,833	100,00

ESI-MS *m/z* (%)

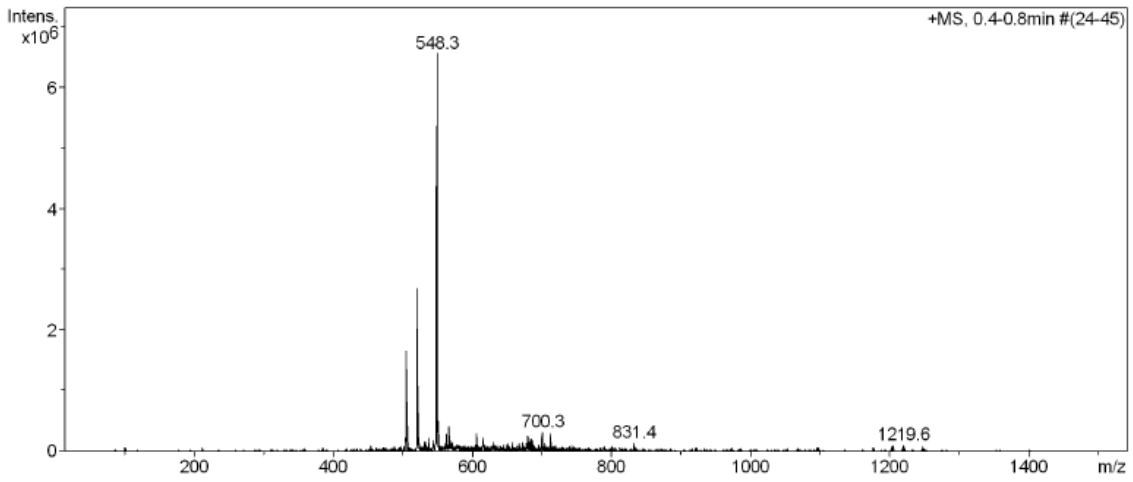

H-Lys-Phe-Lys-Lys-Leu-Phe(4-B(OH)$_2$)-Leu-Leu-NH$_2$ (33)

HPLC (λ = 220 nm)

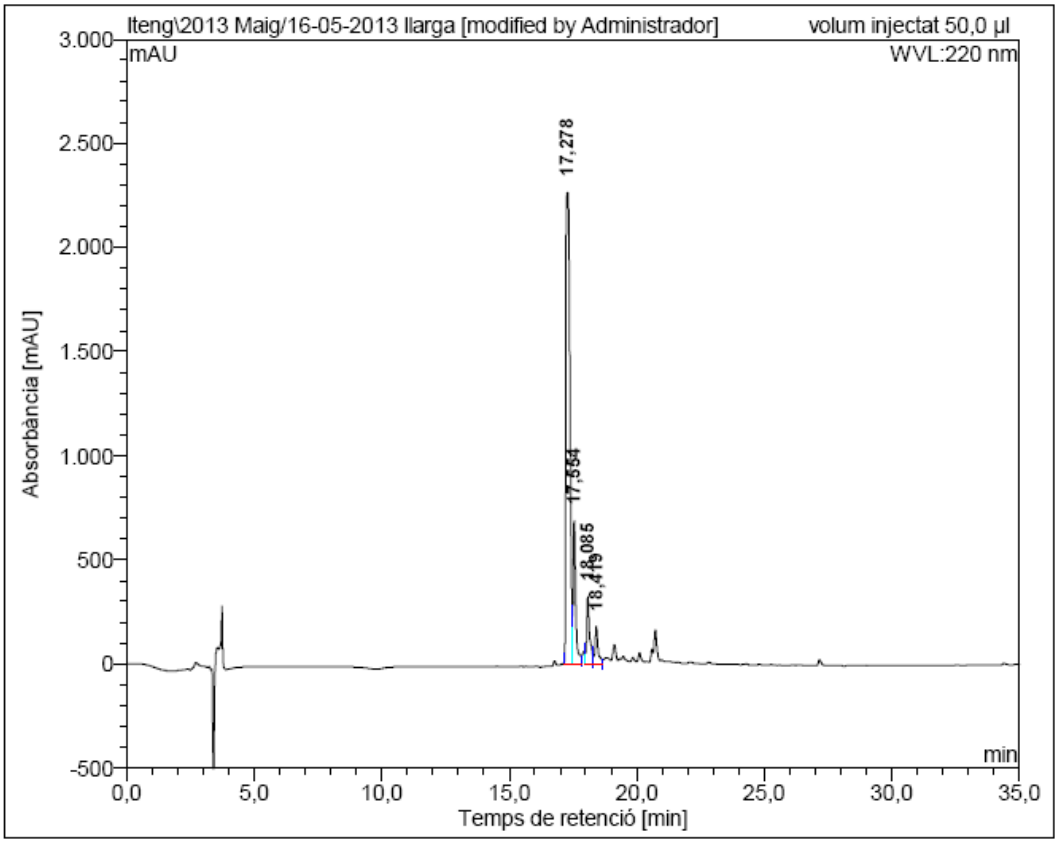

No.	Ret.Time (detected) min	Height mAU	Area mAU*min	Rel.Area %
1	17,28	2261,990	421,391	73,73
2	17,55	685,214	82,328	14,40
3	18,09	321,183	43,697	7,65
4	18,42	179,417	24,123	4,22
Total:		3447,804	571,540	100,00

ESI-MS *m/z* (%)

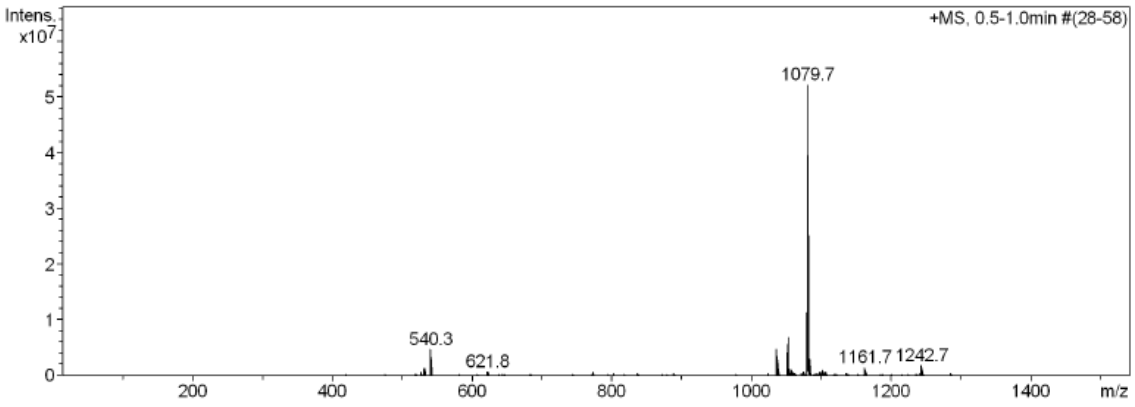

H-Lys-Lys-Phe-Lys-Lys-Leu-Phe(4-B(OH)$_2$)-Leu-Leu-NH$_2$ (34)

HPLC (λ = 220 nm)

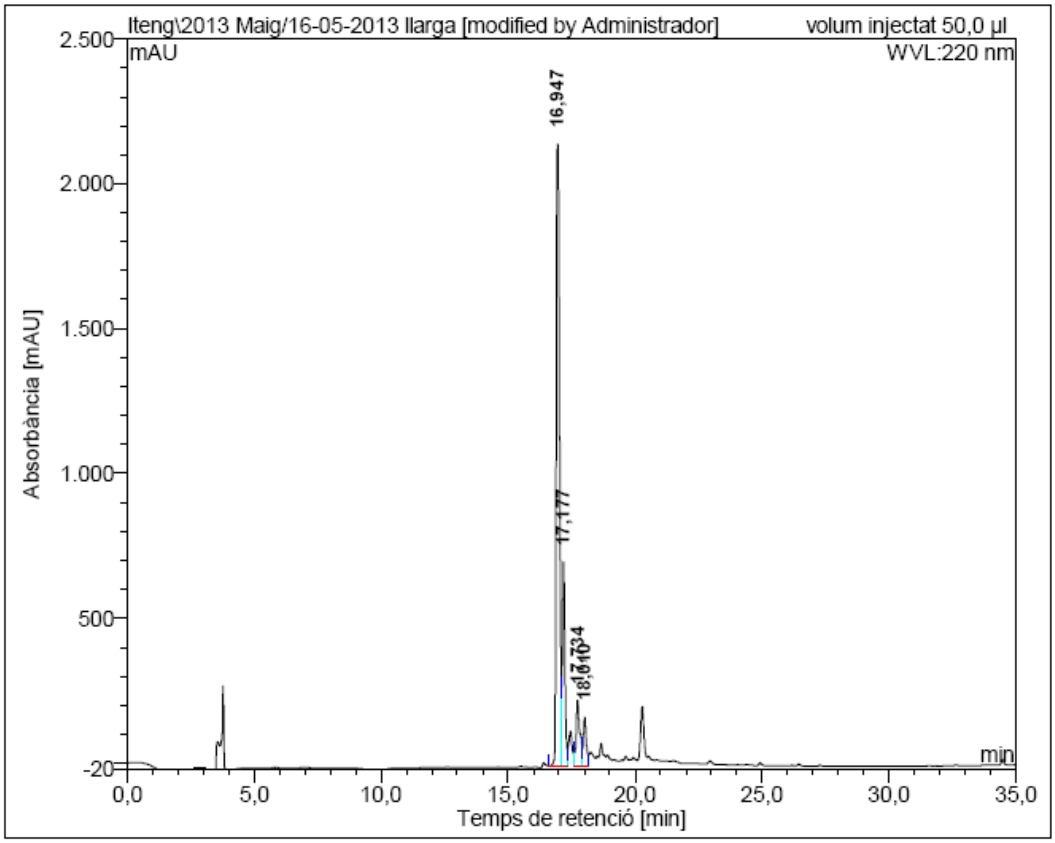

No.	Temps retenció min	alçada mAU	Area mAU*min	Area relativa %
1	16,95	2151,734	330,884	69,59
2	17,18	707,177	82,974	17,45
3	17,73	230,318	38,502	8,10
4	18,01	171,388	23,136	4,87
Total:		3260,617	475,496	100,00

ESI-MS *m/z* (%)

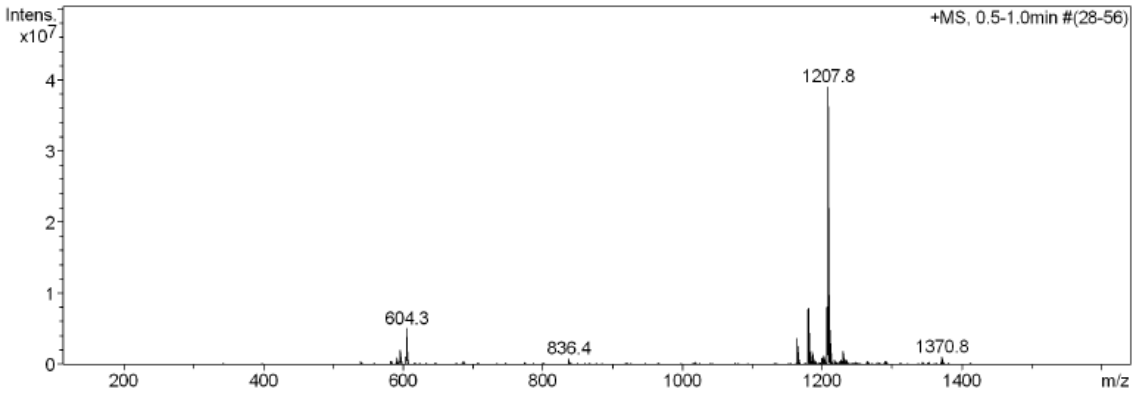

H-Lys-Lys-Leu-Phe(4-B(OH)$_2$)-NH$_2$ (35)

HPLC (λ = 220 nm)

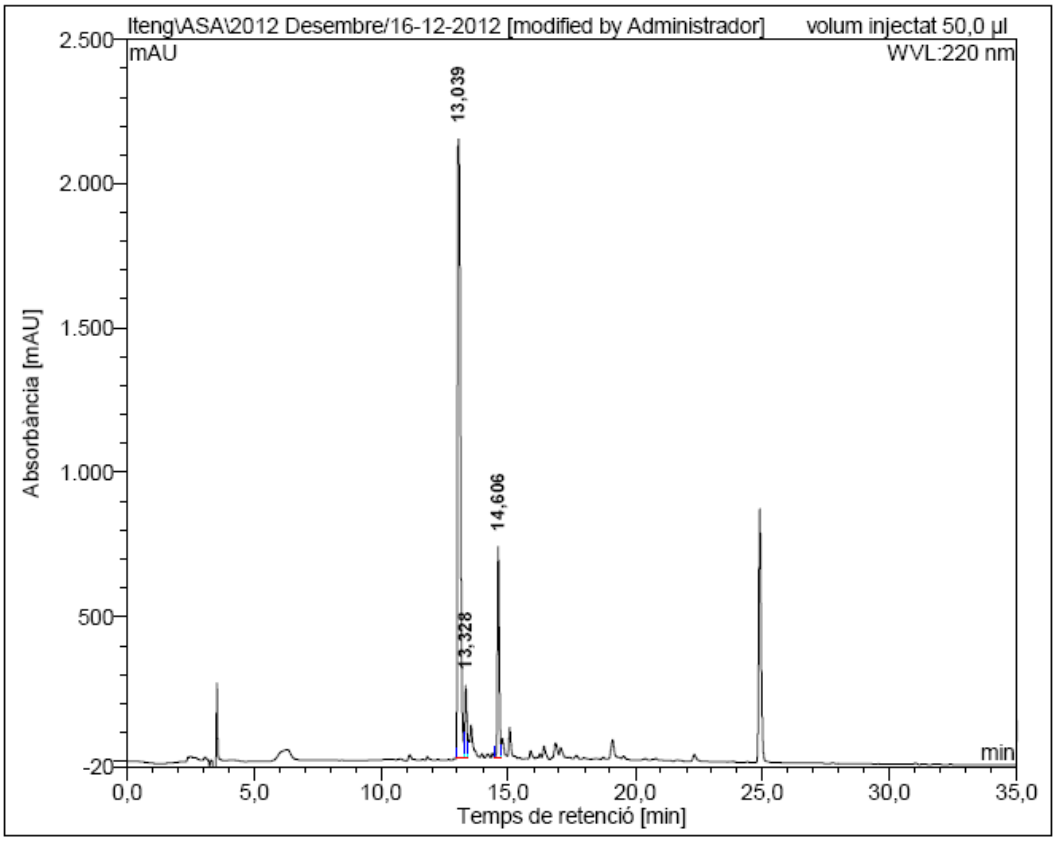

No.	Temps retenció min	alçada mAU	Area mAU*min	Area relativa %
1	13,04	2145,982	287,717	76,78
2	13,33	252,846	22,776	6,08
3	14,61	733,047	64,217	17,14
Total:		3131,874	374,709	100,00

ESI-MS *m/z* (%)

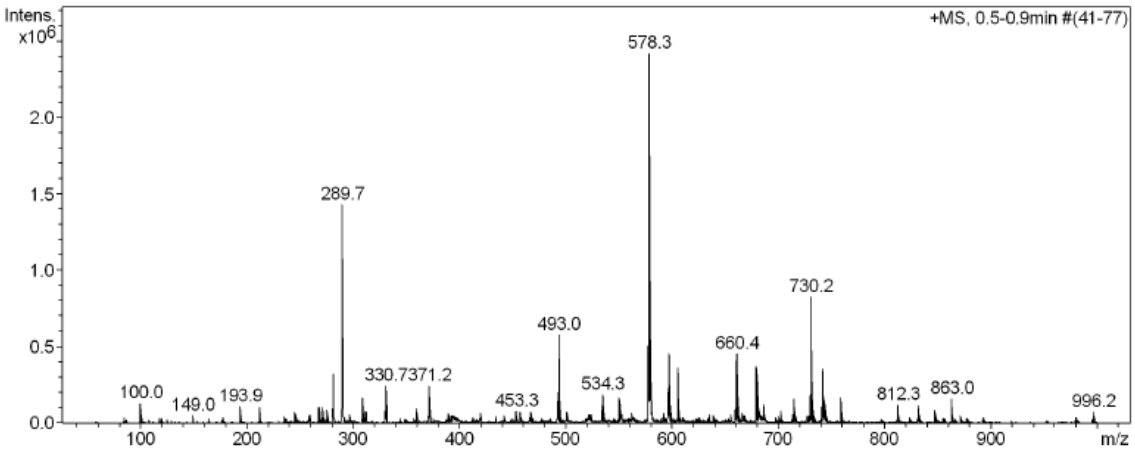

H-Leu-Phe(4-B(OH)$_2$)-NH$_2$ (36)

HPLC (λ = 220 nm)

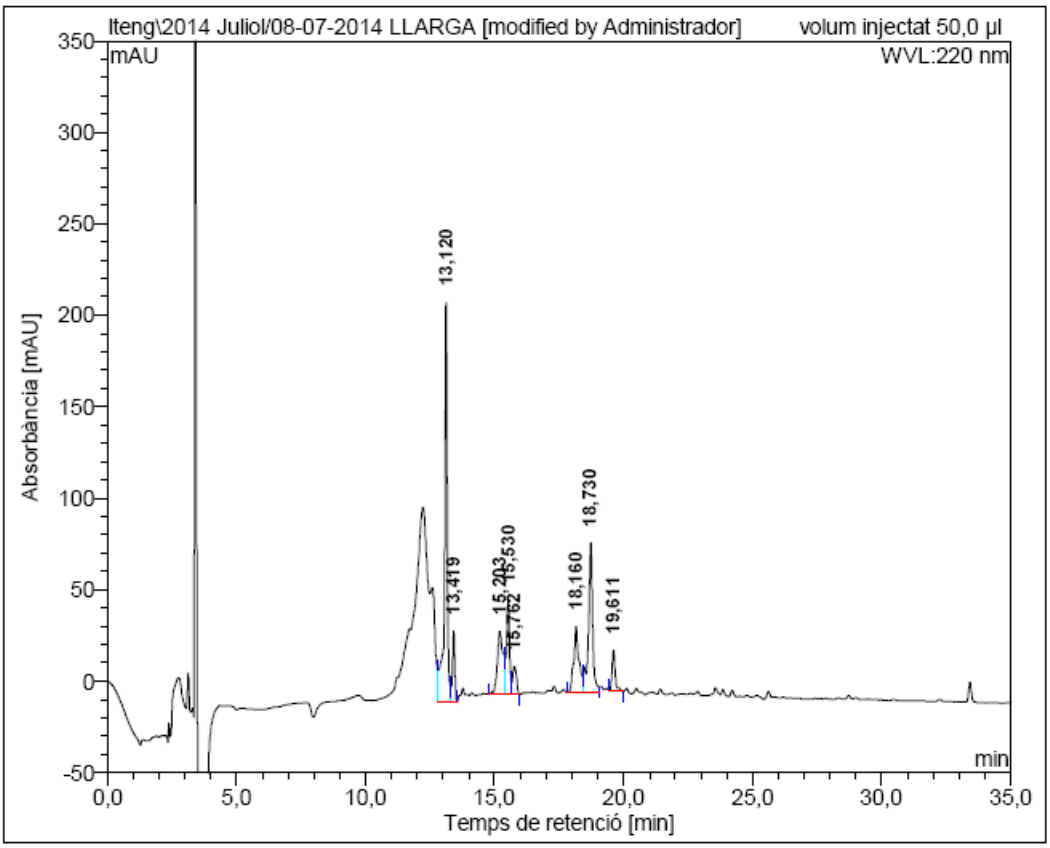

No.	mps retenc min	alçada mAU	Area mAU*min	Area relativa %
1	13,12	218,280	27,424	35,20
2	13,42	38,915	4,128	5,30
3	15,20	34,588	9,619	12,35
4	15,53	51,995	6,657	8,54
5	15,76	15,202	2,623	3,37
6	18,16	36,024	8,344	10,71
7	18,73	81,648	15,823	20,31
8	19,61	22,542	3,292	4,23
Total:		499,195	77,909	100,00

ESI-MS *m/z* (%)

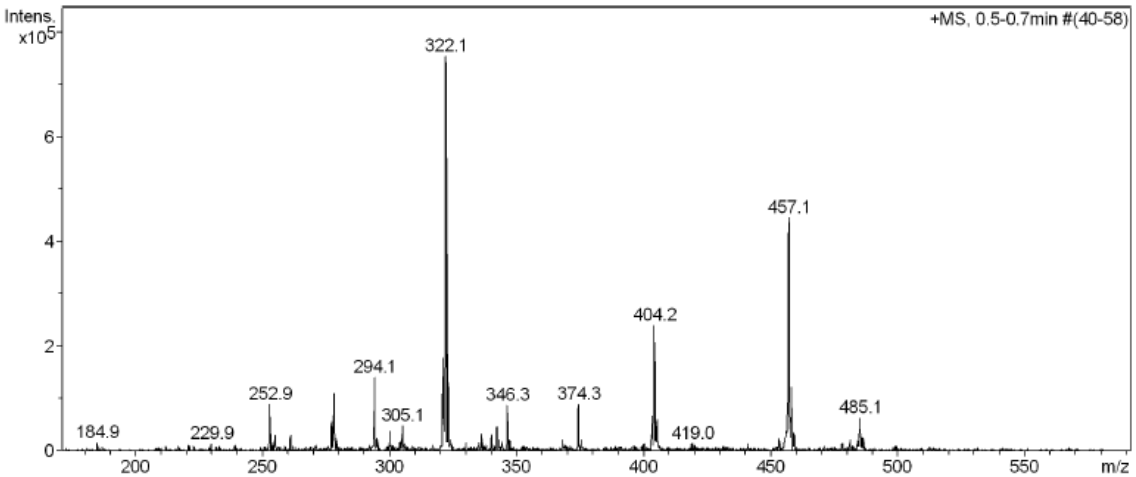

H-Lys-Phe-Lys-Lys-Leu-Phe(4-B(OH)$_2$)-NH$_2$ (37)

HPLC (λ = 220 nm)

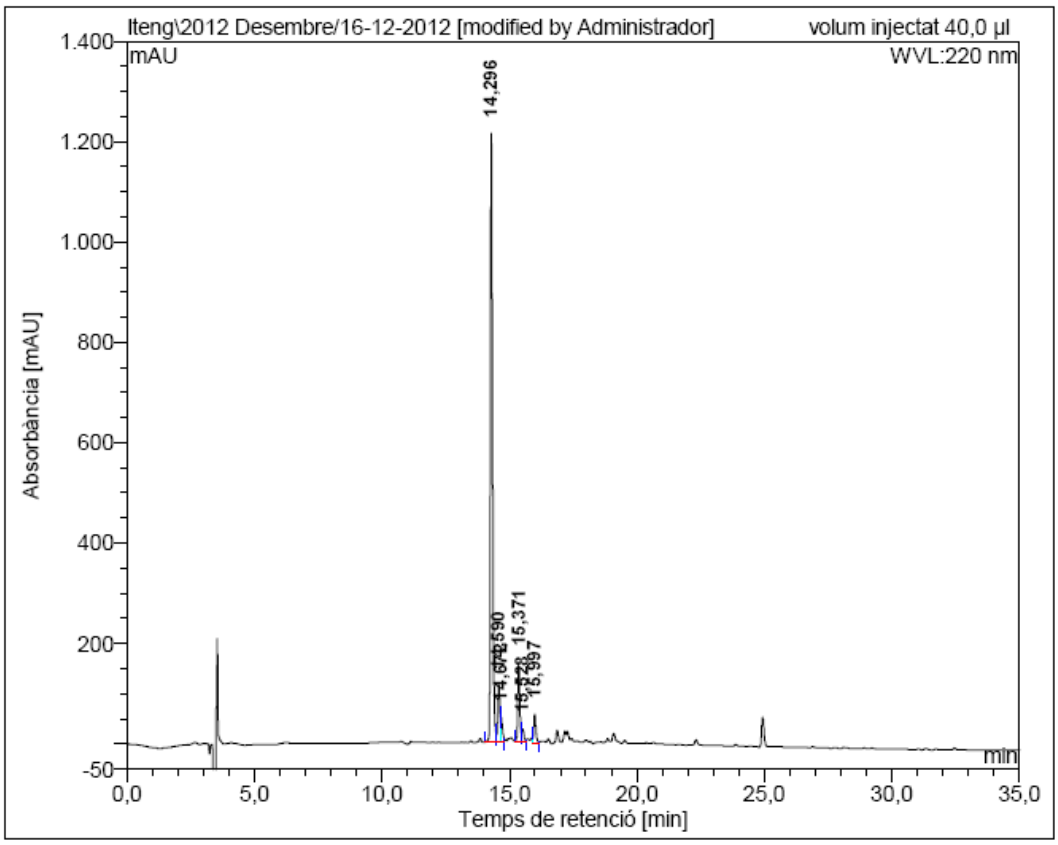

No.	Ret.Time (detected) min	Height mAU	Area mAU*min	Rel.Area %
1	14,30	1211,832	114,779	75,26
2	14,59	114,253	10,361	6,79
3	14,67	50,172	4,231	2,77
4	15,37	159,635	15,246	10,00
5	15,53	25,808	2,575	1,69
6	16,00	56,431	5,324	3,49
Total:		1618,131	152,515	100,00

ESI-MS *m/z* (%)

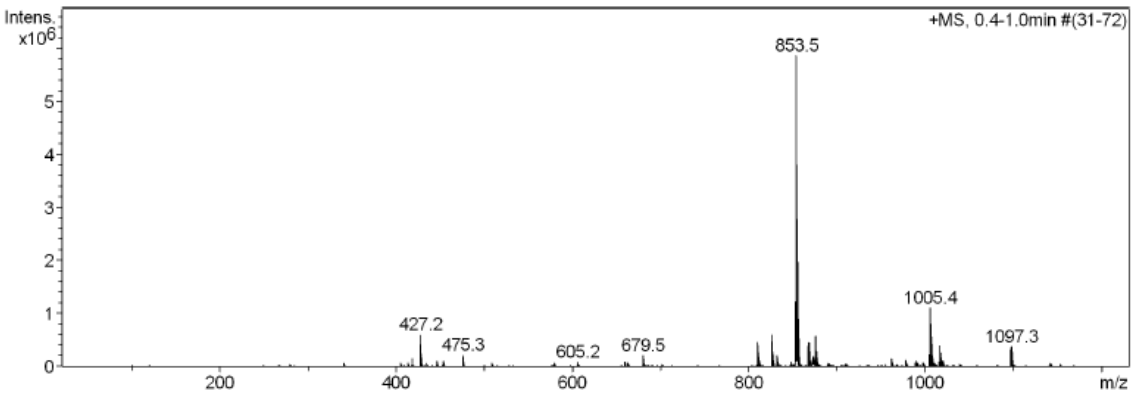

H-Lys-Lys-Leu-Phe(4-B(OH)$_2$)-Lys-Lys-Leu-Lys-Lys-NH$_2$ (38)

HPLC (λ = 220 nm)

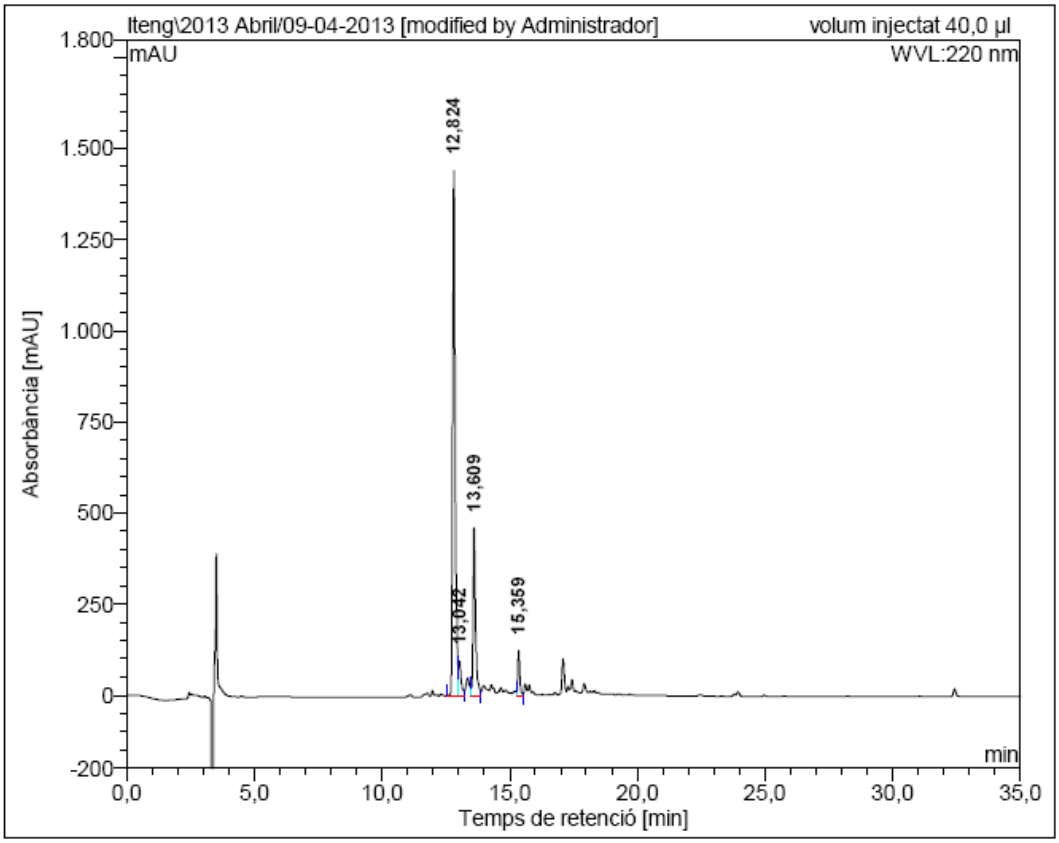

No.	Ret.Time (detected) min	Height mAU	Area mAU*min	Rel.Area %
1	12,82	1439,632	174,135	69,70
2	13,04	94,653	11,083	4,44
3	13,61	461,429	52,658	21,08
4	15,36	123,577	11,947	4,78
Total:		2119,290	249,824	100,00

ESI-MS *m/z* (%)

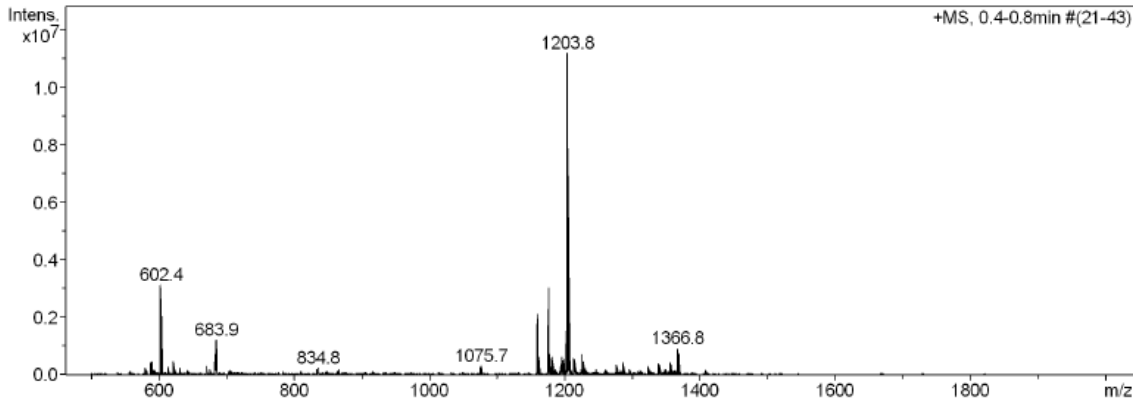

H-Leu-Phe(4-B(OH)$_2$)-Lys-Lys-Leu-Lys-Lys-NH$_2$ (39)

HPLC (λ = 220 nm)

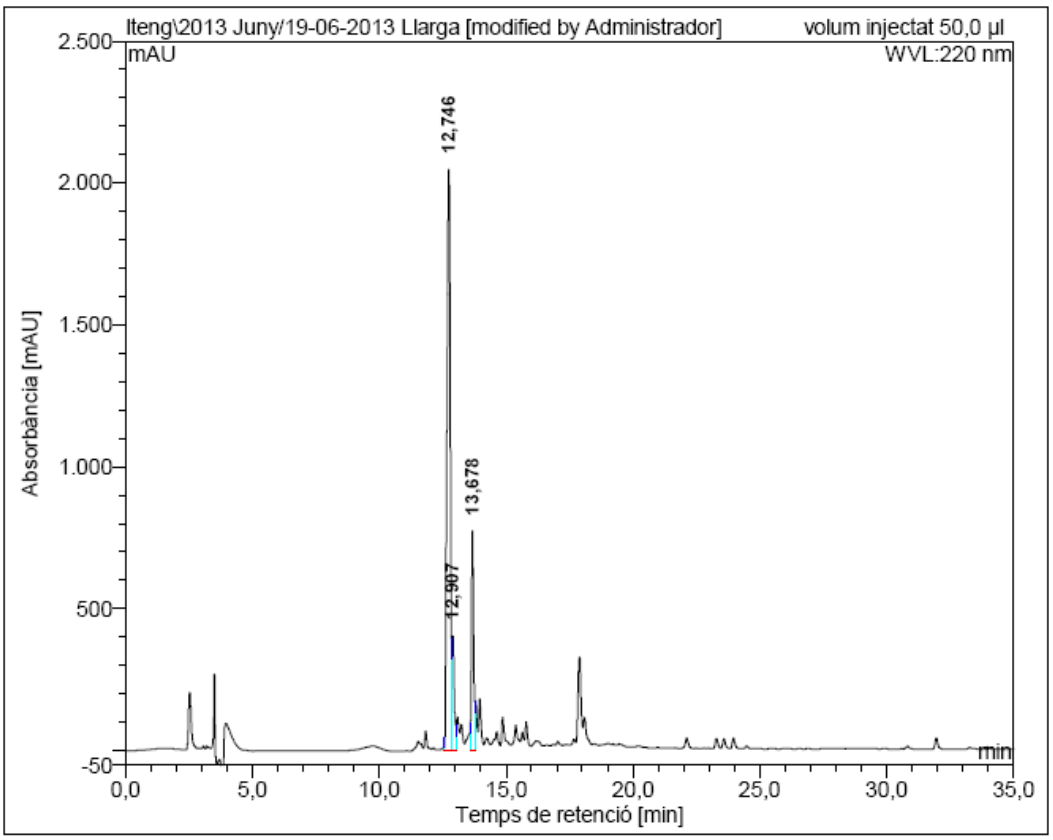

No.	Ret.Time (detected) min	Height mAU	Area mAU*min	Rel.Area %
1	12,75	2044,374	318,153	73,58
2	12,91	400,298	37,577	8,69
3	13,68	770,818	76,653	17,73
Total:		3215,490	432,382	100,00

ESI-MS *m/z* (%)

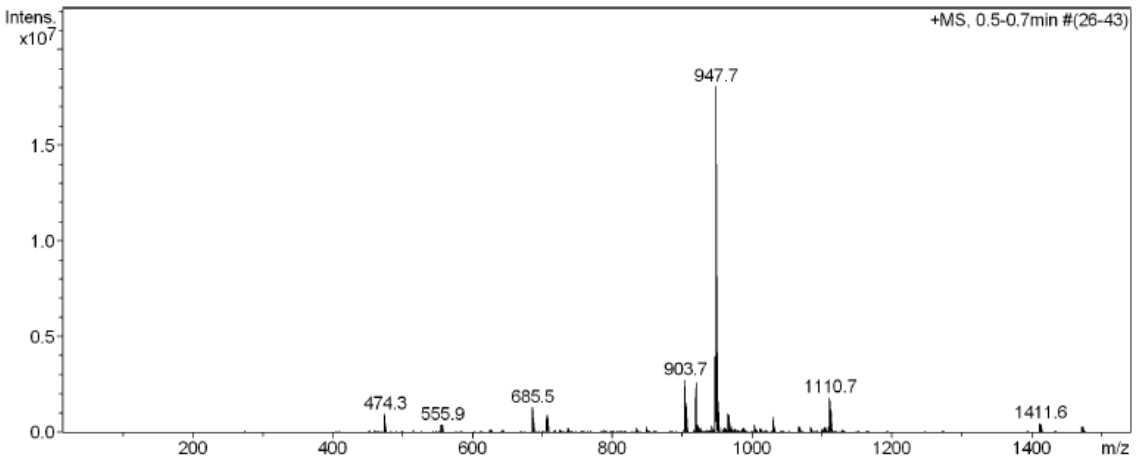

Linear peptides 42-52

H-His(5-Br)-Lys-Lys-Leu-Phe(4-B(OH)$_2$)-Leu-Leu-NH$_2$ (42)

HPLC (λ = 220 nm)

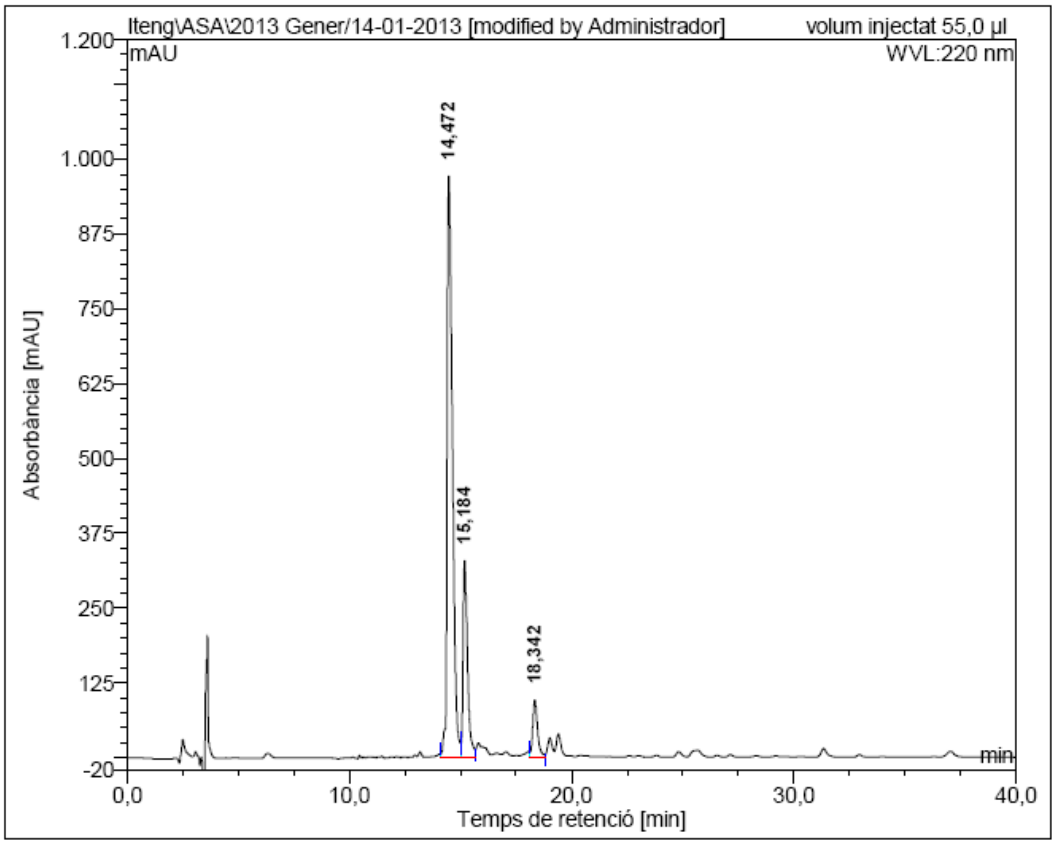

No.	Temps retenció min	alçada mAU	Area mAU*min	Area relativa %
1	14,47	971,681	272,946	72,83
2	15,18	329,691	77,206	20,60
3	18,34	96,872	24,635	6,57
Total:		1398,244	374,786	100,00

ESI-MS *m/z* (%)

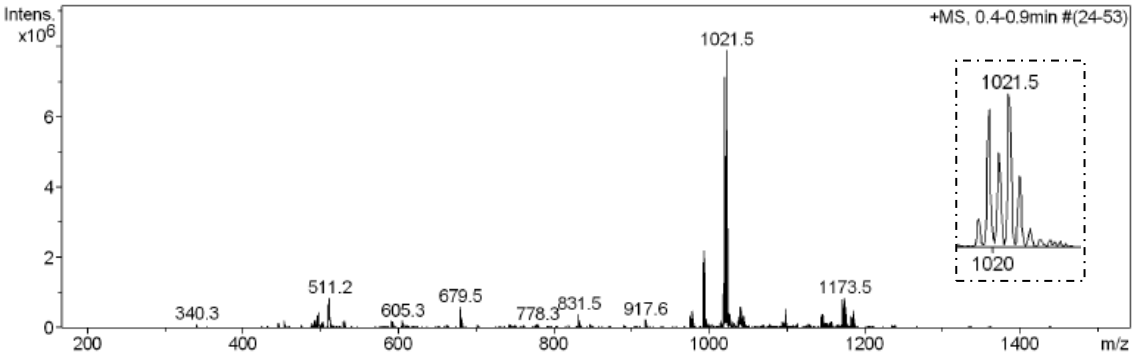

H-His(5-Br)-Leu-Phe(4-B(OH)$_2$)-Leu-Leu-NH$_2$ (43)

HPLC (λ = 220 nm)

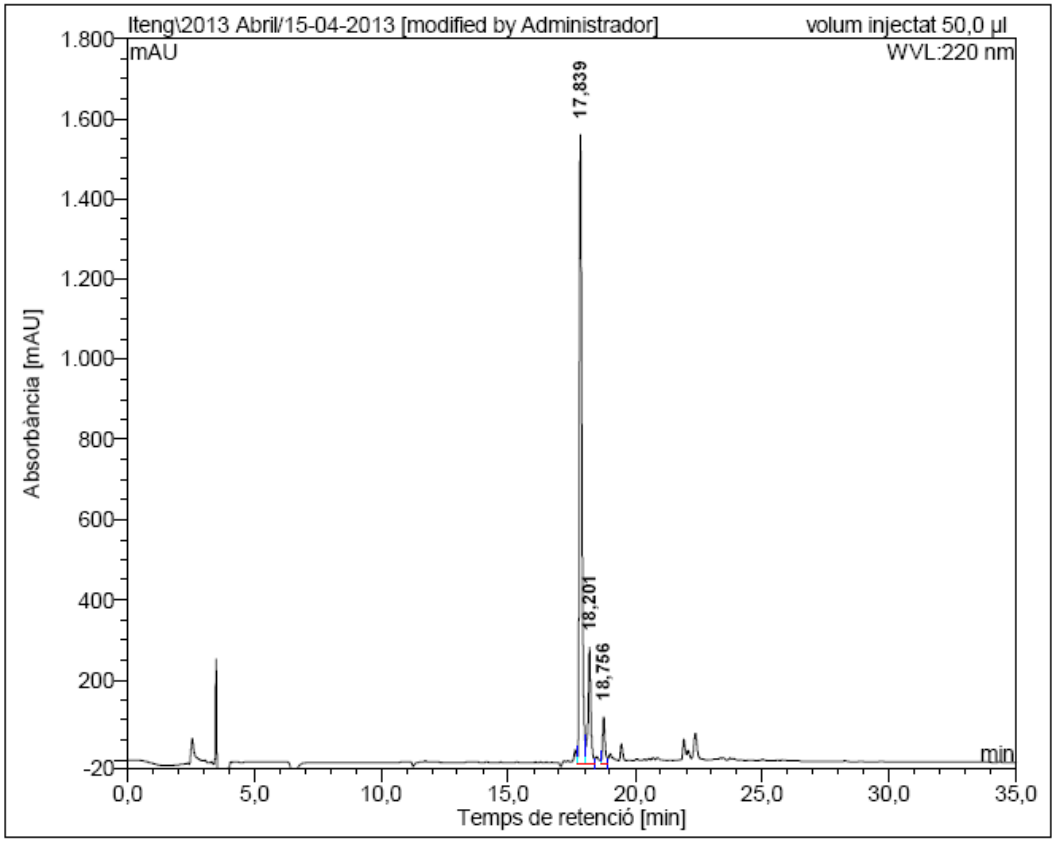

No.	Temps retenció min	alçada mAU	Area mAU*min	Area relativa %
1	17,84	1570,991	187,059	78,65
2	18,20	292,035	36,750	15,45
3	18,76	118,551	14,013	5,89
Total:		1981,578	237,822	100,00

ESI-MS *m/z* (%)

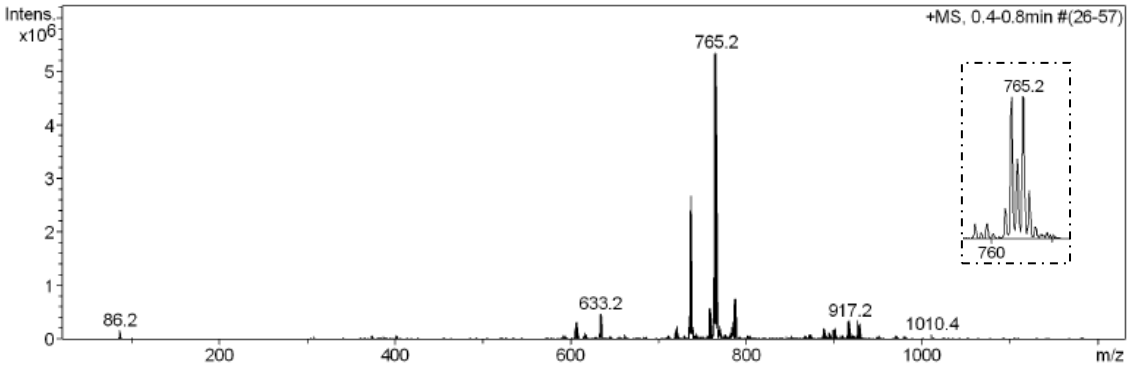

H-His(5-Br)-Lys-Phe-Lys-Lys-Leu-Phe(4-B(OH)$_2$)-Leu-Leu-NH$_2$ (44)

HPLC (λ = 220 nm)

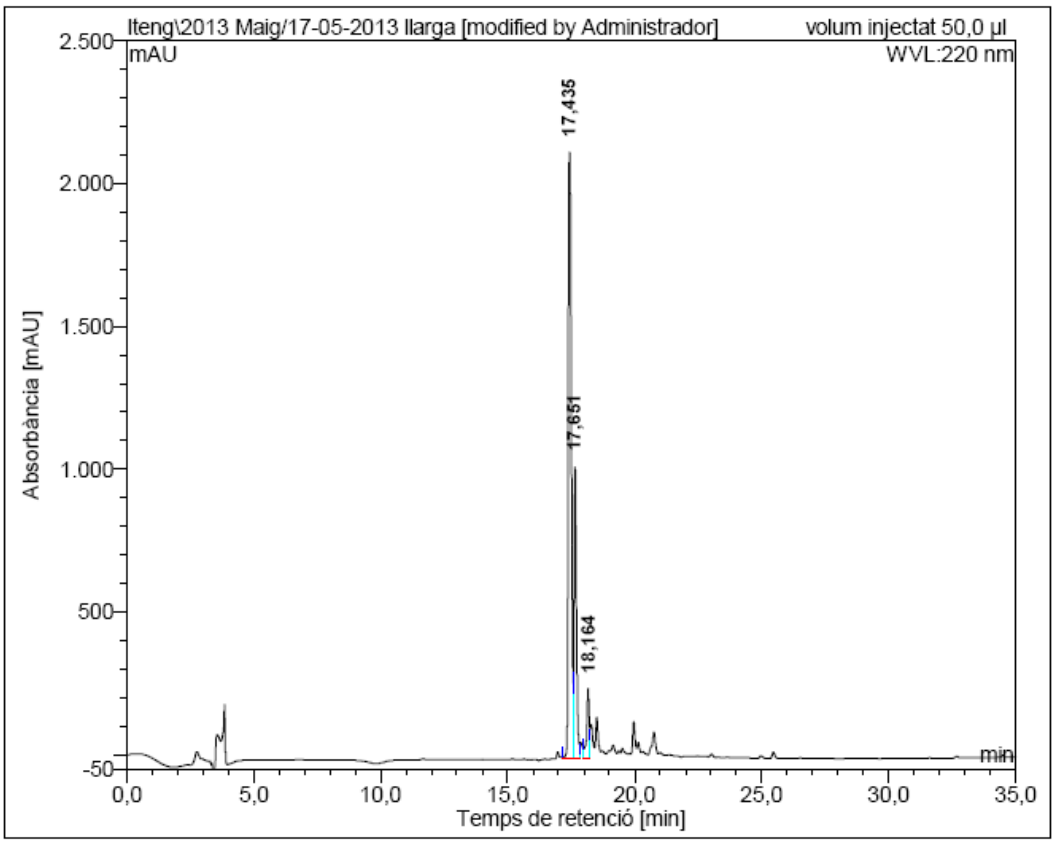

No.	Temps retenció min	alçada mAU	Area mAU*min	Area relativa %
1	17,44	2123,081	289,781	66,94
2	17,65	1022,895	113,294	26,17
3	18,16	245,252	29,792	6,88
Total:		3391,229	432,867	100,00

ESI-MS *m/z* (%)

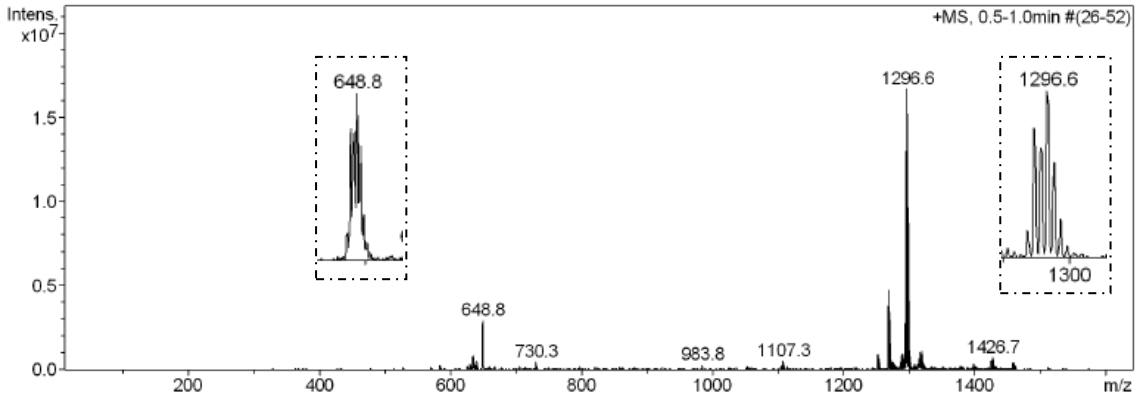

H-His(5-Br)-Lys-Lys-Phe-Lys-Lys-Leu-Phe(4-B(OH)$_2$)-Leu-Leu-NH$_2$ (45)

HPLC (λ = 220 nm)

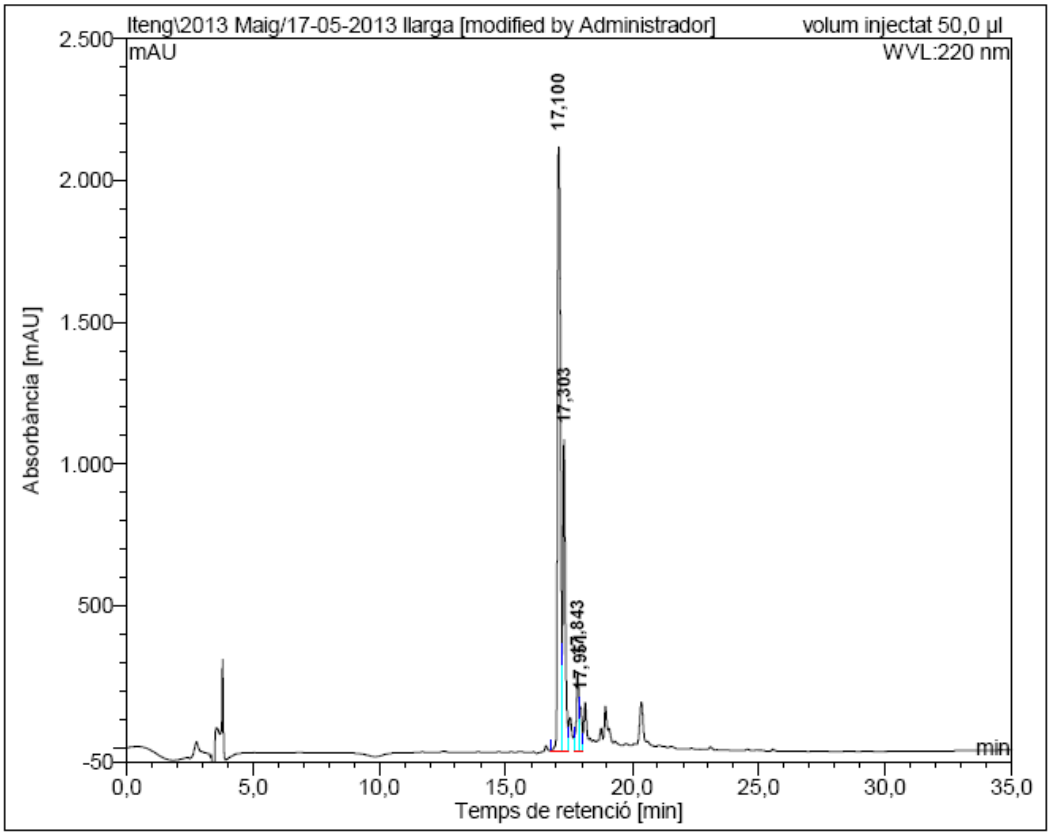

No.	Temps retenció min	alçada mAU	Area mAU*min	Area relativa %
1	17,10	2128,218	294,264	62,57
2	17,30	1097,946	124,187	26,41
3	17,84	277,472	35,976	7,65
4	17,95	156,595	15,863	3,37
Total:		3660,230	470,290	100,00

ESI-MS *m/z* (%)

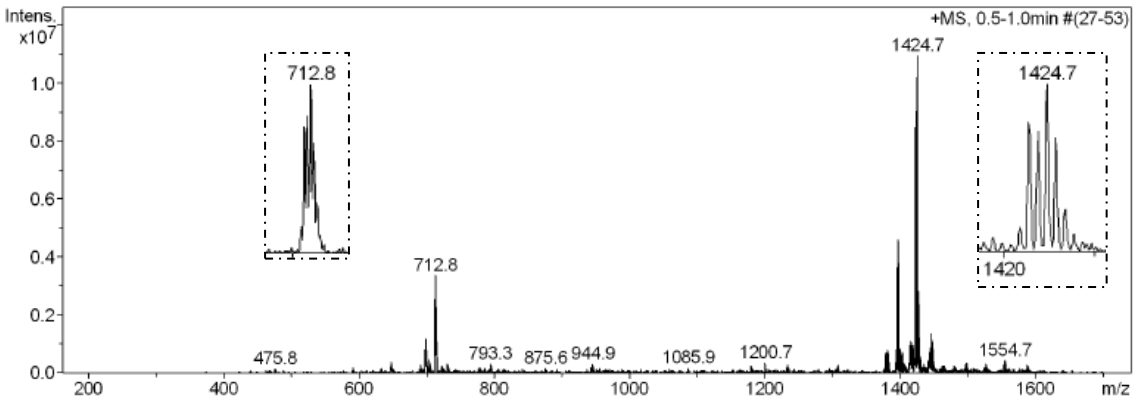

H-His(5-Br)-Lys-Lys-Leu-Phe(4-B(OH)$_2$)-NH$_2$ (46)

HPLC (λ = 220 nm)

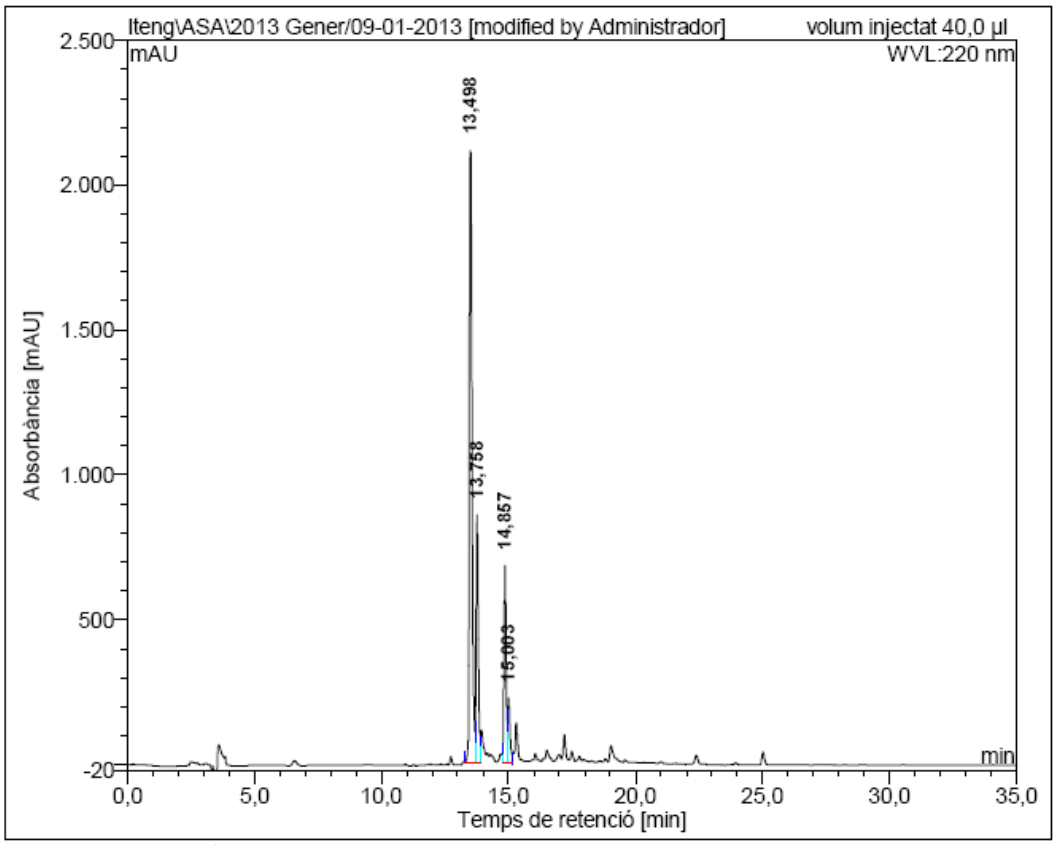

No.	Temps retenció min	alçada mAU	Area mAU*min	Area relativa %
1	13,50	2116,408	268,856	60,23
2	13,76	857,720	87,607	19,63
3	14,86	682,721	65,776	14,73
4	15,00	226,554	24,160	5,41
Total:		3883,403	446,398	100,00

ESI-MS *m/z* (%)

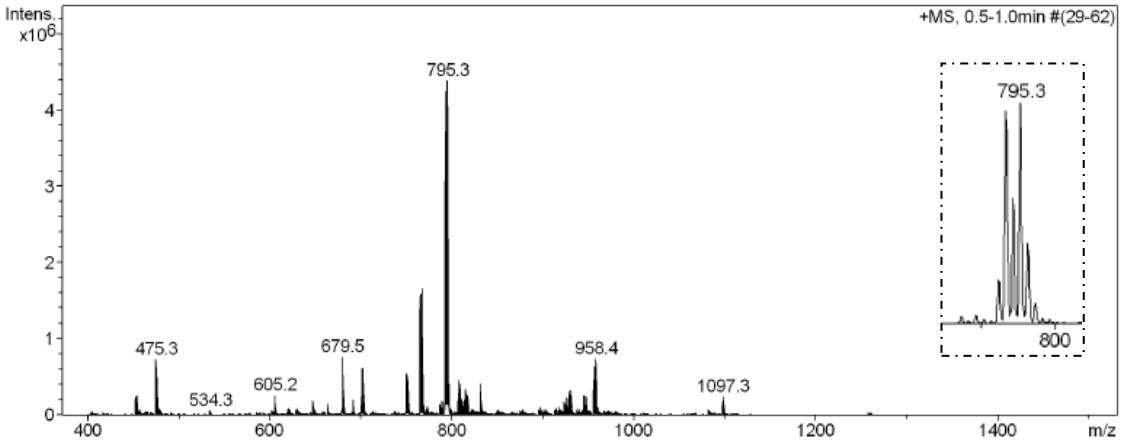

H-His(5-Br)-Leu-Phe(4-B(OH)$_2$)-NH$_2$ (47)

HPLC (λ = 220 nm)

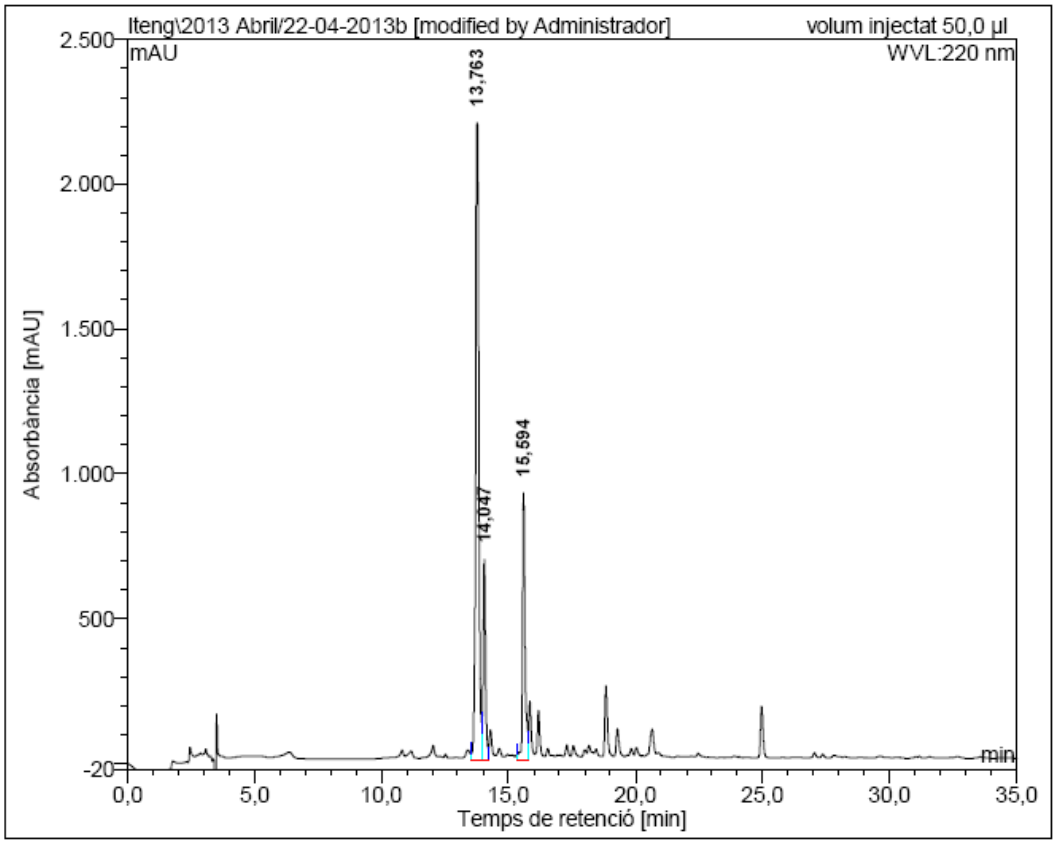

No.	Temps retenció min	alçada mAU	Area mAU*min	Area relativa %
1	13,76	2202,275	329,746	63,84
2	14,05	694,580	77,876	15,08
3	15,59	923,886	108,885	21,08
Total:		3820,741	516,507	100,00

ESI-MS *m/z* (%)

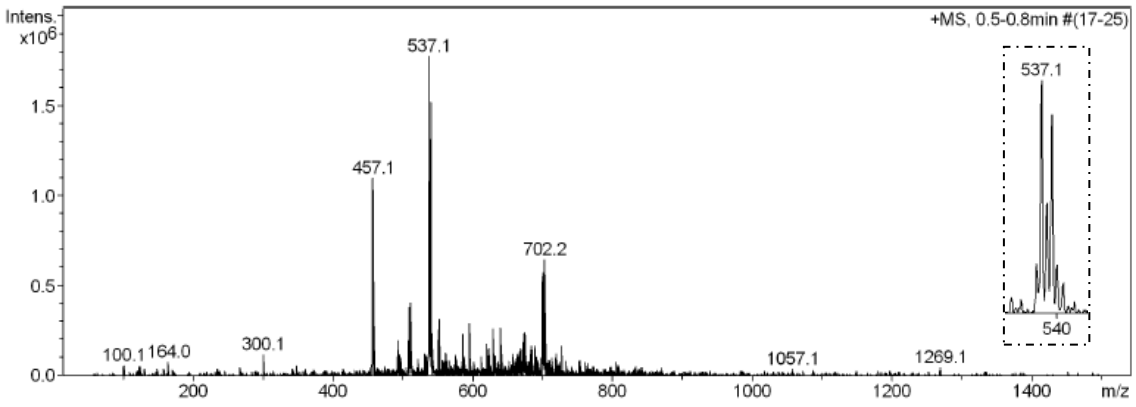

H-His(5-Br)-Lys-Phe-Lys-Lys-Leu-Phe(4-B(OH)$_2$)-NH$_2$ (48)

HPLC (λ = 220 nm)

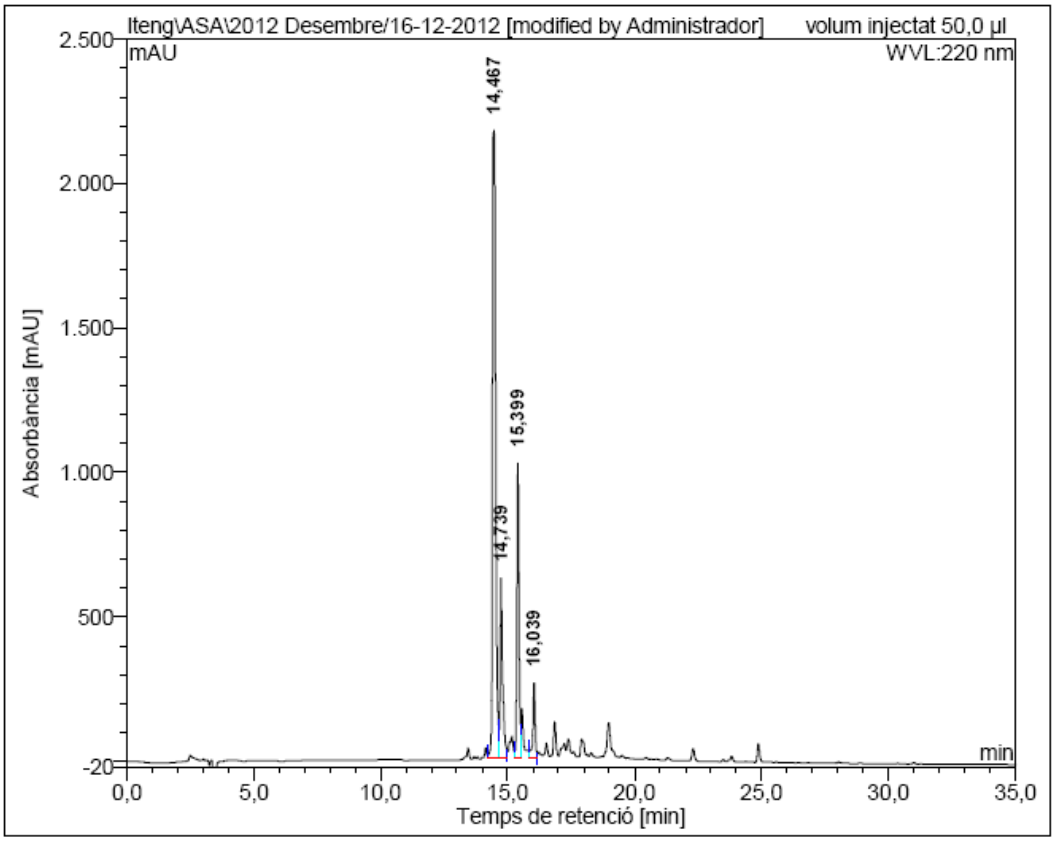

No.	Temps retenció min	alçada mAU	Area mAU*min	Area relativa %
1	14,47	2172,865	319,159	61,83
2	14,74	623,823	72,917	14,13
3	15,40	1021,615	97,041	18,80
4	16,04	260,165	27,106	5,25
Total:		4078,468	516,223	100,00

ESI-MS *m/z* (%)

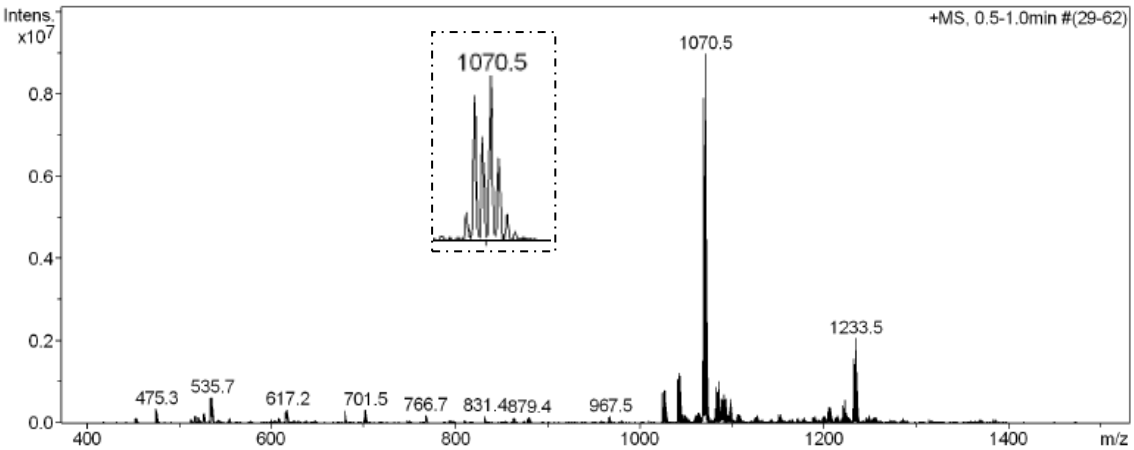

H-His(5-Br)-Lys-Lys-Leu-Phe(4-B(OH)$_2$)-Lys-Lys-Leu-Lys-Lys-NH$_2$ (49)

HPLC (λ = 220 nm)

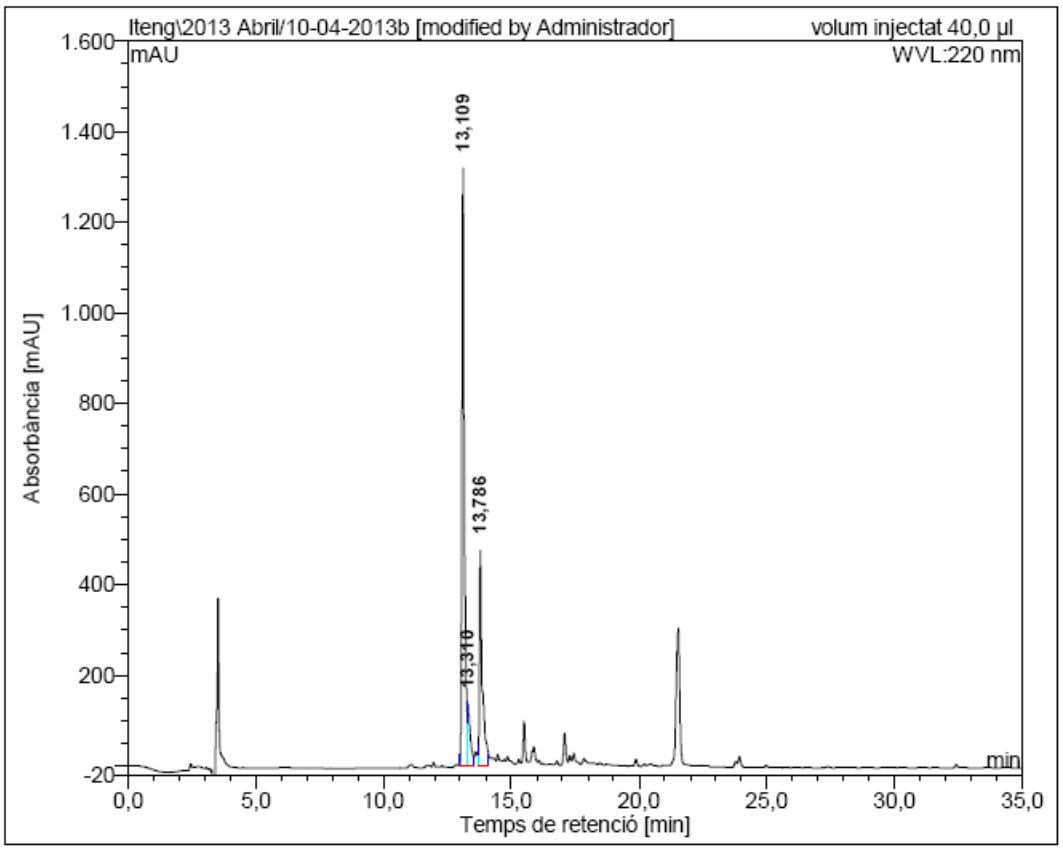

No.	Temps retenció min	alçada mAU	Area mAU*min	Area relativa %
1	13,11	1318,518	140,246	64,24
2	13,31	134,393	17,398	7,97
3	13,79	474,674	60,676	27,79
Total:		1927,585	218,319	100,00

ESI-MS *m/z* (%)

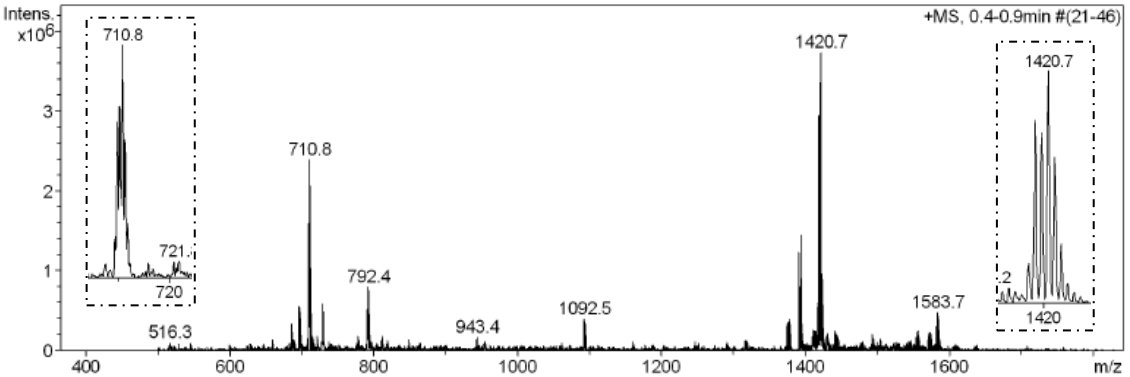

H-His(5-Br)-Leu-Phe(4-B(OH)$_2$)-Lys-Lys-Leu-Lys-Lys-NH$_2$ (50)

HPLC (λ = 220 nm)

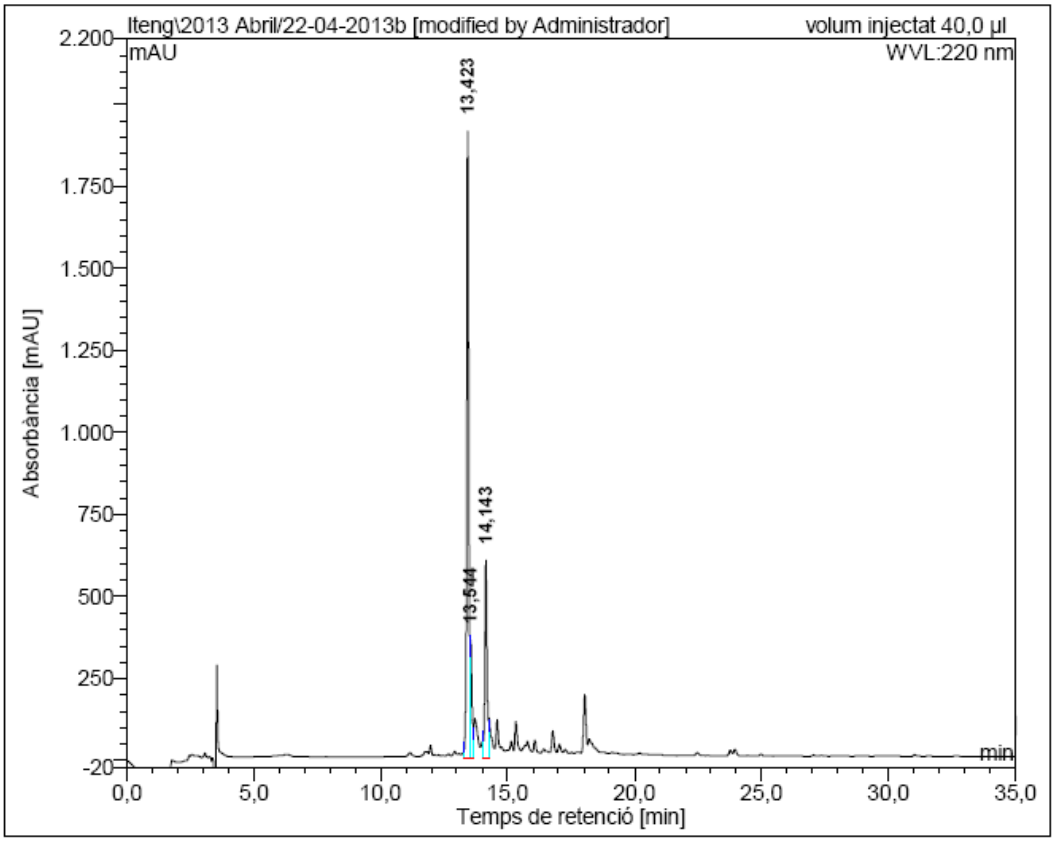

No.	Temps retenció min	alçada mAU	Area mAU*min	Area relativa %
1	13,42	1908,217	184,261	67,79
2	13,54	357,749	29,774	10,95
3	14,14	601,254	57,777	21,26
Total:		2867,219	271,812	100,00

ESI-MS *m/z* (%)

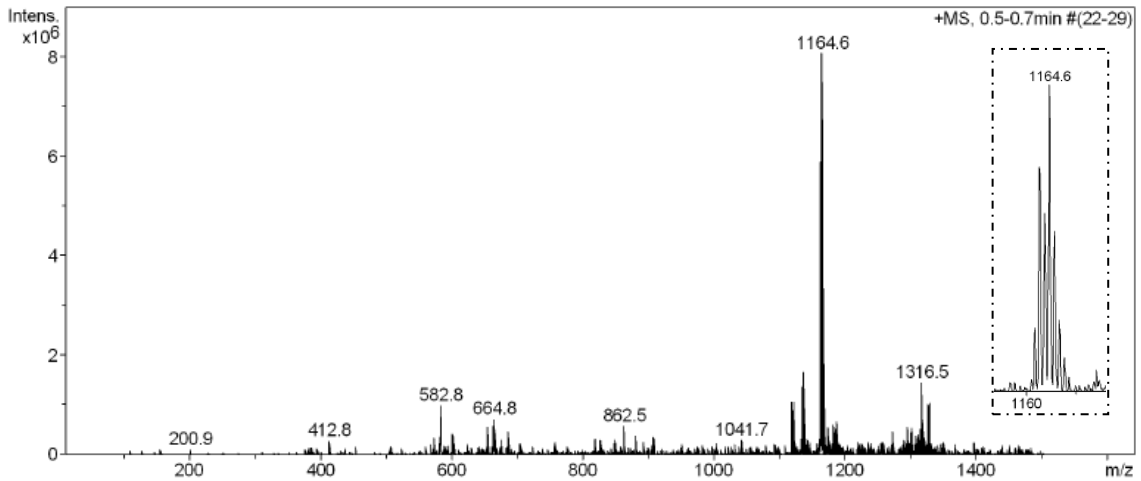

H-His(5-Br,1-Me)-Lys-Lys-Leu-Phe(4-B(OH)$_2$)-Leu-Leu-NH$_2$ and H-His(5-Br,3-Me)-Lys-Lys-Leu-Phe(4-B(OH)$_2$)-Leu-Leu-NH$_2$ (51)

HPLC (λ = 220 nm)

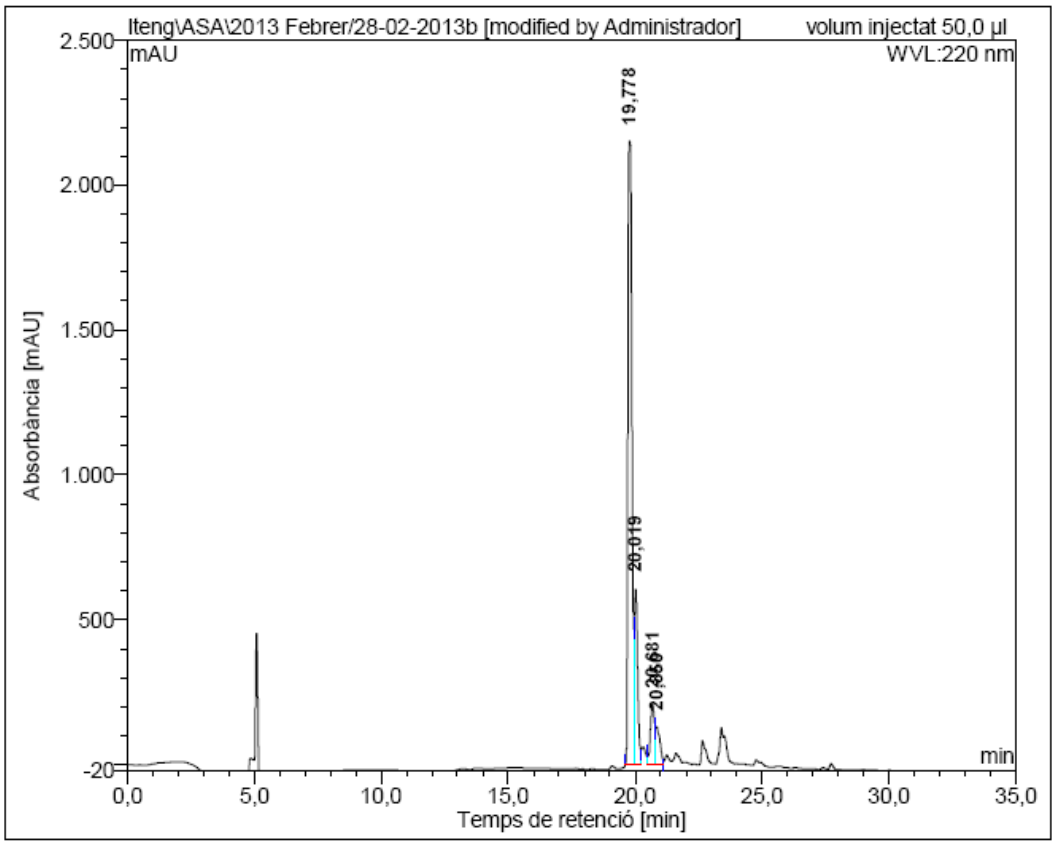

No.	Temps retenció min	alçada mAU	Area mAU*min	Area relativa %
1	19,78	2152,209	389,082	70,86
2	20,02	604,127	93,733	17,07
3	20,68	208,092	42,530	7,75
4	20,85	131,029	23,726	4,32
Total:		3095,457	549,071	100,00

ESI-MS *m/z* (%)

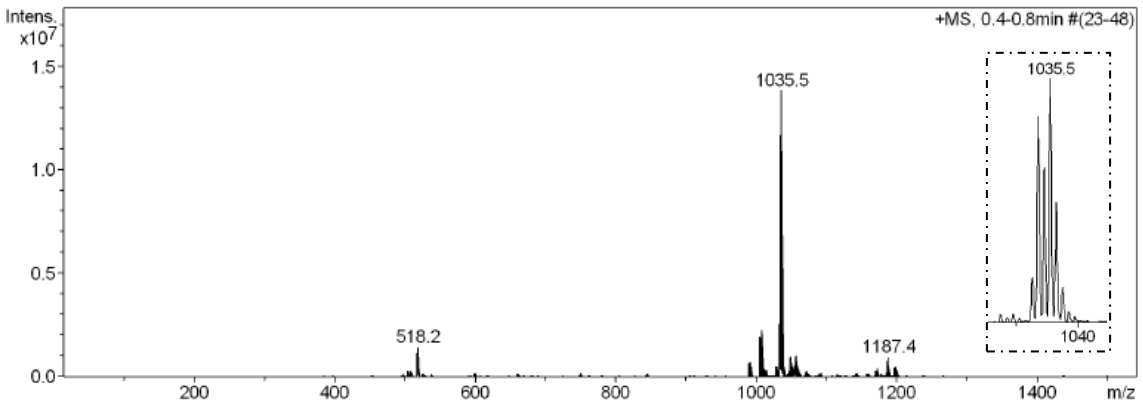

H-His(5-Br,1-Me)-Lys-Lys-Leu-Phe(4-B(OH)$_2$)-NH$_2$ and H-His(5-Br,3-Me)-Lys-Lys-Leu-Phe(4-B(OH)$_2$)-NH$_2$ (52)

HPLC (λ = 220 nm)

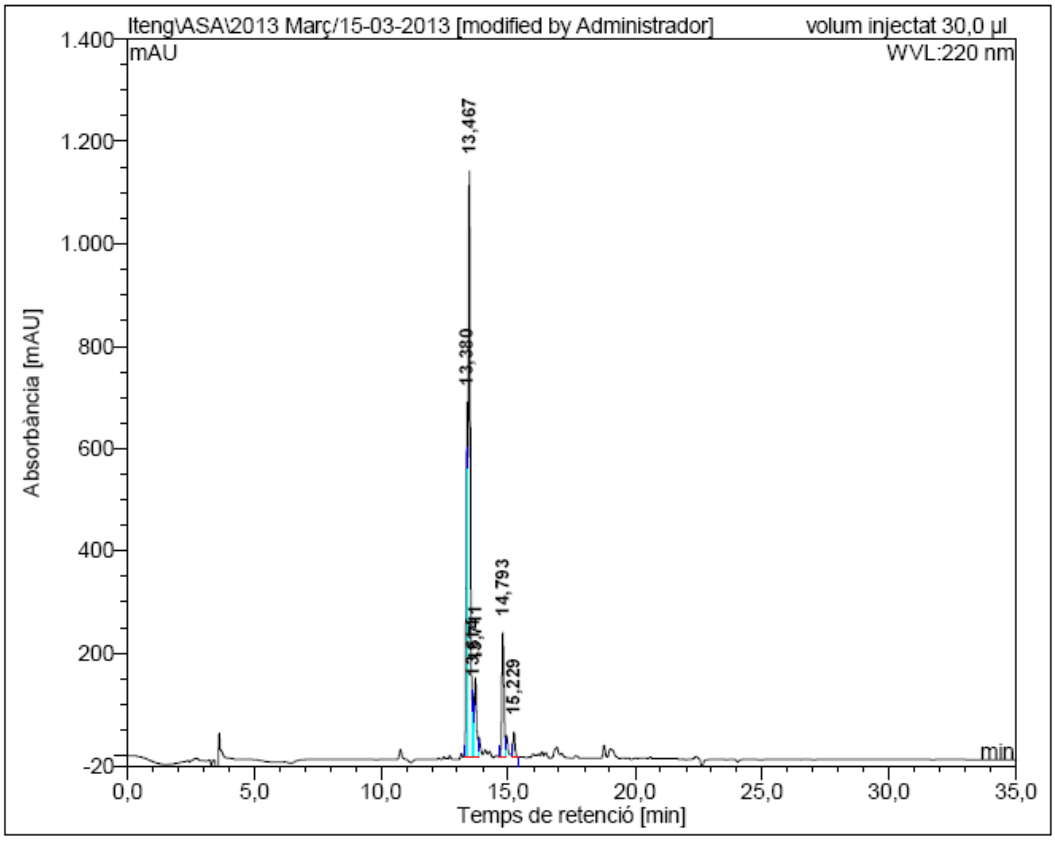

No.	Temps retenció min	alçada mAU	Area mAU*min	Area relativa %
1	13,38	691,984	45,195	22,30
2	13,47	1143,169	107,416	53,01
3	13,61	124,222	8,246	4,07
4	13,71	153,837	13,872	6,85
5	14,79	244,282	23,141	11,42
6	15,23	50,135	4,757	2,35
Total:		2407,629	202,627	100,00

ESI-MS *m/z* (%)

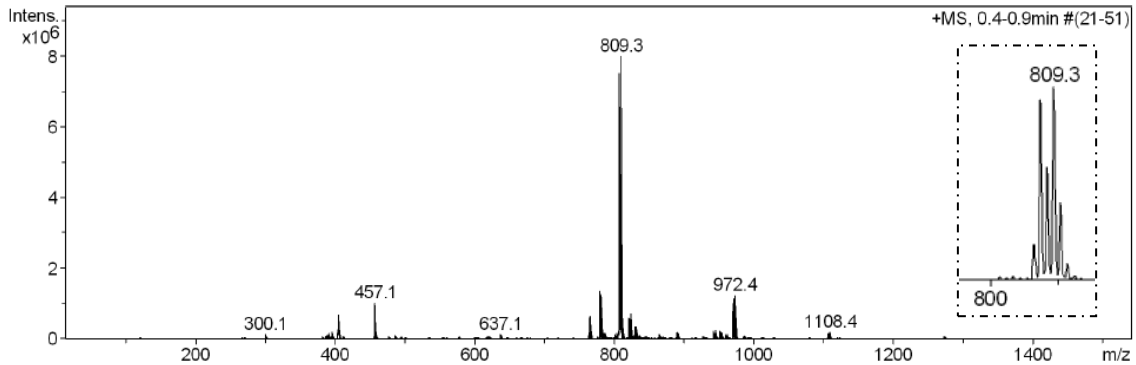

3. Linear peptides containing a 5-bromohistidine at the C-terminus

Linear peptides 65-68

H-Phe(4-B(OH)$_2$)-Leu-His(5-Br)-Leu-Leu-NH$_2$ (65)

HPLC (λ = 220 nm)

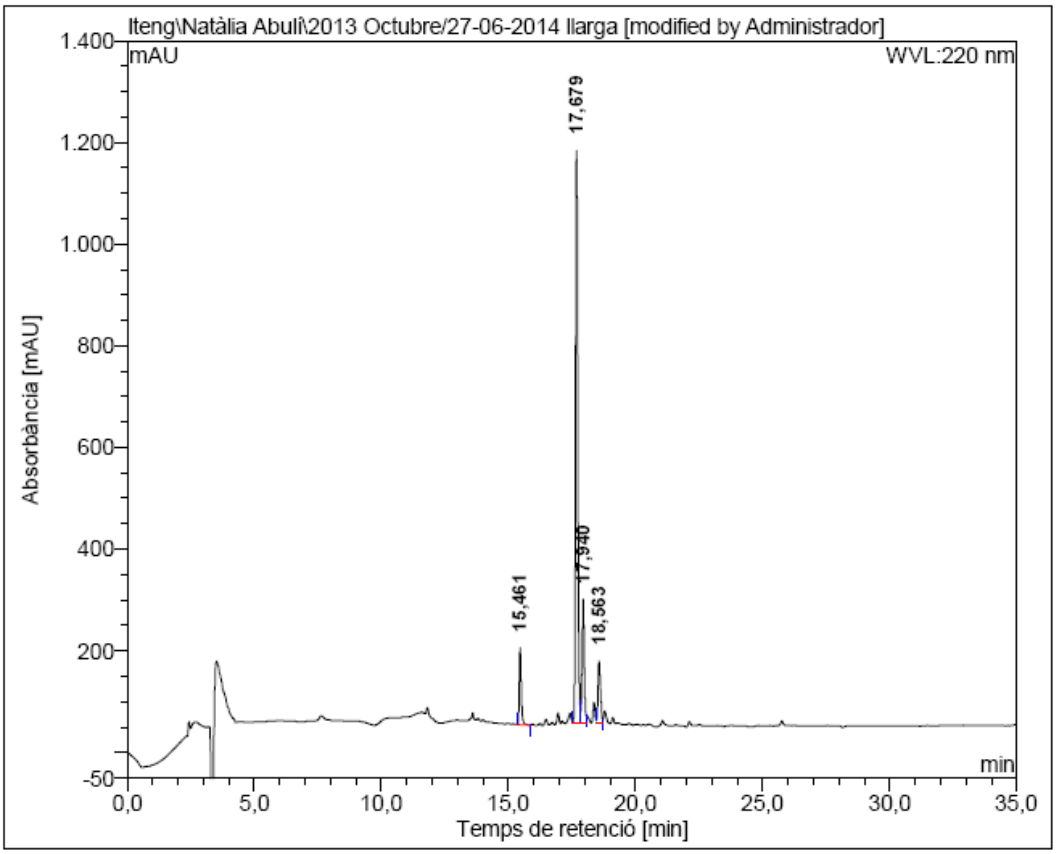

No.	mps retenc min	alçada mAU	Area mAU*min	Area relativa %
1	15,46	150,590	13,563	8,15
2	17,68	1125,930	114,800	68,95
3	17,94	244,440	23,545	14,14
4	18,56	123,146	14,596	8,77
Total:		1644,106	166,505	100,00

ESI-MS *m/z* (%)

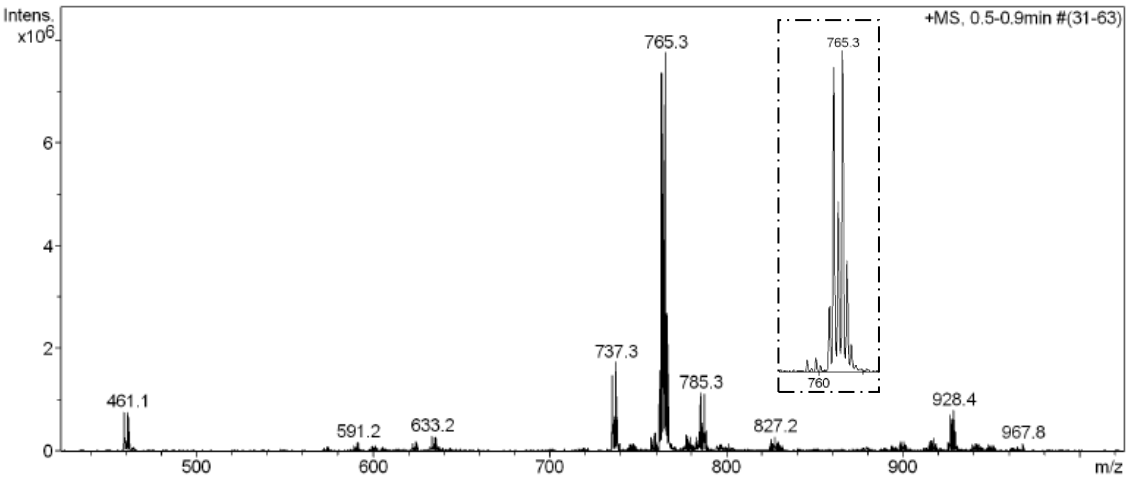

H-Phe(4-B(OH)$_2$)-Lys-Lys-Leu-His(5-Br)-Leu-Leu-NH$_2$ (66)

HPLC (λ = 220 nm)

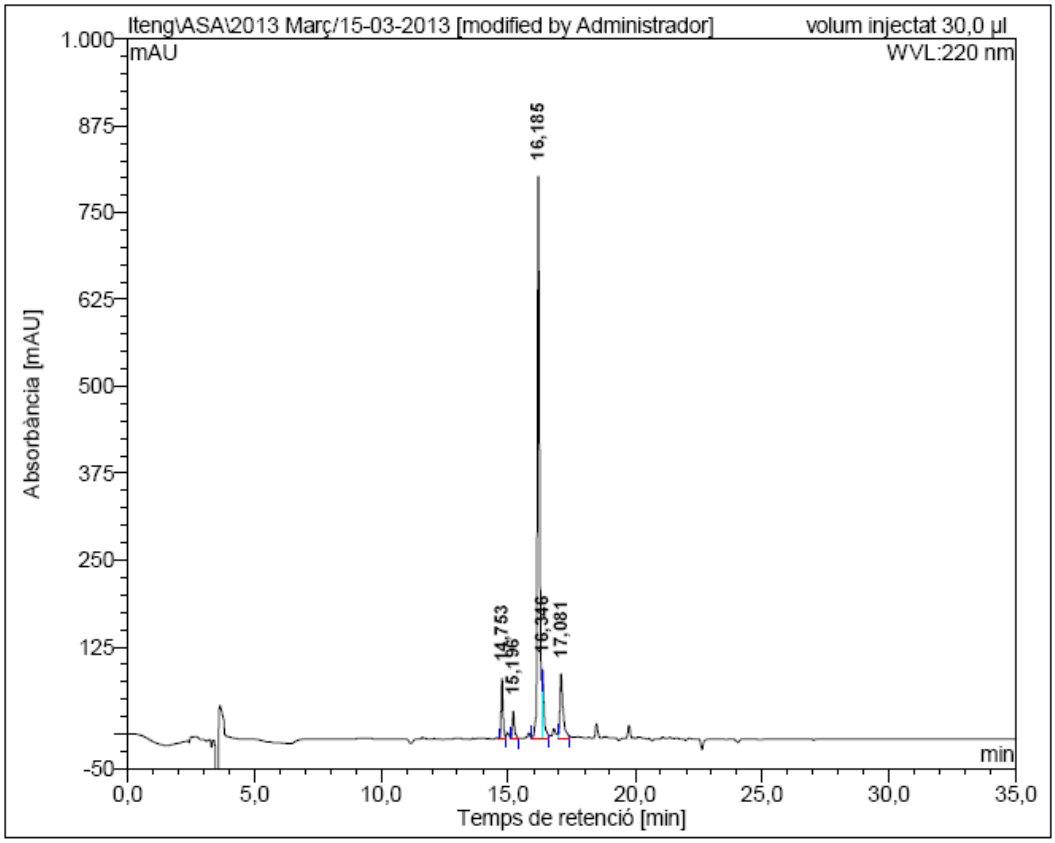

No.	Temps retenció min	alçada mAU	Area mAU*min	Area relativa %
1	14,75	87,717	7,780	6,52
2	15,20	40,240	4,033	3,38
3	16,18	809,753	82,250	68,88
4	16,35	100,805	11,514	9,64
5	17,08	93,934	13,829	11,58
Total:		1132,449	119,406	100,00

ESI-MS *m/z* (%)

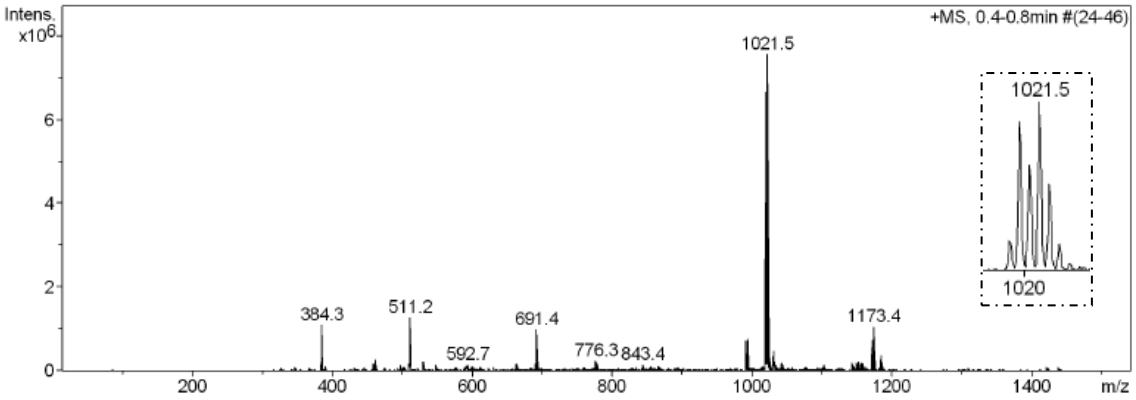

H-Phe(4-B(OH)$_2$)-Leu-His(5-Br)-NH$_2$ (67)

HPLC (λ = 220 nm)

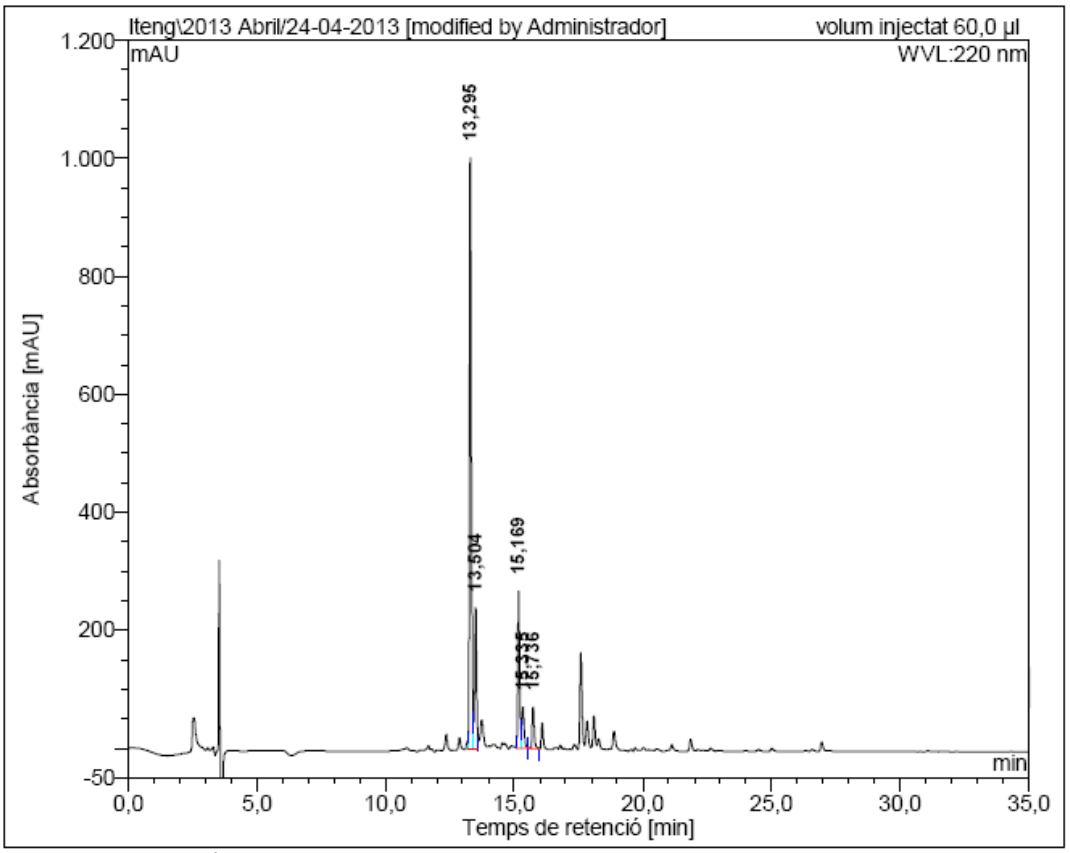

No.	Temps retenció min	alçada mAU	Area mAU*min	Area relativa %
1	13,29	1000,535	86,368	59,72
2	13,50	238,430	20,852	14,42
3	15,17	267,008	23,437	16,20
4	15,34	70,494	7,341	5,08
5	15,74	71,197	6,633	4,59
Total:		1647,664	144,631	100,00

ESI-MS *m/z* (%)

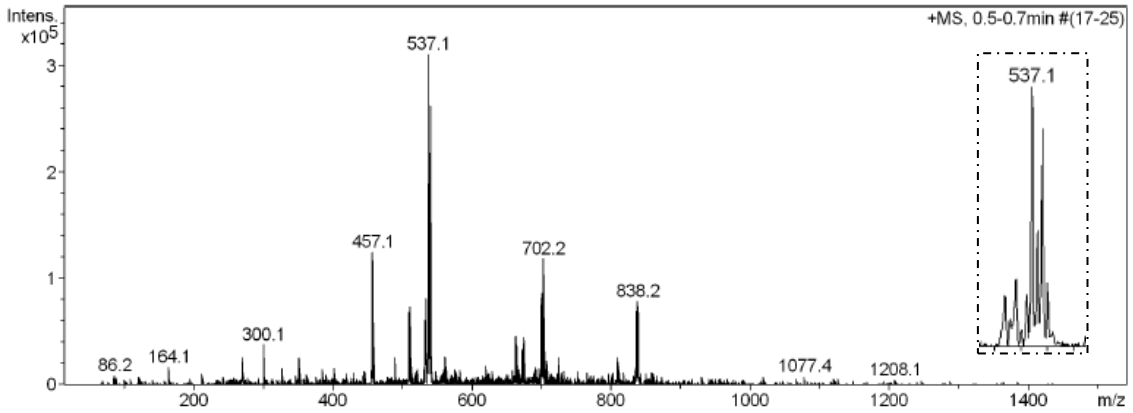

H-Phe(4-B(OH)$_2$)-Lys-Lys-Leu-His(5-Br)-NH$_2$ (68)

HPLC (λ = 220 nm)

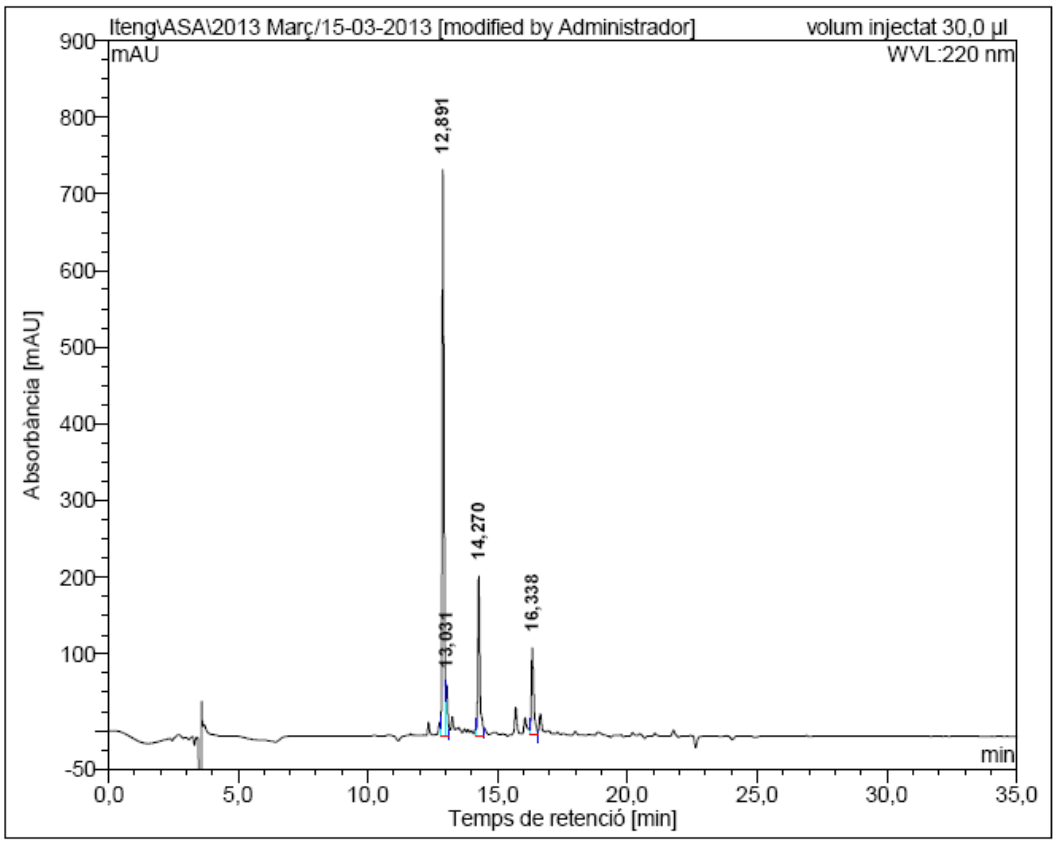

No.	Temps retenció min	alçada mAU	Area mAU*min	Area relativa %
1	12,89	737,752	59,428	61,78
2	13,03	66,151	5,313	5,52
3	14,27	207,672	19,235	20,00
4	16,34	113,248	12,221	12,70
Total:		1124,823	96,197	100,00

ESI-MS *m/z* (%)

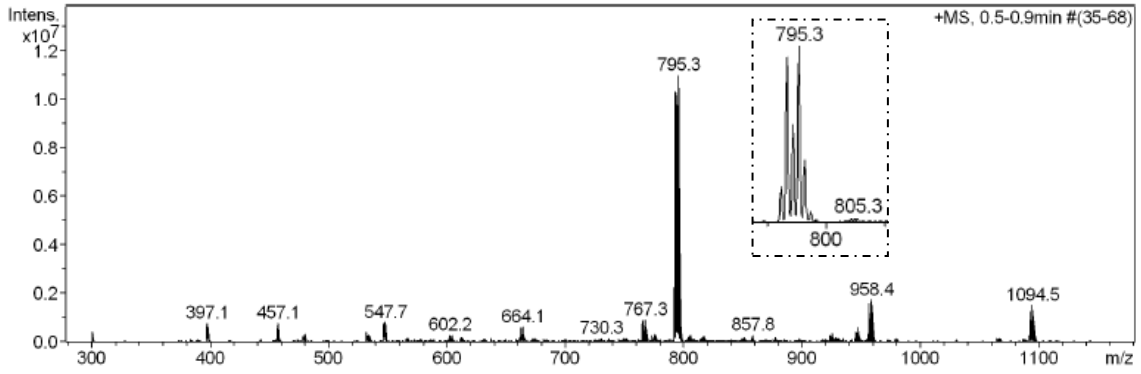

4. Biaryl cyclic peptides

Biaryl cyclic peptide BPC750

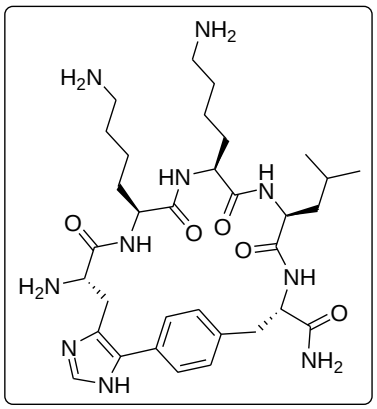

Crude peptide

HPLC-MS

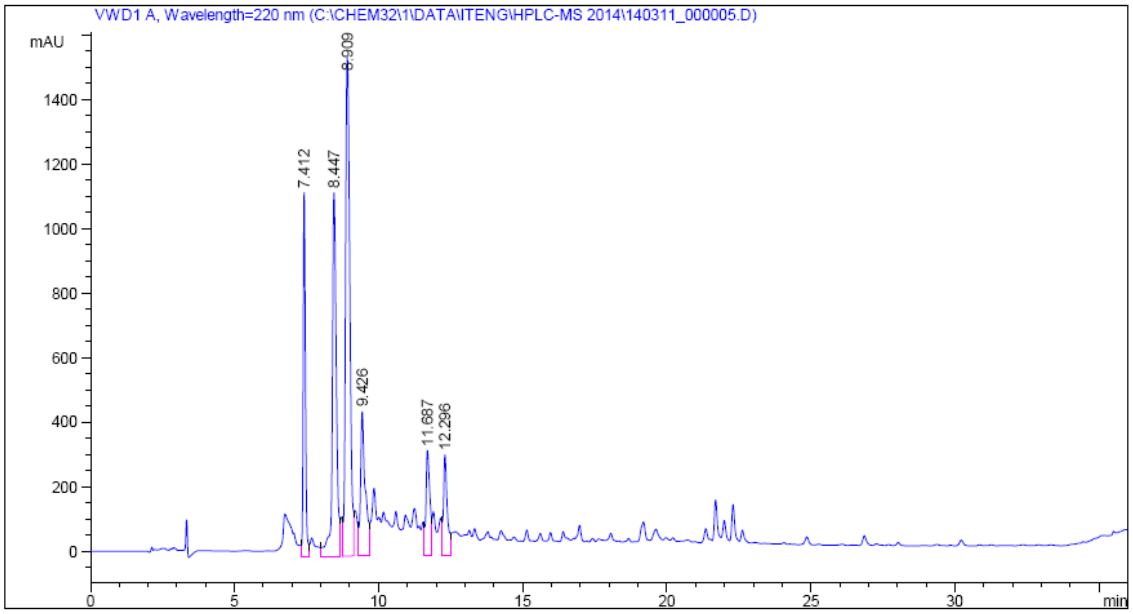

Peak #	RetTime [min]	Type	Width [min]	Area mAU *s	Height [mAU]	Area %
1	7.412	VV	0.0833	6091.82568	1130.35437	13.7311
2	8.447	VV	0.1473	1.09971e4	1127.61829	24.7876
3	8.909	VV	0.1644	1.62089e4	1547.88965	36.5352
4	9.426	VV	0.1593	5122.47119	449.02802	11.5461
5	11.687	VV	0.1391	3084.87329	327.16312	6.9534
6	12.296	VV	0.1311	2860.06030	313.74521	6.4466

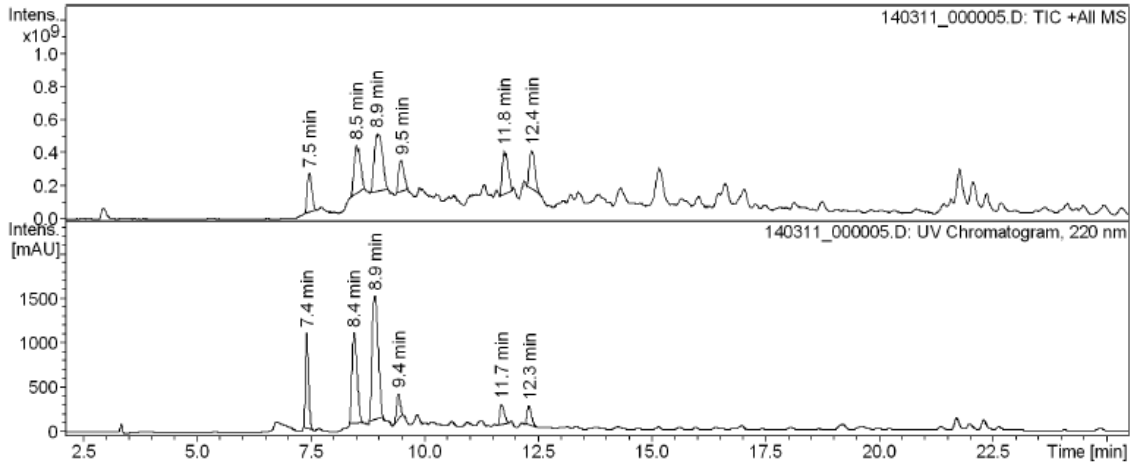
Intens.
x10^9
1.0
0.8
0.6
0.4
0.2
0.0
140311_000005.D: TIC +All MS
7.5 min
8.5 min
8.9 min
9.5 min
11.8 min
12.4 min
Intens.
[mAU]
1500
1000
500
0
140311_000005.D: UV Chromatogram, 220 nm
7.4 min
8.4 min
8.9 min
9.4 min
11.7 min
12.3 min
2.5
5.0
7.5
10.0
12.5
15.0
17.5
20.0
22.5
Time [min]

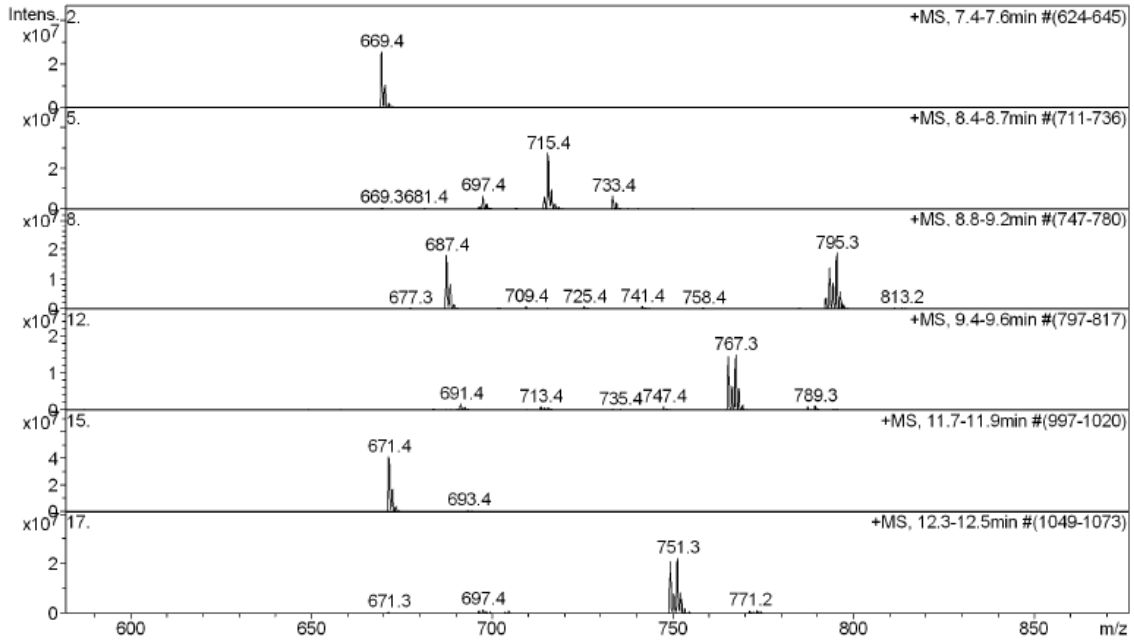
Intens.
2.
x10^7
669.4
+MS, 7.4-7.6min #(624-645)
5.
715.4
669.3681.4
697.4
733.4
+MS, 8.4-8.7min #(711-736)
8.
687.4
795.3
677.3
709.4
725.4
741.4
758.4
813.2
+MS, 8.8-9.2min #(747-780)
12.
767.3
691.4
713.4
735.4747.4
789.3
+MS, 9.4-9.6min #(797-817)
15.
671.4
693.4
+MS, 11.7-11.9min #(997-1020)
17.
751.3
671.3
697.4
771.2
+MS, 12.3-12.5min #(1049-1073)
600
650
700
750
800
850
m/z

Biaryl cyclic peptide BPC752

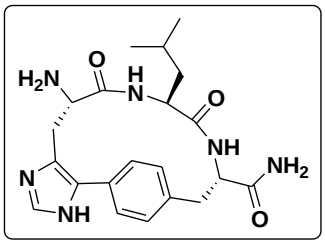

Crude peptide

HPLC (λ = 220 nm)

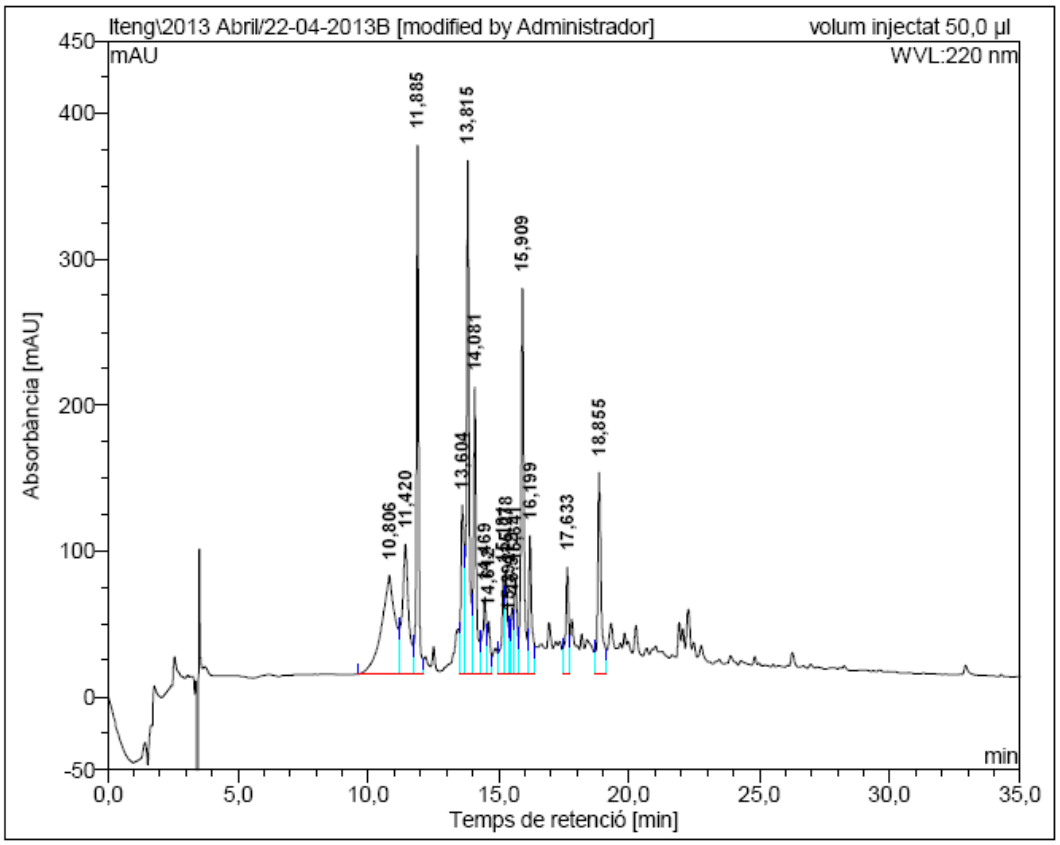

No.	Ret.Time (detected) min	Height mAU	Area mAU*min	Rel.Area %
1	10,81	67,735	39,819	12,83
2	11,42	88,886	25,708	8,28
3	11,89	362,653	36,267	11,68
4	13,60	115,814	17,407	5,61
5	13,81	352,075	40,603	13,08
6	14,08	196,500	24,666	7,95
7	14,47	52,921	9,589	3,09
8	14,61	36,201	4,565	1,47
9	15,18	65,212	8,761	2,82
10	15,28	71,640	7,637	2,46
11	15,39	32,366	2,098	0,68
12	15,51	45,345	4,861	1,57
13	15,64	65,719	9,303	3,00
14	15,91	264,358	33,504	10,79
15	16,20	94,729	13,326	4,29
16	17,63	73,430	10,746	3,46
17	18,85	137,990	21,568	6,95
Total:		2123,574	310,427	100,00

ESI-MS *m/z*

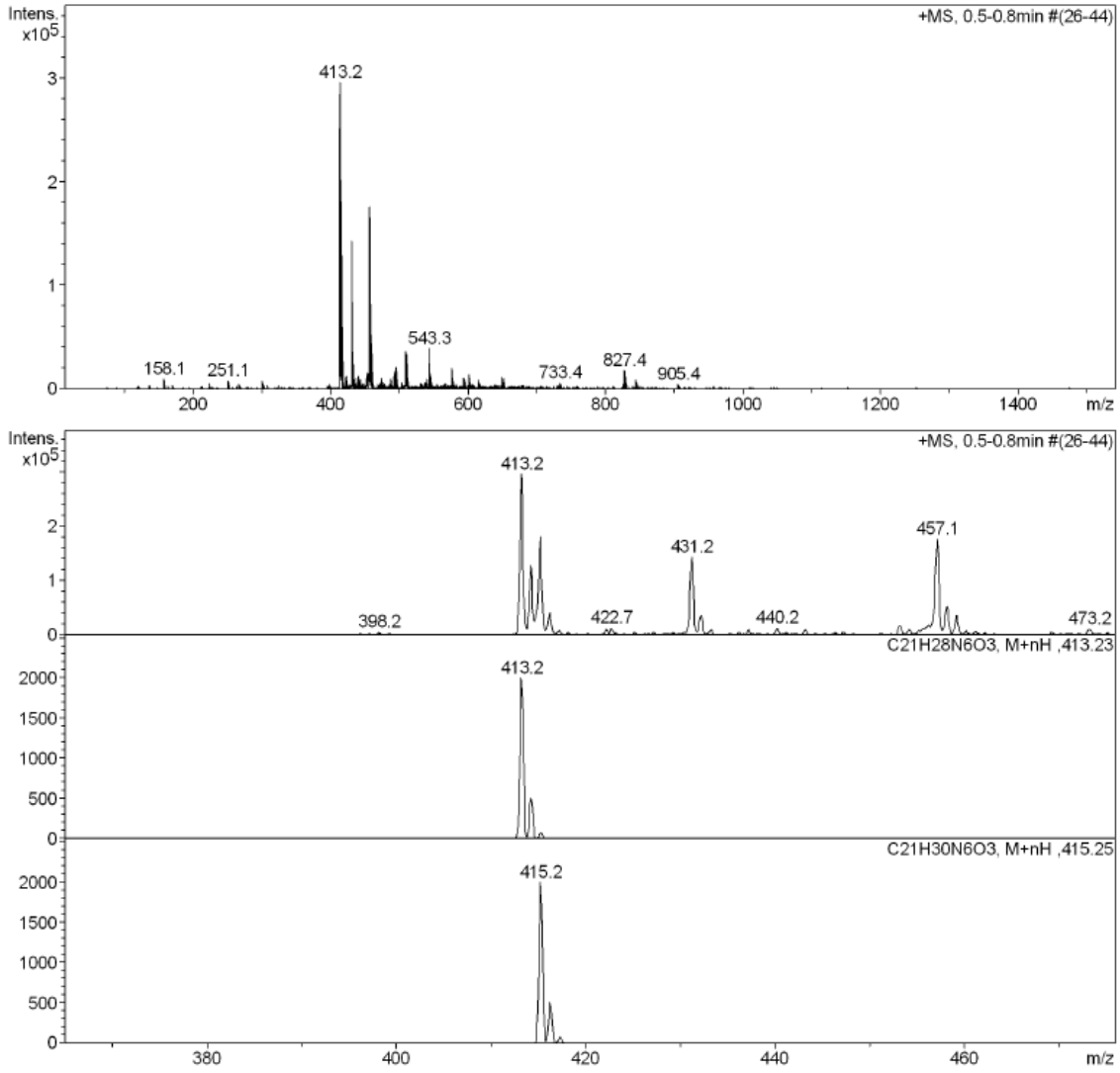
Intens.
x10^5
+MS, 0.5-0.8min #(26-44)
413.2
543.3
158.1
251.1
733.4
827.4
905.4
m/z
Intens.
x10^5
+MS, 0.5-0.8min #(26-44)
413.2
457.1
431.2
398.2
422.7
440.2
473.2
C21H28N6O3, M+nH ,413.23
413.2
C21H30N6O3, M+nH ,415.25
415.2
m/z

Purified peptide

HPLC (λ = 220 nm)

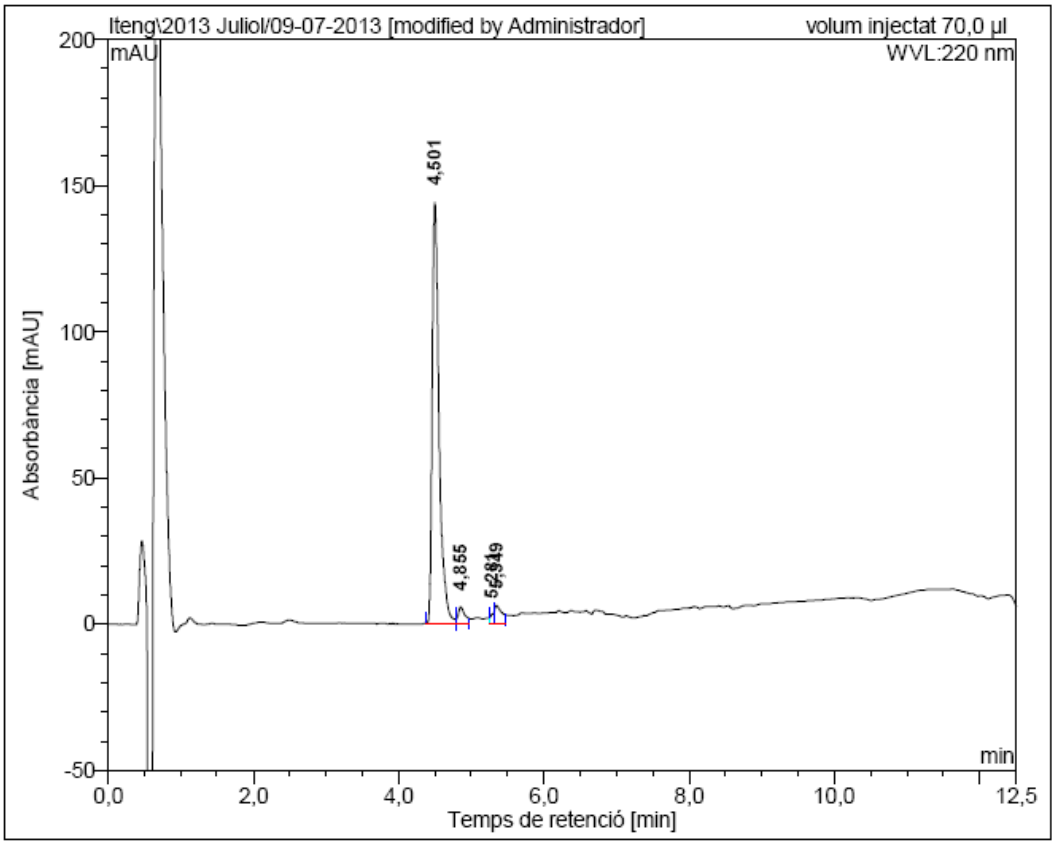

No.	Temps retenció min	alçada mAU	Area mAU*min	Area relativa %
1	4,50	143,979	15,775	91,43
2	4,86	5,697	0,593	3,44
3	5,28	3,110	0,147	0,85
4	5,35	6,142	0,739	4,28
Total:		158,928	17,254	100,00

ESI-MS *m/z*

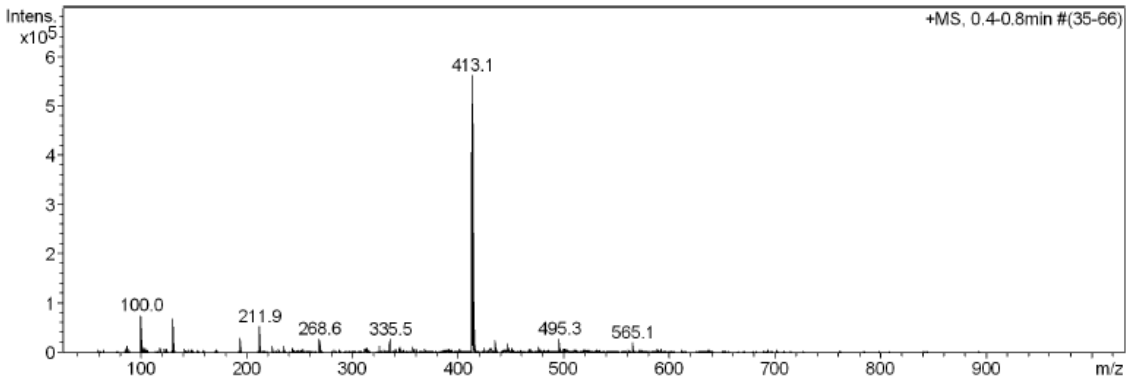

HRMS (ESI) *m/z*

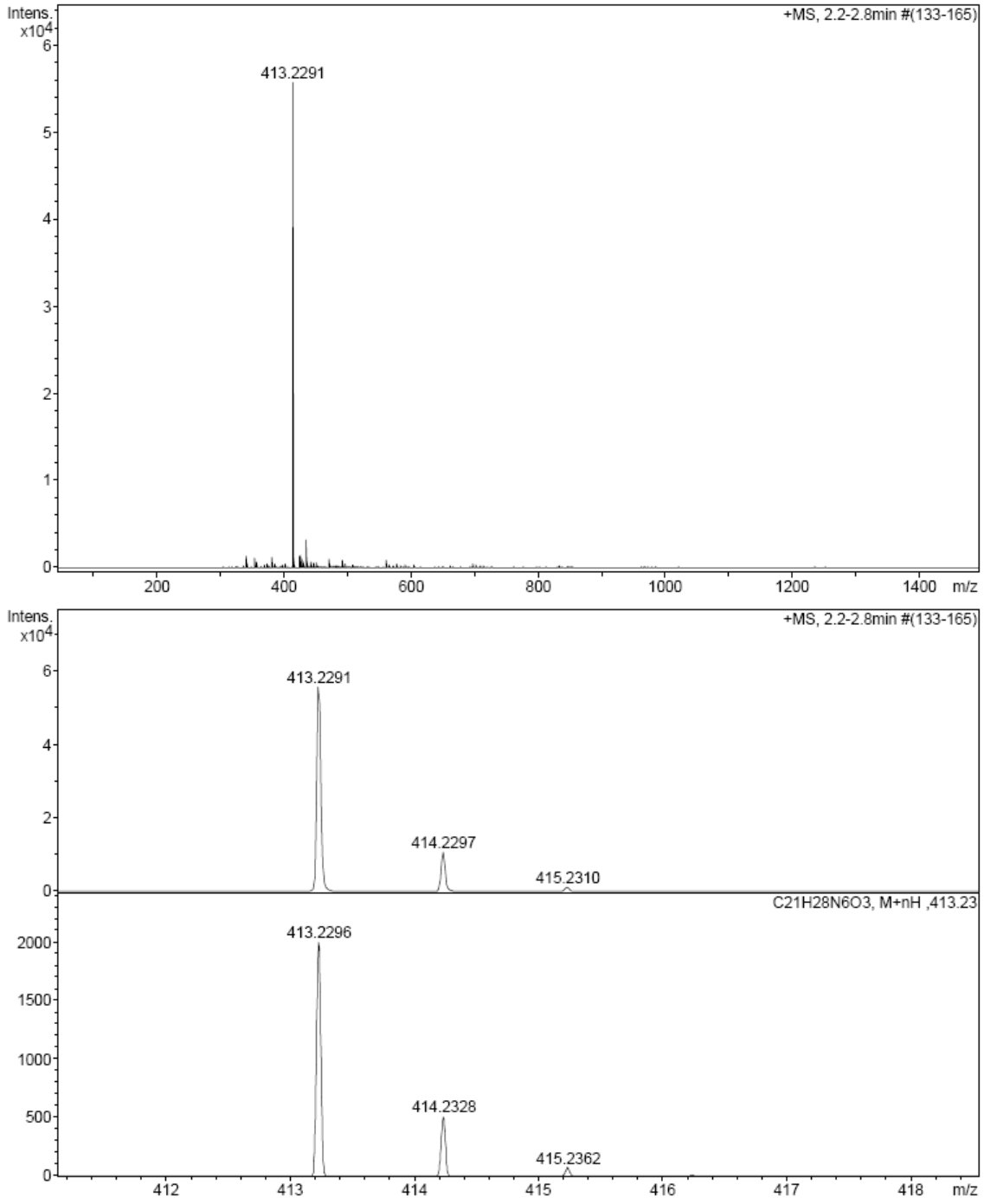
Intens.
x10^4
+MS, 2.2-2.8min #(133-165)
413.2291
m/z
Intens.
x10^4
+MS, 2.2-2.8min #(133-165)
413.2291
414.2297
415.2310
C21H28N6O3, M+nH ,413.23
413.2296
414.2328
415.2362
m/z

Biaryl cyclic peptide BPC754

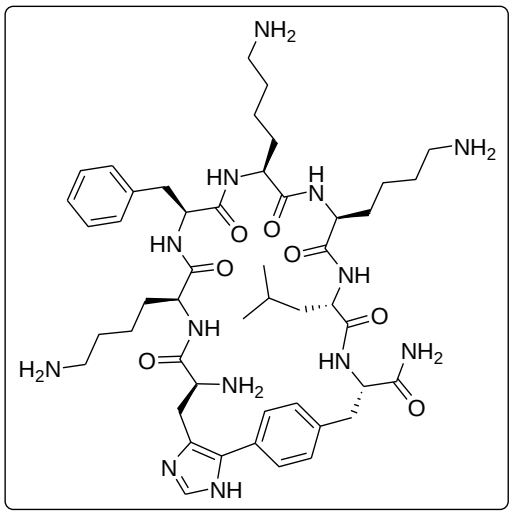

Crude peptide

HPLC-MS

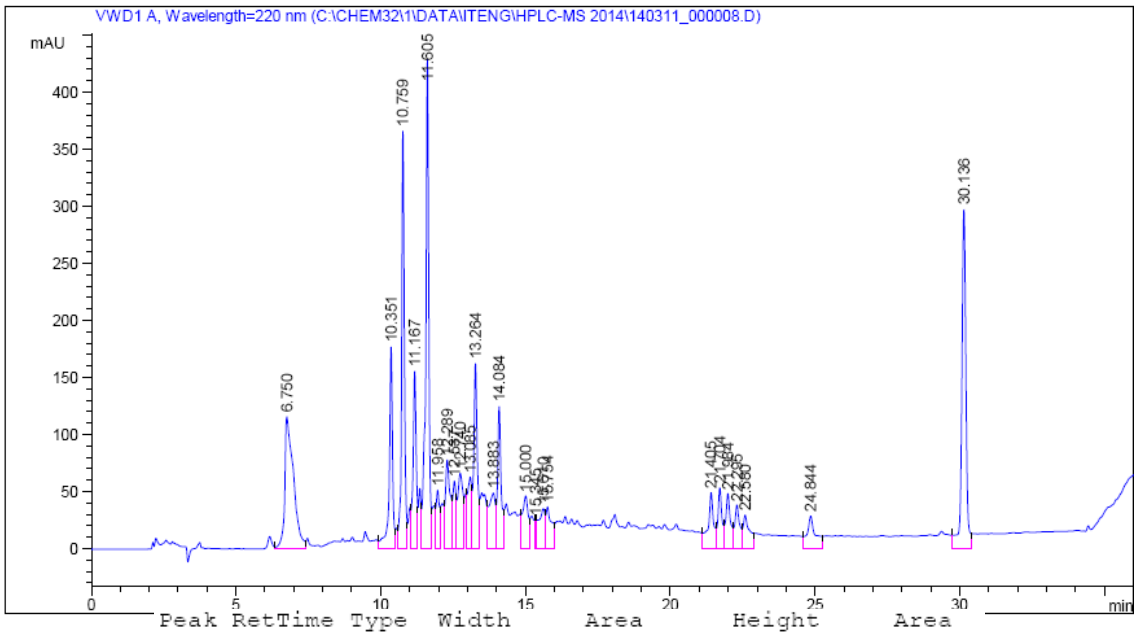

Peak #	RetTime [min]	Type	Width [min]	Area mAU *s	Height [mAU]	Area %
1	6.750	VV	0.2748	2436.85669	115.72290	9.5602
2	10.351	VV	0.1151	1416.69934	177.25807	5.5580
3	10.759	VV	0.1002	2460.76538	366.33887	9.6540
4	11.167	VV	0.1139	1229.50891	155.88240	4.8236
5	11.605	VV	0.1091	3265.17871	429.18002	12.8099
6	11.958	VV	0.1112	406.35226	51.36128	1.5942
7	12.289	VV	0.1615	916.02960	78.12401	3.5937
8	12.537	VV	0.1233	517.23932	59.44904	2.0292
9	12.740	VV	0.1759	827.75629	66.45026	3.2474
10	13.085	VV	0.1363	616.67255	62.85778	2.4193
11	13.264	VV	0.1260	1430.30591	162.53557	5.6113
12	13.883	VV	0.1970	729.80591	49.01923	2.8632
13	14.084	VV	0.1218	1069.71179	124.87048	4.1967
14	15.000	VV	0.1929	646.58832	46.46993	2.5367
15	15.345	VV	0.0572	101.93134	25.27822	0.3999
16	15.610	VV	0.2083	548.65179	35.44394	2.1525
17	15.754	VV	0.1829	513.40479	36.86473	2.0142
18	21.405	VV	0.1826	660.66632	49.29629	2.5919
19	21.704	VV	0.1377	520.64948	53.76215	2.0426
20	21.984	VV	0.1671	584.98578	48.45042	2.2950
21	22.295	VV	0.1653	459.66428	38.55211	1.8033
22	22.580	VV	0.2188	495.48987	29.79371	1.9439
23	24.844	VB	0.2793	606.73853	28.79135	2.3803
24	30.136	VV	0.1537	3027.88574	297.47565	11.8789

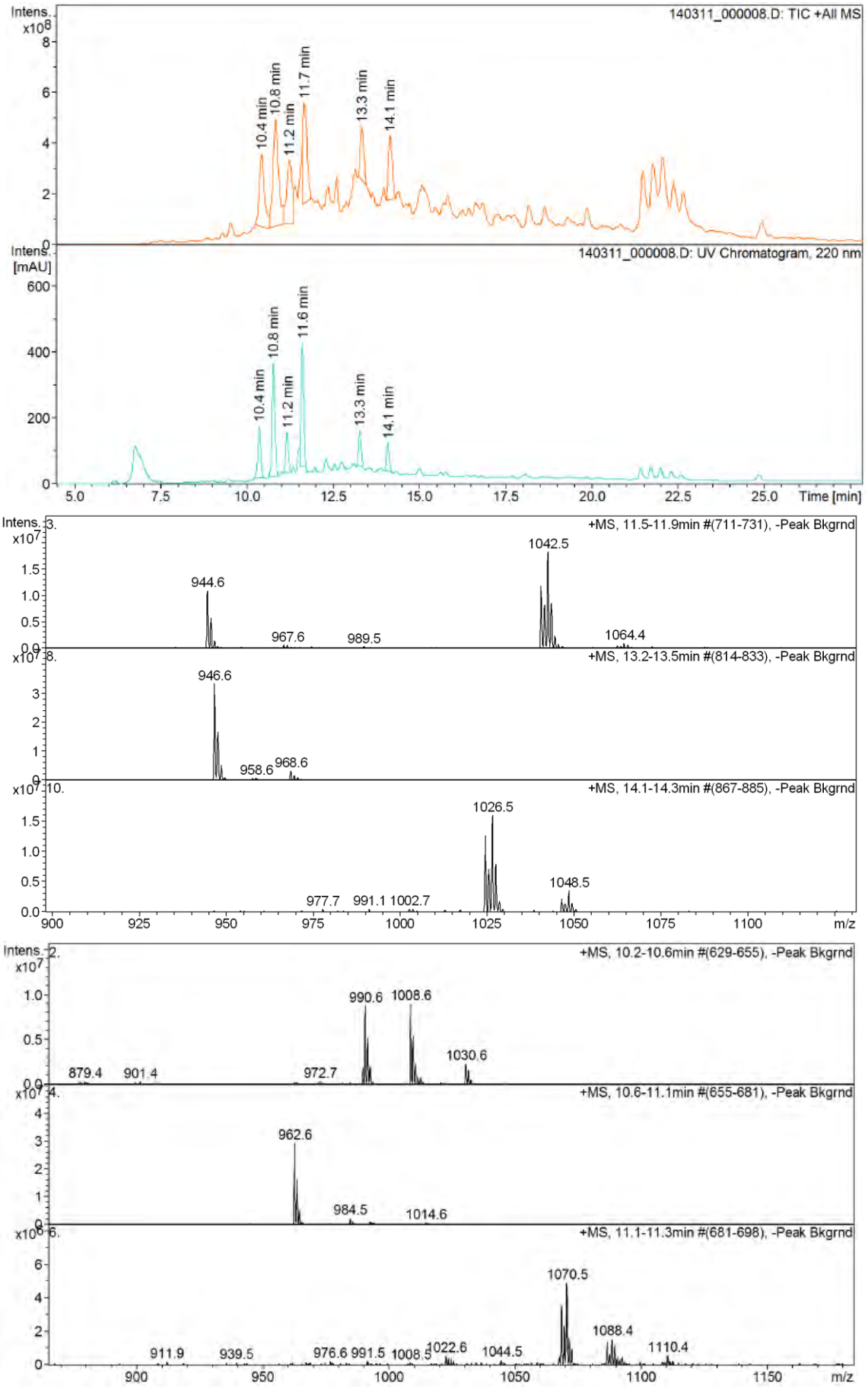
140311_000008.D: TIC +All MS
10.4 min
10.8 min
11.2 min
11.7 min
13.3 min
14.1 min
140311_000008.D: UV Chromatogram, 220 nm
10.4 min
10.8 min
11.2 min
11.6 min
13.3 min
14.1 min
Time [min]
+MS, 11.5-11.9min #(711-731), -Peak Bkgrnd
944.6
967.6
989.5
1042.5
1064.4
+MS, 13.2-13.5min #(814-833), -Peak Bkgrnd
946.6
958.6
968.6
+MS, 14.1-14.3min #(867-885), -Peak Bkgrnd
977.7
991.1
1002.7
1026.5
1048.5
m/z
+MS, 10.2-10.6min #(629-655), -Peak Bkgrnd
879.4
901.4
972.7
990.6
1008.6
1030.6
+MS, 10.6-11.1min #(655-681), -Peak Bkgrnd
962.6
984.5
1014.6
+MS, 11.1-11.3min #(681-698), -Peak Bkgrnd
911.9
939.5
976.6
991.5
1008.5
1022.6
1044.5
1070.5
1088.4
1110.4
m/z

Biaryl cyclic peptide BPC758

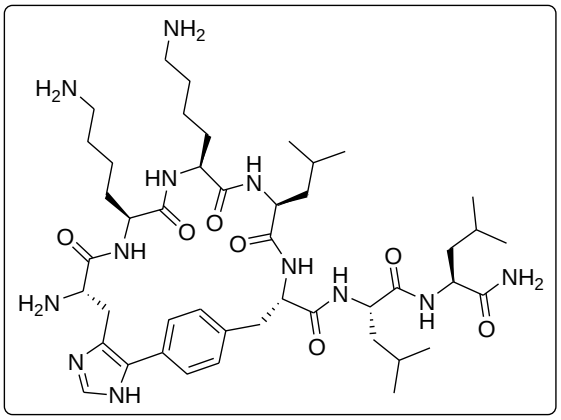

Crude peptide

HPLC (λ = 220 nm)

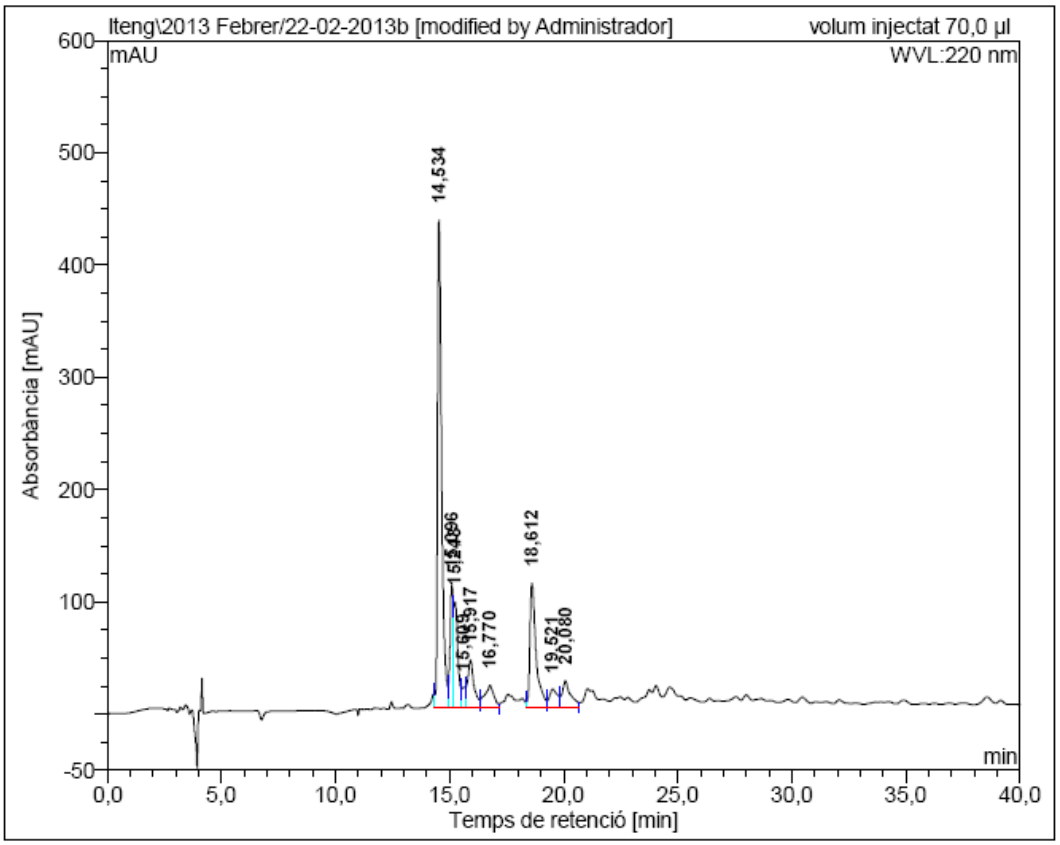

No.	Ret.Time (detected) min	Height mAU	Area mAU*min	Rel.Area %
1	14,53	434,600	91,968	43,87
2	15,10	109,483	18,945	9,04
3	15,24	94,202	18,884	9,01
4	15,61	18,539	3,142	1,50
5	15,92	42,588	14,068	6,71
6	16,77	20,220	9,791	4,67
7	18,61	110,789	35,451	16,91
8	19,52	16,617	7,121	3,40
9	20,08	24,008	10,288	4,91
Total:		871,045	209,659	100,00

ESI-MS *m/z*

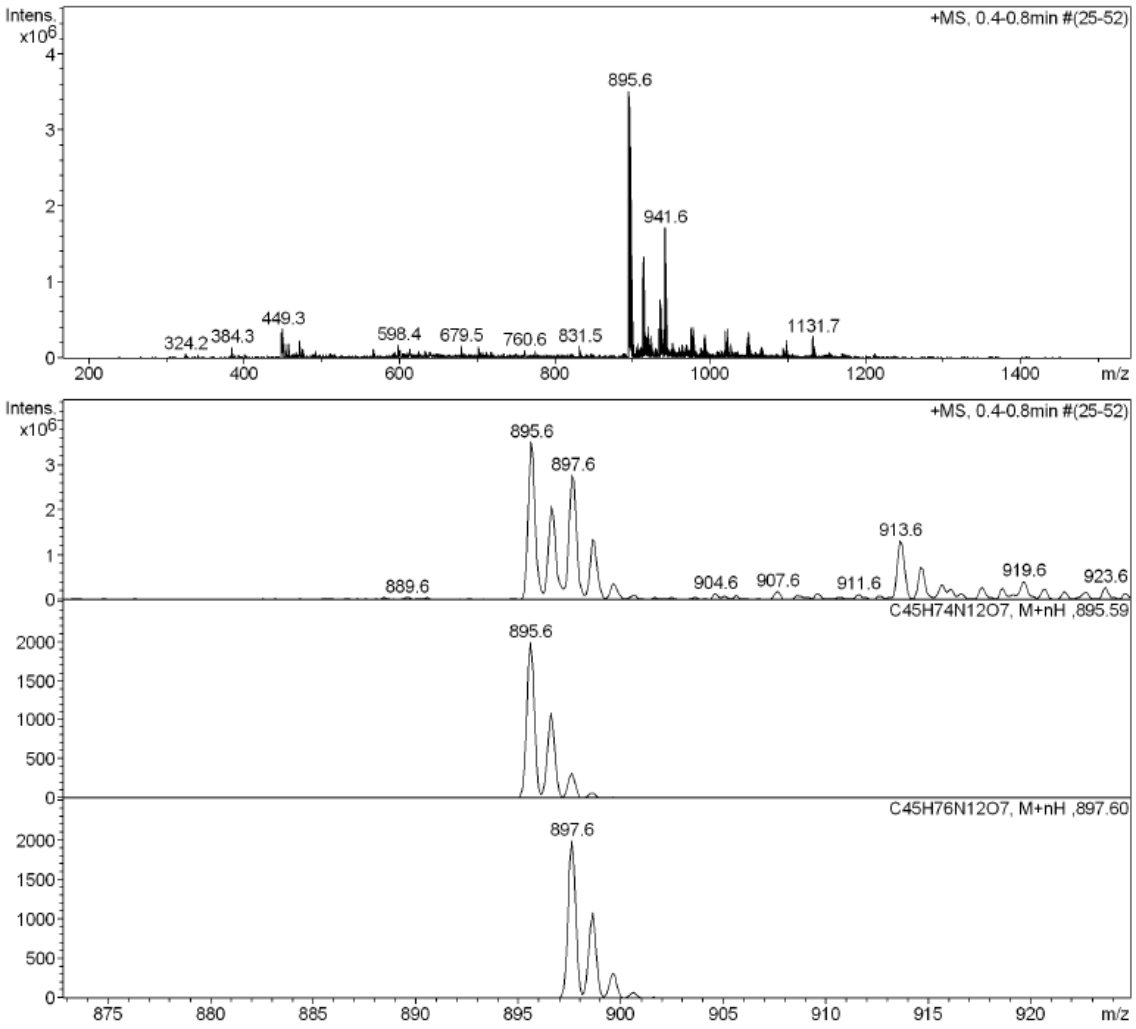
Intens.
x10^6
+MS, 0.4-0.8min #(25-52)
895.6
941.6
449.3
324.2
384.3
598.4
679.5
760.6
831.5
1131.7
m/z
889.6
897.6
904.6
907.6
911.6
913.6
919.6
923.6
C45H74N12O7, M+nH ,895.59
C45H76N12O7, M+nH ,897.60

Purified peptide

HPLC (λ = 220 nm)

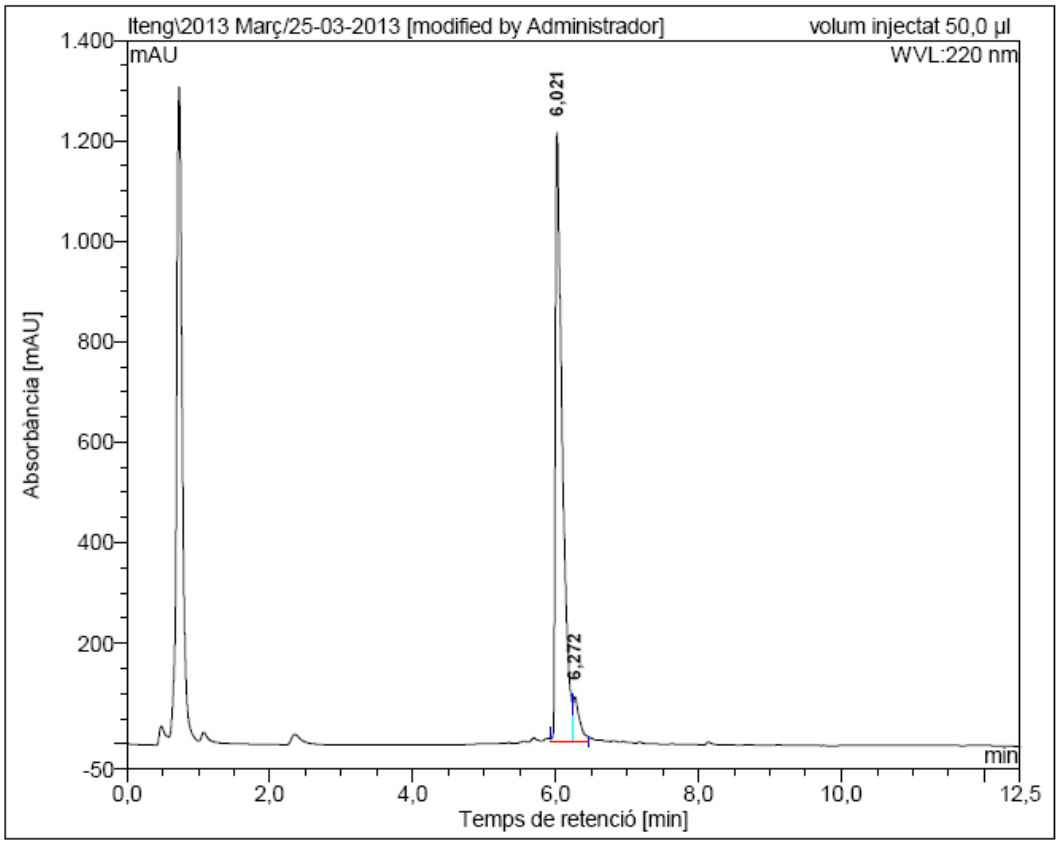

No.	Ret.Time (detected) min	Height mAU	Area mAU*min	Rel.Area %
1	6,02	1212,412	135,755	93,45
2	6,27	90,649	9,510	6,55
Total:		1303,060	145,265	100,00

ESI-MS *m/z*

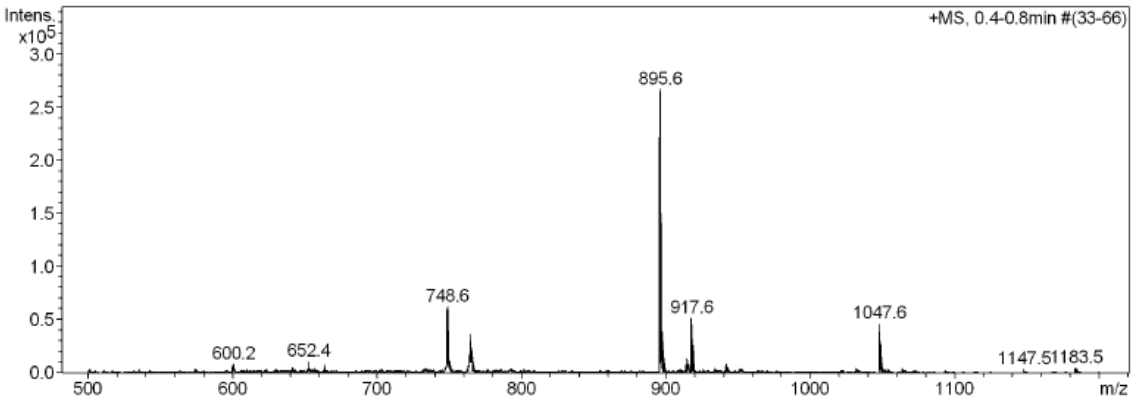

HRMS (ESI) *m/z*

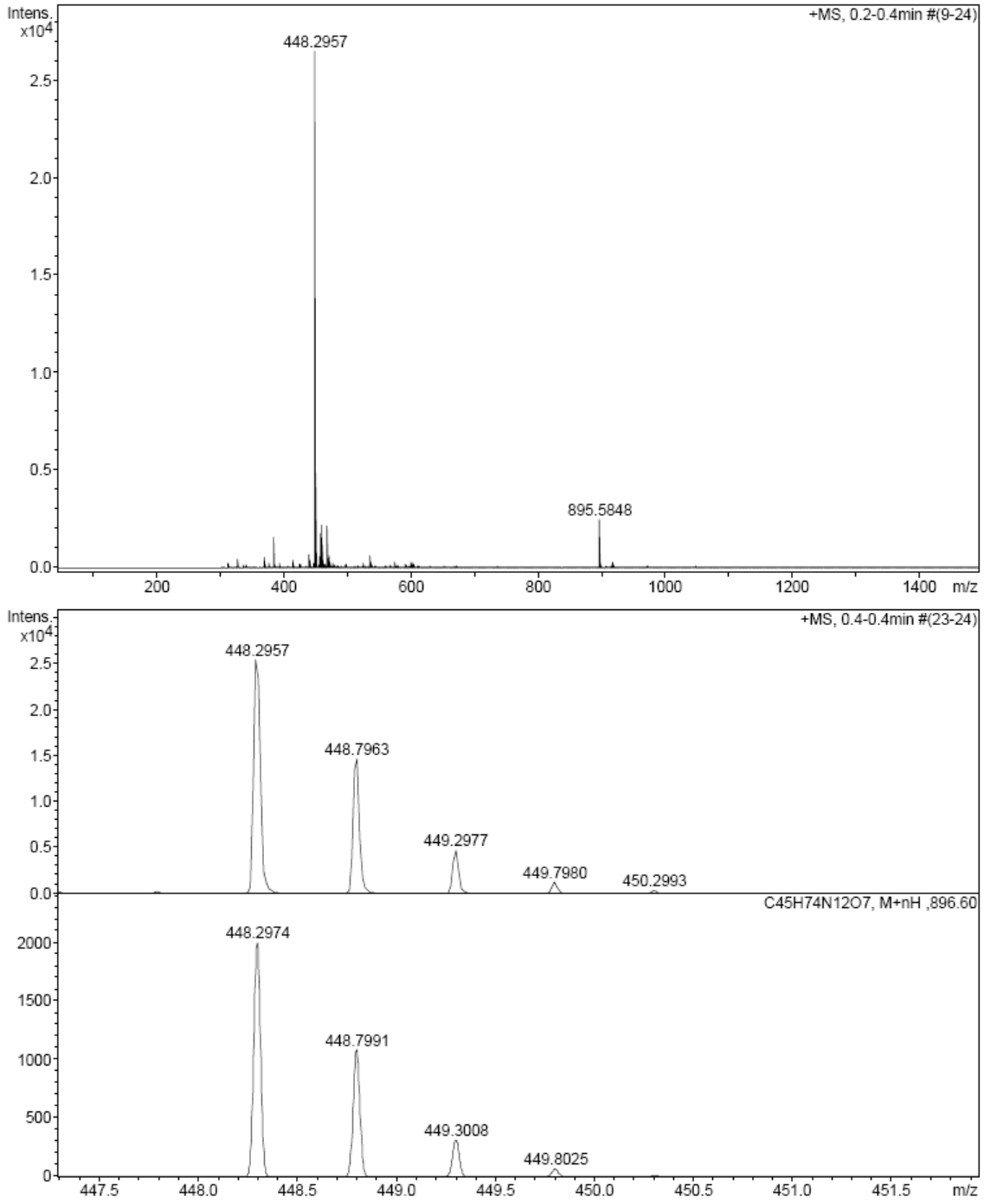
Intens.
x10^4
+MS, 0.2-0.4min #(9-24)
448.2957
895.5848
m/z
+MS, 0.4-0.4min #(23-24)
448.2957
448.7963
449.2977
449.7980
450.2993
C45H74N12O7, M+nH ,896.60
448.2974
448.7991
449.3008
449.8025

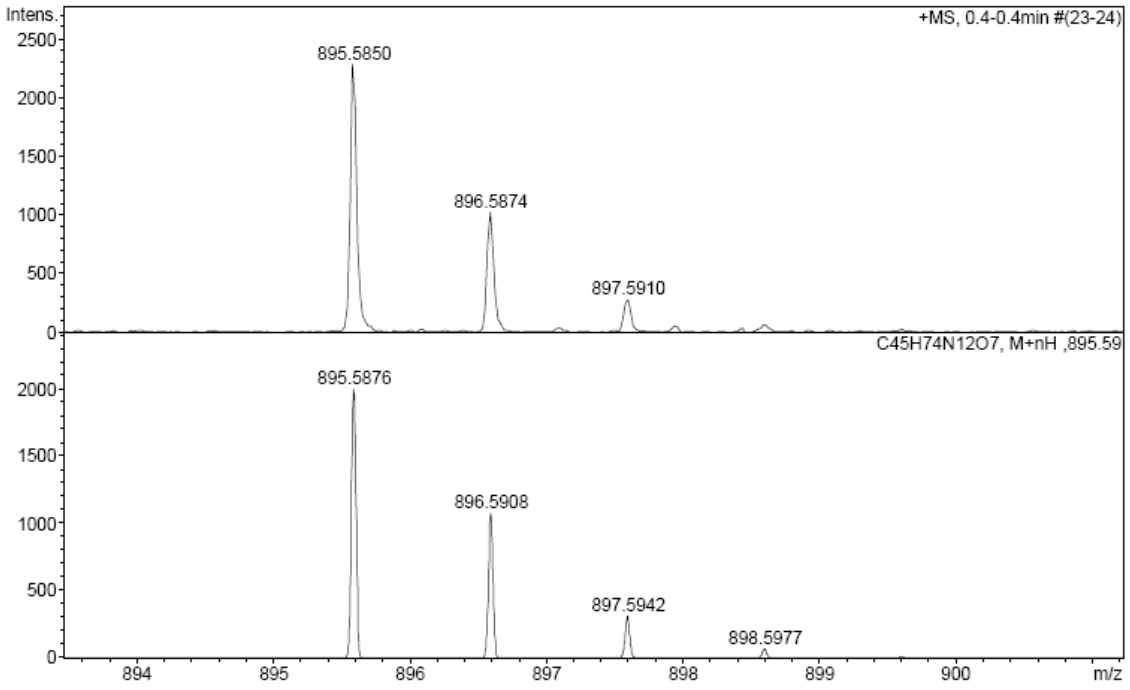
Intens.
+MS, 0.4-0.4min #(23-24)
2500
2000
1500
1000
500
0
895.5850
896.5874
897.5910
C45H74N12O7, M+nH ,895.59
895.5876
896.5908
897.5942
898.5977
894
895
896
897
898
899
900
m/z

Biaryl cyclic peptide BPC760

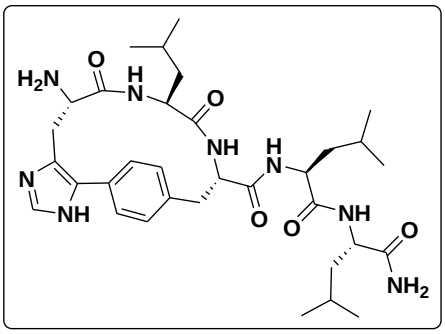

Crude peptide

HPLC (λ = 220 nm)

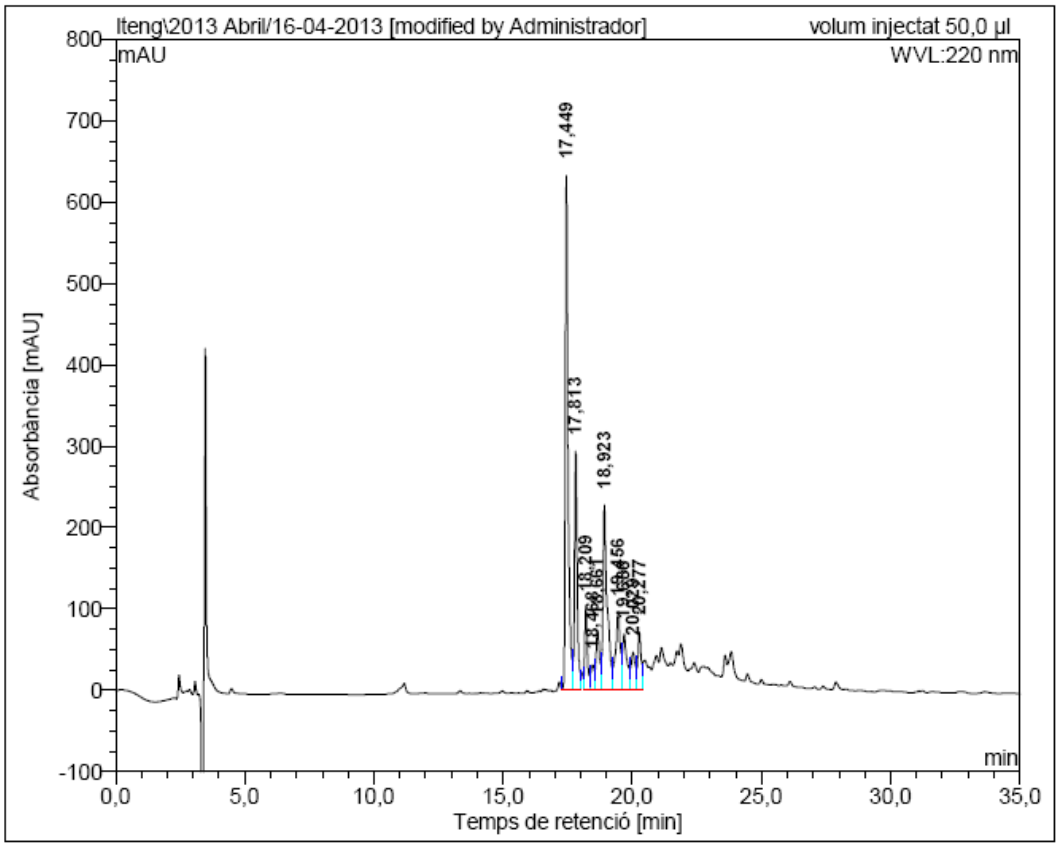

No.	Ret.Time (detected) min	Height mAU	Area mAU*min	Rel.Area %
1	17,45	633,138	80,596	33,02
2	17,81	294,027	35,351	14,48
3	18,21	100,846	11,903	4,88
4	18,47	31,369	5,399	2,21
5	18,66	72,766	11,378	4,66
6	18,92	227,598	44,586	18,26
7	19,46	96,788	20,694	8,48
8	19,69	69,308	14,226	5,83
9	20,03	46,705	8,722	3,57
10	20,28	71,151	11,257	4,61
Total:		1643,697	244,111	100,00

ESI-MS *m/z*

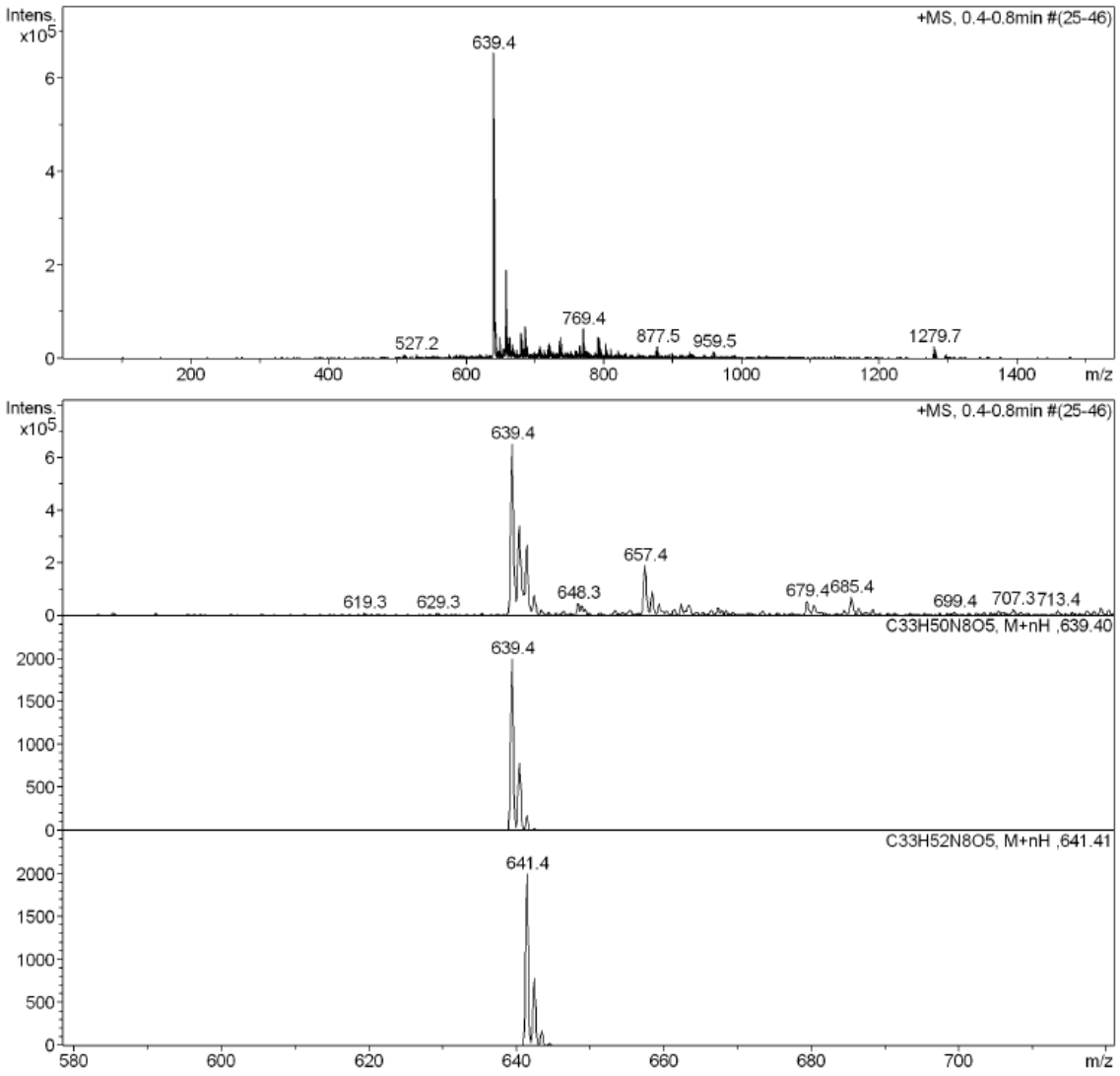
Intens.
x10^5
+MS, 0.4-0.8min #(25-46)
639.4
769.4
527.2
877.5
959.5
1279.7
m/z
619.3
629.3
648.3
657.4
679.4
685.4
699.4
707.3
713.4
C33H50N8O5, M+nH ,639.40
C33H52N8O5, M+nH ,641.41
641.4

Purified peptide

HPLC (λ = 220 nm)

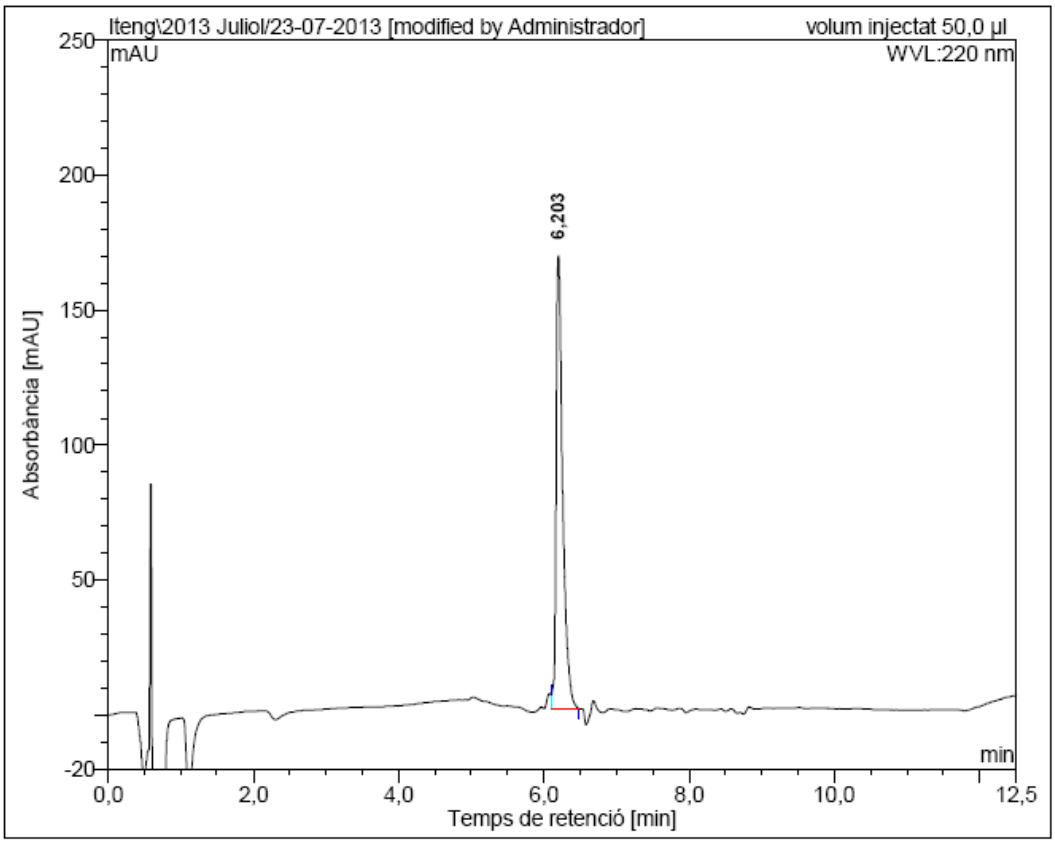

No.	Temps retenció min	alçada mAU	Area mAU*min	Area relativa %
1	6,20	167,614	17,599	100,00
Total:		167,614	17,599	100,00

ESI-MS *m/z*

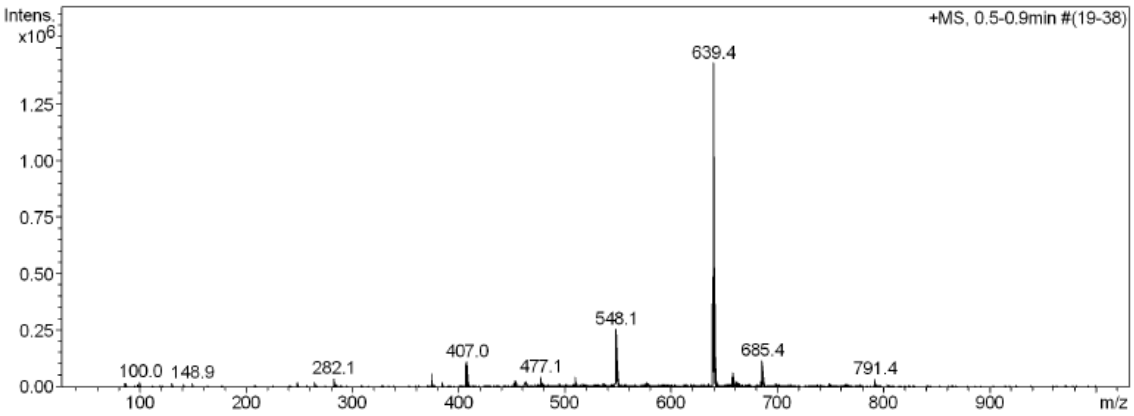

HRMS (ESI) *m/z*

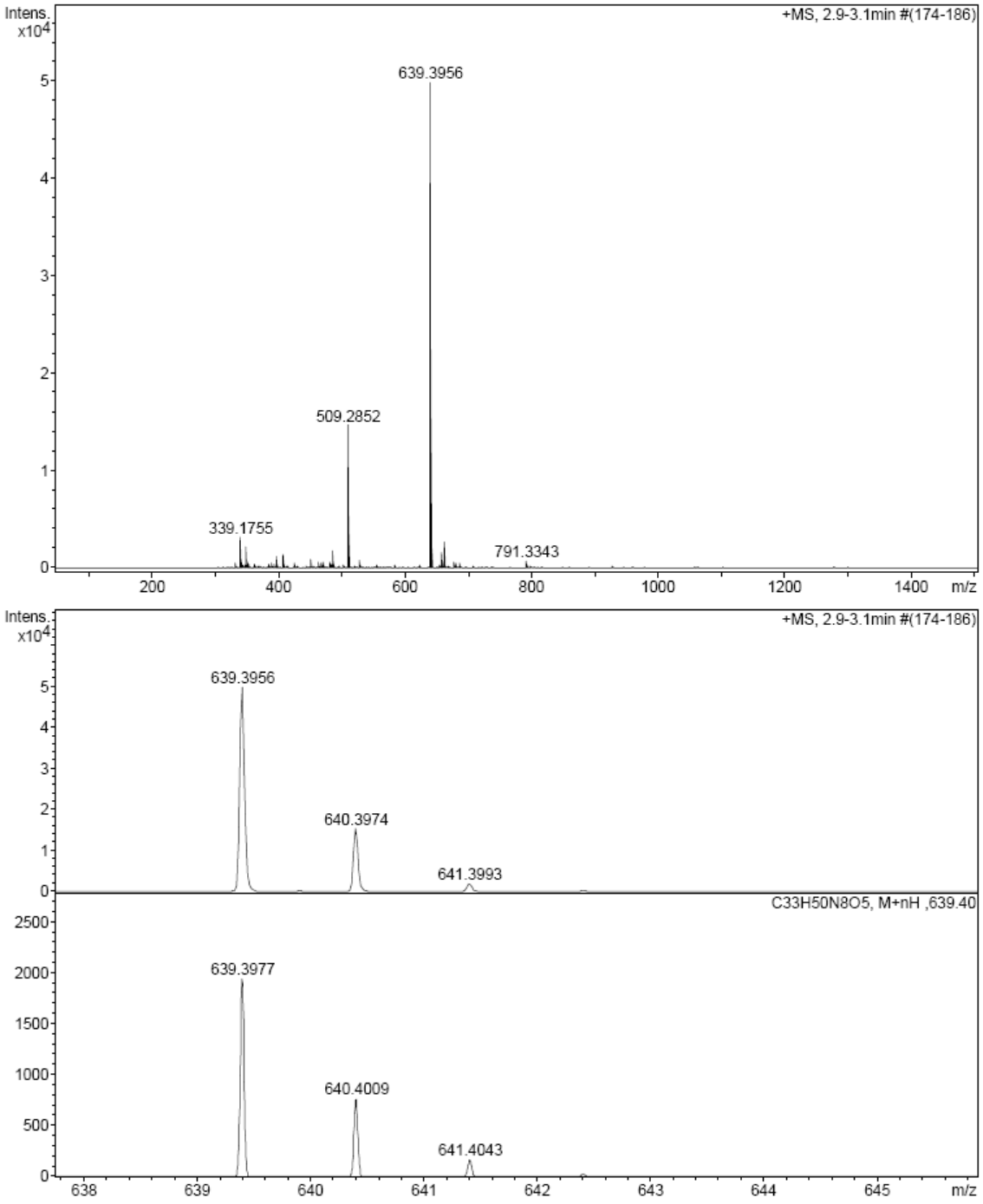
Intens.
x10^4
+MS, 2.9-3.1min #(174-186)
639.3956
509.2852
339.1755
791.3343
m/z
C33H50N8O5, M+nH ,639.40
639.3977
640.4009
641.4043
640.3974
641.3993

Biaryl cyclic peptide

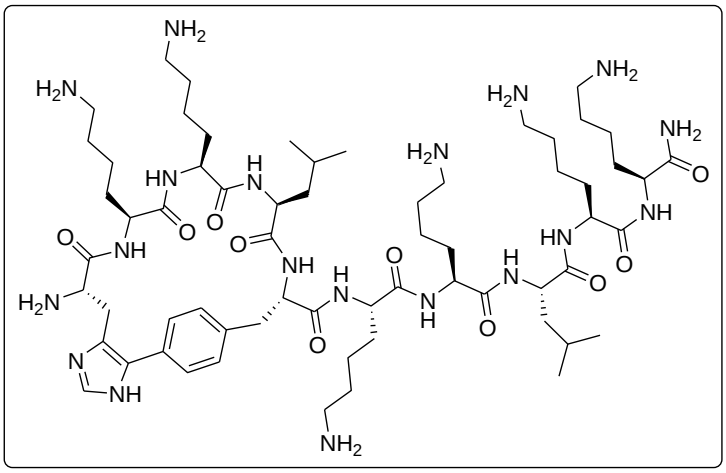

Crude peptide

HPLC-MS

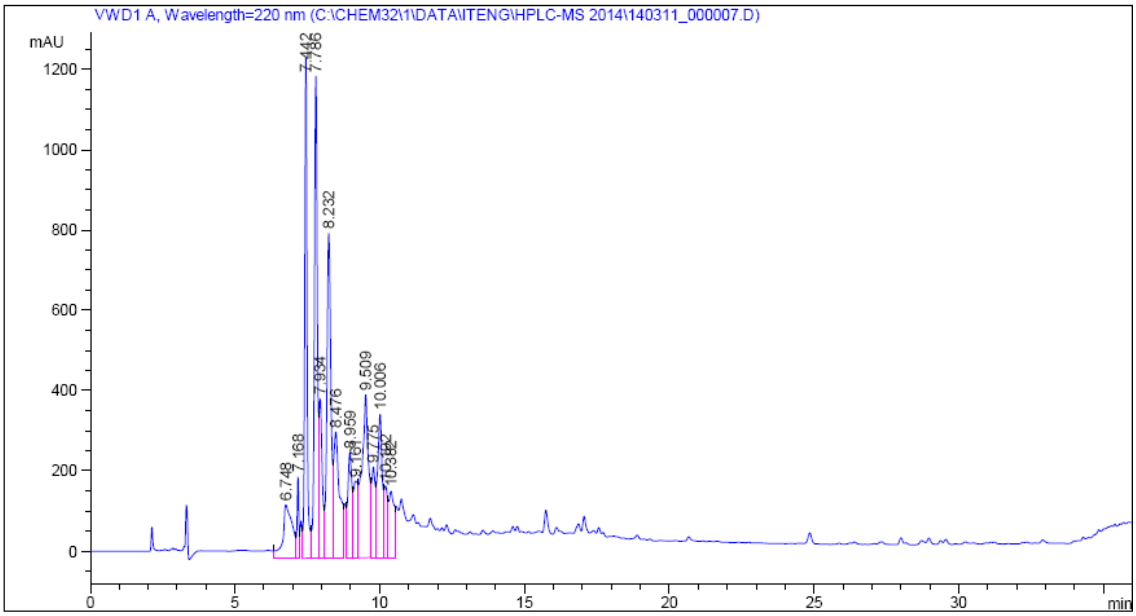

Peak #	RetTime [min]	Type	Width [min]	Area mAU *s	Height [mAU]	Area %
1	6.748	VV	0.2960	3093.33081	134.50415	5.4689
2	7.168	VV	0.0617	848.69824	203.63239	1.5005
3	7.442	VV	0.0848	7050.54102	1247.95276	12.4651
4	7.786	VV	0.1085	8630.72852	1202.50708	15.2588
5	7.934	VV	0.1153	3133.33008	397.27182	5.5396
6	8.232	VV	0.1474	7908.92432	810.08838	13.9826
7	8.476	VV	0.2014	4521.06348	314.12454	7.9930
8	8.959	VV	0.1476	2731.50439	262.48453	4.8292
9	9.161	VV	0.1607	2039.62585	191.51099	3.6060
10	9.509	VV	0.2164	6786.29004	406.93433	11.9979
11	9.775	VV	0.1217	1961.92700	225.94171	3.4686
12	10.006	VV	0.1636	4166.88965	357.56644	7.3669
13	10.192	VV	0.1277	1626.58411	179.30522	2.8757
14	10.382	VV	0.1686	2063.01465	165.59039	3.6473

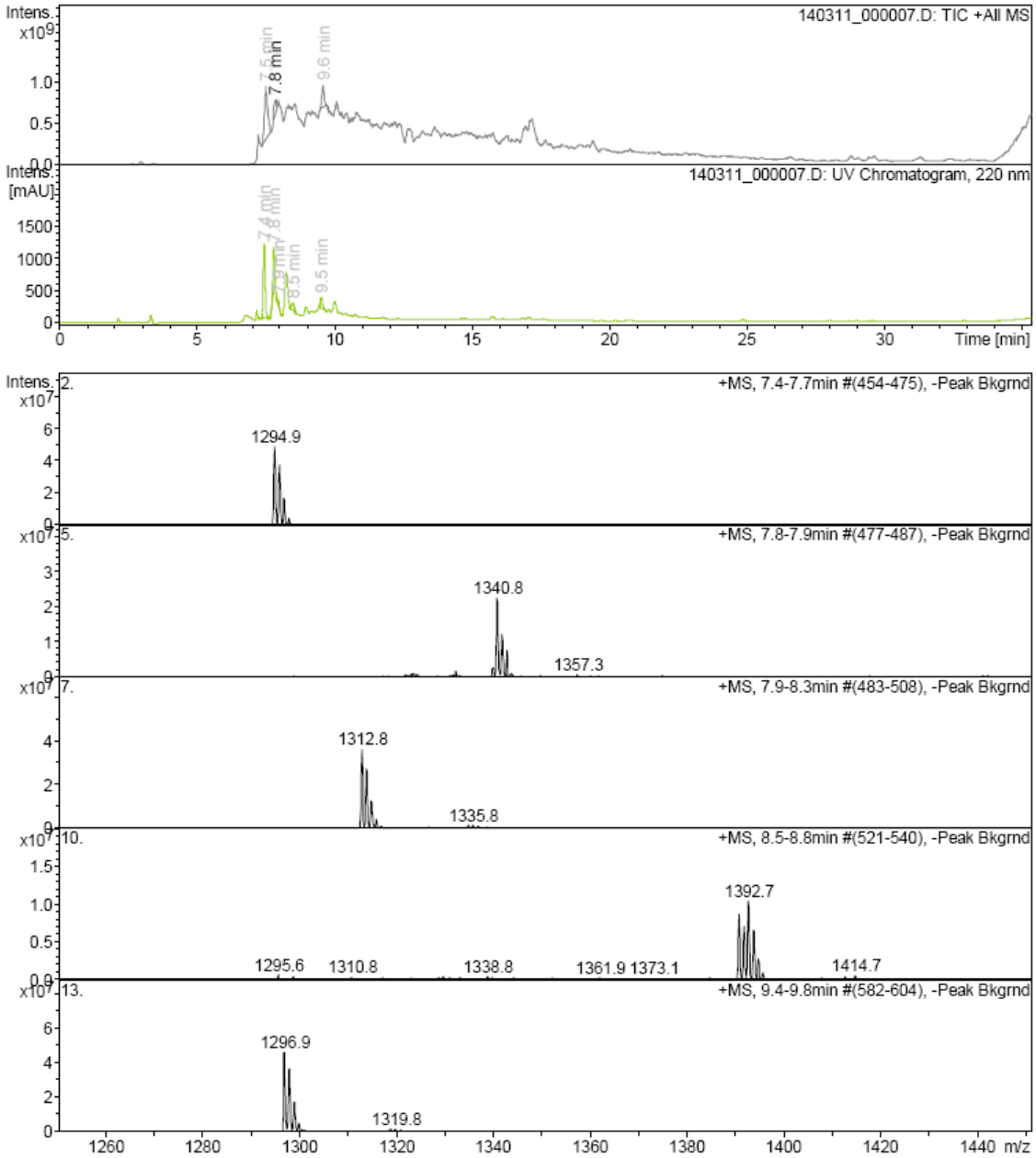
Intens.
x10^9
140311_000007.D: TIC +All MS
7.8 min
9.6 min
Intens.
[mAU]
140311_000007.D: UV Chromatogram, 220 nm
9.5 min
Time [min]
Intens.
2.
+MS, 7.4-7.7min #(454-475), -Peak Bkgrnd
1294.9
5.
+MS, 7.8-7.9min #(477-487), -Peak Bkgrnd
1340.8
1357.3
7.
+MS, 7.9-8.3min #(483-508), -Peak Bkgrnd
1312.8
1335.8
10.
+MS, 8.5-8.8min #(521-540), -Peak Bkgrnd
1392.7
1295.6
1310.8
1338.8
1361.9 1373.1
1414.7
13.
+MS, 9.4-9.8min #(582-604), -Peak Bkgrnd
1296.9
1319.8
m/z

Biaryl cyclic peptide BPC768

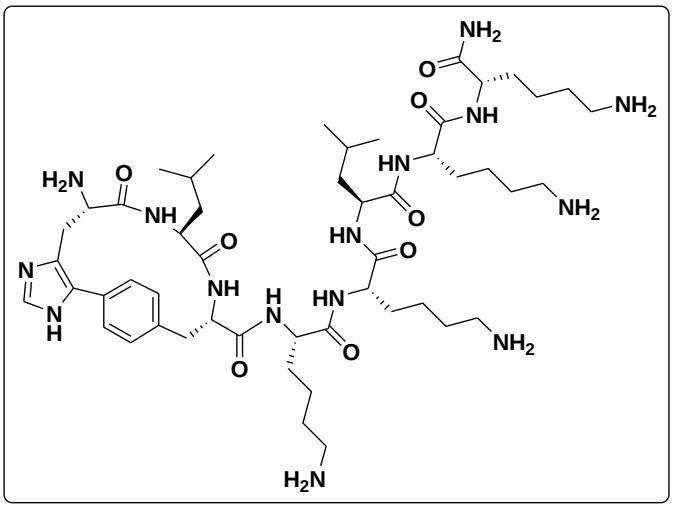

Crude peptide

HPLC (λ = 220 nm)

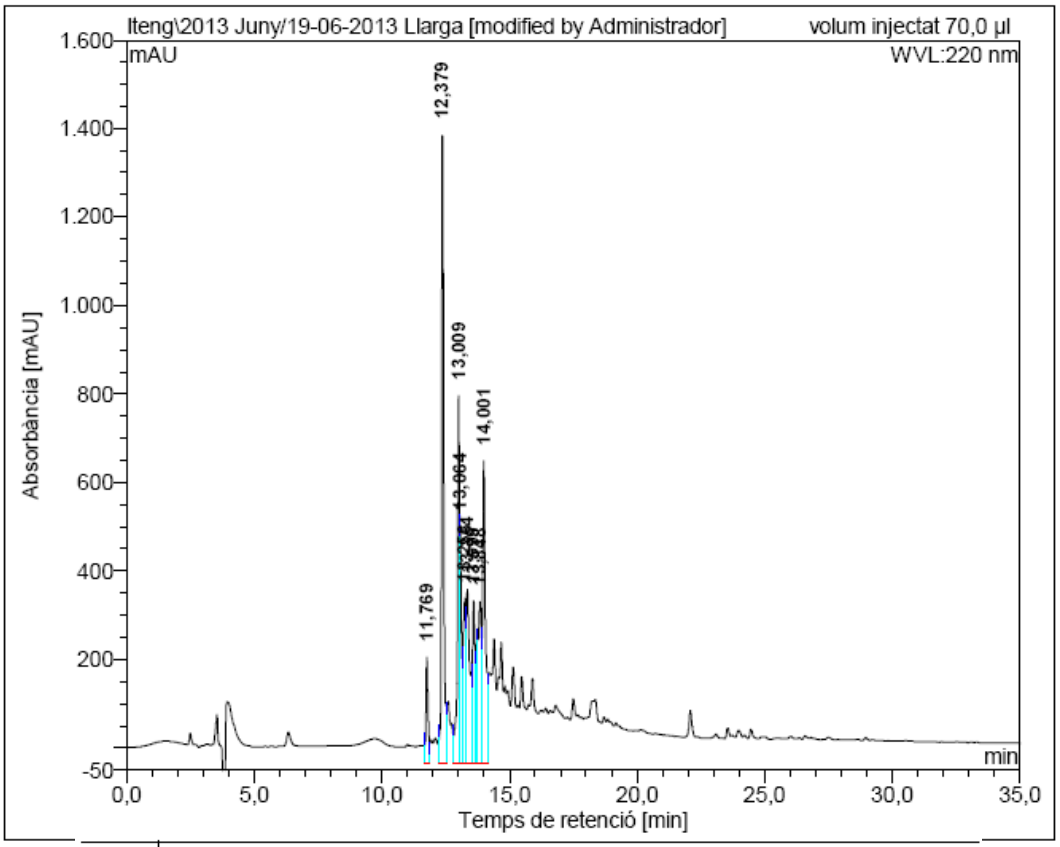

No.	Ret.Time (detected) min	Height mAU	Area mAU*min	Rel.Area %
1	11,77	238,763	23,895	4,19
2	12,38	1418,100	136,606	23,93
3	13,01	830,041	81,479	14,27
4	13,06	535,019	35,108	6,15
5	13,26	373,101	47,587	8,34
6	13,35	392,087	60,658	10,62
7	13,60	368,172	47,257	8,28
8	13,85	365,540	48,124	8,43
9	14,00	684,085	90,182	15,80
Total:		5204,908	570,896	100,00

ESI-MS *m/z*

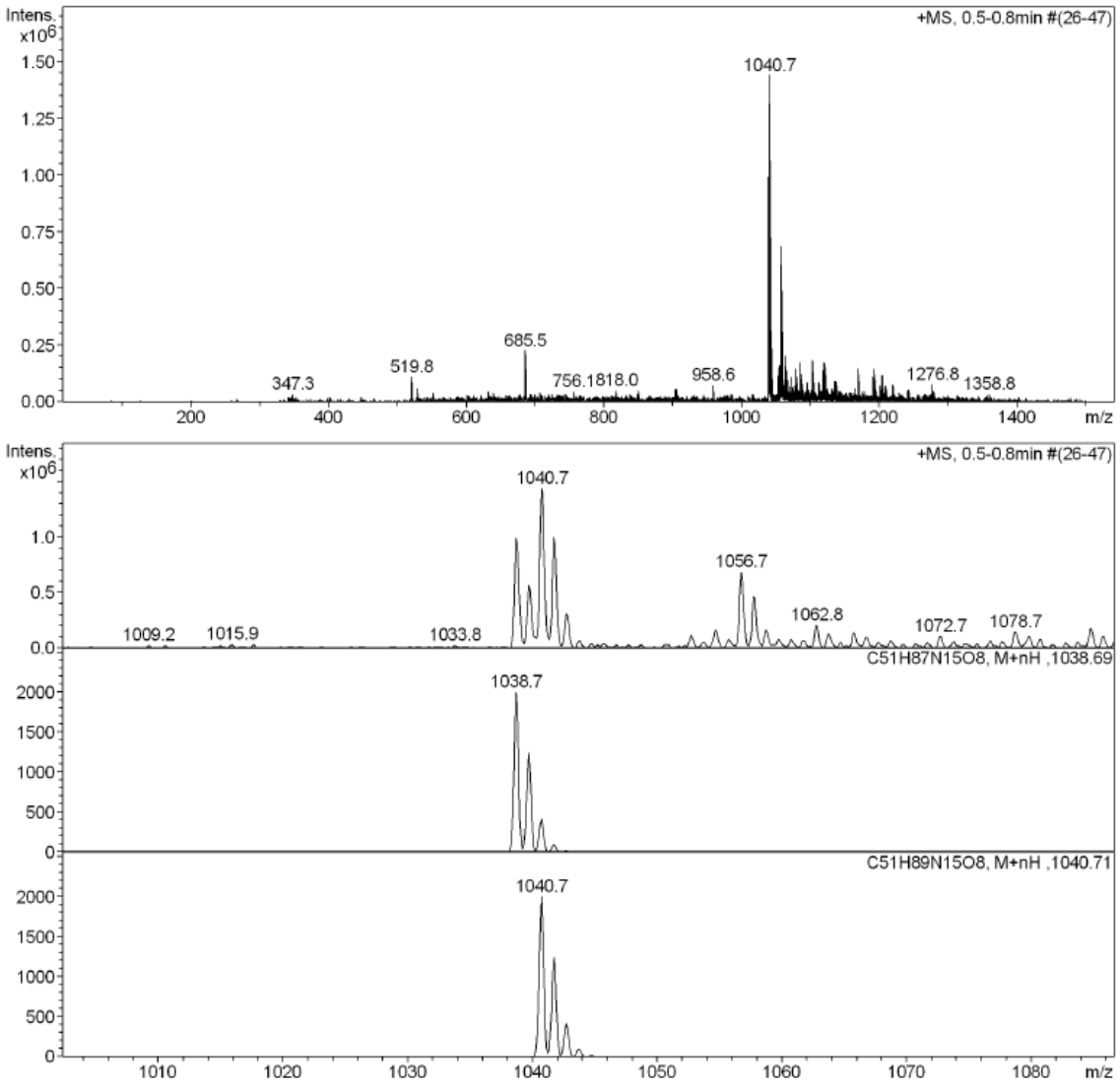
Intens.
x10^6
+MS, 0.5-0.8min #(26-47)
1040.7
685.5
519.8
347.3
756.1818.0
958.6
1276.8
1358.8
m/z
1040.7
1056.7
1062.8
1072.7
1078.7
1009.2
1015.9
1033.8
C51H87N15O8, M+nH ,1038.69
1038.7
C51H89N15O8, M+nH ,1040.71
1040.7

Biaryl cyclic peptide BPC772a-b

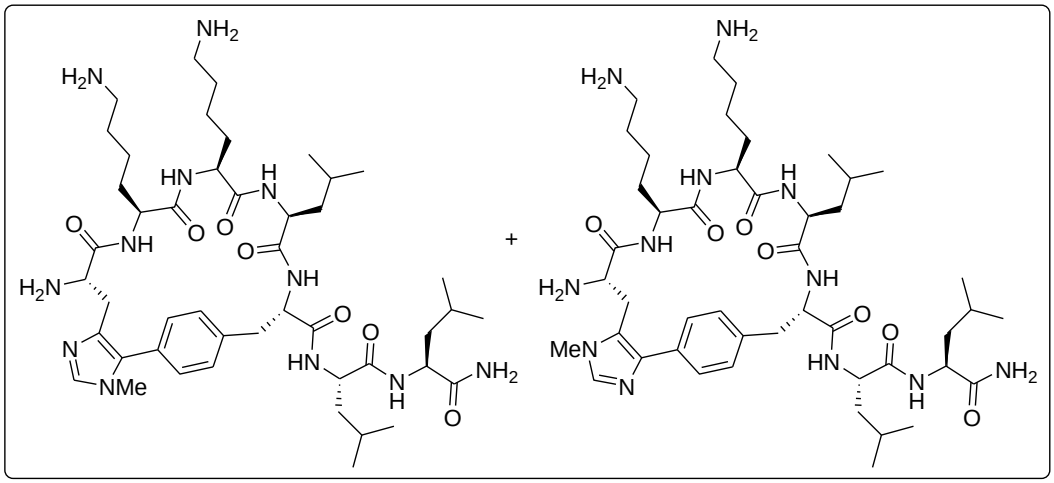

Crude peptide

HPLC (λ = 220 nm)

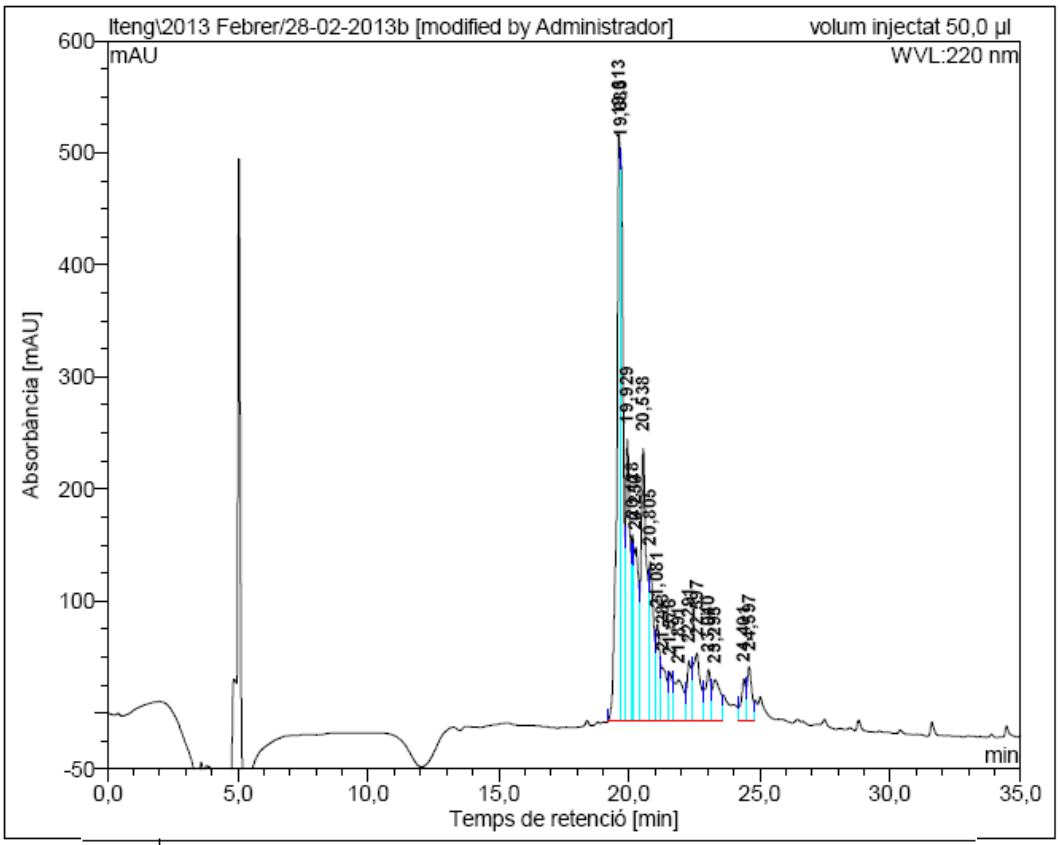

No.	Ret.Time (detected) min	Height mAU	Area mAU*min	Rel.Area %
1	19,61	524,461	77,476	17,54
2	19,68	505,230	63,229	14,31
3	19,93	250,555	45,699	10,35
4	20,13	165,303	19,955	4,52
5	20,25	154,200	29,820	6,75
6	20,54	242,520	57,657	13,05
7	20,81	141,170	28,109	6,36
8	21,08	85,778	16,253	3,68
9	21,28	46,905	10,587	2,40
10	21,58	43,140	8,213	1,86
11	21,89	36,066	14,522	3,29
12	22,29	53,048	10,183	2,31
13	22,60	59,819	19,809	4,48
14	23,04	45,563	11,924	2,70
15	23,29	36,051	11,324	2,56
16	24,40	37,100	6,924	1,57
17	24,60	47,585	10,025	2,27
Total:		2474,496	441,709	100,00

ESI-MS *m/z*

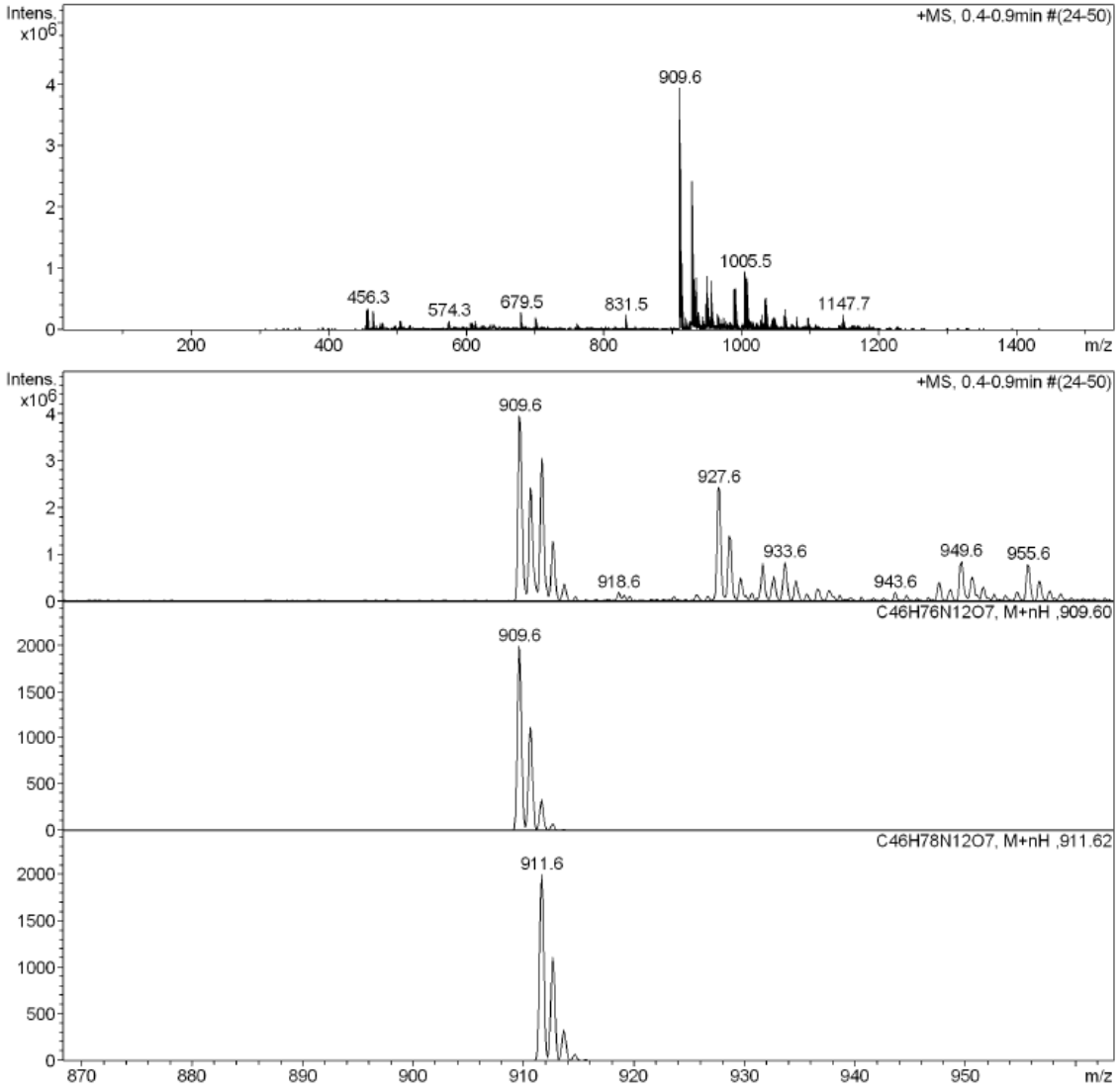
Intens.
x10^6
+MS, 0.4-0.9min #(24-50)
909.6
1005.5
456.3
574.3
679.5
831.5
1147.7
m/z
927.6
933.6
949.6
955.6
918.6
943.6
C46H76N12O7, M+nH ,909.60
C46H78N12O7, M+nH ,911.62
911.6

Purified peptide

HPLC (λ = 220 nm)

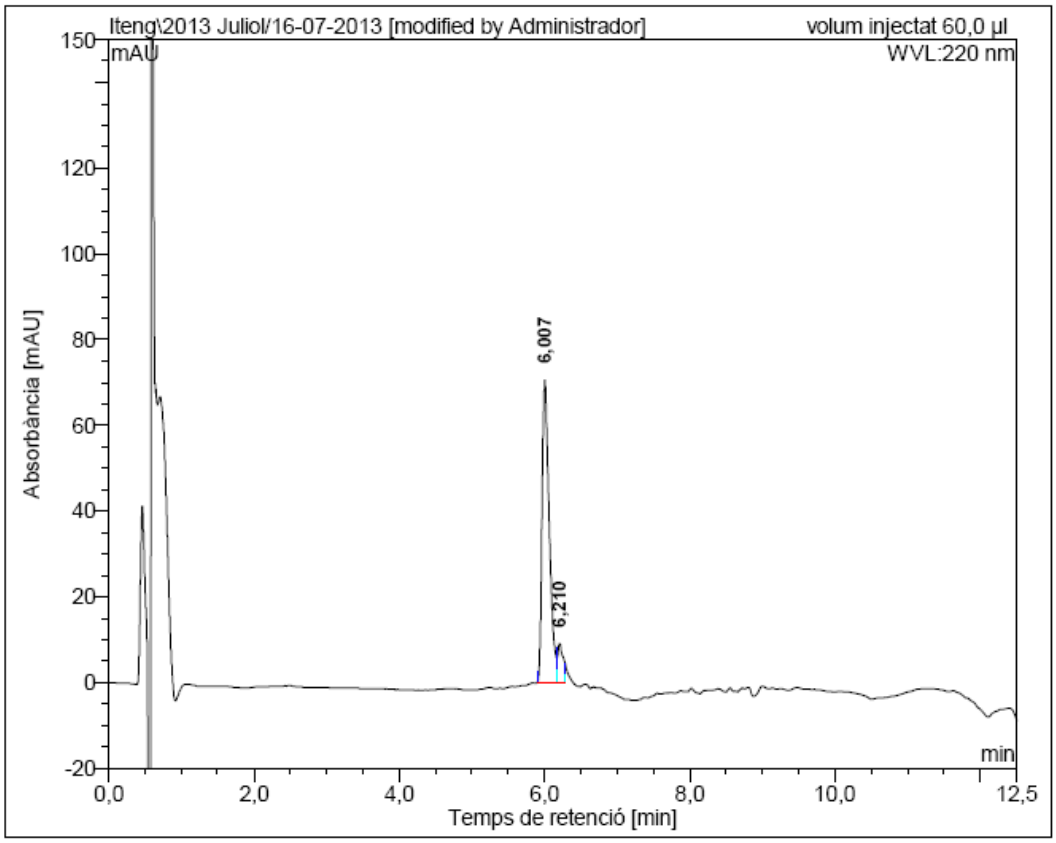

No.	Temps retenció min	alçada mAU	Area mAU*min	Area relativa %
1	6,01	70,521	8,107	90,97
2	6,21	9,096	0,805	9,03
Total:		79,617	8,912	100,00

ESI-MS *m/z*

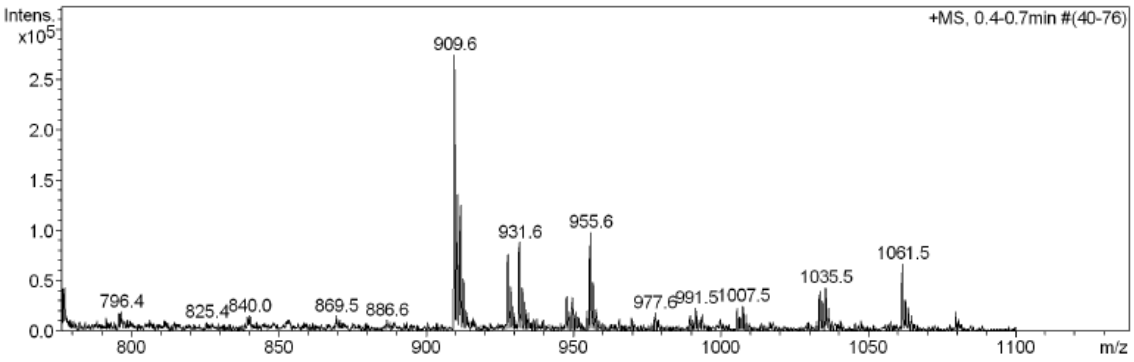

HRMS (ESI) *m/z*

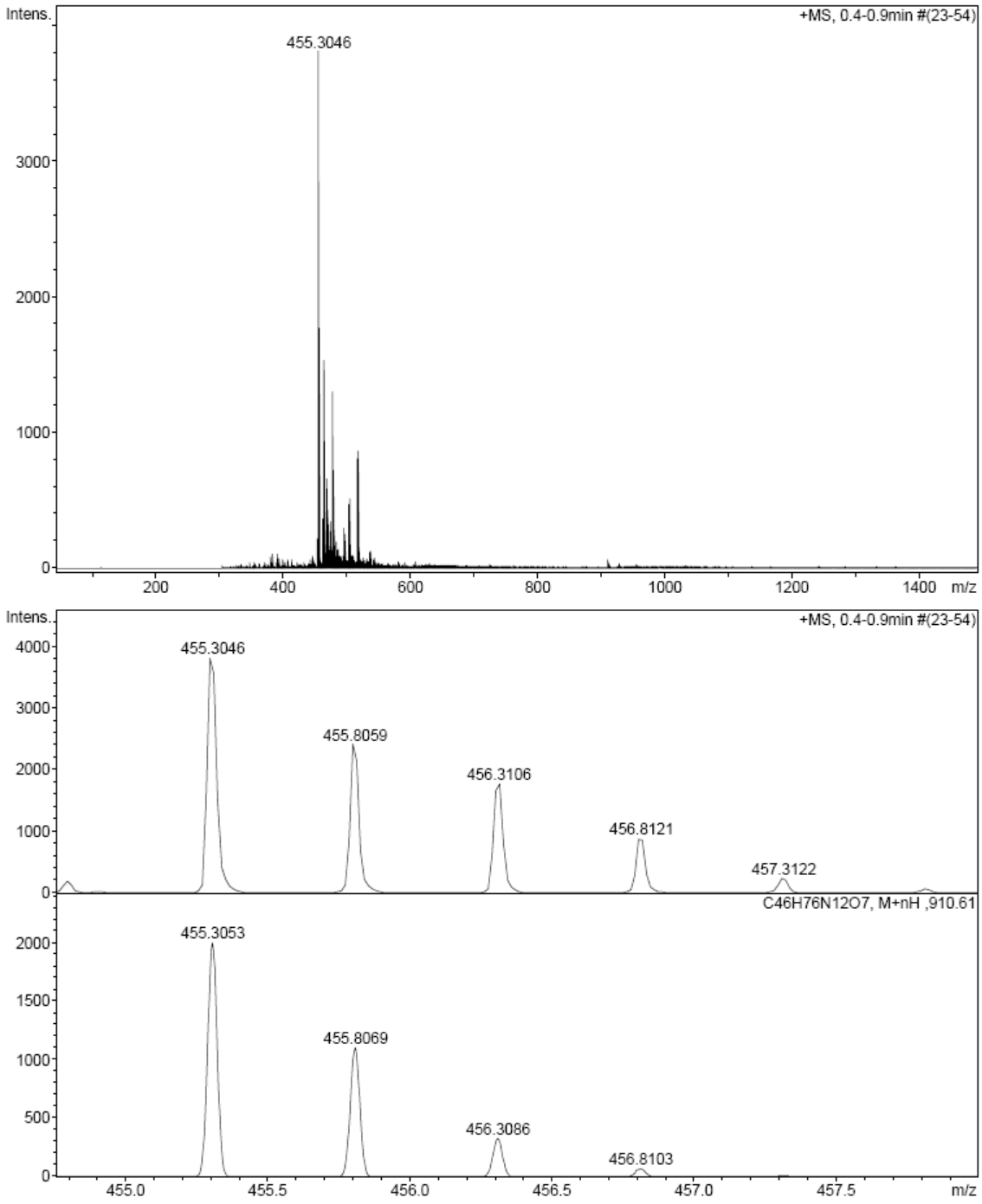
Intens.
+MS, 0.4-0.9min #(23-54)
455.3046
3000
2000
1000
0
200
400
600
800
1000
1200
1400
m/z
Intens.
+MS, 0.4-0.9min #(23-54)
4000
3000
2000
1000
0
455.3046
455.8059
456.3106
456.8121
457.3122
C46H76N12O7, M+nH ,910.61
2000
1500
1000
500
0
455.3053
455.8069
456.3086
456.8103
455.0
455.5
456.0
456.5
457.0
457.5
m/z

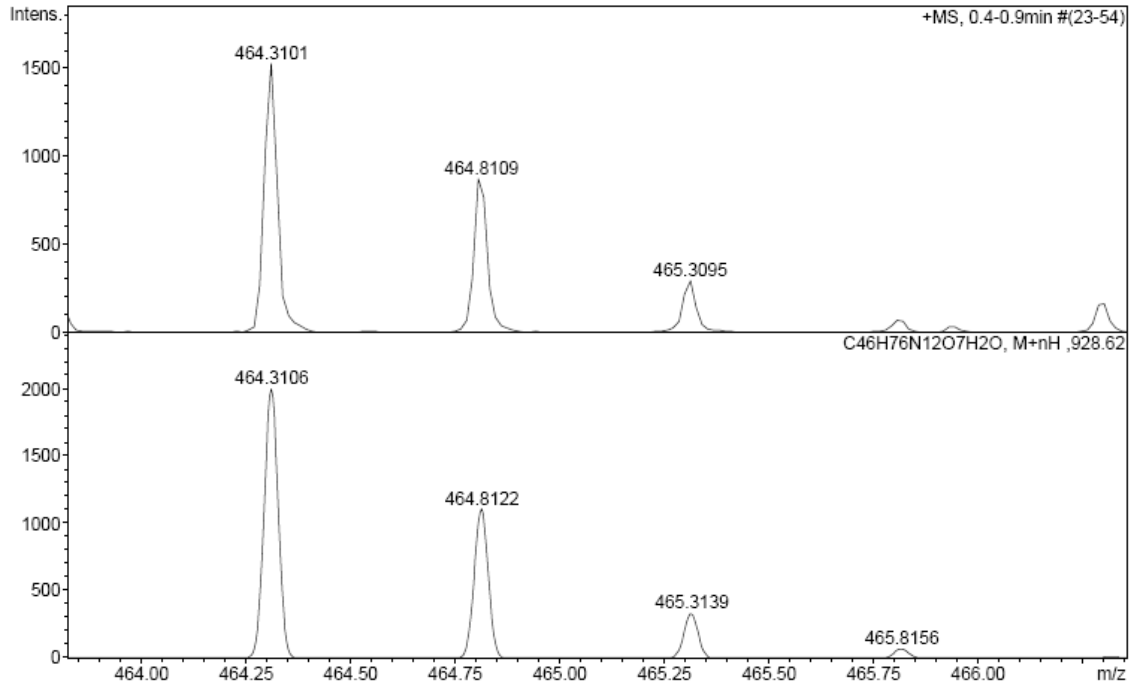
Intens.
+MS, 0.4-0.9min #(23-54)
464.3101
464.8109
465.3095
C46H76N12O7H2O, M+nH ,928.62
464.3106
464.8122
465.3139
465.8156
m/z

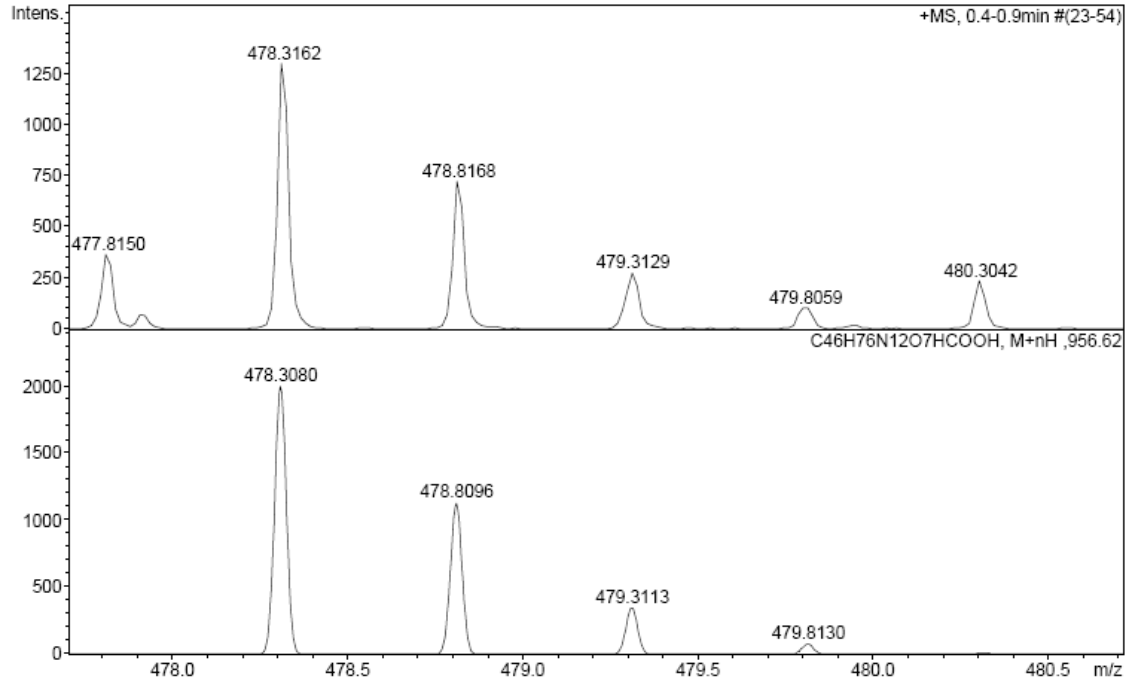
Intens.
+MS, 0.4-0.9min #(23-54)
478.3162
478.8168
477.8150
479.3129
479.8059
480.3042
C46H76N12O7HCOOH, M+nH ,956.62
478.3080
478.8096
479.3113
479.8130
m/z

Biaryl cyclic peptide BPC776

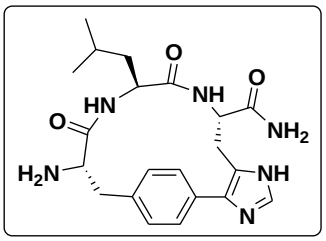

Crude peptide

HPLC-MS

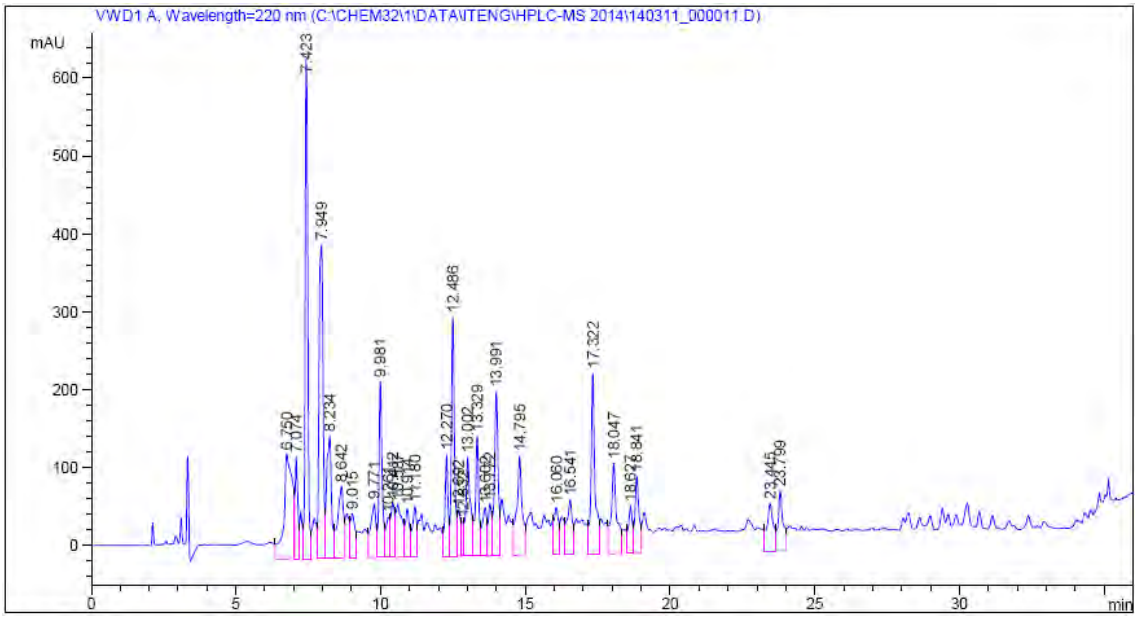

Peak #	RetTime [min]	Type	Width [min]	Area mAU *s	Height [mAU]	Area %
1	6.750	VV	0.2713	2828.60107	134.62878	6.7463
2	7.074	VV	0.0841	833.35919	131.46922	1.9876
3	7.423	VV	0.1010	4117.70166	642.55029	9.8208
4	7.949	VV	0.1333	3901.68726	403.00427	9.3056
5	8.234	VV	0.1559	1827.96033	157.37077	4.3597
6	8.642	VV	0.1924	1362.23376	92.39401	3.2490
7	9.015	VV	0.1598	653.28125	57.05331	1.5581
8	9.771	VV	0.1688	878.62640	69.05244	2.0955
9	9.981	VV	0.1128	1767.62805	226.60815	4.2158
10	10.261	VV	0.1208	440.09689	51.88609	1.0496
11	10.412	VV	0.1400	698.64526	69.82861	1.6663
12	10.587	VV	0.1986	1039.70911	68.05606	2.4797
13	10.914	VV	0.1433	646.02167	62.02747	1.5408
14	11.180	VV	0.1367	634.71820	65.32581	1.5138
15	12.270	VV	0.1101	986.98505	130.45277	2.3540
16	12.486	VV	0.1108	2311.62524	308.22406	5.5133
17	12.692	VV	0.1162	486.13641	59.17364	1.1594
18	12.832	VV	0.0691	211.99649	44.13979	0.5056
19	13.002	VV	0.1557	1441.38025	127.01097	3.4377
20	13.329	VV	0.1187	1283.17358	154.55151	3.0604
21	13.602	VV	0.1531	670.10645	62.32004	1.5982
22	13.772	VV	0.1172	547.55017	67.02190	1.3059
23	13.991	VV	0.1273	1854.02173	210.98880	4.4219
24	14.795	VV	0.1758	1670.21570	127.80444	3.9835
25	16.060	VV	0.1434	621.88965	61.12788	1.4832
26	16.541	VV	0.1724	898.69904	70.32449	2.1434
27	17.322	VV	0.1386	2272.34863	232.85262	5.4196
28	18.047	VV	0.1861	1595.75232	116.40776	3.8059
29	18.627	VV	0.1430	615.28558	60.72224	1.4675
30	18.841	VV	0.1412	988.53967	99.07055	2.3577
31	23.445	VV	0.2057	920.98322	61.34428	2.1966
32	23.799	VV	0.1638	921.35706	77.28230	2.1975

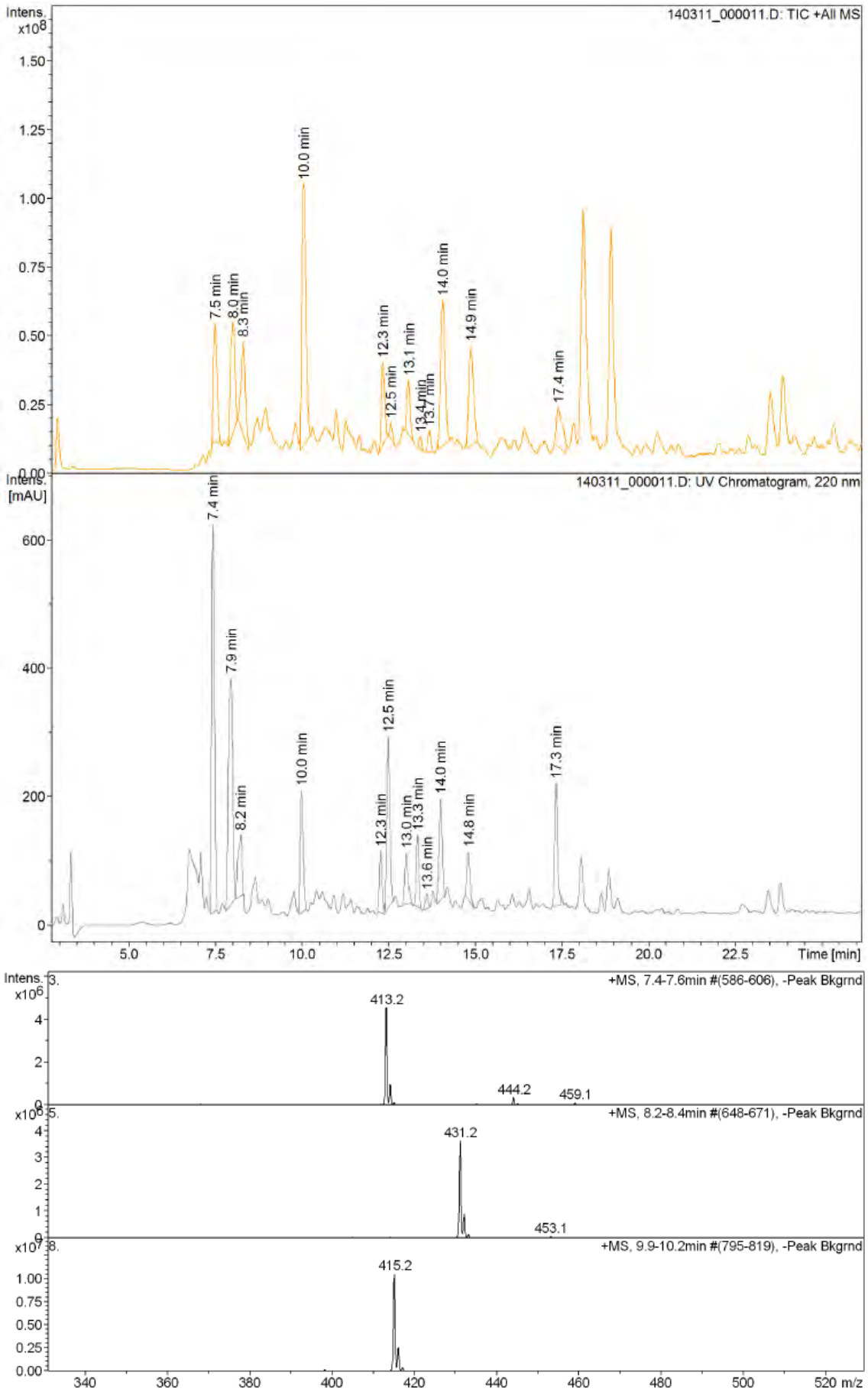
Intens.
x10^8
140311_000011.D: TIC +All MS
7.5 min
8.0 min
8.3 min
10.0 min
12.3 min
12.5 min
13.1 min
13.4 min
13.7 min
14.0 min
14.9 min
17.4 min
Intens.
[mAU]
140311_000011.D: UV Chromatogram, 220 nm
7.4 min
7.9 min
8.2 min
10.0 min
12.3 min
12.5 min
13.0 min
13.3 min
13.6 min
14.0 min
14.8 min
17.3 min
Time [min]
Intens.
x10^6
3.
+MS, 7.4-7.6min #(586-606), -Peak Bkgrnd
413.2
444.2
459.1
x10^6
5.
+MS, 8.2-8.4min #(648-671), -Peak Bkgrnd
431.2
453.1
x10^7
8.
+MS, 9.9-10.2min #(795-819), -Peak Bkgrnd
415.2
m/z

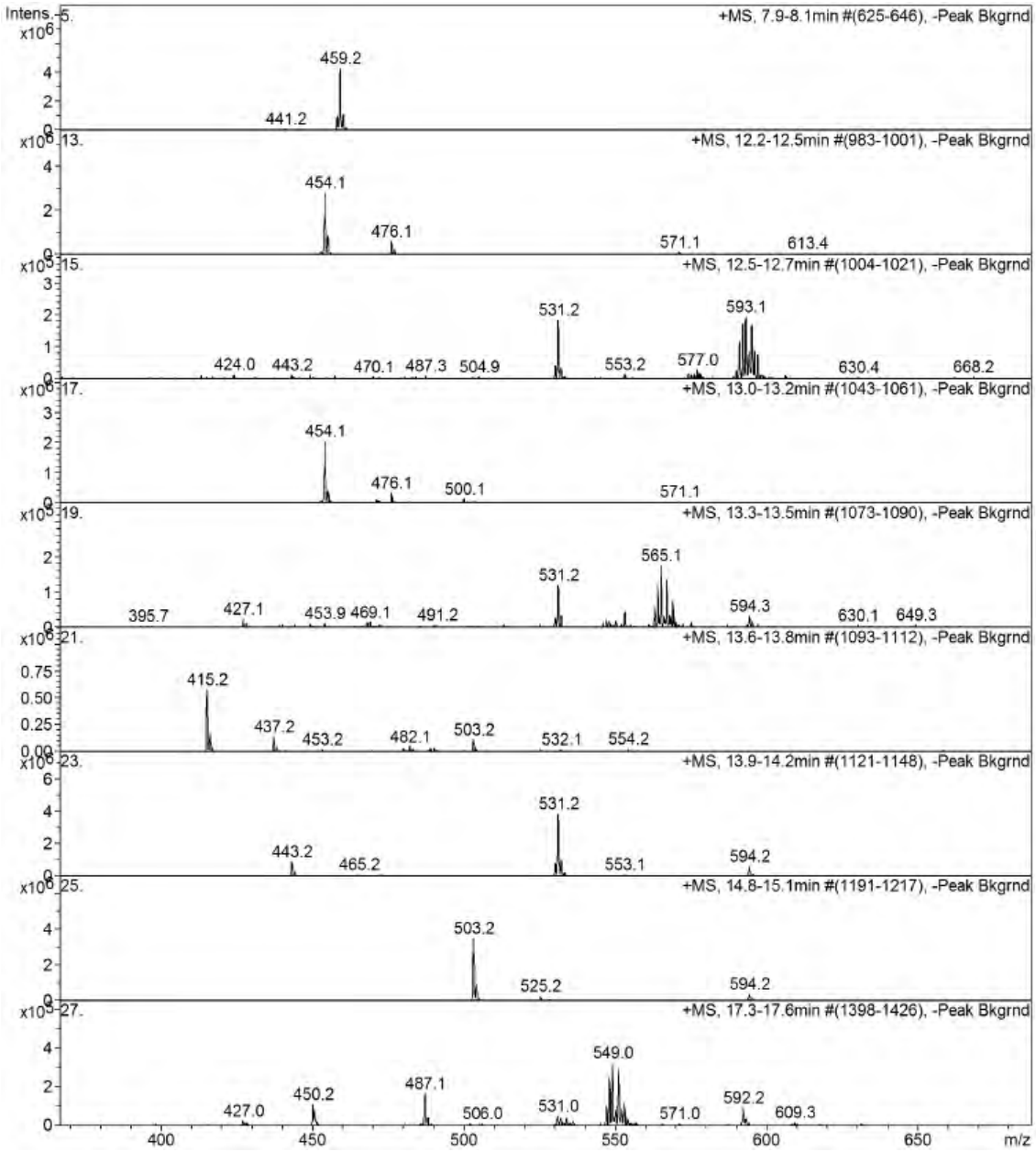
Intens.
5.
+MS, 7.9-8.1min #(625-646), -Peak Bkgrnd
459.2
441.2
13.
+MS, 12.2-12.5min #(983-1001), -Peak Bkgrnd
454.1
476.1
571.1
613.4
15.
+MS, 12.5-12.7min #(1004-1021), -Peak Bkgrnd
531.2
593.1
424.0
443.2
470.1
487.3
504.9
553.2
577.0
630.4
668.2
17.
+MS, 13.0-13.2min #(1043-1061), -Peak Bkgrnd
454.1
476.1
500.1
571.1
19.
+MS, 13.3-13.5min #(1073-1090), -Peak Bkgrnd
565.1
531.2
395.7
427.1
453.9
469.1
491.2
594.3
630.1
649.3
21.
+MS, 13.6-13.8min #(1093-1112), -Peak Bkgrnd
415.2
437.2
453.2
482.1
503.2
532.1
554.2
23.
+MS, 13.9-14.2min #(1121-1148), -Peak Bkgrnd
531.2
443.2
465.2
553.1
594.2
25.
+MS, 14.8-15.1min #(1191-1217), -Peak Bkgrnd
503.2
525.2
594.2
27.
+MS, 17.3-17.6min #(1398-1426), -Peak Bkgrnd
549.0
487.1
450.2
427.0
506.0
531.0
571.0
592.2
609.3
400
450
500
550
600
650
m/z

Biaryl cyclic peptide BPC780

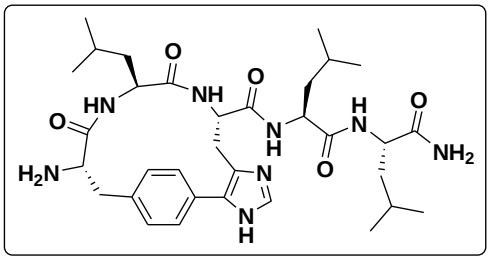

Crude peptide

HPLC (λ = 220 nm)

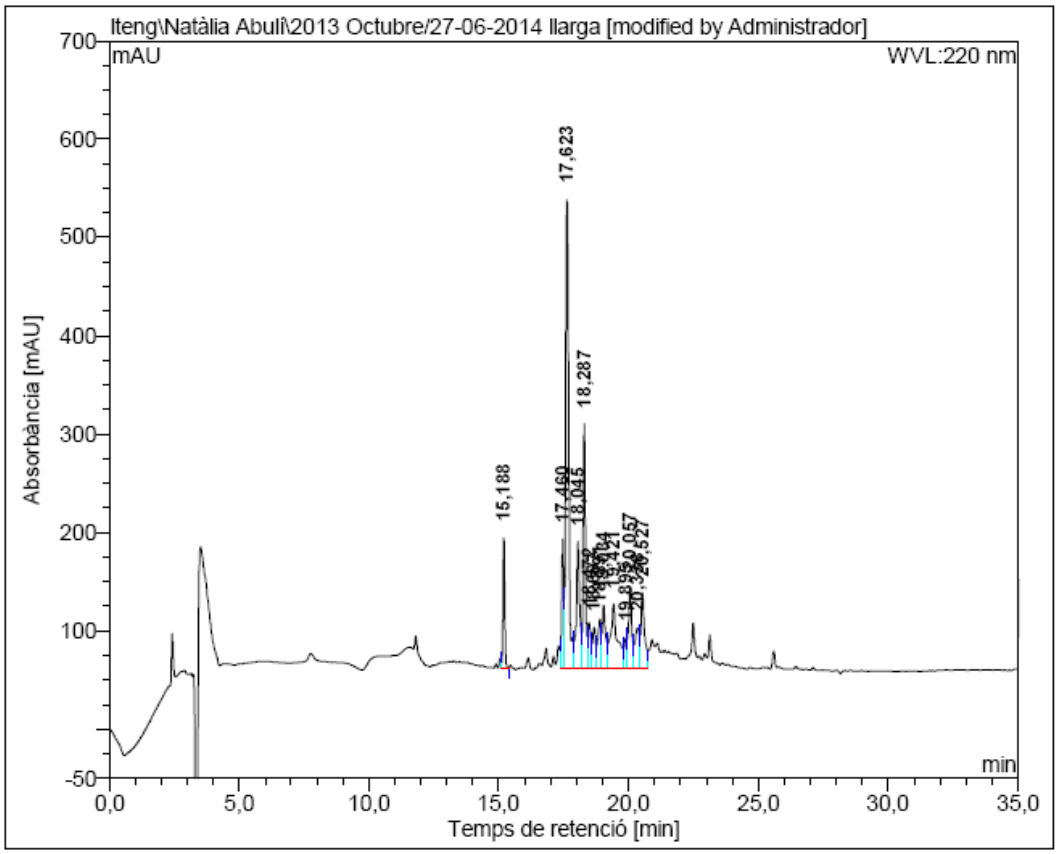

No.	mps retenc min	alçada mAU	Area mAU*min	Area relativa %
1	15,19	132,505	10,712	4,88
2	17,46	131,277	12,860	5,86
3	17,62	475,800	65,994	30,06
4	18,05	128,365	19,288	8,79
5	18,29	248,492	24,593	11,20
6	18,47	46,282	6,542	2,98
7	18,67	41,718	5,701	2,60
8	18,89	49,815	7,530	3,43
9	19,03	63,987	9,609	4,38
10	19,42	64,971	20,247	9,22
11	19,90	30,628	3,948	1,80
12	20,06	82,955	12,475	5,68
13	20,34	41,011	7,934	3,61
14	20,53	76,630	12,075	5,50
Total:		1614,437	219,507	100,00

ESI-MS *m/z*

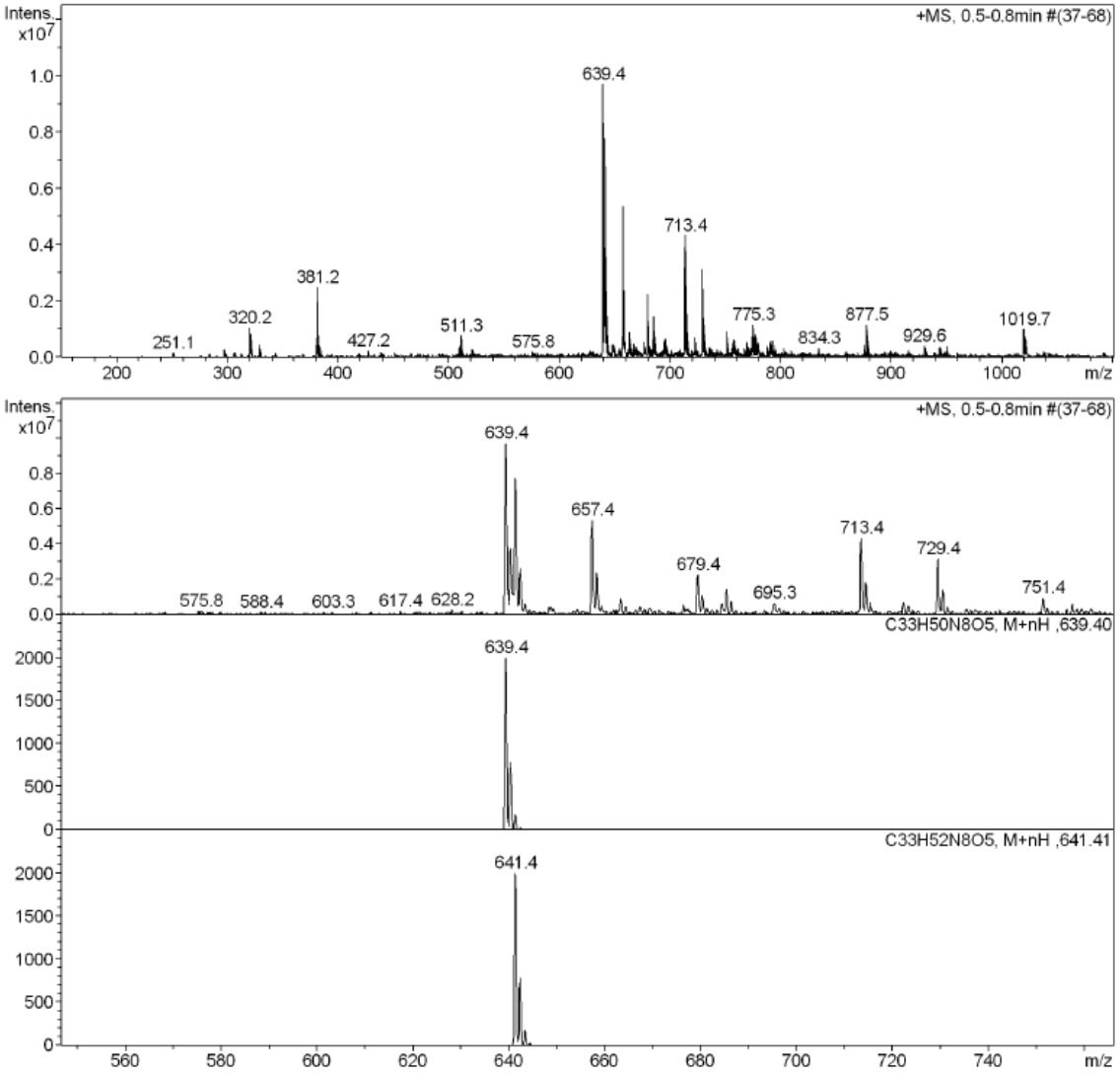
Intens.
x10^7
+MS, 0.5-0.8min #(37-68)
639.4
713.4
381.2
320.2
775.3
877.5
511.3
1019.7
251.1
427.2
575.8
834.3
929.6
m/z
+MS, 0.5-0.8min #(37-68)
639.4
657.4
713.4
729.4
679.4
751.4
575.8
588.4
603.3
617.4
628.2
695.3
C33H50N8O5, M+nH ,639.40
639.4
C33H52N8O5, M+nH ,641.41
641.4
m/z

Purified peptide

HPLC (λ = 220 nm)

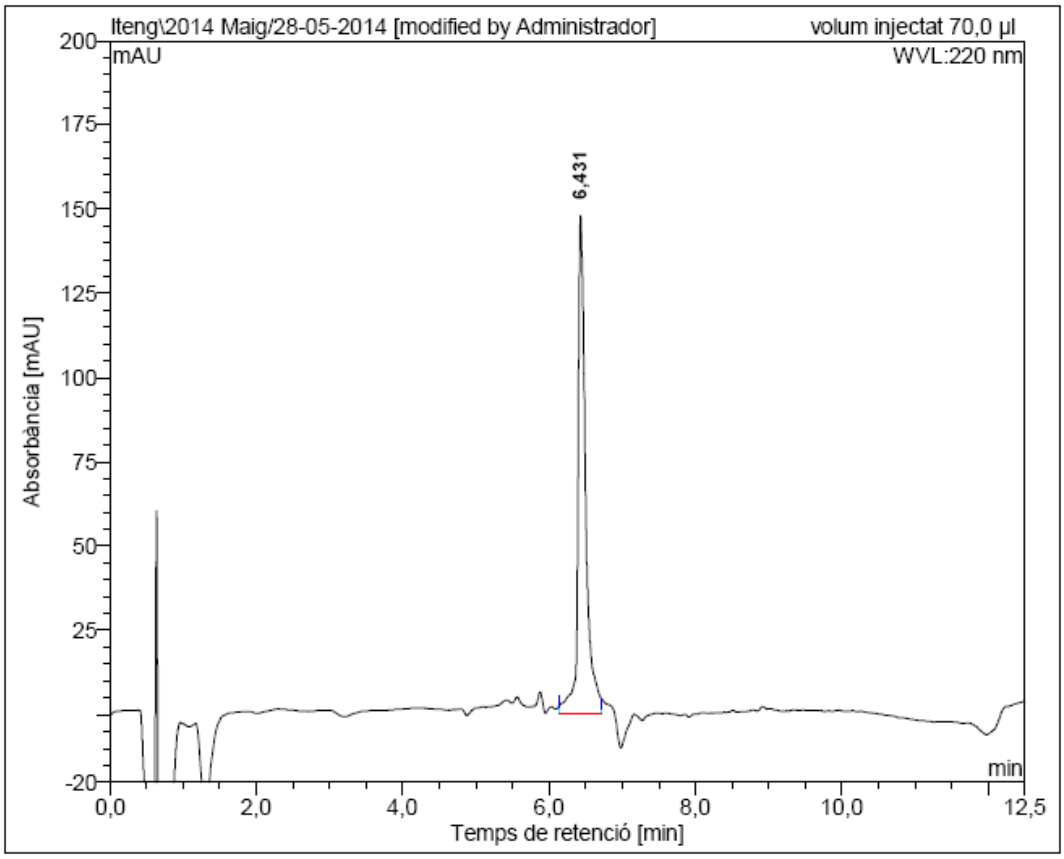

No.	mps retenc min	alçada mAU	Area mAU*min	Area relativa %
1	6,43	147,801	18,056	100,00
Total:		147,801	18,056	100,00

ESI-MS *m/z*

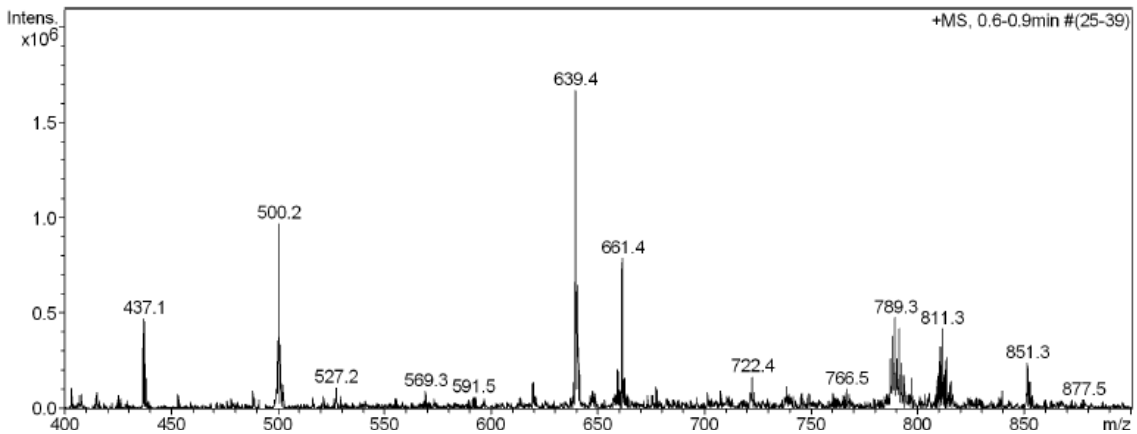

HRMS (ESI) *m/z*

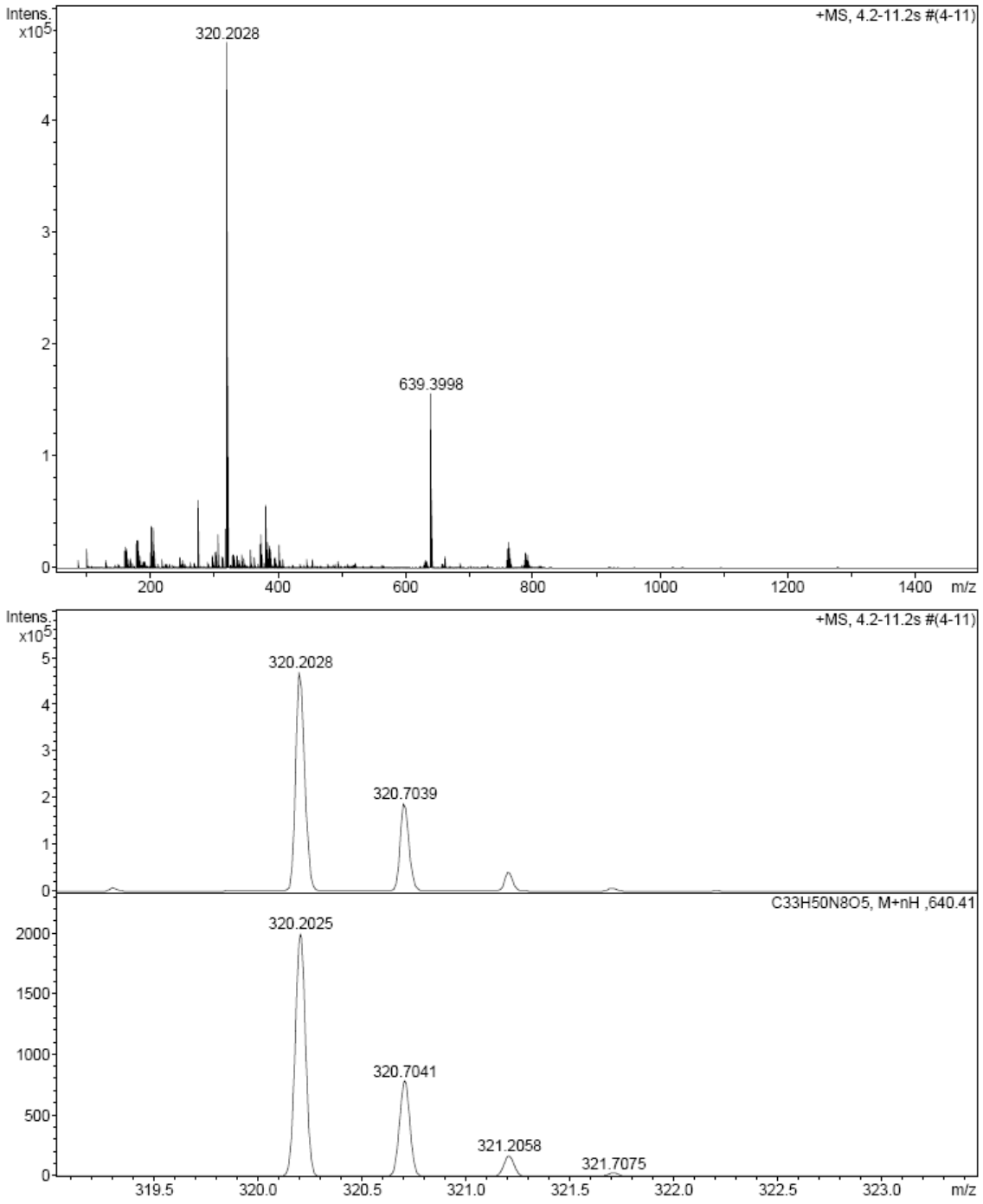
Intens.
x10^5
+MS, 4.2-11.2s #(4-11)
320.2028
639.3998
m/z
320.2028
320.7039
C33H50N8O5, M+nH ,640.41
320.2025
320.7041
321.2058
321.7075

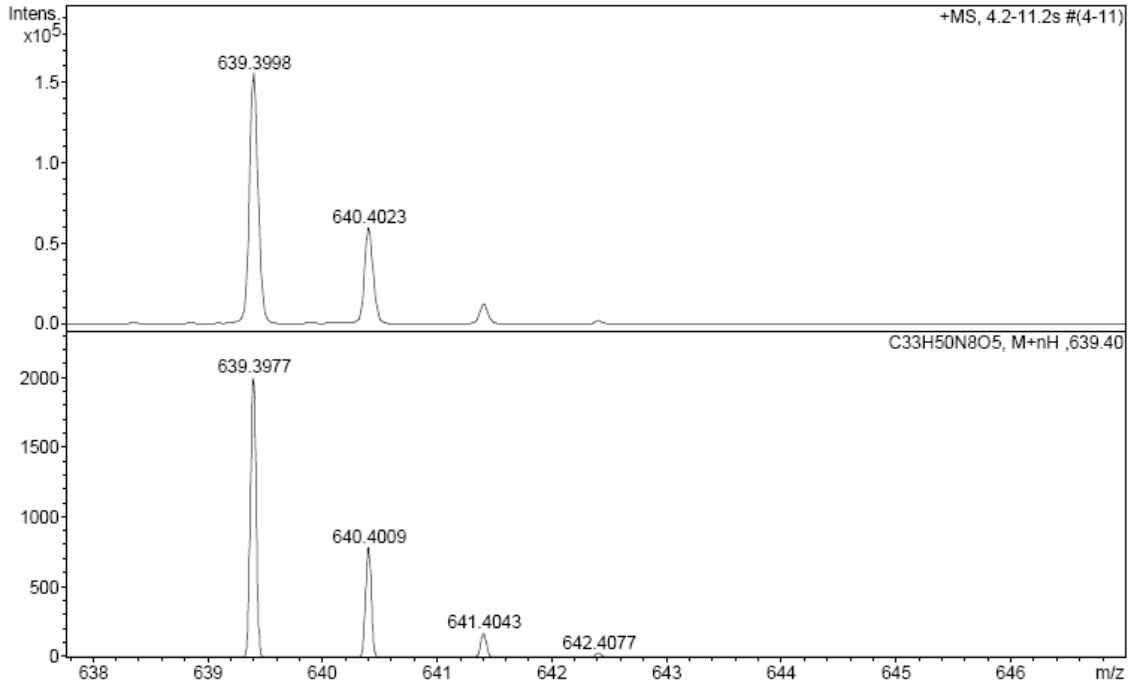
Intens.
x10^5
+MS, 4.2-11.2s #(4-11)
639.3998
640.4023
C33H50N8O5, M+nH ,639.40
639.3977
640.4009
641.4043
642.4077
m/z

Biaryl cyclic peptide 55

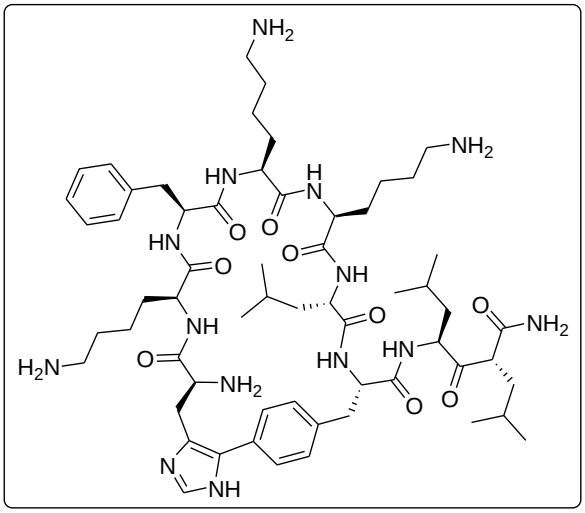

Crude peptide

HPLC-MS

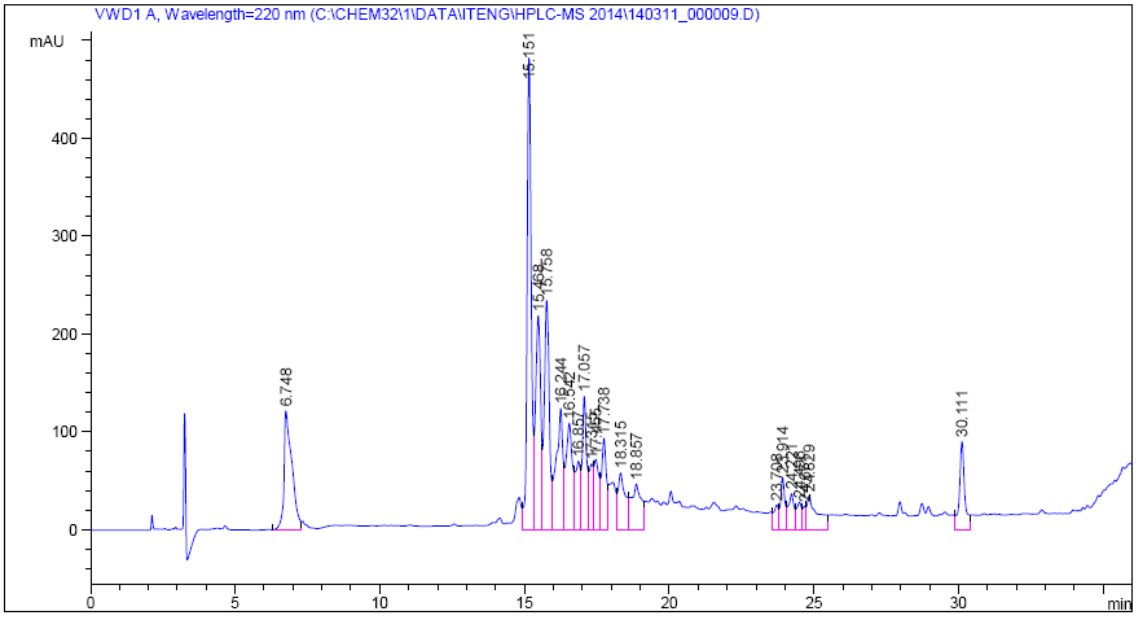

Peak #	RetTime [min]	Type	Width [min]	Area mAU *s	Height [mAU]	Area %
1	6.748	VV	0.2514	2332.99634	121.65116	8.4242
2	15.151	VV	0.1549	4842.08691	482.54626	17.4843
3	15.468	VV	0.1987	2747.25146	219.16302	9.9201
4	15.758	VV	0.1843	2855.62427	234.41689	10.3114
5	16.244	VV	0.2202	2068.99121	124.45097	7.4709
6	16.542	VV	0.2140	1703.85986	109.24957	6.1525
7	16.857	VV	0.1611	820.70386	70.24554	2.9635
8	17.057	VV	0.1558	1497.07422	136.34161	5.4058
9	17.315	VV	0.1290	612.16577	67.55420	2.2105
10	17.455	VV	0.1749	911.26105	72.18242	3.2905
11	17.738	VV	0.1682	1112.20056	93.30350	4.0161
12	18.315	VV	0.2442	1067.07324	58.27025	3.8531
13	18.857	VV	0.3049	1129.83972	47.05492	4.0797
14	23.708	VV	0.1532	278.42035	25.58371	1.0053
15	23.914	VV	0.1509	562.53143	53.27354	2.0312
16	24.221	VV	0.1890	517.06415	37.06379	1.8671
17	24.496	VV	0.1691	348.78543	28.46888	1.2594
18	24.671	VV	0.1032	173.76953	24.47163	0.6275
19	24.829	VV	0.3494	948.87653	34.71935	3.4263
20	30.111	VV	0.1855	1163.29834	90.16402	4.2006

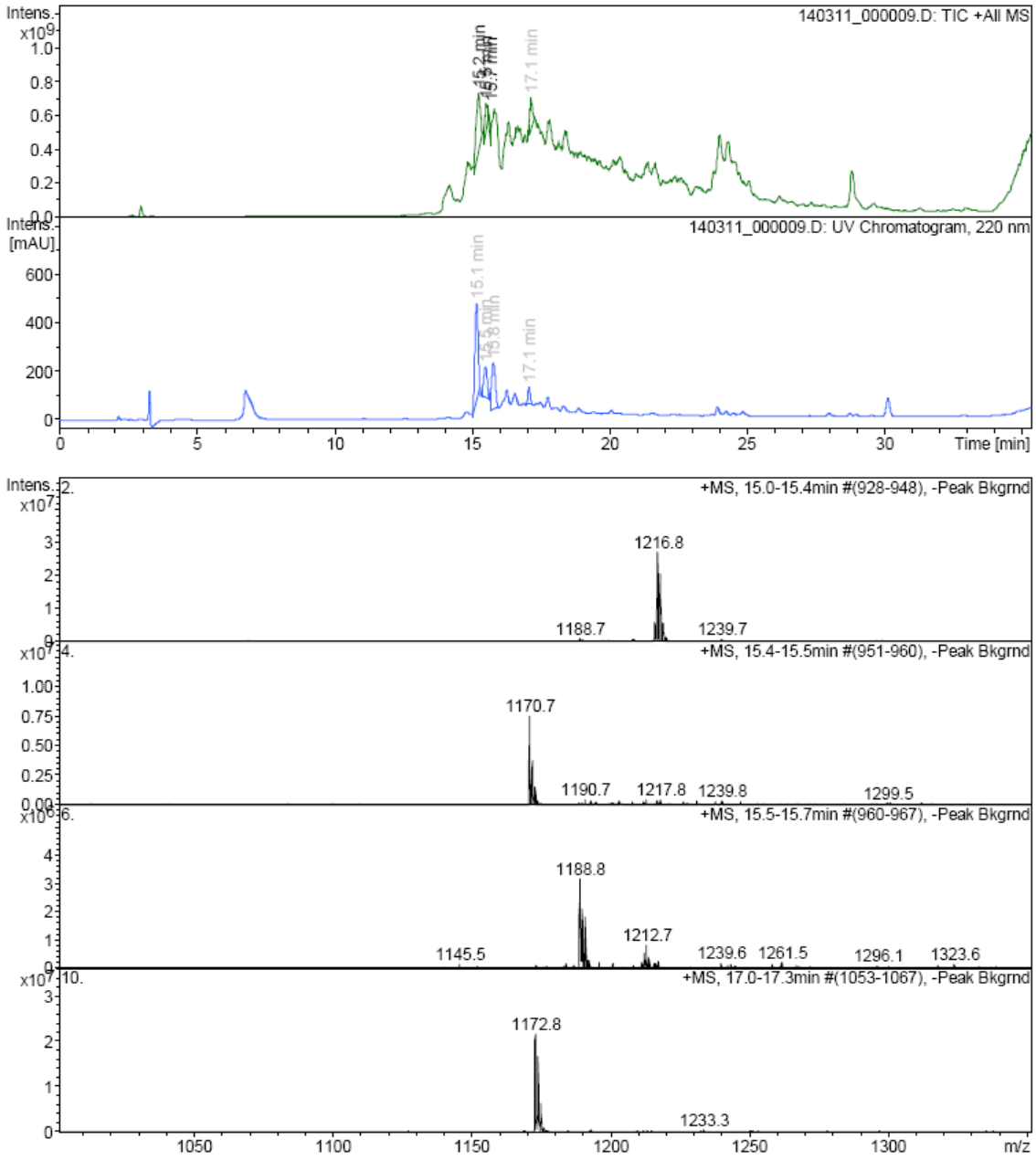
140311_000009.D: TIC +All MS
Intens.
x10^9
1.0
0.8
0.6
0.4
0.2
0.0
15.1 min
17.1 min
140311_000009.D: UV Chromatogram, 220 nm
Intens.
[mAU]
600
400
200
0
15.1 min
17.1 min
0
5
10
15
20
25
30
Time [min]
+MS, 15.0-15.4min #(928-948), -Peak Bkgrnd
x10^7
3
2
1
0
1216.8
1188.7
1239.7
+MS, 15.4-15.5min #(951-960), -Peak Bkgrnd
x10^7
1.00
0.75
0.50
0.25
0.00
1170.7
1190.7
1217.8
1239.8
1299.5
+MS, 15.5-15.7min #(960-967), -Peak Bkgrnd
x10^7
4
3
2
1
0
1188.8
1212.7
1145.5
1239.6
1261.5
1296.1
1323.6
+MS, 17.0-17.3min #(1053-1067), -Peak Bkgrnd
x10^7
3
2
1
0
1172.8
1233.3
1050
1100
1150
1200
1250
1300
m/z

Biaryl cyclic peptide 56

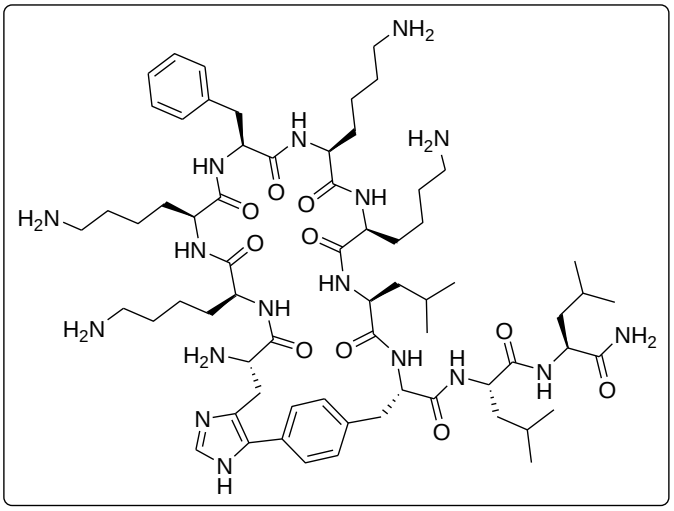

Crude peptide

HPLC-MS

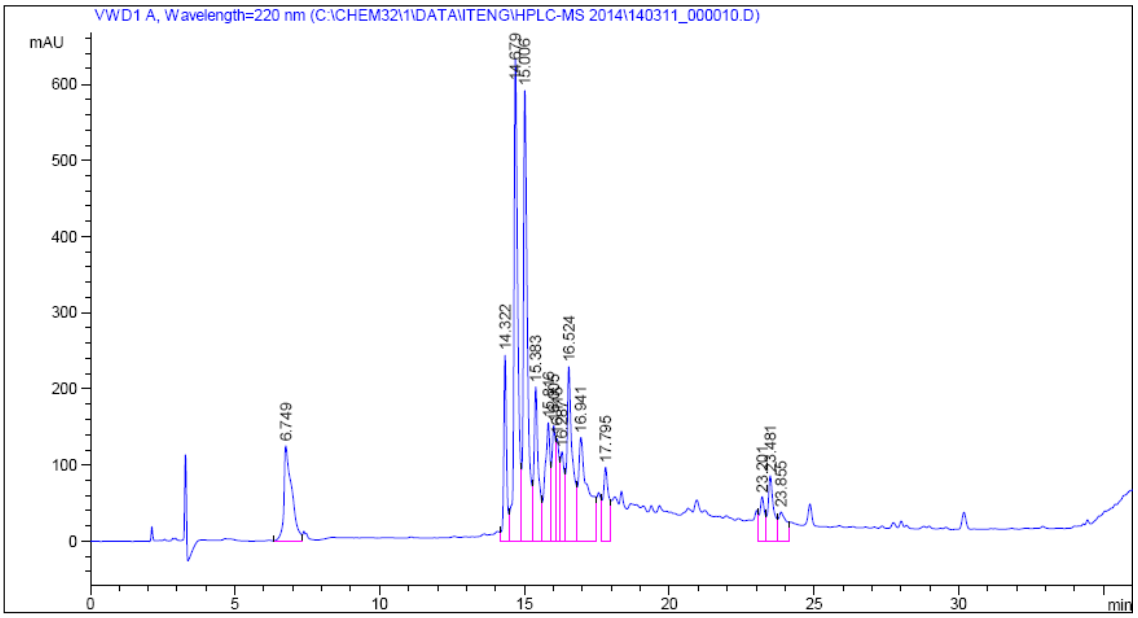

Peak #	RetTime [min]	Type	Width [min]	Area mAU *s	Height [mAU]	Area %
1	6.749	VV	0.2477	2356.51929	124.95012	6.9872
2	14.322	VV	0.1012	1660.79211	244.13057	4.9244
3	14.679	VV	0.1375	5962.11963	633.32465	17.6781
4	15.006	VV	0.1444	5772.50488	591.85944	17.1158
5	15.383	VV	0.1558	2247.94507	202.42946	6.6653
6	15.816	VV	0.1692	1944.38867	155.49596	5.7652
7	16.005	VV	0.1224	1305.90234	151.57753	3.8721
8	16.116	VV	0.1125	1045.92627	134.53891	3.1012
9	16.287	VV	0.1345	1119.77917	117.44226	3.3202
10	16.524	VV	0.1859	3163.70044	228.98468	9.3806
11	16.941	VV	0.3118	3193.69849	136.02122	9.4695
12	17.795	VV	0.1882	1347.57068	97.03305	3.9956
13	23.201	VV	0.1652	680.07434	58.29771	2.0165
14	23.481	VV	0.1918	1182.07629	85.52626	3.5049
15	23.855	VV	0.2539	743.11310	38.07728	2.2034

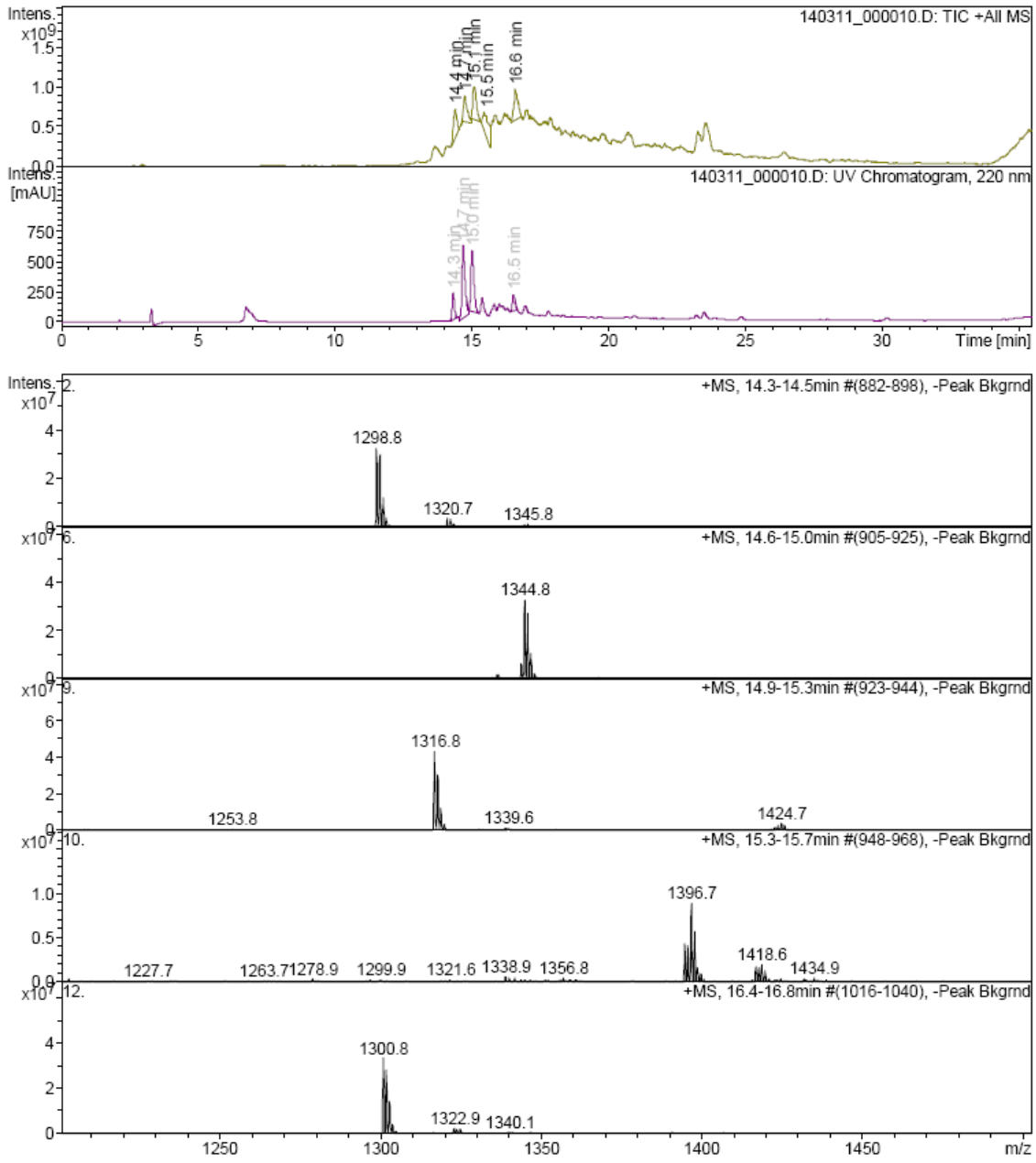
Intens.
x10^9
1.5
1.0
0.5
0.0
140311_000010.D: TIC +All MS
14.4 min
14.7 min
15.1 min
15.5 min
16.6 min
Intens.
[mAU]
750
500
250
0
140311_000010.D: UV Chromatogram, 220 nm
14.3 min
14.7 min
15.0 min
16.5 min
0
5
10
15
20
25
30
Time [min]
Intens.
x10^7
2.
+MS, 14.3-14.5min #(882-898), -Peak Bkgrnd
1298.8
1320.7
1345.8
6.
+MS, 14.6-15.0min #(905-925), -Peak Bkgrnd
1344.8
9.
+MS, 14.9-15.3min #(923-944), -Peak Bkgrnd
1316.8
1253.8
1339.6
1424.7
10.
+MS, 15.3-15.7min #(948-968), -Peak Bkgrnd
1396.7
1227.7
1263.7
1278.9
1299.9
1321.6
1338.9
1356.8
1418.6
1434.9
12.
+MS, 16.4-16.8min #(1016-1040), -Peak Bkgrnd
1300.8
1322.9
1340.1
1250
1300
1350
1400
1450
m/z

Biaryl cyclic peptide 57a-b

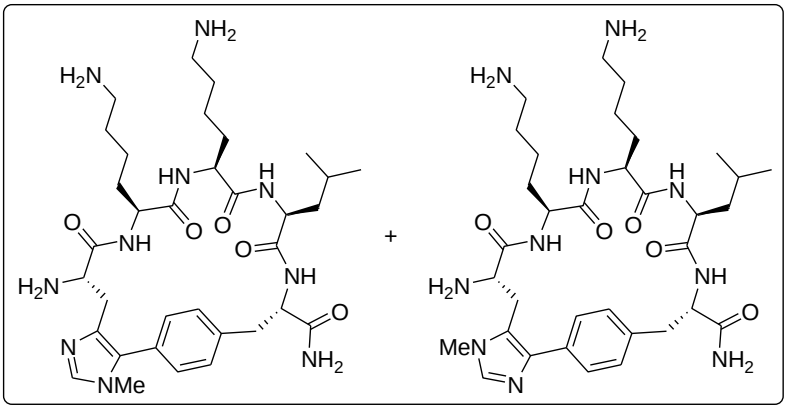

Crude peptide

HPLC-MS

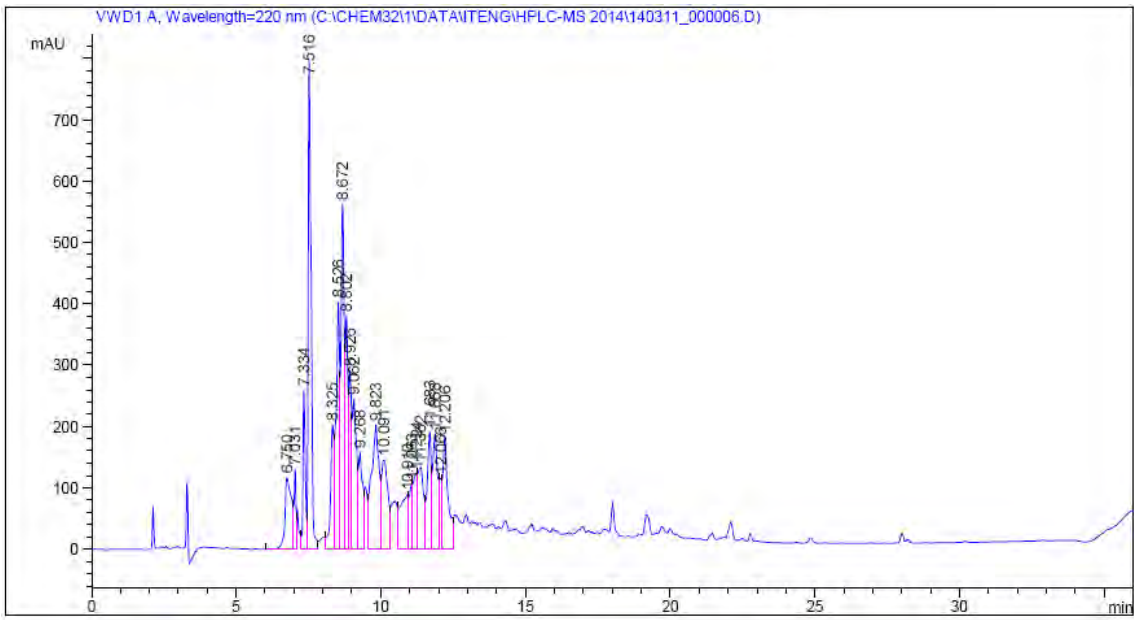

Peak #	RetTime [min]	Type	Width [min]	Area mAU *s	Height [mAU]	Area %
1	6.750	BV	0.2158	1866.83252	116.68562	4.0698
2	7.031	VV	0.0645	573.52557	130.17807	1.2503
3	7.334	VV	0.0789	1430.52893	259.47272	3.1186
4	7.516	VV	0.0981	5611.85889	797.64447	12.2342
5	8.325	VV	0.1162	1609.62708	202.09883	3.5091
6	8.526	VV	0.1234	3559.24780	402.95096	7.7594
7	8.672	VV	0.1114	4243.54736	561.95996	9.2512
8	8.802	VV	0.0913	2400.87573	379.49326	5.2341
9	8.926	VV	0.0983	1981.09094	291.32977	4.3189
10	9.062	VV	0.1332	2421.47876	244.06172	5.2790
11	9.268	VV	0.1332	1566.18860	157.87715	3.4144
12	9.823	VV	0.2329	3731.86255	202.05812	8.1357
13	10.091	VV	0.2037	2291.79028	144.67885	4.9962
14	10.910	VV	0.2471	1725.34375	88.80429	3.7614
15	11.063	VV	0.0900	643.27496	105.61656	1.4024
16	11.224	VV	0.1353	1267.61169	123.97361	2.7635
17	11.362	VV	0.2042	1903.72388	133.50212	4.1502
18	11.683	VV	0.1368	1864.79932	191.74327	4.0654
19	11.868	VV	0.1746	2265.73218	187.32533	4.9394
20	12.066	VV	0.0692	570.66882	115.70674	1.2441
21	12.206	VV	0.1741	2340.67407	182.82645	5.1028

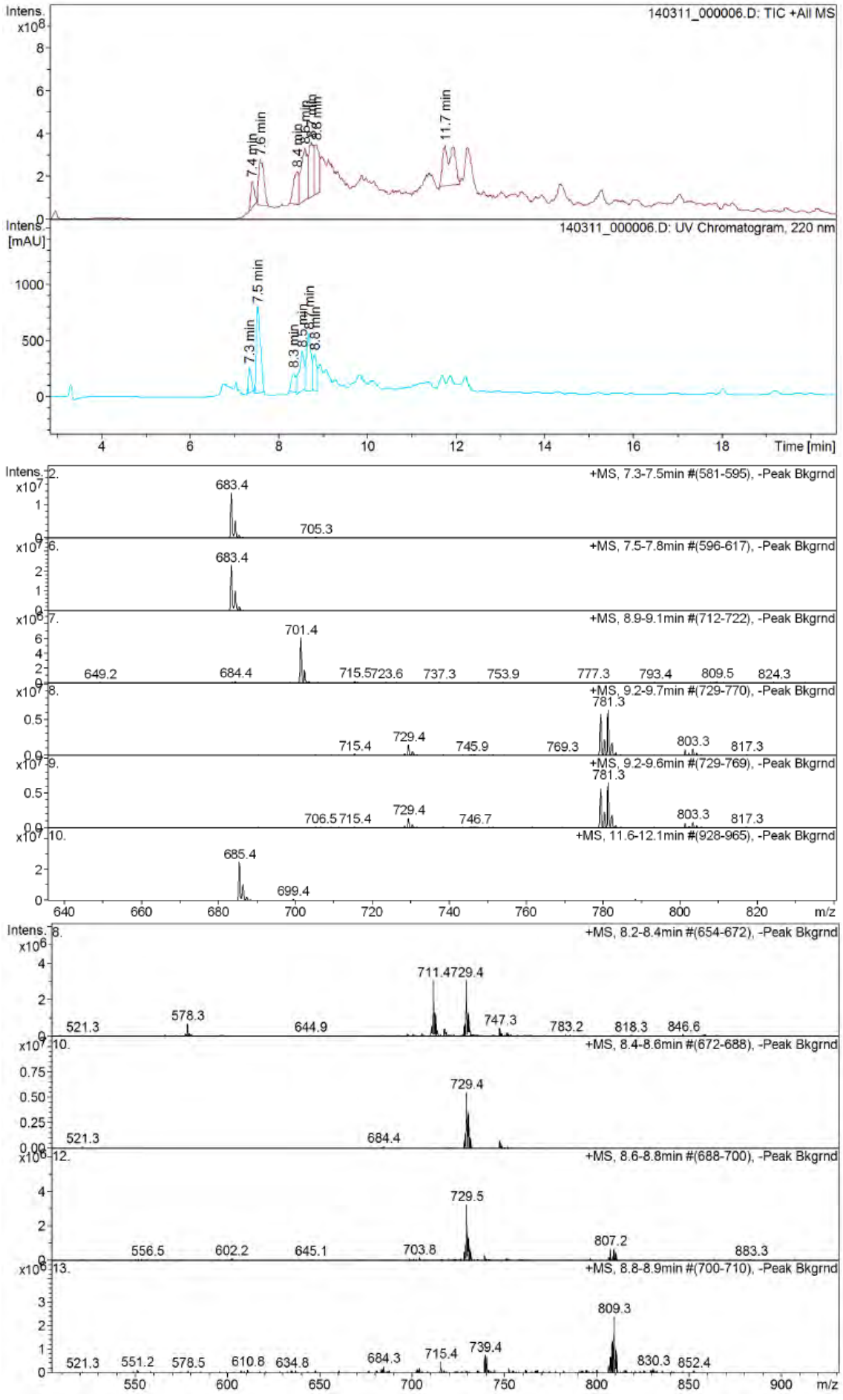
140311_000006.D: TIC +All MS
7.4 min
7.6 min
8.4 min
11.7 min
140311_000006.D: UV Chromatogram, 220 nm
7.3 min
7.5 min
8.3 min
Time [min]
+MS, 7.3-7.5min #(581-595), -Peak Bkgrnd
683.4
705.3
+MS, 7.5-7.8min #(596-617), -Peak Bkgrnd
683.4
+MS, 8.9-9.1min #(712-722), -Peak Bkgrnd
701.4
+MS, 9.2-9.7min #(729-770), -Peak Bkgrnd
781.3
729.4
+MS, 9.2-9.6min #(729-769), -Peak Bkgrnd
781.3
729.4
+MS, 11.6-12.1min #(928-965), -Peak Bkgrnd
685.4
699.4
m/z
+MS, 8.2-8.4min #(654-672), -Peak Bkgrnd
711.4729.4
+MS, 8.4-8.6min #(672-688), -Peak Bkgrnd
729.4
+MS, 8.6-8.8min #(688-700), -Peak Bkgrnd
729.5
807.2
+MS, 8.8-8.9min #(700-710), -Peak Bkgrnd
809.3
739.4
m/z

SUPPORTING INFORMATION

Solid-phase Peptide Macrocyclization via a Microwave-Assisted Suzuki-Miyaura Reaction Between a Histidine and a Tyrosine Derivative

Iteng Ng-Choi, Marta Planas* and Lidia Feliu*

TABLE OF CONTENTS

Copies of HPLC, MS and NMR spectra

1. Synthesis of amino acids

H-Tyr(3-I,Me)-OMe

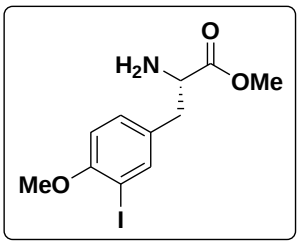

HPLC (λ = 220 nm)

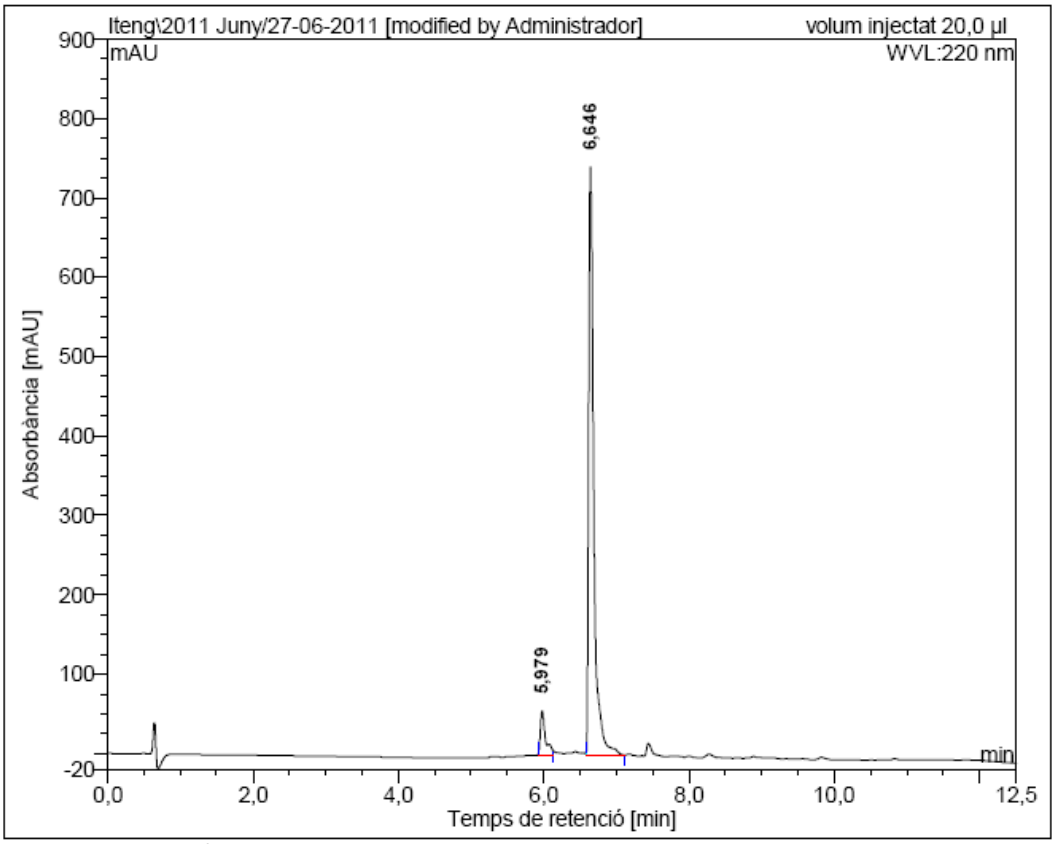

No.	Temps retenció min	alçada mAU	Area mAU*min	Area relativa %
1	5,98	55,426	4,665	7,15
2	6,65	740,599	60,541	92,85
Total:		796,025	65,206	100,00

^{1}H-NMR (400 MHz, $CDCl_3$) δ (ppm)

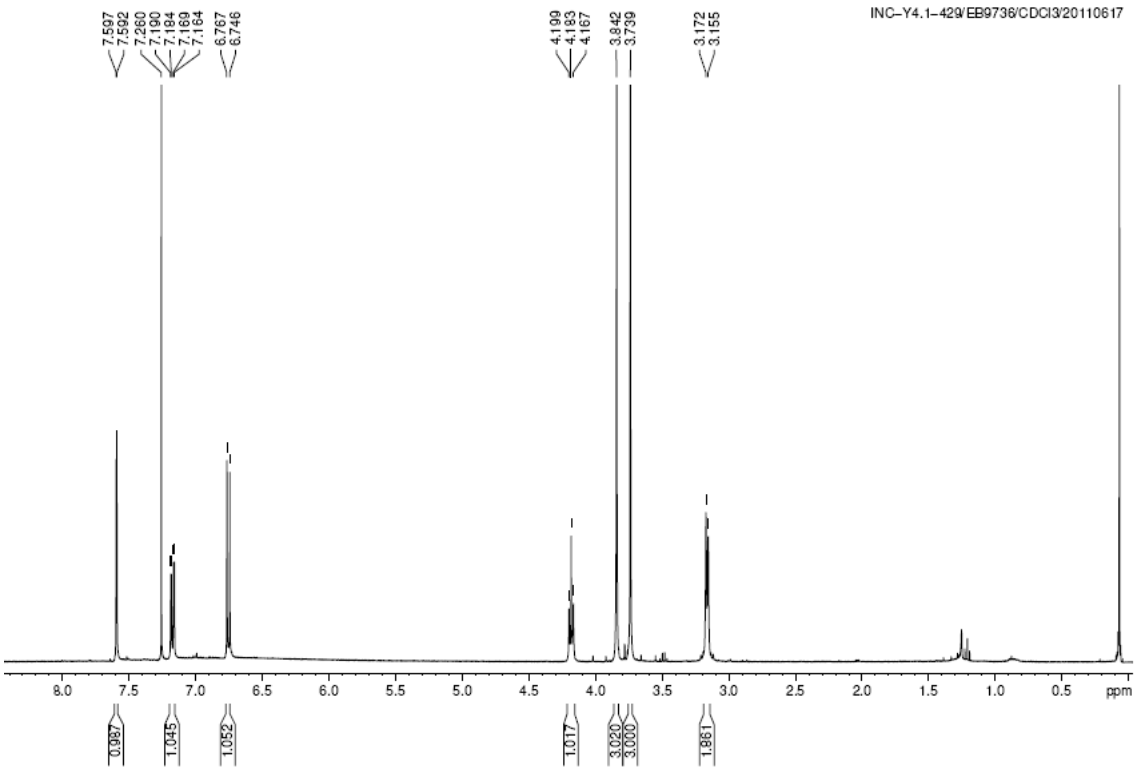

^{13}C-NMR (75 MHz, DMSO-d_6) δ (ppm)

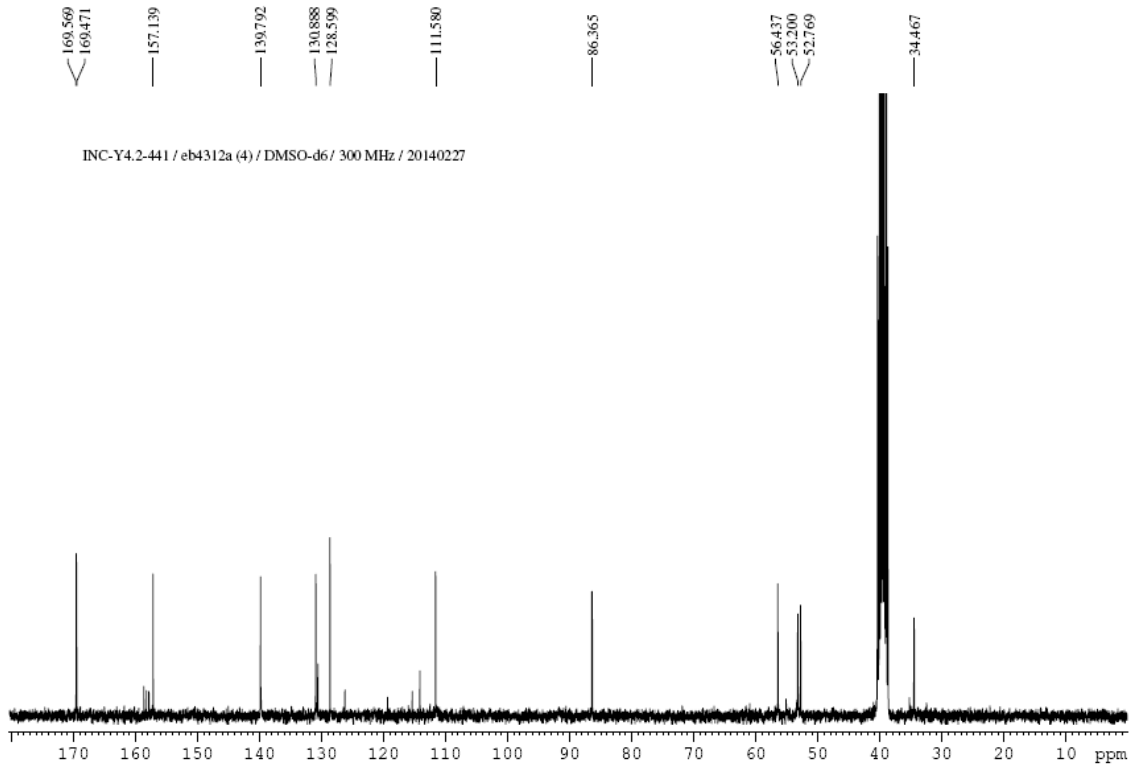

H-Tyr(3-I,Me)-OH

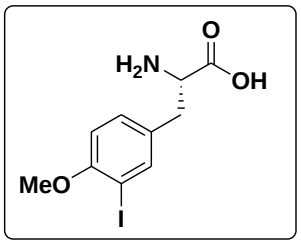

HPLC (λ = 220 nm)

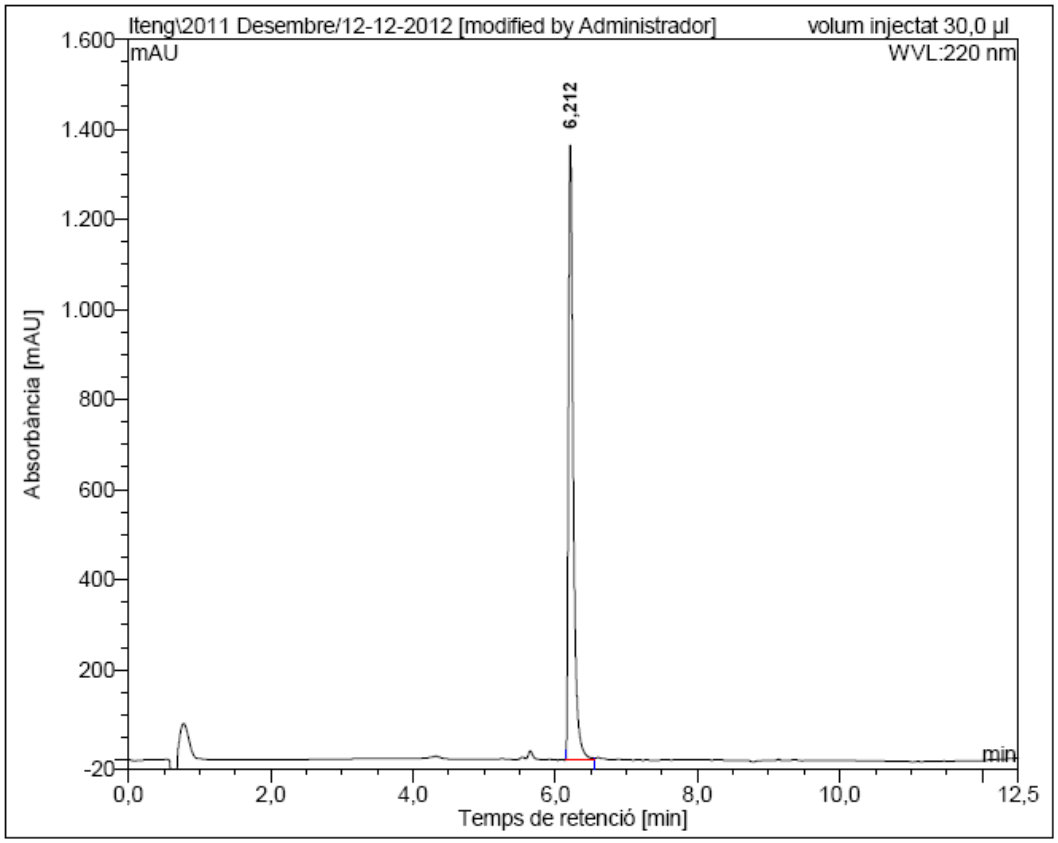

No.	Temps retenció min	alçada mAU	Area mAU*min	Area relativa %
1	6,21	1365,180	107,408	100,00
Total:		1365,180	107,408	100,00

^{1}H-NMR (300 MHz, DMSO-d_6) δ (ppm)

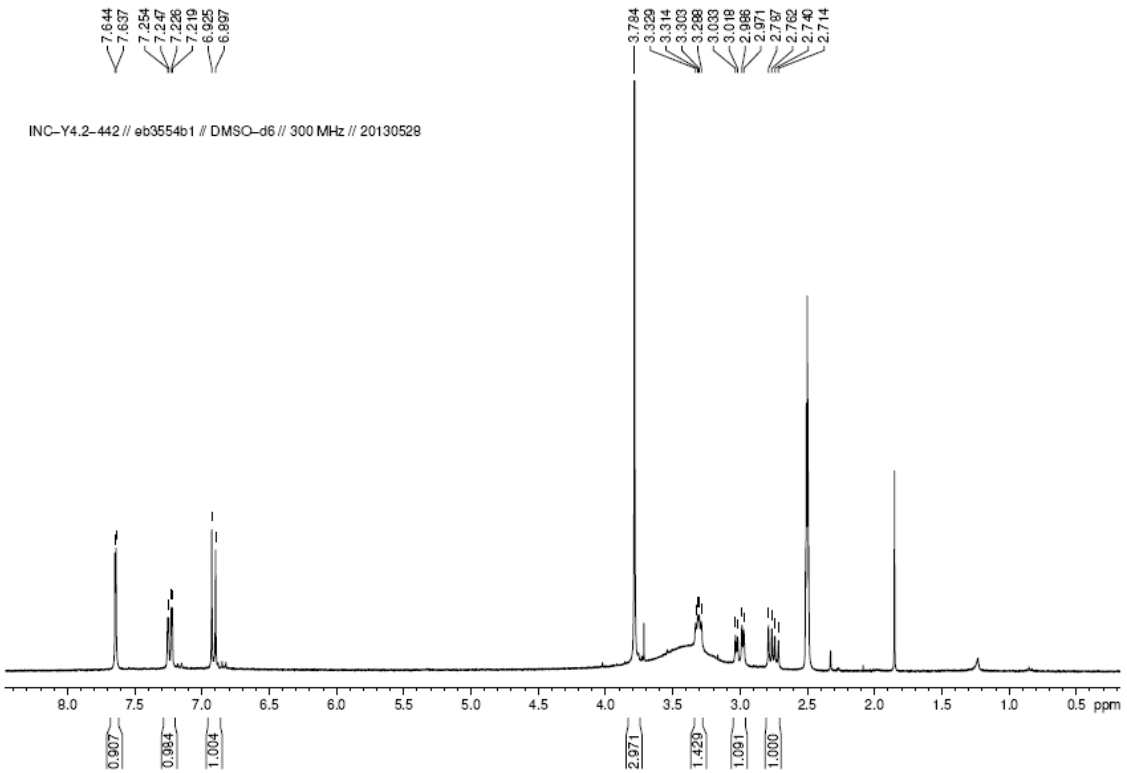

^{13}C-NMR (75 MHz, DMSO-d_6) δ (ppm)

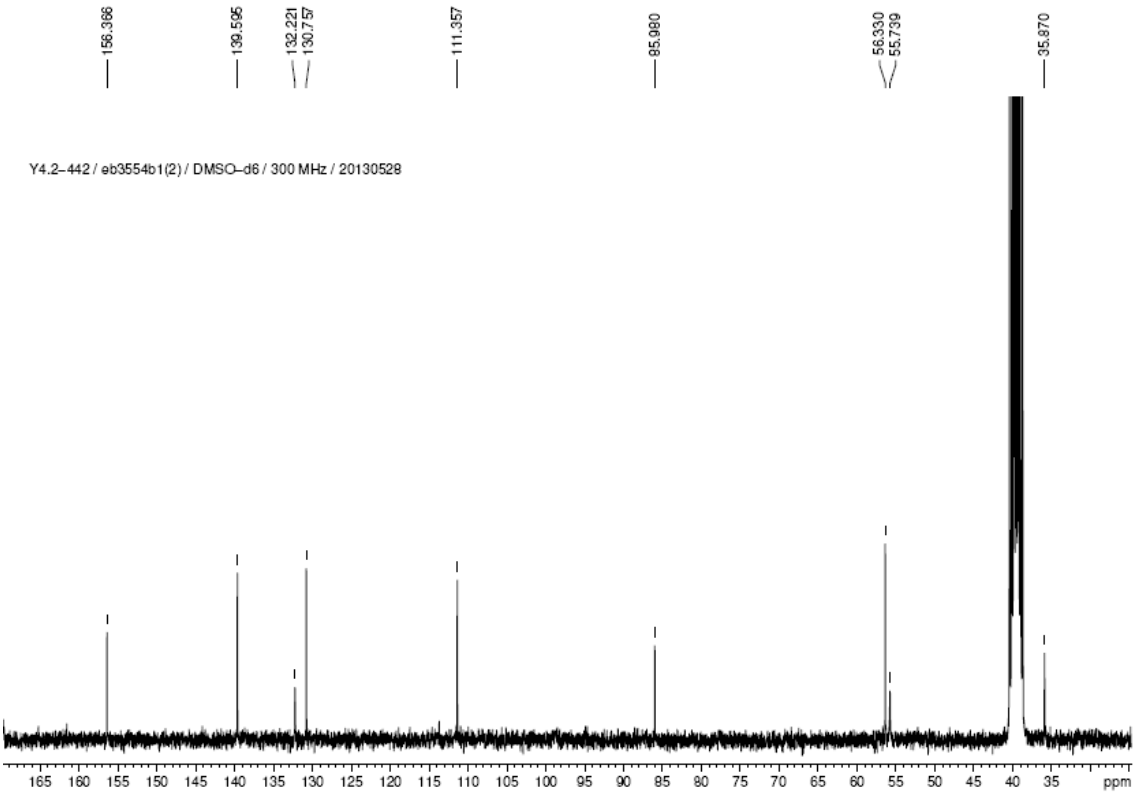

Fmoc-Tyr(3-I,Me)-OH (2)

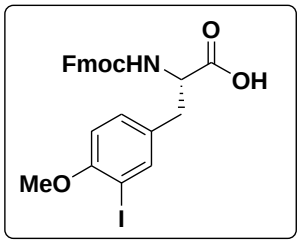

HPLC (λ = 220 nm)

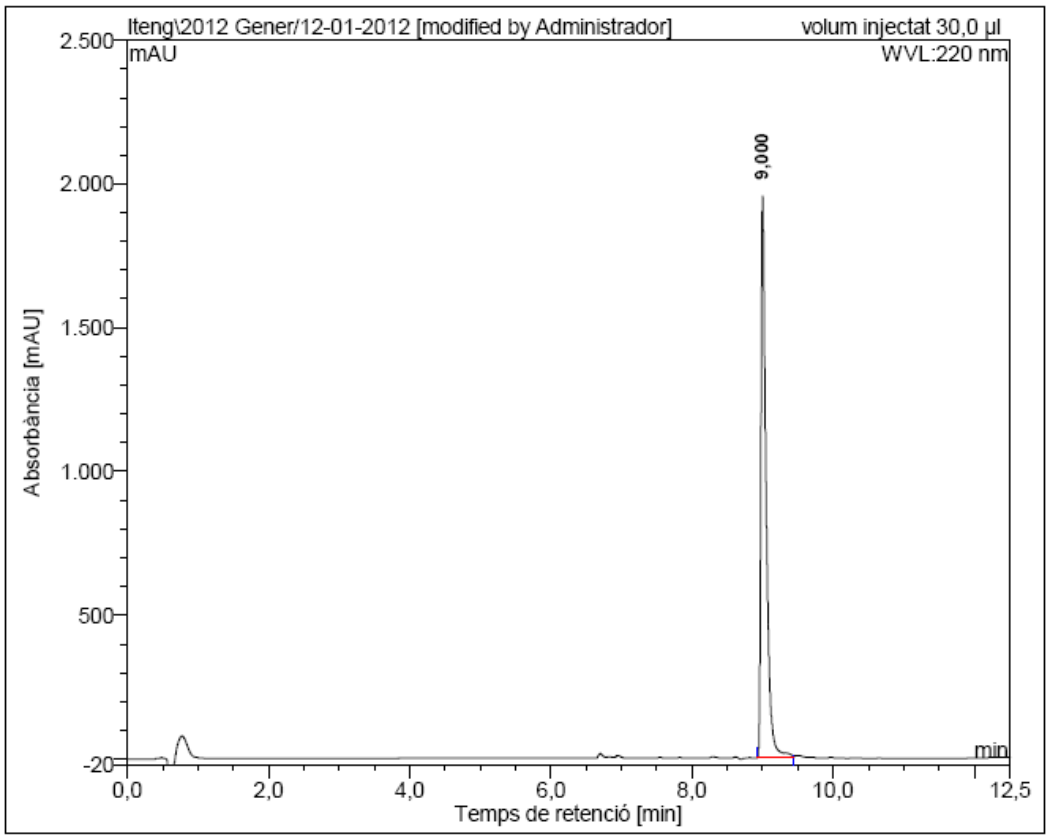

No.	Temps retenció min	alçada mAU	Area mAU*min	Area relativa %
1	9,00	1954,245	167,666	100,00
Total:		1954,245	167,666	100,00

^{1}H-NMR (300 MHz, DMSO-d_6) δ (ppm)

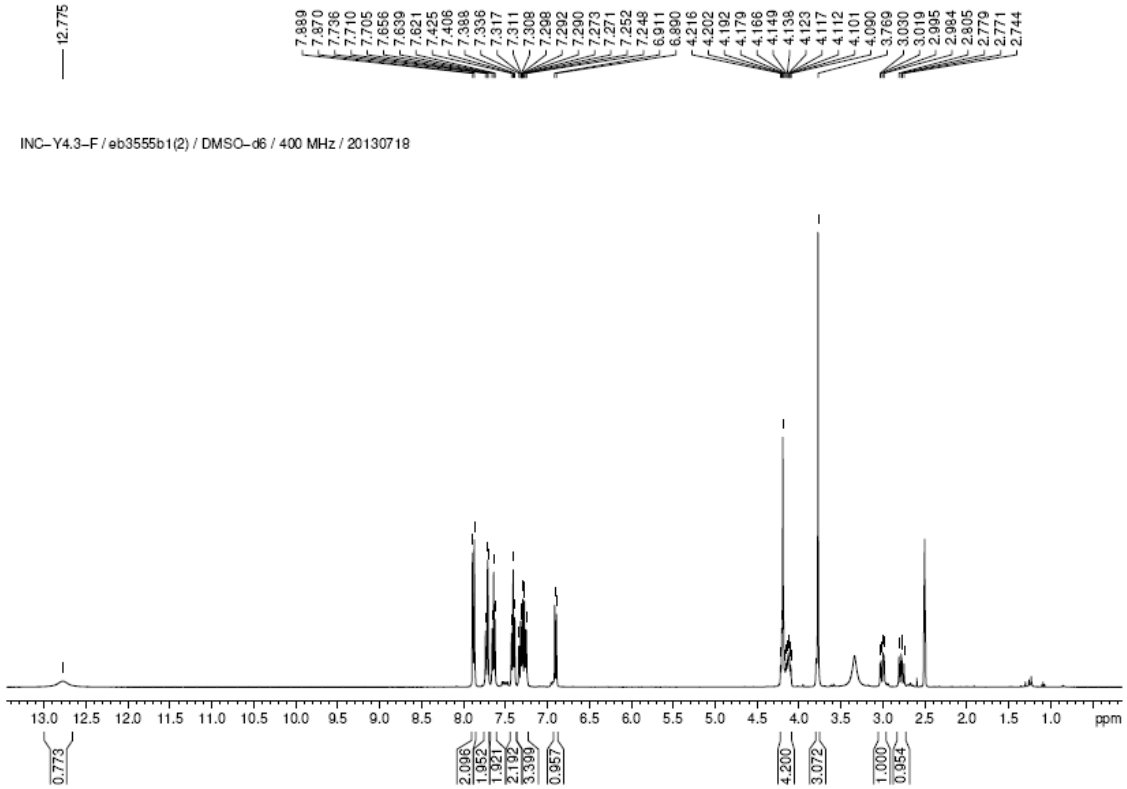

^{13}C-NMR (75 MHz, DMSO-d_6) δ (ppm)

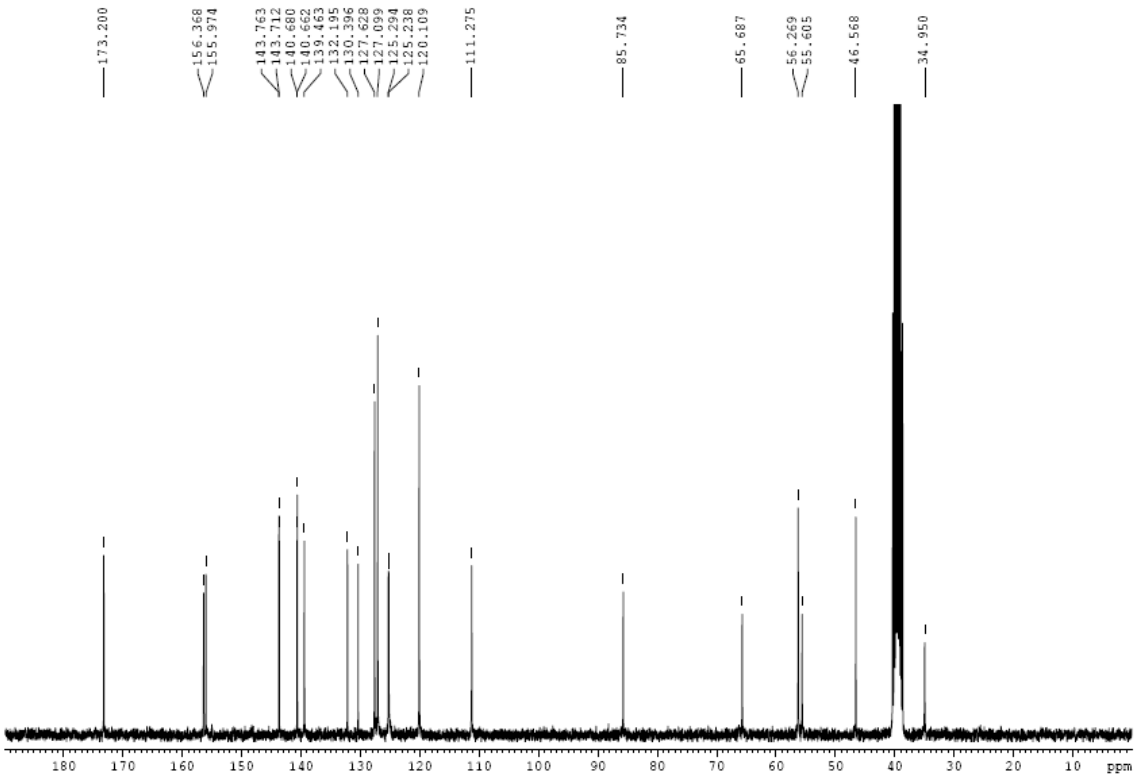

Boc-Tyr(3-B(OH)$_2$,Me)-OMe

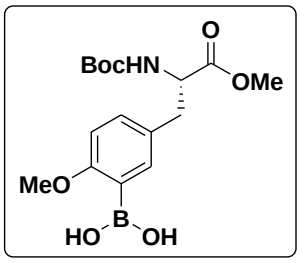

HPLC (λ = 220 nm)

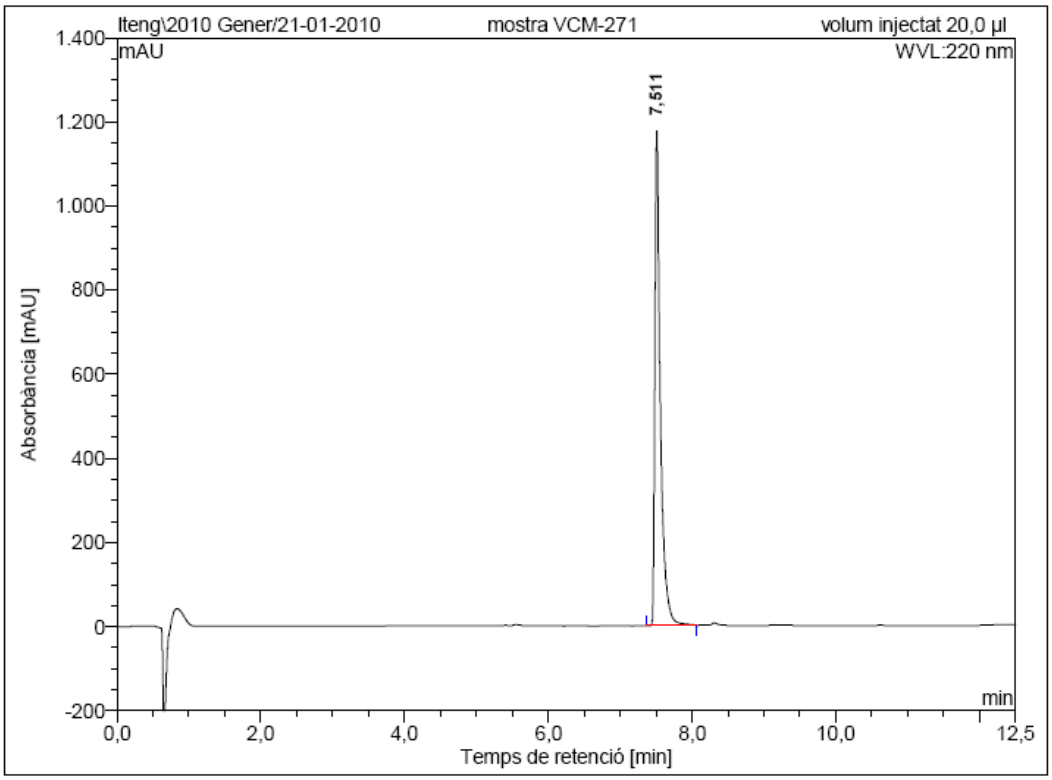

No.	Temps retenció min	alçada mAU	Area mAU*min	Area relativa %
1	7,51	1175,909	105,036	100,00
Total:		1175,909	105,036	100,00

^{1}H-NMR (400 MHz, $CDCl_3$) δ (ppm)

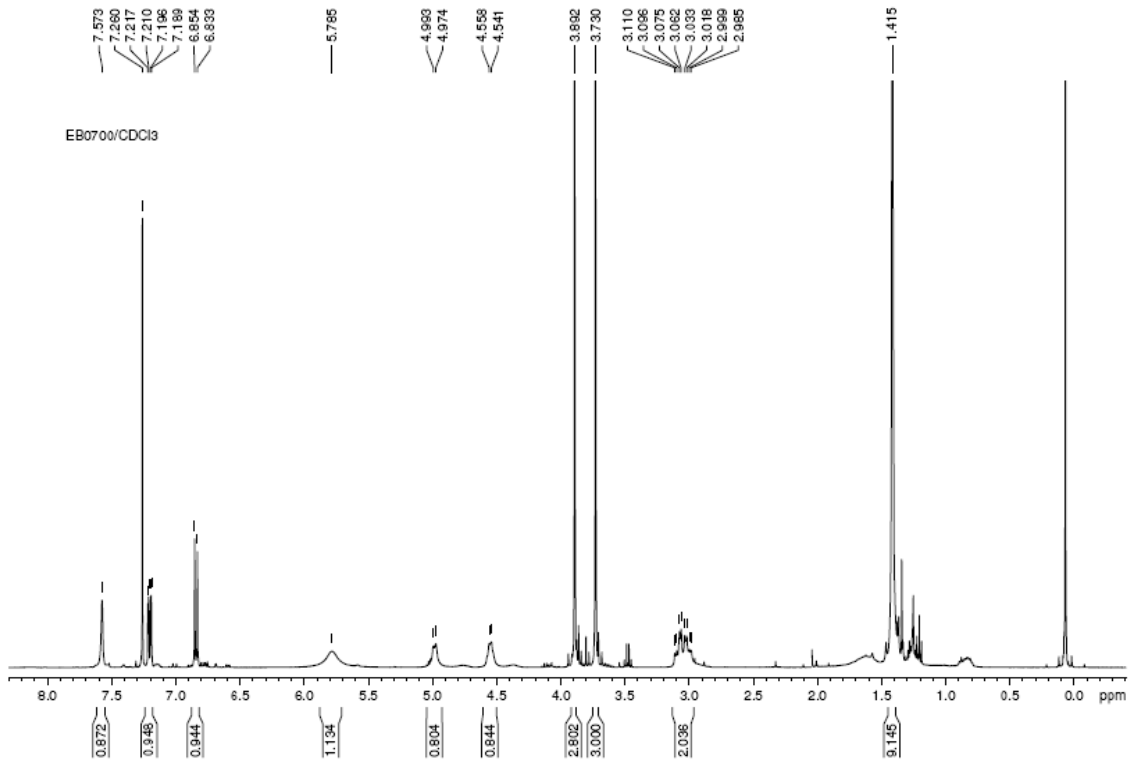

^{13}C-NMR (75 MHz, $CDCl_3$) δ (ppm)

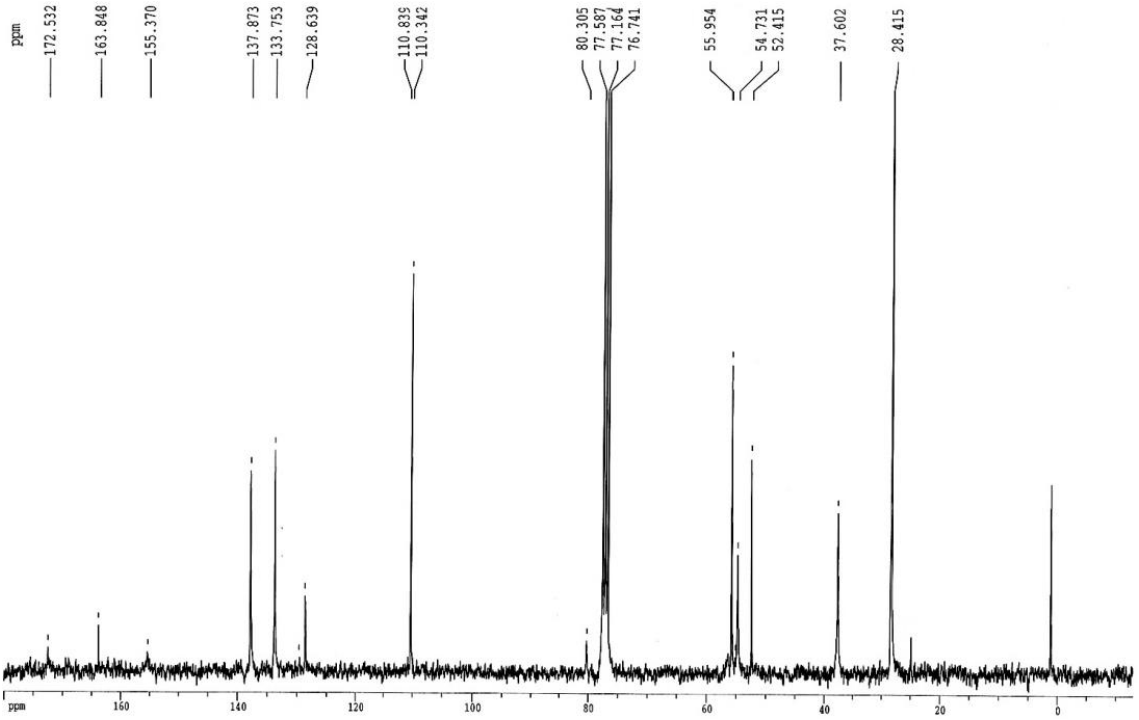

Boc-Tyr(3-B(OH)$_2$,Me)-OH (14)

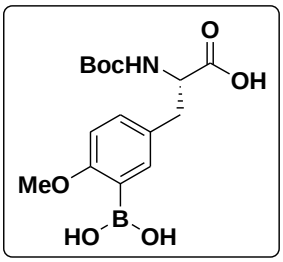

HPLC (λ = 220 nm)

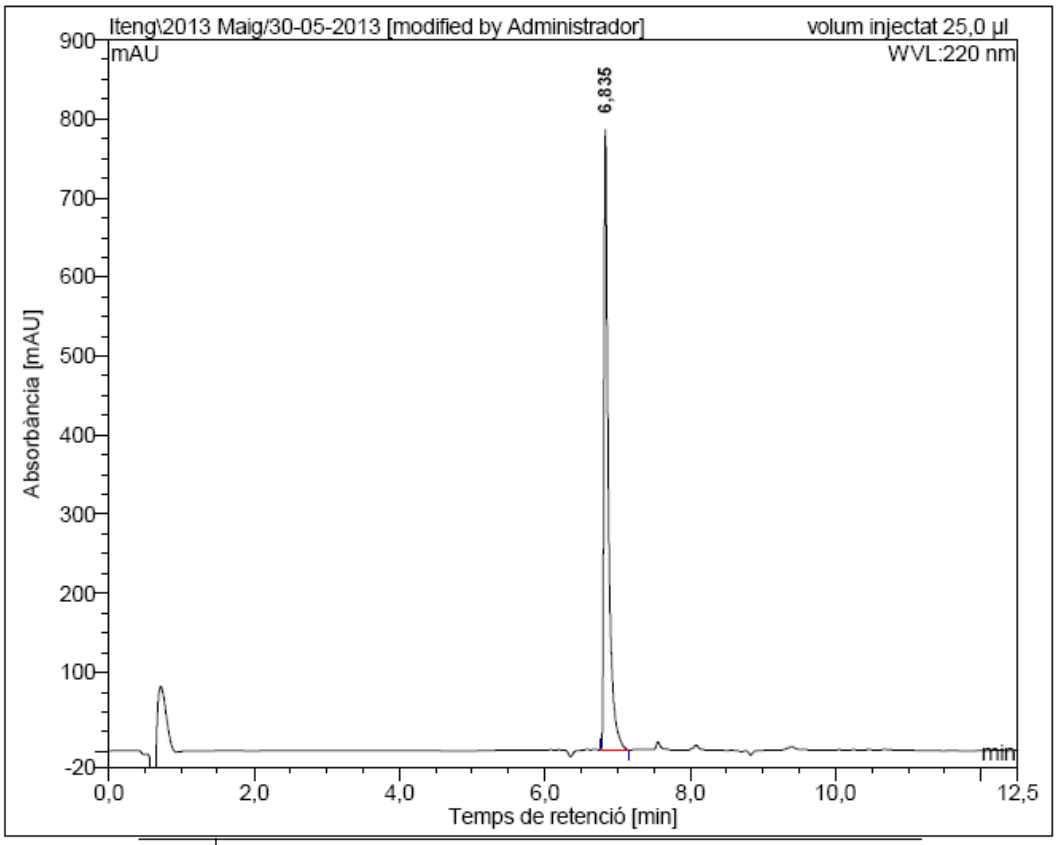

No.	Temps retenció min	alçada mAU	Area mAU*min	Area relativa %
1	6,84	785,715	55,818	100,00
Total:		785,715	55,818	100,00

^{1}H-NMR (400 MHz, $CDCl_3$) δ (ppm)

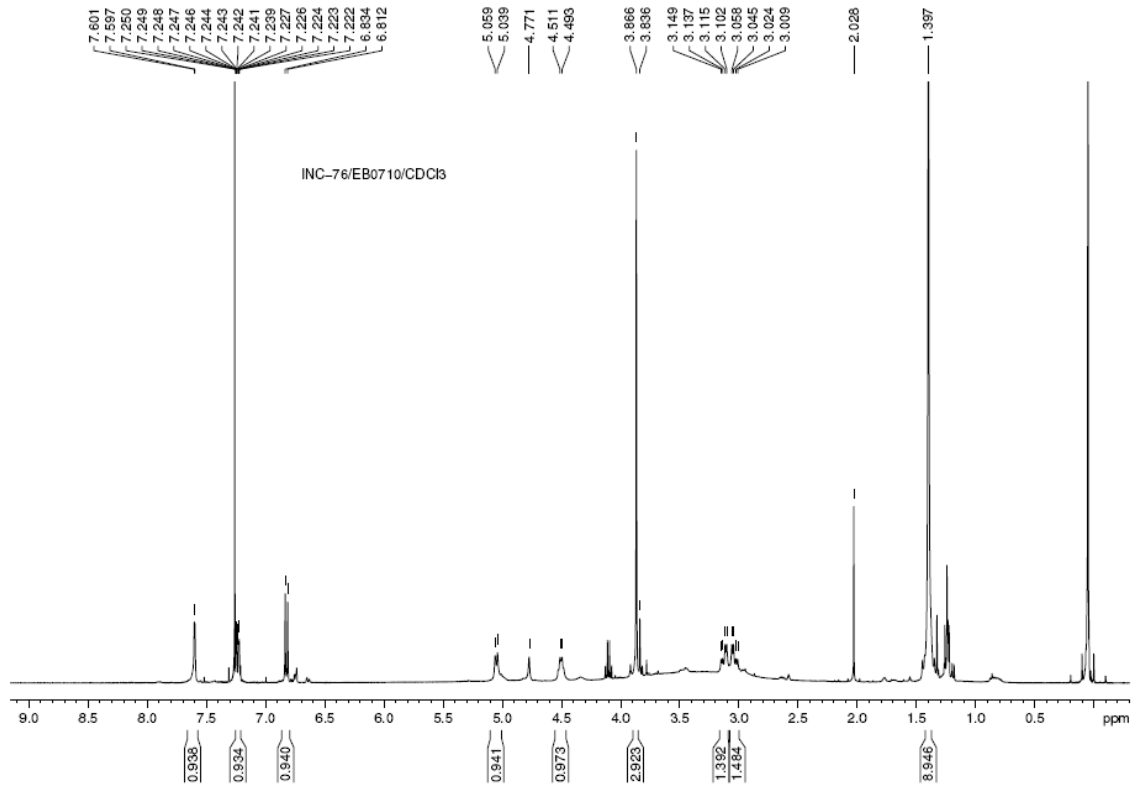

^{13}C-NMR (75 MHz, $CDCl_3$) δ (ppm)

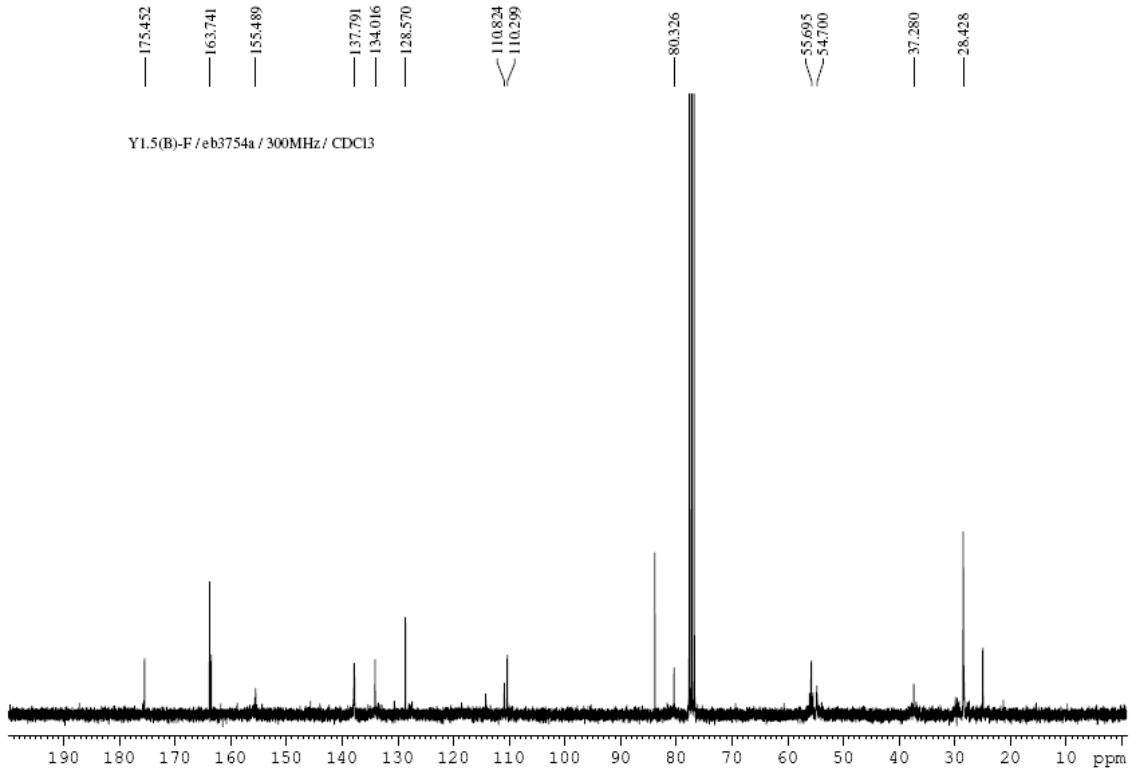

2. Linear peptides containing a 5-bromohistidine at the N-terminus

Iodopeptides

H-Lys-Lys-Leu-Tyr(3-I,Me)-Leu-Leu-NH_2

HPLC (λ = 220 nm)

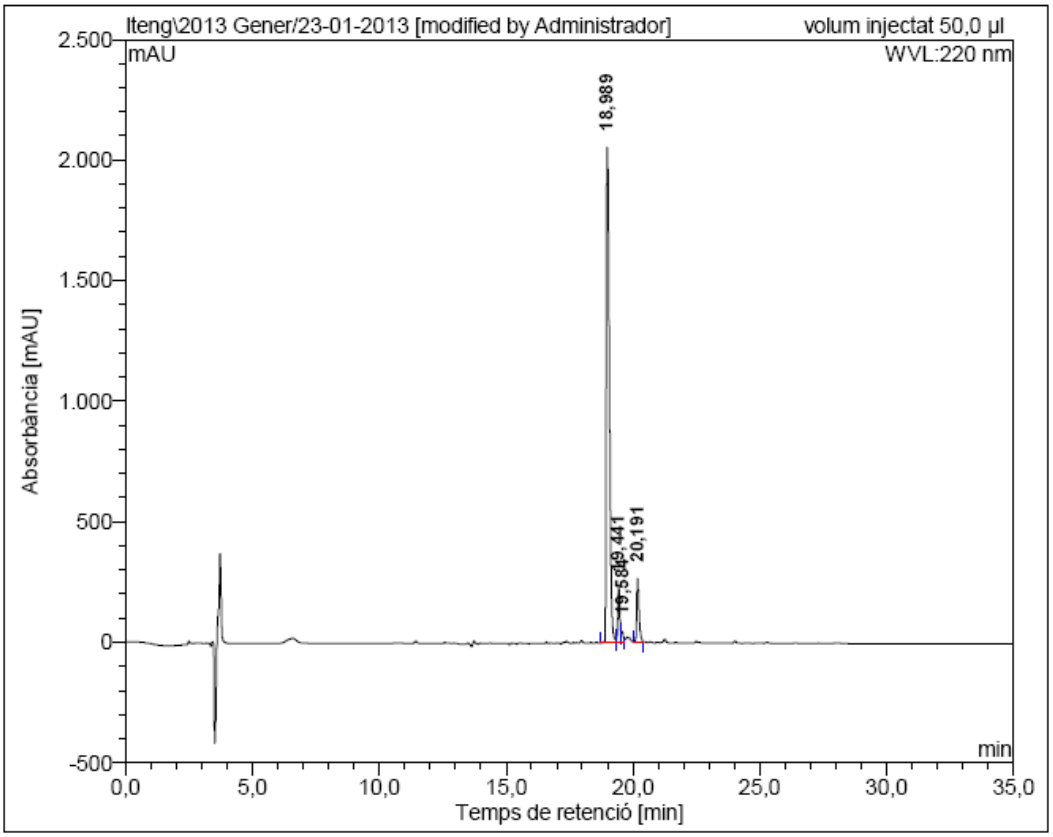

No.	Ret.Time (detected) min	Height mAU	Area mAU*min	Rel.Area %
1	18,99	2056,045	298,060	84,31
2	19,44	229,605	22,280	6,30
3	19,58	47,970	4,238	1,20
4	20,19	267,888	28,958	8,19
Total:		2601,509	353,535	100,00

ESI-MS *m/z*

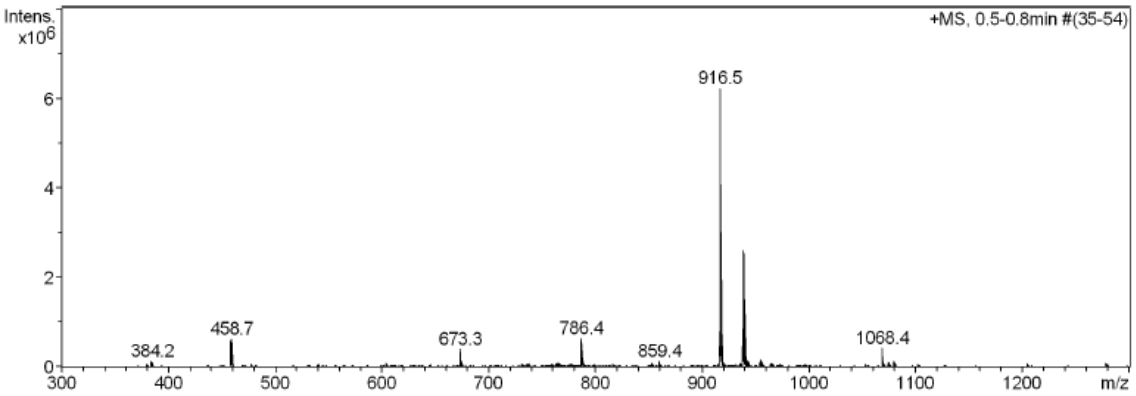

H-Lys-Lys-Leu-Tyr(3-I,Me)-NH_2

HPLC (λ = 220 nm)

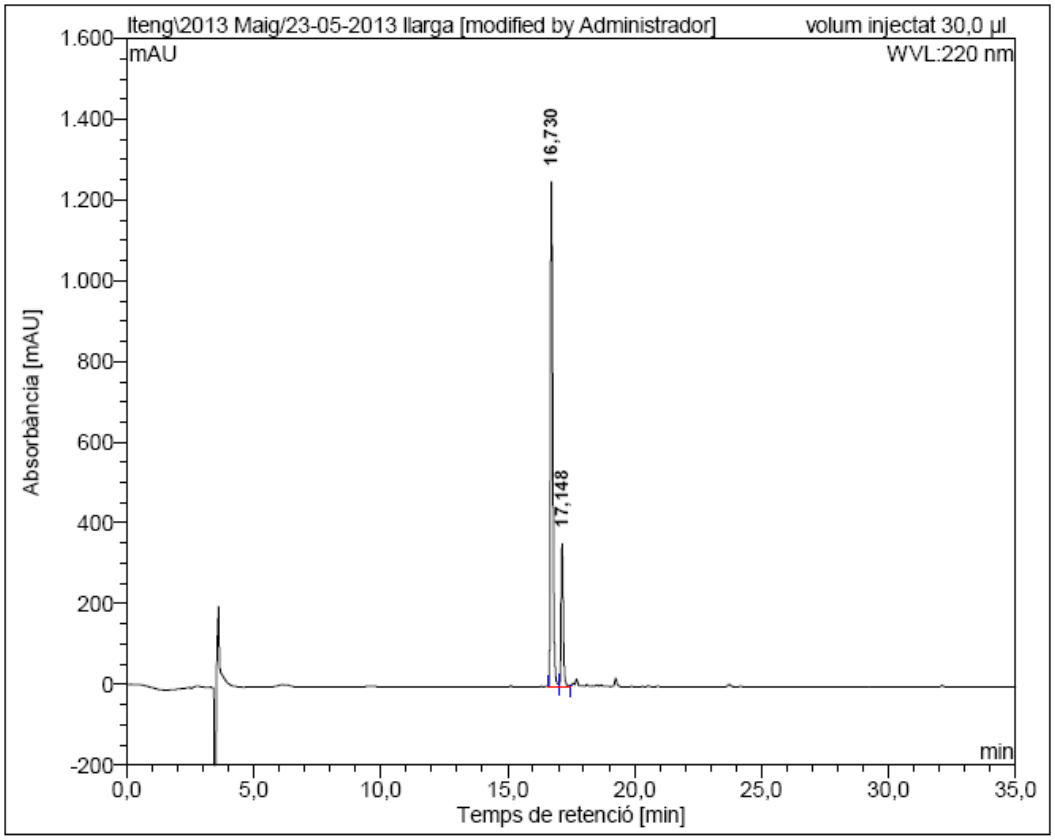

No.	Ret.Time (detected) min	Height mAU	Area mAU*min	Rel.Area %
1	16,73	1252,197	136,402	80,17
2	17,15	354,935	33,736	19,83
Total:		1607,131	170,138	100,00

ESI-MS *m/z*

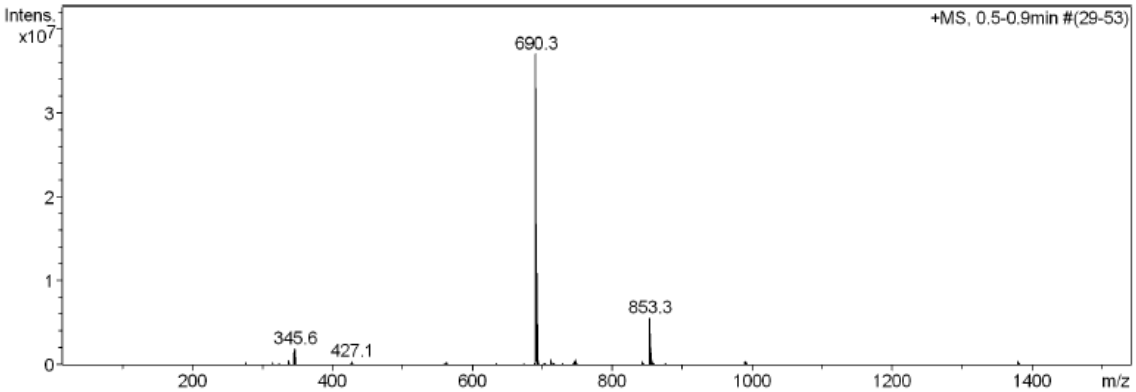

H-Leu-Tyr(3-I,Me)-NH_2

HPLC (λ = 220 nm)

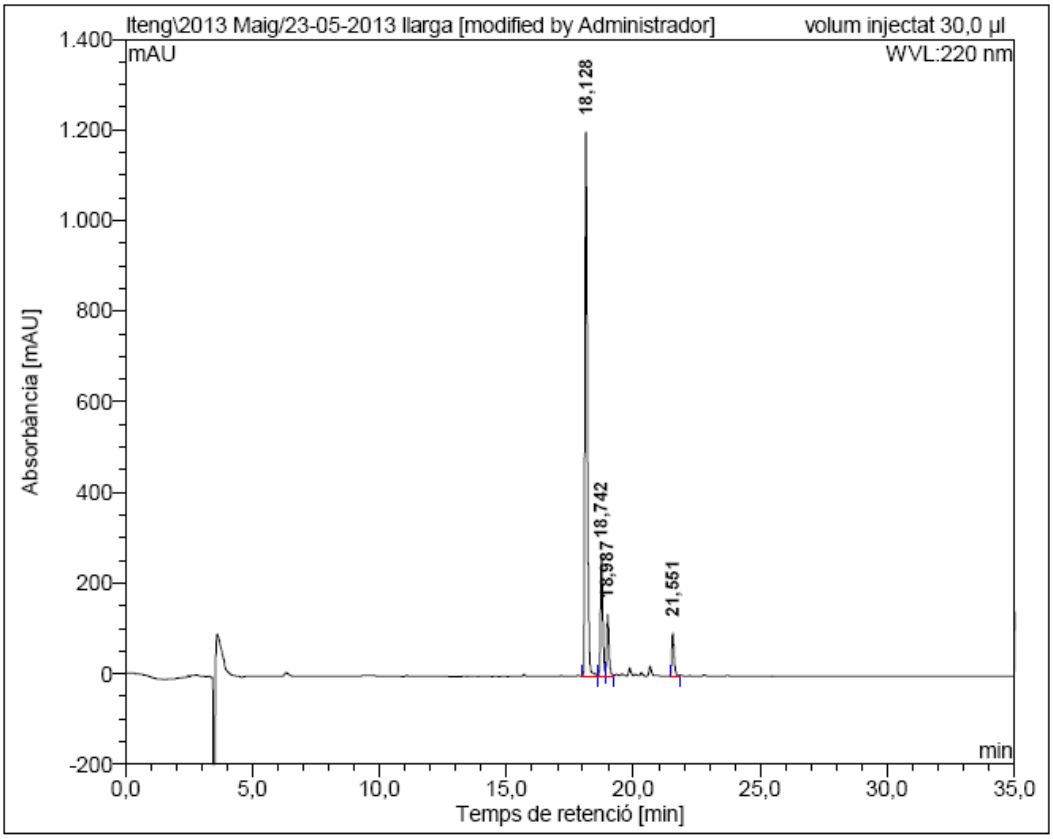

No.	Ret.Time (detected) min	Height mAU	Area mAU*min	Rel.Area %
1	18,13	1200,834	134,917	72,05
2	18,74	268,250	27,832	14,86
3	18,99	135,638	14,374	7,68
4	21,55	94,692	10,123	5,41
Total:		1699,414	187,247	100,00

ESI-MS *m/z*

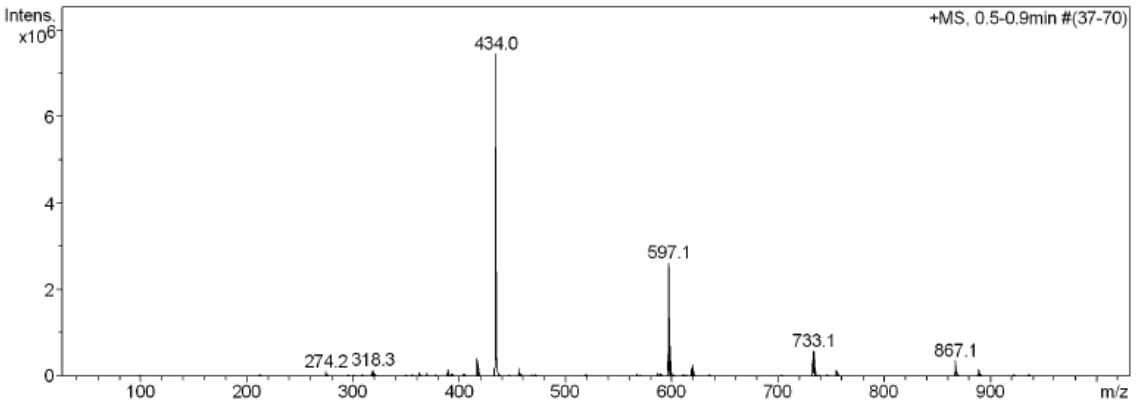

Boronopeptides

H-Lys-Lys-Leu-Tyr(3-B(OH)$_2$,Me)-Leu-Leu-NH$_2$

HPLC (λ = 220 nm)

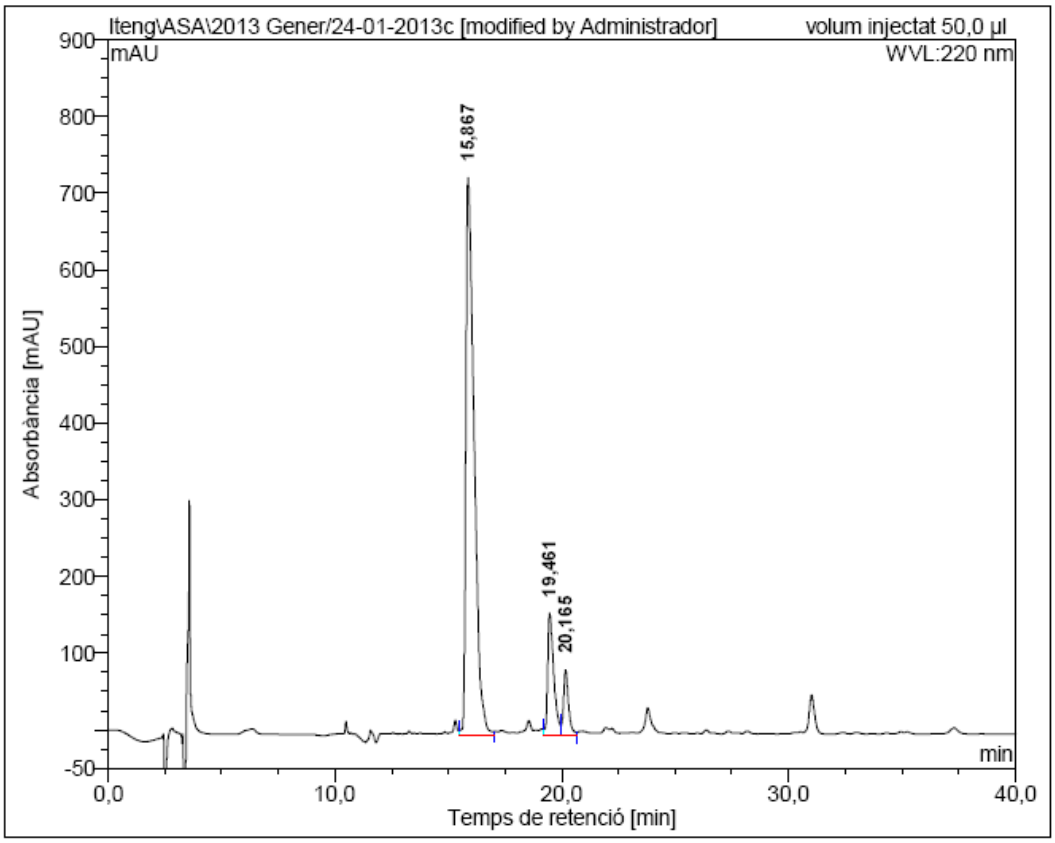

No.	Temps retenció min	alçada mAU	Area mAU*min	Area relativa %
1	15,87	726,276	305,360	81,20
2	19,46	157,853	49,202	13,08
3	20,16	84,035	21,497	5,72
Total:		968,164	376,059	100,00

ESI-MS *m/z*

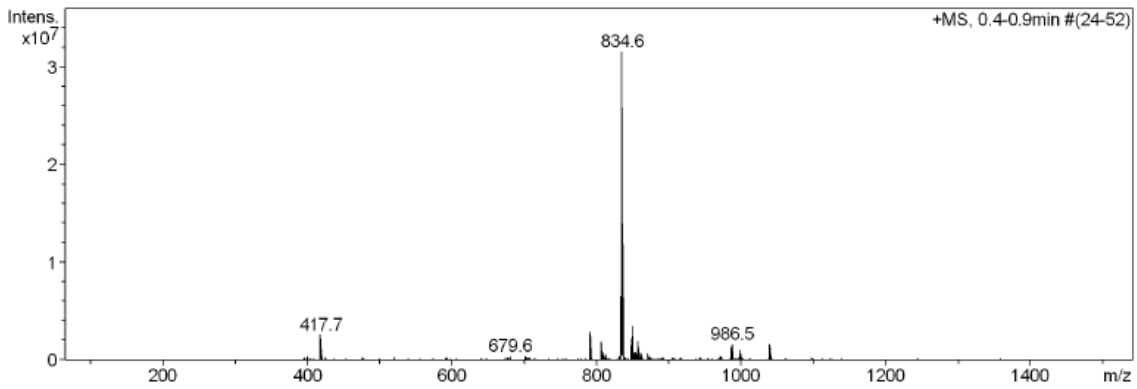

H-Lys-Lys-Leu-Tyr(3-B(OH)$_2$,Me)-NH$_2$

HPLC (λ = 220 nm)

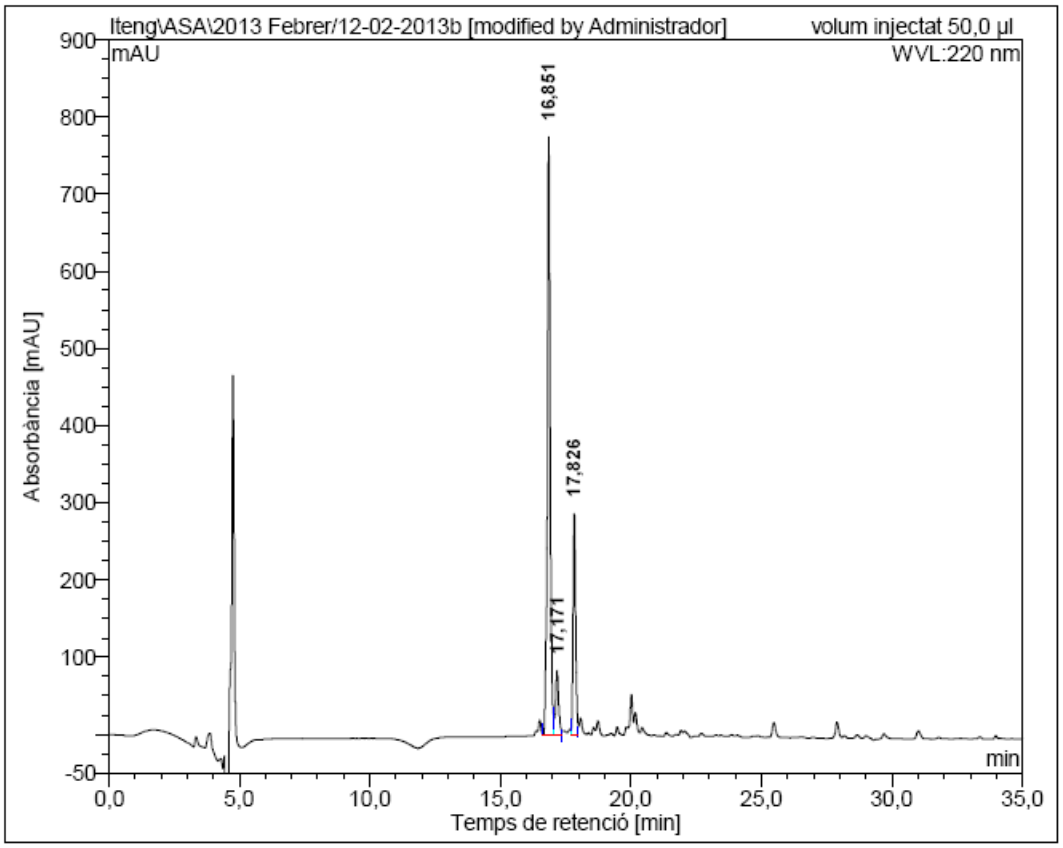

No.	Temps retenció min	alçada mAU	Area mAU*min	Area relativa %
1	16,85	774,615	99,643	69,39
2	17,17	83,236	10,964	7,64
3	17,83	286,322	32,982	22,97
Total:		1144,173	143,589	100,00

ESI-MS *m/z*

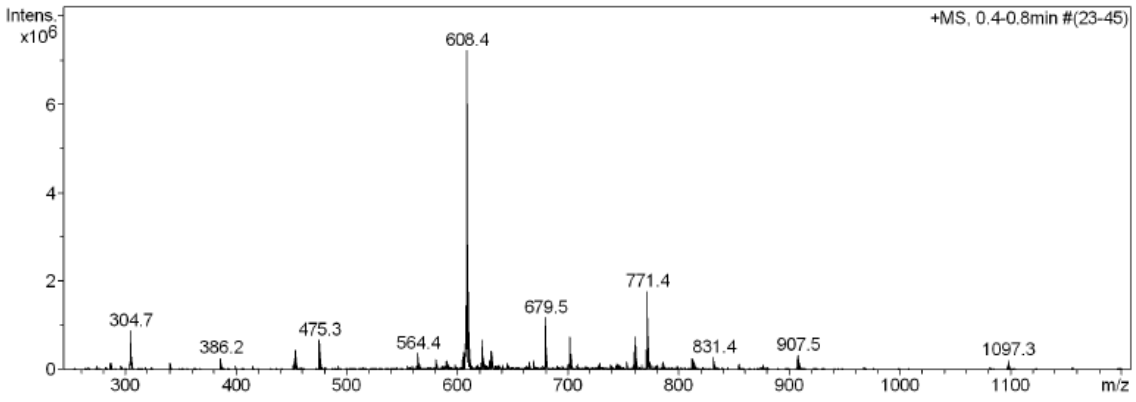

H-Leu-Tyr(3-B(OH)$_2$,Me)-NH$_2$

HPLC (λ = 220 nm)

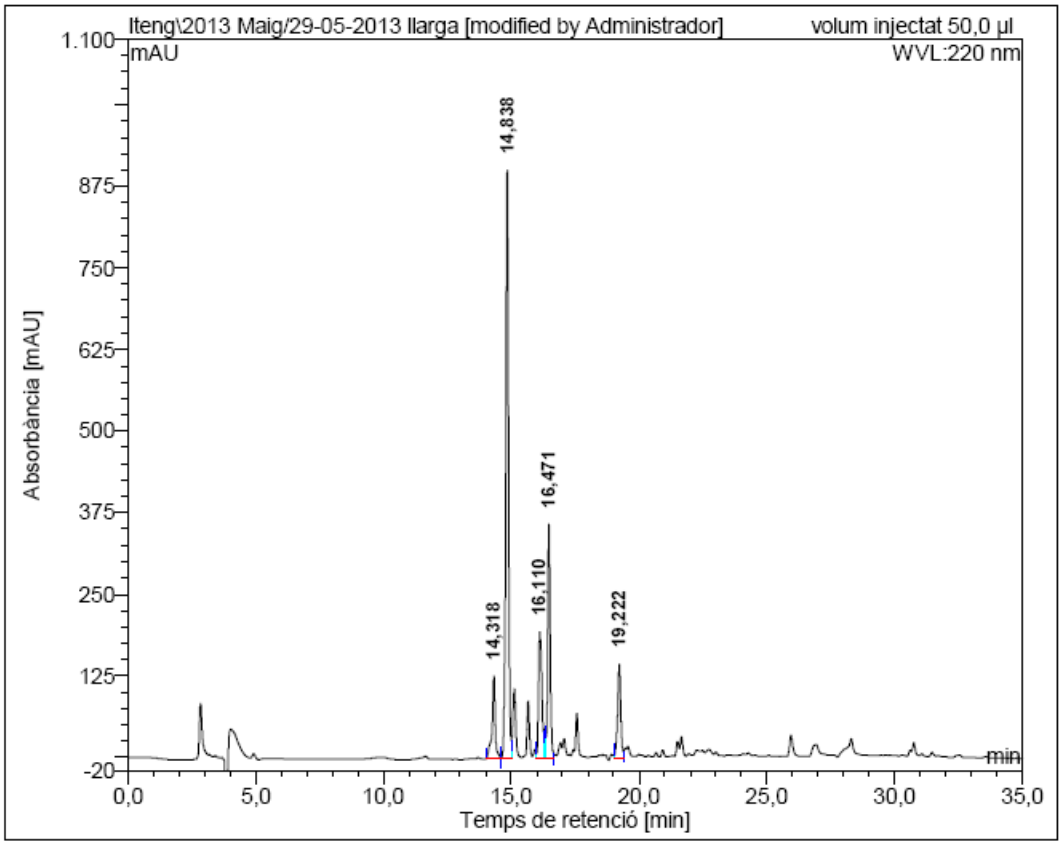

No.	Temps retenció min	alçada mAU	Area mAU*min	Area relativa %
1	14,32	127,195	18,514	8,52
2	14,84	901,488	107,875	49,64
3	16,11	194,294	29,476	13,56
4	16,47	359,536	40,377	18,58
5	19,22	144,411	21,067	9,69
Total:		1726,924	217,308	100,00

ESI-MS *m/z*

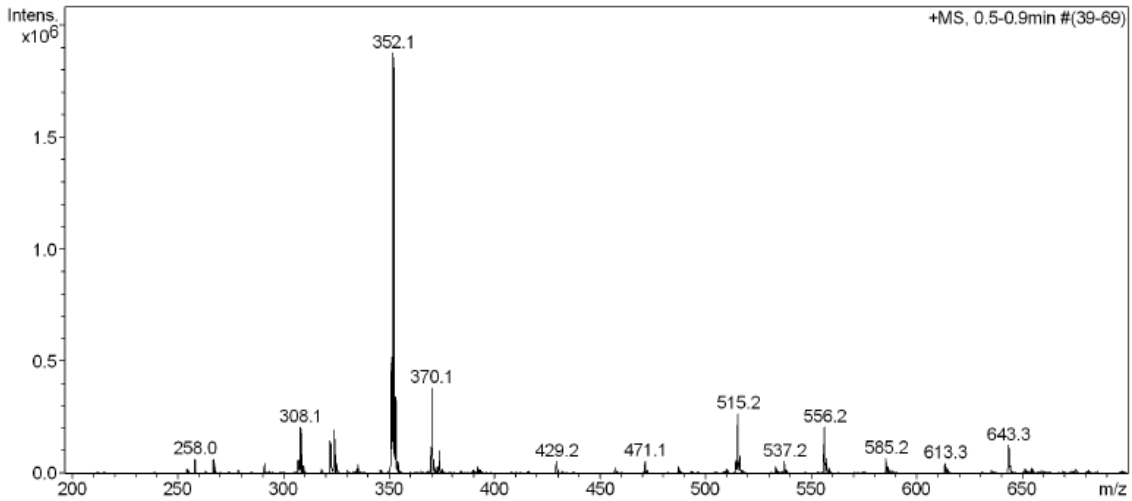

Linear peptides 6, 11 and 12

H-His(5-Br)-Lys-Lys-Leu-Tyr(3-B(OH)$_2$,Me)-Leu-Leu-NH$_2$ (6)

HPLC (λ = 220 nm)

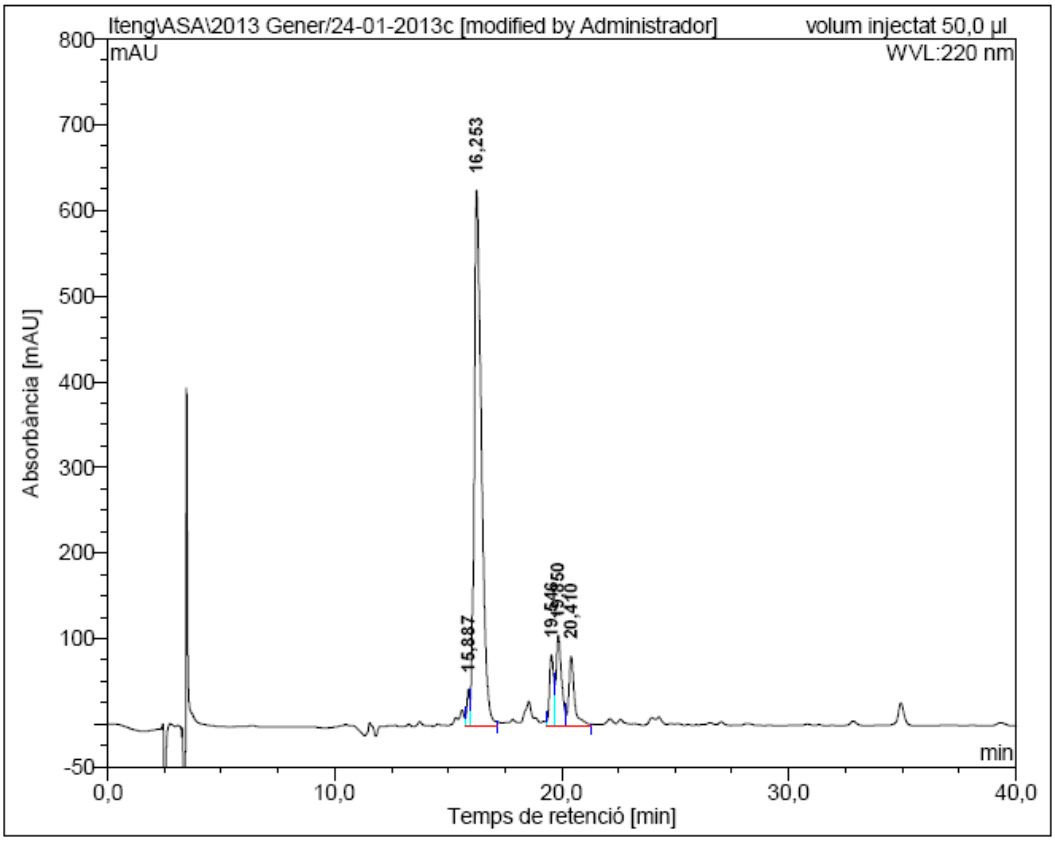

No.	Temps retenció min	alçada mAU	Area mAU*min	Area relativa %
1	15,89	43,379	6,515	2,08
2	16,25	625,846	233,110	74,50
3	19,55	83,433	18,835	6,02
4	19,85	106,261	30,236	9,66
5	20,41	81,673	24,219	7,74
Total:		940,592	312,915	100,00

ESI-MS *m/z*

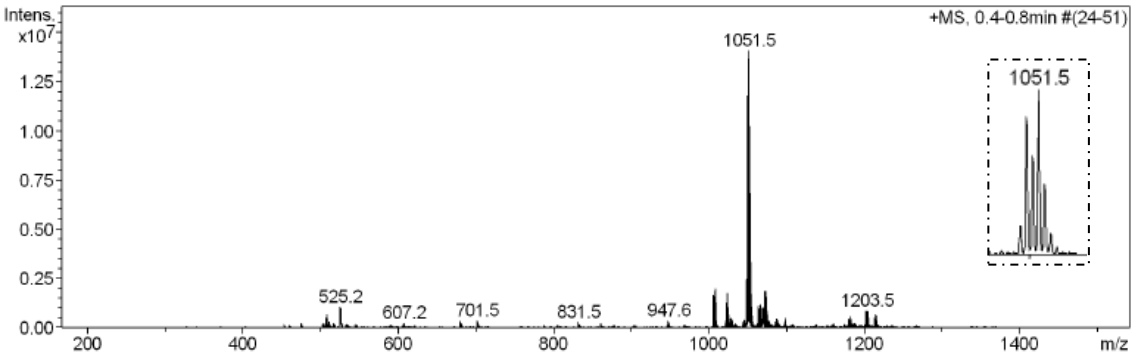

H-His(5-Br)-Lys-Lys-Leu-Tyr(3-B(OH)$_2$,Me)-NH$_2$ (11)

HPLC (λ = 220 nm)

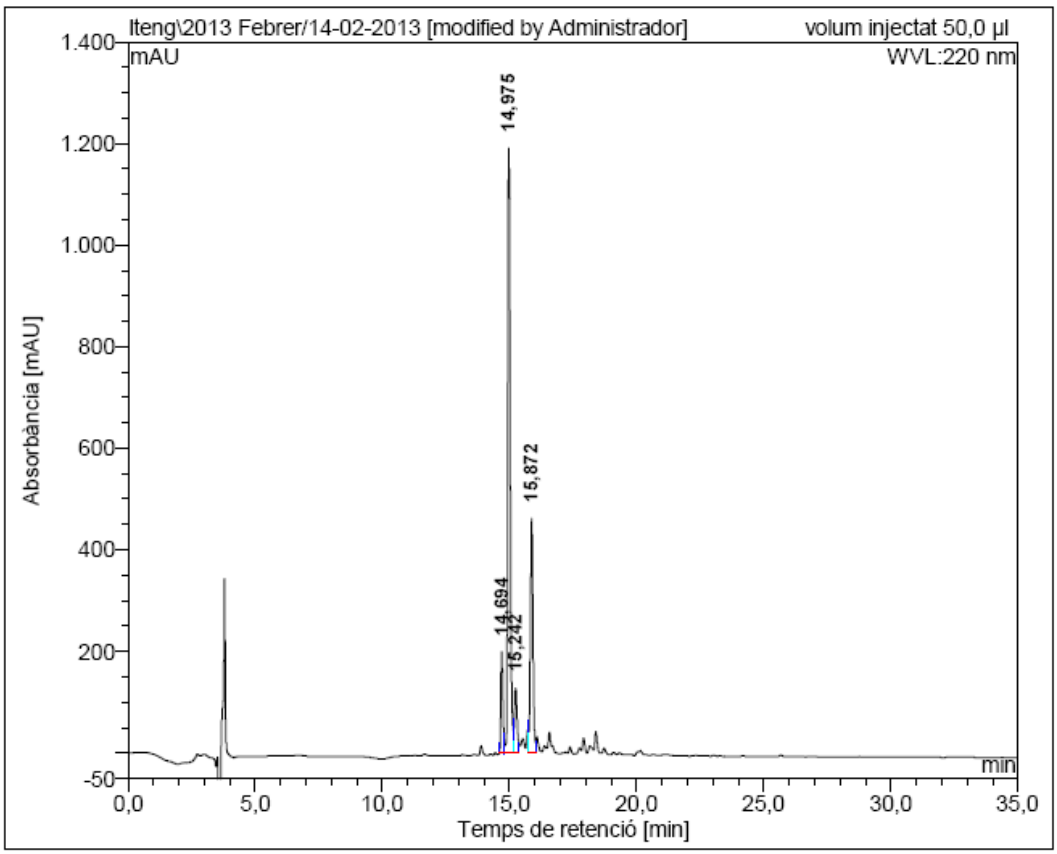

No.	mps retenc min	alçada mAU	Area mAU*min	Area relativa %
1	14,69	198,242	18,914	8,74
2	14,97	1189,635	129,925	60,07
3	15,24	127,395	14,461	6,69
4	15,87	462,216	52,995	24,50
Total:		1977,488	216,294	100,00

ESI-MS *m/z*

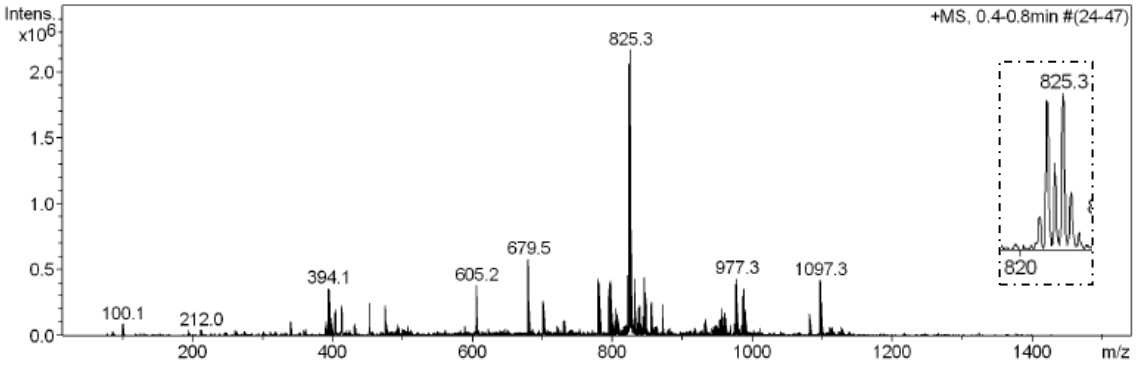

H-His(5-Br)-Leu-Tyr(3-B(OH)$_2$,Me)-NH$_2$ (12)

HPLC (λ = 220 nm)

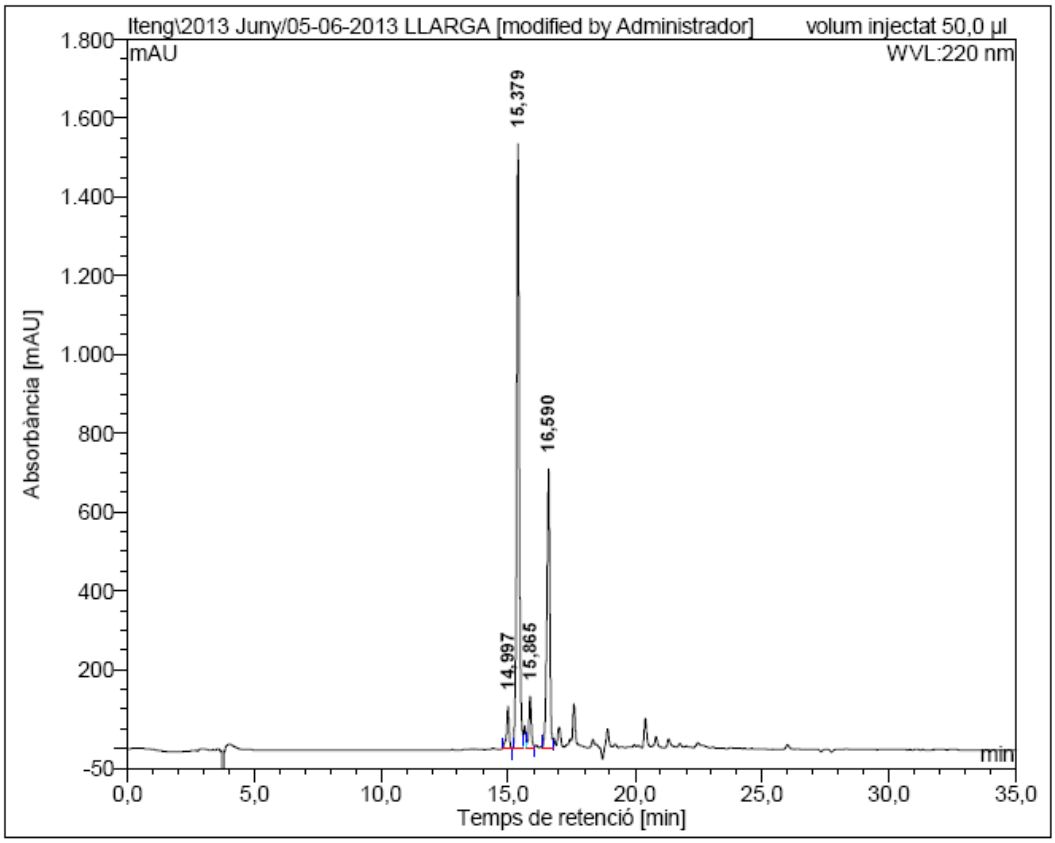

No.	Temps retenció min	alçada mAU	Area mAU*min	Area relativa %
1	15,00	107,126	12,474	4,14
2	15,38	1535,282	180,548	59,95
3	15,87	132,738	14,889	4,94
4	16,59	708,665	93,272	30,97
Total:		2483,811	301,183	100,00

ESI-MS *m/z*

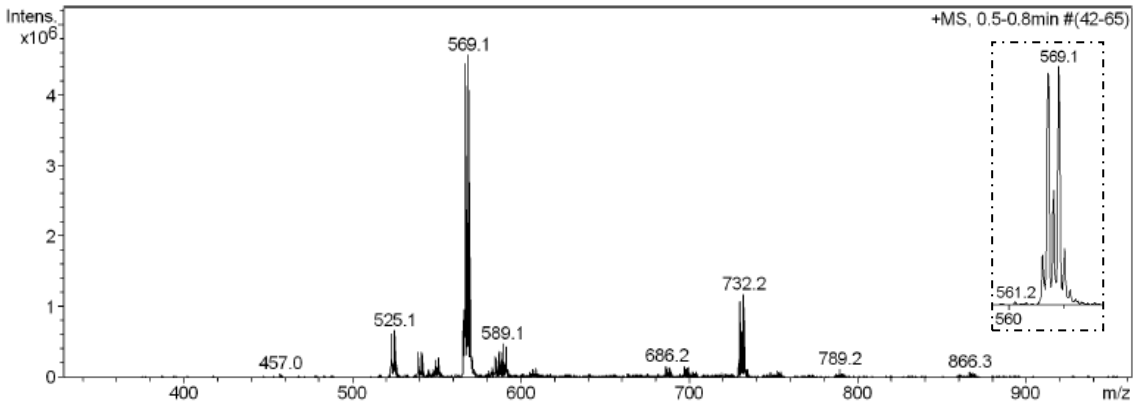

3. Linear peptides containing a 5-bromohistidine at the C-terminus

Linear peptides 15, 18 and 19

H-Tyr(3-B(OH)$_2$,Me)-Lys-Lys-Leu-His(5-Br)-Leu-Leu-NH$_2$ (15)

HPLC (λ = 220 nm)

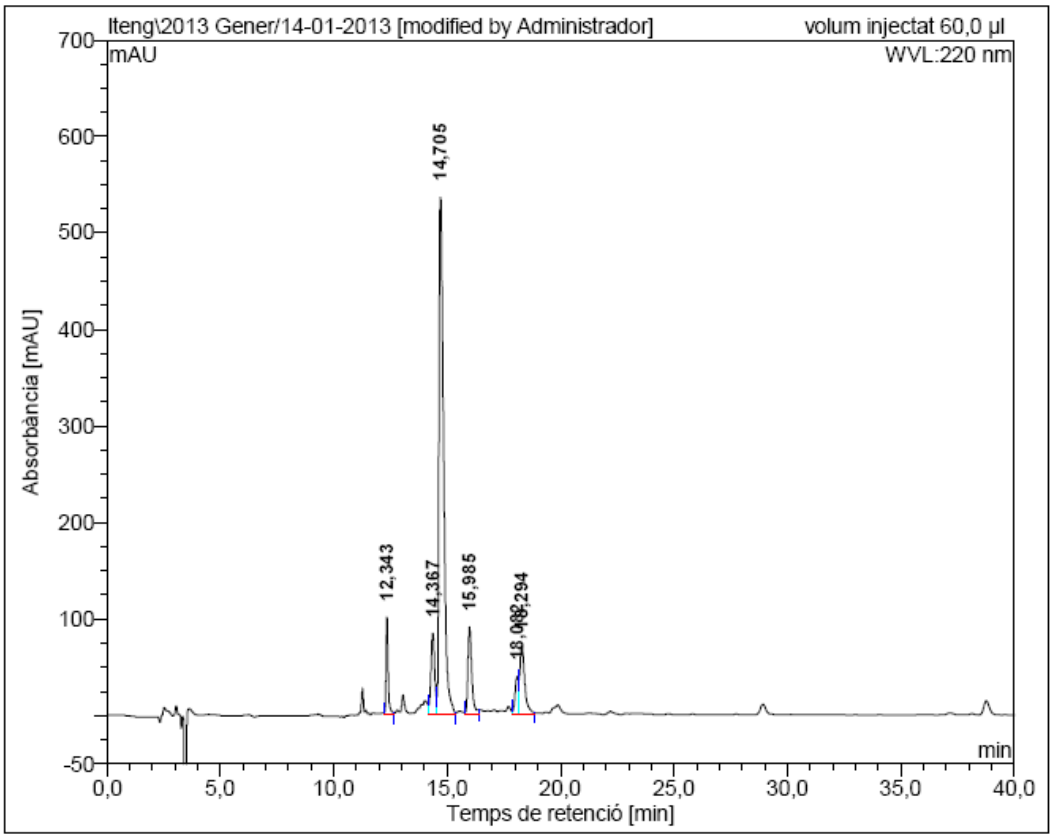

No.	Ret.Time (detected) min	Height mAU	Area mAU*min	Rel.Area %
1	12,34	100,069	10,617	5,52
2	14,37	82,945	15,852	8,24
3	14,70	535,044	124,600	64,73
4	15,99	89,563	17,507	9,10
5	18,08	37,962	6,311	3,28
6	18,29	70,759	17,590	9,14
Total:		916,342	192,478	100,00

ESI-MS *m/z*

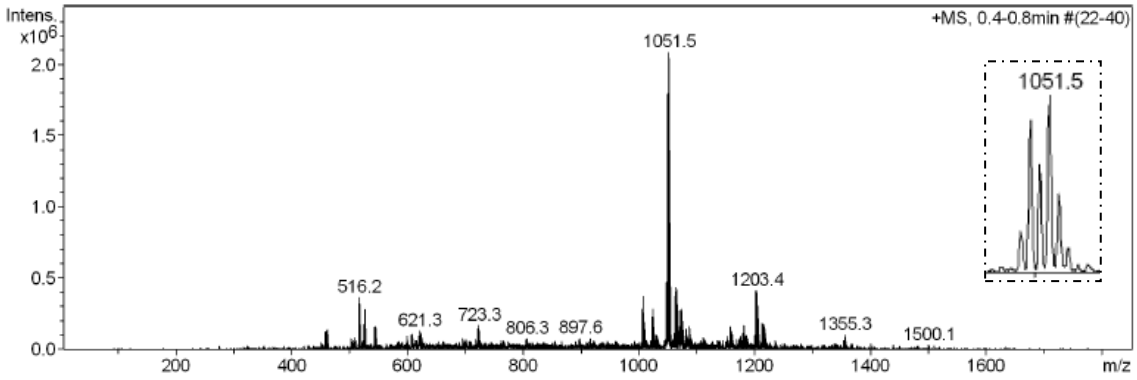

H-Tyr(3-B(OH)$_2$,Me)-Lys-Lys-Leu-His(5-Br)-NH$_2$ (18)

HPLC (λ = 220 nm)

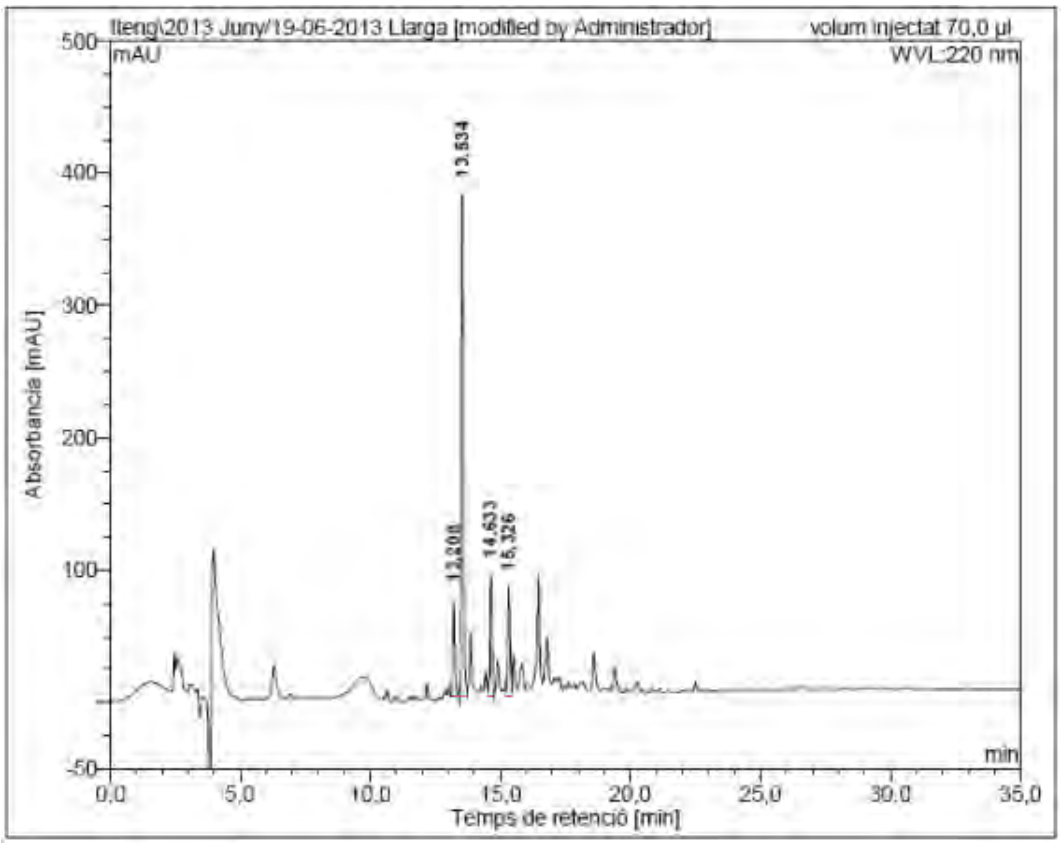

No.	Temps retenció min	alçada mAU	Area mAU*min	Area relativa %
1	13,21	73,766	6,734	11,83
2	13,53	379,129	33,445	58,73
3	14,63	92,186	8,702	15,28
4	15,33	82,561	8,066	14,16
Total:		627,643	56,947	100,00

ESI-MS *m/z*

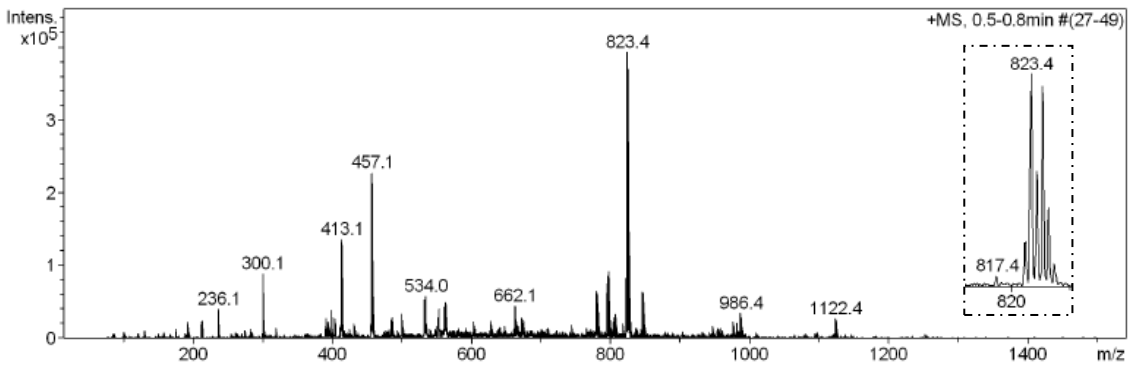

H-Tyr(3-B(OH)$_2$,Me)-Leu-His(5-Br)-NH$_2$ (19)

HPLC (λ = 220 nm)

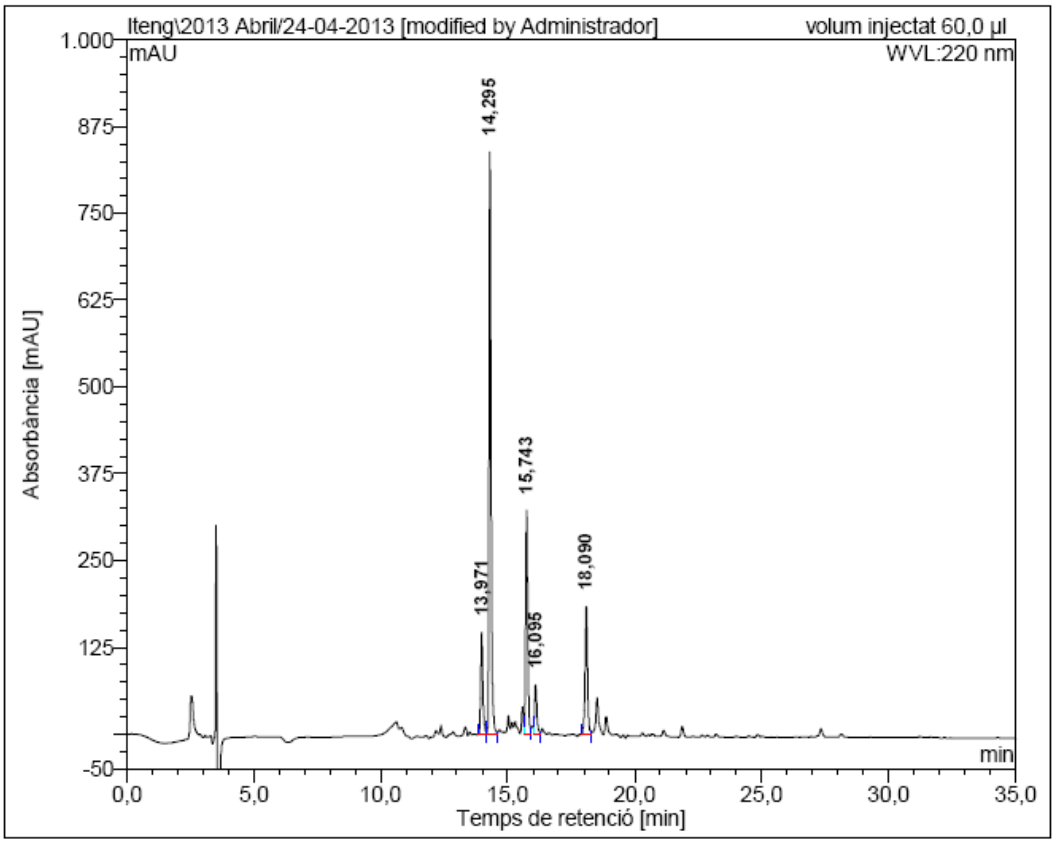

No.	Temps retenció min	alçada mAU	Area mAU*min	Area relativa %
1	13,97	147,473	14,483	9,49
2	14,29	838,971	79,145	51,86
3	15,74	322,926	30,223	19,80
4	16,10	72,078	7,899	5,18
5	18,09	184,247	20,861	13,67
Total:		1565,695	152,612	100,00

ESI-MS *m/z*

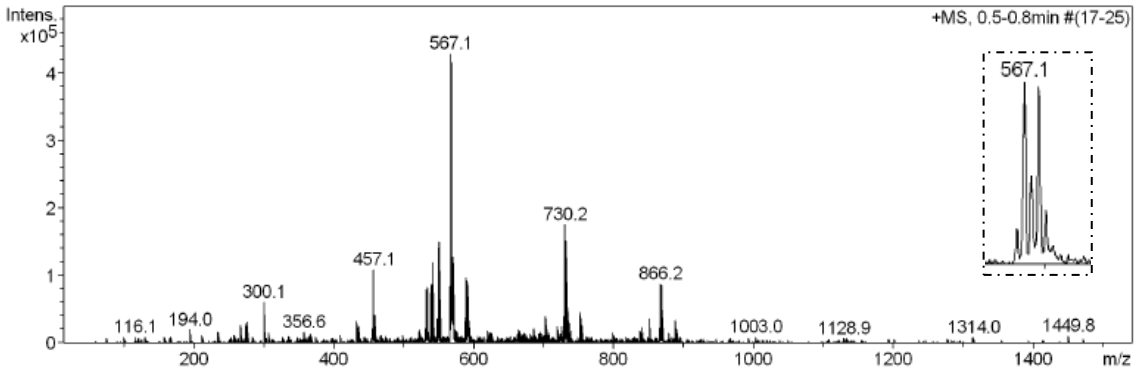

4. Biaryl cyclic peptides

Biaryl cyclic peptide BPC782

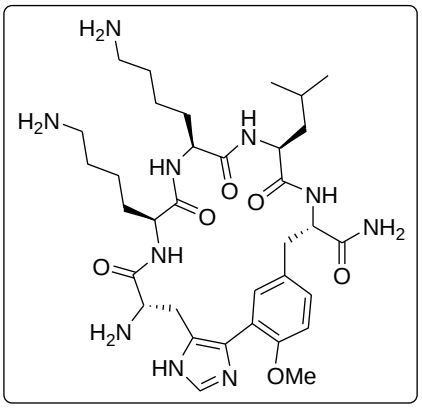

Crude peptide

HPLC (λ = 220 nm)

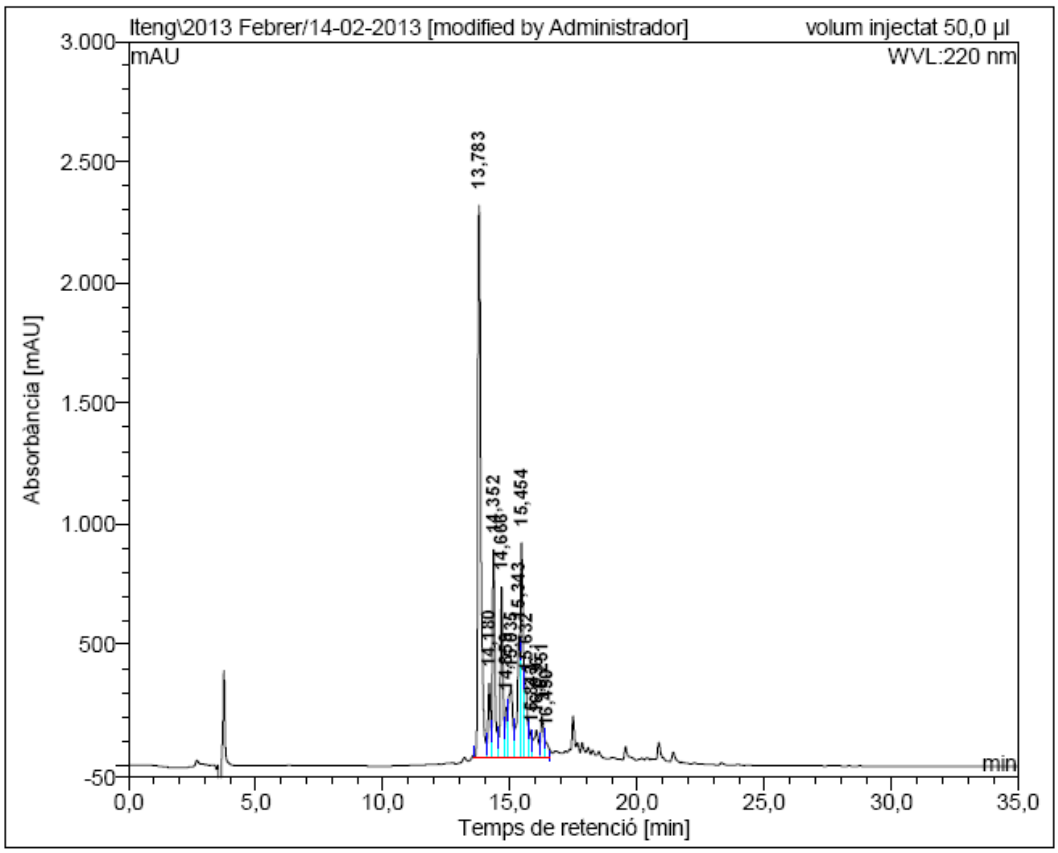

No.	mps retenc min	alçada mAU	Area mAU*min	Area relativa %
1	13,78	2285,235	309,241	35,08
2	14,18	305,579	34,639	3,93
3	14,35	860,249	98,844	11,21
4	14,67	705,102	80,114	9,09
5	14,86	207,490	20,139	2,28
6	15,04	296,594	60,882	6,91
7	15,34	501,548	55,174	6,26
8	15,45	889,294	109,101	12,38
9	15,63	290,360	41,773	4,74
10	15,84	74,409	13,242	1,50
11	16,04	112,437	24,083	2,73
12	16,25	170,636	23,122	2,62
13	16,45	56,716	11,227	1,27
Total:		6755,648	881,581	100,00

ESI-MS *m/z*

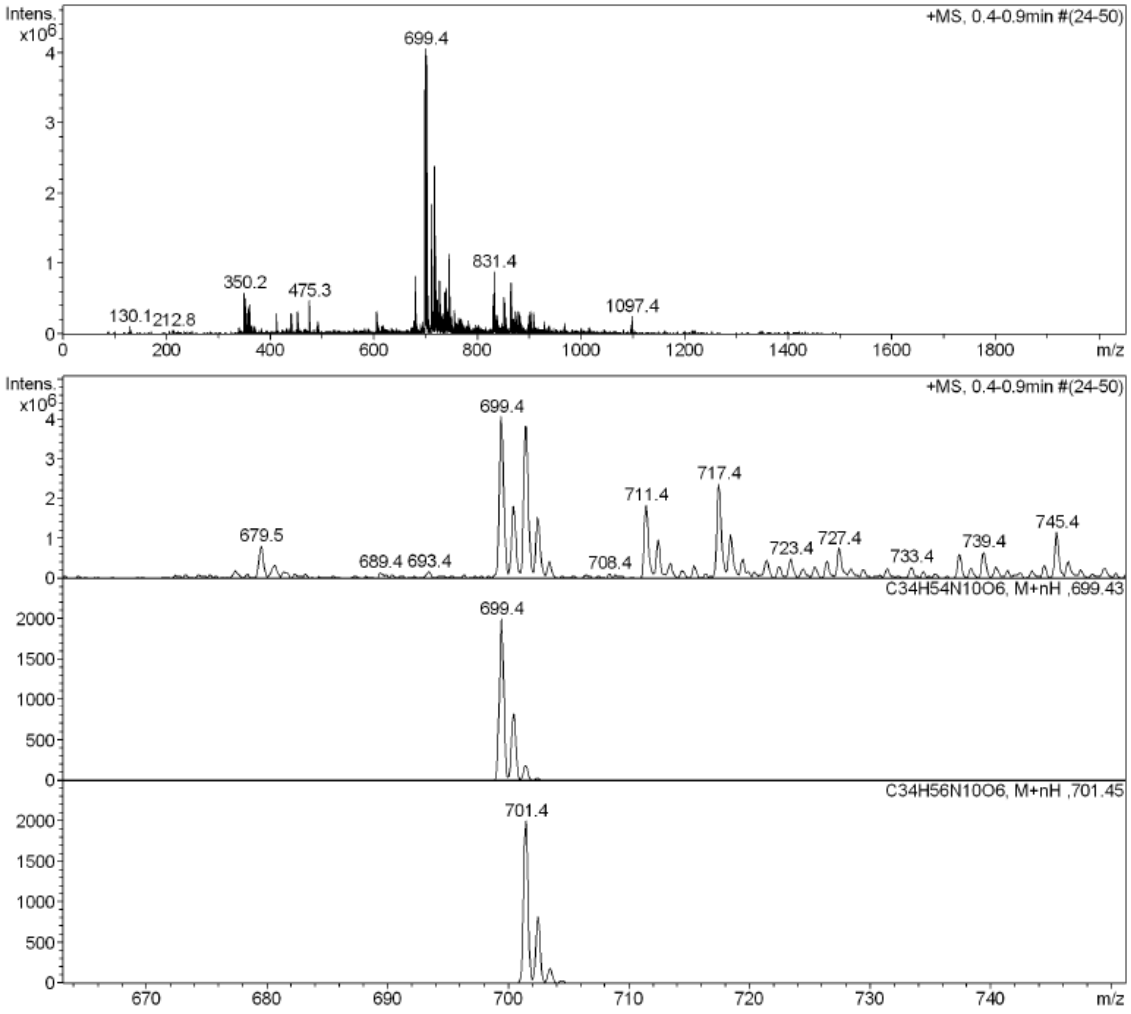
Intens.
x10^6
+MS, 0.4-0.9min #(24-50)
699.4
831.4
350.2
475.3
130.1
212.8
1097.4
m/z
679.5
689.4
693.4
708.4
711.4
717.4
723.4
727.4
733.4
739.4
745.4
C34H54N10O6, M+nH ,699.43
C34H56N10O6, M+nH ,701.45
701.4

Purified peptide

HPLC (λ = 220 nm)

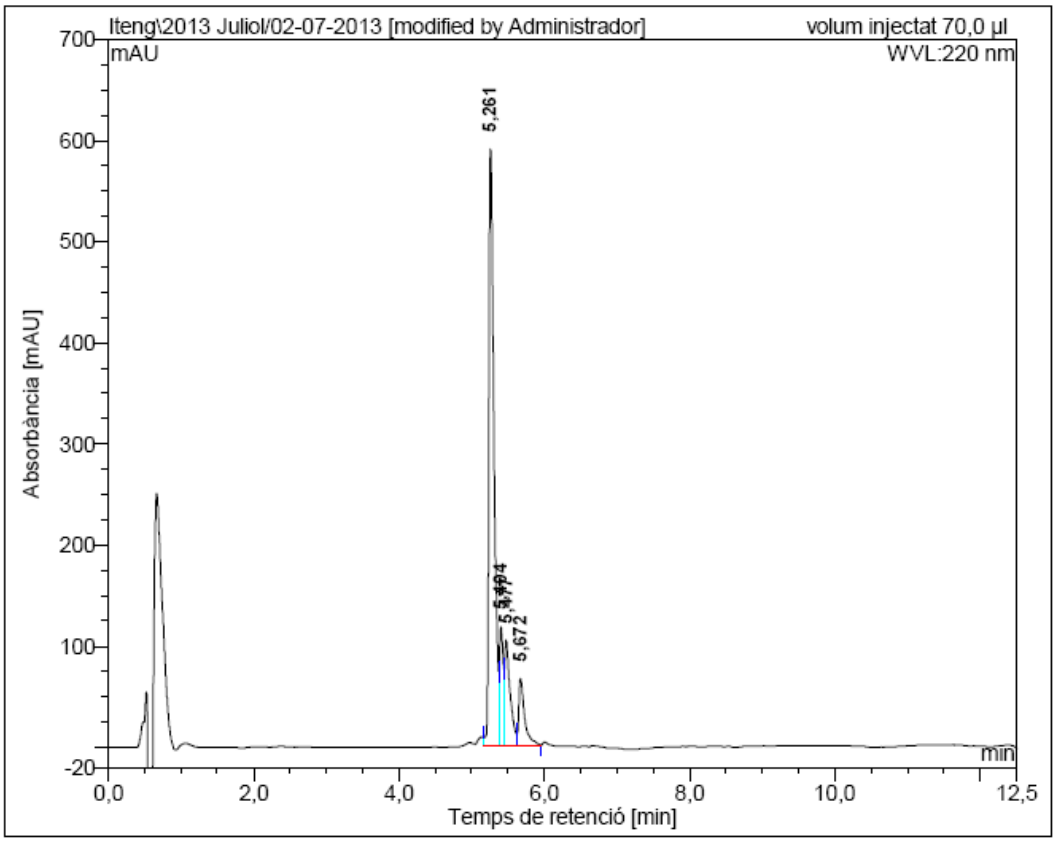

No.	Temps retenció min	alçada mAU	Area mAU*min	Area relativa %
1	5,26	589,198	48,420	68,26
2	5,40	116,763	7,171	10,11
3	5,48	103,711	9,207	12,98
4	5,67	65,509	6,136	8,65
Total:		875,180	70,934	100,00

ESI-MS *m/z*

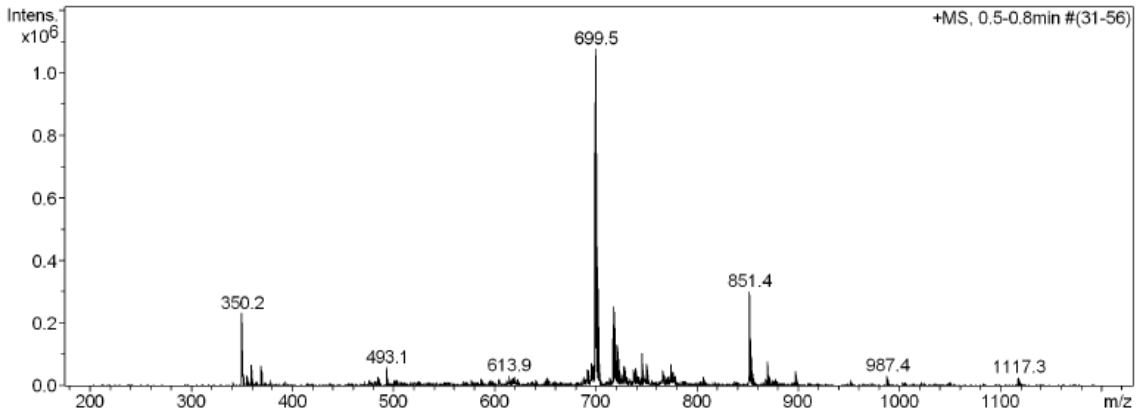

HRMS (ESI) *m/z*

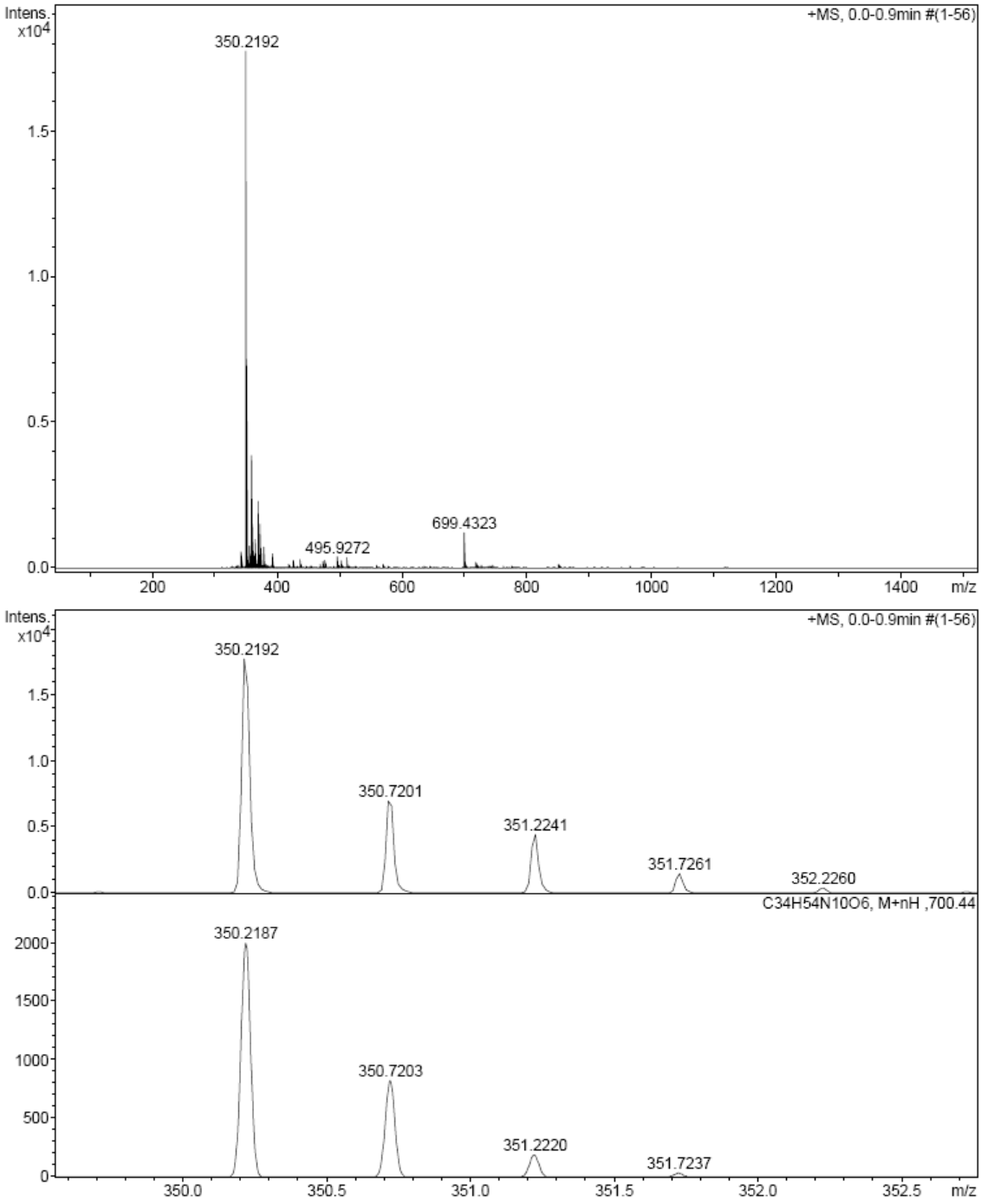
Intens.
x10^4
+MS, 0.0-0.9min #(1-56)
350.2192
699.4323
495.9272
m/z
350.2192
350.7201
351.2241
351.7261
352.2260
C34H54N10O6, M+nH ,700.44
350.2187
350.7203
351.2220
351.7237

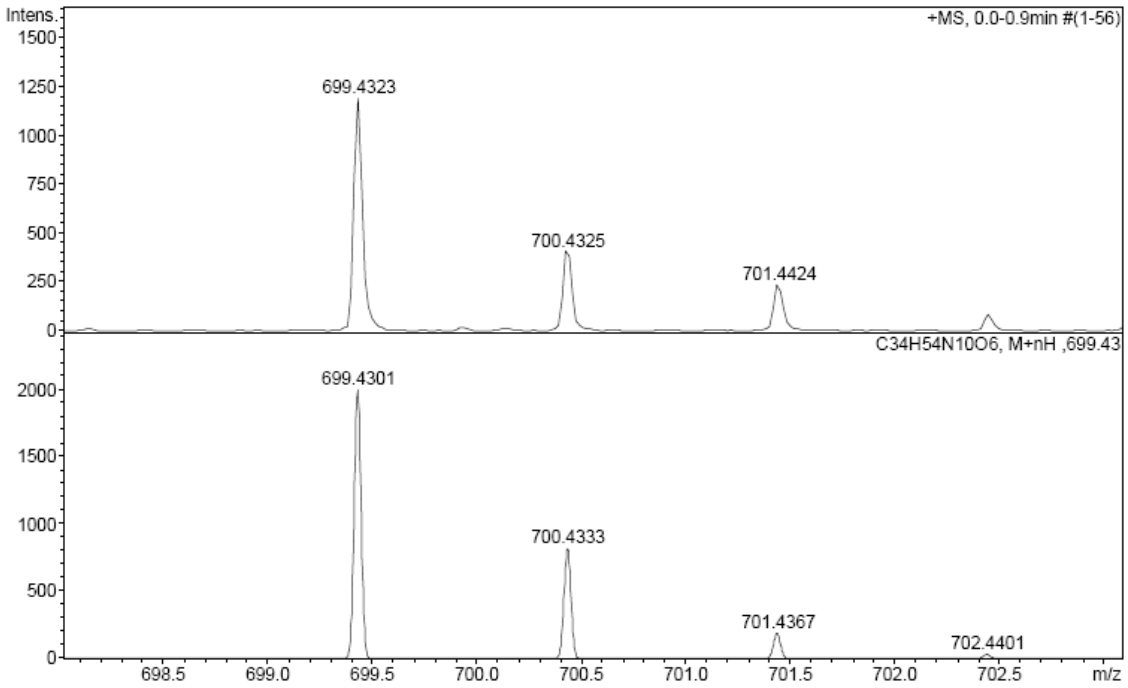
Intens.
+MS, 0.0-0.9min #(1-56)
699.4323
700.4325
701.4424
C34H54N10O6, M+nH ,699.43
699.4301
700.4333
701.4367
702.4401
m/z

Biaryl cyclic peptide BPC784

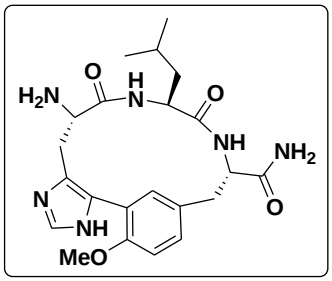

Crude peptide

HPLC (λ = 220 nm)

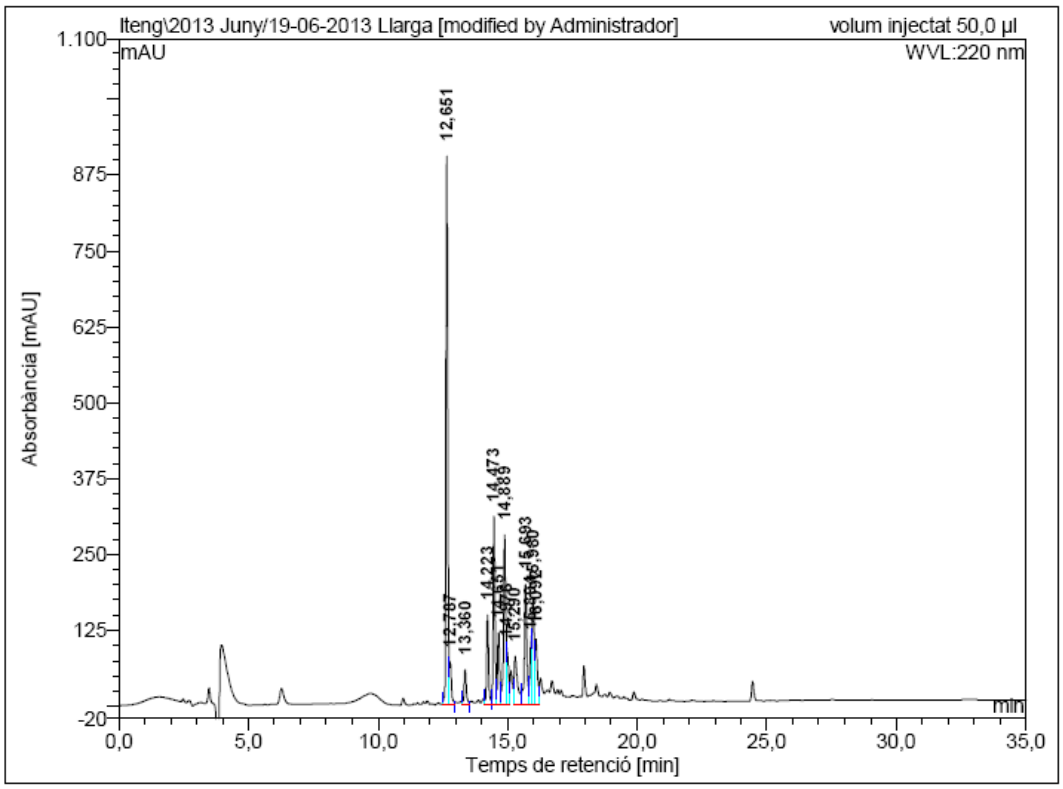

No.	Temps retenció min	alçada mAU	Area mAU*min	Area relativa %
1	12,65	904,411	73,486	30,28
2	12,79	70,868	5,979	2,46
3	13,36	58,457	5,664	2,33
4	14,22	148,459	13,287	5,47
5	14,47	311,026	26,988	11,12
6	14,65	119,023	10,866	4,48
7	14,89	280,246	28,659	11,81
8	14,98	87,448	6,717	2,77
9	15,29	80,019	12,739	5,25
10	15,69	198,139	21,538	8,87
11	15,89	98,573	8,423	3,47
12	15,98	177,269	16,759	6,90
13	16,09	108,732	11,620	4,79
Total:		2642,672	242,725	100,00

ESI-MS *m/z*

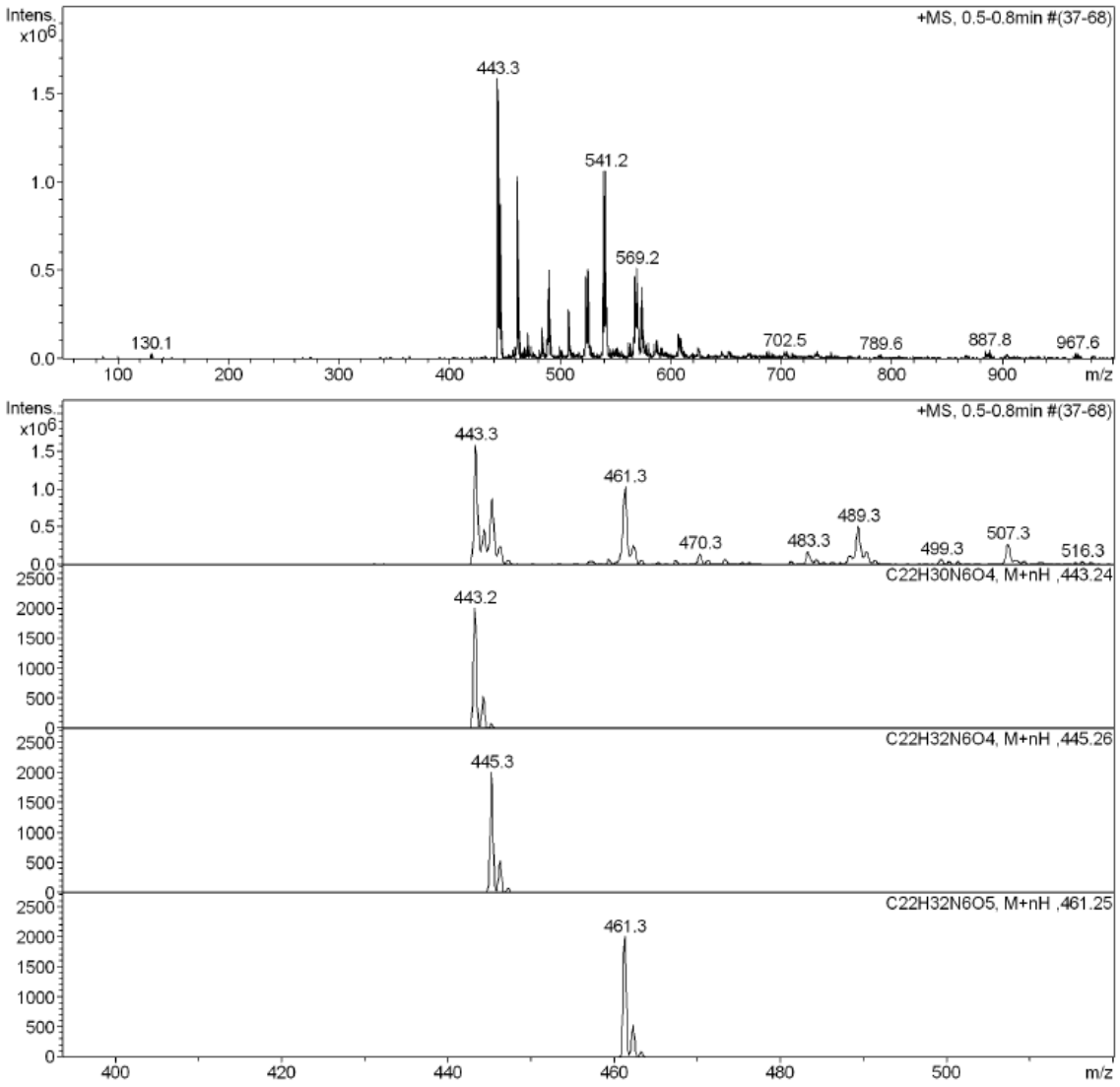
Intens.
x10^6
+MS, 0.5-0.8min #(37-68)
443.3
541.2
569.2
130.1
702.5
789.6
887.8
967.6
m/z
461.3
489.3
470.3
483.3
499.3
507.3
516.3
C22H30N6O4, M+nH ,443.24
443.2
C22H32N6O4, M+nH ,445.26
445.3
C22H32N6O5, M+nH ,461.25
461.3

Purified peptide

HPLC (λ = 220 nm)

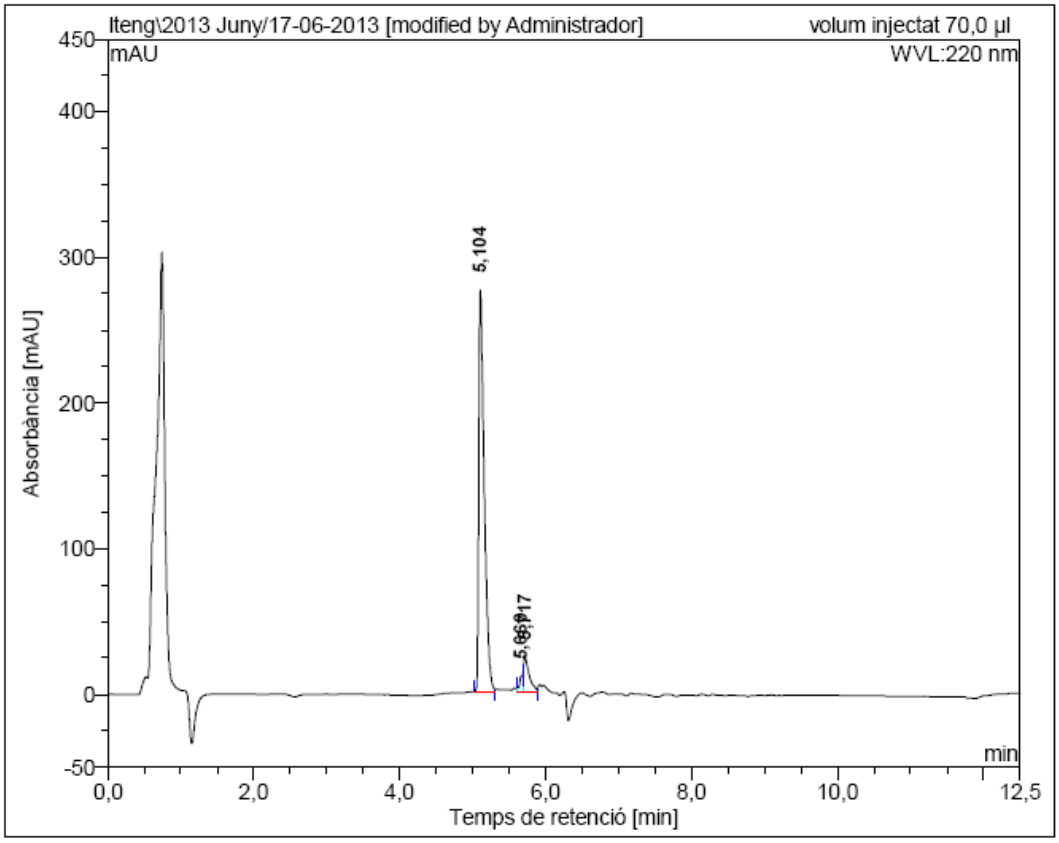

No.	Ret.Time (detected) min	Height mAU	Area mAU*min	Rel.Area %
1	5,10	275,484	24,087	89,89
2	5,66	10,347	0,491	1,83
3	5,72	24,509	2,217	8,27
Total:		310,340	26,795	100,00

ESI-MS *m/z*

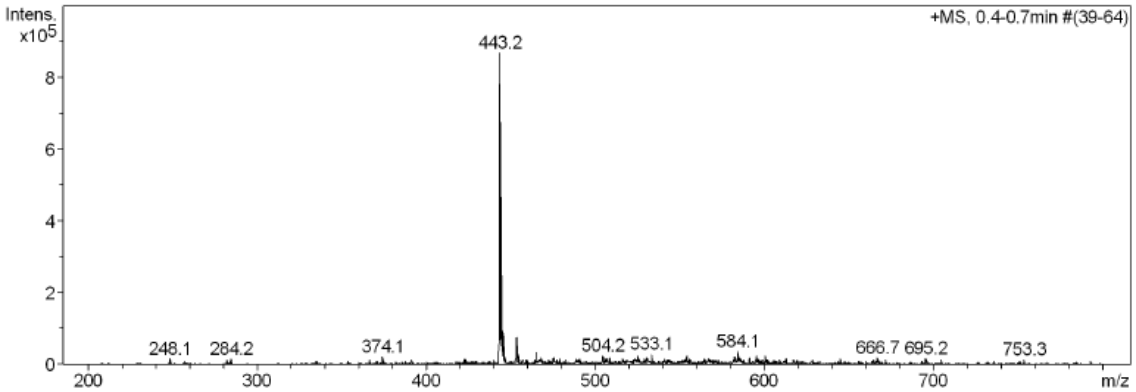

HRMS (ESI) *m/z*

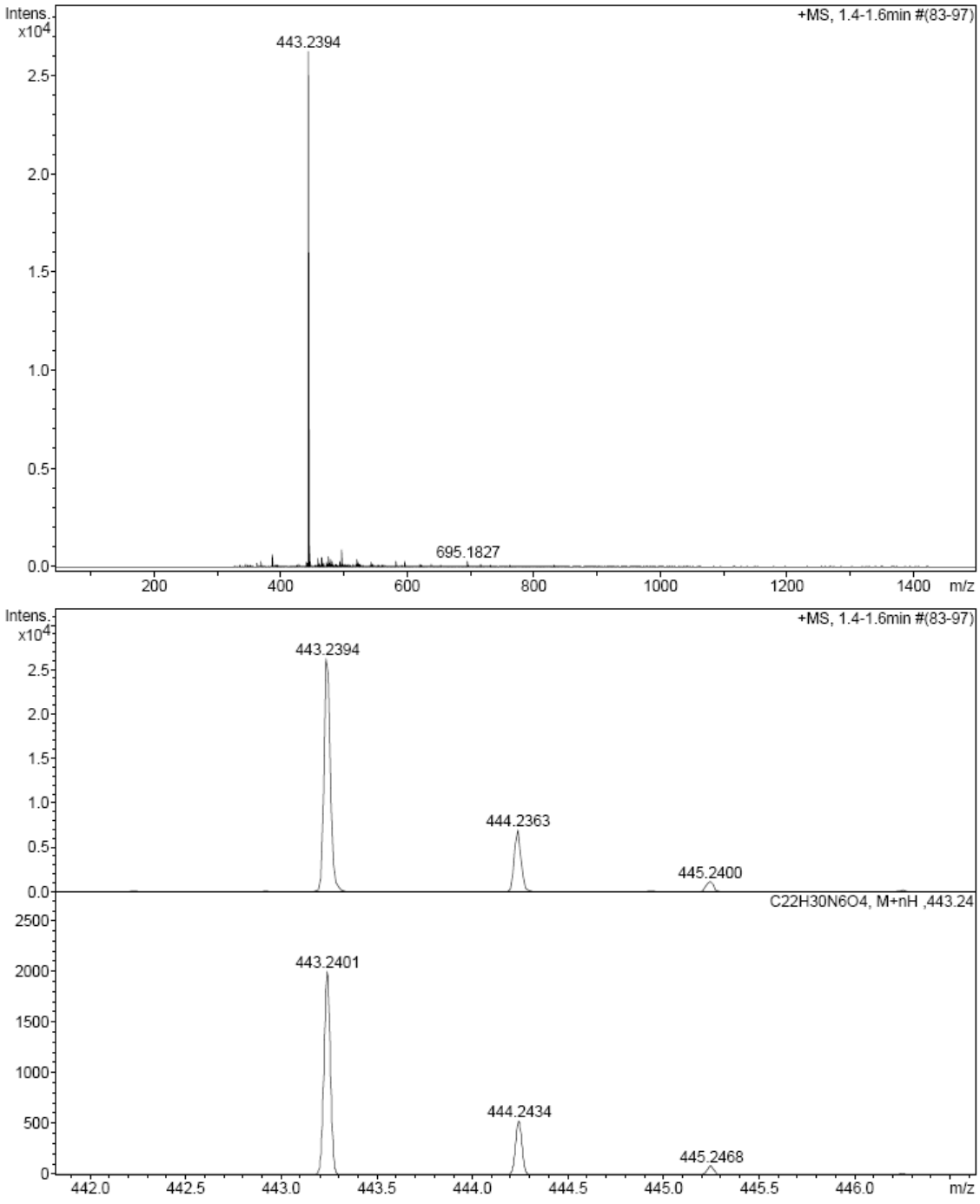
Intens.
x10^4
+MS, 1.4-1.6min #(83-97)
443.2394
695.1827
m/z
Intens.
x10^4
+MS, 1.4-1.6min #(83-97)
443.2394
444.2363
445.2400
C22H30N6O4, M+nH ,443.24
443.2401
444.2434
445.2468
m/z

Biaryl cyclic peptide BPC786

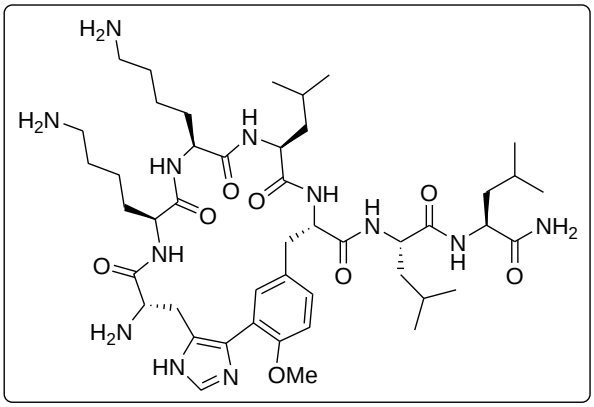

Crude peptide

HPLC (λ = 220 nm)

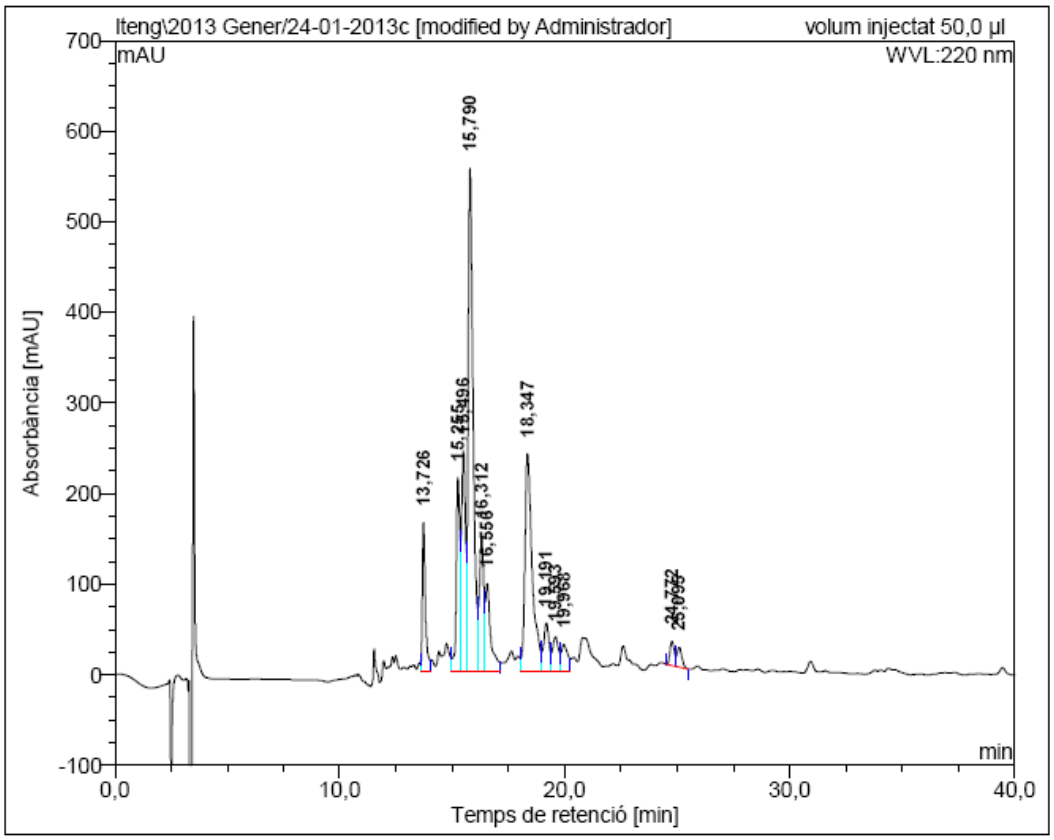

No.	Ret.Time (detected) min	Height mAU	Area mAU*min	Rel.Area %
1	13,73	163,593	26,186	5,72
2	15,26	213,352	40,991	8,95
3	15,50	243,001	49,947	10,91
4	15,79	554,171	141,978	31,01
5	16,31	149,331	34,045	7,44
6	16,56	96,403	26,628	5,82
7	18,35	239,491	90,436	19,75
8	19,19	52,667	15,029	3,28
9	19,59	37,413	11,590	2,53
10	19,97	29,068	9,495	2,07
11	24,77	26,820	6,121	1,34
12	25,09	21,816	5,443	1,19
Total:		1827,127	457,889	100,00

ESI-MS *m/z*

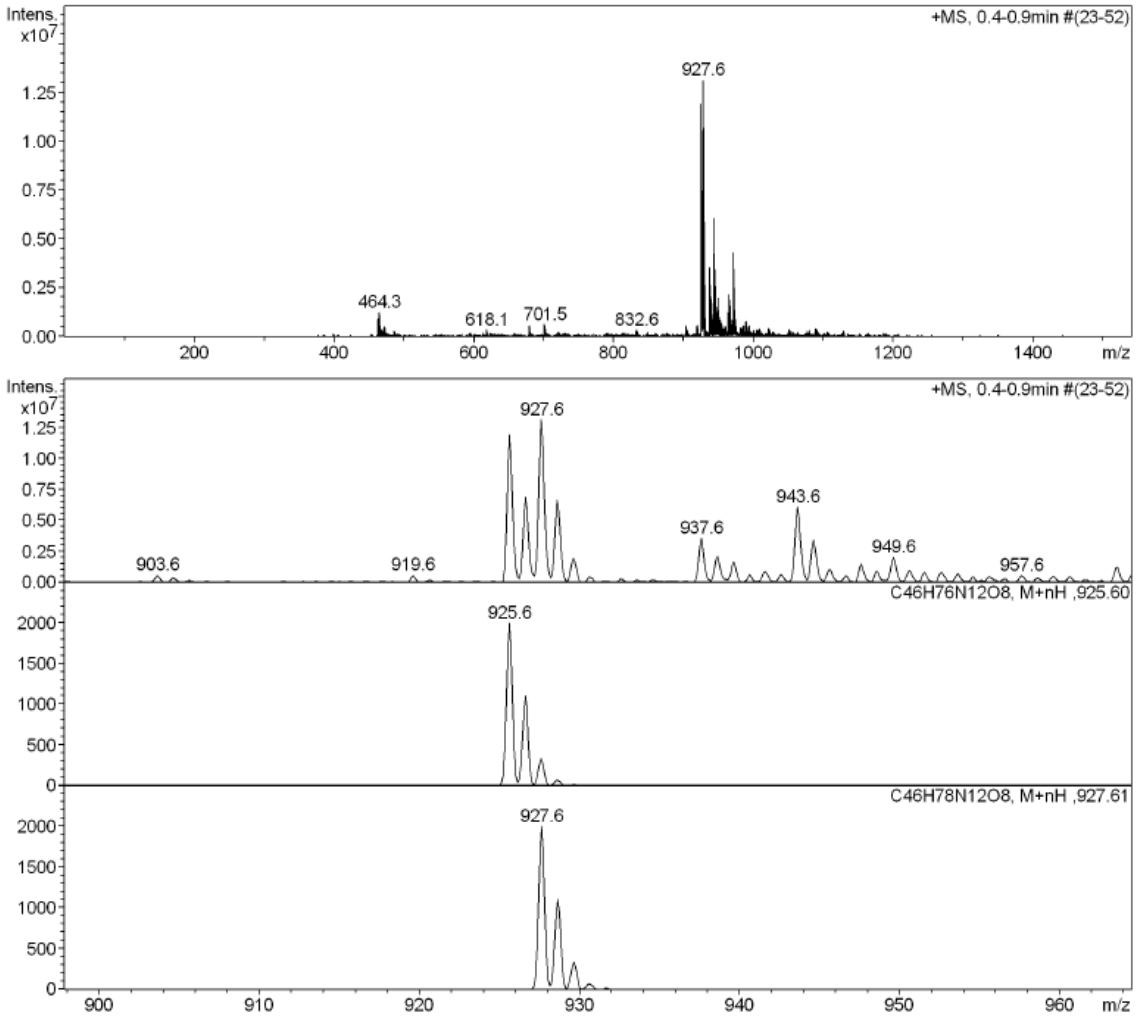
Intens.
x10^7
+MS, 0.4-0.9min #(23-52)
927.6
464.3
618.1
701.5
832.6
m/z
903.6
919.6
937.6
943.6
949.6
957.6
C46H76N12O8, M+nH ,925.60
925.6
C46H78N12O8, M+nH ,927.61

Purified peptide

HPLC (λ = 220 nm)

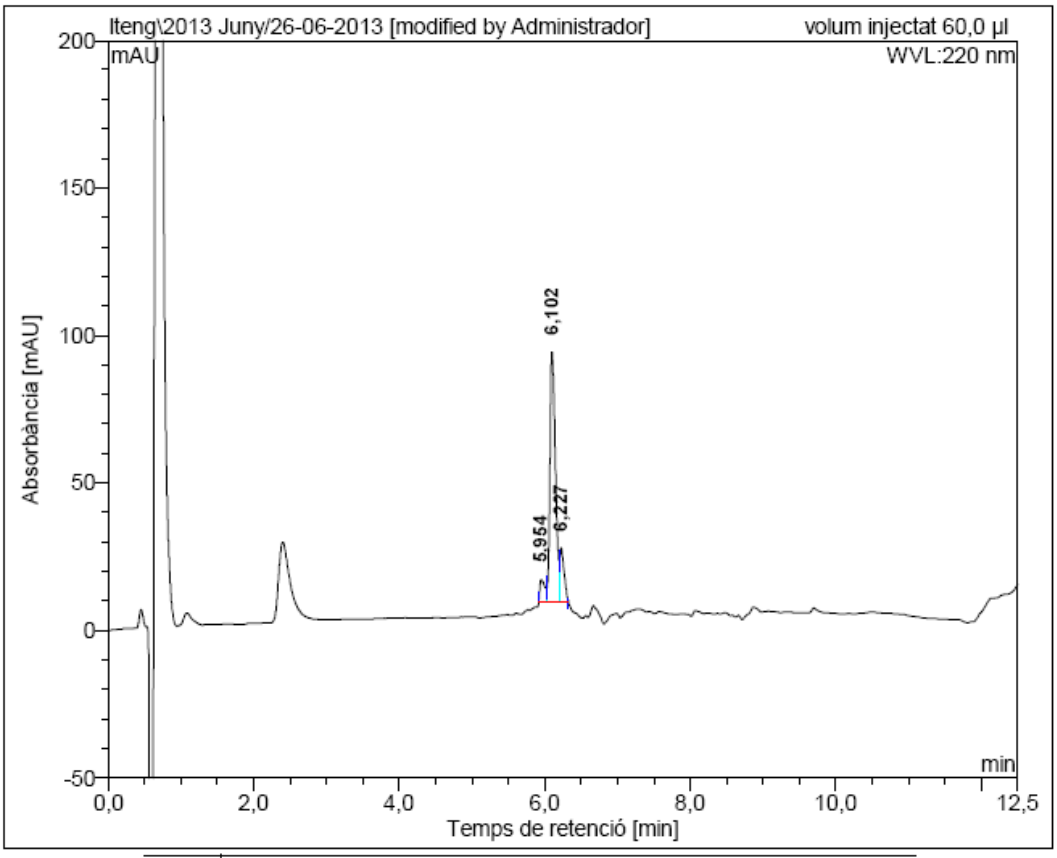

No.	mps retenc min	alçada mAU	Area mAU*min	Area relativa %
1	5,95	7,592	0,647	6,98
2	6,10	84,855	7,314	78,93
3	6,23	18,405	1,306	14,09
Total:		110,852	9,267	100,00

ESI-MS *m/z*

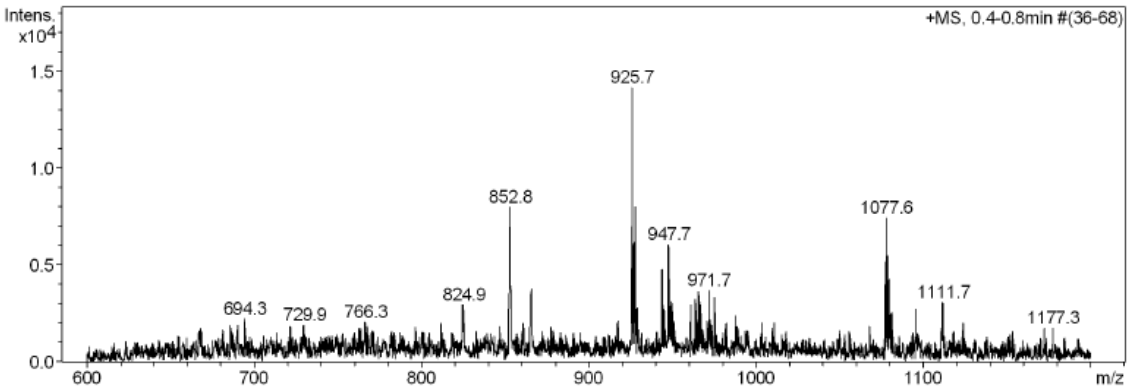

HRMS (ESI) *m/z*

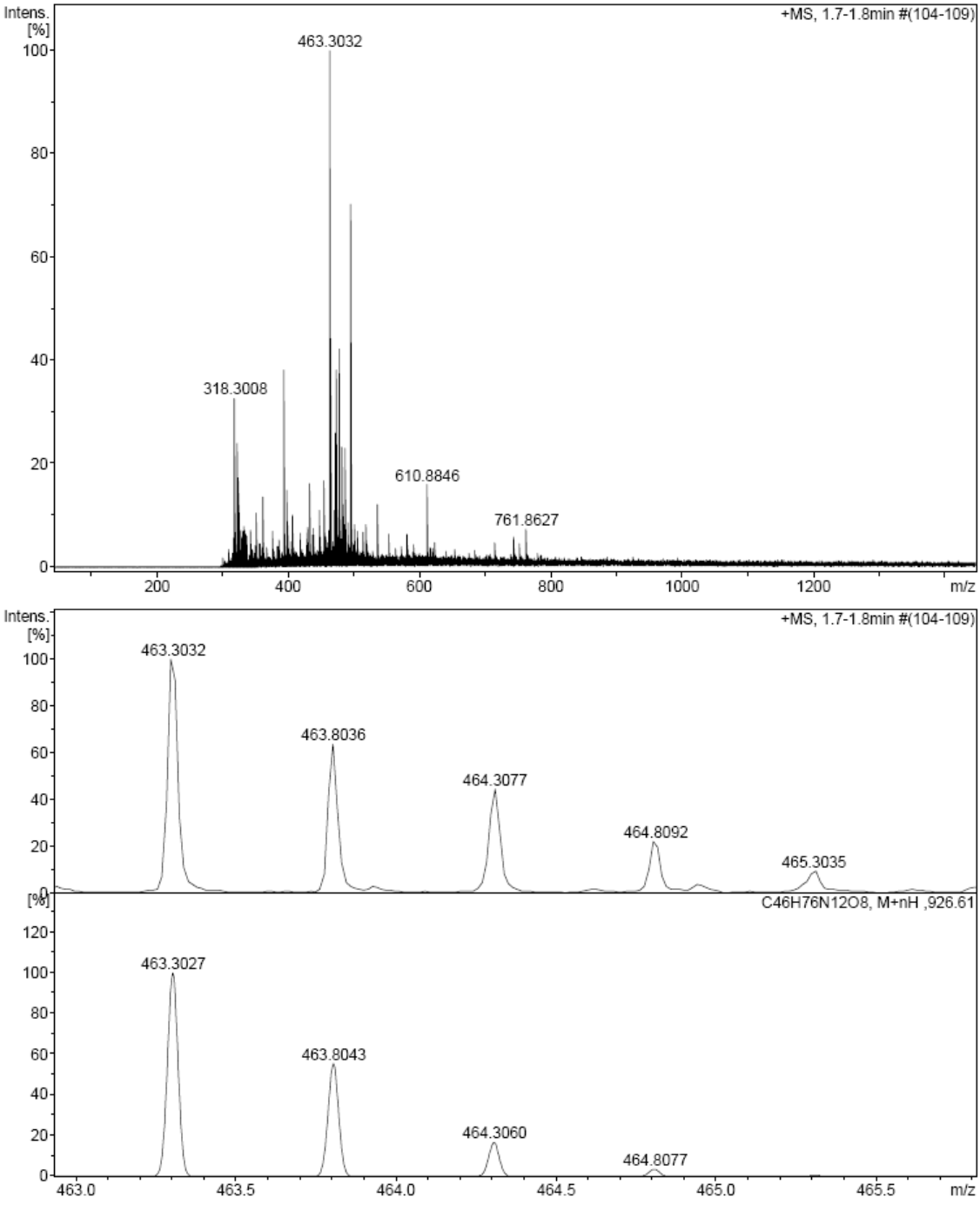
Intens.
[%]
+MS, 1.7-1.8min #(104-109)
463.3032
318.3008
610.8846
761.8627
m/z
+MS, 1.7-1.8min #(104-109)
463.3032
463.8036
464.3077
464.8092
465.3035
C46H76N12O8, M+nH ,926.61
463.3027
463.8043
464.3060
464.8077

Biaryl cyclic peptide BPC788

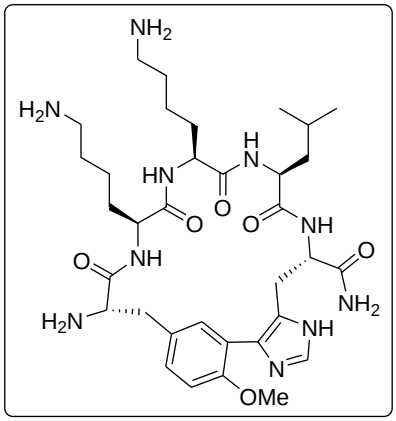

Crude peptide

HPLC (λ = 220 nm)

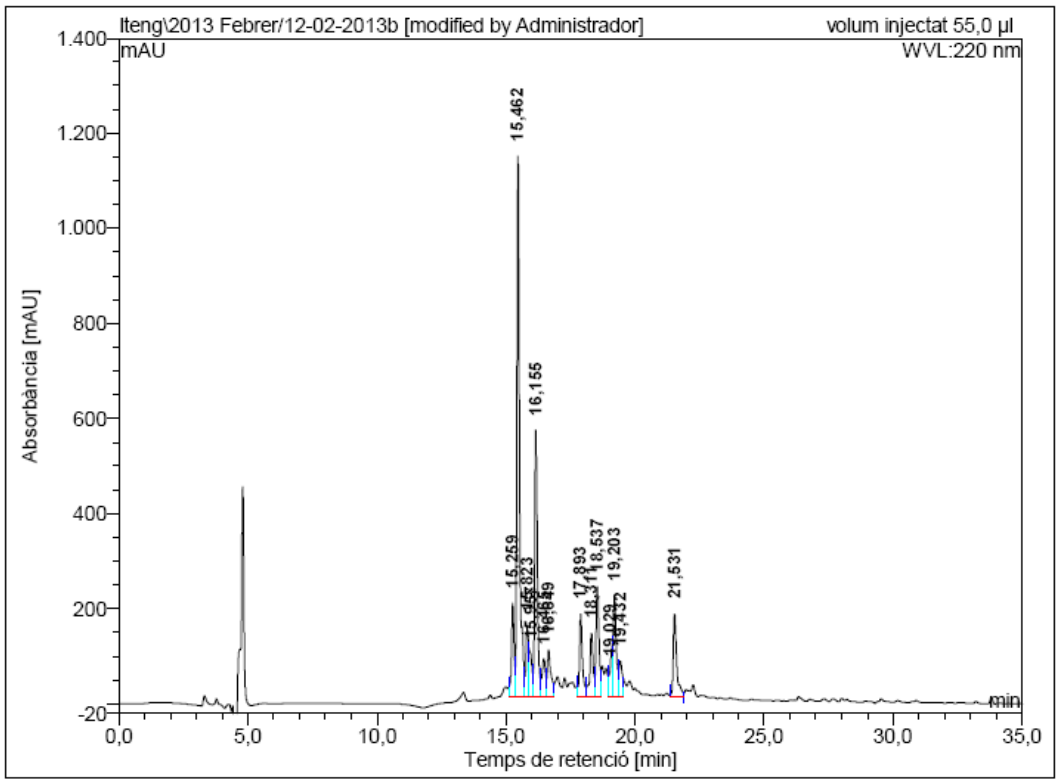

No.	Temps retenció min	alçada mAU	Area mAU*min	Area relativa %
1	15,26	195,624	23,594	5,39
2	15,46	1134,824	139,320	31,81
3	15,82	148,551	18,551	4,24
4	15,96	88,308	9,920	2,26
5	16,15	560,030	67,816	15,48
6	16,47	78,810	12,197	2,78
7	16,65	97,212	15,154	3,46
8	17,89	173,103	23,360	5,33
9	18,31	131,344	18,993	4,34
10	18,54	229,616	30,405	6,94
11	19,03	51,492	10,623	2,43
12	19,20	210,840	29,429	6,72
13	19,43	74,029	11,427	2,61
14	21,53	172,146	27,200	6,21
Total:		3345,929	437,990	100,00

ESI-MS *m/z*

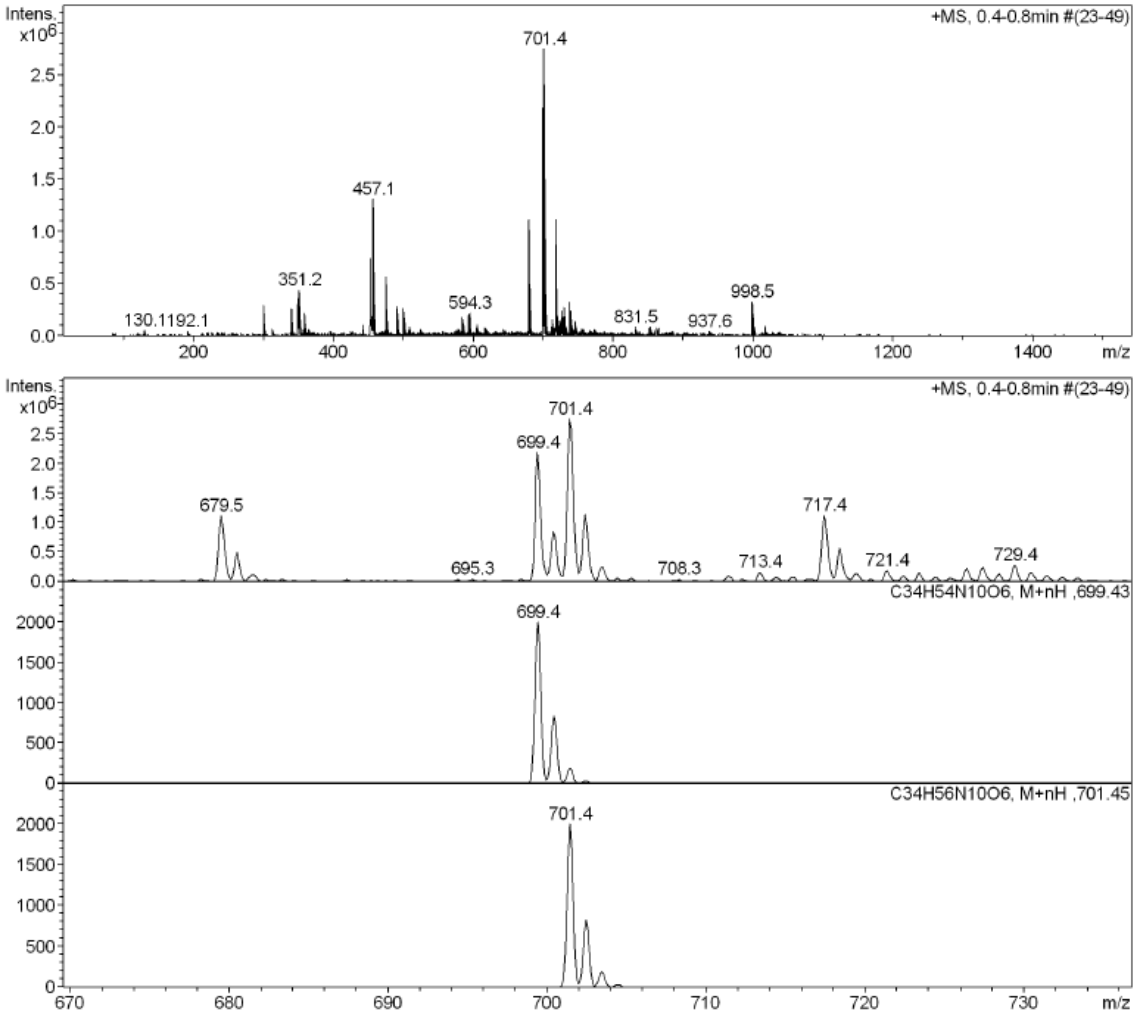
Intens.
x10^6
+MS, 0.4-0.8min #(23-49)
701.4
457.1
351.2
594.3
998.5
130.1192.1
831.5
937.6
200
400
600
800
1000
1200
1400
m/z
679.5
699.4
695.3
708.3
713.4
717.4
721.4
729.4
C34H54N10O6, M+nH ,699.43
C34H56N10O6, M+nH ,701.45
670
680
690
700
710
720
730

Purified peptide

HPLC (λ = 220 nm)

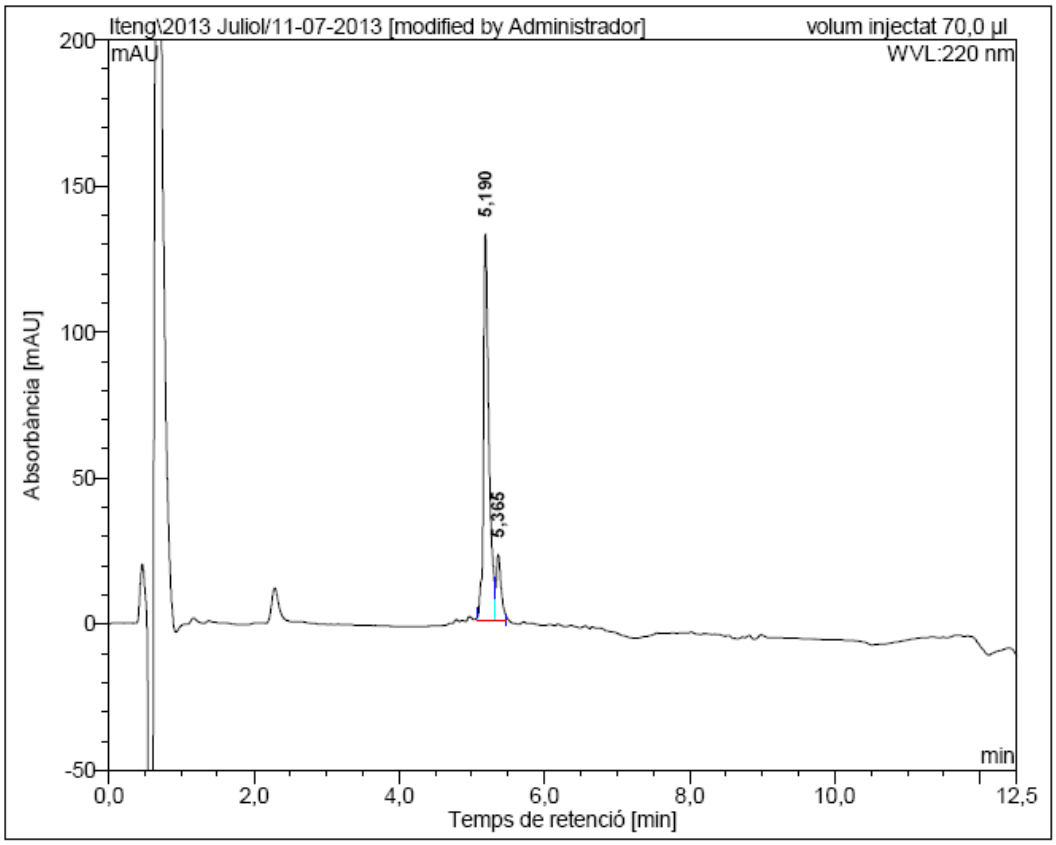

No.	Temps retenció min	alçada mAU	Area mAU*min	Area relativa %
1	5,19	132,359	11,530	87,13
2	5,36	22,654	1,704	12,87
Total:		155,013	13,233	100,00

ESI-MS *m/z*

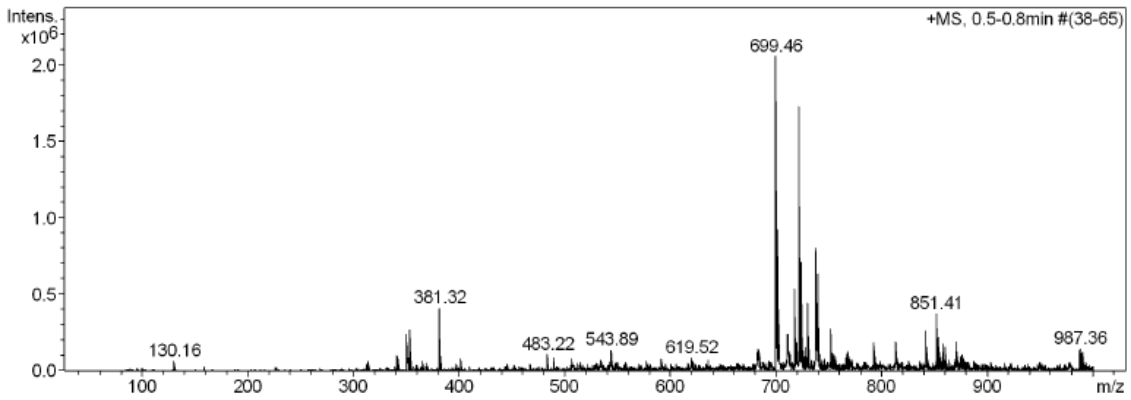

HRMS (ESI) *m/z*

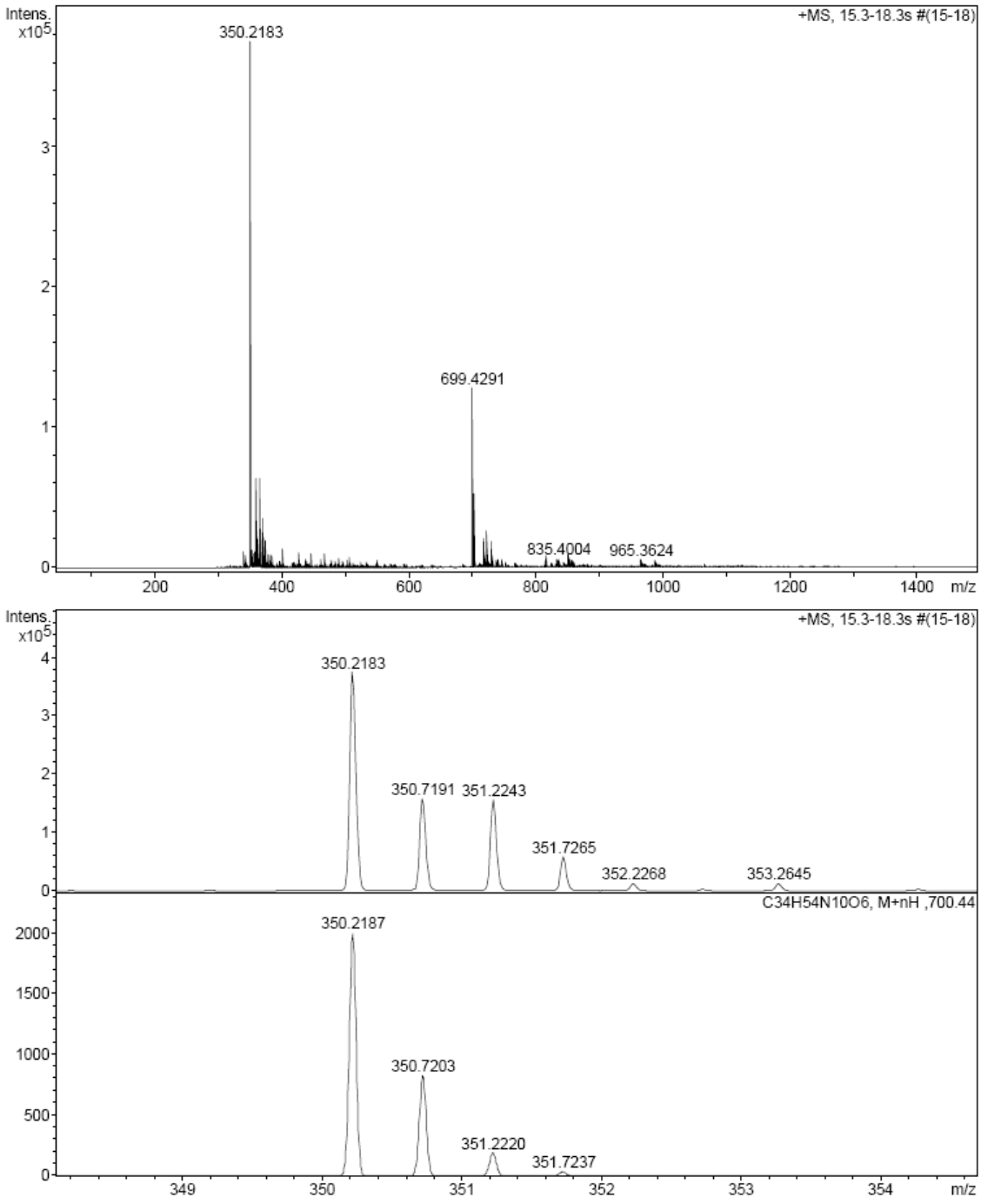
Intens.
x10^5
+MS, 15.3-18.3s #(15-18)
350.2183
699.4291
835.4004
965.3624
m/z
350.2183
350.7191
351.2243
351.7265
352.2268
353.2645
C34H54N10O6, M+nH ,700.44
350.2187
350.7203
351.2220
351.7237

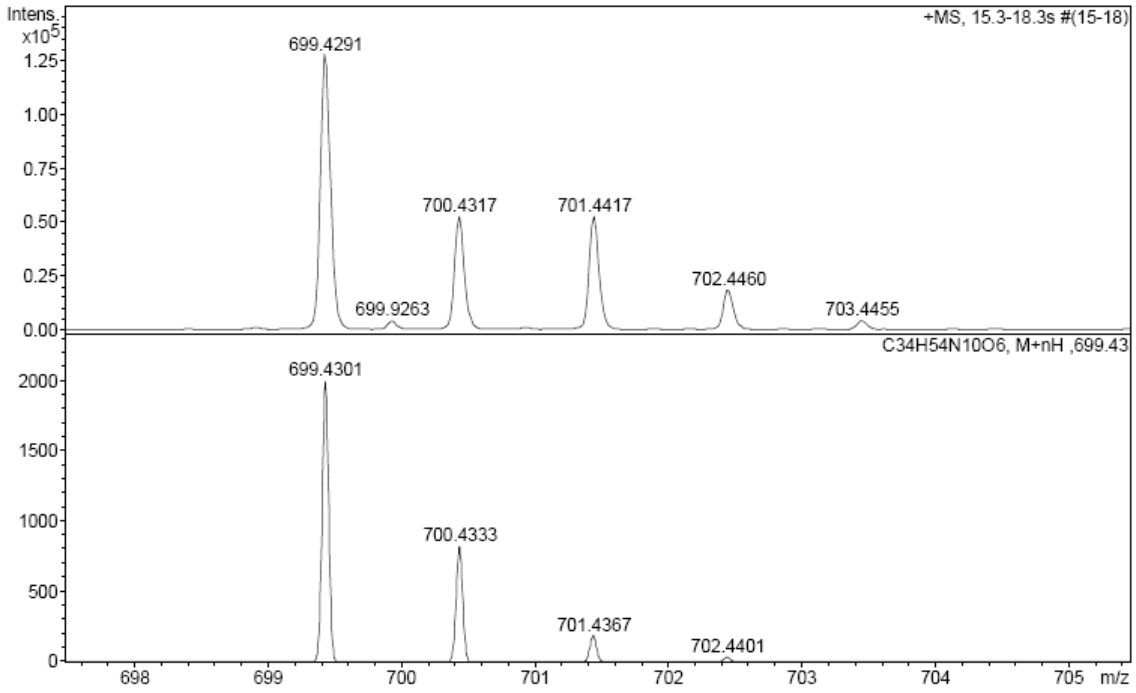
Intens.
x10^5
1.25
1.00
0.75
0.50
0.25
0.00
+MS, 15.3-18.3s #(15-18)
699.4291
700.4317
701.4417
699.9263
702.4460
703.4455
C34H54N10O6, M+nH ,699.43
2000
1500
1000
500
0
699.4301
700.4333
701.4367
702.4401
698
699
700
701
702
703
704
705
m/z

Biaryl cyclic peptide BPC790

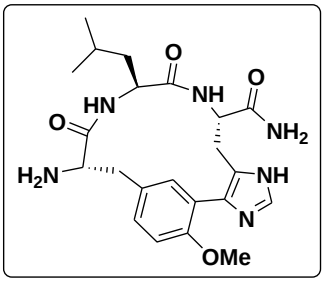

Crude peptide

HPLC (λ = 220 nm)

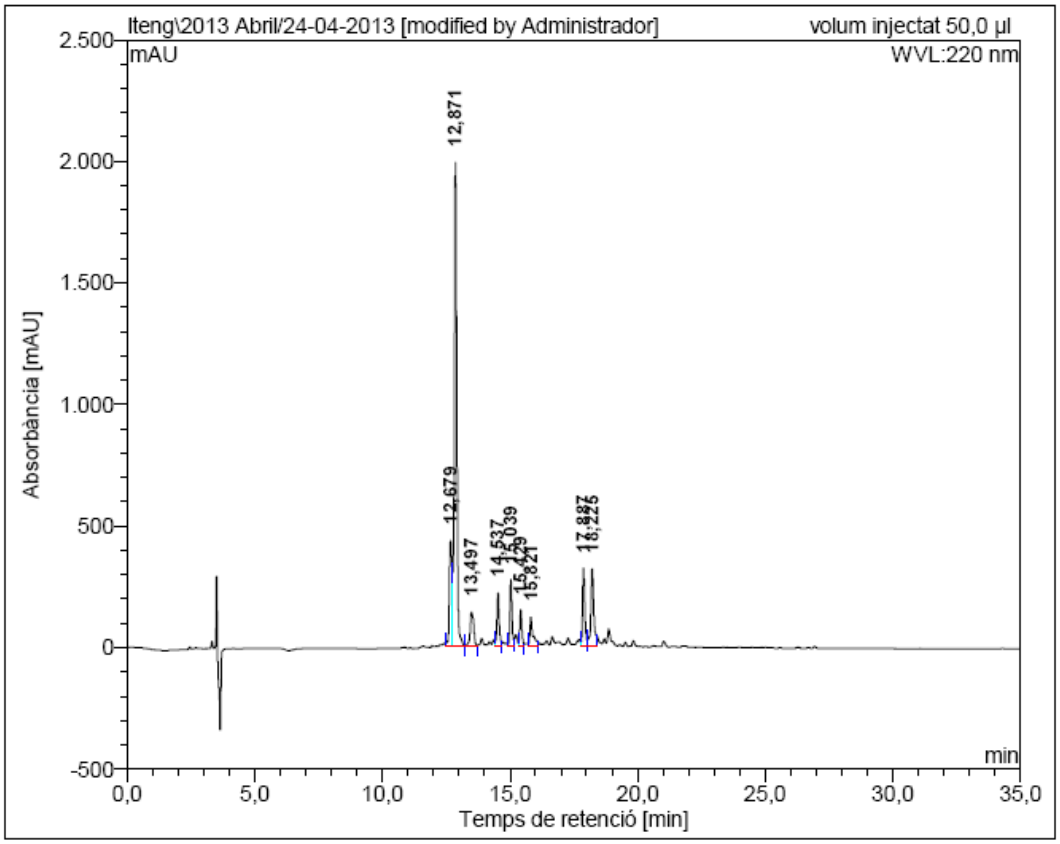

No.	Ret.Time (detected) min	Height mAU	Area mAU*min	Rel.Area %
1	12,68	437,348	51,801	11,40
2	12,87	1989,446	223,804	49,26
3	13,50	140,613	22,806	5,02
4	14,54	219,963	22,570	4,97
5	15,04	274,278	26,590	5,85
6	15,43	149,734	14,866	3,27
7	15,82	119,062	17,584	3,87
8	17,89	321,575	33,837	7,45
9	18,22	318,133	40,438	8,90
Total:		3970,153	454,297	100,00

ESI-MS *m/z*

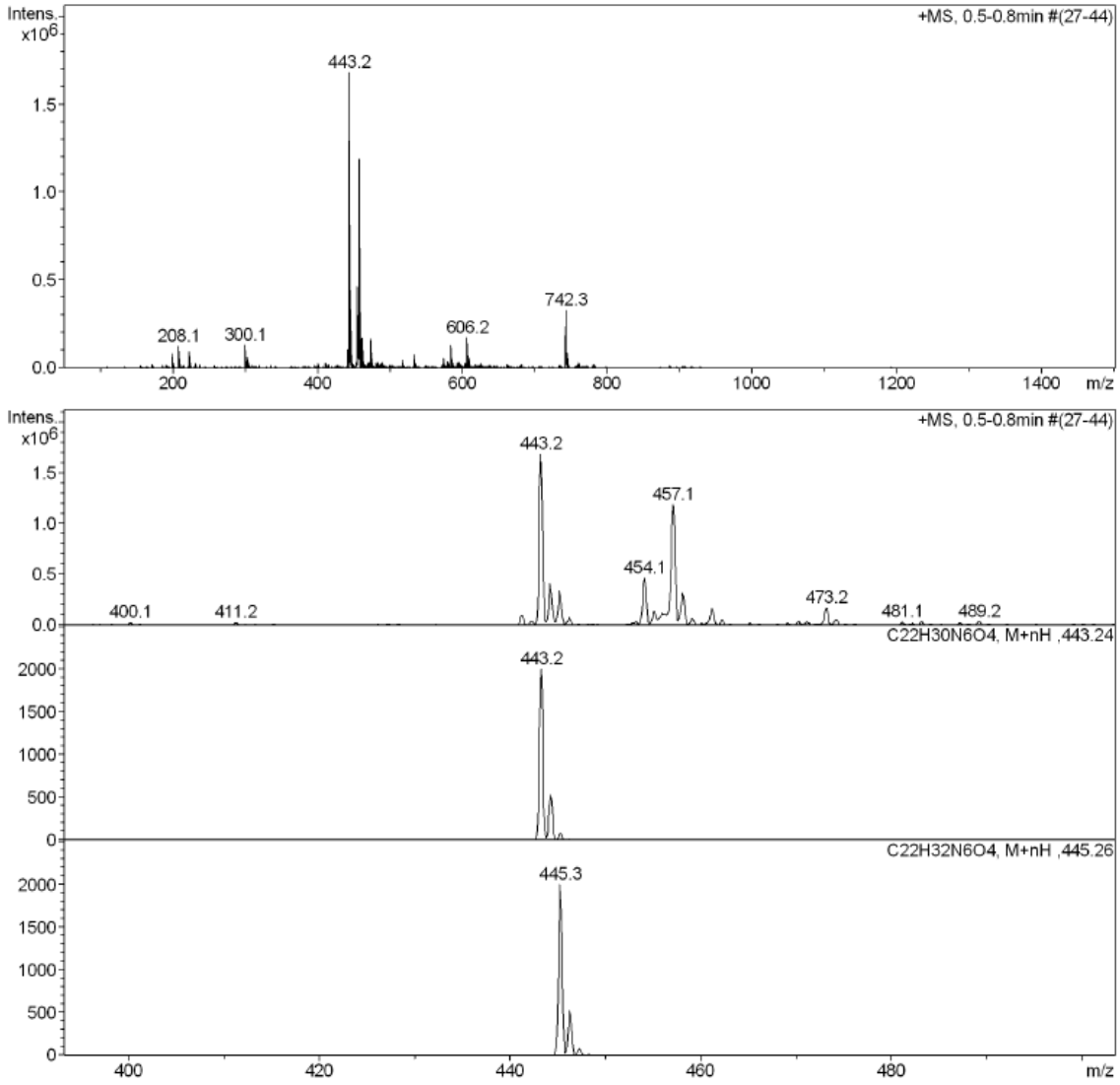
Intens.
x10^6
+MS, 0.5-0.8min #(27-44)
443.2
742.3
606.2
208.1
300.1
m/z
457.1
454.1
473.2
400.1
411.2
481.1
489.2
C22H30N6O4, M+nH ,443.24
C22H32N6O4, M+nH ,445.26
445.3

Purified peptide

HPLC (λ = 220 nm)

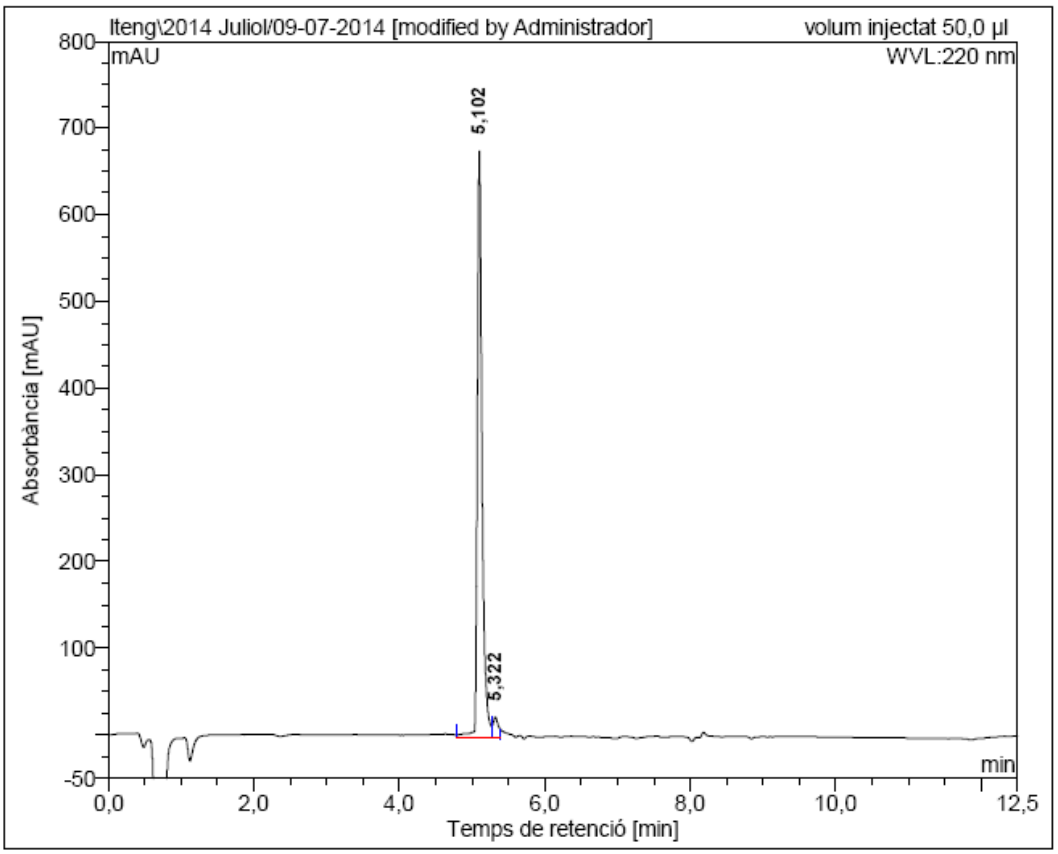

No.	mps retenc min	alçada mAU	Area mAU*min	Area relativa %
1	5,10	675,370	51,090	96,38
2	5,32	23,032	1,917	3,62
Total:		698,403	53,007	100,00

ESI-MS *m/z*

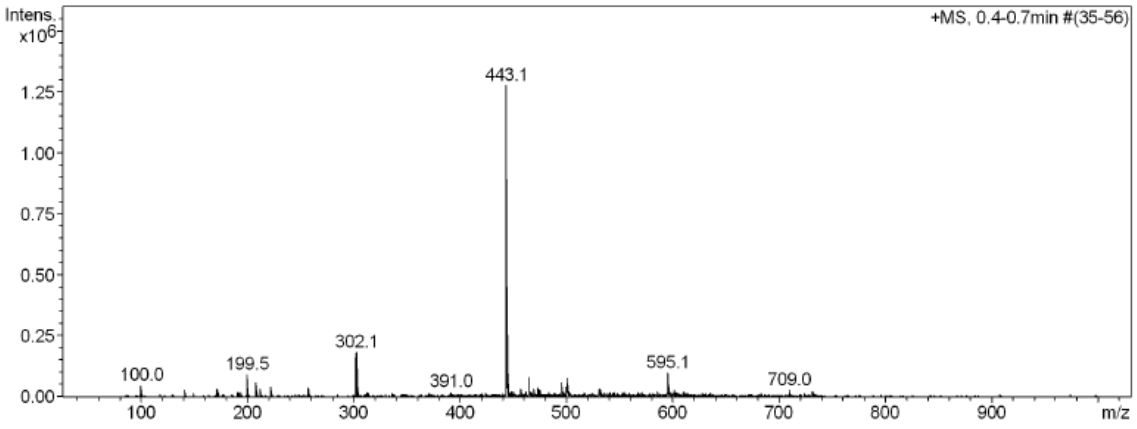

HRMS (ESI) *m/z*

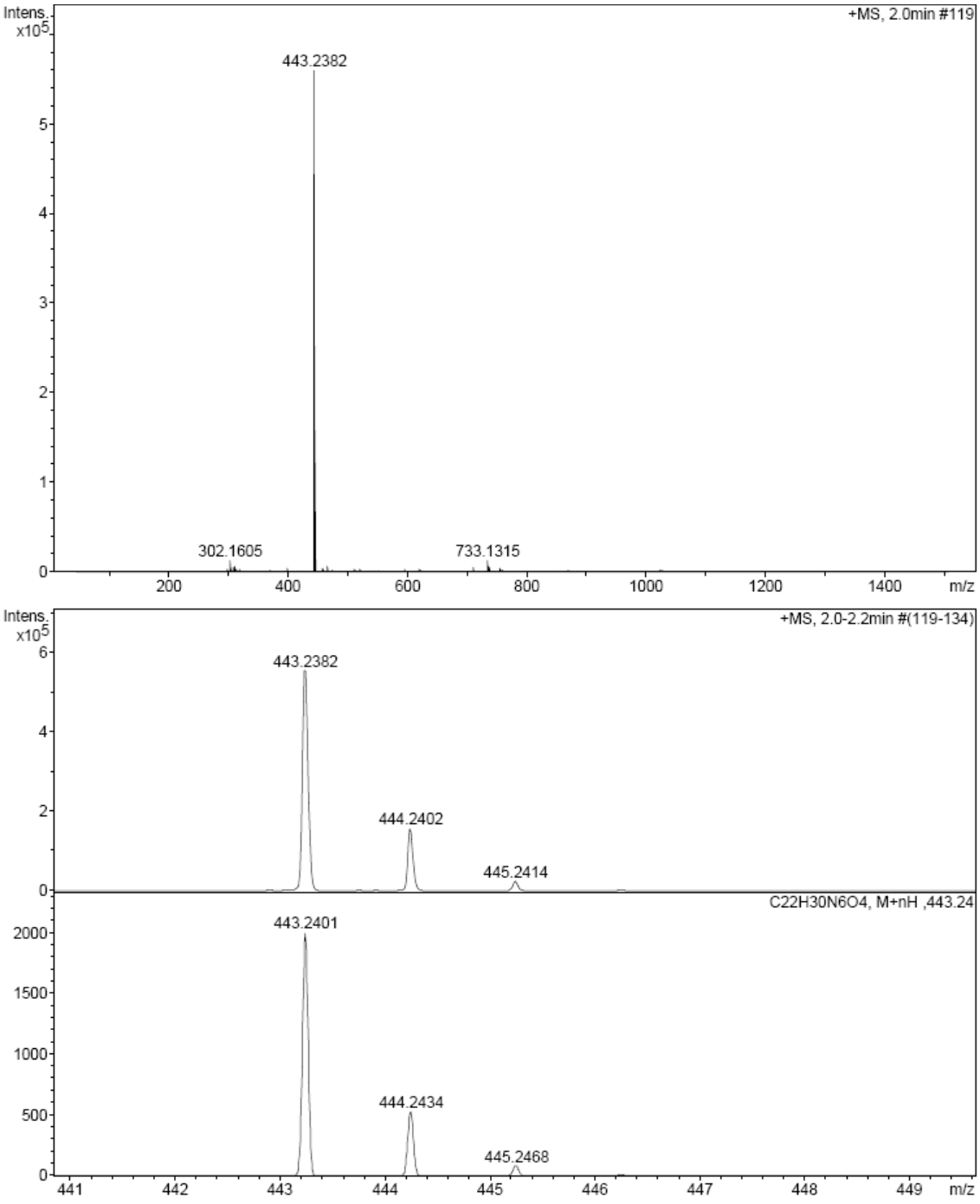
Intens.
x10^5
+MS, 2.0min #119
443.2382
302.1605
733.1315
m/z
+MS, 2.0-2.2min #(119-134)
443.2382
444.2402
445.2414
C22H30N6O4, M+nH ,443.24
443.2401
444.2434
445.2468
m/z

^{1}H-NMR (400 MHz, CD_3OD) δ (ppm)

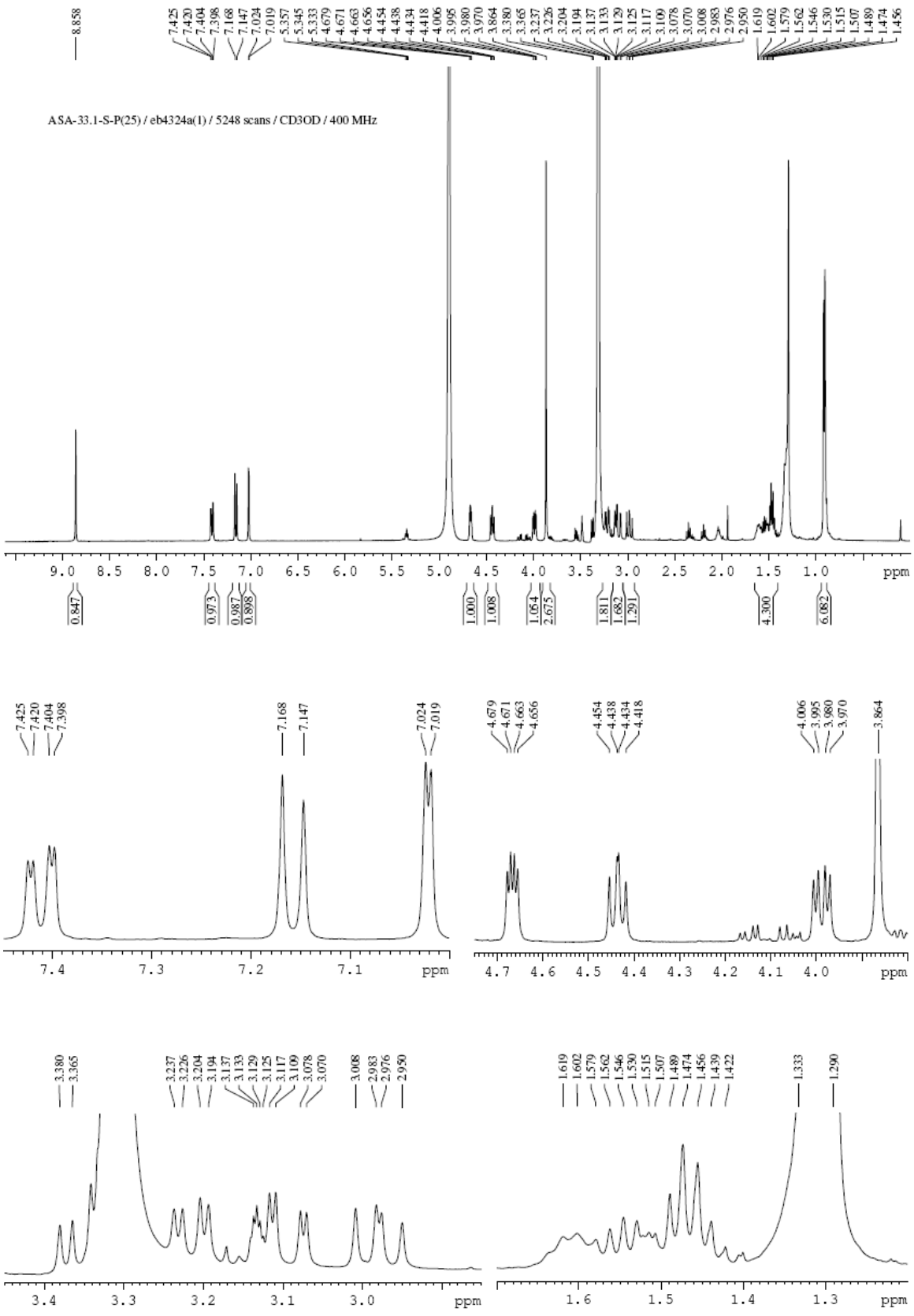

COSY (400 MHz, CD_3OD) δ (ppm)

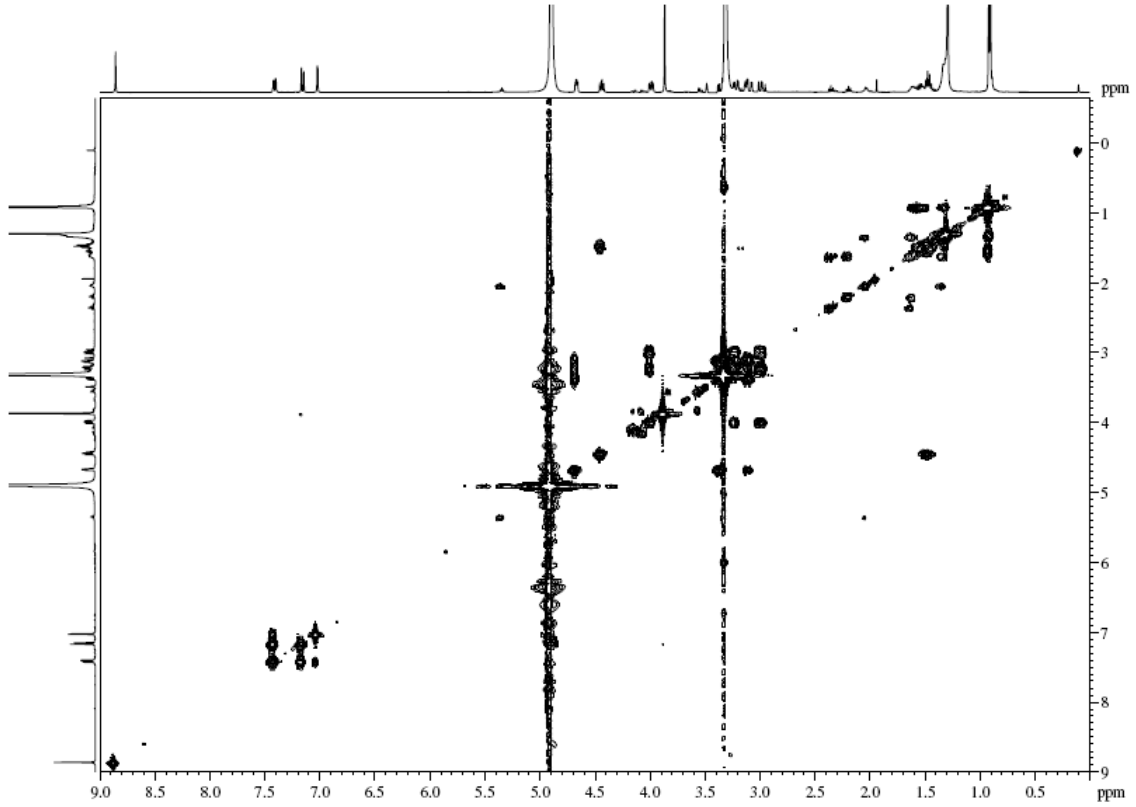

Biaryl cyclic peptide BPC792

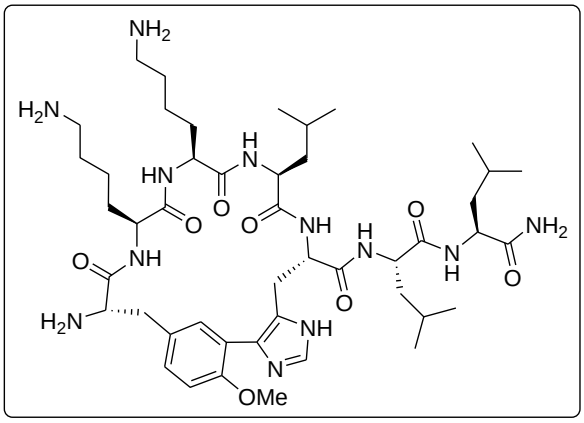

Crude peptide

HPLC (λ = 220 nm)

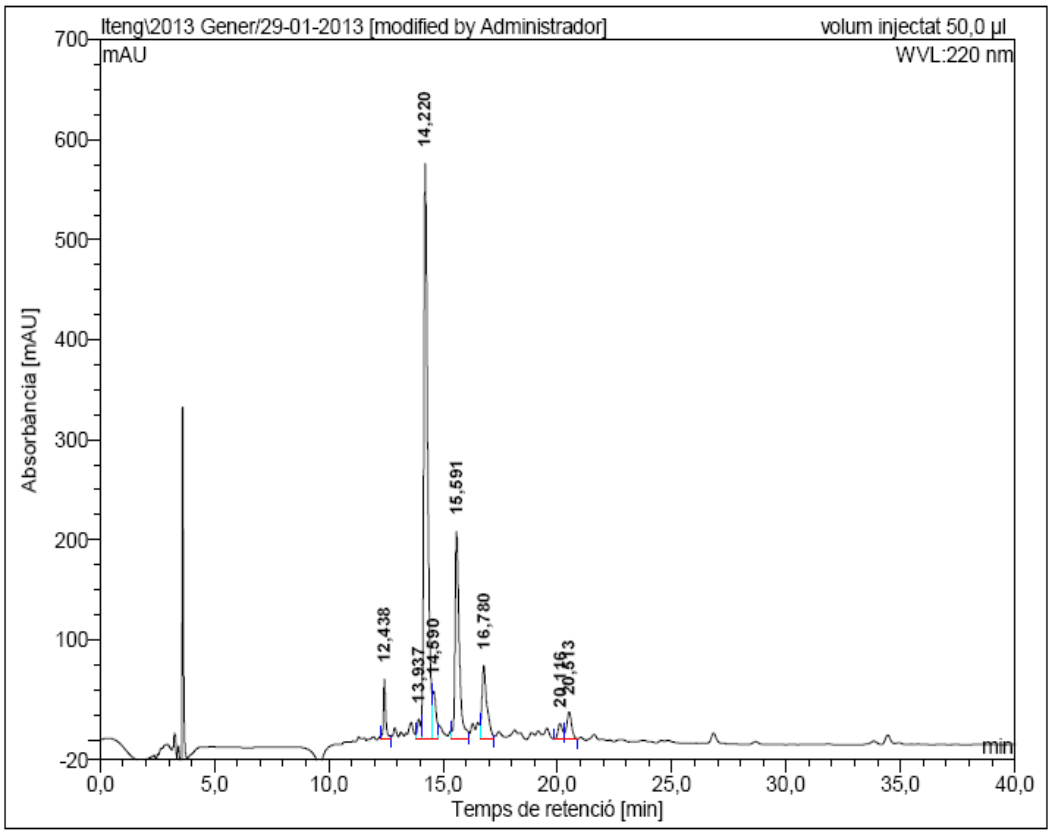

No.	Temps retenció min	alçada mAU	Area mAU*min	Area relativa %
1	12,44	59,896	7,175	3,47
2	13,94	19,816	3,190	1,54
3	14,22	575,761	114,276	55,21
4	14,59	47,557	8,206	3,96
5	15,59	207,683	44,748	21,62
6	16,78	73,736	19,136	9,24
7	20,12	15,386	3,563	1,72
8	20,51	27,082	6,703	3,24
Total:		1026,918	206,998	100,00

ESI-MS *m/z*

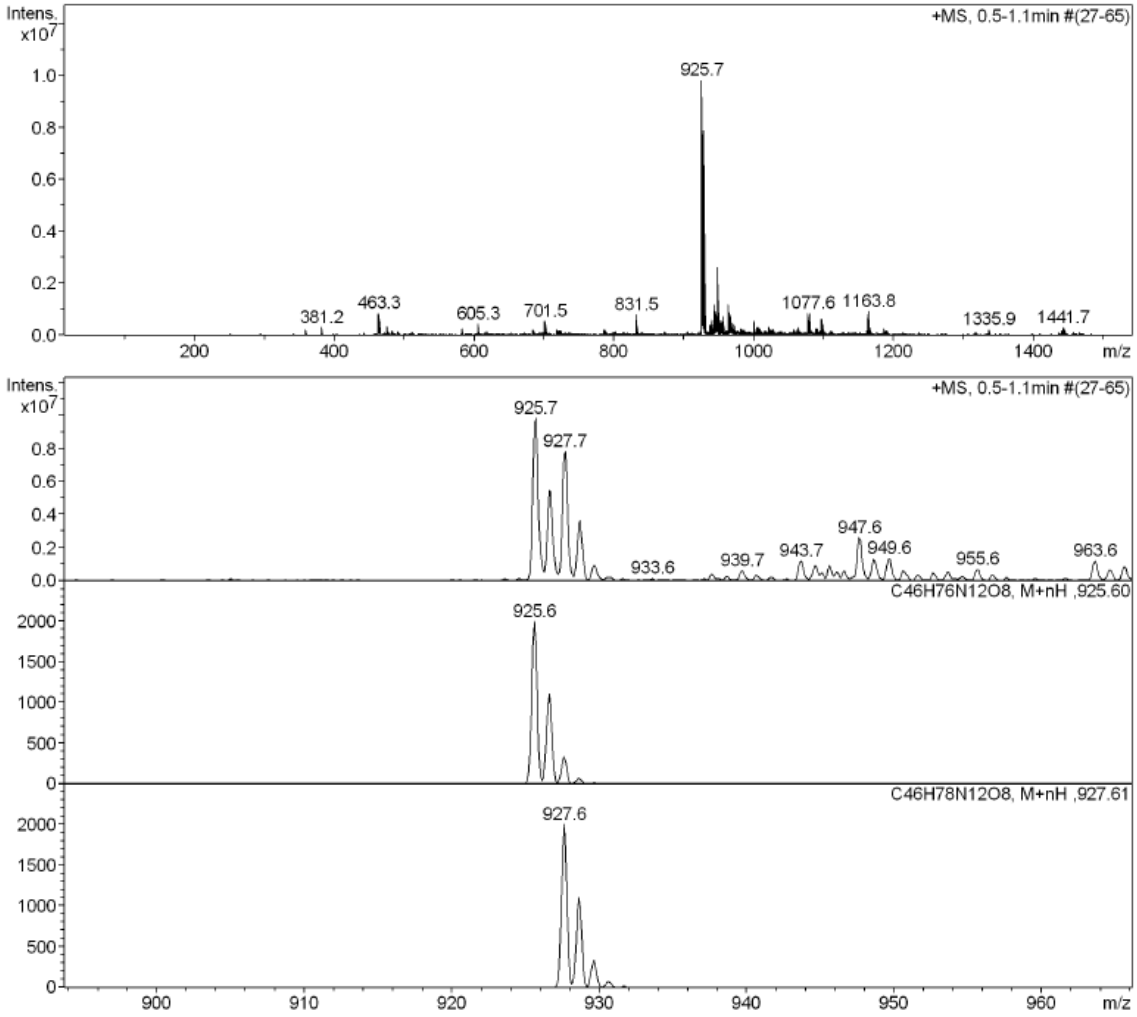
Intens.
x10^7
+MS, 0.5-1.1min #(27-65)
925.7
381.2
463.3
605.3
701.5
831.5
1077.6
1163.8
1335.9
1441.7
m/z
925.7
927.7
933.6
939.7
943.7
947.6
949.6
955.6
963.6
C46H76N12O8, M+nH ,925.60
925.6
C46H78N12O8, M+nH ,927.61
927.6

Purified peptide

HPLC (λ = 220 nm)

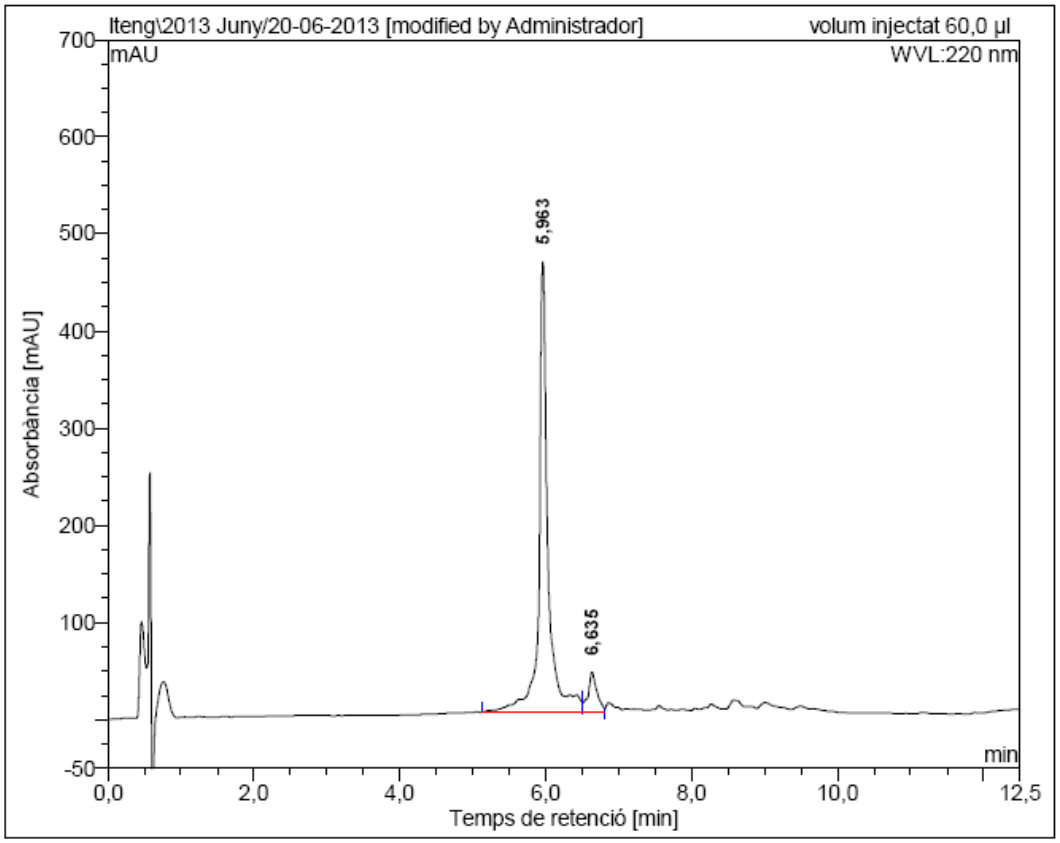

No.	Ret.Time (detected) min	Height mAU	Area mAU*min	Rel.Area %
1	5,96	463,902	66,134	91,91
2	6,63	41,055	5,821	8,09
Total:		504,957	71,955	100,00

ESI-MS *m/z*

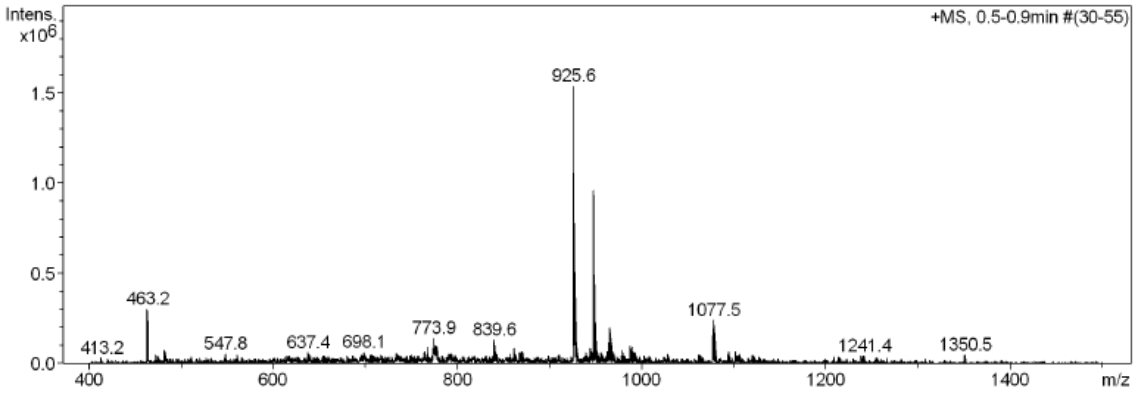

HRMS (ESI) *m/z*

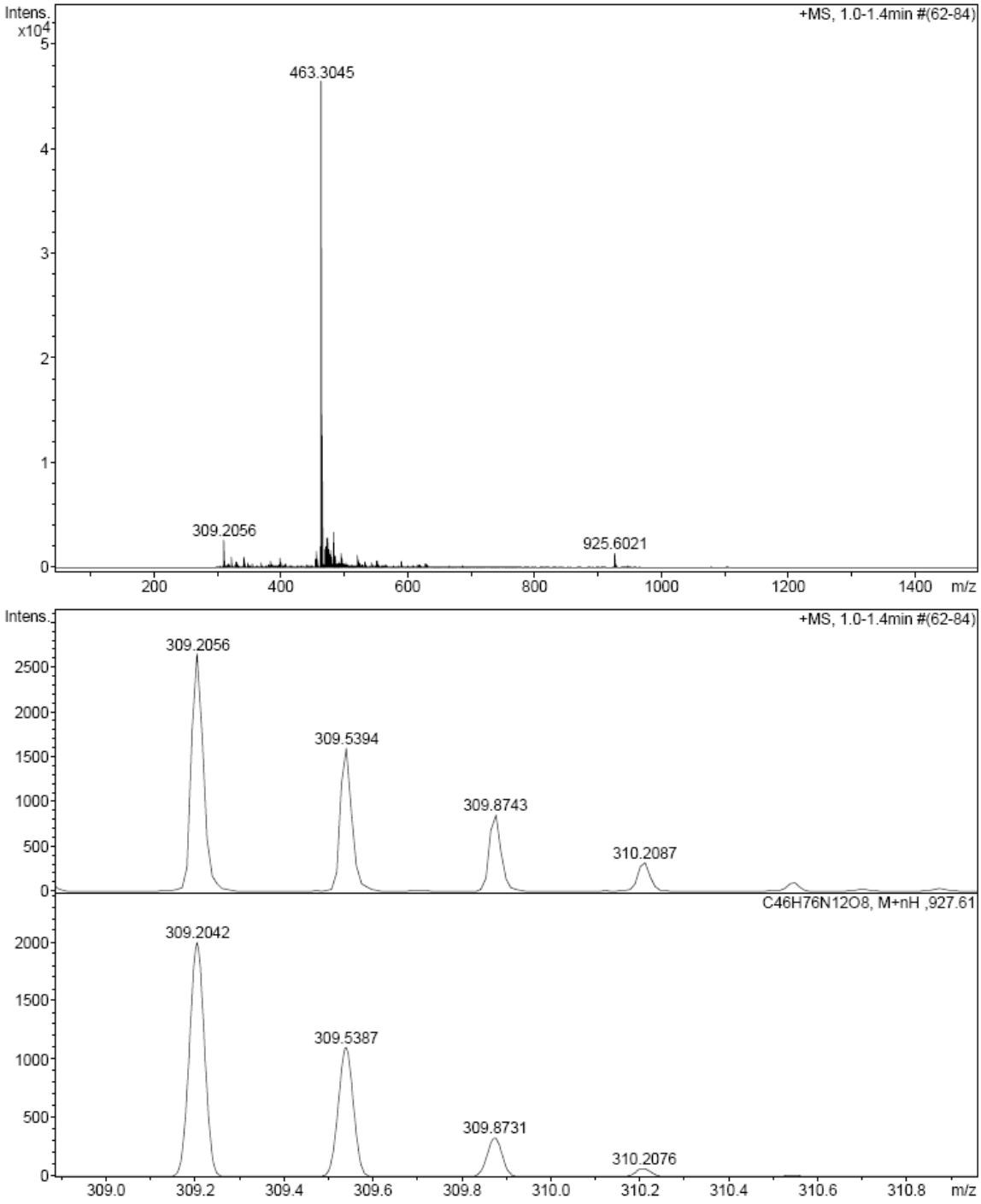
Intens.
x10^4
+MS, 1.0-1.4min #(62-84)
463.3045
309.2056
925.6021
m/z
Intens.
+MS, 1.0-1.4min #(62-84)
309.2056
309.5394
309.8743
310.2087
C46H76N12O8, M+nH ,927.61
309.2042
309.5387
309.8731
310.2076
m/z

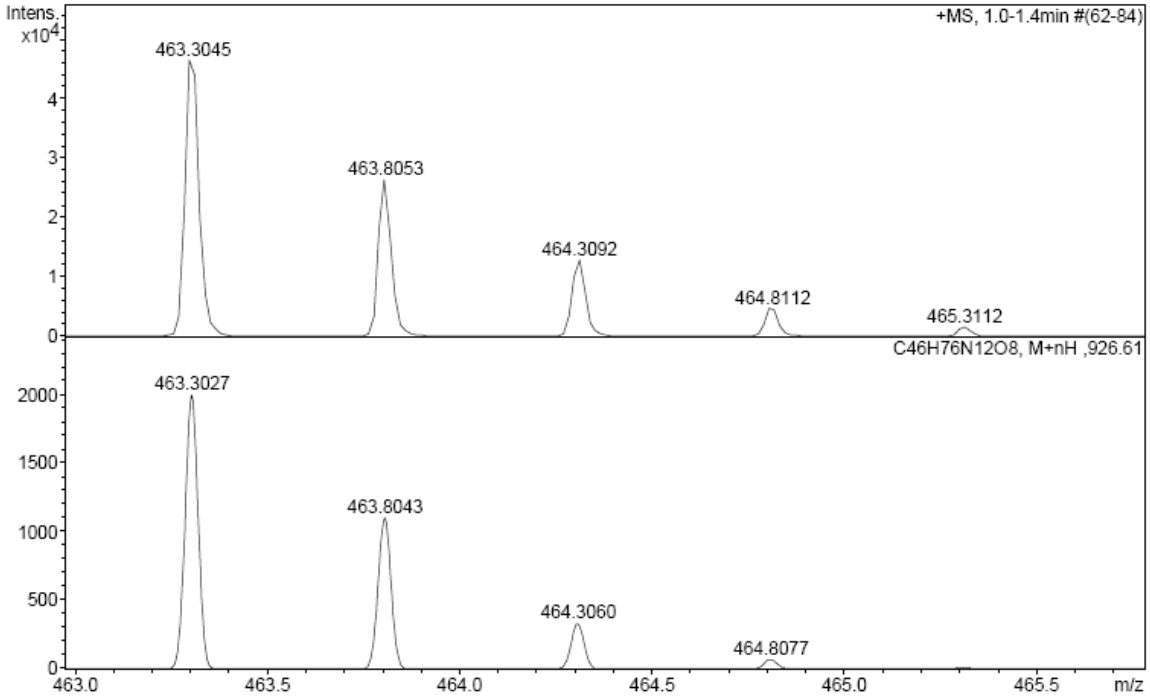
Intens.
x10^4
+MS, 1.0-1.4min #(62-84)
463.3045
463.8053
464.3092
464.8112
465.3112
C46H76N12O8, M+nH ,926.61
463.3027
463.8043
464.3060
464.8077
m/z

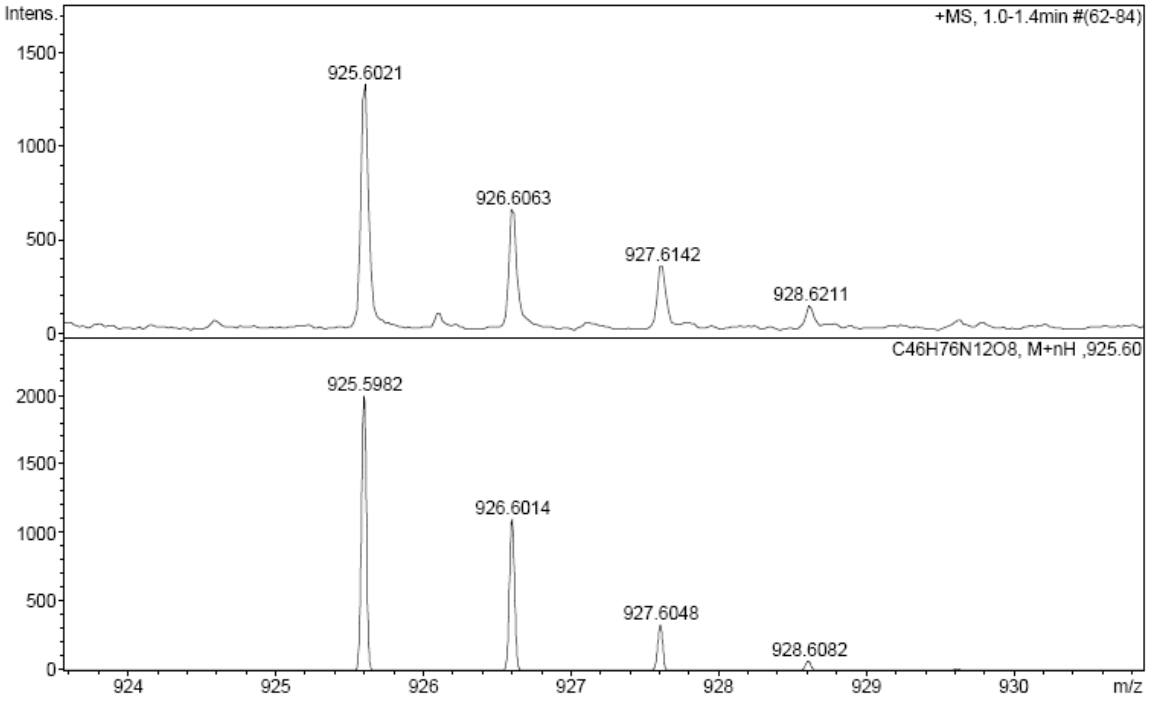
Intens.
+MS, 1.0-1.4min #(62-84)
925.6021
926.6063
927.6142
928.6211
C46H76N12O8, M+nH ,925.60
925.5982
926.6014
927.6048
928.6082
m/z

SUPPORTING INFORMATION CHAPTER 6

Solid-Phase Synthesis of Biaryl Cyclic Lipopeptides Derived from Arylomycins

Iteng Ng-Choi, Eduard Figueras, Lidia Feliu* and Marta Planas*

TABLE OF CONTENTS

Copies of HPLC, MS and NMR spectra

1. Synthesis of amino acids

Boc-Phg(4-OH)-OH

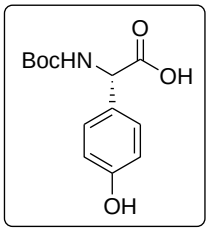

HPLC (λ = 220 nm)

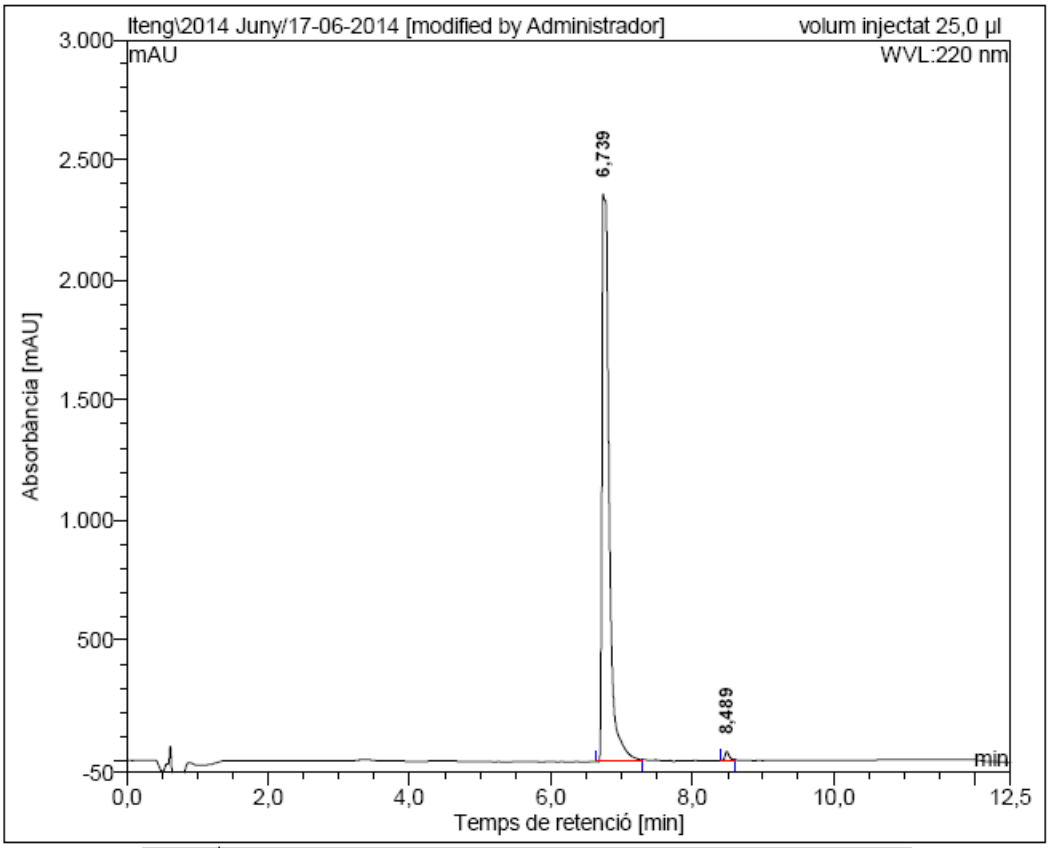

No.	mps retenc min	alçada mAU	Area mAU*min	Area relativa %
1	6,74	2364,188	281,091	98,73
2	8,49	42,804	3,618	1,27
Total:		2406,992	284,710	100,00

Boc-Phg(3-I,4-OH)-OH

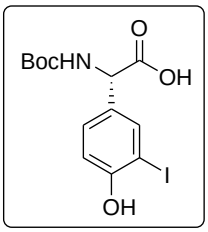

HPLC (λ = 220 nm)

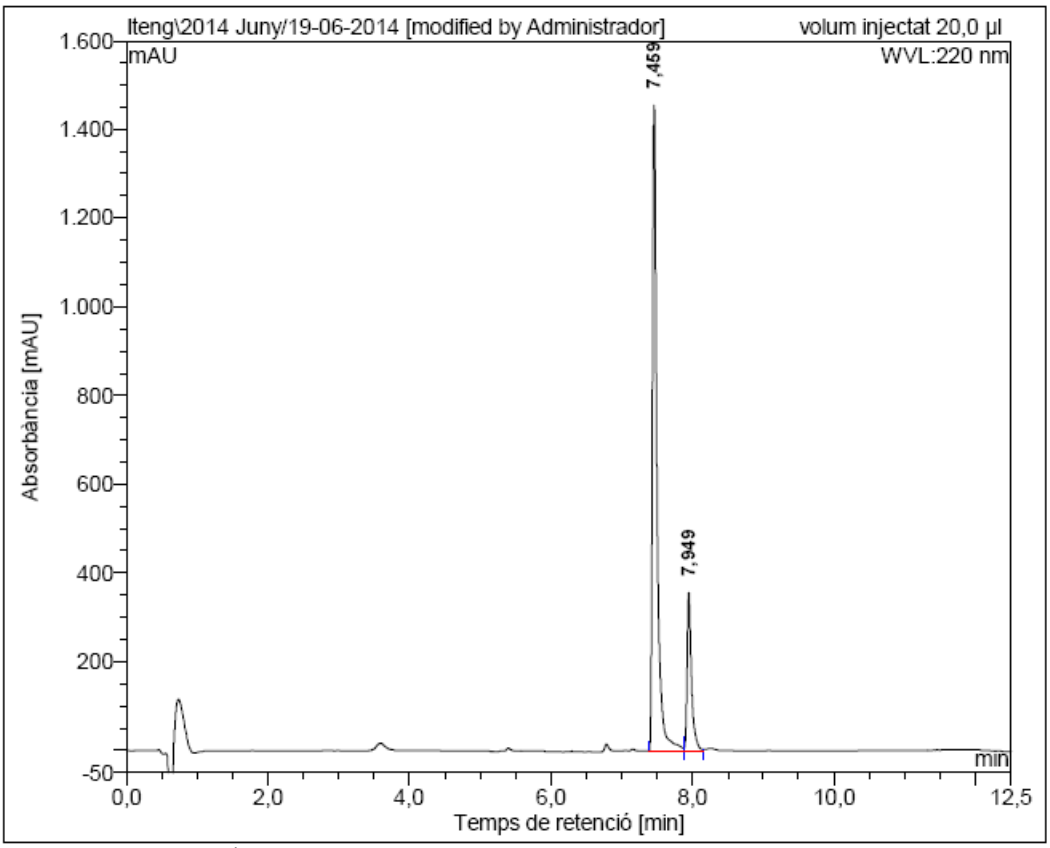

No.	mps retenc min	alçada mAU	Area mAU*min	Area relativa %
1	7,46	1455,755	108,441	80,62
2	7,95	357,846	26,063	19,38
Total:		1813,602	134,504	100,00

Boc-Phg(3-I,4-OMe)-OMe

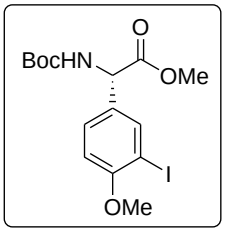

HPLC (λ = 220 nm)

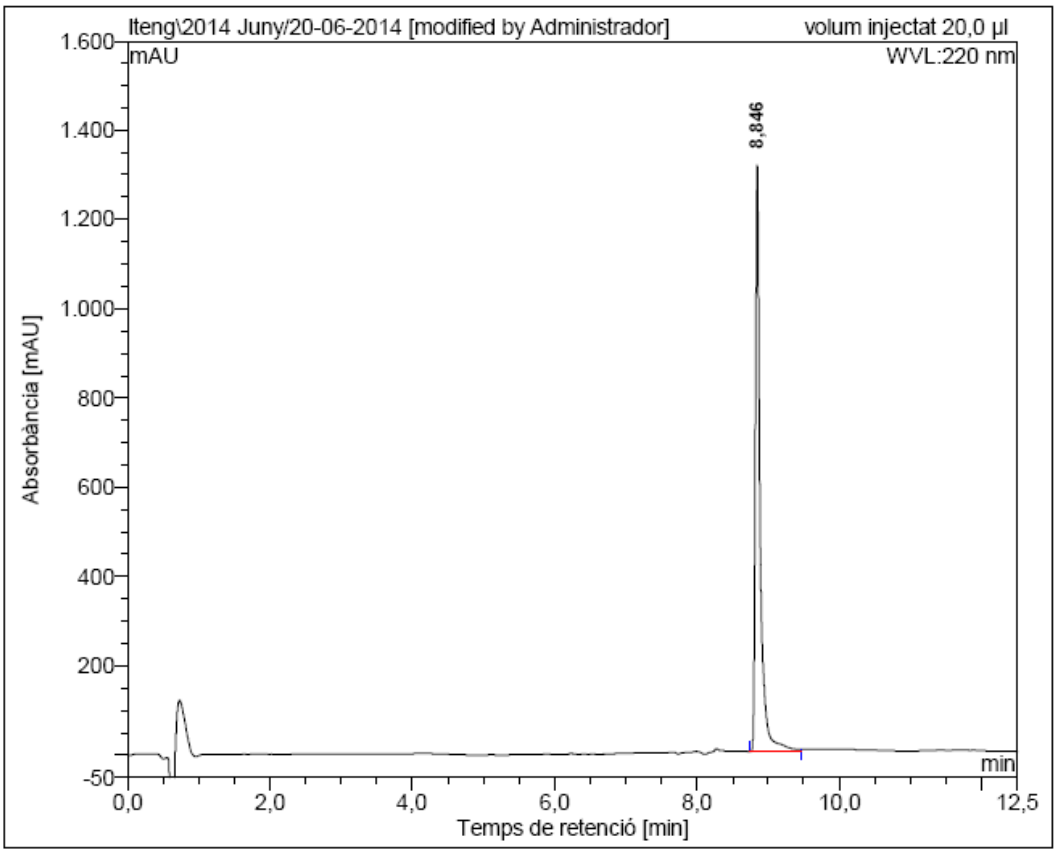

No.	mps retenc min	alçada mAU	Area mAU*min	Area relativa %
1	8,85	1313,420	103,151	100,00
Total:		1313,420	103,151	100,00

ESI-MS *m/z*

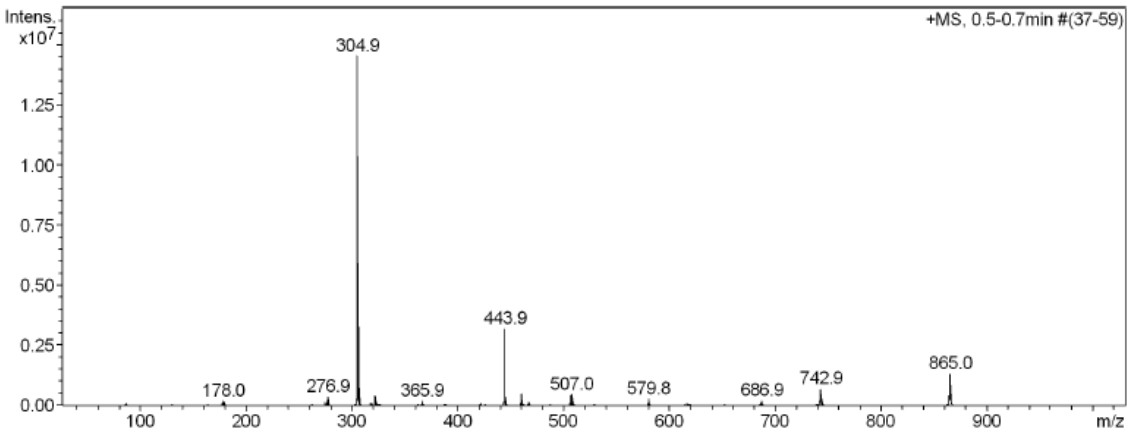

^{1}H-NMR (300 MHz, $CDCl_3$) δ (ppm)

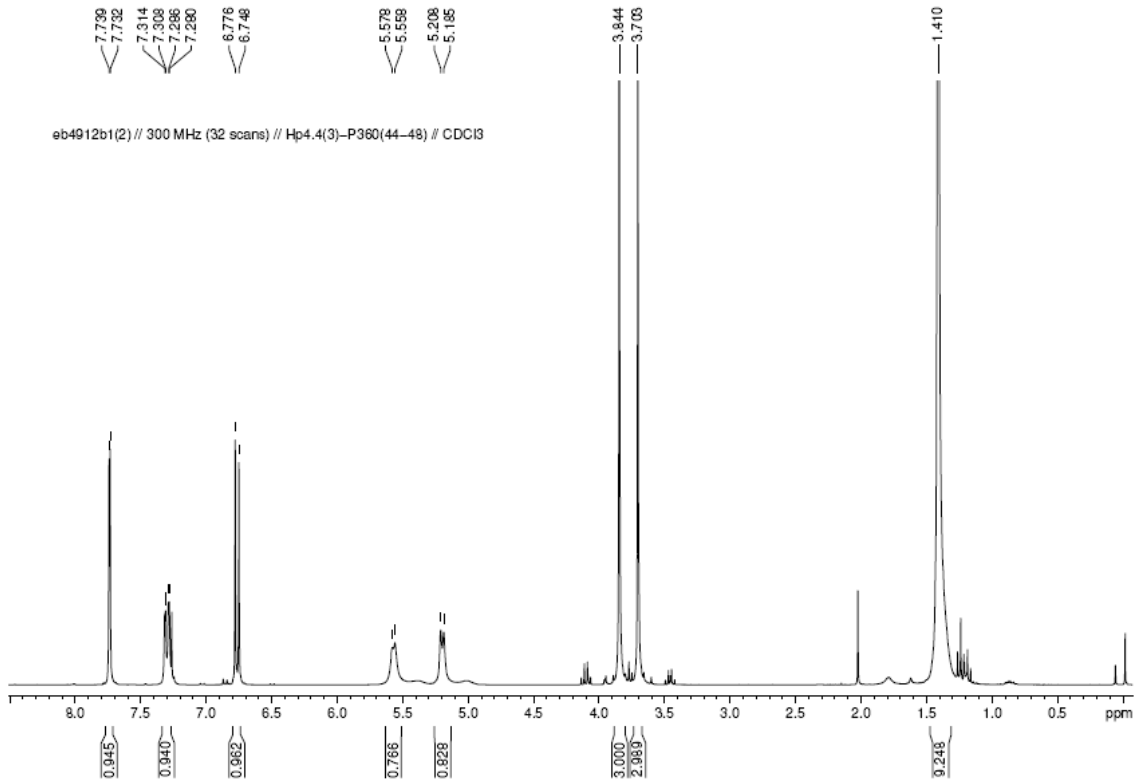

^{13}C-NMR (75 MHz, $CDCl_3$) δ (ppm)

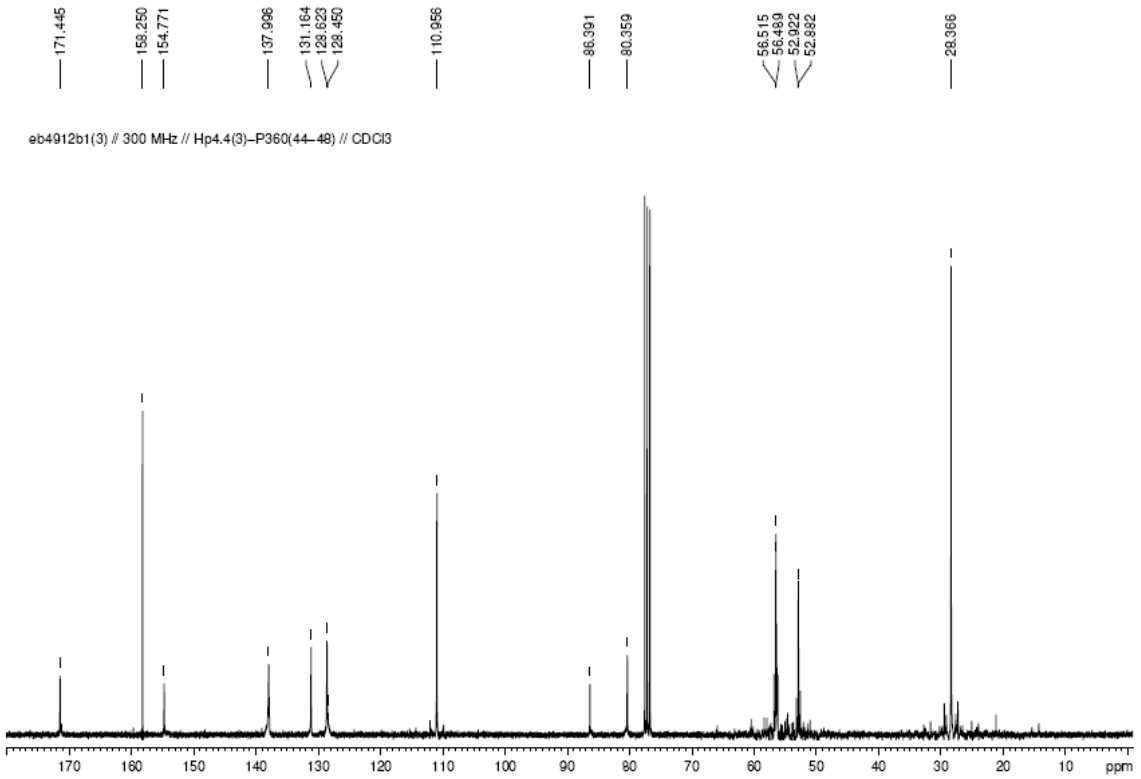

Boc-Phg(3-I,4-OMe)-OH

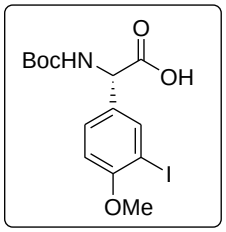

HPLC (λ = 220 nm)

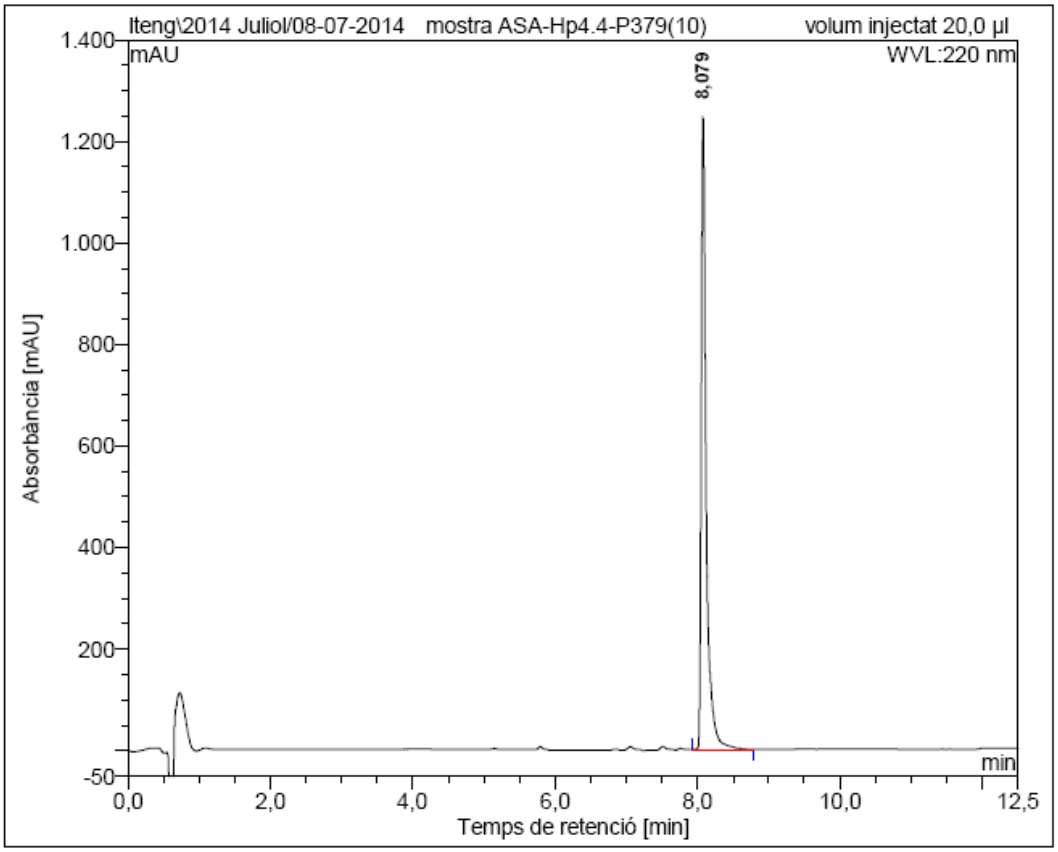

No.	mps retenc min	alçada mAU	Area mAU*min	Area relativa %
1	8,08	1244,995	99,756	100,00
Total:		1244,995	99,756	100,00

ESI-MS *m/z*

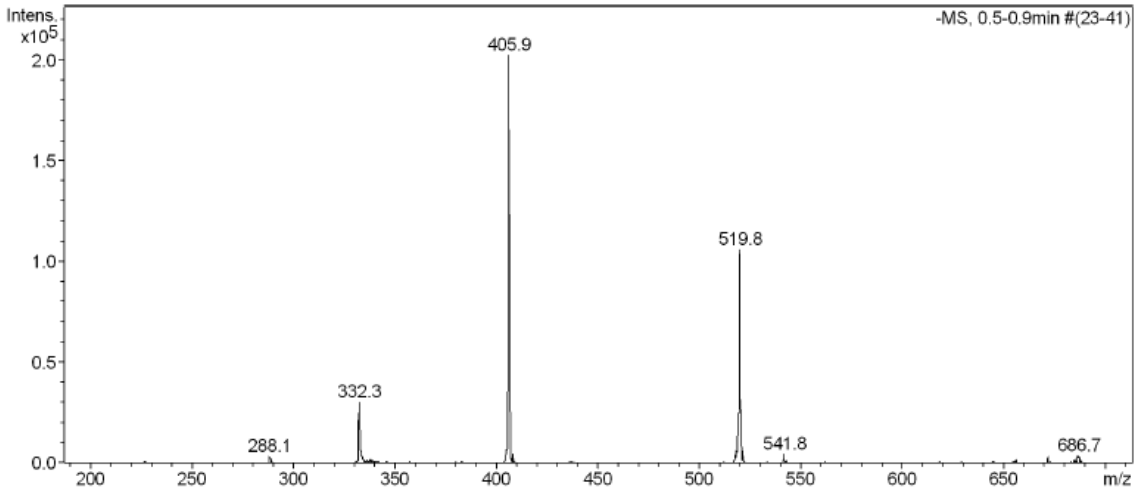

^{1}H-NMR (300 MHz, $CDCl_3$) δ (ppm)

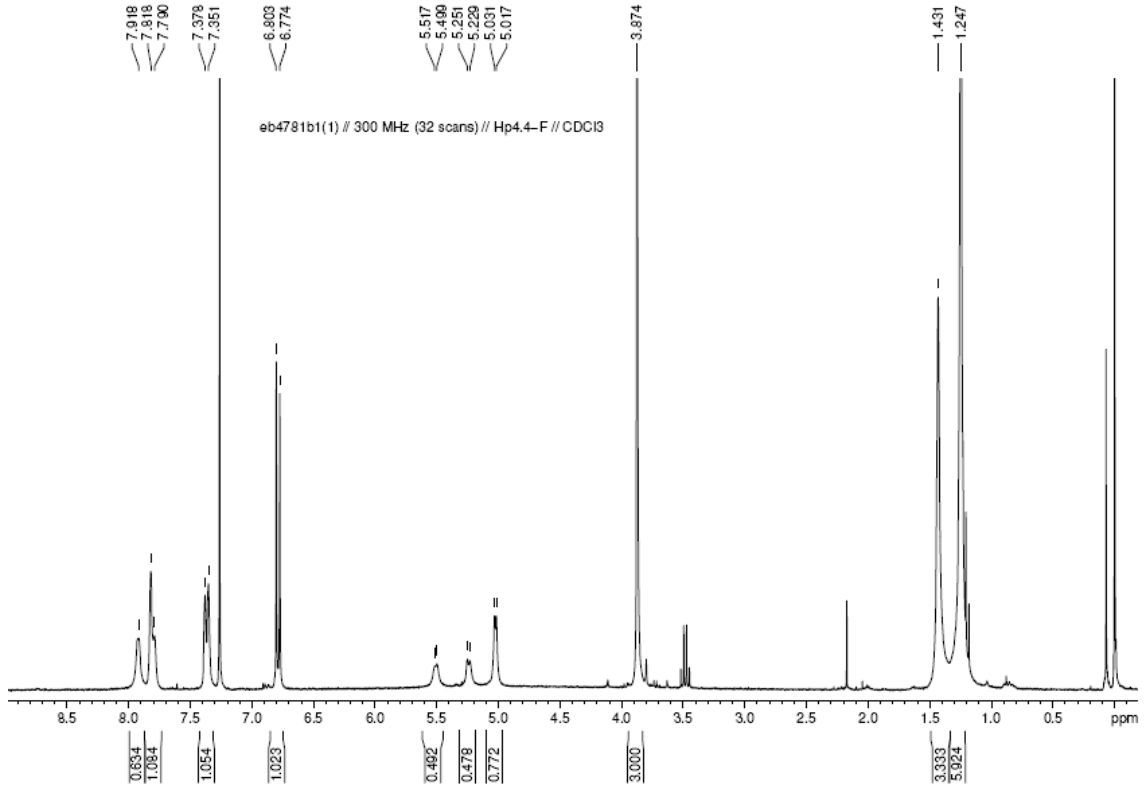

2. Synthesis of linear dipeptides

Fmoc-Ala-Tyr(3-I,Me)-NH_2

HPLC (λ = 220 nm)

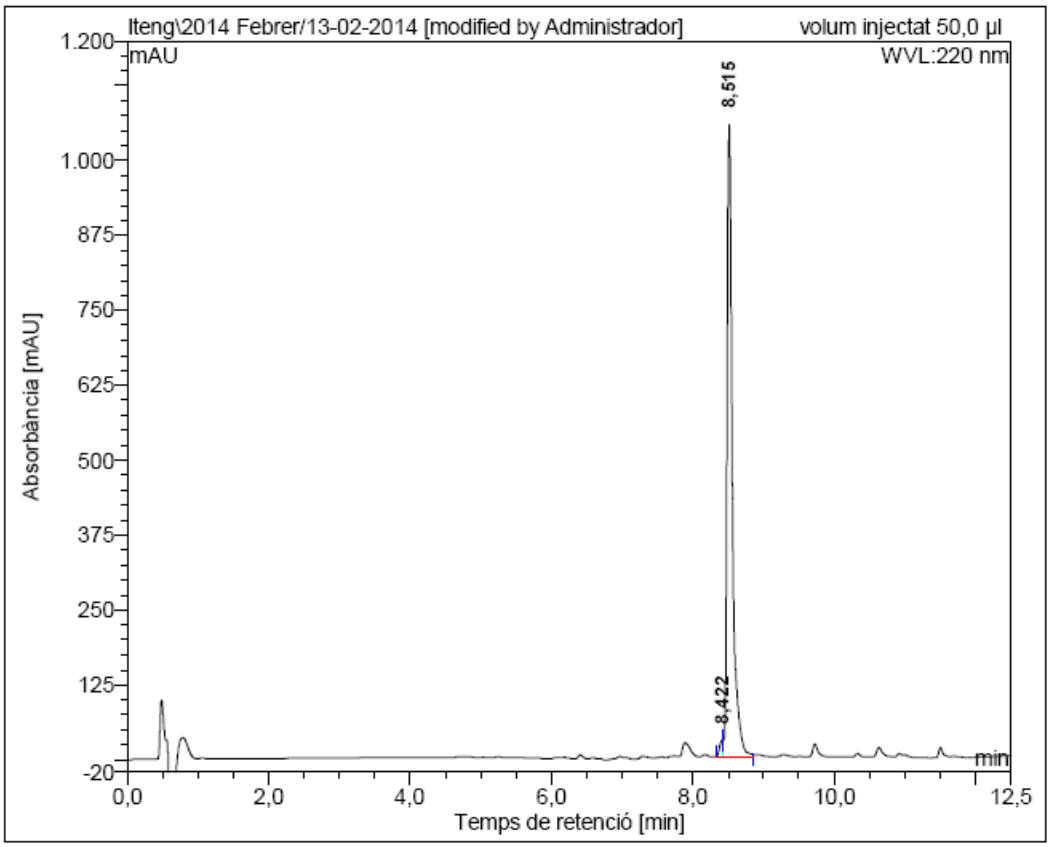

No.	mps retenc min	alçada mAU	Area mAU*min	Area relativa %
1	8,42	28,977	1,621	1,74
2	8,51	1054,974	91,429	98,26
Total:		1083,951	93,050	100,00

H-Ala-Tyr(3-I,Me)-NH_2

HPLC (λ = 220 nm)

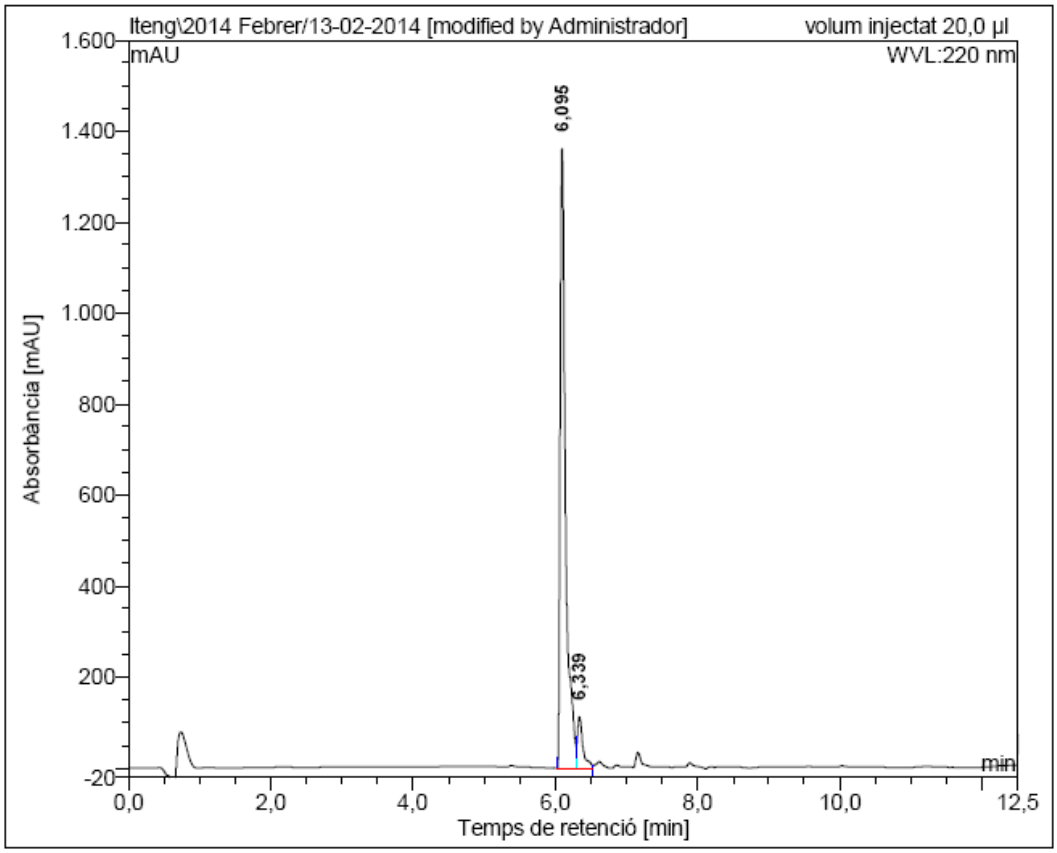

No.	mps retenc min	alçada mAU	Area mAU*min	Area relativa %
1	6,10	1361,691	120,422	92,00
2	6,34	112,716	10,467	8,00
Total:		1474,407	130,889	100,00

ESI-MS *m/z*

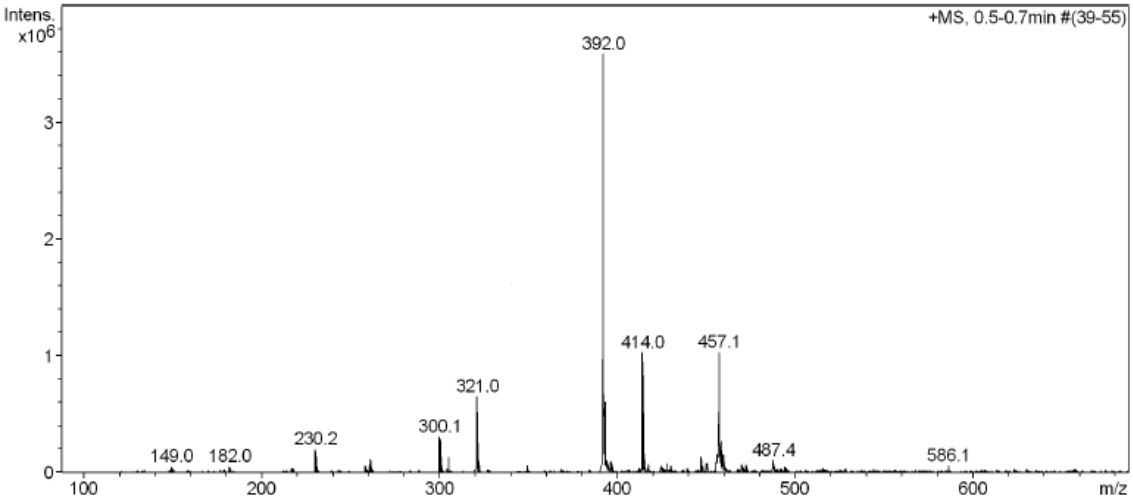

H-Ala-Tyr(3-B(OH)$_2$,Me)-NH$_2$

HPLC (λ = 220 nm)

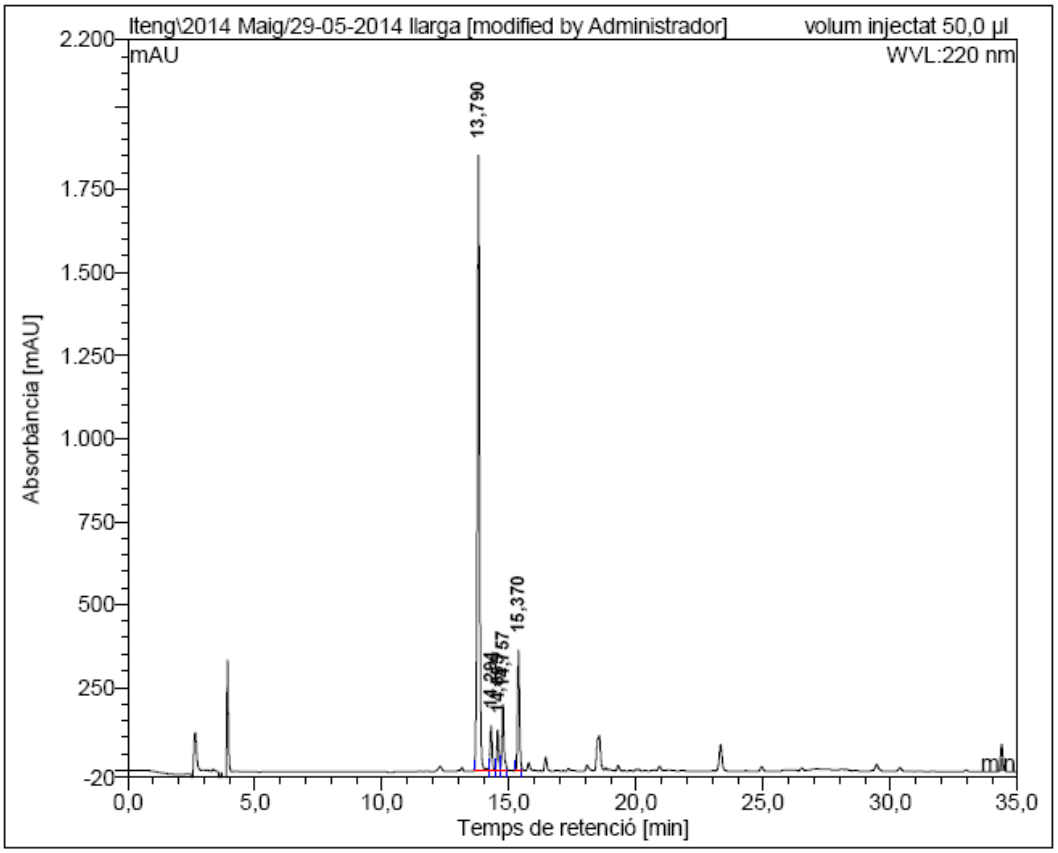

No.	mps retenc min	alçada mAU	Area mAU*min	Area relativa %
1	13,79	1852,744	194,745	71,78
2	14,29	135,520	12,490	4,60
3	14,55	123,196	11,067	4,08
4	14,76	200,682	19,334	7,13
5	15,37	364,017	33,688	12,42
Total:		2676,159	271,324	100,00

ESI-MS *m/z*

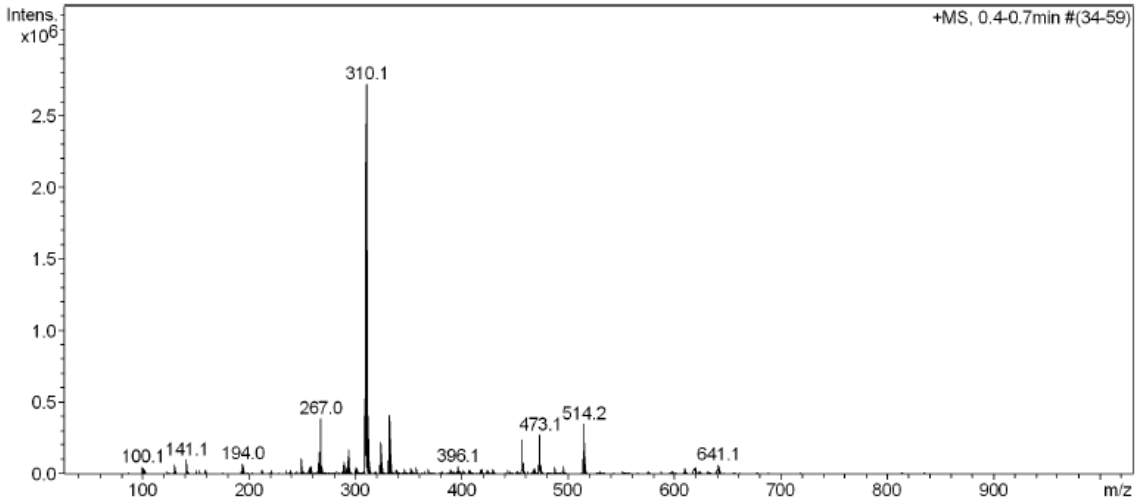

3. Synthesis of linear tripeptides

H-Phe(4-I)-Ala-Tyr(3-B(OH)$_2$,Me)-NH$_2$

HPLC (λ = 220 nm)

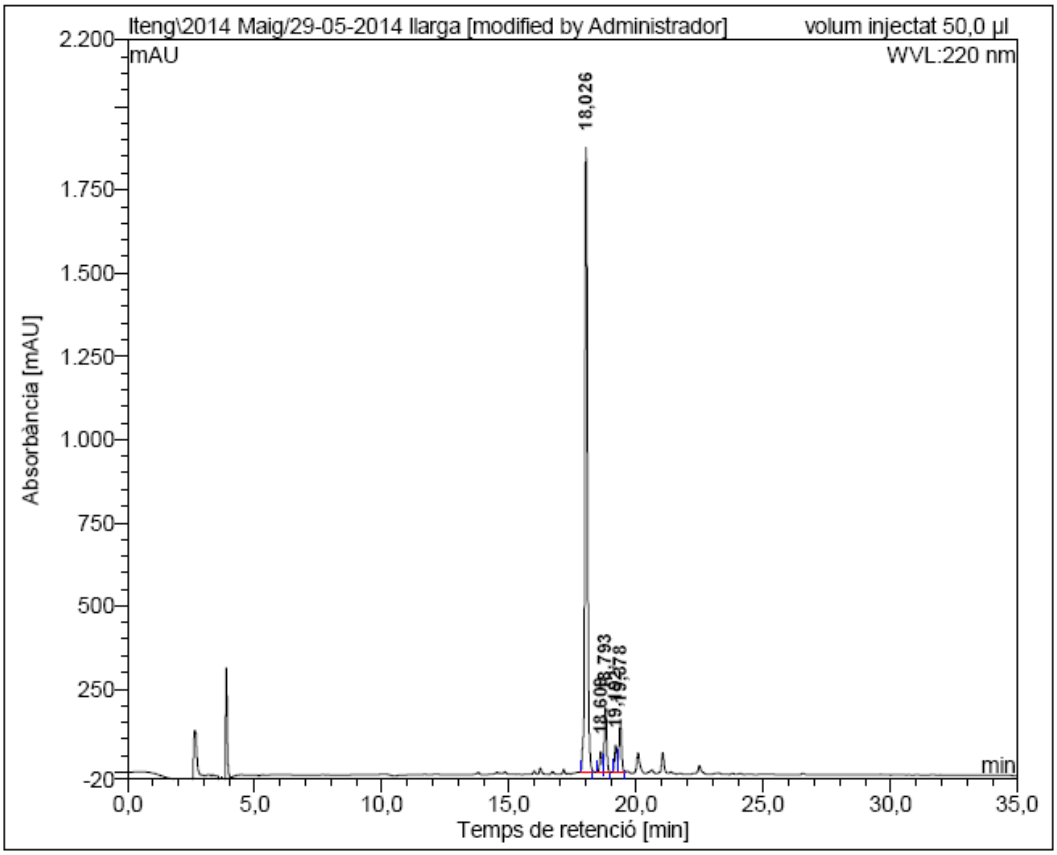

No.	mps retenc min	alçada mAU	Area mAU*min	Area relativa %
1	18,03	1879,065	227,742	80,63
2	18,61	64,538	7,106	2,52
3	18,79	194,847	20,688	7,32
4	19,19	84,000	9,655	3,42
5	19,38	160,742	17,248	6,11
Total:		2383,192	282,439	100,00

ESI-MS *m/z*

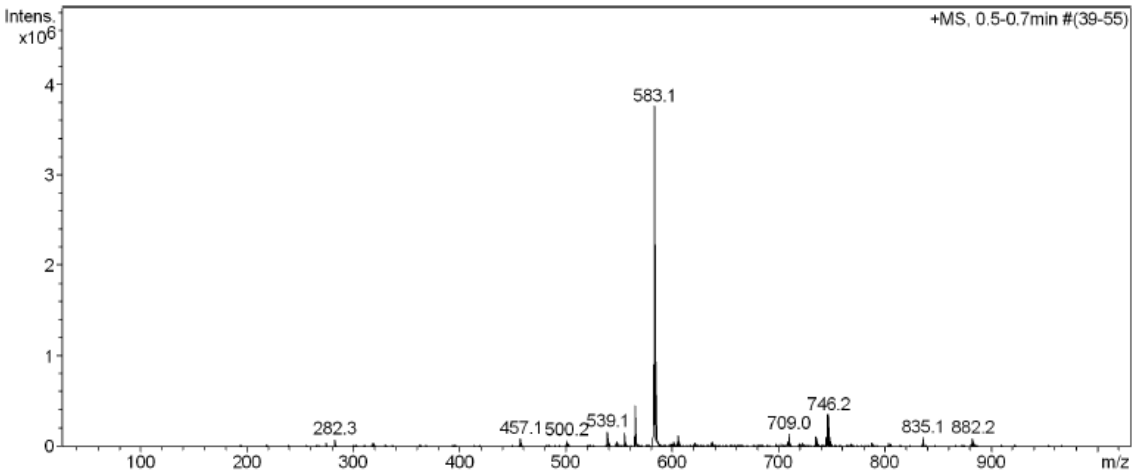

H-Tyr(3-I,Me)-Ala-Tyr(3-B(OH)$_2$,Me)-NH$_2$

HPLC (λ = 220 nm)

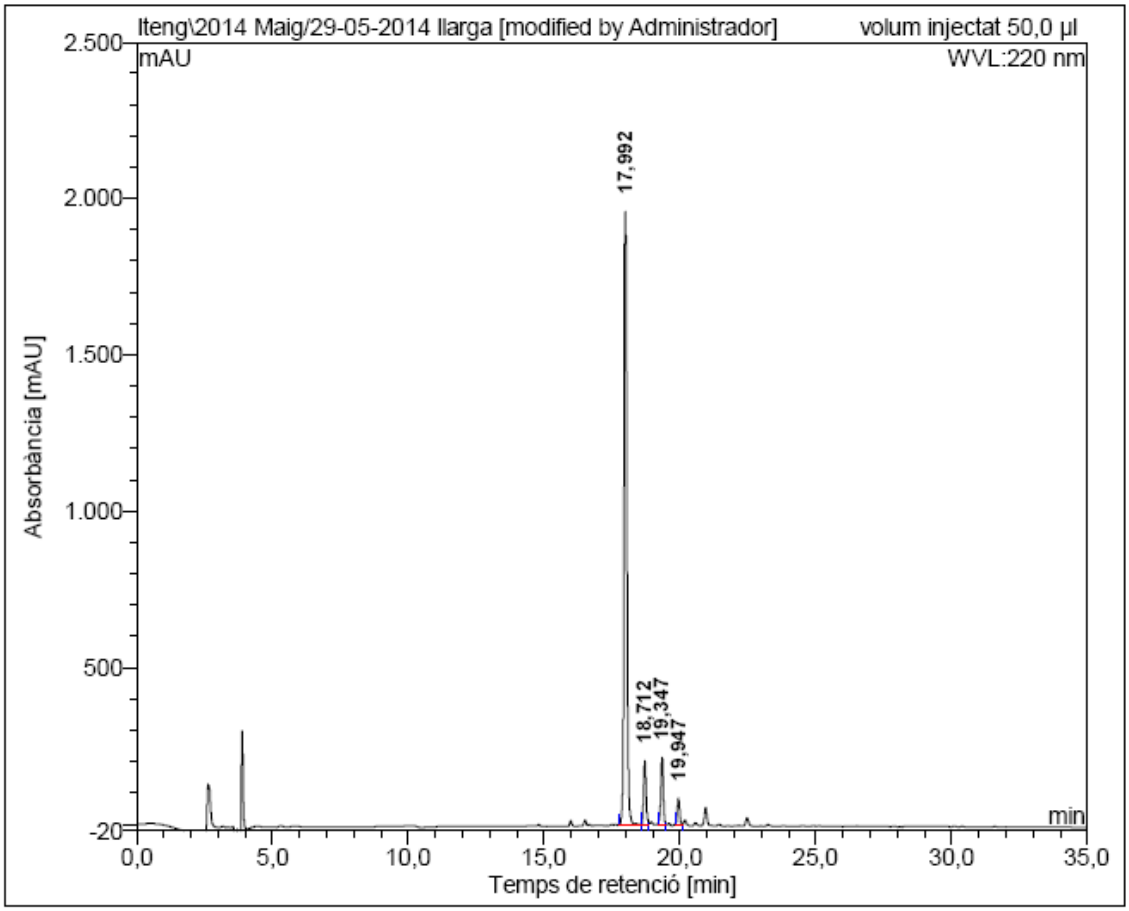

No.	mps retenc min	alçada mAU	Area mAU*min	Area relativa %
1	17,99	1959,798	252,855	82,44
2	18,71	204,680	22,459	7,32
3	19,35	216,346	22,905	7,47
4	19,95	85,552	8,495	2,77
Total:		2466,375	306,714	100,00

ESI-MS *m/z*

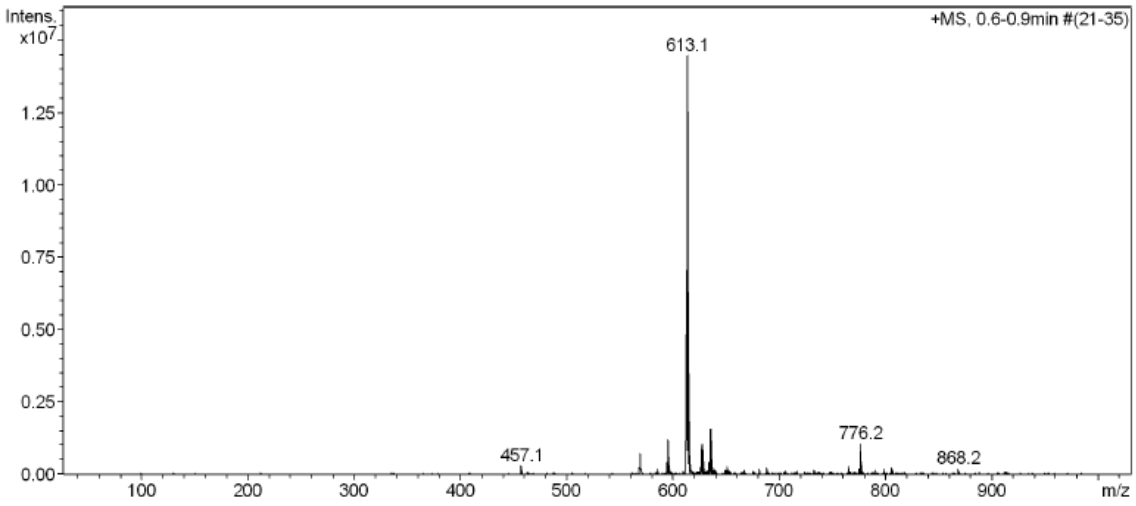

H-His(5-Br)-Ala-Tyr(3-B(OH)$_2$,Me)-NH$_2$

HPLC (λ = 220 nm)

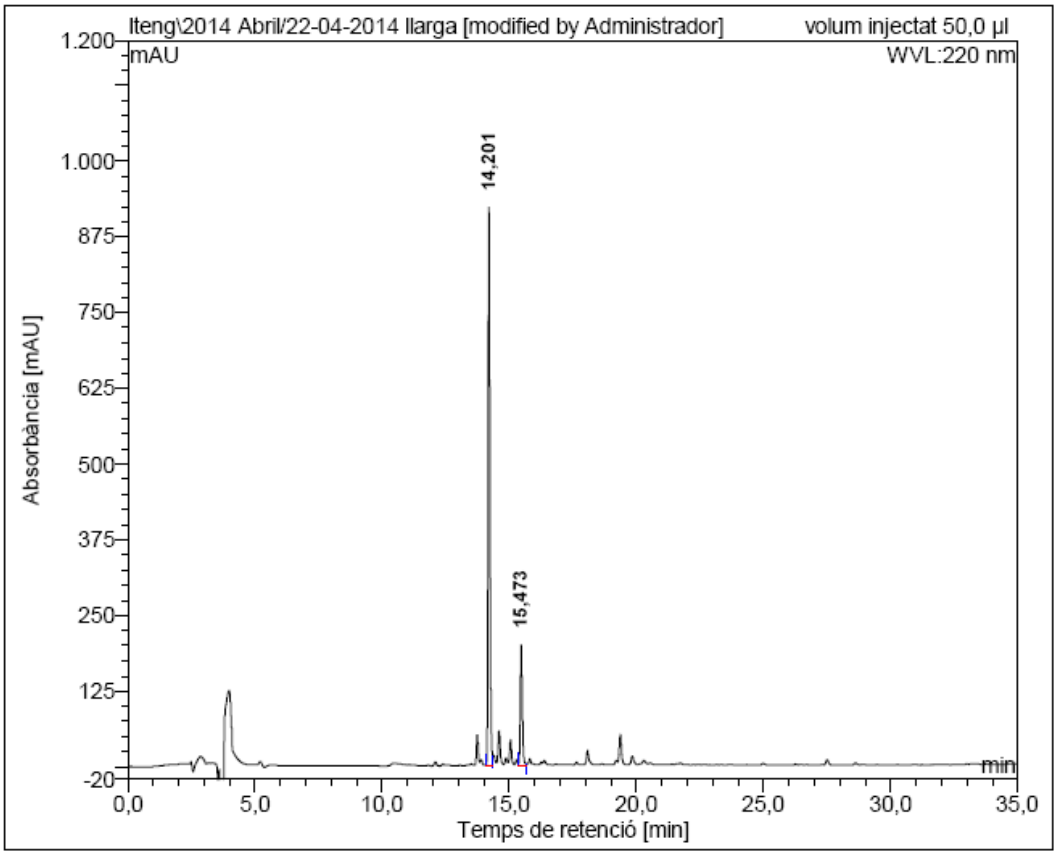

No.	mps retenc min	alçada mAU	Area mAU*min	Area relativa %
1	14,20	920,730	77,098	81,50
2	15,47	198,439	17,504	18,50
Total:		1119,169	94,602	100,00

ESI-MS *m/z*

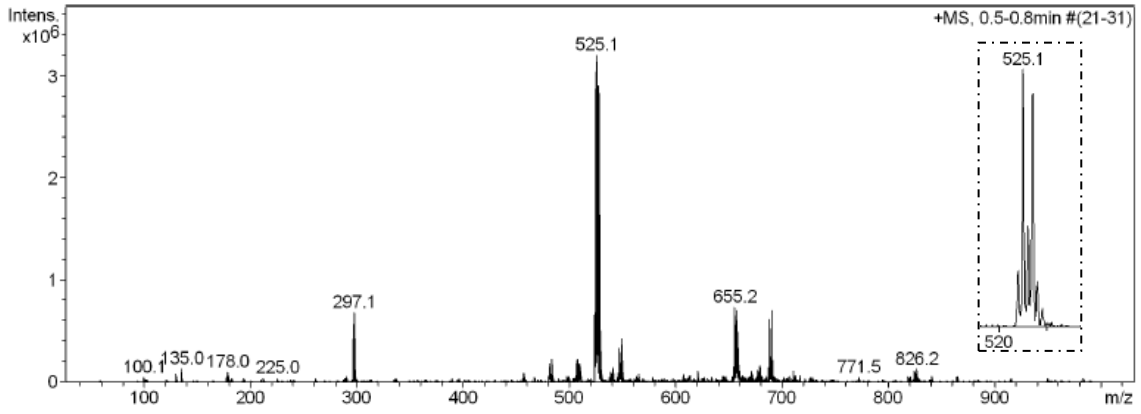

H-Phg(3-I,4-OMe)-Ala-Tyr(3-B(OH)$_2$,Me)-NH$_2$

HPLC (λ = 220 nm)

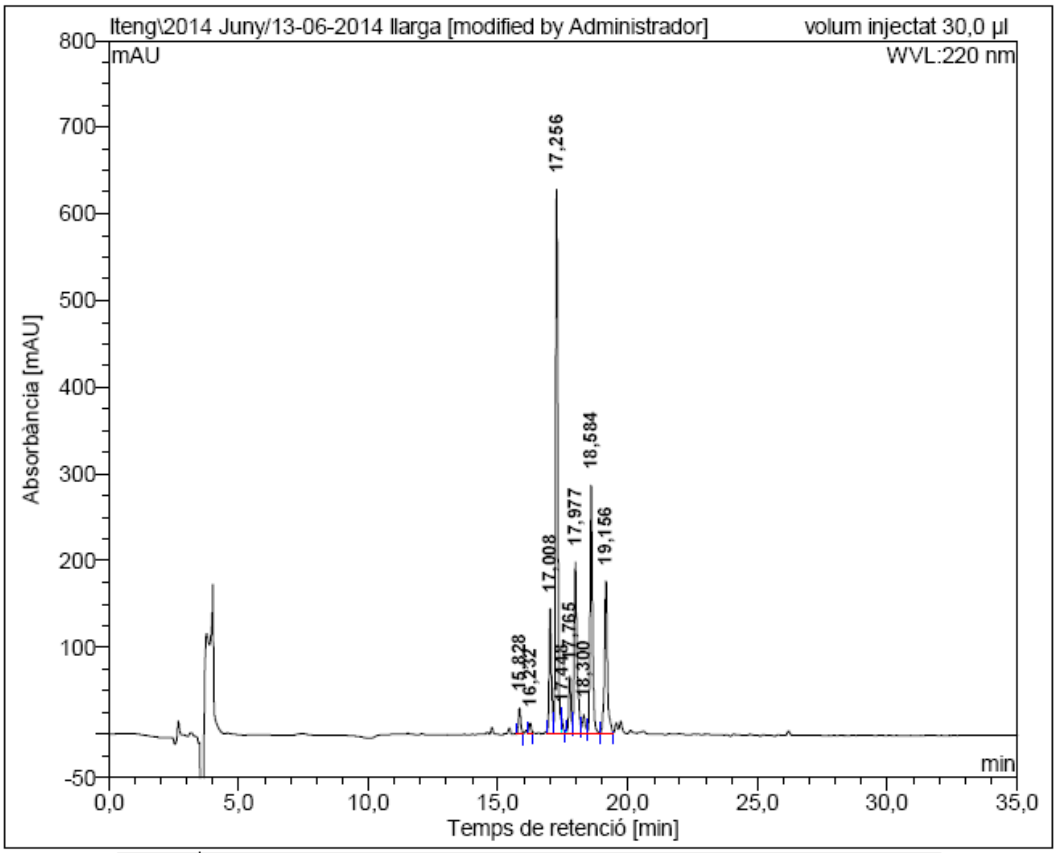

No.	mps retenc min	alçada mAU	Area mAU*min	Area relativa %
1	15,83	30,247	3,017	1,74
2	16,23	13,109	1,453	0,84
3	17,01	144,768	14,920	8,59
4	17,26	627,829	62,813	36,15
5	17,45	17,975	1,626	0,94
6	17,77	66,721	6,859	3,95
7	17,98	198,483	25,145	14,47
8	18,30	22,297	3,001	1,73
9	18,58	286,613	32,020	18,43
10	19,16	176,650	22,917	13,19
Total:		1584,692	173,772	100,00

ESI-MS *m/z*

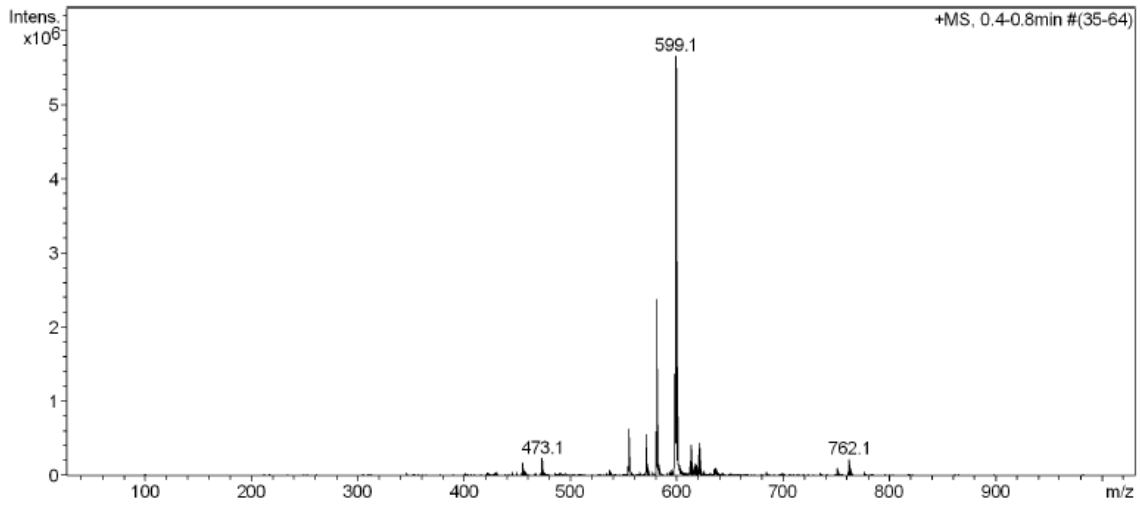

4. Synthesis of biaryl cyclic tripeptides

Biaryl cyclic peptide incorporating a Phe-Tyr linkage 17

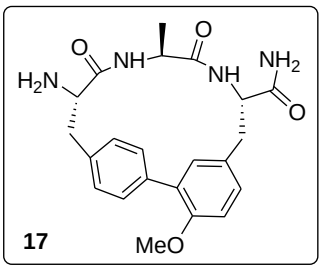

Crude peptide 17

HPLC (λ = 220 nm)

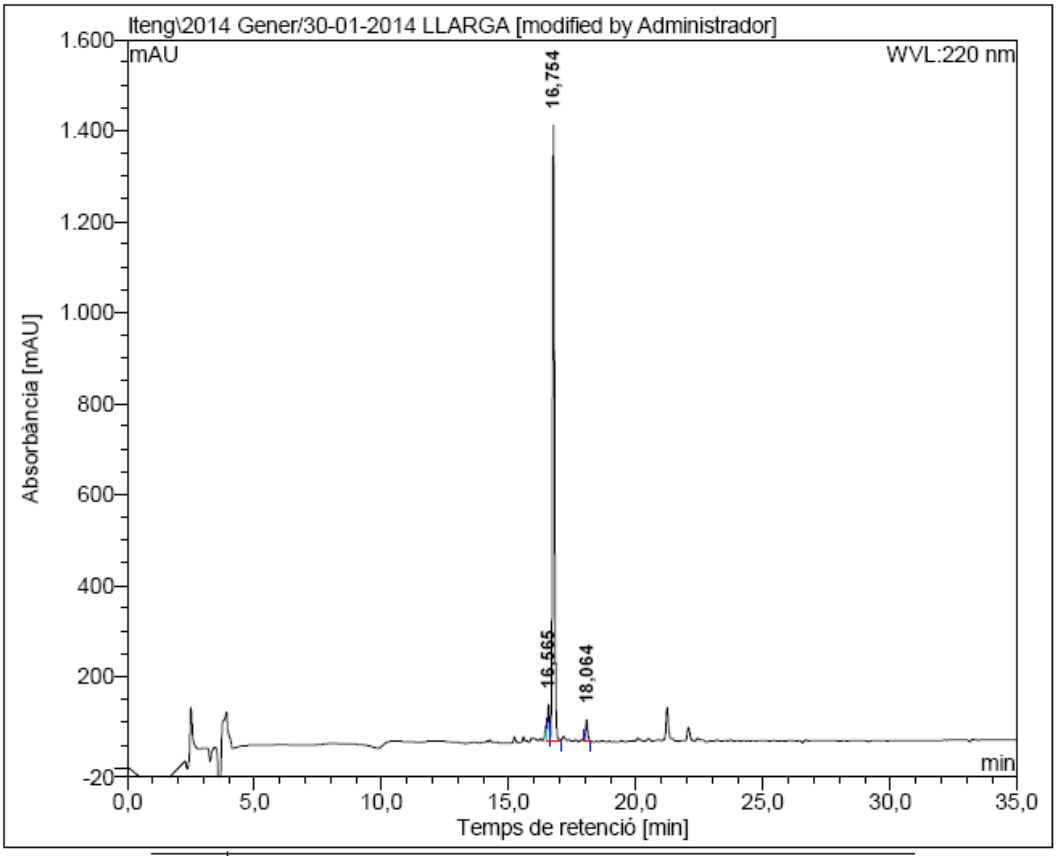

No.	mps retenc min	alçada mAU	Area mAU*min	Area relativa %
1	16,56	81,473	7,021	5,08
2	16,75	1353,326	126,723	91,64
3	18,06	47,162	4,540	3,28
Total:		1481,962	138,284	100,00

ESI-MS *m/z*

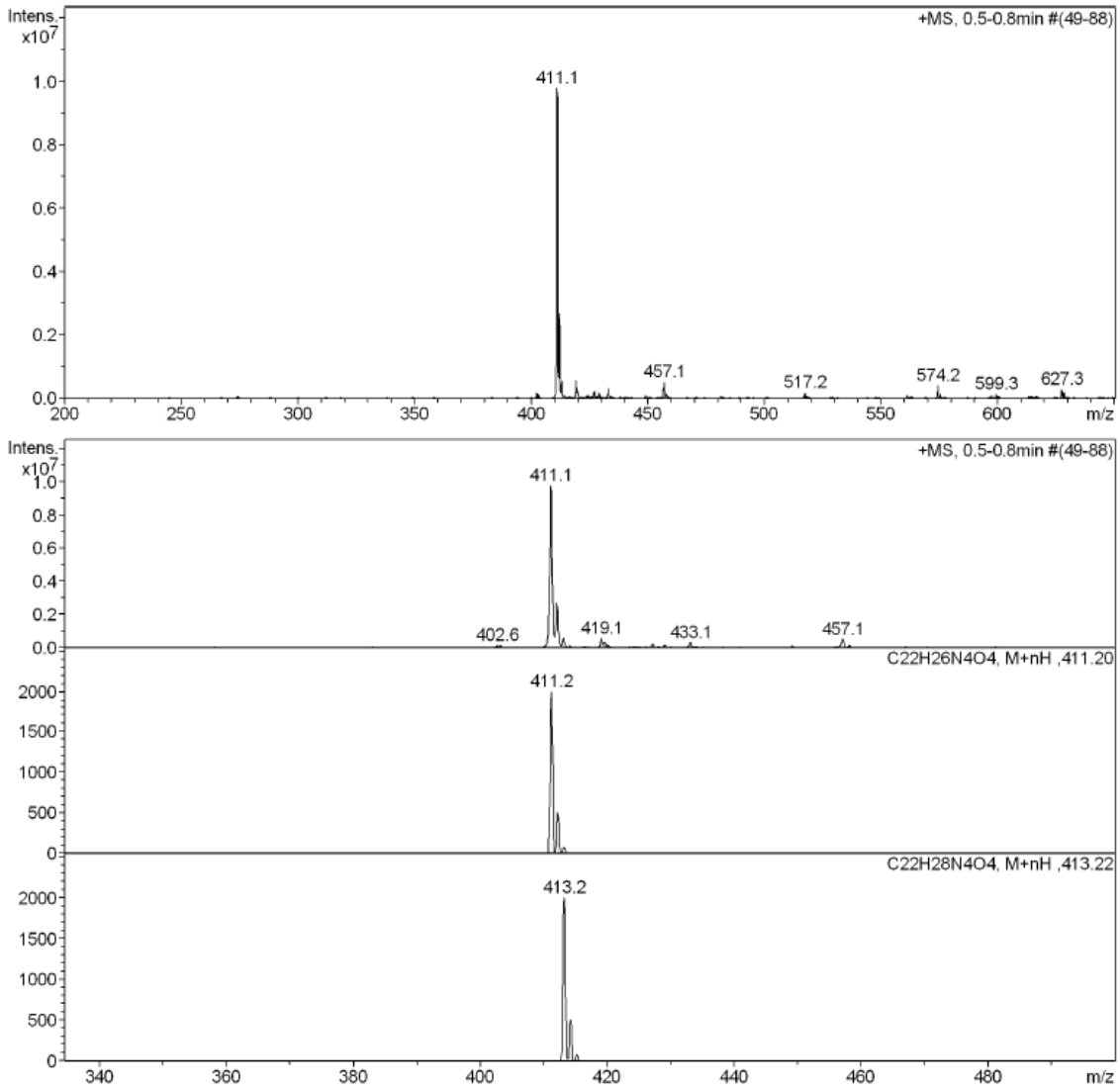
Intens.
x10^7
+MS, 0.5-0.8min #(49-88)
411.1
457.1
517.2
574.2
599.3
627.3
m/z
402.6
419.1
433.1
C22H26N4O4, M+nH ,411.20
411.2
C22H28N4O4, M+nH ,413.22
413.2

Purified peptide 17

HPLC (λ = 220 nm)

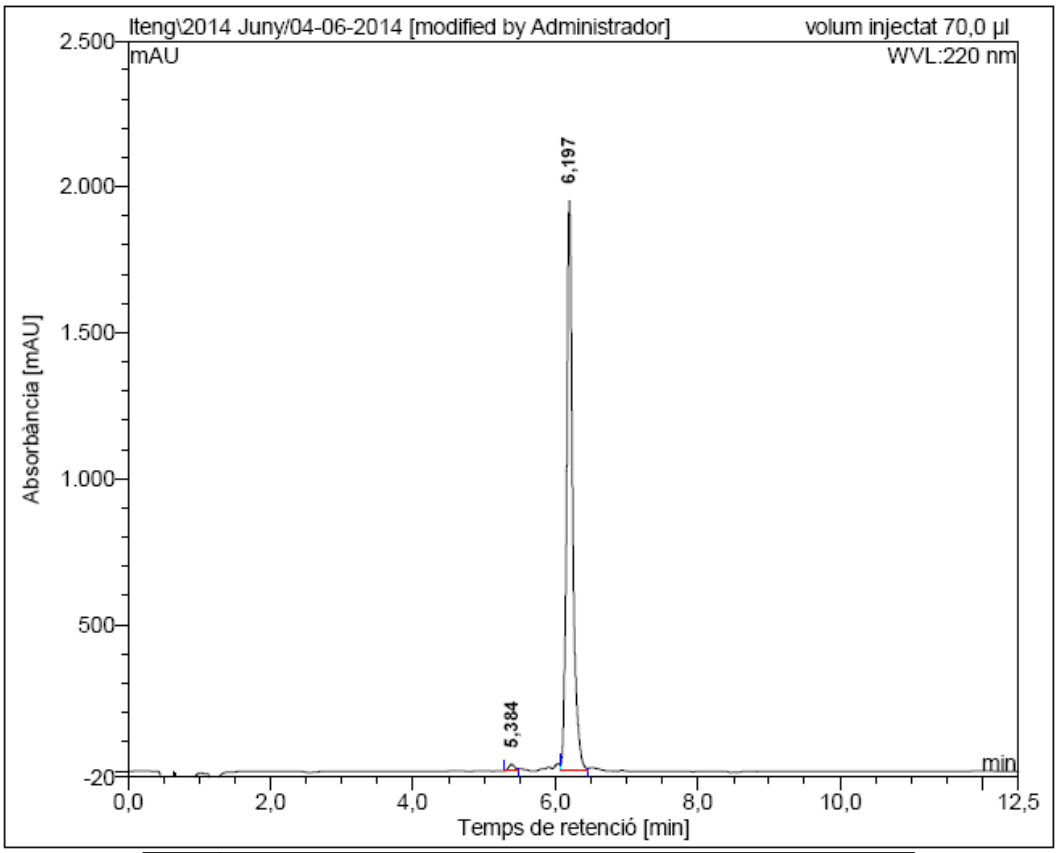

No.	mps retenc min	alçada mAU	Area mAU*min	Area relativa %
1	5,38	22,021	2,233	1,14
2	6,20	1951,418	194,203	98,86
Total:		1973,439	196,436	100,00

ESI-MS *m/z*

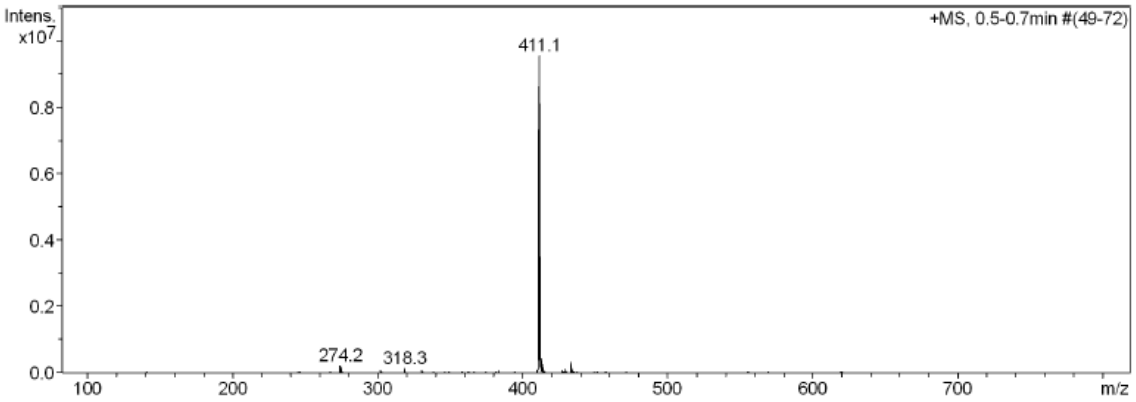

HRMS (ESI) *m/z*

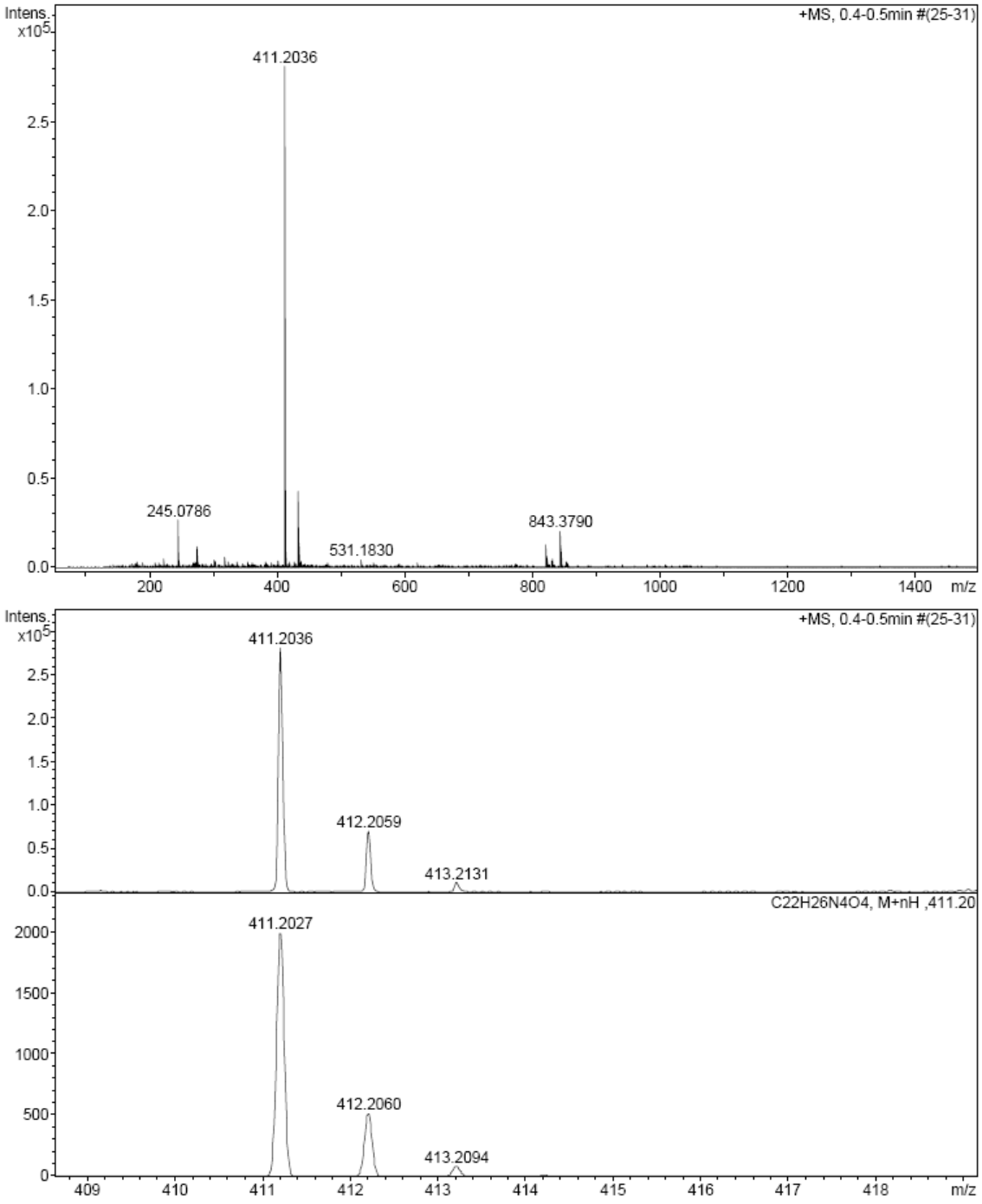
Intens.
x10^5
+MS, 0.4-0.5min #(25-31)
411.2036
245.0786
531.1830
843.3790
m/z
C22H26N4O4, M+nH ,411.20
411.2027
412.2059
412.2060
413.2131
413.2094

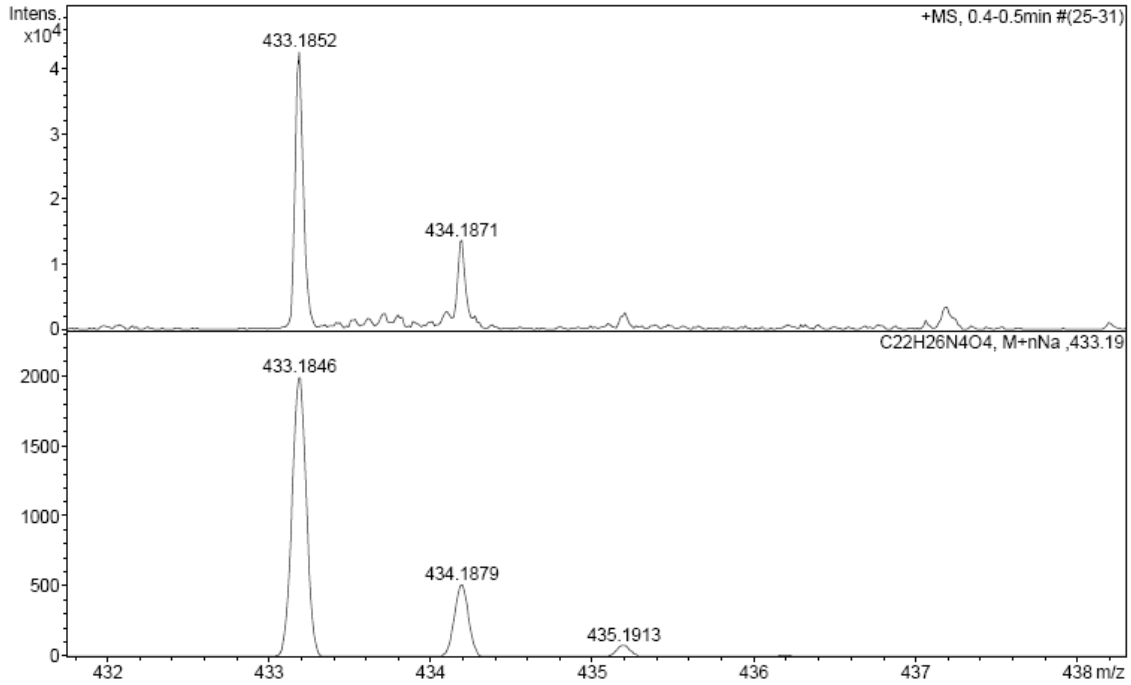

^{1}H-NMR (400 MHz, CD_3OD) δ (ppm)

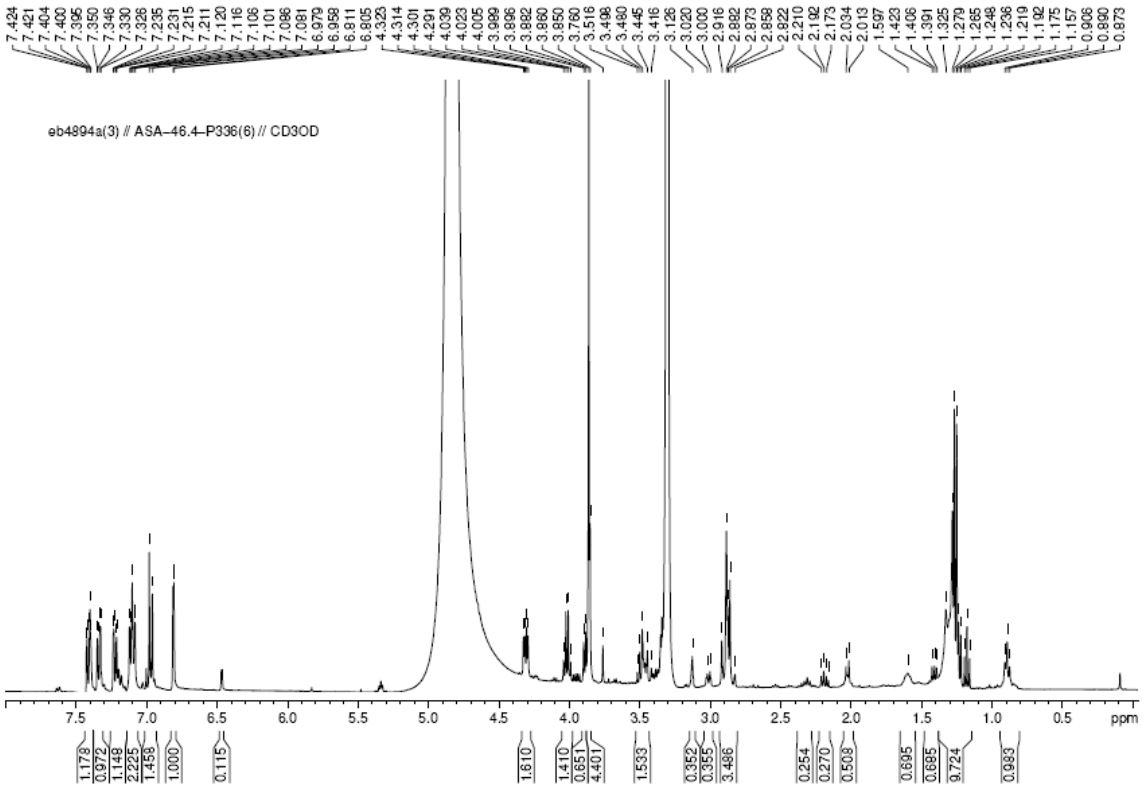

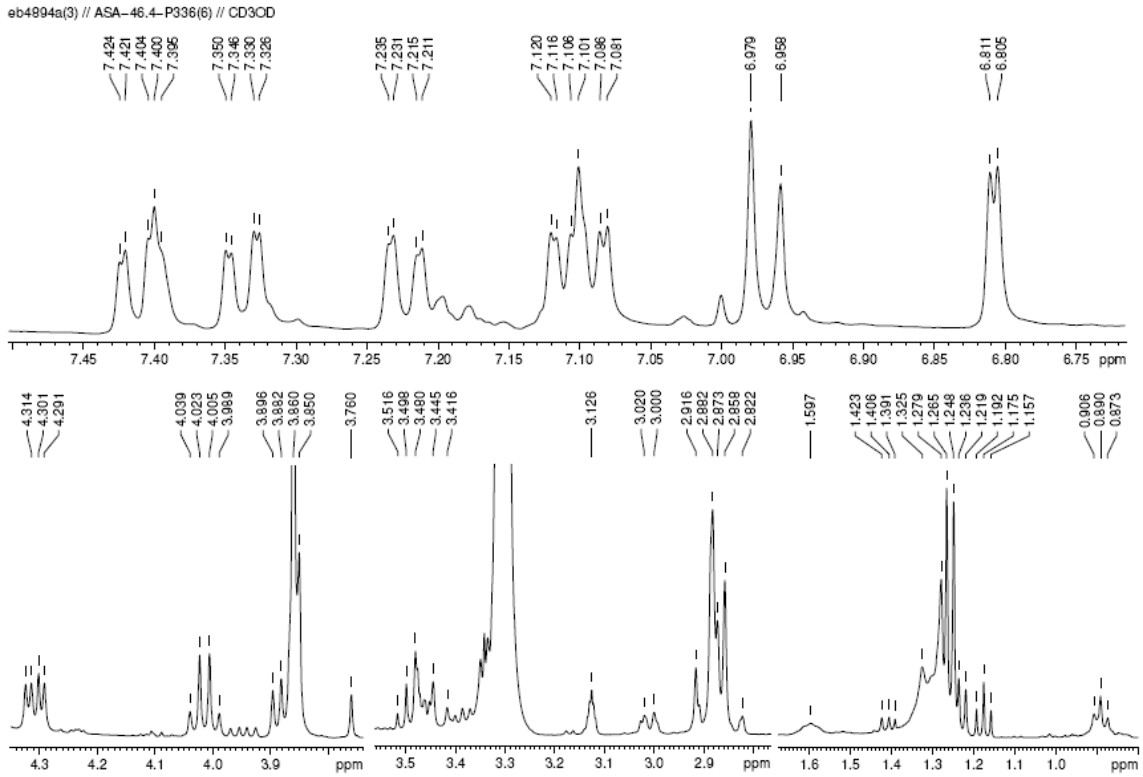

COSY (400 MHz, CD_3OD) δ (ppm)

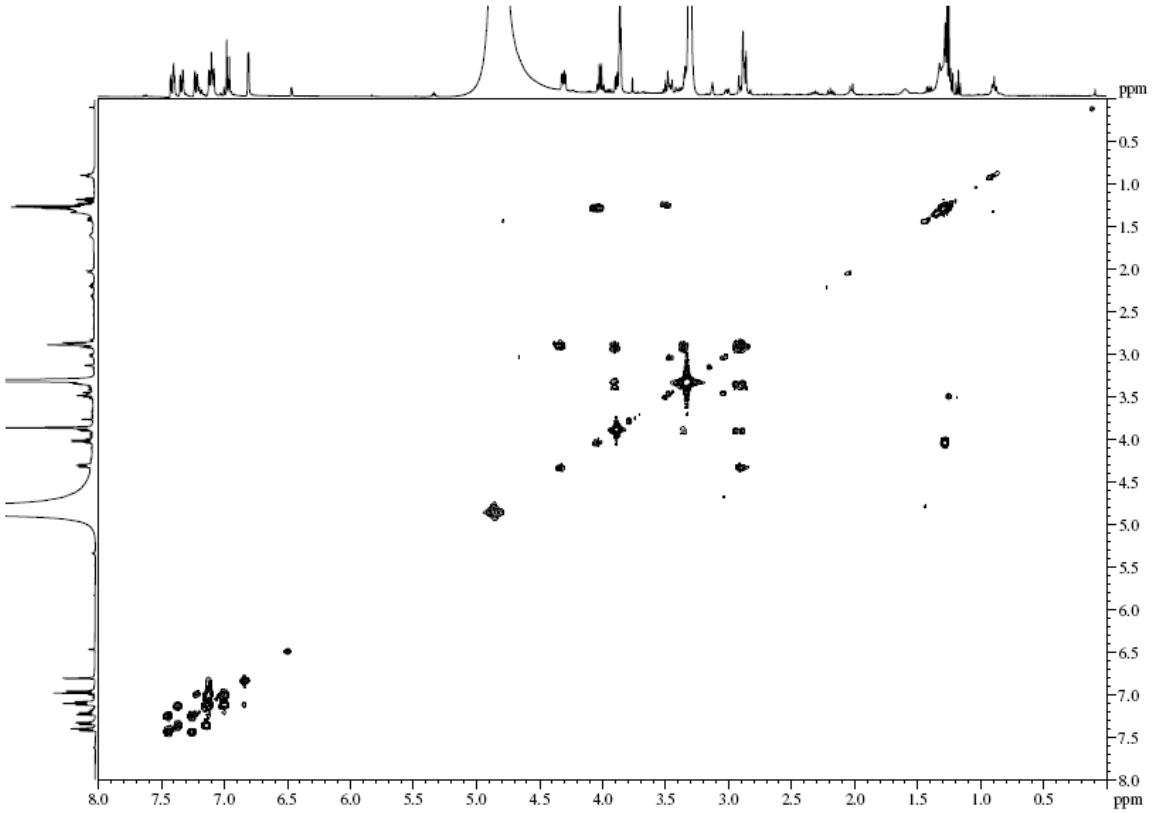

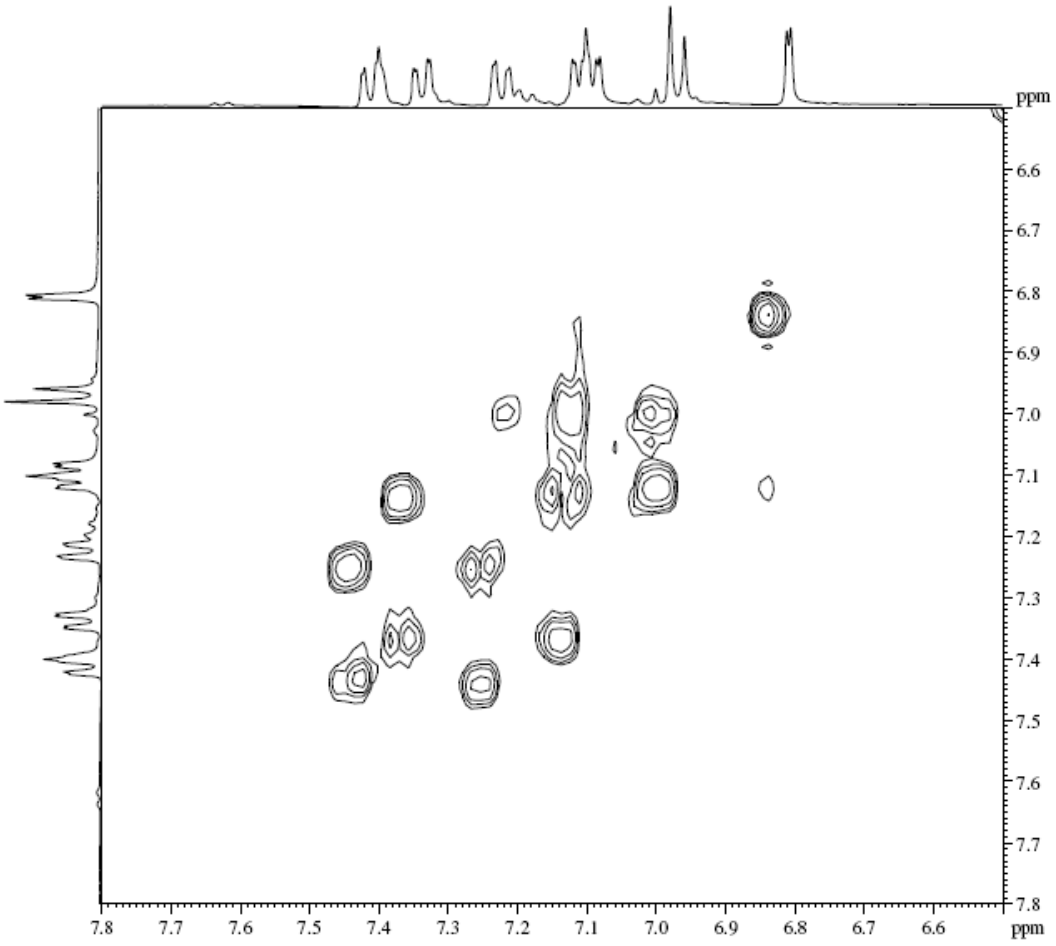
ppm
6.6
6.7
6.8
6.9
7.0
7.1
7.2
7.3
7.4
7.5
7.6
7.7
7.8
7.8
7.7
7.6
7.5
7.4
7.3
7.2
7.1
7.0
6.9
6.8
6.7
6.6
ppm

Biaryl cyclic peptide incorporating a Tyr-Tyr linkage 23

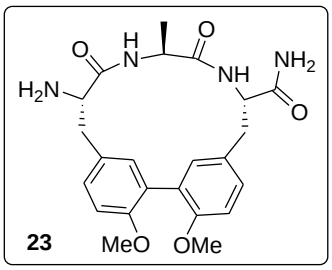

Crude peptide 23

HPLC (λ = 220 nm)

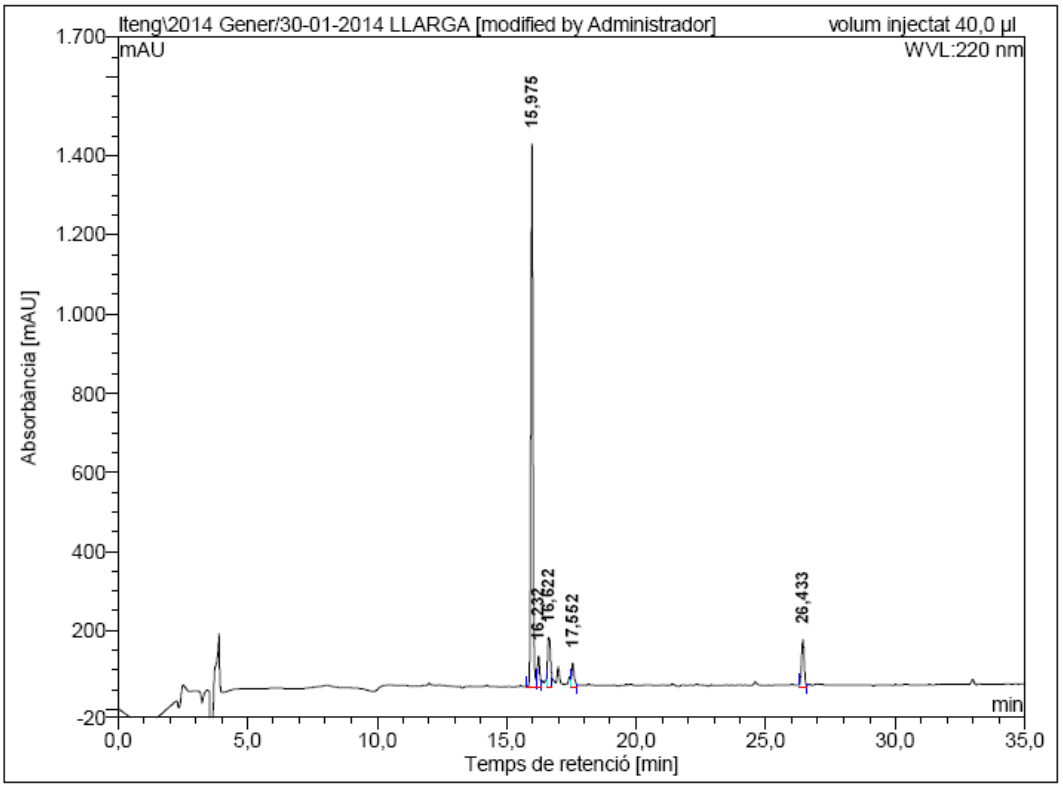

No.	Temps retenció min	alçada mAU	Area mAU*min	Area relativa %
1	15,97	1373,053	121,452	72,90
2	16,23	76,679	7,674	4,61
3	16,62	124,288	17,062	10,24
4	17,55	59,655	6,647	3,99
5	26,43	118,045	13,762	8,26
Total:		1751,721	166,598	100,00

ESI-MS *m/z*

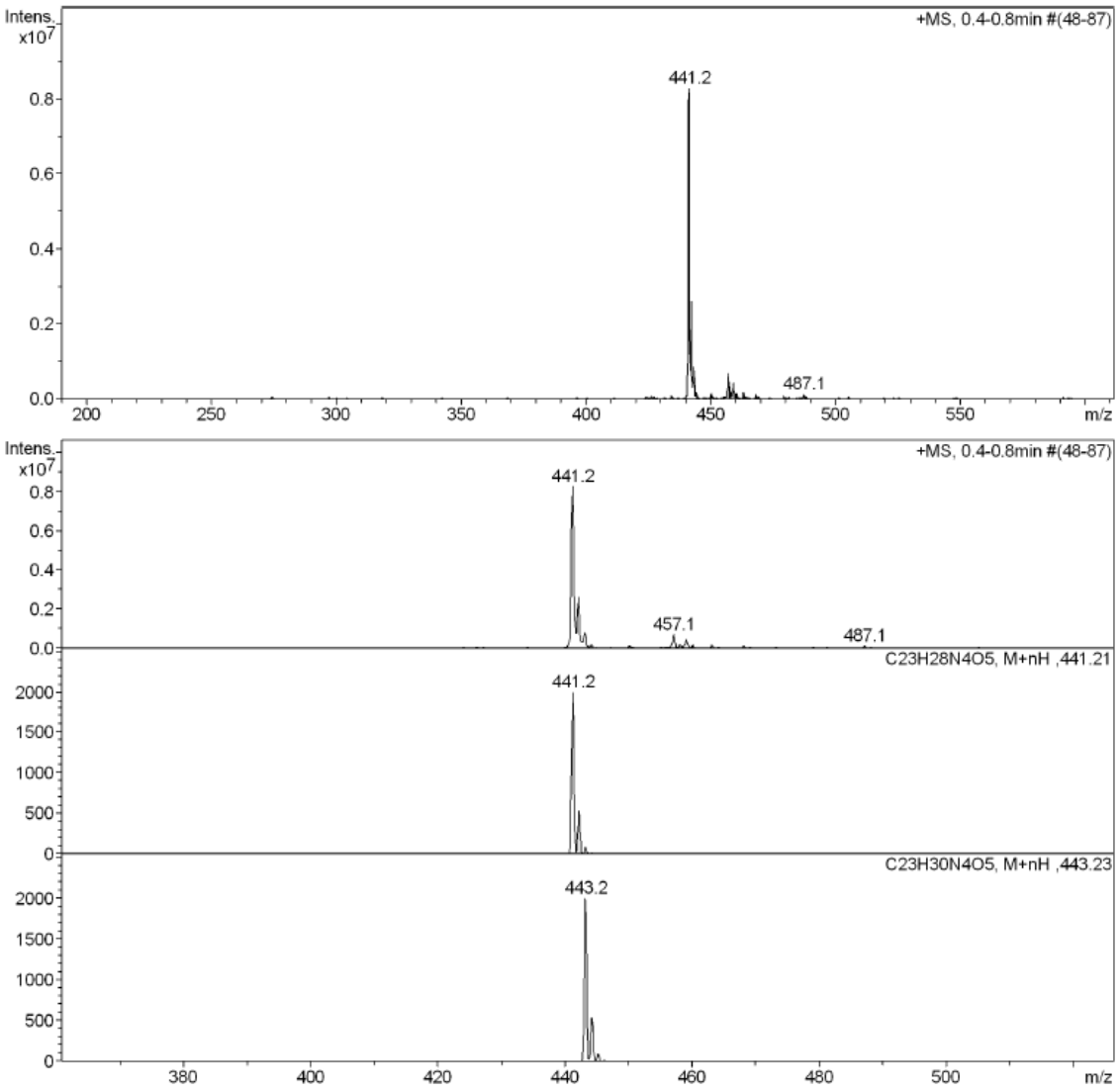
Intens.
x10^7
+MS, 0.4-0.8min #(48-87)
441.2
487.1
m/z
457.1
C23H28N4O5, M+nH ,441.21
C23H30N4O5, M+nH ,443.23
443.2

Purified peptide 23

HPLC (λ = 220 nm)

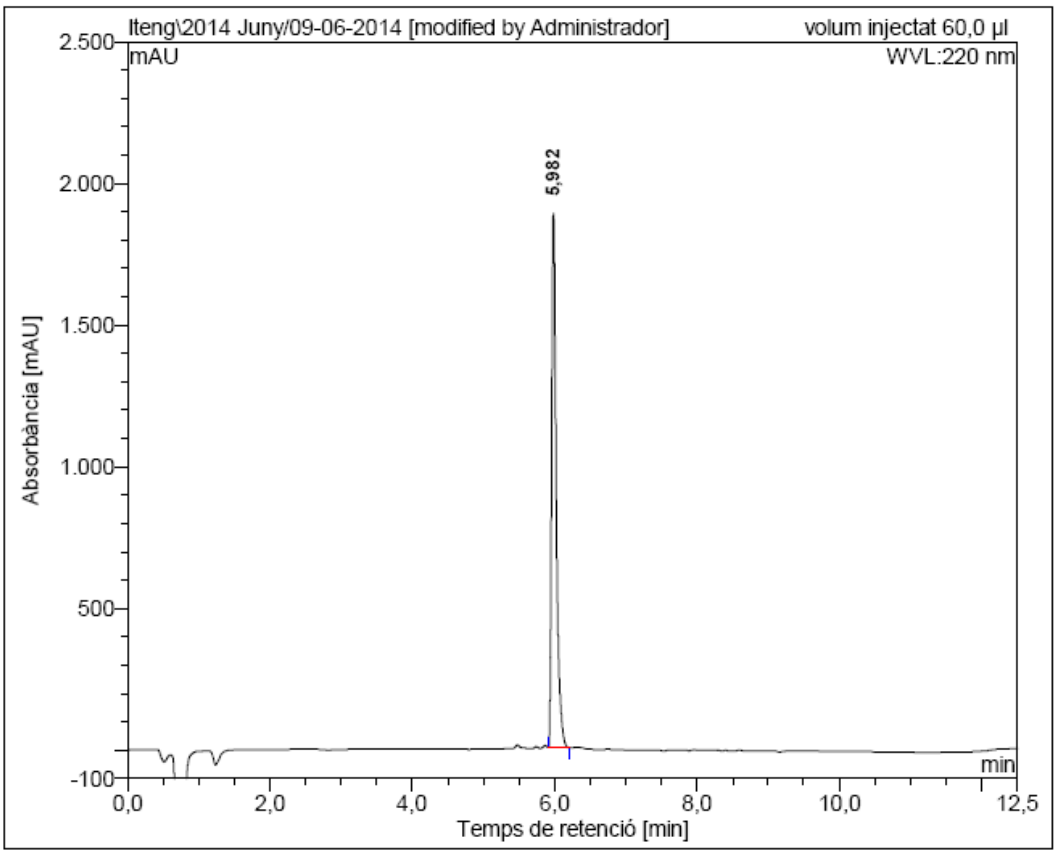

No.	mps retenc min	alçada mAU	Area mAU*min	Area relativa %
1	5,98	1885,745	142,011	100,00
Total:		1885,745	142,011	100,00

ESI-MS *m/z*

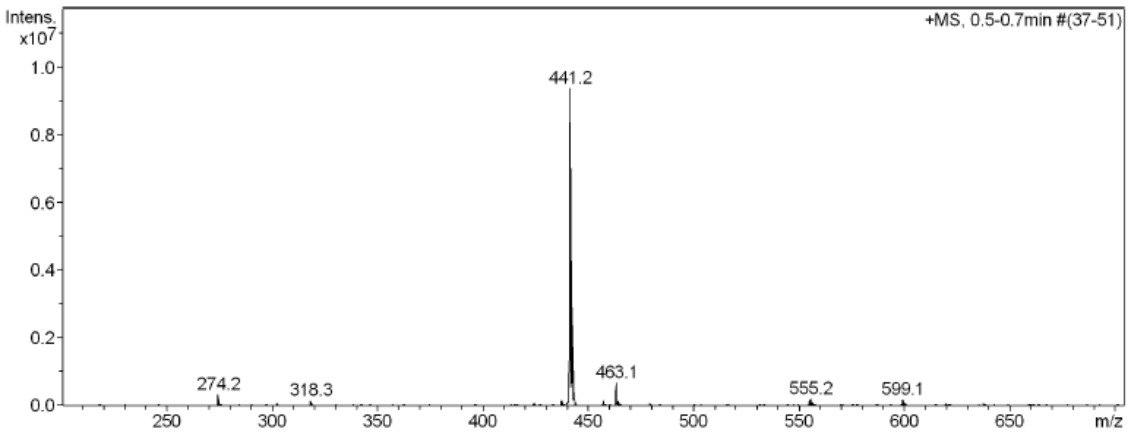

HRMS (ESI) *m/z*

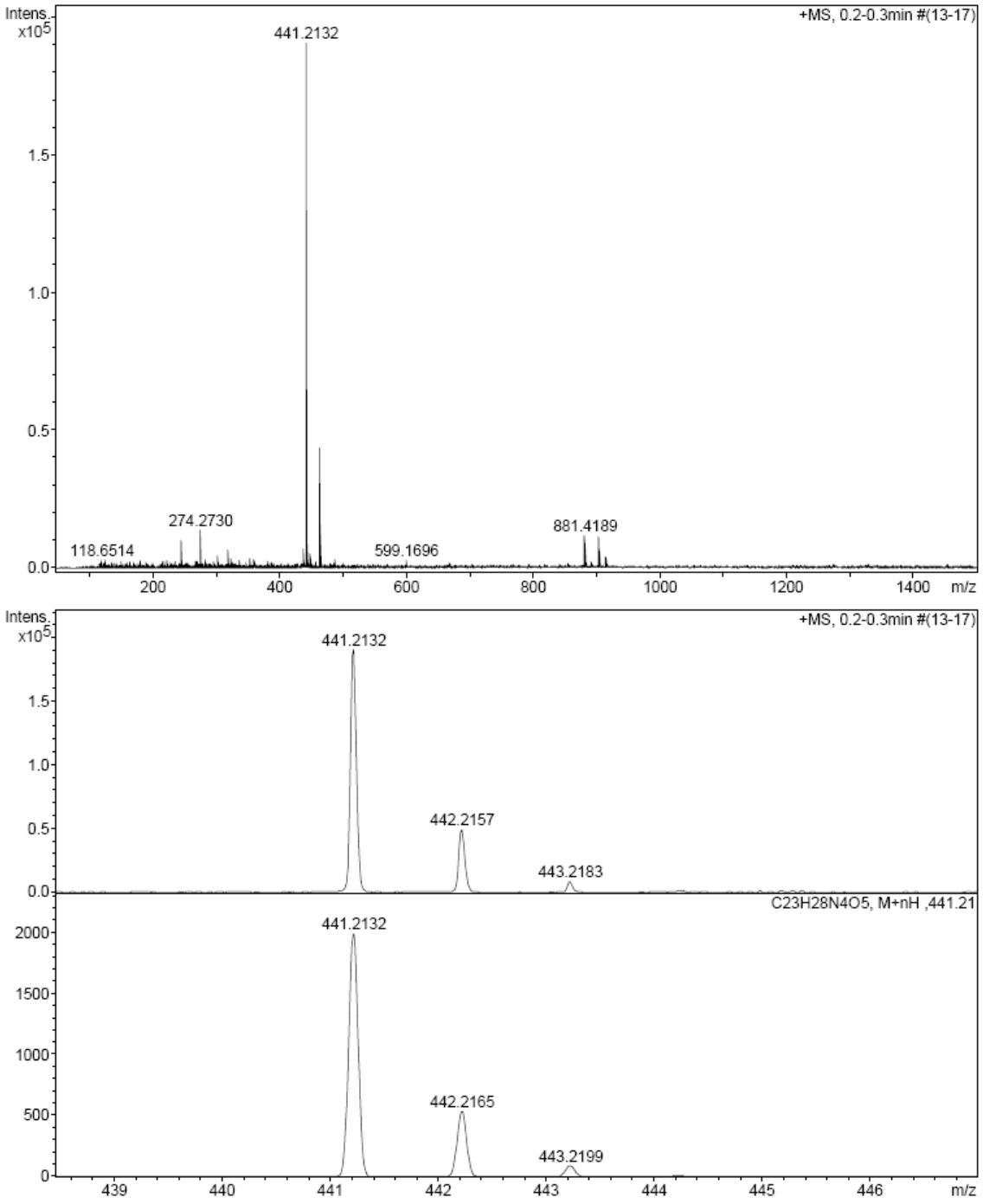
Intens.
x10^5
+MS, 0.2-0.3min #(13-17)
441.2132
274.2730
118.6514
599.1696
881.4189
m/z
442.2157
443.2183
C23H28N4O5, M+nH ,441.21
442.2165
443.2199

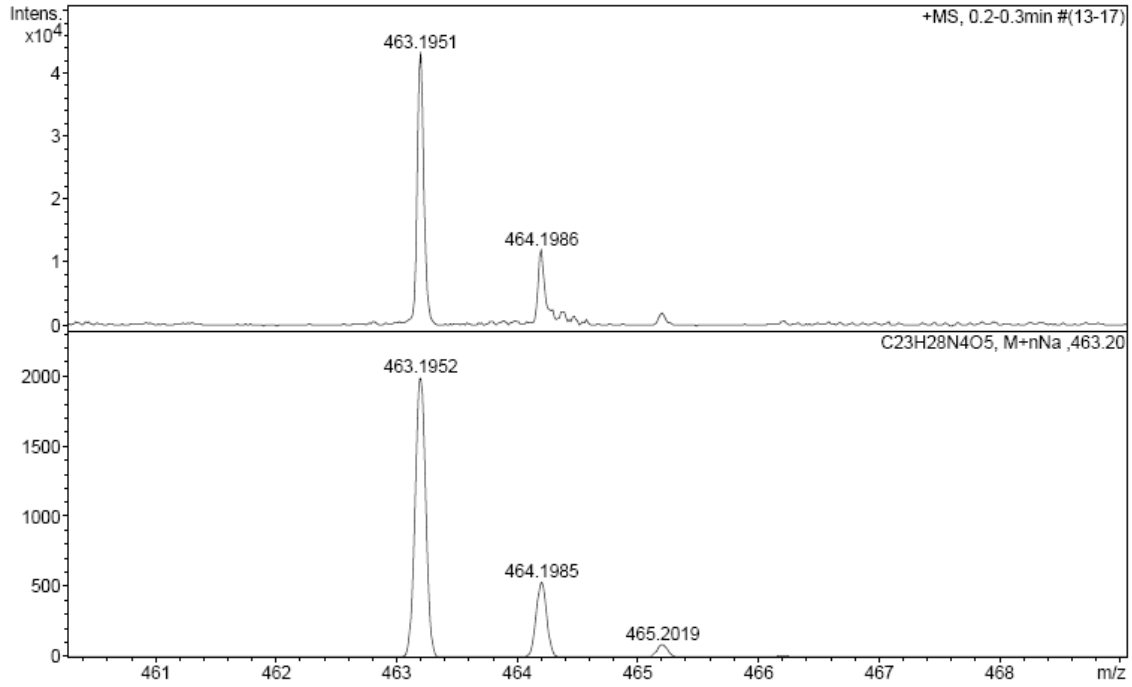

^{1}H-NMR (400 MHz, CD_3OD) δ (ppm)

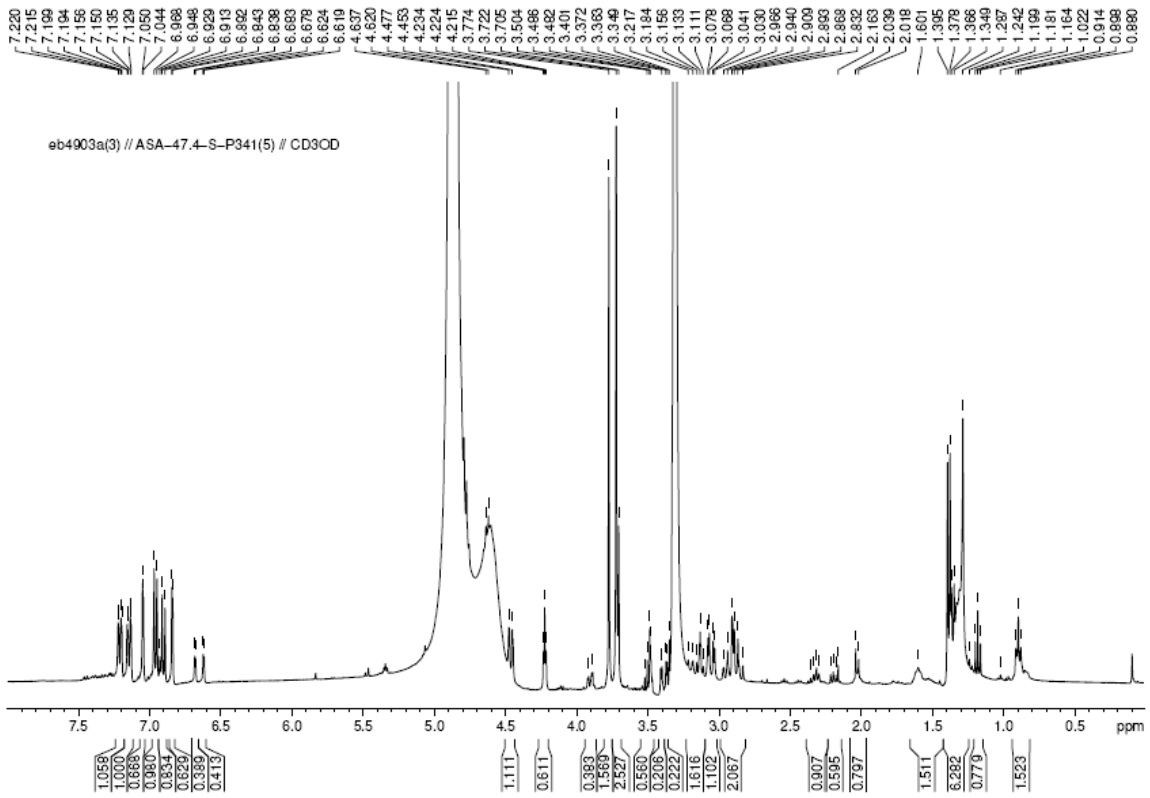

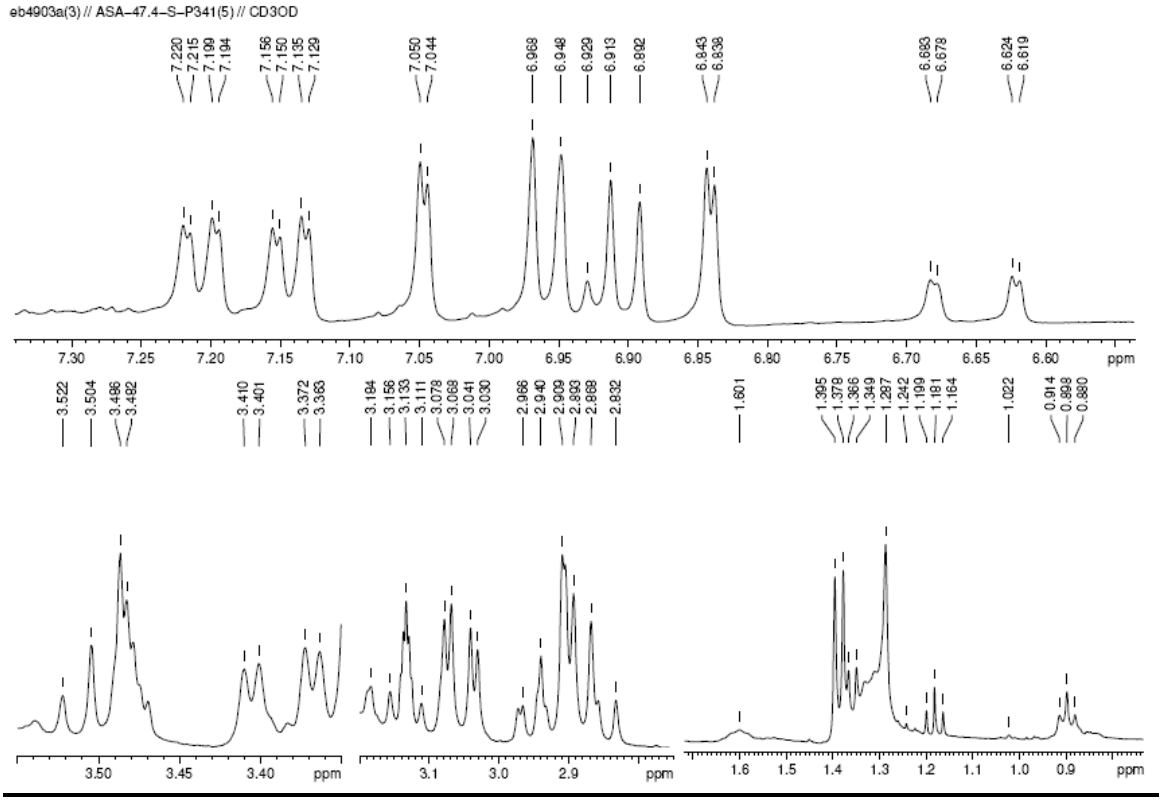

COSY (400 MHz, CD_3OD) δ (ppm)

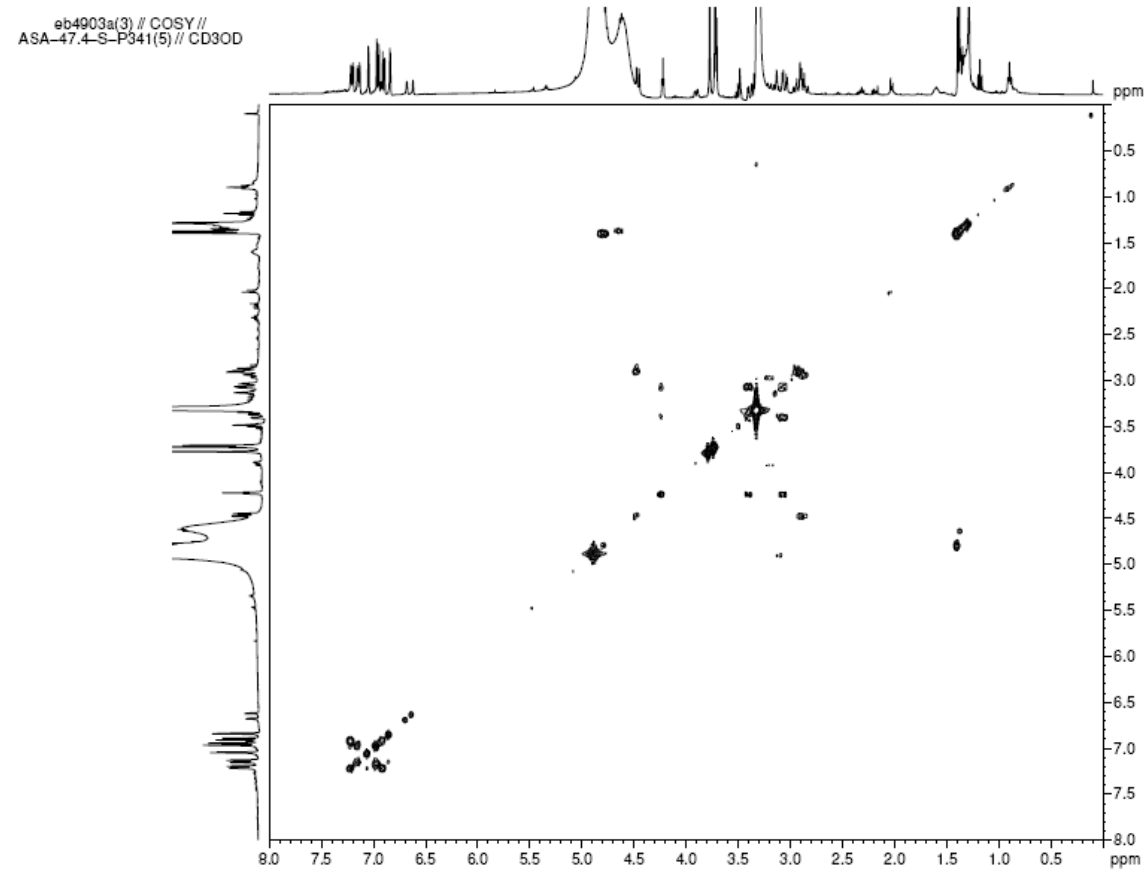

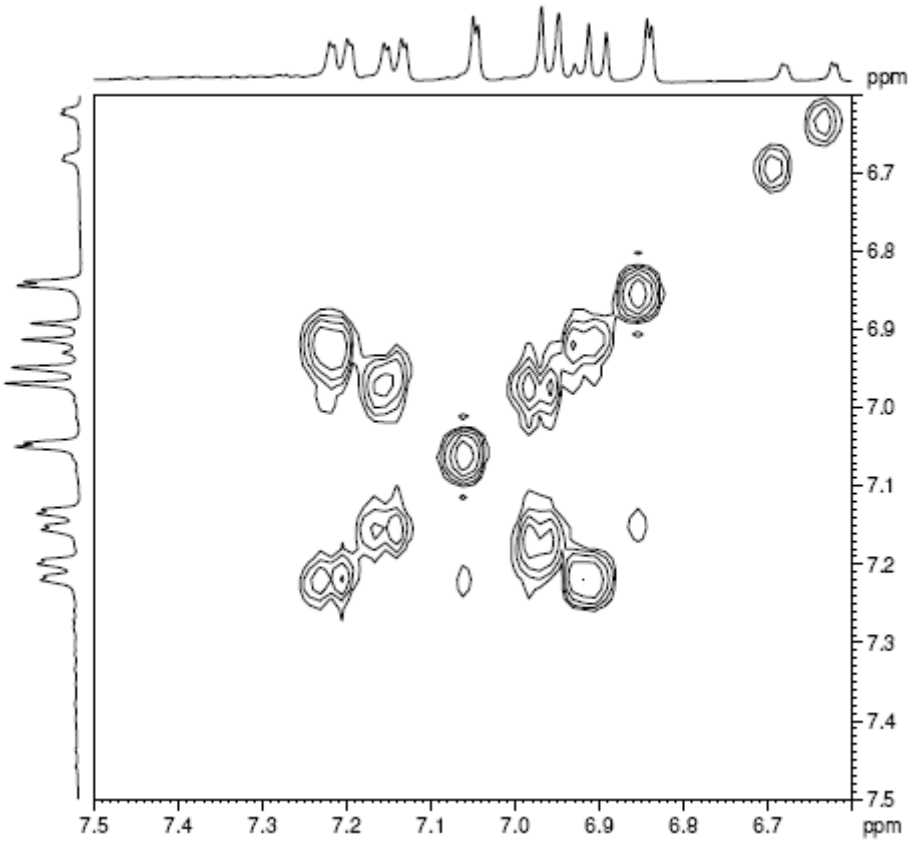
ppm
6.7
6.8
6.9
7.0
7.1
7.2
7.3
7.4
7.5
7.5
7.4
7.3
7.2
7.1
7.0
6.9
6.8
6.7
ppm

Biaryl cyclic peptide incorporating a His-Tyr linkage

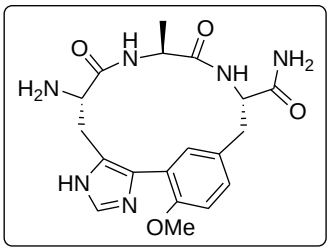

Crude peptide

HPLC (λ = 220 nm)

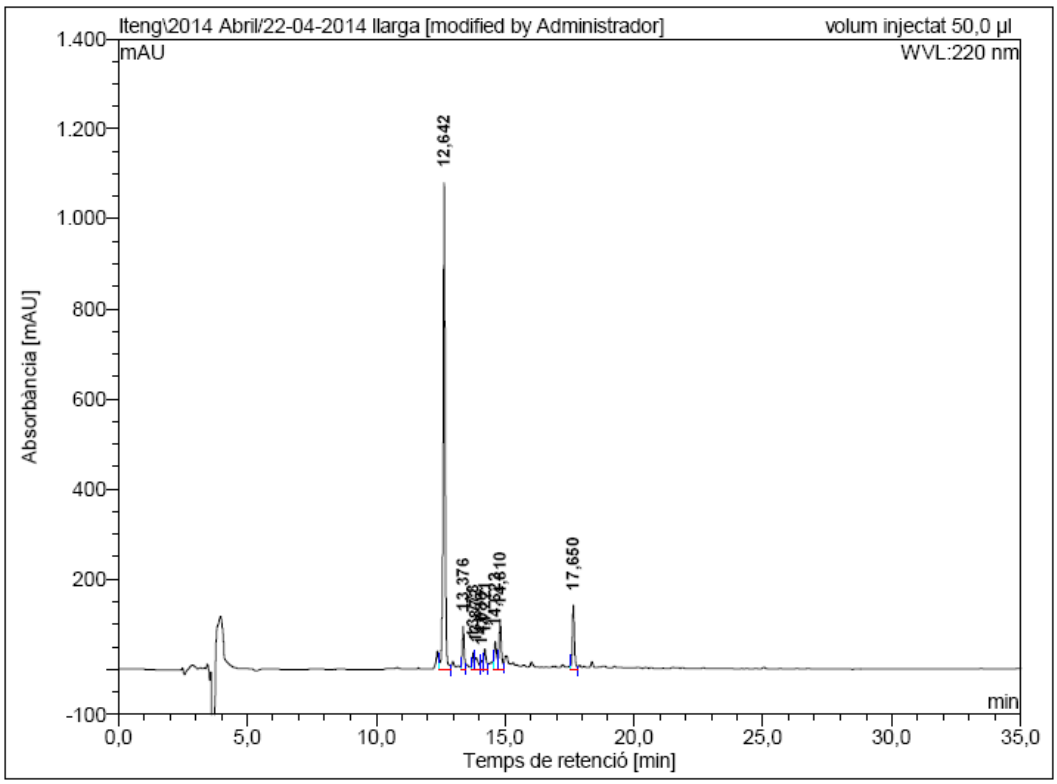

No.	Temps retenció min	alçada mAU	Area mAU*min	Area relativa %
1	12,64	1079,063	97,111	64,80
2	13,38	95,288	8,144	5,43
3	13,77	36,589	3,407	2,27
4	13,87	26,006	3,536	2,36
5	14,09	19,059	1,827	1,22
6	14,22	45,251	4,876	3,25
7	14,62	61,589	6,725	4,49
8	14,81	110,187	10,922	7,29
9	17,65	142,490	13,316	8,89
Total:		1615,522	149,864	100,00

ESI-MS *m/z*

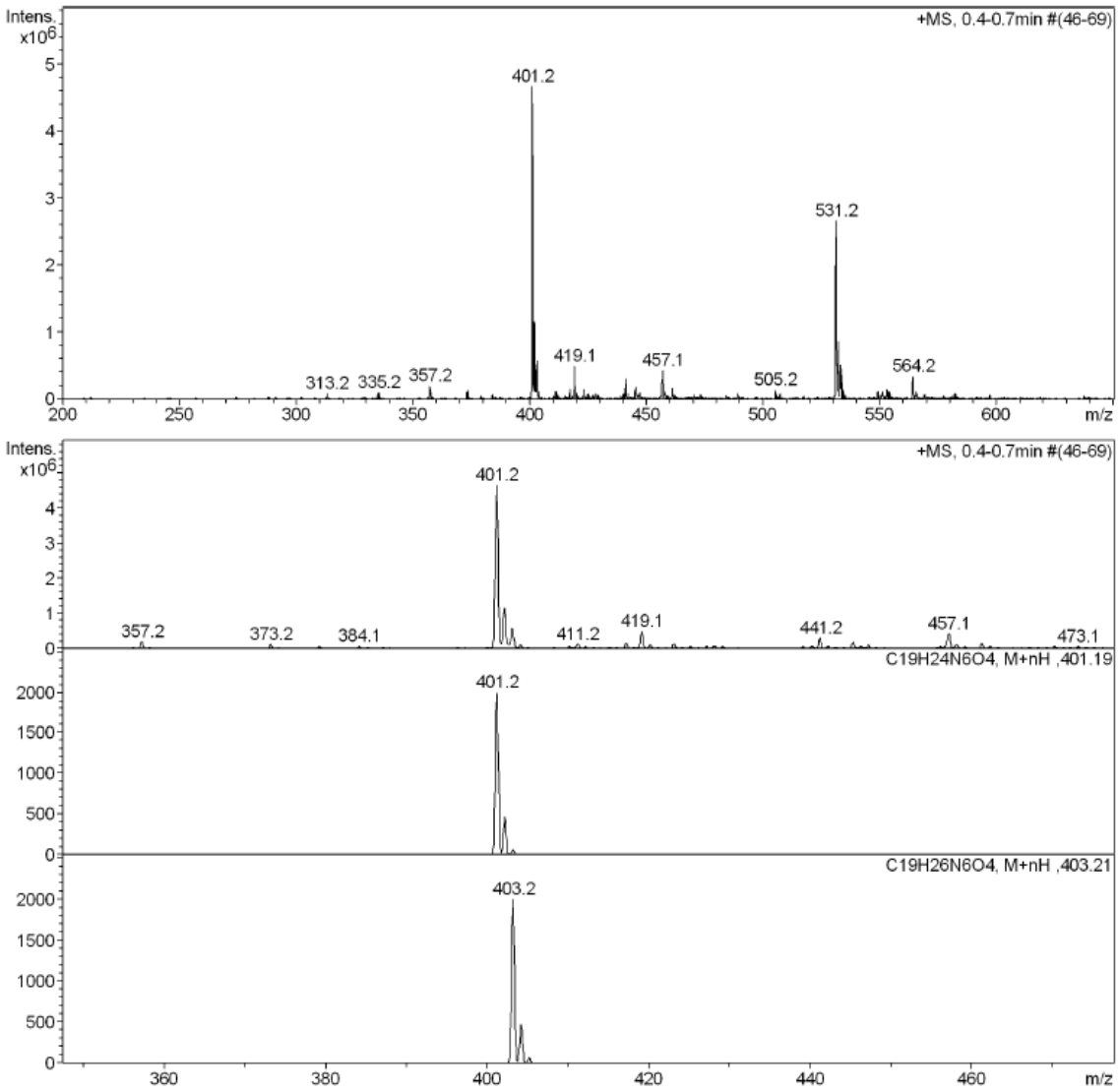
Intens.
x10^6
+MS, 0.4-0.7min #(46-69)
401.2
531.2
419.1
457.1
313.2
335.2
357.2
505.2
564.2
m/z
Intens.
x10^6
+MS, 0.4-0.7min #(46-69)
401.2
357.2
373.2
384.1
411.2
419.1
441.2
457.1
473.1
C19H24N6O4, M+nH ,401.19
401.2
C19H26N6O4, M+nH ,403.21
403.2
m/z

Purified peptide

HPLC (λ = 220 nm)

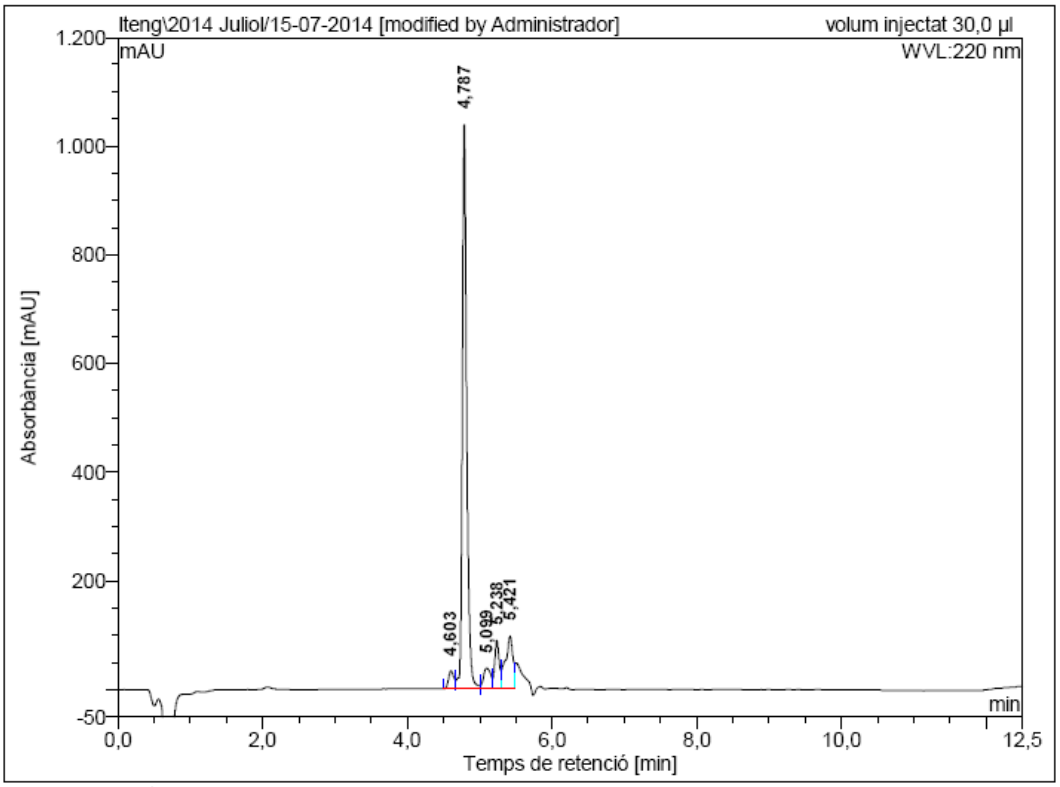

No.	Temps retenció min	alçada mAU	Area mAU*min	Area relativa %
1	4,60	33,089	2,927	2,95
2	4,79	1037,489	74,288	74,77
3	5,10	37,979	4,325	4,35
4	5,24	88,992	6,474	6,52
5	5,42	96,895	11,339	11,41
Total:		1294,443	99,354	100,00

ESI-MS *m/z*

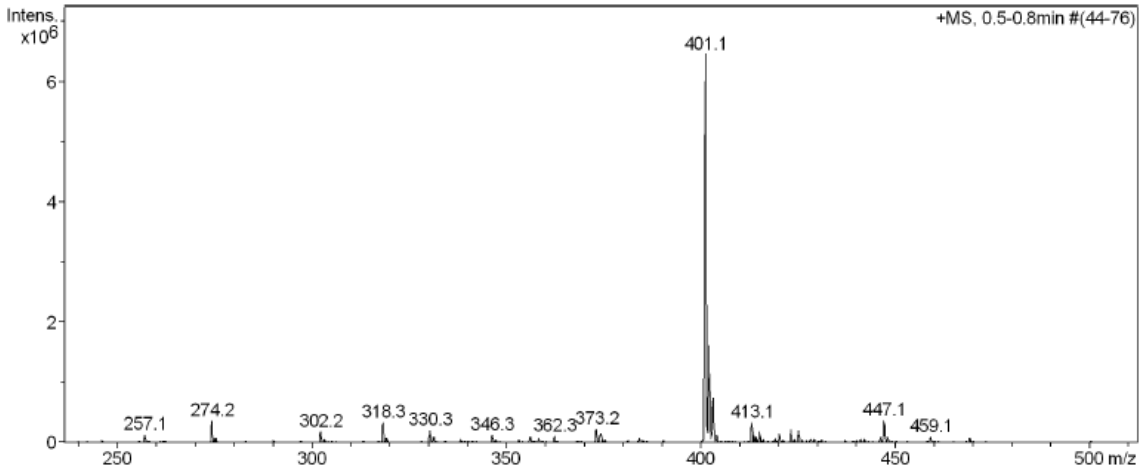

HRMS (ESI) *m/z*

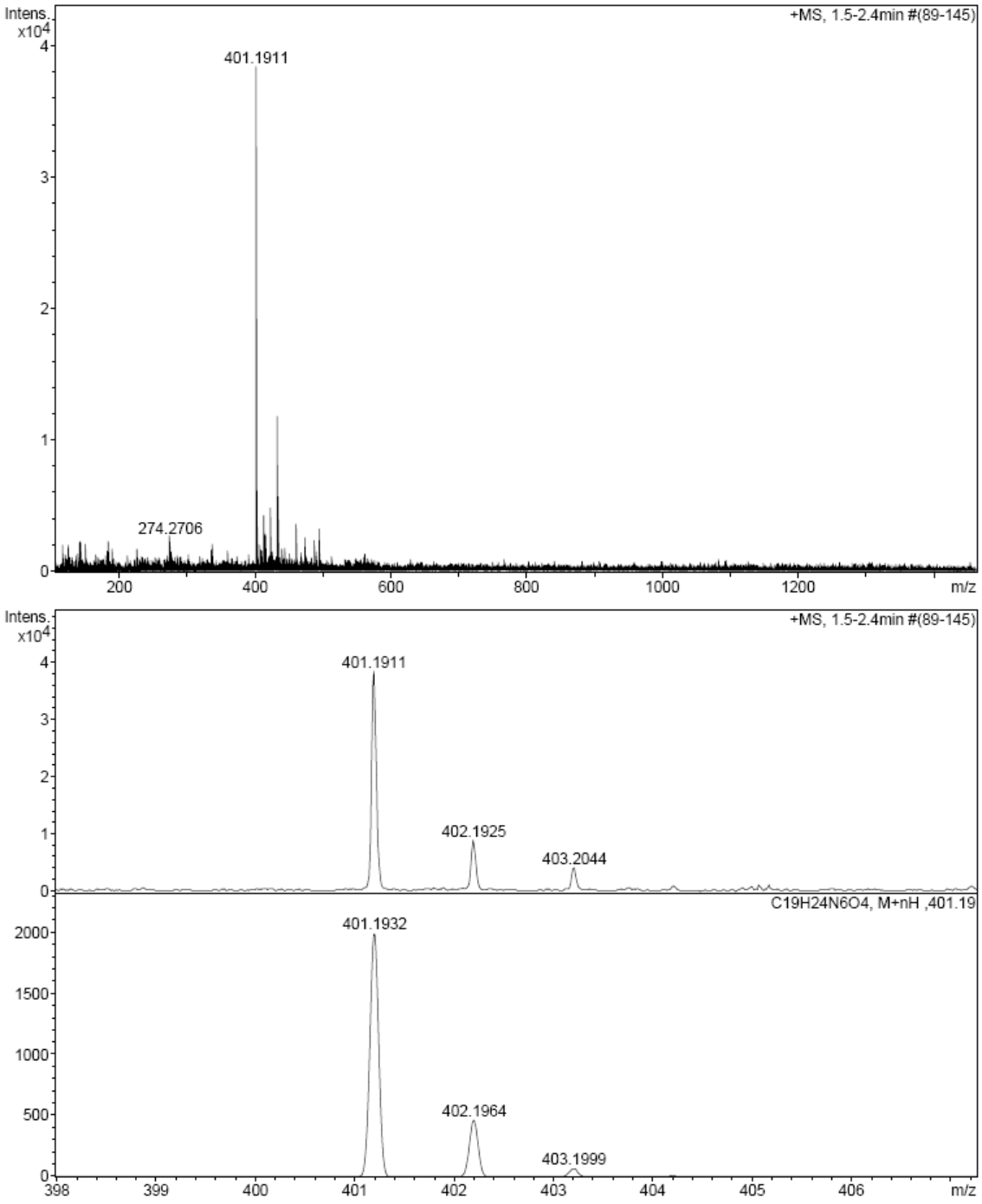
Intens.
x10^4
+MS, 1.5-2.4min #(89-145)
401.1911
274.2706
m/z
Intens.
x10^4
+MS, 1.5-2.4min #(89-145)
401.1911
402.1925
403.2044
C19H24N6O4, M+nH ,401.19
401.1932
402.1964
403.1999
m/z

^{1}H-NMR (400 MHz, CD_3OD) δ (ppm)

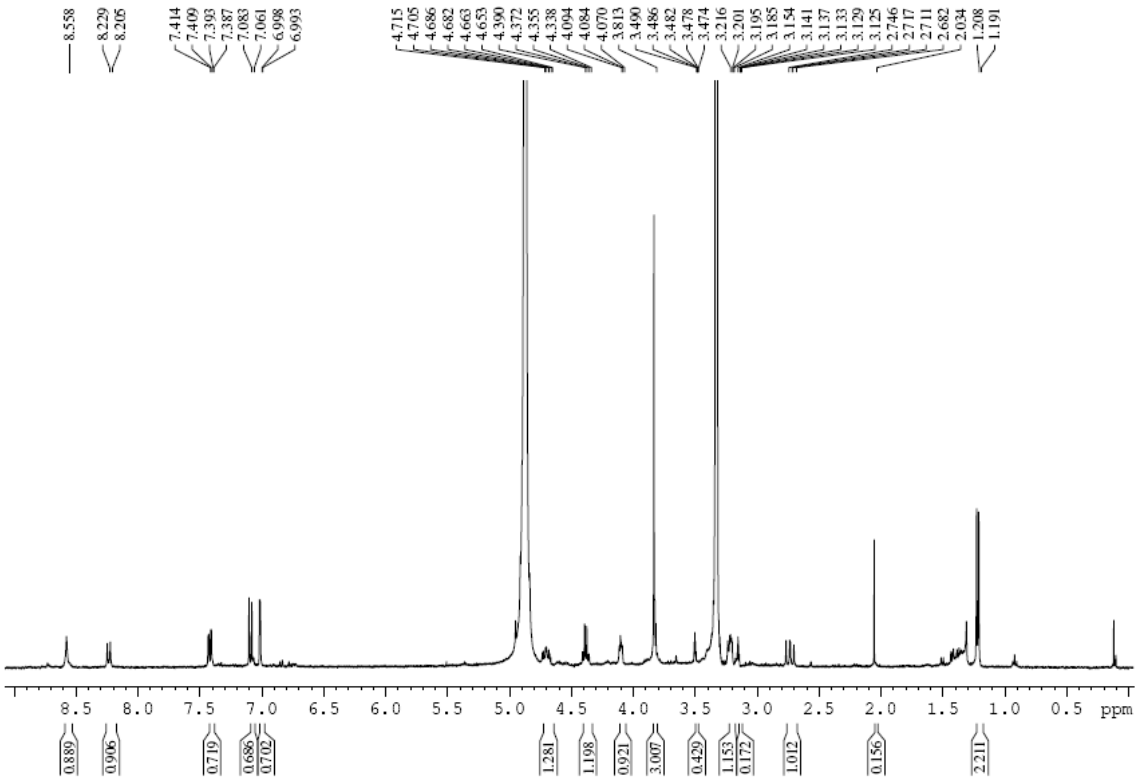

COSY (400 MHz, CD_3OD) δ (ppm)

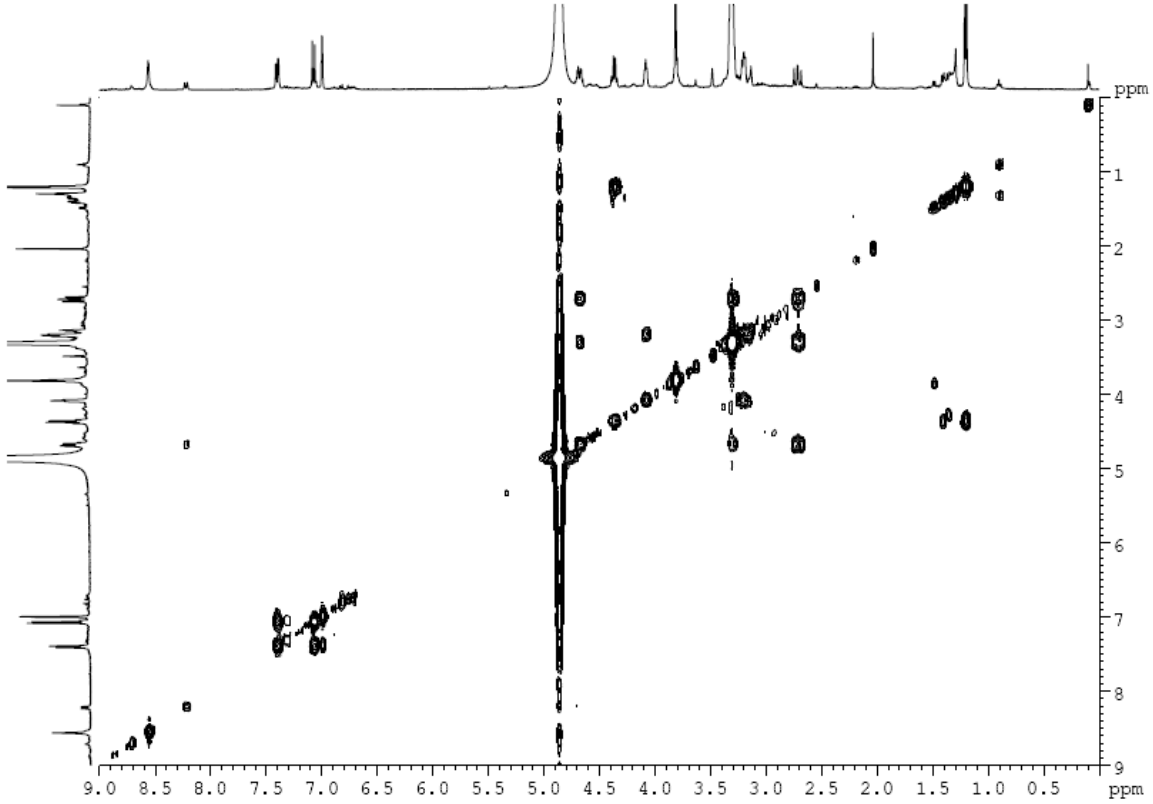

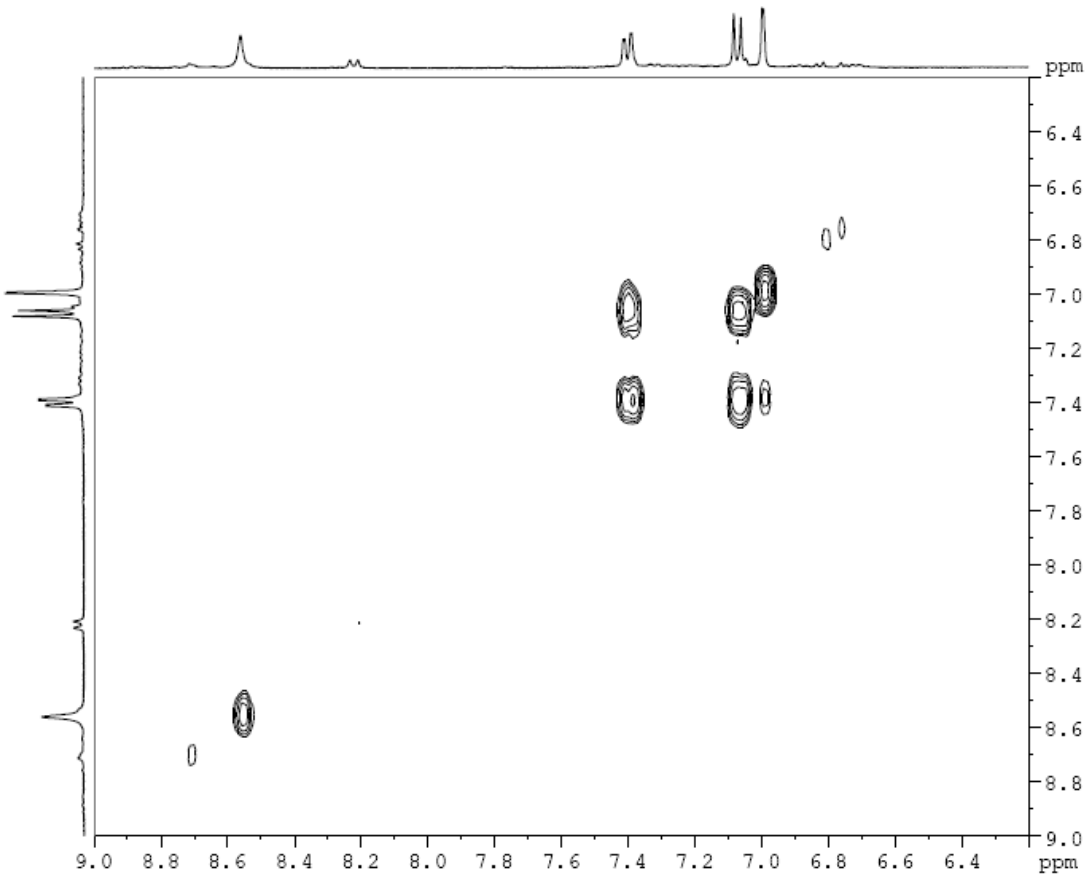

Biaryl cyclic peptide incorporating a Phg-Tyr linkage 32

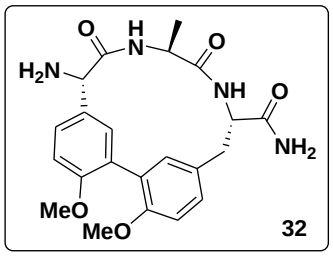

Crude peptide 32

HPLC (λ = 220 nm)

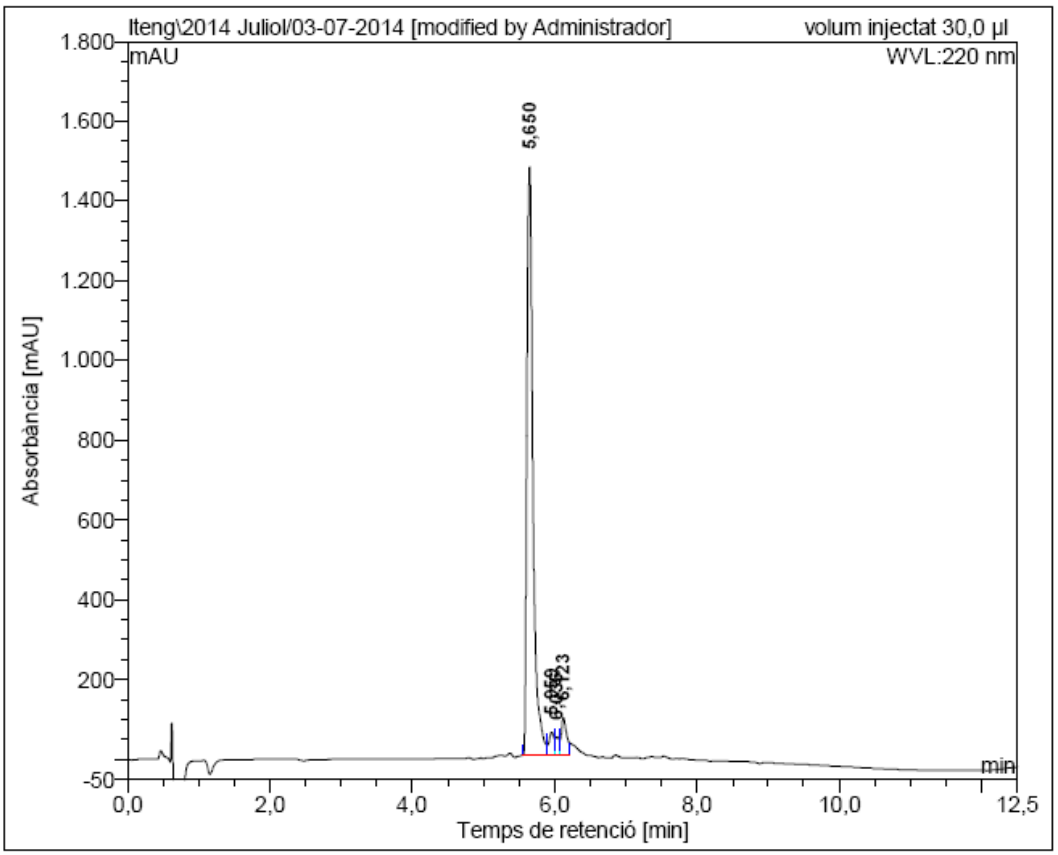

No.	mps retenc min	alçada mAU	Area mAU*min	Area relativa %
1	5,65	1473,576	145,842	89,96
2	5,96	57,438	5,248	3,24
3	6,04	46,476	2,702	1,67
4	6,12	93,865	8,318	5,13
Total:		1671,354	162,111	100,00

ESI-MS *m/z*

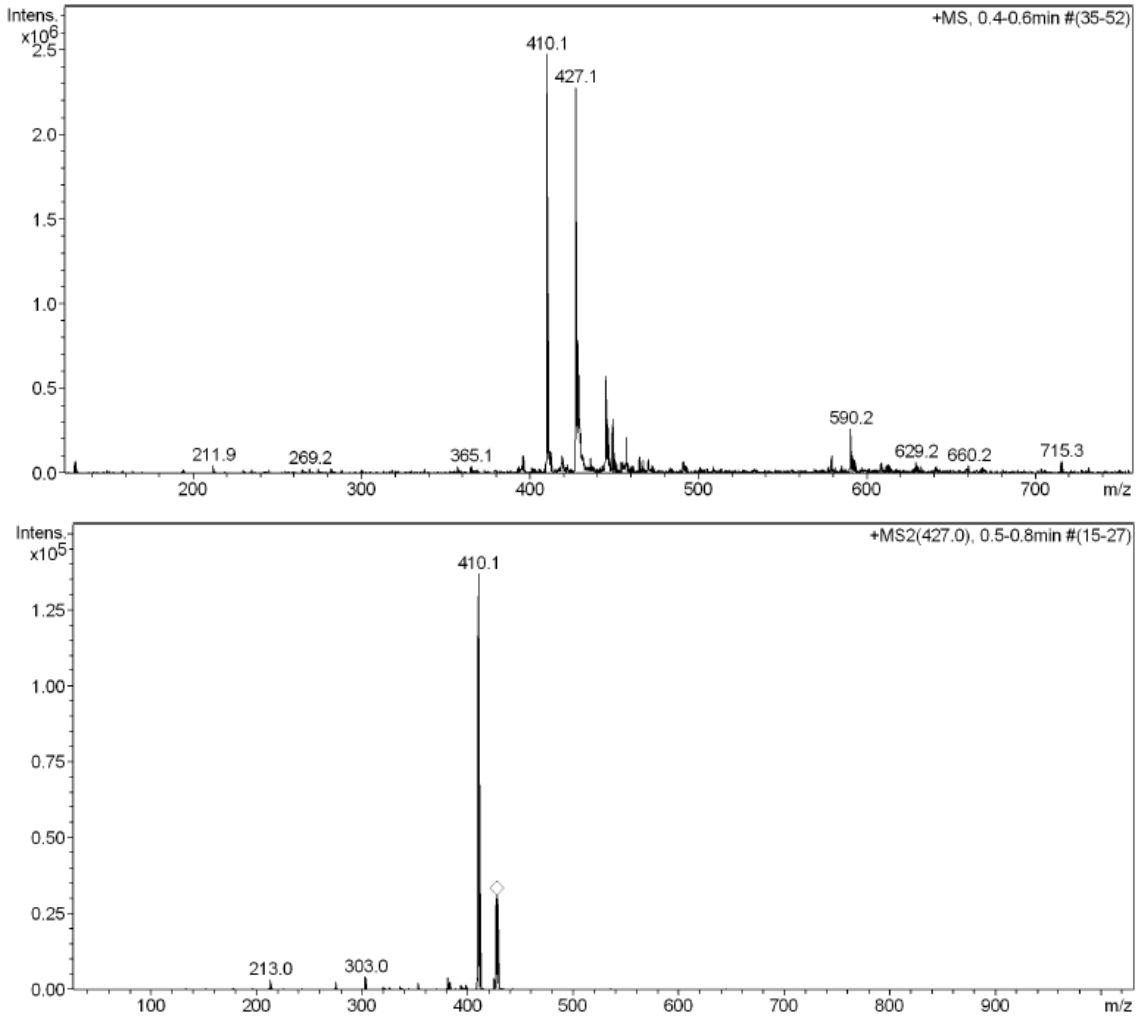
Intens.
x10^6
+MS, 0.4-0.6min #(35-52)
410.1
427.1
590.2
211.9
269.2
365.1
629.2
660.2
715.3
m/z
Intens.
x10^5
+MS2(427.0), 0.5-0.8min #(15-27)
410.1
213.0
303.0
m/z

Purified peptide 32

HPLC (λ = 220 nm)

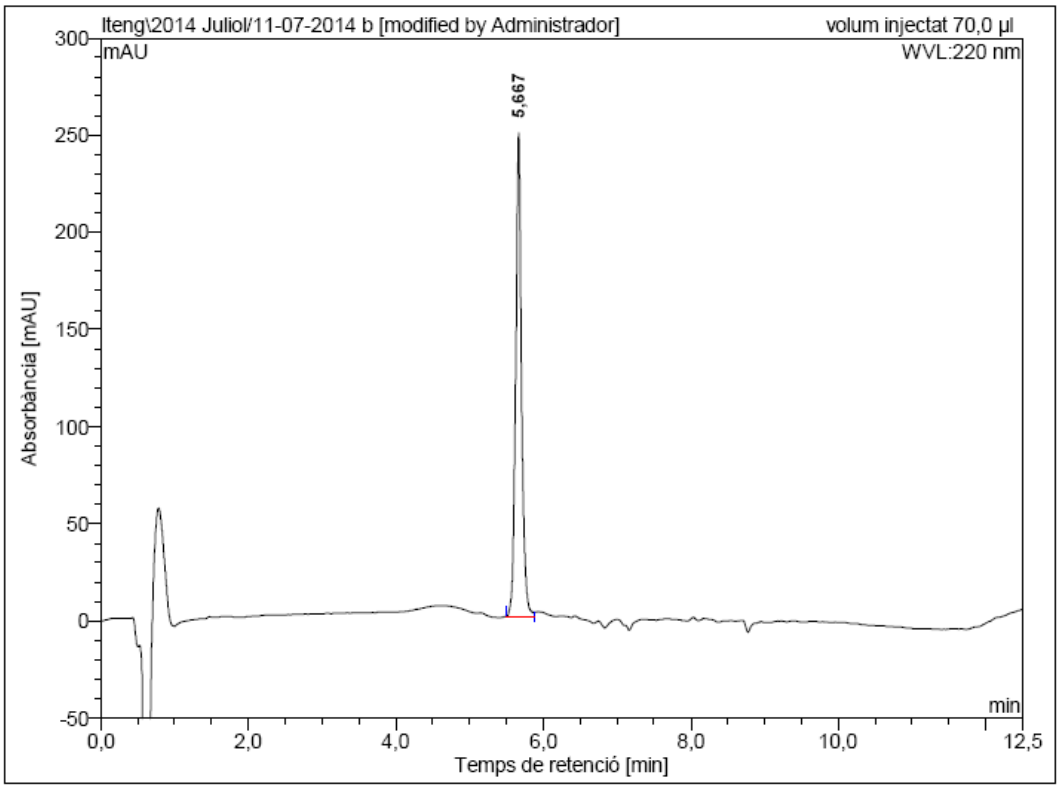

No.	Temps retenció min	alçada mAU	Area mAU*min	Area relativa %
1	5,67	248,630	22,908	100,00
Total:		248,630	22,908	100,00

ESI-MS *m/z*

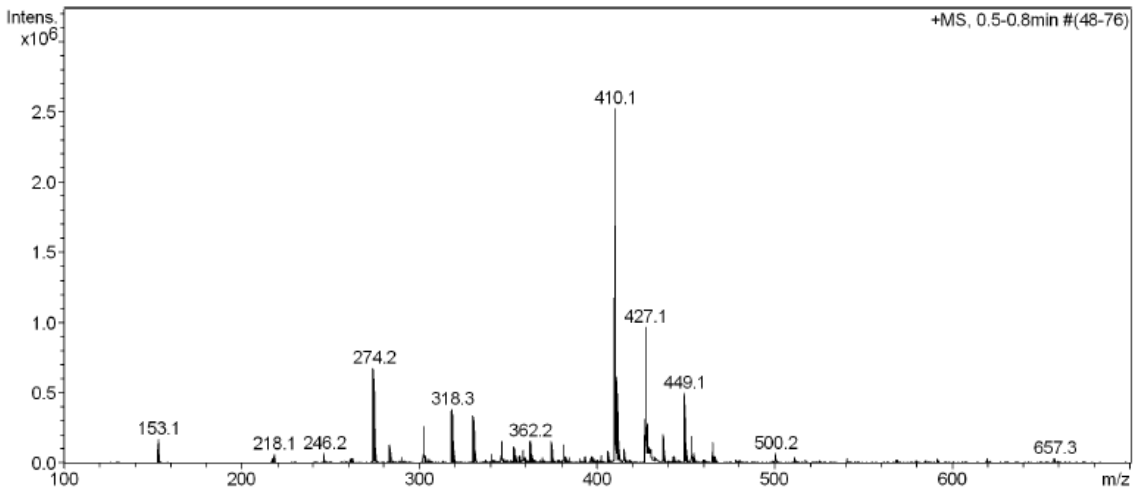

HRMS (ESI) *m/z*

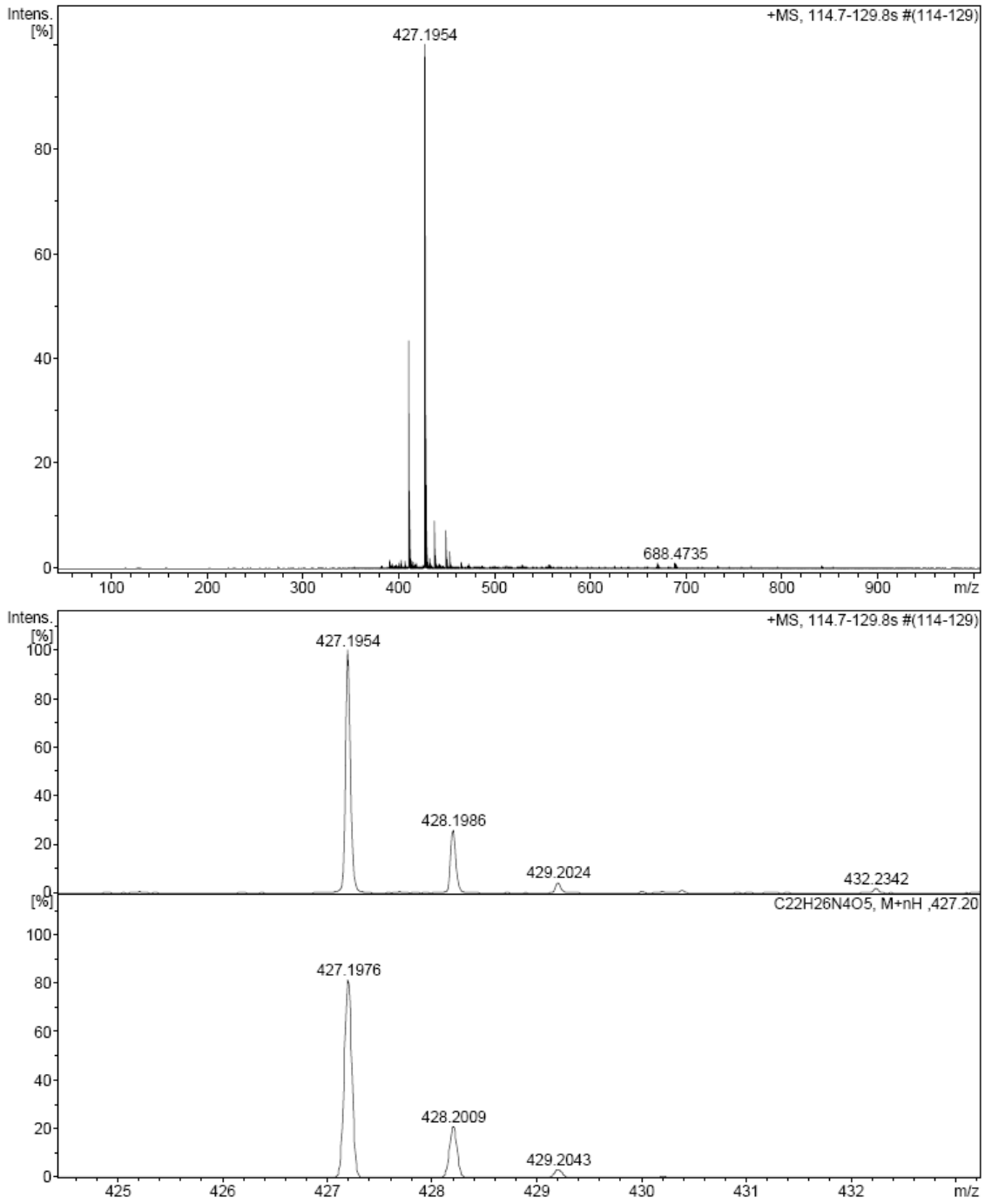
Intens.
[%]
+MS, 114.7-129.8s #(114-129)
427.1954
688.4735
m/z
Intens.
[%]
+MS, 114.7-129.8s #(114-129)
427.1954
428.1986
429.2024
432.2342
C22H26N4O5, M+nH ,427.20
427.1976
428.2009
429.2043
m/z

5. Synthesis of N-methylated biaryl cyclic tripeptides

N-Methylated biaryl cyclic tripeptide incorporating a Phe-Tyr linkage 19

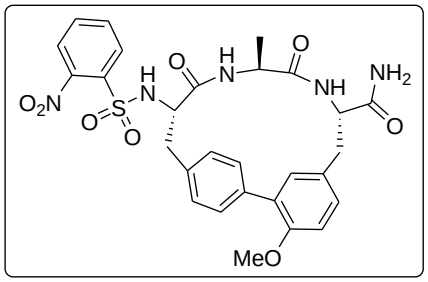

HPLC (λ = 220 nm)

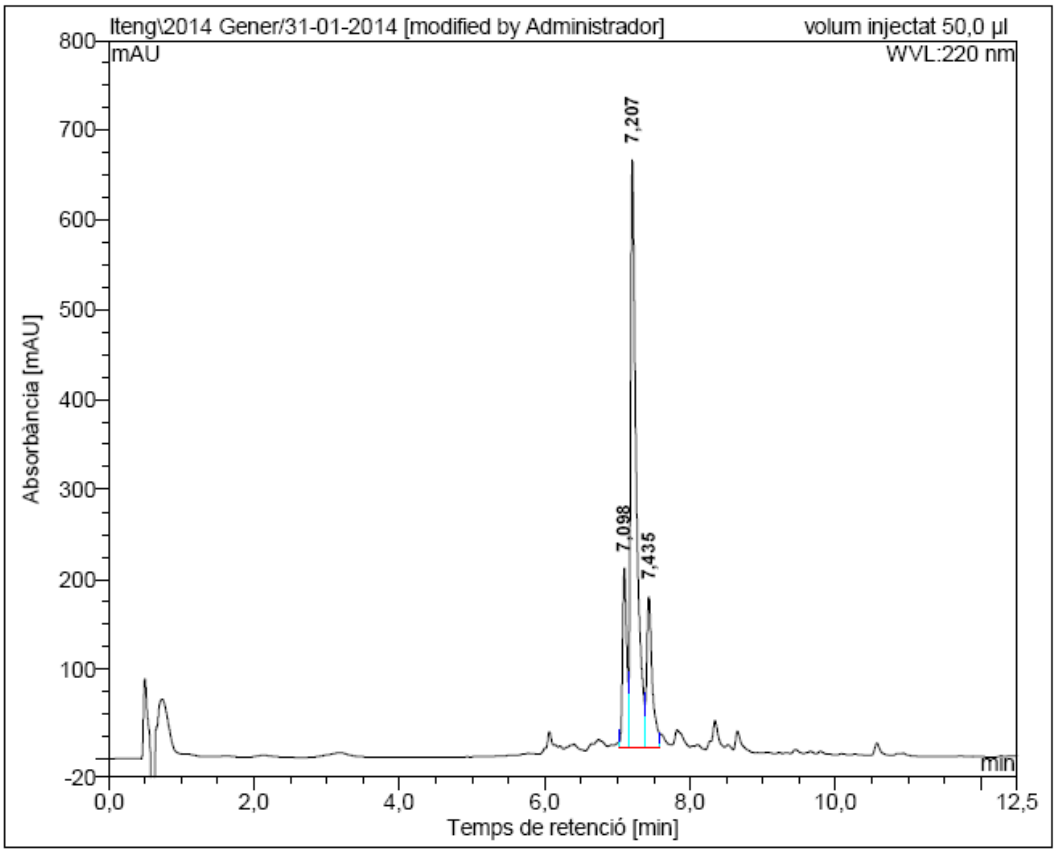

No.	mps retenc min	alçada mAU	Area mAU*min	Area relativa %
1	7,10	199,711	13,177	14,78
2	7,21	654,254	61,279	68,72
3	7,43	167,874	14,719	16,51
Total:		1021,839	89,176	100,00

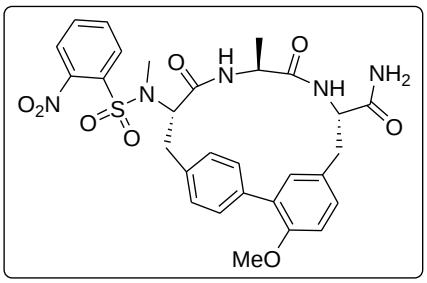

HPLC (λ = 220 nm)

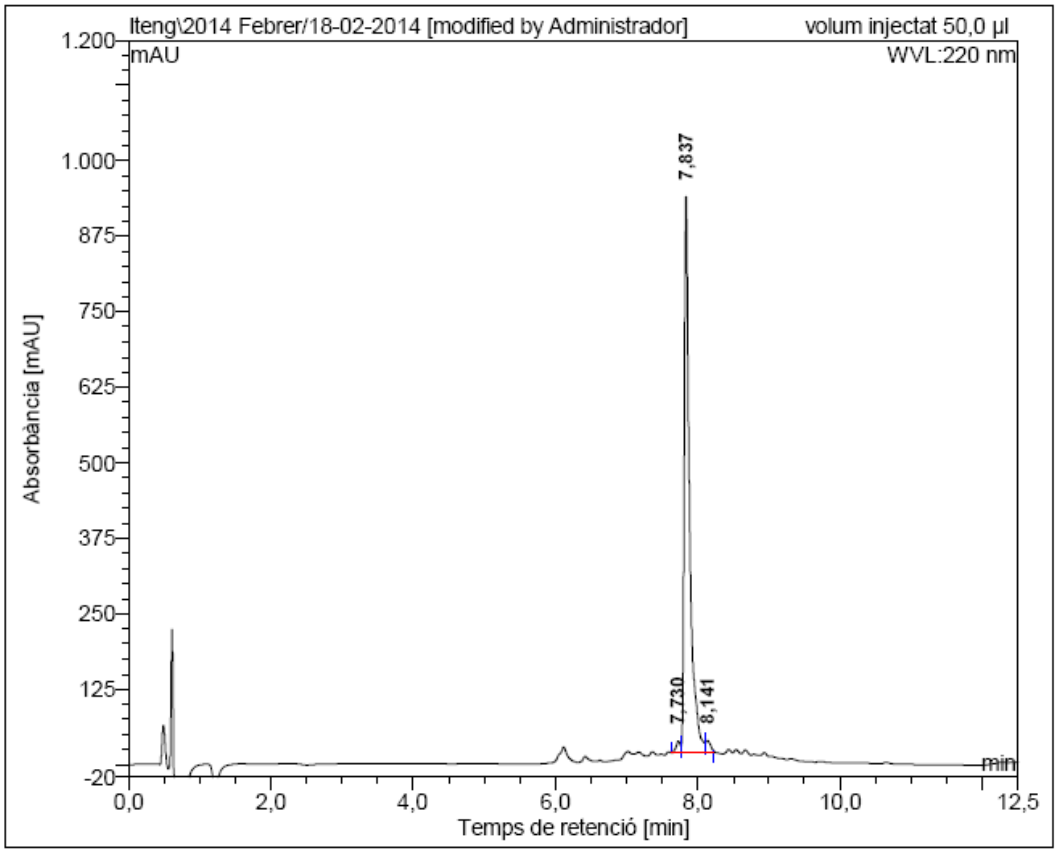

No.	mps retenc min	alçada mAU	Area mAU*min	Area relativa %
1	7,73	19,670	1,363	1,62
2	7,84	920,875	81,140	96,28
3	8,14	20,818	1,770	2,10
Total:		961,362	84,274	100,00

ESI-MS *m/z*

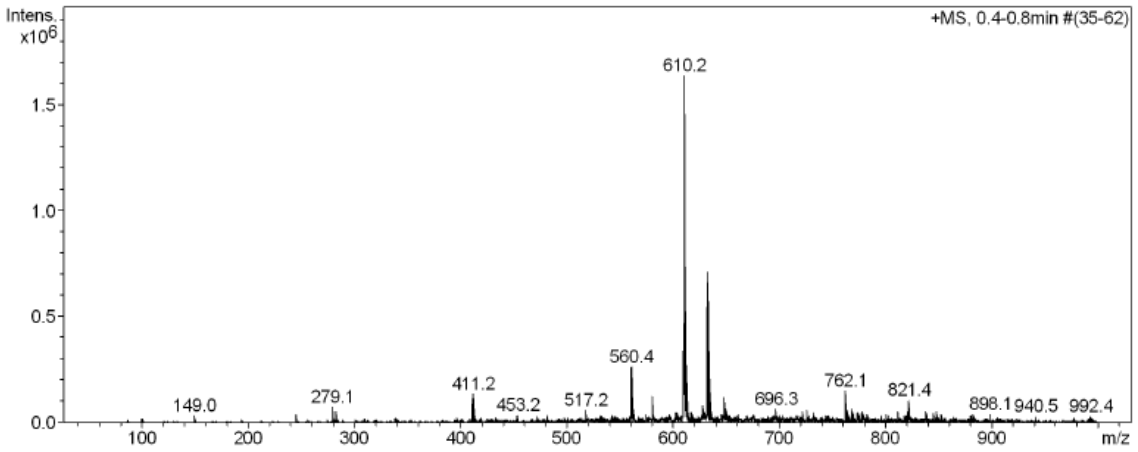
Intens.
x10^6
+MS, 0.4-0.8min #(35-62)
610.2
1.5
1.0
0.5
0.0
560.4
411.2
279.1
149.0
453.2
517.2
696.3
762.1
821.4
898.1
940.5
992.4
100
200
300
400
500
600
700
800
900
m/z

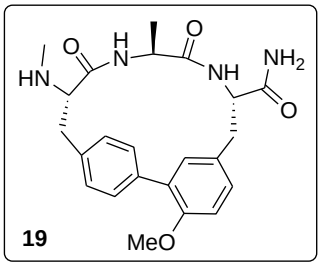

HPLC (λ = 220 nm)

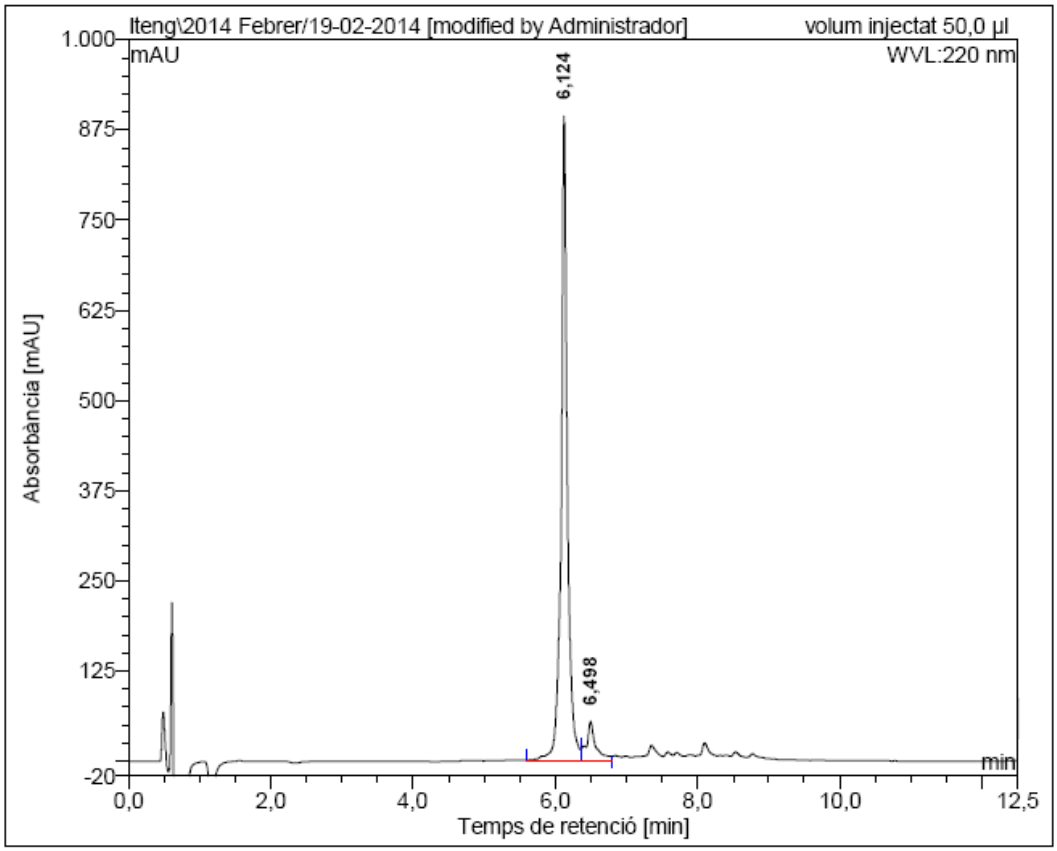

No.	mps retenc min	alçada mAU	Area mAU*min	Area relativa %
1	6,12	892,681	90,768	91,87
2	6,50	53,474	8,034	8,13
Total:		946,155	98,801	100,00

ESI-MS *m/z*

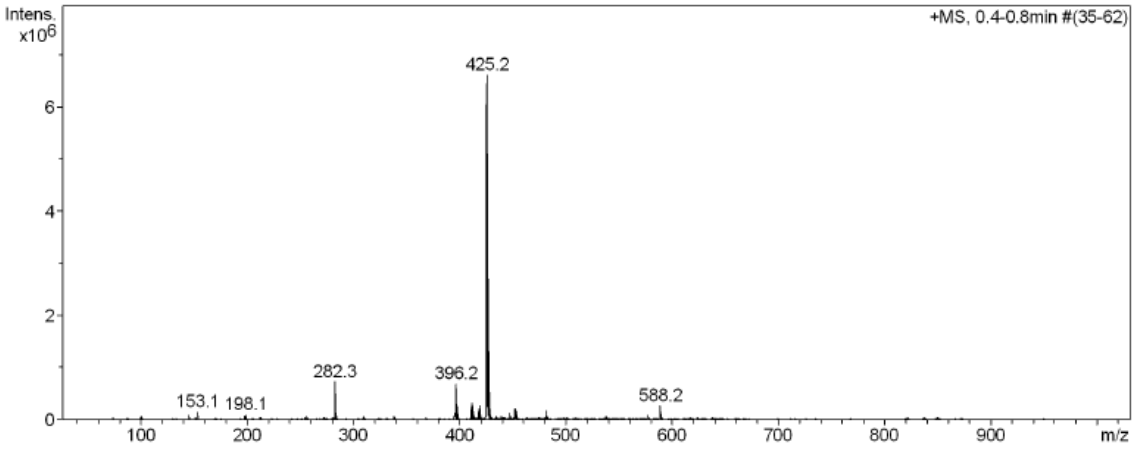

N-Methylated biaryl cyclic tripeptide incorporating a Tyr-Tyr linkage

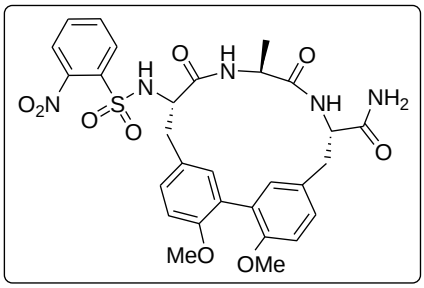

HPLC (λ = 220 nm)

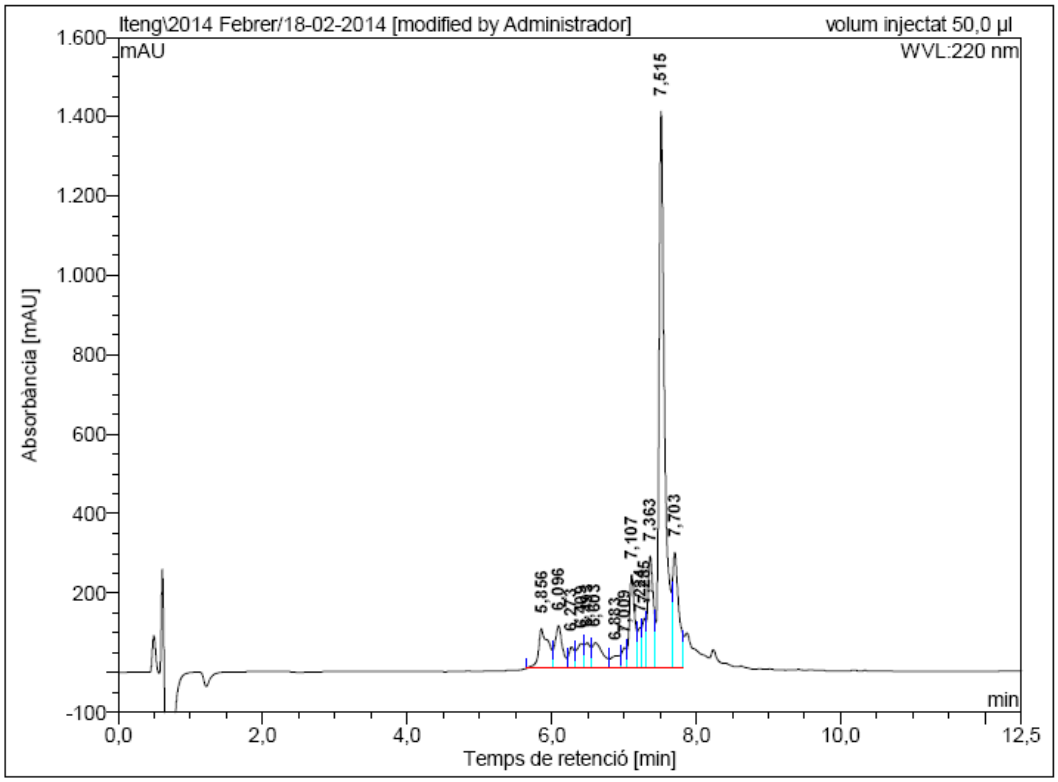

No.	Temps retenció min	alçada mAU	Area mAU*min	Area relativa %
1	5,86	98,764	15,645	5,54
2	6,10	106,985	12,742	4,51
3	6,27	53,581	4,946	1,75
4	6,41	61,689	6,327	2,24
5	6,49	63,467	6,162	2,18
6	6,60	63,842	11,076	3,92
7	6,88	31,189	4,445	1,57
8	7,01	51,081	4,294	1,52
9	7,11	235,757	20,820	7,37
10	7,22	102,381	5,616	1,99
11	7,28	125,589	7,228	2,56
12	7,36	281,208	25,934	9,18
13	7,52	1401,820	128,603	45,51
14	7,70	291,388	28,757	10,18
Total:		2968,741	282,596	100,00

ESI-MS *m/z*

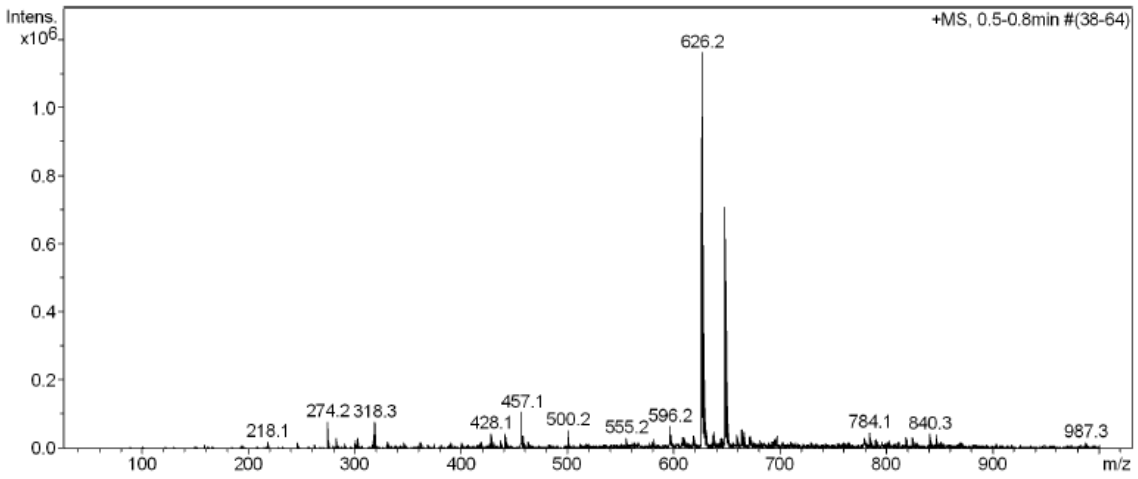
Intens.
x10^6
+MS, 0.5-0.8min #(38-64)
626.2
1.0
0.8
0.6
0.4
0.2
0.0
218.1
274.2
318.3
428.1
457.1
500.2
555.2
596.2
784.1
840.3
987.3
100
200
300
400
500
600
700
800
900
m/z

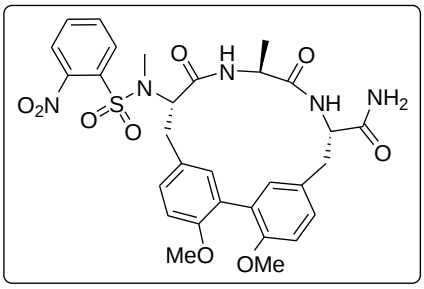

HPLC (λ = 220 nm)

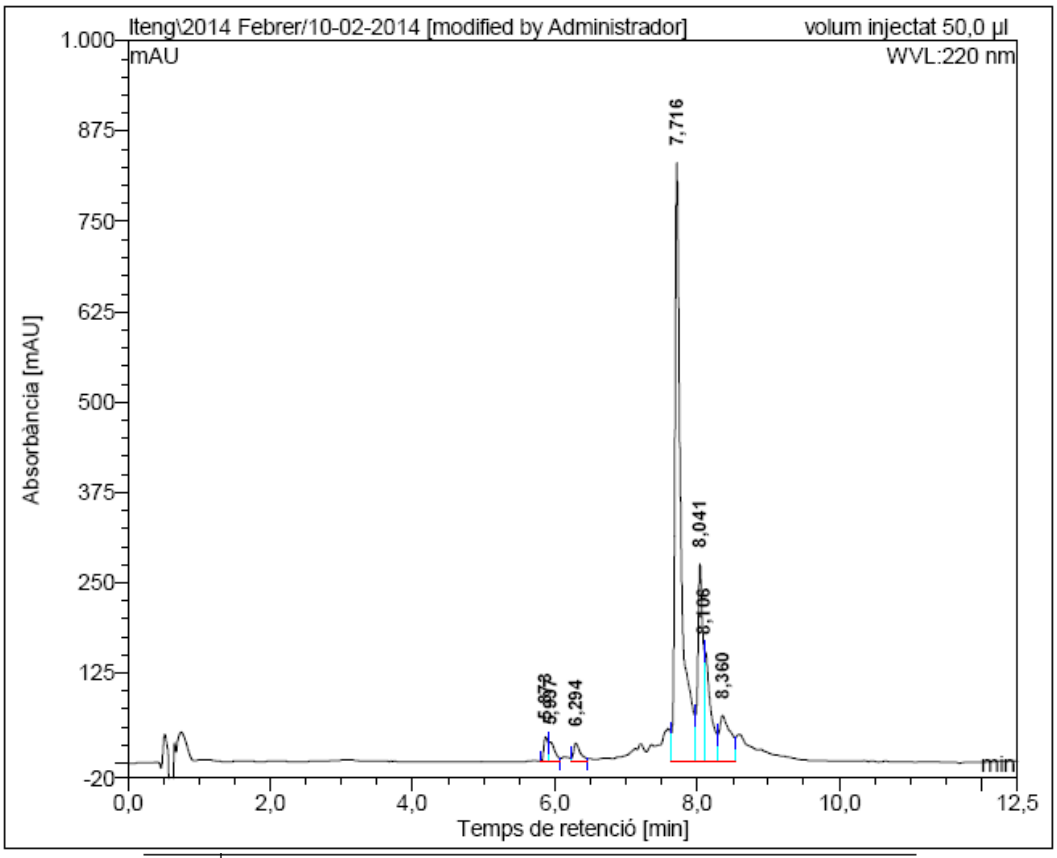

No.	mps retenc min	alçada mAU	Area mAU*min	Area relativa %
1	5,87	33,409	2,258	1,59
2	5,94	26,655	2,519	1,78
3	6,29	25,033	2,776	1,96
4	7,72	827,855	84,582	59,73
5	8,04	273,170	22,835	16,12
6	8,11	152,612	15,356	10,84
7	8,36	63,050	11,293	7,97
Total:		1401,784	141,618	100,00

ESI-MS *m/z*

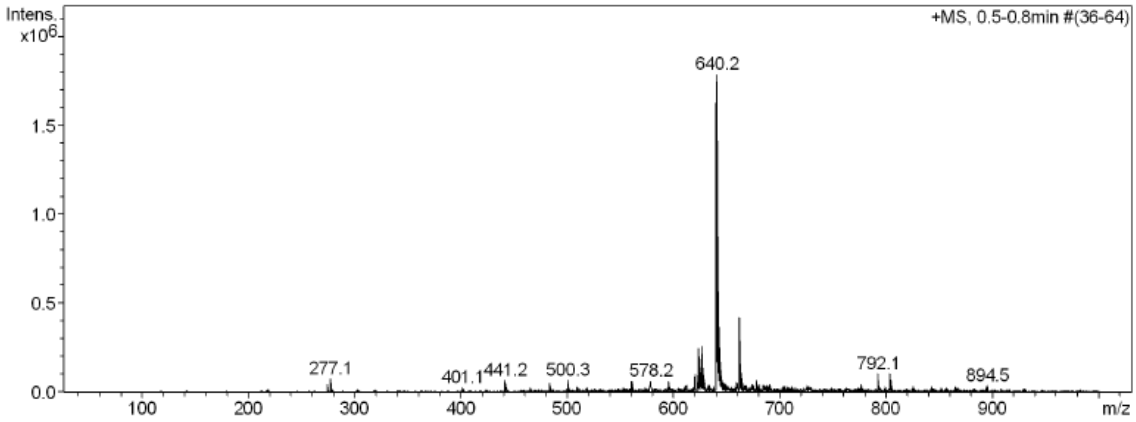
Intens.
x10^6
+MS, 0.5-0.8min #(36-64)
640.2
1.5
1.0
0.5
0.0
277.1
401.1
441.2
500.3
578.2
792.1
894.5
100
200
300
400
500
600
700
800
900
m/z

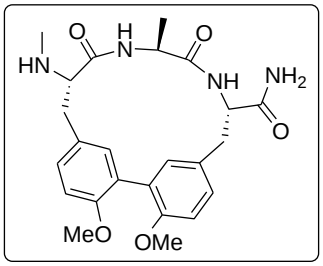

HPLC (λ = 220 nm)

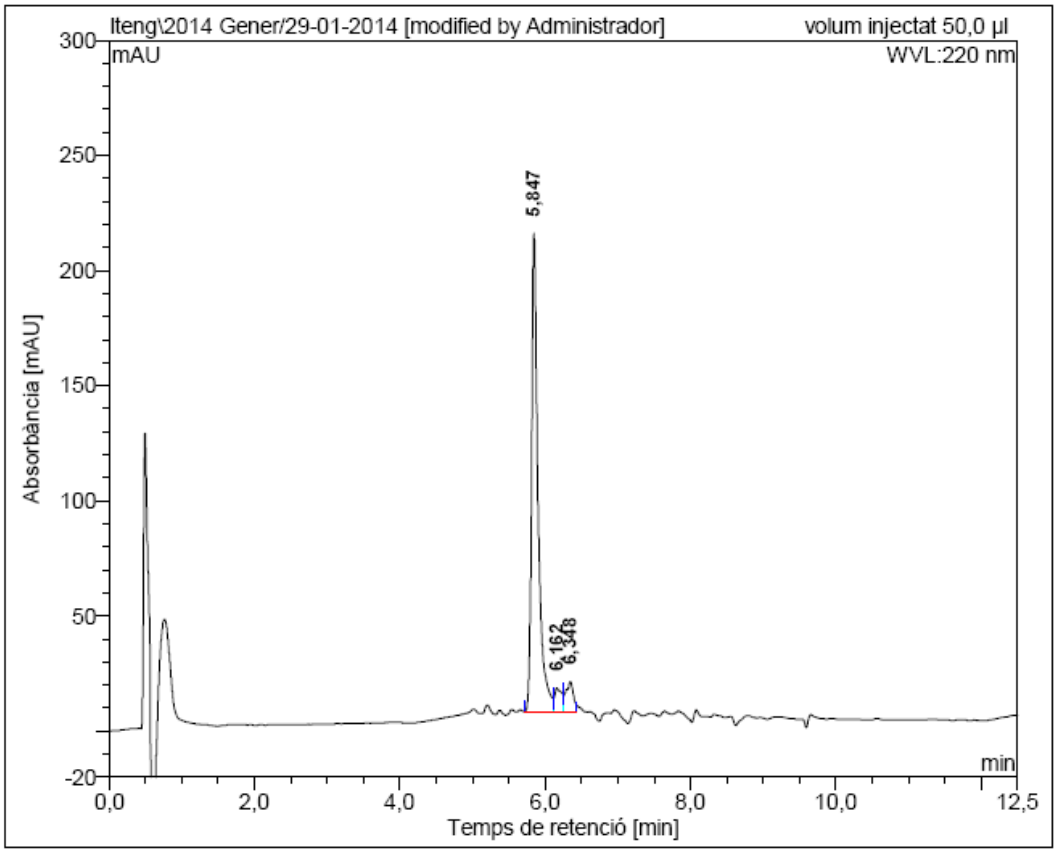

No.	mps retenc min	alçada mAU	Area mAU*min	Area relativa %
1	5,85	207,559	21,510	89,04
2	6,16	10,180	1,119	4,63
3	6,35	12,916	1,528	6,33
Total:		230,655	24,157	100,00

ESI-MS *m/z*

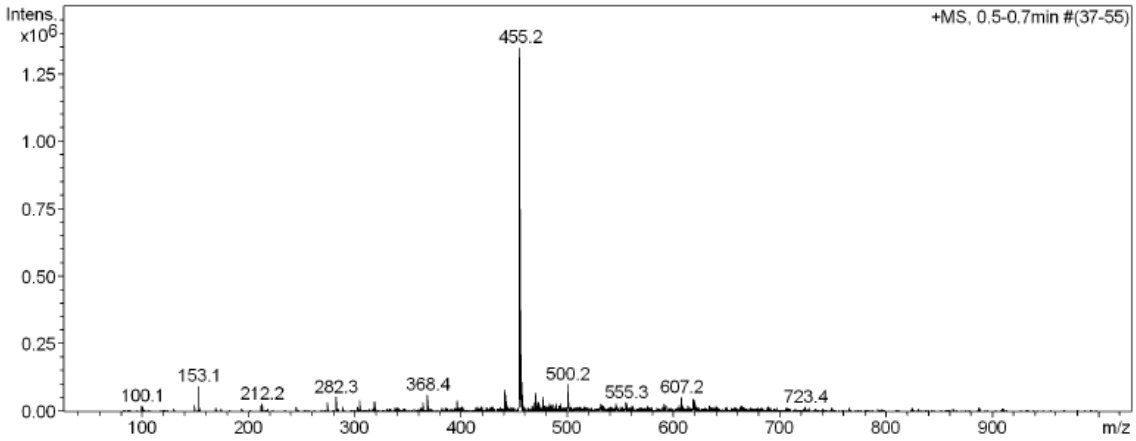
Intens.
x10^6
1.25
1.00
0.75
0.50
0.25
0.00
+MS, 0.5-0.7min #(37-55)
455.2
153.1
100.1
212.2
282.3
368.4
500.2
555.3
607.2
723.4
100
200
300
400
500
600
700
800
900
m/z

N-Methylated biaryl cyclic tripeptide incorporating a His-Tyr linkage

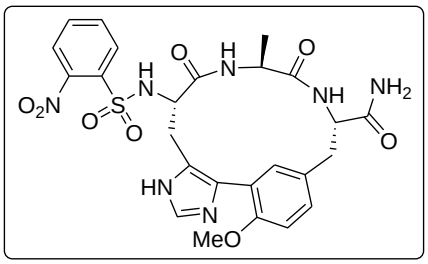

HPLC (λ = 220 nm)

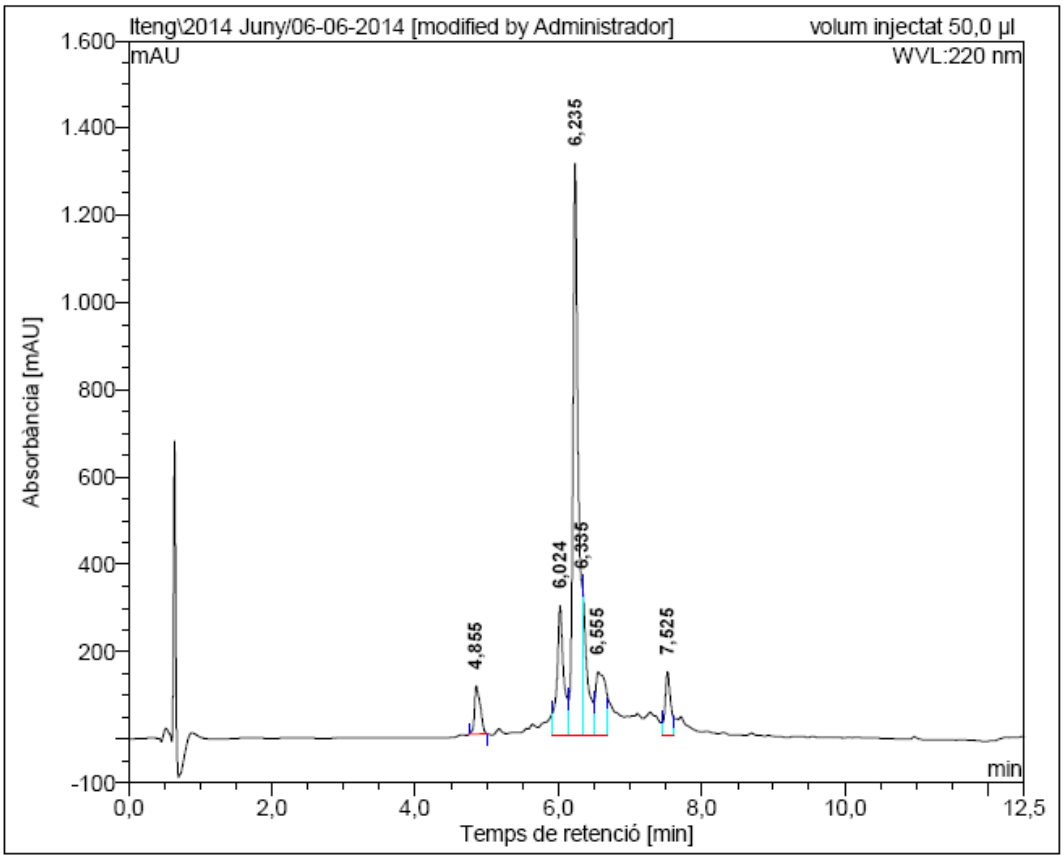

No.	mps retenc min	alçada mAU	Area mAU*min	Area relativa %
1	4,85	110,555	10,327	4,73
2	6,02	295,086	31,273	14,34
3	6,23	1308,893	114,801	52,63
4	6,34	339,713	26,025	11,93
5	6,56	144,070	23,480	10,76
6	7,52	144,574	12,238	5,61
Total:		2342,892	218,144	100,00

ESI-MS *m/z*

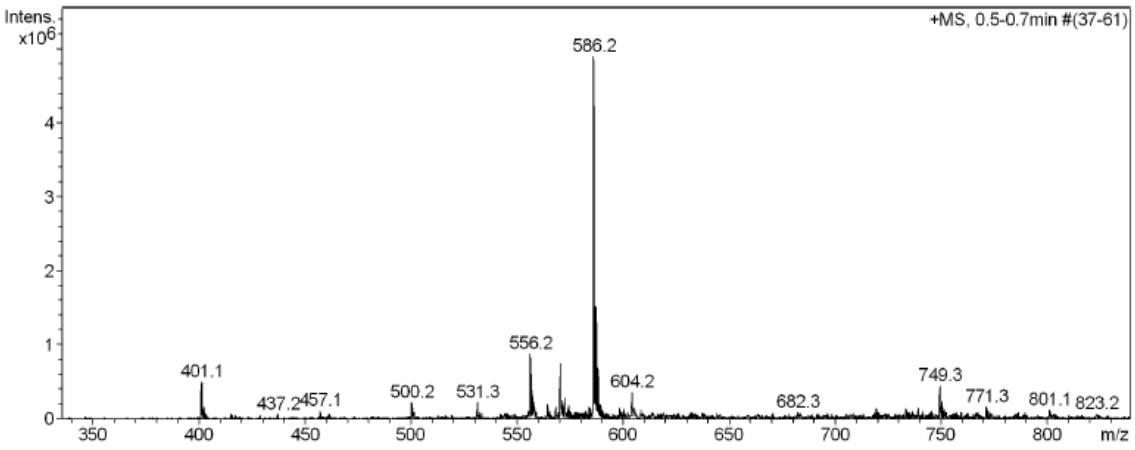
Intens.
x10^6
+MS, 0.5-0.7min #(37-61)
586.2
556.2
401.1
604.2
749.3
437.2
457.1
500.2
531.3
682.3
771.3
801.1
823.2
m/z

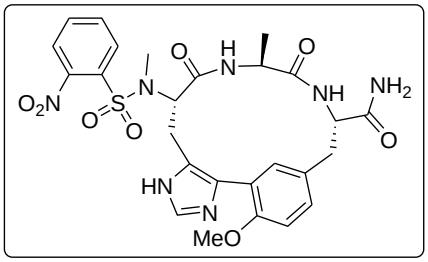

HPLC (λ = 220 nm)

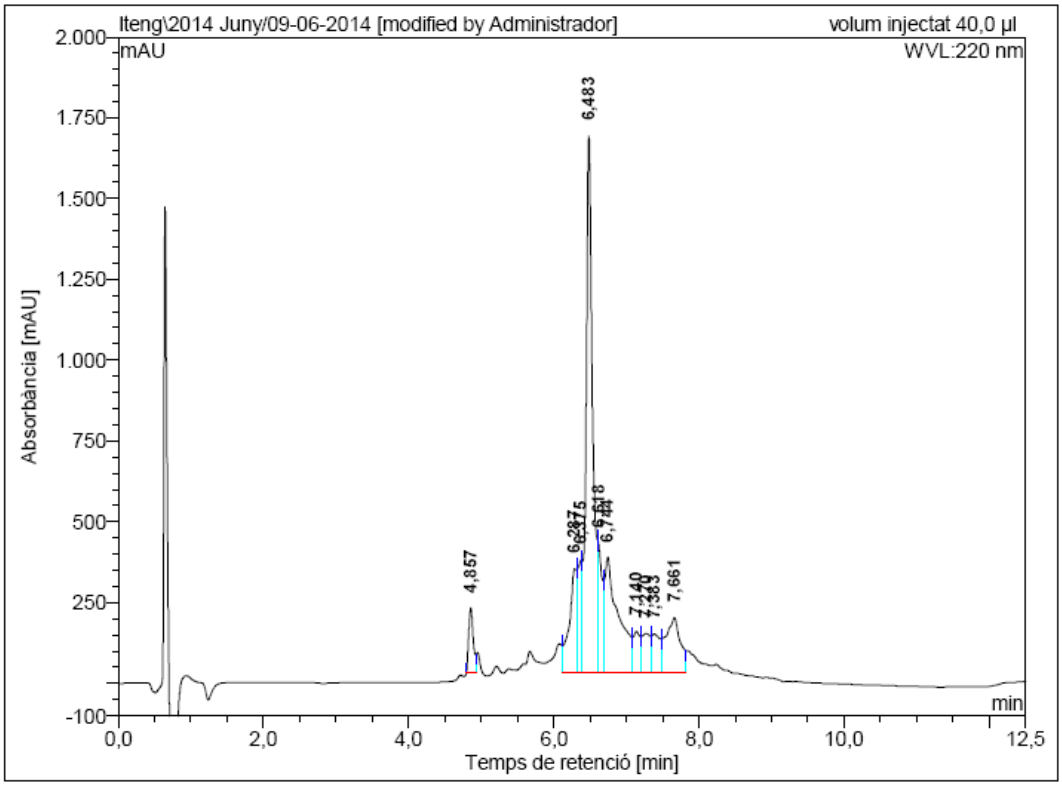

No.	Temps retenció min	alçada mAU	Area mAU*min	Area relativa %
1	4,86	201,847	15,006	3,34
2	6,29	321,972	39,833	8,86
3	6,38	348,939	21,464	4,78
4	6,48	1660,715	178,301	39,68
5	6,62	401,204	26,306	5,85
6	6,74	358,727	80,967	18,02
7	7,14	128,332	14,487	3,22
8	7,27	122,922	16,757	3,73
9	7,38	120,714	16,347	3,64
10	7,66	170,751	39,870	8,87
Total:		3836,123	449,337	100,00

ESI-MS *m/z*

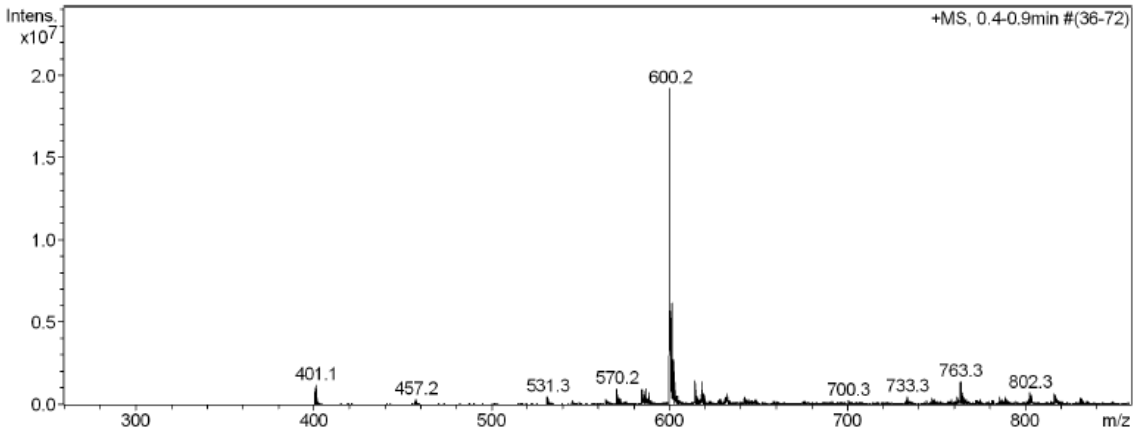
Intens.
x10^7
+MS, 0.4-0.9min #(36-72)
2.0
1.5
1.0
0.5
0.0
600.2
401.1
457.2
531.3
570.2
700.3
733.3
763.3
802.3
300
400
500
600
700
800
m/z

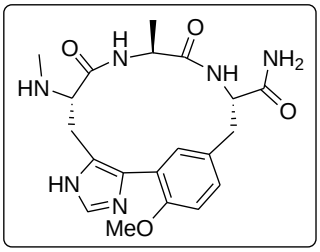

HPLC (λ = 220 nm)

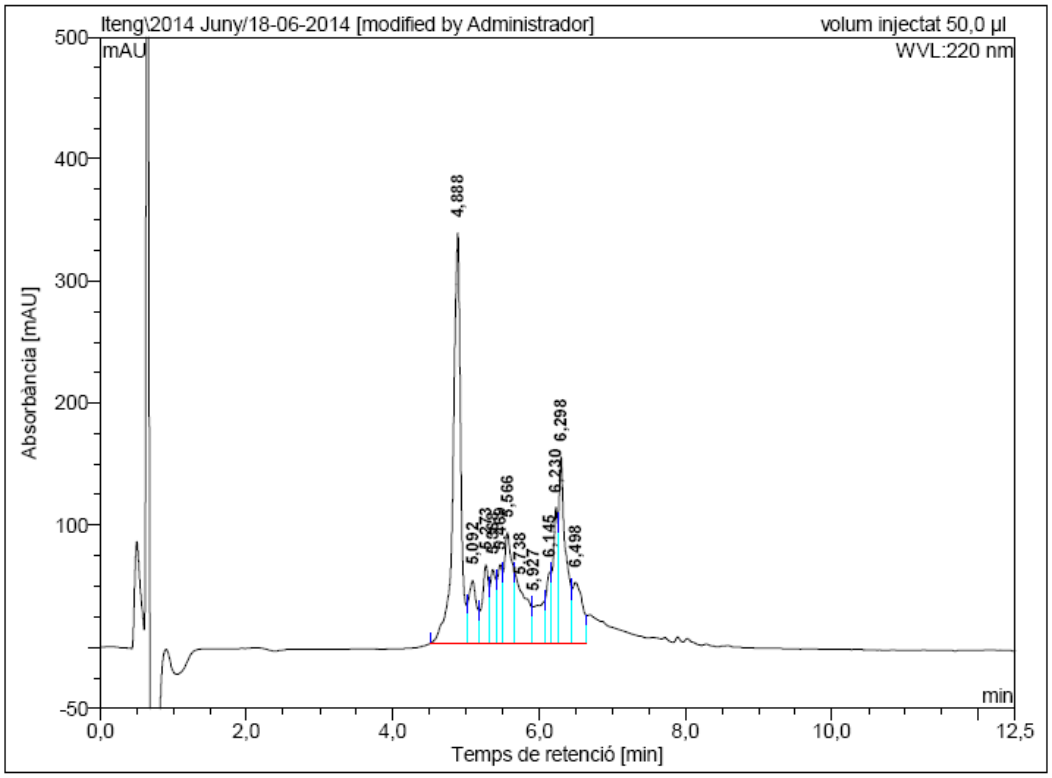

No.	Temps retenció min	alçada mAU	Area mAU*min	Area relativa %
1	4,89	335,518	40,374	31,78
2	5,09	50,834	6,490	5,11
3	5,27	63,633	6,395	5,03
4	5,37	59,937	5,163	4,06
5	5,47	63,972	5,133	4,04
6	5,57	90,116	11,560	9,10
7	5,74	43,433	9,401	7,40
8	5,93	29,505	5,677	4,47
9	6,15	57,802	4,354	3,43
10	6,23	111,186	7,782	6,12
11	6,30	152,213	17,414	13,71
12	6,50	49,440	7,318	5,76
Total:		1107,587	127,061	100,00

ESI-MS *m/z*

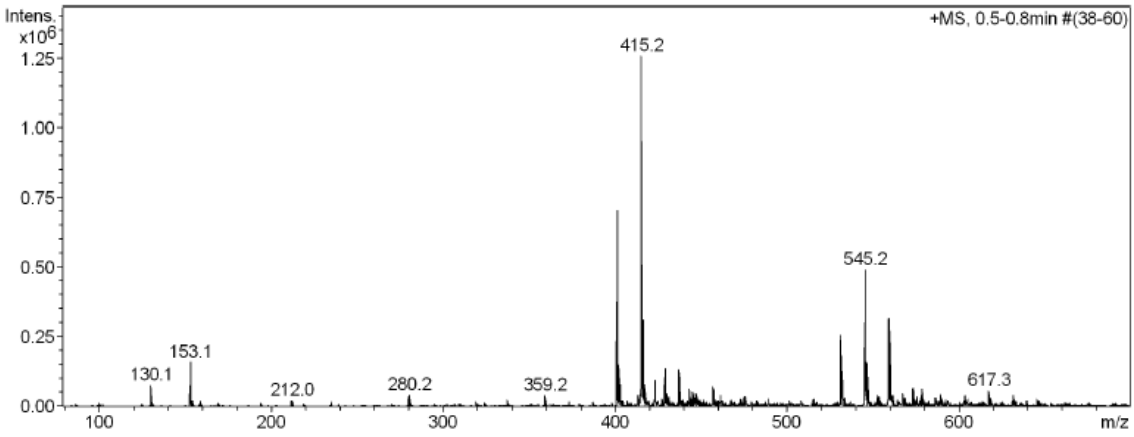
Intens.
x10^6
1.25
1.00
0.75
0.50
0.25
0.00
+MS, 0.5-0.8min #(38-60)
415.2
545.2
153.1
130.1
212.0
280.2
359.2
617.3
100
200
300
400
500
600
m/z

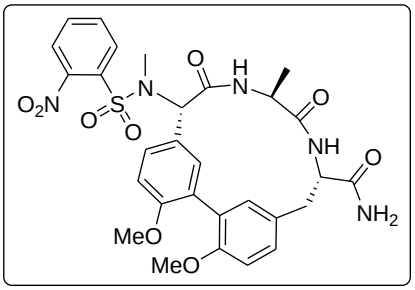

HPLC (λ = 220 nm)

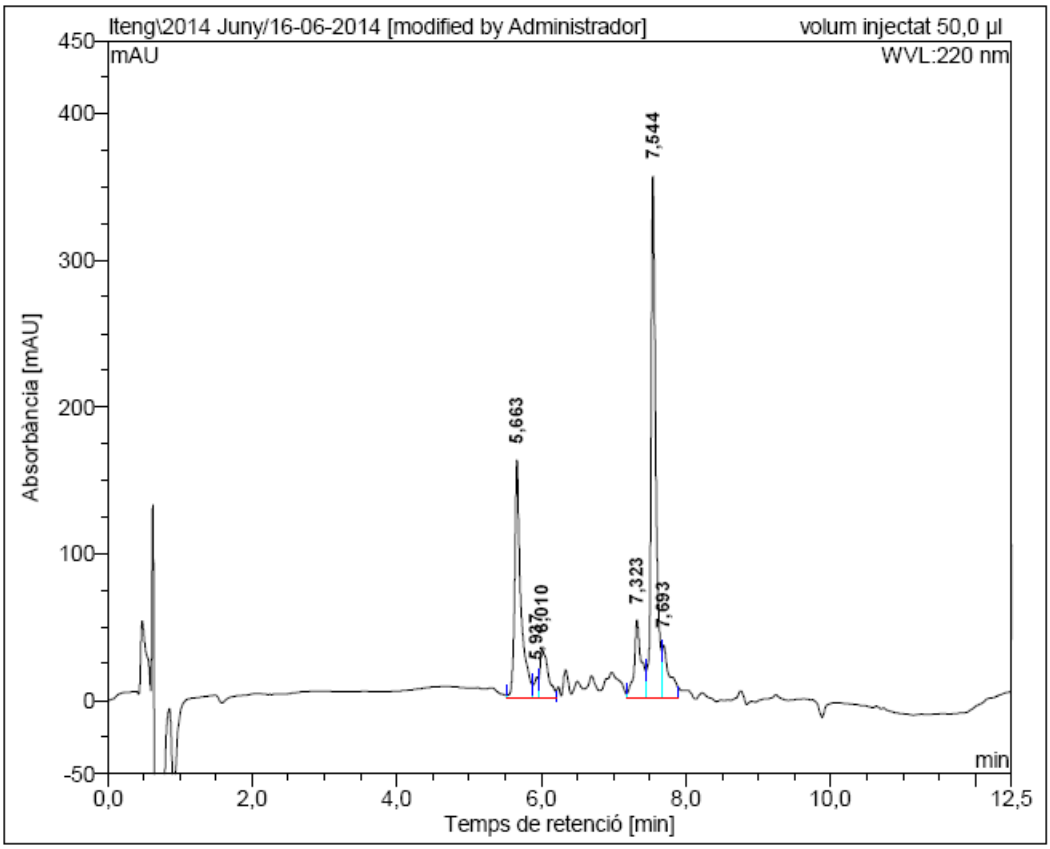

No.	mps retenc min	alçada mAU	Area mAU*min	Area relativa %
1	5,66	162,638	16,386	27,38
2	5,94	15,005	0,924	1,54
3	6,01	34,047	4,494	7,51
4	7,32	53,875	6,383	10,66
5	7,54	356,238	27,166	45,39
6	7,69	36,371	4,502	7,52
Total:		658,175	59,855	100,00

ESI-MS *m/z*

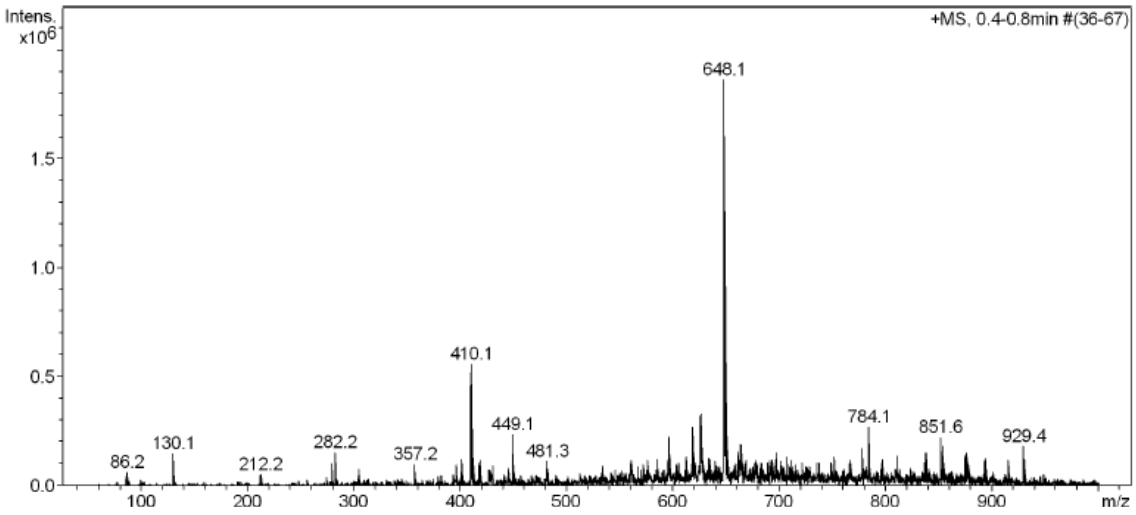
Intens.
x10^6
+MS, 0.4-0.8min #(36-67)
648.1
410.1
784.1
851.6
929.4
449.1
481.3
130.1
282.2
357.2
86.2
212.2
1.5
1.0
0.5
0.0
100
200
300
400
500
600
700
800
900
m/z

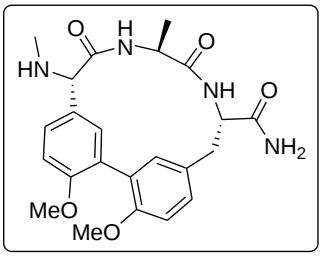

HPLC (λ = 220 nm)

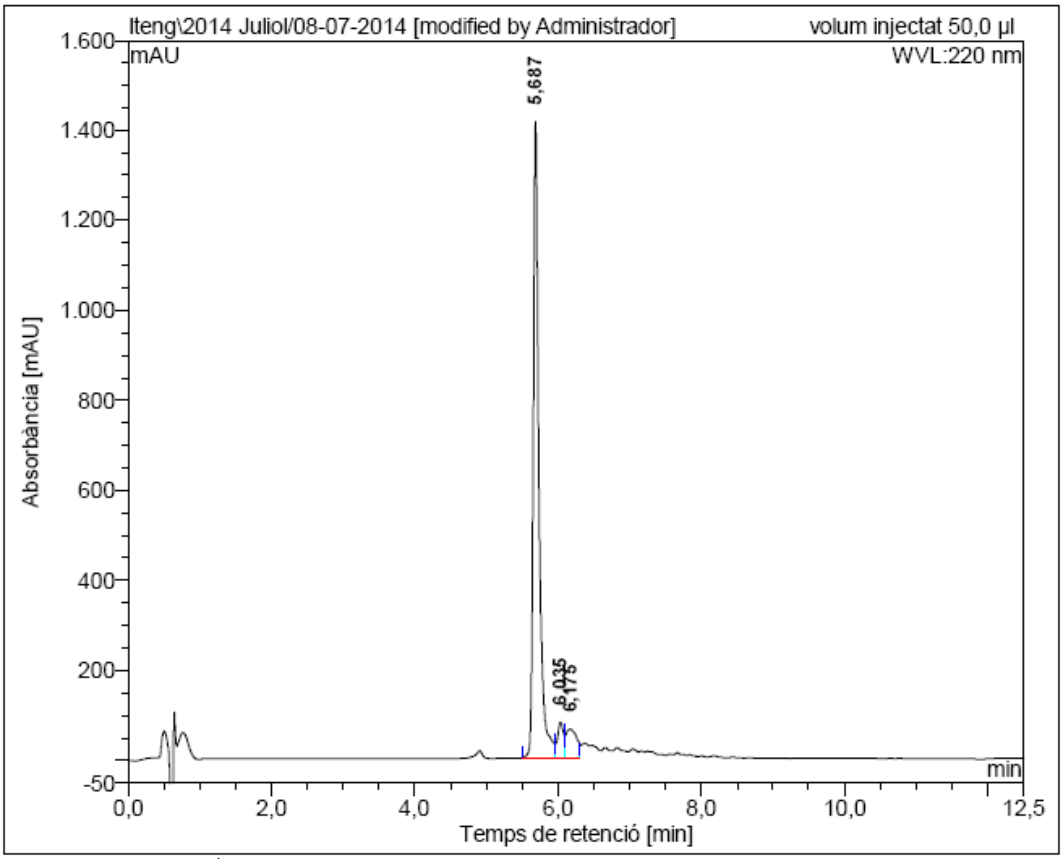

No.	mps retenc min	alçada mAU	Area mAU*min	Area relativa %
1	5,69	1414,041	129,583	87,44
2	6,04	78,805	7,594	5,12
3	6,17	63,202	11,025	7,44
Total:		1556,048	148,202	100,00

ESI-MS *m/z*

6.

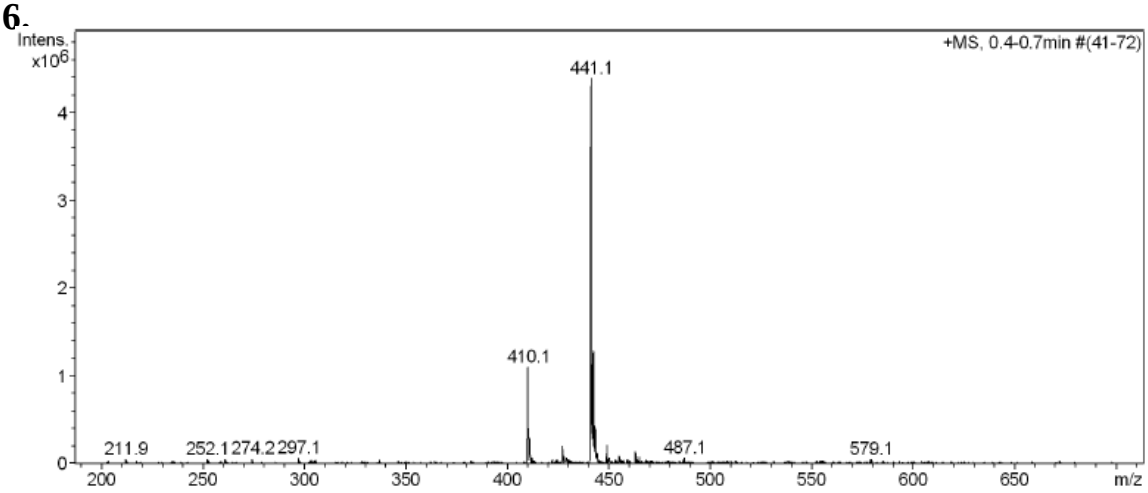
Intens.
x10^6
+MS, 0.4-0.7min #(41-72)
441.1
410.1
211.9
252.1
274.2
297.1
487.1
579.1
m/z

Synthesis of tailed biaryl cyclic hexapeptides

Tailed biaryl cyclic hexapeptide resulting from the cleavage of resin 20

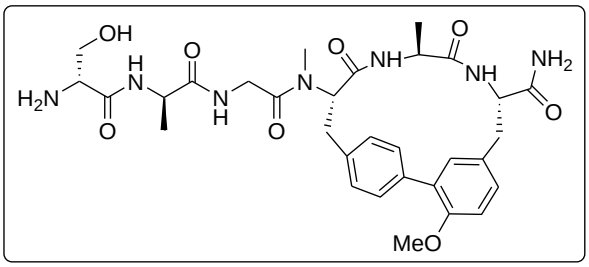

HPLC (λ = 220 nm)

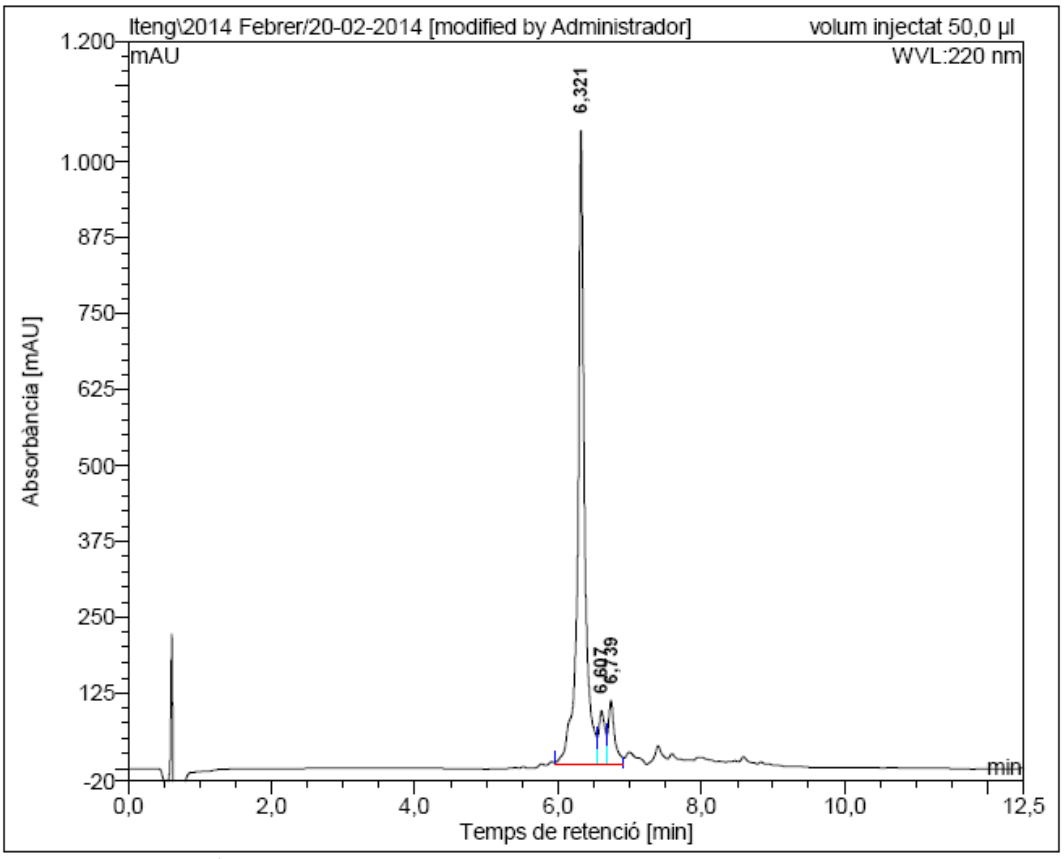

No.	mps retenc min	alçada mAU	Area mAU*min	Area relativa %
1	6,32	1044,578	116,151	85,44
2	6,61	88,234	8,985	6,61
3	6,74	105,298	10,803	7,95
Total:		1238,110	135,939	100,00

ESI-MS *m/z*

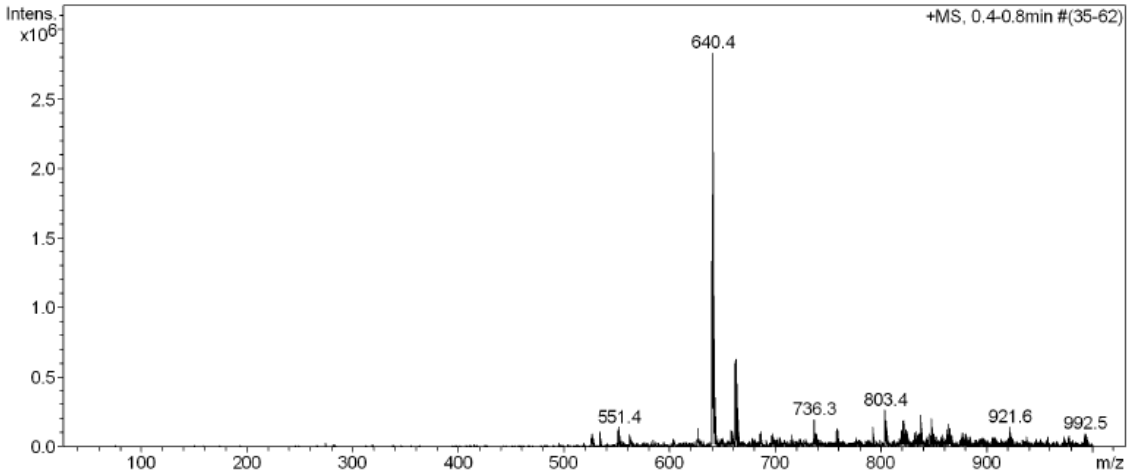
Intens.
x10^6
+MS, 0.4-0.8min #(35-62)
640.4
551.4
736.3
803.4
921.6
992.5
2.5
2.0
1.5
1.0
0.5
0.0
100
200
300
400
500
600
700
800
900
m/z

Tailed biaryl cyclic hexapeptide resulting from the cleavage of resin 25

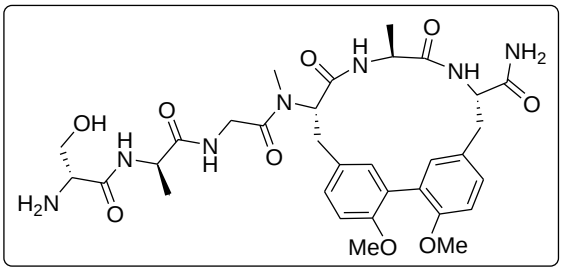

HPLC (λ = 220 nm)

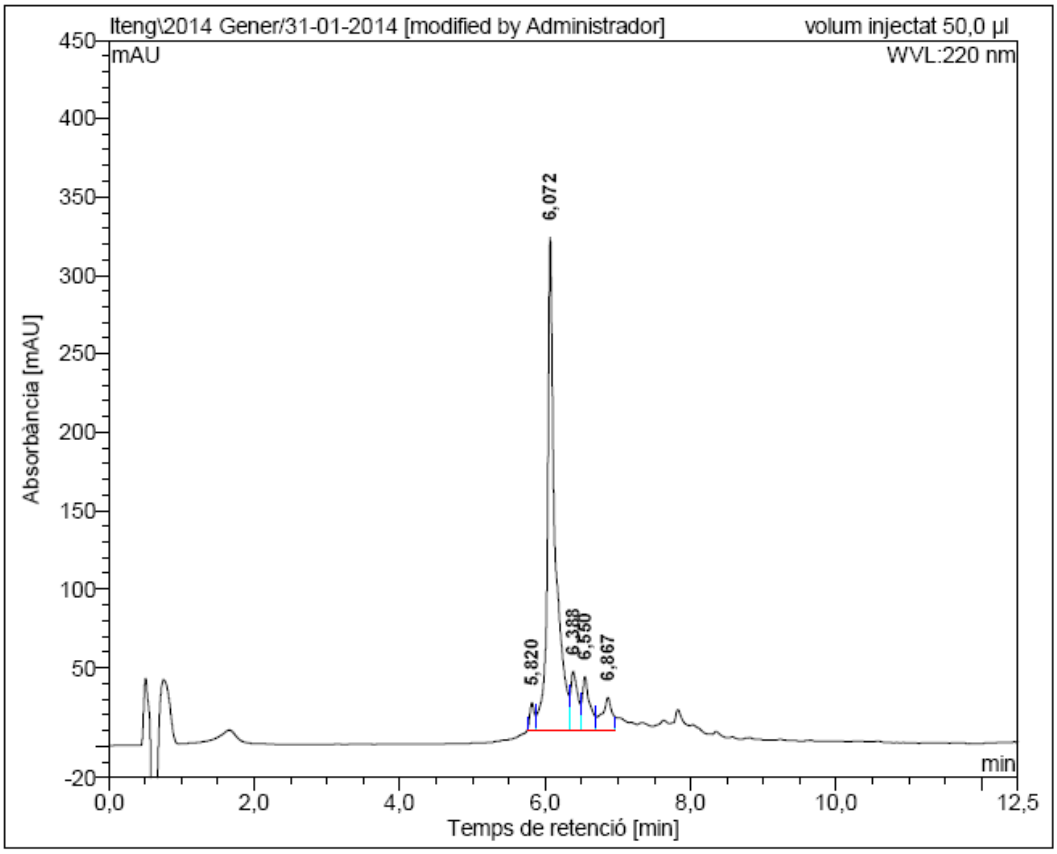

No.	mps retenc min	alçada mAU	Area mAU*min	Area relativa %
1	5,82	17,832	1,234	2,36
2	6,07	314,377	39,001	74,72
3	6,39	38,011	4,324	8,28
4	6,55	34,679	4,236	8,12
5	6,87	21,206	3,401	6,52
Total:		426,106	52,196	100,00

ESI-MS *m/z*

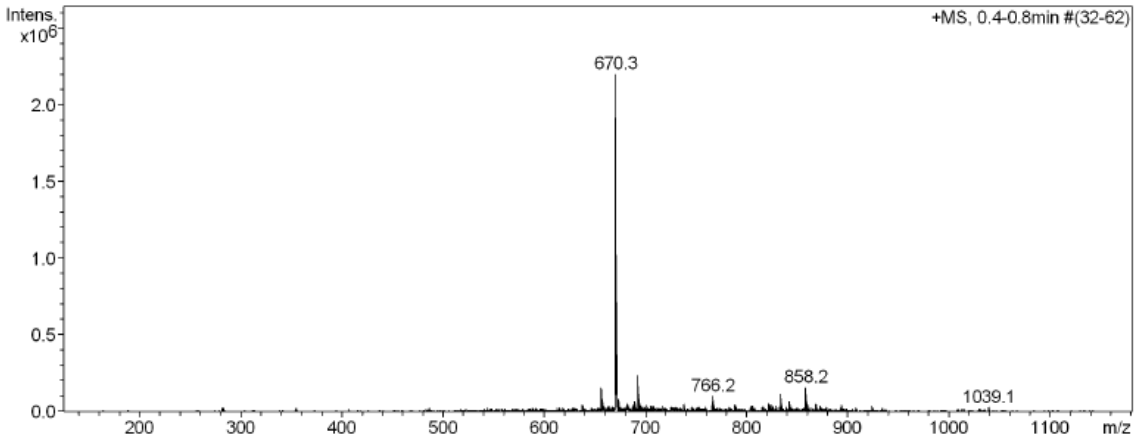
Intens.
x10^6
+MS, 0.4-0.8min #(32-62)
670.3
766.2
858.2
1039.1
2.0
1.5
1.0
0.5
0.0
200
300
400
500
600
700
800
900
1000
1100
m/z

Tailed biaryl cyclic hexapeptide resulting

from the cleavage of resins 29

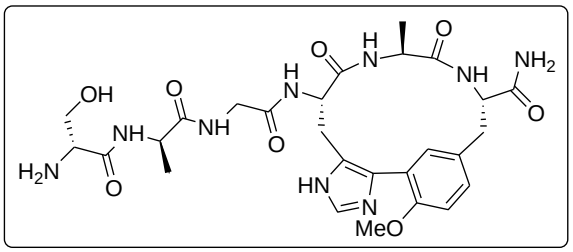

HPLC (λ = 220 nm)

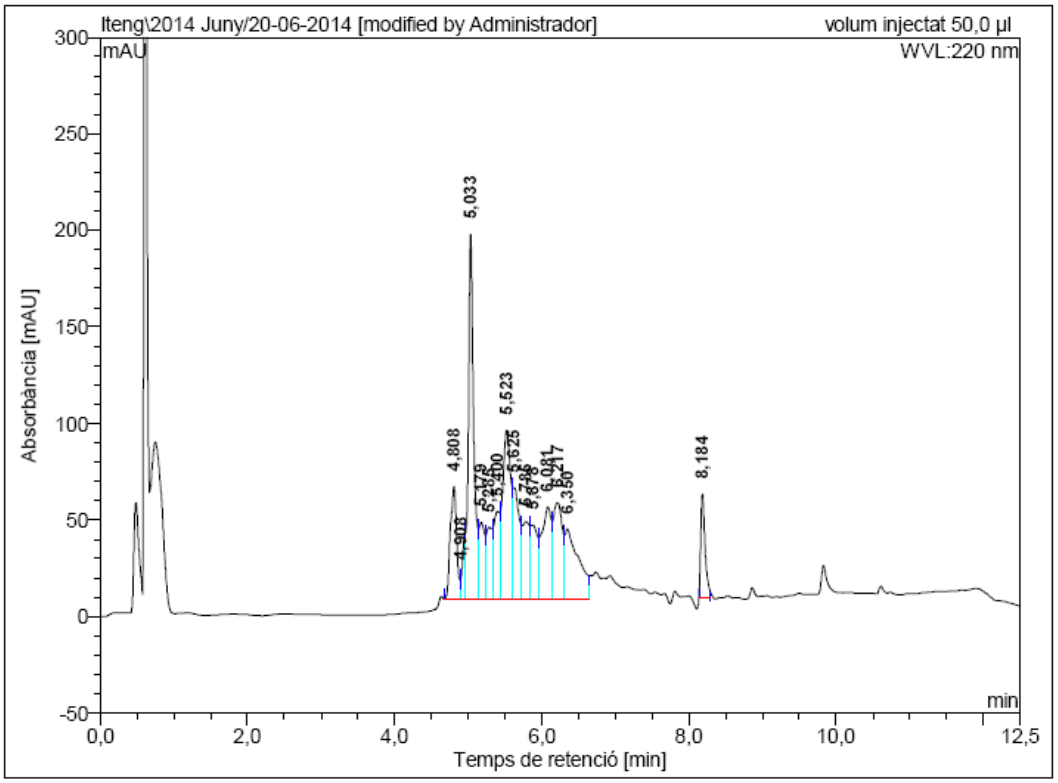

No.	Temps retenció min	alçada mAU	Area mAU*min	Area relativa %
1	4,81	58,186	5,711	6,53
2	4,91	12,212	1,814	2,07
3	5,03	188,605	15,808	18,07
4	5,18	39,715	3,308	3,78
5	5,28	37,359	3,700	4,23
6	5,40	45,354	4,510	5,15
7	5,52	87,473	11,363	12,99
8	5,63	57,714	6,270	7,17
9	5,78	40,155	4,828	5,52
10	5,88	38,395	4,048	4,63
11	6,08	47,647	7,274	8,31
12	6,22	49,853	6,892	7,88
13	6,35	36,320	8,237	9,41
14	8,18	53,905	3,738	4,27
Total:		792,893	87,500	100,00

ESI-MS *m/z*

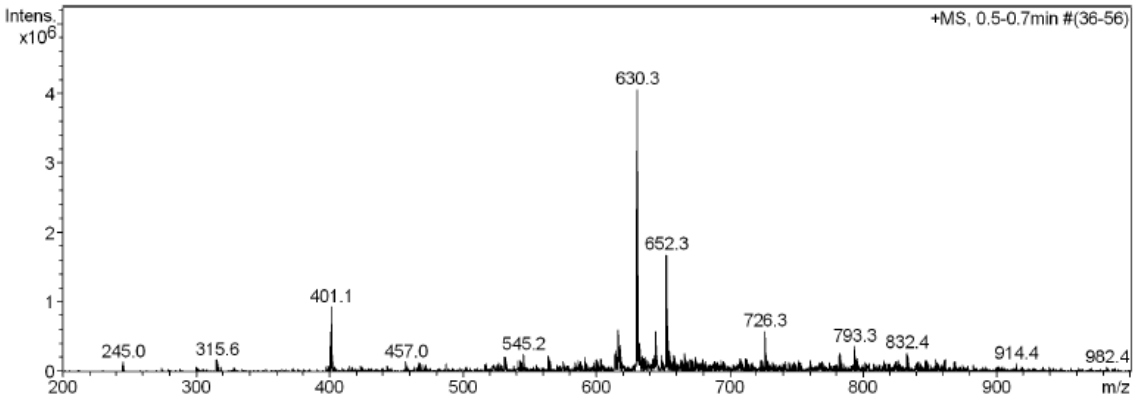
Intens.
x10^6
+MS, 0.5-0.7min #(36-56)
630.3
652.3
401.1
726.3
793.3
832.4
914.4
982.4
245.0
315.6
457.0
545.2
m/z

Tailed biaryl cyclic hexapeptide resulting from the cleavage of resin 34

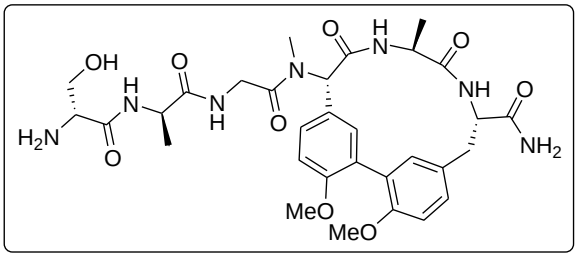

HPLC (λ = 220 nm)

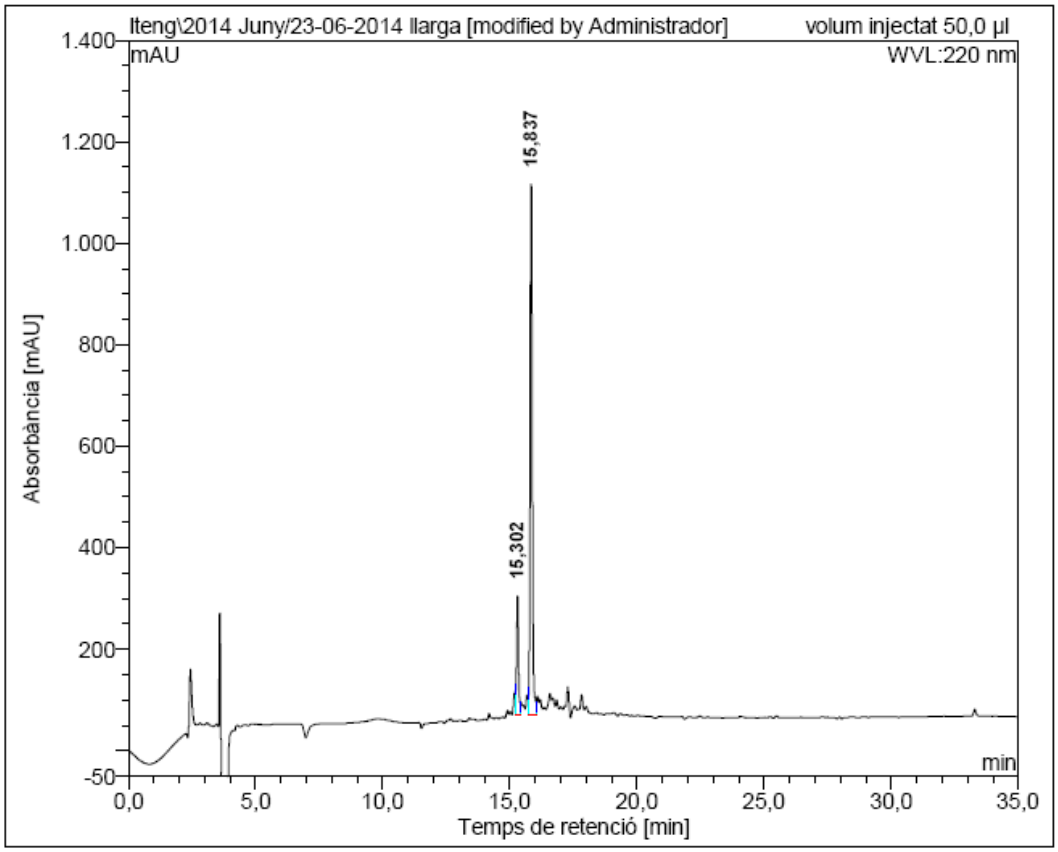

No.	mps retenc min	alçada mAU	Area mAU*min	Area relativa %
1	15,30	232,651	20,726	17,36
2	15,84	1043,963	98,646	82,64
Total:		1276,614	119,372	100,00

ESI-MS *m/z*

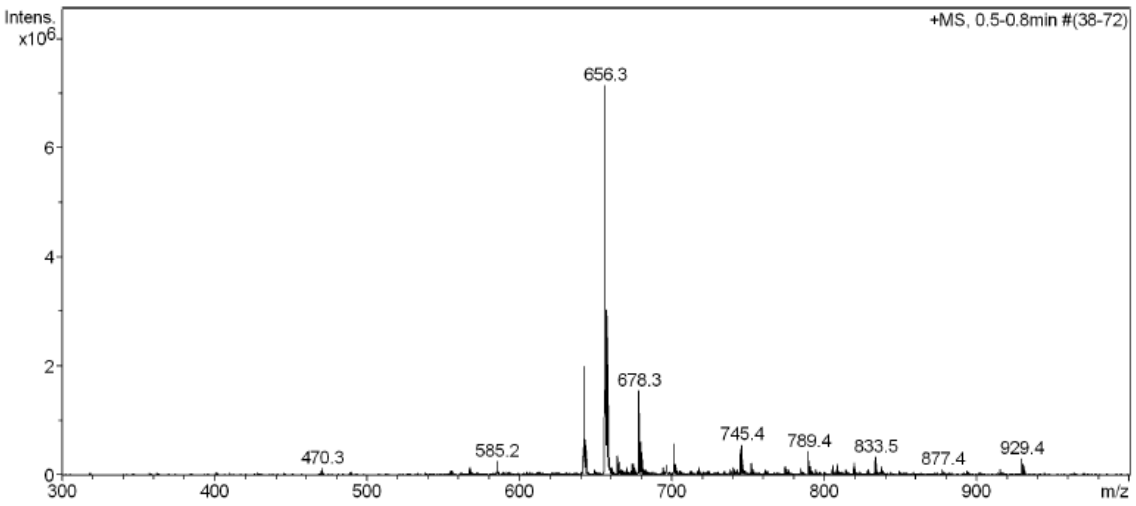
Intens.
x10^6
+MS, 0.5-0.8min #(38-72)
656.3
678.3
745.4
789.4
833.5
877.4
929.4
470.3
585.2
m/z

7. Synthesis of N-methylated tailed biaryl cyclic hexapeptides 21, 26, 30, 35

N-Methylated tailed biaryl cyclic hexapeptide incorporating a Phe-Tyr linkage 21

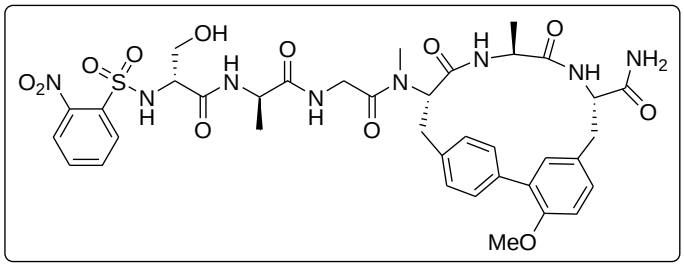

HPLC (λ = 220 nm)

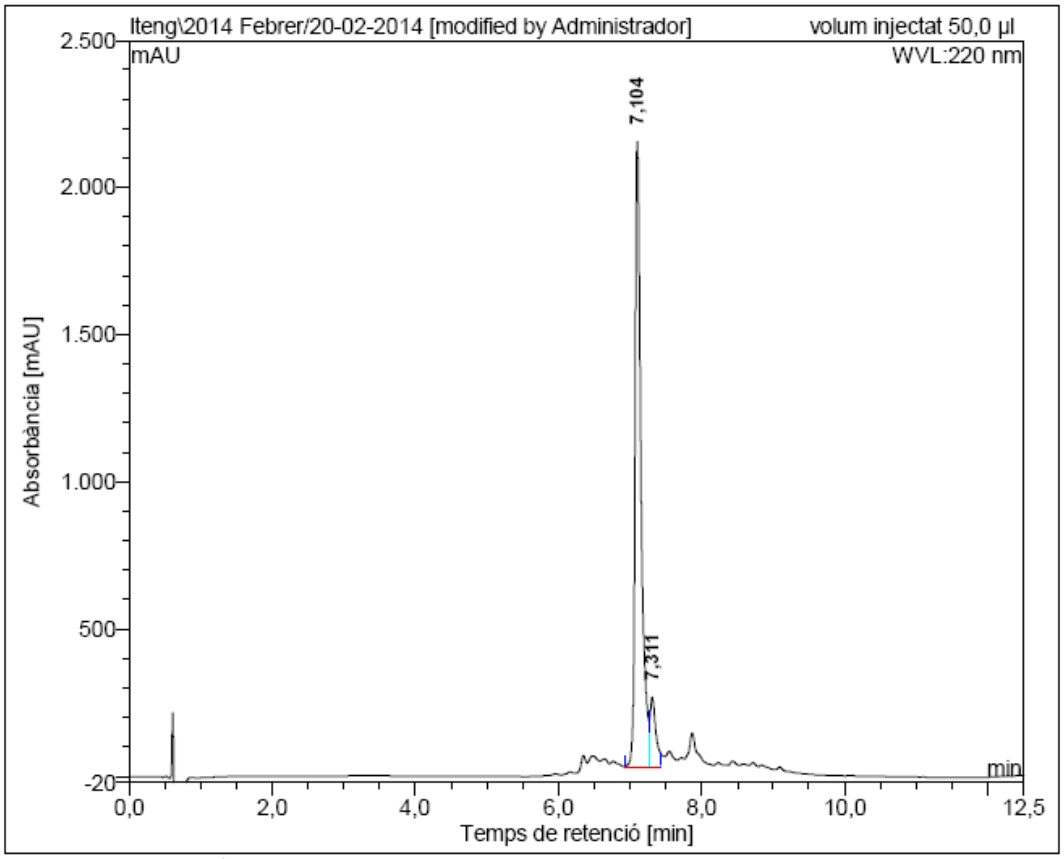

No.	mps retenc min	alçada mAU	Area mAU*min	Area relativa %
1	7,10	2122,684	206,072	89,97
2	7,31	236,478	22,981	10,03
Total:		2359,162	229,053	100,00

ESI-MS *m/z*

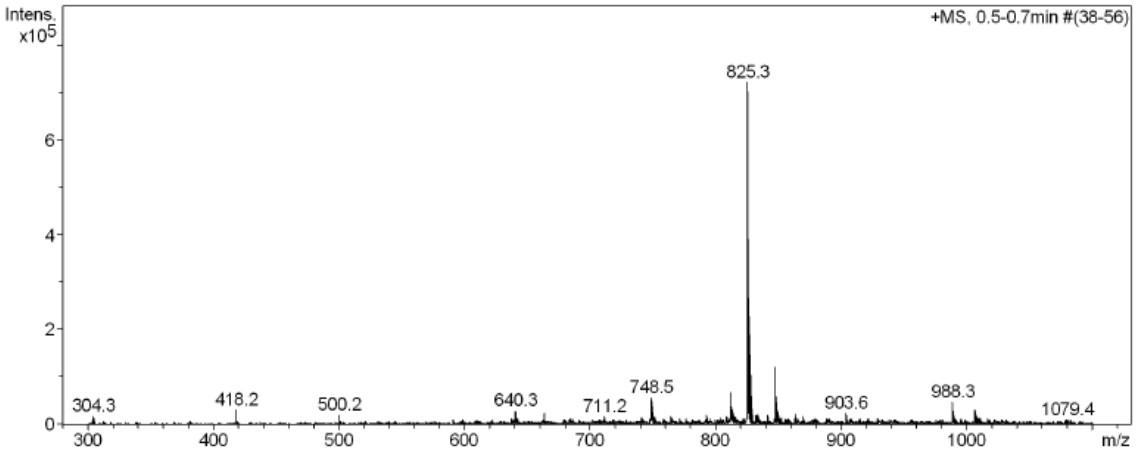
Intens.
x10^5
+MS, 0.5-0.7min #(38-56)
825.3
304.3
418.2
500.2
640.3
711.2
748.5
903.6
988.3
1079.4
m/z

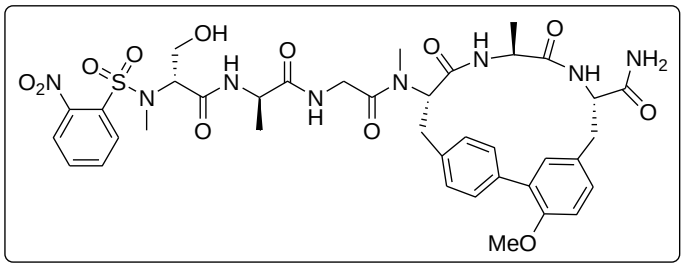

HPLC (λ = 220 nm)

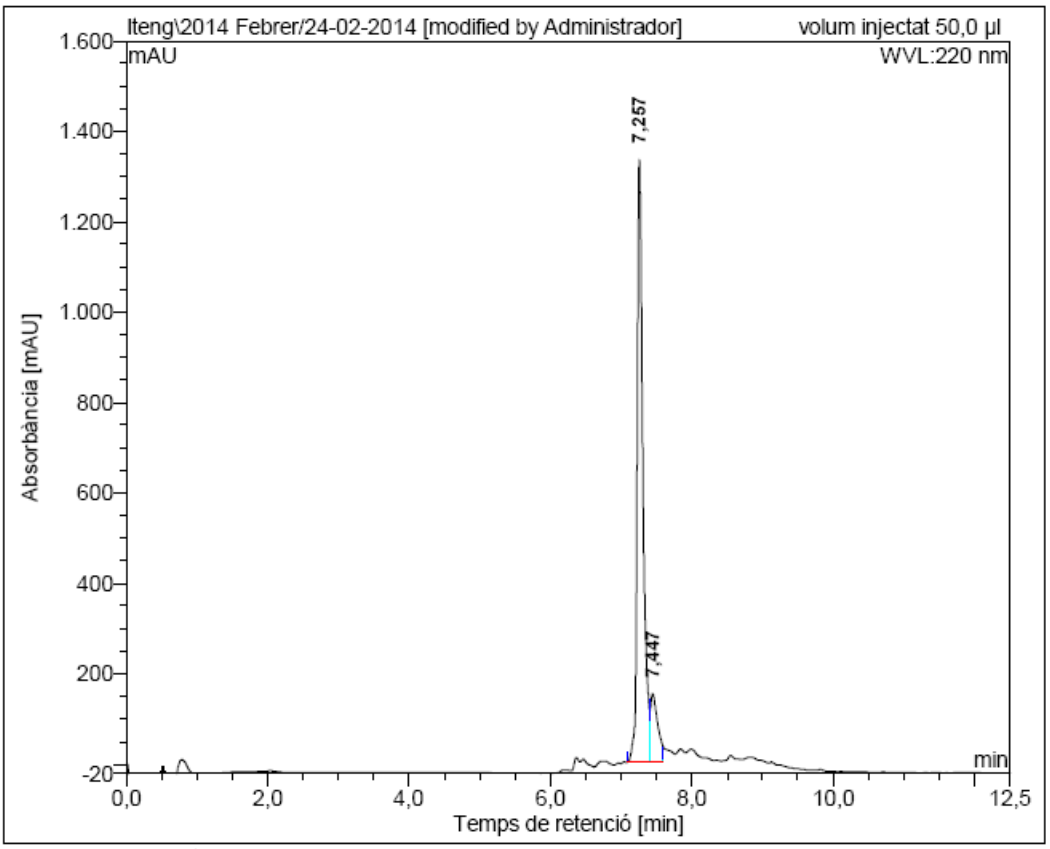

No.	mps retenc min	alçada mAU	Area mAU*min	Area relativa %
1	7,26	1333,166	126,892	87,43
2	7,45	151,743	18,252	12,57
Total:		1484,910	145,144	100,00

ESI-MS *m/z*

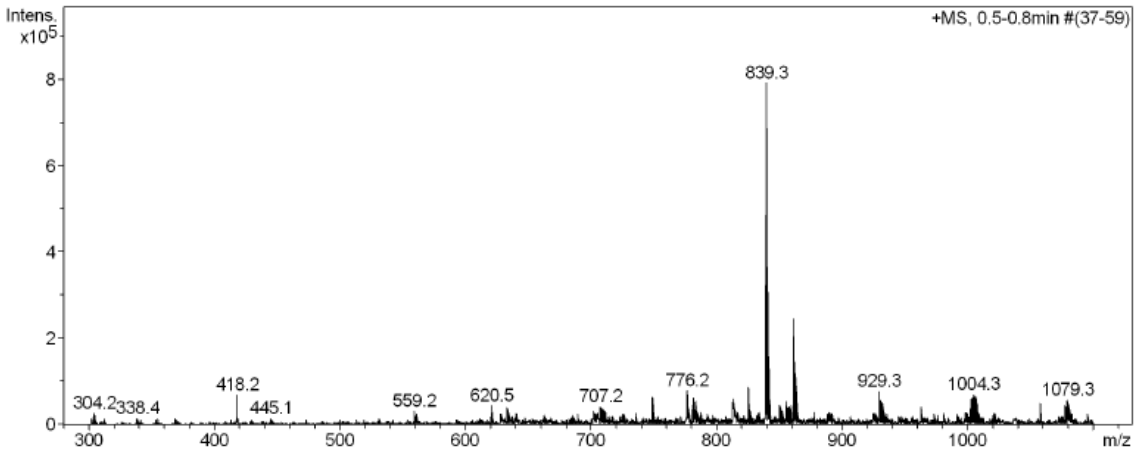
Intens.
x10^5
+MS, 0.5-0.8min #(37-59)
839.3
304.2
338.4
418.2
445.1
559.2
620.5
707.2
776.2
929.3
1004.3
1079.3
m/z

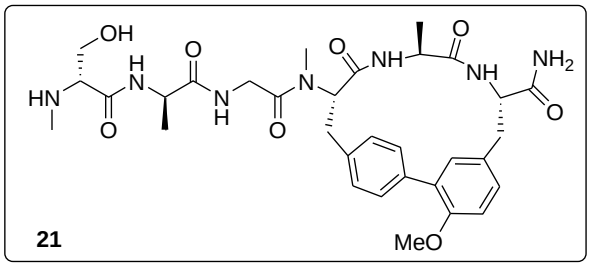

21

Crude peptide 21

HPLC (λ = 220 nm)

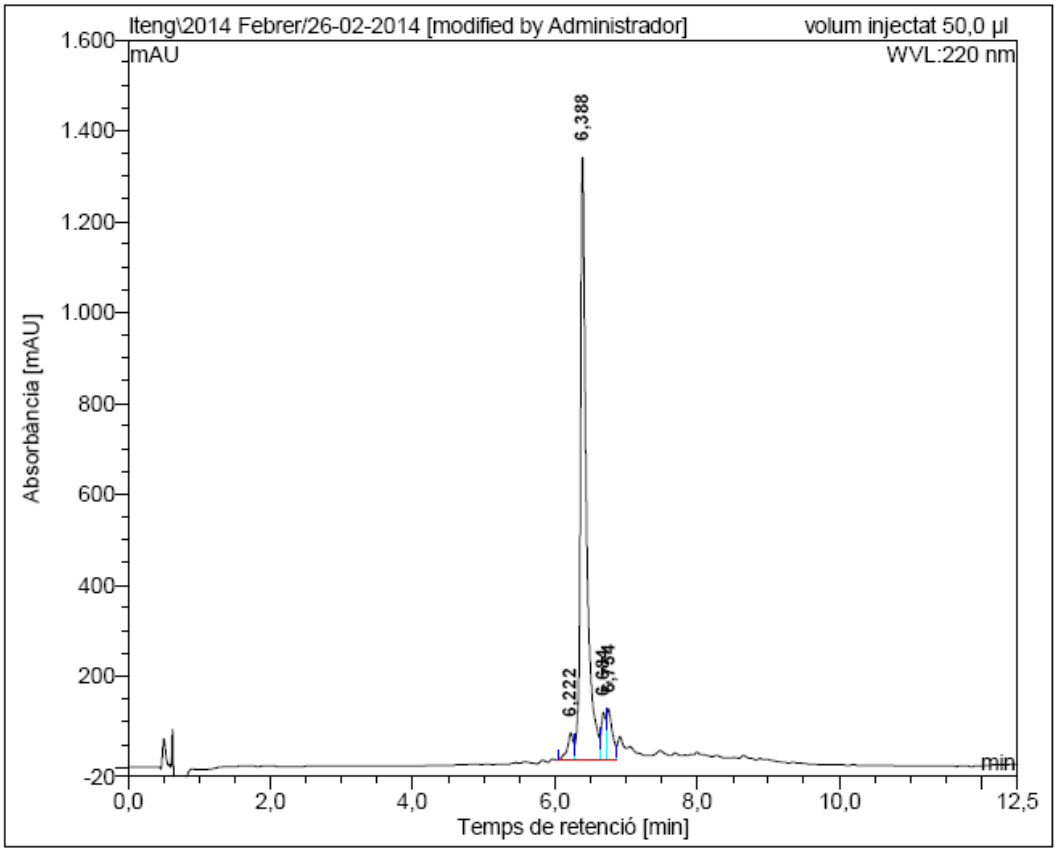

No.	mps retenc min	alçada mAU	Area mAU*min	Area relativa %
1	6,22	59,632	5,838	3,82
2	6,39	1325,127	128,541	84,21
3	6,68	105,184	7,227	4,73
4	6,75	112,055	11,040	7,23
Total:		1601,999	152,646	100,00

ESI-MS *m/z*

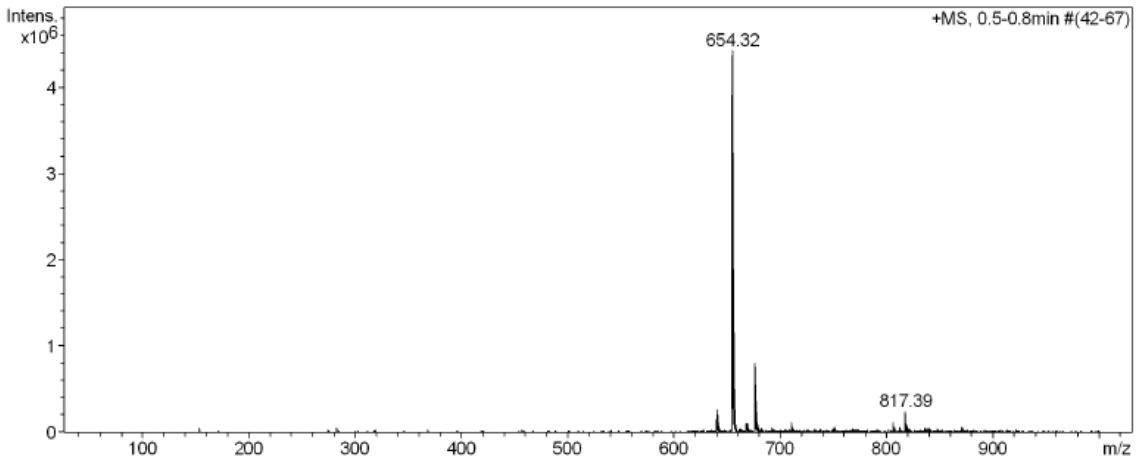
Intens.
x10^6
+MS, 0.5-0.8min #(42-67)
654.32
817.39
0
1
2
3
4
100
200
300
400
500
600
700
800
900
m/z

Purified peptide 21

HPLC (λ = 220 nm)

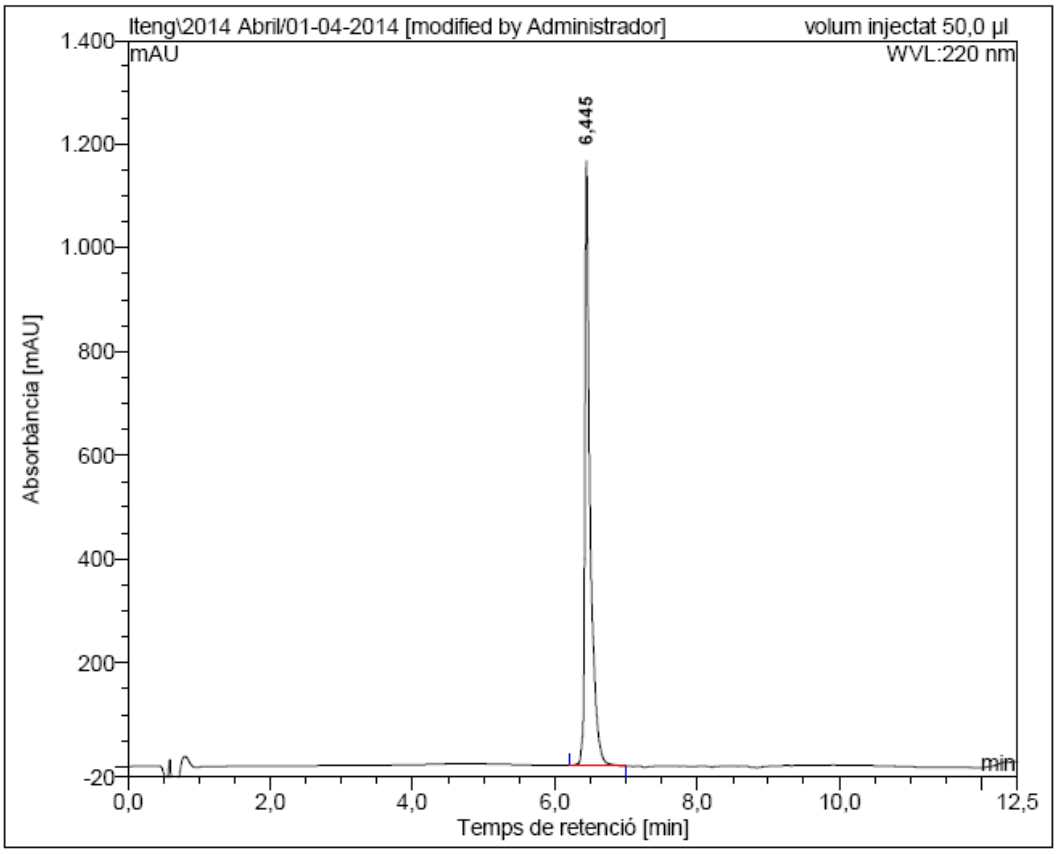

No.	mps retenc min	alçada mAU	Area mAU*min	Area relativa %
1	6,45	1166,432	101,619	100,00
Total:		1166,432	101,619	100,00

ESI-MS *m/z*

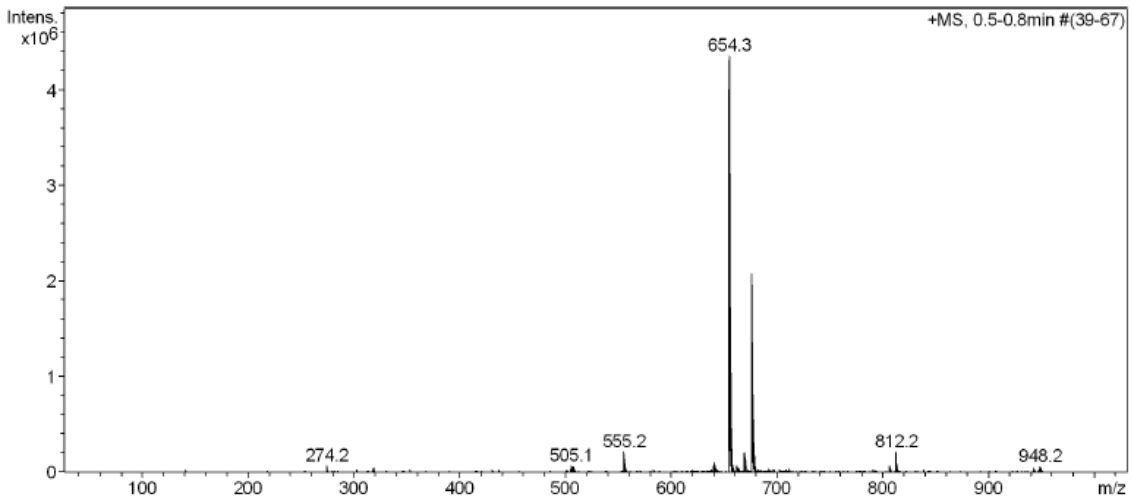

HRMS (ESI) *m/z*

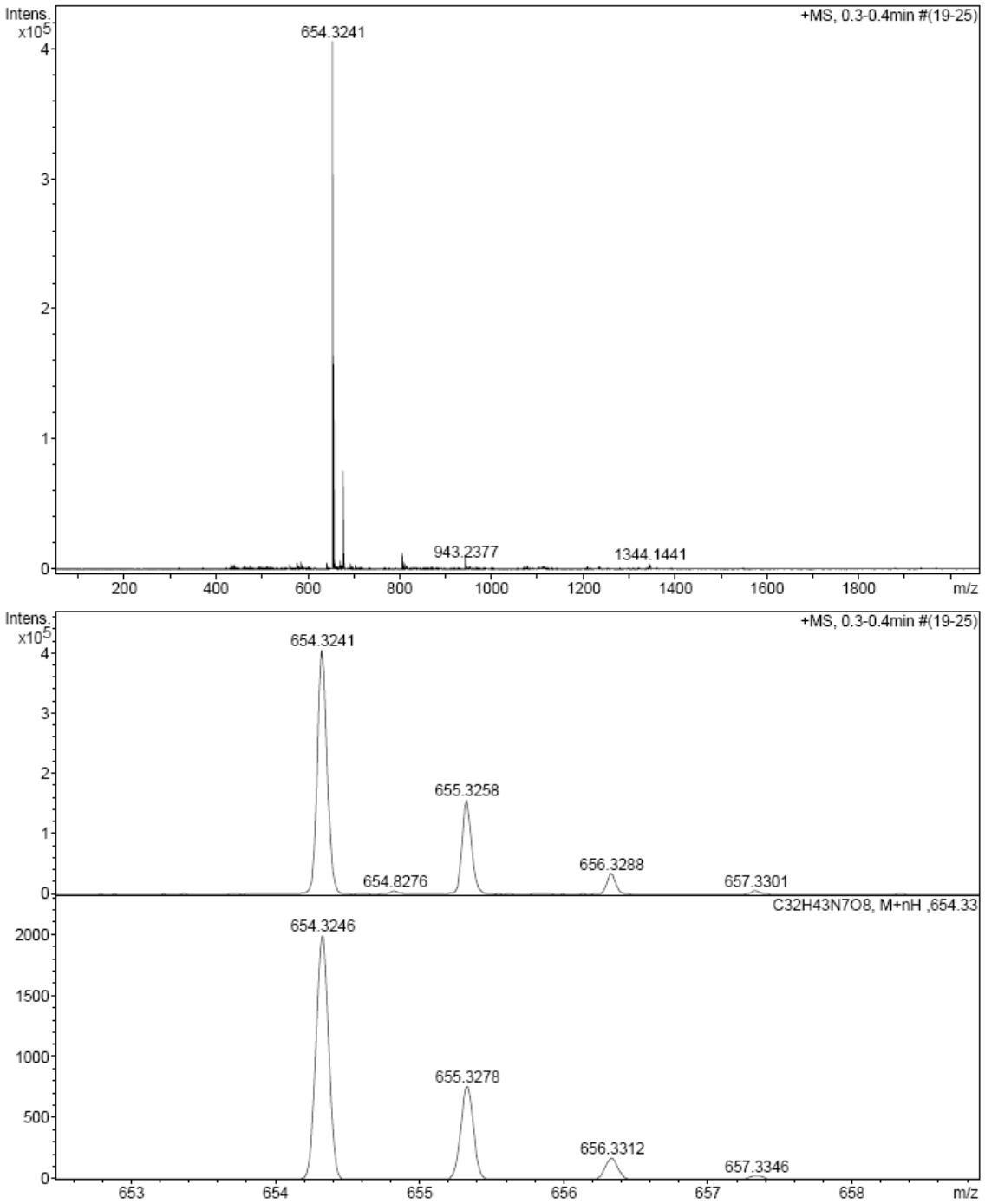
Intens.
x10^5
+MS, 0.3-0.4min #(19-25)
654.3241
943.2377
1344.1441
m/z
Intens.
x10^5
+MS, 0.3-0.4min #(19-25)
654.3241
655.3258
654.8276
656.3288
657.3301
C32H43N7O8, M+nH ,654.33
654.3246
655.3278
656.3312
657.3346
m/z

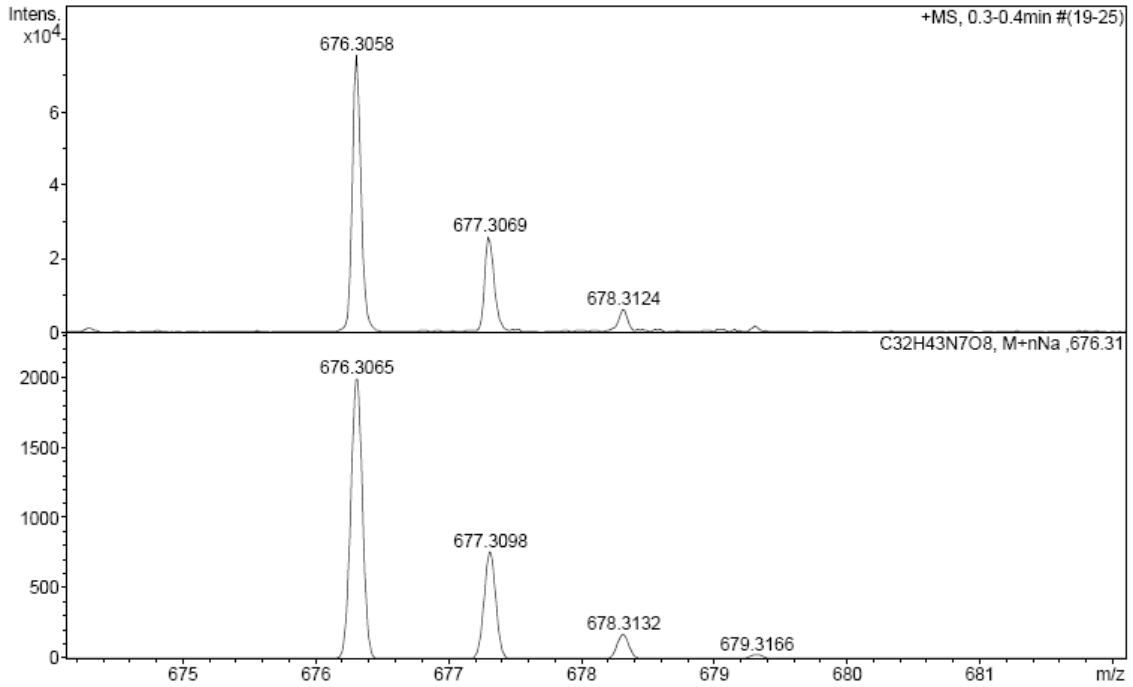

^{1}H-NMR (400 MHz, CD_3OD) δ (ppm)

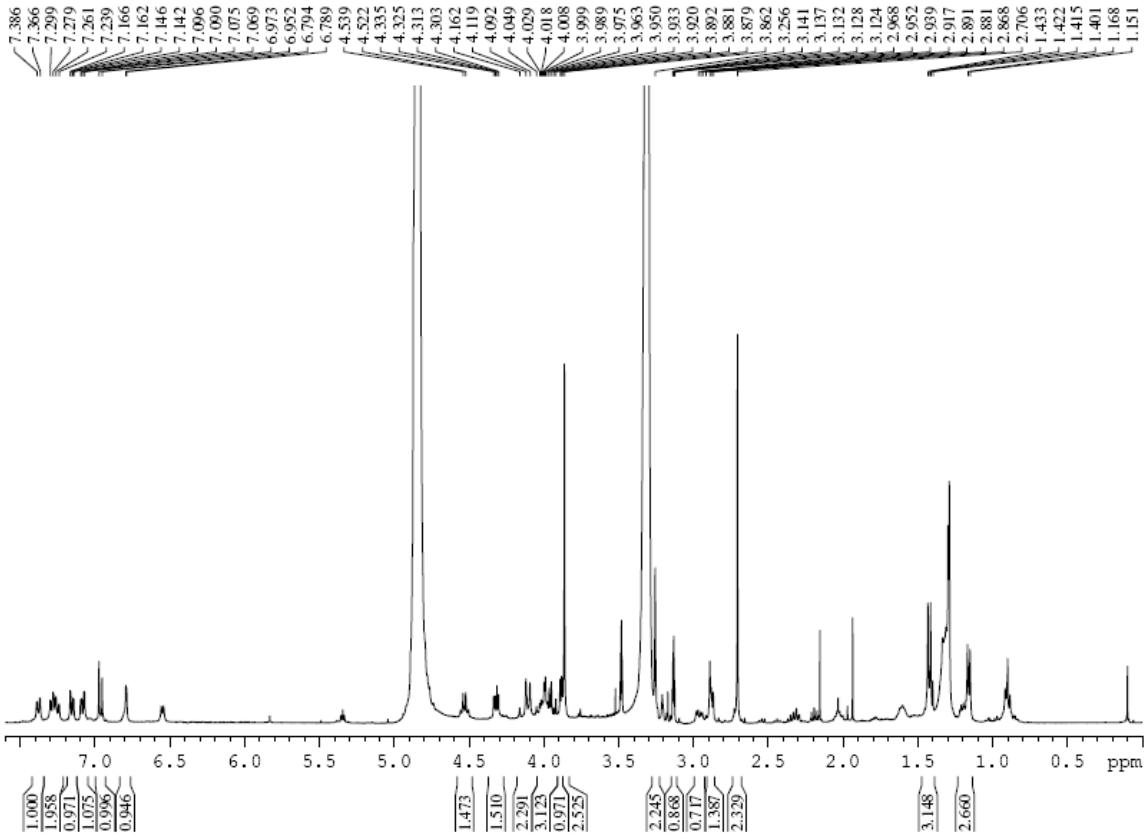

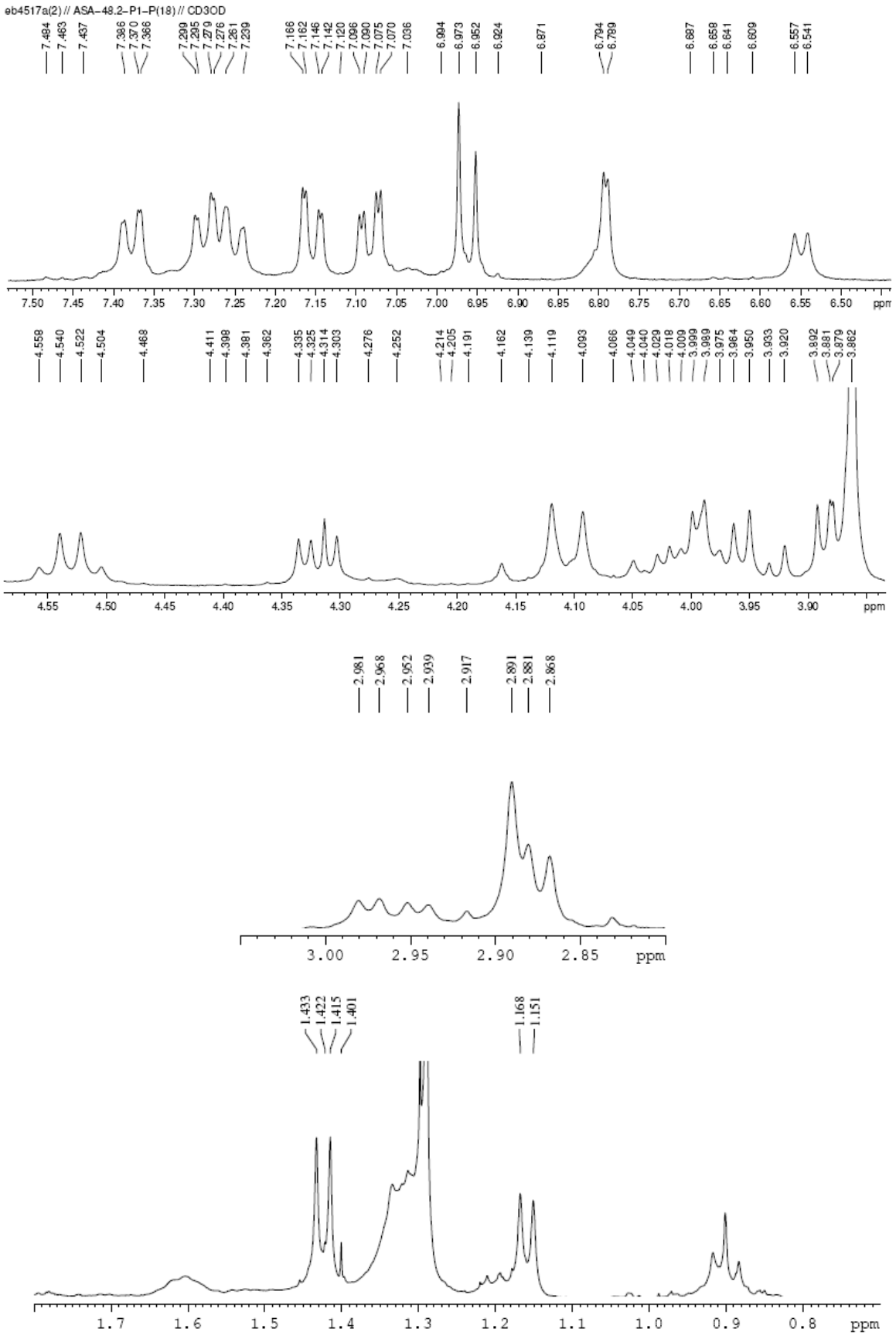
eb4517a(2) // ASA-48.2-P1-P(18) // CD3OD
7.494
7.463
7.437
7.386
7.370
7.366
7.299
7.295
7.279
7.276
7.261
7.239
7.166
7.162
7.146
7.142
7.120
7.096
7.090
7.075
7.070
7.036
6.994
6.973
6.952
6.924
6.871
6.794
6.789
6.687
6.658
6.641
6.609
6.557
6.541
7.50 7.45 7.40 7.35 7.30 7.25 7.20 7.15 7.10 7.05 7.00 6.95 6.90 6.85 6.80 6.75 6.70 6.65 6.60 6.55 6.50 ppm
4.558
4.540
4.522
4.504
4.468
4.411
4.398
4.381
4.362
4.335
4.325
4.314
4.303
4.276
4.252
4.214
4.205
4.191
4.162
4.139
4.119
4.093
4.066
4.049
4.040
4.029
4.018
4.009
3.999
3.989
3.975
3.964
3.950
3.933
3.920
3.892
3.881
3.879
3.862
4.55 4.50 4.45 4.40 4.35 4.30 4.25 4.20 4.15 4.10 4.05 4.00 3.95 3.90 ppm
2.981
2.968
2.952
2.939
2.917
2.891
2.881
2.868
3.00 2.95 2.90 2.85 ppm
1.433
1.422
1.415
1.401
1.168
1.151
1.7 1.6 1.5 1.4 1.3 1.2 1.1 1.0 0.9 0.8 ppm

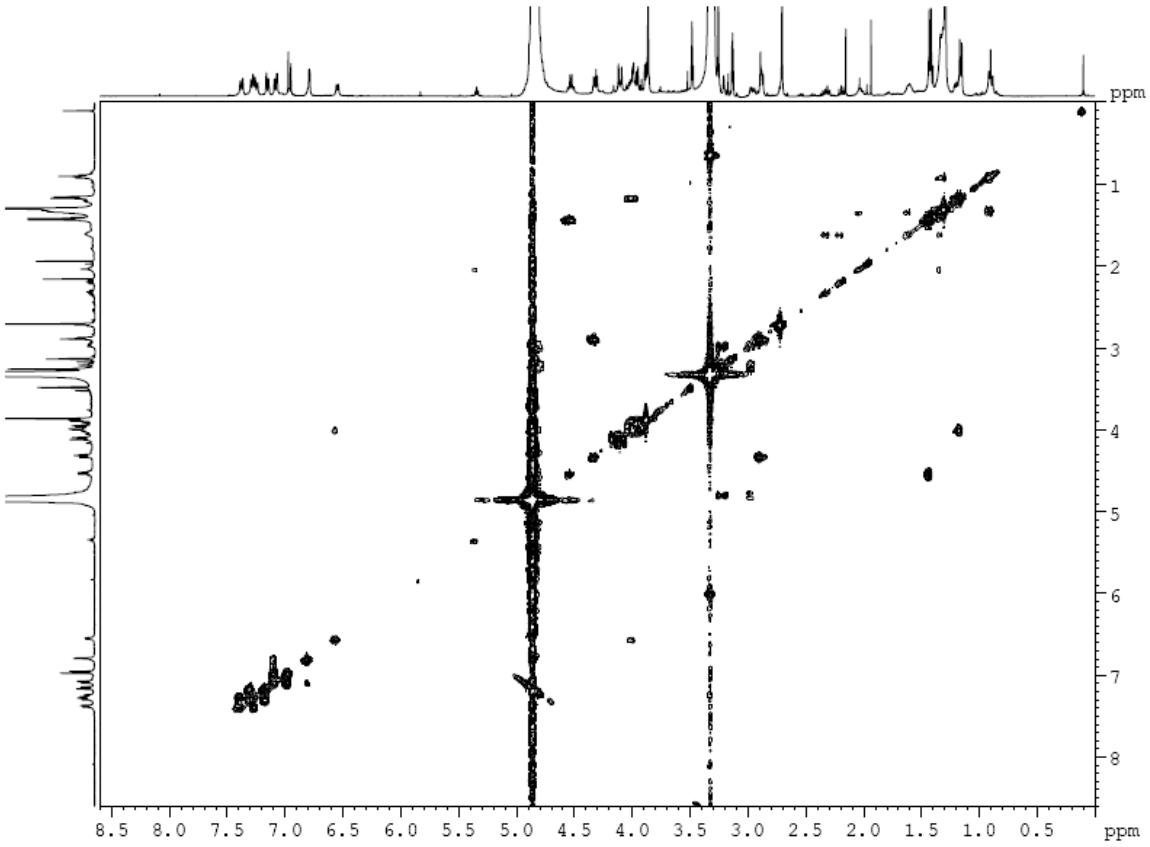
ppm
1
2
3
4
5
6
7
8
8.5 8.0 7.5 7.0 6.5 6.0 5.5 5.0 4.5 4.0 3.5 3.0 2.5 2.0 1.5 1.0 0.5
ppm

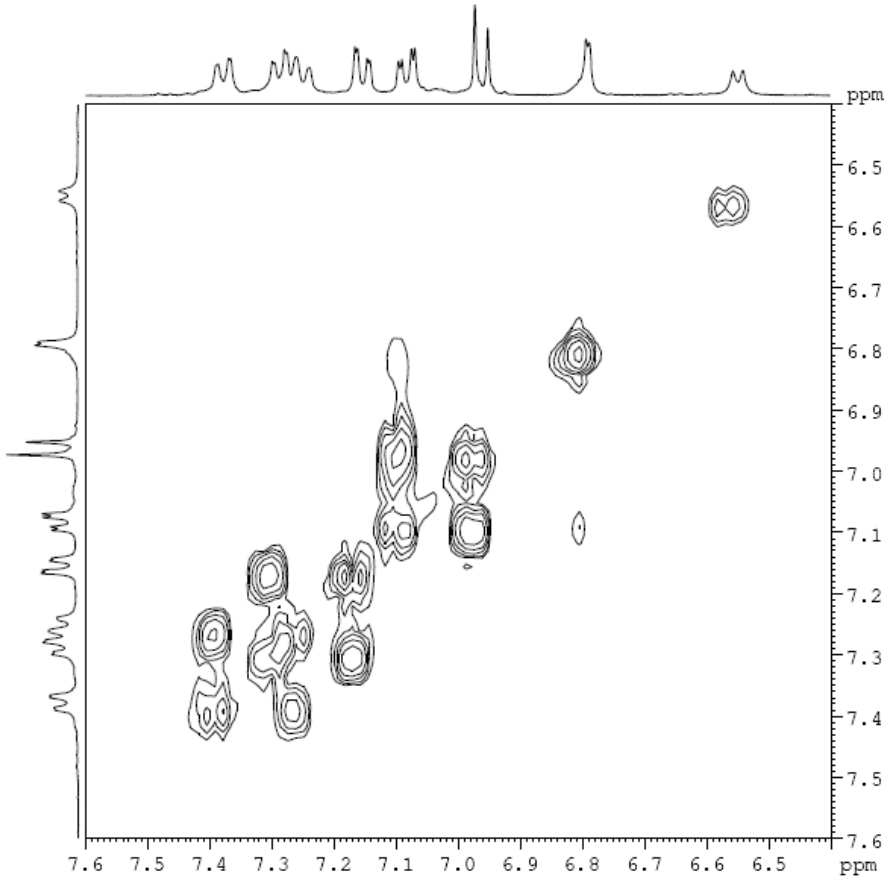
ppm
6.5
6.6
6.7
6.8
6.9
7.0
7.1
7.2
7.3
7.4
7.5
7.6
7.6 7.5 7.4 7.3 7.2 7.1 7.0 6.9 6.8 6.7 6.6 6.5
ppm

N-Methylated tailed biaryl cyclic hexapeptide incorporating a Tyr-Tyr linkage 26

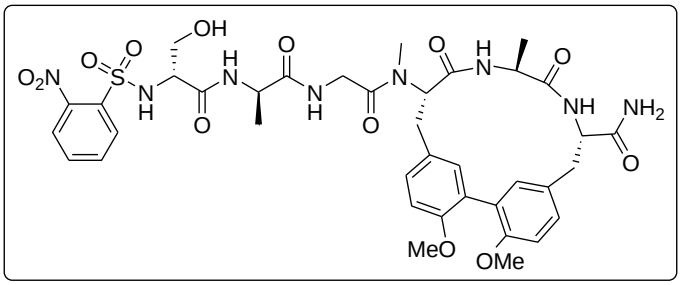

HPLC (λ = 220 nm)

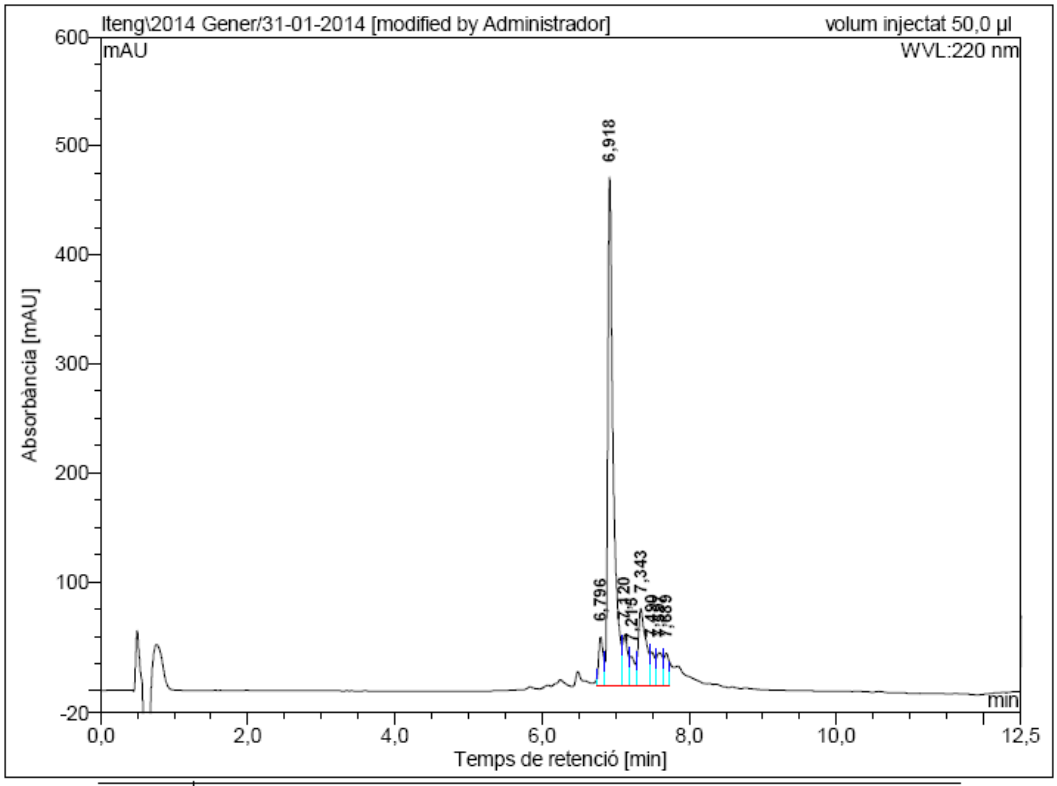

No.	Temps retenció min	alçada mAU	Area mAU*min	Area relativa %
1	6,80	45,309	3,300	4,98
2	6,92	466,863	40,751	61,51
3	7,12	47,017	3,671	5,54
4	7,22	27,350	2,470	3,73
5	7,34	71,403	8,236	12,43
6	7,49	31,371	2,558	3,86
7	7,60	30,793	3,177	4,79
8	7,69	30,264	2,091	3,16
Total:		750,369	66,253	100,00

ESI-MS *m/z*

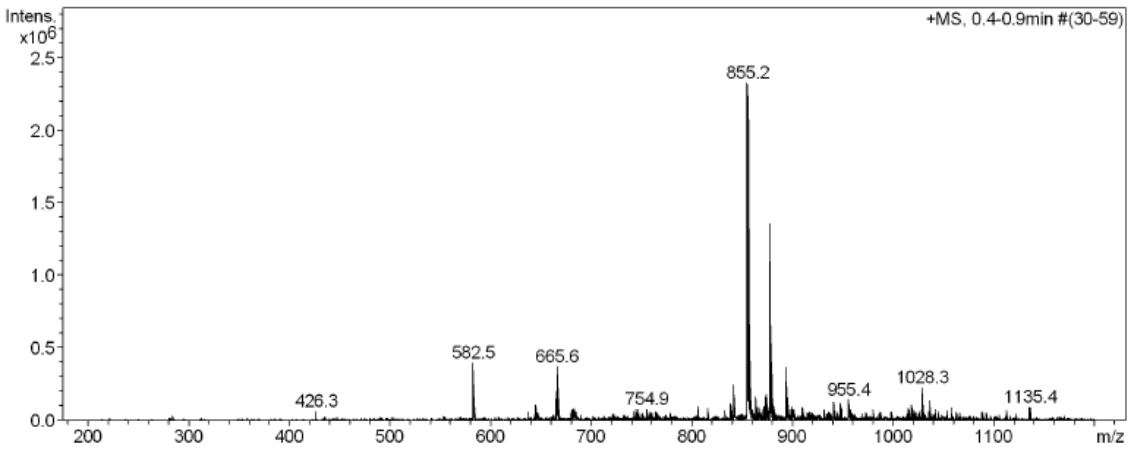
Intens.
x10^6
+MS, 0.4-0.9min #(30-59)
855.2
582.5
665.6
426.3
754.9
955.4
1028.3
1135.4
m/z

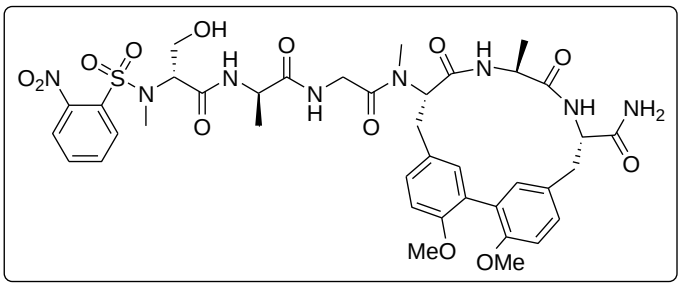

HPLC (λ = 220 nm)

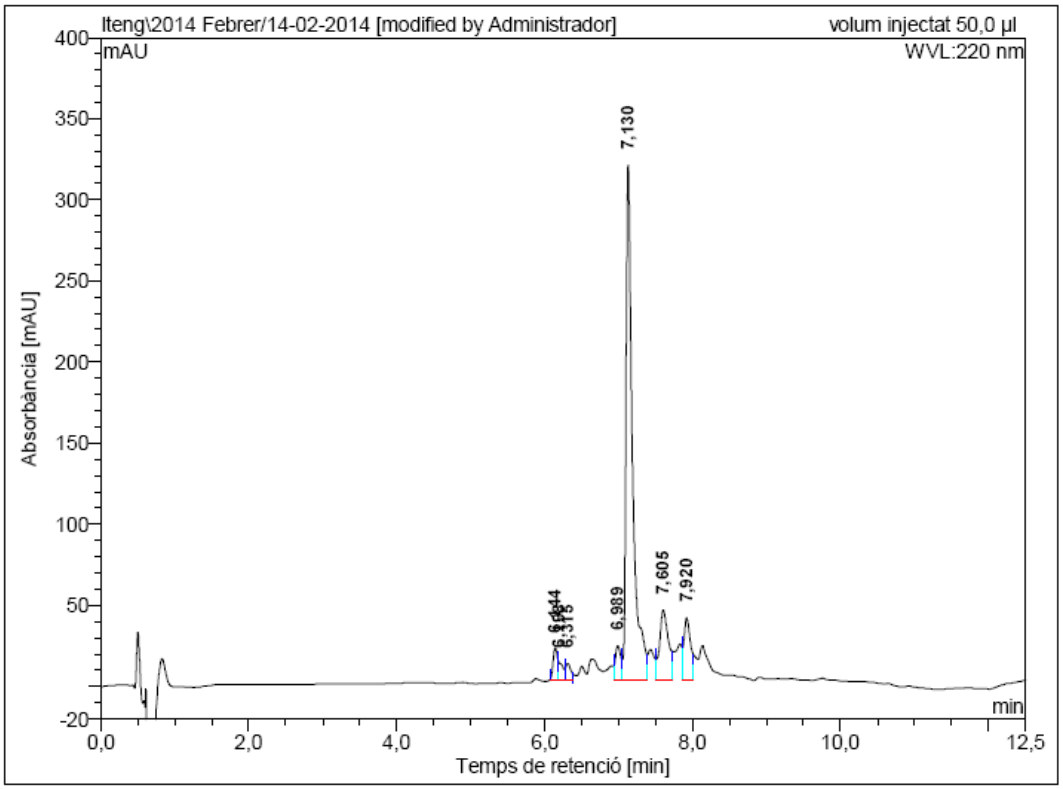

No.	Temps retenció min	alçada mAU	Area mAU*min	Area relativa %
1	6,14	19,849	1,340	2,84
2	6,20	10,348	0,755	1,60
3	6,31	10,144	0,832	1,77
4	6,99	21,008	1,697	3,60
5	7,13	317,214	32,616	69,23
6	7,60	43,166	5,815	12,34
7	7,92	38,343	4,060	8,62
Total:		460,072	47,115	100,00

ESI-MS *m/z*

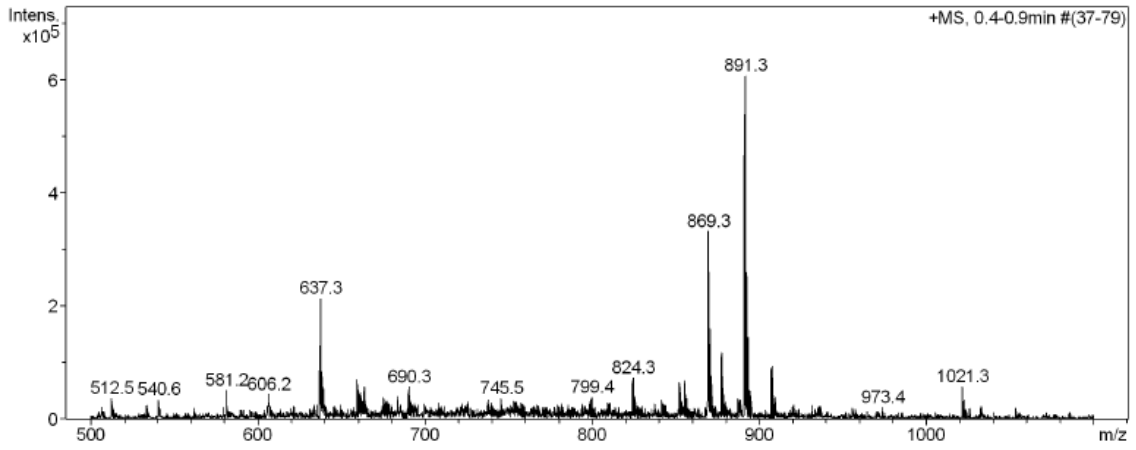
Intens.
x10^5
+MS, 0.4-0.9min #(37-79)
6
4
2
0
891.3
869.3
637.3
824.3
1021.3
690.3
512.5
540.6
581.2
606.2
745.5
799.4
973.4
500
600
700
800
900
1000
m/z

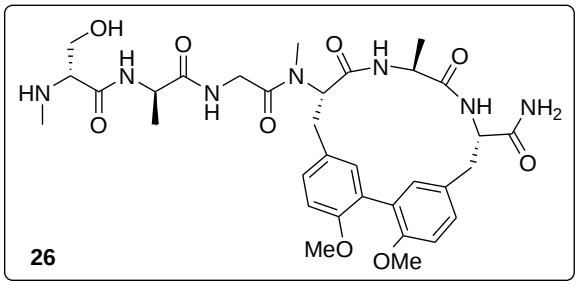

26

Crude peptide 26

HPLC (λ = 220 nm)

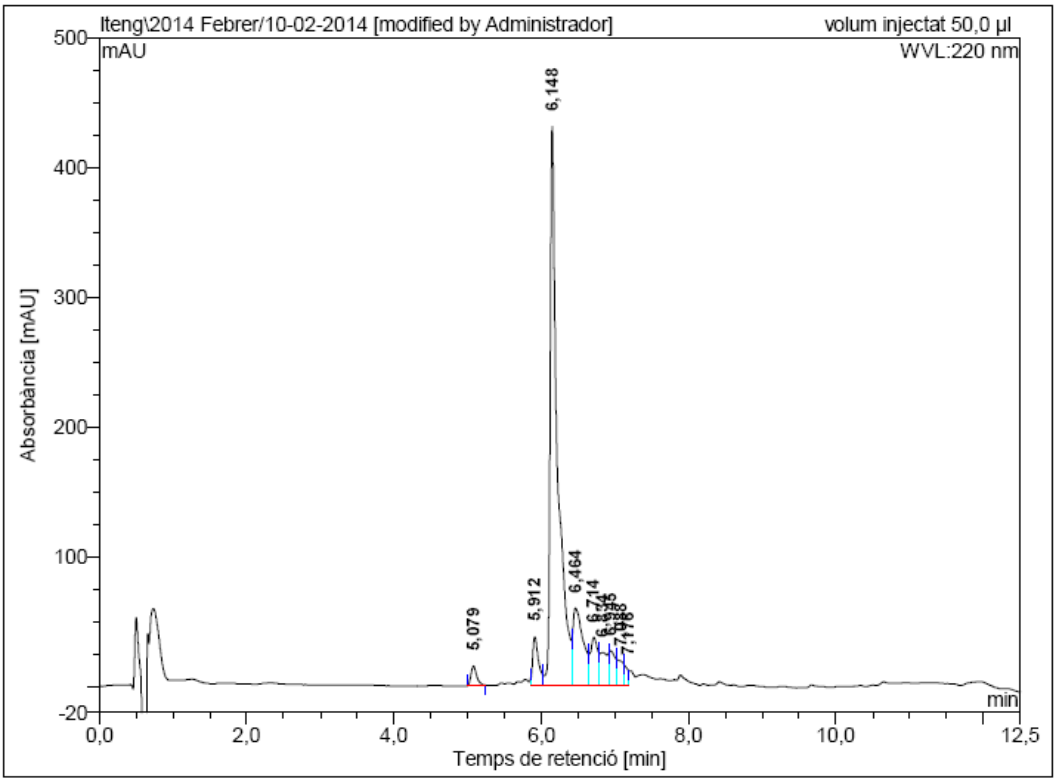

No.	Temps retenció min	alçada mAU	Area mAU*min	Area relativa %
1	5,08	14,867	1,358	1,74
2	5,91	37,353	3,426	4,39
3	6,15	430,264	50,619	64,88
4	6,46	59,572	9,663	12,39
5	6,71	37,236	4,369	5,60
6	6,83	25,666	3,163	4,05
7	6,95	26,592	2,541	3,26
8	7,09	18,597	1,890	2,42
9	7,18	11,993	0,987	1,27
Total:		662,140	78,016	100,00

ESI-MS *m/z*

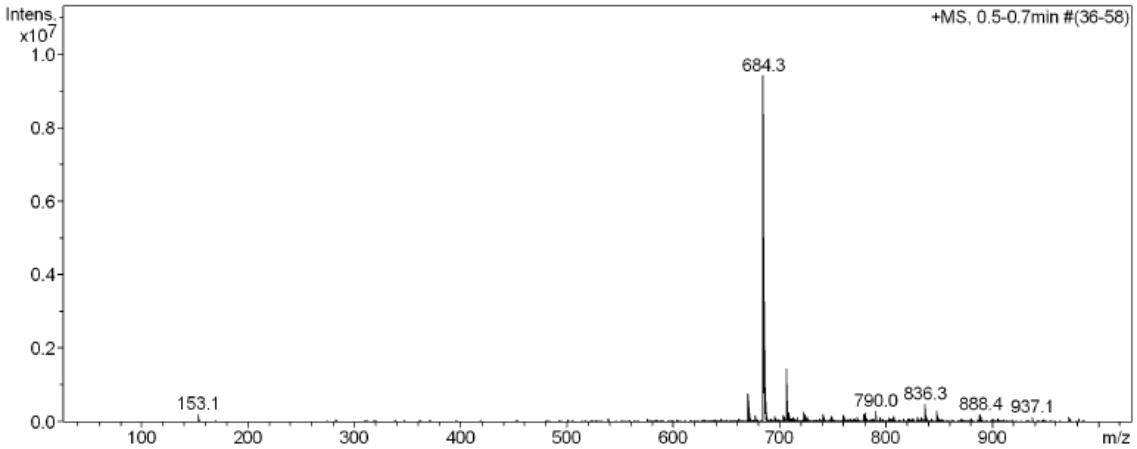
Intens.
x10^7
1.0
0.8
0.6
0.4
0.2
0.0
+MS, 0.5-0.7min #(36-58)
684.3
153.1
790.0
836.3
888.4
937.1
100
200
300
400
500
600
700
800
900
m/z

Purified peptide 26

HPLC (λ = 220 nm)

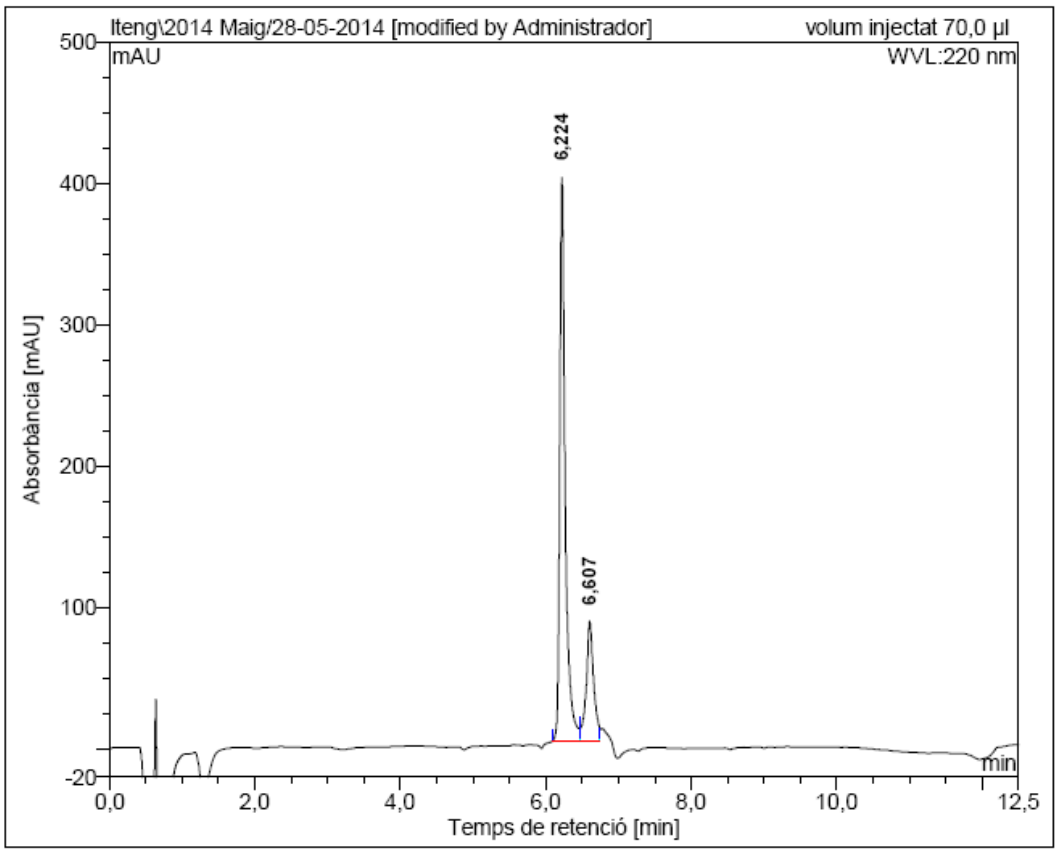

No.	mps retenc min	alçada mAU	Area mAU*min	Area relativa %
1	6,22	398,008	34,766	78,00
2	6,61	84,297	9,808	22,00
Total:		482,305	44,574	100,00

ESI-MS *m/z*

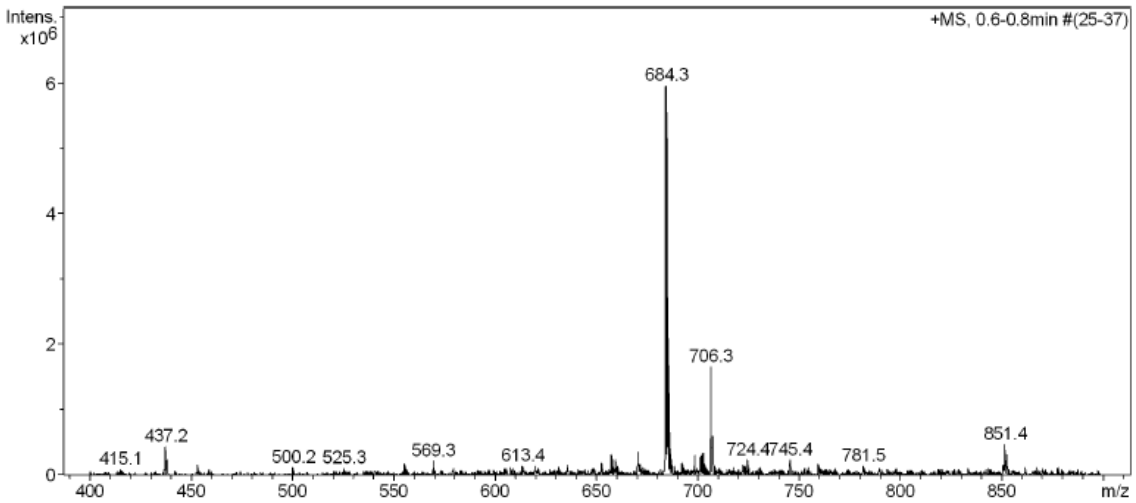

HRMS (ESI) *m/z*

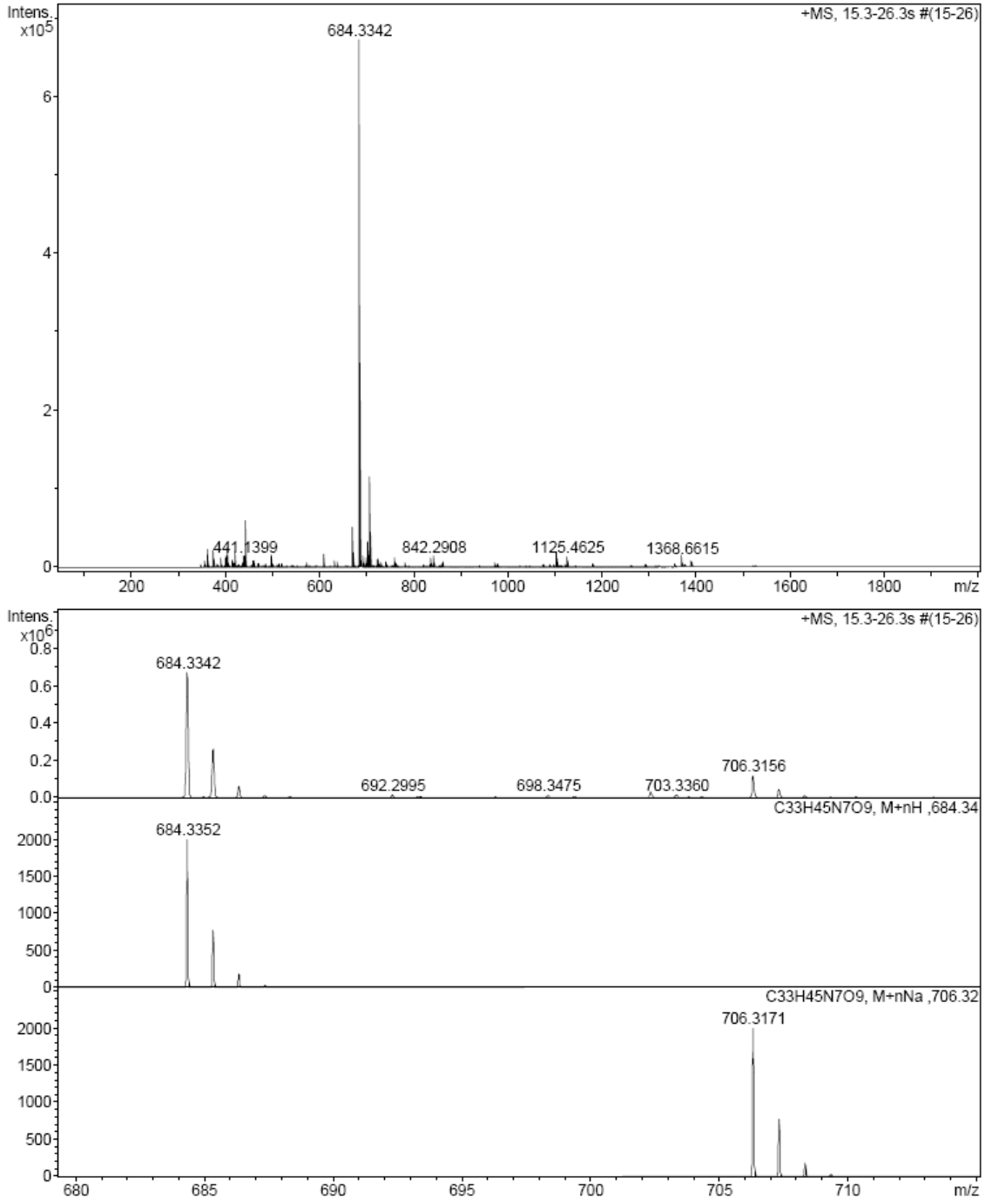
Intens.
x10^5
+MS, 15.3-26.3s #(15-26)
684.3342
441.1399
842.2908
1125.4625
1368.6615
m/z
Intens.
x10^6
+MS, 15.3-26.3s #(15-26)
684.3342
692.2995
698.3475
703.3360
706.3156
C33H45N7O9, M+nH ,684.34
684.3352
C33H45N7O9, M+nNa ,706.32
706.3171
m/z

N-Methylated tailed biaryl cyclic hexapeptide incorporating a His-Tyr linkage 30

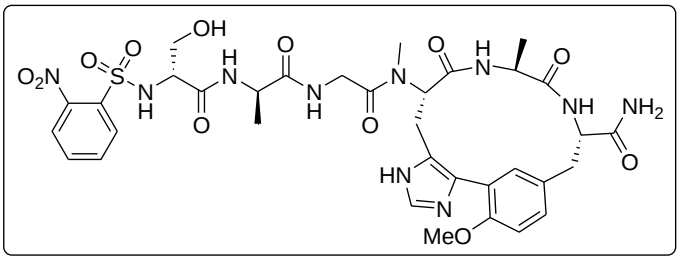

HPLC (λ = 220 nm)

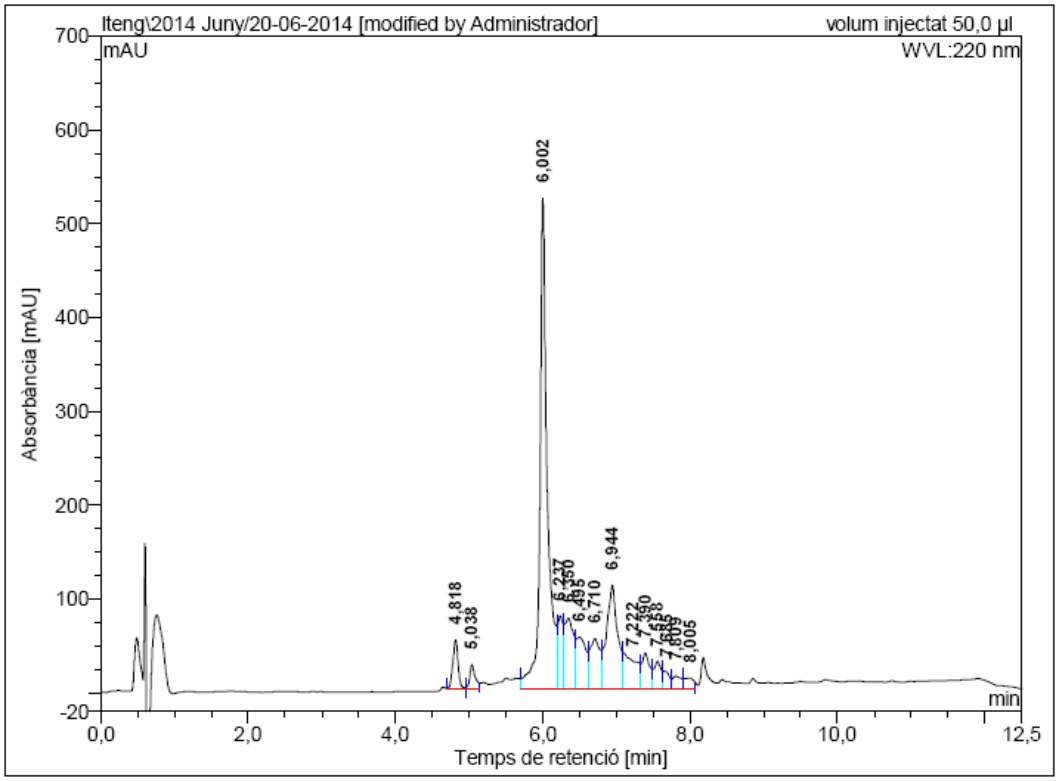

No.	Temps retenció min	alçada mAU	Area mAU*min	Area relativa %
1	4,82	51,832	4,231	3,00
2	5,04	25,221	2,141	1,52
3	6,00	523,571	60,818	43,13
4	6,24	77,446	6,399	4,54
5	6,35	75,227	10,465	7,42
6	6,50	54,659	8,119	5,76
7	6,71	53,026	8,466	6,00
8	6,94	110,160	19,482	13,82
9	7,22	29,050	7,601	5,39
10	7,39	37,577	4,473	3,17
11	7,56	28,932	3,368	2,39
12	7,68	17,316	1,874	1,33
13	7,81	13,181	1,838	1,30
14	8,00	11,234	1,722	1,22
Total:		1108,432	140,997	100,00

ESI-MS *m/z*

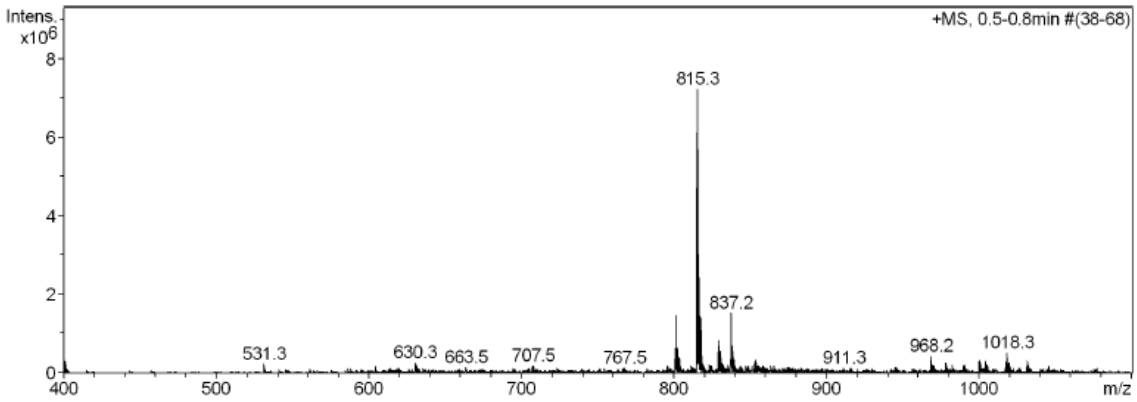
Intens.
x10^6
+MS, 0.5-0.8min #(38-68)
815.3
837.2
531.3
630.3
663.5
707.5
767.5
911.3
968.2
1018.3
m/z

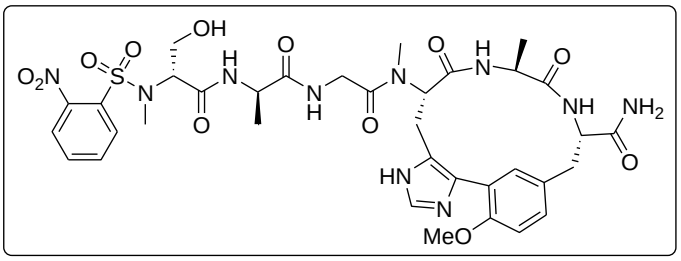

HPLC (λ = 220 nm)

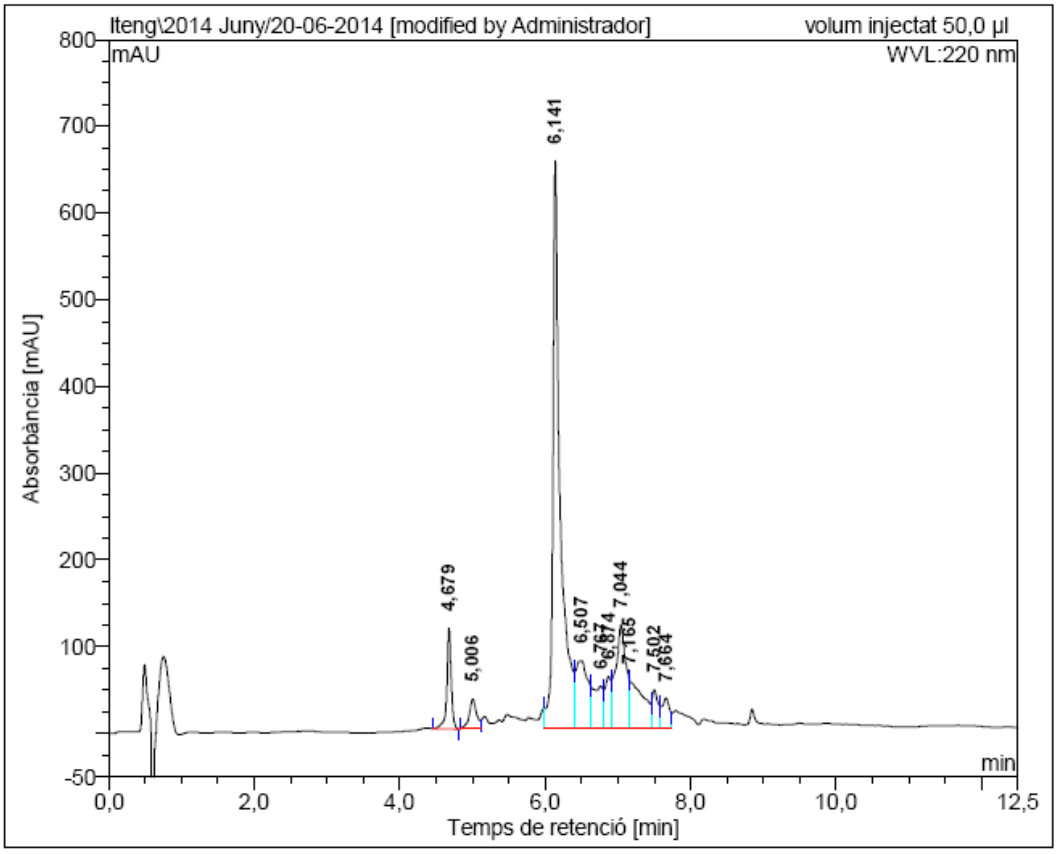

No.	mps retenc min	alçada mAU	Area mAU*min	Area relativa %
1	4,68	116,027	8,090	5,06
2	5,01	34,471	3,986	2,49
3	6,14	654,546	77,744	48,59
4	6,51	78,599	14,585	9,12
5	6,77	49,356	8,439	5,27
6	6,87	60,221	5,491	3,43
7	7,04	119,688	20,573	12,86
8	7,17	55,482	12,367	7,73
9	7,50	44,803	4,595	2,87
10	7,66	35,391	4,116	2,57
Total:		1248,583	159,985	100,00

ESI-MS *m/z*

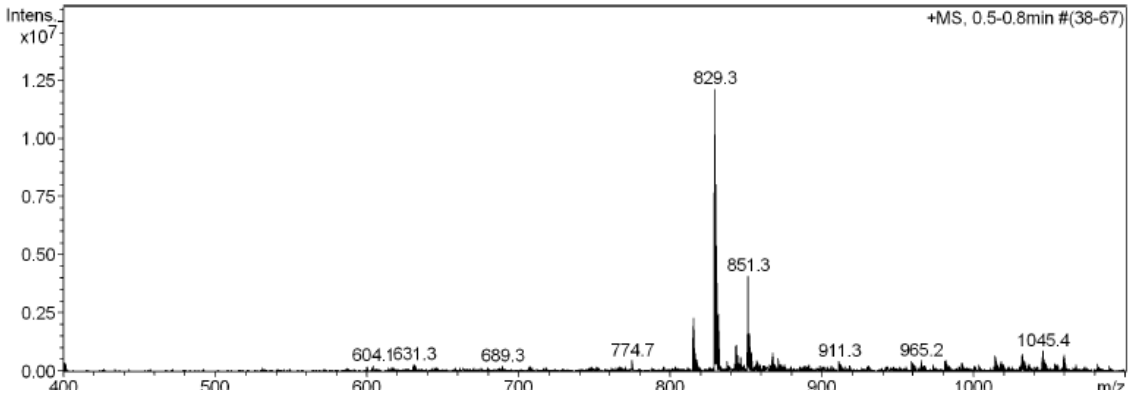
Intens.
x10^7
1.25
1.00
0.75
0.50
0.25
0.00
+MS, 0.5-0.8min #(38-67)
829.3
851.3
604.1631.3
689.3
774.7
911.3
965.2
1045.4
400
500
600
700
800
900
1000
m/z

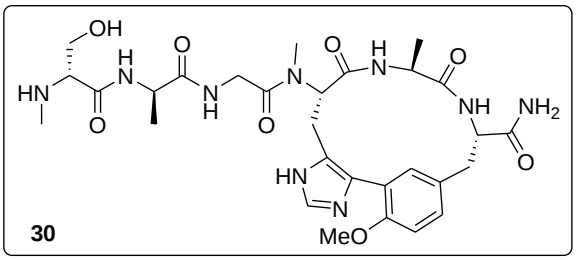

30

Crude peptide 30

HPLC (λ = 220 nm)

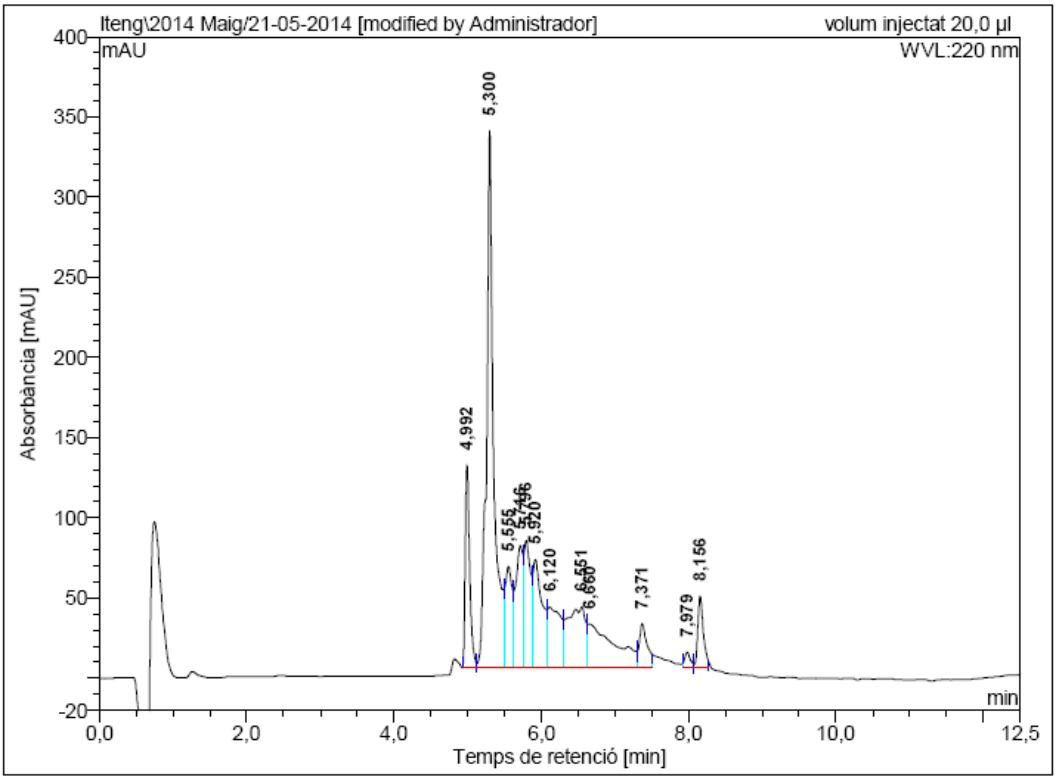

No.	Temps retenció min	alçada mAU	Area mAU*min	Area relativa %
1	4,99	126,198	8,748	7,39
2	5,30	334,670	37,511	31,68
3	5,56	63,090	7,512	6,34
4	5,72	76,067	8,273	6,99
5	5,80	79,182	8,457	7,14
6	5,92	67,385	10,094	8,52
7	6,12	37,676	7,882	6,66
8	6,55	37,736	10,451	8,83
9	6,66	27,141	11,399	9,63
10	7,37	27,387	3,334	2,82
11	7,98	9,482	0,847	0,72
12	8,16	44,587	3,897	3,29
Total:		930,602	118,403	100,00

ESI-MS *m/z*

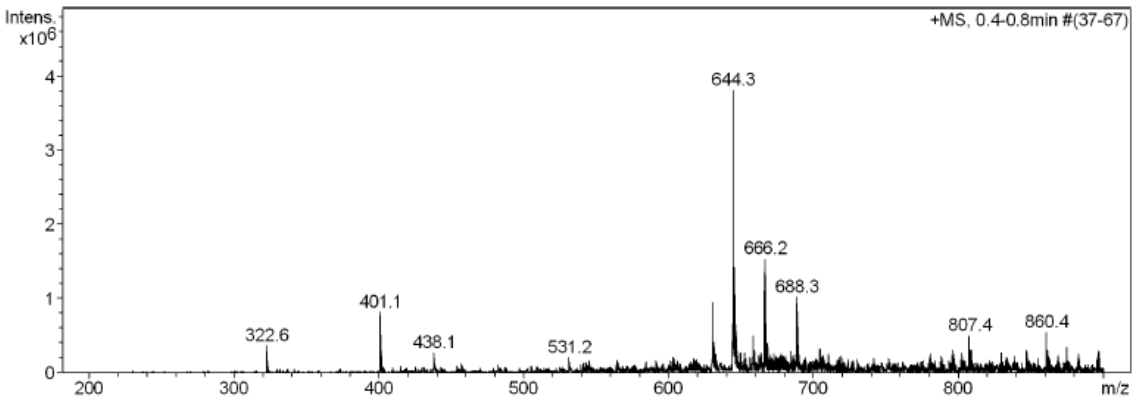
Intens.
x10^6
+MS, 0.4-0.8min #(37-67)
644.3
666.2
688.3
401.1
322.6
438.1
531.2
807.4
860.4
m/z

Purified peptide 30

HPLC (λ = 220 nm)

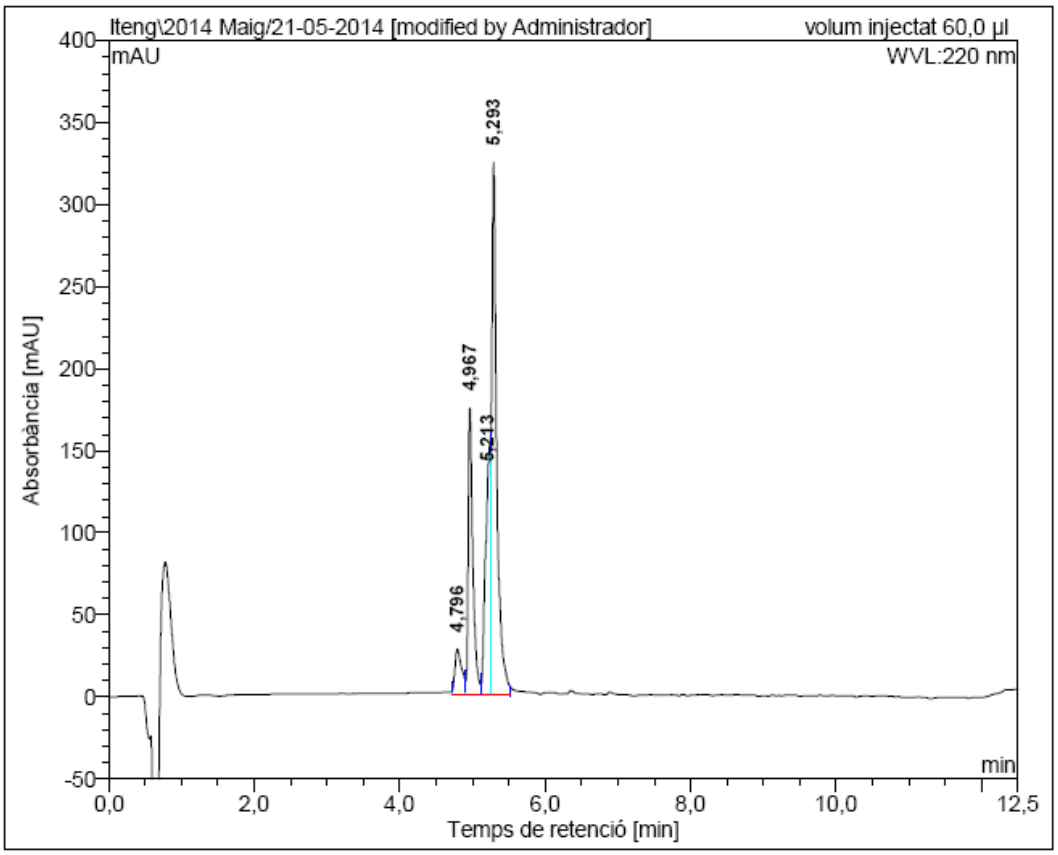

No.	mps retenc min	alçada mAU	Area mAU*min	Area relativa %
1	4,80	27,695	3,096	5,75
2	4,97	174,440	12,758	23,72
3	5,21	131,483	11,129	20,69
4	5,29	324,495	26,808	49,84
Total:		658,113	53,791	100,00

ESI-MS *m/z*

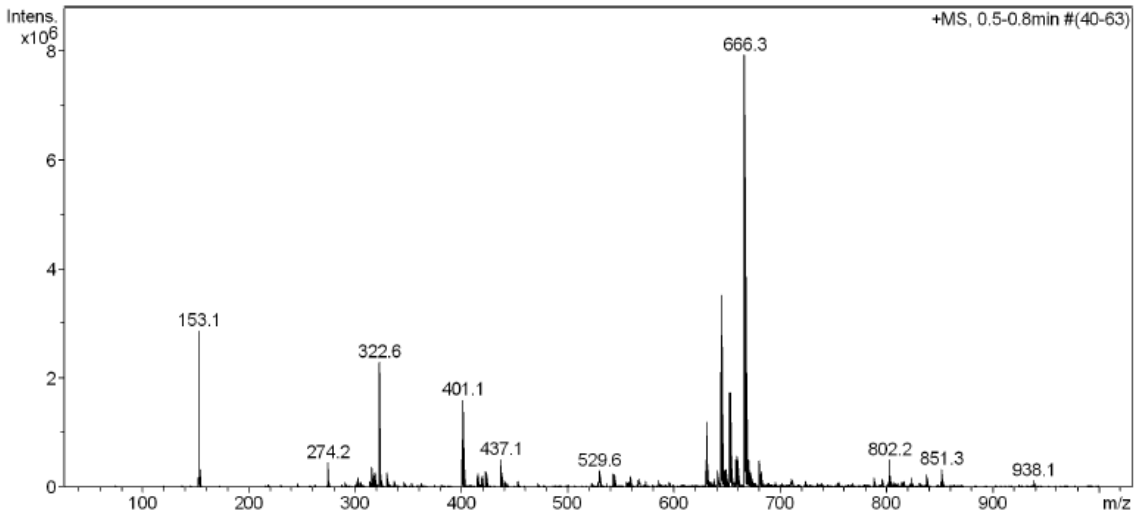

HRMS (ESI) *m/z*

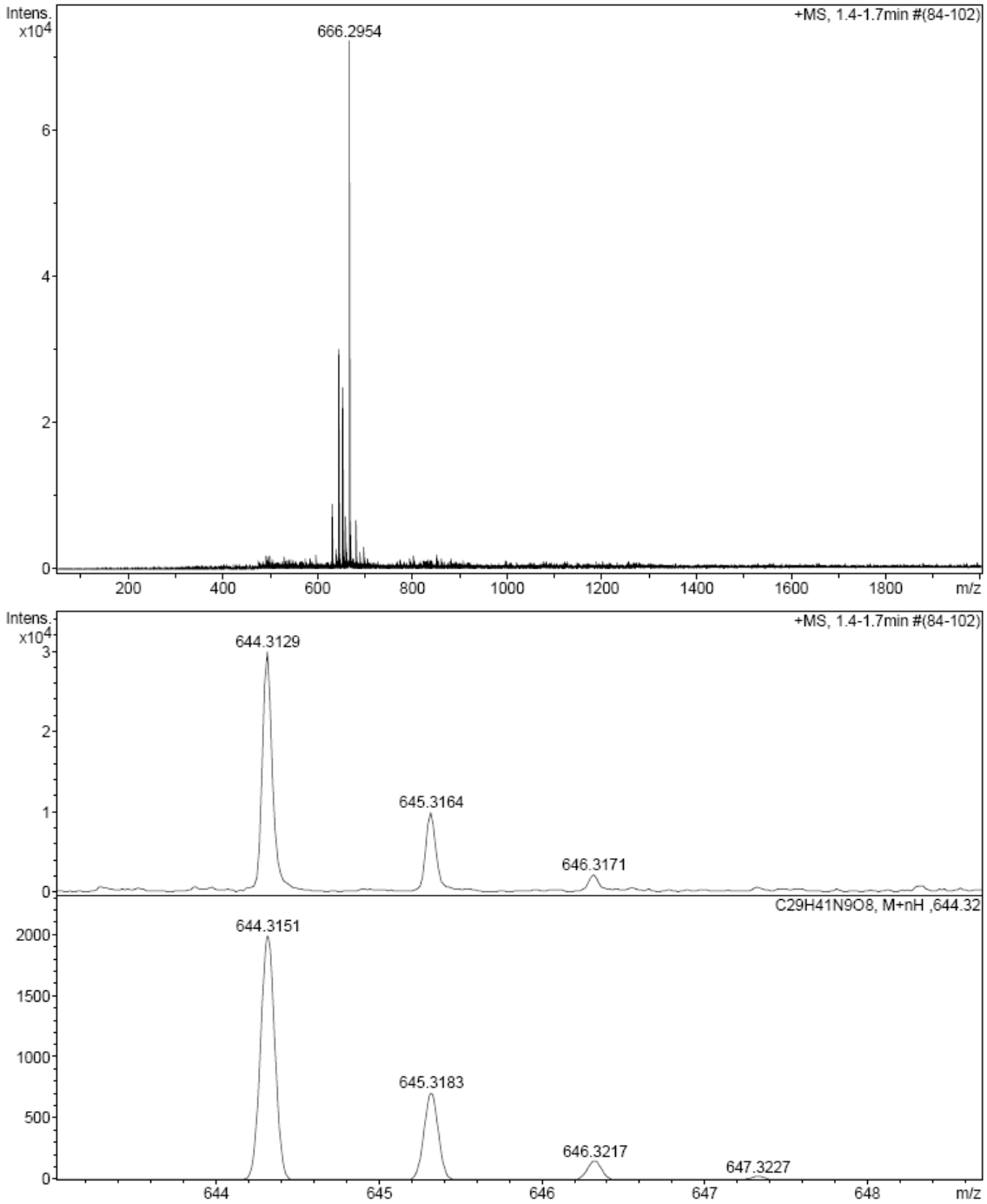
Intens.
x10^4
+MS, 1.4-1.7min #(84-102)
666.2954
6
4
2
0
200
400
600
800
1000
1200
1400
1600
1800
m/z
Intens.
x10^4
+MS, 1.4-1.7min #(84-102)
644.3129
645.3164
646.3171
3
2
1
0
C29H41N9O8, M+nH ,644.32
644.3151
645.3183
646.3217
647.3227
2000
1500
1000
500
0
644
645
646
647
648
m/z

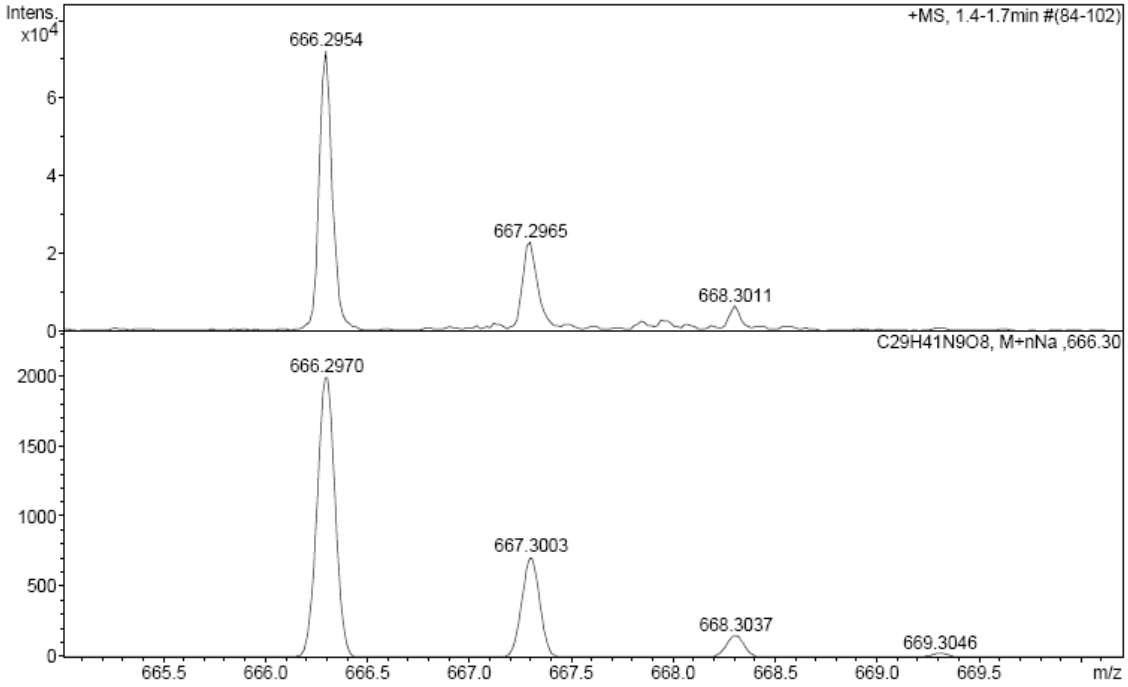
Intens.
x10^4
+MS, 1.4-1.7min #(84-102)
666.2954
667.2965
668.3011
C29H41N9O8, M+nNa ,666.30
666.2970
667.3003
668.3037
669.3046
m/z

N-Methylated tailed biaryl cyclic hexapeptide incorporating a Phg-Tyr linkage 35

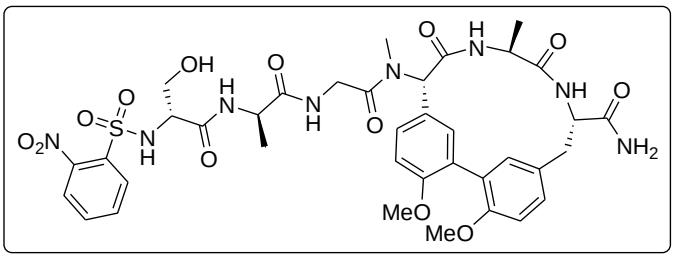

HPLC (λ = 220 nm)

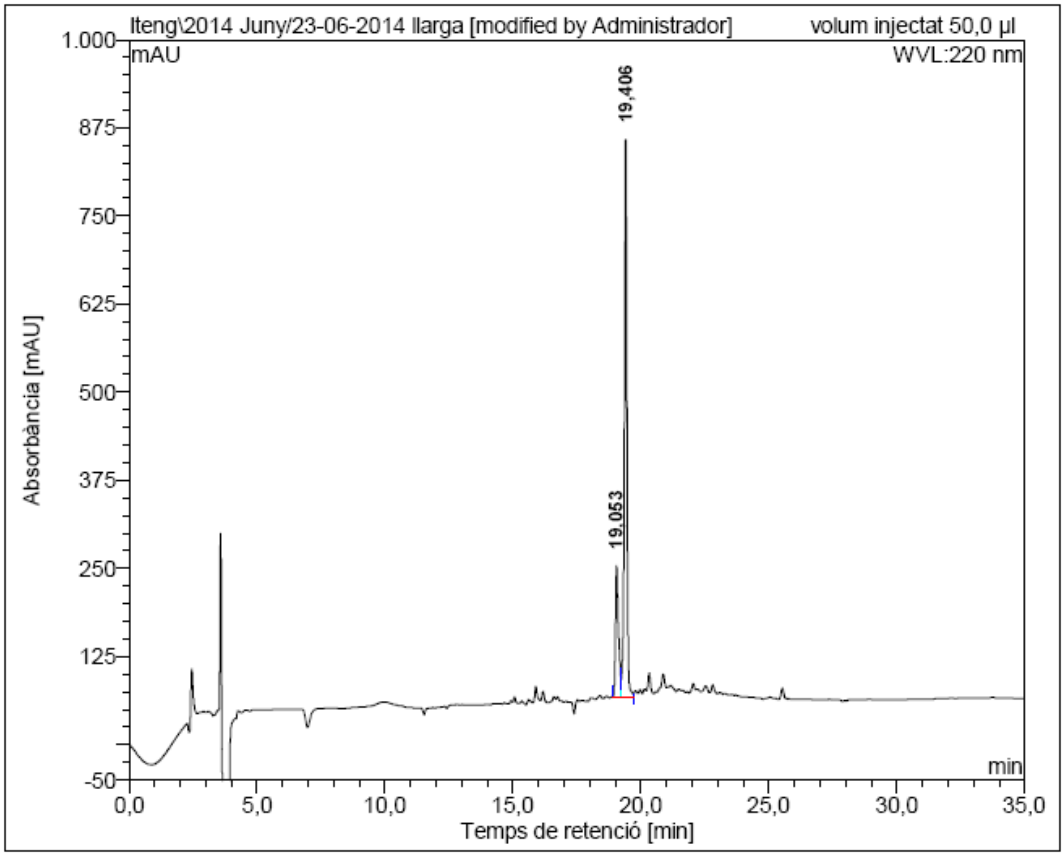

No.	mps retenc min	alçada mAU	Area mAU*min	Area relativa %
1	19,05	186,345	25,147	21,91
2	19,41	790,681	89,621	78,09
Total:		977,026	114,768	100,00

ESI-MS *m/z*

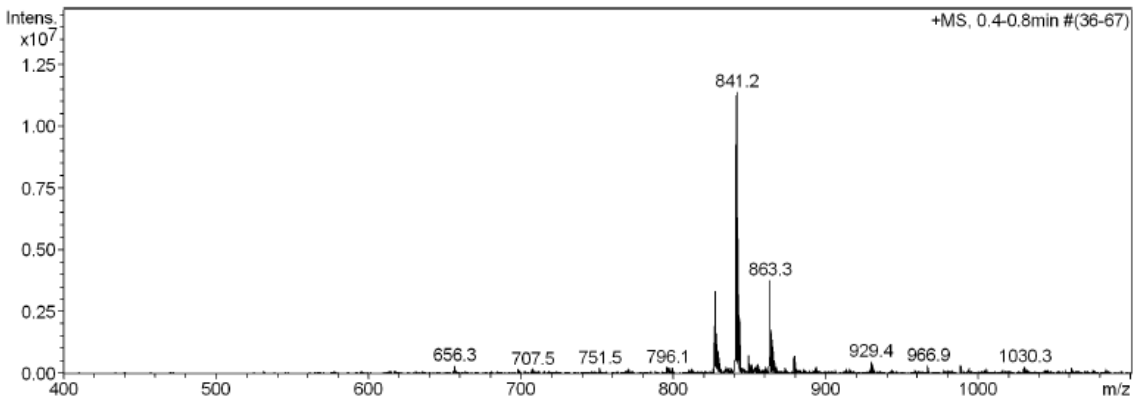
Intens.
x10^7
1.25
1.00
0.75
0.50
0.25
0.00
+MS, 0.4-0.8min #(36-67)
841.2
863.3
656.3
707.5
751.5
796.1
929.4
966.9
1030.3
400
500
600
700
800
900
1000
m/z

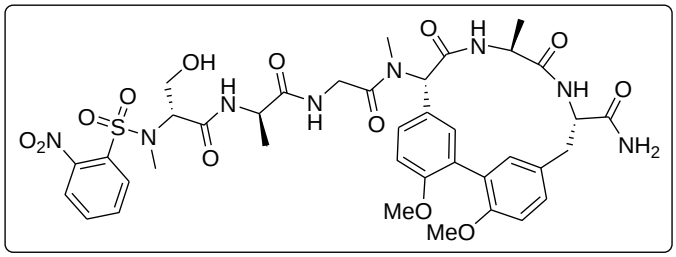

HPLC (λ = 220 nm)

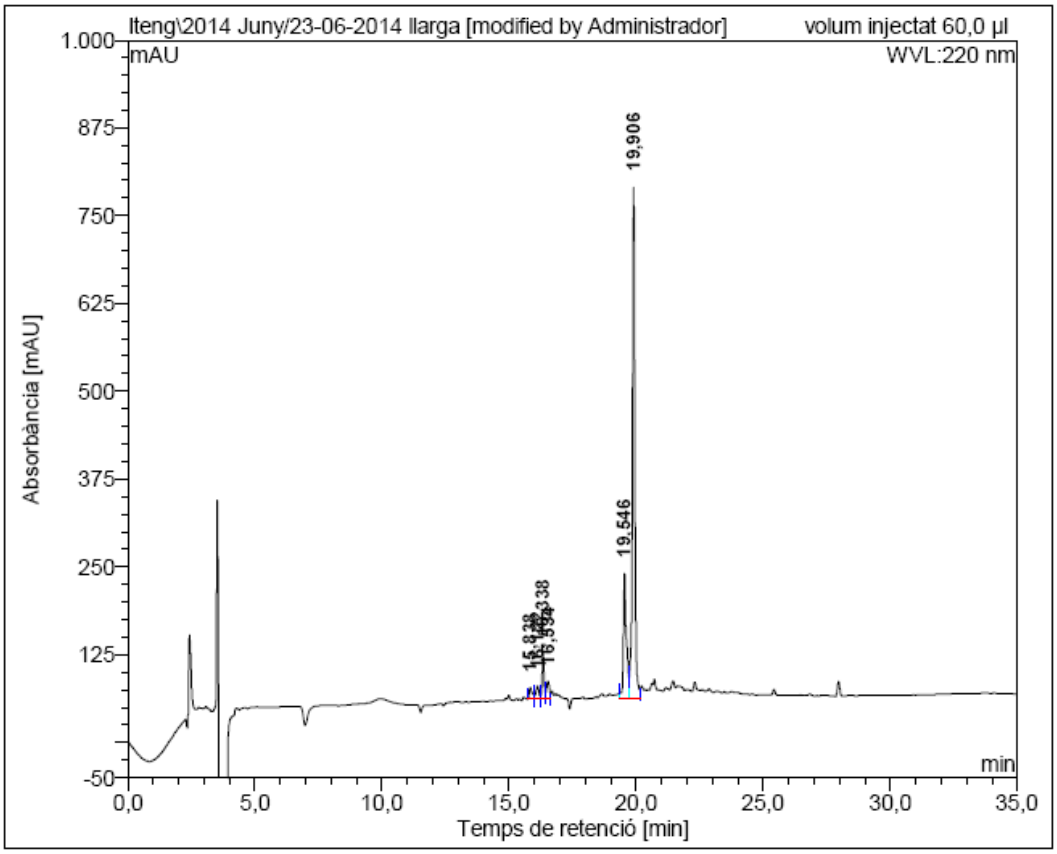

No.	mps retenc min	alçada mAU	Area mAU*min	Area relativa %
1	15,84	16,167	2,274	1,87
2	16,12	18,748	2,505	2,06
3	16,34	65,559	6,124	5,02
4	16,53	25,305	3,450	2,83
5	19,55	178,546	25,263	20,72
6	19,91	728,053	82,285	67,50
Total:		1032,379	121,901	100,00

ESI-MS *m/z*

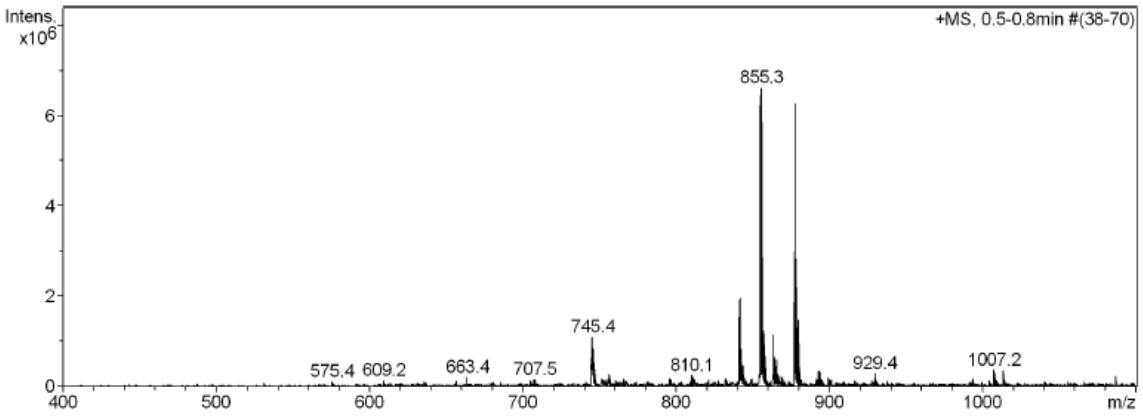
Intens.
x10^6
+MS, 0.5-0.8min #(38-70)
855.3
745.4
575.4
609.2
663.4
707.5
810.1
929.4
1007.2
m/z

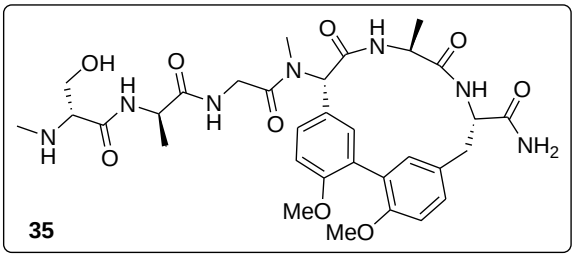

35

Crude peptide 35

HPLC (λ = 220 nm)

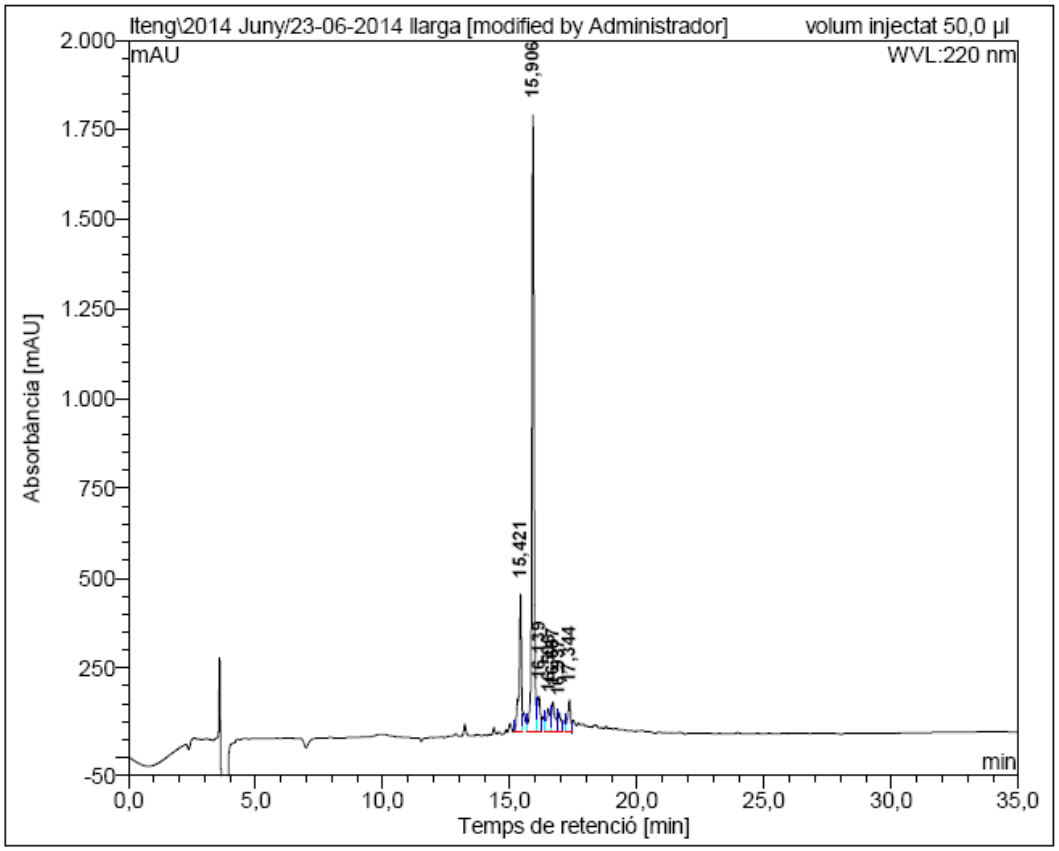

No.	mps retenc min	alçada mAU	Area mAU*min	Area relativa %
1	15,42	380,244	41,295	15,60
2	15,91	1716,652	170,577	64,44
3	16,14	96,269	13,119	4,96
4	16,51	61,613	9,133	3,45
5	16,69	79,827	13,319	5,03
6	16,94	51,124	6,497	2,45
7	17,34	87,333	10,770	4,07
Total:		2473,061	264,711	100,00

ESI-MS *m/z*

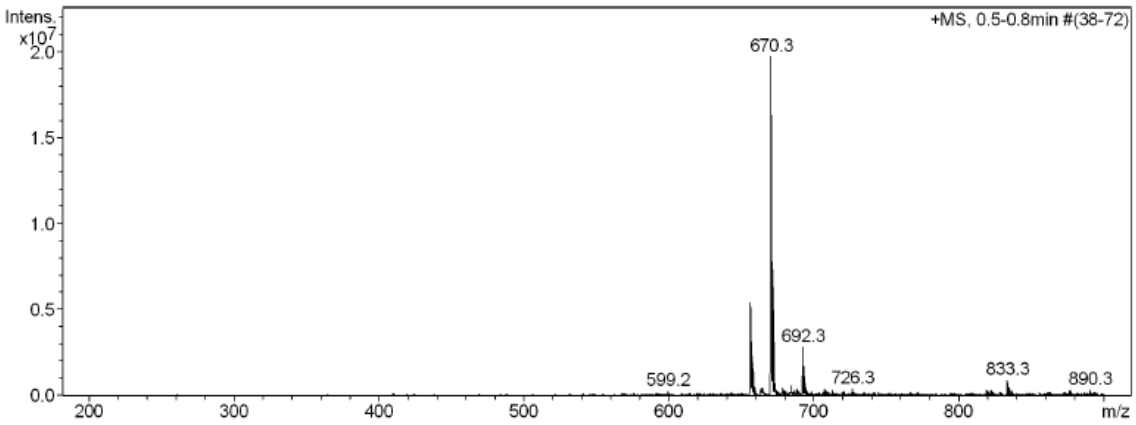
Intens.
x10^7
2.0
1.5
1.0
0.5
0.0
+MS, 0.5-0.8min #(38-72)
670.3
692.3
599.2
726.3
833.3
890.3
200
300
400
500
600
700
800
m/z

Purified peptide 35

HPLC (λ = 220 nm)

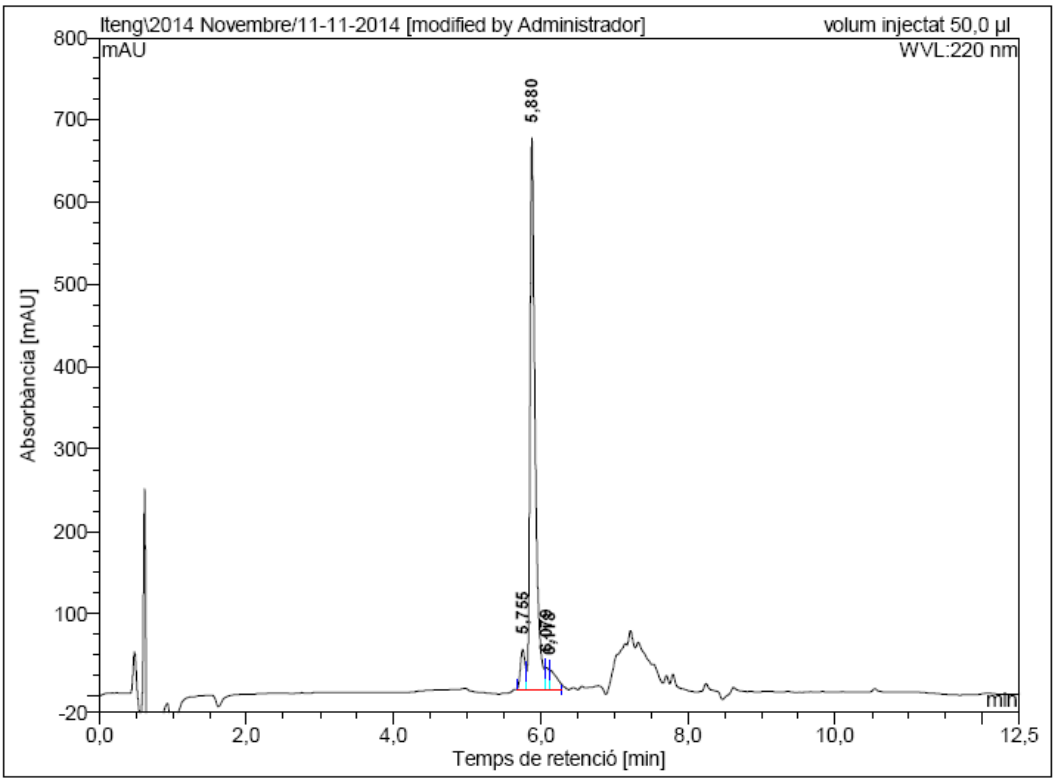

No.	Temps retenció min	alçada mAU	Area mAU*min	Area relativa %
1	5,75	48,507	3,581	5,73
2	5,88	670,252	54,610	87,44
3	6,08	26,470	1,523	2,44
4	6,12	23,145	2,743	4,39
Total:		768,375	62,458	100,00

ESI-MS *m/z*

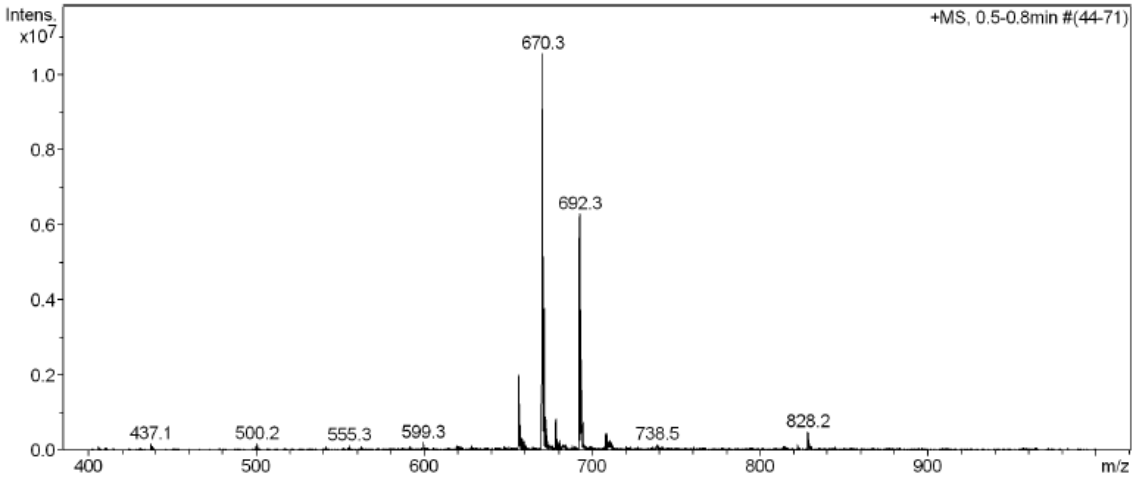

HRMS (ESI) *m/z*

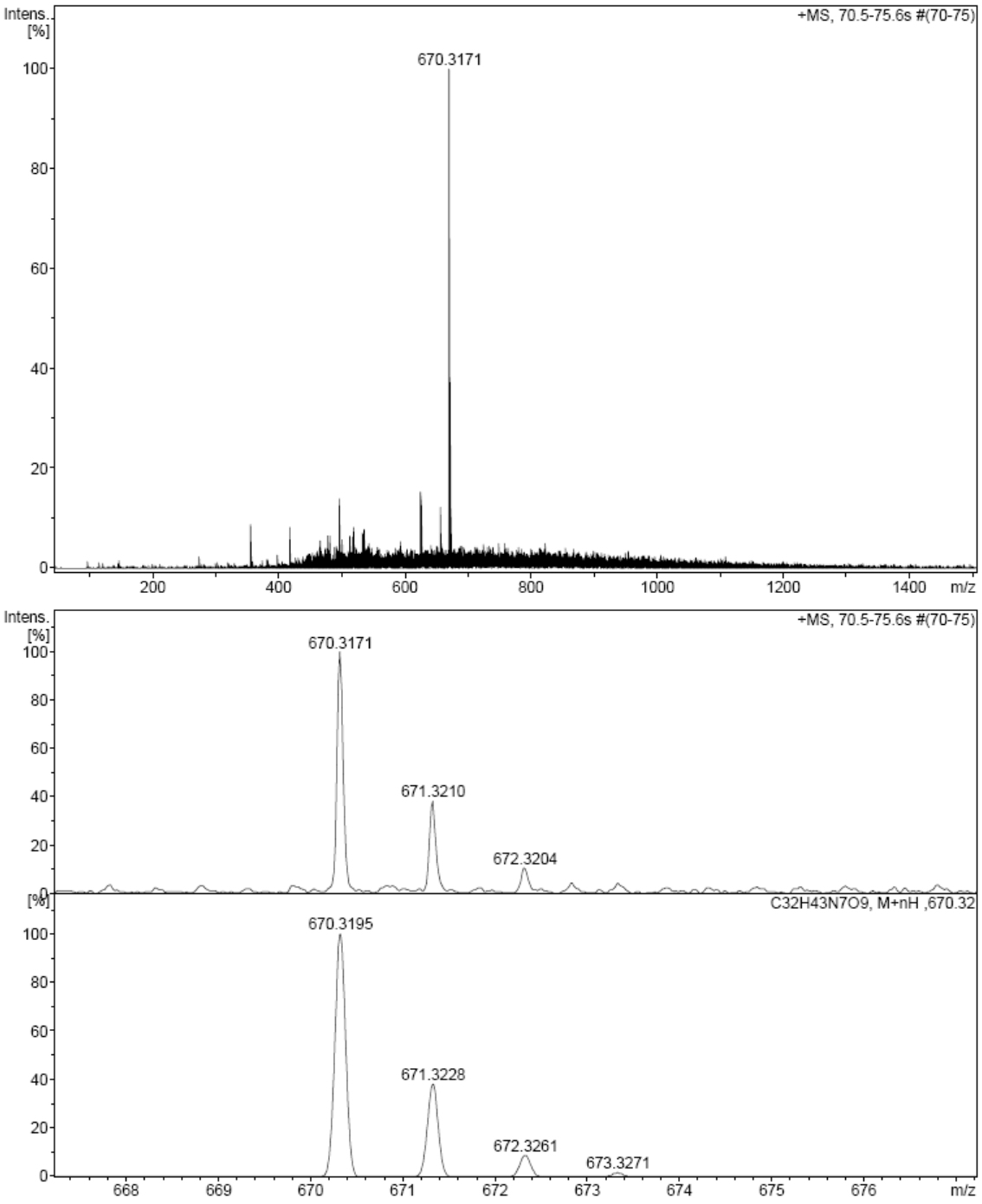
Intens.
[%]
+MS, 70.5-75.6s #(70-75)
670.3171
100
80
60
40
20
0
200
400
600
800
1000
1200
1400
m/z
Intens.
[%]
+MS, 70.5-75.6s #(70-75)
670.3171
671.3210
672.3204
C32H43N7O9, M+nH ,670.32
670.3195
671.3228
672.3261
673.3271
668
669
670
671
672
673
674
675
676

8. Synthesis of tailed biaryl cyclic lipohexapeptides

Tailed biaryl cyclic lipopeptide incorporating a Phe-Tyr linkage 1

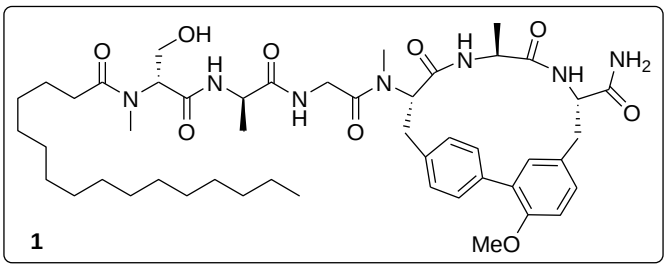

1

HRMS (ESI) *m/z*

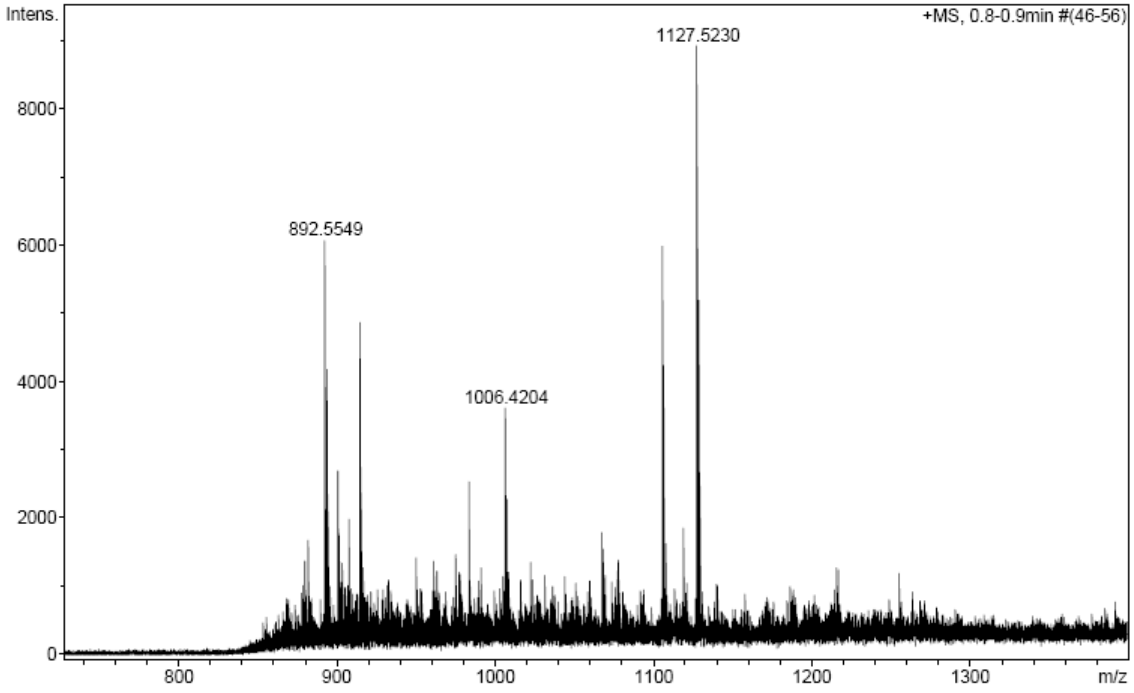

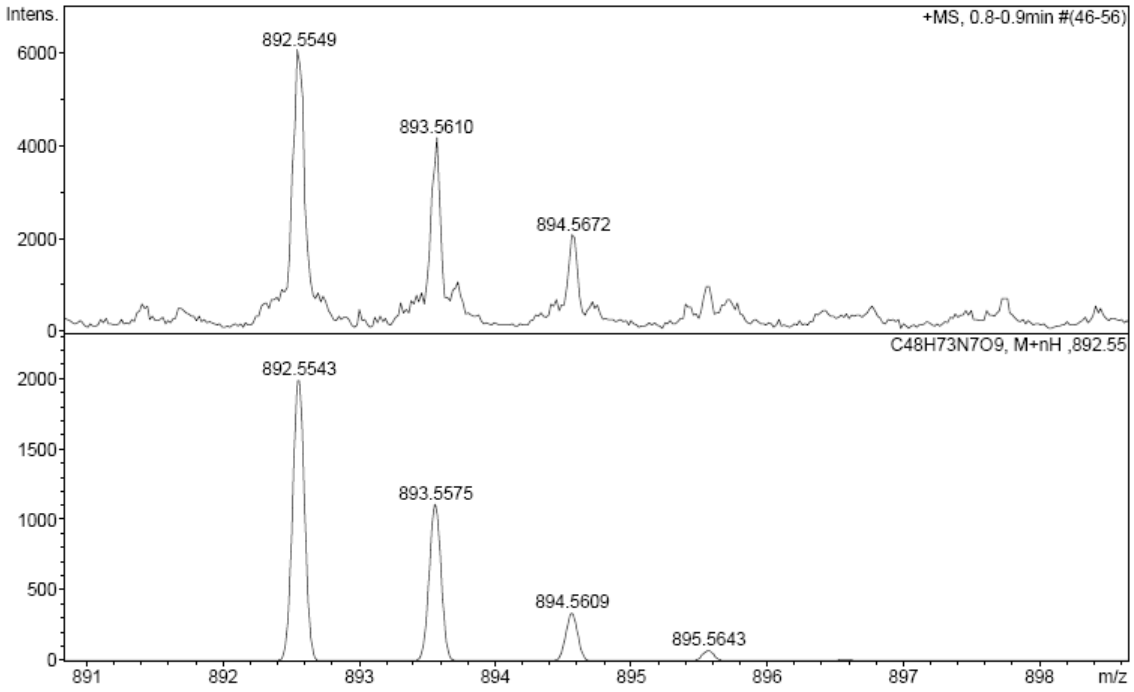

Tailed biaryl cyclic lipopeptide incorporating a His-Tyr linkage 3

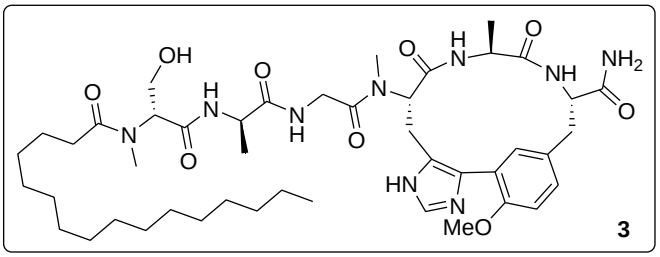

HRMS (ESI) *m/z*

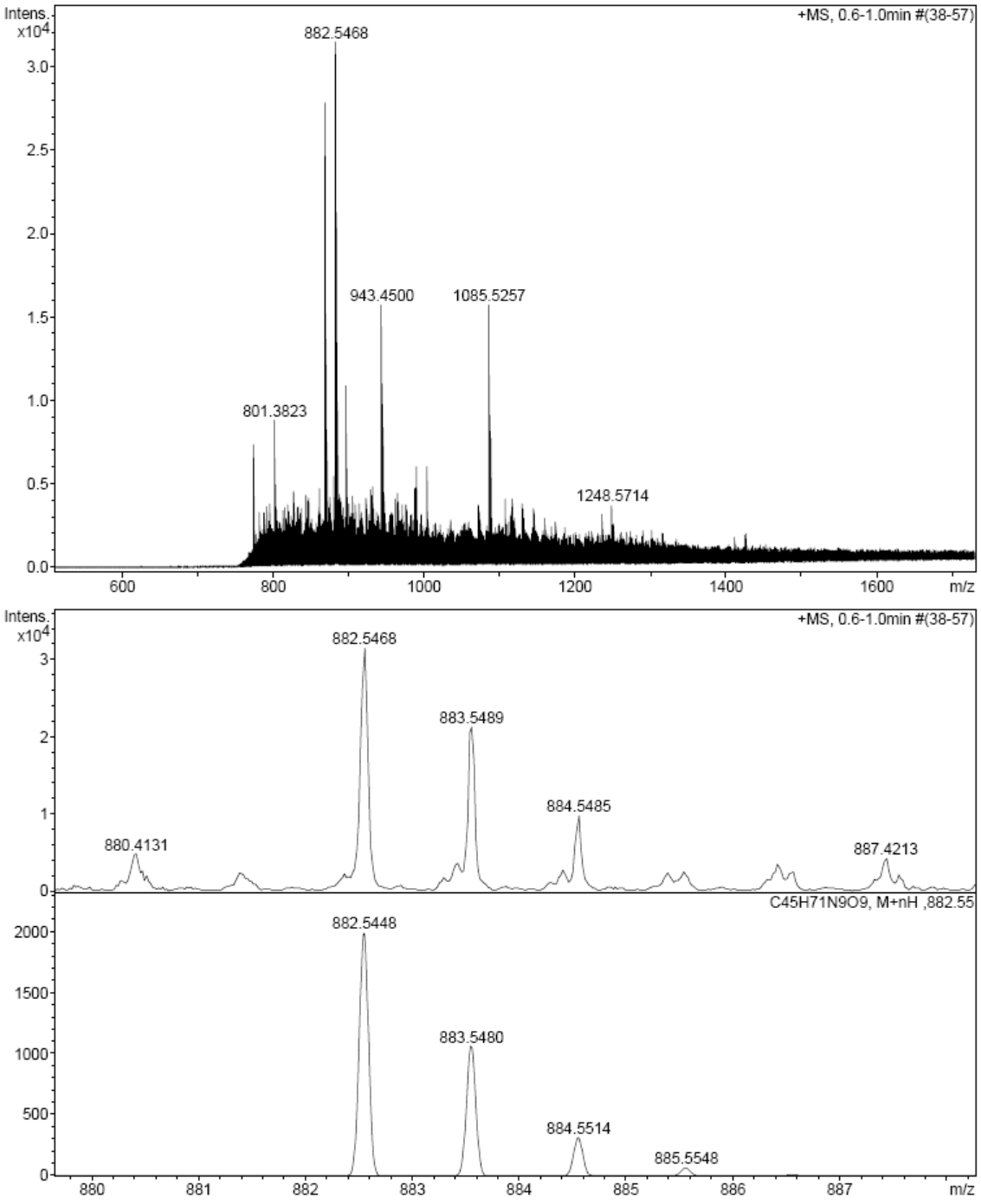

Tailed biaryl cyclic lipopeptide incorporating a Phg-Tyr linkage 4

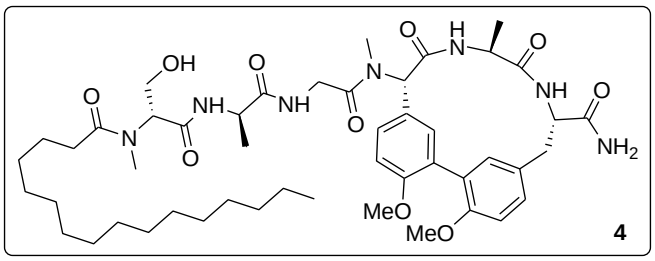

HRMS (ESI) *m/z*

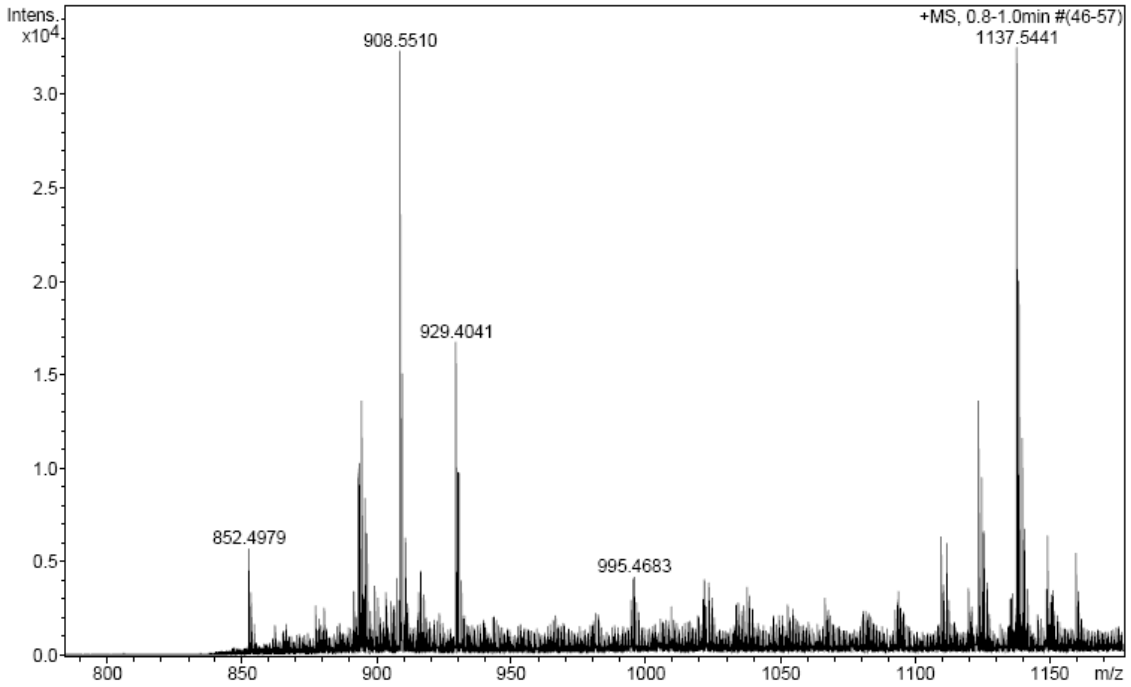

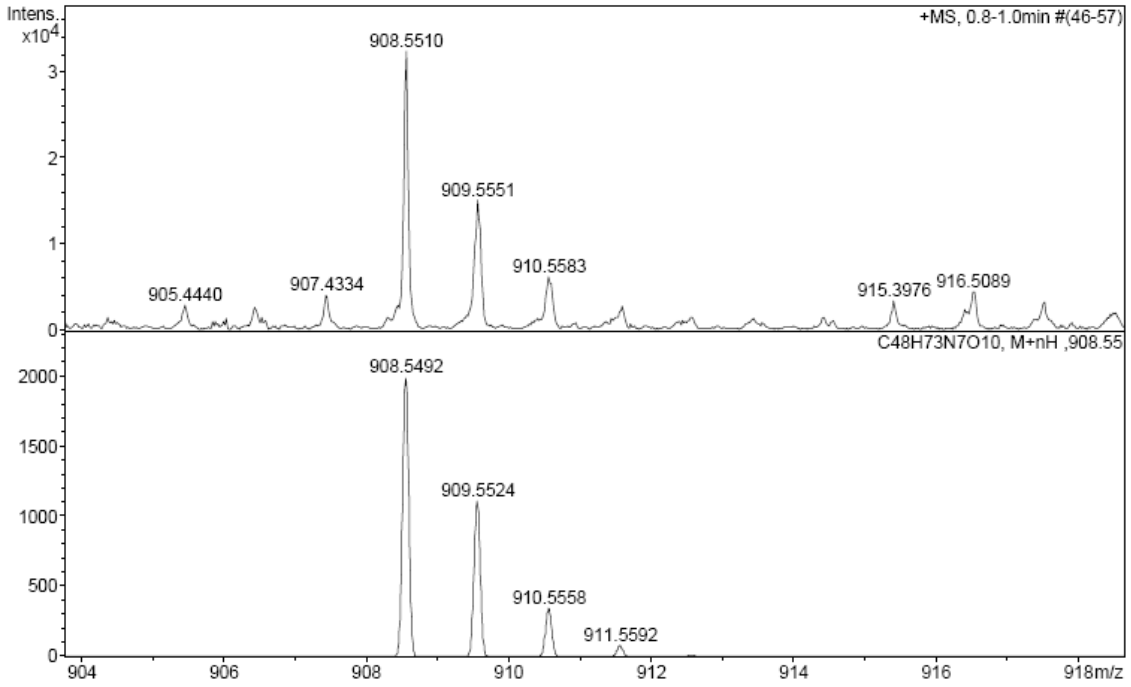

9. Synthesis of tailed biaryl cyclic lipoheptapeptides

Tailed biaryl cyclic lipopeptide incorporating a Phe-Tyr linkage 40

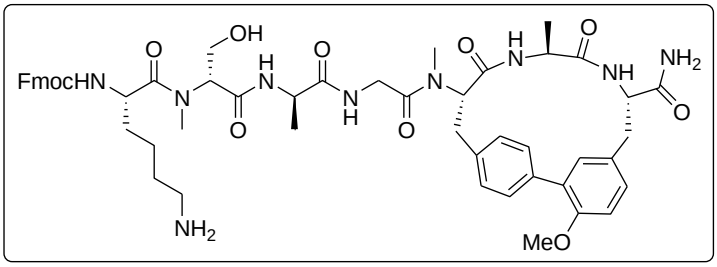

HPLC (λ = 220 nm)

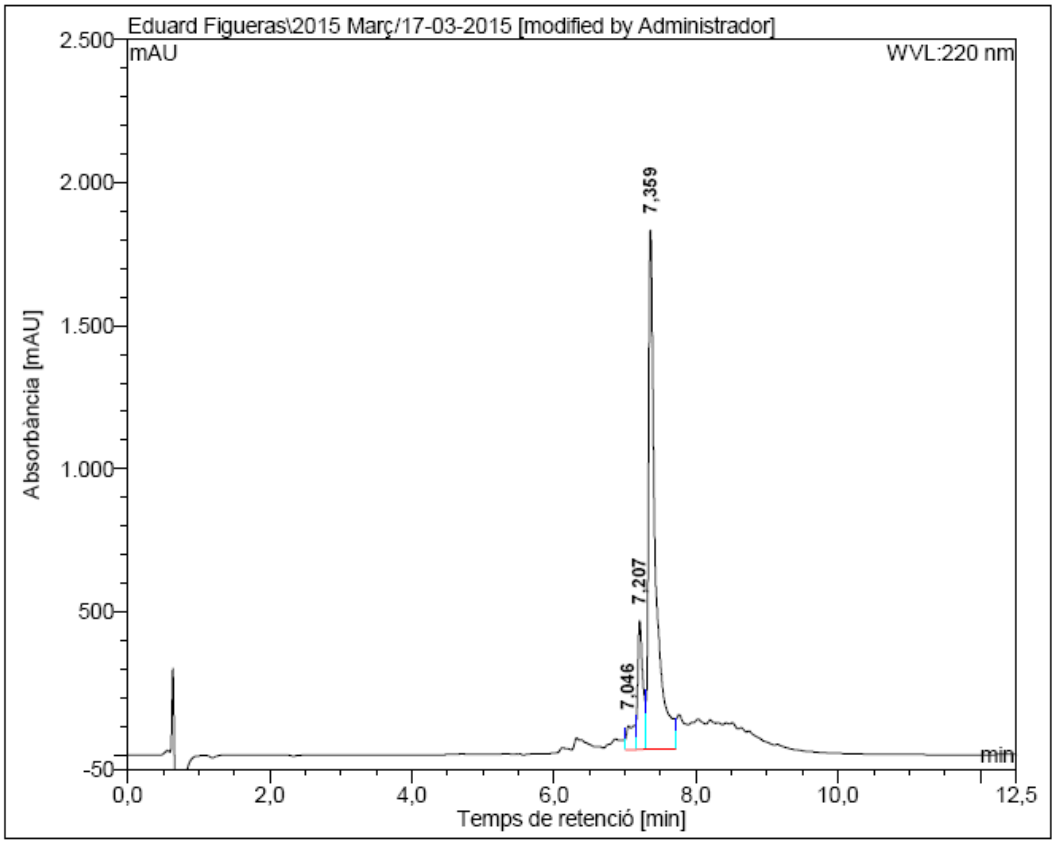

No.	Temps retenció min	alçada mAU	Area mAU*min	Area relativa %
1	7,05	82,264	10,291	4,03
2	7,21	450,938	38,471	15,08
3	7,36	1812,558	206,396	80,89
Total:		2345,760	255,158	100,00

ESI-MS *m/z*

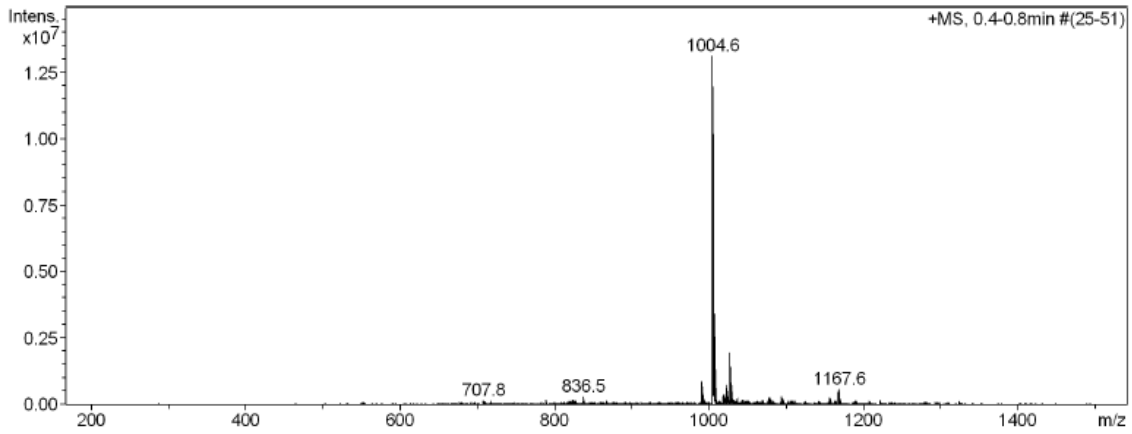
Intens.
x10^7
1.25
1.00
0.75
0.50
0.25
0.00
+MS, 0.4-0.8min #(25-51)
1004.6
707.8
836.5
1167.6
200
400
600
800
1000
1200
1400
m/z

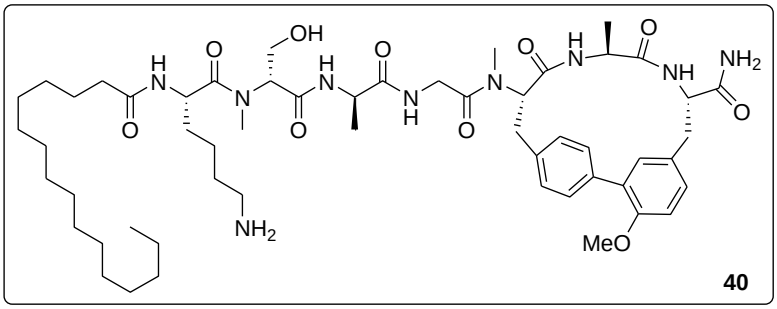

40

Crude peptide 40

HPLC (λ = 220 nm)

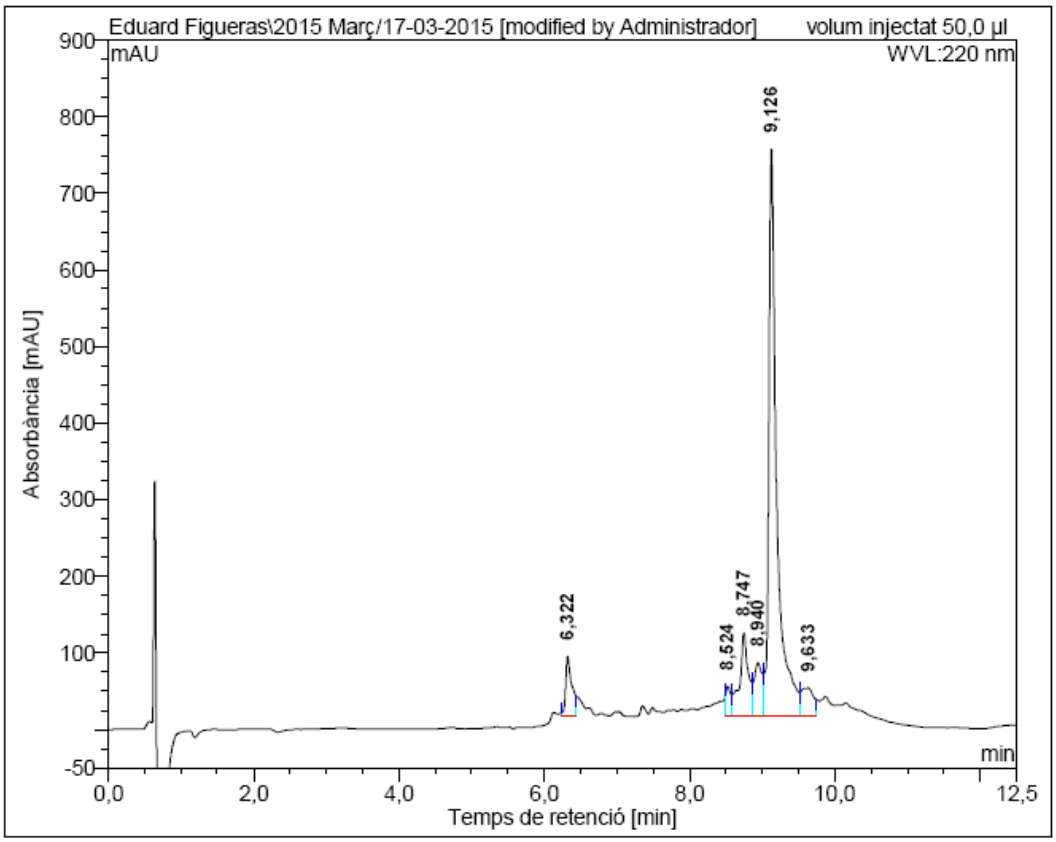

No.	Temps retenció min	alçada mAU	Area mAU*min	Area relativa %
1	6,32	78,455	7,685	5,62
2	8,52	38,870	3,098	2,27
3	8,75	108,918	15,535	11,37
4	8,94	69,874	8,599	6,29
5	9,13	740,201	94,298	68,99
6	9,63	37,067	7,470	5,47
Total:		1073,384	136,685	100,00

ESI-MS *m/z*

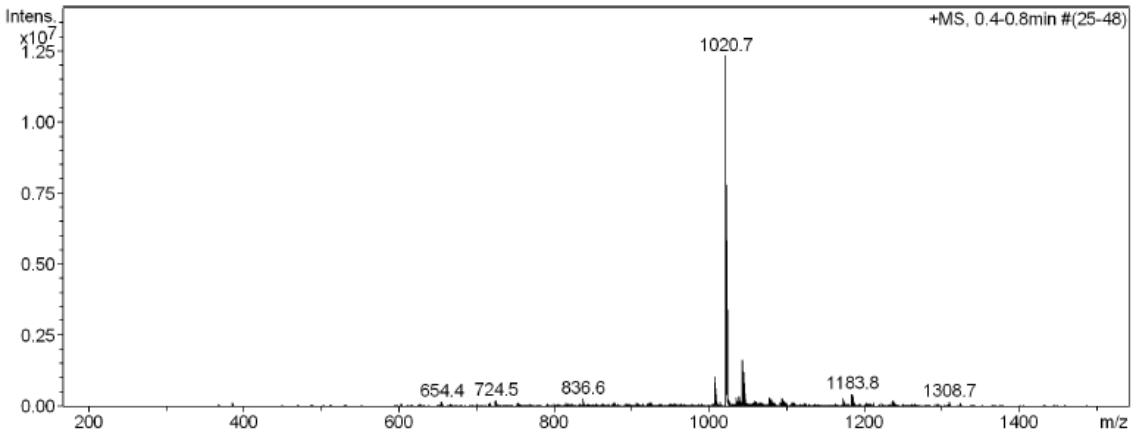

Purified peptide 40

HPLC (λ = 220 nm)

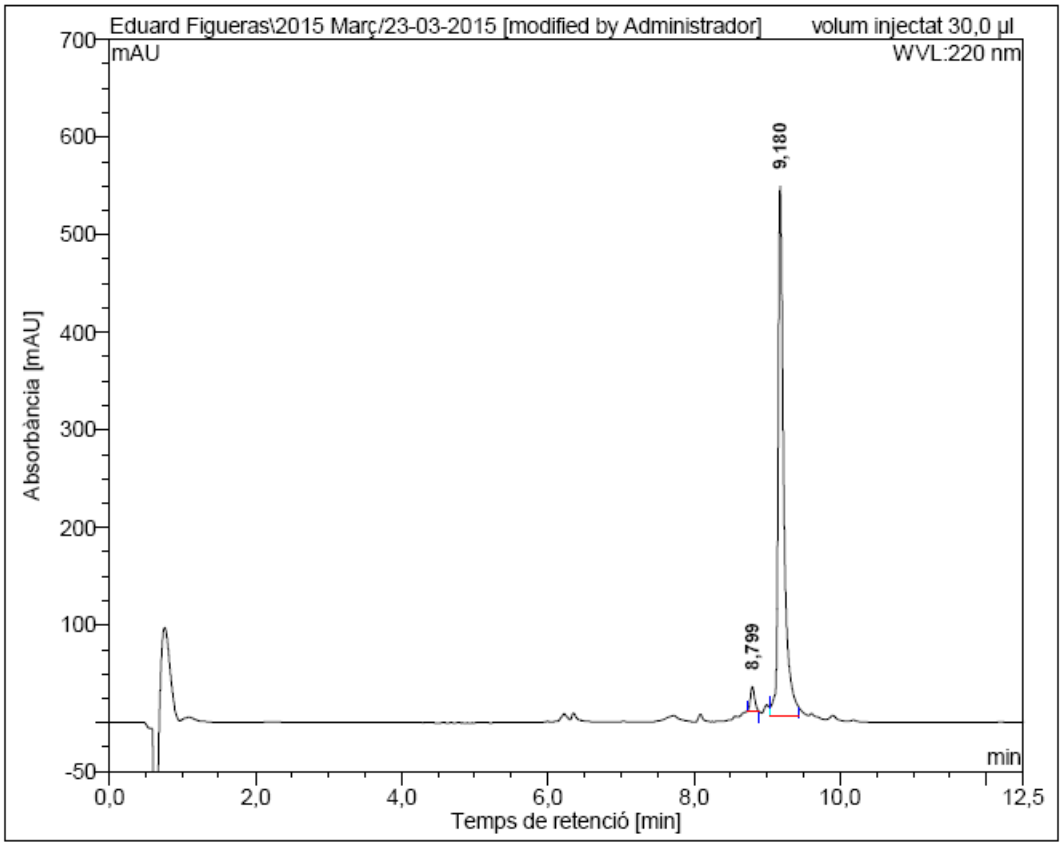

No.	Temps retenció min	alçada mAU	Area mAU*min	Area relativa %
1	8,80	25,457	1,734	3,43
2	9,18	542,396	48,801	96,57
Total:		567,853	50,535	100,00

ESI-MS *m/z*

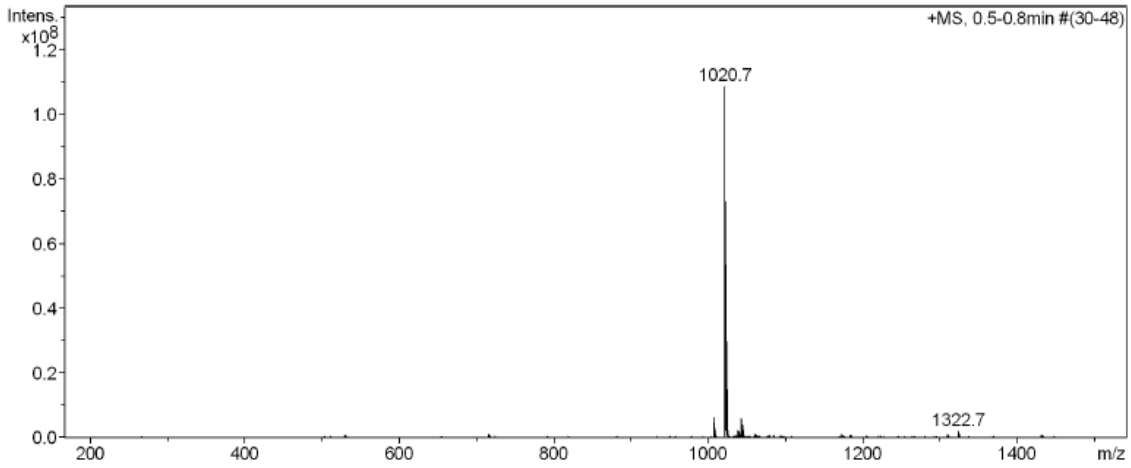

HRMS (ESI) *m/z*

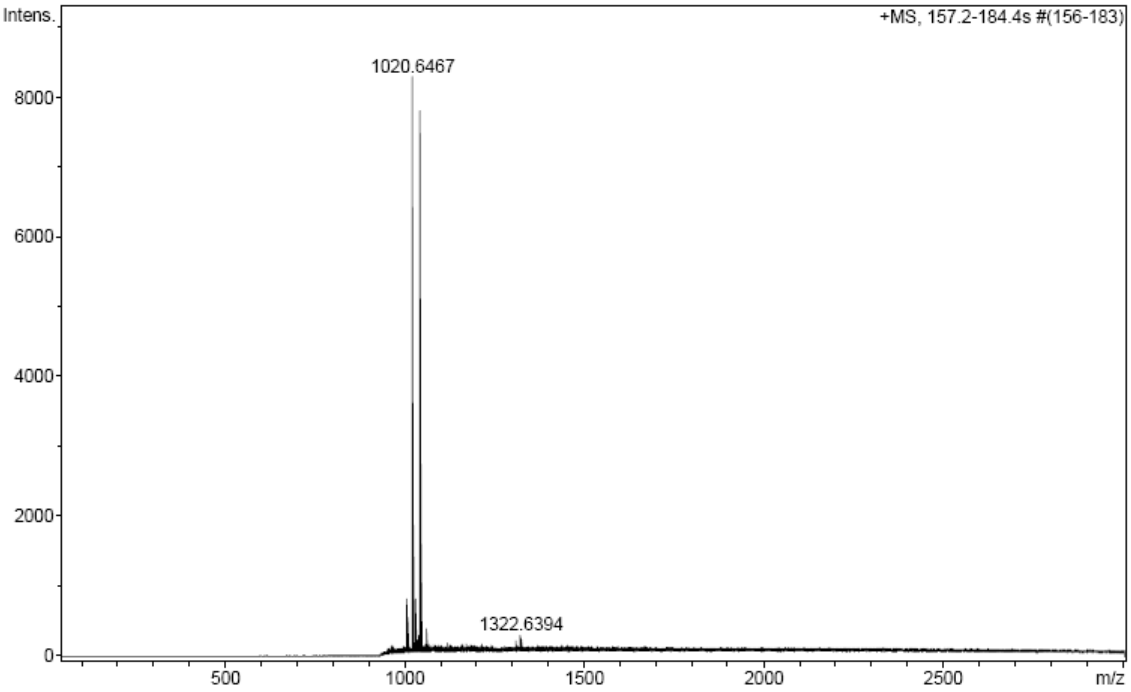

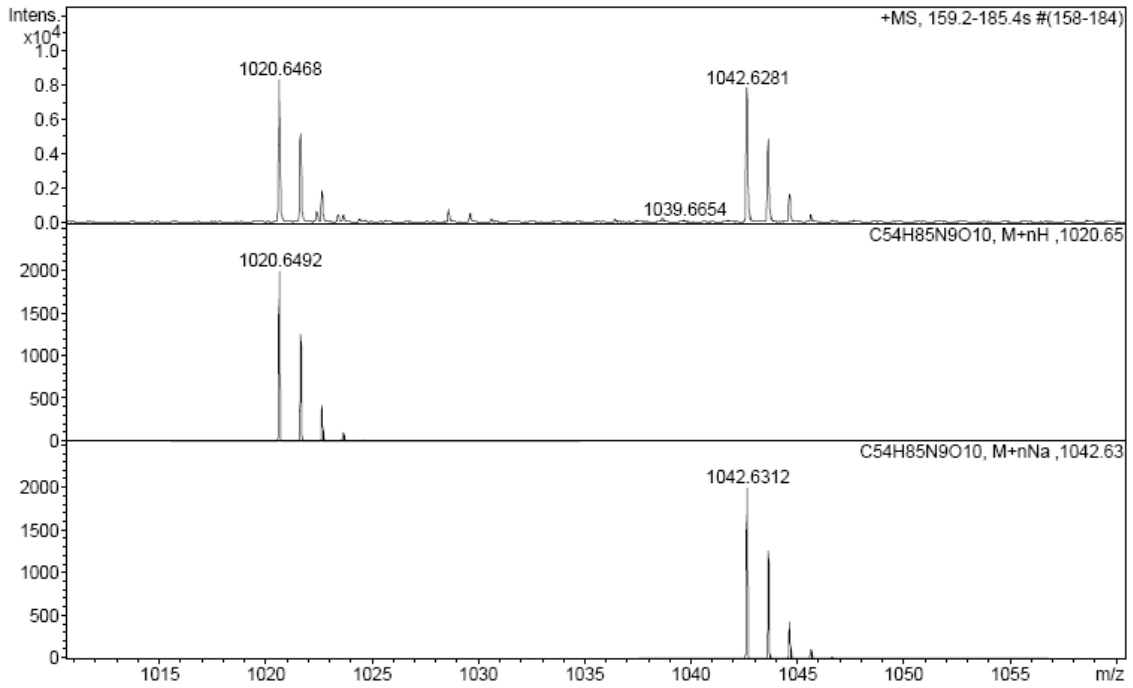

^{1}H-NMR (400 MHz, CD_3OD) δ (ppm)

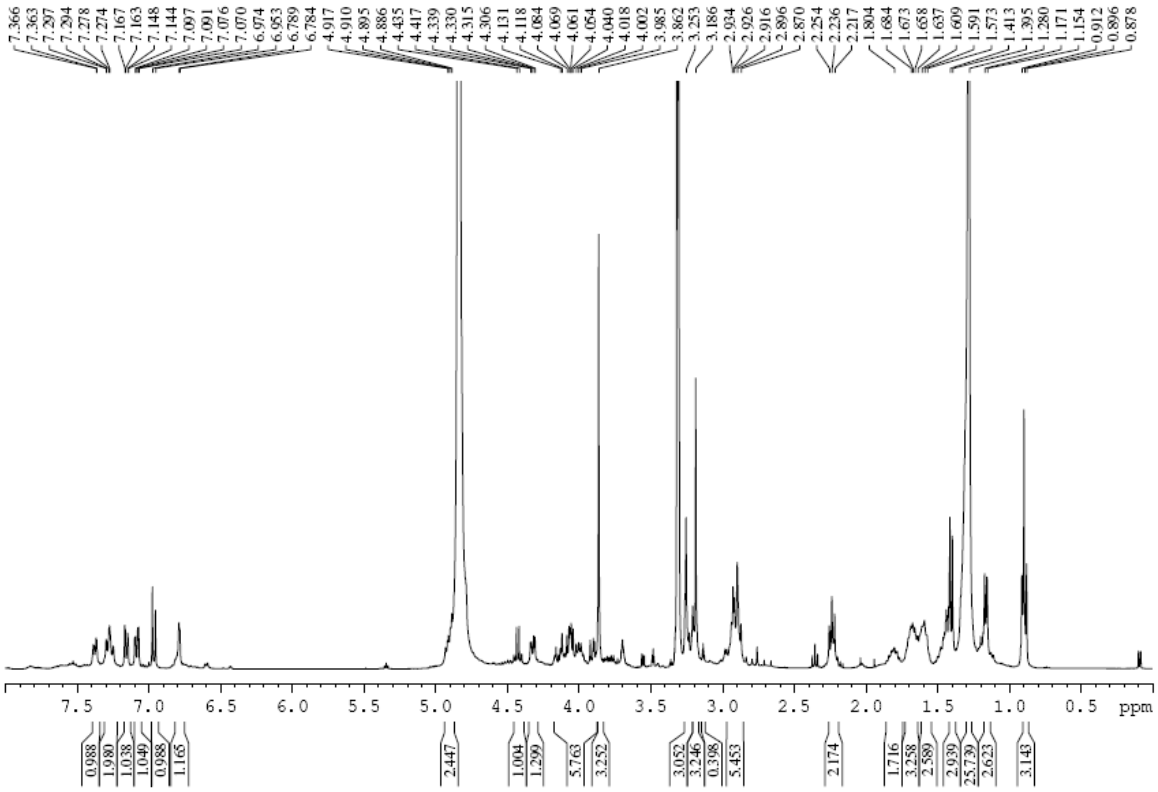

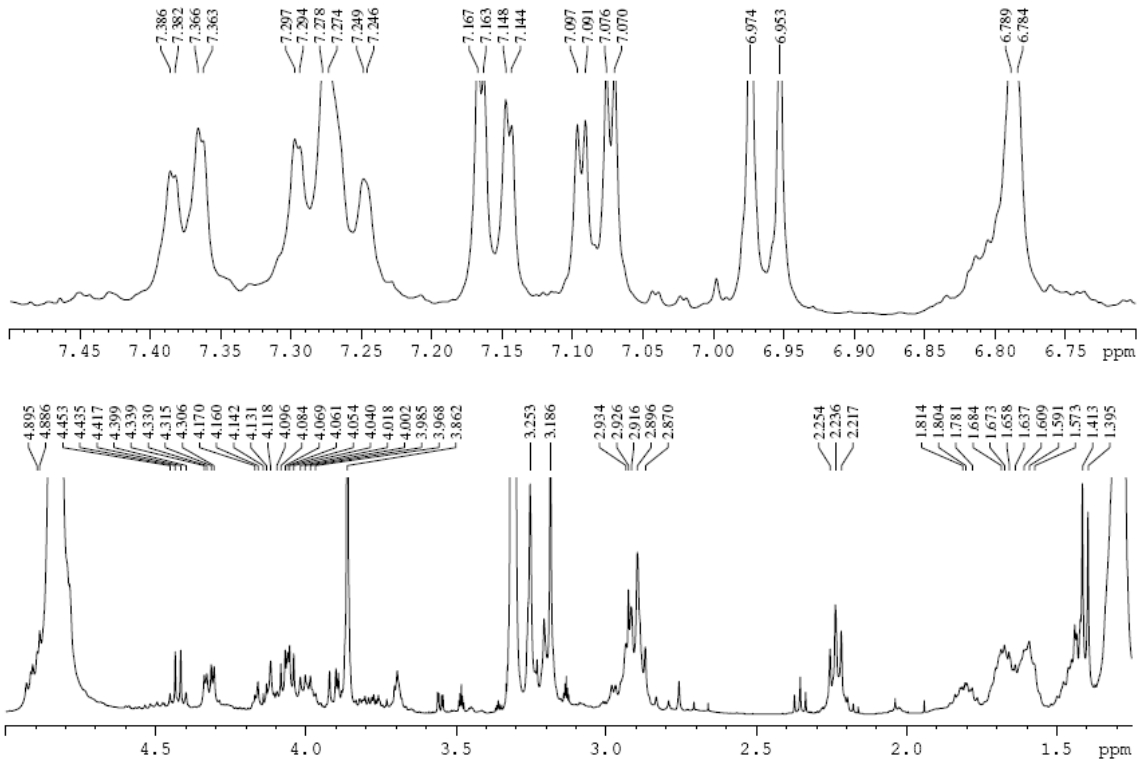

COSY (400 MHz, CD_3OD) δ (ppm)

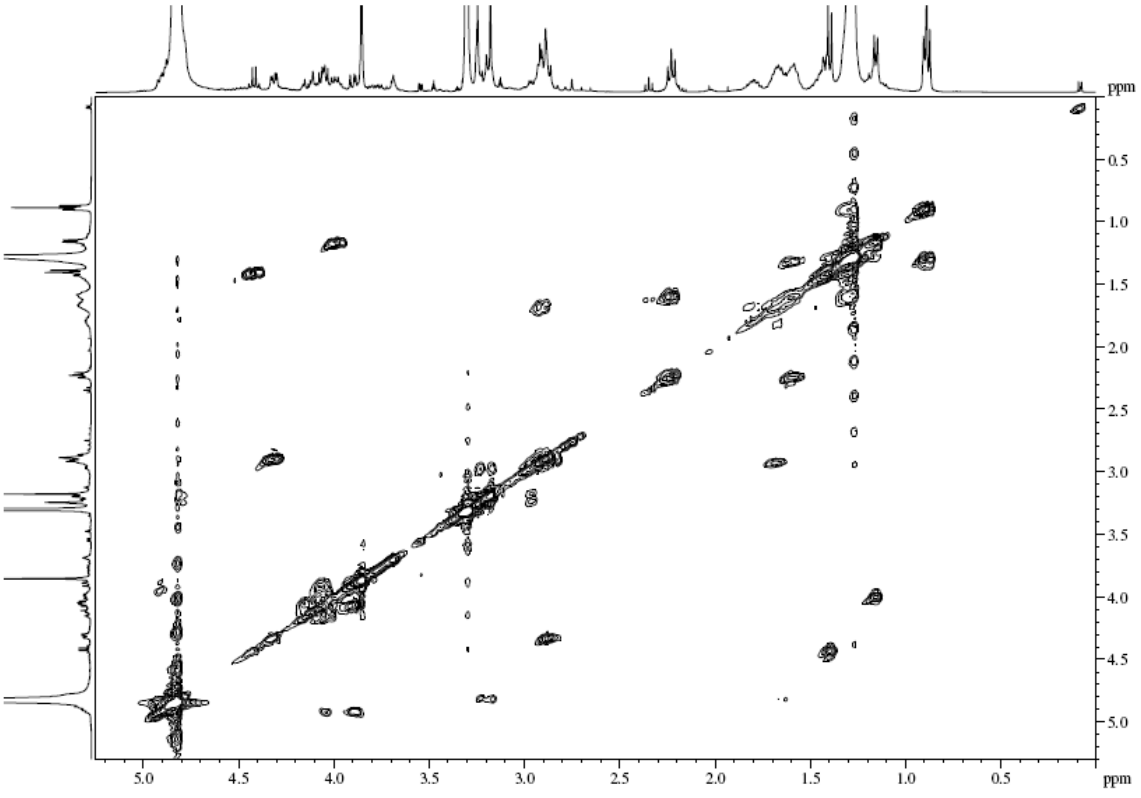

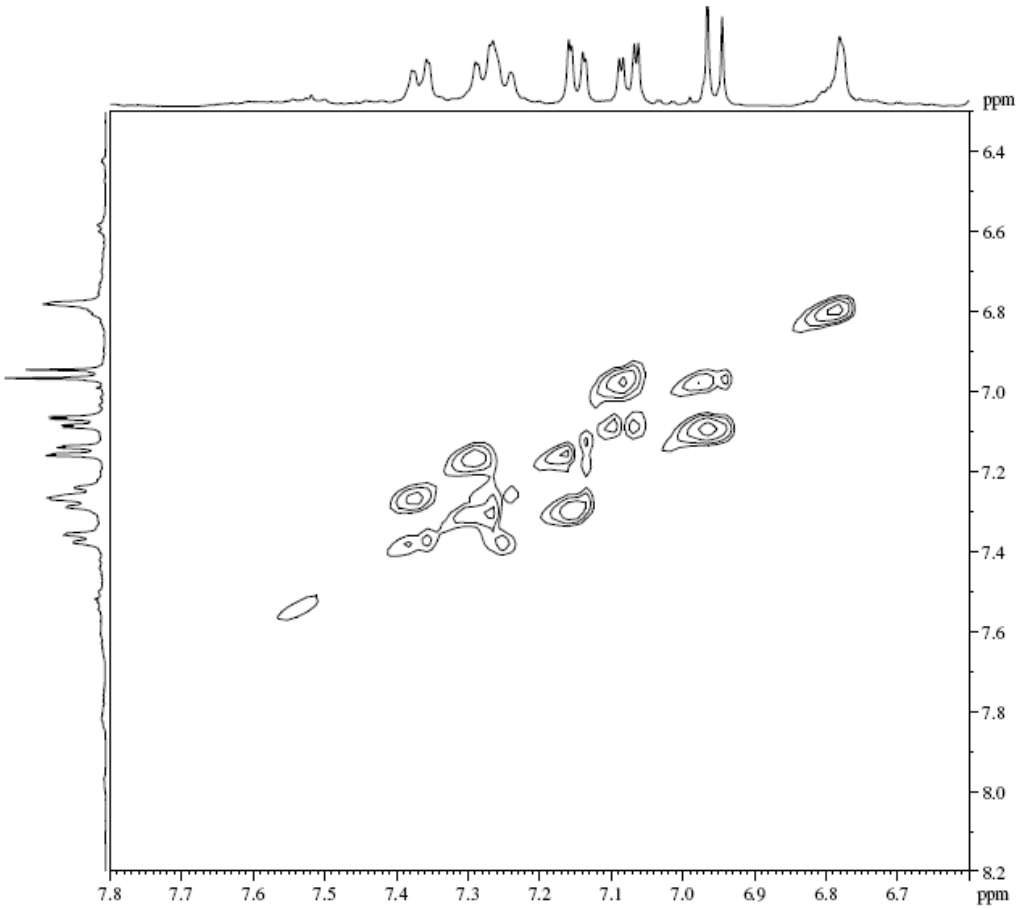

NOESY (400 MHz, CD_3OD) δ (ppm)

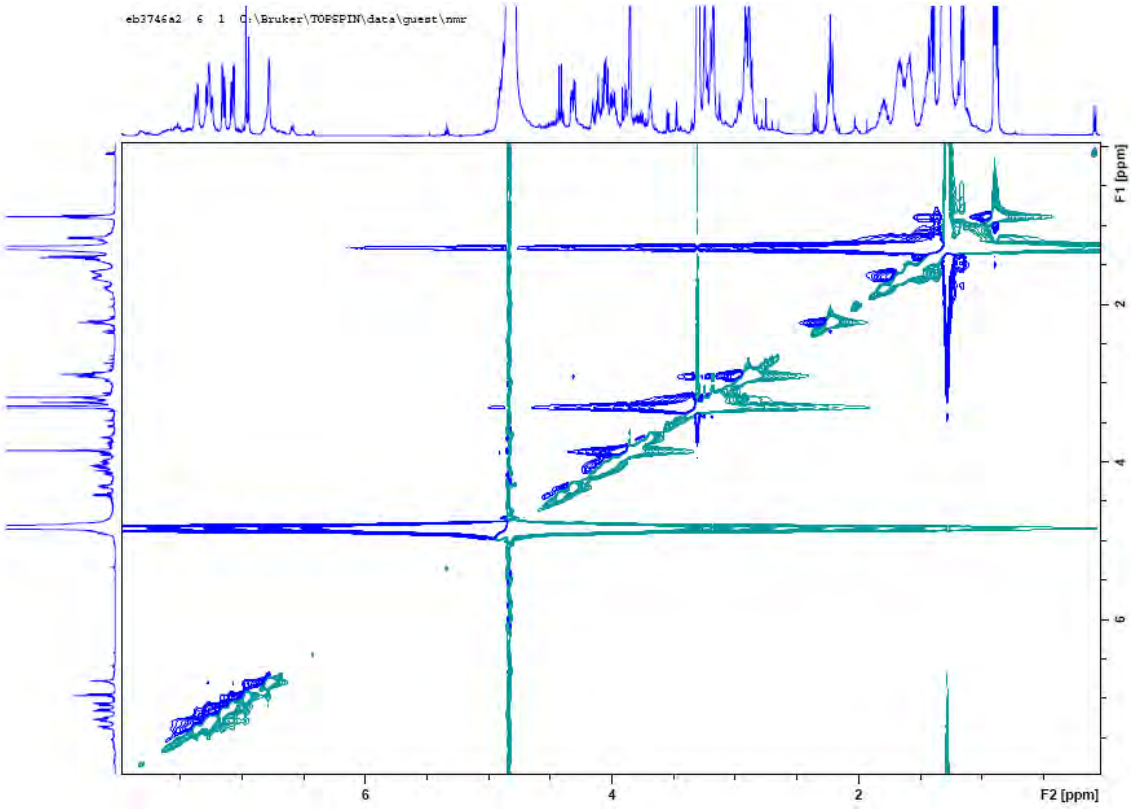

Tailed biaryl cyclic lipopeptide incorporating a Tyr-Tyr linkage 41

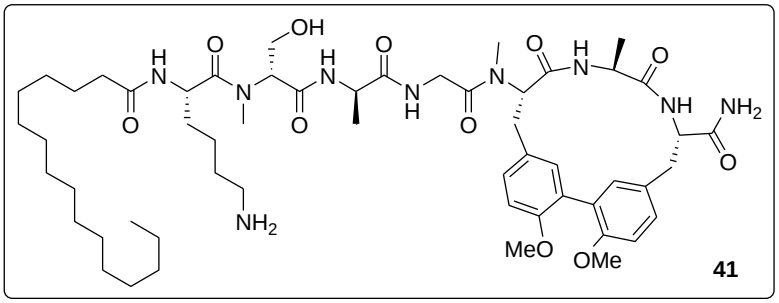

Crude peptide 41

HPLC (λ = 220 nm)

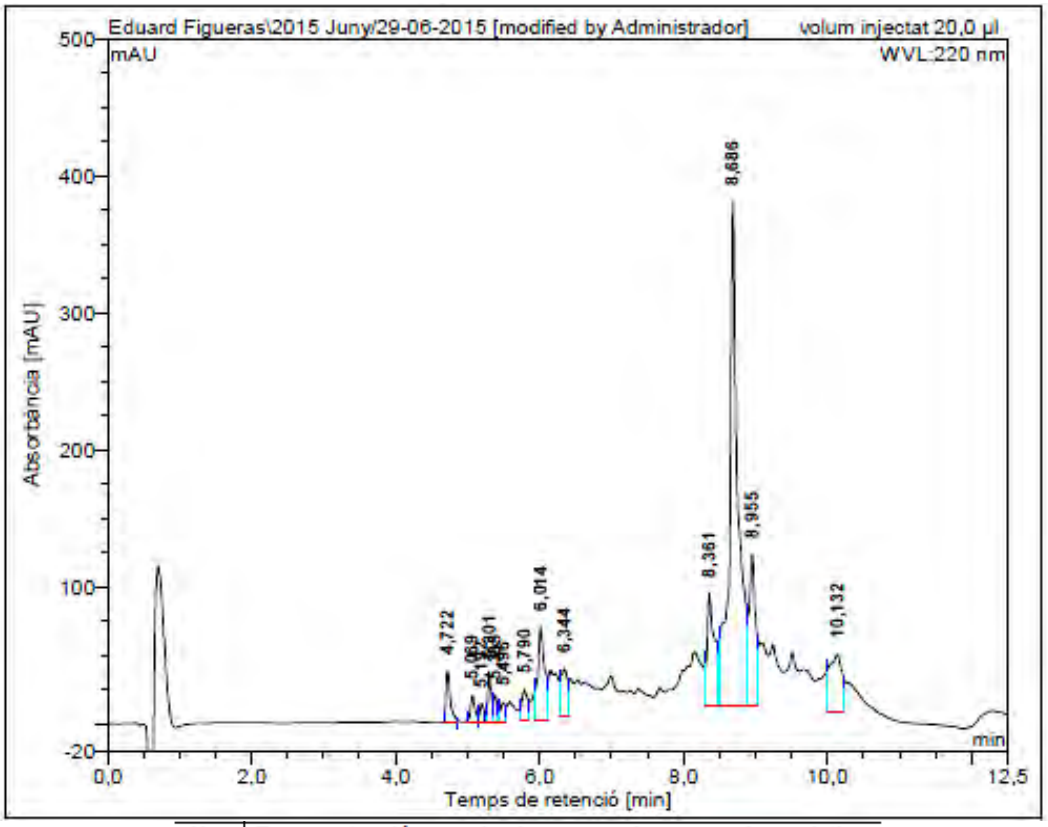

No.	Temps retenció min	alçada mAU	Area mAU*min	Area relativa %
1	4,72	36,783	2,536	2,50
2	5,07	18,858	1,295	1,28
3	5,19	13,202	0,862	0,85
4	5,30	33,732	2,092	2,06
5	5,39	19,164	0,935	0,92
6	5,50	14,431	1,028	1,01
7	5,79	22,899	2,255	2,22
8	6,01	68,334	7,377	7,27
9	6,34	35,026	3,826	3,77
10	8,36	81,777	9,114	8,98
11	8,69	368,226	51,598	50,85
12	8,95	110,767	10,765	10,61
13	10,13	41,158	7,779	7,67
Total:		864,358	101,462	100,00

ESI-MS *m/z*

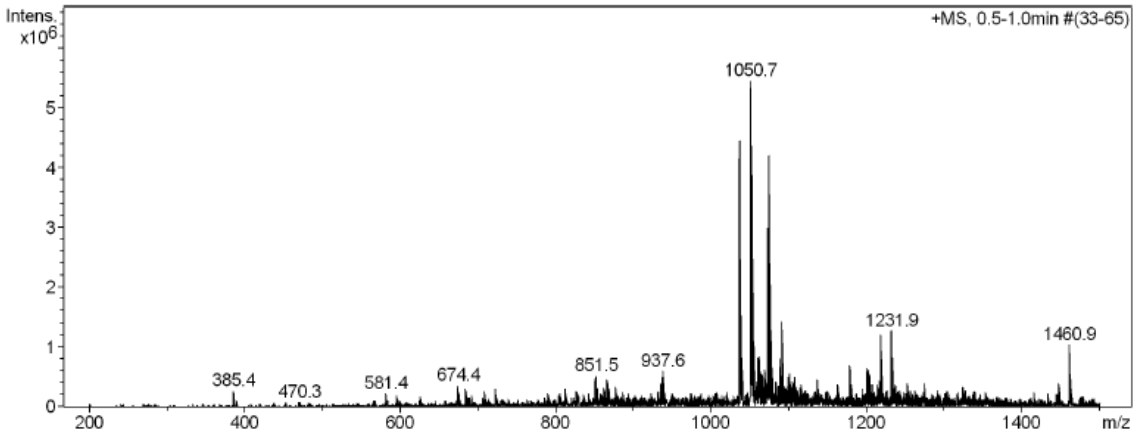

Purified peptide 41

HPLC (λ = 220 nm)

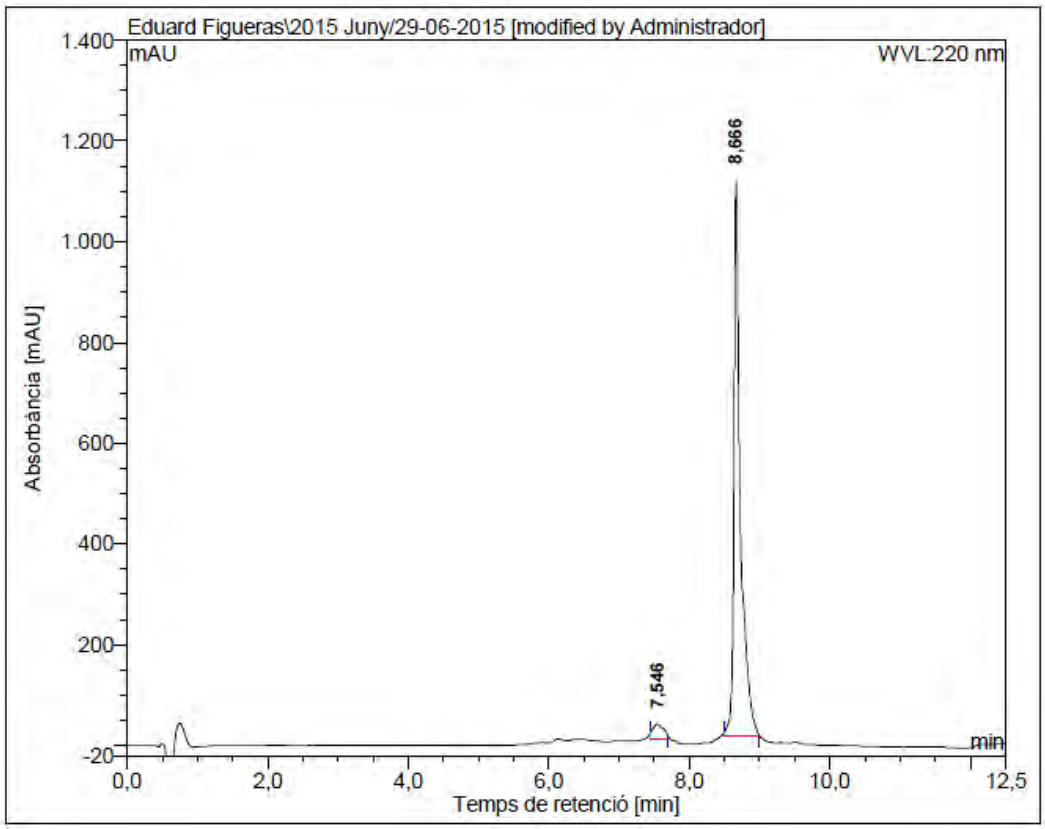

No.	Temps retenció min	alçada mAU	Area mAU*min	Area relativa %
1	7,55	29,941	5,277	4,22
2	8,67	1103,636	119,757	95,78
Total:		1133,577	125,034	100,00

ESI-MS *m/z*

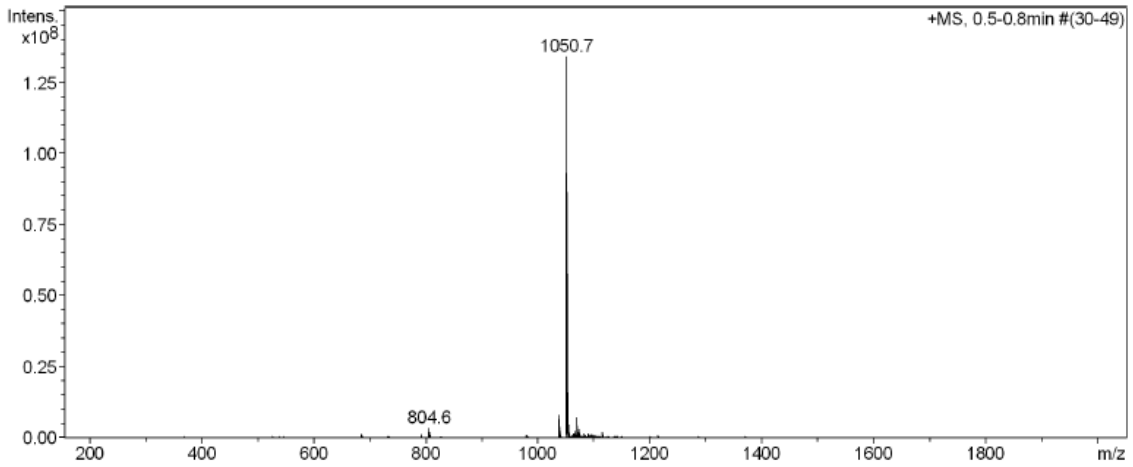

HRMS (ESI) *m/z*

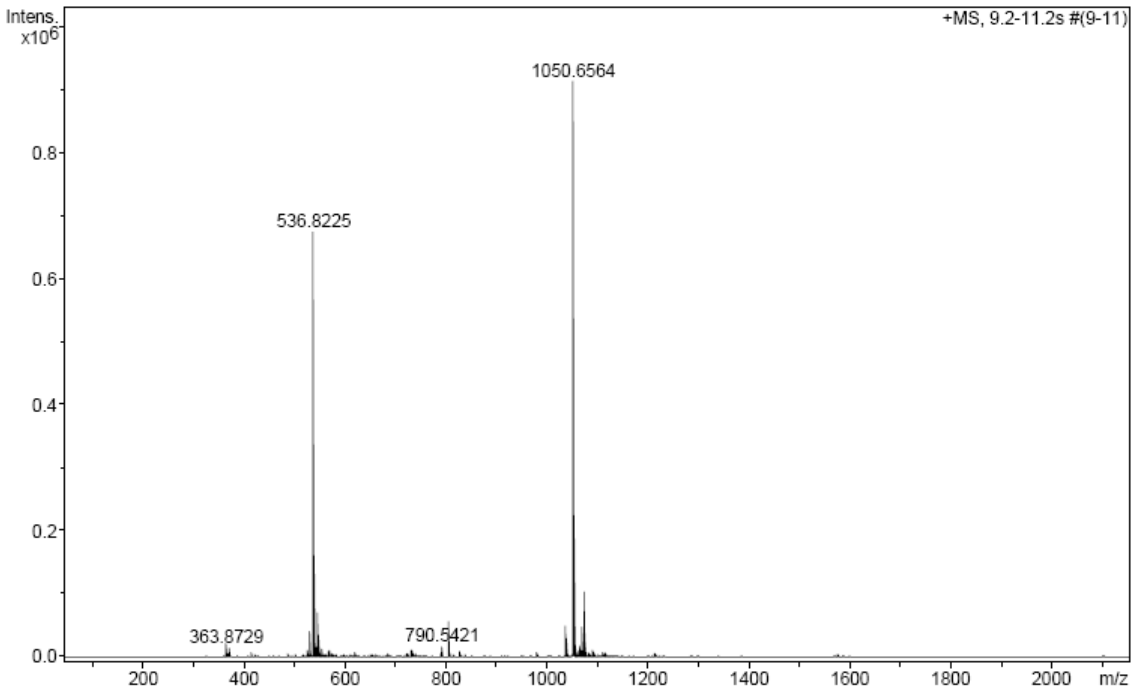

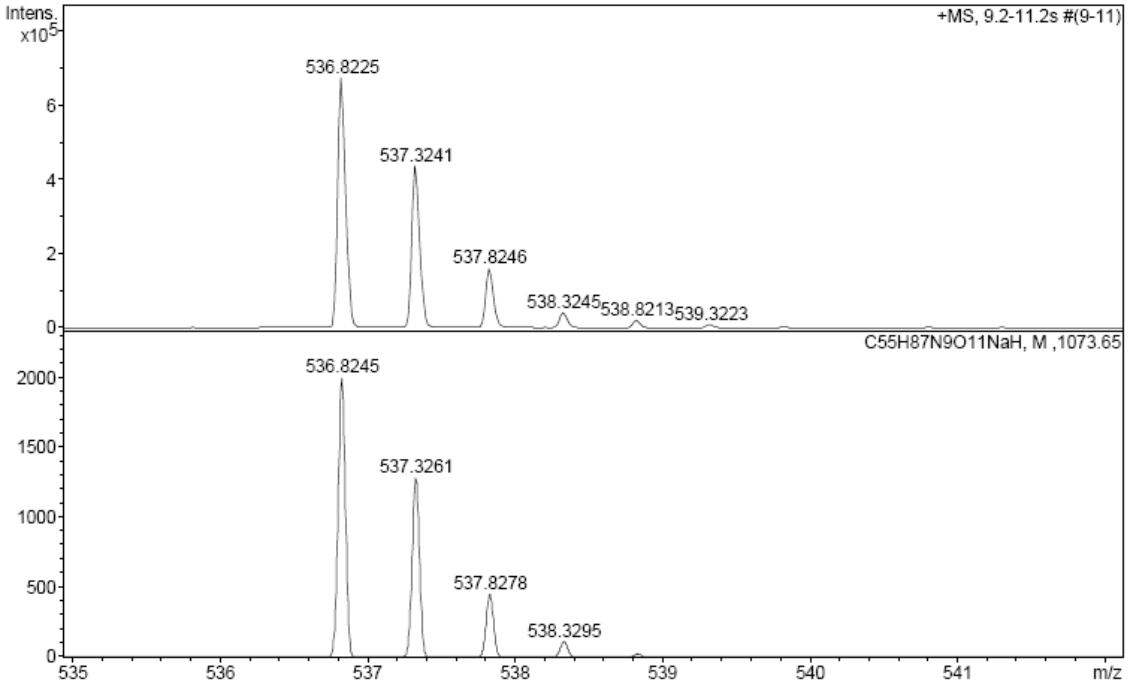
Intens.
x10^5
+MS, 9.2-11.2s #(9-11)
536.8225
537.3241
537.8246
538.3245
538.8213
539.3223
C55H87N9O11NaH, M ,1073.65
536.8245
537.3261
537.8278
538.3295
m/z

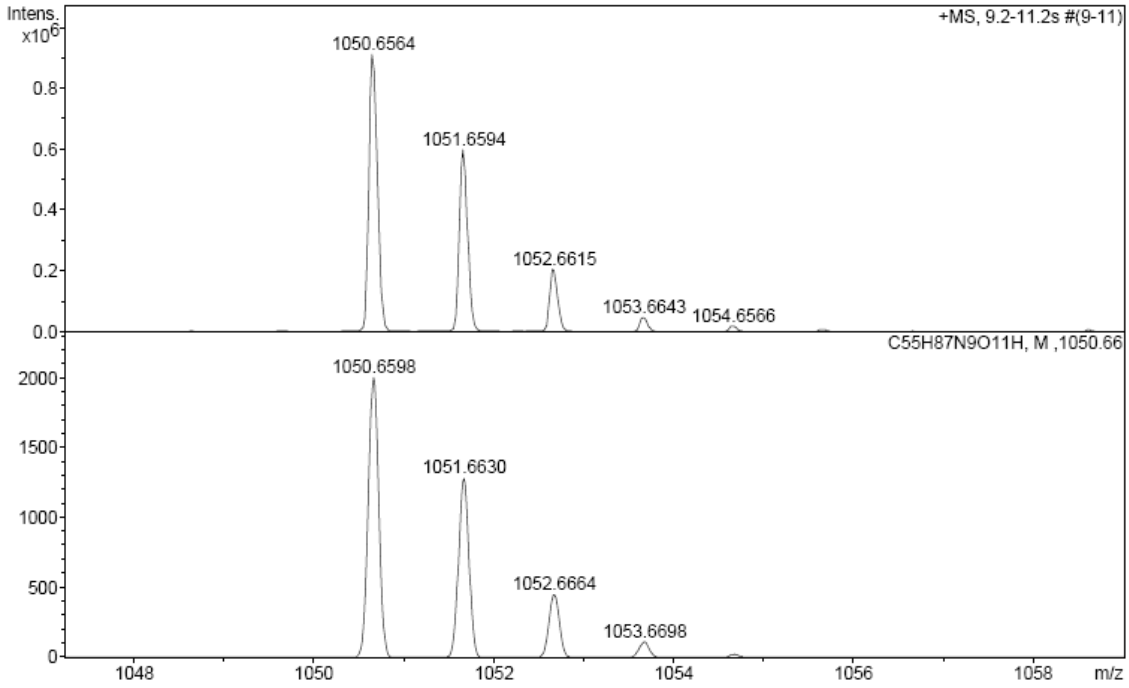
Intens.
x10^6
+MS, 9.2-11.2s #(9-11)
1050.6564
1051.6594
1052.6615
1053.6643
1054.6566
C55H87N9O11H, M ,1050.66
1050.6598
1051.6630
1052.6664
1053.6698
m/z

Tailed biaryl cyclic lipopeptide incorporating a His-Tyr linkage 42

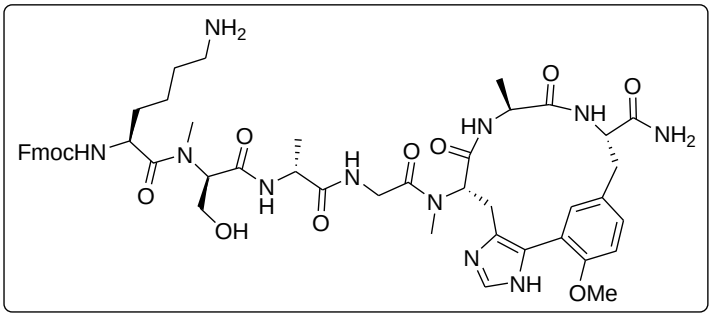

HPLC (λ = 220 nm)

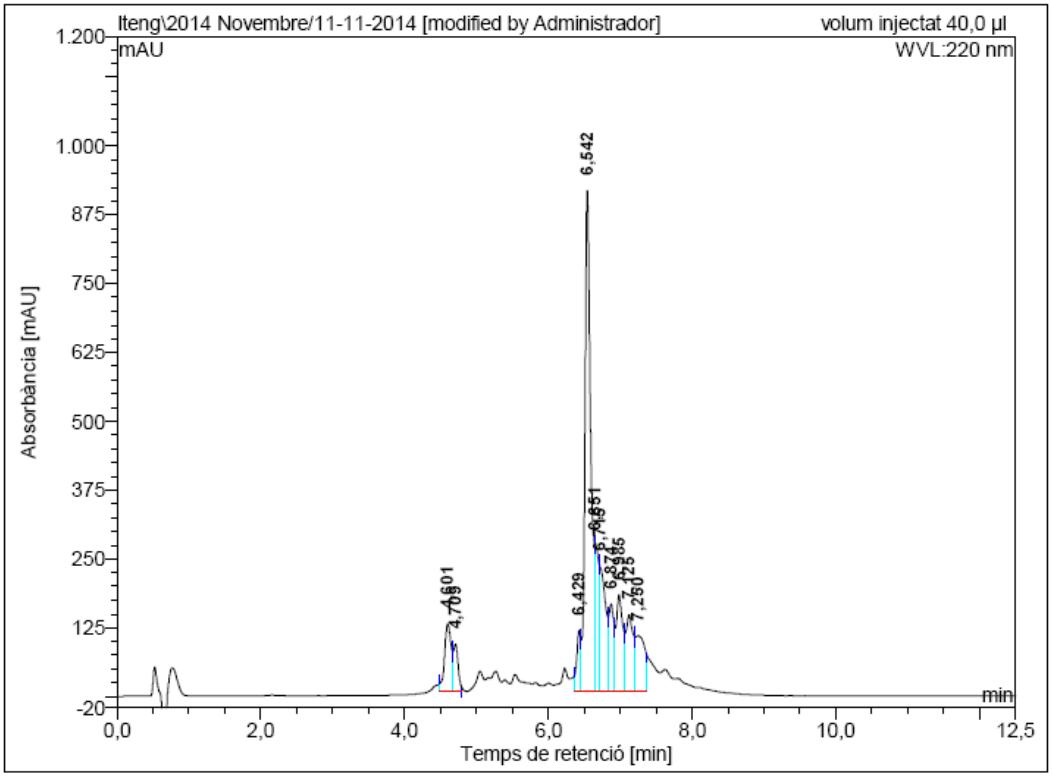

No.	Temps retenció min	alçada mAU	Area mAU*min	Area relativa %
1	4,60	122,780	13,329	6,17
2	4,71	85,820	6,713	3,11
3	6,43	110,677	7,113	3,29
4	6,54	909,695	86,818	40,21
5	6,65	266,560	15,720	7,28
6	6,72	228,587	21,981	10,18
7	6,87	158,850	14,079	6,52
8	6,98	175,457	19,449	9,01
9	7,12	139,539	16,192	7,50
10	7,25	101,547	14,540	6,73
Total:		2299,513	215,935	100,00

ESI-MS *m/z*

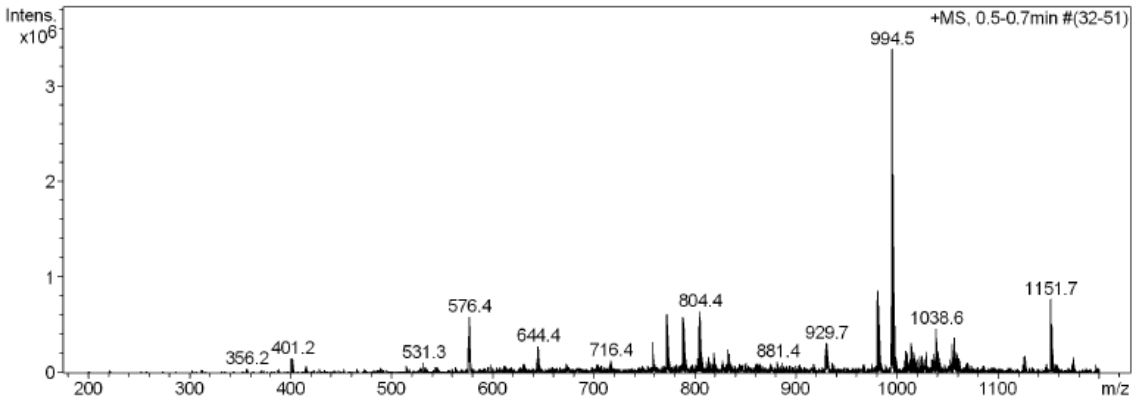
Intens.
x10^6
+MS, 0.5-0.7min #(32-51)
994.5
576.4
804.4
1151.7
1038.6
644.4
929.7
356.2
401.2
531.3
716.4
881.4
m/z

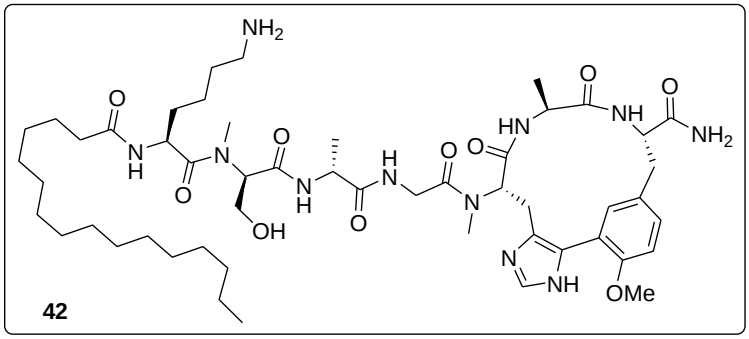

42

Crude peptide 42

HPLC (λ = 220 nm)

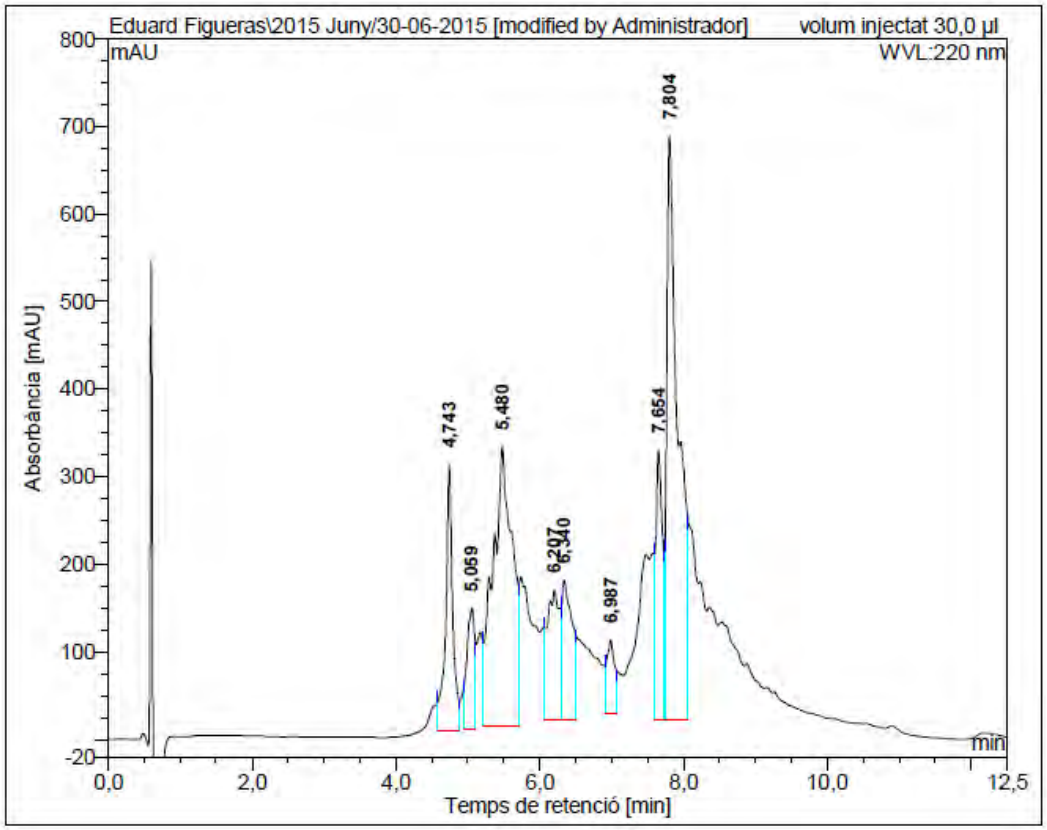

No.	Temps retenció min	alçada mAU	Area mAU*min	Area relativa %
1	4,74	304,216	33,541	8,96
2	5,06	138,744	17,870	4,77
3	5,48	318,845	100,151	26,75
4	6,21	148,703	28,614	7,64
5	6,34	160,007	25,234	6,74
6	6,99	83,117	10,523	2,81
7	7,65	308,114	32,900	8,79
8	7,80	665,807	125,555	33,54
Total:		2127,553	374,390	100,00

ESI-MS *m/z*

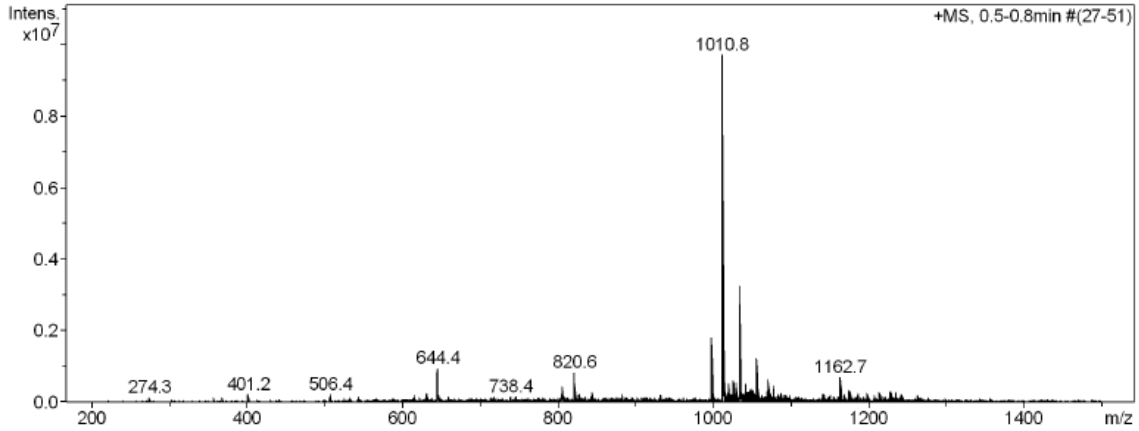

HRMS (ESI) *m/z*

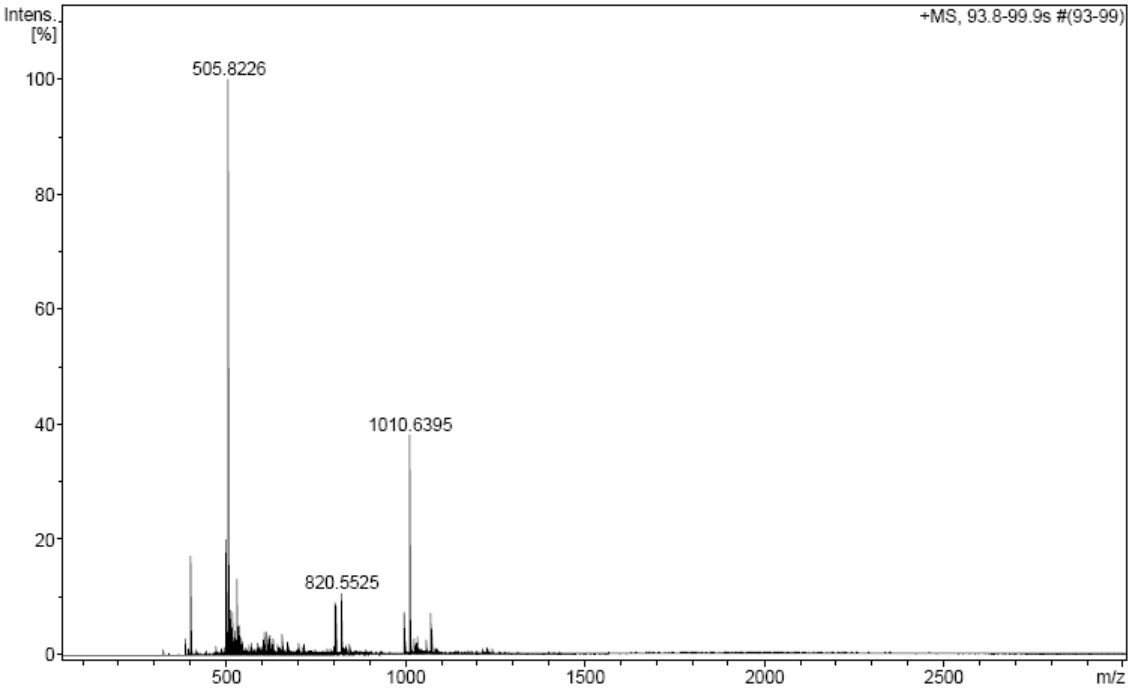

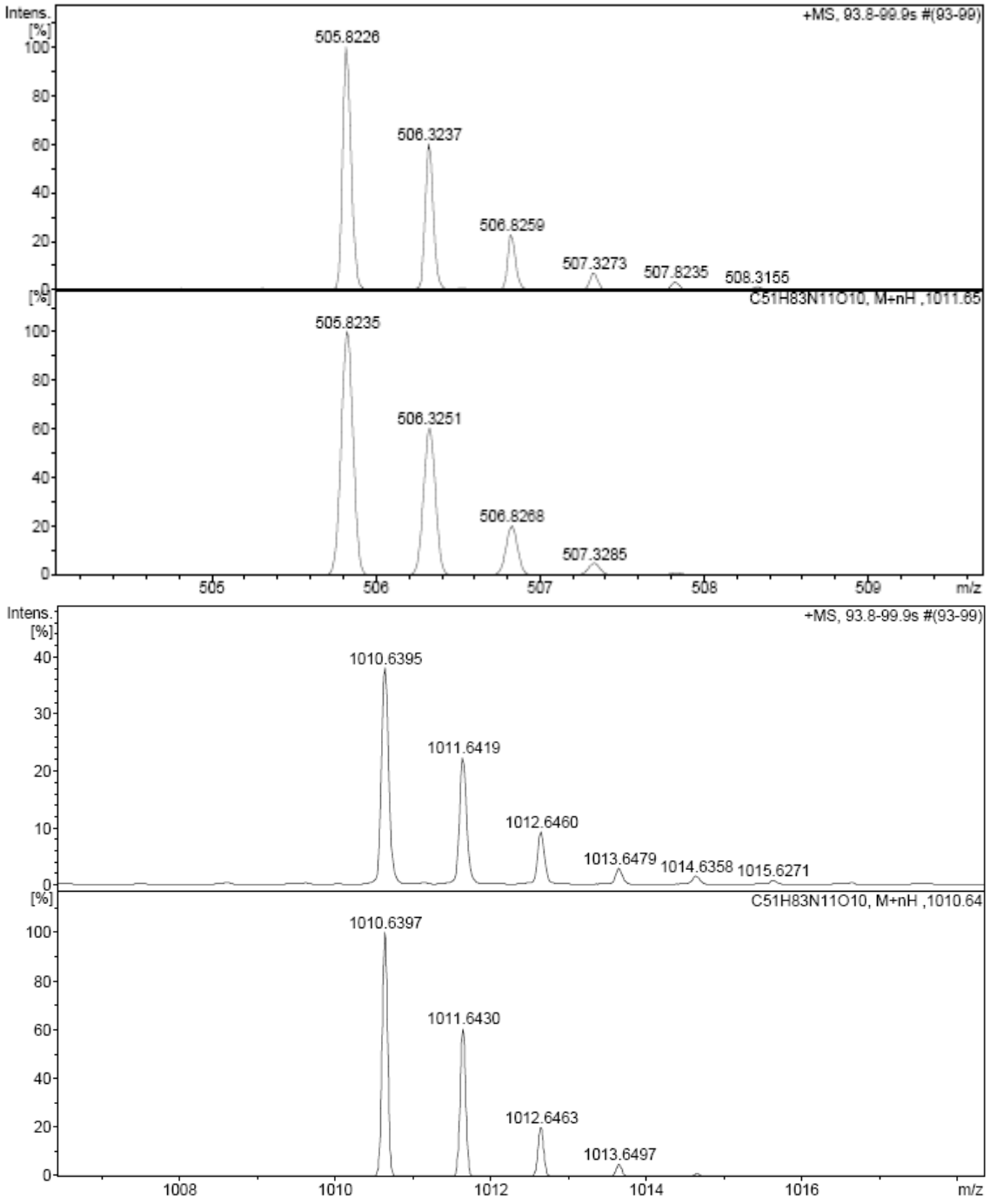
Intens.
[%]
+MS, 93.8-99.9s #(93-99)
505.8226
506.3237
506.8259
507.3273
507.8235
508.3155
C51H83N11O10, M+nH ,1011.65
505.8235
506.3251
506.8268
507.3285
505
506
507
508
509
m/z
+MS, 93.8-99.9s #(93-99)
1010.6395
1011.6419
1012.6460
1013.6479
1014.6358
1015.6271
C51H83N11O10, M+nH ,1010.64
1010.6397
1011.6430
1012.6463
1013.6497
1008
1010
1012
1014
1016
m/z

Purified peptide 42

HPLC (λ = 220 nm)

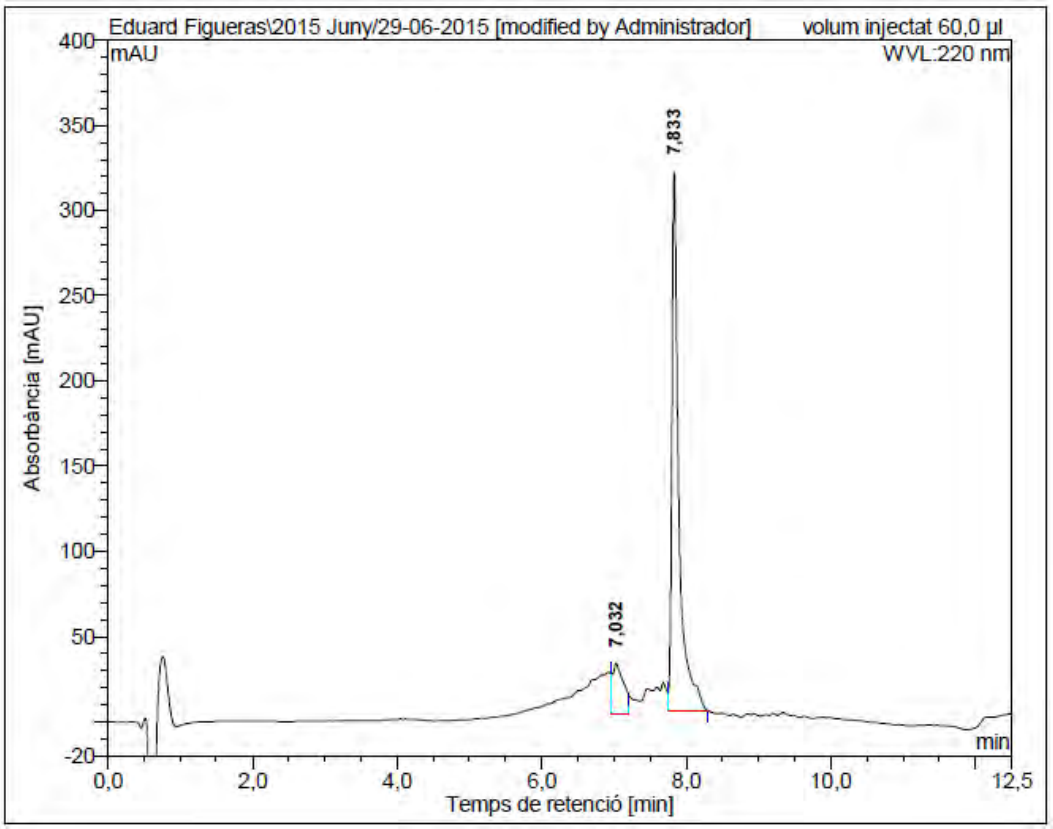

No.	Temps retenció min	alçada mAU	Area mAU*min	Area relativa %
1	7,03	29,632	5,530	13,40
2	7,83	316,273	35,746	86,60
Total:		345,905	41,277	100,00

ESI-MS *m/z*

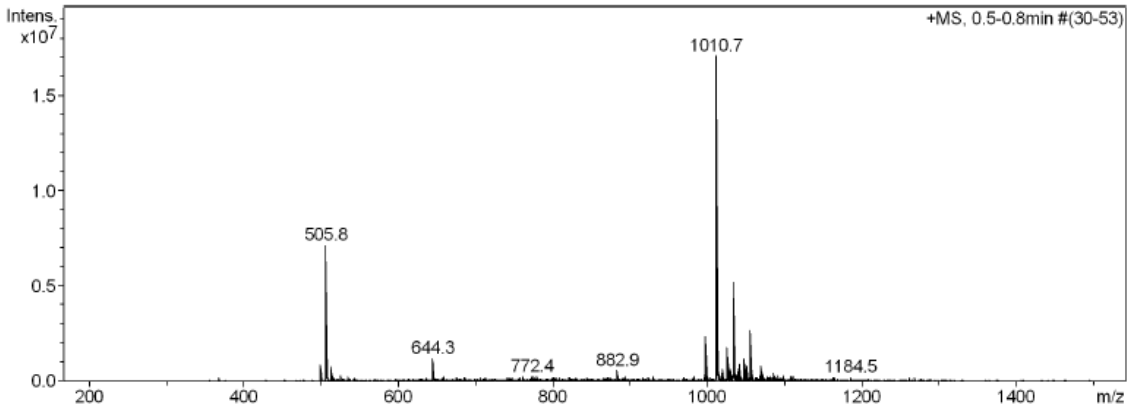

HRMS (ESI) *m/z*

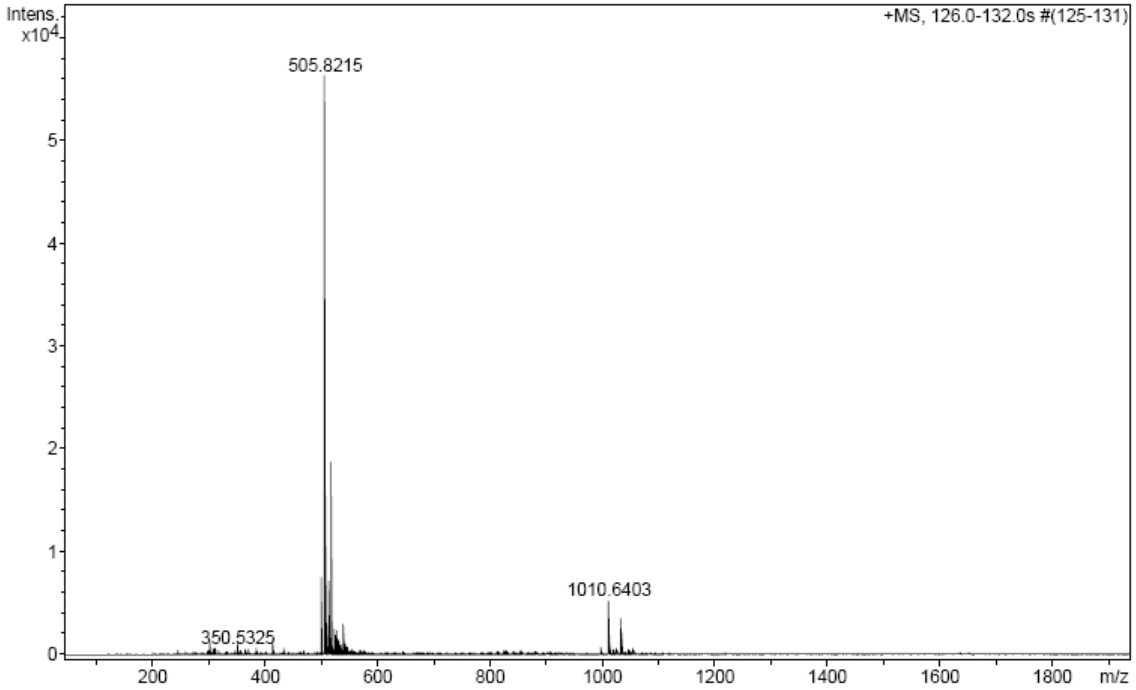

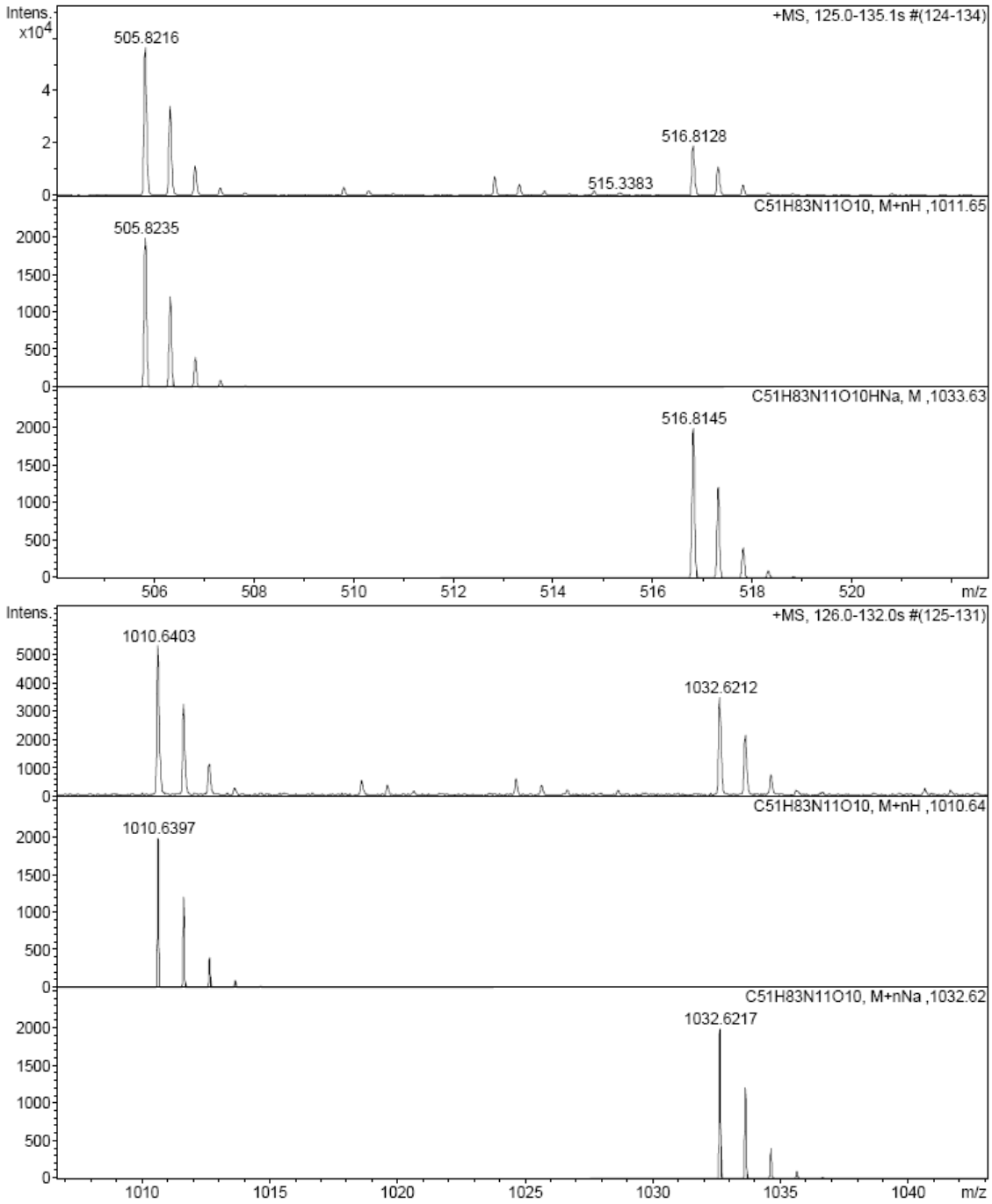
Intens.
x10^4
+MS, 125.0-135.1s #(124-134)
505.8216
516.8128
515.3383
C51H83N11O10, M+nH ,1011.65
505.8235
C51H83N11O10HNa, M ,1033.63
516.8145
m/z
Intens.
+MS, 126.0-132.0s #(125-131)
1010.6403
1032.6212
C51H83N11O10, M+nH ,1010.64
1010.6397
C51H83N11O10, M+nNa ,1032.62
1032.6217
m/z

Tailed biaryl cyclic lipopeptide incorporating a Phg-Tyr linkage 43

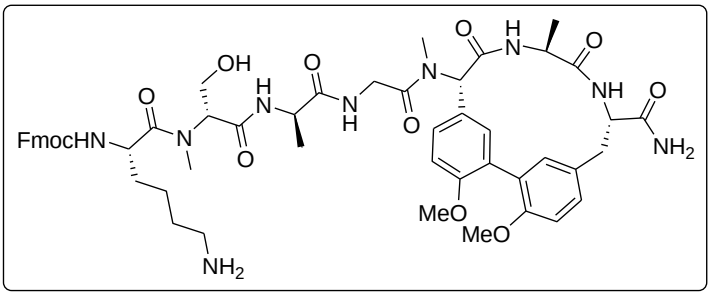

HPLC (λ = 220 nm)

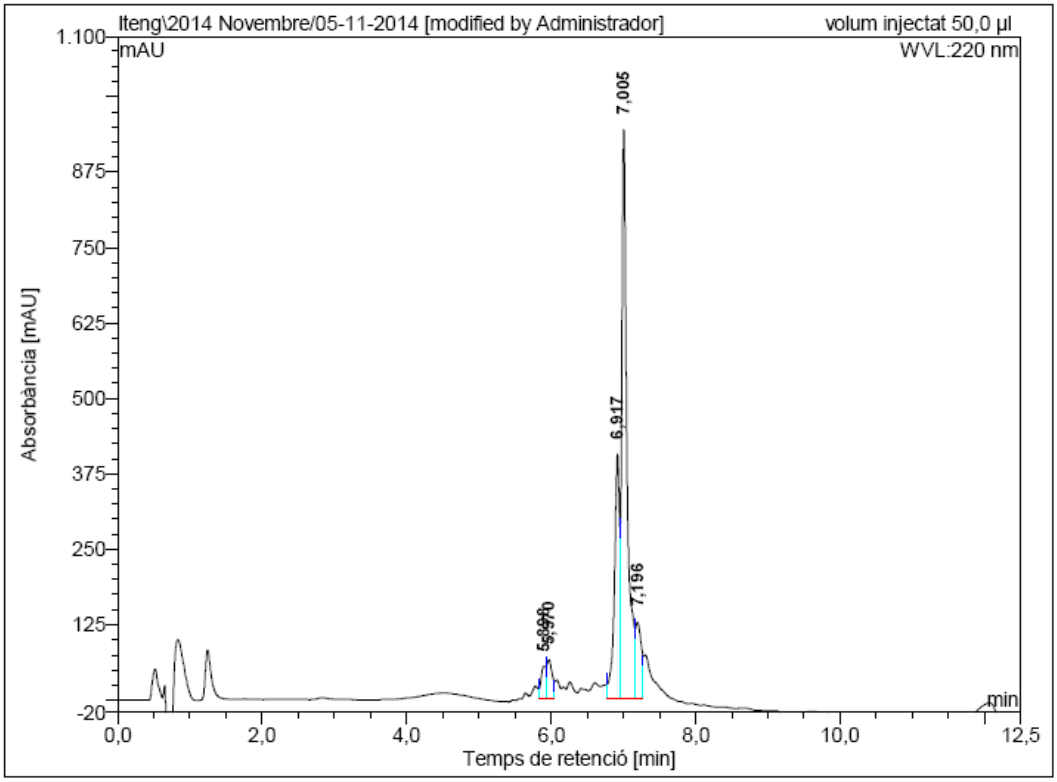

No.	Temps retenció min	alçada mAU	Area mAU*min	Area relativa %
1	5,90	52,854	3,932	2,90
2	5,97	63,542	5,832	4,31
3	6,92	403,950	32,092	23,69
4	7,01	941,737	81,754	60,36
5	7,20	125,669	11,845	8,74
Total:		1587,751	135,455	100,00

ESI-MS *m/z*

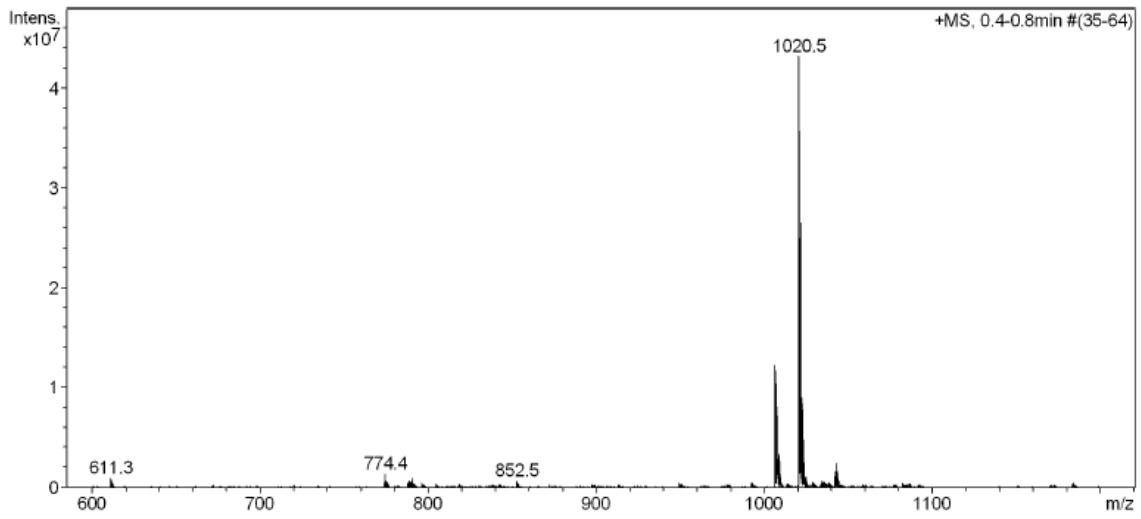

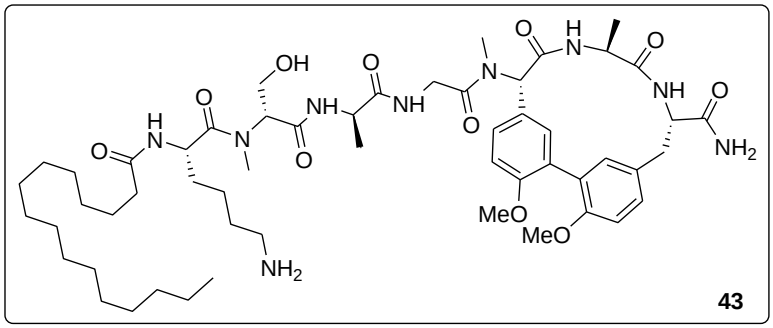

43

Crude peptide 43

HPLC (λ = 220 nm)

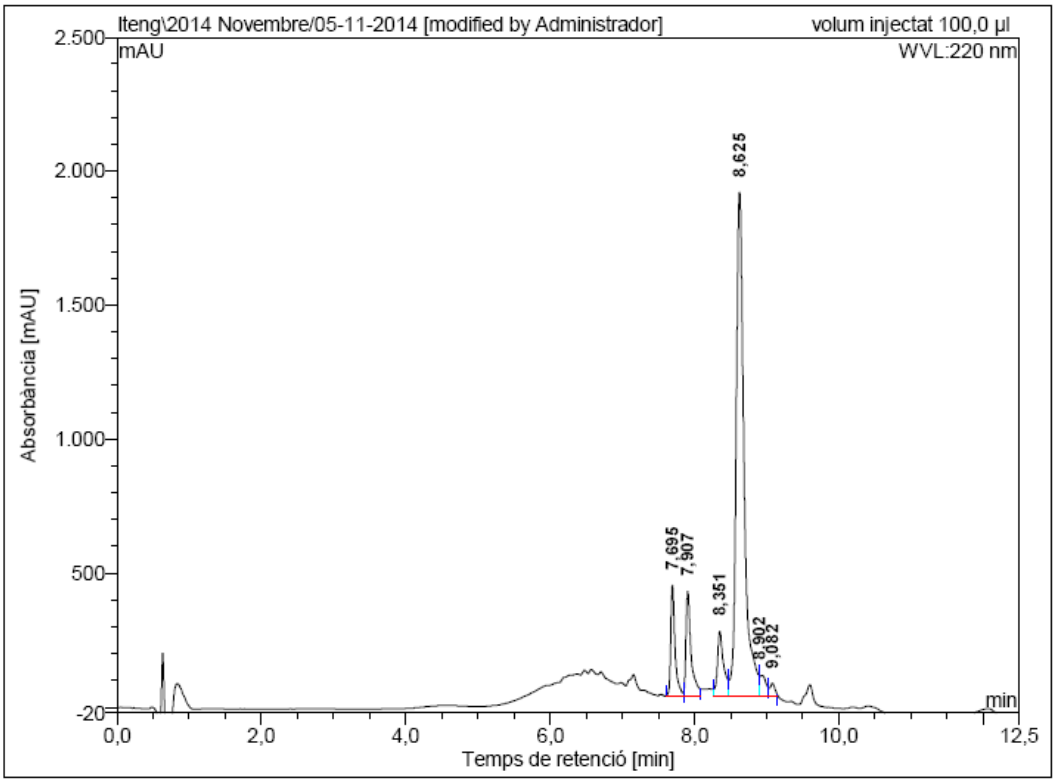

No.	Temps retenció min	alçada mAU	Area mAU*min	Area relativa %
1	7,69	412,866	28,835	8,53
2	7,91	390,594	32,019	9,47
3	8,35	241,212	23,865	7,06
4	8,62	1879,247	241,683	71,46
5	8,90	76,940	7,811	2,31
6	9,08	47,592	3,977	1,18
Total:		3048,451	338,189	100,00

ESI-MS *m/z*

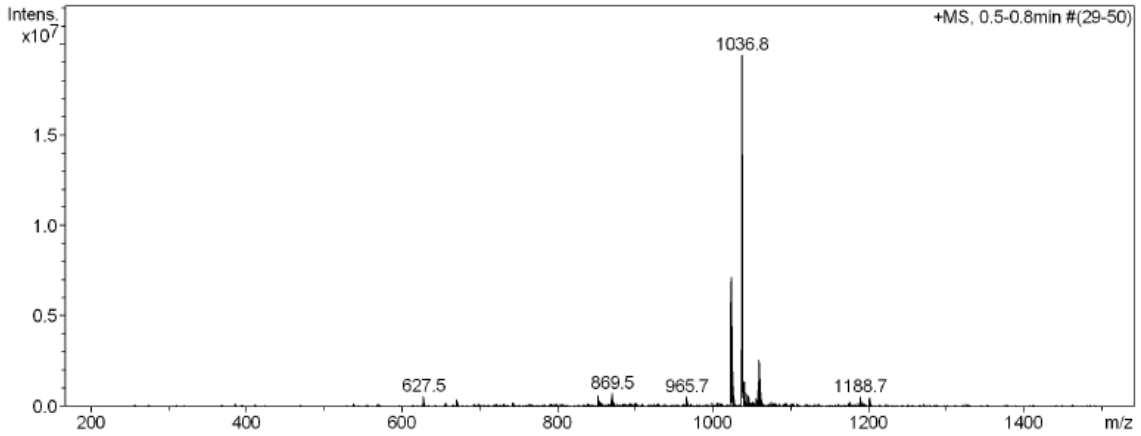

HRMS (ESI) *m/z*

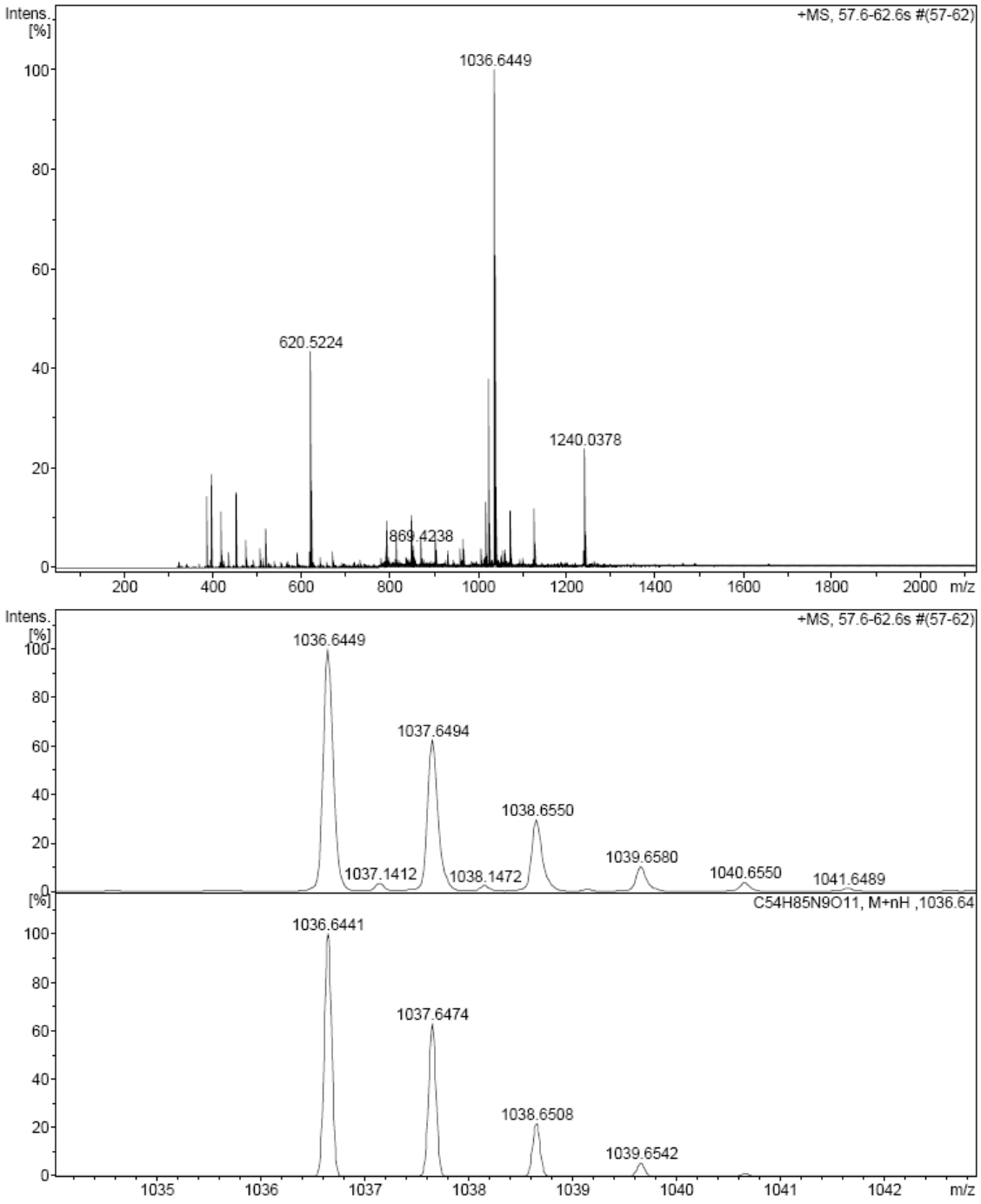

SUPPORTING INFORMATION CHAPTER 7

Solid-phase Synthesis of Analogues of the Northern and Southern Hemispheres of Aciculitins

Iteng Ng-Choi, Marta Planas* and Lidia Feliu*

TABLE OF CONTENTS

Copies of HPLC, MS and NMR spectra

1. Synthesis of amino acids

Boc-Tyr(3-B(OH)$_2$,Me)-OMe

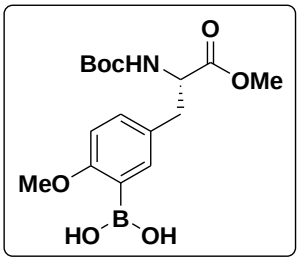

HPLC (λ = 220 nm)

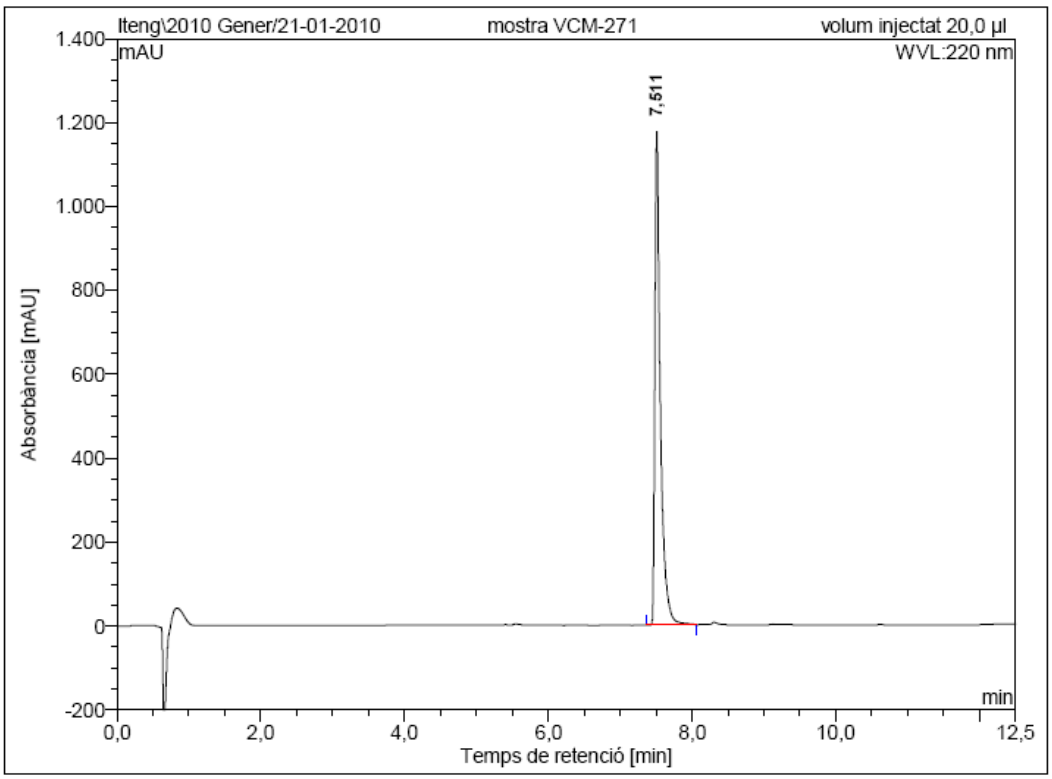

No.	Temps retenció min	alçada mAU	Area mAU*min	Area relativa %
1	7,51	1175,909	105,036	100,00
Total:		1175,909	105,036	100,00

^{1}H-NMR (400 MHz, $CDCl_3$) δ (ppm)

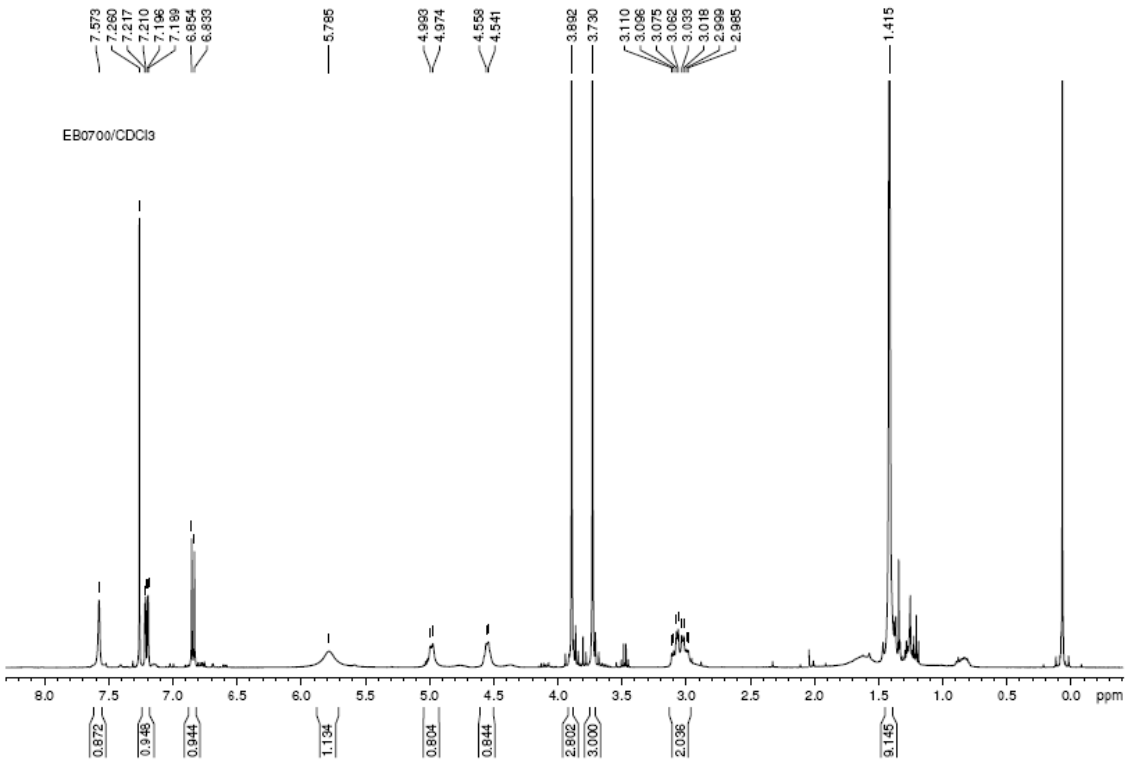

^{13}C-NMR (75 MHz, $CDCl_3$) δ (ppm)

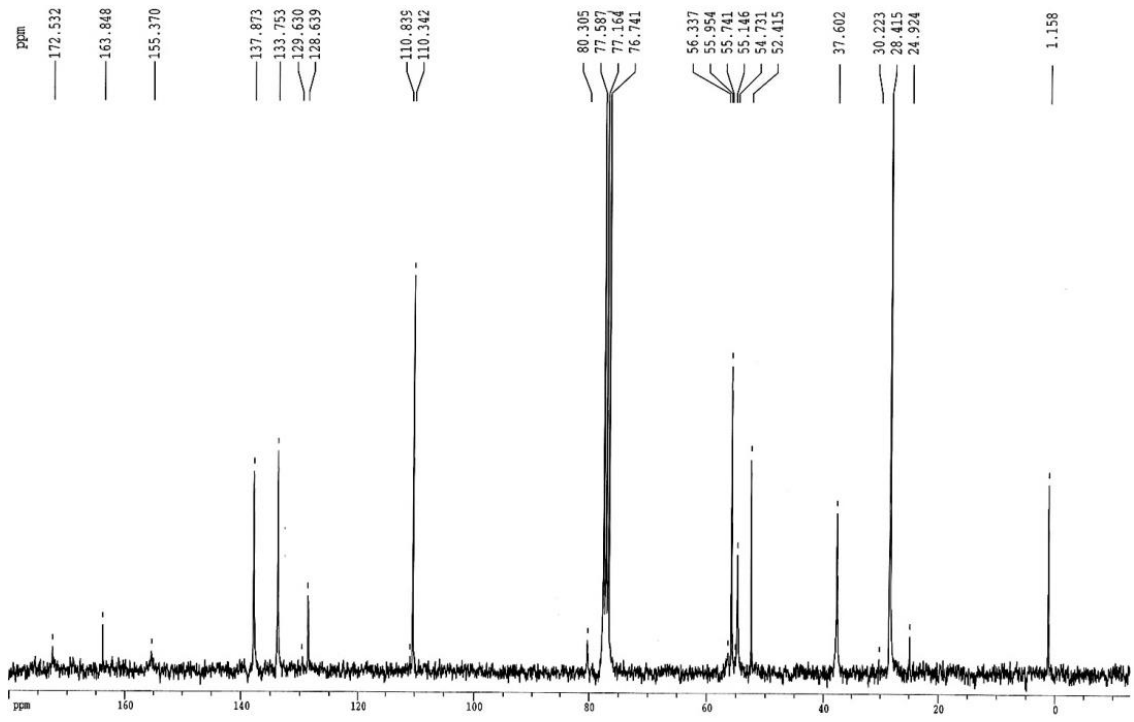

Boc-Tyr(3-B(OH)$_2$,Me)-OH

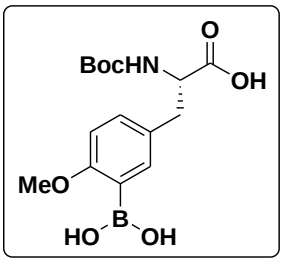

HPLC (λ = 220 nm)

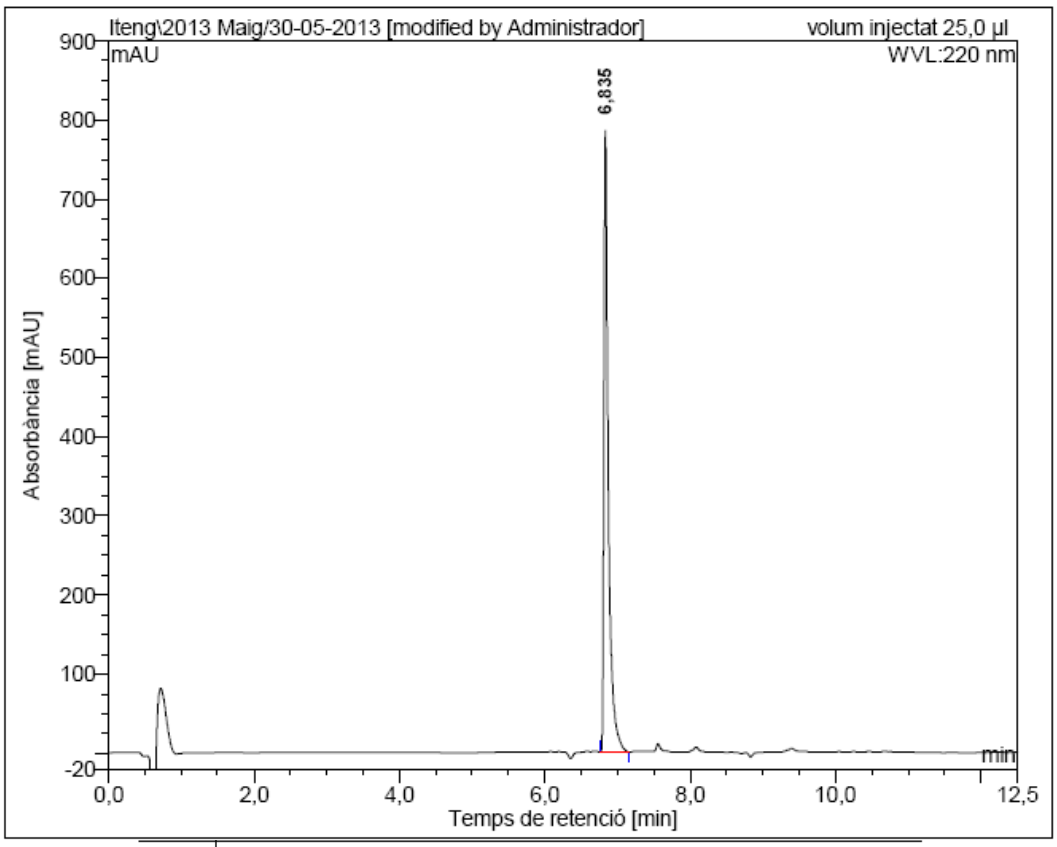

No.	Temps retenció min	alçada mAU	Area mAU*min	Area relativa %
1	6,84	785,715	55,818	100,00
Total:		785,715	55,818	100,00

^{1}H-NMR (400 MHz, $CDCl_3$) δ (ppm)

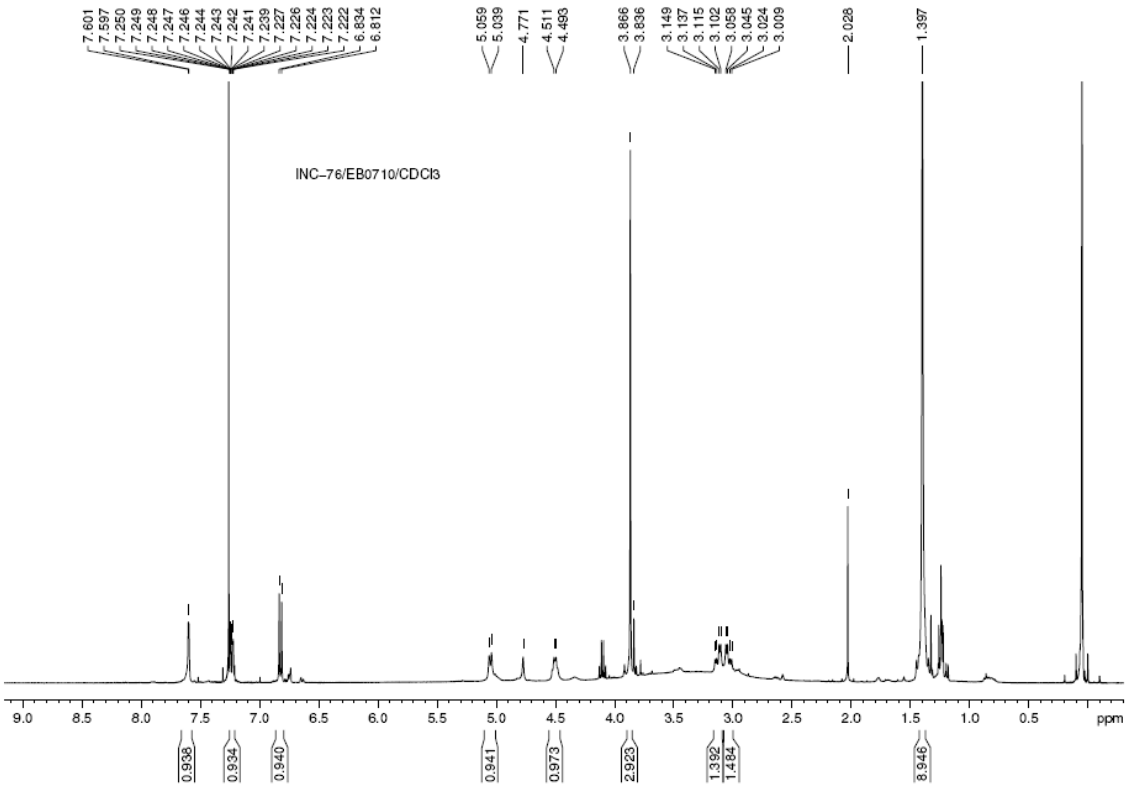

^{13}C-NMR (75 MHz, $CDCl_3$) δ (ppm)

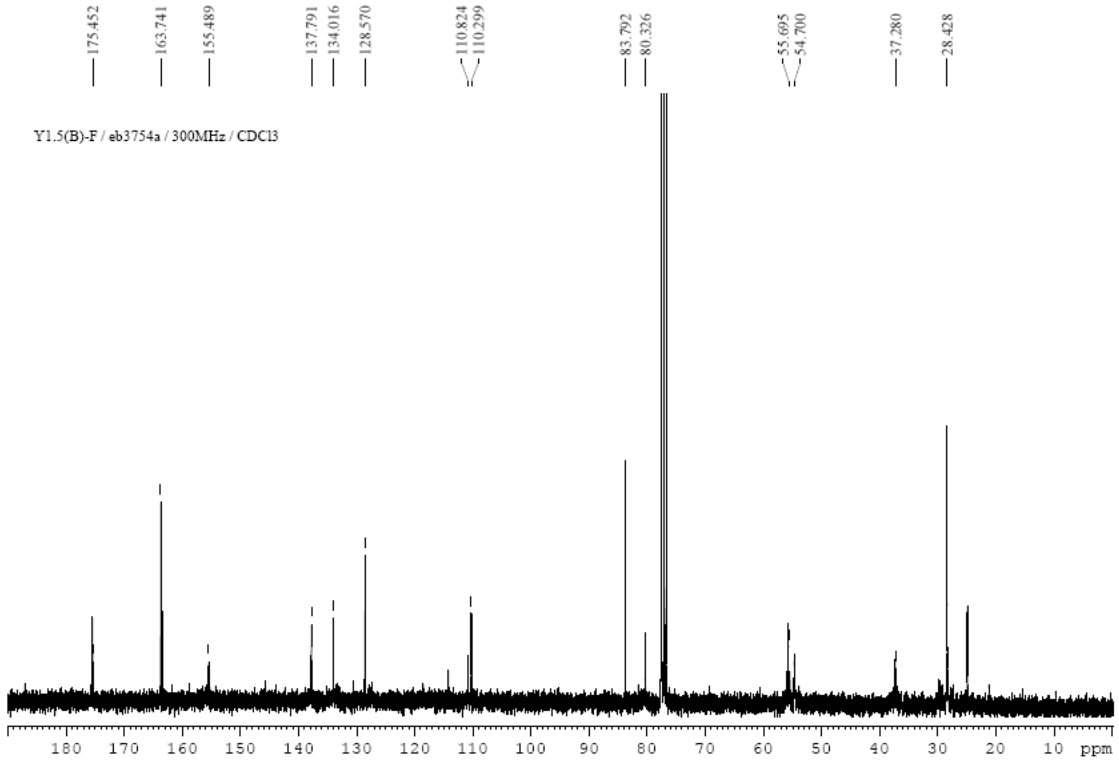

2. Linear peptides containing a 5-bromohistidine at the C-terminus

H-Tyr(3-B(OH)$_2$,Me)-Ala-Gln-Gly-Gln-His(5-Br)-βAla-NH$_2$ (5) from resin 4

HPLC (λ = 220 nm)

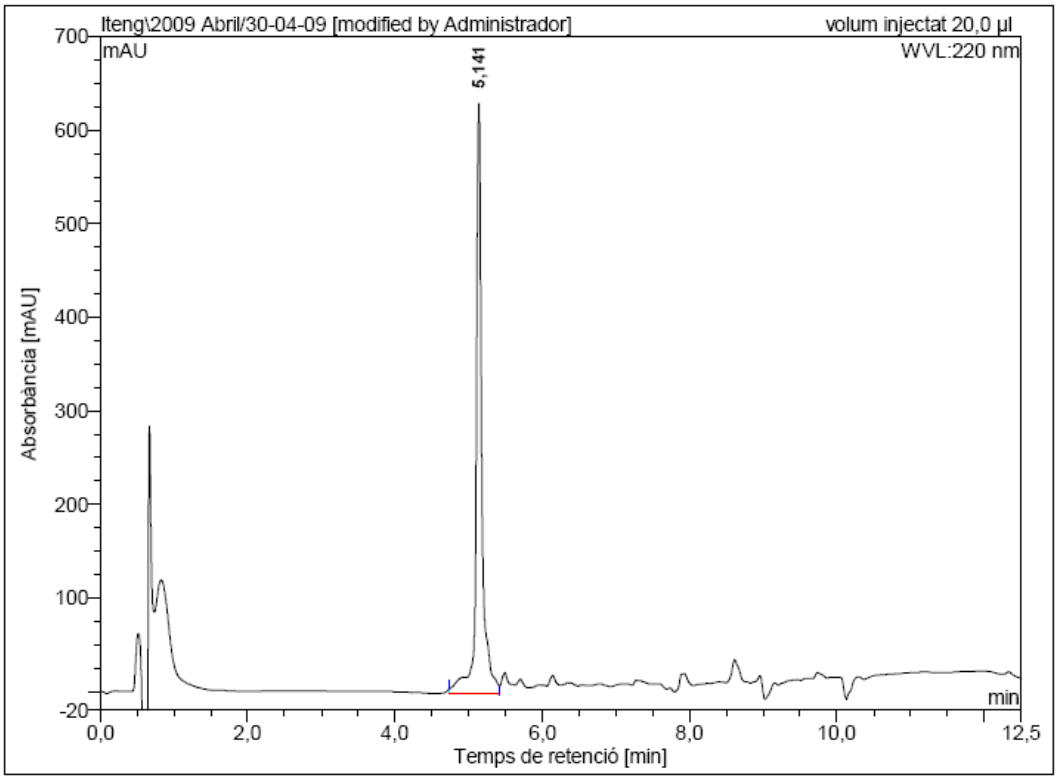

No.	Temps retenció min	alçada mAU	Area mAU*min	Area relativa %
1	5,14	630,701	57,783	100,00
Total:		630,701	57,783	100,00

ESI-MS *m/z*

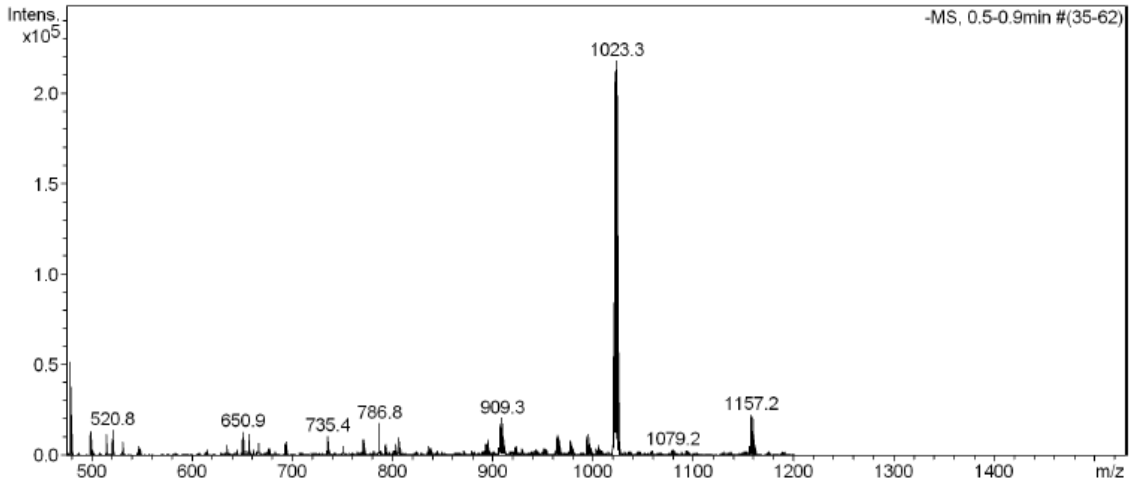

H-Tyr(3-B(OH)$_2$,Me)-Ala-Gln-Gly-Gln-His(5-Br)-βAla-NH$_2$ (5) from resin 7

HPLC (λ = 220 nm)

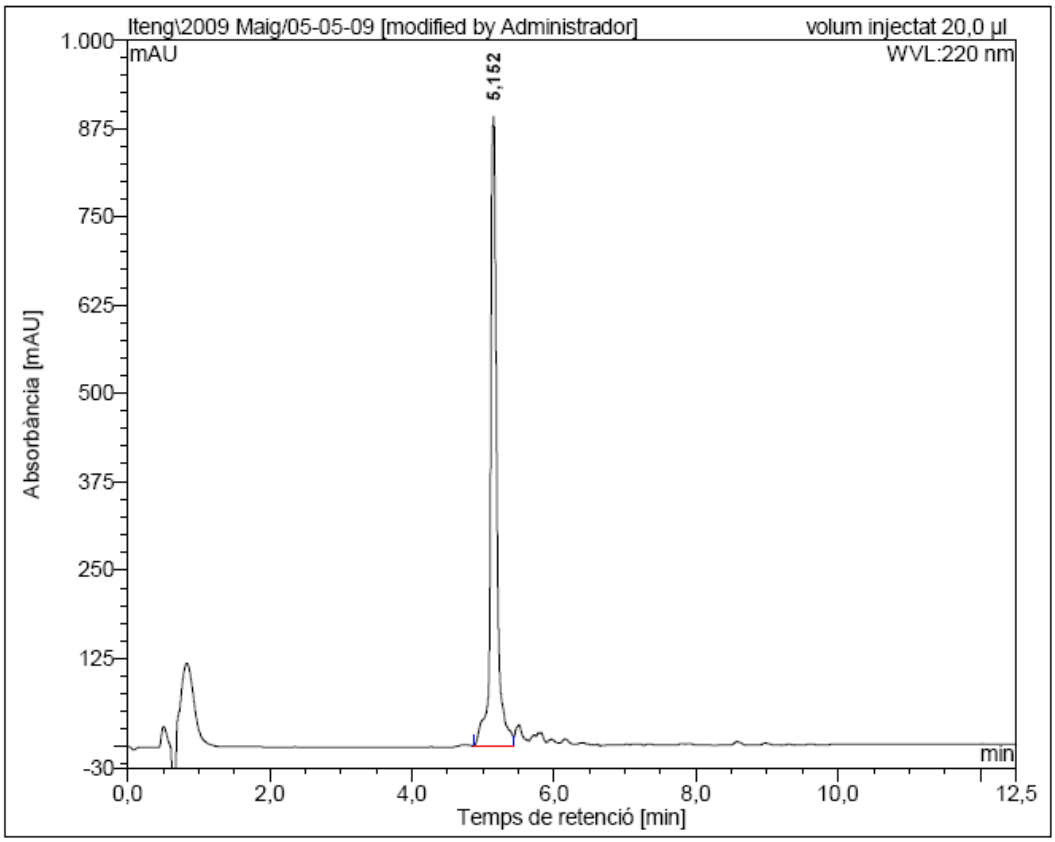

No.	Temps retenció min	alçada mAU	Area mAU*min	Area relativa %
1	5,15	890,111	91,360	100,00
Total:		890,111	91,360	100,00

ESI-MS *m/z*

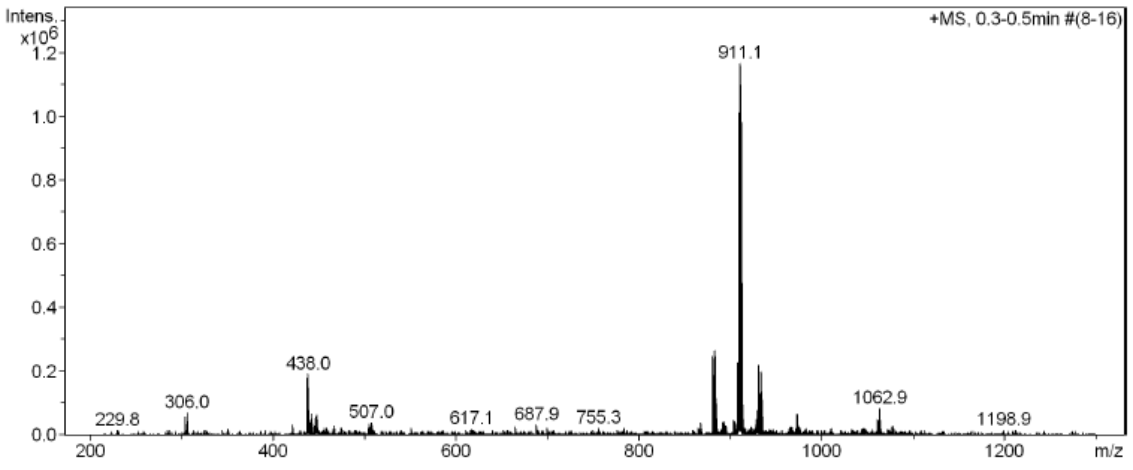

H-Tyr(3-B(OH)$_2$,Me)-Ala-D-Glu-Gly-D-Glu-His(5-Br)-βAla-NH$_2$ from resin 9

HPLC (λ = 220 nm)

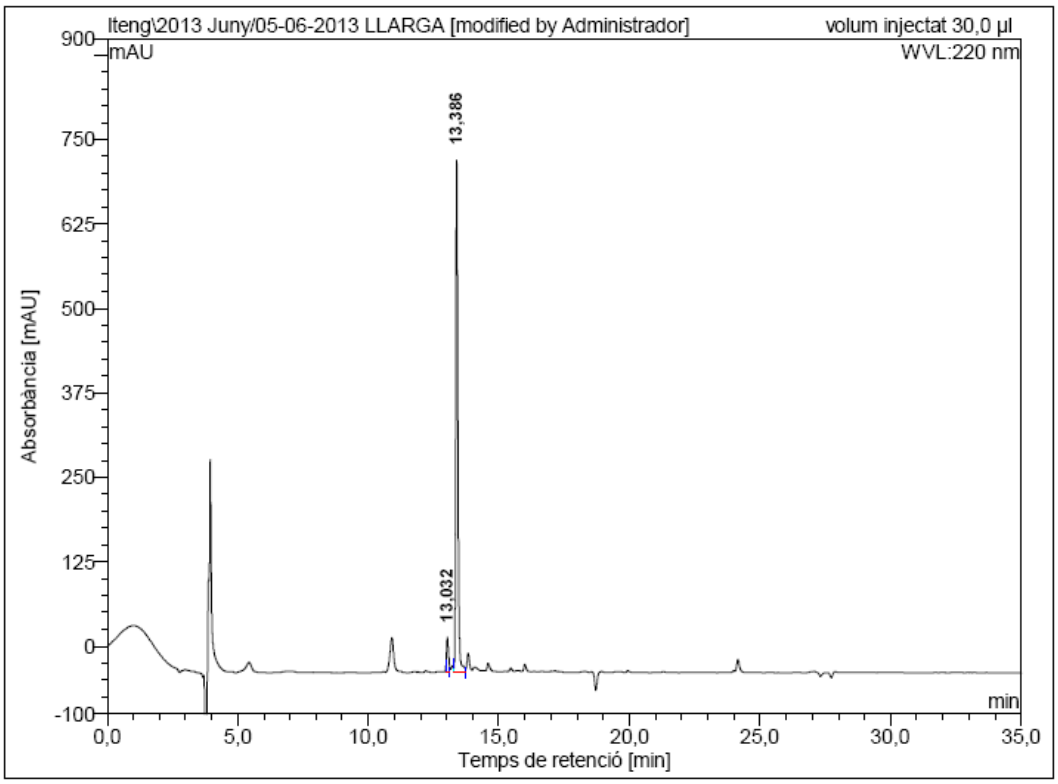

No.	Temps retenció min	alçada mAU	Area mAU*min	Area relativa %
1	13,03	50,576	4,405	5,82
2	13,39	757,020	71,262	94,18
Total:		807,596	75,667	100,00

ESI-MS *m/z*

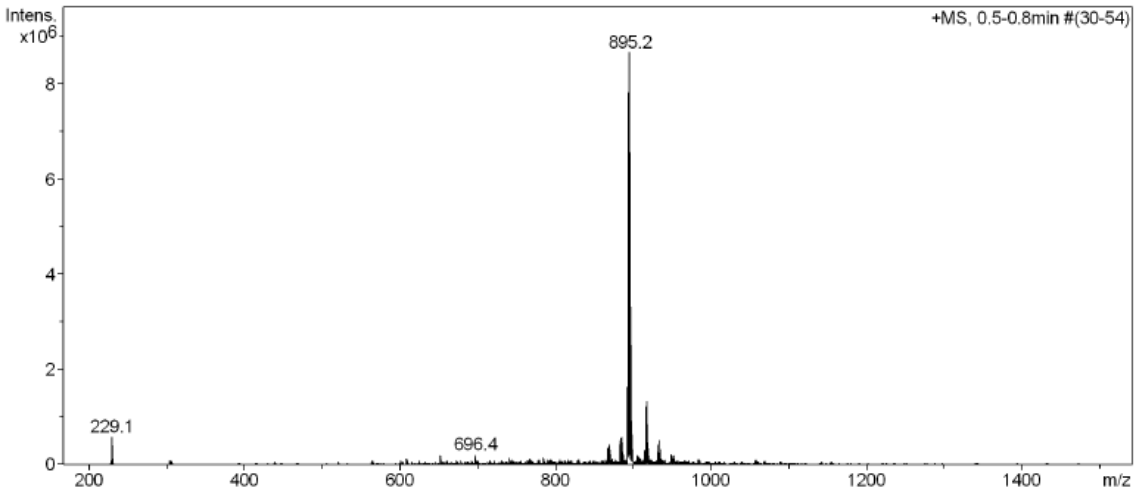

3. Linear peptides containing a 5-bromohistidine at the N-terminus

Fmoc-βAla-Thr-Tyr(3-I,Me)-Ala-Gln-NH_2

HPLC (λ = 220 nm)

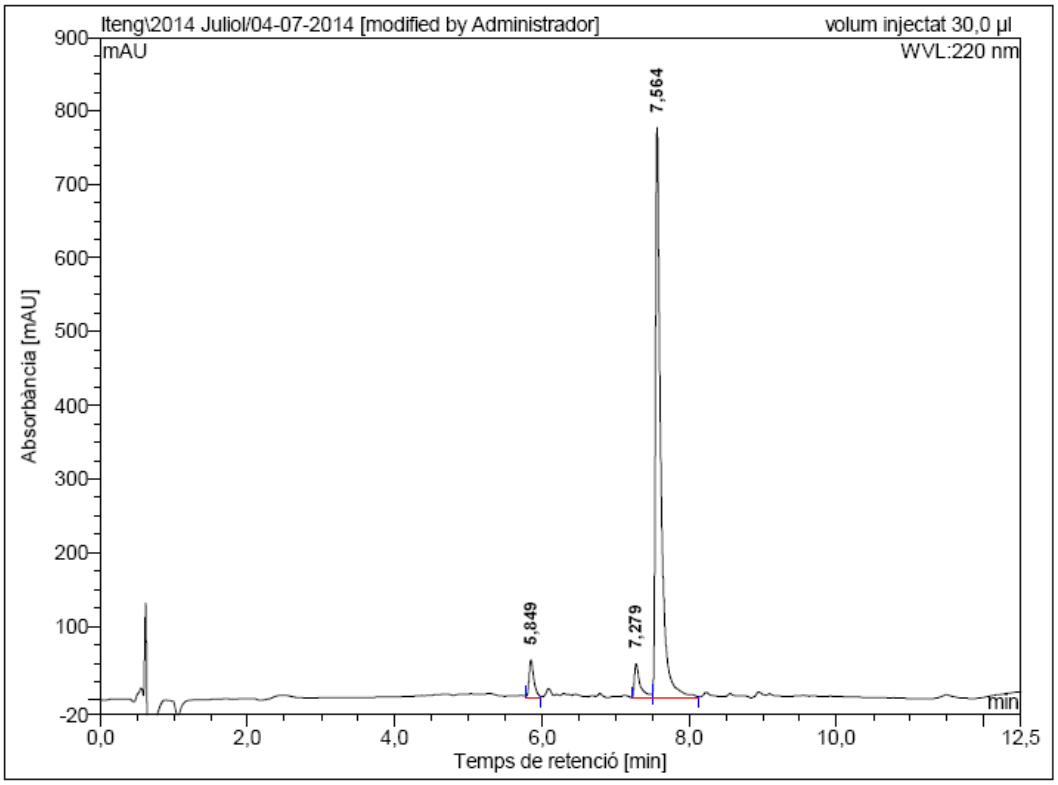

No.	Temps retenció min	alçada mAU	Area mAU*min	Area relativa %
1	5,85	51,496	3,924	5,37
2	7,28	45,732	4,162	5,70
3	7,56	774,233	64,951	88,93
Total:		871,461	73,037	100,00

H-βAla-Thr-Tyr(3-I,Me)-Ala-Gln-NH_2 from resin 11

HPLC (λ = 220 nm)

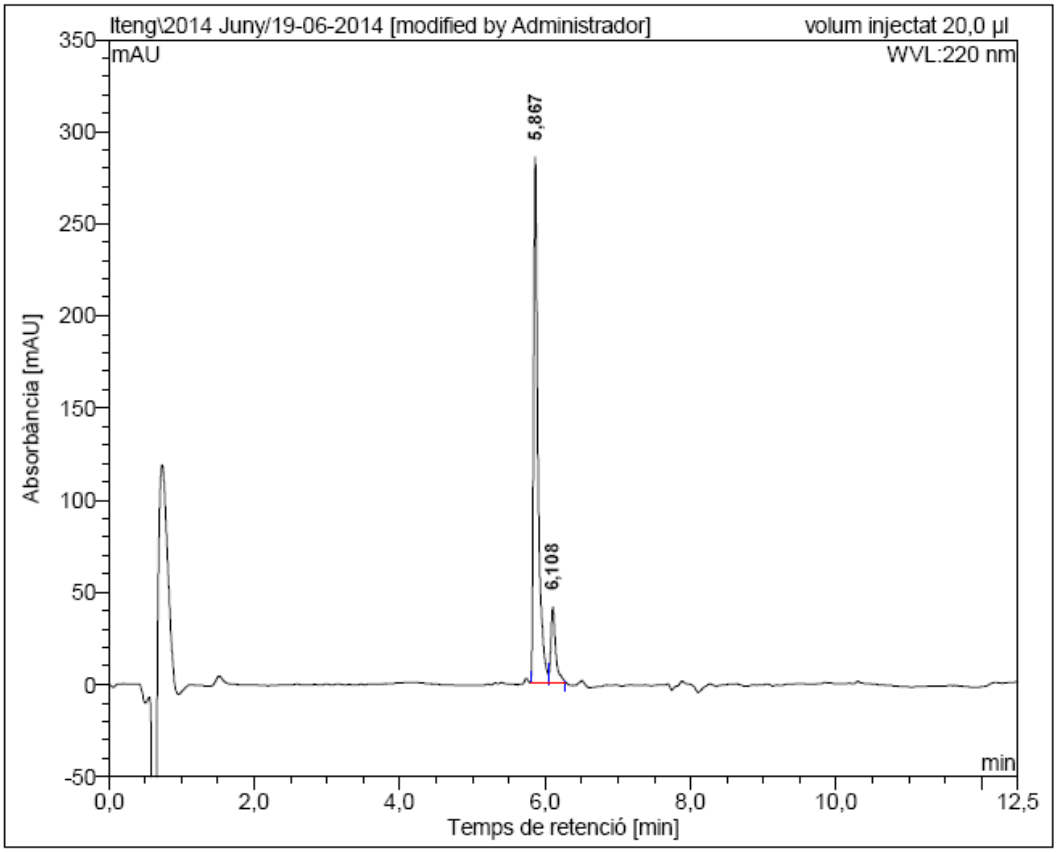

No.	mps retenc min	alçada mAU	Area mAU*min	Area relativa %
1	5,87	285,117	20,257	86,74
2	6,11	40,756	3,096	13,26
Total:		325,874	23,353	100,00

H-βAla-Thr-Tyr(3-B(OH)$_2$,Me)-Ala-Gln-NH$_2$ from resin 12

HPLC (λ = 220 nm)

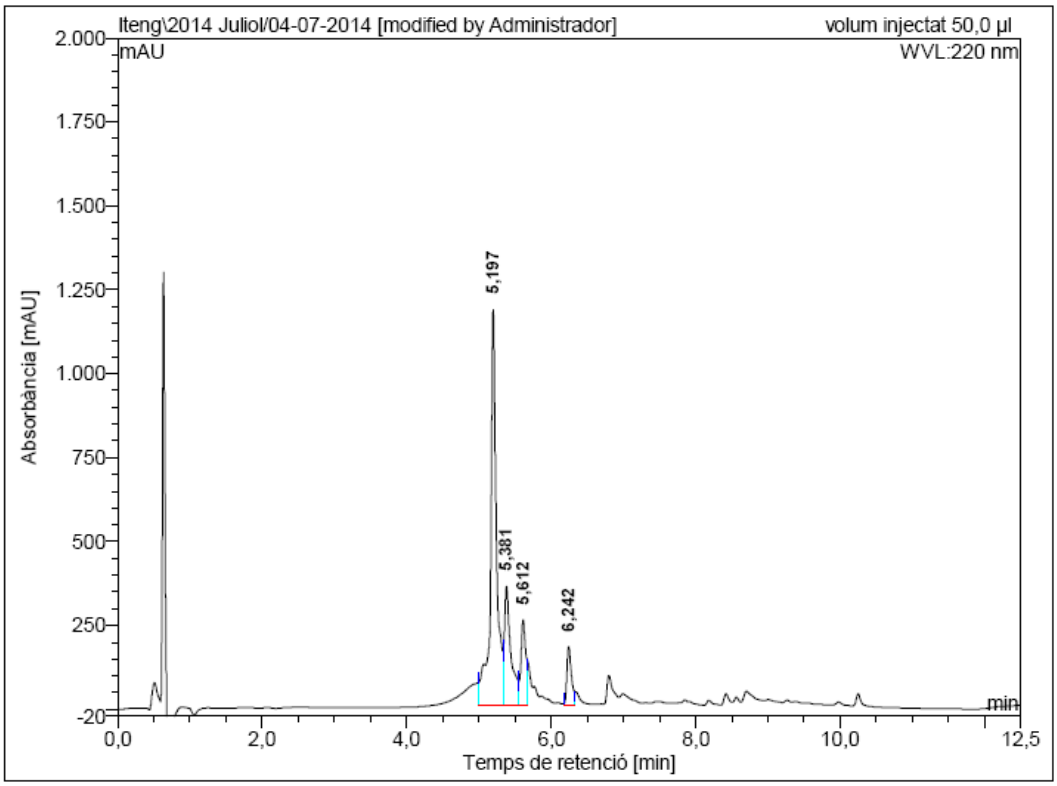

No.	Temps retenció min	alçada mAU	Area mAU*min	Area relativa %
1	5,20	1176,839	112,987	62,06
2	5,38	351,559	38,061	20,90
3	5,61	252,385	18,738	10,29
4	6,24	172,306	12,283	6,75
Total:		1953,089	182,069	100,00

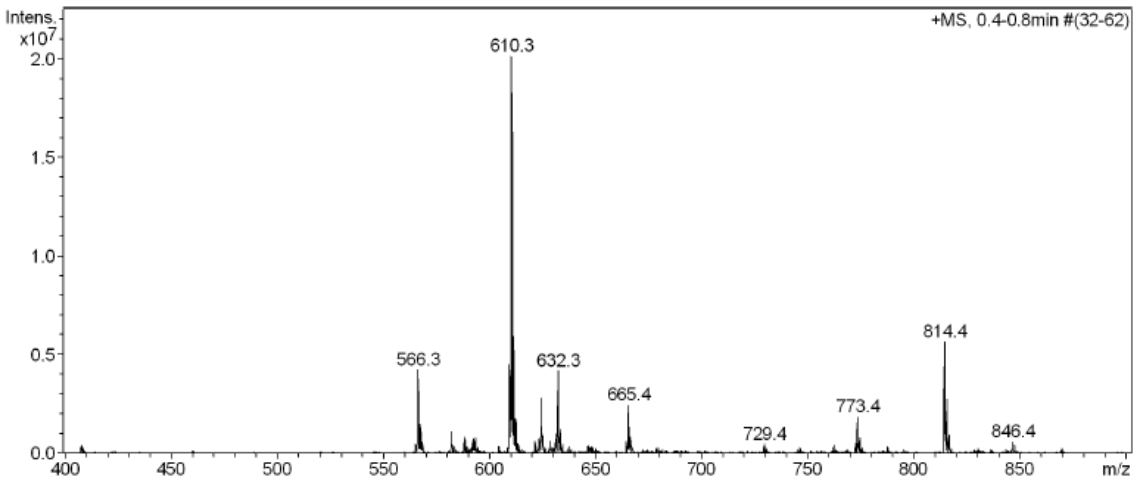

H-His(5-Br)-βAla-Thr-Tyr(3-B(OH)$_2$,Me)-Ala-Gln-NH$_2$ from resin 10

HPLC (λ = 220 nm)

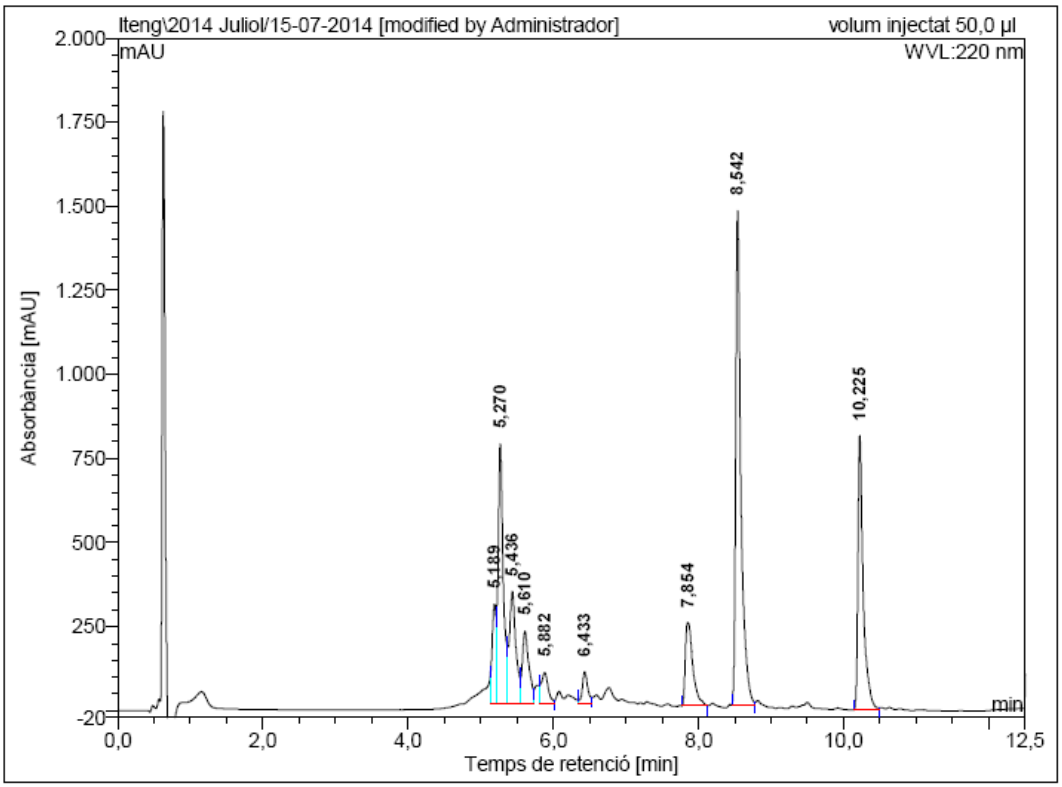

No.	Temps retenció min	alçada mAU	Area mAU*min	Area relativa %
1	5,19	296,410	18,218	4,75
2	5,27	773,653	66,725	17,41
3	5,44	333,803	34,388	8,97
4	5,61	215,616	22,862	5,97
5	5,88	92,718	10,782	2,81
6	6,43	94,594	8,324	2,17
7	7,85	246,677	29,195	7,62
8	8,54	1470,225	123,689	32,27
9	10,22	816,253	69,068	18,02
Total:		4339,949	383,251	100,00

ESI-MS *m/z*

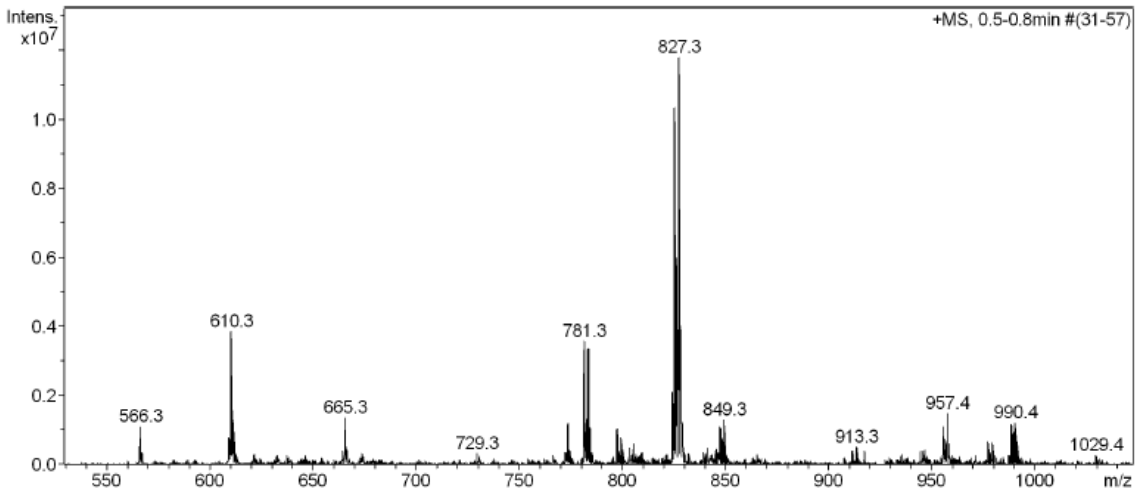
Intens.
x10^7
+MS, 0.5-0.8min #(31-57)
827.3
610.3
781.3
566.3
665.3
729.3
849.3
913.3
957.4
990.4
1029.4
1.0
0.8
0.6
0.4
0.2
0.0
550
600
650
700
750
800
850
900
950
1000
m/z

4. Biaryl cyclic peptides

Biaryl cyclic peptide 1

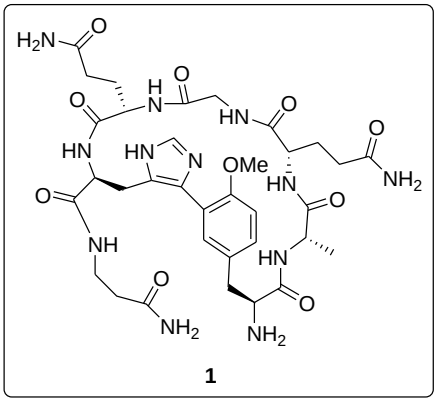

1

Crude peptide 1

T = 20 °C

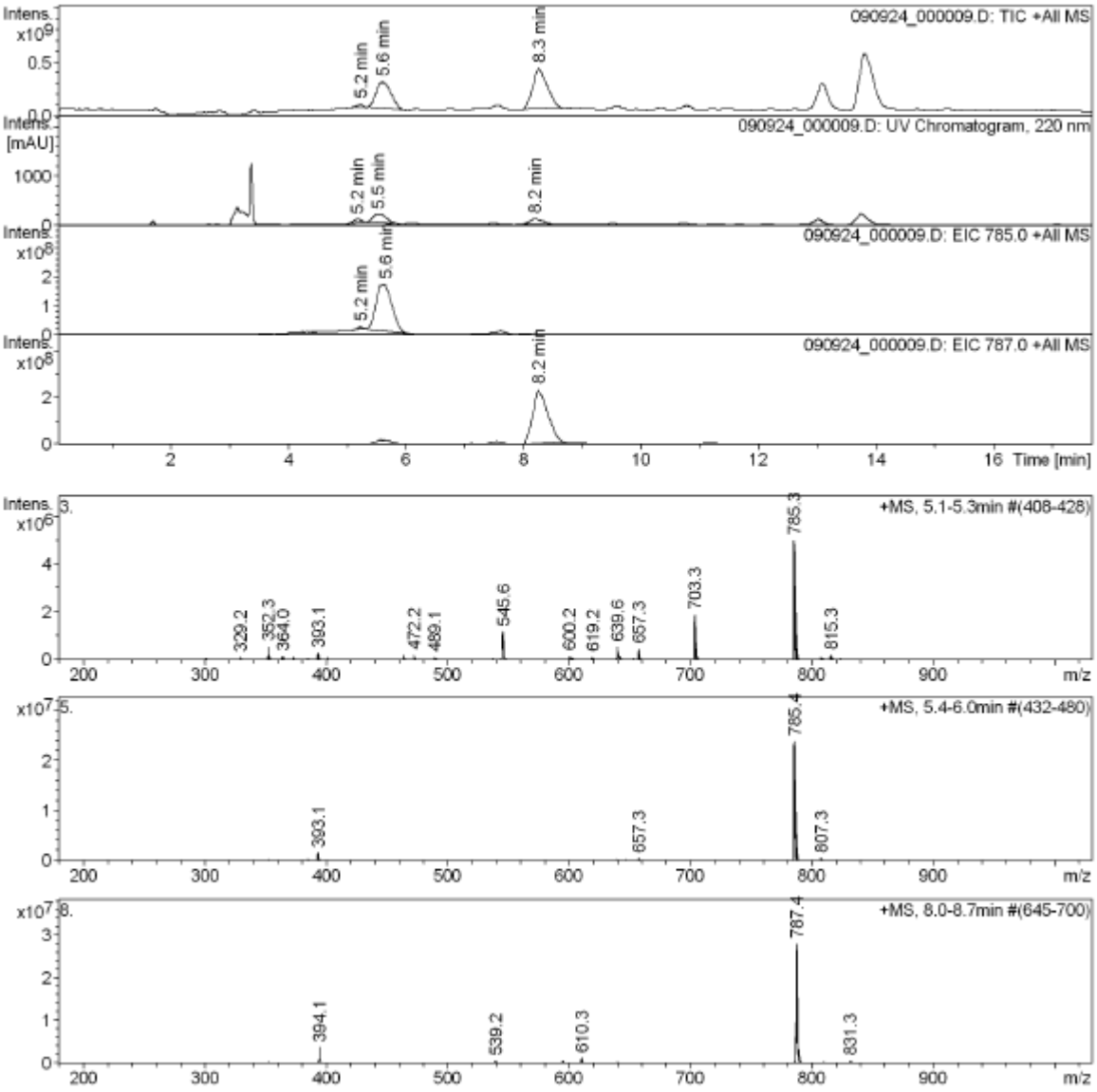

T = 25 ºC

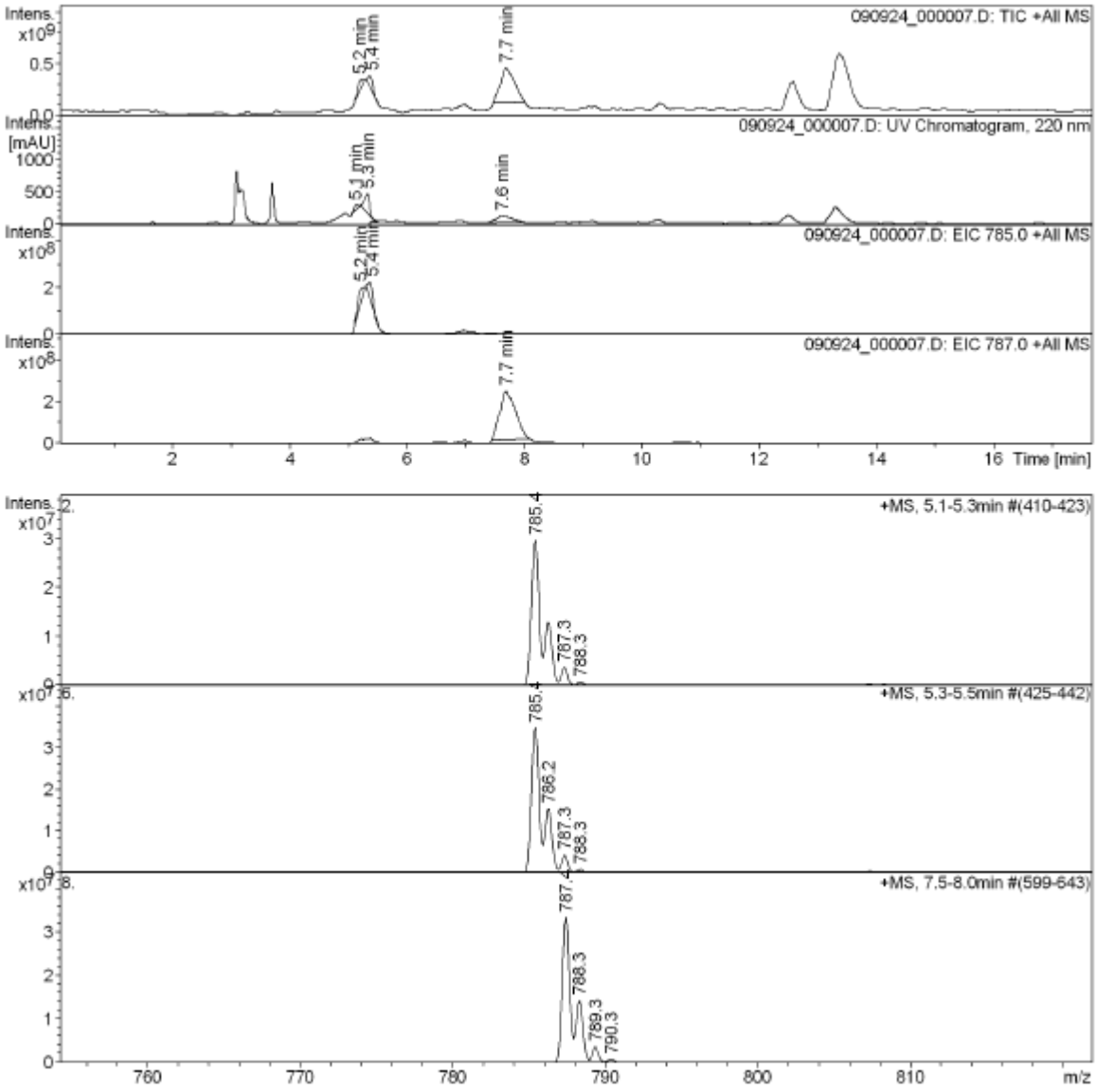
090924_000007.D: TIC +All MS
5.2 min
5.4 min
7.7 min
090924_000007.D: UV Chromatogram, 220 nm
5.1 min
5.3 min
7.6 min
090924_000007.D: EIC 785.0 +All MS
090924_000007.D: EIC 787.0 +All MS
Time [min]
+MS, 5.1-5.3min #(410-423)
+MS, 5.3-5.5min #(425-442)
+MS, 7.5-8.0min #(599-643)
m/z

T = 40 ºC

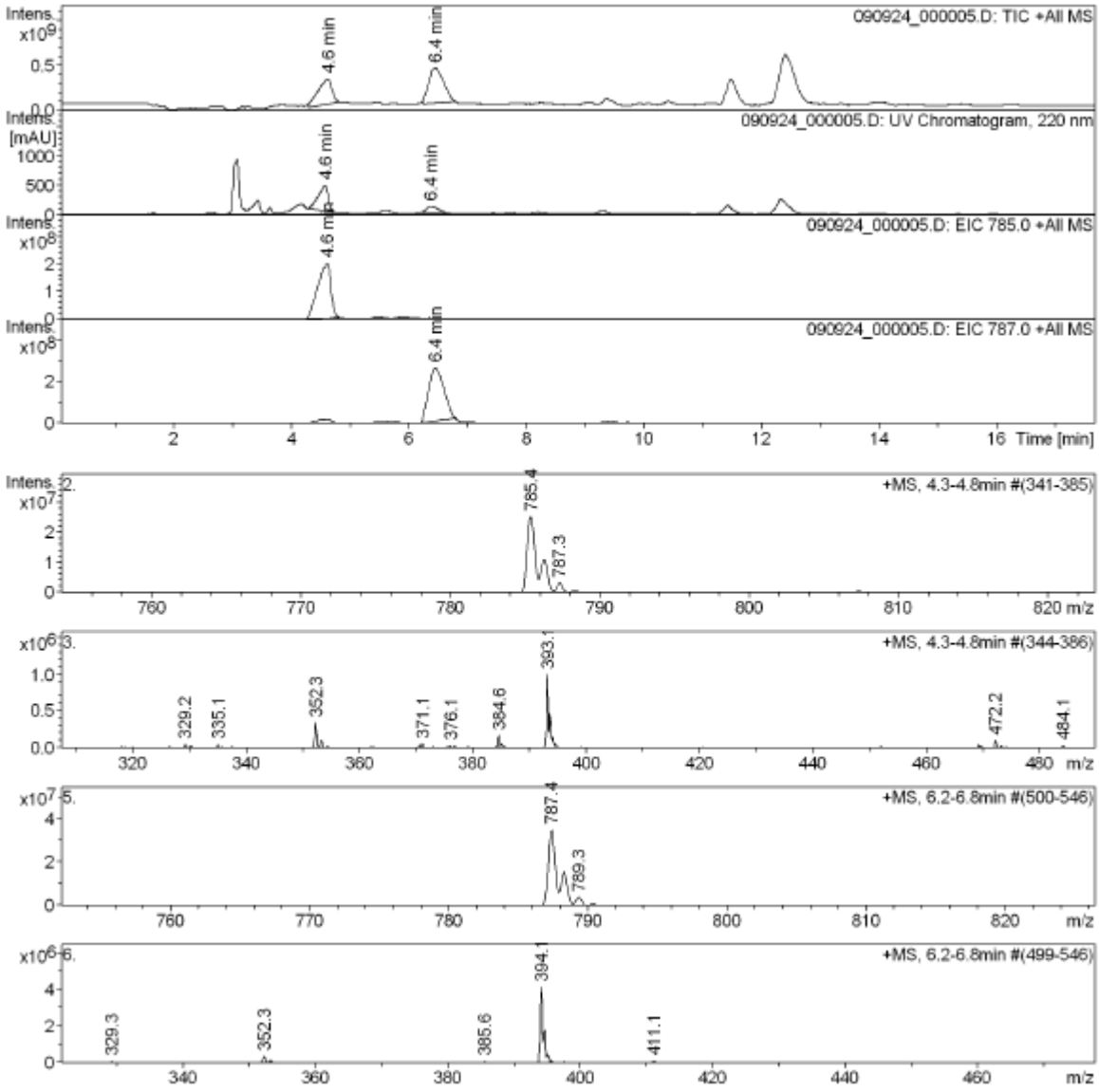
090924_000005.D: TIC +All MS
4.6 min
6.4 min
090924_000005.D: UV Chromatogram, 220 nm
090924_000005.D: EIC 785.0 +All MS
090924_000005.D: EIC 787.0 +All MS
Time [min]
+MS, 4.3-4.8min #(341-385)
785.4
787.3
+MS, 4.3-4.8min #(344-386)
329.2
335.1
352.3
371.1
376.1
384.6
393.1
472.2
484.1
+MS, 6.2-6.8min #(500-546)
787.4
789.3
+MS, 6.2-6.8min #(499-546)
329.3
352.3
385.6
394.1
411.1
m/z

T = 60 °C

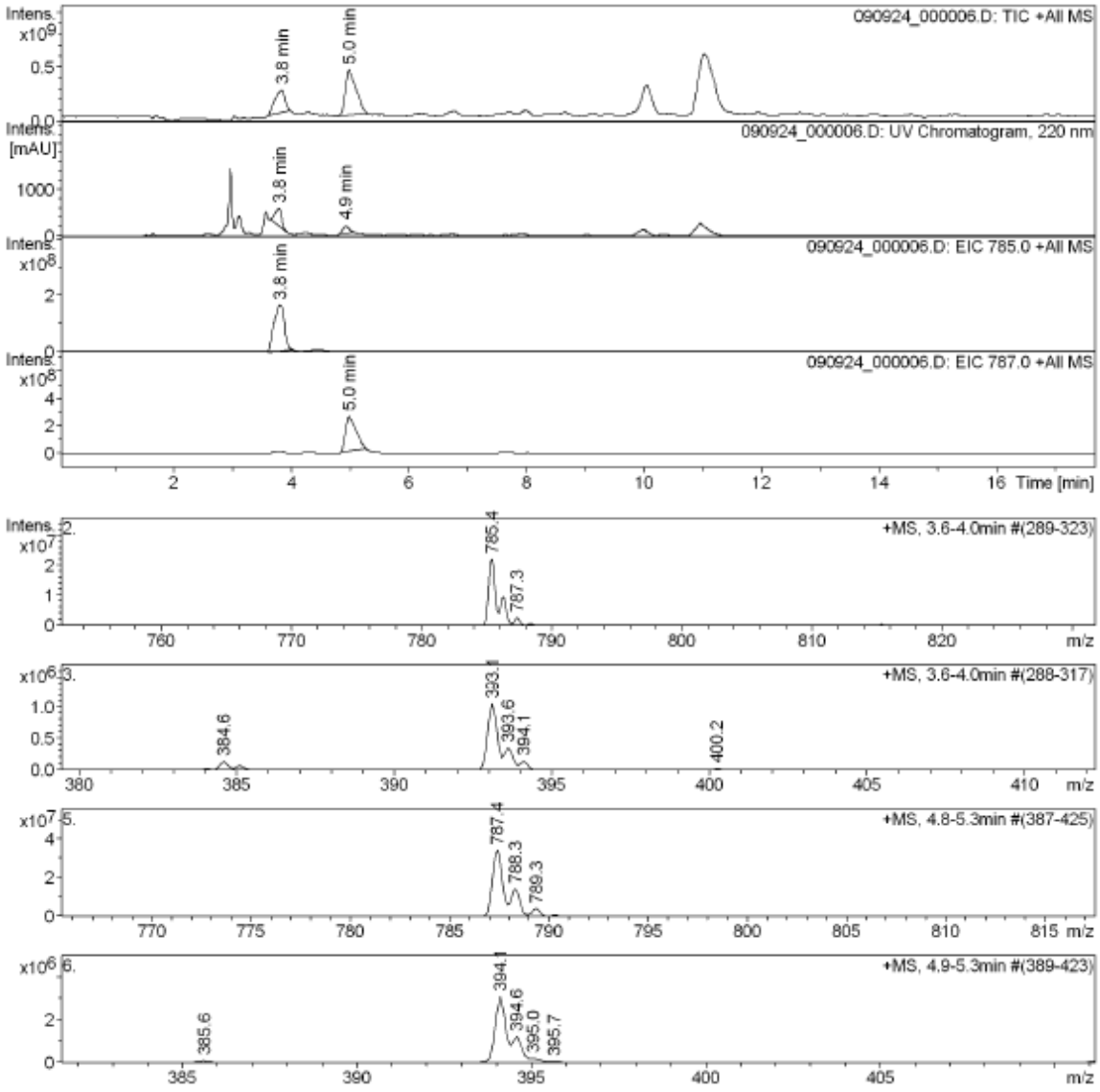
090924_000006.D: TIC +All MS
3.8 min
5.0 min
090924_000006.D: UV Chromatogram, 220 nm
3.8 min
4.9 min
090924_000006.D: EIC 785.0 +All MS
3.8 min
090924_000006.D: EIC 787.0 +All MS
5.0 min
Time [min]
+MS, 3.6-4.0min #(289-323)
785.4
787.3
+MS, 3.6-4.0min #(288-317)
384.6
393.1
393.6
394.1
400.2
+MS, 4.8-5.3min #(387-425)
787.4
788.3
789.3
+MS, 4.9-5.3min #(389-423)
385.6
394.1
394.6
395.0
395.7
m/z

Monomode CEM microwave

HPLC (λ = 220 nm)

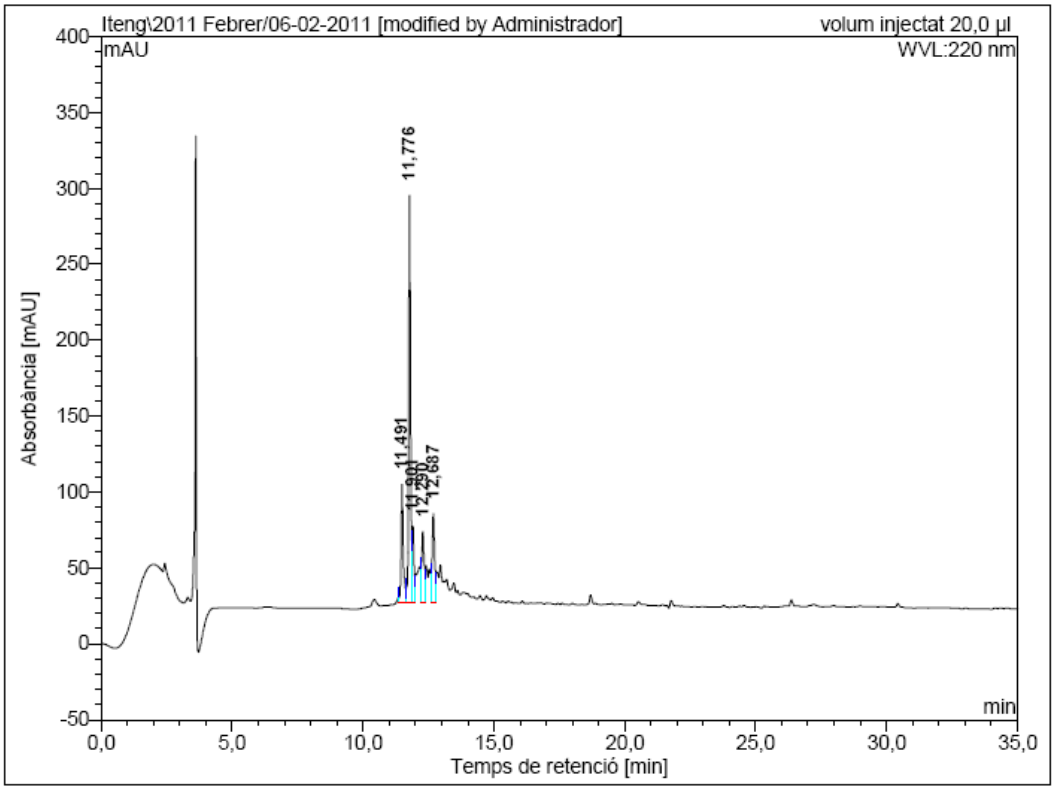

No.	Temps retenció min	alçada mAU	Area mAU*min	Area relativa %
1	11,49	77,567	7,666	16,69
2	11,78	268,067	21,927	47,73
3	11,90	50,339	4,230	9,21
4	12,29	46,884	5,216	11,35
5	12,69	58,519	6,898	15,02
Total:		501,376	45,938	100,00

ESI-MS *m/z*

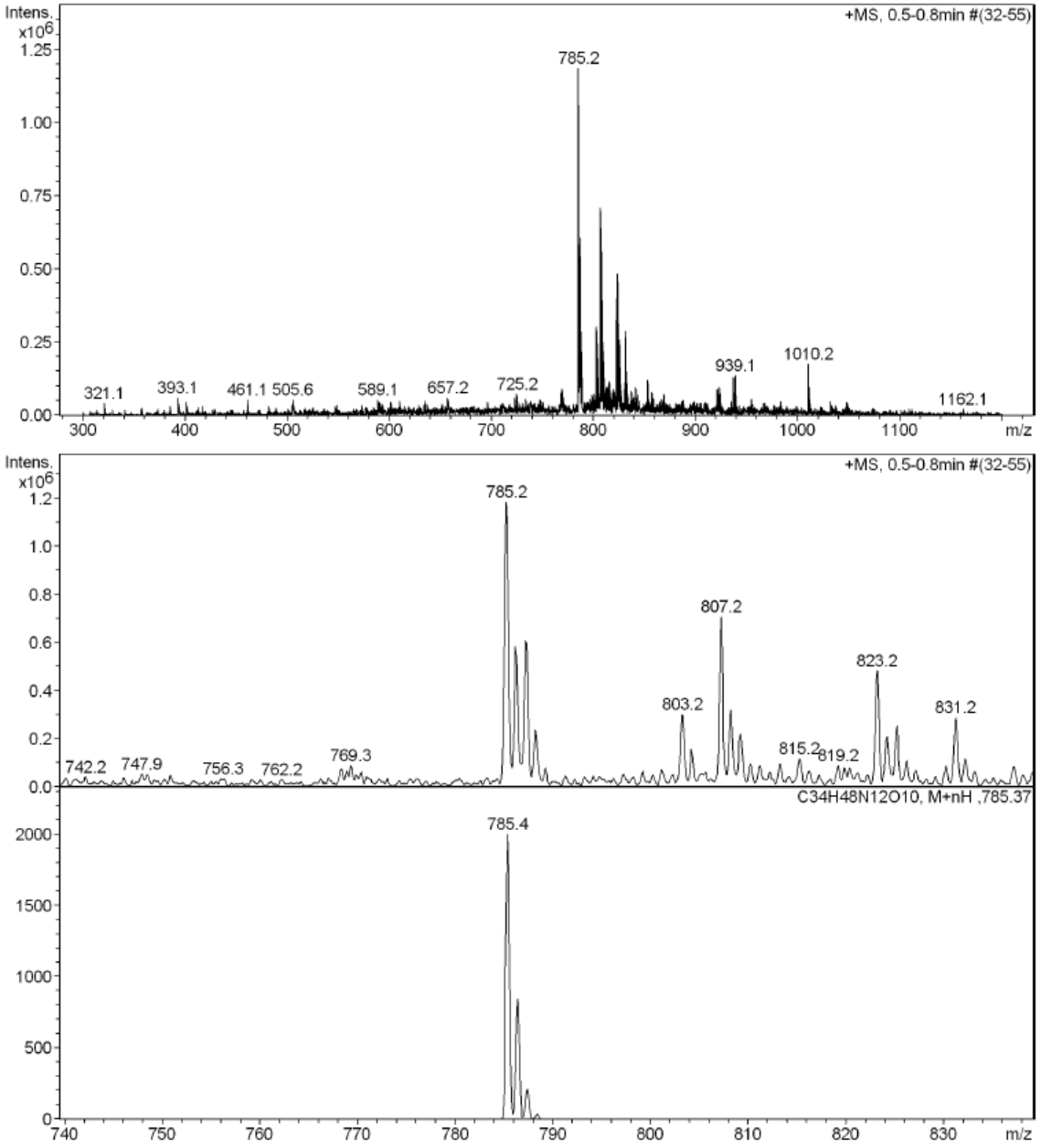
Intens.
x10^6
+MS, 0.5-0.8min #(32-55)
785.2
939.1
1010.2
321.1
393.1
461.1
505.6
589.1
657.2
725.2
1162.1
m/z
807.2
823.2
803.2
831.2
742.2
747.9
756.3
762.2
769.3
815.2
819.2
C34H48N12O10, M+nH ,785.37
785.4

Purified peptide 1

HPLC (λ = 220 nm)

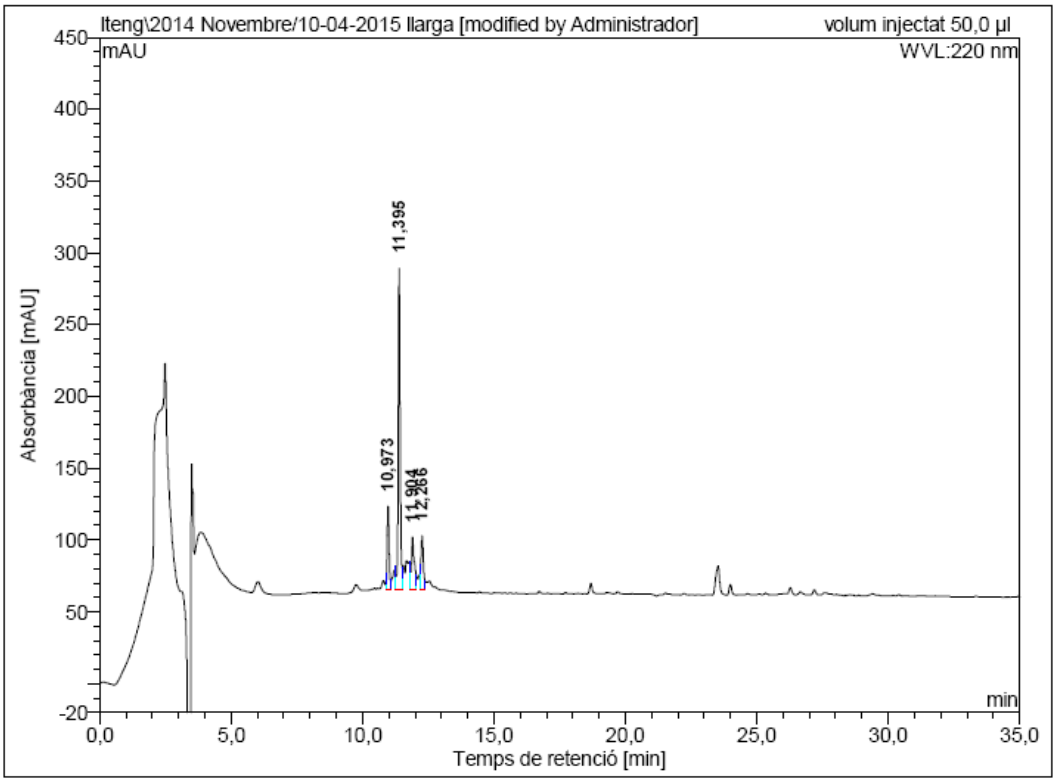

No.	Temps retenció min	alçada mAU	Area mAU*min	Area relativa %
1	10,97	58,212	4,718	14,58
2	11,39	224,171	19,010	58,73
3	11,90	36,999	4,627	14,30
4	12,27	37,877	4,012	12,40
Total:		357,259	32,366	100,00

ESI-MS *m/z*

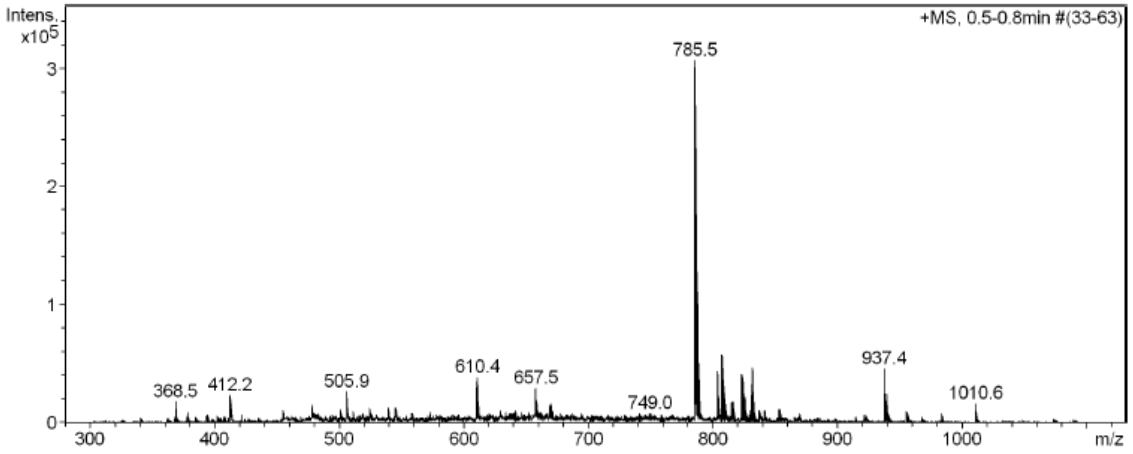

HRMS (ESI) *m/z*

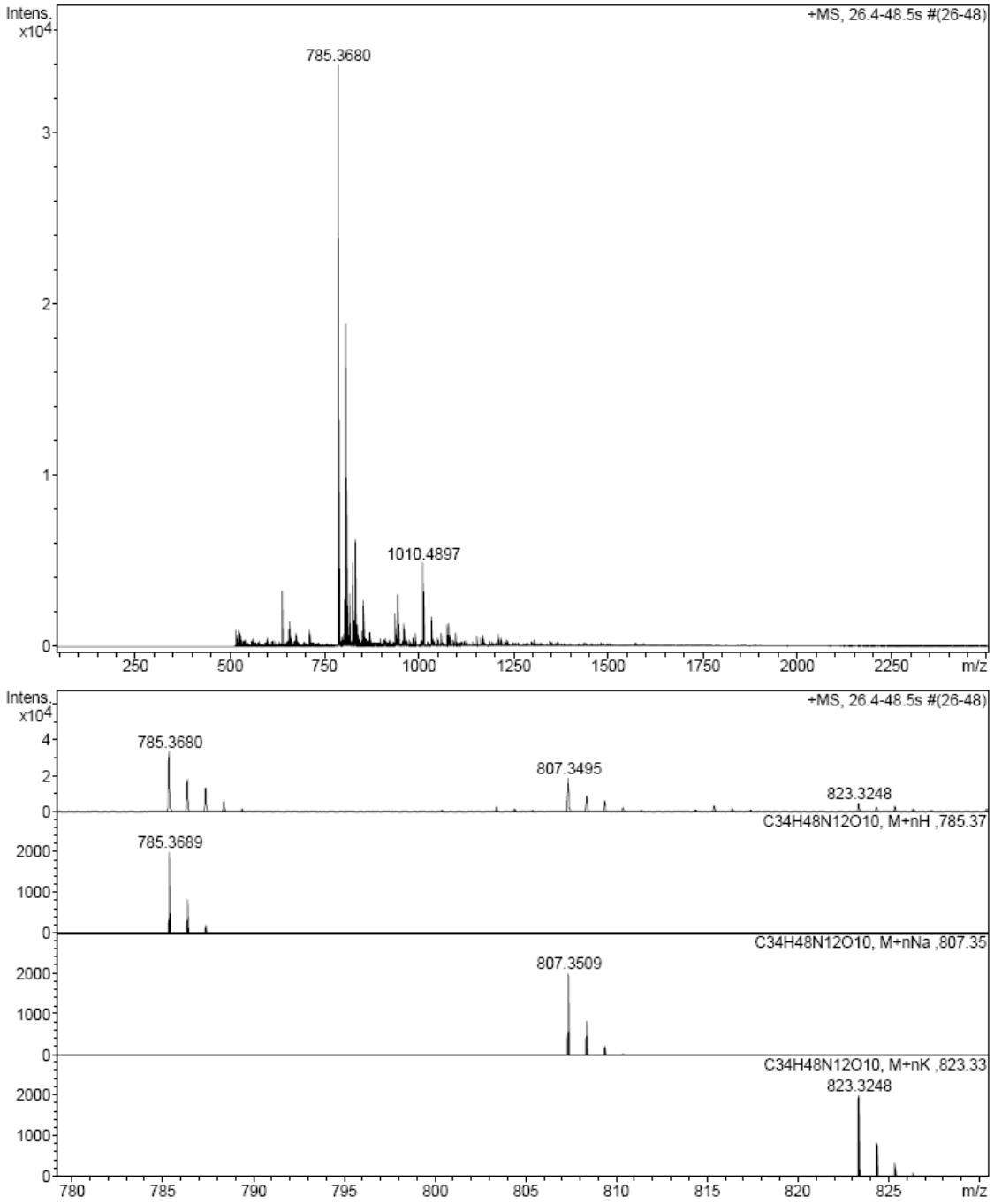
Intens.
x10^4
+MS, 26.4-48.5s #(26-48)
785.3680
1010.4897
m/z
785.3680
807.3495
823.3248
C34H48N12O10, M+nH ,785.37
785.3689
C34H48N12O10, M+nNa ,807.35
807.3509
C34H48N12O10, M+nK ,823.33
823.3248

Biaryl cyclic peptide 2

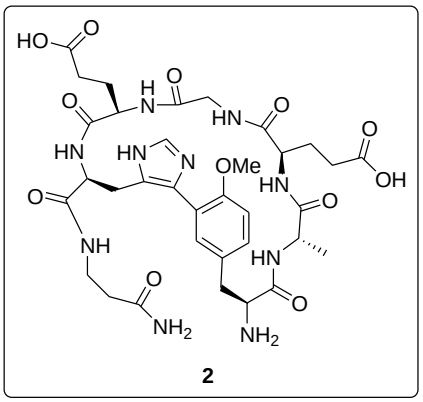

2

Crude peptide 2

HPLC (λ = 220 nm)

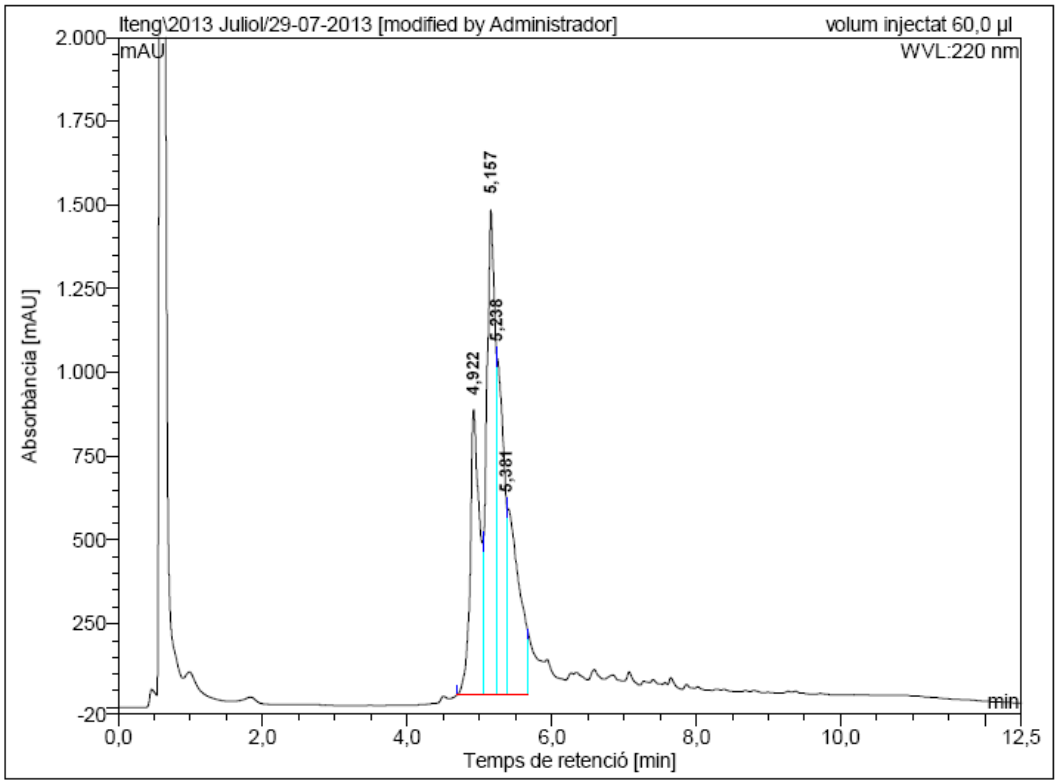

No.	Temps retenció min	alçada mAU	Area mAU*min	Area relativa %
1	4,92	850,878	127,271	23,17
2	5,16	1447,020	196,795	35,82
3	5,24	1006,171	116,870	21,27
4	5,38	558,750	108,464	19,74
Total:		3862,819	549,401	100,00

ESI-MS *m/z*

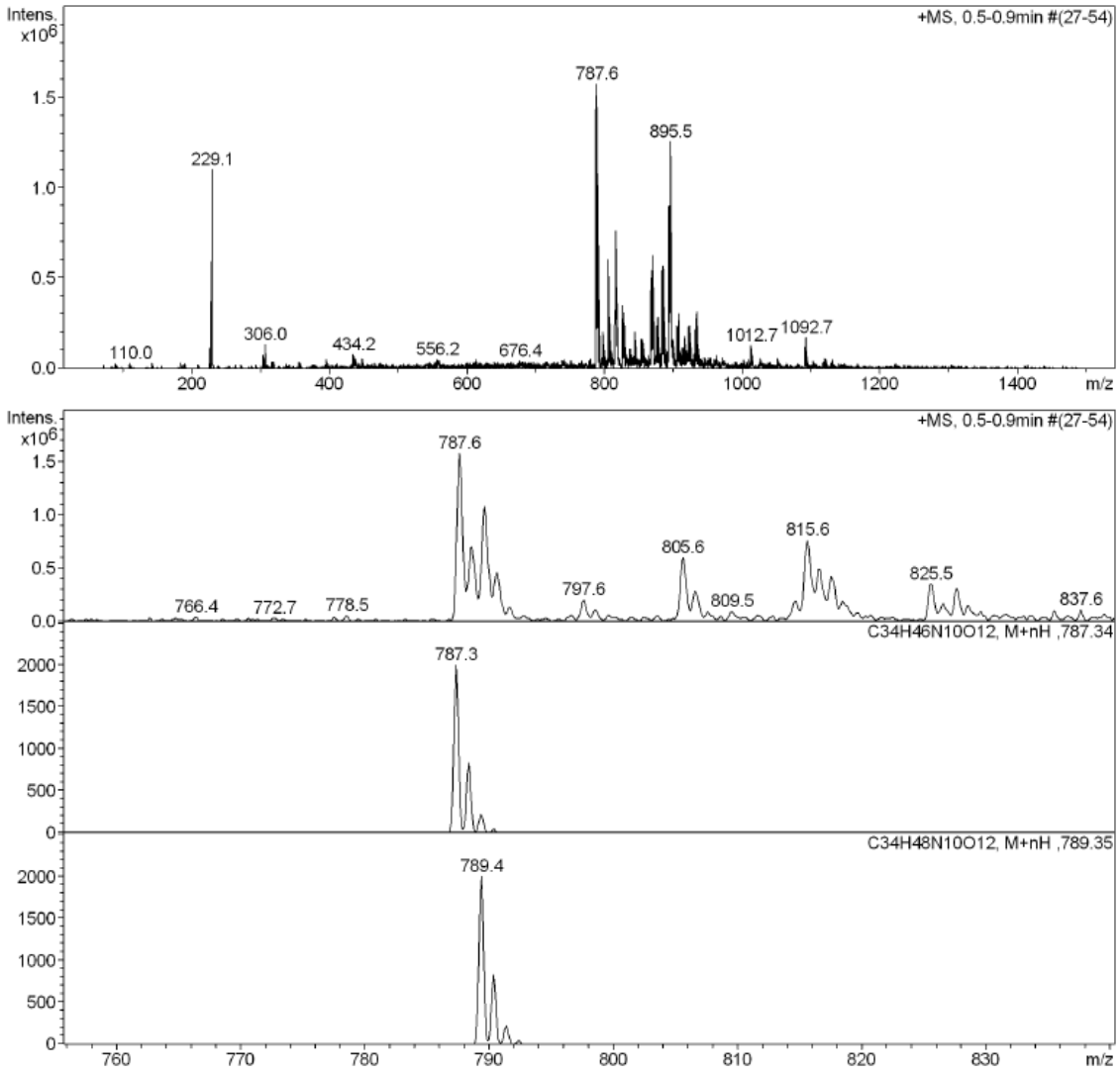
Intens.
x10^6
+MS, 0.5-0.9min #(27-54)
787.6
895.5
229.1
110.0
306.0
434.2
556.2
676.4
1012.7
1092.7
m/z
766.4
772.7
778.5
797.6
805.6
809.5
815.6
825.5
837.6
C34H46N10O12, M+nH ,787.34
787.3
C34H48N10O12, M+nH ,789.35
789.4

Purified peptide 2

HPLC (λ = 220 nm)

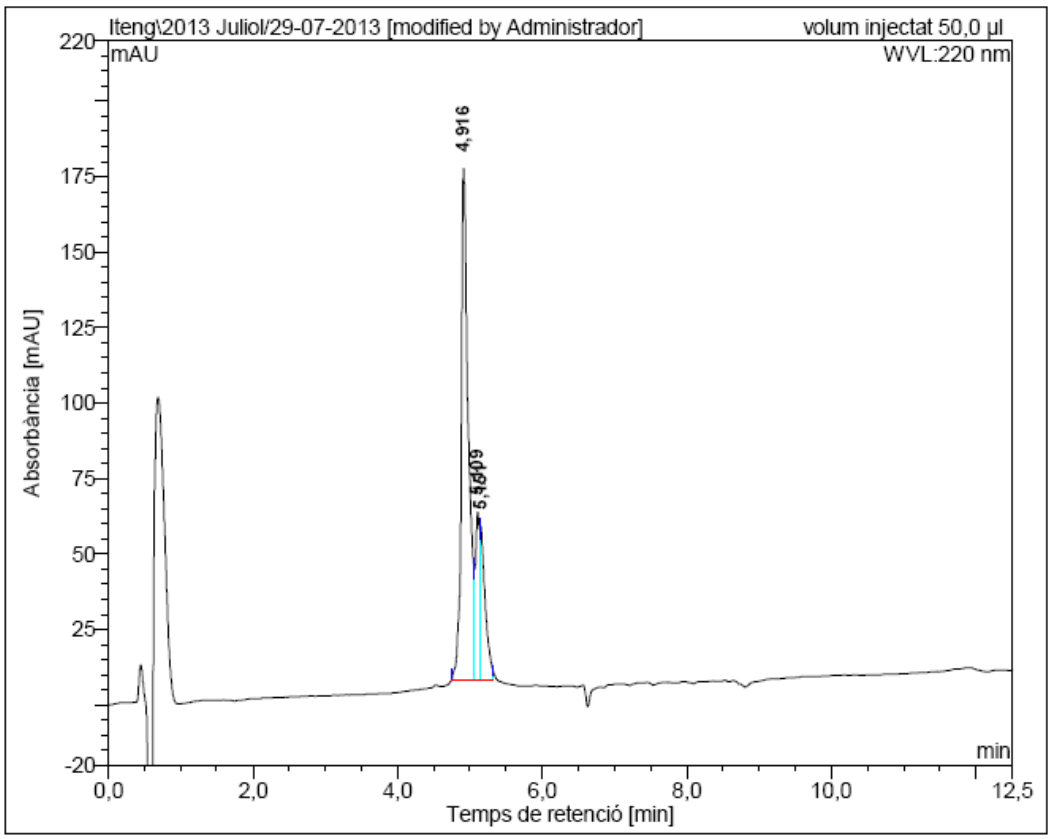

No.	Temps retenció min	alçada mAU	Area mAU*min	Area relativa %
1	4,92	169,180	19,366	71,21
2	5,11	55,405	3,426	12,60
3	5,15	50,749	4,405	16,20
Total:		275,334	27,197	100,00

ESI-MS *m/z*

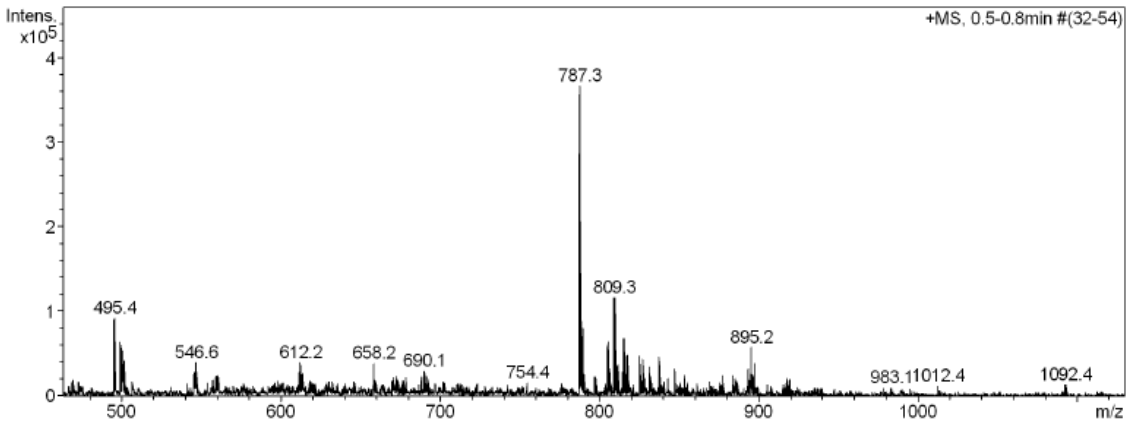

HRMS (ESI) *m/z*

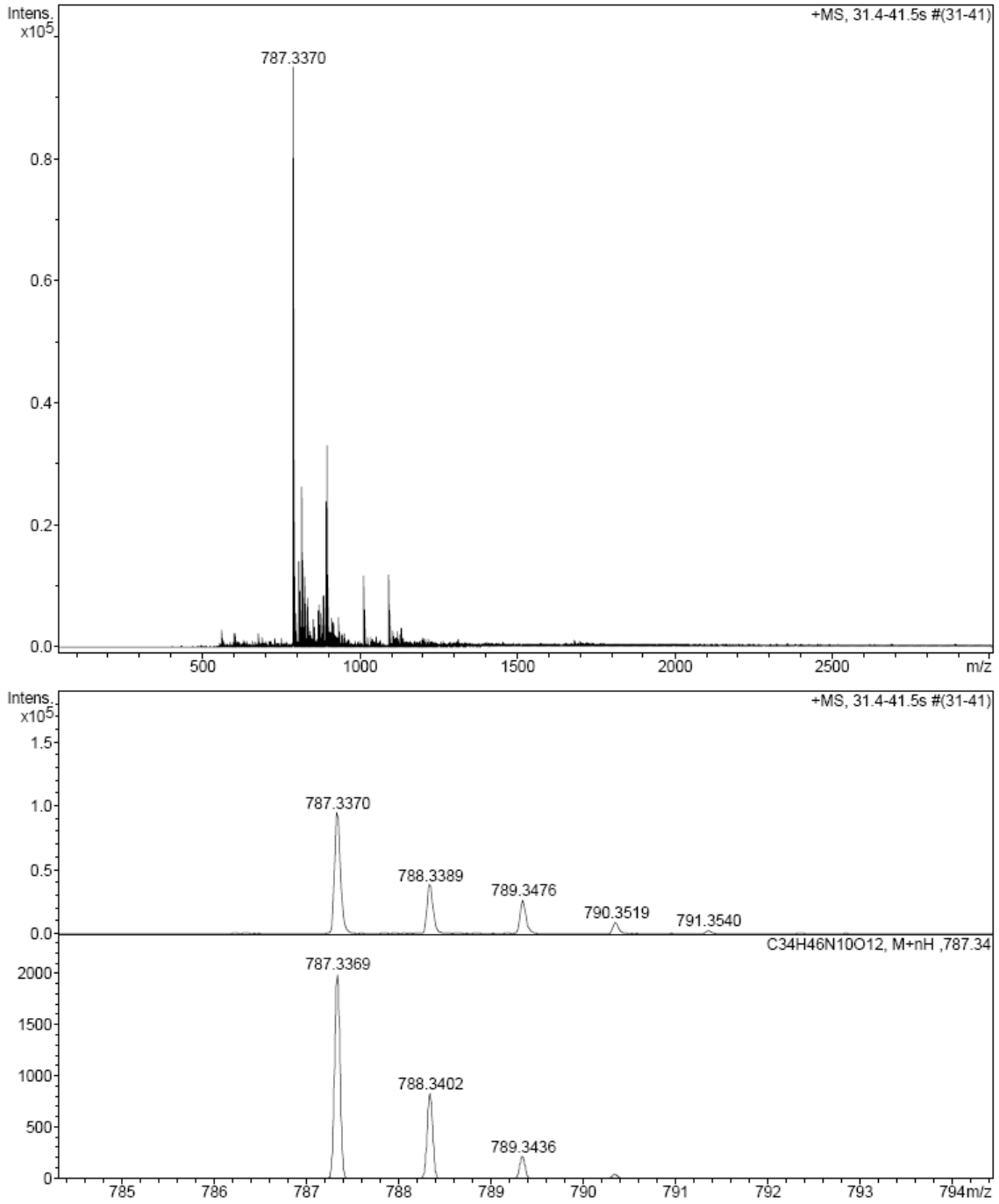
Intens.
x10^5
+MS, 31.4-41.5s #(31-41)
787.3370
0.8
0.6
0.4
0.2
0.0
500
1000
1500
2000
2500
m/z
Intens.
x10^5
+MS, 31.4-41.5s #(31-41)
1.5
1.0
0.5
0.0
787.3370
788.3389
789.3476
790.3519
791.3540
C34H46N10O12, M+nH ,787.34
2000
1500
1000
500
0
787.3369
788.3402
789.3436
785
786
787
788
789
790
791
792
793
794m/z

Biaryl cyclic peptide 3

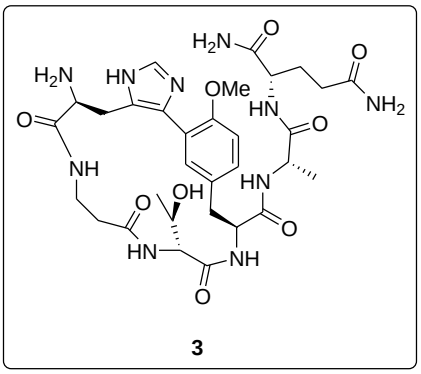

3

Crude peptide 3

HPLC (λ = 220 nm)

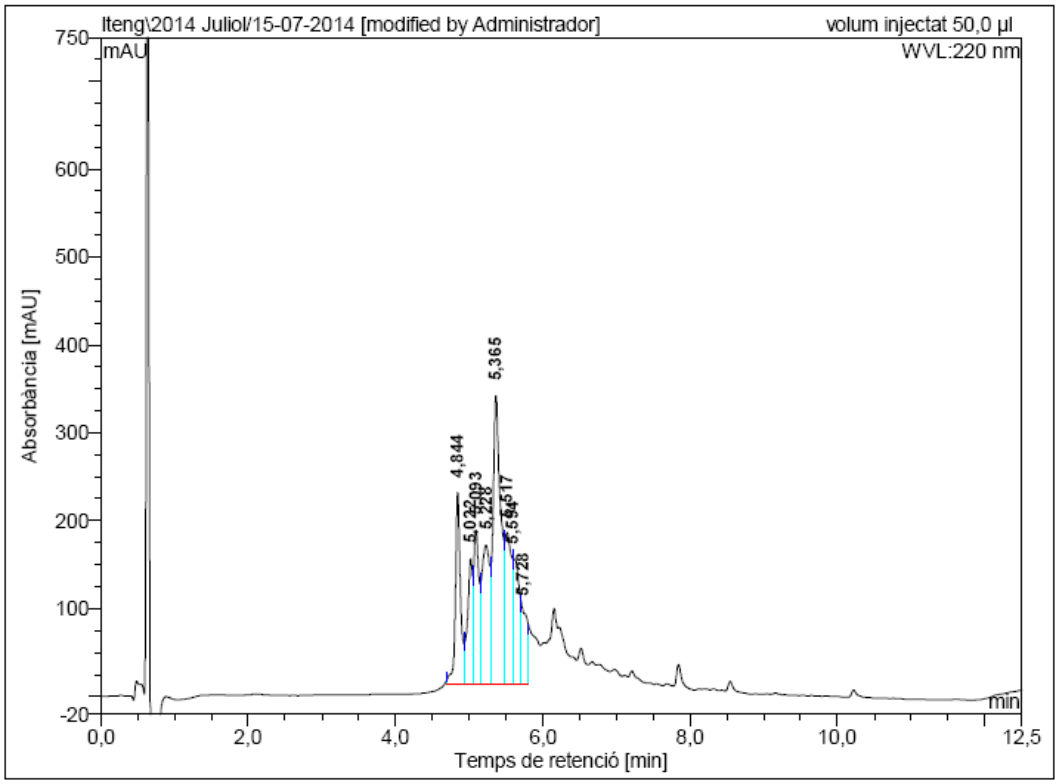

No.	Temps retenció min	alçada mAU	Area mAU*min	Area relativa %
1	4,84	217,476	17,828	12,35
2	5,02	142,189	10,665	7,39
3	5,09	173,990	14,316	9,91
4	5,23	157,321	19,451	13,47
5	5,36	327,356	41,984	29,07
6	5,52	171,837	17,740	12,28
7	5,59	141,466	14,826	10,27
8	5,73	82,788	7,601	5,26
Total:		1414,423	144,411	100,00

ESI-MS *m/z*

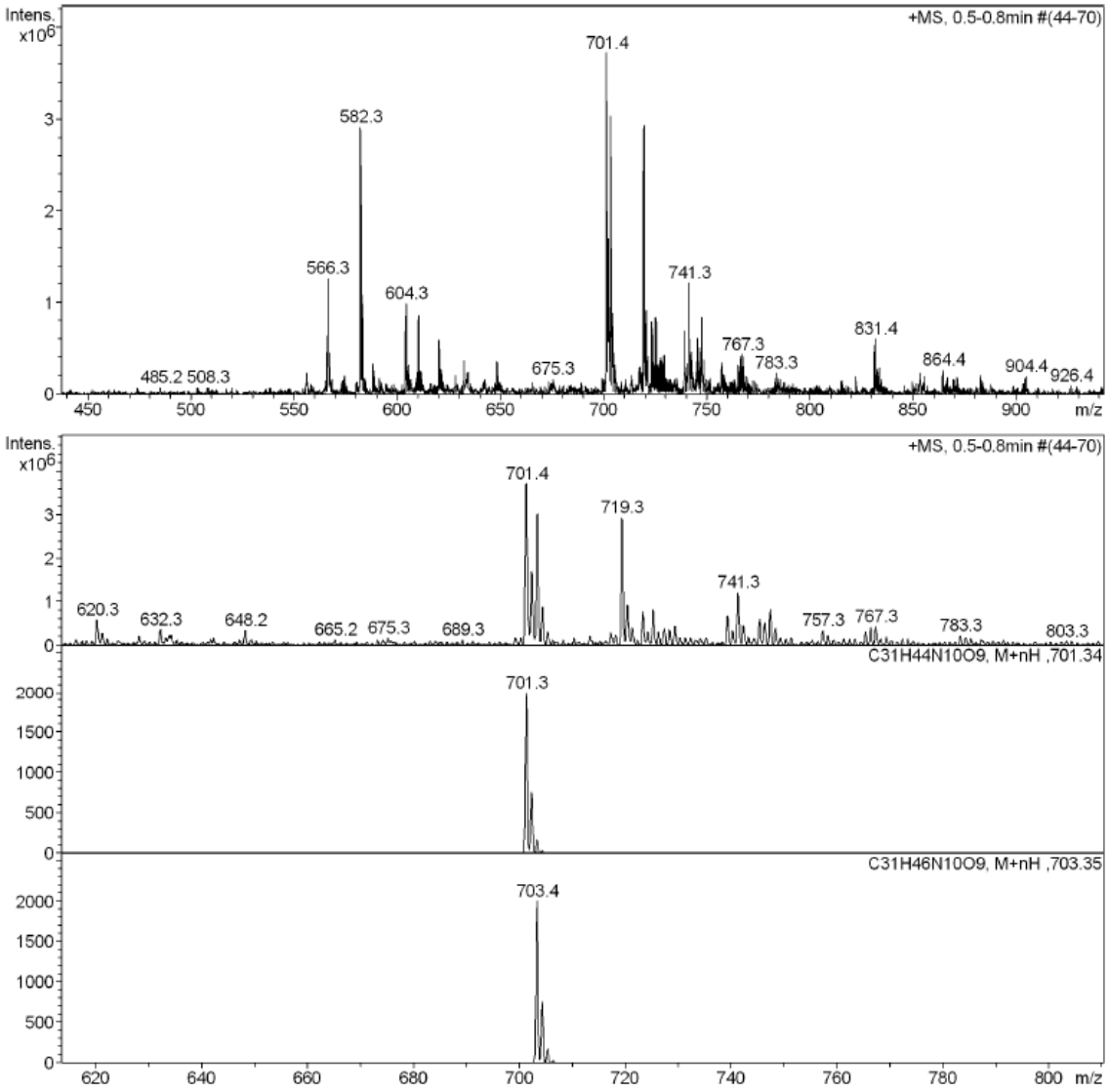
Intens.
x10^6
+MS, 0.5-0.8min #(44-70)
701.4
582.3
566.3
604.3
741.3
831.4
767.3
783.3
485.2 508.3
675.3
864.4
904.4
926.4
m/z
Intens.
x10^6
+MS, 0.5-0.8min #(44-70)
701.4
719.3
741.3
620.3
632.3
648.2
665.2
675.3
689.3
757.3
767.3
783.3
803.3
C31H44N10O9, M+nH ,701.34
701.3
C31H46N10O9, M+nH ,703.35
703.4
m/z

Purified peptide 3

HPLC (λ = 220 nm)

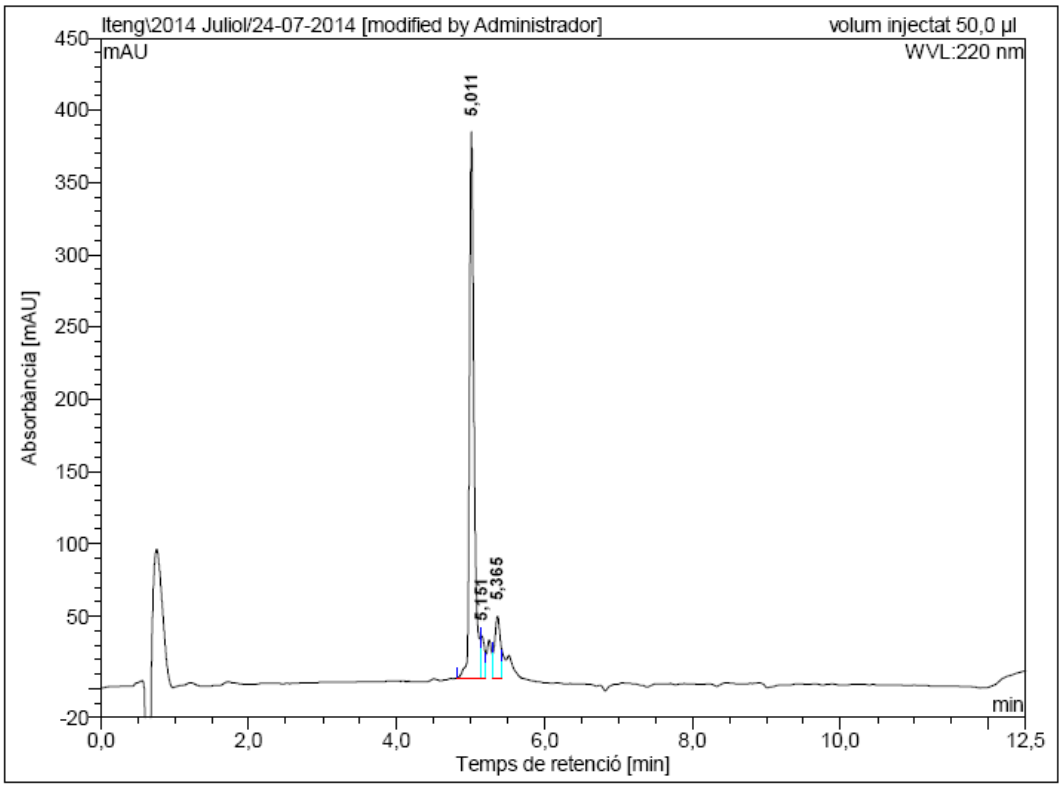

No.	Temps retenció min	alçada mAU	Area mAU*min	Area relativa %
1	5,01	377,844	27,004	83,71
2	5,15	28,803	1,672	5,18
3	5,36	42,554	3,584	11,11
Total:		449,202	32,259	100,00

ESI-MS *m/z*

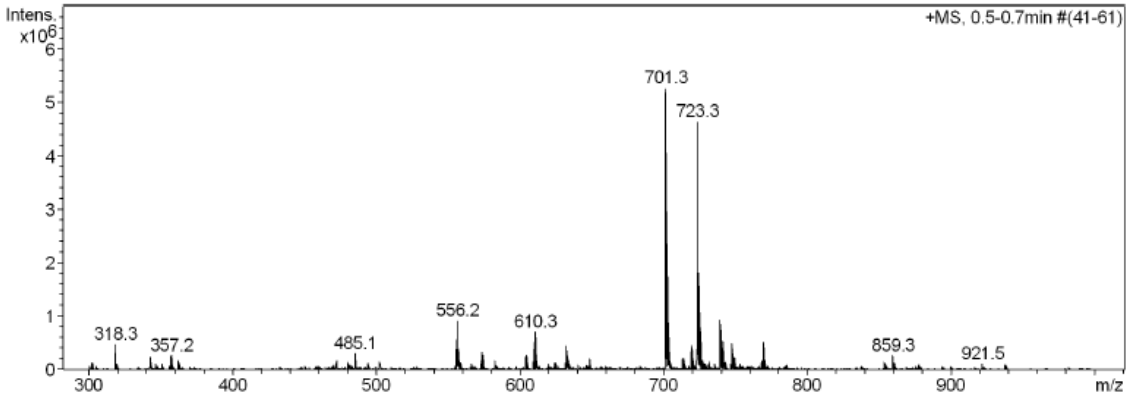

HRMS (ESI) *m/z*

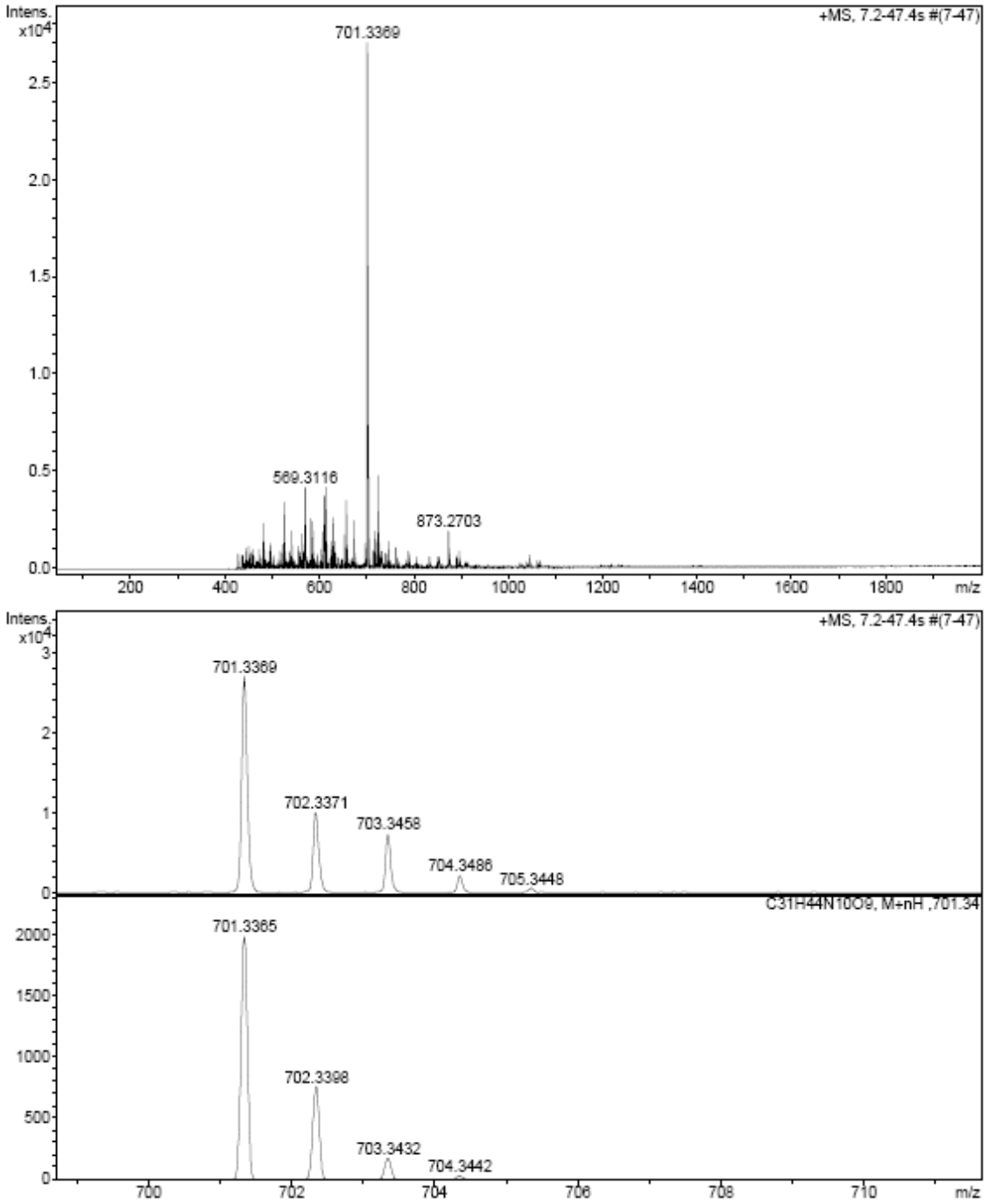
Intens.
x10^4
+MS, 7.2-47.4s #(7-47)
701.3369
569.3116
873.2703
m/z
Intens.
x10^4
+MS, 7.2-47.4s #(7-47)
701.3369
702.3371
703.3458
704.3486
705.3448
C31H44N10O9, M+nH ,701.34
701.3365
702.3398
703.3432
704.3442
m/z

SUPPORTING INFORMATION CHAPTER 8

Solid-phase synthesis of biaryl bicyclic peptides analogues of aciculitins

Iteng Ng-Choi[1], Lidia Feliu[1]* and Marta Planas[1]*

TABLE OF CONTENTS

Copies of HPLC, MS and NMR spectra

1.Synthesis of Fmoc-Glu-O*p*NB

Fmoc-Glu(O*t*Bu)-O*p*NB

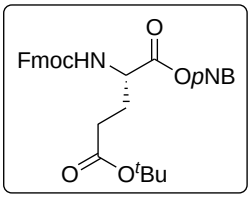

HPLC (λ = 220 nm)

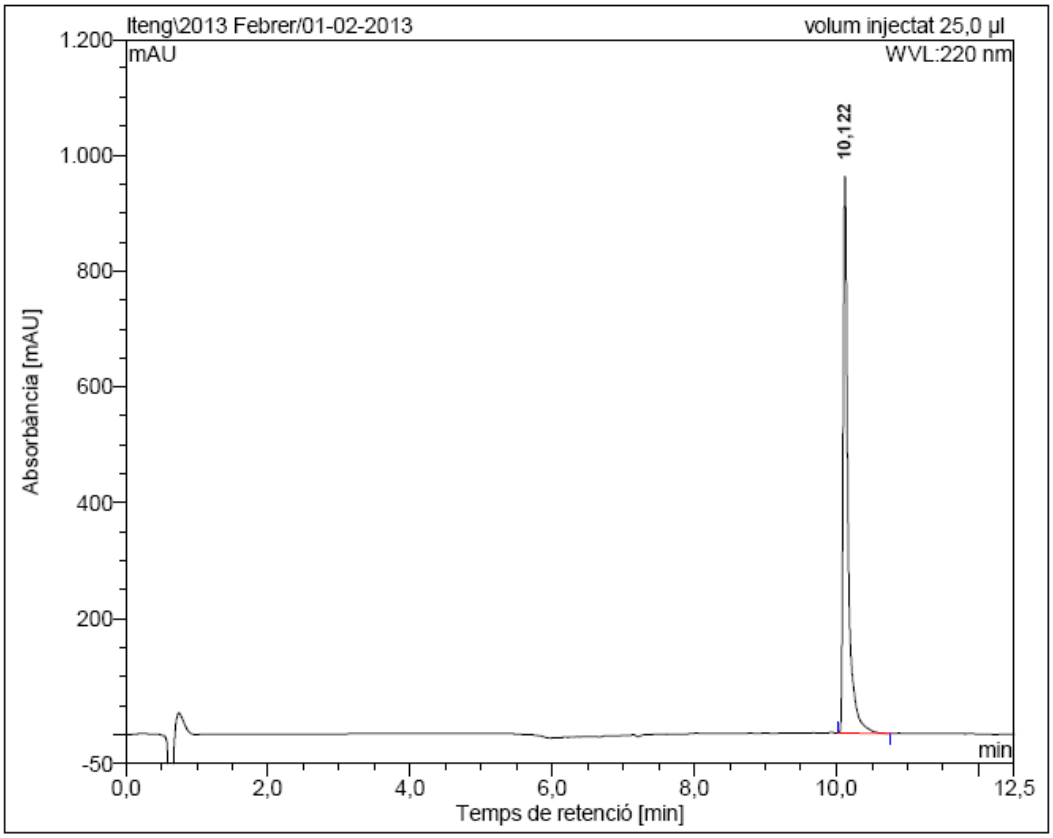

No.	Ret.Time (detected) min	Height mAU	Area mAU*min	Rel.Area %
1	10,12	960,063	76,164	100,00
Total:		960,063	76,164	100,00

^{1}H-NMR (400 MHz, $CDCl_3$) δ (ppm)

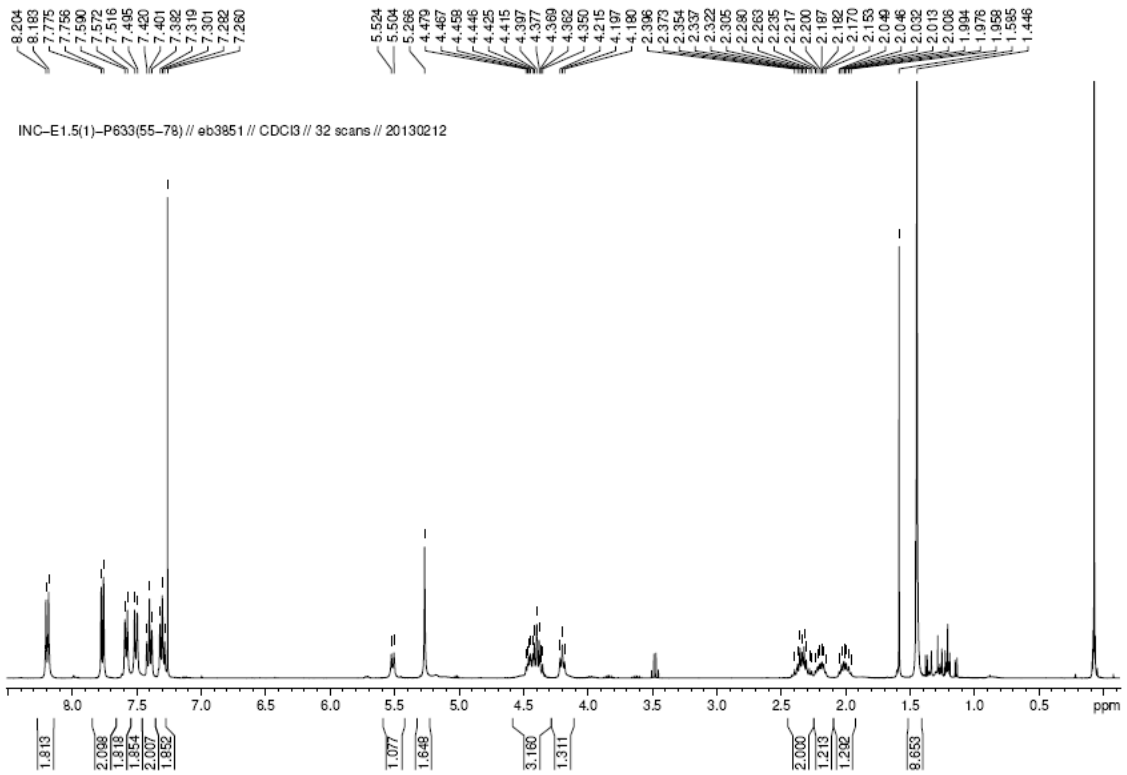

Fmoc-Glu-O*p*NB

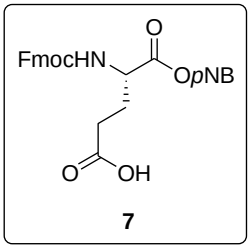

7

HPLC (λ = 220 nm)

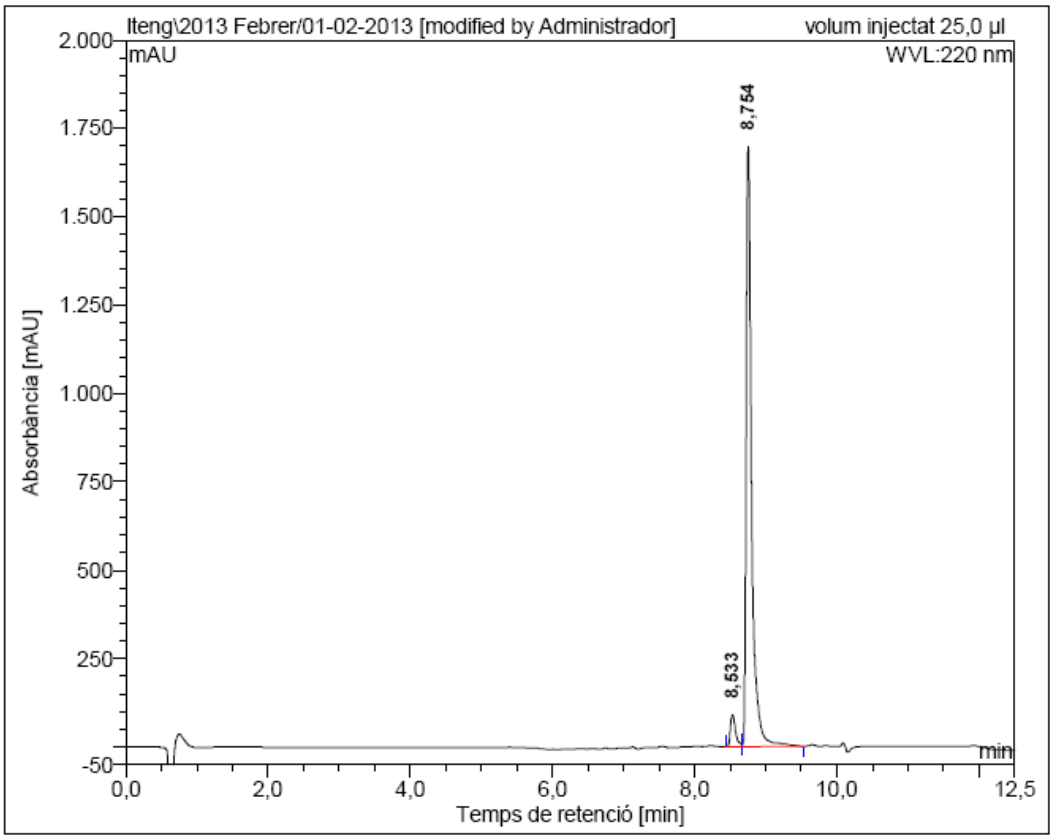

No.	Ret.Time (detected) min	Height mAU	Area mAU*min	Rel.Area %
1	8,53	90,891	7,731	4,81
2	8,75	1698,022	152,928	95,19
Total:		1788,913	160,659	100,00

^{1}H-NMR (400 MHz, $CDCl_3$) δ (ppm)

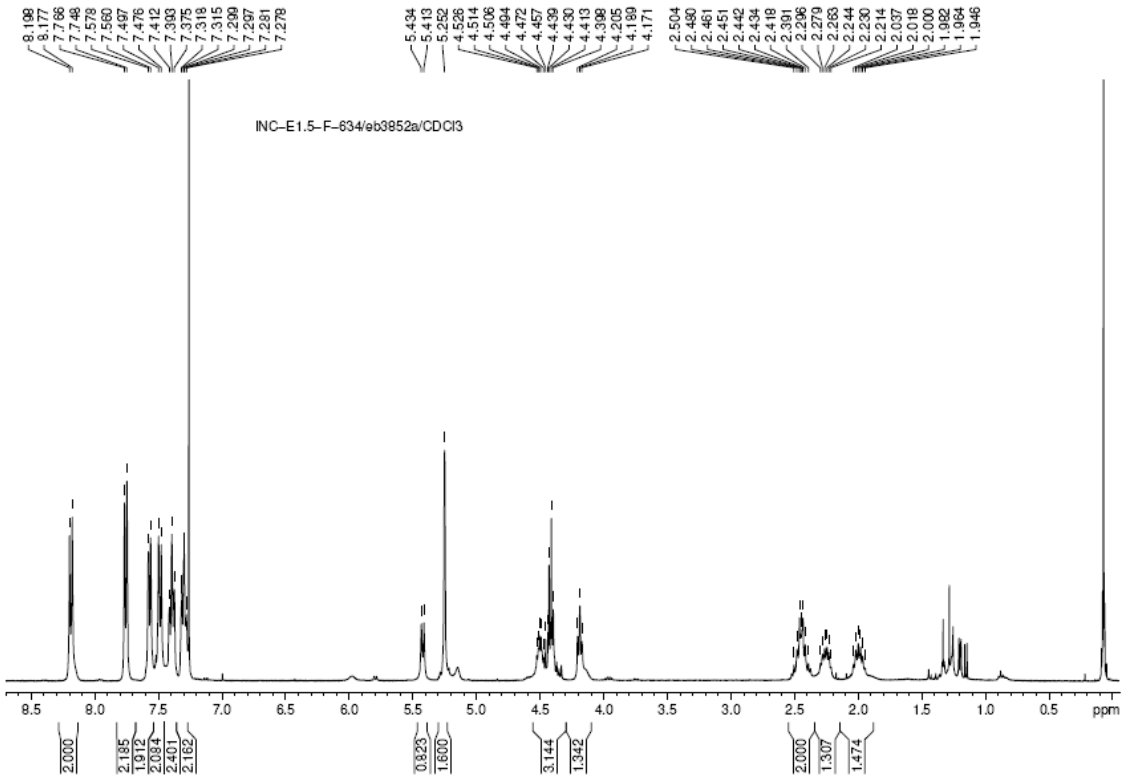

2. Linear peptides

H-Ala-Gln-Leu-Gln-Phe(4-I)-βAla-Gln-OpNB

HPLC (λ = 220 nm)

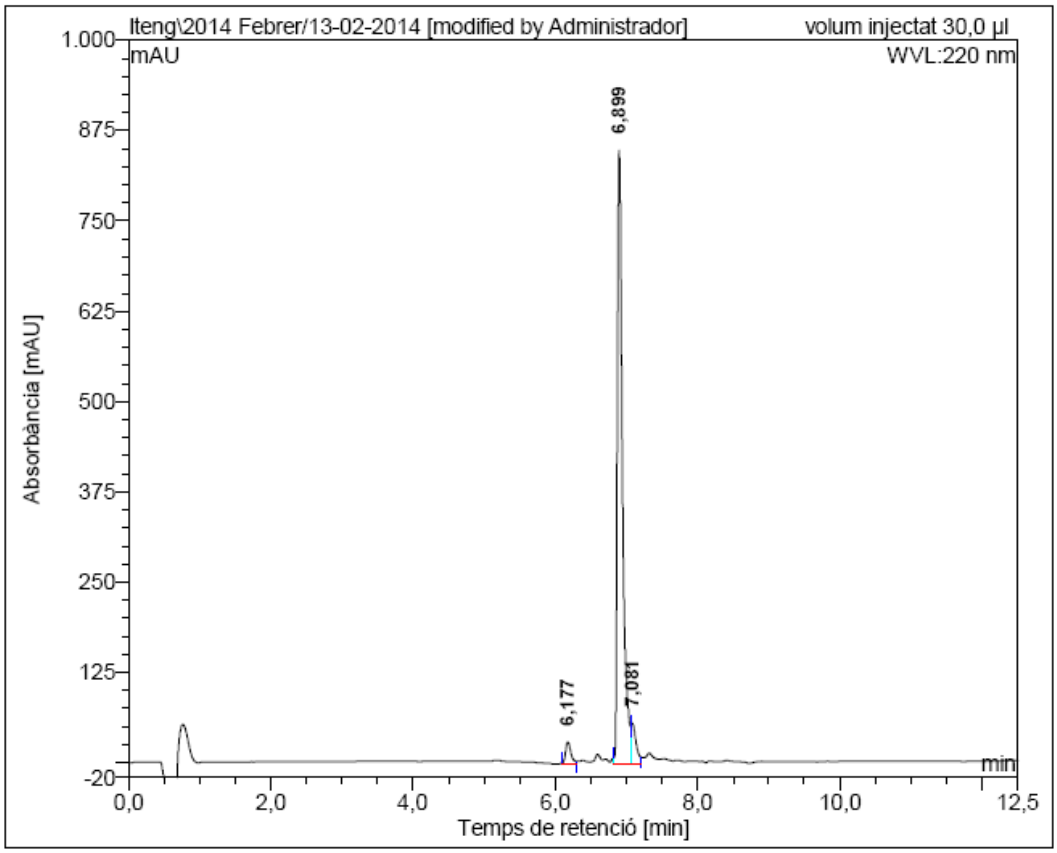

No.	mps retenc min	alçada mAU	Area mAU*min	Area relativa %
1	6,18	29,659	2,585	3,27
2	6,90	848,820	71,490	90,35
3	7,08	56,053	5,048	6,38
Total:		934,532	79,123	100,00

H-Phe(4-B(OH)$_2$)-Ala-Gln-Leu-Gln-Phe(4-I)-βAla-Gln-O*p*NB

HPLC (λ = 220 nm)

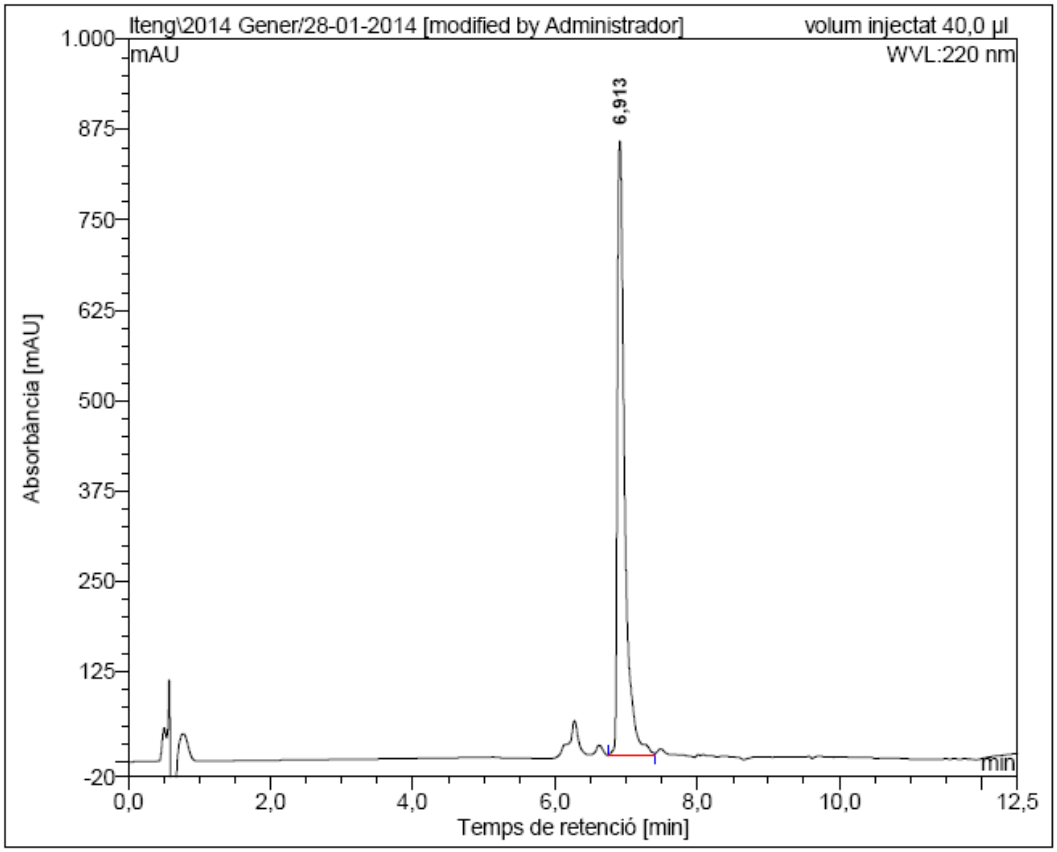

No.	mps retenc min	alçada mAU	Area mAU*min	Area relativa %
1	6,91	849,530	101,466	100,00
Total:		849,530	101,466	100,00

ESI-MS *m/z*

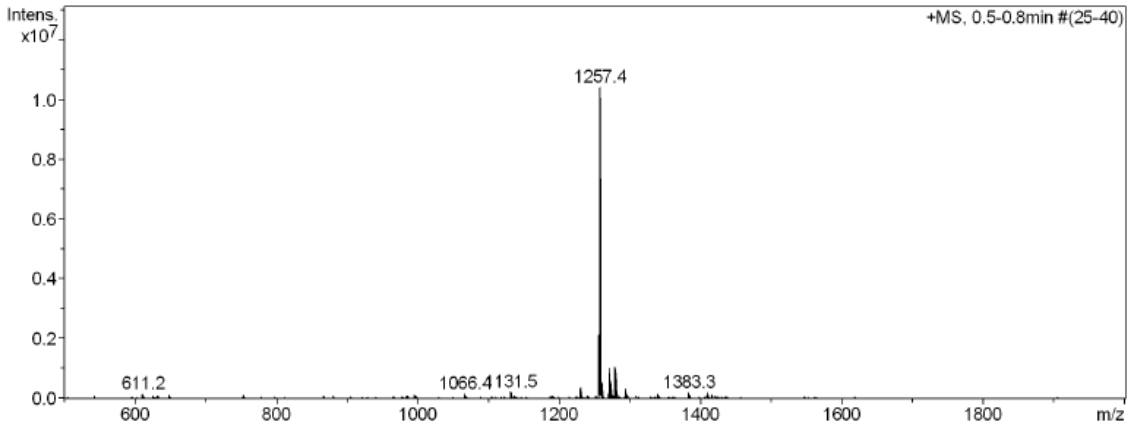

H-Ala-Gln-Gly-Gln-Phe(4-I)-βAla-Gln-O*p*NB

HPLC (λ = 220 nm)

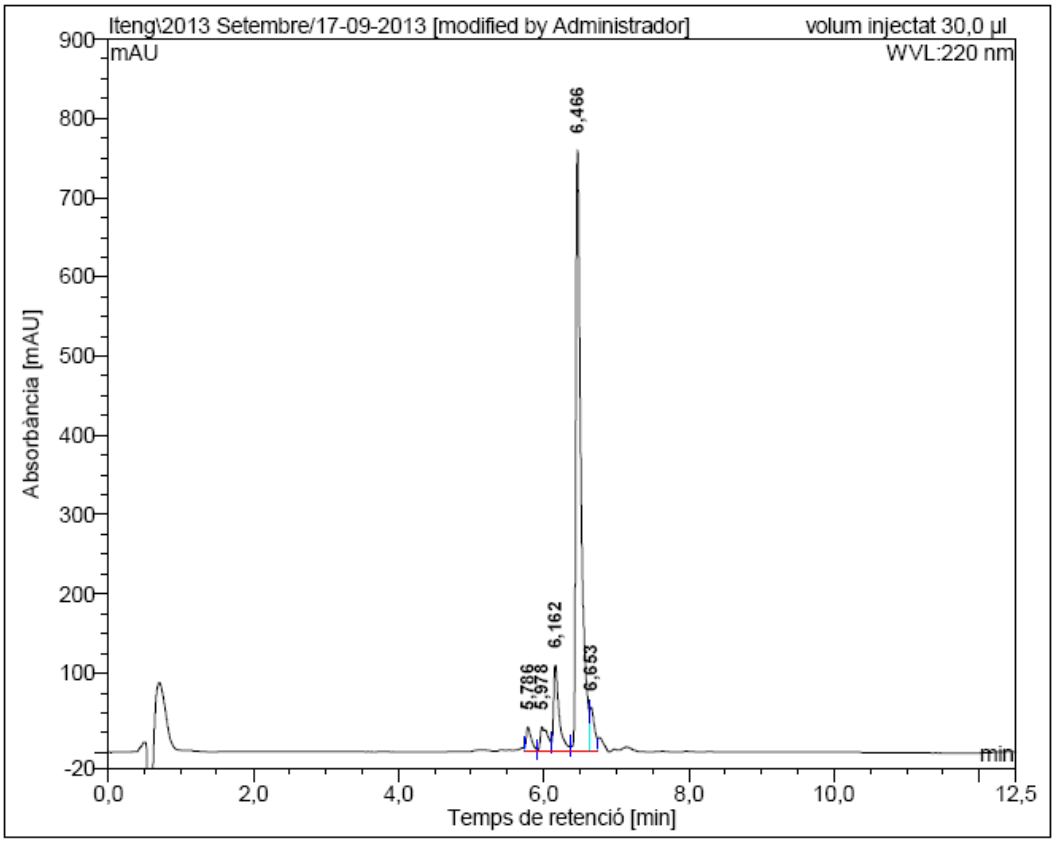

No.	Temps retenció min	alçada mAU	Area mAU*min	Area relativa %
1	5,79	30,651	2,569	3,09
2	5,98	30,669	3,678	4,42
3	6,16	109,277	9,703	11,66
4	6,47	758,789	62,930	75,59
5	6,65	56,126	4,373	5,25
Total:		985,511	83,253	100,00

H-Tyr(3-B(OH)$_2$,Me)-Ala-Gln-Gly-Gln-Phe(4-I)-βAla-Gln-OpNB

HPLC (λ = 220 nm)

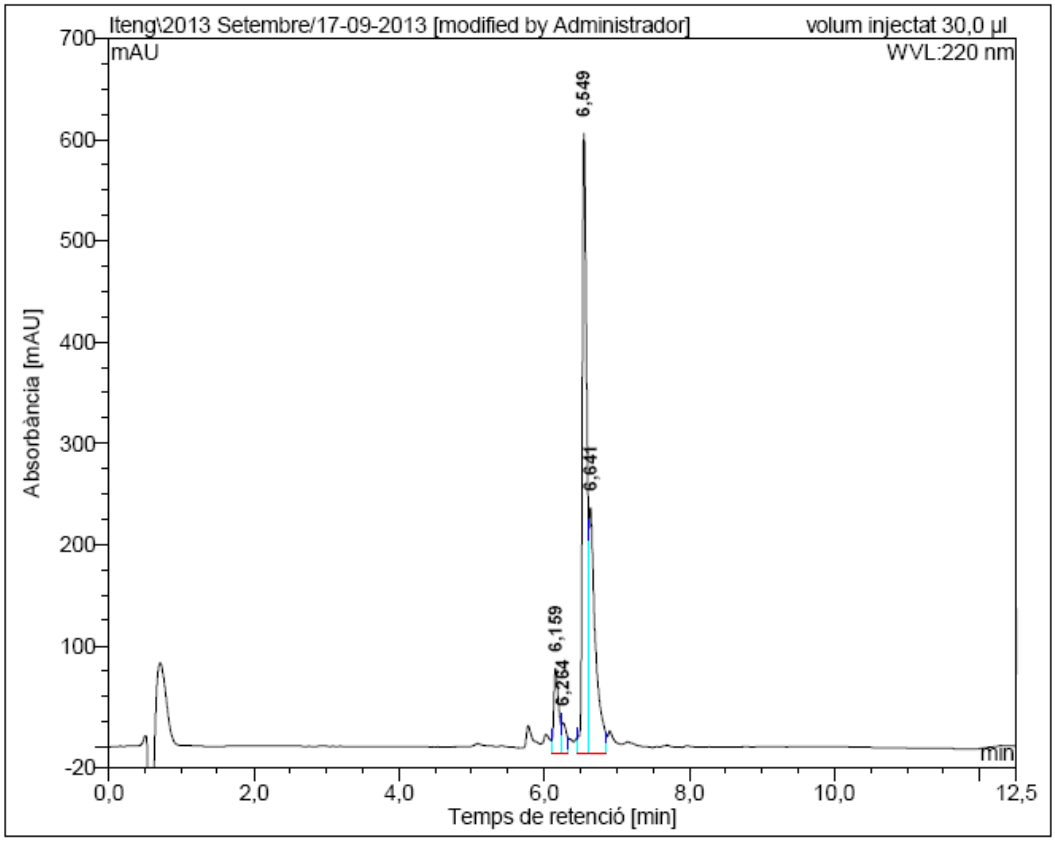

No.	Temps retenció min	alçada mAU	Area mAU*min	Area relativa %
1	6,16	84,816	6,659	8,56
2	6,26	31,339	2,498	3,21
3	6,55	613,516	44,469	57,15
4	6,64	243,783	24,186	31,08
Total:		973,453	77,812	100,00

ESI-MS *m/z*

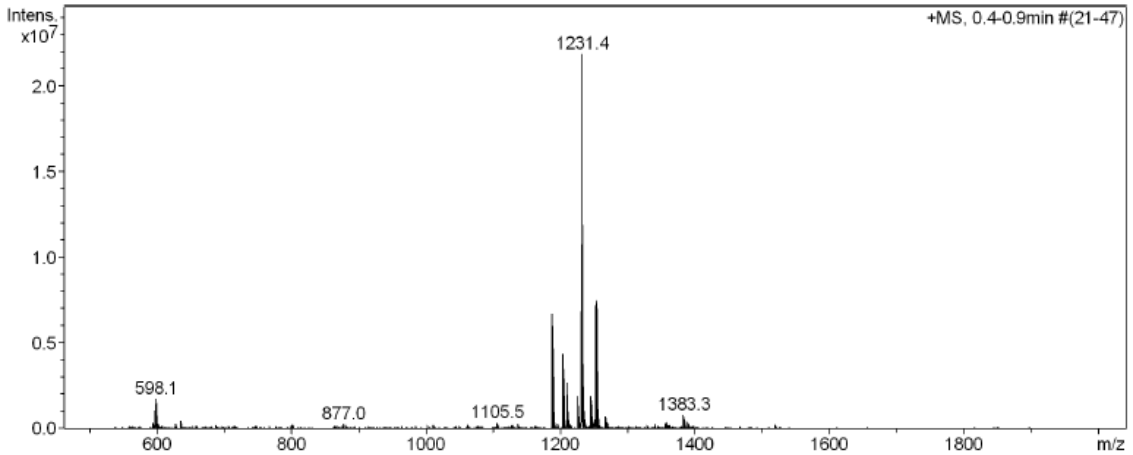

H-Ala-Gln-Leu-Gln-His(5-Br)-βAla-Gln-O*p*NB

HPLC (λ = 220 nm)

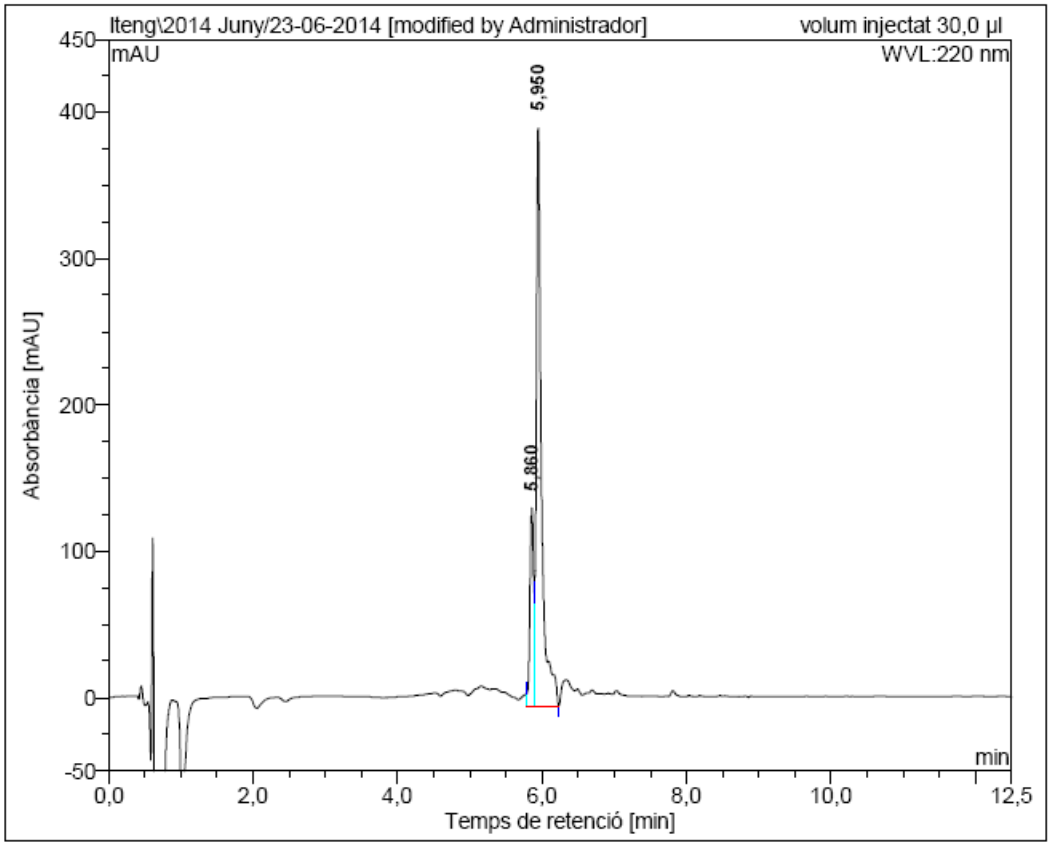

No.	mps retenc min	alçada mAU	Area mAU*min	Area relativa %
1	5,86	135,273	8,093	19,44
2	5,95	395,206	33,537	80,56
Total:		530,479	41,630	100,00

H-Tyr(3-B(OH)$_2$,Me)-Ala-Gln-Leu-Gln-His(5-Br)-βAla-Gln-O*p*NB

HPLC (λ = 220 nm)

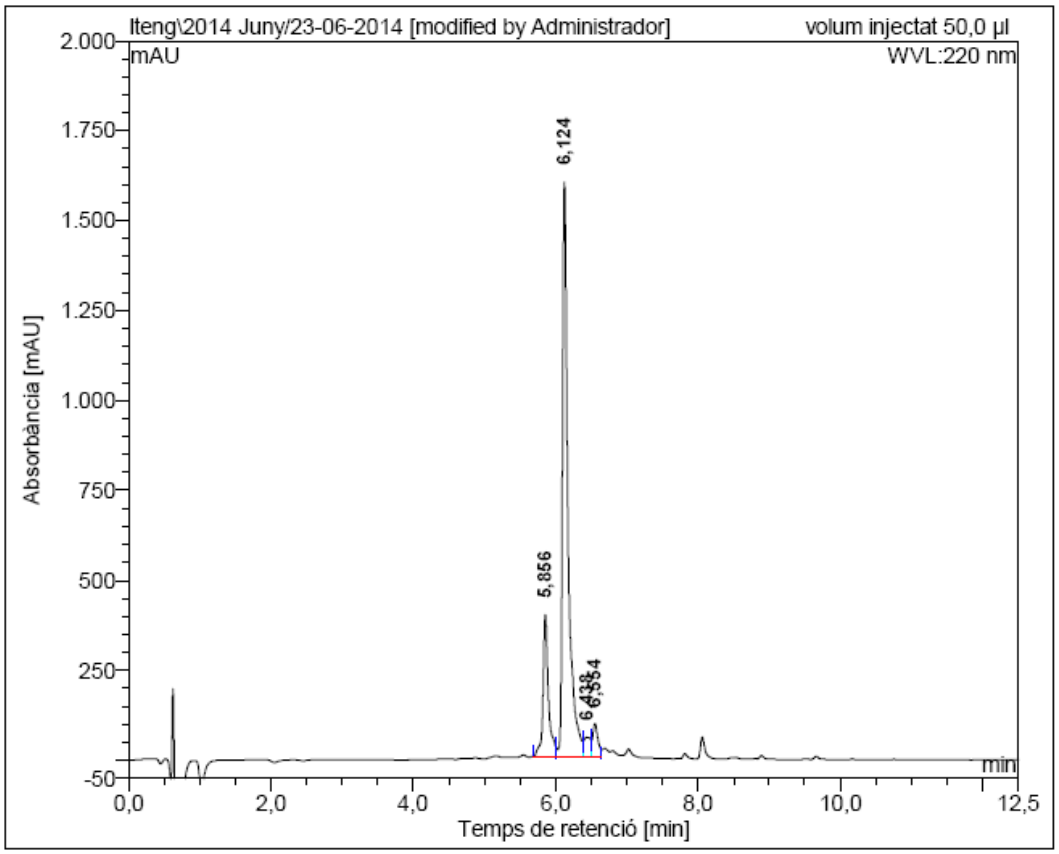

No.	mps retenc min	alçada mAU	Area mAU*min	Area relativa %
1	5,86	393,842	34,569	17,61
2	6,12	1596,461	148,206	75,50
3	6,44	53,352	5,876	2,99
4	6,55	91,554	7,661	3,90
Total:		2135,209	196,312	100,00

ESI-MS *m/z*

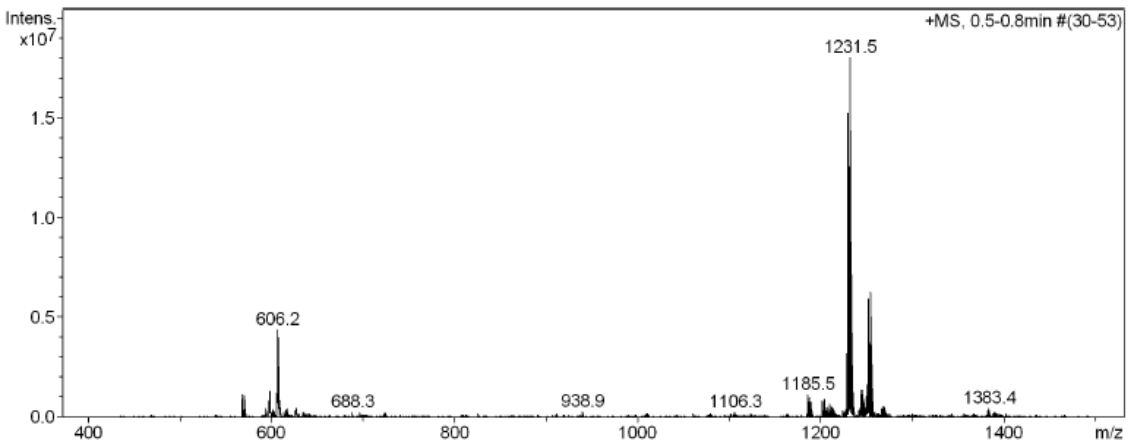

H-Ala-Gln-Leu-Gln-Tyr(3-I,Me)-βAla-Gln-O*p*NB

HPLC (λ = 220 nm)

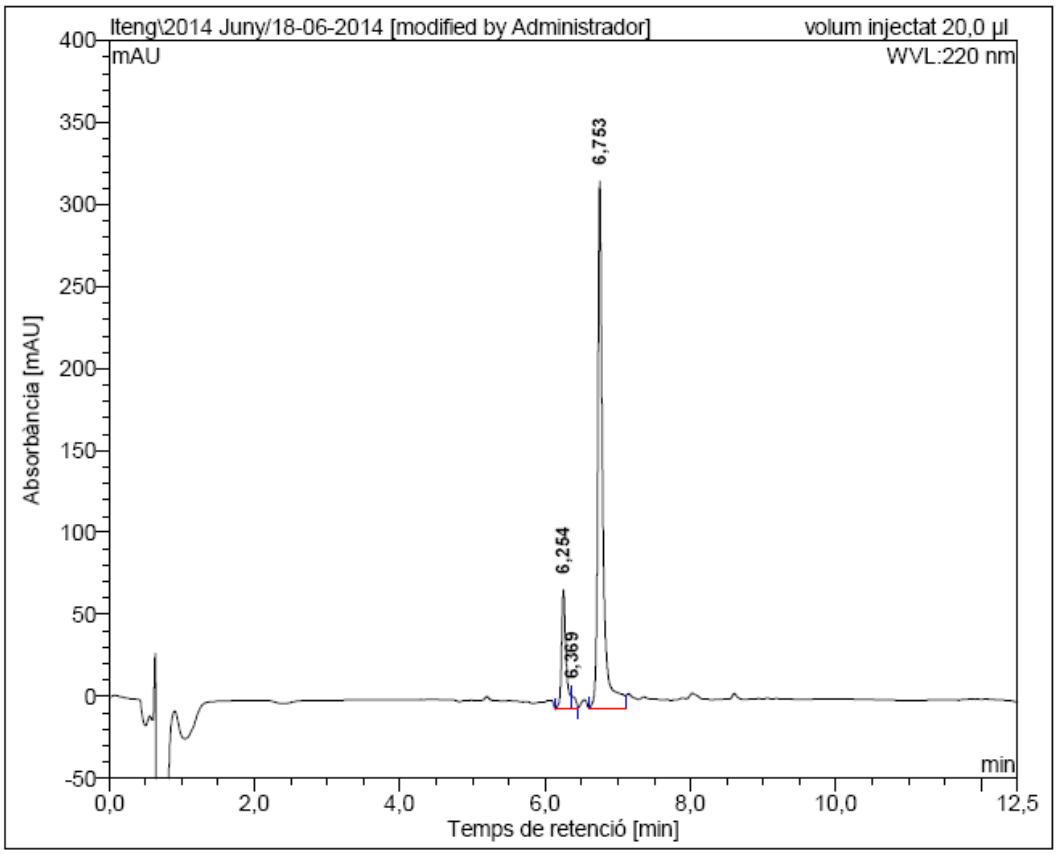

No.	mps retenc min	alçada mAU	Area mAU*min	Area relativa %
1	6,25	72,436	5,216	16,24
2	6,37	7,728	0,482	1,50
3	6,75	322,094	26,416	82,26
Total:		402,258	32,114	100,00

H-Tyr(3-B(OH)$_2$,Me)-Ala-Gln-Leu-Gln-Tyr(3-I,Me)-βAla-Gln-O*p*NB

HPLC (λ = 220 nm)

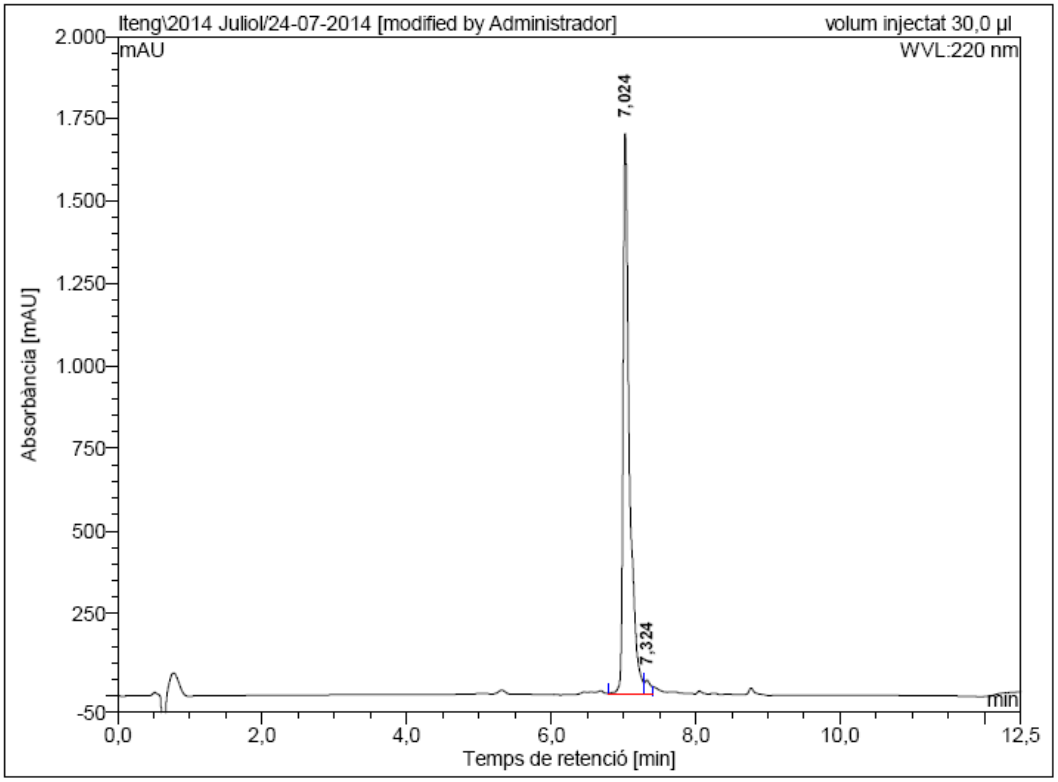

No.	Temps retenció min	alçada mAU	Area mAU*min	Area relativa %
1	7,02	1698,450	172,454	97,99
2	7,32	40,394	3,533	2,01
Total:		1738,844	175,987	100,00

ESI-MS *m/z*

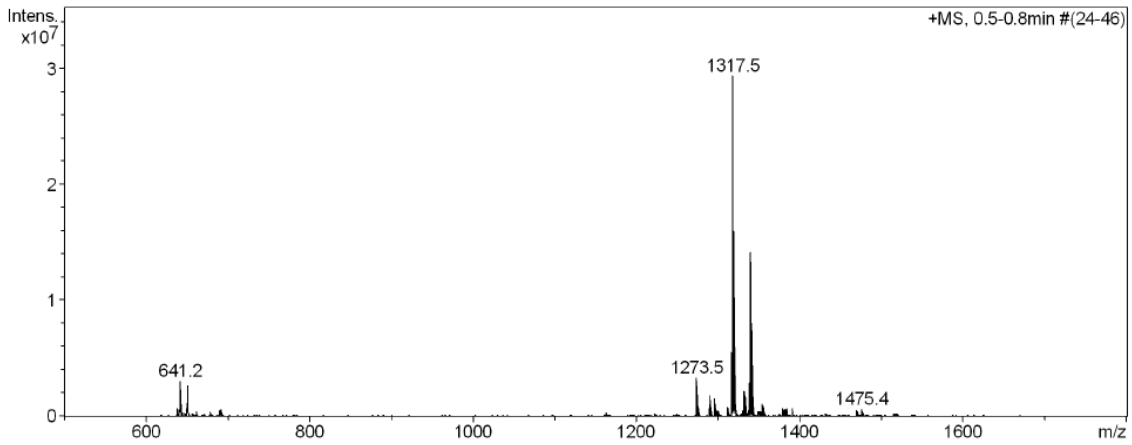

3. Biaryl monocyclic peptides 7, 10, 14 and 15, 18

Biaryl monocyclic peptide 7

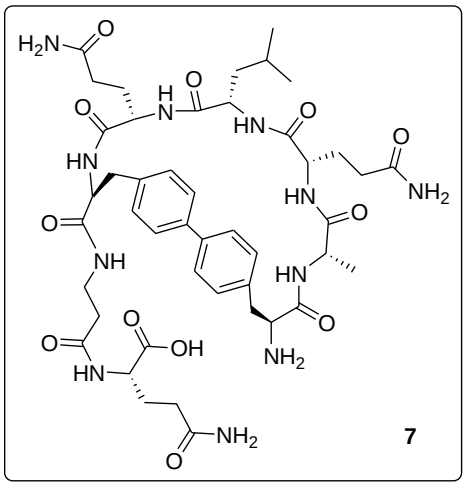

HPLC (λ = 220 nm)

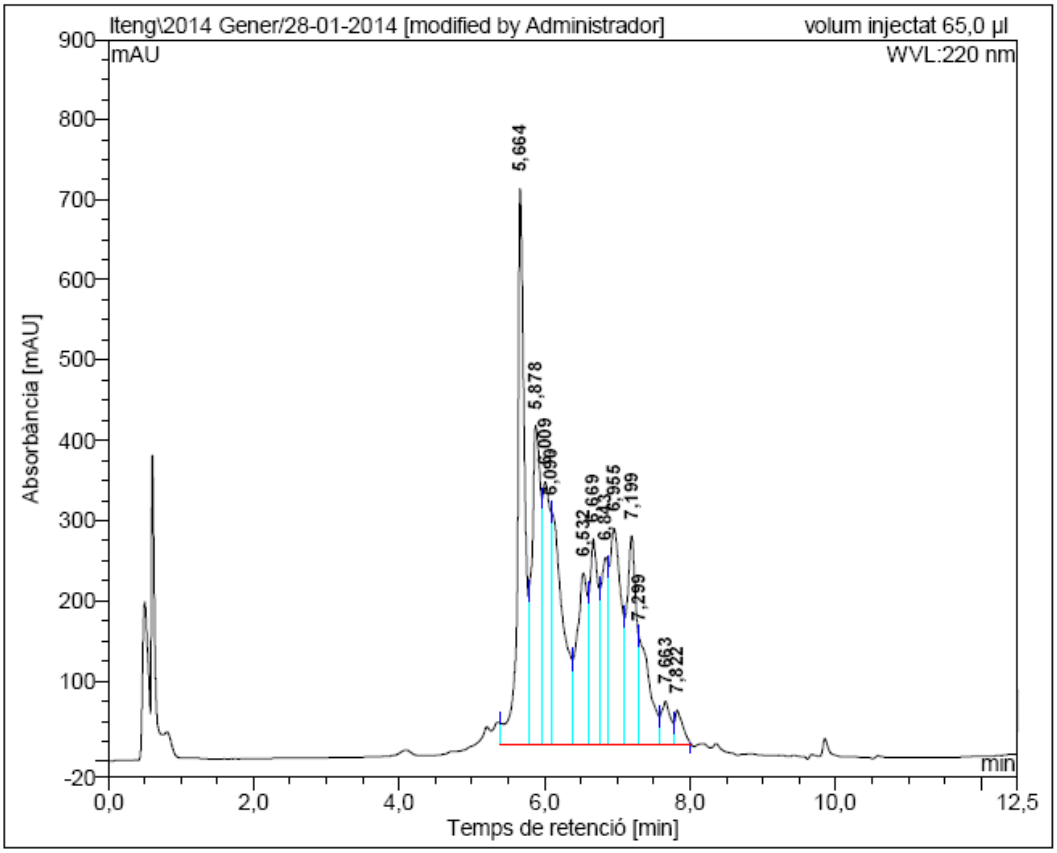

No.	mps retenc min	alçada mAU	Area mAU*min	Area relativa %
1	5,66	693,919	80,158	17,73
2	5,88	398,048	55,909	12,36
3	6,01	328,041	37,187	8,22
4	6,09	290,723	55,853	12,35
5	6,53	214,240	38,462	8,50
6	6,67	257,148	31,678	7,00
7	6,84	234,025	28,814	6,37
8	6,95	269,532	47,536	10,51
9	7,20	260,849	39,585	8,75
10	7,30	134,234	23,338	5,16
11	7,66	54,812	8,059	1,78
12	7,82	43,314	5,649	1,25
Total:		3178,885	452,228	100,00

ESI-MS *m/z*

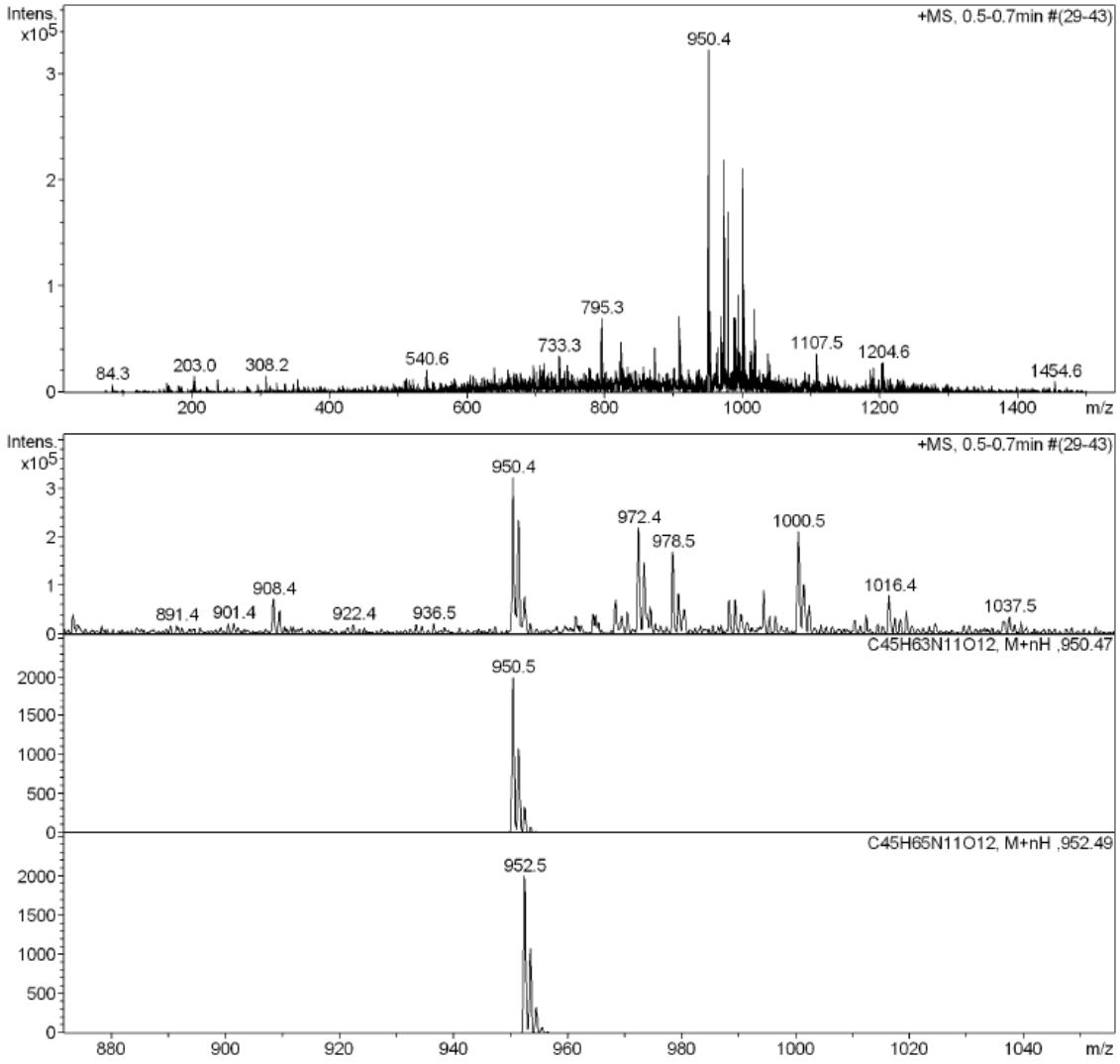
Intens.
x10^5
+MS, 0.5-0.7min #(29-43)
950.4
795.3
733.3
1107.5
1204.6
84.3
203.0
308.2
540.6
1454.6
m/z
+MS, 0.5-0.7min #(29-43)
950.4
972.4
978.5
1000.5
908.4
891.4
901.4
922.4
936.5
1016.4
1037.5
C45H63N11O12, M+nH ,950.47
950.5
C45H65N11O12, M+nH ,952.49
952.5

Biaryl monocyclic peptide 10

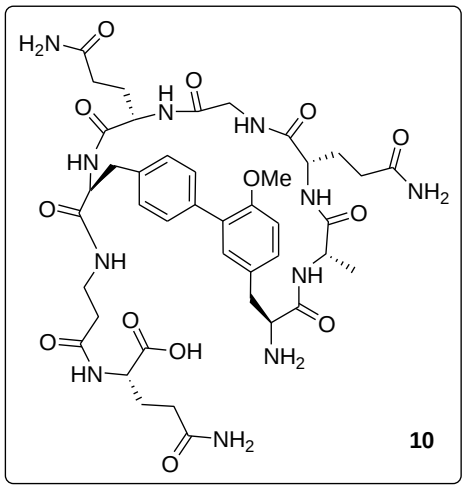

HPLC (λ = 220 nm)

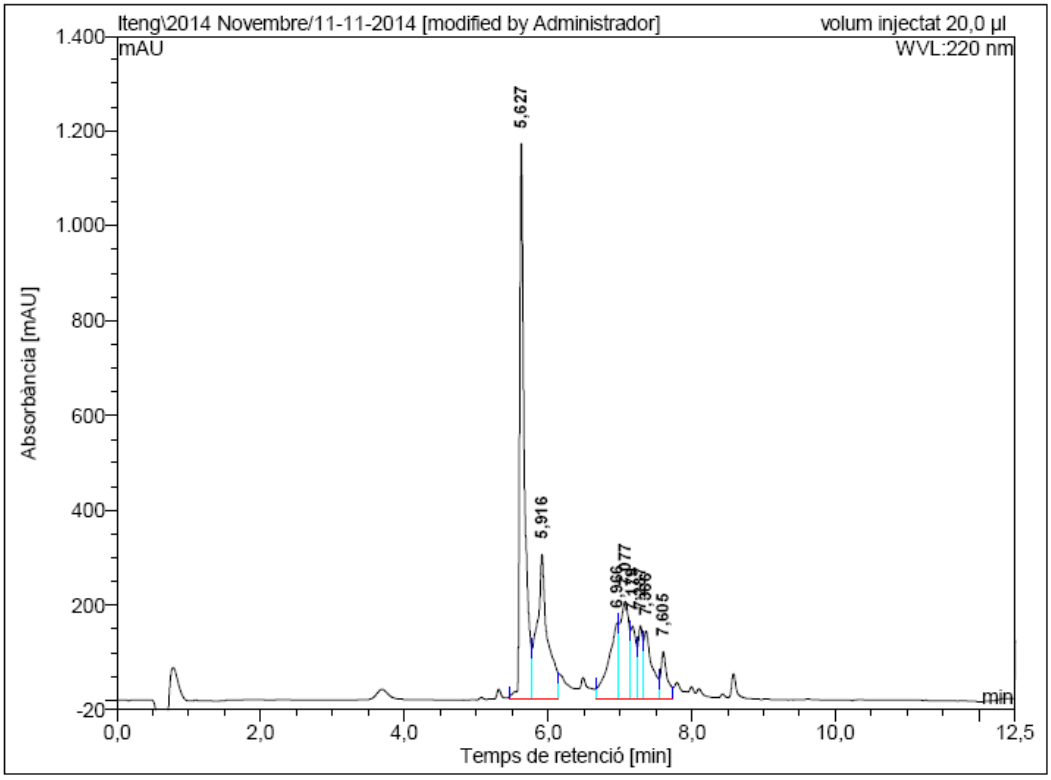

No.	Temps retenció min	alçada mAU	Area mAU*min	Area relativa %
1	5,63	1172,287	90,776	35,80
2	5,92	306,356	52,987	20,89
3	6,97	161,377	26,929	10,62
4	7,08	206,978	28,140	11,10
5	7,18	154,595	13,317	5,25
6	7,29	155,577	11,478	4,53
7	7,37	144,208	19,127	7,54
8	7,60	100,922	10,842	4,28
Total:		2402,301	253,598	100,00

ESI-MS *m/z*

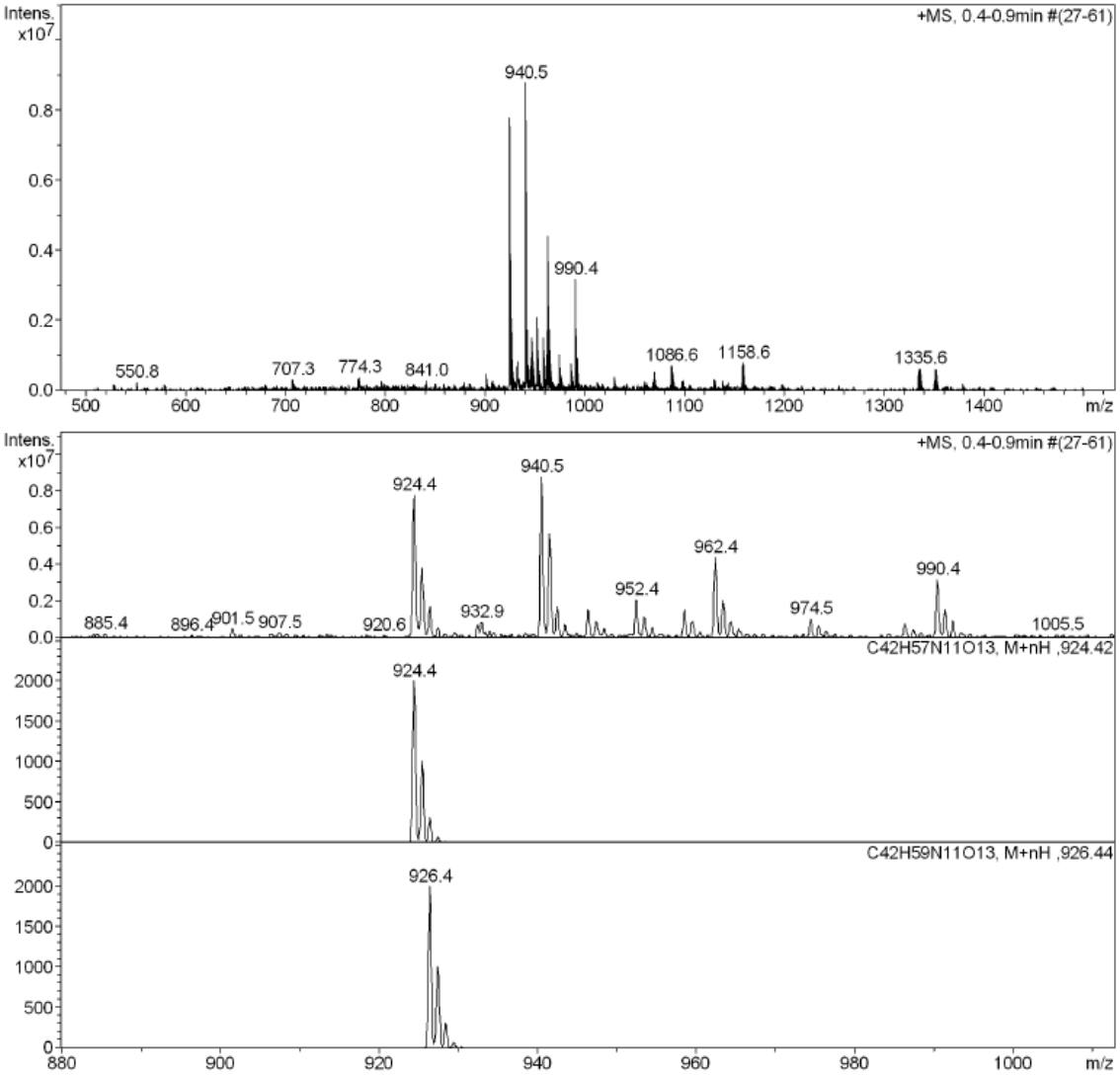
Intens.
x10^7
+MS, 0.4-0.9min #(27-61)
940.5
990.4
550.8
707.3
774.3
841.0
1086.6
1158.6
1335.6
m/z
924.4
940.5
962.4
990.4
952.4
974.5
885.4
896.4
901.5
907.5
920.6
932.9
1005.5
C42H57N11O13, M+nH ,924.42
C42H59N11O13, M+nH ,926.44
926.4

Biaryl cyclic peptides 14 and 15

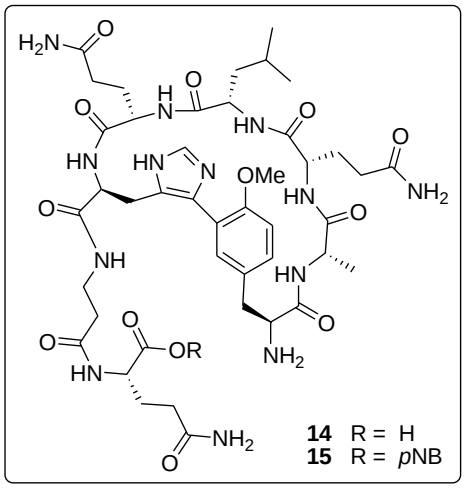

HPLC (λ = 220 nm)

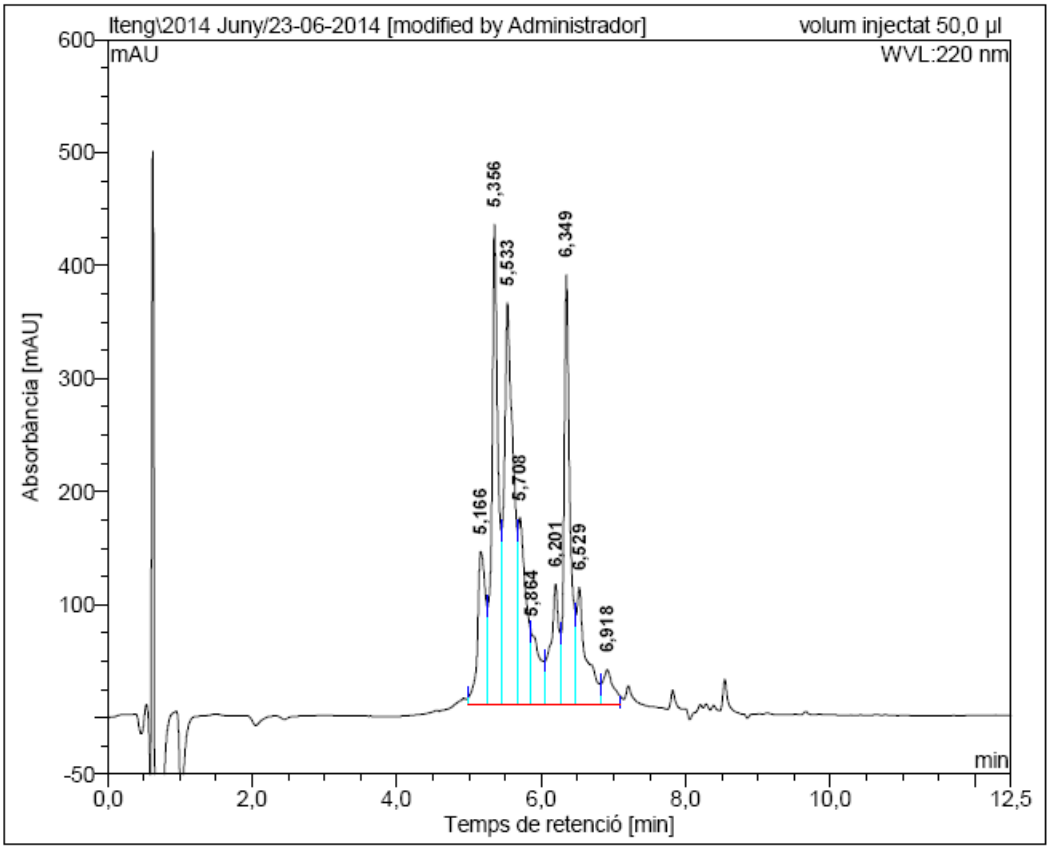

No.	mps retenc min	alçada mAU	Area mAU*min	Area relativa %
1	5,17	134,941	17,791	8,18
2	5,36	424,469	42,178	19,40
3	5,53	354,981	53,905	24,80
4	5,71	164,984	21,542	9,91
5	5,86	62,830	9,340	4,30
6	6,20	105,970	14,256	6,56
7	6,35	379,434	37,235	17,13
8	6,53	102,882	15,883	7,31
9	6,92	30,340	5,240	2,41
Total:		1760,832	217,371	100,00

ESI-MS *m/z*

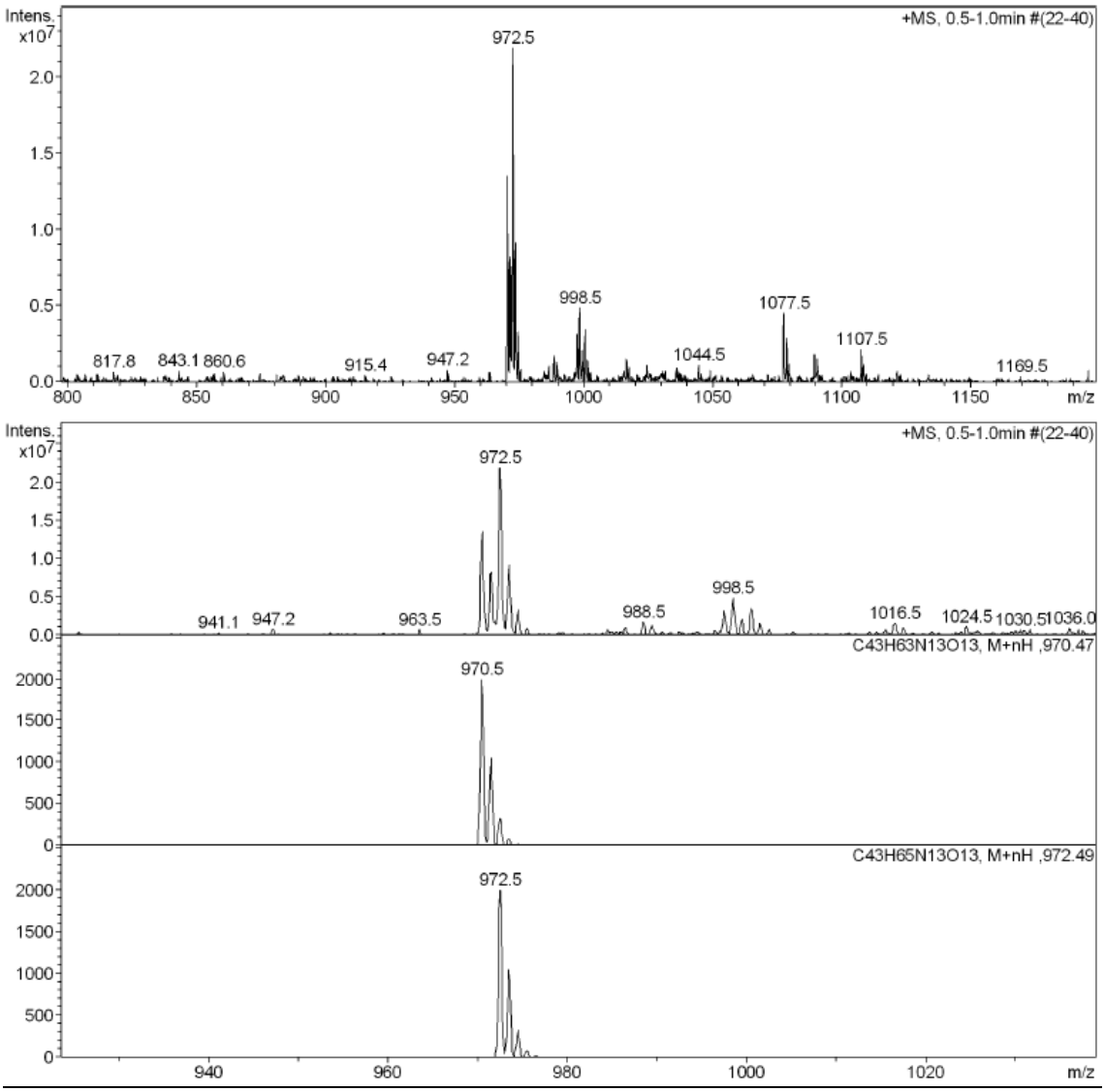
Intens.
x10^7
+MS, 0.5-1.0min #(22-40)
972.5
998.5
1077.5
1107.5
1044.5
817.8
843.1
860.6
915.4
947.2
1169.5
m/z
941.1
963.5
988.5
1016.5
1024.5
1030.5
1036.0
C43H63N13O13, M+nH ,970.47
970.5
C43H65N13O13, M+nH ,972.49

Biaryl monocyclic peptide 18

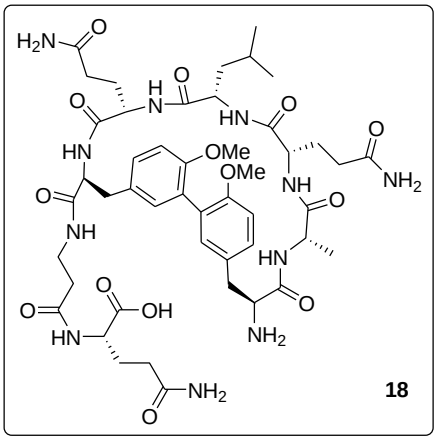

HPLC (λ = 220 nm)

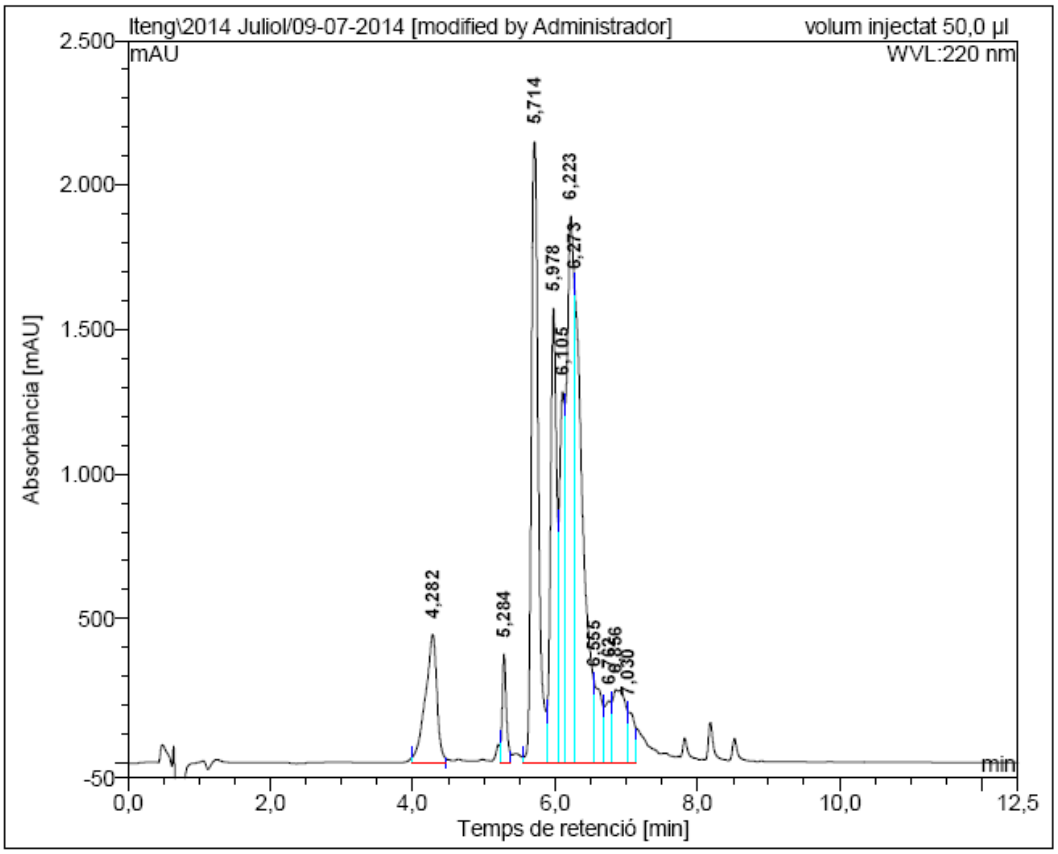

No.	mps retenc min	alçada mAU	Area mAU*min	Area relativa %
1	4,28	443,481	84,118	7,03
2	5,28	375,948	26,007	2,17
3	5,71	2147,748	246,370	20,58
4	5,98	1571,558	160,207	13,38
5	6,11	1282,747	97,631	8,16
6	6,22	1890,043	220,412	18,41
7	6,27	1646,613	235,950	19,71
8	6,56	274,338	30,443	2,54
9	6,76	213,917	23,673	1,98
10	6,86	253,748	54,173	4,53
11	7,03	175,102	17,986	1,50
Total:		10275,243	1196,971	100,00

ESI-MS *m/z*

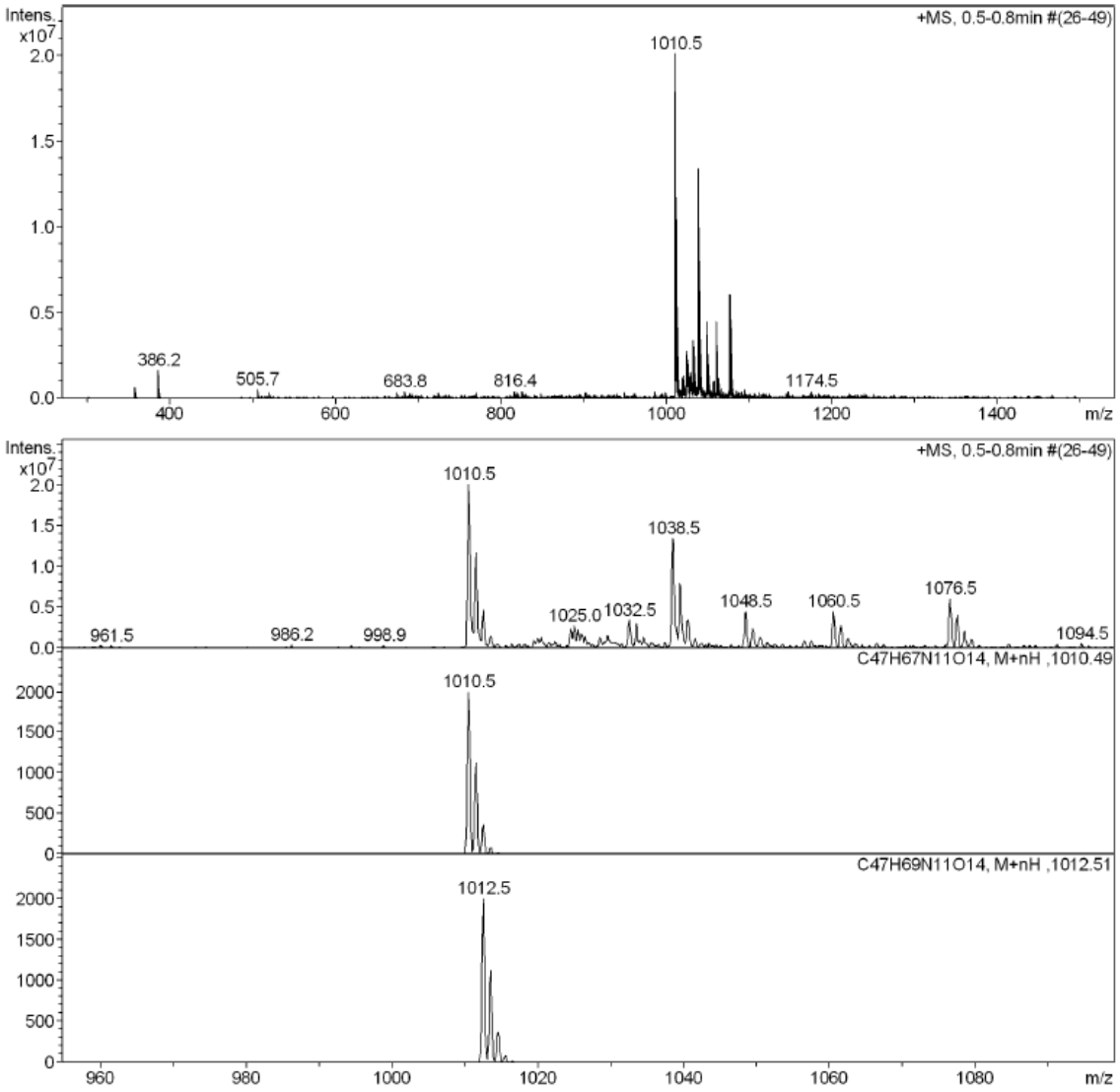
Intens.
x10^7
+MS, 0.5-0.8min #(26-49)
1010.5
386.2
505.7
683.8
816.4
1174.5
m/z
1038.5
1076.5
1025.0
1032.5
1048.5
1060.5
961.5
986.2
998.9
1094.5
C47H67N11O14, M+nH ,1010.49
C47H69N11O14, M+nH ,1012.51
1012.5

4. Biaryl bicyclic peptides 1-4

Biaryl bicyclic peptide 1

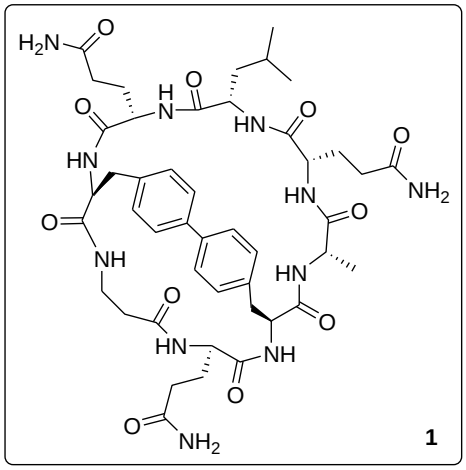

HPLC (λ = 220 nm)

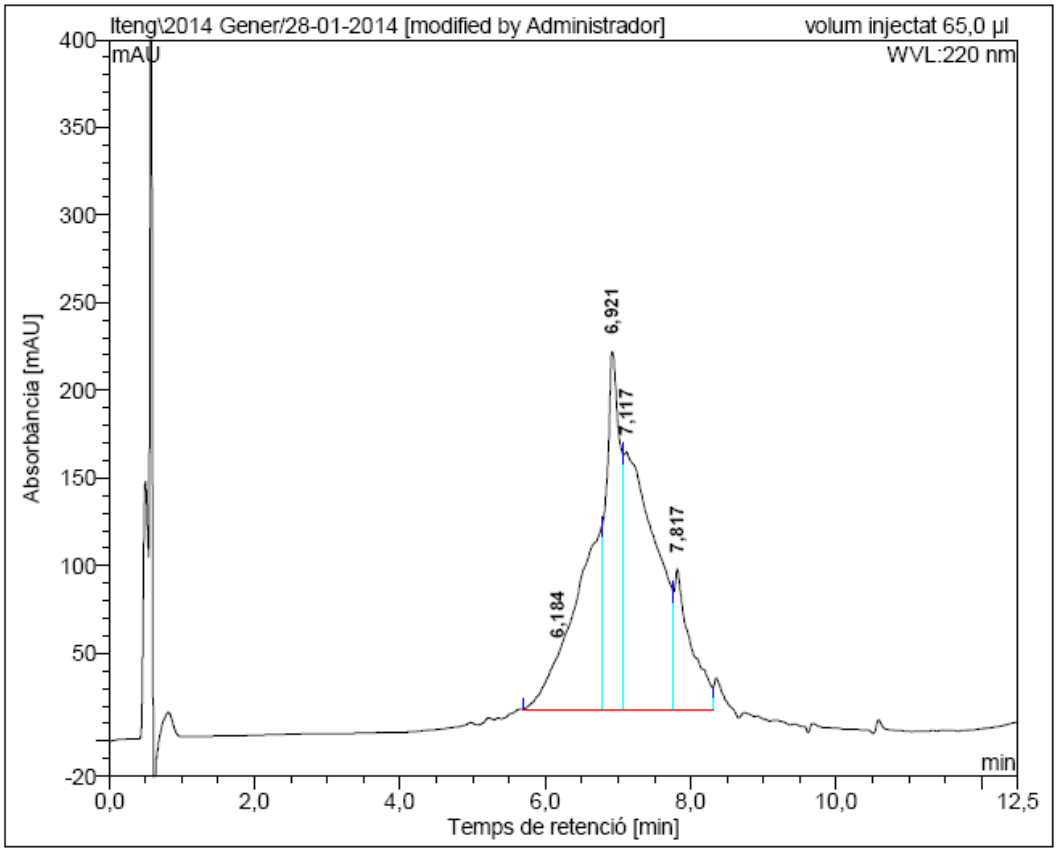

No.	mps retenc min	alçada mAU	Area mAU*min	Area relativa %
1	6,18	31,344	47,202	24,83
2	6,92	203,859	44,684	23,51
3	7,12	146,649	76,901	40,46
4	7,82	79,824	21,275	11,19
Total:		461,677	190,063	100,00

ESI-MS *m/z*

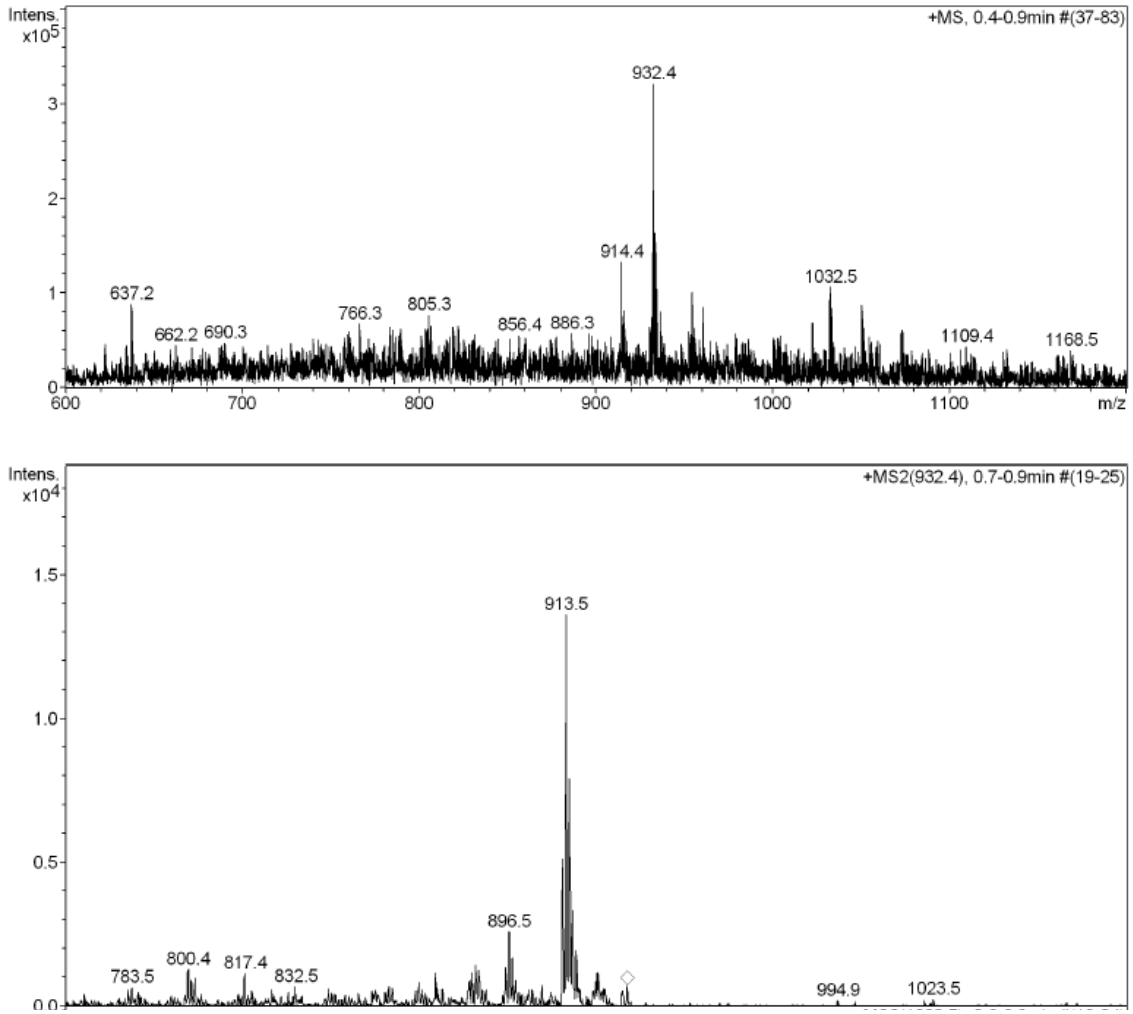
Intens.
x10^5
+MS, 0.4-0.9min #(37-83)
932.4
914.4
1032.5
637.2
662.2
690.3
766.3
805.3
856.4
886.3
1109.4
1168.5
600
700
800
900
1000
1100
m/z
Intens.
x10^4
+MS2(932.4), 0.7-0.9min #(19-25)
913.5
896.5
783.5
800.4
817.4
832.5
994.9
1023.5

Biaryl bicyclic peptide 2

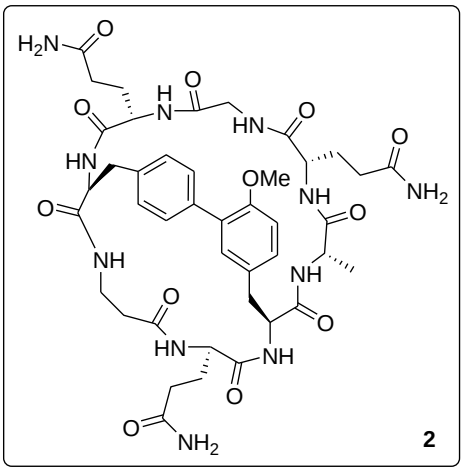

HPLC (λ = 220 nm)

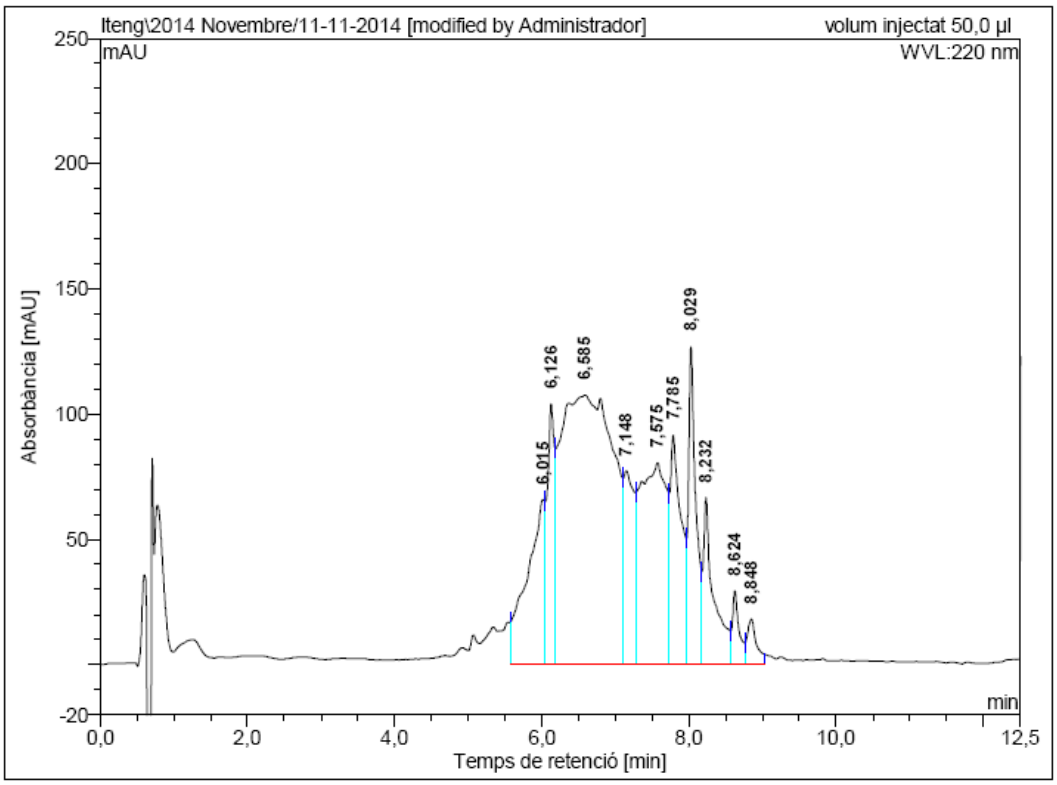

No.	Temps retenció min	alçada mAU	Area mAU*min	Area relativa %
1	6,02	65,568	18,478	8,65
2	6,13	103,808	11,122	5,21
3	6,58	107,364	89,810	42,03
4	7,15	77,132	12,625	5,91
5	7,57	80,330	33,471	15,67
6	7,79	91,242	15,582	7,29
7	8,03	126,519	15,664	7,33
8	8,23	66,352	11,030	5,16
9	8,62	29,175	3,176	1,49
10	8,85	17,984	2,706	1,27
Total:		765,475	213,662	100,00

ESI-MS *m/z*

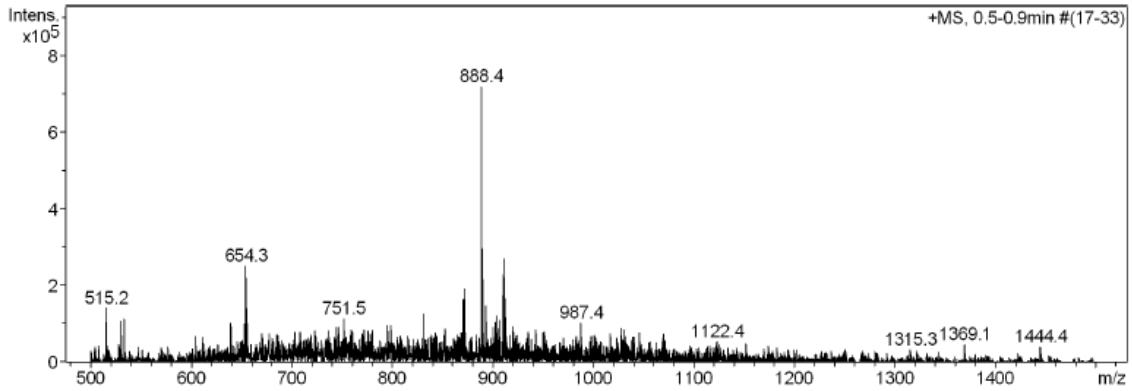
Intens.
x10^5
+MS, 0.5-0.9min #(17-33)
888.4
654.3
515.2
751.5
987.4
1122.4
1315.3
1369.1
1444.4
m/z

Biaryl bicyclic peptide 3

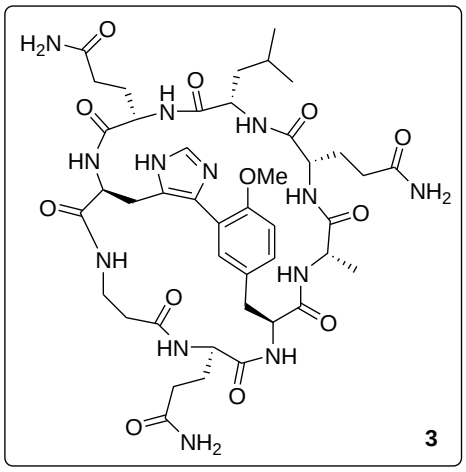

HPLC (λ = 220 nm)

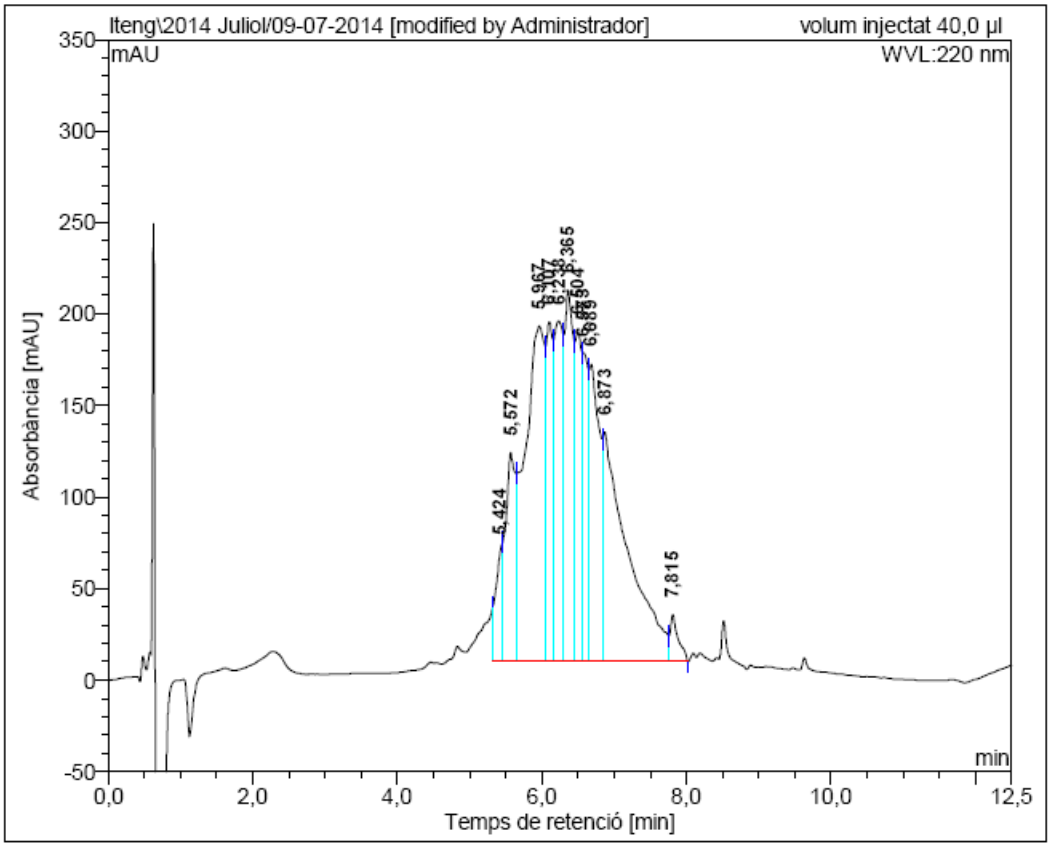

No.	mps retenc min	alçada mAU	Area mAU*min	Area relativa %
1	5,42	59,806	6,674	2,46
2	5,57	113,956	17,670	6,52
3	5,97	182,968	57,835	21,35
4	6,11	185,475	19,535	7,21
5	6,24	185,647	26,003	9,60
6	6,37	202,727	28,291	10,44
7	6,50	179,918	19,766	7,30
8	6,57	168,441	14,526	5,36
9	6,69	162,106	26,115	9,64
10	6,87	125,017	51,088	18,86
11	7,81	25,279	3,372	1,24
Total:		1591,340	270,876	100,00

ESI-MS *m/z*

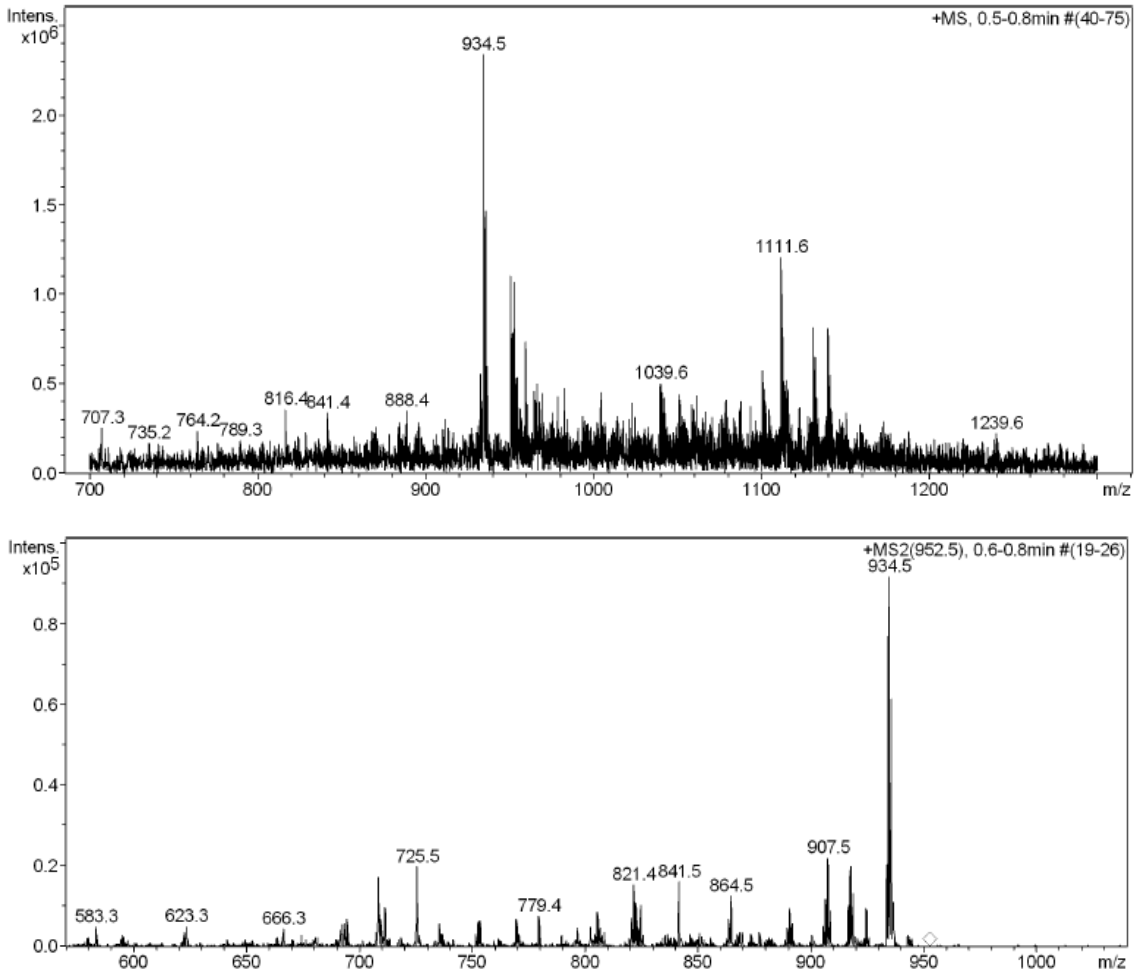
Intens.
x10^6
+MS, 0.5-0.8min #(40-75)
934.5
1111.6
1039.6
816.4
841.4
888.4
707.3
735.2
764.2
789.3
1239.6
m/z
Intens.
x10^5
+MS2(952.5), 0.6-0.8min #(19-26)
934.5
907.5
725.5
821.4
841.5
864.5
779.4
583.3
623.3
666.3
m/z

Biaryl bicyclic peptide 4

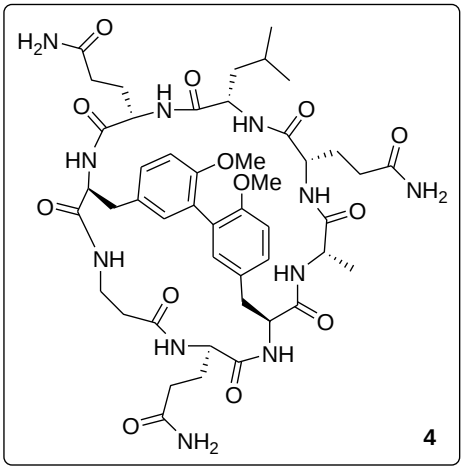

HPLC (λ = 220 nm)

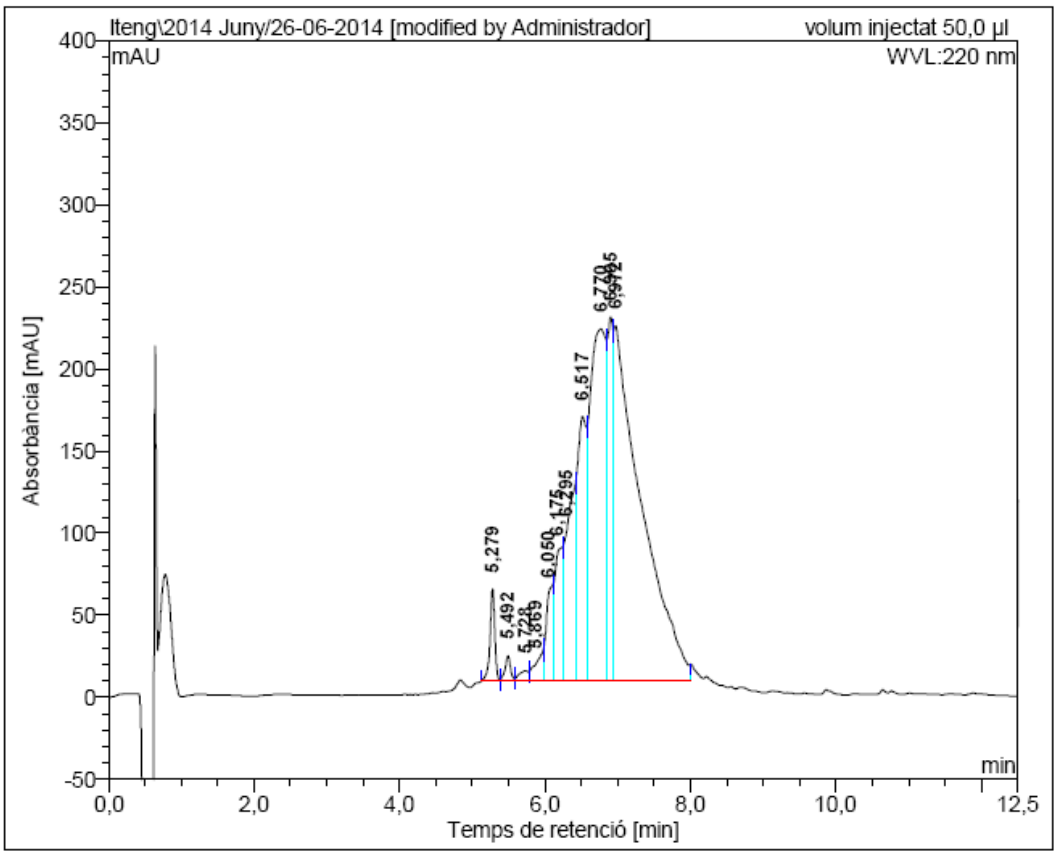

No.	mps retenc min	alçada mAU	Area mAU*min	Area relativa %
1	5,28	55,926	4,215	1,80
2	5,49	15,134	1,317	0,56
3	5,73	6,218	0,889	0,38
4	5,87	9,783	2,208	0,94
5	6,05	52,697	6,250	2,66
6	6,18	78,081	9,224	3,93
7	6,30	90,107	18,007	7,67
8	6,52	161,280	22,758	9,70
9	6,77	214,654	54,598	23,26
10	6,90	221,751	20,464	8,72
11	6,97	216,577	94,808	40,39
Total:		1122,206	234,739	100,00

ESI-MS *m/z*

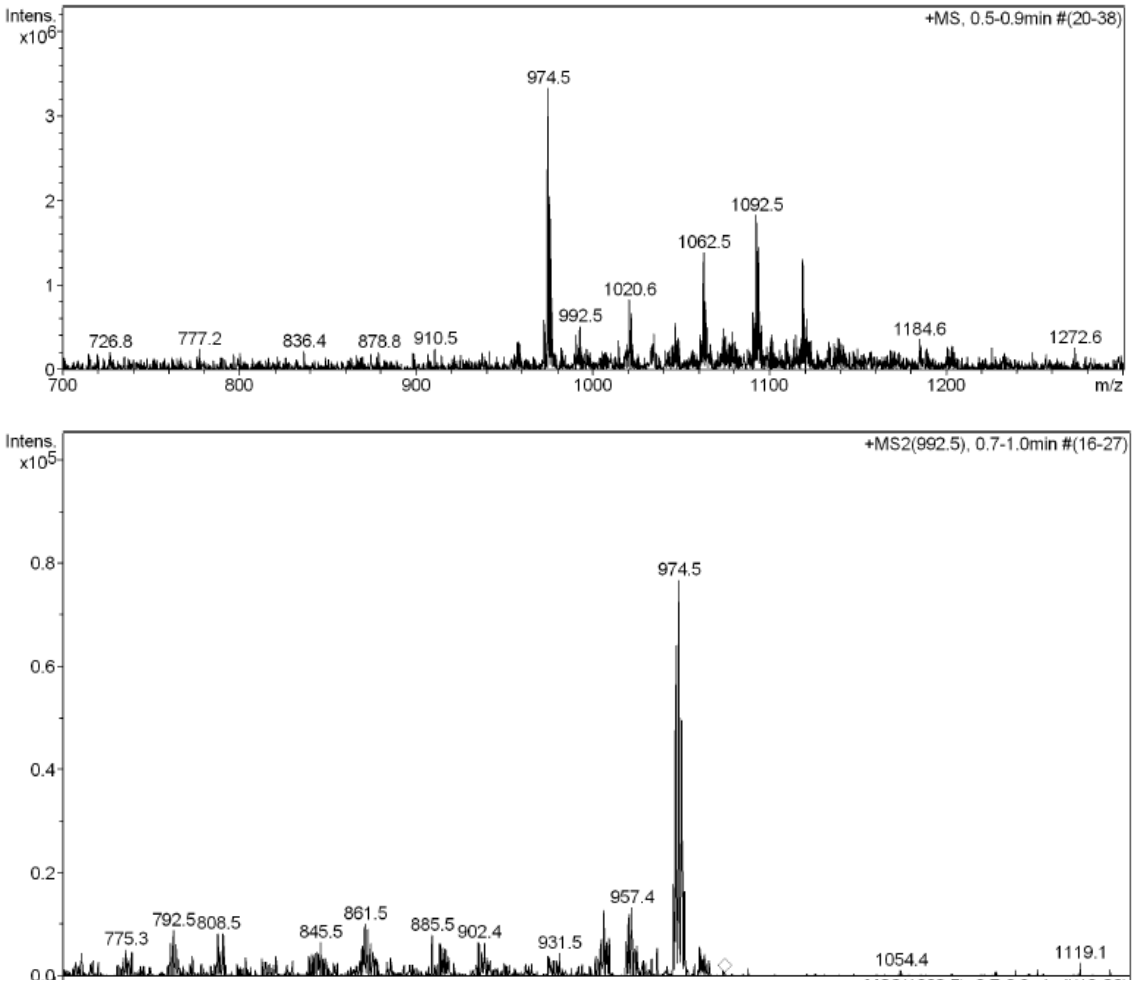
Intens.
x10^6
+MS, 0.5-0.9min #(20-38)
974.5
1092.5
1062.5
1020.6
992.5
726.8
777.2
836.4
878.8
910.5
1184.6
1272.6
700
800
900
1000
1100
1200
m/z
Intens.
x10^5
+MS2(992.5), 0.7-1.0min #(16-27)
974.5
957.4
792.5
808.5
775.3
861.5
845.5
885.5
902.4
931.5
1054.4
1119.1